

ANNUAL REVIEW OF NUCLEAR SCIENCE

Co-editors:

EMILIO SEGRÈ
University of California

LEONARD I. SCHIFF
Stanford University

Associate Editors:

GERHART FRIEDLANDER
Brookhaven National Laboratory

WALTER E. MEYERHOF
Stanford University

VOLUME 9

1959

PUBLISHED BY
ANNUAL REVIEWS, INC.
IN CO-OPERATION WITH THE
NATIONAL RESEARCH COUNCIL
OF THE NATIONAL ACADEMY OF SCIENCES

ON SALE BY
ANNUAL REVIEWS, INC.
PALO ALTO, CALIFORNIA, U.S.A.

Engin.

QC

770

.A65

Vol. 9

ANNUAL REVIEWS, INC.
PALO ALTO, CALIFORNIA, U.S.A.

© 1959 BY ANNUAL REVIEWS, INC.
ALL RIGHTS RESERVED

Library of Congress Catalog Card Number: 53-995

FOREIGN AGENCY

Maruzen Company, Limited
6 Tori-Nichome Nihonbashi
Tokyo

PRINTED AND BOUND IN THE UNITED STATES OF AMERICA BY
THE GEORGE BANTA COMPANY, INC.

PREFACE

In presenting the ninth volume of this Review to the public we can not fail to express again our thanks to the authors. They have gone to great pains to summarize a tremendous and ever-growing body of knowledge, trying to make it accessible to their fellow scientists. The great labor involved is one of the most meritorious we can think of at the present state of nuclear science, and the unselfish sacrifice in time and effort by the contributors entitles them to the gratitude of all the readers.

No great changes in editorial policy are to be recorded this year.

Unfortunately nuclear science which has suffered in recent years such grave and untimely losses must add another unexpected death. Wolfgang Pauli died on December 15, 1958, at the age of 58. With him theoretical physics lost one of its most illustrious exponents: the discoverer of the exclusion principle. Apart from this most fundamental contribution to all physics, nuclear science remembers him also as the theoretical discoverer of the neutrino and the nuclear spin and as one of the keenest minds to plumb the secrets of the nucleus.

To Joann Huddleston, our editorial assistant, the editors and the editorial committee are indebted for competent and devoted help throughout the preparation of this volume.

EMILIO SEGRÈ

ERRATA

Volume 8

We regret that the names of E. M. Burbidge and G. R. Burbidge were consistently spelled Burbridge in this volume.

CONTENTS

	PAGE
NUCLEAR PHOTODISINTEGRATION, <i>D. H. Wilkinson</i>	1
THE PION-NUCLEON INTERACTION AND DISPERSION RELATIONS, <i>Geoffrey F. Chew</i>	29
STRANGE PARTICLES, <i>L. Okun'</i>	61
THE EXPERIMENTAL CLARIFICATION OF THE LAWS OF β -RADIOACTIVITY, <i>E. J. Konopinski</i>	99
HIGH-ENERGY NUCLEAR REACTIONS, <i>J. M. Miller and J. Hudis</i> . .	159
TECHNETIUM AND ASTATINE CHEMISTRY, <i>Edward Anders</i>	203
SOLVENT EXTRACTION IN RADIOCHEMICAL SEPARATIONS, <i>Henry Freiser and George H. Morrison</i>	221
NUCLEAR FISSION, <i>I. Halpern</i>	245
ELECTRONICS ASSOCIATED WITH NUCLEAR RESEARCH, <i>H. W. Kendall</i>	343
HIGH-TEMPERATURE PLASMA RESEARCH AND CONTROLLED FUSION, <i>R. F. Post</i>	367
FAST REACTORS, <i>Leonard J. Koch and Hugh C. Paxton</i>	437
ECONOMICS OF NUCLEAR POWER, <i>James A. Lane</i>	473
VERTEBRATE RADIOBIOLOGY (EMBRYOLOGY), <i>Roberts Rugh</i> . . .	493
BIOCHEMICAL EFFECTS OF IONIZING RADIATION, <i>Margery G. Ord and L. A. Stocken</i>	523
CELLULAR RADIOBIOLOGY, <i>K. C. Atwood</i>	553
INDEXES	593

Annual Reviews, Inc., the National Research Council, and the Editors of this publication assume no responsibility for the statements expressed by the contributors to this *Review*.

NUCLEAR PHOTODISINTEGRATION¹

By D. H. WILKINSON

Clarendon Laboratory, Oxford, England

INTRODUCTION

Nuclear photodisintegration was last reviewed in this series by Levinger (1) in 1954. We shall take his review as our starting point and refer to earlier material only if necessary for the sense of the present treatment or if it was there overlooked or has acquired a new importance; we shall not be historical and shall resist the temptation to be consistent. Other reviews have appeared elsewhere in the meantime (2, 2a, 2b), and a useful bibliography is available (3). Because of this the present references have not been made by any means exhaustive. The examples quoted are those that seem to illustrate most directly and completely the point under discussion.

We shall concentrate chiefly on experimental results that bear fairly directly on the photodisintegration mechanisms themselves and shall not touch the large body of data of a systematic kind that so far does not seem to illuminate a specifically photonuclear aspect of theory. Similarly, we shall only mention those researches among the light nuclei that bear on photonuclear models and we do not pretend to treat those whose chief interest is for nuclear structure or some more general matter such as isotopic spin. There is a need for detailed data in the light nuclei to compare with detailed computations which, however, are as yet only exceptionally available. Photofission is omitted. So is the contentious matter of the "breaks" or fine structure in the photonuclear cross section; this is of interest in its own right but has little importance for the present discussion of the photoreaction mechanism.

PHOTODISINTEGRATION OF THE DEUTERON

The discussion of the radiative properties of the two-nucleon systems has been made much more meaningful by the recent development of nucleon-nucleon potentials that account successfully for the phenomena of n - p and p - p scattering in the energy range up to 200 Mev or so. Chief among these are the Gammel-Thaler (4) and Signell-Marshak (5) potentials. They contain hard cores and strong, explicit, *ad hoc* spin-orbit terms of the velocity-dependent LS type. The latter are necessary to account for the polarization data which cannot be fitted by any combination of purely central and tensor forces (6). Both potentials retain a tensor term which is strongly indicated by meson theory. The chief difference between them is that the Signell-Marshak (5) potential starts off from a meson-theoretic potential of the Gartenhaus (7) type (central plus tensor), while the Gammel-Thaler (4)

¹ The survey of literature pertaining to this chapter was concluded in March, 1959.

potential has as its starting point an empirical set of phase shifts at one energy. The differences between the predictions of these two potentials are remarkably slight except for the triple-scattering parameters which are not yet well determined by experiment.

Any computation of interest in the two-nucleon problem should be redone using these potentials. Unfortunately the first experimental datum whose accuracy has been significantly improved in recent years has not yet received such adequate theoretical treatment. This is the radiative capture cross section of protons for thermal neutrons which, at 2200 m./sec. [(8); see (8a) for experimental references] is now given as:

$$\sigma_{ap} = 0.3315 \pm 0.0017 \text{ barn.}$$

Since this cross section is now known with considerable accuracy, it can be used as a test for the contribution to the (*M*1) *n-p* capture of mesonic exchange currents which would themselves be specified by a detailed theory. This contribution would manifest itself as a discrepancy between experiment and the simple theory which involves only the initial and final state nucleon wavefunctions and the free nucleon magnetic moments. Such a calculation is now due and would be of considerable interest, since preliminary work (9) suggests that the exchange contribution may well be 5 to 10 per cent. [See Berger (10) for a discussion of the exchange contribution to *M*1 photodisintegration at moderate energies.]

There are no photodisintegration measurements proper of increased precision below $E_\gamma \simeq 20$ Mev (E_γ = gamma-ray energy) although new data (11, 11a) give a confirmation of earlier results (12, 12a) and a reassurance of the adequacy of the standard (effective range) treatment of the total cross section (13, 14, 14a) at these energies. However, even at these low energies an interesting discrepancy with the first-order theory (14, 14a) ($E1 \text{ } ^3S \rightarrow ^3P$ plus *M*1 $\text{ } ^3S \rightarrow ^1S$) of the angular distribution is clear. If we represent the differential cross section folded about 90° as:

$$d\sigma/d\Omega = A + B \sin^2 \theta$$

then the first-order theory predicts $A/B \sim 0.02$ above the lowest energies. Experiment (11, 11a) for $E_\gamma = 20\text{--}25$ Mev gives $A/B = 0.12 \pm 0.01$. This discrepancy increases with increasing gamma-ray energy (15, 15a, 15b): the 0° or 180° differential cross section remains almost constant at about $A = 4\text{--}5 \mu\text{barn/ster.}$, while the 90° cross section declines smoothly from about $A+B = 50 \mu\text{barn/ster.}$ at 20 Mev to $5 \mu\text{barn/ster.}$ at 250 Mev. The comparison with first-order theory (14, 14a) for the total cross section σ_t is good up to about $E_\gamma = 50$ Mev, but beyond that a discrepancy develops rapidly. Already at $E_\gamma = 150$ Mev experiment is five times as big as theory. A pronounced resonancelike behaviour at $E_\gamma \simeq 250$ Mev suggests strongly that the $T=3/2$, $J=3/2$ isobar found in π -*p* scattering at a pion energy of about 180 Mev [see e.g. (16)] is participating actively in the photodisintegration process (17, 17a). This isobar is seen also as a resonance in pion photoproduction from hydrogen [see e.g. (18)] as expected at $E_\gamma \simeq 320$ Mev. In the deu-

teron photodisintegration one may crudely think of the photoproduction of a pion from one nucleon followed by resonant $3/2, 3/2$ scattering from that nucleon and absorption by the other. It is also important to consider (19) s -wave photopion production followed by $3/2, 3/2$ scattering from the second nucleon and re-absorption by the first. The detailed description of this process is not yet clear and is beyond the scope of the present review, but the phenomenon suffices to teach us that explicit account must be made of mesonic contributions to deuteron photodisintegration above 200 Mev. This was only to be expected, but it is important to ask at how low an energy one must in fact renounce a description of the process purely in terms of the nucleon wavefunctions, i.e., how long will Siegert's theorem hold (1)?

We have noted a serious discrepancy with first-order theory even at $E_\gamma \simeq 20$ Mev, and by $E_\gamma \simeq 70$ Mev the isotropic term is indeed dominating the cross section although the isotropic $M1$ contribution (14, 14a) is tiny. Early attempts to explain this were unsuccessful, and Austern (20) was led to the conclusions that the Siegert theorem was invalid above $E_\gamma \simeq 20$ Mev and that some specifically mesonic model such as that of Wilson (21) was already necessary at those very low energies. With the development of the successful nucleon-nucleon potentials (4, 5) this supposition has been tested with surprising results. De Swart & Marshak (22), using the Signell-Marshak potential (5), and Nicholson & Brown (23), using the Gammel-Thaler potential (4), have calculated the differential cross section for $E1$ absorption alone, assuming Siegert's theorem to be valid but taking account of the $D \rightarrow P$ and $D \rightarrow F$ transitions from a 3D_1 ground state component of intensity specified by those potentials (about 7 per cent). This component is rather larger than that normally assumed (about 3 per cent) (13) but cannot be said to be in conflict with the experimental electric quadrupole and magnetic dipole moments. The calculations were done at $E_\gamma = 22, 54$ and 80 Mev (22), and 130 Mev (23). It is found that a very large isotropic component in fact results from pure $E1$ transitions. This is caused largely by interference between the final 3F and 3P states as can be seen from Table I taken from De Swart & Marshak (22), and so the initial D state plays a role out of proportion to its intensity. (Tensor coupling between the 3P_2 and 3F_2 final states is ignored.) The tensor splitting of the final 3P states is seen to be quite inadequate by itself.

Agreement with experiment is excellent and there is no need to question Siegert's theorem if the large D state admixture in the ground state remains acceptable. Agreement at $E_\gamma = 130$ Mev (23) is also quite good although the theoretical total cross section may be too small by about 10 to 15 per cent.

Such calculations using only $E1$ absorption must be extended to allow for $M1$ and $E2$ contributions. Although these may have only a slight effect on the total cross section, they can modify the angular distributions very considerably. These calculations have been made for gamma-ray energies from 20 to 200 Mev by Zernik, Rustgi & Breit (24) in the most comprehensive computations so far presented. A potential of the Signell-Marshak (5)

type was again used with some modification of the parameters (25). The experimental cross section, including the forward peaking resulting from interference between final states of opposite parity, is well reproduced and it is clear that considerably refined experiments will be needed in this energy range if a breakdown of Siegert's theorem is to be detected. Similarly, confidence in the potentials used in the computation must be increased; it should be emphasized that these were in no way adjusted to give best fit for the photodisintegration problem, but were taken over as derived from the

TABLE I
EXPERIMENTAL DEUTERON PHOTODISINTEGRATION CROSS SECTIONS*
COMPARED WITH $E1$ THEORY
[according to De Swart & Marshak (22)]

Photon energy	22.4 Mev			53.5 Mev			80 Mev		
	A	B	σ_t	A	B	σ_t	A	B	σ_t
Experiment	4.8 ± 0.8	47 ± 8	465 ± 50	5.1 ± 0.9	9.5 ± 1.5	140 ± 15	4.5 ± 0.8	3.9 ± 0.6	88 ± 10
First order theory (14, 14a)†	0	55	460	0	12.7	107	0	5.8	48
$^2S_1 \rightarrow ^2P_{0,1,2}$	0.4	52	442	0.2	12.8	110	0.6	5.6	54
$^2S_1 + ^2D_1 \rightarrow ^2P_{0,1,2}$	1.5	52	453	1.7	12.5	126	1.4	6.0	68
$^2S_1 + ^2D_1 \rightarrow ^2P_{0,1,2} + ^2F_3$	4.1	50	470	4.7	10.5	147	4.1	4.3	88

* Cross sections in μbarn .

† No interaction in the final state.

scattering data. A precise measurement of total cross section in the region where the $M1$ contribution has become small would be very useful.

Newton (26) has shown how the low-energy photodisintegration data themselves eliminate a possible class of long-tailed potentials that are otherwise consistent with the remaining low-energy data.

Zernik, Rustgi & Breit (24) have also considered nucleon polarization effects as have Czyz & Sawicki (27) whose work they correct. See also De Swart, Czyz & Sawicki (27a). Some general considerations from a restricted starting point have also been given (28). The polarization depends sensitively upon the approximations used and has a maximum value of about 20 per cent. It is to be noted that only when both parities are present in the final state can nonzero polarization be found at 90° . No experimental data are yet available on polarization.

Successful sum-rule calculations, including considerations about $M1$ transitions, have been carried out (29, 29a, 30) although, since detailed calcu-

lations are available, their chief value is to gather all the experiments into a single datum (and incidentally to be themselves tested with a view to later application to complex nuclei). The bremsstrahlung-weighted integrated (E_1) cross section is found to be:

$$\sigma_{-1}^{E_1} = \int_0^\infty \sigma_t^{E_1} E_\gamma^{-1} dE_\gamma$$

where $\sigma_t^{E_1}$ is the total E_1 cross section. However, it is determined solely by the mean square radius R^2 of the positions of the nucleons:

$$\sigma_{-1}^{E_1} = \frac{4\pi^2}{3} \left(\frac{e^2}{\hbar c} \right) \frac{ZN}{A-1} R^2.$$

This is true for H^2 , H^3 , He^3 and He^4 , dependent only on the space-symmetry of the ground state wavefunctions. The experimental data for deuterium after correction for the $M1$ contribution yield $R = 1.95 \times 10^{-13}$ cm. To find the r.m.s. radius R_c of the charge distribution as seen for example by a probing charge, we must add suitably the r.m.s. radius of the proton itself: $R_p = 0.77 \times 10^{-13}$ cm. (31). From $R_c^2 = R^2 + R_p^2$ we then find $R_c = 2.10 \times 10^{-13}$ cm. which is in good agreement with that directly determined by fast electron scattering (31). This constitutes a nice comparison between two totally different forms of experimentation.

PHOTODISINTEGRATION OF THE VERY LIGHT NUCLEI

Considerable new experimental material has recently become available on the photodisintegration of the lightest nuclei, particularly of He^4 (32 to 32c). Unfortunately there has not been a corresponding increase in our ability to give a detailed theoretical treatment and the time is not ripe for an extensive discussion. The difficulty is connected with the failure of variational calculations to reproduce the ground state properties of these nuclei. Characteristically, the calculations produce too small an r.m.s. size for He^4 ($R \simeq 1.0 \times 10^{-13}$ cm.). This is reflected in a gross discrepancy between the experimental and theoretical values for the bremsstrahlung-weighted integrated cross section σ_{-1} (see above) (30, 33); the experimental r.m.s. size is $R = 1.46 \times 10^{-13}$ cm. This figure accords well with the value $R = 1.41 \times 10^{-13}$ cm. derived from the elastic scattering of fast electrons by helium (31) (where due allowance has been made for the finite size of the proton—see above). This agreement places the responsibility squarely upon theory. Considerable progress has been made in the corresponding problem for $A=3$ (34, 34a) by the introduction of hard cores into the nucleon-nucleon potential, but here we have very little experimental photonuclear data. Similar theoretical treatment is clearly demanded for He^4 (35).

Sum rules for H^3 and He^3 have been given (36).

SUM RULES FOR COMPLEX NUCLEI

The various sum rules form a valuable adjunct to detailed models. In the hands of Levinger and others (37, 38 to 38c), they have helped our under-

standing of the relationships between models and of the importance of correlations in the photonuclear problem. Some reference to this will be made later.

The integral σ_0 of the total absorption cross section σ_t (which we understand to exclude elastic scattering) has been treated (39) using dispersion relations. This automatically includes all multipoles and absorption mechanisms.

$$\sigma_0 = \int_0^{E_\gamma'} \sigma_t dE_\gamma.$$

If E_γ' is set somewhere in the region of the meson threshold (by which time Siegert's theorem is certainly invalid), the result is very closely related to the usual $E1$ sum rule in which $E_\gamma' = \infty$. The precise reason for this coincidence is obscure; but the result is very valuable in indicating that the conventional use of the sum rules is unlikely to lead far astray, particularly when extra powers of E_γ are included in the denominator of the integrand. There is further comment later on this matter.

Sum rules for $E2$ transitions have recently been considered (40, 40a).

THE GIANT RESONANCE REGION

The last few years have seen a considerable improvement in the accuracy with which the total nuclear absorption cross section σ_t as a function of gamma-ray energy is known. This has come about chiefly from greater skill in the stabilization of betatron energies, a better handling of the bremsstrahlung problem (41), and a willingness to amass many millions of counts for the analysis of a single excitation function. The results are for the most part, however, still not as accurate as is needed. The advent of new techniques, particularly careful direct absorption studies (42) and methods of monochromatization of bremsstrahlung sources (43, 43a), is likely to effect a yet further great improvement in the next few years. Direct absorption studies are particularly urgently needed as they remove the uncertainty that always attends the correction of neutron yields for multiple emission. They also remove the necessity for measuring many separate partial cross sections which frequently makes work in the light elements rather unsure—though the partial cross sections themselves are often of great value.

Because of this hope that better results will be forthcoming, the present general situation (44, 45) in the giant resonance region will not now be extensively reviewed. Throughout the greater part of the periodic table, σ_t shows a strongly-resonant form peaking at $E_m \simeq 80 A^{-\frac{1}{2}}$ Mev and with a width Γ of the order of 5–7 Mev. At lower mass numbers E_m falls below this line and is roughly constant at about 20–23 Mev below $A \simeq 40$. It is clear that the absorption in this resonance is chiefly $E1$ because the integrated cross section, σ_0 , over it is comparable with the maximum allowed by the $E1$ sum rule (1, 37).

For some time there have been two chief attempts to explain this giant

resonance phenomenon. They are the collective (Migdal-Goldhaber-Teller) model and the shell or independent particle model (IPM); their early history has been summarized (1). The collective model for spherical nuclei has been little further developed in recent years although an attempt has been made (46) to relate its parameters to the two-nucleon force and it has been refined (47) by the introduction of Coulomb and compressibility effects. The IPM has received detailed treatment (48, 49).

ABSORPTION ACCORDING TO THE IPM²

A very great many shell model $E1$ transitions are in general possible at all sorts of energies. How then can they be expected to cluster together to form the giant resonance? The germ of the solution is seen by considering the simplest shell model, namely, an isotropic harmonic oscillator; all $E1$ transitions then have just the oscillator spacing. When the level positions are examined in a more realistic potential, all resemblance to the harmonic oscillator seems lost; the levels are jumbled together and the selection rules special to the harmonic oscillator no longer hold. For $E1$ transitions, however, the harmonic oscillator can still be seen through the jumble. This comes about because: (a) levels of a given sequence such as $1s$, $1p$, $1d$, \dots or $2s$, $2p$, $2d$, \dots still follow each other at more-or-less equal intervals near the top of the Fermi surface; (b) the matrix elements are much greater for the transitions that were allowed for the harmonic oscillator (one quantum jumps) than for those which were forbidden (multiple quantum jumps). The first point is attributable to the finiteness of the potential well. For an infinite square well the successive level spacings within a sequence increase with l , but the finite well has the effect of depressing the higher levels relative to the lower and so tends to restore equality of spacing. The second point is made in Table II which gives the square of the $E1$ radial overlap integral measured in units of the nuclear radius squared for an infinite square well (48). Again the results for a finite well would be closer to those for the harmonic oscillator.

The finite well and the $E1$ operator, together with the Pauli principle which restricts the shells of interest to those near the Fermi surface, conspire to restore much of the simplicity of the harmonic oscillator for this present problem. In this way it can be understood how the IPM can give rise to an $E1$ absorption of resonant form. Similarly we should expect this IPM resonance effectively to exhaust the $E1$ sum rule (37) since this is certainly true for the harmonic oscillator. At first sight this seems surprising since the form of that sum rule:

$$\sigma_0^{E1} = \int_0^\infty \sigma_t^{E1} dE_\gamma = 2\pi^2 \frac{e^2 \hbar}{mc} \frac{NZ}{A} (1 + \text{exchange terms}^3)$$

² IPM = independent particle model.

³ The exchange term arises from two-body Majorana exchange forces. Its empirical value is 0.6–0.8 if we cut short our evaluation of the integral at about the meson

implies the involvement of all the nucleons of the nucleus, and the low-lying states α seem inhibited from contributing by the Pauli principle if the higher states β to which they would make their strong $E1$ transitions are already full. This dilemma is resolved by remembering that in the definition of the oscillator strength as it enters the sum rule (37) a downward transition counts negatively. Thus, the negative contribution to the integrated cross section that would have resulted from the transitions $\beta \rightarrow \alpha$ is also removed for the same reason that prevents the transitions $\alpha \rightarrow \beta$: the states α are also full if the higher states β are. Thus, the nucleons in states α effectively make their positive contribution to the integrated cross section by cancelling the negative contribution from the downward transitions from the states β . In this way we can think of the contribution from a lower shell being passed upwards from shell to shell until it comes to the Fermi surface. The chief IPM transitions take place from the closed shells that lie within an "oscillator spacing" of the Fermi surface. It is important to remember that the valence nucleons of the unfilled shells are relatively few in number and make relatively little contribution to the cross section. Similarly, many of the transitions that contribute in important measure to the absorption process are to bound states and do not lead directly to the continuum. The value of the binding energy is of little account in discussing the primary absorption process.

A final point of detail in understanding how the IPM transitions can be so strong as to exhaust the sum rule is that a transition from a closed shell may be several times stronger than a single-particle transition. This in itself is a sort of collective effect but one wholly within the framework of the shell

threshold as we must since Siegert's theorem, on which the sum rule is based, will certainly be invalid by then. It is a weakness of this $E1$ sum rule that we do not know what to do about the breakdown of this theorem. The exchange term can be understood semiquantitatively on the IPM (50) as being associated with the velocity-dependence of the potential—see later. Its introduction into the collective model is obscure. In the dispersion theory treatment (39), σ_0 includes all multipoles, Siegert's theorem is not invoked, and the integral is explicitly taken only to the meson threshold μ . The result is just the first, no-exchange Thomas-Reiche-Kuhn (37), term in the above expression for σ_0^{E1} plus a contribution from above the meson threshold which represents chiefly real meson production:

$$\int_0^\mu \sigma_i dE_\gamma = \frac{2\pi^2 e^2 \hbar N Z}{mc A} + \int_\mu^\infty (Z\sigma_p + N\sigma_n - \sigma_i) dE_\gamma$$

where σ_p , σ_n are the gamma-ray absorption cross sections for the free proton and neutron. In a sense this enables one to account for the mesonic contribution to the sum rule either in the form of virtual mesons which produce the exchange forces that help to determine σ_i at the actual gamma-ray energies over which we evaluate the integral (viz. below the meson threshold) or alternatively in the form of real meson production in the range of gamma-ray energy above that at which we cut short our evaluation of σ_0 .

TABLE II

RADIAL OVERLAP INTEGRALS FOR AN INFINITE SQUARE WELL

(D is the square of the radial overlap integral measured in units of the nuclear radius)

1[l] to 1[l+1]	l	0	1	2	3	4	5	6
	D	0.28	0.38	0.44	0.49	0.53	0.56	0.58

2[l] to 2[l+1]	l	0	1	2	3
	D	0.23	0.28	0.33	0.37

3[l] to 3[l+1]	l	0	1
	D	0.22	0.25

1[l] to 2[l-1]	l	1	2	3	4	5
	D	0.09	0.07	0.05	0.04	0.04

1[l] to 2[l+1]	l	0	1	2	3
	D	0.001	0.002	0.002	0.003

2[l] to 3[l-1]	l	1	2
	D	0.12	0.09

model. It results from the correlations which the process of antisymmetrization imposes between the equivalent particles of a given shell (51). This is illustrated by tabulating in Table III the strengths S of the three possible types of transition from closed shells in jj coupling in terms of the single-particle transition strength between the same orbits such as was given in Table II for a particular well. This makes S roughly equal to the strength of the transition in single-particle (Weisskopf) units. The shell to which the transition is made is taken as initially empty. S depends only on l and is independent of the well shape.

It is seen that transitions that have no (classical) reversal of intrinsic

TABLE III

STRENGTHS OF TRANSITIONS FROM CLOSED SHELLS IN TERMS OF THE
TRANSITION STRENGTH FOR A SINGLE PARTICLE

Transition	S
$l + \frac{1}{2} \rightleftharpoons l + 1 + \frac{1}{2}$	$\frac{(l+1)(l+2)}{2l+3}$
$l + \frac{1}{2} \rightleftharpoons l + 1 - \frac{1}{2}$	$\frac{l+1}{(2l+3)(2l+1)}$
$l - \frac{1}{2} \rightleftharpoons l + 1 - \frac{1}{2}$	$\frac{l(l+1)}{2l+1}$

spin are enhanced over the single particle value while that in which the spin is reversed is inhibited. This is another factor that tends to sharpen the over-all absorption since the latter transition is at a greater energy than the former. Notice that S increases with l , that the largest l values are to be found in the sequence $1s, 1p, 1d, \dots$, viz. the nodeless radial wavefunctions, and that the radial overlap integral (Table II) is biggest for this sequence. This explains why the greatest contribution (typically 50 to 60 per cent) to the IPM picture of the giant resonance comes from the nodeless to nodeless transitions $1[l] \rightarrow 1[l+1]$. Transitions of the type $2[l] \rightarrow 2[l+1]$ contribute typically about 20 to 25 per cent. Thus 70 to 85 per cent of all the IPM $E1$ absorption is given by transitions between successive states of the $1 \rightarrow 1$ and $2 \rightarrow 2$ sequences. Table IV illustrates how close together in energy such transitions in fact take place in a calculation using a finite square well (49) for Au. The energy units are arbitrary. When these transitions, and the others that make appreciable contributions, are weighted proportionally to their contribution they form a distribution of full width at half maximum (derived from the variance, assuming a Gaussian distribution) of 0.28 in the units of Table IV. Since the empirical value of E_m for Au is about 14 Mev, this corresponds to a theoretical spread of about 3.9 Mev in the IPM states.

It is likely, however, that a more realistic IPM computation using a well with a rounded edge instead of a square well would yield an even tighter grouping of transitions. This is qualitatively true because the rounding of the edge is a move towards the harmonic oscillator potential where all the transitions are degenerate. More quantitatively, such exact computations as have been done for level positions in rounded wells can be examined (52) and it can be seen that in going from the square to the rounded-off well the levels with no radial nodes move up relative to those with nodes so that the energy differences in the $1 \rightarrow 1$ sequence increase relative to those in the $2 \rightarrow 2$

TABLE IV

ENERGY OF IPM TRANSITIONS IN A FINITE SQUARE WELL FOR Au^{197} AFTER RAND (49). THE ENERGY SCALE IS IN ARBITRARY UNITS

Transition	Energy
Neutrons: $1 h_{9/2} \rightarrow 1 i_{11/2}$	1.08
$1 h_{11/2} \rightarrow 1 i_{13/2}$	0.83
$1 i_{13/2} \rightarrow 1 j_{15/2}$	0.87
$2 f_{5/2} \rightarrow 2 g_{7/2}$	1.22
$2 f_{7/2} \rightarrow 2 g_{9/2}$	1.05
Protons: $1 g_{7/2} \rightarrow 1 h_{9/2}$	0.96
$1 h_{11/2} \rightarrow 1 i_{13/2}$	0.78
$2 p_{1/2} \rightarrow 2 d_{3/2}$	1.05
$2 d_{3/2} \rightarrow 2 f_{5/2}$	1.11
$2 d_{5/2} \rightarrow 2 f_{7/2}$	0.97

sequence. As can be seen from Table IV, such a move will tighten the clustering.

It can now be seen that the clustering of the IPM transitions is tight enough for them to represent the giant resonance. An important question is the absolute value of the energy at which they take place. To settle this the scale and depth of the potential must be fixed first of all. These can be taken from the results on elastic proton and neutron scattering (53, 53a). The radius of the square well for the photonuclear computations is taken as equal to the half-way point of the Saxon-Woods potential used to analyse the elastic scattering results. This corresponds to a radius $R=r_0 \times A^{1/3}$, where $r_0=1.2 \times 10^{-13}$ cm. for the present purpose, consistent with the scattering data (53, 53a). These results also show that the potential is velocity-dependent and the experiments are consistent with a linear fall of the real part of the potential with increasing nucleon energy. This means that, near the Fermi surface, the velocity dependence can be represented by an effective nucleon mass $m^* \neq m$, where m is the free mass. The many-body (Brueckner) treatment of nuclear matter [see e.g. (54); (54a)] suggests $m^* \simeq m/2$, and the elastic scattering results are not inconsistent with this although they are not accurate enough to fix m^* at all well. It was realized early in the IPM treatment of the giant resonance that the use of a small effective mass was essential to success. Wilkinson (48) has used $m^*=0.5 m$, and Rand (49) has used $m^*=0.55 m$. Both used $r_0=1.2 \times 10^{-13}$ cm. and finite square wells adjusted to give the correct binding energies.⁴ Table V shows the results of these computations for 18 monoisotopic or almost monoisotopic elements which

⁴ The further into the continuum a level is moved, the more will it be depressed relative to its position in an infinite well so we might qualitatively expect that tightly-bound nuclei may have higher E_m values. There is some indication of this (55).

TABLE V

MEASURED (45) AND CALCULATED ENERGIES E_m AND WIDTHS Γ OF THE GIANT RESONANCE IN A NUMBER OF MONOISOTOPIC ELEMENTS

E_m (theo. 1) gives the calculated position using a finite square well of radius constant $r_0 = 1.2 \times 10^{-13}$ cm. and an effective mass $m^* = 0.5 m$ (see text). E_m (theo. 2) includes the effects of the pairing energy. The experimental values (exp.) have been taken from reference (45).

The theoretical widths Γ (theo.) have been computed using a width of 3 Mev for the various IPM transitions that superpose to make up the resonance. The widths in the rare earth region are discussed separately in the text and are presented in Table VI.

Isotope	E_m (theo. 1) Mev	E_m (theo. 2) Mev	E_m (exp.) Mev	Γ (theo.) Mev	Γ (exp.) Mev
V ⁵¹	16.8	19.9	18.4	7.3	4.9
Mn ⁵⁵	16.4	19.5	19.2	7.2	6.5
Co ⁵⁹	16.4	19.4	18.0	7.3	5.4
As ⁷⁵	16.3	19.0	16.4	9.4	7.6
Y ⁸⁹	15.7	18.3	17.1	6.5	5.2
Nb ⁹³	15.4	17.9	17.0	6.8	6.0
Rh ¹⁰³	14.1	16.6	16.3	6.5	7.5
I ¹²⁷	13.6	15.8	15.2	6.6	4.5
Cs ¹³³	13.9	16.1	16.0	6.4	6.0
La ¹³⁹	13.7	15.8	15.5	6.8	3.2
Pr ¹⁴¹	13.5	15.6	15.0	5.8	4.7
Tb ¹⁵⁹	13.0	15.0	14.2	see Table VI	
Ho ¹⁶⁵	12.7	14.7	13.3	see Table VI	
Tm ¹⁶⁹	12.7	14.6	13.8	see Table VI	
Lu ¹⁷⁵	12.4	14.3	15.0	see Table VI	
Ta ¹⁸¹	12.0	13.9	13.9	see Table VI	
Au ¹⁹⁷	11.7	13.5	13.5	5.5	3.4
Bi ²⁰⁹	11.9	13.7	13.2	5.4	4.5

have formed the subject of a recent careful experimental study (45). The two theoretical studies (48, 49) have been combined in column E_m (theo. 1). Rand's results (49) have been slightly modified to $m^* = 0.5m$, and the earlier calculations (48) have been redone using Rand's better method of allowing for the change of effective mass across the nuclear boundary. The theoretical transition energies have all been diminished by 10 per cent from the values given by the simple computation to allow for relativistic effects (49). Before comparing them with experiment, the theoretical results must be adjusted to allow for the effect of the pairing energy [see e.g. (56)] necessary to break up the closed shells that are chiefly responsible for the absorption. The pairing energy has been estimated from such data as are available and declines smoothly from about 3.0 Mev near $A = 50$ to about 1.8 Mev near $A = 200$.

(These are effective values representing a suitable average over the various shells involved.) Column E_m (theo. 2) shows the effect of these corrections and is to be compared with the experiments in column E_m (exp.). The agreement is excellent. It must be emphasized that this agreement between experimental and calculated giant resonance positions is entirely contingent upon the use of a small effective mass.⁵

Rough agreement between the theoretical and experimental integrated cross sections now follow from the sum rules and the fact that the resonances are rather sharp. In that case, $E_m \simeq \bar{E}_{-1}$, the harmonic energy. But $\bar{E}_{-1} = \sigma_0/\sigma_{-1}$ while σ_{-1} is rather model-insensitive (37)⁶ so σ_0 should be determined chiefly by the position of the resonance and if agreement is obtained on E_m it will be obtained on σ_0 . This is borne out by detailed computation (48, 49). It could alternatively have been argued that since exchange forces increase σ_0 without affecting σ_{-1} then they must raise \bar{E}_{-1} , hence E_m . This suggests a general equivalence of exchange force, and velocity-dependent potential (effective mass) approaches to the problem of raising E_m and σ_0 . This equivalence has been investigated for the particular case of the Van Vleck potential whose velocity dependence is caused largely by Majorana exchange forces (50).

So far the IPM model has been discussed solely from the point of view of a pure real potential. In fact, it must be allowed that there is also an imaginary part. This, crudely speaking, has the effect of blurring the positions of the single-particle states by dissolving them into a multitude of compound nucleus states over a region of order $2W$ in width, where W is related to the imaginary part of the potential. This effect is complicated in the present problem because, thinking of the situation naively and pictorially, both the excited nucleon and the hole in the closed shell from which it was excited have finite mean free paths against the breakdown of their simple orbital motions and so both contribute to the lack of definition of the transition energy. There is fair information on excited particles (53) but very little on the damping of holes. To some degree the effects are complementary in that if the broken shell is deep lying the hole would be expected to be quickly damped but in that case the excited particle will be near the Fermi surface where its mean free path is long. Another difficulty is that such information as there is about W relates chiefly to states of low orbital angular momentum which contribute chiefly to scattering, whereas the present interest is chiefly in states of high l -value found in the important $1 \rightarrow 1$ sequence. It is difficult to guess which way this will affect the effective value of W . Because of these

⁵ This effect has been disputed by Agranovitch & Stavinski (55); their treatment of the effective mass seems inconsistent and their handling of the excited states is not acceptable, since they base it on the Lane-Thomas-Wigner method which gives poor results for nucleon scattering.

⁶ In particular, Okamoto (57) has recently shown that the effect of dynamical correlations on σ_{-1} using a Fermi-gas (simple IPM) model with account taken of the two-body forces is only a few per cent (decrease). The effect on σ_0 is also small.

uncertainties it is impossible to estimate with confidence the spread of the strength functions of the many IPM transitions. The smearing should clearly be a few Mev for each transition, and for purposes of illustration we shall use 3 Mev. This figure is consistent with available knowledge of the optical model parameters in the regions involved. With this assumption the total widths expected for the giant resonance on the IPM picture can be computed. This is done also in Table V where the data of Rand (49) have been slightly modified and supplemented where necessary. The nuclei in the rare-earth region have been omitted for reasons to be discussed shortly. The comparison between the experimental (45) and theoretical widths reveals a fair measure of agreement. There is, however, a clear tendency for the IPM widths to be too large. This may be attributable to the choice of too large a width, 3 Mev, for the individual transitions. It may also be caused by the need for computations with a rounded well which, as noted before, will sharpen the energy distribution of the IPM. The explanation may be a more fundamental one, however, namely the inadequacy of the simple IPM picture.

THE COLLECTIVE MODEL AND DEFORMED NUCLEI

At this point we leave the IPM description and turn to examine the alternative, collective model of the absorption process (1). In this essentially classical model, the neutron and proton fluids run through each other in bulk in opposite directions to constitute the resonance. Two extreme approximations may be pictured: (a) the proton and neutron fluids move through each other as individually rigid spheres; (b) the envelope of the nucleus remains fixed and the oscillating fluids adjust themselves so that their combined density at each point is constant. Approximation (a) leads to $E_m \sim A^{-1/6}$ and approximation (b) to $E_m \sim A^{-1/3}$. Approximation (b) is favoured by experiment for the greater part of the periodic table. This model is not clearly enough defined and its relation to quantum mechanics is too obscure to form the basis for an absolute prediction about E_m at the moment. The estimates that can be made (1, 47) by the borrowing of data from other parts of nuclear physics yield E_m values of the right order. Since the collective model, from the beginning, pictures the giant resonance as a single vibration, it has no difficulty in explaining the sharpness of the resonance. On the other hand it is equally unable of itself to give a quantitative account of the actual width. It is a model merely of the absorption mechanism and can say nothing quantitative about the "viscous forces" that break down the simple two-fluid motion and give the resonance its width. Attempts have been made to represent this width as resulting from a coupling between the collective resonance and individual nucleon properties (58 to 58b), but they have met criticism (59).

This discussion of both models has been limited to spherical nuclei. Many nuclei are in fact strongly deformed, especially in the region of the rare earths. In this circumstance the collective model makes an immediate and

exciting prediction (60, 60a). In a uniaxial ellipsoid two frequencies of oscillation now appear, a slow vibration for motion in the major axis and a faster vibration for motion in a minor axis (positive deformation). The giant resonance should therefore split into two, and the magnitude ΔE of the splitting is obviously related to the eccentricity ϵ of the ellipsoid. (Define $\epsilon = (R_1 - R_2)/R_0$ where R_1 and R_2 are the major and minor axes and R_0 is the radius of a sphere with the same volume as the ellipsoid.) As is to be expected, the frequency of the vibration varies inversely as the dimension of the box which contains it and in detail it is found that (60):

$$\begin{aligned}\Delta E &= \frac{1}{2}\epsilon E_m && \text{for approximation (a)} \\ &= \epsilon(1 - \epsilon)E_m && \text{for approximation (b)}\end{aligned}$$

(these are Okamoto's version; Danos' is essentially equivalent). E_m is the "unperturbed" resonance energy. When the finite width of the individual lines is taken into account, a broadening of the resonance for slightly-deformed nuclei and perhaps even a splitting for strongly-deformed nuclei might be expected.

It has been known for some time (61, 61a) that Γ is small in the region of magic and especially of doubly-magic nuclei. This was understood (48) from the IPM viewpoint as a result of the absence of diminution at such nuclei both of transitions from the valence nucleons, which would not be sharply grouped in energy, and also of the wide variety of couplings possible between the excited single-particle core state and the valence nucleons. Not until the suggestion of the collective model (60, 60a) of an actual possible splitting of the resonance was particular attention paid to the opposite region, namely, that remote from closed shells. A survey of the rare-earth region has in fact (62) shown that the giant resonances are there anomalously broad. A very careful and beautiful series of measurements (63) then revealed an actual splitting into two of the resonances for Tb^{159} and Ta^{181} . The experimental widths and splittings may now be compared with the two predictions of the collective model. This is done in Table VI adapted from Okamoto (60a), who derived values of ϵ for the various elements from spectroscopic and Coulomb excitation data. In computing Γ , a natural line width of 3.9 Mev has been used since this represents the observed widths for spherical nuclei in this region [the mean of recent results (45, 62) being taken]. The agreement is in general very satisfying particularly if approximation (b) is assumed to be valid. It is to be remembered that this is the approximation that gives $E_m \sim A^{-1/3}$ which, of the two, is the better representation of the data in the heavy elements. There is thus some internal consistency in the use of this approximation.

THE IPM FOR DEFORMED NUCLEI

What has the IPM to say? It is clear that in strongly deformed nuclei the simple calculations so far described do not apply. The individual j 's are no longer good quantum numbers but are replaced by the Ω 's, the projection

TABLE VI

RESONANCE WIDTHS IN THE RARE EARTHS

Experimental (62, 63) giant resonance widths Γ (exp.) and splittings ΔE (exp.) in the rare-earth region compared with the two predictions (a) and (b) of the collective model in approximations (a) and (b) and with the IPM prediction.

Element	ΔE (a) Mev	ΔE (b) Mev	ΔE (IPM) Mev	Γ (a) Mev	Γ (b) Mev	Γ (IPM) Mev	ΔE (exp.) Mev	Γ (exp.) Mev
Sm	1.2	2.1	(3.0)	5.1	6.0	8.0	—	8.6
Tb	3.1	4.0	4.6	7.0	7.9	10.6	3.8	8.7
Ho	2.3	3.3	4.6	6.2	7.2	10.0	—	7.5
Er	2.5	3.5	4.5	6.4	7.4	9.6	—	8.5
Yb	2.2	3.2	4.2	6.1	7.1	9.4	—	7.0
Ta	1.8	2.8	(3.5)	5.7	6.7	8.1	3.0	6.0

of the j 's on the nuclear symmetry axis. The previous $2j+1$ fold degeneracy with respect to the magnetic substates is lifted, and now many transitions of different energy are possible for each one before. This should be expected to broaden the resonance. The IPM calculation may now be done again using the results of Nilsson (64) for the level sequence in a deformed potential. The resonance is indeed found (65) to broaden as ϵ increases. Furthermore, for large values of ϵ it actually splits into two. The detailed results are also found in Table VI. It is seen that if anything the IPM exaggerates the phenomenon although it can be seen that the approximations made would tend to operate in this sense. A different IPM treatment has been given (66) with similar results. Detailed examination of the IPM calculation reveals another interesting point of similarity with the collective picture. It is that the transitions contributing to the upper peak are chiefly of high Ω while those in the lower peak are of low Ω . Classically, low Ω corresponds to nucleon motion along the major axis while high Ω represents motion in the minor axes—the same correlation between axis of motion and peak position as in the collective model. One cannot, therefore, expect clear discrimination to be made between the models on the basis of experiments with aligned nuclei or polarized gamma-rays.

RAPPROCHEMENT OF THE MODELS

The collective and IPM models seem very different and yet it has been seen that they make very similar predictions in many cases, even to details. Is this accident? A unified description was discussed qualitatively (67). More recently Brink (68) has demonstrated that the similarities are probably not accidental and that the two models are basically the same. He considered the harmonic oscillator version of the IPM, probably reasonably valid for light nuclei, and pointed out that in this case an exact separation

of the ground state wavefunction Φ_0 may be effected in the form:

$$\Phi_0 = \Psi_p \chi_n \zeta(\vec{R}) \beta_0(\vec{r})$$

where Ψ_p contains only the relative co-ordinates of the protons among themselves, χ_n similarly for the neutrons, $\zeta(\vec{R})$ describes the mass centre of the whole nucleus and $\beta_0(\vec{r})$ describes the separation of the mass centres of the proton and neutron groups. Furthermore, the IPM $E1$ operator can be re-written:

$$e \sum_i (\vec{r}_i - \vec{R}) = e \frac{NZ}{A} \vec{r}.$$

If one now operates on Φ_0 with the right-hand version of the $E1$ operator, the only term affected is $\beta_0(\vec{r})$ which is transformed into $\beta_1(\vec{r})$, viz. an $l=1$ state of relative motion of the neutron and proton mass centres instead of their initial $l=0$ motion. Ψ_p and χ_n are unaffected; the $E1$ operator merely sets the neutron and proton groups into motion relative to each other without changing either one. This is precisely approximation (a) of the collective model, and so a formal identity between the apparently conflicting models is established. Although there are many $E1$ IPM transitions superposed to form the giant resonance, the $E1$ operator arranges the excited states to have just the right relative phases to duplicate the collective motion of all neutrons vibrating against all protons.

In a potential representing a heavy nucleus, this special property is lost. However if the various IPM transitions are blurred by the 3 Mev or so as a result of the effective imaginary potential, so that they overlap to a large degree, then the effect will persist. By the time the initial phase relationship which produces the relationship between the models has been lost, any simple initial motion has been broken down anyway. It might therefore be said that the collective and IPM models are indistinguishable from each other for about the first few times 10^{-22} sec., after which time the region is entered about which the collective model does not attempt to speak, namely, that of the de-excitation processes.

Levinger (69) has extended an early treatment by Migdal (70) of approximation (b) of the collective model. He shows that if the neutron and proton fluids are represented as two degenerate Fermi gases (i.e., a simple IPM) then a complete correspondence in all respects including resonance energy between the fluid and shell pictures is found for distorted as well as spherical nuclei. This valuable result supplements Brink's Identity in a useful way.⁷

⁷ We must hope that the explicit introduction of exchange forces does not upset this harmony. We have seen that exchange is essential to our understanding of E_m and σ_0 and yet it cannot be introduced into the collective model in a systematic way without effectively rewriting it in particle language. Thus Fujita (67) has argued qualitatively that we can understand how exchange forces raise E_m in the collective model because in the excited state particles will tend to meet each other in relative

There is still point in asking which model provides the better picture for the initial absorption. The IPM account, as it has been presented, is a first-order picture and has neglected the effects of interaction between the many superposed transitions. These interactions may well be strong [see e.g. (71)] and the transitions may be pulled together by them to show a tighter grouping than expected by the raw IPM. This would then represent a real collective phenomenon. To test this, raw IPM calculations should be carried out in as realistic a manner as possible to ascertain the sharpness of grouping. This requires the use of a complex potential—the effect of the imaginary part of the potential on the transition energies has not been well investigated yet. A rounded edge must be used and, in certain regions of the periodic table, a distorted potential. This test for collective effects should be applied in the region of the doubly closed shells where the narrowest resonances are found. Another test is to seek cases where the IPM calculation predicts an unusually wide resonance in a region where distortions are small. If this shows up in practice (As^{76} is a possible case—see Table V) it will argue for the raw IPM picture and against the importance of strong collective effects. This theoretical work remains to be done. If the experimental giant resonance turns out to have structure (other than that associated with a deformation) on a much coarser scale than that possibly resulting from the many compound nucleus levels, this fact will argue for the IPM. In general terms, the raw IPM expects the giant resonance to be bumpy and the collective model expects it to be smooth. Similarly the IPM expects that there may be considerable differences between neighbouring nuclei or different isotopes of the same element because the IPM states can be profoundly altered by the addition of a single nucleon through their coupling to it. This should be best seen in the light elements because the overlap between a given nucleon and the rest is greatest there because of the finite range of the effective residual interaction. This expectation is well borne out by C^{13} (72). Its giant resonance has $E_m \simeq 25$ Mev, $\Gamma \simeq 9$ Mev as compared with $E_m \simeq 22$ Mev, $\Gamma \simeq 3$ Mev for C^{12} . Carbon 13 also shows a supplementary small bump at lower energy as do Be^9 (73 to 73b) and the lighter elements generally. The addition of a very few nucleons can also have a large effect on Γ in the rare earths where the deformation increases greatly between $N=88$ and $N=90$ (N =neutron number). In fact Γ for Eu^{153} ($N=90$) is markedly larger than for Eu^{151} ($N=88$) (74).

PHOTOREACTION PRODUCTS

So far only the absorption of the gamma radiation has been discussed. The decay can be decoupled from this absorption by a forgetting process that the collective model would call nuclear viscosity and the IPM would

p -states more frequently than in the ground state. Since Majorana exchange forces are repulsive in p -states and attractive in s -states, this will raise the energy of the collective state. But this is rather special pleading and it is fair to say that the increase of E_m and σ_0 remain somewhat obscure on the collective model.

call the imaginary part of the optical model potential. If this happens, the decay follows some statistical prescription that is of no interest here. This is usual, at least in the heavier nuclei. Alternatively the decay may pick out some special feature of the initial excitation. In particular the emission of the faster nucleons picks out those parts of the wavefunction of the intermediate state that may be written as a product of the wavefunctions of low-lying residual states and the departing nucleon. This is directly related to the absorption process on the IPM which then makes rather clear predictions about such fast nucleon emission. This is similar to the early "direct emission" of Courant (75) which could not give large enough cross sections because of its neglect of the possibility of resonance effects. A crude account is given on the IPM (48) by picturing a nucleon as being raised by the absorption process into the appropriate IPM state from which it may escape directly into the laboratory (width Γ_f) or alternatively be amalgamated into a statistically-decaying compound nucleus through the action of the imaginary part of the potential (width $2W$). If the contribution of the initial transition in question to the absorption cross section is σ' , we expect the cross section for this "resonance direct" emission to be of order $\sigma'\Gamma_f/2W$. This estimate, which is in good accord with experiment (48), pretends that excitation and amalgamation form a sequence in time whereas in fact they do not; one should more properly think of absorption of gamma radiation straight into an eigenstate of the compound system, viz.: into one of the many complex compound nucleus states into which the ideal shell model state is dissolved. However, if the strength function of the IPM state is narrow (small W), the simple picture retains fair validity (76; see also 76a). If IPM states are to be found in the region of the giant resonance, then resonance direct emission will take place through those states in more or less the amount given by the above crude estimate regardless of what may be the detailed mechanism of the resonance.* This is an important point which shows that success of the IPM in predicting the details of fast-nucleon emission does not necessarily prove that it is a complete description of the absorption process. On the other hand, what it does demonstrate is that the shell model states that the IPM regards as chiefly contributing to the giant resonance are in fact to be found in it. If some element of collective motion is found to be necessary to explain the absorption itself, then the shell model expansion of the collective state is rich in those IPM states that bear complete responsi-

* Brown & Levinger (76) also consider $E2$ effects (40, 40a) within the IPM framework and show them capable of producing (by interference with the $E1$ transitions) the peaking forward of 90° usually observed in (γ, p) reactions for the more energetic protons, although the $E2$ contribution to the total cross section is small. This $E1$ - $E2$ interference should be absent for neutrons since their effective charge is tiny for $E2$ transitions (contrast the $E1$ case), and so the fast neutrons, although anisotropic, should be symmetrical about 90° . This difference of behaviour of fast neutrons and fast protons is beautifully seen in the work of Johansson (77). In another possible form of $E2$ absorption, the photon excites collective quadrupole surface oscillations which then couple with single nucleons (78, 78a).

bility for the absorption on the raw IPM picture. Again a *rapprochement* is found between the models though, of course, the collective model can say nothing in its own right about nucleon emission but must be expanded in IPM terms.

Many experiments on the emission both of fast protons (79 to 79f) and fast neutrons (80 to 80d), viz. above the more-or-less isotropic "Maxwellian" region, have given results in general agreement with the IPM prediction and do not even approximately correspond with the prediction of the statistical model. Some detailed IPM comparisons have been attempted for photoneutrons from Bi (81), from Al (82), from Cr and Ta (83), and for photoprotons from Ag (84)—with results both for cross-section and angular distribution⁹ that agree rather better with the IPM than might have been expected. Detailed comparisons are usually hazardous because it is difficult to know over what range of excitation in the residual nucleus the transitions from a particular initial shell model state will spread. If there are valence nucleons, then the coupling of the hole in the inner shell to these nucleons may take place in several ways; if the transition is from the valence shells themselves, then there may be many parent states for a given intermediate state. In the original discussion (48) of this process, it was assumed that the effective spread of parent states for each IPM transition was about 8 Mev. Recent work (86) suggests that this figure may be high, viz. the real situation may be closer to the primitive one in which the explicit effect of all particle-particle forces is neglected. With the development of plane-polarized bremsstrahlung and other (reaction) sources of gamma radiation, further data with which to test the IPM may be expected—viz. distributions in azimuthal angle ϕ of photoproducts. These have not yet been computed but it may be noted that no terms higher than $\cos^2 \phi$ can be found for any multipole because the photon's spin is only \hbar .

So far, the detailed predictions of the IPM as regards both intermediate "giant resonance" and residual states have been worked out only for O^{16} (87). This has been done using harmonic oscillator wavefunctions taking into account the effective residual particle-hole interactions and using intermediate coupling. There are obviously five IPM transitions of importance forming the giant resonance states $1p^{-1}$ ($2s$, $1d$). The two most important ones (totalling 94 per cent of the summed transition strength) are theoretically at about 22.6 and 25.2 Mev. The experimental resonance is at about 23.5 Mev. Furthermore, the theoretical IPM predictions about the relative populations of the residual states in $O^{16}(\gamma, p)N^{15}$ and the angular distribution of the proton groups are in excellent accord with experiment¹⁰ (88). This good ac-

⁹ The angular distributions for the individual $E1$ transitions are easily written down (48, 75) but interference terms between them may be important and are more complicated to deal with (85). These will tend to average out if taken over a range of E_γ .

¹⁰ The attempt to explain these phenomena in terms of an alpha-particle subunit model (89) does not seem to lead to any detailed predictions.

cord with theory in the only case where it has been properly worked out is most pleasing but further testing comparison is urgently needed. It may be forthcoming in N^{15} (90, 90a). A similar but much less complete comparison has been made for $C^{12}(\gamma, p)B^{11}$ in the giant resonance region (91, 91a), again with results that agree with the IPM predictions (92).

Because of the close connection on the IPM between absorption and fast-nucleon emission, the excitation functions for fast nucleons are expected to show the giant resonances to some degree and this they do (81). But the width for their emission depends on their angular momentum, being, at a given excitation, less for the high l values that chiefly contribute to the giant resonance. It is quite possible, therefore, that the transitions most important for giving fast nucleons will be those of low final l , that are not the most important for the absorption (48). Because of this an exact comparison is not expected between the giant resonance and the fast nucleon excitation function which may show a displaced resonance or subsidiary resonances (93).

Other evidence for a direct emission process (with which is included the "quasi-deuteron" process—see later) comes from the high (γ, n) cross section that persists long past the $(\gamma, 2n)$ and $(\gamma, 3n)$ thresholds. This is totally inconsistent with the statistical prediction (94).

Products other than single nucleons will probably tend to come from the more complicated ("statistical") parts of the intermediate state wavefunction. In particular it seems that alpha-particle emission more nearly follows the prediction of the statistical model as would be expected, though here again the yield may exceed statistical expectation in the heavier nuclei (95 to 95c). The same is true, at least in the medium weight nuclei, for tritons also (96). Deuteron emission, which is sometimes much more frequent than suggested by the statistical model, may be described as a pick-up by the excited nucleon of a further nucleon from the core (97). Fast deuteron emission might, therefore, also be related to the giant resonance and this would be interesting to study.

In the heavy nuclei, neutrons form the great bulk of the final products, and the problem of disentangling σ_t from the yield curve is one of correct allowance for multiple emission (94). In lighter nuclei, proton yields become important. It has sometimes been argued that the neutron and proton cross sections will follow each other and so a determination of the neutron cross section fixes E_m . In some light nuclei, however, it appears that neutron and proton yields may peak at energies several Mev apart—this is best shown in A^{40} (98) where the branching is also much more strongly in favour of protons than would have been anticipated. This behaviour is rather mysterious. It may result in part from the different absorption energies expected for neutrons and protons on the IPM and in part from the effects of isotopic spin (99) and isotopic spin impurity (100). The magnitude of the effect is surprising but it must be watched for carefully in discussing systematics in the light nuclei.

PHOTON SCATTERING

Measurements of elastic scattering of photons through 120° by a wide range of elements have been made (101). As a function of photon energy this cross section is in general double-peaked. The first peak is just at the particle thresholds below which energy photon scattering is the only possible process. Above these thresholds photon scattering is severely attenuated by the heavy-particle competition but rises to its second peak (about 10–15 mbarn in heavy elements if a $1 + \cos^2 \theta$ angular distribution characteristic of $E1$ radiation is assumed) which follows the giant resonance in form quite closely. For $A < 50$ or so, this behaviour no longer holds and the elastic scattering appears to peak at substantially higher energies than E_m . This is not understood. At $E_\gamma \simeq 30$ Mev the cross section is not much greater than the Thomson scattering for Z free protons. The elastic scattering can be related to the total absorption, using dispersion relations (39). The theoretical relations appear to be followed in these measurements. In particular if σ_t has a resonant form it should, near its peak, be related to the scattering σ_s by $\sigma_t^2/\sigma_s \simeq 6\pi\lambda^2$ and this relation is adequately satisfied by a number of elements (101).

A detailed comparison of elastic scattering with the smoothed σ_t will reveal whether or not σ_t is really smooth or is made up of sharp peaks. The measurements are consistent with a truly smooth σ_t at least for the heavier elements in the region of the giant resonance. These scattering measurements, since they are so generally related to the absorption, are almost model-independent and tell little about the mechanism of photon absorption. A recent measurement of elastic scattering by Ta (102) has been valuable in revealing that this photon-nucleus interaction, as would be expected for that deformed nucleus (103), is tensor in character.

Work on the inelastic scattering of photons is difficult and the only significant experiments refer to isomer excitation. In the region above the giant resonance, inelastic scattering may become a considerable fraction of the total cross section according to one report (104). This would be most difficult to understand.

ABOVE THE GIANT RESONANCE

A photon carries much energy but little momentum. The much higher momentum that corresponds to this same energy when it is transferred to a nucleon in a photoabsorption process must therefore be supplied by interaction between nucleons in the nucleus. When the photon energy is low—below about 20 Mev—this interaction can be between one nucleon and the rest of the nucleus as a whole, i.e., IPM states are adequate to supply the momentum (48); but when it is high, close interactions between pairs of nucleons are necessary in the absorption act. This quasi-deuteron model (105, 105a), which has been much elaborated (106, 106a), therefore predicts that such pairs of nucleons should emerge from the nucleus when the gamma-

ray energy is high. This is beautifully confirmed for n - p pairs¹¹ (108 to 108b) at $E_\gamma \simeq 150$ –300 Mev where quasi-deuteron absorption appears to account for the whole of the cross section. This model also predicts the photoproton spectrum at high energy. Measurements for $E_\gamma = 45$ to 110 Mev (109) show remarkable quantitative agreement with these predictions for Li, Be, and C. In general at higher energies the proton abundance would be expected to fall rapidly above $E_p \simeq \frac{1}{2}E_\gamma$ and this is reflected in many investigations (110 to 110c). There is, as yet, little work with neutrons (111, 111a).

The transition from IPM absorption to the quasi-deuteron condition is a gradual one, of course, and is well seen in the Russian work of (110 to 110c). The interference between these two modes should be a very interesting study.¹²

¹¹ Note that only n - p pairs have an electric dipole moment. Emission of p - p pairs should be and is much less probable (107).

¹² Note that there is nothing mysterious in the photon being "given its choice" between absorption in an IPM state or in a high-momentum pair; the simultaneous and complementary existence of these two apparently conflicting states of motion is fundamental to the Brueckner approach to nuclear matter (54, 54a).

LITERATURE CITED

1. Levinger, J. S., *Ann. Rev. Nuclear Sci.*, **4**, 13 (1954)
2. Titterton, E. W., *Progr. in Nuclear Phys.*, **4**, 1 (1955)
- 2a. Bishop, G. R., and Wilson, R., *Encyclopedia Phys.*, **42**, 309 (Springer, Berlin, Germany, 1957)
- 2b. DeSabbata, V., *Nuovo cimento*, **5**, Suppl. No. 1, 243 (1957)
3. Toms, M. E., *Bibliography of Photoneuclear Reactions* (Naval Research Laboratory, Washington, D. C.)
4. Gammel, J. L., and Thaler, R. M., *Phys. Rev.*, **107**, 291, 1337 (1957)
5. Signell, P. S., and Marshak, R. E., *Phys. Rev.*, **106**, 832 (1957); **109**, 1229 (1958)
6. Gammel, J. L., Christian, R. S., and Thaler, R. M., *Phys. Rev.*, **105**, 311 (1957)
7. Gartenhaus, S., *Phys. Rev.*, **107**, 291 (1957)
8. Baker, A. R., and Wilkinson, D. H., *Phil. Mag.*, **3**, 647 (1958)
- 8a. Baker, A. R., *Proc. Roy. Soc. (London)*, **A248**, 539 (1958)
9. Austern, N., *Phys. Rev.*, **92**, 670 (1953)
10. Berger, J. M., *Phys. Rev.*, **94**, 1698 (1954)
11. Whetstone, A., and Halpern, J., *Phys. Rev.*, **109**, 2072 (1958)
- 11a. Allen, L., *Phys. Rev.*, **98**, 705 (1955)
12. Barnes, C. A., Carver, J. H., Stafford, G. H., and Wilkinson, D. H., *Phys. Rev.*, **86**, 359 (1952)
- 12a. Wilkinson, D. H., *Phys. Rev.*, **86**, 373 (1952)
13. Hulthén, L., and Sugawara, M., *Encyclopedia Phys.*, **39**, 1 (Springer, Berlin, Germany, 1957)
14. Schiff, L. I., *Phys. Rev.*, **78**, 733 (1950)
- 14a. Marshall, J. F., and Guth, E., *Phys. Rev.*, **78**, 738 (1950)
15. Whalin, E. A., Schriever, B. D., and Hanson, A. O., *Phys. Rev.*, **101**, 377 (1956)
- 15a. Keck, J. C., and Tollestrup, A. V., *Phys. Rev.*, **101**, 360 (1956)
- 15b. Keck, J. C., Littauer, R. M., O'Neill, G. K., Perry, A. M., and Woodward, W. M., *Phys. Rev.*, **93**, 827 (1954)
16. Lindenbaum, S. J., *Ann. Rev. Nuclear Sci.*, **7**, 317 (1957)
17. Austern, N., *Phys. Rev.*, **85**, 283 (1952); **100**, 1522 (1955)
- 17a. Feld, B. T., *Nuovo cimento*, **2**, Suppl. No. 1, 145 (1955)
18. McDonald, W. S., Peterson, V. Z., and Corson, D. R., *Phys. Rev.*, **107**, 577 (1957)
19. Zachariasen, F., *Phys. Rev.*, **101**, 371 (1956)
20. Austern, N., *Phys. Rev.*, **108**, 973 (1957)
21. Wilson, R. R., *Phys. Rev.*, **104**, 218 (1956)
22. De Swart, J. J., and Marshak, R. E., *Phys. Rev.*, **111**, 272 (1958)
23. Nicholson, A. F., and Brown, G. E., *Proc. Phys. Soc. (London)*, **73**, 221 (1959)
24. Zernik, W., Rustgi, M. L., and Breit, G. (In press)
25. Fischer, C. R., Pyatt, K. D., Hull, M. H., and Breit, G., *Bull. Am. Phys. Soc.* [II], **3**, 183 (1958)
26. Newton, R. G., *Phys. Rev.*, **107**, 1025 (1957)
27. Czyż, W., and Sawicki, J., *Phys. Rev.*, **110**, 900 (1958)
- 27a. De Swart, J. J., Czyż, W., and Sawicki, J., *Phys. Rev. Letters*, **2**, 51 (1959)
28. Kawaguchi, M., *Phys. Rev.*, **111**, 1314 (1958)
29. Rustgi, M. L., and Levinger, J. S., *Prog. Theoret. Phys. (Kyoto)*, **18**, 100 (1957)
- 29a. Levinger, J. S., *Phys. Rev.*, **97**, 970 (1955)
30. Foldy, L. L., *Phys. Rev.*, **107**, 1303 (1957)

31. Hofstadter, R., *Ann. Rev. Nuclear Sci.*, **7**, 231 (1957)
32. Gorbunov, A. N., and Spiridonov, V. M., *Zhur. Ekspl. i Teoret. Fiz.* (Transl.), **6**, 16 (1958); **7**, 596, 600 (1958)
- 32a. Fuller, E. G., *Phys. Rev.*, **96**, 1306 (1954)
- 32b. De Saussure, G., and Osborne, L. S., *Phys. Rev.*, **99**, 843 (1955)
- 32c. Livesey, D. L., and Main, I. G., *Nuovo cimento*, **10**, 590 (1958)
33. Rustgi, M. L., and Levinger, J. S., *Phys. Rev.*, **106**, 530 (1957)
34. Kikuta, T., Morita, M., and Yamada, M., *Prog. Theoret. Phys. (Kyoto)*, **15**, 222 (1956)
- 34a. Blatt, J. M., and Derrick, G., *Nuclear Phys.*, **8**, 602 (1958)
35. Bransden, B. H., Douglas, A. C., and Robertson, H. H., *Phil. Mag.*, **2**, 1211 (1957)
36. Rustgi, M. L., *Phys. Rev.*, **106**, 1256 (1957)
37. Levinger, J. S., and Bethe, H. A., *Phys. Rev.*, **78**, 115 (1950)
38. Levinger, J. S., and Kent, D. C., *Phys. Rev.*, **95**, 418 (1954)
- 38a. Levinger, J. S., *Phys. Rev.*, **97**, 122 (1955); *Phys. Rev.*, **101**, 733 (1956); *Phys. Rev.*, **107**, 554 (1957)
- 38b. Migdal, A., *Zhur. Ekspl. i Teoret. Fiz.*, **15**, 81 (1945)
- 38c. Khokhlov, Yu. K., *Doklady Akad. Nauk U.S.S.R.*, **97**, 239 (1954)
39. Gell-Mann, M., Goldberger, M. L., and Thirring, W. E., *Phys. Rev.*, **95**, 1612 (1954)
40. Levinger, J. S., Rustgi, M. L., and Okamoto, K., *Phys. Rev.*, **106**, 1191 (1957)
- 40a. Khokhlov, Yu. K., *Zhur. Ekspl. i Teoret. Fiz.* (Transl.), **5**, 88 (1957)
41. Penfold, A. S., and Leiss, J. E., *Analysis of Photo Cross Sections* (University of Illinois, Champaign, Ill., 1958)
42. Koch, H. W., *Proc. Conf. Nuclear Meson Phys., Glasgow, 1954*, 155 (1955) (Pergamon Press, London, 1955)
43. Goldemberg, J., *Phys. Rev.*, **93**, 1426 (1954)
- 43a. Tzara, C., *Compt. rend.*, **245**, 56 (1957)
44. de Souza Santos, M. D., Goldemberg, J., Pieroni, R. R., Silva, E., Borello, D. A., Villaca, S. S., and Lopes, J. L., *Proc. Intern. Conf. Peaceful Uses Atomic Energy, Geneva, 1955*, **2**, 169 (1956)
45. Katz, L., and Chidley, B. G., *Proc. Conf. Low and Medium Energy Nuclear Reactions, Moscow, 1957*, 371 (1958)
46. Fujii, S., and Takagi, S., *Prog. Theoret. Phys. (Kyoto)*, **14**, 402 (1955)
47. Araújo, J. M., *Nuovo cimento*, **12**, 780 (1954)
48. Wilkinson, D. H., *Proc. Conf. Nuclear Meson Phys., Glasgow, 1954*, 161 (1954); *Physica*, **22**, 1039 (1956)
49. Rand, S., *Phys. Rev.*, **107**, 208 (1957)
50. Levinger, J. S., Austern, N., and Morrison, P., *Nuclear Phys.*, **3**, 456 (1957)
51. Lane, A. M., and Wilkinson, D. H., *Phys. Rev.*, **97**, 1199 (1955)
52. Ross, A. A., Lawson, R. D., and Mark, H., *Phys. Rev.*, **104**, 401 (1956)
53. Fernbach, S., *Revs. Modern Phys.*, **30**, 414 (1958)
- 53a. Glassgold, A. E., *Revs. Modern Phys.*, **30**, 419 (1958)
54. Weisskopf, V. F., *Nuclear Phys.*, **3**, 423 (1957)
- 54a. Gomes, L. C., Walecka, J. D., and Weisskopf, V. F., *Ann. Phys. (N. Y.)*, **3**, 241 (1958)
55. Agranovitch, V. M., and Stavinski, V. S., *Zhur. Ekspl. i Teoret. Fiz.* (Transl.), **7**, 48 (1958)

56. Mayer, M. G., and Jensen, J. H. D., *Elementary Theory of Nuclear Shell Structure* (John Wiley & Sons, Inc., New York, N. Y., 1955)
57. Okamoto, K. (In press)
58. Wildermuth, K., *Z. Naturforsch.*, **10**, 447 (1955)
- 58a. Wildermuth, K., and Wittern, H., *Z. Naturforsch.*, **12**, 39 (1957)
- 58b. Fujii, S., and Takagi, S., *Prog. Theoret. Phys. (Kyoto)*, **14**, 405 (1955)
59. Danos, M., *Bull. Am. Phys. Soc. [II]*, **2**, 354 (1957)
60. Danos, M., *Nuclear Phys.*, **5**, 23 (1958)
- 60a. Okamoto, K., *Phys. Rev.*, **110**, 1113 (1958)
61. Nathans, R., and Halpern, J., *Phys. Rev.*, **73**, 437 (1954)
- 61a. Nathans, R., and Yergin, P. F., *Phys. Rev.*, **98**, 1296 (1955)
62. Fuller, E. G., Petree, B., and Weiss, M. S., *Phys. Rev.*, **112**, 554 (1958)
63. Fuller, E. G., and Weiss, M. S., *Phys. Rev.*, **112**, 560 (1958)
64. Nilsson, S. G., *Kgl. Danske Videnskab. Selskab, Mat.-fys. Medd.*, **29**, No. 16 (1955)
65. Wilkinson, D. H., *Phil. Mag.*, **3**, 567 (1958)
66. Soga, M., and Fujita, J., *Nuovo cimento*, **6**, 1494 (1957)
67. Fujita, J., *Prog. Theoret. Phys. (Kyoto)*, **14**, 400 (1955); **16**, 112 (1956)
68. Brink, D., *Nuclear Phys.*, **4**, 215 (1957)
69. Levinger, J. S., *Nuclear Phys.*, **8**, 428 (1958)
70. Migdal, A., *Zhur. Eksptl. i Teoret. Fiz.*, **8**, 331 (1944)
71. Ferrell, R. A., and Visscher, W. M., *Phys. Rev.*, **102**, 450 (1956)
72. Cook, B. C., *Phys. Rev.*, **106**, 300 (1957)
73. Nathans, R., and Halpern, J., *Phys. Rev.*, **92**, 940 (1953)
- 73a. Barber, W. C., *Phys. Rev.*, **111**, 1642 (1958)
- 73b. Haslam, R. N. H., Katz, L., Crosby, E. H., Summers-Gill, R. G., and Cameron, A. G. W., *Can. J. Phys.*, **31**, 210 (1953)
74. Cook, B. C. (Communication to Washington Photonuclear Conf., 1958)
75. Courant, E. D., *Phys. Rev.*, **82**, 703 (1951)
76. Brown, G. E., and Levinger, J. S., *Proc. Phys. Soc. (London)*, **71**, 733 (1958)
- 76a. Bloch, C., *Nuclear Phys.*, **4**, 503 (1957)
77. Johansson, S. A. E., *Phys. Rev.*, **97**, 434 (1955)
78. Akhiezer, A. I., and Sitenko, A. G., *Physica*, **22**, 1149 (1956)
- 78a. Sawicki, J., *Nuclear Phys.*, **6**, 525 (1958)
79. Toms, M. E., and Stephens, W. E., *Phys. Rev.*, **92**, 362 (1953)
- 79a. Weinstock, E. V., and Halpern, J., *Phys. Rev.*, **94**, 1651 (1954)
- 79b. Leikin, E. M., Osokina, R. M., and Ratner, B. S., *Nuovo cimento*, **3**, Suppl. No. 1, 105 (1956)
- 79c. Osokina, R. M., and Ratner, B. S., *Zhur. Eksptl. i Teoret. Fiz. (Transl.)*, **5**, 1 (1957)
- 79d. Ferrero, F., Hanson, A. O., Malvano, R., and Tribuno, C., *Nuovo cimento*, **6**, 585 (1957)
- 79e. Keszthelyi, L., and Erö, J., *Nuclear Phys.*, **8**, 650 (1958)
- 79f. Toms, M. E., and Stephens, W. E., *Phys. Rev.*, **98**, 626 (1955)
80. Price, G. A., *Phys. Rev.*, **93**, 1279 (1954)
- 80a. Zatsepina, G. N., Lazareva, L. E., and Pospelov, A. N., *Zhur. Eksptl. i Teoret. Fiz. (Transl.)*, **5**, 21 (1957)
- 80b. Ferrero, F., Gonella, L., Malvano, R., Tribuno, C., and Hanson, A. O., *Nuovo cimento*, **5**, 242 (1957)

- 80c. Toms, M. E., and Stephens, W. E., *Phys. Rev.*, **108**, 77 (1957)
- 80d. Bertozzi, W., Paolini, F. R., and Sargent, C. P., *Phys. Rev.*, **110**, 790 (1958)
81. Ferrero, F., Hanson, A. O., Malvano, R., and Tribuno, C., *Nuovo cimento*, **4**, 418 (1958)
82. Ferrero, F., Malvano, R., Menardi, S., and Terracini, O., *Nuclear Phys.*, **9**, 32 (1958)
83. Cortini, G., Milone, C., Rubbino, A., and Ferrero, F., *Nuovo cimento*, **9**, 85 (1958)
84. Lokan, K. H., *Proc. Phys. Soc. (London)*, **73**, 697 (1959)
85. Eichler, J., and Weidenmüller, H. A. (In press)
86. Agodi, A., *Nuovo cimento*, **8**, 516 (1958)
87. Elliott, J. P., and Flowers, B. H., *Proc. Roy. Soc. (London)*, **A242**, 57 (1957)
88. Johansson, S. A. E., and Forkman, B., *Arkiv. Fys.*, **12**, 359 (1957)
89. Wilhelmsson, H., and Nilsson, M., *Nuclear Phys.*, **4**, 234 (1957)
90. Rhodes, J. L., and Stephens, W. E., *Phys. Rev.*, **110**, 1415 (1958)
- 90a. Halbert, E. C., and French, J. B., *Phys. Rev.*, **105**, 1563 (1957)
91. Cohen, L. D., Mann, A. K., Patton, B. J., Reibel, K., Stephens, W. E., and Winhold, E. J., *Phys. Rev.*, **104**, 108 (1956)
- 91a. Penner, S., and Leiss, J. E., *Natl. Bur. Standards (U. S.) Rept. No. 6219* (1958)
92. Mann, A. K., Stephens, W. E., and Wilkinson, D. H., *Phys. Rev.*, **97**, 1184 (1955)
93. Ferrero, F., Malvano, R., and Tribuno, C., *Nuovo cimento*, **6**, 385 (1957)
94. Carver, J. H., Edge, R. D., and Lokan, K. H., *Proc. Phys. Soc. (London)*, **A70**, 415 (1957)
95. Greenberg, L. H., Taylor, J. G. V., and Haslam, R. N. H., *Phys. Rev.*, **95**, 1540 (1954)
- 95a. Erdős, P., Jordan, P., and Stoll, P., *Helv. Phys. Acta*, **28**, 322 (1955)
- 95b. Heinrich, F., Wäffler, H., and Walter, M., *Helv. Phys. Acta*, **29**, 3 (1956)
- 95c. Erdős, P., Scherrer, P., and Stoll, P., *Helv. Phys. Acta*, **30**, 639 (1957)
96. Heinrich, F., and Wäffler, H., *Helv. Phys. Acta*, **29**, 232 (1956)
97. Sawicki, J., and Czyż, W., *Nuclear Phys.*, **4**, 248, 695 (1957)
98. Penfold, A. S., and Garwin, E. L. (In press)
99. Morinaga, H., *Phys. Rev.*, **97**, 444 (1955)
100. Barker, F. C., and Mann, A. K., *Phil. Mag.*, **2**, 5 (1957)
101. Fuller, E. G., and Hayward, E., *Phys. Rev.*, **101**, 692 (1956)
102. Fuller, E. G., and Hayward, E., *Phys. Rev. Letters*, **1**, 465 (1958)
103. Baldin, A. M., *Nuclear Phys.*, **9**, 237 (1958)
104. Bogdankevich, O. V., Lazareva, L. E., and Nicolaev, F. A., *Zhur. Eksptl. i Teoret. Fiz.* (Transl.), **4**, 320 (1957)
105. Khokhlov, Yu. K., *Zhur. Eksptl. i Teoret. Fiz.*, **23**, 241 (1952)
- 105a. Levinger, J. S., *Phys. Rev.*, **84**, 43 (1951)
106. Dedrick, K. G., *Phys. Rev.*, **100**, 58 (1955)
- 106a. Gottfried, K., *Nuclear Phys.*, **5**, 557 (1958)
107. Palfrey, T. R. (Communication to Chicago Photonuclear Conf., 1956)
108. Barton, M. Q., and Smith, J. H., *Phys. Rev.*, **110**, 1143 (1958)
- 108a. Odian, A. C., Stein, P. C., Wattenberg, A., Feld, B. T., and Weinstein, R. M., *Phys. Rev.*, **102**, 837 (1956)
- 108b. Wattenberg, A., Odian, A. C., Stein, P. C., Wilson, H., and Weinstein, R. M., *Phys. Rev.*, **104**, 1710 (1956)
109. Whitehead, C., McMurray, W. R., Aitken, M. J., Middlemas, N., and Collie, C. H., *Phys. Rev.*, **110**, 941 (1958)

- 110. Kliger, G. K., Riabinkin, V. I., Chuvilo, I. V., and Shevchenko, V. G., *Physica*, **22**, 1142 (1956)
- 110a. Chuvilo, I. V., and Shevchenko, V. G., *Zhur. Eksptl. i Teoret. Fiz.* (Transl.), **5**, 1090 (1957); **7**, 410 (1958)
- 110b. Feld, B. T., Goldbole, R. D., Odian, A., Scherb, F., Stein, P. C., and Wattenberg, A., *Phys. Rev.*, **94**, 1000 (1954)
- 110c. Bazhanov, E. B., Volkov, Yu. M., Komar, A. P., Kulchitsky, L. A., Chizhov, V. P., and Yavor, I. P., *Proc. Conf. Low and Medium Energy Nuclear Reactions, Moscow, 1957*, 463 (1958); see *Zhur. Eksptl. i Teoret. Fiz.* (Transl.), also **2**, 107 (1958) and **4**, 432 (1957)
- 111. Baranov, P. S., and Goldanskii, V. I., *Zhur. Eksptl. i Teoret. Fiz.* (Transl.), **1**, 613 (1955)
- 111a. Baranov, P. S., Goldanskii, V. I., and Roganov, V. S., *Phys. Rev.*, **109**, 1801 (1958)

THE PION-NUCLEON INTERACTION AND DISPERSION RELATIONS¹

BY GEOFFREY F. CHEW²

Lawrence Radiation Laboratory, University of California, Berkeley, California

1. INTRODUCTION

This article is concerned with the problem of strong coupling as it is manifested in the properties of the "ordinary" particles, pions and nucleons. It is not possible to separate such a discussion cleanly from strange particles, which also undergo strong interactions; but at the current level of understanding of the pion-nucleon interaction the complications arising from strange particles can be minimized.

Although it seems likely that the masses of the pion (μ) and the nucleon (M) are consequences of strong coupling, no attempt is made here to discuss the masses in this sense. Let us consider μ and M to be given parameters. The same is true for the pion-nucleon (g) and pion-pion (λ) coupling constants, even though future developments may show these quantities to be not really fundamental. The problem, then, is to relate the cross sections for the various interactions involving pions and nucleons to the four constants μ , M , g , and λ . We shall restrict ourselves to processes in which there are two ingoing and two outgoing particles. These processes are the following:

1. $\pi + \pi \leftrightarrow \pi + \pi$ Pion-pion scattering.
2. $\pi + \pi \leftrightarrow N + \bar{N}$ Nucleon pair production in pion-pion collisions and nucleon-antinucleon annihilation to produce two pions.
3. $\pi + N \leftrightarrow \pi + N$ or $\pi + \bar{N} \leftrightarrow \pi + \bar{N}$ Pion-nucleon or pion-antinucleon scattering.
4. $N + N \leftrightarrow N + N$ Nucleon-nucleon scattering.
5. $N + \bar{N} \leftrightarrow N + \bar{N}$ Nucleon-antinucleon scattering.

The above processes are different manifestations of three fundamental matrix elements that can be represented as shown in Figure 1. Here the wiggly lines refer to pions and the straight lines to nucleons. Any pair of lines may represent the ingoing two particles, with the other pair representing the outgoing; and going opposite to the direction of an arrow simply means changing particle to antiparticle with a change of sign of the four-momen-

¹ The survey of literature pertaining to this review was concluded in March, 1959.

² This article was written under contract with the U. S. Atomic Energy Commission under Contract No. W-7405-eng-48 and carries the number UCRL-8670.

tum. Thus Figure 1(b) includes both process 2 and process 3, while Figure 1(c) includes processes 4 and 5.

It is instructive also to consider diagrams of the type of Figures 1(a) and 1(b) with one of the pions replaced by a photon. Such diagrams correspond to the following processes:

- | | |
|--|---|
| 6. $\gamma + \pi \leftrightarrow \pi + \pi$ | Photopion production from pions and radiative capture of a pion by a pion. |
| 7. $\gamma + \pi \leftrightarrow N + \bar{N}$ | Nucleon pair production in photopion collisions and nucleon-antinucleon annihilation to produce a pion plus a photon. |
| 8. $\gamma + N \leftrightarrow \pi + N$ or
$\gamma + \bar{N} \leftrightarrow \pi + \bar{N}$ | Photopion production from nucleon (or antinucleon) and radiative capture of a pion by a nucleon. |

These last three processes will require for their description at least one additional parameter, the elementary electric charge e .

The above four-particle reactions are to be discussed here by means of spectral representations, often referred to as "dispersion relations." Actually these representations have much more content and utility than the original dispersion relations of electromagnetic theory, but they developed out of attempts to generalize the Kramers-Kronig equations (1, 2). The systematic derivation of the new dispersion relations is complicated and not at all suitable to a review of this kind; therefore we restrict ourselves to a short qualitative description of the main ingredients.

The current justification of dispersion relations rests on two fundamental physical assumptions that have become prominent only within the past 10 years, even though their origin is much older. Extensive use is also made of standard symmetry principles and associated conservation laws that are recognized as important in all areas of particle physics; these principles will be taken for granted and no special mention made of them.³ The two distinctive principles are:

(a) Signals never propagate with a velocity faster than that of light, no matter how short the distance involved. This is the principle of "microscopic causality." In the language of local quantum field theory, it is expressed by saying that the commutator of two Heisenberg field operators, taken at different space-time points, vanishes if the separation between these points is spacelike. Without use of the framework of local field theory no precise way is known of formulating microcausality.

(b) The totality of all possible physical states of the universe forms a complete set of basis vectors in the quantum mechanical sense. That is to say,

³ It will be assumed that for the strong coupling phenomena with which we are concerned, charge conjugation invariance and parity conservation are separately valid, as well as charge independence.

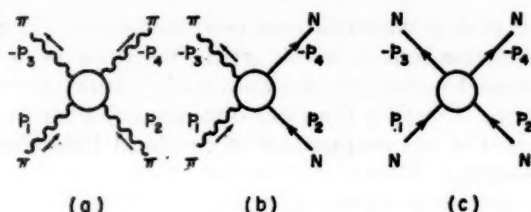


FIG. 1. The three fundamental diagrams of the pion-nucleon system. Outgoing particles are assigned negative momenta in accordance with the convention of Section 2.

an arbitrary state vector may be expressed as a linear superposition of vectors, each representing a possible physical state with a total energy-momentum four vector that is positive timelike. This "spectral condition," although it sounds extremely plausible, is not universally accepted, the conjecture having often been made that local field theory is inconsistent unless "ghost" states, with no direct physical interpretation, are included.

The usual starting point in the derivation of a dispersion relation is the reduction formula, first given in a general form by Lehmann, Zimmermann & Symanzik (3) and for the special case of π - N scattering by Low (4). The reduction formula allows one to write the amplitude for an arbitrary transition in terms of the Fourier transform of a matrix element of a commutator of two Heisenberg field operators. The energy variable occurs only in the imaginary exponent, multiplying the space-time co-ordinate; and the vanishing of the commutator outside the light cone then allows one to extend the energy dependence into the complex plane. Goldberger was the first to use such an approach (5), which after this crucial step leads immediately to dispersion relations. Later it was realized that a rigorous justification of Goldberger's extension into the complex plane was not really easy to achieve except for zero-mass particles scattered in the forward direction. Symanzik (6) was the first to solve the nonzero mass problem, and Bogoliubov (7) then showed that the extension was justifiable even for nonforward scattering if the particle mass were formally made imaginary and sufficiently large in absolute value. However, the difficult problem remained of investigating the behavior of the amplitude as a function of particle mass; it was necessary, of course, to show that dispersion relations continue to hold as the mass is made real and equal to its actual physical value.

Bogoliubov developed methods of proof appropriate to certain special cases (7), but these have now been superseded by the work of Bremermann, Oehme & Taylor (8), based on the theory of many complex variables, and by the work of Jost & Lehmann (9) and of Dyson (10), based on more familiar but still tricky mathematics.

Although the details of the derivation cannot be given here, the Dyson representation (10), which expresses conditions *a* and *b* in a form suitable

to the deduction of dispersion relations, is written down. No specific use of Dyson's representation is made in this article, but it serves to illustrate the kind of connection between physics and mathematics that characterizes dispersion relations. Consider the (four-dimensional) Fourier transform of the matrix element of the commutator of two local Heisenberg operators, $j(x/2)$ and $h(-x/2)$:

$$F(q) = \int d^4x e^{iqx} \langle P, \alpha | [j(x/2), h(-x/2)] | Q, \beta \rangle. \quad 1.1.$$

The matrix element here connects two physical states whose total energy-momentum four vectors are P and Q , respectively. The indices α and β refer to the other degrees of freedom needed to complete the specification of these states. According to the microcausality assumption *a*, the matrix element vanishes for $x^2 = x_0^2 - \vec{x}^2 < 0$, that is, for spacelike separation of the two operator-arguments.

Assumption *b* comes into play if one inserts a complete set of "intermediate" physical states between the operators j and h . It may then be seen by using displacement operators, which shift the arguments of j and h to the origin, that $F(q)$ vanishes unless $[\frac{1}{2}(P+Q)+q]$ is the energy-momentum of a state $|n\rangle$ for which both the matrix elements

$$\langle P, \alpha | j(0) | n \rangle \quad \text{and} \quad \langle n | h(0) | Q, \beta \rangle \quad 1.2.$$

fail to vanish, or $\frac{1}{2}[(P+Q)-q]$ is the energy-momentum of a state for which both

$$\langle P, \alpha | h(0) | n \rangle \quad \text{and} \quad \langle n | j(0) | Q, \beta \rangle \quad 1.3.$$

fail to vanish. The four-momenta of the states $|n\rangle$ are all positive timelike; m_1 designates the smallest mass of a state satisfying 1.2 and m_2 the corresponding smallest mass for 1.3. Assumption *b* thus leads to the property that $F(q)$ vanishes except for

$$\frac{P_0 + Q_0}{2} + q_0 \geq 0 \quad \text{and} \quad \left(\frac{P + Q}{2} + q \right)^2 \geq m_1^2 \quad 1.4.$$

or

$$\frac{P_0 + Q_0}{2} - q_0 \geq 0 \quad \text{and} \quad \left(\frac{P + Q}{2} - q \right)^2 \geq m_2^2.$$

Dyson was able to prove that, for $F(q)$ to satisfy the condition 1.4 and at the same time be the Fourier transform of a function that vanishes for space-like argument, it is necessary and sufficient that $F(q)$ can be represented as

$$F(q) = \int d^4u \int_0^\infty d\kappa^2 \epsilon(q_0 - u_0) \delta[(q - u)^2 - \kappa^2] \phi(u, \kappa^2). \quad 1.5.$$

The integrations here extend over a region such that the vectors

$$\frac{P + Q}{2} + u \quad \text{and} \quad \frac{P + Q}{2} - u$$

both lie in the forward light cone, while κ is positive and larger than either

$$m_1 - \sqrt{\left(\frac{P+Q}{2} + u\right)^2} \quad \text{or} \quad m_2 - \sqrt{\left(\frac{P+Q}{2} - u\right)^2}.$$

Within this region $\phi(u, \kappa^2)$ is arbitrary.

Previously Lehmann & Jost had deduced a somewhat similar representation for the special case $m_1 = m_2$ (9). The Jost-Lehmann representation will not be written down, but historically it represented a significant step in the understanding of dispersion relations. The alternative approach to the problem through the theory of many complex variables, exploited by Bremermann, Oehme & Taylor (8), yields the same results as those achieved through the Dyson representation. These results have been summarized recently by Goldberger (11).

For the reader who wishes to see all the essential steps in a complete and yet economical derivation of the pion-nucleon dispersion relation, the following use of the published literature is recommended: (a) Read the first and about half of the second section of (8), up to the point where dispersion relations have been obtained for imaginary mass. (b) Switch here to a recent paper by Lehmann (12) which uses the Dyson representation not only to carry out the necessary extension in the mass variable but also to justify the use of Legendre polynomials in implementing dispersion relations. (c) If any strength remains, read the Dyson paper (10).

It should be stated at this point that interest in dispersion relations as a tool for strong coupling physics was first aroused by the 1955 papers of Goldberger (5) and Karplus & Ruderman (13), although at that time the mathematical difficulties involved in giving a systematic derivation were not realized. At present it remains true that the methods of implementation of dispersion relations are elementary and quite unrelated to the sophisticated mathematical techniques required for their derivation. Such a situation may not persist indefinitely, but it motivates the decision to avoid in this review the mathematics of derivation.

In the following section, certain important kinematical questions are dealt with, preparatory to a general statement of the rules for formulating dispersion relations. The rules are then given in Sections 3, 4, and 5 in such a way as to cover not only those relations that have been rigorously derived, but also many relations conjectured on the basis of perturbation theory.

2. KINEMATICAL PRELIMINARIES

Energy and angle variables.—In order to describe the scattering amplitudes for processes with two ingoing and two outgoing particles, one needs in addition to spin and charge variables at least two invariants that correspond to the energy and angle of scattering in the barycentric system. To maintain a maximum symmetry let us assign four-momenta p_1, p_2, p_3, p_4 , all of which correspond formally to ingoing particles. Two of these momenta will always be negative timelike, representing the actual outgoing particles, while the

other two are positive timelike and represent the incoming particles. Energy-momentum conservation is stated through the condition

$$p_1 + p_2 + p_3 + p_4 = 0 \quad 2.1.$$

while the particle masses are introduced through the four constraints,

$$p_i^2 = m_i^2. \quad 2.2.$$

For the purposes of dispersion relations it is convenient to define three invariants

$$s_1 = (p_1 + p_4)^2 = (p_2 + p_3)^2$$

$$s_2 = (p_2 + p_4)^2 = (p_1 + p_3)^2$$

$$s_3 = (p_3 + p_4)^2 = (p_1 + p_2)^2$$

each of which is the square of the total energy in the barycentric system for a particular pairing of incoming and outgoing particles.⁴ For example, when p_1 and p_2 are incoming and p_3 and p_4 outgoing, the total energy is $\sqrt{s_3}$. In this case s_1 and s_2 may be interpreted as squares of four-momentum transfers. It is easy to show that the physical range of an s variable when it is the square of an energy does not overlap the range when it is the square of a momentum transfer. In particular, in the former case s is always positive and extends to $+\infty$, while in the latter it may be negative and extends to $-\infty$.

The three variables s_1, s_2, s_3 are not independent of one another, but with the constraints 2.1 and 2.2 they can be shown to satisfy the relation

$$s_1 + s_2 + s_3 = m_1^2 + m_2^2 + m_3^2 + m_4^2. \quad 2.3.$$

Any two of the s 's may be considered as independent variables, with the third determined by 2.3. In the dispersion-relation approach it is necessary for the s variables to be extended not only to nonphysical regions of the real axis but also throughout the complex plane. Condition 2.3 requires that in such extensions the sum of the imaginary parts of the three s variables shall vanish.

In the theory of dispersion relations, the substitution rule plays an important part. This rule was discovered in perturbation theory [see, e.g., Jauch & Rohrlich (14, p. 161)] and relates the different channels corresponding to a single diagram. For the purposes of this review this rule will be expressed by the statement that a single analytic function describes all three channels contained in the same diagram. In particular, the physical amplitude for the process when particles 1 and 2 are ingoing is the boundary value of an analytic function as the variable s_3 approaches the positive real axis in its physical energy range, with one of the other two s variables held fixed at a physical value in the momentum transfer range, while the amplitudes for particles 1 and 3 or 1 and 4 ingoing are obtained from corresponding limits of the same function taken with the variables s_2 or s_1 , respectively. Condition 2.3 is to be obeyed, so that one is dealing in the limiting process with a single complex variable. However, the general rule has meaning only

⁴ We shall refer to each possible pairing as a "channel." For each diagram there are three channels.

if the two independent s variables can both be extended into the complex plane. The above statement of the substitution rule has been rigorously proved only in a few special cases, but the general form of perturbation theory makes it extremely plausible.

An invariance principle related to the substitution rule, that follows when there are two or more identical particles among the four involved in a particular process, is the so-called "crossing symmetry." Exchanging two identical particles at most changes the sign of the amplitude, but such an interchange means exchanging two of the s variables, leaving the third alone. For example, suppose particles 1 and 3 are identical. Then, depending on whether these are bosons or fermions, the amplitude is either symmetric or antisymmetric under an exchange of p_1 and p_3 , which means interchanging s_1 and s_3 , leaving s_2 alone.⁵ If p_1 and p_3 are both incoming or both outgoing (i.e., $\sqrt{s_2}$ is the energy), the symmetry in question is familiar and directly related to the Pauli principle. If one is incoming and the other outgoing, however, the symmetry cannot be so identified and is a special characteristic of field theory. In this case, if one starts with physical values of the s variables, the exchange in question necessarily leads to nonphysical values because of the above-mentioned nonoverlapping nature of the energy and momentum-transfer ranges. Thus, the general crossing symmetry has meaning only when a continuation of the amplitude into unphysical regions is possible.

Charge and spin variables.—The possibility of degrees of freedom of spin and charge has so far been ignored. It will now be explained how internal degrees of freedom may always be absorbed into invariant matrices, whose coefficients are invariant functions of the s variables only. The number of such functions depends on the complexity of the internal degrees of freedom: For processes associated with Figure 1(a), three independent functions are required, Figure 1(b) requires four functions, and Figure 1(c) 10 functions. Remarkably enough, replacing a pion with a photon in Figure 1(a) or 1(b) has a very different effect in the two cases. Figure 1(a) with a photon requires just a single invariant function, while Figure 1(b) with a photon requires twelve. We shall now write down for the simpler problems the invariant matrices required and point out the implications of crossing symmetry for the corresponding invariant functions.

The four-pion problem is one of the simplest because there are no spins and all three branches of the diagram correspond to the same process, $\pi\text{-}\pi$ scattering.⁶ Each pion has a charge degree of freedom, however, and this is described in the conventional way [see, e.g., Bethe & de Hoffman (16, p. 49)] by an index that takes values 1, 2, 3. For the pion with momentum p_1 , associate the charge index α , with p_2 the index β , with p_3 the index γ ,

⁵ Note that such an exchange is consistent with the constraint 2.3.

⁶ For a more complete discussion of the $\pi\text{-}\pi$ problem, see Chew & Mandelstam (15).

and with p_4 the index λ . It is assumed that (p_1, α) and (p_2, β) are incoming, with $(-p_3, \gamma)$ and $(-p_4, \lambda)$ outgoing. The scattering amplitude may then be considered a matrix in a nine-dimensional charge space that is the product of two three-dimensional spaces. The requirement of charge independence leads to the conclusion that only three independent matrices are allowed, corresponding to the fact that only three values of total I spin occur for the two-pion system: $I=0, 1, 2$. It is convenient to choose as the three fundamental matrices

$$\begin{aligned}(X_1)_{\gamma\lambda, \alpha\beta} &= \delta_{\alpha\beta}\delta_{\gamma\lambda} \\ (X_2)_{\gamma\lambda, \alpha\beta} &= \delta_{\alpha\gamma}\delta_{\beta\lambda} \\ (X_3)_{\gamma\lambda, \alpha\beta} &= \delta_{\beta\gamma}\delta_{\alpha\lambda}\end{aligned}\tag{2.4}$$

and to write the complete amplitude as

$$X_1 A(s_1, s_2, s_3) + X_2 B(s_1, s_2, s_3) + X_3 C(s_1, s_2, s_3).\tag{2.5}$$

The operation of particle exchange involves both the charge and the momentum. Since all four particles are identical bosons, the following crossing relations follow:

$$\begin{aligned}A &\leftrightarrow A & s_1 &\leftrightarrow s_2 \\ B &\leftrightarrow C & & \\ A &\leftrightarrow B & s_2 &\leftrightarrow s_3 \\ C &\leftrightarrow C & &\end{aligned}\tag{2.6}$$

plus other relations that are redundant in content. The first of the above two lines simply represents the Pauli principle, but the second puts on the pion-pion scattering amplitude a type of dynamical requirement unknown outside field theory.

With the definite assignment of $(p_1\alpha)$ and $(p_2\beta)$ as incoming particles it is possible to express A , B , and C in terms of the conventional amplitudes A^I for scattering in states of well-defined I spin. The relations turn out to be

$$\begin{aligned}A^0 &= 3A + B + C \\ A^1 &= B - C \\ A^2 &= B + C.\end{aligned}\tag{2.7}$$

In the barycentric system, if the magnitude of the three-momentum of any pion is called q and the angle of scattering θ , the physical meaning of the s variables is

$$\begin{aligned}s_1 &= -2q^2(1 + \cos \theta) \\ s_2 &= -2q^2(1 - \cos \theta) \\ s_3 &= 4(q^2 + \mu^2).\end{aligned}\tag{2.8}$$

The exchange of s_1 and s_2 thus corresponds to changing $\cos \theta$ to $-\cos \theta$; and the first line of 2.6, when applied to 2.7, says no more and no less than that A^0 and A^2 are even functions of $\cos \theta$ while A^1 is an odd function. The second line of 2.6, however, which relates to the exchange of s_2 and s_3 , expresses a condition on the energy and angular dependence considered together.

A final essentially kinematical feature of the pion-pion problem is the connection between the amplitudes A^I and conventional phase shifts. The formula here is ambiguous as to normalization, but the dependence on energy and angle is unique [Chew & Mandelstam(15)]. We choose to normalize so that

$$A^I(q^2, \cos \theta) = \frac{\sqrt{q^2 + \mu^2}}{q} \sum_l (2l+1) e^{i\delta_l^I} \sin \delta_l^I P_l(\cos \theta) \quad 2.9.$$

where δ_l^I is the phase shift for a state of angular momentum l and isotopic spin I . The phase shifts are real for $s_3 < 16\mu^2$ ($q^2 < 3\mu^2$) and complex at higher energies, where production of two additional pions becomes possible. Single-pion production is forbidden by a combination of charge-conjugation invariance and charge independence,⁷ which in general forbids the production of any odd number of pions. As noted above, only even l values occur in 2.9 for $I=0, 2$, while only odd l values occur for $I=1$.

The two processes described by Figure 1(b), pion-nucleon scattering and nucleon pair production in pion-pion collisions, are physically quite different even though they are limits of the same analytic function. Since the scattering problem is the more familiar of the two, this notation will be adjusted to conform with existing literature on pion-nucleon scattering [Chew *et al.* (18)].

Let us then assign to the incident and outgoing pions the momenta p_1 and $-p_3$ and the charge indices α and β , respectively. The corresponding nucleon momenta are p_2 and $-p_4$, but the degrees of freedom of the nucleon charge and spin will be suppressed in the conventional way [see, e.g., Chew (19)]. The invariant amplitude may then be written as a sum of four terms,

$$\delta_{\beta\alpha} [-A^0(s_1, s_2, s_3) + \frac{1}{2} i \gamma \cdot (p_1 - p_3) B^0(s_1, s_2, s_3) + \frac{1}{2} [\tau_\beta, \tau_\alpha] [-A^1(s_1, s_2, s_3) + \frac{1}{2} i \gamma \cdot (p_1 - p_3) B^1(s_1, s_2, s_3)]] \quad 2.10.$$

with the crossing relations, following from symmetry under interchange of the two pions,

$$\begin{aligned} A^0 &\leftrightarrow A^0 & A^1 &\leftrightarrow -A^1 & s_1 &\leftrightarrow s_3. \\ B^0 &\leftrightarrow -B^0 & B^1 &\leftrightarrow B^1. \end{aligned} \quad 2.11.$$

The connection between the amplitudes $A^{0,1}$, $B^{0,1}$ and those corresponding to states of well-defined I spin A^I , B^I where $I=\frac{1}{2}, \frac{3}{2}$, is given by the formulas

$$\begin{aligned} A^{1/2} &= A^0 + 2A^1 & B^{1/2} &= B^0 + 2B^1 \\ A^{3/2} &= A^0 - A^1 & B^{3/2} &= B^0 - B^1 \end{aligned} \quad 2.12.$$

while the three s variables are related to the barycentric-system momentum q and the scattering angle θ (or equivalently to the total energy in the barycentric system W and the square of the momentum transfer, Δ^2) by

⁷ The so-called G parity of Lee & Yang (17), which for states containing only pions is even or odd depending on whether the total number of pions is even or odd. States with nonzero baryon number generally do not have well-defined G parity.

$$\begin{aligned}
 s_3 &= (\sqrt{M^2 + q^2} + \sqrt{\mu^2 + q^2})^2 = W^2 \\
 s_2 &= -2q^2(1 - \cos \theta) = -\Delta^2 \\
 s_1 &= 2M^2 + 2\mu^2 - W^2 + \Delta^2.
 \end{aligned}
 \tag{2.13}$$

Finally, the connection to phase shifts is needed. This is given conveniently in terms of functions f_1^I and f_2^I , defined by

$$\begin{aligned}
 f_1^I &= \frac{1}{q} \sum_l [e^{i\delta_{l+}^I} \sin \delta_{l+}^I P_{l+1}'(\cos \theta) - e^{i\delta_{l-}^I} \sin \delta_{l-}^I P_{l-1}'(\cos \theta)] \\
 f_2^I &= \frac{1}{q} \sum_l [e^{i\delta_{l+}^I} \sin \delta_{l-}^I - e^{i\delta_{l-}^I} \sin \delta_{l+}^I] P_l'(\cos \theta)
 \end{aligned}
 \tag{2.14}$$

where $P_l'(\cos \theta)$ is the first derivative of the Legendre polynomial. The quantities $\delta_{l\pm}^I$ are phase shifts for scattering in states of isotopic spin I , orbital angular momentum l , and total angular momentum $l \pm \frac{1}{2}$. These phase shifts can be complex for $W > M + 2\mu$, where pion production becomes possible. The relation between the f 's and the A and B amplitudes is given by

$$\begin{aligned}
 4\pi f_1 &= \frac{(W + M)^2 - \mu^2}{4W^2} [A + (W - M)B] \\
 4\pi f_2 &= \frac{(W - M)^2 - \mu^2}{4W^2} [-A + (W + M)B]
 \end{aligned}
 \tag{2.15}$$

where, as in the pion-pion problem, the choice of normalization is an arbitrary one.

Now let us consider the same fundamental amplitude from the point of view of nucleon pair production. Here one must distinguish between k , the barycentric system three-momentum of an incident pion, and K , that of an outgoing nucleon. Since p_1 and p_3 are now both ingoing, with $-p_2$ and $-p_4$ outgoing,

$$\begin{aligned}
 s_2 &= 4(k^2 + \mu^2) = 4(K^2 + M^2) \\
 s_1 &= -k^2 - K^2 + 2kK \cos \Theta \\
 s_3 &= -k^2 - K^2 - 2kK \cos \Theta
 \end{aligned}
 \tag{2.16}$$

where Θ is the angle in the barycentric system between an incident pion and an outgoing nucleon.

Again there are two isotopic spin values, but this time $I=0, 1$, and the amplitudes for these states turn out to be just the quantities already labeled with the superscripts 0, 1. The remaining requirement is the equivalent of formulas 2.14 and 2.15. Since off-diagonal elements of the S matrix are involved, the process cannot be described simply in terms of phase shifts, but a partial-wave decomposition is still appropriate. Frazer & Fulco (20) found that for total angular momentum J , the orbital angular momentum of the $N\bar{N}$ system can be either $J+1$ or $J-1$, while the isotopic spin is 0 for J even and 1 for J odd. Frazer & Fulco (20) worked out the formulas connecting the transition amplitudes in states of definite J to the invariant amplitudes $A^{0,1}$ and $B^{0,1}$, but these formulas will not be given here because of their complication.

Even more complicated are the internal degrees of freedom in the problem of nucleon-nucleon or nucleon-antinucleon scattering. The relevant formulas have been worked out by Goldberger, Nambu & Oehme (21), among others, and involve 10 independent scalar functions. In the NN channel, if p_1 and p_2 are associated with the incoming nucleons and $-p_3$ and $-p_4$ with the outgoing, again there are relations of the type 2.8:

$$\begin{aligned}s_1 &= -2q^2(1 + \cos \theta) \\ s_2 &= -2q^2(1 - \cos \theta) \\ s_3 &= 4(q^2 + M^2)\end{aligned}\tag{2.17}$$

where q is the barycentric three-momentum and θ the angle of scattering. These relations switch over in the $N\bar{N}$ channel, where p_4 becomes an ingoing antinucleon and $-p_2$ an outgoing antinucleon, to

$$\begin{aligned}s_1 &= 4(K^2 + M^2) \\ s_2 &= -2K^2(1 - \cos \Theta) \\ s_3 &= -2K^2(1 + \cos \Theta)\end{aligned}\tag{2.18}$$

where now K is the barycentric momentum and Θ the angle of scattering. There is of course a second $N\bar{N}$ channel where $\sqrt{s_2}$ is the energy.

It is out of the question to go deeply into the NN and $N\bar{N}$ problem in this review. Suffice it to say that the same general approach may be used as in the $\pi\pi$ and πN problems. For the details of formulation, (21) should be consulted. The important results obtained to date will be described later.

The replacement of a pion by a photon in Figure 1(a) leads to the only problem in the group under consideration where a single invariant function suffices. The process in question is $\gamma + \pi \rightarrow 2\pi$, and it can be shown [Wong (22)] that G parity⁷ allows only the $I=1$ state and, therefore, only odd J values of the two-pion system. Furthermore, gauge invariance eliminates all electric multipoles, so that for each J value there is just one transition amplitude.

Putting a photon in place of a pion in Figure 1(b) gives rise to a complicated problem that requires 12 invariant functions [Chew *et al.* (23)]. The most familiar channel here is $\gamma + N \rightarrow \pi + N$, where all possible isotopic and angular momentum states of the final pion-nucleon system may be produced by both electric and magnetic transitions. Formulas for the invariant matrices as well as the connection between multipole transition amplitudes and invariant amplitudes are given in (23).

3. POLES IN SCATTERING AMPLITUDES

One of the most important practical consequences to date of the dispersion-relation approach to strong-coupling physics is the recognition of the presence in scattering amplitudes of poles, whose residues have not only a simple physical meaning but also great practical utility. One might almost say that everything so far understood theoretically about strong-coupling phenomena flows from these poles.

There are three different aspects of "polology" that deserve emphasis: (a) The existence and positions of the poles can be predicted simply on the basis of particle masses and internal quantum numbers, spin, parity, etc. (b) The residues of poles in different amplitudes or in different regions of the same amplitude are often simply related. In particular, "fundamental" coupling constants are usually defined directly in terms of residues. (c) Poles dominate the behavior of the scattering amplitude in their immediate neighborhood. On these three pillars a very substantial theoretical structure can be erected.

To implement the third aspect of "polology" it is of course necessary to know something about the other singularities, generally branch points, of the scattering amplitude in the complex plane. A good definition of the subject of "dispersion relations" is that it is the study of the location and nature of these singularities. Of course if enough were known about all the singularities one could construct the complete function, but at present we are far from such a situation, at least in practice. We are just now achieving a comfortable familiarity with the poles and beginning to understand what to do about the nearest branch points.

Location of poles.—The existence of poles in a few particular amplitudes has been rigorously proved in the course of deriving dispersion relations by the methods discussed in the introduction. [See, for example, Symazik (6).] Perturbation theory, however, suggests a broad rule that covers not only the poles rigorously derived but many others—some already established experimentally. The rule is the following, as applied to the problem of two incoming and two outgoing particles:⁸ If the two incoming particles and the two outgoing particles in any of the three channels of a diagram can be "connected" by a stable⁹ single particle of mass m_0 , then there will be a pole when the s variable corresponding to the square of the total four-momentum in this channel is equal to m_0^2 . By "connected" it is meant that the initial two-particle state and the final two-particle state can both assume all the same quantum numbers as the single particle in question. From the requirement of stability for the intermediate particle it follows that poles, although on the real axis, are never in the physical energy region. If they were, the single particle responsible for the pole could decay via strong interactions into either of the two-particle states to which it couples. It also can be shown that poles are always outside the physical momentum-transfer region.

Let us investigate the diagrams of Figure 1 from the point of view of poles. In Figure 1(a) there are no poles at all, if electromagnetic effects are ignored, because a two-pion state has quantum numbers different from any known particle except the photon. Of course there may exist a still undiscovered boson of mass less than 2μ , baryon number and strangeness zero, iso-

⁸ The more general rule is stated in Sect. III of (24).

⁹ Since we are neglecting weak and electromagnetic interactions, all the usually discussed "elementary" particles are to be counted as stable.

topic spin 0, 1, or 2 with the appropriate even or odd spin, and with even G parity. If so, there will be poles in the pion-pion scattering amplitude in addition to the photon pole,¹⁰ which is to be ignored in a strictly strong-coupling approach.

Figure 1(b) similarly contains no pole from the channel where two pions are incoming or outgoing; but from the two channels where one pion and one nucleon occur, poles arise at $s_1 = M^2$ and $s_3 = M^2$, respectively, corresponding to a single nucleon connecting initial and final states. Figure 1(c) has three poles, one from each channel. The two-nucleon channel gives rise to a pole at $s_3 = M_D^2$, corresponding to the deuteron, while the nucleon-antinucleon channels give rise to poles at $s_1 = \mu^2$ and $s_2 = \mu^2$, both corresponding to the pion.

TABLE I

THE POSITIONS OF POLES (m_0) AND LOWEST BRANCH POINTS ($\sqrt{s_0}$)
ARISING FROM THE VARIOUS CHANNELS OF FIGURE 1

Channel	m_0	$\sqrt{s_0}$
1. $\pi + \pi \leftrightarrow \pi + \pi$	—	2μ
2. $\pi + \pi \leftrightarrow N + \bar{N}$	—	2μ
3. $\pi + N \leftrightarrow \pi + N$	M	$M + \mu$
4. $N + N \leftrightarrow N + N$	M_D	$2M$
5. $N + \bar{N} \leftrightarrow N + \bar{N}$	μ	2μ
6. $\gamma + \pi \leftrightarrow \pi + \pi$	—	2μ
7. $\gamma + \pi \leftrightarrow N + \bar{N}$	μ	2μ
8. $\gamma + N \leftrightarrow \pi + N$	M	$M + \mu$

In the diagram obtained by replacing a pion of Figure 1(a) by a photon there are no poles, but Figure 1(b) with a photon has three, one from each channel. The channels containing one nucleon and a pion or one nucleon and a photon each give nucleon poles, while the channel containing $\gamma + \pi$ on one side and $N\bar{N}$ on the other gives a pion pole. Table I summarizes the location of poles in the pion-nucleon problem.

Residues and coupling constants.—Now, what about the residues? Again the rigorous dispersion-relation derivations have given for a few special cases an answer to this question that agrees with the rule suggested by perturbation theory. This rule is as follows:¹¹ (a) Pretend (whether you believe it or not) that all four external particles and the connecting particle are elementary and associated with local fields in the conventional sense. Construct from these fields invariant trilinear "interactions," satisfying all known symmetry requirements, that represent the two-particle to one-particle

¹⁰ The photon pole for charged particles manifests itself in the Coulomb part of the amplitude that becomes infinite at zero momentum transfer.

¹¹ A generalization of this rule for processes involving more than four particles is given in (24).

transitions in question. Associate with each trilinear interaction a real coefficient which may be called a "coupling constant." (b) Calculate the contribution to the scattering amplitude by conventional second-order perturbation theory. There will be one Feynman diagram for each connecting particle, the poles appearing automatically from the propagators of the connectors. The residues of these poles may be identified with the residues of the corresponding poles in the complete scattering amplitude, which are thus in general proportional to the product of two coupling constants.

Two important properties of the residues may be inferred from the above recipe. First: The residues are real. Second: The residue of a pole in one s variable does not depend on the remaining s variables. Thus, not only is the residue proportional to products of coupling constants; it also is completely determined by these constants.

Note that no statement is being made about the validity of perturbation theory or even about the legitimacy of the concept of an interaction propor-

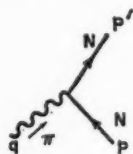


FIG. 2. The pion-nucleon vertex.

tional to the product of local fields. We are simply giving a recipe that is convenient because the rules of perturbation calculation are familiar. It is perfectly possible to formulate a recipe for the residues that avoids a specification of the form of the interaction and makes no use of the apparatus of perturbation theory [see, e.g., Symanzik (6)]. Such a formulation, however, would require the development of elaborate notation otherwise unnecessary in this review.

The most important coupling constant in our problem is that describing the three-pronged vertex of Figure 2. Except for trivial and known factors, the square of this constant determines the residue of all the poles of Figures 1(b) and 1(c) except that involving the deuteron. It also appears linearly in the residues of the poles of Figure 1(b) when a photon replaces a pion.¹² The vertex of Figure 2 in general depends on the three invariants q^2 , p^2 , p'^2 ; and the pion-nucleon coupling constant may be defined¹³ as the value of this vertex function when all three particles are on the mass shell, i.e., $p^2 = p'^2 = M^2$, $q^2 = \mu^2$. These conditions are guaranteed to be satisfied when residues

¹² The pion-nucleon coupling constant also occurs in the residues of poles for processes involving more than four particles. See, e.g., Chew & Low (24).

¹³ When electromagnetic effects are considered, one must define three constants, one for the processes $\pi^+ + n \leftrightarrow p$ and $n \leftrightarrow p + \pi^-$, one for the process $\pi^0 + p \leftrightarrow p$, and one for $\pi^0 + n \leftrightarrow n$. These three constants are expected to differ by a few per cent.

are calculated according to the above rules because two of the three particles are "external" and the internal particle momentum is considered at the point where its propagator is infinite, i.e., on its mass shell. From this point of view it is immaterial whether the coupling constant is introduced through the pseudoscalar "interaction"

$$g\bar{\psi}\gamma_5\tau_i\psi\phi_i \quad 3.1.$$

or the pseudovector "interaction"

$$\frac{f}{\mu}\bar{\psi}\gamma_5\gamma_\mu\tau_i\psi\frac{\partial\phi_i}{\partial x_\mu} \quad 3.2.$$

where ψ is the nucleon field and ϕ the pion field. When all three particles are on the mass shell, the two forms are identical for

$$f = \frac{\mu}{2M} g. \quad 3.3.$$

Much less familiar is the coupling constant associated with the vertex of Figure 3, whose square determines the residue of the deuteron pole in Figure



FIG. 3. The nucleon-deuteron vertex.

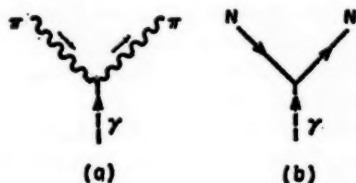


FIG. 4a. The pion-photon vertex.
FIG. 4b. The nucleon-photon vertex.

1(c). Actually this vertex involves two scalar functions, associated with the presence in the deuteron of both S - and D -wave components, and the corresponding "coupling constant" also has two parts. It can be shown [Goldberger *et al.* (21)] that the S part is much larger than the D and bears a simple relation to the triplet effective range of the neutron-proton system. Since the latter has been rather accurately measured, it is possible to calculate the residue of the deuteron pole.

In order to calculate the residues of Figure 1(b), with a photon replacing a pion, it is necessary to consider also the three-pronged vertices of Figure 4. The coupling constant for Figure 4(a) is just e , the charge of the pion; but—as for Figure 3—an analysis of the nucleon-photon vertex Figure 4(b) shows that two constants are required (actually four, because the photon distinguishes between neutron and proton), this time corresponding to the nucleon charge and anomalous magnetic moment. The anomalous moments are very important, but since they are accurately known there is no difficulty in calculating the required residues [Chew *et al.* (23)].

Extrapolation to the neighborhood of a pole—"polology."—It is obvious that

in the immediate vicinity of a pole, a scattering amplitude is completely determined by the pole's residue. Since these residues are fixed by a few constants, "polology" leads to many definite and interesting predictions about scattering amplitudes. The predictions, however, always involve some kind of extrapolation of experimental data because, as has been seen, poles invariably lie in nonphysical regions.

In order to formulate extrapolation procedures it is necessary to know something about the other singularities of the scattering amplitude. This question will not be reached until the next section, but here an extremely simple type of extrapolation [Chew (25)] may be described that is legitimate when a sufficiently large region of the complex plane, including a physical range of the real axis as well as the neighborhood of the pole, is singularity-free. This situation is believed to prevail¹⁴ for an s variable in the region of its momentum-transfer range when one of the other s variables is held fixed at a physical point in the energy range.

Inspection of the kinematical relations of Section 2 (e.g., formula 2.17) shows that when the energy is held fixed, the remaining s variables are linearly related to $\cos \theta$ with real coefficients. One may therefore speak of a $\cos \theta$ complex plane in which the poles are in one-to-one correspondence with those of the momentum-transfer s variables (which are really only a single variable because of 2.3). The physical region in $\cos \theta$ is of course the interval -1 to $+1$ on the real axis.

It is trivial to compute the location in the $\cos \theta$ plane of the poles enumerated above. They all lie on the real axis but outside the physical interval; in Table II the positions are given.

In every case, the position of the pole approaches the end of the physical region, $\cos \theta = \pm 1$, as the energy becomes very large; but at a finite energy the distance from the end of the physical interval to the pole varies sharply from case to case. At currently accessible energies the only poles near enough to allow practical extrapolations are those associated with pions in channels 4, 5, and 8.¹⁵

Since the neighborhood of the physical region in the $\cos \theta$ plane is free from singularities, the real and the imaginary parts of the scattering amplitude are separately analytic functions. Now, these poles all lie on the real axis and have real residues; thus, they occur only in the extension of the real part of the amplitude.¹⁶ A possible extrapolation procedure may then be

¹⁴ Lehmann (12) has given a rigorous proof of analyticity properties in the momentum-transfer variable that almost, but not quite, guarantees the domain of analyticity required here.

¹⁵ It will also be seen in the next section that the nearest branch points lie relatively close to the nucleon poles and further add to the difficulty of extrapolation in these cases.

¹⁶ The imaginary part of the amplitude has only branch points, which in the next section will be seen to be further from the physical region than the nearest branch points in the real part.

TABLE II

THE POSITIONS OF POLES EXPRESSED IN TERMS OF $\cos \theta$. THE CHANNEL INDICATED IS THAT WHOSE ANGULAR DISTRIBUTION CONTAINS THE POLE. THE CHANNEL THAT GIVES RISE TO A POLE, IN THE SENSE OF TABLE I, IS ALWAYS DIFFERENT FROM THE CHANNEL THAT CONTAINS THIS POLE IN $\cos \theta$

Channel	Position of Pole in $\cos \theta$
1. $\pi + \pi \leftrightarrow \pi + \pi$	—
2. $\pi + \pi \leftrightarrow N + \bar{N}$	$\pm \frac{M^2 + k^2 + K^2}{2kK}$
3. $\pi + N \leftrightarrow \pi + N$	$- \sqrt{\left(1 + \frac{M^2}{q^2}\right)\left(1 + \frac{\mu^2}{q^2}\right)} + \frac{\mu^2}{2q^2}$
4. $N + N \leftrightarrow N + N$	$\pm \left(1 + \frac{\mu^2}{2q^2}\right)$
5. $N + \bar{N} \leftrightarrow N + \bar{N}$	(a) $+ \left(1 + \frac{\mu^2}{2K^2}\right)$ (b) $- \left(1 + \frac{M_D^2}{2K^2}\right)$
6. $\gamma + \pi \leftrightarrow \pi + \pi$	—
7. $\gamma + \pi \leftrightarrow N + \bar{N}$	$\pm \sqrt{\frac{P^2 + M^2}{P^2}}$
8. $\gamma + N \leftrightarrow \pi + N$	(a) $+ \sqrt{\frac{q^2 + \mu^2}{q^2}}$ (b) $- \sqrt{\frac{q^2 + M^2}{q^2}}$

based on the following: Consider the function $f_R(z)$, which is the real part of any one of the scalar amplitudes discussed above, evaluated at a fixed physical energy for one of the s variables. The dependence on the other two s variables is expressed through $z = \cos \theta$. Then in a region of the complex plane which includes the physical interval $-1 < z < +1$, as well as the position of the pole $z = z_0$, the function

$$g_R(z) = (z - z_0)f(z) \quad 3.4.$$

is analytic. Further, $g_R(z_0) = \lambda$, where λ is the residue of the pole.¹⁷ At the same time, if $f_I(z)$ is the imaginary part of the amplitude, then

$$g_I = (z - z_0)f_I(z) \quad 3.5.$$

¹⁷ The residue λ is proportional to g^2 in the case of the poles 4 and 5a and to eg in the case of 8a.

is analytic in at least as large a region, with $g_I(z_0) = 0$. The cross section, with an appropriate normalizing factor that does not contain z , is given by¹⁸

$$\sigma(z) = f_R^2(z) + f_I^2(z); \quad 3.6.$$

therefore

$$G(z) = (z - z_0)^2 \sigma(z) \quad 3.7.$$

is an analytic function throughout this same region with the value λ^2 at $z = z_0$.

The function $G(z)$ can be measured experimentally in the interval $-1 < z < +1$ and fitted with a polynomial in z , or—what is equivalent but more convenient—a polynomial in $z - z_0$.¹⁹

$$G(z) = a_0 + a_1(z - z_0) + a_2(z - z_0)^2 + \dots \quad 3.8.$$

The coefficient a_0 in this expansion evidently is equal to λ^2 , so that one has a direct method of confronting the theory with experiment.

Sufficient experimental data exist already to have allowed application of this procedure by Cziffra & Moravcsik (26) to the "backward" pion pole in neutron-proton scattering at average neutron energies (lab) of 90 and 400 Mev. The broad spread in the incident-neutron energy spectrum prevents these data from yielding an accurate value for the pion-nucleon coupling constant, but the residue obtained agrees satisfactorily with other determinations of f^2 , which are to be discussed below. Eventually, it may be expected that backward $n\bar{p}$ scattering at a well-defined energy will yield an accurate determination of f^2 , which in this case is related to the coefficient a_0 in 3.8 by the formula [Chew (25)]

$$f^4 = (q^4/M^4)(q^2 + M^2)a_0. \quad 3.9.$$

Taylor, Moravcsik & Uretsky (28) have investigated the pion pole in photopion production from nucleons by the same method. The data here are poor, but the existence of the pole can be established and a rough value for f^2 obtained. The "forward" pion poles in nucleon-nucleon and nucleon-antinucleon scattering will probably be harder to exploit because the imaginary part of the amplitude tends to be larger than the real part near the forward direction at high energies. This familiar diffraction effect means that the interesting part of the cross section, containing the pole, is only a small fraction of what is measured.²⁰

¹⁸ With internal degrees of freedom there will be generally more than one scalar amplitude, but since all have the same properties of analyticity, the procedure outlined is still valid.

¹⁹ The question of how high an order of polynomial should be used depends on the energy, the angular interval of the experiment, and the accuracy, as well as the location of the nearest branch point. The most careful study of this question to date has been by Cziffra & Moravcsik (26) and by Frazer (27).

²⁰ Extrapolations to poles in angular distributions can be and are being carried out for many processes not considered here because they involve strange or complex particles or more than four particles all together. The basic principles involved are always the same.

It is also possible to extrapolate to poles, starting from the energy region of the real axis. These energy extrapolations can be done either at fixed momentum transfer, fixed angle, or at fixed angular momentum; but in all cases one must contend with a branch point lying at the lower end of the physical interval, between the experimental data and the pole. It is possible to get around this branch point, but the necessary techniques are much less direct than in the angle extrapolations. Often the term "effective range" theory is used to describe techniques of extrapolation in the energy variable. An example of the effective-range type of extrapolation is that proposed by Chew & Low (29) in connection with *P*-wave pion-nucleon scattering. The Chew-Low procedure was very crude, however, since (among other circumstances) there really is no pole in the amplitude they considered. These authors approximated a pair of neighboring branch points by a simple pole, a procedure that is exact only for an infinitely heavy nucleon. Also, singularities associated with the pion-pion interaction were ignored.

4. DISPERSION RELATIONS AT FIXED MOMENTUM TRANSFER

Let us now consider the extension of an *s* variable into the complex plane when one of the other *s* variables is held fixed in the physical momentum-transfer range of the real axis. This situation is the opposite of that discussed above in which the fixed variable was in the energy range. Holding the momentum transfer fixed is actually the more familiar condition historically and the one for which nearly all the rigorous derivations have been given.

As was the practice in discussing poles, we give without proof a prescription for extension into the complex plane that includes all the systematically derived results as well as others conjectured on the basis of perturbation theory. Consider any invariant scattering amplitude $A(s_1, s_2, s_3)$, after the internal degrees of freedom have been removed, and suppose that s_2 is held fixed on the real axis in the momentum-transfer range. The remaining two variables are linearly related through 2.3, and it is convenient to break the amplitude into two parts

$$A(s_1, s_2, s_3) = A_1^{s_2}(s_1) + A_2^{s_2}(s_3) \quad 4.1.$$

each of which is a function of a single variable. The rule for this decomposition has, of course, not yet been given. It is closely tied to the extension rule, which is as follows:

The functions $A_1^{s_2}(z)$ and $A_2^{s_2}(z)$ are associated with the channels in which s_1 and s_3 , respectively, act as energy variables. Each may contain simple poles²¹ of the type described above, with residues that are independent of s_2 . The remainder of the function in each case can be represented by an integral along the real axis of the form

$$\frac{1}{\pi} \int_{s_0}^{\infty} ds' \frac{\rho^{s_2}(s')}{s' - z} \quad 4.2.$$

²¹ In practice as seen in Table I, the particular channels which are concerned in the pion-nucleon problem have at most one pole each.

where $\rho^{*2}(s')$ is real for s_2 sufficiently small in absolute value, and the lower limit s_0 is the square of the lightest mass of a multiparticle state that has the quantum numbers of the channel in question. Table I gives the values of s_0 for the various channels.

The above prescription evidently allows an extension to complex z and corresponds to the statement that $A_2^{*1}(z)$ and $A_3^{*1}(z)$ are each real analytic functions in the cut plane with singularities confined to poles and branch points on the real axis [e.g. (19, Sect. 40)]. The cut is chosen to run along the positive real axis from the lowest branch point to $+\infty$. Also implied by 4.2, although not necessarily true in practice, is the vanishing of these functions at infinity; but the latter requirement may be relaxed by the technique of subtraction. The necessity for subtractions in dispersion relations is discussed in a systematic way by Bogoliubov *et al.* (7, p. 5). To avoid complicating the formulas, it will be assumed in this general discussion that subtractions are unnecessary, although in practical applications it is necessary to be careful about this point.

For values of s_2 such that ρ^{*2} is real (see discussion following Eq. 5.8), it follows that $\rho^{*2}(s')$ is just the imaginary part of the function in question as z approaches the positive real axis from above, that is, in the limit $z \rightarrow s' + i\epsilon$. The complete representation of the function is thus given by

$$A_{1,3}^{*2}(z) = \frac{\lambda_{1,3}}{m_{01,3}^2 - z} + \frac{1}{\pi} \int_{s_{01,3}}^{\infty} ds' \frac{\text{Im} A_{1,3}^{*2}(s')}{s' - z}. \quad 4.3.$$

In order to illustrate the foregoing, consider the diagram 1(a), for which there are no poles, and let s_2 be fixed at a small real negative value. Each of the three independent $\pi\pi$ amplitudes A , B , C may then be broken into two parts as in 4.1, and each of these parts has an integral representation of the type 4.3. The complete function can then be written, for example, as

$$A(s_1, s_2, s_3) = \frac{1}{\pi} \int_{4\mu^2}^{\infty} ds'_3 \frac{\text{Im} A_3^{*2}(s'_3)}{s'_3 - s_3} + \frac{1}{\pi} \int_{4\mu^2}^{\infty} ds'_1 \frac{\text{Im} A_1^{*2}(s'_1)}{s'_1 - s_1} \quad 4.4.$$

where s_1 and s_3 may be complex but obey the relation $s_1 + s_2 + s_3 = 4\mu^2$, so that either may be eliminated in terms of the other. Suppose one wants to apply 4.4 in the region where s_3 is positive real and larger than $4\mu^2$, i.e., in the physical-energy region for s_3 . It is then appropriate to eliminate s_1 , and the physical scattering amplitude may be defined by²²

$$^2A^{*2}(s_3) = \lim_{z \rightarrow s_3 + i\epsilon} \frac{1}{\pi} \int_{4\mu^2}^{\infty} ds' \left\{ \frac{\text{Im} A_3^{*2}(s')}{s' - z} + \frac{\text{Im} A_1^{*2}(s')}{s' - (4\mu^2 - s_2 - z)} \right\}. \quad 4.5.$$

The denominator of the second term cannot vanish for $s_2 > -4\mu^2$, so that the imaginary part of the expression comes entirely from the vanishing of

²² Note carefully the difference between $^3A^{*2}(s_3)$ and $A_3^{*2}(s_3)$. The former is the complete amplitude, while the latter is only one of two parts. Their imaginary parts are the same, but not their real parts.

the first denominator,²³ and thus

$$Im^3 A^{*2}(s_3) = Im A_1^{*2}(s_3). \quad 4.6.$$

By considering the physical energy region for s_1 in a similar way one would find

$$Im^1 A^{*2}(s_1) = Im A_1^{*2}(s_1); \quad 4.7.$$

therefore, both terms in the integrand of the dispersion integral can be expressed in terms of imaginary parts of complete scattering amplitudes. Since the imaginary part of 4.5 is satisfied identically once relation 4.6 is used, the final dispersion relation is usually written for the real part only:

$$Re^3 A^{*2}(s_3) = \frac{P}{\pi} \int_{\mu^2}^{\infty} ds' \left\{ \frac{Im^3 A^{*2}(s')}{s' - s_3} + \frac{Im^1 A^{*2}(s')}{s' - 4\mu^2 + s_2 + s_3} \right\}. \quad 4.8.$$

Entirely similar procedures may be used to obtain dispersion relations at fixed momentum transfers for any of the processes 1 to 8. When poles occur, these are simply to be added to the dispersion integrals. The general relation then has the form.

$$Re^3 A^{*2}(s_3) = \frac{\lambda_3}{m_{03}^2 - s_3} + \frac{\lambda_1}{m_{01}^2 - \left(\sum_{i=1}^4 m_i^2 - s_2 - s_3 \right)} + \frac{P}{\pi} \int_{s_{03}}^{\infty} ds'_3 \frac{Im^3 A^{*2}(s'_3)}{s'_3 - s_3} \\ + \frac{P}{\pi} \int_{s_{01}}^{\infty} ds'_1 \frac{Im^1 A^{*2}(s'_1)}{s'_1 - \left(\sum_{i=1}^4 m_i^2 - s_2 - s_3 \right)}. \quad 4.9.$$

It is characteristic that in the second or "crossed" term of a dispersion relation the imaginary part of the amplitude for a different channel occurs. Sometimes crossing symmetry allows one to express this amplitude in terms of the channel originally chosen for investigation. In the π - π scattering problem, for example, the crossing relations 2.6 tell that, under the exchange of s_1 and s_3 , $A \leftrightarrow C$. Thus the numerator of the crossed term can be written $Im^3 C^{*2}(s')$, which may be more convenient for practical applications.

The possibility of using crossing symmetry often determines which s variable is to be held fixed. In pion-nucleon scattering one nearly always holds s_2 fixed, rather than s_1 , because of the more useful relations that result. Holding s_1 fixed leads to a crossed term involving the channel $\pi + \pi \leftrightarrow N + \bar{N}$, about which little is known experimentally. In the nucleon-nucleon dispersion relations nothing can be done to avoid the nucleon-antinucleon channel, and as a result the relation has been difficult to apply.

In the dispersion relation 4.9 it is nearly always true that, near the lower limits of the integrations, nonphysical values of s'_3 and s'_1 occur for a fixed

²³ Here one may use the rule

$$\frac{1}{s' - (s_3 + i\epsilon)} = P \frac{1}{s' - s_3} + i\pi \delta(s' - s_3)$$

where P signifies that the principal value of the integral is to be taken.

value of s_2 . In pion-pion scattering, for example, the minimum physical value of s_3 for a fixed (negative) s_2 is $4\mu^2 - s_2$ and thus larger than the lower limit of the dispersion integral except in the case of forward scattering, where $s_2 = 0$. These nonphysical intervals give rise to most of the difficulty in proving dispersion relations, because it must be shown that the imaginary parts of the amplitudes in question have a meaning throughout the entire region of integration. The conjecture was made very early that the needed extension of the imaginary part of the amplitude could be achieved through conventional Legendre polynomial expansions such as 2.9, but it is necessary for these expansions to converge for a range of $\cos \theta$ that exceeds the physical range -1 to $+1$ on the negative side. A proof of this convergence has recently been given by Lehmann (12) for the cases in which rigorous derivations are possible.

Rigorous derivations have been given only for channels $\pi + \pi \leftrightarrow \pi + \pi$ with either s_1 or s_2 fixed, $\pi + N \leftrightarrow \pi + N$ with s_2 fixed, and $\gamma + N \leftrightarrow \pi + N$ with the momentum transfer to the nucleon fixed [Goldberger (11)]. In addition, proofs have so far been possible only for rather small magnitudes of the fixed momentum transfer. It is expected that future developments will extend the rigorous derivations, both in the number of channels and the range of momentum transfer. In the meantime most theorists are disposed to use perturbation theory as a guide to the actual limitations of the dispersion-relation approach, and perturbation theory leads to relations of the type 4.9 for all eight channels. There do appear to be some restrictions on the momentum-transfer range in which the above simple considerations are valid, but (as will be seen in the next section) these limitations do not cause any real difficulty.

By far the most useful²⁴ of the fixed momentum-transfer dispersion relations is that for pion-nucleon scattering in the forward direction. Not only is there no unphysical range here, but also—by luck—a direct measurement of the needed integrands can be achieved through the “optical theorem” relating the total cross section to the imaginary part of the forward amplitude. The formulas for this application were first worked out by Goldberger, Miyazawa & Oehme (30); and their relation to the invariant amplitudes $A^{0,1}$ and $B^{0,1}$, introduced above in formula 2.10, may be found in (19).

An enormous experimental effort has gone into testing the forward-direction pion-nucleon dispersion relations, and some doubts raised [Puppi & Stanghellini (31)] concerning the extent to which they are satisfied by the data. As the errors involved are better understood, however, the apparent discrepancies between theory and experiment diminish, and the current belief by most workers who have carefully studied the question is that the relations are experimentally satisfied. [See, e.g., Schnitzer & Salzman (32). References to other work on the verification of the forward πN relation can

²⁴ Pion-pion scattering has thus far eluded direct observation because of the relatively short lifetime of the particles.

be found in these articles.] Since the only quantity in these relations that is not directly measurable is the residue of the nucleon pole, we have here a relatively accurate means of determining the pion-nucleon coupling constant. The result is

$$f^2 = 0.08 \pm .01. \quad 4.9.$$

None of the other channels (except $\pi\pi \leftrightarrow \pi\pi$) on this list has dispersion relations without unphysical regions of integration, but serious efforts have been made nonetheless to investigate $N + N \leftrightarrow N + N$ [Matsuyama (33) and Grisaru (34)] and $\gamma + N \leftrightarrow \pi + N$ [Chew *et al.* (23)] because large parts of the dispersion integrals for these two channels can be determined experimentally. The methods so far used in such attempts, however, are "dirty" and certain to undergo radical improvement in the near future. It is preferable not to discuss these methods here and the interested reader is referred to the original articles. The conclusion from all investigations made to date of these two channels is that the experimental data probably satisfy the dispersion relations, with poles whose residues are roughly determined and correspond to values of f^2 in agreement with 4.9.

5. THE MANDELSTAM REPRESENTATION

The rule for extending the two independent s variables simultaneously into the complex plane has been given by Mandelstam (35). This prescription is based mainly on perturbation theory, and a long time may elapse before the rule is given the rigorous basis that now underlies some of the fixed momentum-transfer dispersion relations. However, Mandelstam's representation has passed many significant theoretical tests of internal consistency, and so far all its experimental consequences seem satisfied. If the representation can be believed, it not only allows many important types of extrapolation to the neighborhood of poles, but it apparently leads to a complete dynamical description of strong-coupling physics in the conventional sense. That is, when the masses and internal quantum numbers of elementary particles, as well as the mutual coupling constants, are known, the representation seems in principle to allow the calculation of all physically interesting quantities.

Let us first write down the representation for the simplest case, that of pion-pion scattering, and then generalize. According to Mandelstam the invariant amplitude $A(s_1, s_2, s_3)$, where the arguments can be complex but satisfy 2.3, may be expressed as follows:

$$A(s_1, s_2, s_3) = \frac{1}{\pi^2} \int \int ds'_1 ds'_2 \frac{\rho_{12}(s'_1, s'_2)}{(s'_1 - s_1)(s'_2 - s_2)} + \frac{1}{\pi^2} \int \int ds'_1 ds'_3 \frac{\rho_{13}(s'_1, s'_3)}{(s'_1 - s_1)(s'_3 - s_3)} \\ + \frac{1}{\pi^2} \int \int ds'_2 ds'_3 \frac{\rho_{23}(s'_2, s'_3)}{(s'_2 - s_2)(s'_3 - s_3)}. \quad 5.1.$$

The weight functions $\rho_{ij}(s'_i, s'_j)$ are real and the integrations in each s' variable go over a region of the positive real axis extending to infinity. For $\pi\pi$ scattering the region in which the weight functions are nonzero is asymptotic to

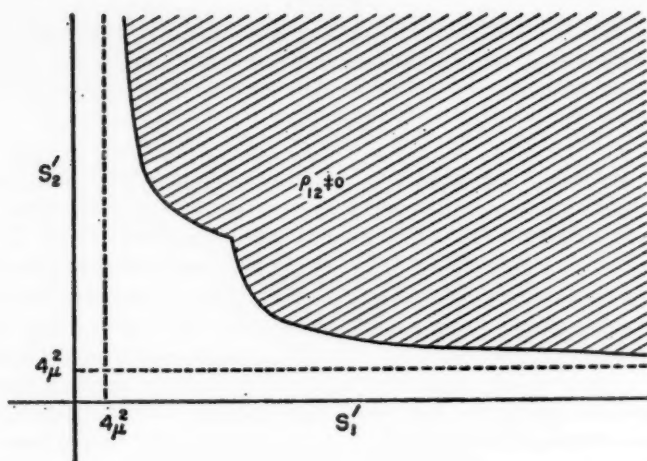


FIG. 5

the limiting values $s_i = 4_\mu^2$, $s_j = 4_\mu^2$. This particular region is shown in Figure 5. The general recipe for calculating boundary curves is not simple [Mandelstam (36)], but the asymptotic limits are always given by the s_0 of Table I. That is, the absolute lower limit of any s' variable of integration, which occurs when the other s' variable with which it is paired goes to infinity, is equal to the lowest mass of a multiparticle state that has the quantum numbers of the channel in question. If single-particle states can occur, then simple poles with constant residues are to be added to 5.1. Also subtractions may be needed if the amplitude does not vanish at infinity for both independent variables. These subtractions do not correspond to the introduction of new arbitrary constants if they are made in only one variable [see Mandelstam (36)].

It is easy to see that holding one s variable fixed at a real value outside its energy range and carrying out one of the two integrations in the Mandelstam representation lead to ordinary dispersion relations. If one wishes to arrive at 4.6, for example, then the first and third terms of 5.1 may be written as

$$\frac{1}{\pi} \int_{s_{10}}^{\infty} ds'_1 \frac{g_{12}^{*2}(s'_1)}{s'_1 - s_1} + \frac{1}{\pi} \int_{s_{20}}^{\infty} ds'_2 \frac{g_{23}^{*2}(s'_2)}{s'_2 - s_2} \quad 5.2.$$

where the new weight functions,

$$g_{2j}^{*2}(s'_j) = \frac{1}{\pi} \int_{s_2^0(s'_j)}^{\infty} ds'_2 \frac{\rho_{j2}(s'_j, s'_2)}{s'_2 - s_2}, \quad j = 1, 3, \quad 5.3.$$

are real for $s_2 < s_{20}$, since the lower limit $s_2^0(s'_j)$ is always larger than s_{20} . This form is then exactly that required for the ordinary dispersion relations at fixed s_2 . For the second term of 5.1 use is made of the identity

$$\begin{aligned} \frac{1}{(s_1' - s_1)(s_3' - s_3)} &= \frac{1}{s_1' + s_3' - s_1 - s_3} \left(\frac{1}{s_1' - s_1} + \frac{1}{s_3' - s_3} \right) \\ &= \frac{1}{s_1' + s_3' - \sum_{i=1}^4 m_i^2 + s_2} \left(\frac{1}{s_1' - s_1} + \frac{1}{s_3' - s_3} \right) \end{aligned} \quad 5.4.$$

to arrive at a similar form. Thus the entire expression 5.1 can be written in the form 5.2 if $g_{12}^{s_2}(s_1')$ is augmented by the integral

$$\frac{1}{\pi} \int_{s_2^0(s_1')}^{\infty} ds_2' \frac{\rho_{12}(s_1', s_2')}{s_1' + s_3' - \sum_{i=1}^4 m_i^2 + s_2} \quad 5.5.$$

and $g_{32}^{s_2}(s_3')$ by a corresponding integral over ds_1' . The complete connection between 5.1 and 4.6 is therefore given by

$$\begin{aligned} Im^3 A^{s_2}(s_3') &= \frac{1}{\pi} \int_{s_2^0(s_3')}^{\infty} ds_2' \frac{\rho_{32}(s_3', s_2')}{s_2' - s_2} + \frac{1}{\pi} \int_{s_1^0(s_3')}^{\infty} ds_1' \frac{\rho_{13}(s_1', s_3')}{s_1' + s_3' - \sum_{i=1}^4 m_i^2 + s_2} \\ Im^1 A^{s_2}(s_1') &= \frac{1}{\pi} \int_{s_2^0(s_1')}^{\infty} ds_2' \frac{\rho_{12}(s_1', s_2')}{s_2' - s_2} + \frac{1}{\pi} \int_{s_3^0(s_1')}^{\infty} ds_3' \frac{\rho_{31}(s_3', s_1')}{s_1' + s_3' - \sum_{i=1}^4 m_i^2 + s_2}. \end{aligned} \quad 5.6.$$

Poles that may appear in the Mandelstam representation are to be carried over without change into the one-dimensional representation, except that a pole in the fixed variable is generally suppressed by making a subtraction, since it becomes just a constant in the reduced equation.

The denominators of the second integrals in 5.6 can vanish if s_2 is sufficiently large and negative, so that the "imaginary parts" defined by these expressions become complex. It can easily be shown, however, that the imaginary parts of the "imaginary parts" cancel out when both terms of 4.6 are calculated because the apparent singularity was introduced artificially through the partial fractions of 5.4.

A second elementary application of the Mandelstam representation is to justify the procedure outlined in Section 3 for extrapolating to the neighborhood of poles. Here the fixed s variable is in the physical-energy range; i.e., real and larger than the s_0 for this channel. It is easy to see by inspection of 5.1 that if the remaining two variables are replaced by $\cos \theta$, then the singularities in the $\cos \theta$ complex plane all lie on the real axis and are outside the physical interval, $-1 < \cos \theta < +1$. Furthermore, the nearest branch points²⁵ are determined by the s_0 values and always lie beyond any poles that occur. Thus there is no impediment to a simple polynomial extrapolation from the physical region.

Many other applications of 5.1 are possible. For example, Cini, Fubini &

²⁵ The nearest right-hand branch point (or left) is given by the equation $s_1(\cos \theta, s_3) = s_{10}$ and the nearest left-hand branch point (or right) by $s_2(\cos \theta, s_3) = s_{20}$, if the fixed variable is s_3 .

Stanghellini (37) have derived dispersion relations at fixed $\cos \theta$, and several workers have deduced dispersion relations for fixed angular momentum. The latter are particularly powerful because they allow a simple incorporation of the unitarity of the S matrix into the problem. When unitarity is added to 5.1, the dynamics of the system seem to be almost completely determined.

In order to get dispersion relations for a given partial-wave amplitude (i.e., for a definite angular momentum), it is necessary to make a projection of 5.1. Taking $\pi\pi$ scattering again as an example and using 2.8 to replace s_1 and s_2 by \cos and s_3 by q^2 , $A(s_1, s_2, s_3)$ may be expanded as follows:

$$A(q^2, \cos \theta) = \sum_{l=0}^{\infty} (2l+1) q^{2l} A_l(q^2) P_l(\cos \theta) \quad 5.8.$$

where

$$q^{2l} A_l(q^2) = \frac{1}{2} \int_{-1}^{+1} dx A(q^2, x) P_l(x). \quad 5.9.$$

Since the dependence of 5.1 on s_1 and s_2 and hence on $\cos \theta$ is contained explicitly in the denominators, one may carry out the integration 5.9 and obtain an expression for $A(q^2)$ in which the singularities in the q^2 complex plane are clearly exhibited.

There are of course no poles in the $\pi\pi$ case, and all the branch points turn out to lie on the real axis [Chew & Mandelstam (15)]. There is a branch point at $q^2=0$, the threshold of the physical region; another at $q^2=3\mu^2$, the threshold for producing two additional pions; and so on. It is convenient, then, to choose a cut running along the positive real axis from 0 to ∞ . On the negative real axis there is a corresponding set of branch points, the first occurring at $q^2=-\mu^2$, the second at $q^2=-4\mu^2$, and so forth, so that a second cut may be chosen to run along the negative real axis from $-\infty$ to $-\mu^2$.

In more complicated channels the branch points may not all lie on the real axis, but their positions can be determined by inspection of 5.1 after the projection is carried out. There are in general three cuts, corresponding to the three channels of a single diagram, but when two or more identical particles appear in the same diagram there may be a coincidence of the singularities arising from different channels. Such a coincidence occurs in the $\pi\pi$ problem just described, where the left-hand cut covers a superposition of two sets of branch points. The results for $\pi+N \leftrightarrow \pi+N$ have been given by McDowell (38); for $\pi+\pi \leftrightarrow N+\bar{N}$ by Frazer & Fulco (20); for $N+N \leftrightarrow N+N$ by Noyes & Wong (39); and for $\gamma+\pi \leftrightarrow \pi+\pi$ by H. Wong (22).

The partial-wave amplitudes may be expressed in each case in terms of integrals along the cuts, where the integrand is the discontinuity in going across the cut and may be written in terms of the imaginary part of the physical amplitude for the channel which gives rise to the cut in question. It is possible, therefore, to consider these relations as coupled integral equations which determine the dynamics of the system.

To illustrate the situation, consider the S -wave part of the amplitude A in pion-pion scattering. This amplitude, by projection according to 5.9 from 5.1, satisfies the dispersion relation

$$A_0(q^2) = \frac{1}{\pi} \int_{\mu^2}^{\infty} dq'^2 \frac{\rho_0(q'^2)}{q'^2 + q^2} + \frac{1}{\pi} \int_0^{\infty} dq'^2 \frac{\text{Im} A_0(q'^2)}{q'^2 - q^2} \quad 5.10.$$

where

$$\rho_0(q'^2) = 2 \int_0^{+q'^2 - \mu^2} \frac{dq''^2}{q'^2} \text{Im} B \left(q''^2, 1 - 2 \frac{q'^2 - \mu^2}{q'^2} \right). \quad 5.11.$$

The other partial A amplitudes, as well as those of B and C , satisfy similar relations; and by taking the linear combinations 2.7 one can form dispersion relations for partial waves of well-defined isotopic spin. At this stage the imaginary part on the right-hand cut, at least for $0 < q^2 < 3\mu^2$, can be very simply expressed in terms of the unitarity condition. That is, since according to 2.9,

$$A_I^I(q^2) = \sqrt{\frac{q^2 + \mu^2}{q^2}} e^{i\delta_I^I} \sin \delta_I^I \quad 5.12.$$

with δ_I^I real in this interval, it follows that

$$\text{Im} A_I^I(q^2) = \sqrt{\frac{q^2}{q^2 + \mu^2}} |A_I^I(q^2)|^2. \quad 5.13.$$

Beyond $q^2 = 3\mu^2$, it is necessary to include inelastic processes in the expression for the imaginary part of the amplitude.

The expression 5.11 for the contribution from the cut along the negative real axis involves the imaginary part of the pion-pion amplitude for $\cos \theta < -1$. By inspection of the boundaries in Figure 5 it can be shown that the polynomial expansion of the imaginary part, for the values of $\cos \theta$ required in 5.11, converges for $q'^2 < 9\mu^2$ [Chew & Mandelstam (15)]. There is no difficulty then in representing the function $\rho_0(q'^2)$ up to this point; beyond it new techniques, such as suggested by Mandelstam (35), must be used. These techniques are too complicated to be described here.

Attempts are currently being made to solve the pion-pion equations in a low-energy approximation in which only S and P waves and only the lowest branch points are considered [Chew & Mandelstam (15)]. The latter simplification corresponds to the neglect of inelastic processes and allows the use of 5.13 throughout the physical region. The former permits an elementary calculation of the contribution from the left-hand (unphysical) cut.

The equations to be solved contain one free parameter, which may be called the pion-pion coupling constant. It is introduced conveniently as the value of the amplitude at the point $s_1 = s_2 = s_3 = \xi = \frac{4}{3}\mu^2$, where the three amplitudes A , B , and C are all real and equal to one another. Precisely, one may define

$$-\lambda = A(\xi, \xi, \xi) = B(\xi, \xi, \xi) = C(\xi, \xi, \xi). \quad 5.14.$$

It is clear that at least one arbitrary constant is needed in the elastic approximation because the equations permit as a solution an amplitude that is zero everywhere. It is not known whether an arbitrary constant would be necessary in a calculation that included inelastic processes, such as $\pi + \pi \rightarrow N + \bar{N}$; however, it will be so difficult to calculate such high-energy effects

accurately that in practice λ will surely play the role of an "independent" constant for a long time to come. At the time of this writing it is known only from the absence of 2π bound state that $-.4 \lesssim \lambda \lesssim +.2$, but experimental efforts are under way which should soon yield some information.

Attempts are also being made to solve the integral equations resulting from the application of Mandelstam's representation to Figures 1(b) and 1(c), and in the final section the relationships of the different channels and their current status of understanding are surveyed. Mandelstam has shown (36) that the results of conventional perturbation theory can be reproduced by iteration of his integral equations; therefore there is a strong inclination to believe that they represent a complete dynamical framework, given the masses and conventional coupling constants. Of course these highly non-linear equations, if they can be solved at all, must be applied to large coupling constants for which the perturbation series is meaningless. Whether the equations have unique solutions in such a situation is not known. Perhaps they have no solutions at all except for certain definite values of the masses and coupling constants!

6. SUMMARY AND CONCLUSION

The reader may wonder why so few concrete results have been given in this review. The reason is that in the author's opinion the results obtained to date are relatively insignificant compared with what will be forthcoming in the next year or two. The power of the generalized dispersion relations, when supplemented by unitarity, has only recently been recognized, and theoretical attempts to utilize this power are in their infancy.

It is true that a large literature on dispersion relations already exists, but this is based almost entirely on fixed momentum-transfer relations which contain only a part of the story. All questions investigated to date will surely be re-examined within the more general framework, and a vast clarification is guaranteed. The current literature is filled with confusion about "subtractions" and extensions in the momentum-transfer variable that there is no point in propagating further in this review.

It is possible already to see the outline of a general line of attack on the pion-nucleon problem that should go quite a distance toward answering the conventional questions. The starting point must be pion-pion scattering, where, as explained above, one can hope to calculate the amplitude up to $q^2 \sim 3\mu^2$ in terms of a single constant λ . Next one would go to the two channels of Figure 1(b), $\pi + N \leftrightarrow \pi + N$ and $\pi + \pi \leftrightarrow N + \bar{N}$, which in such an approach must be considered simultaneously and for which the $\pi\pi$ interaction must already be known.

One of the most misleading aspects of the history of pion-nucleon theory is the partial success of attempts to understand low-energy pion-nucleon scattering without any inclusion of a pion-pion interaction [Chew & Low (29)]. Such success appears now to be largely accidental; it had the beneficial effect of reviving interest in field theory for strong-coupling phenomena; but

if pion-pion scattering at very low kinetic energies were as strong as it must be at higher energies, simple models of the pion-nucleon interaction would not work. These models, of course, have never even pretended to answer such basic questions as why the S -wave pion-nucleon phase shifts are small.

It is perhaps worth spelling out the interrelation of the three processes $\pi + \pi \leftrightarrow \pi + \pi$, $\pi + N \leftrightarrow \pi + N$, and $\pi + \pi \leftrightarrow N + \bar{N}$ in the Mandelstam framework. If one derives dispersion relations for pion-nucleon partial waves, then there are two left-hand unphysical cuts, one corresponding to pion-nucleon scattering itself and one to the channel $\pi + \pi \leftrightarrow N + \bar{N}$. Keeping only the former leads to integral equations roughly of the kind proposed by Chew & Low (29), provided the inelastic branch points are ignored.²⁶

The nearest portion of the other cut requires a knowledge of the amplitude for $\pi + \pi \leftrightarrow N + \bar{N}$ at energies for this process between 2μ and 4μ . Such an energy region is unphysical, and fortunately so, because if the dispersion relations for this amplitude are derived, the contribution from the right-hand cut in the corresponding interval is controlled entirely by pion-pion elastic scattering. Precisely, the unitarity condition for this interval is that the phase of a partial-wave amplitude for $\pi + \pi \leftrightarrow N + \bar{N}$ is the same as the phase of the corresponding elastic pion-pion amplitude. This information, together with a knowledge of the contribution from the left-hand cuts,²⁷ is sufficient to determine the amplitude for $\pi + \pi \leftrightarrow N + \bar{N}$, provided always that higher branch points are neglected.

The coupled integral equations that must be solved in carrying out Mandelstam's program are complicated but apparently manageable with fast electronic computers. There is reason to hope, then, that low-energy pion-nucleon scattering can be roughly calculated in terms of the two constants λ and g^2 . The neglect of higher branch points, of course, limits the accuracy of the calculation and precludes a treatment of high-energy scattering by this method.

It is perhaps worth emphasizing the philosophy behind the approximation of neglecting high-energy singularities. The underlying motivation lies in the property of an analytic function that its behavior in a small region is dominated by near-by singularities. The dispersion relations make this feature very clear, since they resemble Coulomb's law for a static potential produced by point charges (poles) and line charges (branch cuts). Faraway charges produce at most a slowly varying potential in a local region; strong variations of potential are produced by near-by charges. It is obvious that in strong-coupling problems no calculation can be exact; some approximation must be made. A program of successive approximations based on the distance

²⁶ To evaluate the contribution of the left-hand pion-nucleon cut an extension to $\cos \theta < -1$ is required, just as in the pion-pion problem, and it may be necessary to introduce a cutoff if this extension is carried out by Legendre polynomials.

²⁷ (The two left-hand cuts here are coincident, both being associated with pion-nucleon scattering.)

of singularities from the region of interest seems to the author more plausible than any other procedure yet proposed.

Many valuable theoretical by-products would flow from a successful integration of Mandelstam's equations for Figure 1(b). A knowledge of the amplitude $\pi + \pi \leftrightarrow N + \bar{N}$ would allow at long last a correct calculation of the two-pion exchange contribution to the nucleon-nucleon interaction. Precisely, one may derive [Noyes & Wong (39)] dispersion relations for partial-wave nucleon-nucleon elastic-scattering amplitudes, where the two left-hand cuts are coincident and associated with the process $N + \bar{N} \leftrightarrow N + \bar{N}$. The nearest contribution comes from the single-pion intermediate state in this process, which is determined entirely by g^2 . The next contribution is from the 2π state and is known as soon as the amplitude for $N + \bar{N} \leftrightarrow 2\pi$ is known. There is some reason to believe that inclusion of these two singularities will allow a rough calculation of low-energy nucleon-nucleon phase shifts without any new parameters. If the faraway left-hand singularities are represented by an adjustable constant,²⁸ one may hope to achieve an accurate theory. It should be emphasized that in the solution of the nucleon-nucleon integral equations, the deuteron pole will appear automatically; it does not have to be inserted as an independent entity. Thus one expects to calculate the binding energy and quadrupole moment of the deuteron, as well as the triplet effective range, in terms of "fundamental" constants.

A second application of the amplitude for $N + \bar{N} \leftrightarrow 2\pi$ is to the problem of nucleon electromagnetic structure [Chew *et al.* (40); Federbush *et al.* (41)]. Here, in conjunction with the vertex function for $\gamma \rightarrow 2\pi$, this amplitude determines the structure and magnitude of the anomalous magnetic moment. The pion-photon vertex function can easily be calculated once the pion-pion scattering amplitude is available.

Also immediately calculable in terms of $\pi\pi$ scattering is the amplitude for $\gamma + \pi \leftrightarrow 2\pi$, which is needed in the problem $\gamma + N \leftrightarrow \pi + N$. One of the two left-hand cuts in the latter case involves photopion production itself, but the other requires $\gamma + \pi \leftrightarrow N + \bar{N}$ which, in turn, involves $\gamma + \pi \leftrightarrow 2\pi$. It should be possible, then, to put the theory of low-energy photopion production from nucleons on a sound basis.

The chain does not end here. With a proper understanding of photopion production one can calculate photon-nucleon elastic scattering, and this latter amplitude may allow a calculation of the neutron-proton mass difference [Cini *et al.* (42)]. Similarly, the charged-neutral pion mass difference may be calculable in terms of $\gamma + \pi \leftrightarrow \gamma + \pi$, which in turn depends on $\gamma + \pi \rightarrow 2\pi$. The chance of achieving quantitatively reliable results from mass calculations is, however, much smaller than that for scattering amplitudes.

Even if, as is unlikely, the calculations outlined here were to yield good results in terms of the four constants μ , M , λ , and g^2 , it must not be supposed

²⁸ This constant may be thought of as equivalent to the hard-core radius of conventional potentials.

that all questions would have been answered. Why should these constants have the particular values that are observed? Why are nucleons and pions the only nonstrange strongly interacting "elementary" particles? Why is the pion pseudoscalar? There is no understanding yet of such questions, and if one starts to consider the hyperons and K particles the number of puzzles multiplies. Exciting as the prospects are for dynamical calculations with the Mandelstam representation, it must be remembered that these calculations are based on conventional field theory, just as it was invented 30 years ago, and that the breakthrough which will yield the origin of elementary particles has not been achieved.

LITERATURE CITED

1. Kronig, R., *J. Opt. Soc. Am.*, **12**, 547 (1926)
2. Kramers, H. A., *Atti Congr. intern. fis., Como*, **2**, 545 (1927)
3. Lehmann, H., Symanzik, K., and Zimmermann, W., *Nuovo cimento*, **1**, 205, (1955); **6**, 319 (1957)
4. Low, F. E., *Phys. Rev.*, **97**, 1392 (1955)
5. Goldberger, M. L., *Phys. Rev.*, **99**, 979 (1955)
6. Symanzik, K., *Phys. Rev.*, **105**, 743 (1957)
7. Bogoliubov, N. N., Medvedev, B. M., and Polivanov, M. K., "Problems of the Theory of Dispersion Relations," lecture notes transl. at Inst. for Advanced Study, Princeton Univ., Princeton, N. J., 1957 (Unpublished)
8. Bremermann, H., Oehme, R., and Taylor, J., *Phys. Rev.*, **109**, 2178 (1958)
9. Jost, R., and Lehmann, H., *Nuovo cimento*, **5**, 1598 (1957)
10. Dyson, F. J., *Phys. Rev.*, **110**, 1460 (1958)
11. Goldberger, M. L., *Proc. Ann. Intern. Conf. High-Energy Phys., Geneva*, 208 (1958)
12. Lehmann, H., *Nuovo cimento*, **10**, 579 (1958)
13. Karplus, R., and Ruderman, M. A., *Phys. Rev.*, **98**, 771 (1955)
14. Jauch, J. M., and Rohrlich, F., *The Theory of Photons and Electrons* (Addison-Wesley Publishing Co., Inc., Cambridge, Mass., 1955)
15. Chew, G. F., and Mandelstam, S., *U. S. Atomic Energy Document, UCRL 8728* (1959)
16. Bethe, H. A., and de Hoffman, F., *Mesons and Fields*, II (Row, Peterson & Co., White Plains, N. Y., 1955)
17. Lee, T. D., and Yang, C. N., *Nuovo cimento*, **3**, 749 (1956)
18. Chew, G. F., Goldberger, M. L., Low, F. E., and Nambu, Y., *Phys. Rev.*, **106**, 1337 (1957)
19. Chew, G. F., *Theory of Pion Scattering and Photoproduction* (To be published in *Handbuch der Physik*, **43**, Springer-Verlag, Heidelberg, Germany); issued in preprint form as *U. S. Atomic Energy Document, UCRL Misc. 1957-45*
20. Frazer, W., and Fulco, J. (Private communication, Berkeley, Calif., 1959)
21. Goldberger, M. L., Nambu, Y., and Oehme, R., *Ann. Phys. (N. Y.)*, **2**, 226 (1957)
22. Wong, H. S., to be published, *Phys. Rev.*, (1959)
23. Chew, G. F., Goldberger, M. L., Low, F. E., and Nambu, Y., *Phys. Rev.*, **106**, 1345 (1957)
24. Chew, G. F., and Low, F. E., *Phys. Rev.*, **113**, 1640 (1959)
25. Chew, G. F., *Phys. Rev.*, **112**, 1380 (1958)

26. Cziffra, P., and Moravcsik, M., *U. S. Atomic Energy Commission Document, UCRL 8707* (1959)
27. Frazer, W. R., *U. S. Atomic Energy Commission Document, UCRL 8621* (1959)
28. Taylor, J., Moravcsik, M., and Uretsky, J., *Phys. Rev.*, **113**, 689 (1959)
29. Chew, G. F., and Low, F. E., *Phys. Rev.*, **101**, 1570 (1956)
30. Goldberger, M. L., Miyazawa, H., and Oehme, R., *Phys. Rev.*, **99**, 986 (1955)
31. Puppi, G., and Stanghellini, A., *Nuovo cimento*, **5**, 1257 (1957)
32. Schnitzer, H., and Salzman, G., *Phys. Rev.*, **112**, 1802 (1958); **113**, 1153 (1959)
33. Matsuyama, S., *Determination of the Pion-Nucleon Coupling Constant by Means of the Nucleon-Nucleon Dispersion Relation* (Univ. of Tokyo Preprint, Tokyo, Japan, 1958)
34. Goldberger, M. L., Grisaru, M., and Oehme, R., *Proc. Ann. Intern. Conf. High Energy Physics, Geneva*, **99** (1958)
35. Mandelstam, S., *Phys. Rev.*, **112**, 1344 (1958)
36. Mandelstam, S., *The Analytic Properties of Scattering Amplitudes in Perturbation Theory*, **99** (Univ. of Calif. Physics Dept., Preprint, Berkeley, Calif., 1959)
37. Cini, M., Fubini, S., and Stanghellini, A., *Fixed Angle Dispersion Relations for Nucleon-Nucleon Scattering* (CERN Preprint, Geneva, Switzerland, 1959)
38. McDowell, S. W., *On the Analytic Properties of Partial Amplitudes* (Univ. of Birmingham Physics Dept., Preprint, Birmingham, Engl., 1959)
39. Noyes, H. P., and Wong, D. (Private communication, Berkeley, Calif., 1959)
40. Chew, G. F., Karplus, R., Gasiorowicz, S., and Zachariasen, F., *Phys. Rev.*, **110**, 265 (1958)
41. Federbush, P., Goldberger, M. L., and Treiman, S. B., *Phys. Rev.*, **112**, 642 (1958)
42. Cini, M., Ferrari, A., and Gatto, R., *Neutron-Proton Mass Difference by Dispersion Theory* (Univ. of Rome Preprint, Rome, Italy, 1958)

STRANGE PARTICLES: DECAYS¹

By L. OKUN'

*Institute of Theoretical and Experimental Physics,
Academy of Sciences, Moscow, U. S. S. R.*

1. INTRODUCTION

This review deals with the theory of weak interactions of elementary particles, with particular attention to leptonic decays of strange particles (K mesons and hyperons). We shall altogether disregard slow processes taking place in nuclei (nuclear β -decay, muon capture in nuclei, hyperfragment decay).

Without attempting to embrace all the trends now existing in the theory of strange particle decays, we shall give below one of the possible approaches. This approach is based on the hypotheses of the compound model of strongly interacting particles and of the universal weak interaction.

Of essential importance in the decays of mesons and baryons are virtual strong interactions. As no consistent theory of strong interactions exists at present, we shall take them into account phenomenologically. We shall not consider small corrections caused by virtual photons.

In Section 2 the properties of weak interactions are discussed. Muon decay is considered in Section 3. In this process the nature of the weak interaction is not obscured by virtual strong interactions. The fourth section deals with interactions between leptons and strongly interacting particles involving no change of strangeness of the latter. These interactions are responsible for such processes as neutron decay, muon capture by the proton, charged pions decays, and several hyperon decays which have not been observed so far. Section 5 considers interactions of leptons with strongly interacting particles, involving a change of strangeness of the latter. They are responsible for the leptonic decays of K mesons and hyperons. Section 6 is devoted to non-leptonic decays of strange particles.

Lack of space has made it impossible to embrace all original theoretical works on the questions considered and even more so to cover all experimental papers. The reader will find more exhaustive information on the questions dealt with in this review in the proceedings of conferences on the physics of elementary particles (1 to 5) and in a number of reviews (6 to 19).

2. PROPERTIES OF WEAK INTERACTION

2.1 Universal Fermi interaction.—It is now widely known that weak interactions are responsible for all known decays of elementary particles (see Table I) except those of the Σ^0 -hyperon and the π^0 -meson. Research into weak interactions, which has become especially intensive since the fundamental paper of Lee & Yang (20) appeared, has resulted in a theory of universal weak interaction set forth in the works of Feynman & Gell-Mann

¹ The survey of literature pertaining to this review was concluded in December, 1958.

TABLE I

MASSES AND LIFETIMES OF ELEMENTARY PARTICLES

Particle family	Particle	Spin	Mass (Mev)	Mean lifetime (sec.)
Photons	γ	1	0	stable
Leptons	$\nu \quad \bar{\nu}$	$\frac{1}{2}$	$< 2 \cdot 10^{-4} \dagger$	stable
	$e^- \quad e^+$	$\frac{1}{2}$	0.510976	stable
	$\mu^- \quad \mu^+$	$\frac{1}{2}$	105.70 ± 0.06	$(2.22 \pm 0.02) \times 10^{-8}$
Mesons	$\pi^+ \quad \pi^-$	0	139.63 ± 0.06	$(2.56 \pm 0.05) \times 10^{-8}$
	π^0	0	135.04 ± 0.16	$(0.0 < \tau < 0.4) \times 10^{-13}$
	$K^+ \quad K^-$	0	494.0 ± 0.20	$(1.224 \pm 0.013) \times 10^{-8}$
	$K^0 \quad \bar{K}^0$	0	497.9 ± 0.6	$K_1^0: \begin{pmatrix} +0.07 \\ 1.05 \\ -0.05 \end{pmatrix} \times 10^{-10} \dagger$
				$K_2^0: \begin{pmatrix} +3.2 \\ 8.1 \\ -2.4 \end{pmatrix} \times 10^{-8} \parallel$
Baryons*	p	$\frac{1}{2}$	938.213 ± 0.01	stable
	n	$\frac{1}{2}$	939.506 ± 0.01	$(1.011 \pm 0.026) \times 10^8 \S$
	Λ^0	$\frac{1}{2}$	1115.2 ± 0.13	$\begin{pmatrix} +0.13 \\ 2.42 \\ -0.12 \end{pmatrix} \times 10^{-10} \dagger$
	Σ^+	$\frac{1}{2}$	1189.3 ± 0.35	$(0.79 \pm 0.08) \times 10^{-10} \dagger$
	Σ^-	$\frac{1}{2}$	1196.4 ± 0.5	$\begin{pmatrix} +0.16 \\ 1.71 \\ -0.14 \end{pmatrix} \times 10^{-10} \dagger$
			$+0.9^\ddagger$	
	Σ^0	$\frac{1}{2}$	1190	$< 10^{-11}$; theory $\sim 10^{-10}$
			-1.9	
	Ξ^-	?	1321 ± 3.5	$(4.6 < \tau < 200) \times 10^{-10}$
	Ξ^0	?	?	?

* Antibaryons have the same spin, mass, and lifetime as baryons.

† See paper by Sakurai where the experimental data are interpreted theoretically (119).

‡ Eisler *et al.* (120); see also Boldt, Caldwell & Pal (121), who give $\tau_{\Lambda^0} = (2.63 \pm 0.21) \times 10^{-10}$ sec. $\tau_{K_1^0} = 9_{-7}^{+6} \times 10^{-8}$ sec. $\tau_{K_2^0} = (1.07 \pm 0.13) \times 10^{-10}$ sec.

§ Sosnovsky *et al.* (122).

|| Bardou *et al.* (123).

¶ Stevenson (124).

** Rosenfeld *et al.* (134).

The rest of the data is from Table 1 of the review by Gell-Mann & Rosenfeld (125).

(21) and Sudarshan & Marshak (22; see also 23, 24). According to this theory and within the framework of Sakata's compound model, L , the density of the weak interaction Lagrangian, has the following form:

$$L = \frac{G}{\sqrt{2}} j_\alpha j_\alpha^\dagger. \quad 1.$$

The current j_α contained in the Lagrangian consists of four terms:

$$j_\alpha = j_\alpha^e + j_\alpha^\mu + j_\alpha^n + j_\alpha^\Lambda \quad 2.$$

of which two are leptonic currents:

$$j_\alpha^e = \bar{\psi}_e \gamma_\alpha (1 + \gamma_5) \psi_e \quad \text{and} \quad j_\alpha^\mu = \bar{\psi}_\mu \gamma_\alpha (1 + \gamma_5) \psi_\mu \quad 3.$$

and two, baryonic currents:

$$j_\alpha^n = \bar{\psi}_n \gamma_\alpha (1 + \gamma_5) \psi_p \quad \text{and} \quad j_\alpha^\Lambda = \bar{\psi}_\Lambda \gamma_\alpha (1 + \gamma_5) \psi_p. \quad 4.$$

The first of the baryonic currents conserves strangeness ($\Delta S=0$), the second changes it ($\Delta S=-1$). In expressions 3 and 4, $\bar{\psi}$ are the operators of particle creation and antiparticle annihilation; ψ are the operators of antiparticle creation and particles annihilation. We regard e^- , μ^- , ν , p , n , and Λ as particles and e^+ , μ^+ , $\bar{\nu}$, \bar{p} , \bar{n} , and $\bar{\Lambda}$ as antiparticles.

$$\gamma_5 = \begin{pmatrix} 1 & 0 \\ 0 & -1 \end{pmatrix}, \quad \vec{\gamma} = \begin{pmatrix} 0 & \vec{\sigma} \\ -\vec{\sigma} & 0 \end{pmatrix}, \quad \gamma_5 = i\gamma_1\gamma_2\gamma_3\gamma_4 = -\begin{pmatrix} 0 & 1 \\ 1 & 0 \end{pmatrix}. \quad 5.$$

Each of the currents 3 and 4 consists of two terms, one vector: $j_\alpha(V) = \bar{\psi} \gamma_\alpha \psi$ and the other axial-vector: $j_\alpha(A) = \bar{\psi} \gamma_\alpha \gamma_5 \psi$.

The weak interaction constant G equals $(1.40 \pm 0.01) \times 10^{-49}$ ergs \times cm.³, if determined by comparing the experimentally measured rate of muon decay with that calculated theoretically (see below). In the system of units $\hbar=c=1$, which we shall employ in the following

$$G = (1.00 \pm 0.01) \cdot 10^{-5} M^{-2} \quad 6.$$

where M is the mass of a proton.²

It can easily be seen that interaction 1 contains all the known weak interactions. Thus, the term $j^e j^{\mu\dagger}$ will give the muon decay; the term $j^e j^{n\dagger}$ will give neutron β -decay; the term $j^n j^{\mu\dagger}$ will cause muon capture by a proton and pion decay; the terms $j^e j^{\Lambda\dagger}$ and $j^\mu j^{\Lambda\dagger}$ will result in leptonic decays of strange particles; and the term $j^n j^{\Lambda\dagger}$ will cause nonleptonic decays of strange particles.³

In addition, interaction 1 should result in a number of processes which have not been observed so far. These processes, in particular, include neutrino-electron scattering (term $j^e j^{e\dagger}$) and proton-neutron scattering with

² To pass from the system of units in which $\hbar=c=1$ to the CGS system, the relations $\hbar/Mc^2 = 7 \cdot 10^{-28}$ sec. and $\hbar/Mc = 2.1 \cdot 10^{-14}$ cm. are convenient.

³ For the sake of brevity here and in a number of cases in the following text, we do not mention separately terms which are the Hermitian conjugate of those under consideration.

nonconservation of parity (term $j^n j^{n+}$). The first of these processes was considered by Feynman & Gell-Mann (21) and Šešter (25); the second, by Zel'dovich (26) who estimated the specific "anapol" electromagnetic interaction (26a) of atomic electrons with the nucleus caused by the interaction $j^n j^{n+}$.

2.2 Sakata model.—Now let us consider in greater detail the baryonic currents j^n and j^Λ . Such a choice of baryonic currents corresponds to the model of strongly interacting particles suggested by Sakata (27). In accordance with this model, only three particles among the strongly interacting particles are truly elementary: the proton, the neutron, and the Λ -hyperon, all the rest of the mesons and baryons being composite (see Table II). The

TABLE II
SAKATA MODEL

Mesons	S	T	Hyperons	S	T
$\pi^+ = p\bar{n}$	0	1	$\Sigma^+ = p\bar{n}\Lambda$	-1	1
$\pi^- = \bar{p}n$	0	1	$\Sigma^- = \bar{p}n\Lambda$	-1	1
$\pi^0 = \frac{1}{\sqrt{2}}(p\bar{p} - n\bar{n})$	0	1	$\Sigma^0 = \frac{1}{\sqrt{2}}(p\bar{p} - n\bar{n})\Lambda$	-1	1
$K^- = \bar{p}\Lambda$	-1	$\frac{1}{2}$	$\Xi^- = \bar{p}\Lambda\Lambda$	-2	$\frac{1}{2}$
$\bar{K}^0 = \bar{n}\Lambda$	-1	$\frac{1}{2}$	$\Xi^0 = \bar{n}\Lambda\Lambda$	-2	$\frac{1}{2}$
$K^+ = p\bar{\Lambda}$	+1	$\frac{1}{2}$			
$K^0 = n\bar{\Lambda}$	+1	$\frac{1}{2}$			

S =strangeness, T =isotopic spin; bar indicates antiparticles.

Sakata model is a generalization for strange particles of the idea of Fermi & Yang (28) concerning the composite π -meson. [Quite similar models were suggested by Levy & Marshak (29) and by Markov (29a).]

If we did not confine ourselves to the framework of the Sakata model, the current j , along with the term $\bar{n}p$, could also contain the terms $\pi^0\pi^+$, $\pi^-\pi^0$, $\bar{\Sigma}^0\Sigma^+$, and others for which $\Delta S=0$ where ΔS is the change in strangeness. Together with the term $\bar{\Lambda}p$ the current would contain the terms $\bar{\Sigma}^0p$, $\bar{\Sigma}^-n$, $K^-\pi^0$, and others for which $\Delta Q=\Delta S=-1$ where ΔQ is the change in charge. Besides, terms would be possible for which $\Delta Q=-\Delta S=-1$, for example, $\bar{n}\Sigma^+$, and terms with $\Delta S=-2$ such as $\bar{\Xi}^-n$.

In conformity with the Sakata model we shall assume that all strong interactions of elementary particles result from a strong four-fermion interaction between a proton, a neutron, and a Λ -hyperon (and their antiparticles). And all slow meson and baryon decays result from the weak interaction of p , n , and Λ with one another and with leptons.

It is well known that one of the main difficulties in considering meson and baryon decays lies in the fact that account has to be taken of strong

interactions which do not as yet lend themselves to consistent computation. Unfortunately, calculations involving four-fermion strong interaction (29b to 29e) are at present no more consistent than calculations within the scope of the conventional meson theory. In this respect the Sakata model does not make things easier. The merit of this model is that as a result of a minimum number of strongly interacting fields the weak interactions within the limits of the Sakata model possess a number of symmetry properties which are not destroyed by strong interactions. In a number of cases this makes possible quite definite forecasts as to the characteristics of various processes (30). The properties possessed by the weak interactions in the Sakata model include the rule $\Delta S = \pm 1$ for nonleptonic decays, the rule $\Delta T = \frac{1}{2}$ for leptonic decays with change of strangeness, similarity of the strangeness conserving vector interaction and the electromagnetic interaction, etc.

Of course, all the properties of the weak interaction that follow from the Sakata model can be postulated (and have actually been postulated) independently of one another and of the Sakata model. This will be seen in the following sections where these properties will be considered in detail. For the time being, only the main properties of weak interaction not connected with the Sakata model will be formulated.

2.3 General properties of weak interaction.—The weak interaction in form 1 possesses the following properties:

(a) It is universal because it has an identical form (V and A) and constant (G) for various pairs of particles. The idea of the universality of weak interactions was first suggested over 10 years ago (31 to 31d) and since then has found several confirmations.

(b) It is noninvariant with respect to inversion of space co-ordinates, as alongside its scalar terms $j(V)j(V)^+$ and $j(A)j(A)^+$ it contains the pseudo-scalar terms $j(V)j(A)^+$ and $j(A)j(V)^+$. The hypothesis of nonconservation of parity in weak interactions put forth by Lee & Yang (20) has been confirmed in recent years in almost all known slow processes.

(c) It is noninvariant with respect to charge conjugation. A number of authors (32 to 32b) have pointed out the possibility of such noninvariance in relation to nonconservation of parity. This has now been verified experimentally.

(d) It is invariant with respect to combined inversion, the latter being the product of space inversion and charge conjugation. The necessity of this invariance was first formulated by Landau (33). Available experimental data evidently bear it out.

(e) It is invariant with respect to the so-called chirality transformation which consists in the exchange $\psi \rightarrow \gamma_5 \psi$, $\bar{\psi} \rightarrow -\bar{\psi} \gamma_5$ for each particle (22, 23, 24, 30a, 50). The physical meaning of this invariance is not clear as yet because the complete Lagrangian, including the rest mass of the particles, is not invariant under chirality transformation and, therefore, the matrix elements of various processes involving strongly interacting particles are not invariant either.

(f) It conserves "leptonic charge" (34 to 34b). If we regard μ^- , e^- , and ν as leptons and μ^+ , e^+ and $\bar{\nu}$ as antileptons, the number of leptons minus the number of antileptons should be conserved in all slow processes. Experimental data confirm this conservation law.

(g) If $m_\nu = 0$, the theory we are describing coincides with the longitudinal neutrino theory (35 to 35b) in which the neutrino is polarized antiparallel, and the antineutrino parallel, to their momenta. However, at the present time, inasmuch as not only the neutrinos but all the particles participate in weak interactions only with two components [in the form $(1 + \gamma_5)\psi$], no special argument can be seen in favor of the mass of the neutrino being strictly equal to zero (36).

(h) A remarkable feature of the currents in 2 is that each of them includes one charged and one neutral particle. This property corresponds to the fact that in nature such processes as $\mu^- + p \rightarrow e^- + p$ (37), $K^+ \rightarrow \pi^+ + e^+ + e^-$, $K^0 \rightarrow e^+ + e^-$ and others involving only two leptons, both charged or both neutral, are evidently forbidden, as is the decay $\mu^+ \rightarrow 2e^+ + e^-$.

2.4 *Is the Fermi interaction a primary one?*—A number of the above considered properties of weak interaction suggest that interaction 1 is not a primary one but is caused by exchange of a charged vector meson between fermion pairs (see Fig. 1). According to this hypothesis (21, 38, 39, 40) the interaction constant of such a vector meson with the above enumerated fermion pairs is the same in all cases, and the effective weak interaction Lagrangian has the form:

$$L' = \frac{G}{\sqrt{2}} \frac{m^2}{m^2 - k^2} \left(\delta_{\alpha\beta} + \frac{k_\alpha k_\beta}{m^2} \right) j_\alpha j_\beta^* \quad 7.$$

where k is the four-dimensional momentum carried by the intermediate meson and m is its mass. It can easily be seen that if the mass of the intermediate meson is large enough, then in all slow processes observed so far, for which $k \ll m$, interaction L' is practically equivalent to L . [The slight difference between these interactions in the decay $\mu \rightarrow e + \nu + \bar{\nu}$ was studied by Lee & Yang (41). In decays of strongly interacting particles, the form factors

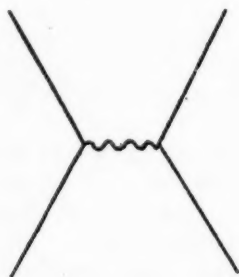


FIG. 1. Feynman diagram of intermediate meson exchange. Wavy line represents intermediate meson. Solid lines represent fermions.

caused by the vector meson are difficult to separate in practice from the form factors caused by the strong interaction.] An objection has been put forth by Feynman & Gell-Mann (42) and also by Feinberg (39) against such a weak interaction model. They showed that an intermediate vector meson would make possible the decay $\mu \rightarrow e + \gamma$ which is forbidden for local four-fermion interaction (in the first order of the perturbation theory with respect to the weak interaction). The decay ratio $\mu \rightarrow e + \gamma / \mu \rightarrow e + \nu + \bar{\nu}$ would be, according to their estimates, $\geq 10^{-4}$, while experimentally this ratio is smaller than 2×10^{-5} (43). It should be pointed out, however, that the theoretical conclusion is based on a calculation with a divergent integral and, therefore, cannot be considered absolutely perfect.

Now let us see how the universal weak interaction manifests itself in different physical processes. We shall begin with the simplest case.

3. INTERACTION BETWEEN LEPTONS

3.1 *Muon decay.*—The only process observed so far involving only leptons is the muon decay:

$$\mu^{\pm} \rightarrow e^{\pm} + \nu + \bar{\nu}. \quad 8.$$

According to formulas 1 to 4 the Lagrangian of the interaction responsible for this process has the form:

$$L = \frac{G}{\sqrt{2}} j_{\alpha}^{\mu} j_{\alpha}^{e*} + \text{h.c.} \quad 9.$$

Disregarding virtual photons,⁴ the amplitude of muon decay will be determined only by Lagrangian 9 and will be equal to

$$\frac{G}{\sqrt{2}} (\bar{u}_e \gamma_{\alpha} (1 + \gamma_5) u_{\mu}) (\bar{\nu}_\nu \gamma_{\alpha} (1 + \gamma_5) u_{\mu}) \quad 10.$$

where u_e , u_{ν} , and u_{μ} are the spinors of the respective particles. The amplitude 10 makes it possible to calculate all the characteristics of muon decay. The total probability of decay equals

$$w = \frac{1}{\tau} = \frac{G^2 \mu^5}{192 \pi^3}. \quad 11.$$

Here μ is the mass of the muon, the mass of the electron being neglected. The spectrum of decay electrons has the form

$$w(\epsilon) d\epsilon = \frac{2}{\tau} (3 - 2\epsilon) \epsilon^2 d\epsilon. \quad 12.$$

Here ϵ is the ratio of the energy of the electron to its maximum energy equal to $\mu/2$ ($0 \leq \epsilon \leq 1$). In case of a general four-fermion interaction, the electron spectrum is characterized by the Michel parameter ρ (45):

$$w(\epsilon) d\epsilon = \frac{12}{\tau} \left[(1 - \epsilon) - \frac{2}{9} \rho (3 - 4\epsilon) \right] \epsilon^2 d\epsilon. \quad 13.$$

⁴ Radiative corrections to muon decay are considered in a paper by Berman (44).

It can easily be seen that spectrum 12 responds to $\rho = 0.75$.

The angular distribution of electrons in the decay of a completely polarized muon:

$$w(e, \vartheta) d\epsilon d(\cos \vartheta) = \frac{1}{\tau} [(3 - 2\epsilon) - \lambda \cos \vartheta (1 - 2\epsilon)] \epsilon^2 d\epsilon d(\cos \vartheta) \quad 14.$$

where ϑ is the angle between the muon spin and the electron momentum and λ equals $+1$ for μ^+ decay and -1 for μ^- decay. The angular distribution of electrons averaged over their energies has the form:

$$w(\vartheta) d(\cos \vartheta) = \frac{1}{2\tau} \left[1 + \frac{\lambda}{3} \cos \vartheta \right] d(\cos \vartheta). \quad 15.$$

In the μ^+ decay the positrons should be polarized parallel to their momentum ($\bar{S} = +1$, where \bar{S} is the degree of longitudinal polarization) while the electrons in the μ^- decay should be polarized antiparallel ($\bar{S} = -1$). Experimental data on μ^+ decay are compared with theory in Table III.

TABLE III
POSITIVE MUON DECAY

Parameter	τ sec. $\times 10^6$	ρ	λ	S
Theory	?	0.75	1	+1
Experiment	2.22 ± 0.02	$0.68 \pm 0.02^*$	$0.98 \pm 0.06^\dagger$	+1*

* See report by Goldhaber at the 1958 Geneva Conference. On the question of the parameter ρ see article by Rosenson (126) which contains a detailed bibliography.

† Ali-Zade *et al.* (127). This paper also contains a detailed bibliography on the measurement of the parameter λ . The sign of λ has not been established by experiment, because the direction of polarization of decaying muons has not been measured as yet. See note added in page proof on page 77.

The deduction of all the formulas in this section, as well as of the formulas for the more general interaction responsible for muon decay, can be found in the papers listed in (46, 46a).

4. LEPTONIC DECAYS OF MESONS AND BARYONS WITHOUT CHANGE OF STRANGENESS

4.1 *Lagrangian and matrix elements.*—According to formulas 1 to 4 the Lagrangian interaction of strongly interacting particles with leptons in which the strangeness of the former does not change has the form:

$$L = \frac{G}{\sqrt{2}} j_a^* j_a^{l+} + \text{h.c.} \quad 16.$$

where the index l indicates one of the two leptonic currents (j^e or j^μ). Interaction 16 gives rise to a number of processes: neutron β -decay, muon capture

by a proton, charged pion decay, leptonic decays of hyperons (or K mesons) during which hyperons (or K mesons) of the same strangeness as those decaying arise, for example: $\Sigma^\pm \rightarrow \Lambda^0 + e^\pm \pm \nu$. Here and in the following, $+\nu$ denotes emission of a neutrino and $-\nu$, emission of an antineutrino.

In all these processes, the virtual strong interactions play a fundamental role and must be taken into account. On the other hand, there is at present no consistent theory of strong interactions. Hence, we are obliged to describe various processes by the phenomenological matrix elements containing the parameters which the future theory of strong interactions will make it possible to compute and which we are now forced to determine by comparing our formulas with experiment. In spite of the obvious insufficiency of this approach, it enables satisfactory systematization of extensive experimental material, as well as a number of interesting predictions.

To minimize the number of unknown parameters included in the matrix elements, extensive use will be made here and in the following sections of the symmetry properties of Lagrangians of strong and weak interactions, because they determine precisely the symmetry properties of the matrix elements. (We remind the reader that we are disregarding virtual electromagnetic interactions.) In particular, we shall base our reasoning extensively on the fact that strong interactions are invariant under charge conjugation, and conserve parity and isotopic spin.

In the above-considered case of muon decay, as well as in all other processes considered in this review, we may confine ourselves to the first order of the perturbation theory with respect to weak interaction.⁵ Therefore, the amplitudes of the various leptonic decays should have the form

$$\frac{G}{\sqrt{2}} (V_\alpha + A_\alpha) \bar{u}_\nu \gamma_\alpha (1 + \gamma_5) u_l \quad 17.$$

where u_l is the electron (muon) spinor, u_ν is the neutrino spinor. The matrix elements V_α and A_α equal

$$V_\alpha = \langle f | j_\alpha(V) | i \rangle, \quad A_\alpha = \langle f | j_\alpha(A) | i \rangle \quad 18.$$

where $|i\rangle$ and $\langle f|$ are the physical states of strongly interacting particles at the beginning and end of the process (currents $j(V)$ and $j(A)$ are determined above in paragraph 2.1). Because of the presence of strong interaction, we cannot calculate V_α and A_α ; we know only that they are four-dimensional vectors (or pseudovectors) constructed, generally speaking, in the most general way from the wave functions and momenta of strongly interacting particles.

In the following we shall be dealing mainly with three types of processes:

(a) Decay of a pseudoscalar meson into leptons (see Fig. 2). In this

⁵ The corollaries which follow from this fact with respect to dispersion relations in the case of weak interactions have been examined by Bogolyubov, Bilenkii & Logunov (47).



FIG. 2. Leptonic decay of a meson. Wavy line represents meson. Loop represents virtual strong interactions. Fermi interaction is acting at O.

case there is one pseudoscalar φ , wave function of the decaying meson, and one four-dimensional vector k , the momentum of the meson, hence

$$V_\alpha = 0, \quad A_\alpha = f\varphi k_\alpha \quad 19.$$

where f is a constant.

For the decay of a scalar meson, V_α and A_α would change places.

(b) Decay of a meson into a pair of leptons and another meson (see Fig. 3). In this case there are two meson wave functions φ_1 and φ_2 , and two four-dimensional vectors k_1 and k_2 , the momenta of the mesons (the total momentum of the leptons $k = k_1 - k_2$); therefore, if the parity of the mesons is the same,

$$V_\alpha = [f_1(k^2)k_1^\alpha + f_2(k^2)k_2^\alpha]\varphi_2^+\varphi_1, \quad A_\alpha = 0 \quad 20.$$

where f_1 and f_2 are functions of the invariant k^2 . (The two other invariants which can be built from k_1 and k_2 equal the squared masses of the mesons.) If the meson parities were different, V_α and A_α would change places in 20.

(c) Decay of a baryon into a pair of leptons and another baryon (see Fig. 4). The baryon wave functions u_1 and u_2 are spinors. Therefore, the matrix elements have a more complex form (48). If the parity of the two baryons is the same, then:

$$V_\alpha = u_2[\gamma_\alpha f_1 + (\gamma_\alpha \hat{k} - \hat{k} \gamma_\alpha) f_2 + k_\alpha f_3] u_1 \quad 21.$$

$$A_\alpha = u_2[\gamma_\alpha g_1 + (\gamma_\alpha \hat{k} - \hat{k} \gamma_\alpha) g_2 + k_\alpha g_3] \gamma_5 u_1. \quad 22.$$

Here f and g are scalar functions depending only on k^2 where k is the four-dimensional momentum transferred to the leptons. The matrixes γ have been defined above (see expression 5), $\hat{k} = k_\alpha \gamma_\alpha$. If the parities of the baryons are different, V_α and A_α change places.

Expressions 17 to 22 refer not only to leptonic decays involving conservation of strangeness of the strongly interacting particles but also to decays in which their strangeness changes (see Sect. 5).

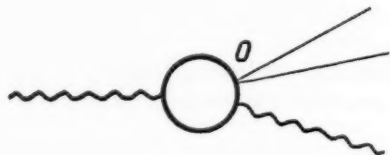


FIG. 3. Decay of a meson into another meson plus leptons. Wavy lines represent mesons. Loop represents virtual strong interactions. Fermi interaction is acting at O.

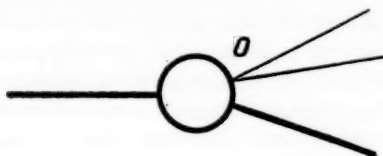


FIG. 4. Decay of a baryon into another baryon plus leptons. Solid lines represent baryons. Loop represents virtual strong interactions. Fermi interaction is acting at O.

In view of the invariance of the weak interaction Lagrangian with respect to transformation of combined inversion, all the functions f and g in 19 to 22 are real.

4.2 Conservation of vector current.—The above theory of weak interactions possesses a remarkable property; it involves a profound analogy between weak interaction 16 and electromagnetic interaction.

In the Sakata model, the interaction of all the mesons and baryons with an electromagnetic field reduces to interaction of a proton with the electromagnetic field, as the other two elementary particles are neutral. The Lagrangian of this interaction has the form:

$$e\bar{\psi}_p\gamma_\alpha\psi_p\cdot A_\alpha$$

where e is the electric charge, A_α is the four-dimensional vector-potential. This interaction may be written as:

$$e\bar{\psi}_p\gamma_\alpha\frac{1+\tau_3}{2}\psi_p\cdot A_\alpha \quad 23.$$

where

$$\tau_3 = \begin{pmatrix} 1 & 0 \\ 0 & -1 \end{pmatrix} \quad \text{and} \quad \psi = \begin{pmatrix} \psi_p \\ \psi_n \end{pmatrix}$$

is a spinor in isotopic space. The nucleon current in 23 consists of two terms: an isotopic scalar, 1, and an isotopic vector, τ_3 .

Now let us consider the interaction of the vector strangeness-conserving current $j^\alpha(V)$ with leptons:

$$\frac{G}{\sqrt{2}}\bar{\psi}_\alpha\gamma_\alpha\psi_p\cdot j^\alpha{}^{1+}.$$

This interaction can be written as

$$\frac{G}{2}\bar{\psi}_\alpha\gamma_\alpha\tau^-\psi\cdot j^\alpha{}^{1+} \quad 24.$$

where

$$\tau^- = \sqrt{2}\begin{pmatrix} 0 & 0 \\ 1 & 0 \end{pmatrix} = \frac{1}{\sqrt{2}}(\tau_x - i\tau_y).$$

Comparing 23 and 24 we see that the isotopic vector part of the electric current of strongly interacting particles $\bar{\psi}\tau_3\gamma_\alpha\psi$ and the weak interaction

vector current $\bar{\psi}\tau\gamma_\alpha\psi$ are different projections of the same isotopic vector. As the strong interaction is isotopically invariant, this property of the Lagrangians of weak and electromagnetic interactions results in the fact that the corresponding matrix elements are also different projections of the same isotopic vector. It follows, therefore, that the matrix elements V_α in paragraph 4.1 must possess the properties of isotopic-vector electromagnetic matrix elements.

Consider decays in which strongly interacting particles at the beginning and at the end of the process belong to the same isotopic multiplet, for example: $n \rightarrow p + e^- + \nu$, $\pi^+ \rightarrow \pi^0 + e^+ + \nu$, $\Sigma^- \rightarrow \Sigma^0 + e^- + \nu$. The vector interaction constant must be the same in all these processes, just as the electric charges of different strongly interacting particles are equal to one another in absolute value. Continuing this analogy, we are obliged to conclude that just as, for instance, the electric charges of the proton and the electron are equal to one another in spite of the fact that the proton possesses strong interactions while the electron does not, the constant of weak vector interaction should not change its value, i.e., should not become renormalized under the influence of strong interactions and should be the same, for instance, in muon and neutron decay. These conclusions refer to the case where the momentum transferred to the leptons is equal to zero ($k=0$). Passing over to momenta $k \neq 0$, we conclude that the form-factors of the weak strangeness-conserving vector interaction resulting from strong interaction are the same as the isotopic-vector form-factors of the electromagnetic interaction.

All these properties of the matrix elements V_α are related to the fact that, as can easily be shown (50),⁴ the Sakata model involves conservation of the vector current $j^\alpha(V)$:

$$\frac{\partial}{\partial x_\alpha} j^\alpha(V) = 0 \quad 25.$$

whence it follows that the matrix elements V_α satisfy the condition

$$k_\alpha V_\alpha = 0 \quad 26.$$

where k is the four-dimensional momentum transferred to the leptons.

In connection with the theory of universal $V-A$ interaction, Feynman & Gell-Mann (21) came to the idea of a conserved vector current and the nonrenormalization connected with it. These authors had postulated the direct vector interaction of pions, K mesons, and other particles with leptons to make the vector current of weak interaction conserved, like electromagnetic current. Ioffe (51) proved that in the ordinary (mesonic) strong interaction model this would lead to nonrenormalization of the weak vector interaction constant. It may be pointed out that the first to suggest that

⁴ The same result was obtained by Feynman for the Fermi-Yang model (without allowance for strange particles) (50a).

there might exist an analogy between weak vector interaction and electrodynamics were Gerštein & Zel'dovich (52) back in the far-off times when it was considered established that only the scalar and the tensor types of interaction were responsible for β -decay. Certain corollaries which follow from the analogy between the γ -transitions and the β -transitions in nuclei were examined by Gell-Mann (53).

In summarizing, it may be said that the analogy between the electromagnetic and the weak vector interactions in the ordinary formulation is brought into the theory from without, while in the Sakata model it follows from the very foundations of theory. Therefore, if experiment were found to refute this analogy, that would mean that the Sakata model is incorrect [see Oppenheimer's remark (54)].

A number of attempts were made to obtain a condition analogous to 25 also for the axial part of the current $j^a(A)$ [see, e.g., Polkinghorn (55)]. It should, however, be pointed out that even if the equation

$$k_a A_a = 0 \quad 27.$$

were fulfilled, no conclusion as to the nonrenormalization of the axial-vector interaction constant would follow from it (56). Besides, Equation 27 contradicts experiment, as it forbids the decays $\pi \rightarrow \mu + \nu$ and $\pi \rightarrow e + \nu$ and gives a larger effective pseudoscalar interaction in the β -decay [Taylor (57) and Goldberger & Treiman (58)].

4.3 G invariance.—Now let us consider an operation representing charge conjugation and a 180° rotation around the second axis in the isotopic spin-space. This transformation, named the G transformation by Lee & Yang (59), transfers $p \rightarrow \bar{n}$, $n \rightarrow -\bar{p}$ and changes the sign of the pion wave function ($\varphi_\pi \rightarrow -\varphi_\pi$) [see for instance Wick's review (15)]. The G transformation was studied in application to weak interactions by Michel (60), Kawaguchi & Nishijima (61), and Weinberg (62). It can easily be shown that under this transformation the current $j^a(V)$ does not change sign, while the current $j^a(A)$ does change sign. As a result of G transformation and Hermitian conjugation, the matrix elements of a number of processes such as the neutron β -decay and muon capture in hydrogen should pass into themselves (with or without a change of sign). It follows from the above that the matrix elements V_a in these cases should not change their sign thereon, while the matrix elements A_a should change sign.

4.4 Neutron decay.—In accordance with the above, the matrix elements of neutron β -decay would have the following form in the most general case (21, 22):

$$V_a = a_p [\gamma_a f_1 + (\gamma_a \hat{k} - \hat{k} \gamma_a) f_2 + k_a f_3] u_n \quad 28.$$

$$A_a = a_p [\gamma_a g_1 + (\gamma_a \hat{k} - \hat{k} \gamma_a) g_2 + k_a g_3] \gamma_5 u_n. \quad 29.$$

However, because of G invariance (Sect. 4.3) $f_3 = 0$ and $g_3 = 0$. As was indicated above (Sect. 4.2), functions f_1 and f_2 equal the isotopic-vector part of the

electric and magnetic nucleon form-factors respectively. In particular, at $k^2=0$, $f_1(0)=1$ and

$$f_2(0) = \frac{\mu_p - \mu_n}{4e} = \frac{3.7}{4M_p}$$

where μ_p and μ_n are the anomalous magnetic moments of the proton and the neutron respectively, e is the electric charge, and M_p is the proton mass. General considerations do not as yet give grounds to say anything with regard to the terms g_1 and g_3 .

In neutron decay, the momentum transmitted to e^- and $\bar{\nu}$ is small ($k \sim 1$ Mev/ c) and, therefore, in 28 and 29 the terms proportional to f_2 and g_3 may be neglected. (It should be noted that the term proportional to g_3 may be neglected at higher energies as well, provided we are dealing with the lepton pair $e\nu$ [for example in the process $e^- + p \rightarrow n + \nu$ at high energies (63)], as the contribution of this term is proportional to the small mass of the electron.) The amplitude of the neutron β -decay acquires the form:

$$\frac{G}{\sqrt{2}} [\bar{u}_p \gamma_\alpha (1 + \alpha \gamma_5) u_n] [\bar{u}_e \gamma_\alpha (1 + \gamma_5) u_\nu] \quad 30.$$

where $\alpha \equiv g_1(0)$ is the only quantity in expression 30 which cannot be predicted theoretically and must be obtained from experimental data. (We already know the value of G from the μ -decay.)

The neutron decay rate calculated from 30 equals

$$w = \frac{1}{\tau} = G^2 (1 + 3\alpha^2) \frac{\Delta^5}{60\pi^3} 0.47. \quad 31.$$

Here $\Delta = 1.293$ Mev. The factor 0.47 makes allowance for the decrease in the decay phase volume attributable to the mass of the electron; for $m_e = 0$ this factor would be equal to 1.

The energy spectrum of the electrons is described by the Fermi spectrum:

$$(\epsilon^2 - m_e^2)^{1/2} (\Delta - \epsilon)^2 d\epsilon \quad 32.$$

where ϵ is the energy of an electron. The dependence of the probability of decay on the angle ϑ between the electron and the antineutrino is described by the formula

$$1 + v\lambda \cos \vartheta \quad 33.$$

where v is the velocity of the electron and

$$\lambda = \frac{1 - \alpha^2}{1 + 3\alpha^2}. \quad 34.$$

The electrons appearing in the decay of a nonpolarized neutron should be polarized antiparallel to their momentum, the degree of this polarization being equal to v , the velocity of the electron (in terms of c). If the decaying neutron is completely polarized, the electron angular distribution should have the form:

$$1 + \nu \rho_e \cos \varphi_e \quad 35.$$

$$1 + \rho_\nu \cos \varphi_\nu \quad 36.$$

where

$$\rho_e = -\frac{2(\alpha^2 - \alpha)}{1 + 3\alpha^2} \quad 37.$$

$$\rho_\nu = \frac{2(\alpha^2 + \alpha)}{1 + 3\alpha^2} \quad 38.$$

$\varphi_e(\varphi_\nu)$ is the angle between the neutron spin and the electron (neutrino) momentum. Experimental and theoretical information on neutron decay are compared in Table IV.

Because of the conservation of combined parity there should be no correlation of the type $\eta[\vec{p}_e \times \vec{p}_\nu]$ where η is the neutron polarization vector, and \vec{p}_e and \vec{p}_ν are the momenta of the electron and the neutrino. Experiment confirms this conclusion (64, 64a).

It can be seen from Table IV that neutron decay experiments agree with the theory of universal $V-A$ -interaction. However, the actual confirmation of this theory is based essentially on the results of investigation of nuclear β -decay [Konopinski (16); Smorodinsky (17)].

If we regard the above theory of weak interaction as correct, we essentially extract only the value of α from neutron decay experiments. We are not yet able to explain why α is so close to unity and why $\alpha > 1$.

4.5 *Muon capture in hydrogen.*—In the process $\mu^- + p \rightarrow n + \nu$, the momentum transferred from the leptons to the nucleons $k \approx m_\mu \approx 100$ Mev/c. Therefore, in expressions 28 and 29, the terms proportional to f_2 and g_2

TABLE IV
 β -DECAY OF NEUTRON

Parameter	$\tau_{\text{exp.}}$	α	λ	ρ_e	ρ_ν
Theory	?	?	-0.08	-0.08	1.00
Experiment	$1011 \pm 26^*$	1.25 ± 0.04	$+0.07 \pm 0.12^\dagger$ $-0.06 \pm 0.13^\ddagger$	$-0.11 \pm 0.02^\S$	$+0.88 \pm 0.15^\S$

* Sosnovsky *et al.* (122).

† Robson (128).

‡ Trebukhovskiy *et al.* (129).

§ Burgy *et al.* (130).

The value α in the table is calculated by formula 31 for the value of τ given in the table. The theoretical values of λ , ρ_e , and ρ_ν were obtained from this value of α by formulas 34, 37, and 38.

which were discarded in considering neutron β -decay now become substantial. (Terms f_3 and g_3 are, of course, equal to 0 as before.) Estimates by the perturbation theory (65, 65a) give $g_3 \sim 12/m_\pi$ where m_π is the pion mass. An examination with the aid of a dispersion technique (48, 49) confirms the reliability of these estimates.

Making use of the Dirac equation for leptons, it can easily be found that the term proportional to g_3 is equivalent to the effective pseudoscalar interaction between leptons and nucleons. Similarly, the term proportional to f_3 , forbidden in the theory under consideration, would be equivalent to the scalar interaction. Calculations of the probability of muon capture by a proton as well as of the angular and spin correlations in this process have been carried out in a number of studies (66 to 70a); in (67) the above-indicated pseudoscalar term g_3 was taken into account, while in (69) the term proportional to f_3 was considered.

4.6 $\pi \rightarrow \mu + \nu$ and $\pi \rightarrow e + \nu$ decays.—The amplitudes of these decays have the form:

$$\frac{G}{\sqrt{2}} f_\pi \varphi k_\alpha (\bar{u}_l \gamma_\alpha (1 + \gamma_5) u_l) \quad 39.$$

where f_π is a constant having the dimensions of mass, k is the four-dimensional momentum of the pion, and φ is its wave function; the index l indicates e or μ . From 39, the corresponding decay rates can easily be obtained

$$w_l = \frac{G^2}{8\pi} f_\pi^2 m_\pi m_l^2 \left(1 - \frac{m_l^2}{m_\pi^2}\right)^2. \quad 40.$$

Comparing 40 with the experimental rate of $\pi \rightarrow \mu$ -decay, we get

$$f_\pi^2 \approx 2 \cdot 10^{-2} M_p^2, \quad f_\pi \approx 0.14 M_p \approx m_\pi. \quad 41.$$

Formula 40 gives the relationship between the rates of the decays $\pi \rightarrow e + \nu$ and $\pi \rightarrow \mu + \nu$ not depending on f_π (71, 71a):

$$\frac{w_e}{w_\mu} = \left(\frac{m_e}{m_\mu}\right)^2 \left(\frac{m_\pi^2 - m_e^2}{m_\pi^2 - m_\mu^2}\right)^2 = 1.36 \cdot 10^{-4}. \quad 42.$$

Until recently, the decay $\pi \rightarrow e + \nu$ could not be detected [e.g. (72)] and its absence was considered one of the most serious objections to the theory of universal Fermi interaction. In late summer of 1958, this decay was finally detected (73, 73a). Its observed decay rate does not contradict 42.

As the pion spin equals 0 and the neutrino (antineutrino) is polarized longitudinally, the muons in the decay $\pi^\pm \rightarrow \mu^\pm \pm \nu$ must be completely polarized longitudinally (μ^- along the direction of the movement, and μ^+ counter to it). The same, of course, refers to e^- and e^+ in $\pi^\pm \rightarrow e^\pm \pm \nu$ decays. Such a polarization of μ^\pm and e^\pm in pion decay may be called "forced" (it will be remembered that in the neutron β -decay which has no such rigorous limitations because of conservation of angular momentum, e^- are polarized antiparallel to their momentum). Neither the sign nor the value of muon

polarization in the π -decay has been measured directly. So far, we can judge of them only indirectly: by the sign and value of asymmetry of the electrons and their polarization in the decay chain $\pi \rightarrow \mu \rightarrow e$. If we assume that muon decay is correctly described by the above theory, it can be established by comparing experimental data with formulas 14 and 15 that the muons in the $\pi \rightarrow \mu$ decay are also polarized in compliance with theory.

4.7 $\pi^+ \rightarrow \pi^0 + e^+ + \nu$ decay.—Owing to the analogy between the vector weak interaction and interaction with the electromagnetic field, the amplitude of the decay $\pi^+ \rightarrow \pi^0 + e^+ + \nu$ equals (21):

$$G\varphi\varphi(k_\alpha^+ + k_\alpha^0)(\bar{u}_e\gamma_\alpha(1 + \gamma_5)u_\mu). \quad 43.$$

Here k^+ and k^0 are the four-dimensional momenta of π^+ - and π^0 -mesons. Such a form of the matrix element can easily be obtained from formula 20 by taking advantage of the condition $k_\alpha V_\alpha = 0$. The decay rate calculated from 43 equals

$$w = \frac{G^2 \Delta^5}{30\pi^3} \approx 0.43 \text{ sec.}^{-1} \quad 44.$$

where

$$\Delta = m_{\pi^+} - m_{\pi^0} = 4.6 \text{ Mev.}$$

Comparing this result with the known lifetime of the π^+ -meson we find:

$$\frac{w(\pi^+ \rightarrow \pi^0 + e^+ + \nu)}{w(\pi^+ \rightarrow \mu^+ + \nu)} \approx 10^{-8}. \quad 45.$$

A theoretical calculation of the process $\pi^+ \rightarrow \pi^0 + e^+ + \nu$ was made by Zel'dovich (74) and Feenberg & Primakoff (75). These authors also consider a possible method of experimental detection of this process.⁷

4.8 $\pi^+ \rightarrow e^+ + \nu + \gamma$ decay.—Along with strong and weak interactions, this decay also involves an electromagnetic interaction. As can easily be seen, both the V and the A parts of the weak interaction contribute to this process. The computation for the A interaction was made by Treiman & Wyld (76) and elaborated by Vaks & Ioffe (77), who also calculated the contribution of the V interaction. [References to other theoretical studies concerning this decay are given in (78).] According to (77), the value $R = w(\pi^+ \rightarrow e^+ + \nu + \gamma)/w(\pi^+ \rightarrow \mu^+ + \nu)$ is equal to:

$$R \approx 3 \times 10^{-8} \text{ for the } V \text{ interaction}$$

$$R \approx 3 \times 10^{-6} \text{ for the } A \text{ interaction.}$$

The latter value refers to radiative decays in which the positron energy $\epsilon \leq 0.9\epsilon_{\max}$ (ϵ_{\max} is the maximum positron energy in the decay). It should be taken into account that the main part of the radiation for the A interaction is concentrated in a narrow angle along the direction of motion of the elec-

⁷ Note added in proof: The polarization sign of negative muons appearing in the π^\pm decays was measured recently (135). In agreement with the theory expounded, the muons proved to be polarized along the momentum.

tron, low-energy photons predominating in this radiation. Therefore, if we observe high-energy photons traveling at 180° to the electron, the contribution of the V interaction can be isolated, this contribution being expressed simply, as is shown in (77) through the known lifetime of the π^0 -meson.

The relation between the decays $\pi^+ \rightarrow e^+ + \nu + \gamma$ (a) and $\pi^0 \rightarrow 2\gamma$ (b) can be established simply if the analogy between the vector Fermi interaction and the electromagnetic interaction is taken into account. Taking advantage of the G transformation, it can easily be shown that the emission of the photon in process (a) and of one of the photons in process (b) is caused by the isotopically scalar part of Lagrangian 23 and that the isotopic vector part of this Lagrangian is responsible for the emission of the second photon in process (b). Thus the isotopic structure of the matrix elements of processes (a) and (b) is also identical (see Fig. 5).

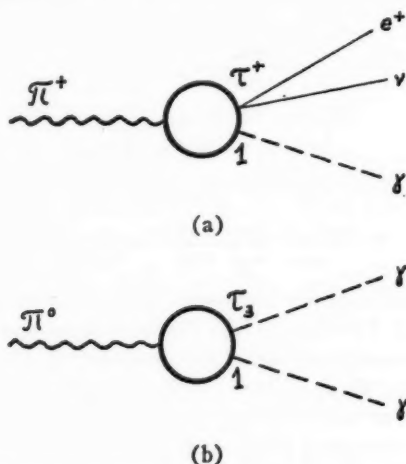


FIG. 5. Diagrams of decays: (a) $\pi^+ \rightarrow e^+ + \nu + \gamma$ and (b) $\pi^0 \rightarrow 2\gamma$

Experiments (78) gave $R < 8.3 \cdot 10^{-6}$. The accuracy of these experiments was insufficient for the effect to be observed.

4.9 *Strange-particle decays.*—The various types of symmetry established above, particularly conservation of the vector current and G invariance, put very rigorous limitations on the decays of strange particles with conservation of strangeness. This refers primarily to decays of the type

$$K^0 \rightarrow K^+ + e^- + \bar{\nu} \quad 46.$$

for which the amplitude equals:

$$\frac{G}{\sqrt{2}} \varphi \varphi (k_a^+ + k_a^0) (\bar{u}_e \gamma_5 (1 + \gamma_5) u_\pi) \quad 47.$$

and the probability of decay $w = G^2 \Delta^5 / 60 \pi^3$. For $\Delta \approx 3.7$ Mev we get $w \approx 0.1$

sec.⁻¹ Observation of these decays is obviously still more complicated than observation of the corresponding pion decays.

The situation with respect to the decay $\Sigma^- \rightarrow \Sigma^0 + e^- + \bar{\nu}$, the "most readily observed" of such β -transitions within the Σ -hyperon triplet, is analogous: it must constitute $\sim 10^{-9}$ of all the Σ^- -hyperon decays.

Probably the only leptonic decays of strange particles with conservation of strangeness which have chances of being detected by present-day experimental techniques are the decays

$$\Sigma^\pm \rightarrow \Lambda^0 + e^\pm \pm \nu. \quad 48.$$

The form of the matrix elements of these decays depends on the relative parity of the Σ -hyperon and the Λ -hyperon. If the parities are the same, then (see formulas 21 and 22):

$$\begin{aligned} V_\alpha &= \bar{u}_\Lambda [\gamma_\alpha f_1 + (\gamma_\alpha \hat{k} - \hat{k} \gamma_\alpha) f_2 + k_\alpha f_3] u_\Sigma \\ A_\alpha &= \bar{u}_\Lambda [\gamma_\alpha g_1 + (\gamma_\alpha \hat{k} - \hat{k} \gamma_\alpha) g_2 + k_\alpha g_3] \gamma_5 u_\Sigma. \end{aligned} \quad 49.$$

If the parities are different, then V_α and A_α change places. From the condition $k_\alpha V_\alpha = 0$ it follows that

$$f_1 = - \frac{f_3 k^2}{M_\Sigma - M_\Lambda} \quad 50.$$

if the parities of Λ and Σ are the same, and

$$g_1 = \frac{g_3 k^2}{M_\Sigma + M_\Lambda} \quad 51.$$

if the parities of Λ and Σ are different. As Šechter (79) pointed out, this results in the fact that with $k \rightarrow 0$ the matrix element $V_\alpha \rightarrow 0$ and is, therefore, small compared to the matrix element A_α which tends towards a finite limit at $k \rightarrow 0$. It should be noted that the matrix element of the radiative decay $\Sigma^0 \rightarrow \Lambda^0 + \gamma$ and of the conversion decay $\Sigma^0 \rightarrow \Lambda^0 + e^+ + e^-$ related to it also equals V_α of formula 49. [See the computation of these processes in the papers of Feinberg (80) and Feldman & Fulton (80a).] Thus, the matrix elements V_α can be determined independently in studying both leptonic and electromagnetic decays.

If in 49 we neglect the terms which tend towards 0 at $k \rightarrow 0$ and presume that $g_1 = 1$, we can estimate the rate of decay 48; in the case of identical parities of Δ - and Σ -hyperons it is expressed by the formula of neutron β -decay

$$w = \frac{3G^2 \Delta^4}{60\pi^3} \quad 52.$$

whence we get:

$$w_{\Sigma^+} = 0.7 \times 10^6 \text{ sec.}^{-1}, \quad w_{\Sigma^-} = 1.1 \times 10^6 \text{ sec.}^{-1}.$$

Taking advantage of the known lifetimes of the Σ -hyperons we get:

$$w_{\Sigma^+ \tau \Sigma^+} = 0.5 \times 10^{-4}, \quad w_{\Sigma^- \tau \Sigma^-} = 1.8 \times 10^{-4}. \quad 53.$$

Though the true values may differ severalfold from these estimates, it can nevertheless be concluded that to observe the decays $\Sigma^\pm \rightarrow \Lambda^0 + e^\pm + \nu$, approximately 10^4 to 10^5 pionic decays of Σ -hyperons must be available. (Up to now, several hundred pionic Σ -hyperon decays have been observed.)

5. LEPTONIC DECAYS OF K MESONS AND HYPERONS WITH CHANGE OF STRANGENESS

5.1 *Allowed and forbidden processes.*—With the exception of several "exotic" decays considered above (paragraph 4.9), the leptonic decays of strange particles are caused by the interactions (see formulas 1 to 4):

$$\frac{G}{\sqrt{2}} j^{\Lambda} j^{e*} + \text{h.c.}, \quad \frac{G}{\sqrt{2}} j^{\Lambda} j^{\mu*} + \text{h.c.} \quad 54.$$

These interactions should result in the following leptonic hyperon decays:

$$\begin{array}{ll} \Lambda \rightarrow p + e^- + \bar{\nu} & (\Lambda_e) \quad \Lambda \rightarrow p + \mu^- + \bar{\nu} \quad (\Lambda_\mu) \\ \Sigma^- \rightarrow n + e^- + \bar{\nu} & (\Sigma_e^-) \quad \Sigma^- \rightarrow n + \mu^- + \bar{\nu} \quad (\Sigma_\mu^-) \\ \Xi^- \rightarrow \Sigma^0 + e^- + \bar{\nu} & \left. \begin{array}{l} \Xi^- \rightarrow \Sigma^0 + \mu^- + \bar{\nu} \\ \Xi^- \rightarrow \Lambda^0 + e^- + \bar{\nu} \\ \Xi^0 \rightarrow \Sigma^+ + e^- + \bar{\nu} \end{array} \right\} (\Xi_e) \quad \left. \begin{array}{l} \Xi^- \rightarrow \Sigma^0 + \mu^- + \bar{\nu} \\ \Xi^- \rightarrow \Lambda^0 + \mu^- + \bar{\nu} \\ \Xi^0 \rightarrow \Sigma^+ + \mu^- + \bar{\nu} \end{array} \right\} (\Xi_\mu). \end{array}$$

Experimentally, two cases of Λ_e -decay and one possible case of Σ_e or Σ_μ decay have been observed. The other leptonic hyperon decays have not been observed so far. Besides, interaction 54 should result in the following K^+ and K^0 meson decays:

$$\begin{array}{ll} K^+ \rightarrow e^+ + \nu & (K_{e2}) \quad K^+ \rightarrow \mu^+ + \nu \quad (K_{\mu2}) \\ K^+ \rightarrow e^+ + \nu + \pi^0 & (K_{e3}^+) \quad K^+ \rightarrow \mu^+ + \nu + \pi^0 \quad (K_{\mu3}^+) \\ K^0 \rightarrow e^+ + \nu + \pi^- & (K_{e3}^0) \quad K^0 \rightarrow \mu^+ + \nu + \pi^- \quad (K_{\mu3}^0) \\ \left. \begin{array}{l} K^+ \rightarrow e^+ + \nu + \pi^0 + \pi^0 \\ K^+ \rightarrow e^+ + \nu + \pi^+ + \pi^- \\ K^0 \rightarrow e^+ + \nu + \pi^- + \pi^0 \end{array} \right\} (K_{e4}) & \left. \begin{array}{l} K^+ \rightarrow \mu^+ + \nu + \pi^0 + \pi^0 \\ K^+ \rightarrow \mu^+ + \nu + \pi^+ + \pi^- \\ K^0 \rightarrow \mu^+ + \nu + \pi^- + \pi^0 \end{array} \right\} (K_{\mu4}). \end{array}$$

The corresponding K^- - and \bar{K}^0 -meson decays are obtained from the K^+ and K^0 -meson decays by substitution for all the particles by antiparticles. It should be pointed out that the K_{e2} decay and the K_{e4} and $K_{\mu4}$ decays have not as yet been observed.

It can easily be seen that interactions 54 may change the strangeness of the strongly interacting particles by $\Delta S = \pm 1$. A strangeness change of $|\Delta S| > 1$ is forbidden. In view of this, the following decays, particularly, are impossible:

$$\begin{array}{ll} \Xi^- \rightarrow n + e^- + \bar{\nu} & \Xi^- \rightarrow n + \mu^- + \bar{\nu} \\ \Xi^0 \rightarrow p + e^- + \bar{\nu} & \Xi^0 \rightarrow p + \mu^- + \bar{\nu}. \end{array}$$

As can be seen from 54, increase of the strangeness of strongly interacting particles in this interaction (transition $\Lambda \rightarrow p$) raises their charge by one unit, while decrease of the strangeness of strongly interacting particles lowers

their charge by one unit (transition $p \rightarrow \Lambda$). For interaction 54, the relation $\Delta Q = \Delta S$ thus exists, where ΔQ and ΔS are the change in charge and strangeness only of strongly interacting particles. It follows, therefore, that the decays

$$\begin{array}{ll} \Sigma^+ \rightarrow n + e^+ + \nu & \Sigma^+ \rightarrow n + \mu^+ + \nu \\ \Xi^0 \rightarrow \Sigma^- + e^+ + \nu & \Xi^0 \rightarrow \Sigma^- + \mu^+ + \nu \\ K^0 \rightarrow \pi^+ + e^- + \bar{\nu} & K^0 \rightarrow \pi^+ + \mu^- + \bar{\nu} \\ \bar{K}^0 \rightarrow \pi^- + e^+ + \nu & \bar{K}^0 \rightarrow \pi^- + \mu^+ + \nu \\ K^+ \rightarrow \pi^+ + \pi^+ + e^- + \bar{\nu} & K^+ \rightarrow \pi^+ + \pi^+ + \mu^- + \bar{\nu} \\ K^0 \rightarrow \pi^+ + \pi^0 + e^- + \bar{\nu} & K^0 \rightarrow \pi^+ + \pi^0 + \mu^- + \bar{\nu} \end{array}$$

for which $\Delta Q = -\Delta S$ must be forbidden. Experimental data are as yet insufficient to enable verification of whether the above processes are actually forbidden.

5.2 Further properties of the Lagrangian and the matrix elements.—It is easy to see that Lagrangian 54 changes the isotopic spin of strongly interacting particles by $\Delta T = \frac{1}{2}$ (the isotopic spin of a proton is $\frac{1}{2}$ and that of a Λ -hyperon, 0). As the strong interaction is isotopically invariant, this property of interaction 54 extends also the matrix elements of the processes caused by this interaction (see K_{e3} and $K_{\mu 3}$ decays). The rule $\Delta T = \frac{1}{2}$ for leptonic decays of strange particles was first suggested by Gell-Mann (81).

Unfortunately, we cannot at present indicate the other symmetry properties of Lagrangian 54. In particular, in contrast to the vector current $j^n(V)$ it is not clear how the conserved current j^A could be constructed. Moreover, as in the case of the axial current $j^A(A)$ such conservation would result in a contradiction with the available experimental data on $K_{\mu 2}$ and $K_{\mu 3}$ decays (58, 82, 82a). Besides as p and Λ belong to different isotopic multiplets, it is not clear how this conservation could result in nonrenormalizability of the corresponding constants. As we shall see below, the interaction constants of 54 actually undergo considerable renormalization.

The fact that p and Λ belong to different isotopic multiplets deprives us of one more symmetry, viz. G invariance (see paragraph 4.3). Thus, the matrix elements 19 to 22 should contain, in the case of leptonic decays of strange particles with nonconservation of strangeness, all the possible terms enumerated in paragraph 4.1.

5.3 Leptonic hyperon decays.—We have already enumerated above the leptonic hyperon decays which should occur in accordance with the theory discussed and the decays which should be forbidden.

The amplitude of leptonic hyperon decay (e.g., Λ_e) has the form

$$\frac{G}{\sqrt{2}} (V_\alpha + A_\alpha) (\bar{u}_e \gamma_\alpha (1 + \gamma_5) u_\nu) \quad 55.$$

where

$$V_\alpha = \bar{u}_p [V_\alpha f_1 + (\gamma_\alpha \hat{k} - \hat{k} \gamma_\alpha) f_2 + k_\alpha f_3] u_\Lambda \quad 56.$$

$$A_\alpha = \bar{u}_p [\gamma_\alpha g_1 + (\gamma_\alpha \hat{k} - \hat{k} \gamma_\alpha) g_2 + k_\alpha g_3] \gamma_5 u_\Lambda. \quad 57.$$

Here all six functions $f(k^2)$ and $g(k^2)$ are unknown and must be obtained from experiment. Of course, if we were in possession of a consistent theory of strong interactions, we could calculate these functions; but there is no such theory as yet and we cannot even calculate the probability of the decay in question, not to speak of its angular distributions, spectra, polarizations, etc.

To get at least an approximate idea of the values of functions f and g , let us calculate the "theoretical" rates of some decays under the assumption that $f_1 = g_1 = 1$ and $f_2 = f_3 = g_2 = g_3 = 0$. Then we get (21, 84; see also 83, 83a).

$$w = \frac{G^2 \Delta^4 C}{15\pi^3} \quad 58.$$

where

$$\Delta = \frac{M_Y^2 - M_N^2}{2M_Y}$$

is the maximum electron energy (M_Y and M_N being the hyperon and nucleon masses), C is a factor taking the recoil into account. If $X = \Delta/M_Y$,

$$C = -\frac{15}{16} X^{-4} (1 - 2X)^2 \log(1 - 2X) - \frac{5}{8} X^{-4} (1 - X)(3 - 6X - 2X^2) \quad 59.$$

with $X=0$, $C=1$, and formula 58 coincides with formula 31 for neutron β -decay if we assume $\alpha=1$ in the latter. At $X=0.5$, $C=2.5$ and formula 58 coincides with formula 11 for muon decay. Decay rates calculated by formula 58 are given in Table V. The spectra and angular distributions of secondary particles in leptonic hyperon decays are calculated for the case $f_2 = f_3 = g_2 = g_3 = 0$ in paper (85).

To date, approximately 1500 Λ -hyperon decays ($\Lambda \rightarrow p + \pi^-$ and $\Lambda \rightarrow n + \pi^0$) and over 200 Σ^- -hyperon decays ($\Sigma^- \rightarrow n + \pi^-$) have been observed in various laboratories (86b). According to Table V, approximately 25 leptonic Λ -

TABLE V
"THEORETICAL" RATES OF LEPTONIC DECAYS OF HYPERONS

Decay	$w_e \text{ sec.}^{-1}$	$w_e \tau$	Decay*	$w_\mu \text{ sec.}^{-1}$	$w_\mu \tau$
$\Lambda^0 \rightarrow p + e^- + \bar{\nu}$	5.8×10^7	1.5×10^{-2}	$\Lambda^0 \rightarrow p + \mu^- + \bar{\nu}$	9.4×10^6	2.4×10^{-3}
$\Sigma^- \rightarrow n + e^- + \bar{\nu}$	3.4×10^8	5.8×10^{-2}	$\Sigma^- \rightarrow n + \mu^- + \bar{\nu}$	1.5×10^8	2.6×10^{-2}
$\Xi^- \rightarrow \Lambda^0 + e^- + \bar{\nu}$	1.2×10^8	6×10^{-2}	$\Xi^- \rightarrow \Lambda^0 + \mu^- + \bar{\nu}$	3.2×10^7	1.6×10^{-2}
$\Xi^- \rightarrow \Sigma^0 + e^- + \bar{\nu}$	1.4×10^7	7×10^{-3}	$\Xi^- \rightarrow \Sigma^0 + \mu^- + \bar{\nu}$	2.1×10^6	1.1×10^{-4}

The decay rates w_e were calculated by formula 58.

* Formula 58 is inapplicable to decays with muon emission. The corresponding decay rates were taken from a paper by Sehler (131).

The lifetimes of Λ - and Σ -hyperons τ_Λ and τ_Σ are from Table I. We have assumed arbitrarily that $\tau_\Sigma = 5 \times 10^{-10} \text{ sec.}$

hyperon decays and about 12 leptonic Σ -hyperon decays must have been observed. But there is only one case known which can be interpreted as a leptonic decay of a Σ -hyperon (86) and two cases of the decay Λ_e (86a, 86b; see also 86c). As the energy liberated in the Σ and Λ -decays is different, it seems quite improbable that the low decay rate value resulted in both cases from the destructive interference of various terms of the matrix elements 56 and 57. Therefore, we must conclude that actually the coefficients f and g in 56 and 57 are much smaller than unity. As will be seen from the following, this conclusion is in qualitative agreement with the conclusions which can be drawn from an examination of $K_{\mu 2}$ and $K_{e 2}$ decays (75, 85a, 99).

5.4 $K_{\mu 2}$ and $K_{e 2}$ decays.—The amplitudes of the decays $K^+ \rightarrow \mu^+ + \nu$ and $K^+ \rightarrow e^+ + \nu$ have the form

$$\frac{G}{\sqrt{2}} f_K \varphi k_\alpha (u_i \gamma_\alpha (1 + \gamma_5) u_l) \quad 60.$$

where k is the 4-momentum of the K meson, φ is its wave function and f_K is an unknown constant. (Compare formula 19.) From 60 it follows that the corresponding decay rates equal

$$w_l = \frac{G^2}{8\pi} f_K^2 m_K m_l^2 \left(1 - \frac{m_l^2}{m_K^2}\right)^2. \quad 61.$$

Comparing this with the experimental rate of $K_{\mu 2}$ decay, we find

$$f_K^2 \approx 0.14 \cdot 10^{-2} M_p^2. \quad 62.$$

Comparing 62 with 41, we get $f_\pi^2/f_K^2 \approx 14$. This does not contradict the conclusion from paragraph 5.3 on the smallness of the effective interaction of strange particles with leptons.

It follows from formula 61 that the $K_{e 2}$ decay must be about 40,000 times less probable than the $K_{\mu 2}$ decay. Experimentally, this ratio is apparently less than 1 per cent (6).

The muons in the $K_{\mu 2}$ decay must be completely longitudinally polarized (μ^- parallel to the momentum and μ^+ counter to it), analogously to the muons in pion decay. This is confirmed by measurement of the electron asymmetry in the chain $K^+ \rightarrow \mu^+ \rightarrow e^+$ (87).

As in the case of the decay $\pi \rightarrow \mu + \nu$, conservation of the current responsible for the $K_{\mu 2}$ and $K_{e 2}$ decays would result in their being forbidden, because from the condition $f k_\alpha k_\alpha = 0$ it follows that $f = 0$ (58).

5.5 $K_{e 3}$ decay.—The amplitudes of the decays $K^+ \rightarrow e^+ + \nu + \pi^0$ and $K^+ \rightarrow \mu^+ + \nu + \pi^0$ have the form:

$$\frac{G}{\sqrt{2}} \varphi_K \varphi_\pi (f_1 p_\alpha + f_2 q_\alpha) (\bar{u}_i \gamma_\alpha (1 + \gamma_5) u_l) \quad 63.$$

where φ_K and φ_π are wave functions and p and q the four-dimensional momenta of the K meson and the pion respectively. Let us consider the $K_{e 3}$ decay in greater detail. Taking into account that $q = p - k_e - k_\nu$, and taking

advantage of the Dirac equation ($\hat{k}\bar{u} = m\bar{u}$) for leptons, we get from 63, neglecting the mass of the electron:

$$\frac{G}{\sqrt{2}} \varphi_{\pi} \varphi_K (f_1 + f_2) \bar{p}_\alpha (\bar{u}_\nu \gamma_\alpha (1 + \gamma_5) u_e). \quad 64.$$

Now, considering the decay of a K meson at rest and denoting $f_1 + f_2 = 2g$, we have:

$$\sqrt{2} G g \varphi_K \varphi_{\pi} m_K (\bar{u}_\nu \gamma_4 (1 + \gamma_5) u_e). \quad 65.$$

The function g , like f_1 and f_2 , depends only on $(p-q)^2$, i.e. on the energy E_π of the pion. To calculate most of the characteristics of the K_{e3} decay, and particularly its decay rate, this dependence must be known. If we assume that $g(E_\pi) = \text{const.}$, then

$$w \approx \frac{G^2 g^2 m_K^5}{768 \pi^3} \cdot 0.6 \quad 66.$$

where w is the decay rate and 0.6 is a factor making allowance for the mass of the pion differing from 0. With $m_\pi = 0$ it would equal unity and with $m_\pi = m_K$ it would equal 0.

Comparing 66 with the experimental decay rate (see Table VI), we have:

$$g^2 \approx 2.5 \times 10^{-2}, \quad g \approx \pm 0.16. \quad 67.$$

Again, as in the cases of leptonic hyperon decays and the $K_{\mu 2}$ decay, the effective coupling in K_{e3} decay proves to be much less than unity.

Assuming $g(E_\pi) = \text{const.}$, the electron spectrum in the K_{e3} decay has the form [Furuichi *et al.* (88)]:

$$w(E_e) dE_e = \frac{G^2 g^2}{2\pi^3} \cdot \frac{m_K (W_e - E_e)^2 E_e^2}{m_K - 2E_e} dE_e. \quad 68.$$

$$0 \leq E_e \leq W_e = \frac{m_K^2 - m_\pi^2}{2m_K}.$$

Upon the decay of neutral K mesons (for example $K_2^0 \rightarrow e^+ + \nu + \pi^-$), the momentum of which is not known, the neutrino energy distribution can be obtained. The neutrino energy E_ν in the rest system of the K meson is related to the energies and momenta of the charged decay products by the expression:

$$E_\nu = \frac{m_K^2 - (E_\pi' + E_e')^2 + (\vec{p}_\pi' + \vec{p}_e')^2}{2m_K} \quad 69.$$

where E_π' , \vec{p}_π' (E_e' , \vec{p}_e') is the energy and momentum of a pion (positron) in the laboratory system. Thus, though the energies and momenta of the charged particles (π^- and e^+) in the rest system of the K meson are unknown in this case, the neutrino energy in this system is known. This was first pointed out by Furuichi (89). As we neglect the electron mass in our calculation, it is not difficult to see that the neutrino spectrum, like that of the electrons, is described by formula 68.

TABLE VI
 BRANCHING RATIOS AND RATES OF K -MESON DECAYS

		K^+		K_1^0	K_2^0
$K\pi_2$	$\pi^+ + \pi^0$	25.6 ± 1.7	$\pi^+ + \pi^-$ $\pi^0 + \pi^0$	78 ± 6 14 ± 6	* *
$K\pi_3$	$\pi^+ + \pi^+ + \pi^-$ $\pi^0 + \pi^0 + \pi^+$	5.66 ± 0.30 1.70 ± 0.32	$\pi^+ + \pi^- + \pi^0$ $\pi^0 + \pi^0 + \pi^0$	† *	~ 15
$K\mu_2$ K_{e2}	$\mu^+ + \nu$ $e^+ + \nu$	58.8 ± 2.0 †	No analogues		
$K\mu_3$ K_{e3}	$\mu^+ + \nu + \pi^0$ $e^+ + \nu + \pi^0$	4.0 ± 0.77 4.19 ± 0.42	$\mu^\pm \pm \nu + \pi^\mp$ $e^\pm \pm \nu + \pi^\mp$	† †	~ 40 ~ 40
$K\mu_4$	$\mu^+ + \nu + \pi^0 + \pi^0$ $\mu^+ + \nu + \pi^+ + \pi^-$ $\mu^- + \bar{\nu} + \pi^+ + \pi^+$	† † †	$\mu^\pm \pm \nu + \pi^\mp + \pi^0$	†	†
$K_{e4}\S$	$e^+ + \nu + \pi^0 + \pi^0$ $e^+ + \nu + \pi^+ + \pi^-$ $e^- + \bar{\nu} + \pi^+ + \pi^+$	† † †	$e^\pm \pm \nu + \pi^\mp + \pi^0$	†	†
		100		92	~ 100
	Decay rate, sec. ⁻¹	0.815×10^8		$0.95 \cdot 10^{10}$	1.24×10^7

* indicates that the process is forbidden because of CP invariance.

† indicates that the process, though not forbidden, theoretically possesses a low decay rate and has not been observed as yet.

‡ indicates that the process is forbidden because of selection rule $\Delta Q = \Delta S$.

The data on the decay of K^+ mesons were taken from the review of Gell-Mann & Rosenfeld (125). According to the paper of Bruin *et al.* (132), the branching ratio for $K_{\mu 3}^+$ equals 3.9 ± 0.5 per cent and that for $K_{e 3}^+$ 5.1 ± 0.8 per cent.

The data on the decay of the K_1^0 meson were taken from the report of Glaser at the 1958 Geneva Conference. The sum of the branching ratios does not equal 100 per cent as the corresponding data were obtained in essentially different experiments.

The data on the decays of the K_2^0 meson were taken from the paper of Bardon *et al.* (123).

§ A theoretical estimate of the $K_{e 4}$ decay rate is contained in the paper of Oneda (133).

Rather a large number of predictions concerning the $K_{e 3}$ decay can be made without knowing the properties of the function $g(E_\pi)$. The first to draw attention to this fact were Pais & Treiman (90). Indeed, the angular distribution of electrons for a fixed pion momentum or, which is equivalent, the electron spectrum for a fixed E_π can be calculated without knowledge

of $g(E_\pi)$. The probability of emission of an electron with energy E_e and of a pion with energy E_π equals (91, 92, 93):

$$w(E_e, E_\pi) dE_e dE_\pi = \frac{G^2 g^2}{8\pi^3} m_K [\bar{K}_\pi^2 - (m_K - E_\pi - 2E_e)^2] dE_e dE_\pi. \quad 70.$$

For the given E_π the electron energy lies within

$$\frac{m_K - E_\pi - \bar{K}_\pi}{2} \leq E_e \leq \frac{m_K - E_\pi + \bar{K}_\pi}{2} \quad 71.$$

for the given E_e we have:

$$\frac{(m_K - 2E_e)^2 + m_\pi^2}{2(m_K - 2E_e)} \leq E_\pi \leq \frac{m_K^2 + m_\pi^2}{2m_K}. \quad 72.$$

Unfortunately, the necessity of selecting pions of a definite energy complicates the experimental problem. [We remind the reader that to date only about 40 cases of K_{e3} decay have been investigated in which neither the energy nor the direction of pion emergence was observed (95).] As Kobzarev (94) has pointed out, a comparison of distribution 70 with experimental data can conveniently be made on a diagram analogous to the Dalitz plot for the τ -decay (see Fig. 6). Slightly modifying Kobzarev's procedure, we shall rewrite formula 70 to make it comparable with the experimental results in which the pion energy is measured but not fixed:

$$w(\bar{K}_\pi, v) \propto (\bar{K}_\pi^2 - v^2) d\bar{K}_\pi dv \quad 73.$$

where $v = |E_e - E_\pi|$.

The region of variation of \bar{K}_π and v allowed by the conservation laws is bounded by the straight lines $\bar{K}_\pi = \bar{K}_{\pi \max} = (m_K^2 - m_\pi^2)/2m_K$ and $\bar{K}_\pi = v$ (see Fig. 7). Let us draw the ray $\bar{K}_\pi = v/a$ ($a \leq 1$). Now if we denote by R the ratio between the number of experimental points at the left of the ray and their total number, we find that

$$R = \frac{3}{2} \left(a - \frac{a^3}{3} \right). \quad 74.$$

It is essential that formula 74 is valid with any arbitrary form of the function $g(E_\pi)$.

The pion energy spectrum may be employed to determine the function $g(E_\pi)$ (91, 92):

$$w(E_\pi) dE_\pi = \frac{G^2 g^2(E_\pi)}{12\pi^3} m_K \bar{K}_\pi^2 dE_\pi. \quad 75.$$

Experimental data available at present on the electron spectrum in the K_{e3} decay do not agree with formula 68. This contradiction cannot be eliminated by changing the form of the function $g(E_\pi)$. As Furuichi, Sawada & Yonezawa (96) have shown, it follows from formula 70 that whatever the function $g(E_\pi)$, the number of "slow" electrons of energy $E_e \leq W_e/2$ (where W_e is the maximum possible energy of the electron) must be less than half the total number of electrons. (This result is obvious from diagram 6 if its

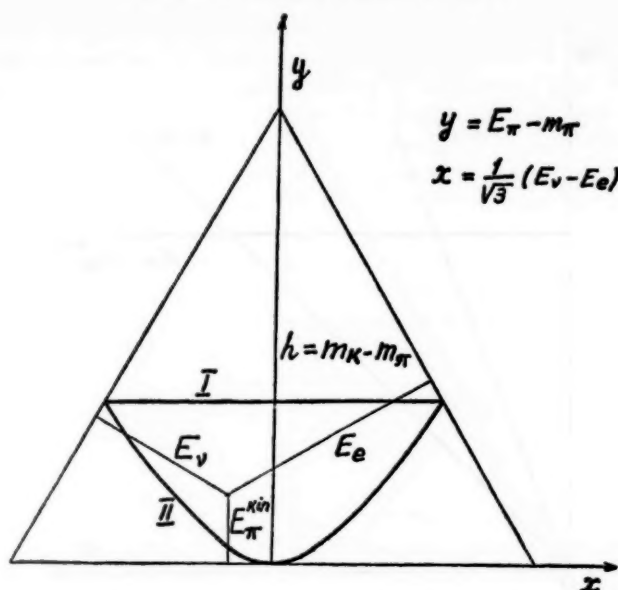


FIG. 6. Kobzarev plot for K_{e3} decay. The region allowed by the conservation laws is bounded by the lines I:

$$y = y_{\max} = \frac{(m_K - m_\pi)^2}{2m_K}$$

and II: $3x^2 = y^2 + 2m_\pi y$.

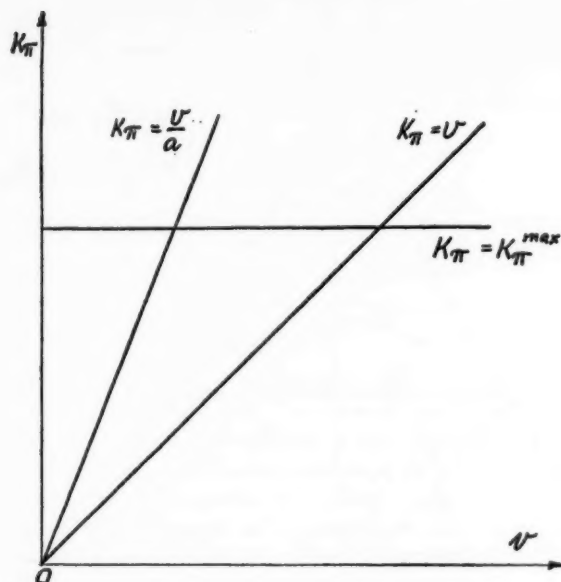
symmetry with respect to the vertical axis is taken into account.) In experiment, the share of "slow" electrons exceeds 0.6 of the total number of electrons. It may, however, be hoped that increasing the statistics will eliminate this contradiction. [The electron spectrum is based on approximately 40 cases; for a list of the experimental studies see (95).]

In concluding, we may point out that the electrons in the K_{e3}^- and \bar{K}_{e3}^0 decays must be completely polarized longitudinally counter to the direction of their motion, while the positrons in the K_{e3}^+ and K_{e3}^0 decays must be polarized in the direction of their motion. The only exceptions are those rare cases when the pion emerges with a zero momentum and the electron and neutrino fly in opposite directions. [If $m_e = 0$ such a case would be strictly forbidden (97).]

5.6 $K_{\mu 3}$ decay.—The amplitude of the $K_{\mu 3}$ decay may be modified, like the amplitude of the K_{e3} decay, to the form:

$$\sqrt{2}G_F \varphi_K \varphi_\pi [g m_K (\bar{u}_\nu \gamma_4 (1 + \gamma_5) u_\mu) - f m_\mu (\bar{u}_\nu (1 - \gamma_5) u_\mu)]. \quad 76.$$

This expression contains two unknown functions of the pion energy

FIG. 7. "Sliding ray" diagram for K_{e3} decay.

E_{π} : $2g=f_1+f_2$ and $2f=f_2$. It is appropriate to emphasize here that the function $g(E_{\pi})$ in 76 is exactly the same as the function $g(E_{\pi})$ in expression 65, owing to the universality of the weak interaction (97, 98, 99). Only the region of allowed energy of the pion in the $K_{\mu 3}$ decay is smaller than in K_{e3} :

$$m_{\pi} \leq E_{\pi} \leq W_{\pi} = \frac{m_K^2 + m_{\pi}^2 - m_{\mu}^2}{2m_K}. \quad 77.$$

If we put $g=\text{const.}$, $f=\text{const.}$, we can calculate the rate of the $K_{\mu 3}$ decay (97, 98, 99):

$$w \approx \frac{G^2 m_K^5}{768} [g^2 \cdot 0.5 - fg \cdot 0.2 + f^2 \cdot 0.05]. \quad 78.$$

At $m_{\mu} \rightarrow 0$: $0.5 \rightarrow 0.6$, $0.2 \rightarrow 0$, $0.05 \rightarrow 0$ and we obtain formula 66 for the K_{e3} decay. Comparing 78 with 66, as has been done by a number of authors (97, 98, 99), we get

$$0.5g^2 - 0.2fg + 0.05f^2 \approx 0.6g^2 \quad 79.$$

since experimentally $w(K_{e3}) \approx w(K_{\mu 3})$ (see Table VI). Equation 79 has two solutions:

$$\frac{f}{g} \approx 4.5; \quad \frac{f}{g} \approx -0.5. \quad 80.$$

It is easy to convince oneself that the different solutions 80 result in different spectra of muons and pions and in different muon polarizations (97 to 101).

This enables selection of one of the solutions 80 by means of an experiment.

The approximation $f = \text{const.}$, $g = \text{const.}$ made above is permissible if f and g depend weakly on E_π . In the theory of universal Fermi interaction, there are grounds for expectation that this dependence will not be strong. Indeed, if, for example, the $K_{\mu 3}^+$ decay takes place because of the decay of the particle pair $p + \bar{\Lambda}$ into $\mu^+ + \nu$, then, as the masses of p and Λ are much higher than the energy carried away by the pion, it may be considered that their leptonic decay will depend weakly on the value of this energy.

If the spectrum of muons is measured at different fixed energies E_π of the pion, the dependence of g and f on E_π can be found. The probability of decay into a pion of energy E_π and a muon of energy E_μ , calculated from amplitude 76, equals (92, 100, 102):

$$w(E_\pi E_\mu) \cdot dE_\pi dE_\mu = \frac{G^2}{4\pi^2} \{ g^2 m_K [2E_\mu E_\nu - m_K(W_\pi - E_\pi)] - 2gfm_\mu^2 E_\nu + f^2 m_\mu^2 (W_\pi - E_\pi) \} dE_\pi dE_\mu. \quad 81.$$

Here

$$W_\pi = \frac{m_K^2 + m_\pi^2 - m_\mu^2}{2m_K}, \quad E_\nu = m_K - E_\pi - E_\mu.$$

With fixed energy E_π the energy E_μ varies over the range

$$\frac{(m_K - E_\pi - p_\pi)^2 + m_\mu^2}{2(m_K - E_\pi - p_\pi)} \leq E_\mu \leq \frac{(m_K - E_\pi + p_\pi)^2 + m_\mu^2}{2(m_K - E_\pi + p_\pi)}. \quad 82.$$

With fixed E_μ :

$$\frac{(m_K - E_\mu - p_\mu)^2 + m_\pi^2}{2(m_K - E_\mu - p_\mu)} \leq E_\pi \leq \frac{(m_K - E_\mu + p_\mu)^2 + m_\pi^2}{2(m_K - E_\mu + p_\mu)}. \quad 83.$$

If we integrate 81 with respect to E_π within the limits of 83, assuming $g = \text{const.}$ and $f = \text{const.}$, we get the muon spectrum:

$$w(E_\mu) dE_\mu = \frac{G^2}{2\pi^2} \frac{\bar{p}_\mu (W_\mu - E_\mu)^2}{(m_K^2 + m_\mu^2 - 2m_K E_\mu)^2} \times [g^2 m_K^3 (m_K E_\mu - 2E_\mu^2 + m_\mu^2) - 2fgm_K^2 m_\mu^2 (m_K - E_\mu) + f^2 m_K m_\mu^2 (m_K E_\mu - m_\mu^2)] dE_\mu \quad 84.$$

where

$$W_\mu = \frac{m_K^2 + m_\mu^2 - m_\pi^2}{2m_K}.$$

Integrating 81 with respect to E_μ within the limits of 82, we get the pion spectrum:

$$w(E_\pi) dE_\pi = \frac{G^2}{2\pi^2} \frac{m_K p_\pi (W_\pi - E_\pi)^2}{(m_K^2 + m_\pi^2 - 2m_K E_\pi)^2} \times \left\{ \frac{g^2}{3} m_K^2 [2p_\pi^2 (m_K^2 + m_\pi^2 - 2m_K E_\pi) + m_\mu^2 (3(m_K - E_\pi)^2 + p_\pi^2)] - 2gfm_\mu^2 m_K (m_K - E_\pi) (m_K^2 + m_\pi^2 - 2m_K E_\pi) + f^2 m_\mu^2 (m_K^2 + m_\pi^2 - 2m_K E_\pi)^2 \right\} dE_\pi \quad 85.$$

where, as before,

$$W_{\pi} = \frac{m_K^2 + m_{\pi}^2 - m_{\mu}^2}{2m_K}.$$

Contrary to the electrons in the K_{e3} decay, the muons in the $K_{\mu 3}$ decay possess not only longitudinal but transverse polarization in the decay plane as well. No muon polarization in the direction normal to the decay plane should exist [see paper by Gatto (103) where the invariants of the $K_{\mu 3}$ decay are investigated, and also papers by Ivanter (104) and Sakurai (108)].

The longitudinal muon polarization (μ^+) as a function of the energy equals (104 to 107; see also 108):

$$P(E_{\mu}) = m_K p_{\mu} \frac{g^2(m_K - 2E_{\mu})m_K + 2fgm_{\mu}^2 - f^2m_{\mu}^2}{g^3(E_{\mu}m_K - 2E_{\mu}^2 + m_{\mu}^2)m_K^2 - 2fgm_{\mu}^2m_K(m_K - E_{\mu}) + f^2m_{\mu}^2(E_{\mu}m_K - m_{\mu}^2)}. \quad 86.$$

Here again use has been made of the approximation $g = \text{const.}$, $f = \text{const.}$ In the case of μ^- the polarization is of the opposite sign. For expressions for transverse muon polarization see papers (109, 110). Experimental data on the muon spectra in $K_{\mu 3}$ decay are very scarce (95). The muon polarization in the $K_{\mu 3}$ decay has not been measured as yet.

5.7 *Relation between leptonic decays of charged and neutral K mesons.*— We have already mentioned that the interaction responsible for the K_{e3} and $K_{\mu 3}$ decays changes the isotopic spin of strongly interacting particles by $\Delta T = \frac{1}{2}$ (see paragraph 5.2). As has been indicated by a number of authors (30, 81, 111), this results in a relationship between the amplitudes of the $K_{\mu 3}(K_{e3})$ decays of charged and neutral K mesons. It proves that the functions f and g contained in the amplitudes of the $K_{\mu 3}$ and K_{e3} decays satisfy the condition:

$$\frac{g_{K^+}}{g_{K^0}} = \frac{f_{K^+}}{f_{K^0}} = \frac{g_{K^-}}{g_{K^0}} = \frac{f_{K^-}}{f_{K^0}} = \frac{1}{\sqrt{2}}. \quad 87.$$

It follows from this relationship that the energy spectra of secondary particles, angular distributions, and polarizations in the $K_{\mu 3}$ decays of $K^+(K^-)$ and $K^0(\bar{K}^0)$ mesons should be similar and the total decay rates should be to each other as 1:2.

When neutral K mesons decay we have to deal not with K^0 and \bar{K}^0 but with their superpositions, K_1^0 and K_2^0 :

$$K_1^0 = \frac{K^0 + \bar{K}^0}{\sqrt{2}}, \quad K_2^0 = \frac{K^0 - \bar{K}^0}{\sqrt{2}} \quad 88.$$

(6, 113). Comparing 88 and 87 we can easily establish the relationship between the $K_{\mu 3}$ -decay rates of K_1^0 and K_2^0 mesons and K^+ meson (111, 112):³

$$\begin{aligned} w(K_1^0 \rightarrow \pi^+ + \mu^- + \bar{\nu}) &= w(K_2^0 \rightarrow \pi^+ + \mu^- + \bar{\nu}) = w(K_1^0 \rightarrow \pi^- + \mu^+ + \nu) \\ &= (K_2^0 \rightarrow \pi^- + \mu^+ + \nu) = w(K^+ \rightarrow \pi^0 + \mu^+ + \nu). \end{aligned} \quad 89.$$

³ This result was obtained also by Gell-Mann (112a).

All that has been said above with respect to $K_{\mu 3}$ decays pertains also to $K_{e 3}$ decays. Taking advantage of known data on the lifetime of the K_1^0 -meson and the $K_{\mu 3}^+$ and $K_{e 3}^+$ -decay rates, as well as of the relation 89, we can easily find that the $K_{\mu 3}$ and $K_{e 3}$ decays must constitute less than 0.1 per cent of all the decays of the K_1^0 meson. For the K_2^0 meson these decays prove to be quite substantial. It follows from 89 that if the K_2^0 meson had no other decays but the $K_{\mu 3}$ and $K_{e 3}$, its lifetime would be about 7×10^{-8} sec. The existence of other decays ($K_{\pi 3}$) lowers this value to $(5-6) \times 10^{-8}$ sec. If the lifetime of the K_2^0 meson and the probabilities of its various decays were determined more accurately (in experiment $\tau_{K_2^0} = 8.1_{-2.4}^{+3.2} \cdot 10^{-8}$ sec.), we could ascertain the truth of theoretical predictions on this point.

5.8 *Interference effects in $K_{e 3}$ and $K_{\mu 3}$ decays.*—As was mentioned in paragraph 5.1, in $K_{\mu 3}$ and $K_{e 3}$ decays the K^0 meson can decay only into $\mu^+\nu$ and $e^+\nu$ and the \bar{K}^0 meson only into $\mu^-\bar{\nu}$ and $e^-\bar{\nu}$. On the other hand, in a beam of neutral K mesons in vacuum there must be a transition from K^0 into \bar{K}^0 (113). Hence, as the beam of neutral K mesons "ages," the ratio of the number of $e^+(\mu^+)$ -decays to the number of $e^-(\mu^-)$ -decays should vary. The possibility of this effect was indicated by Zel'dovich (114) and by Treiman & Sachs (115). In the theory considered herein, the ratios e^-/e^+ and μ^-/μ^+ should be identical and equal to the ratio of the number of \bar{K}^0 mesons to the number of K^0 mesons:

$$R(t) = \frac{n(\mu^-)}{n(\mu^+)} = \frac{n(e^-)}{n(e^+)} = \frac{n(\bar{K}^0)}{n(K^0)} = \frac{e^{-t/\tau_1} + e^{-t/\tau_2} - 2e^{-t/2\tau_1 - t/2\tau_2} \cos \Delta m t}{e^{-t/\tau_1} + e^{-t/\tau_2} + 2e^{-t/2\tau_1 - t/2\tau_2} \cos \Delta m t} \quad 90.$$

where t is the time elapsed from the moment of formation of the K^0 mesons to the moment of observation, τ_1 and τ_2 are the lifetimes of the K_1^0 and K_2^0 mesons, Δm is the difference of their masses.

No oscillations of leptonic decays as described by formula 90 have been observed as yet. As to the ratio of the number of \bar{K} mesons to the number of K mesons, it was determined by measuring the \bar{K} meson capture in substance with the formation of a hyperon (116), which made it possible to establish Δm , the difference of masses of the K_1^0 and K_2^0 mesons. It proved that $(1/\Delta m) \approx 10^{-10}$ sec.

6. WEAK NONLEPTONIC INTERACTIONS

6.1 *The Lagrangian and the selection rules.*—A detailed examination of nonleptonic decays of strange particles is contained in a number of reviews, particularly in that of Gell-Mann & Rosenfeld (6). Therefore, only the selection rules for this interaction, which follow from the Sakata model, will be considered here.

The weak interaction Lagrangian responsible for the nonleptonic decays of strange particles has the form (see formula 1):

$$\frac{G}{\sqrt{2}} j_a^\Lambda j_a^\Lambda + \text{h.c.} \quad 91.$$

All the particles contained in this Lagrangian possess strong interactions and, therefore, not much can be said as yet about the properties of the matrix elements resulting from Lagrangian 91. Still, a thing or two may be said.

Lagrangian 91 can cause only transitions with $\Delta S = \pm 1$, because it corresponds to transitions $\Lambda \bar{\Sigma}$ nucleon. Hence, it follows that the slow decays

$$\Xi^- \rightarrow n + \pi^-, \quad \Xi^0 \rightarrow p + \pi^-, \quad \Xi^0 \rightarrow n + \pi^0$$

in which $\Delta S = +2$ must be forbidden. Indeed, these decays have never been detected. However, it must be taken into account that till now only one case of Ξ^0 -hyperon has been observed and that the number of Ξ^- -hyperons observed is just a little over 10.

A more weighty argument in favor of the rule $\Delta S = \pm 1$ is the experimentally established value of the mass difference of the K_1^0 and the K_2^0 mesons. This mass difference is proportional to the matrix elements of the transition $K^0 \rightarrow \bar{K}^0$ which takes place in vacuum under the influence of the weak interaction. Let the direct slow transitions with $|\Delta S| > 1$ be forbidden, as is the case in the weak interaction model under consideration. Then the difference of masses will be attributable to processes which contain the weak interactions twice, such as

$$K^0 \xrightarrow{G} N + \bar{N} \xrightarrow{G} \bar{K}^0.$$

Here, both transitions contain the weak interaction constant; thus, the mass difference proves to be proportional to G^2 and of the same order as the inverse lifetime of the K_1^0 meson: $\Delta m \sim (1/\tau_1)$, where $\tau_1 \approx 10^{-10}$ sec. [see for instance (114)].

As was noted by Pontecorvo and the author (117), if transitions with $|\Delta S| = 2$ were allowed, the difference of masses of K_1^0 and K_2^0 mesons would be proportional to G and not to G^2 , and would be five to seven orders greater [$\Delta m \sim (1/\tau)$, where $\tau \approx 10^{-17}$ sec.]. In the above-mentioned experiment (116) it was established that $1/\Delta m \approx 10^{-10}$ sec. In agreement with the above, this means that transitions with $|\Delta S| = 2$ are forbidden in the first order of the perturbation theory with respect to weak interaction.

The isotopic spin change caused by Lagrangian 91 can equal only $\Delta T = 1/2, 3/2$. Greater ΔT are forbidden because $T_\Lambda = 0$ and the value of T for a system of two nucleons and one antinucleon into which the Λ -hyperon can pass can equal $1/2$ or $3/2$, according to 91. This property of the Lagrangian should also be shared by the amplitudes of the corresponding processes because the strong interactions are isotopically invariant (we neglect virtual photons).

If we assume that the amplitude with $\Delta T = 3/2$ is much smaller than that with $\Delta T = 1/2$, we can speak of the approximate rule ΔT for nonleptonic decays of strange particles. This rule, first suggested by Gell-Mann & Pais (118), has been investigated in a number of theoretical papers (6, 14) and is in remarkable agreement with all experimental data on nonleptonic de-

cays of strange particles. It should be stressed that no special grounds for the rule $\Delta T = 1/2$ can be seen within the framework of the theory under consideration.

7. CONCLUSIONS

The theory of weak interactions of elementary particles described in this review is based on two hypotheses: (a) Hypothesis of the universal Fermi $V-A$ interaction between particles. (b) Hypothesis of the composite model of strongly interacting particles.

The first of these hypotheses is a far-reaching generalization of experimental results obtained mainly in the β -decay and in the decays of the pion and muon. As to the second hypothesis, it should be emphasized that we have utilized it in a somewhat conventional sense. The point is that before the theory of strong interactions is created (and perhaps even within the framework of this future theory) we are unable to distinguish "primary" elementary particles and interactions from "secondary" ones. (For instance, if we proceed from a model in which Ξ^- , Ξ^0 , and Λ have been selected as the elementary particles, while all the other particles are composite, all the consequences of such a model coincide exactly with those following from the Sakata model.) That is why we have based our reasoning on the Sakata model only in so far as use could be made of the symmetry properties characteristic of it and of the conservation laws and selection rules connected with it.

From the contents of the review it can be seen that there is at present not a single experimental fact which seriously contradicts the theory described. It should, however, be remembered that in a number of cases the experimental data are still either very indefinite or entirely lacking.

LITERATURE CITED

1. *Proc. Ann. Rochester Conf. High-Energy Nuclear Phys.*, **6** (New York, N. Y., 1956)
2. *Proc. Ann. Rochester Conf. High-Energy Nuclear Phys.*, **7** (New York, N. Y., 1956)
3. *Proc. CERN Ann. Intern. Conf. High-Energy Phys.* (Geneva, Switzerland, 1958)
4. *Proc. Padua-Venice Conf. Mesons Newly Discovered Particles* (Italy, September, 1957)
5. *Proc. Intern. Conf. Elementary Particles* (Pisa, Italy, 1955); *Nuovo cimento*, **4**, Suppl., 848 (1957)
6. Gell-Mann, M., and Rosenfeld, A. H., *Ann. Rev. Nuclear Sci.*, **7**, 407-78 (1957)
7. Franzinetti, G., and Morpurgo, G., *Nuovo cimento*, **6**, Suppl., 469-804 (1957)
8. Dalitz, R. H., *Repts. Progr. Phys.*, **20**, 163-304 (1957)
9. Lee, T. D., and Yang, C. N., *Brookhaven Natl. Lab. Rept.*, No. 443 (BNL (T-91) (1957)
10. Markov, M. A., *Hyperons and K-Mesons* (State Publishers of Physical and Mathematical Literature, Moscow, U.S.S.R., 1958)
11. Nishijima, R., *Fortschr. Phys.*, **4**, 519-59 (1956)
12. Frisch, O. R., and Skyrme, T. H. R., *Progr. in Nuclear Phys.*, **6**, 267 (1957)
13. D'Espagnat, B., and Prentki, J., in *Progress in Elementary Particle and Cosmic Ray Physics*, **4** (North-Holland Publ. Co., Amsterdam, Holland, 1958)
14. Okun', L. B., *Uspekhi Fiz. Nauk*, **61**, 535-60 (1957)
15. Wick, G. C., *Ann. Rev. Nuclear Sci.*, **8**, 1-48 (1958)
16. Konopinski, E. J., *Ann. Rev. Nuclear Sci.*, **9**, 1 (1959)
17. Smorodinsky, Ya. A., *Uspekhi Fiz. Nauk.*, **67**, 43 (1959)
- 17a. Okonov, E. O., *Uspekhi Fiz. Nauk*, **67**, 245 (1959)
18. Yang, C. N., *Science*, **127**, 565 (1958)
- 18a. Lee, T. D., *Science*, **127**, 569 (1958)
19. Gell-Mann, M., and Rosenbaum, E. R., *Sci. Am.*, **197**, 72 (1957)
20. Lee, T. D., and Yang, C. N., *Phys. Rev.*, **104**, 254 (1956)
21. Feynman, R. P., and Gell-Mann, M., *Phys. Rev.*, **109**, 193 (1958)
22. Sudarshan, E. C. G., and Marshak, R. E., Report to *Padua-Venice Conf. Mesons Newly Discovered Particles* (Italy, September, 1957)
23. Sakurai, J. J., *Nuovo cimento*, **7**, 649 (1958)
24. Sudarshan, E. C. G., and Marshak, R. E., *Phys. Rev.*, **109**, 1860 (1958)
25. Šešter, V. M., *Zhur. Ekspl. i Teoret. Fiz.*, **34**, 257 (1958)
26. Zel'dovich, Ya. B., *Zhur. Ekspl. i Teoret. Fiz.*, **36**, 964 (1959)
- 26a. Zel'dovich, Ya. B., *Zhur. Ekspl. i Teoret. Fiz.*, **33**, 1531 (1957)
27. Sakata, S., *Progr. Theoret. Phys. (Kyoto)*, **16**, 686 (1956)
28. Fermi, E., and Yang, C. N., *Phys. Rev.*, **76**, 1739 (1949)
29. Levy, M. M., and Marshak, R. E., *Nuovo cimento*, **11**, 366 (1954)
- 29a. Markov, M. A., *On the Classification of Elementary Particles* (Acad. of Sci. U.S.S.R., Moscow, Russia, 1955); Report to *Ann. Rochester Conf. High-Energy Nuclear Phys.*, **6** (New York, N. Y., 1956)
- 29b. Tanaka, S., *Progr. Theoret. Phys. (Kyoto)*, **16**, 625, 631 (1956)
- 29c. Maki, Z., *Progr. Theoret. Phys. (Kyoto)*, **16**, 667 (1956)
- 29d. King, R. W., and Peaslee, D. C., *Phys. Rev.*, **106**, 360 (1957)
- 29e. Polubarinov, I. V., *Nuclear Phys.*, **8**, 444 (1958)

30. Okun', L. B., *Zhur. Eksptl. i Teoret. Fiz.*, **34**, 469 (1958); Report to *Padua-Venice Conf. Mesons Newly Discovered Particles* (Italy, September, 1957)
- 30a. Fujii, K., and Iwata, K., *Progr. Theoret. Phys. (Kyoto)*, **19**, 475 (1958); **20**, 126 (1958)
31. Puppi, G., *Nuovo cimento*, **5**, 505 (1948)
- 31a. Klein, O., *Nature*, **161**, 897 (1948)
- 31b. Lee, T. D., Rosenbluth, M., and Yang, C. N., *Phys. Rev.*, **75**, 905 (1949)
- 31c. Tiomno, J., and Wheeler, J. A., *Revs. Modern Phys.*, **21**, 144 (1949)
- 31d. Pontecorvo, B., *Phys. Rev.*, **72**, 246 (1947)
32. Yang, C. N., *Revs. Modern Phys.*, **29**, 231 (1957)
- 32a. Ioffe, B. L., Okun', L. B., and Rudik, A. P., *Zhur. Eksptl. i Teoret. Fiz.*, **32**, 396 (1957)
- 32b. Lee, T. D., Oehme, R., and Yang, C. N., *Phys. Rev.*, **106**, 340 (1957)
33. Landau, L. D., *Zhur. Eksptl. i Teoret. Fiz.*, **32**, 405 (1957); *Nuclear Phys.*, **3**, 127 (1957)
34. Konopinski, E. J., and Mahmoud, H. M., *Phys. Rev.*, **92**, 1045 (1953)
- 34a. Zel'dovich, Ya. B., *Doklady Akad. Nauk U.S.S.R.*, **91**, 1317 (1953)
- 34b. Marx, G., *Acta Phys. Hung.*, **3**, 55 (1953)
35. Salam, A., *Nuovo cimento*, **5**, 299 (1957)
- 35a. Landau, L. D., *Zhur. Eksptl. i Teoret. Fiz.*, **32**, 405 (1957)
- 35b. Lee, T. D., and Yang, C. N., *Phys. Rev.*, **105**, 1671 (1957)
36. Sakurai, J. J., *Phys. Rev. Letters*, **1**, 40 (1958)
37. Steinberger, J., and Wolfe, H. B., *Phys. Rev.*, **100**, 1490 (1955)
38. Schwinger, J., *Ann. Phys. (N. Y.)*, **2**, 407 (1957)
39. Feinberg, G., *Phys. Rev.*, **110**, 1482 (1958)
40. Byers, N., and Peierls, R. E., *Nuovo cimento*, **10**, 520 (1958)
41. Lee, T. D., and Yang, C. N., *Phys. Rev.*, **108**, 1611 (1957)
42. Feynman, R. P., and Gell-Mann, M., Meeting of the American Phys. Soc., December, 1958 (Unpublished)
43. Lokanathan, S., and Steinberger, J., *Phys. Rev.*, **98**, 240 (1955)
44. Berman, S. M., *Phys. Rev.*, **112**, 267 (1958)
45. Michel, L., *Proc. Phys. Soc. (London)*, **A63**, 514, 1371 (1950)
46. Kinoshita, T., and Sirlin, A., *Phys. Rev.*, **108**, 844 (1957)
- 46a. Okun', L. B., and Šešter, V. M., *Nuovo cimento*, **10**, 359 (1958); *Zhur. Eksptl. i Teoret. Fiz.*, **34**, 1250 (1958)
47. Bogolyubov, N. N., Bilenskiĭ, S. M., and Logunov, A. A., *Doklady Akad. Nauk U.S.S.R.*, **115**, 89 (1957); *Nucl. Phys.*, **5**, 383 (1958)
48. Goldberger, M. L., and Treiman, S. B., *Phys. Rev.*, **111**, 354 (1958)
49. Goldberger, M. L., and Treiman, S. B., *Phys. Rev.*, **110**, 1178 (1958)
50. Okun', L. B., Report to *CERN Ann. Intern. Conf. High-Energy Phys.* (Geneva, Switzerland, 1958)
- 50a. Feynman, R. P. (Private communication)
51. Ioffe, B. L., *Zhur. Eksptl. i Teoret. Fiz.*, **34**, 1343 (1958)
52. Gerštein, S. S., and Zel'dovich, Ya. B., *Zhur. Eksptl. i Teoret. Fiz.*, **29**, 698 (1955)
53. Gell-Mann, M., *Phys. Rev.*, **111**, 362 (1958)
54. Oppenheimer, J., in *Proc. CERN Ann. Intern. Conf. High-Energy Phys.*, 257 (Geneva, Switzerland, 1958)
55. Polkinghorne, J. C., *Nuovo cimento*, **8**, 179, 781 (1958)

56. Blin-Stoyle, R. J., *Nuovo cimento*, **10**, 132 (1958)
57. Taylor, J. C., *Phys. Rev.*, **110**, 1216 (1958)
58. Goldberger, M. L., and Treiman, S. B., *Phys. Rev.*, **110**, 1478 (1958)
59. Lee, T. D., and Yang, C. N., *Nuovo cimento*, **3**, 749 (1956)
60. Michel, L., in *Progress in Cosmic Ray Physics*, **1** (North-Holland Publ. Co., Amsterdam, Holland, 1952)
61. Kawaguchi, M., and Nishijima, K., *Phys. Rev.*, **108**, 905 (1957)
62. Weinberg, S., *Phys. Rev.*, **112**, 1375 (1958)
63. Berestetsky, V. B., and Pomeranchuk, I. Ya., *Zhur. Eksptl. i Teoret. Fiz.*, **36**, 1321 (1959)
64. Clark, M. A., Robson, J. M., and Nathans, R., *Phys. Rev. Letters*, **1**, 100 (1958)
- 64a. Burgy, H. T., Krohn, V. E., Novey, T. B., Ringo, G. R., and Telegdi, V. L., *Phys. Rev. Letters*, **1**, 324 (1958)
65. Weinberg, S., *Phys. Rev.*, **106**, 1301 (1957)
- 65a. Lopes, J. L., *Phys. Rev.*, **109**, 509 (1958)
66. Shapiro, I. S., Dolinsky, E. I., and Blokhintsev, L. D., *Nuclear Phys.*, **4**, 273 (1957)
67. Wolfenstein, L., *Nuovo cimento*, **8**, 882 (1958)
68. Huang, K., Yang, C. N., and Lee, T. D., *Phys. Rev.*, **108**, 1340 (1958)
69. Chou, H.-C., and Mayevsky, V., *Zhur. Eksptl. i Teoret. Fiz.*, **35**, 1581 (1958)
70. Zel'dovich, Ya. B., and Gerstein, S. S., *Zhur. Eksptl. i Teoret. Fiz.*, **35**, 821 (1958)
- 70a. Gerstein, S. S., *Zhur. Eksptl. i Teoret. Fiz.*, **34**, 463 (1958)
71. Ruderman, M. A., and Finkelstein, R. J., *Phys. Rev.*, **76**, 1458 (1949)
- 71a. D'Espagnat, B., *Compt. rend.*, **228**, 744 (1949)
72. Anderson, H. L., and Lattes, C. M. G., *Nuovo cimento*, **6**, 1356 (1957)
73. Fazzini, T., Fidecaro, G., Merrison, A. W., Paul, H., and Tollestrup, A. W., *Phys. Rev. Letters*, **1**, 247 (1958)
- 73a. Impeduglia, G., Plano, R., Prodell, A., Samios, N., Schwartz, M., and Steinberger, J., *Phys. Rev. Letters*, **1**, 249 (1958)
74. Zel'dovich, Ya. B., *Doklady Akad. Nauk U.S.S.R.*, **97**, 421 (1954)
75. Feenberg, E., and Primakoff, H., *Phil. Mag.*, **3**, 328 (1958)
76. Treiman, S. B., and Wyld, H. W., *Phys. Rev.*, **101**, 1552 (1956)
77. Vaks, V. G., and Ioffe, B. L., *Zhur. Eksptl. i Teoret. Fiz.*, **35**, 221 (1958); *Nuovo cimento*, **10**, 342 (1958)
78. Burkhardt, G. H., Cassels, J. M., Rigby, M., Wetherell, A. M., and Wormald, I. R., *Proc. Phys. Soc. (London)*, **72**, 44 (1958)
79. Šehter, V. M. (Private communication)
80. Feinberg, G., *Phys. Rev.*, **109**, 1019 (1958)
- 80a. Feldman, G., and Fulton, T., *Nuclear Phys.*, **8**, 106 (1958)
81. Gell-Mann, M., in *Proc. Ann. Rochester Conf. High-Energy Nuclear Phys.*, **6**, (New York, N. Y., 1956)
82. Weinberg, S., Marshak, R. E., Okubo, S., Sudarshan, E. C., and Teutsch, W. B., *Phys. Rev. Letters*, **1**, 25 (1958)
- 82a. Marshak, R., Report to CERN Ann. Intern. Conf. High-Energy Phys. (Geneva, Switzerland, 1958)
83. Finkelstein, R. J., *Phys. Rev.*, **88**, 555 (1952)
- 83a. Markov, M., and Stakhanov, V., *Zhur. Eksptl. i Teoret. Fiz.*, **28**, 740 (1955)
84. Behrends, R. E., and Fronsdaal, C., *Phys. Rev.*, **106**, 345 (1957)

85. Šehter, V. M., *Zhur. Eksptl. i Teoret. Fiz.*, **35**, 458 (1958)
- 85a. Šehter, V. M., *Zhur. Eksptl. i Teoret. Fiz.*, **36**, 1299 (1959)
86. Hornbostel, J., and Salant, E. O., *Phys. Rev.*, **102**, 502 (1956)
- 86a. Crawford, F. S., Jr., Cresti, M., Good, M. L., Kalbfleisch, G. R., Stevenson, M. L., and Ticho, H. K., *Phys. Rev. Letters*, **1**, 377 (1958)
- 86b. Nordin, P., Orear, J., Reed, L., Rosenfeld, A. H., Solmitz, F. T., Taft, H. D., and Tripp, R. D., *Phys. Rev. Letters*, **1**, 380 (1958)
- 86c. Eisler, F., Plano, R., Prodell, A., Samios, N., Schwartz, M., Steinberger, J., Conversi, M., Franzini, P., Mannelli, I., Santangelo, R., and Silvestrini, V., *Phys. Rev.*, **112**, 979 (1958)
87. Coombes, C. A., Cork, B., Galbraith, W., Lambertson, G. R., and Wenzel, W. A., *Phys. Rev.*, **108**, 1348 (1957)
88. Furuichi, S., Kodama, T., Ogawa, S., Sugahara, Y., Wakasa, A., and Yonezawa, M., *Prog. Theoret. Phys. (Kyoto)*, **17**, 89 (1957)
89. Furuichi, S., *Nuovo cimento*, **7**, 269 (1958)
90. Pais, A., and Treiman, S. B., *Phys. Rev.*, **105**, 1616 (1957)
91. Okun', L. B., *Zhur. Eksptl. i Teoret. Fiz.*, **33**, 525 (1957)
92. McDowell, S. W., *Nuovo cimento*, **6**, 1445 (1957)
93. Ivanter, I. G., *Zhur. Eksptl. i Teoret. Fiz.*, **34**, 1202 (1958)
94. Kobzarev, I. Yu., *Zhur. Eksptl. i Teoret. Fiz.*, **34**, 1347 (1958)
95. Bruin, M., Holthuizen, D. J., and Jongejans, B., *Nuovo cimento*, **9**, 422 (1958)
96. Furuichi, S., Sawada, S., and Yonezawa, M., *Nuovo cimento*, **10**, 541 (1958)
97. Gatto, R., *Phys. Rev.*, **111**, 1426 (1957)
98. Streater, R. F., and Taylor, J. C., *Nuclear Phys.*, **7**, 276 (1958)
99. Fujii, A., and Kawaguchi, M., *Phys. Rev.*, **113**, 1159 (1959)
100. Zachariasen, F., *Phys. Rev.*, **110**, 1481 (1958)
101. Matinian, S. G., and Okun', L. B., *Zhur. Eksptl. i Teoret. Fiz.*, **36**, 1317 (1959)
102. Matinian, S. G., *Zhur. Eksptl. i Teoret. Fiz.*, **33**, 797 (1957)
103. Gatto, R., *Prog. Theoret. Phys. (Kyoto)*, **19**, 146 (1958)
104. Ivanter, I. G., *Zhur. Eksptl. i Teoret. Fiz.*, **35**, 111 (1958)
105. Werle, J., *Nuclear Phys.*, **4**, 171 (correction 4, 693) (1957)
106. Furuichi, S., Sawada, S. and Yonezawa, M., *Nuovo cimento*, **6**, 1416 (1957)
107. Okun', L. B., *Nuclear Phys.*, **5**, 455 (1958)
108. Sakurai, J. J., *Phys. Rev.*, **109**, 980 (1958)
109. Werle, J., *Nuclear Phys.*, **6**, 1 (1958)
110. McDowell, S. W., *Nuovo cimento*, **9**, 258 (1958)
111. Okubo, S., Marshak, R. E., Sudarshan, E. C. G., Teutsch, W. B., and Weinberg, S., *Phys. Rev.*, **112**, 665 (1958)
112. Kobzarev, I. Yu., and Okun', L. B., *Zhur. Eksptl. i Teoret. Fiz.*, **34**, 763 (1958)
- 112a. Gell-Mann, M. (Private communication)
113. Gell-Mann, M., and Pais, A., *Phys. Rev.*, **97**, 1387 (1955)
114. Zel'dovich, Yu. B., *Zhur. Eksptl. i Teoret. Fiz.*, **30**, 1168 (1956)
115. Treiman, S. B., and Sachs, R. G., *Phys. Rev.*, **103**, 1545 (1956)
116. Boldt, E., Caldwell, D. O., and Pal, Y., *Phys. Rev. Letters*, **1**, 150 (1958)
117. Okun', L. B., and Pontecorvo, B. M., *Zhur. Eksptl. i Teoret. Fiz.*, **32**, 1587 (1957)
118. Gell-Mann, M., and Pais, A., *Proc. Conf. Nuclear Meson Phys., Glasgow, 1954*, 342 (Pergamon, London, Engl., 1955)

REFERENCES FOR TABLES

119. Sakurai, J. J., *Phys. Rev. Letters*, **1**, 40 (1958)
120. Eisler, F., Plano, R., Prodell, A., Samios, N., Schwartz, N., Steinberger, J., Bassi, P., Borelli, V., Puppi, G., Tocraka, H., Waloschek, P., Zoboli, V., Conversi, M., Franzini, P., Mannelli, I., Santangelo, R., and Silvestrini, V., *Nuovo cimento*, **10**, 150 (1958)
121. Boldt, E., Caldwell, D. O., and Pal, Y., *Phys. Rev. Letters*, **1**, 148 (1948)
122. Sosnovsky, A. N., Spivak, P. E., Prokofyev, Y. A., Kutikov, I. E., Dobrynin, Y. P., *Zhur. Ekspl. i Teoret. Fiz.*, **35**, 1059 (1958)
123. Bardon, M., Lande, K., Lederman, L. M., and Chinowsky, W., *Ann. Phys.*, **5**, 156 (1958)
124. Stevenson, M. L., *Phys. Rev.*, **111**, 1707 (1958)
125. Gell-Mann, M., and Rosenfeld, A. H., *Ann. Rev. Nuclear Sci.*, **7**, 407 (1957)
126. Rosenson, L., *Phys. Rev.*, **109**, 958 (1958)
127. Ali-Zade, S. A., Gurevich, I. I., Dobretsov, Yu. P., Nikol'sky, B. A., and Surkova, L. V., *Zhur. Ekspl. i Teoret. Fiz.*, **36**, 1327 (1959)
128. Robson, J. M., *Can. J. Phys.*, **36**, 1450 (1958)
129. Trebukhovskiy, Y. V., Vladimirovskiy, V. V., Grigoryev, V. K., and Yergakov, V. A., *Zhur. Ekspl. i Teoret. Fiz.*, **36**, 1314 (1959)
130. Burgy, M. T., Krohn, V. E., Novey, T. B., Ringo, G. R., and Telegdi, V. L., *Phys. Rev.*, **110**, 1214 (1958)
131. Šešter, V. M., *Zhur. Ekspl. i Teoret. Fiz.*, **36**, 1299 (1959)
132. Bruin, M., Holthuisen, D. J., and Yongejans, B., *Nuovo cimento*, **9**, 422 (1958)
133. Oneda, S., *Nuclear Phys.*, **4**, 27 (1958)
134. Rosenfeld, A. H., Solmitz, F. T., and Tripp, R. D., *Phys. Rev. Letters*, **2**, 111 (1959)
135. Love, W. A., Marder, S., Nadelhaft, J., Siegel, R. T., and Taylor, A. E., *Phys. Rev. Letters*, **2**, 107 (1959)

THE EXPERIMENTAL CLARIFICATION OF THE LAWS OF β -RADIOACTIVITY¹

By E. J. KONOPINSKI²

Physics Department, Indiana University, Bloomington, Indiana

The understanding of β -radioactivity has undergone a revolution since its last review in this Annual (1). The revolution began with a startling hypothesis, advanced by T. D. Lee and C. N. Yang (2), that nature discriminates between right and left in generating radiations through the weak, "decay," interactions. The hypothesis was first confirmed by observations on nuclear β -decay (3) and has a wide variety of implications for it. It leads to the expectation of phenomena which no one previously suspected of existing, such as polarization of the emitted electrons. New types of experimentation become feasible, increasing the variety of ways in which β -radioactivity may be studied. It is therefore appropriate to begin the present review with a discussion of the basic Lee-Yang hypothesis (subsection, The Overthrow of Parity Conservation).

Even if the Lee-Yang hypothesis had not been verified, the conclusions about the β -radioactivity would have undergone a thorough revision. Quite coincidentally, earlier conclusions concerning the directional correlation of the emitted electrons and neutrinos have been upset [especially through the work of Allen and his collaborators (4)]. The issue so laid open began to be settled by an ingenious experiment devised by Goldhaber, Grodzins & Sunyar (5), as will be related.

The ferment associated with these upsets of old ideas generated a whole series of brilliant experiments in America, Europe, and Israel. The consequence has been an almost "word-for-word" spelling out of the laws of β -radiation, directly by the experimental observations, without the necessity of elaborate mathematical analysis. Just how the "spelling out" proceeds will be reviewed in the section, The Key Experiments. Only after this will consideration of the more mathematical formulations begin.

The theoretical formulation is still essentially Fermi's (1, 6). This poses an interesting question. How can it happen that Fermi's theory can still be retained, even though, for over 20 years, it appeared to give no hint of such now established facts as that the β -electrons are polarized? It will be seen that the theory nevertheless remains largely intact, and moreover, in the latest turn of events, Fermi's original form of it is more closely correct than various modifications tried in the meantime. As Fermi suggested, the decay radiations are generated in proportion to the product of two (four-vector) currents, each current being associated with the intertransformation of a charged and a neutral particle (neutron \leftrightarrow proton, electron \leftrightarrow neutrino).

¹ The survey of literature pertaining to this chapter was concluded March 1, 1959.

² Supported by National Science Foundation during major part of the work.

The change that must be made is to allow only the participation of spin states classifiable as "left-handed" (subsection, The $V-A$ Law). In this classification, "right-handed" antiparticles must be regarded as equivalent to "left-handed" normal particles.

In the sense meant here, a spin state is classified as "left-handed" when the particle's spin is antiparallel to its motion, in the limit that this approaches the velocity of light. The polarization is complete only for the neutrinos, which travel only with the speed of light. Thus, only neutrinos with a left-handed "helicity" are generated (or antineutrinos with right-handed helicity). If the Fermi interactions remain the only sources of neutrinos, then it will presumably never be necessary to describe any with more than half the internal degrees of freedom ascribed to other spin $1/2$ particles. The distinction neutrino-antineutrino can be identified with left-vs. right-helicity. Alternatively, one can drop the neutrino-antineutrino distinction and speak of purely left-handed and purely right-handed neutrinos (the subsection, The Two-Component Neutrino Theory).

The Fermi Theory can be successfully extended to processes other than just nuclear β -decay, by substituting an appropriate current for the (neutron \leftrightarrow proton) or (electron \leftrightarrow neutrino) current. When a (muon \leftrightarrow neutrino) current is substituted for the (neutron \leftrightarrow proton) current, one has the muon-decay. When, instead, the (muon \leftrightarrow neutrino) current replaces the (electron \leftrightarrow neutrino) current, the capture of muons by nuclei can be explained. Pion decay is accounted for as the virtual splitting of the pion into a nucleon-antinucleon pair which then decays by the Fermi processes (see the section, The Universal Fermi Interaction).

Problems remain in connection with the modifications of the nucleonic states caused by their strong interactions with the pion field. Their definitive solution will probably have to await a more completely calculable theory of the pion-nucleon interactions (see the final subsections).

PARITY AND CHARGE SYMMETRY

THE OVERTHROW OF PARITY CONSERVATION

The expectation that nature should indifferently give rise to right- and left-handed situations is embodied in the principle of parity conservation. The expectation is best clarified by contrasting a specific experimental arrangement with another, constructed like a mirror image of the original one. It is well illustrated by the first experiment which actually upset the expectation. This pioneering experiment was performed by Wu, Ambler, Hayward, Hoppes, and Hudson at the National Bureau of Standards (3).

The most essential features of the experiment were these: A sample of radioactive cobalt, Co^{60} , cooled to a very low temperature ($\sim 0.01^\circ\text{K}$.) to avoid disturbance by thermal agitation, was placed within a solenoidal, electrically-conducting coil. Without current in the coil, the Co source emits

electrons isotropically. The startling finding was that with current flowing in the coil more electrons are emitted in one direction, parallel to the axis of the coil, than in the opposite direction. A schematic representation of the finding is depicted in the upper half of Figure 1.

The coiled arrows in Figure 1 represent the direction of the current. The arrows emanating from the source point are intended to represent the pattern of emitted intensities in a qualitative way, greater intensities being represented by longer arrows. The broad arrows on the sides, marked "B," give

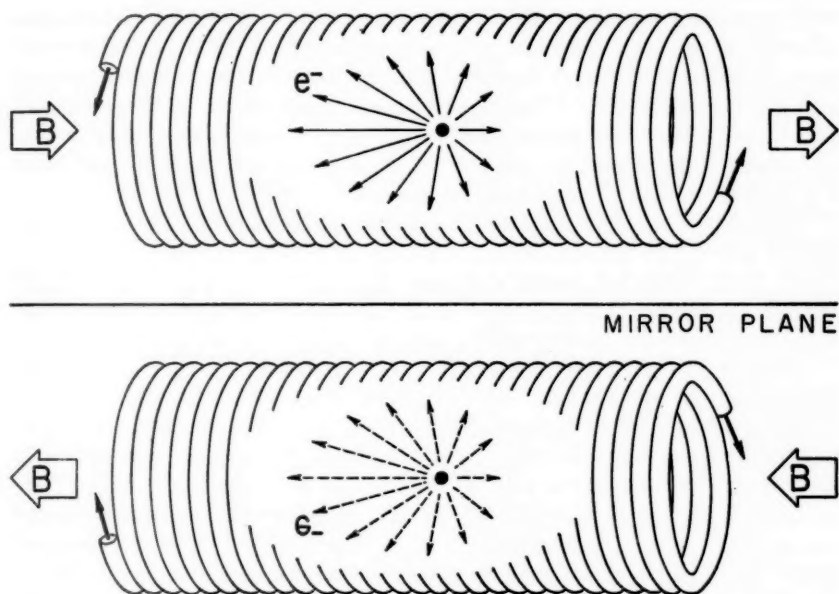


FIG. 1

the direction of the magnetic field within the solenoid. This field is expected to align the spin vectors, I , of the Co^{60} nuclei. One then interprets the finding of this experiment as a preference for electron emission antiparallel to the nuclear spin direction.

Whatever its interpretation, the finding was considered a startling one on the following grounds. Suppose we compare the experimental arrangement in the upper half of Figure 1 with one constructed like its mirror image in the horizontal plane dividing Figure 1, and shown in the lower half of the figure. (Notice that the broad arrows giving the magnetic field directions need not be mirror images, since they merely represent helpful conventions for judging the magnetic effects of the concrete currents.) One is thus led to expect a preponderance of electron emissions leftwards, as

shown, in the mirror-image experiment. What one actually observes is the reverse; the mirrored intensity pattern, as drawn in the lower half of Figure 1, is not the one found! The mirrored experiment can obviously be carried out merely by reversing the current in the original arrangement, and the expectation on this basis is that the intensity pattern should be reversed also. The point is that both expectations should have been fulfilled, and that would have been done by a finding of a left-and-right symmetry of the emissions in the first place. The actual finding of any left-right asymmetry immediately destroyed the expectations based on the mirroring.

The expectation that the mirror-image of an experiment should also represent a correct experiment may be compared to the expectation that the experiment should give the same results if it were done in another room of the same laboratory ("invariance under translation" in homogeneous space), or if the complete experimental set-up were rotated into a new orientation ("invariance to rotation" in isotropic space), or if it were done at a different time ("invariance to translation in time").

The invariance of a system-as-a-whole (an *isolated* system) to translations in time and space requires that its energy and linear momentum be conserved. The invariance under rotations requires conservation of the total angular momentum, around any axis. Similarly, the expectation of invariance under reflections is said to require "parity" conservation.

The effects of parity conservation are not conspicuous in classical phenomena, largely because one is usually concerned with arrangements having a mixed parity. Nevertheless, the parity conservation requirement has always been complied with by all the stronger interactions; only the weak, decay interactions have now been shown to contradict the principle. An instance of parity conservation in the stronger, electromagnetic interactions is provided in the same experiment, described above, which revealed parity non-conservation in the β -decay. The decay of Co^{60} is followed by γ -radiation, and this has the fore-and-aft symmetry expected from a parity-conserving process, according to the analysis above.

The fact that the violations of the parity principle are exceptional gives rise to a new question; Pauli (in a private communication) has put it as "Why should God be only weakly left-handed?" with emphasis on the fact that only in the weak interactions is the "ambidexterity" lost. Some degree of comfort is restored by a suggestion put forward by several authors (7a to d). In effect, the suggestion is that the conception of mirroring presented above is not complete, that the mirror-image of a charge should be conceived as a charge of the opposite sign—and, indeed, that the mirror-image of every particle is its antiparticle. On this view, the correct way to test for invariance under reflections, in the Co^{60} experiment, involves replacing the source with an anti- Co^{60} source! Of course, a test like this is not in immediate prospect, and so the suggestion may seem safe from contradiction; there is, however, a formal chain of inference through which a test is more feasible, and it will be touched upon below.

Meanwhile, one can reassure oneself that the suggested "joint-parity" principle, according to which the mechanical mirroring should be accompanied by a "charge conjugation," does not interfere with the understanding of the ordinary, parity-conserving, electromagnetic interactions. All purely electromagnetic effects are proportional to the product of two charges. A simultaneous sign change of both the "factor" charges changes nothing. Even a lone electron, when decelerated and so emitting radiation, emits it with an intensity depending on its own charge, $-e$, but only through the combination $\alpha = e^2/\hbar c$. Electromagnetic interactions are invariant to charge-conjugation separately; hence adherence to the joint-parity principle still permits them to exhibit ordinary parity-conservation, as formerly understood.

FORMAL ASPECTS OF PARITY AND CHARGE CONJUGATION

In developing a formal description of parity, it is more convenient to speak of "space inversion," i.e. reflections in a point, rather than reflections in a plane mirror like that of Figure 1. It can be seen that inversion through an appropriate point in the plane halving Figure 1 will produce an image differing from the plane reflection drawn only in that it will be rotated through 180° around a vertical axis. Invariance to rotations can be taken for granted (angular momentum is still conserved!), so space inversions really test for the same invariances as do reflections in a plane. At the same time, the formal expression of a space inversion is briefer. One can represent positions in space by vectors \mathbf{r} originating in the inversion point. Then the space inversion can be described as the substitution $\mathbf{r} \rightarrow -\mathbf{r}$. The operation of space inversion will be symbolized by the letter P , so that $Pf(\mathbf{r}) \equiv f(-\mathbf{r})$ when $f(\mathbf{r})$ is any function occurring in the description.

All "polar vectors," i.e. all which must behave as does \mathbf{r} itself, change sign in space inversion. The momentum vector, $\mathbf{p} = m\mathbf{v}$, giving the direction of a given electron emission, is such a polar vector. This is because the velocity $\mathbf{v} = d\mathbf{r}/dt$ must change sign when \mathbf{r} does: $P\mathbf{v} = -\mathbf{v}$.

The arrows standing for the magnetic field, \mathbf{B} , represent examples of "axial vectors," ones with a behavior opposite to that of polar vectors under space inversions: $P\mathbf{B} = +\mathbf{B}$. The magnetic field must keep a definite screw-sense relative to the circulating current, once a specific convention for representing it is adopted. Another example of an axial vector is the orbital angular momentum $\mathbf{L} = \mathbf{r} \times \mathbf{p}$, of an electron about the inversion point. Under space inversions, while $P\mathbf{r} = -\mathbf{r}$ and $P\mathbf{p} = -\mathbf{p}$, $P\mathbf{L} = (-\mathbf{r}) \times (-\mathbf{p}) = +\mathbf{L}$.

The effect of the magnetic field on the Co^{60} nuclei is to align their intrinsic spins, \mathbf{I} (known to be five units in magnitude), along the direction of the field. Nuclei without spin (i.e. having $I=0$) could not show any kind of anisotropy; it is only through polarizing nuclei already possessing individual axes like \mathbf{I} that the magnetic field can have appreciable influence on the

directions of the high-speed electrons. The intensity patterns which are found can be described as proportional to

$$1 + A\hat{I} \cdot \mathbf{v}/c = 1 + A(v/c)\cos\theta_{eI}, \quad 1.$$

where \hat{I} is the unit vector in the direction of the nuclear spin I , while θ_{eI} is the angle of the electron's direction with the spin axis. When the coefficient A is defined through the expression 1, $A = -1$ is the conclusion for the Co^{60} experiment.³

We find a component of intensity proportional to $I \cdot \mathbf{v}$. Note that I is an angular momentum, like L above; hence $PI = +I$ and $PI \cdot \mathbf{v} = -I \cdot \mathbf{v}$. Thus, we find a component of intensity, a number of observed particles, which changes sign under space inversions, despite the fact that a space inversion can be regarded as a mere change from a right- to a left-handed frame of reference. The number in question is not an ordinary scalar, but a pseudoscalar. It is characteristic of parity nonconserving processes that they generate pseudoscalar components of intensity.

We may represent parity conservation by $P=1$, to indicate that operation with P , like multiplication with unity, changes nothing. Then $P \neq 1$, as for $P(1 + A\hat{I} \cdot \mathbf{v}/c) = 1 - A\hat{I} \cdot \mathbf{v}/c$ when $A \neq 0$, will represent a parity nonconserving result.

We may also introduce a "charge conjugation operator," C , and represent invariance to the exchange of particles with antiparticles by $C=1$. The joint-parity principle, suggested above, can be symbolized by $CP=1$. Since $P \neq 1$ has been found for the β -decay, the joint-parity principle implies $C \neq 1$ for such processes; there should be no invariance under charge conjugation alone. As mentioned above, the electromagnetic interactions have a higher degree of symmetry than the decay interactions; for them, not only is $CP=1$, but also $C=1$ and $P=1$, individually.

To verify the joint-parity principle for the decay interactions, it will be necessary to find an experimental verification of noninvariance to charge conjugation, i.e. $C \neq 1$; more than that, experiments will have to show that $C \neq 1$ in such a way that it complements $P \neq 1$, to give $CP=1$.

To avoid having to use antinucleon sources in testing behavior under charge conjugation, one must resort to longer chains of inference. A useful one is provided by the so-called "CPT theorem" (8a, b, c). This theorem establishes a relation between C , P , and a third operation T called "time reversal," with the effect $Tf(t) = f(-t)$, when operating on any element of description in time. The burden of the theorem is that $CPT=1$ is a conse-

* It is an overstatement of the actual experimental accuracy (3) to say that the angular distribution 1 was measured and that $A = -1$ was found. Actually measured was simply the ratio of intensities observed along the axis of the magnetic field, before and after reversing the current. The result was consistent with $A = -1$. We do not take the space to present an evaluation of the accuracy achieved here because our analysis will require only semiquantitative use of the result.

quence of the ordinary Lorentz-invariance to the proper transformations in space-time.

On the basis of the *CPT* theorem, one will have verified the joint-parity principle, $CP=1$, if one shows that the experiments require $T=1$, i.e. invariance under time-reversal. A discussion of how experiments on β -decay are able to check this will be left until after the detailed formalism is introduced. The next section will first treat those points which can be profitably discussed before the detailed formalism is expounded.

THE KEY EXPERIMENTS

All the nuclear β -processes can be represented in the "Normal Relation":

$$p + e^- \leftrightarrow n + \nu. \quad 2.$$

According to the conventional nomenclature, each symbol here stands for a "normal" particle, as against an antiparticle. In orbital electron (e^-) capture, a proton (p) of the nucleus is transformed into a neutron (n), with the emission of a monoenergetic neutrino (ν). In positron (e^+) emission, the electron is captured out of the ambient "vacuum sea of negative-energy electrons," thus producing a "hole" which is observed as a positron. In negatron emission, a neutron captures a neutrino out of a "vacuum sea," to produce an antineutrino ($\bar{\nu}$). When a pair of "leptons"⁴ is emitted, i.e. (e^+ , ν) or (e^- , $\bar{\nu}$) as in the last two processes, then these particles share the energy released (W_0) on a largely statistical basis, so that one observes a continuous spectrum of electron energies, with an "end-point" kinetic energy $W_0 - mc^2$. All the facts of these descriptions, as well as many more which will be introduced when needed, have been established for decades; hence the "key experiments" responsible for them will not be reviewed here. It is the experiments which have revealed facts which are new since the last review of the subject (1), which will be given more detailed attention.

FERMI AND *GT* RADIATIONS

A salient characteristic of the β -processes is that each entails the participation of four "fermions," i.e. particles of spin 1/2. When a pair of leptons⁴ is emitted, they form a state which can be analyzed into a "singlet" and a "triplet." In the singlet substate, the individual lepton spins are antiparallel, so that the total spin is $S=0$. In the triplet state, they are parallel and $S=1$. The total spin S is all the angular momentum which is carried away from the nucleus in the so-called "allowed" cases of β -decay. To radiate orbital angular momentum (L) as well, the lepton wave must be distributed so that its mean distance from the nucleus is large compared to the nuclear radius for the momenta available in nuclear β -decay ($L = r_e \times p_e + r_\nu \times p_\nu$). When the main body of the wave must thus be produced at a substantial

⁴ "Lepton" is a generic name for any spin $\frac{1}{2}$ particle lighter than a nucleon.

distance from its source, its rate of production is small, and completely negligible in cases of allowed decay.

Allowed ($L=0$) transitions occur only when a final nuclear state (differing from the initial one by an $n \leftrightarrow p$ substitution) is energetically available, having an angular momentum (nuclear spin) $I_f = I_i + S$. The singlet radiation obviously requires $I_f = I_i$; this is known as a "Fermi selection rule" and a decay interaction which generates singlet radiation in allowed decay is known as "Fermi coupling." In triplet radiation $I_f = I_i + 1$, and so $I_f = I_i$ or $I_i \pm 1$, in magnitude. The requirement $\Delta I = I_f - I_i = 0, \pm 1$ is known as a "Gamow-Teller," or "GT," selection rule. Clearly, one cannot achieve an angular momentum balance with triplet radiation if both $I_i = I_f = 0$, even though $\Delta I = 0$ in this case. Thus, a prohibition of $0 \rightarrow 0$ transitions is also part of the GT selection rules. This circumstance permits one to have cases of pure Fermi radiation ($0 \rightarrow 0$ transitions), as well as the cases of pure GT radiation in which $\Delta I = \pm 1$. (We now see that the $5 \rightarrow 4$ transition of Co^{60} yields pure GT radiation.) The allowed, $\Delta I = 0$ cases in which $I_i \neq 0$ consist of both Fermi and GT radiations, in proportions depending on the relative ease with which the requisite final nuclear states can be formed by the Fermi and GT couplings, respectively. Anyone acquainted with radiation theory will recognize the factors here mentioned as ones usually embodied in so-called "source moments."

Because singlet and triplet states are orthogonal to each other, one expects the two types of radiation not to interfere with each other, when both are emitted as in the allowed $\Delta I = 0$ cases. This is a valid expectation as long as the formation of the states observed is not restricted, as when the observations are limited to nuclei with a given polarization. (When the Co^{60} experiment, above, is repeated for a case like Mn^{55} , which undergoes a $6 \rightarrow 6$ transition (9a, b), then Fermi-GT interference occurs. Fermi radiation can contribute to the anisotropy of the electron's angular distribution only through such interference; this is because allowed Fermi radiation, by itself, takes no angular momentum from the nucleus, hence is uninfluenced by its spin direction.) Ordinary sources, of unpolarized nuclei, yield only non-interfering superpositions of the Fermi and GT radiations.

One should find the relative strengths of the Fermi and GT couplings by comparing decay rates of nuclei which are allowed to emit different relative amounts of singlet and triplet radiations. The decay rates also depend on other factors, extraneous to the primary coupling strengths—notably, on the particular energy available, and on the particular nuclear coulomb field affecting the electron, in any given case. Ways to correct for such incidental differences have long been known (1); the standard way is to compare " ft -values," = "comparative half lives," instead of the directly observed decay rates. Thus, the observed half life of the neutron (10) is 11.7 ± 0.3 min., while its "comparative half life" is $(ft)_n = 1170 \pm 35$ sec. The purely Fermi, $0 \rightarrow 0$, transition of O^{14} has $(ft)_0 = 3160 \pm 12$ sec. (11a, b).

The coupling strengths of the Fermi and GT interactions are represented by the squares of "coupling constants": $|C_F|^2$ and $|C_{GT}|^2$, respectively. Both contribute to the $I_i = \frac{1}{2} \rightarrow I_f = \frac{1}{2}$ neutron decay. A given neutron has only one final spin state available when it produces the spinless Fermi radiation: a proton of the same orientation as the neutron. However, when the neutron generates GT radiation, one finally has $S=1$ with three possible orientations and, with each, the two possible orientations ($\pm 1/2$) of the proton; these six states are produced from both possible orientations of the initial neutron, hence one has three final states per given neutron, resulting from GT radiation. Now one expects a decay rate proportional to

$$(ft)_n^{-1} \sim |C_F|^2 + 3|C_{GT}|^2 \quad 3.$$

for the neutron.

On the same scale, one must give a weight 2 to the purely Fermi radiation of O^{14} ; the initial spin $I_i=0$, here, has been analyzed to be a resultant from two equivalent protons in the O^{14} nucleus. Either of these may transform, in making the same energy available for the β -process. Consequently,

$$\frac{(ft)_n^{-1}}{(ft)_o^{-1}} = \frac{|C_F|^2 + 3|C_{GT}|^2}{2|C_F|^2} = \frac{3160 \pm 12}{1170 \pm 35}.$$

Supporting the O^{14} datum are several analogous $0 \rightarrow 0$ cases, e.g. Al^{26} with $ft = 3050 \pm 60$ sec. and Cl^{34} with $ft = 3110 \pm 70$ sec. (11a, b). The conclusion is that

$$|C_{GT}|^2/|C_F|^2 = 1.47 \pm 0.06. \quad 4.$$

Explaining the deviation of this value from unity is a concern of many theorists (12a to d).

THE ELECTRON POLARIZATION

In the preceding section we briefly summarized what is known about the relative orientation of the electron and neutrino spins. Now, we inquire into the orientation of the electron's spin relative to its own direction of motion, i.e. the polarization of the electron wave.

That the negatrons emitted by Co^{60} must have a net polarization became evident as soon as it was discovered that they have a preferred direction of emission. This direction was found, as described above, to be backwards to the initial nuclear spin, $I_i=5$. One unit of angular momentum had to be radiated ($I_f=4$), hence the total radiated spin, $S=1$, is directed preferentially opposite to the electron's velocity. A "left-handed," longitudinal polarization is the result for the negatrons, at least in the GT radiation emitted in this case.

The difficult, initial polarization of the nuclei, which was utilized in the Co^{60} experiment, is fortunately unnecessary for the study of longitudinal electron polarization. Actually needed is only a definition of the electron's velocity direction, v , which is obtained by the position of the counter relative

to the unpolarized source, and then a detection of the spin orientation relative to v . Since the direction of motion serves as the "quantization axis" for the spin orientations, $\pm \frac{1}{2}$, one has polarization if there is an excess of either of these two orientations, and a nonvanishing excess is then appropriately described as a right- or left-handed longitudinal polarization, respectively. Slightly more formally, one can speak of a spin axis direction given by the Pauli unit vector σ , and then, on the model of the relation 1, one might expect a distribution proportional to:

$$1 + \alpha \sigma \cdot v/c, \quad 5.$$

where α is a constant coefficient characteristic of the case of decay. For Co^{60} , because $A = -1$ is nominally found for relation 1, one would expect (and does find below) that $\alpha = -1$, the left-handed polarization of the Co^{60} negatrons already alluded to. Actually measured, however, are the excesses or deficiencies of spin orientations parallel, vs. antiparallel, to the motion (eigenvalues, $\sigma_z = \pm 1$), i.e. the polarization:

$$P = \frac{d\lambda_+ - d\lambda_-}{d\lambda_+ + d\lambda_-} = \alpha \frac{v}{c}. \quad 6.$$

Here, $d\lambda_+$ and $d\lambda_-$ are the rates at which the two spin orientations appear. The more formal expression 5 only has the advantage that it exhibits the characteristic pseudoscalar character of an intensity component which violates parity conservation. Thus, the detection of the electron polarization also served to destroy the old parity principle, for the decay interactions.

Frauenfelder and his colleagues at Illinois (13) seem to have been the first to detect the existence of the β -electron polarization. They did it first for the pure GT , negatron radiation of Co^{60} . The method of polarization analysis which they undertook works only for transverse polarizations, in a way indicated in the right half of the diagram in Figure 2. Negatrons with "upward" spins, incident on the scatterer as indicated, are preferentially scattered to the right. Such rightward orbits have orbital angular momenta directed "down," opposite to the electron spin. It is known from atomic spectroscopy that there is an appreciable "spin-orbit coupling," in the fields of heavy atoms like gold, which makes orbits with opposing spin and orbital momenta more stable, i.e. the coupling then adds to the attractive force of the nucleus for the electron. The increased force results in increased deflections of the appropriately oriented electrons. The experiment is actually carried out by comparing the numbers scattered to counters placed symmetrically, to the left and right of the path (at $-\vartheta_R$, as well as $+\vartheta_R$, in the diagram).

To use the type of polarization analysis just outlined, the investigators had first to change the electron polarization from a longitudinal to a transverse one. They did this by deflecting the beam through roughly 90° by electrically charged plates, as indicated in Figure 2. The spin is essentially

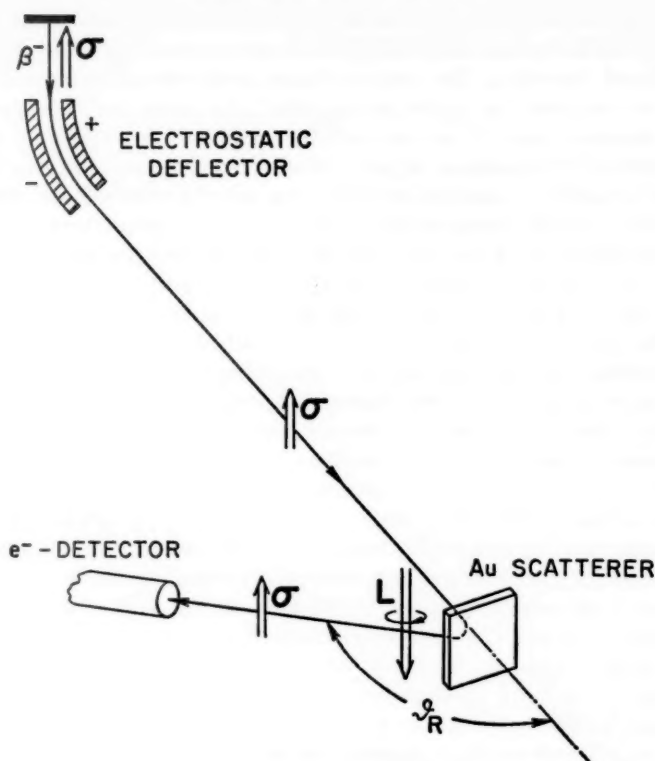


FIG. 2

unaffected by electrostatic forces; hence the direction of motion is turned relative to the spin direction until the two are transverse to each other.

The above method was also used by groups in Holland (14) and France (15), while groups in England (16) and Russia (17) used crossed electric and magnetic fields to twist the spin from the longitudinal into the transverse orientation, without deflecting the beam direction. A group in Israel (18) used 90° deflections in the electrostatic fields of light atoms to turn the beam, without appreciably turning the spin. Here, a double scattering is needed (first in Al, then Au), but the consequent loss of intensity is partially offset by using first-scatterings from a whole semicircular strip of Al. Electrons entering and emerging on opposite sides of the diameter, in going from source to final scattering, will have been deflected through 90° at any part of the strip.

In some experiments (19a, b), electron-electron, instead of electron-nuclear, scattering was used for the polarization analysis. One can distin-

guish the electron-electron scattering from the much more intense nuclear scatterings by detecting the knocked-out target electron in coincidence with the scattered β -particle. The polarization is analyzed by using magnetized iron as the scatterer; as might be expected, the scattering is largest when the two electrons meet in an antiparallel state. One can therefore find the polarization of the incident β -particle by observing the difference in the scattered intensity caused by reversing the magnetization from parallel to antiparallel with the incident beam. Actually, one cannot arrange to have the magnetization lie in the same line as the beam. The magnetized scatterer must be thin if both the colliding electrons are to emerge for the detection, and one cannot force a magnetization normal to the plane sides of a thin sheet. The sheet is magnetized parallel to itself instead, and the β -particles are allowed to have oblique incidence on it. Most of the effect still remains, under these conditions. The electron-electron, or "Møller scattering," method has the virtue that it applies directly to longitudinal polarizations; no preliminary spin-twisting is needed.

Goldhaber introduced the method of observing the "bremsstrahlung" radiated by the β -particles as they are decelerated in a target material. It is not surprising to learn that radiation from stopping a longitudinally spinning particle, as observed in a forward direction, is circularly polarized. The sense of the polarization will be the same as the sense of the spin of the decelerated electron. The analysis is reduced to a matter of detecting the circular polarization of the γ -ray. How that is done will be outlined in connection with the description of the Goldhaber-Grodzins-Sunyar experiment, below.

The γ -rays emitted by a nucleus left in an excited state after β -decay will also be circularly polarized. Study of β - γ correlations with detection of the circular polarization can reveal more about the β -process than just the spin state of the β -particle. Several groups (20a to d) have made such studies.

The last method has the virtue that it works equally well for negatrons and positrons. For the latter particles, the bremsstrahlung method is modified to the detection of the radiation from the positron-electron annihilations in flight (21a, b). The annihilation quanta are circularly polarized, like the bremsstrahlung. One can avoid having to analyze the circular polarization by simply measuring the difference in rates of annihilation in magnetized iron, caused by reversing the magnetization in the iron (22a, b). Finally, one can study the formation of positronium (atoms of $e^+ + e^-$) in a magnetized gas (23). Positronium formed with the positron and electron spin antiparallel ("singlet" state) decays by annihilation 30 times as rapidly as the "triplet" state in which the particles are parallel. The radiated "line width" is broader for the shorter-lived state and so one can detect the polarization of the positrons by finding the effect on the line width caused by reversing the magnetic field applied to the capturing electrons.

The result of the intense activity was the showing that in both Fermi and *GT* radiation, whether pure or mixed, negatrons are left-handedly and positrons right-handedly polarized:

$$\mathcal{P} = \pm v/c \quad (\alpha = \pm 1) \quad \text{for } e^{\pm} \quad 7.$$

within 2 per cent or so. The polarization tends to disappear for slow electrons (as $v \rightarrow 0$) because the process loses the directionality needed to define a "quantization axis." One can have a complete polarization ($\mathcal{P} = \pm 1$) only for particles without rest-mass, like neutrinos, which travel with light velocity ($v/c \rightarrow 1$).

The finding of $\mathcal{P} = -v/c$ for the *GT*, negatron radiation of Co^{60} has already been mentioned (13, 14). Pure *GT* positrons were obtained from Na^{22} (23) and the positive polarization found. Pure Fermi radiation is obtainable only from positron emitters; the positive polarization was found (21) for both Ga^{66} and Cl^{34} . Finally, measurements were made on numerous cases of mixed Fermi and *GT* radiations (13, 14, 16a, 21b). All have finally become consistent with the conclusion 7.

The result that negatrons and positrons have opposite polarizations is to be expected from the particle-antiparticle relationship, as discussed in connection with the Normal Relation 2 of the β -processes. The difference actually exhibits the noninvariance of the β -processes under charge-conjugation.

THE ELECTRON-NEUTRINO CORRELATION

The information reviewed so far bears on the quantities $\hat{\mathbf{l}} \cdot \mathbf{v}/c$, $\hat{\boldsymbol{\sigma}} \cdot \mathbf{v}/c$ and $\hat{\boldsymbol{\sigma}} \cdot \hat{\boldsymbol{\sigma}}_n$. The first two expressions represent the fact that something has been learned about the electron's emission direction and about its spin orientation relative to that direction (polarization). To be considered next are the corresponding properties for the neutrino. As indicated, something has already been learned about the neutrino's spin orientation σ_n relative to that of the electron; that was implicit in the comparison of the Fermi and *GT* radiations. There remains the problem of the neutrino's emission direction, which will be represented by a unit vector $\hat{\mathbf{q}}$ to play the same role as did \mathbf{v}/c for the electron, since the neutrino has the velocity of light. The study of \mathbf{q} , together with the information about $\hat{\boldsymbol{\sigma}} \cdot \hat{\boldsymbol{\sigma}}_n$, should immediately permit conclusions about $\hat{\boldsymbol{\sigma}}_n \cdot \hat{\mathbf{q}}$, i.e. about the neutrino's polarization.

Consider, first, the expectation for pure Fermi radiation under the alternative assumptions that the neutrino will have a right-handed polarization or a left-handed one. In order to state the conclusion for neutrinos, rather than antineutrinos, we should consider cases of positron emission. (Our expectations for negatron-plus-antineutrino emission will follow in the way indicated in the discussion of the Normal Relation 2.) Fermi radiation will consist of positrons, which we now know to be right-handed in a degree v/c , and neutrinos with antiparallel spins. If the neutrino is right-handed,

therefore, it will be preferentially emitted in a direction opposite to that of the positron: a negative correlation between the positron and neutrino emission directions should result. A similar argument will yield the expectation of a positive correlation for left-handed neutrinos emitted in Fermi radiation. These results are represented in Figure 3.

An interaction which yields the Fermi radiation with a right-handed neutrino is known as the scalar (S) coupling, while one yielding a left-hand neutrino is called the vector (V) coupling. If both types of coupling should

FERMI RADIATION

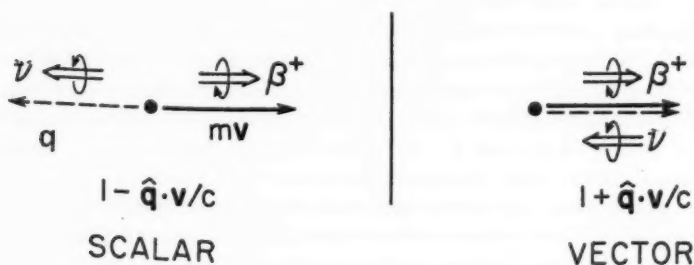


FIG. 3

exist, then the coupling strength introduced earlier should be written: $|C_F|^2 = |C_S|^2 + |C_V|^2$. In general, a positron-neutrino (or electron-anti-neutrino) correlation,

$$\sim 1 + a_F(v/c) \cos \vartheta_{\nu\bar{\nu}}, \quad 8.$$

may be expected, with

$$a_F = (|C_V|^2 - |C_S|^2) / (|C_V|^2 + |C_S|^2), \quad 9.$$

for Fermi radiation. A positive correlation a_F will imply a resultant left-handed polarization of the neutrinos.

The argument for pure GT radiation proceeds in exactly the same way. This time, positrons and neutrinos with parallel spins must be produced; hence a positive correlation would imply a right-handed polarization of the neutrinos. An interaction yielding right-handed neutrinos (with the right-handed positrons), in GT radiation, is called the tensor (T) coupling, while a pseudovector (A) coupling produces left-handed neutrinos. We obtain a correlation coefficient,

$$a_{GT} = \frac{1}{3} (|C_T|^2 - |C_A|^2) / (|C_T|^2 + |C_A|^2), \quad 10.$$

with $|C_T|^2 + |C_A|^2 = |C_{GT}|^2$, in general. The extra factor $\frac{1}{3}$ enters because the possibility of three orientations for the total spin $S=1$ of the GT radiation tends to wash out the correlation.

No experiment has yet been feasible with pure Fermi emitters; hence superpositions $F+GT$ must be considered. We introduce the "Fermi frac-

tion," x , giving the part of the total radiation consisting of Fermi radiation. An example of how it can be evaluated is provided by the case of the neutron; from the expression 3,

$$x_n = |C_F|^2 / |C_F|^2 + 3|C_{GT}|^2. \quad 11.$$

Thus $x_n = 1/4$, if the Fermi and GT coupling strengths are equal; if one takes seriously the deviation from unity in the ratio 4, then $x_n = 0.20 \pm 0.02$. For

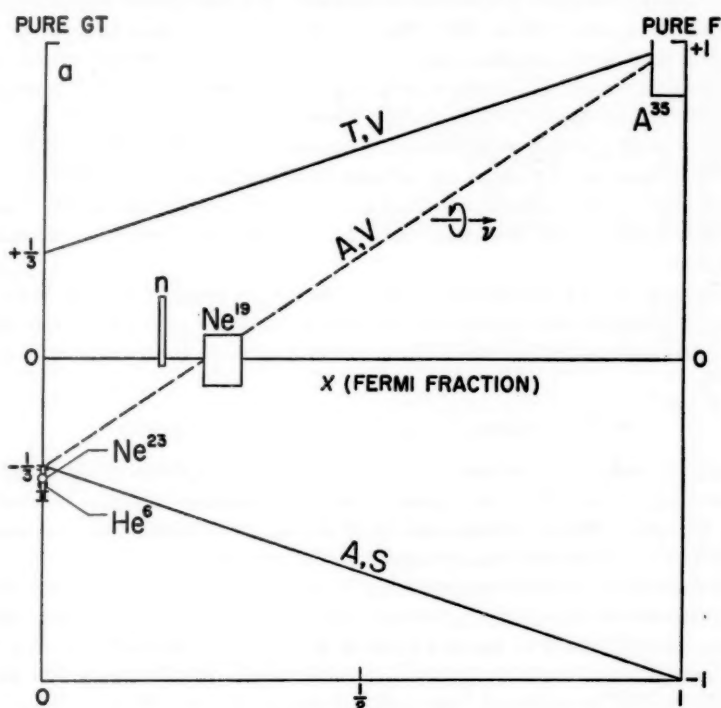


FIG. 4

Ne^{19} , one has $x = 0.28 \pm 0.03$ (11a, b), and A^{35} is practically a pure Fermi emitter with $x = 0.95 \pm 0.05$ (24). In terms of x , we expect a correlation coefficient:

$$a = a_F x + a_{GT}(1 - x), \quad 12.$$

for cases of Fermi and GT superposition. The comparison of cases with various Fermi fractions, x , should yield a straight line when a is plotted against x . Since $-1/3 < a_{GT} < +1/3$ while $-1 < a_F < +1$, the straight line should lie in the region delimited in Figure 4. The points and rectangles labelled Ne^{19} , He^6 , n^0 , A^{35} and Ne^{23} represent, within their margins of uncertainty, results of the most reliable electron-recoil correlation measurements.

The neutron datum is Robson's (25). All the others used in Figure 4 are

the latest results obtained by Allen *et al.* (26). They leave little doubt that $a_F = +1$ and $a_{GT} = -\frac{1}{2}$, characteristic of the vector (V) and pseudovector (A) couplings, respectively. According to the analysis above, this signifies that the neutrinos are left-handed (antineutrinos right-handed) in nuclear β -emissions.

The neutron measurement was obtained by 1955, and there were data on Ne^{19} even earlier (27a, b, c), less accurate but not critically different from the new result of Figure 4. At that early time, the only other datum available was that $a_{GT} \approx +\frac{1}{2}$ for He^6 (28a, b). This was the main reason for the conclusion that the β -coupling has an ST , rather than VA , form, which held sway for some years. This conclusion was first upset by the A^{35} measurements, at the University of Illinois (4). Then a demonstration that pure GT radiation actually produces left-handed neutrinos was offered by Goldhaber, Grodzins & Sunyar (5), using an independent technique to be described in the next section. Meanwhile, a critical re-evaluation of the early He^6 experiment has satisfactorily accounted for what is now considered its erroneous result (28b).

Nuclear recoil measurements on Li^8 (29a, b) are not included in Figure 4 because the final nucleus breaks up into two α -particles, and this fact renders the analysis somewhat different. It is consistent with the conclusions from Figure 4.

THE GOLDHABER-GRODZINS-SUNYAR EXPERIMENT

These investigators devised a way of inferring the nuclear recoil direction by observing the emission of a γ -ray from the recoiling nucleus, instead of relying on the difficult techniques of observing the small nuclear recoils directly as in the experiments reported in the preceding section.

The observations were made on Eu^{152} , an isomer with spin $I_i = 0$, which decays into Sm^{152} by capturing orbital electrons. Some of the decays leave the daughter nucleus in an excited state of spin $I_f = 1$, and are distinguishable by the coincidental emission of the characteristic γ -ray (energy, 961 kev), which de-excites the nucleus into its ground state $I_0 = 0$. The pertinent portions of the decay scheme are shown in the energy level diagram of Figure 5.

The diagrams in the right half of Figure 5 represent the alternatives for the neutrino- and subsequent γ -emissions, corresponding to the tensor (right handed neutrino) and pseudovector (left-handed neutrino) couplings. Only these could generate the pure GT transition here. The resultant nuclear spin, $I_f = 1$, must be antiparallel to the neutrino spin, since the neutrino has only the aid of $\frac{1}{2}$ unit of captured electron spin, in conserving the initial angular momentum $I_i = 0$. This means that if the neutrino is left-handed (case A) the nuclear spin I_f must be antiparallel to the nuclear recoil direction. The converse would be true for right-handed neutrinos (case T).

Next, consider the "forward" γ -rays, i.e. those emitted into the same direction as the nuclear recoil. They must carry away the entire unit of the nuclear angular momentum in order to leave it in the $I_0 = 0$ ground state.

They must, therefore, be left-circularly polarized in the case of the left-handed neutrino emission and right-circularly polarized if they follow upon a right-handed neutrino emission. One is, therefore, left with the problem of distinguishing the "forward" γ -rays, without the necessity of observing the nuclear recoil direction, and then finding the sense of the circular polarization of these γ -rays.

The investigators restricted their observations to the "forward" γ -rays by requiring them to undergo resonance scattering in order to enter the de-

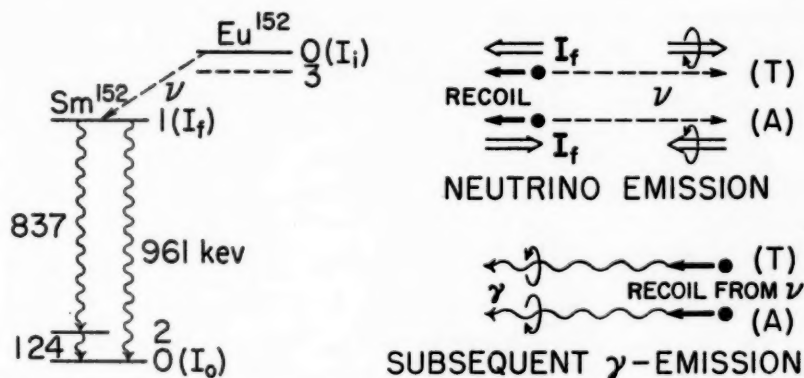


FIG. 5

tector and be recorded. Atoms of the same species as the daughter, Sm^{152} , were used for the scattering, which becomes anomalously large when the γ -ray energy "resonates" with the transition from the normal state ($I_0=0$) to the $I_f=1$ excited state. Resonance requires a very precise matching of the excitation energy supplied by the incident γ -ray with the 961 keV gap between the nuclear levels. Part of the incident γ -energy must be spent in supplying recoil energy to the target nucleus, and so only the "forward" γ -rays which bring the energy of recoil from the neutrino, besides the 961 keV excitation energy, can produce resonance. The resonance scattering consists of a resonance absorption and immediate re-emission; hence the scattered γ -rays will consist of an 837 keV, as well as the 961 keV, component (see the level scheme in Fig. 5). Both were observed in the detector.

The problem remaining is to detect the sense of the circular polarization which the γ -rays possess before they undergo the scattering. The method used for this was devised earlier, to detect the circular polarization of "bremsstrahlung" emitted during the deceleration of polarized electrons (see The Electron Polarization). Before being allowed to approach the resonance scatterer, the γ -rays were forced to pass through magnetized iron. When the magnetic field in the iron has the same direction as the γ -ray beam, the left-circularly polarized γ -rays are transmitted more readily than right-circularly

polarized ones. Thus, by observing the effect of reversing the magnetic field, on the transmitted γ -ray intensity, one can decide whether the γ -rays had been right- or left-circularly polarized.

The direction of the magnetic effect can be understood roughly as follows. Electrons spinning antiparallel to the γ -ray angular momentum can intercept it the more easily because they can absorb the γ -angular momentum simply by flipping their own spins. The electron spins are parallel to the angular momentum of left-circularly polarized γ -rays when the magnetic field has the same direction as the beam.⁵ This was the field direction in which the better transmission was actually found, showing that the "forward" γ -rays from Eu^{152} are left-circularly polarized.

The conclusion of the Goldhaber-Grodzins-Sunyar experiment is that left-handed neutrinos are emitted in pure GT β -transitions. Quantitatively, they found about 68 per cent as large an effect as to be expected with a complete left-circular polarization of the γ -rays. However, there are enough mechanisms for depolarization in the experiment for this result to be entirely consistent with a complete left-handed polarization of the neutrino as concluded in the preceding subsection.

THE DECAY OF POLARIZED NEUTRONS

The experiments reviewed so far have revealed that both the negatrons and neutrinos emitted in β -decay are formed in left-handed states of polarization, i.e. longitudinally polarized, with spin antiparallel to the direction of motion. Antineutrinos and positrons correspondingly emerge right-handed, in consistency with the antiparticle relationships outlined under 2. Nothing has been concluded so far as to any possible polarizations of the nucleons as they participate in β -processes. To obtain the most direct information about this, one should observe a process in which only one nucleon is involved: the free neutron decay.

One would like to observe directly the polarization of the product proton, relative to its own direction of motion, as it was done for the electron. However, for the recoil proton, $v/c \lesssim 0.04$, so its direction of motion makes a very poor "quantization axis." One must be satisfied with less direct inferences about the proton polarization.

Information can be gained if one starts with neutrons of a definite polarization. Observations on such neutrons were made at the Argonne National Laboratory (30) and at Atomic Energy of Canada, Ltd., laboratory in Chalk River, Ontario (31). Both groups used thermal neutron beams from reactors. The Argonne group polarized the neutrons by reflecting them from magnetized cobalt mirrors. The Chalk River group obtained partially

⁵ The oversimplified discussion, here, applies clearly only to the forward scattering, whereas the total cross-section is involved in a transmission experiment. However, at the energies pertinent to the experiment here, the scattering is predominantly forward. I am indebted to Dr. M. Goldhaber for pointing this out to me.

polarized neutrons by filtering the beam through magnetized iron, which preferentially scatters out the neutrons with spins parallel to the magnetic field, leaving primarily antiparallel ones. The neutron decays are identified by requiring coincidences between an electron detector and a proton detector.

One can see that such observations define three vectors, at least roughly: the neutron spin vector $I = \frac{1}{2}\hbar\hat{I}$; the electron velocity v ; the proton recoil direction. The last of these is usually replaced, in theoretical considerations, by the antineutrino direction, as given by the unit vector \hat{q} . It is of course deducible from momentum conservation.

The observed intensity must be a scalar, with pseudoscalar components proportional to I . By forming all possible, independent, scalar, and pseudoscalar products of the three vectors involved, one is led to expect the intensity to be proportional to:

$$1 + a\hat{q} \cdot v/c + \hat{I} \cdot [Av/c + B\hat{q} + Dv \times \hat{q}/c]. \quad 13.$$

One expects the largest, "first-order" effects, characterizing allowed transitions, to be linear in each of the vectors; hence the correlation coefficients, a , A , B , and D are assumed to be constants.

The electron-neutrino correlation, a , had been measured some years ago, by Robson at Chalk River, using an unpolarized neutron beam ($\hat{I}=0$). It has already been reported, above, as having a near-vanishing value (Fig. 4).

The coefficient, A , giving the electron's angular distribution relative to the neutron spin axis \hat{I} was measured by one of three experiments carried out at the Argonne Laboratory. In this "Experiment A," the electron and proton detectors were placed on opposite sides of the neutron beam so that the line from one to the other was parallel to the polarization vector I . By finding the effect of reversing the polarization, one is finding the "fore-and-aft" asymmetry of the electron emissions relative to the nuclear spin, exactly as in the Co^{60} experiment described first. The recorded electron directions v are parallel to I ; hence the term $\sim A$ in expression 13 is maximized, while the term $\sim D$ has a vanishing average. Antineutrinos both parallel and antiparallel to I contribute to the registered events, so the term $\sim B$ is far from its maximum, but correction for it is necessary and was possible after completion of the "Experiment B," to be considered next. The final conclusion from "Experiment A" was

$$A \approx -0.11 \pm 0.02. \quad 14.$$

In changing from "Experiment A" to "B" the neutron polarization was turned through 90° , relative to the line of the counters. The final arrangement is represented schematically in Figure 6. The neutron beam was normal to the plane represented by the plane of the figure, and has a thin rectangular, cross section as indicated. The neutron polarization was parallel to the long side of the cross-sectional rectangle. A system of slits was interposed between beam and proton detector for this experiment. The slits were

slanted downward so as to accept only protons recoiling from antineutrino emissions preferentially upward.

The bias for antineutrinos emitted parallel to the neutron polarization maximizes the effect of the term $\sim B$, which measures the antineutrino angular distribution just as A measures the electron's angular distribution, in the intensity expression 13. Now, the effect of reversing the neutron polarization measures B , and the result obtained was:

$$B \approx 0.88 \pm 0.15. \quad 15.$$

Thus, the antineutrino's direction is almost fully correlated with the neutron spin direction ($B \rightarrow +1$) in contrast to the near-isotropy of the electron's

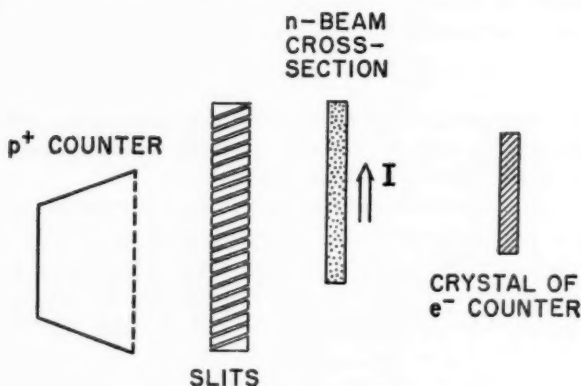


FIG. 6

direction, relative to the antineutrino ($a \rightarrow 0$), as well as relative to the neutron spin ($A \rightarrow 0$).

In the "Experiment D," as it was carried out at the Argonne Laboratory, the same arrangement was used as in "Experiment B" of Figure 6, except that the slit system was turned through 90° around its axis with the electron counter. Now, the proton recoils admitted by the slits correspond to antineutrinos preferentially directed normally to the plane formed by the two vectors: the neutron spin I and the electron velocity v . Thus, $\hat{n} \times v$ has been made approximately parallel to I and the effect of reversing the latter will serve to measure the term $\sim D$, in the expression 13. No effect could be established to exist, as indicated by the reported result:

$$D \approx -0.04 \pm 0.07, \quad 16.$$

essentially zero. The Chalk River experiment, referred to above, differed from the Argonne arrangement by an attempt to use better defined solid

angles; it produced a measure of the limits on D somewhat earlier^{*} (31), given by $|D| < 0.3$, essentially.

The attempts to measure the coefficient D are actually tests of invariance under time reversal. This can be seen, on the formal side, from the definition of the coefficient D by the expression 13. In a reversal of motions, the vectors I , v and $q = q\hat{q}$ all have their signs reversed. This means that the triple product term proportional to D also changes sign and the emitted intensity is not invariant to the reversals unless $D=0$. The Argonne experimenters explain their result more graphically. They compare their experimental set-up, as outlined above, with another so arranged as to detect all the motions reversed. The contrasted arrangements are indicated by the two parts of Figure 7. Clearly, the experiment with motions reversed, of Figure 7(b), can

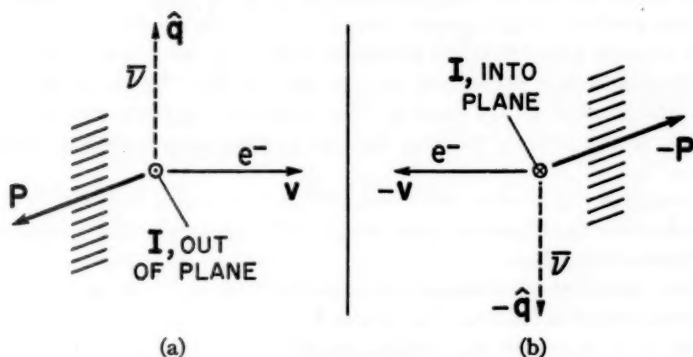


FIG. 7

be done merely by reversing the neutron spin I in the original set-up, of Figure 7 (a), since that reproduces the reversed set-up except for its spatial orientation. Thus, when no effect attributable to reversing the neutron spin is observed, this indicates an invariance to time reversal.

The conclusion of all the observations on the neutron decay is that the only substantial correlation is between the neutron-spin orientation and the emission direction of the antineutrino; the expression 13 degenerates into approximately $1 + \hat{I} \cdot \hat{q}$. Since antineutrinos were shown to be right-handed, the antineutrino tends to carry away all the neutron's angular momentum by itself; the proton and electron angular momenta must cancel each other. This still makes nothing explicit concerning a possible polarization of the proton relative to its direction of motion.

A clue to the latter question lies in the contrast between the large angular

^{*} Still earlier indications that time-reversal invariance is nearly valid were obtained from analyses of β - γ correlations in cases of Fermi and GT superposition, by Boehm & Wapstra (32) and by Ambler *et al.* (33).

anisotropy $A \approx -1$ shown by the electrons from Co^{60} , and the near-isotropy $A \approx 0$ of their emission by the neutron. The two cases differ in that Co^{60} emits pure GT radiation while the neutron also emits Fermi radiation. The latter, by itself, is isotropic, since it takes no angular momentum from the nucleus and so "pays no attention" to the nuclear spin direction. It can cancel out the anisotropy of the GT radiation only by interfering with it, and this is ostensibly what happens in the case of the neutron.

The effectiveness of the Fermi wave in cancelling the anisotropy characteristic of the GT waves argues that the Fermi wave pattern must be given about equal weight. Now, while a GT wave gives no particular preference to the proton recoil direction, the Fermi wave does. It should be recalled that the Fermi wave forms a singlet state of the electron and anti-neutrino, hence correlates the directions of those oppositely spinning particles, giving preference to a proton recoil opposite to the leptonic direction. We have already noted that the proton and electron spins must oppose each other. The result is a preference for the proton, like the electron, to have its spin antiparallel to its motion. One thus also expects the proton to participate in the process through the left-handed components of its states of motion!

The argument here is far from convincing, but it puts into words as well as seems feasible the closer analysis which will be possible after introduction of the detailed formalism.

A fairly simple description of the superposition of Fermi and GT waves can be constructed as follows. The singlet Fermi wave should be proportional to the spin state $\chi_s = 2^{-1/2} (\alpha_e \beta_\nu - \beta_e \alpha_\nu)$ where α, β denote up and down spins in the conventional manner. The triplet of GT states will be proportional to $\chi_t^0 = 2^{-1/2} (\alpha_e \beta_\nu + \beta_e \alpha_\nu)$, $\chi_t^{+1} = \alpha_e \alpha_\nu$ and $\chi_t^{-1} = \beta_e \beta_\nu$.

Next, we must take only the right-handed antineutrino and left-handed electron components of these states. The projection operator for the antineutrino is fairly obviously $\frac{1}{2}(1 + \boldsymbol{\sigma}_\nu \cdot \hat{\mathbf{q}})$, since this cancels the left-handed parts of the wave, a second application makes no further change and is orthogonal to the operation $\frac{1}{2}(1 - \boldsymbol{\sigma}_\nu \cdot \hat{\mathbf{q}})$ which completes the set. (It must be remembered that $\hat{\mathbf{q}}$ is a unit vector.) The left-handed electron projection operator is as simple to construct only for $v/c \rightarrow 1$: $(\frac{1}{2})(1 - \boldsymbol{\sigma}_e \cdot \mathbf{v}/c)$. However, this should be sufficient since we expect the relation 13 to depend on the electron velocity as shown, regardless of its magnitude.

We can now say that the Fermi wave is proportional to the amplitude:

$$(F) = \frac{1}{2} C_V (1 - \boldsymbol{\sigma}_e \cdot \mathbf{v}/c) (1 + \boldsymbol{\sigma}_\nu \cdot \hat{\mathbf{q}}) \chi_s. \quad 17.$$

This wave leaves the nucleon with its spin unaffected. The intensity of the GT wave depends on operations on the neutron spin, given by an operator $\boldsymbol{\sigma}$ insuring conservation of the angular momentum. When the component with spin projection zero on the neutron spin axis (taken to be the z -axis) is emitted:

$$(GT)_0 = \frac{1}{2} C_A [(1 - \boldsymbol{\sigma}_e \cdot \mathbf{v}/c) (1 + \boldsymbol{\sigma}_\nu \cdot \hat{\mathbf{q}}) \chi_t^0] \langle \sigma_z \rangle, \quad 18.$$

where $\langle \sigma_z \rangle$ is the matrix element between neutron and proton spin states. $\langle \sigma_z \rangle$ is equal to unity for a product proton parallel to the initial neutron, just as for the zero angular momentum Fermi wave, and vanishes otherwise.

To emit a lepton wave with a unit spin projection, $\sim \chi_i^1$, the neutron spin must be flipped:

$$(GT)_1 = \frac{1}{4} C_A [(1 - \hat{\sigma}_z \cdot \mathbf{v}/c)(1 + \hat{\sigma}_z \cdot \hat{\mathbf{q}}) \chi_i^1] \cdot 2^{-1/2} \langle \sigma_z - i\sigma_y \rangle. \quad 19.$$

That $2^{-1/2}(\sigma_z - i\sigma_y)$ serves as a "destruction operator" for z -components of angular momentum is familiar. $\langle \sigma_z - i\sigma_y \rangle = 2$ for a proton produced antiparallel to the initial neutron, $= 0$ otherwise. Thus, the component $(GT)_1$ can interfere with neither the Fermi wave, nor $(GT)_0$. The component $(GT)_{-1} \sim \chi_i^{-1}$ cannot be produced at all, since it requires initial angular momentum directed oppositely to that of the neutron under consideration.

Straightforward calculation will now show that

$$|(F)|^2 = \frac{1}{4} |C_V|^2 (1 + \hat{\mathbf{q}} \cdot \mathbf{v}/c), \quad 20.$$

the electron-neutrino correlation expected for Fermi waves! The expected independence of the neutron spin direction is also found.

For the pure GT intensity we obtain:

$$|(GT)_0|^2 + |(GT)_1|^2 = \frac{3}{4} |C_A|^2 [1 - \frac{1}{4} \hat{\mathbf{q}} \cdot \mathbf{v}/c + \frac{3}{4} (\hat{\mathbf{q}}_z - v_z/c)]. \quad 21.$$

Averaging over the z -directions (i.e. the neutron spin), as for an unpolarized source, we get the expected electron-neutrino correlation coefficient $a_{GT} = -\frac{1}{3}$. Notice also that if the intensities 20 and 21 are integrated over all neutrino and electron directions, we get the expected ratio $3|C_A|^2/|C_V|^2$ for the GT to Fermi radiation from the neutron (relation 3).

Finally, it is of interest to look at the intensity component arising from the $(F)(GT)_0$ interference:

$$(F^*)(GT)_0 + (F)(GT)_0^* = -\frac{1}{4} C_V^* C_A \left[\frac{v_z}{c} + \hat{\mathbf{q}}_z + i \left(\frac{\mathbf{v}}{c} \times \hat{\mathbf{q}} \right)_z \right] + \text{c.c.} \quad 22.$$

Adding together 20, 21, 22 produces just the intensity expression 13, multiplied with one-fourth of

$$\xi_n = |C_V|^2 + 3|C_A|^2, \quad 23.$$

and with the following identifications of the correlation coefficients:

$$\xi_n a = |C_V|^2 - |C_A|^2, \quad 24.$$

$$\xi_n A = -2|C_A|^2 - (C_V C_A^* + C_V^* C_A), \quad 25.$$

$$\xi_n B = +2|C_A|^2 - (C_V C_A^* + C_V^* C_A), \quad 26.$$

$$\xi_n D = i(C_V C_A^* - C_V^* C_A). \quad 27.$$

We see borne out here the assertion that the Fermi wave influences dependence on the nuclear spin (through A , B , D) only via interference with the GT wave $\sim C_A$.

We see also that no electron-neutrino correlation ($a=0$) is to be expected of equal Fermi and GT coupling strengths. If we use the result 4,

then $\xi_n \approx (5.4 \pm 0.2) |C_V|^2$ and $a \approx -0.087 \pm 0.015$, as against a measured value of $a = +0.09 \pm 0.11$. In any case, a near-vanishing correlation is expected.

We see further that $B - A = 4 |C_A|^2 / \xi_n$ also depends only on the absolute value of coupling strengths. $B - A = +1$ if $|C_A|^2 = |C_V|^2$ and $B - A = 1.09 \pm 0.05$ with the ratio given by expression 4. The measurements 14 and 15 give $B - A = 0.99 \pm 0.17$.

The remaining results depend on the relative phases, as well as the magnitudes, of C_V , C_A . Putting $C_A/C_V = \rho e^{i\alpha}$, we have

$$B + A = - \frac{4\rho \cos \alpha}{1 + 3\rho^2} = +0.77 \pm 0.17, \quad 28.$$

$$D = - \frac{2\rho \sin \alpha}{1 + 3\rho^2} = -0.04 \pm 0.07. \quad 29.$$

The result for D puts limits on the phase difference α of about 8° to either side of $\alpha = 0$ or $\alpha = \pi$. The result for $B + A$ definitely puts the phase difference into the neighborhood of $\alpha = \pi$, although with a wider range of uncertainty.

We have already seen that invariance under the time reversal requires $D = 0$. We see from 29 that this is equivalent to $\alpha = 0$ or π , i.e. a real ratio of the coupling constant C_V , C_A . An overall absolute phase of the coupling constants is meaningless, in view of their use, as in 17 and 18, as multipliers of waves with arbitrary absolute phase. Thus, we can say that $D = 0$ is equivalent to a reality of the coupling constants and that a choice of real coupling constants is equivalent to assuming invariance under time reversal. (See also Footnote 7.)

An important outcome of these considerations has been the result $C_A/C_V = \rho e^{i\pi}$ with $\rho^2 = 1.47 \pm 0.06$ according to 4, so that

$$C_A = - (1.21 \pm 0.03) C_V. \quad 30.$$

Thus, $C_A = -C_V$ nearly, and we shall eventually learn to interpret this as signifying that the nucleons, like the leptons, participate in β -processes preferentially through the left-handed components of their states of motion.

This review of key experiments demonstrates how nearly directly they lead to the important conclusion: all the fermions participating in the β -processes do so only in the left-handed components of their states of motion (with antiparticles correspondingly in right-handed states)! They also favor an invariance to time reversal, hence through the *CPT* theorem, the joint-parity principle. More quantitatively convincing demonstrations require introduction of the detailed formulation to be reviewed next.

THE FERMI THEORY

The theoretical framework into which the phenomena attending β -decay have always been successfully fitted was supplied by Fermi (6) as long ago as 1934. The latest turn of events makes it important to re-examine Fermi's original hypothesis.

Fermi constructed his theory on the model of the theory of electromagnetic radiation. The latter is generated in proportion to the four-vector current $j_\mu = \bar{\psi}\gamma_\mu\psi$. Fermi therefore assumed that the nucleons generate β -radiation in proportion to the current associated with the neutron-to-proton transformation (or its reverse):

$$J_\mu = \bar{\psi}\tau_+\gamma_\mu\psi \text{ and } J_\mu^* = \bar{\psi}\tau_-\gamma_\mu\psi, \quad 31.$$

where ψ is the (bi-) spinor describing a nucleon and τ_\pm are the well-known isotopic spin operators which formally substitute a proton (neutron) for a neutron (proton) state. The expression 31 can equally well be written

$$J_\mu = \bar{\psi}_p\gamma_\mu\psi_n \text{ and } J_\mu^* = \bar{\psi}_n\gamma_\mu\psi_p, \quad 32.$$

where $\psi_{p(n)}$ describes a proton (neutron) if one agrees to treat as identical the neutron and proton coordinates of the transforming nucleon. Then the symmetry of the relationships in 2, plus the requirements of relativistic invariance, lead to the hypothesis for the coupling energy density:

$$h = g(\bar{\psi}_p\gamma_\mu\psi_n) \cdot (\bar{\psi}_e\gamma_\mu\psi_\nu) + \text{c.c.}, \quad 33.$$

where g is Fermi's fundamental coupling constant, responsible for the magnitude of the interaction, and to be determined by the observed rates of β -decay.

Covariant densities other than the four-vector current can be constructed within the Dirac description of the "internal states" of spin 1/2 particles. The latter can be analyzed into just five independent "states of internal motion" described by a scalar, a tensor, a pseudovector, and a pseudoscalar, besides the four-vector used by Fermi. There is no a priori reason for not expecting β -radiation to be generated by any of these; hence arbitrary linear combinations of them have been investigated. One introduces each with an arbitrary coefficient, C_X , to represent its possible strength as a fraction of g :

$$h = g\sum_X C_X (\bar{\psi}_p O_X \psi_n) \cdot (\bar{\psi}_e O_X \psi_\nu) + \text{c.c.}, \quad 34.$$

with $O_S = 1$, $O_V = \gamma_\mu$, $O_T = \gamma_\mu\gamma_\nu$, $O_A = i\gamma_5\gamma_\mu$, $O_P = \gamma_5$. Ever since this possible generalization of Fermi's theory was recognized, evidence which could serve to measure the five coupling strengths $C_{S,V,T,A,P}$ has been sought.

The so-called "even" coupling forms constituting 34 were the ones conventionally used until Yang and Lee advanced their hypothesis. An alternative set of five coupling forms, called the "odd" couplings, had long been known. The possibility of their existence arose because, for example, one cannot really say whether $\bar{\psi}_e O_S \psi_\nu \equiv \bar{\psi}_e \psi_\nu$ is a scalar and $\bar{\psi}_e O_P \psi_\nu \equiv \bar{\psi}_e \gamma_5 \psi_\nu$ a pseudoscalar, or vice versa. This is because no one can say how a spinor ψ is supposed to behave in a space inversion as regards phase, and the behavior of scalars and pseudoscalars differs only in phase. (The phases generated by proper transformations are another matter; such phases are continuous with the identity transformation and so can be checked against the absence of the phase change in that limit.) Thus an alternative for the scalar contribution to the coupling energy density is obtained by the replacement of

$(\bar{\psi}_p O_S \psi_n)(\bar{\psi}_e O_S \psi_\nu)$ with $(\psi_p O_S \psi_n)(\bar{\psi}_e O_P \psi_\nu) \equiv (\bar{\psi}_p O_S \psi_n)(\bar{\psi}_e O_S \gamma_5 \psi_\nu)$. There is here just a replacement of ψ_ν by $\gamma_5 \psi_\nu$. One gets the full complement of five "odd" coupling forms by replacing ψ_ν by $\gamma_5 \psi_\nu$ everywhere in 34.

To understand how the "odd" couplings differ from the "even" ones physically, one may compare the way they generate neutrino waves. One can always analyze the waves according to the right- and left-handedness of the neutrino; one then finds that the way "odd" and "even" couplings differ is that they generate the right- and left-handed neutrino waves with opposite relative phases. The change makes no observable difference (for a vanishing neutrino rest mass) if only the "odd" couplings or only the "even" couplings exist. For this reason, they were regarded as equivalent, alternative ways in which one could choose to formulate the theory. Each of the alternatives, by itself, leads to results entirely consistent with the old parity conservation principle.

The possibility that the "odd" couplings could coexist with the even ones was rejected on grounds which seemed secure at the time. The radiations generated by each of the two types of coupling, if both exist, can interfere with each other, and the interference components of the radiation violate the old parity-conservation principle.

Now, of course, the situation is changed. The coexistence of the "odd" with the "even" couplings is actually needed in order to represent the observed violations of the parity conservation principle. We therefore generalize 34 to include the "odd" couplings, with the five new coupling coefficients $C'_{S,V,T,A,P}$:

$$h = g \Sigma_X (\bar{\psi}_p O_X \psi_n) \cdot [\bar{\psi}_e O_X (C_X + C_X' \gamma_5) \psi_\nu] + \text{c.c.} \quad 35.$$

It is the ready modifiability of the Fermi Theory, in respects like these, which has enabled it to survive even so fundamental an upset as that of the old parity conservation principle.

It is well to consider also another point at which an upset may still be in store for the formulation. It was formerly presumed that the coupling constants like C_X , C_X' must be real. This guarantees that the results will be invariant under time reversal.⁷ An example of the equivalence of time-reversal invariance to the reality of the coupling constants has already been reviewed. Since the upset of the invariance to space-inversion (the old parity-conservation), one should be suspicious of requirements of invariance under the improper transformations. It is well to retain the possibility that the coupling constants are complex, and leave the matter to experimental test. That will give us 20 coupling parameters to determine, viz. the real and imaginary parts of the 10 coupling constants C_X , C_X' .

⁷ This should not be surprising if one compares the terms of expression 35 written explicitly with those represented by "c.c." The latter, being complex conjugates of the explicitly written ones, are exactly the same except that ψ_p , ψ_e are interchanged with ψ_n , ψ_ν . (See 32, for example.) They therefore represent the reverse process. Thus, one may well expect that invariance under time reversal will require the constants C_X^* , $C_X'^*$ of the "c.c. terms" to be the same as C_X , C_X' .

THE RESTRICTION TO LEFT-HANDED LEPTON STATES

We now want to make use of the experimental evidence reviewed in the preceding sections to determine the coupling constants C_X , C_X' , in the general interaction form 35. To do this, we first study the effect on the neutrino wave of the operation $C_X + C_X'\gamma_5$, in 35. It can be analyzed as

$$(C_X + C_X'\gamma_5)\psi = (C_X + C_X')\phi^+ + (C_X - C_X')\phi^-, \quad 36.$$

where

$$\phi^\pm = \frac{1}{2}(1 \pm \gamma_5)\psi \quad 37.$$

are orthogonal projections of ψ , by virtue of the properties of the operators $\frac{1}{2}(1 \pm \gamma_5)$. The orthogonality follows from $\gamma_5^2 = 1$ and $(1 + \gamma_5)(1 - \gamma_5) = 0$. Notice also that $\frac{1}{2}(1 \pm \gamma_5)\phi^\pm = \phi^\pm$. Next we consider the physical properties of these substates of the motion.

The leptons freed in β -decay obey the Dirac equation:

$$W\psi = (c\alpha \cdot \mathbf{p} + \beta mc^2)\psi. \quad 38.$$

If one multiplies this with $\pm \gamma_5/(2W)$, one gets expressions for the parts $\pm \frac{1}{2}\gamma_5\psi$ of ϕ^\pm . Adding $\frac{1}{2}\psi$, and using the facts that $\gamma_5\alpha = -\alpha$, $\psi = \phi^+ + \phi^-$, $\gamma_5\phi^\pm = \pm \phi^\pm$ and $c\mathbf{p}/W = \mathbf{v}/c$, gives us:

$$\phi^\pm = \frac{1}{2}(1 \mp \mathbf{v} \cdot \mathbf{c}/c)\psi \mp [mc^2/(2W)]\beta(\phi^+ - \phi^-). \quad 39.$$

For neutrinos, with $m=0$ and $v=c$:

$$\phi^\pm = \frac{1}{2}(1 \pm \gamma_5)\psi_\nu = \frac{1}{2}(1 \mp \mathbf{v} \cdot \hat{\mathbf{q}})\psi_\nu, \quad 40.$$

where \mathbf{q} is a unit vector in the direction of the neutrino momentum. We have here states describing left- and right-handedly polarized neutrinos. ϕ^\pm in 39 describes states with preferential polarizations of the same kind, modified only in that $m \neq 0$, hence $v < c$, as for electrons.

As might be expected, the same operation which separates out the left-handed neutrinos also forms the right-handed states of antineutrinos. If $\psi_\nu = C\psi_\nu$ describes an antineutrino with the same dynamical properties as the neutrino, ψ_ν (C is the well-known charge-conjugation operation), then

$$\phi_\nu^\pm = \frac{1}{2}(1 \pm \gamma_5)\phi_\nu = \frac{1}{2}C(1 \mp \gamma_5)\psi_\nu = C\phi_\nu^\mp, \quad 41.$$

since the charge-conjugation operator anticommutes with γ_5 . This means that, whereas ϕ_ν^+ describes left-handed neutrinos, ϕ_ν^+ describes right-handed antineutrinos.

Now, the experimental finding that only left-handed neutrino states are generated in β -decay means that one must suppress ϕ_ν^- in 36, and so choose

$$C_X' = C_X. \quad 42.$$

Expression 35 for the coupling now becomes:

$$h = g\Sigma_X C_X (\bar{\psi}_\nu O_X \psi_n) [\psi_e \dagger \beta O_X (1 + \gamma_5) \psi_\nu] + \text{c.c.}, \quad 43.$$

after using the equivalence $\bar{\psi}_e = \psi_e \dagger \beta$, where $\psi_e \dagger$ is the hermitean conjugate of ψ_e .

We want to investigate next the effect of the operator $(1+\gamma_5)$ in 43 on the electron wave ψ_e . To do this, we must transpose the operations βO_X with $(1+\gamma_5)$. Since γ_5 anticommutes with β and every γ_μ ,

$$\beta O_{S,T,P}(1+\gamma_5) = (1-\gamma_5)\beta O_{S,T,P} \text{ and } \beta O_{V,A}(1+\gamma_5) = (1+\gamma_5)\beta O_{V,A}$$

(see the definitions of the O_X below 34). If it is now recognized that

$$\psi^\dagger(1\pm\gamma_5) = 2(\phi^\pm)^\dagger \quad 44.$$

follows from 37, the interaction form 43 becomes:

$$\begin{aligned} h = & 2g\Sigma_{S,T,P} C_X(\bar{\psi}_p O_X \psi_n) \cdot [(\phi_e^-)^\dagger \beta O_X \psi_\nu] + \text{c.c.} \\ & + 2g\Sigma_{V,A} C_X(\bar{\psi}_p O_X \psi_n) \cdot [(\phi_e^+)^\dagger \beta O_X \psi_\nu] + \text{c.c.} \end{aligned} \quad 45.$$

This means that the scalar, tensor, and pseudoscalar interactions generate right-handed electrons with the left-handed neutrinos (or right-handed anti-neutrinos), while the vector and pseudovector (A) interactions generate left-handed electrons—at least in the limit $v \rightarrow c$. These results conform to the discussions connected with the experiments, above.

The experiments showed that the electrons have a left-handed polarization to the degree v/c . If this is taken to hold for $v \rightarrow c$, then one arrives at the conclusion that the right-handed states ϕ^- in 45 must be suppressed; hence

$$C_{S,T,P} = 0. \quad 46.$$

Only the vector and pseudovector couplings seem to be operative in β -decay.

Since $\frac{1}{2}(1+\gamma_5)\phi^+ = \phi^+$, one may write

$$(\phi_e^+)^\dagger \beta O_{V,A} \psi_\nu = \frac{1}{2}(\phi_e^+)^\dagger \beta O_{V,A}(1+\gamma_5)\psi_\nu = (\phi_e^+)^\dagger \beta O_{V,A} \phi_\nu^+$$

in 45. Further, $O_A \equiv i\gamma_5\gamma_\mu = i\gamma_5 O_V$ and $\gamma_\mu\phi^+ = \phi^+$; hence 43 can now be written:

$$h = 2g[\psi_p^\dagger(C_V - C_A\gamma_5)\beta\gamma_\mu\psi_n] \cdot (\phi_e^\dagger\beta\gamma_\mu\phi_\nu) + \text{c.c.} \quad 47.$$

The superscripts on ϕ_e, ϕ_ν have been suppressed since the opposite projections ϕ_e, ν^- are no longer relevant for β -decay.

One can reassure oneself that the electron polarization will have the right magnitude $\mathcal{P} = \pm v/c$ for e^\pm , when $v < c$.

In the relevant observations, the nuclei are unpolarized and the neutrino spins and directions undifferentiated; hence the rates will be proportional to

$$\Sigma_{\sigma\nu} |\phi_e^\dagger \beta \gamma_\mu \phi_\nu|^2. \quad 48.$$

From the well-known property of the spin sums,

$$\Sigma_\sigma \psi \psi^\dagger = \frac{1}{2} \left(1 + \frac{c\alpha \cdot p + \beta mc^2}{W} \right), \quad 49.$$

it follows for the neutrino that

$$\Sigma_{\sigma\nu} \phi_\nu \phi_\nu^\dagger = \frac{1}{2} (1 + \gamma_5) (1 + \alpha \cdot \hat{q}). \quad 50.$$

The term linear in the neutrino direction \hat{q} averages to zero under the conditions of the observations. Hence,

$$\Sigma_{\sigma\tau} |\phi_\sigma \dagger \beta \gamma_\mu \phi_\tau|^2 = \frac{1}{2} \phi_\sigma \dagger \beta \gamma_\mu (1 + \gamma_5) \gamma_\mu \beta \phi_\sigma = \frac{1}{2} \phi_\sigma \dagger \phi_\sigma, \quad 51.$$

independent of the particular γ_μ -component.

In the ordinary representation in which

$$\gamma_5 = - \begin{pmatrix} 0 & 1 \\ 1 & 0 \end{pmatrix}, \quad 52.$$

the negatron state of definite momentum has the amplitude:

$$\psi_\sigma = \sqrt{\frac{W + mc^2}{2W}} \begin{pmatrix} \chi_\sigma \\ \frac{c\delta \cdot \mathbf{p}}{W + mc^2} \chi_\sigma \end{pmatrix}, \quad 53.$$

where $\chi_{\pm\frac{1}{2}} = \alpha$ and β , the two-component Pauli spin wave functions. Now

$$\phi_\sigma = \frac{1}{2}(1 + \gamma_5)\psi_\sigma = \begin{pmatrix} u_\sigma \\ -u_\sigma \end{pmatrix} \quad 54.$$

with

$$u_\sigma = \frac{1}{2} \sqrt{\frac{W + mc^2}{2W}} \left(1 - \frac{c\delta \cdot \mathbf{p}}{W + mc^2} \right) \chi_\sigma. \quad 55.$$

Now, 51 becomes

$$\frac{1}{2} \phi_\sigma \dagger \phi_\sigma = u_\sigma \dagger u_\sigma = \frac{1}{2} \chi_\sigma \dagger (1 - c\delta \cdot \mathbf{p}/W) \chi_\sigma \quad 56.$$

Since $c\mathbf{p}/W \equiv \mathbf{v}/c$, one obtains an intensity proportional to

$$\frac{1}{2} [1 - \langle \delta \rangle \cdot \mathbf{v}/c] \quad 57.$$

where $\langle \delta \rangle \equiv \chi_\sigma \dagger \delta \chi_\sigma$. This has just the degree of polarization sought, and the right sign for negatrons. For positrons, ψ is replaced by $C\psi$; hence, whereas $\phi_\sigma \dagger \phi_\sigma = \frac{1}{2} \psi \dagger (1 + \gamma_5) \psi$ for the negatrons,

$$\phi_\sigma \dagger \phi_\sigma = \frac{1}{2} \psi \dagger C \dagger (1 + \gamma_5) C \psi = \frac{1}{2} \psi \dagger (1 - \gamma_5) \psi, \quad 58.$$

if the same ψ is used as in 53. One again gets the form $\frac{1}{2} \phi_\sigma \dagger \phi_\sigma = u_\sigma \dagger u_\sigma$, but u_σ differs from 55 in that $\chi_{-\sigma}$ replaces χ_σ . This will obviously give a polarization for the positrons opposite to that for the electrons.

The reducibility of the projection ϕ to two-component wave functions u , as in 54, is a general property which has been emphasized by Feynman & Gell-Mann (34). If one separates the "space" and "time" components of the four-vector $\gamma_\mu (-i\beta\alpha, \beta)$, in the interaction form 47, one can write it in terms of the two-component functions u_σ, u_τ as:

$$\begin{aligned} h = & 4g [\psi_p \dagger (C_V - C_A \gamma_5) \psi_n] (u_\sigma \dagger u_\tau) + \text{c.c.} \\ & + 4g [\psi_p \dagger (C_A - C_V \gamma_5) \psi_n] \cdot (u_\sigma \dagger \delta u_\tau) + \text{c.c.} \end{aligned} \quad 59.$$

THE V-A LAW

The evidence about the leptons, as used in the foregoing, has brought the Fermi coupling to the degree of definition represented by the expression 47, and its mathematical equivalent, 59. There remains the determination

of the relationship between the vector and pseudovector couplings; i.e., C_V vs. C_A .

In order to round out the development as directly as possible, we are going to take for granted, for the time being, the identity of the coupling constants as introduced into the coupling energy density expression 35, and as used in the interpretations in the section on The Key Experiments. The path of development actually taken in the literature was to derive the theoretical expectations for experimental results which follow from the general form 35. One then has very lengthy expressions in which all 10 complex coupling constants C_X , C_X' serve as unknown parameters. The experimental measurements were, in effect, used to provide a sufficient number of simultaneous equations to determine the parameters. Most of this will be bypassed with the treatment of the preceding subsection. However, the expectations from the incompletely determined form 47 (arbitrary C_V , C_A) will still be presented in the next subsection. That will provide the justification for the identification of the coupling constants which is adhered to in the remainder of this subsection.

The observations on the neutron decay, as reviewed above, indicate that, at least in a first approximation:

$$C_A = -C_V. \quad 60.$$

With this, the operator on the nucleonic states in the interaction form 47 becomes:

$$(C_V - C_A\gamma_5)\beta\gamma_\mu = C_V(1 + \gamma_5)\beta\gamma_\mu = \frac{1}{2}C_V(1 + \gamma_5)\beta\gamma_\mu(1 + \gamma_5). \quad 61.$$

It is seen that this projects out just the left-handed nucleonic states, $\phi = \frac{1}{2}(1 + \gamma_5)\psi$ for participation in the interaction. It constitutes the demonstration, promised above, that $C_A = -C_V$ may be interpreted in this way. Notice that when the participation of one nucleonic state is restricted to its left-handed component, so, automatically, is the other. There exists no "polar" four-vector current during a transformation between states of opposite helicity!

Now, the coupling energy density has been brought to the simple and definite form:

$$h = \sqrt{8}G(\phi_p^\dagger\beta\gamma_\mu\phi_n)(\phi_e^\dagger\beta\gamma_\mu\phi_\nu) + \text{c.c.}, \quad 62.$$

where $4gC_V$ has been replaced by $\sqrt{8}G$ to conform to a customary normalization. Because this rests on the presumption $C_A = -C_V$, it is called the "V-A Law."

We see that, in the way outlined here, we are back to Fermi's original assumption 33, at least in the particular that the coupling is proportional to four-vector currents associated with the process. However, the full currents in the states ψ are not operative, contrary to what Fermi had presumed. Only the part of the currents in the so-called "left-handed component states," $\phi = \frac{1}{2}(1 + \gamma_5)\psi$, is now found to generate β -radiation. Of course,

Fermi himself had no basis for expecting that only the left-handed parts of the currents are involved.

There remains an important discrepancy between the simple $V-A$ Law 62 and the experimental facts. On the basis of the experimental analyses as carried out above, the discrepancy is expressed in the form of an inequality in magnitude of the vector and pseudovector coupling constants. The data as evaluated in the section on Fermi and GT radiation indicated that $C_A \approx -1.2C_V$ (see 30).

With the discrepancy put into this form, one retains the expression 47 for the coupling law. This deviates from the $V-A$ Law in two respects. First, it renormalizes the coupling strength in the $V-A$ Law from G to $\frac{1}{2}G(1 - C_A/C_V)$. Second, it adds a contribution from the right-handed nucleonic states, $\phi^- = \frac{1}{2}(1 - \gamma_5)\psi$, with a coupling strength about 10 per cent as great as that in the left-handed states of the $V-A$ Law.

The representation of the discrepancy between the $V-A$ Law and the data, in the form 30, is quite arbitrary. It is incidental to insisting on fitting the data to the form 47 alone, without allowance for the intrusion of effects which are extraneous to the β -interaction proper but which may modify its operations. For instance, it is generally believed that a neutron spends a substantial part of its existence as a proton plus a negatively charged pion cloud. Certainly, the negatron-emitting power of a neutron may be modified by this. Such modifications are of a class referred to as "renormalization effects." It is at least open to doubt that "renormalization effects" will take just the form of a contribution from right-handed nucleonic states, as the above method of representing the discrepancy implies.

The idea that the fundamental β -interaction, aside from "renormalization effects," is to be represented by the $V-A$ Law was explicitly advanced by Marshak & Sudarshan (35), independently by Feynman & Gell-Mann (34), and also by Sakurai (36). Their various papers pointed out various theoretical beauties of the $V-A$ Law in support of its acceptability: "chiral invariance," "two-component" representation of all spinor fields, invariance under "mass-reversal." Perhaps such theoretical properties lend attractiveness to the $V-A$ Law, but the authors themselves do not claim that they compel its acceptance. At least equally persuasive arguments for other forms of the coupling law were advanced years ago, before the data pointed to the $V-A$ Law; such arguments as Critchfield and Wigner's (37) for an " $S-A-P$ Law," Jensen & Stech's (38) for an " $S-T+P$ Law," and many others, still appear cogent enough that one is tempted to regret their incompatibility with experimental facts. On the other hand, the positive assertion of the hypothesis that sources of discrepancy with the $V-A$ Law are to be looked for in effects extraneous to the β -interaction proper has great value in clearing the way for their investigation.

Unfortunately, there as yet exists no definitive treatment of the "renormalization effects" for nucleons. Such progress as has been made will be reported briefly in the final sections. Meanwhile, current practice will be

followed by presenting the results of the theory in the form 47; i.e., retaining the distinction between the coupling coefficient magnitudes C_V and C_A . One then obtains the results of the $V-A$ Law (neglecting "renormalization effects," of course) simply by putting $C_A = -C_V$. At the same time, we retain some sort of measure of the extraneous effects through the disparity between $|C_A|$ and $|C_V|$, which will persist as long as those effects are neglected in the comparisons with experiments.

EXPECTATIONS FOR ALLOWED ELECTRON EMISSIONS

The main concern here is to present the theoretical expectations for the types of measurements discussed as The Key Experiments, above, in order to legitimize the interpretations made there on a more intuitive basis. Everything to be presented in this subsection is deduced from the β -coupling in the form 47 or its equivalent, 59. The more generalized results which follow from the form 35 (still allowing participation of right-handed lepton states) are available in the literature (2, 39) but continue to have interest chiefly to specialists concerned with checking present experimental conclusions to a further degree.

The restriction to concern with what are called The Key Experiments here entails neglect of much valuable work. That is partly necessitated by the sheer volume of it. For instance, extensive studies have been made of many types of correlations between β - and γ -radiations which have yielded valuable confirmations of, and sometimes even partial anticipations of, the results of The Key Experiments. However, any worthwhile exposition of them would require long excursions and distractions from the main theme here, the fundamental character of the β -coupling.

It may also be noticed that forbidden decays are given no attention here, whereas they formerly were given an important role in helping delineate the character of the β -coupling (1). This comes about largely because so many new ways have been found to study the generally more simply interpretable allowed decays. A forbidden transition in general comprises superpositions of, and interferences between, contributions from at least three "nuclear β -moments." That makes the results sensitive to uncertainties about the detailed structure of the nuclear states. Only the purely GT , "unique forbidden" decays are about as directly interpretable as the allowed decays. However, they yield no further information of equal importance.

Examination of the coupling energy 59 makes clear the form which the results for the radiation rates will take in the cases of allowed transitions. The latter are the cases in which the nucleons can be treated in nonrelativistic approximation and the variation of the lepton waves over the nuclear domain can be neglected, without having the results vanish because of the consequent selection rules. For nonrelativistic nucleons, the terms in which γ_5 is explicit, in the form 59, can be dropped. Further, the electron and neutrino amplitudes $u_{e,\nu}$ can be evaluated at any one point in the nucleus. Then, the transition matrix element of 59 becomes:

$$\langle h \rangle = 2g[C_V \langle 1 \rangle (u_e^\dagger u_\nu)_0 + C_A \langle \sigma \rangle \cdot (u_e^\dagger \sigma u_\nu)_0]. \quad 63.$$

Here $\langle \sigma \rangle$ is the matrix element between the initial and final nuclear states of the nucleonic spin unit vector, while $\langle 1 \rangle$ is merely an overlap integral between those states. The expression $\langle 1 \rangle = 0$ unless $I_f = I_i$; hence the vector coupling $\sim C_V$ yields the Fermi radiation as anticipated. $\langle \sigma \rangle = 0$ unless the GT selection rules are obeyed; hence the radiation generated by the pseudovector coupling $\sim C_A$ is indeed to be identified as GT radiation. The further computation of the decay rates $d\lambda \sim |\langle h \rangle|^2$ from 63, is straightforward.

First to be quoted will be a rate for producing radiation with all orientations of the leptonic spins included. This may be compared with experiments in which the initial nuclear spins $I \equiv I_i$ are polarized and the electron and neutrino directions detected, but the polarizations of the leptons are undifferentiated. The rate per unit electron momentum is then:

$$d\lambda/dp = [g^2/(16\pi^2\hbar^7c)] F(Z, W) p^2 q^2 d\Omega_e d\Omega_\nu \times \xi \{ 1 + a\hat{q} \cdot \mathbf{v}/c + d[\langle I^2 - 3M^2 \rangle / I(2I - 1)] \\ [\frac{1}{2} \hat{q} \cdot \mathbf{v}/c - (\hat{I} \cdot \hat{q})(\hat{I} \cdot \mathbf{v}/c)] + (\langle M \rangle / I) \hat{I} \cdot [A\mathbf{v}/c + B\hat{q} - D\hat{q} \times \mathbf{v}/c] \}. \quad 64.$$

Here, $F(Z, W)$ is the well-known (1) function which takes into account the distortion of the electron wave by the nuclear charge. In this expression, $d\Omega_{e,\nu}$ are solid angle elements into which the electron and neutrino momenta p and q emerge. The last two lines of the formula are a generalization to arbitrary nuclei of the distribution 13 already found for the neutron, not from the formal law 47 but on more intuitive grounds. One new type of term $\sim d$ enters. It exists only for initially polarized nuclei with $I > \frac{1}{2}$, and can be detected only through observations on the recoils of such polarized nuclei. That type of experiment has not yet become feasible. To apply the whole formula 64 to a particular case, the prepared nuclear polarization, as measured by the statistical averages $\langle M \rangle$ and $\langle M^2 \rangle$ of the nuclear spin projection, must be known. In the above expression, \hat{I} is the unit vector in the direction of the nuclear polarization axis. The formula was first derived by Yang and Lee for the special case of $I \rightarrow I - 1$ transitions, and the general results seem to have been published first by Jackson, Treiman & Wyld (39). Further coulombic distortions than those included in $F(Z, W)$ are present in the results of the more general law 35 but disappear for the exclusively left-handed leptonic states here. The famous "Fierz Interference" terms (1) also disappear for the same reason.

The relations of the coefficients in 64 to the coupling constants of the law 47 are:

$$\xi = |C_V|^2 |\langle 1 \rangle|^2 + |C_A|^2 |\langle \sigma \rangle|^2, \quad 65.$$

$$\xi a = |C_V|^2 |\langle 1 \rangle|^2 - \frac{1}{2} |C_A|^2 |\langle \sigma \rangle|^2, \quad 66.$$

$$\xi d = -\Delta |C_A|^2 |\langle \sigma \rangle|^2, \quad 67.$$

$$\xi(A - B) = \pm 2\Delta |C_A|^2 |\langle \sigma \rangle|^2 \text{ for } e^\pm, \quad 68.$$

$$\xi(A + B) = -2(C_V C_A^* + C_A C_V^*) \langle 1 \rangle \langle \sigma \rangle \sqrt{I/I + 1}, \quad 69.$$

$$\xi D = i(C_V C_A^* - C_A C_V^*) \langle 1 \rangle \langle \sigma \rangle \sqrt{I/I + 1}. \quad 70.$$

The precise definition of $\langle \sigma \rangle$ is given by:

$$\langle \sigma \rangle = \langle I_f M | \sigma_z | I_f M \rangle / \langle I_f 1 M 0 | I_f 1 I M \rangle, \quad 71.$$

in which the denominator is the vector-addition coefficient for $I = I_f + 1$. The quantities Δ and Λ arise from combinations of vector-addition coefficients:

	Δ	Λ
$I \rightarrow I - 1$	1	1
$I \rightarrow I$	$1/(I + 1)$	$-(2I - 1)/(I + 1)$
$I \rightarrow I + 1$	$-I/(I + 1)$	$I(2I - 1)/(I + 1)(2I + 3)$

These are the same as defined by Jackson, Treiman & Wyld.

The most detailed type of measurement to which the result 64 applies has been carried out for neutrons only. For these $\langle 1 \rangle = 1$, $\langle \sigma \rangle = \sqrt{3}$ and $d = 0$. Then, formula 64 yields exactly the results discussed in the subsection, The Decay of Polarized Neutrons.

Other measurements on polarized nuclei only detected the electrons; hence 64 must be integrated over all neutrino directions for comparison with them:

$$\langle d\lambda/dp \rangle d\Omega_e = [g^2/(4\pi^4 \hbar^7 c)] F p^2 q^2 \xi \{1 + A(\langle M \rangle/I) \hat{I} \cdot \mathbf{v}/c\}. \quad 72$$

This yields the angular distribution 1 for completely polarized nuclei, when $\langle M \rangle = I$. $A = -1$ for pure GT negatron emitters undergoing an $I \rightarrow I - 1$ transition, like Co^{60} , while $A = \pm \Delta$ for GT radiation in general.

Most measurements are made on unpolarized nuclei, for which $\langle M \rangle = 0$ and $\langle M^2 \rangle = \frac{1}{3} \langle I^2 \rangle = \frac{1}{3} I(I + 1)$. Then 64 becomes:

$$d\lambda/(dp d\Omega) = [g^2/(4\pi^4 \hbar^7 c)] F p^2 q^2 \xi (1 + a \hat{q} \cdot \mathbf{v}/c). \quad 73.$$

This yields the electron-neutrino correlations exactly as discussed in connection with Figure 4. When the recoil goes undetected, one gets the electron spectrum:

$$d\lambda/dp = [g^2/(\pi^3 \hbar^7 c)] F p^2 q^2 \xi, \quad 74.$$

having the "statistical shape" (1), $\sim p^2 q^2$, modified only by the coulomb distortion, F . Finally, a last integration gives the half life, t :

$$\lambda = \ln 2/t = [g^2/(\pi^3 \hbar^7 c)] \xi (mc)^5 f, \quad 75.$$

from which the "comparative half life,"

$$ft = t(mc)^{-5} \int_0^{p_0} dp F p^2 q^2 \quad 76.$$

is derived.

The expectations for ordinary electron polarization measurements have already been discussed in the subsection, Restriction to Left-Handed Lepton States. They are independent of the ratio C_A/C_V . There are additional electron polarizations, both longitudinal and transverse to the electron's direction, which should be found for polarized nuclear sources. These

were predicted to occur long ago by Tolhoek & de Groot (40), since their appearance does not require violations of parity conservation. No attempts to detect them seem to have been made as yet.

THE NATURE OF THE NEUTRINO

The preceding sections concentrated on the form of the β -interaction. In the exposition certain conceptions about the neutrino were taken for granted. Concurrent developments will now be reviewed which may be regarded as directed toward clarifying the nature of the neutrino.

First, there has been an essential confirmation of the existence of neutrinos! This will be the subject of the next subsection. The evidence that neutrinos are chargeless, massless, and with spin $1/2$ has been known too long to warrant discussion here. There have been fresh developments which concern the difference between neutrinos and antineutrinos—discussed in terms of lepton conservation and the two-component theory, which will be the subjects of further subsections.

ANTINEUTRINO CAPTURE

The assumption that neutrinos carry away part of the energy, momentum, and angular momentum radiated in β -processes was needed to account for parts otherwise "missing," and this was long the only evidence for the existence of neutrinos. Reines, Cowan and their associates (41) obtained more concrete evidence when they showed that the neutrinos can be detected after they leave their sources, through effects they produce.

The feat was achieved by exposing huge tanks of proton-rich liquid scintillator to the radiation from a reactor. The intense negatron β -radioactivity in the reactor should produce a large flux of antineutrinos, according to the Normal Relation 2. The recapture of these particles should be able to reverse negatron decay, like that of the neutron itself, in the process:



This is expected to occur very rarely because of the characteristic slowness of β -interactions. (The capture of negatrons is much more easily observable, in suitable cases, only because an electron in an atomic orbit spends long times in the vicinity of the nucleus.) The investigators were nevertheless able to prove the occurrence of the process 77. They detected both its products, in delayed coincidence, the delay needed being found to correspond to the time required for the neutrons to slow down and be captured by cadmium impregnating the liquid. It is through the capture γ -rays released by the excited Cd nuclei that the product neutrons were detected. The characteristic scintillations caused by the positrons and the Cd γ -rays were viewed by banks of photomultiplier tubes. The emergent pulses were highly discriminated for the right energies and the right delay times. The quantitative results have been presented most recently in a way directly comparable to a certain theoretical cross section.

The theoretical cross section is evaluated by calculating the positron production rate per proton when a unit current density of antineutrinos is incident. Before the discovery of the leptonic polarizations, the antineutrino current was represented as consisting, half-and-half, of both the possible polarizations. In consequence, the antineutrinos were expected to be oriented correctly, for each accessible "channel" of reaction, in only half the incidence on the average. Now, the incident beam is no longer regarded as being divided up into two polarizations. All antineutrinos emitted in negatron decay are now believed to be oriented in exactly the same way, with their spins parallel to their direction of motion. They cannot be depolarized except through their annihilation; hence all those arriving at a given proton have the same longitudinal polarization. This must be correct for the process, if it goes at all. As a result, the new expectations for the cross section are double the old ones. The cross section following from the interaction 47 is now expected to be:

$$\sigma_p = [2g^2/(\pi\hbar^4c^3)]\langle pW \rangle (|C_V|^2 + 3|C_A|^2). \quad 78.$$

It is appropriate to use the comparative half life $(ft)_n$ of the inverse process, the neutron decay, as a measure of $g^2(|C_V|^2 + 3|C_A|^2)$, and this yields:

$$\sigma_p = [2\pi^2 \ln 2 / (ft)_n] \langle pW \rangle \hbar^3 / [(mc)^5 c^2]. \quad 79.$$

The quantity $\langle pW \rangle$ is the product of the positron momentum and energy, averaged over the spectrum of incident antineutrino energies.

A large uncertainty in the evaluation of $\langle pW \rangle$ stems from the difficulty of determining the energy distribution of the antineutrinos from the reactor. It is done by measuring the negatron spectra characteristic of fission products and their daughters (42a, b), then using the theoretical relations between the negatron and corresponding antineutrino energies. The latest re-evaluation (43 a, b) resulted in a firm lower limit $\sigma_p > 7(10)^{-44}$ cm.² and a "best value" of $14 (10)^{-44}$ cm.² The latter corresponds to an average of about $eq = 2.7$ Mev for the antineutrinos of sufficient energy to surpass the threshold, 1.8 Mev, of the reaction 77. The theoretical expectations, thus evaluated, are to be compared with an experimental value $\sigma_p = (11 \pm 4) 10^{-44}$ cm.² reported most recently (43a, b). At least, no inconsistency shows up in this extremely difficult experiment.

THE NEUTRINO-ANTINEUTRINO DISTINCTION

Experiments involving the recapture of (anti) neutrinos gained interest as possible checks on the presumed distinction between neutrino and antineutrino. The fact that both are expected to be chargeless, without rest-mass, and with spin 1/2 begins to make it difficult to conceive of any intrinsic difference between them. The distinction was introduced in the first place only because the Dirac theory of spin 1/2 particles admits, together with each state ψ , a "charge-conjugate" state $C\psi$, even for neutral particles (vide the antineutron!). The charge-conjugacy of fermions is fairly representable

by the "hole picture," which underlies the interpretations given the Normal Relation 2. However, it is equally well possible to formulate a description of the neutrino, by "self-charge-conjugate" states, which makes no distinction between it and its antiparticle, so that $\bar{\nu} \equiv \nu$. That was shown long ago by Majorana (44).

Attributions of "intrinsic" properties have meaning only as a way of representing behavior during interactions. The Normal Relation 2 leads one to expect at least this difference of interactions: antineutrinos should be absorbable by protons but not by neutrons, whereas neutrinos should have the converse behavior. Thus, the putative antineutrinos emitted by reactors should be captured by protons, as discussed in the preceding subsection, but should fail to induce reversals of positron decay or orbital electron capture, which require absorptions by neutrons.

Attempts directed at testing this distinction were made by Davis (45). He exposed thousand-gallon quantities of a chlorine compound to reactor fluxes and looked for evidences of the hypothetical reaction:



The argon is a well-known isotope which decays by the orbital electron capture:



The hypothetical reaction 80 is clearly not simply a reversal of 81 and is not expected to take place unless $\bar{\nu} \equiv \nu$. Davis could report no evidence that it does take place and was able to put an upper limit on its occurrence: about one-ninth of what was anticipated if every antineutrino were as effective as a neutrino is expected to be.

Meanwhile, the significance of the Davis experiment has been altered by the discovery of the lepton polarizations. Whatever neutral leptons are emitted in negatron decay, as in reactors, are now believed to be exclusively "right-handed." Furthermore, the neutral leptons from orbital electron capture, as in 81, are believed to be exclusively "left-handed," and only the recapture of such left-handed particles is expected to be able to reverse that reaction. Thus, Davis should obtain a null result just to be consistent with the findings about polarizations, regardless of the status of the neutrino-antineutrino distinction!

The same sort of reinterpretation also applies to the attempts to observe neutrinoless double β -decay (46). The simultaneous emission of two negatrons is expected from nuclei which gain stability in the transformation of two neutrons, but not when only one transforms. The process is evaluated as going through a virtual intermediate state in which one of the neutrons has become a proton, and a negatron has appeared together with a neutral lepton. There can be a "neutrinoless" final state if that neutral lepton can be absorbed in the transformation of the second neutron, to produce the second negatron. Such a neutrinoless double β -decay has two main factors

favoring its detectability, relative to processes in which two neutral leptons are also final products. In the first place, a neutral lepton which is reabsorbed can have an arbitrary energy in the temporary intermediate state, and this greatly enlarges the "phase space" available to the process. Secondly, when the two negatrons are given all the energy released, then the sum of their energies forms a well-defined peak. Such a peak is much more easily distinguished above background than is the continuous spectrum to be expected when the energy is shared with final neutral leptons. Nevertheless, the existence of the process could not be proved (46). For instance, a lower limit of of $4 (10)^{18}$ years (47) could be placed on the observable half life of Nd^{150} , yet the theoretical estimates (46) for its lifetime against neutrinoless decay range from $2 (10)^{13}$ years to an extreme of $2 (10)^{17}$ years.

At one time, one would have said that a nonoccurrence of the neutrinoless decay signifies that the antineutrino resulting from the first neutron's decay is distinct from the neutrino needed for the transformation of the second neutron. Now, however, we may say that, regardless of the neutrino-antineutrino distinction the intermediate neutral lepton should not be absorbed by the second neutron because it has the wrong longitudinal polarization. These reinterpretations apparently rob investigators of what had seemed to be the most direct way to check on the neutrino-antineutrino distinction.

THE PRINCIPLE OF LEPTON CONSERVATION

The Normal Relation $p + e^- \leftrightarrow n + \nu$ was meant to imply that the emission of a positron is to be treated like the absorption of a negatron so that the process, in effect, substitutes a neutrino for an electron. Similarly, negatron emission is to be treated as following upon a neutrino absorption. Always, a lepton is to appear for each that disappears (48), so that the Normal Relation can be said to embody a principle of lepton conservation. It is characterized by a maintenance of the lepton-antilepton difference in each process.

The principle in question is sometimes formalized in a way resembling that used for electric charge conservation. One assigns a unit of "leptonic charge" to each negatron and neutrino, and a negative unit to each positron and antineutrino. Then a requirement of "leptonic charge conservation" is equivalent to maintaining the lepton-antilepton difference.

Of course, the considerations here are predicated on a neutrino-antineutrino distinction; but even if these particles are distinct, the principle of lepton conservation does not necessarily follow. It is true that all the forms of β -interaction discussed in the section The Fermi Theory were automatically lepton-conserving. However, interaction forms which violate the principle of lepton conservation are easily constructed.

The discussion of non-lepton-conserving interactions has been revived quite recently (49a, b, c). To construct a general one, it is only necessary to add, to each term of the coupling form 35, another term in which the neutrino

field ψ_ν is replaced by its charge conjugate $C\psi_\nu$. The new terms may have arbitrary coupling strengths $D_X, D_{X'}$, in place of $C_X, C_{X'}$, with the result:

$$h = g \sum_X \{ \bar{\psi}_p O_X \psi_n \} \{ \bar{\psi}_\nu O_X [(C_X + C_X' \gamma_5) + (D_X + D_X' \gamma_5) C] \psi_\nu \} + \text{c. c.} \quad 82.$$

Physically, this will allow neutrinos and antineutrinos to replace each other in every process, i.e. the Normal Relation 2 is supplemented to:

$$p + e^- \leftrightarrow n + (\nu \text{ or } \bar{\nu}). \quad 83.$$

One might say that, with this, the property of being a neutrino vs. an antineutrino is no longer a "good quantum number." By choosing $D_X, D_{X'}$ equal to $C_X, C_{X'}$ one has the equivalent of a "Majorana neutrino," i.e. $\bar{\nu} \equiv \nu$.

The generalization to the non-lepton-conserving interaction 82 results only in certain formal changes for "one-step processes," involving only one neutrino absorption or emission:

$$C_X^* C_X^{(\prime)} \rightarrow C_X^* C_X^{(\prime)} + D_X^* D_X^{(\prime)}. \quad 84.$$

There is only this renaming of the coupling constant combinations which occur. After all, for the one-step processes there is only a renaming of the neutral lepton, without any test of its neutrino vs. antineutrino character. Whatever they may be called, the neutral leptons emerging in negatron decay must be left-handed, those in positron decay, right-handed. Null results are still to be expected in the Davis experiment and in searches for neutrinoless double β -decay, simply because these would require neutral leptons of the "wrong" polarization.

The intrusion of $D_X, D_{X'}$ does not change the implications of The Key Experiments for the coupling constants $C_X, C_{X'}$, as given in 42, 46, and 60. The latter are now supplemented with:⁸

$$D_X' = D_X, D_{S,T,P} = 0 \quad \text{and} \quad D_A \approx -D_V. \quad 85.$$

The interpretation still stands that it is primarily the left-handed states, of

⁸ It is perhaps not clear how two pieces of information e.g. both $D_A \approx -D_V$ and $C_A \approx -C_V$, can follow from the same data which yielded only $C_A \approx -C_V$ when the D_X 's were presumed nonexistent. Consider the experimental finding of near-isotropy in the angular distribution of the electrons from the neutron, both relative to the neutral lepton and to the (\sim parallel) neutron spin, i.e. $a \approx 0$ and $A \approx 0$, from which $C_A \approx -C_V$ was formerly deduced through 28. Introduce the substitutions $R = C_A + C_V$, $L = C_A - C_V$, $\bar{R} = D_A + D_V$, $\bar{L} = D_A - D_V$ into the expressions 24, 25, as generalized according to 84:

$$\begin{aligned} \xi_n a &= -\frac{1}{2} [LR^* + L^*R + \bar{L}\bar{R}^* + \bar{L}^*\bar{R}] \approx 0 \\ \xi_n A &\approx -|R|^2 - |\bar{R}|^2 \approx 0. \end{aligned}$$

The last is one equation giving two results. $R \approx 0$ and $\bar{R} \approx 0$! Of course, the conclusion $D_A \approx -D_V$ is subject to the same qualifications as $C_A \approx -C_V$, discussed in preceding sections.

all the particles as they enter the relation 2 or 83, which participate in β -interactions.

One may still hope to check on the validity of the lepton conservation principle in the one of the two-step processes reviewed above which is not nullified by misfits of the neutral lepton polarization: the capture by protons. The neutral leptons from the reactor will consist of neutrinos and antineutrinos in the ratio $|D_A|^2$ to $|C_A|^2$, insofar as $D_V \approx -D_A$, $C_V \approx -C_A$. The neutrinos will be captured by protons in proportion to $|D_A|^2$, while the antineutrinos are captured proportionally to $|C_A|^2$. In consequence, the theoretical cross-section 78 is now to be multiplied by

$$(|C_A|^4 + |D_A|^4) / |C_A|^2(|C_A|^2 + |D_A|^2). \quad 86.$$

This can deviate from unity by no more than 18 per cent, at $|D_A|^2 \approx 0.4|C_A|^2$, so the present experimental accuracy is insufficient for the check. The experiment is expected to give the same results whether $D_A = 0$ or $D_A = C_A$ so it cannot discriminate against a "Majorana neutrino" $\bar{\nu} \equiv \nu$.

THE TWO-COMPONENT NEUTRINO THEORY

So far, we have sought a necessary, rather than merely sufficient, description of the neutrino. Treating it like a massless and chargeless electron has led to giving it four "internal" degrees of freedom, requiring representation by a four-component (Dirac spinor) field. Two correspond to spin orientations, and the remaining two are the ones which permit a neutrino-antineutrino distinction. It is the latter possibility which generated the question of lepton conservation. We might have started with some even more generalized conception, e.g., admitting more than four "internal" freedoms, and that would have generated more questions—*ad infinitum*! This is an argument for starting from an opposite point of view, by asking only what conception of the neutrino is sufficient for describing its so far evident behavior.

We have seen that present experimental knowledge is compatible with both of two "extremes." On the one hand, we can adopt a "Dirac neutrino," distinct from its antineutrino ($\bar{\nu} \neq \nu$), and with it a principle of lepton conservation. On the other hand, there is no evidence against a Majorana neutrino $\bar{\nu} \equiv \nu$ which may be regarded as yielding a "maximum" of lepton non-conservation. The capture of neutral leptons by protons should, in principle, be able to distinguish an intermediate degree of lepton non-conservation ($0 < |D_A| < |C_A|$) but not lepton conservation ($D_A = 0$) from the "Majorana" case ($D_A = C_A$).

From the point of view of sufficiency, the "Majorana neutrino" may seem to have the advantage. It requires giving the neutrino only the two "internal" degrees of freedom for spin, sufficiently described by a (spinor) field with only two components.⁹ Then the findings about the lepton polari-

⁹ The reduction from the four-component Dirac spinor, ψ , can be carried out in analogy to 37 and 54. Putting $D_A = C_A$, in 82, projects out just the part $\frac{1}{2}(1+C)\psi$, of

zations mean that the only distinction between the neutral leptons emitted in negatron and positron decay is that they are in left- and right-handed states, respectively.

This advantage of the Majorana picture is only an apparent one, however. It is equally simple to maintain the neutrino-antineutrino distinction, but let it coincide with the left- and right-handedness (50a, b, c). Speaking of a right-handed neutral lepton would then be equivalent to speaking of the antineutrino. There is the appealing result that the intrinsic difference between a neutrino and antineutrino is that the first is left-handed and the other right-handed. Again, only a two-component spinor field is sufficient to describe the particle (e.g., u_ν of 59). Now, the occurrence of only left-handed normal lepton states, together with only right-handed charge-conjugate states, automatically yields lepton conservation.

The two-component neutrino theory in the last guise was the one suggested by Lee & Yang (51), Landau (52), and Salam (53) almost immediately after the discovery of the parity nonconservation. One can get the field equations for the two-component neutrino from the Dirac equation 38, specialized to zero mass ($m \rightarrow 0$, $p \rightarrow q$, $W \rightarrow cq$). Applying the operation $\frac{1}{2}(1 + \gamma_5)$ to the result projects out $\phi_\nu = \frac{1}{2}(1 + \gamma_5)\psi_\nu$, obeying $q\phi_\nu = \alpha \cdot q \phi_\nu$, since γ_5 commutes with α . Because $\alpha = -\sigma\gamma_5$ and $\gamma_5\phi_\nu = \phi_\nu$, the field equation becomes:

$$q\phi_\nu = -\sigma \cdot q \phi_\nu. \quad 87.$$

This can be satisfied by a two-component field because the ordinary, two-dimensional Pauli representation of σ is adequate.¹⁰ The equation for the antineutrino state, $\phi_{\bar{\nu}} = C\phi_\nu$, follows from operating on 87 with the charge-conjugation operator C which anticommutes with σ :

$$q\phi_{\bar{\nu}} = +\sigma \cdot q \phi_{\bar{\nu}}. \quad 88.$$

These equations make clear that a positive energy (cq) neutrino must have $\sigma \cdot q < 0$, while a positive-energy antineutrino has $\sigma \cdot q > 0$, i.e. spins antiparallel and parallel to the direction of motion, respectively.

An equation of the type 87 was discussed long ago by Weyl (54) as a mathematical curiosity. It was rejected as of no physical interest by Pauli (55) because of its inconsistency with parity conservation ($\sigma \cdot q$ is a pseudo-scalar!). One can picture a neutrino, spinning antiparallel to its direction of motion, approaching a mirror. The reflection is a particle spinning parallel

$\psi_\nu = \frac{1}{2}(1 - C)\psi_\nu + \frac{1}{2}(1 + C)\psi_\nu$, where $C^2 = 1$ so that $(1 - C)(1 + C) = 0$. The two parts $\frac{1}{2}(1 \pm C)\psi_\nu$ are invariantly independent, each requiring only two of the four components for its description, in a suitable representation.

¹⁰ Some readers will recall that Dirac was driven to a four-component field by the impossibility of constructing four mutually anticommuting, two-dimensional matrices to represent α and β . (Thus, the antiparticle was born!) However, when $m = 0$, β does not enter the field equation and only three mutually anticommuting Pauli matrices need be formed.

to its motion, hence an antineutrino instead of a neutrino, in the present description. This "built-in," maximal violation of the old parity conservation principle led to the short-lived idea that it is just the participation of neutrinos which introduces parity violations into processes. The idea was unwelcome from the beginning, because there are apparent parity violations also in processes not involving neutrinos—like the decay of K mesons into pions. Moreover, it turns out (50 a, b, c) that there is no necessary connection between parity violation and a two-component theory of the neutrino. Within the framework of the latter type of description, one is free to drop the neutrino-antineutrino distinction so that the right-handed particle can also be treated as a neutrino, simply in a different state of spin. It was no accident that the experiments discussed above could not distinguish the two "extremes" of lepton-nonconservation, i.e. between treating the left-handed particle as a neutrino, the right-handed one as an antineutrino, and treating both helicities as different states of a Majorana neutrino. In favor of retaining the neutrino-antineutrino distinction, there is the symmetry this gives to the description in terms of lepton conservation.

We conclude that a two-component theory of the neutrinos is adequate¹¹ for describing their behavior of the nuclear β -processes. We shall also see that it is adequate for describing them in all other known processes (next section), since any given instance of these seems to generate only a left-handed one or only a right-handed one.

THE UNIVERSAL FERMI INTERACTION

The nuclear β -decay processes, which are the primary concern of this review, belong to a class known as the "weak interactions." The latter are distinguished from "strong interactions," like those between pions and nucleons, and also from the "intermediate," electromagnetic interactions. The weak interactions, in general, are those held responsible for the slow decays of elementary particles, like the free pion decay, and the decay of K particles into pions, as well as the nuclear β -decays. When the decay rates are reduced to coupling strengths, then these strengths are characteristically many order of magnitude smaller than is the dimensionless electromagnetic "coupling strength," $e^2/\hbar c = 1/137$. For instance, the nuclear β -decay constant, G of the $V-A$ Law 62, must have a magnitude such that $G^2 \approx 10^{-23}$ in dimensionless units ($\hbar = m = c = 1$), in order to give the correct neutron lifetime via 75.

Nuclear β -decay is just one example of a whole subclass of weak interactions which are known as "Fermi interactions." Also included in the subclass are muon capture by nucleons, muon decay, and, less certainly, the

¹¹ There are occasional attempts to treat several, if not all, the "fundamental" particles as alternative states of some single, comprehensive "matter field." The four-component description of the neutrino seems to fit better into most of these schemes, but, of course, these have been too speculative to make that a valid argument in favor of retaining the four-component description.

"leptonic modes" of hyperon decay. The characteristic feature of any Fermi interaction is supposed to be the simultaneous participation of four fermions (spin $\cdot 1/2$ particles). Quite early (56a to d) it began to be evident that all the Fermi interactions require about the same coupling strength. It then became natural to make the hypothesis of a "universal Fermi interaction," by which not only the strength but also the form (e.g., the $V\text{-}A$ Law) is taken to be the same for all Fermi interactions.

It is beyond the scope of this review to give full treatment to all the Fermi interactions. However, some attention will be given to those about which the information is least fragmentary, because of the light they may throw on the nuclear β -processes.

PION DECAY

The decay of pions into electrons and neutrinos,

$$\pi^\pm \rightarrow e^\pm + (\nu \text{ or } \bar{\nu}), \quad 89.$$

was sought for many years before its recent discovery (57a, b). The basis for having expected it (58) was simply this. The known, strong interaction of pions with nucleons leads to the expectation that a pion will frequently fluctuate into temporary, virtual states consisting of nucleon-antinucleon pairs. For example, a positive pion may temporarily split into a proton-antineutron pair:

$$\pi^+ \leftrightarrow p + \bar{n}. \quad 90.$$

Now, as reference to the Normal Relation 2 shows, there is a chance for the temporary state to decay according to

$$p + \bar{n} \rightarrow e^+ + \nu. \quad 91.$$

The final state here can develop consistently with energy conservation, and the long failure to find it had presented a critical problem. The problem is related to the concerns of this review through the presumed occurrence of the step 91 in the decay.

Evaluating the expectations for the two-step process of pion decay, as here conceived, will require the introduction of two types of coupling, h and h_π . By h is meant the β -decay coupling responsible for the step 91, as given by 47, say. The expression h_π is the pion-nucleon coupling responsible for the step 90. The best current theory of it is that it is proportional to the pseudoscalar pion field and that it involves the nucleons only by also being proportional to the pseudoscalar density,

$$h_\pi \sim i\psi_p^\dagger \beta \gamma_5 \psi_n \sim + h_\pi^*. \quad 92.$$

The further clarification (58) of what is involved is perhaps best discussed by considering a familiar expression from which the rate of the two-step process may be calculated:

$$\lambda = \frac{2\pi}{\hbar} \rho(E_f) \sum_{\sigma_e, \sigma_\nu} \left| \sum_i \frac{\langle f | h | i \rangle \langle i | h_\pi | 0 \rangle}{E_i - E_0} \right|^2. \quad 93.$$

Here, $\rho(E_f)$ is the number of final states available per unit energy. E_f is the final energy while $E_0 = m_\pi c^2$ is the initial energy, of the pion at rest. They must match according to

$$E_f = W + cq = W + cp = m_\pi c^2 = E_0, \quad 94.$$

where W and cq are the positron and neutrino energies; clearly, the positron and neutrino momenta must be equal and opposite: $q = -p$. The E_i 's are energies of the intermediate states. The summation over these states, Σ_i , will include¹² summation over nuclear spins σ_p , σ_n and also integration over all possible nucleonic momenta $p_p = -p_n$. The latter integration will diverge as $p_p \rightarrow \infty$, a familiar difficulty in problems dealing with intermediate states, and one which has not yet been satisfactorily solved. This discussion, therefore, is concerned first with what can be said independently of this divergence in the theoretical absolute rate.

The pion decays into positrons are now compared with the decays into muons:

$$\pi^+ \rightarrow \mu^+ + \nu. \quad 95.$$

This process is observed to occur about 10,000 times (57 a, b) as often as the decay into electrons, and its competition is what had made it difficult to detect the electron decay mode. The pion-to-muon decay can be expected on much the same basis as the pion-to-electron decay. The capture of muons by nucleons had long been known and can be presumed to occur according to:

$$p + \mu^- \leftrightarrow n + \nu, \quad 96.$$

i.e., in exactly the same way as the orbital electron capture of the Normal Relation 2, except that the negative muon replaces the negatron. With this presumption, the calculation of the pion-to-muon rate goes in exactly the same way as for the pion-to-electron rate. The troublesome divergent integrals which occur, involving as they do only the intermediate nucleons, are exactly the same in the two cases. Thus, the ratio of the two modes of decay becomes finite, and unambiguous to calculate.

We proceed by noting first that the final stage amplitude in the expression 93 becomes, on the present presumptions, proportional to (see 47):

$$\Sigma_{\sigma_p, \sigma_n} \langle f | h | i \rangle \langle i | h_\pi | 0 \rangle \sim g [\phi_n \beta \gamma_\mu \phi] \Sigma_{\sigma_p, \sigma_n} [\psi_n^\dagger \beta \gamma_\mu (C_V - C_A \gamma_5) \psi_p] (\psi_p^\dagger \beta \gamma_5 \psi_n), \quad 97.$$

¹² Included among the possible intermediate states must be some which occur with the couplings h and h_π acting in the reverse order $\sim \langle f | h_\pi | i' \rangle \langle i' | h | 0 \rangle$. The intermediate states i' will be ones in which the pion has not yet disappeared (h_π has not yet acted) but a "vacuum fluctuation" generated by h has caused the appearance of a neutron-antiproton pair, i.e. $\pi^+ \rightarrow \pi^+ + (n + \bar{p} + e^+ + \nu)$ is the first step. The final state $e^+ + \nu$ appears after the pion absorbs the nucleon pair through the coupling h_π . The occurrence of these alternative intermediate states can influence the way in which the absolute rate diverges, but it does not alter significantly the remaining discussion in the text.

where the unlabeled ϕ may be either the positron or positive muon spinor. The summation over the nucleon spins, σ_p, σ_n , vanishes except for the component $\gamma_\mu \rightarrow \gamma_4 \equiv \beta$; this is to be expected, since the nucleon state must be rotationally invariant in order to have the zero angular momentum characteristic of the pion. Then the decay rate will be proportional to:

$$\lambda \sim \sum_{\sigma_p, \sigma_n} |\phi_v \phi|^\dagger = \frac{1}{2}(1 + \hat{q} \cdot \mathbf{v}/c) = \frac{1}{2}(1 - v/c), \quad 98.$$

since $\mathbf{q} = -\mathbf{p}$. The preference for a positive correlation of the neutrino and electron directions, in $0 \rightarrow 0$ transitions, has already been discussed in the subsection, Electron-Neutrino Correlations. However, the momentum conservation here demands an exactly negative correlation, hence the minimum value $\frac{1}{2}(1 - v/c)$, for the spin sum.

The result 98 is just what can account for the large preponderance of muon over electron emissions by pions. The electron requires about 100 Mev less of the pion mass-energy for its formation than does the muon; hence the electron's velocity is much closer to the speed of light: $1 - v_e/c \rightarrow 0$. The precise ratio of the electron to muon emissions is obtained after the statistical factor is also taken into account:

$$\rho = \frac{4\pi p^2 dp}{(2\pi\hbar)^3 dE_0} = \frac{1}{2\pi^2 \hbar^3 c} \frac{p^2}{1 + v/c}, \quad 99.$$

since $dE_0 = dW + cd\mathbf{p} = cd\mathbf{p}(1 + v/c)$, according to the energy conservation relation 94. Now,

$$\frac{\lambda_e}{\lambda_\mu} = \frac{[p^2/1 + v/c]_e}{[p^2/1 + v/c]_\mu} \cdot \frac{1 - v_e/c}{1 - v_\mu/c} = \left(\frac{m_\pi}{m_\mu}\right)^2 \frac{(m_\pi^2 - m_e^2)^2}{(m_\pi^2 - m_\mu^2)^2}, \quad 100.$$

after using $W = c\sqrt{p^2 + m^2} = c^2(m_\pi^2 + m^2)/2m_\pi$, which also follows from 94. When one puts $m_\mu/m_e = 206.9$ and $m_\pi/m_e = 273.3$, the result is $\lambda_e/\lambda_\mu = 1.3(10)^{-4}$, which agrees with the reported observations, well within their margins of uncertainty.

It is interesting to see that, on the above theory, pions are sources of left-handedly polarized positrons and positive muons (and right-handed negative particles) in contrast to ordinary β -decay, which produces the opposite helicities of the charged leptons. One can show this simply by omitting the summation over the positron or muon spin in the expression 98:

$$\sum_{\sigma_p} |\phi_v \phi|^\dagger = \frac{1}{4} \left[1 + \hat{q} \cdot \mathbf{v}/c + (\boldsymbol{\delta} \cdot \mathbf{v}/c) \left(1 + \frac{c\hat{q} \cdot \mathbf{p}}{W + mc^2} \right) + \boldsymbol{\delta} \cdot \hat{q} mc^2/W \right], \quad 101.$$

where $\boldsymbol{\delta}$ is the unit vector in the direction of the positron or muon spin. Now, if one were to average this expression over random neutrino directions, $\langle \hat{q} \rangle = 0$, as one must for the polarization measurements on the positrons of ordinary β -decay, then one would get the right-handed positrons then observed, i.e., an intensity proportional to $1 + \boldsymbol{\delta} \cdot \mathbf{v}/c$. However, in the pion decay, here, the neutrino's direction is restricted to $\hat{q} = -\mathbf{v}/v$ by momentum conservation. With this, the intensity 101 reduces to:

$$\sum_{\sigma_p} |\phi_v \phi|^\dagger = \frac{1}{4}(1 - v/c)(1 - \boldsymbol{\delta} \cdot \mathbf{v}/v), \quad 102.$$

and this corresponds to left-handed positrons or muons. That happens despite the fact that $\phi \equiv \frac{1}{2}(1 + \gamma_5)\psi$ is a "right-handed" antiparticle state, although only "to the degree v/c ." This necessity for the positrons and muons of π^+ -decay to be left-handedly polarized can be blamed for the fact that the process tends to vanish as $v \rightarrow c$, which is the limit in which the right-handed positron rule of ordinary β -decay is fully enforced. The rule that the neutrinos be left-handed is, by contrast, strictly enforced, since they always have the speed of light. Thus, the whole situation arises out of the fact that the neutrino and positive particle, emerging from the pion disintegration, must have their spins oppositely directed to conserve the pion's zero spin, and their momenta must be oppositely directed to conserve the momentum.

The discussion so far has been largely restricted to positive pion decay only to avoid confusion. It would have gone in exactly the same way for negative charges, with the conclusion that the negative leptons from π^- -decay are right-handedly polarized, i.e., the opposite of positive leptons from π^+ -decay, and of negative electrons from ordinary β -decay. The expectation has been most directly confirmed by a recent experiment (59) in which the muon spin was transferred to B^{12} nuclei by allowing the muons to be captured by C^{12} . The asymmetry of the β -decay from the polarized B^{12} reveals its sense of polarization in just the way that the Co^{60} experiment, described first in this article, reveals the nuclear polarization in that case.

The next consideration will be the extent to which it has been possible to confirm that pions decay at just the rate expected from the above theory. When the calculation is straightforwardly carried out, along the lines discussed in connection with the "perturbation-theoretic" expression 93, the result is (for muon emission):

$$\lambda = [g^2 | C_A |^2 c^4 / (2\pi^4 \hbar^7)] [M^2 m_\mu^2 (m_\pi^2 - m_\mu^2)^2 / m_\pi^3] \cdot (G_\pi^2 / 4\pi) J_0^2. \quad 103.$$

Here, G_π is the coupling constant for the pion-nucleon interaction of 92, normalized in such a way that $G_\pi^2 / 4\pi \approx 15$ is the dimensionless magnitude indicated by such data as the pion-nucleon scattering. If plane waves of momentum $P = p_p = -p_n$ are used for the intermediate state, then J_0 is the divergent integral

$$J_0 = \int_0^\infty dP P^2 / (P^2 + M^2 c^2)^{3/2}, \quad 104.$$

which was mentioned in connection with the discussion of 93.

Clearly the use of plane waves to describe the intermediate nucleons is unjustifiable, in view of the known strong interactions between nucleons. Indeed the interaction is strong enough to put into doubt the whole "perturbation-theoretic" approach of 93. Goldberger & Treiman (60) tried to avoid such oversimplifications with a "dispersion-theoretic" approach in an attempt to find quantitative relations on only a basis of general invariance properties. They succeeded in relating the intermediate state amplitude concerned in the pion decay to the phase shifts in nucleon-antinucleon

scattering. As a result, the integral J_0 , in the rate expression 103, is replaced by

$$J_0 \rightarrow J/[1 + J(G_\pi^2/2\pi^2)], \quad 105.$$

where J differs from J_0 of 104 by the inclusion of a factor in the integrand which is a function of the phase-shifts mentioned. The value of J remains ambiguous, but the investigators were able to conclude that $J(G_\pi^2/2\pi^2) \gg 1$. This has the consequence that, in a fair approximation, the J_0 of the formula 103 can be replaced by the finite number $2\pi^2/G_\pi^2 \approx 1/10$. One now has a definite estimate for the pion lifetime $\tau_\pi = 1/\lambda$. Taking the pseudovector coupling strength as indicated by the neutron lifetime and the finding 30, a calculated value $\tau_\pi = 3.2(10)^{-8}$ sec. emerges. This is in perhaps too good an agreement with the observed mean life $\tau_\pi = (2.9 \pm 0.3) 10^{-8}$ sec. (61).

One surprise may be the occurrence in 103 of only the pseudovector coupling constant, C_A , and not the vector coupling constant, C_V , which was still included in the expression 97. One can readily calculate that, of the terms of 97 which survive the requirement of rotational invariance occasioned by the zero spin of the pion,

$$C_V \Sigma_{\sigma_p, \sigma_n} (\psi_n^\dagger \psi_p) (\psi_p^\dagger \beta \gamma_5 \psi_n) = 0, \quad 106.$$

while

$$C_A \Sigma_{\sigma_p, \sigma_n} (\psi_n^\dagger \gamma_5 \psi_p) (\psi_p^\dagger \beta \gamma_5 \psi_n) = C_A \cdot 2Mc/(P^2 + M^2c^2)^{1/2}, \quad 107.$$

the latter, for the plane waves used for 104. The vanishing of the vector contribution can be ascribed to the fact that the pion-nucleon coupling produces an intermediate nucleon-antinucleon pair of odd relative parity, and this violates the selection rule for a nonvanishing vector coupling contribution. The same thing would happen with a scalar (S) or tensor (T) β -coupling law (58). Thus, if the discovery of the right ratio of electron to muon emission by pions had come earlier, it would have provided a strong argument that a law including A -coupling, rather than the formerly accepted ST coupling, is the proper one. Besides the pseudovector (A) β -coupling, only a pseudoscalar (P) coupling could have given a pion decay, and the latter possibility is discussed in the next subsection.

It should still be pointed out that the discussion in this subsection was based on the presumption that it is the negative muon which is to be treated as a normal particle, like the negatron, while the positive muon is identified as the antimuon. Actually, an interchange of roles would make no difference to the results either for the μ -capture represented by 96 or for the pion decay. Moreover, because these processes are of first order in the β -coupling, a generalization to a nonconservation of leptons would also make no difference to the physical results.

PSEUDOSCALAR β -COUPLING

The results on pion decay, just reviewed, may serve to settle the question as to whether a pseudoscalar (P) form of β -coupling exists, besides the V

and A forms. The P -coupling was discarded, above, when $C_P=0$ was adopted in 46, in order to guarantee that only left-handed normal leptons would be generated. However, if one considers with more care the nuclear β -decay experiments which exhibited the helicity of the leptons, then it appears that in all those cases the P -coupling did not have a chance to show itself, even if it should exist.

The largest effects of the P -coupling can become observable only in transitions between nuclear states of opposite parity, conventionally classified as "once-forbidden." Even in these, competition from the Fermi and GT radiations is to be expected. This circumstance makes it difficult to prove either the presence or absence of a P -coupling in nuclear β -decay.

Now, as Ruderman & Finkelstein (58) already showed, if any pseudoscalar β -coupling existed, at all comparable with the pseudovector coupling, then it would predominate in pion decay and, moreover, cause the pions to emit more electrons than muons, contrary to what is observed.

That result is easy to understand from a direct comparison of the characteristics of a pseudoscalar (P), as against pseudovector (A) β -coupling, as revealed by the relations 45. The P -coupling would generate a lepton and antilepton (one charged, the other neutral) with the same helicity, whereas the A coupling generates opposite helicities of the two particles. When the two particles must be emitted into opposite directions, as in the pion decay, then the A -coupling has difficulty preserving the zero angular momentum and this results in the small factor $\sim(1-v/c)$ in the intensity, saved from vanishing only because the "handedness" is never quite complete except in the limit $v \rightarrow c$. On the other hand, there is no similar difficulty for the P -coupling, and this shows itself by a replacement of the factor $(1-v/c)$ by $(1+v/c)$. The electron-to-muon ratio 100 becomes, for the P -coupling:

$$\left(\frac{\lambda_e}{\lambda_\mu}\right)_P = \frac{p_e^2}{p_\mu^2} = \left(\frac{m_\pi^2 - m_e^2}{m_\pi^2 - m_\mu^2}\right)^2 = 5.5, \quad 108.$$

more than 10,000 times as large as the ratio observed.

The last result is not a conclusive argument against the P -coupling unless it can also be shown that the absolute rate generated by the P -coupling is comparable to that caused by the A -coupling present. The factor in the intensity 107, for the A -coupling, is replaced by

$$C_P \Sigma_{\sigma p, \sigma n} |\psi_n^\dagger \beta \gamma_5 \psi_p|^2 = 2C_P, \quad 109.$$

for the P -coupling. Here, the divergent absolute rate is much less damped (as $P \rightarrow \infty$). Treiman & Wyld (62) make the more quantitative estimate that

$$|C_P| \lesssim (m_e/M) |C_A| \approx 5(10)^{-4} |C_A| \quad 110.$$

is necessary for conformity to the observations on the pion decay.

MUON DECAY

We have just reviewed a process by which both the states $(\mu + \nu)$ and $(e + \nu)$ are reached from $\pi \leftrightarrow (p + \bar{n})$, and so it is scarcely a surprise that they

should also be able to reach each other, in the form of muon decay:

$$\mu \rightarrow e + \nu + \bar{\nu}. \quad 111.$$

The nucleonic state was found coupled to $(e+\nu)$ in proportion to the current $(\phi_\nu \dagger \beta \gamma_\mu \phi_e)$, and to $(\mu+\nu)$ through $(\phi_\nu \dagger \beta \gamma_\mu \phi_\mu)$. One may then expect the muon decay to be generated by the coupling:

$$h = \sqrt{8}G(\phi_\mu \dagger \beta \gamma_\mu \phi_\nu)(\phi_\nu \dagger \beta \gamma_\mu \phi_e) + \text{c.c.}, \quad 112.$$

where, as in the $V-A$ Law 62, each $\phi = \frac{1}{2}(1+\gamma_5)\psi$ is the "left-handed" projection of ψ . The coupling here can be shown mathematically equivalent, within an absolute phase, to

$$h = \sqrt{8}G(\phi_\mu \dagger \beta \gamma_\mu \phi_e)(\phi_\nu \dagger \beta \gamma_\mu \phi_\nu) + \text{c. c.}, \quad 113.$$

which is the form more commonly used in the literature (63 a, b, c). The invariance under this permutation is a special property of the $V-A$ Law.

It is straightforward to calculate the decay rate generated by the $V-A$ Law 112 or 113. The result is given here for a polarized muon having its spin in the direction of the unit vector δ_μ . The rate of producing electrons of energy $W \gg m_e c^2$ in the range dW , per unit solid angle, is:

$$d\lambda/(\lambda dW d\Omega) = [G^2/(4\pi^4 \hbar^7 c^6)] W_0 W^2 [W_0 - \frac{1}{2}W \pm \frac{1}{2}(\delta_\mu \cdot v/c)(2W - W_0)]. \quad 114.$$

The upper and lower signs attached to δ_μ refer to positively and negatively charged decays, respectively. $W_0 = \frac{1}{2}m_\mu c^2(1 + m_e^2/m_\mu^2)$ is the maximum energy the electrons may have, almost exactly half the muon rest energy, hence $W_0 = 103.5 \text{ } m_e c^2$. The expression v/c is a unit vector in the limit $W \gg m_e c^2$ here.

The energy spectrum of the electrons, integrated over all directions, is simply proportional to $W^2(W_0 - \frac{1}{2}W)$. This increases monotonically with energy, to a maximum at the end-point $W = W_0$. Thus the favored correlation is for the neutrino and antineutrino to emerge codirectionally, so as to give the recoil electron a maximum momentum.

Pseudoscalar intensity components average out in the spectrum, so calculations of it which were done before the discovery of parity nonconservation are still valid. Michel (64) generalized the first calculations, by Wheeler & Tiomno (56d), and showed that the spectra to be expected from a coupling as general as the form 35 form a family characterized by a single parameter ρ (for $W \gg m_e c^2$):

$$d\lambda/(\lambda dW) = (12/W_0^4) W^2 [W_0 - W + \frac{1}{2}\rho(\frac{1}{2}W - W_0)]. \quad 115.$$

Measurements of the spectrum are generally reported in terms of experimental ρ values which make this form of spectrum agree with the observations. The latest reports give values ranging from $\rho = 0.65 \pm 0.05$ (65a, b, c) to $\rho = 0.79 \pm 0.03$ (66). The theoretical result from the $V-A$ Law, above, corresponds to $\rho = 3/4$.

The polarized muons needed for observing the angular distribution of the electrons are available as products of pion decay. It was seen in the sub-

section on Pion Decay, that the emergent muons are expected to be longitudinally polarized antiparallel to their directions of emission when they are positive, and parallel to it when negative. Now, the factor of $\pm \frac{1}{2} \mathbf{s}_\mu \cdot \mathbf{v}/c$ in the electron intensity 114 is positive for the 81 per cent of the electrons having more than half the endpoint energy $\frac{1}{2} W_0$. Indeed, when integrated over all energies, the expression 114 yields the angular distribution:

$$d\lambda/d\Omega = [G^2/(4\pi^4\hbar^7c^6)](W_0^5/6)[1 \pm \frac{1}{2} \mathbf{s}_\mu \cdot \mathbf{v}/c]. \quad 116.$$

There is thus a preference for positron emission parallel to the muon spin, and for negatron emission antiparallel to it. In both cases, the preferred electron direction is opposite to the motion of the muon as it emerges from the pion. This is indicated for the positively charged case in Figure 8. This

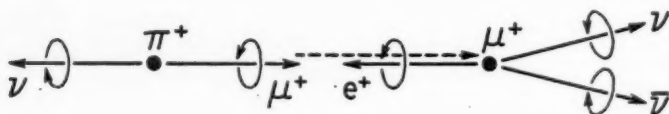


FIG. 8

conforms to the very first observations on the electron directions, by Garwin, Lederman & Weinrich (67), which constituted the first proof of parity non-conservation in weak interactions other than the nuclear β -decay. Precise measurements are difficult because there are mechanisms by which the muons can be depolarized before they decay. However, the results continue to conform more and more quantitatively with the expectations from the V - A Law.

The expected helicities of the product particles are, of course, exactly as in ordinary β -decay. This conforms to observations (68) on the bremsstrahlung of the electrons: the positrons are found to be right-handed, the negatrons left-handed. One can get a simple expression for the distribution of polarized electrons from unpolarized muons, as generated by the V - A Law:

$$d\lambda/(dWd\Omega) = [G^2/(8\pi^4\hbar^7c^6)]W_0W^2(W_0 - \frac{3}{2}W)(1 \pm \mathbf{s}_e \cdot \mathbf{v}/c), \quad 117.$$

for positrons and negatrons, respectively. This is the basis of the theoretical expectations.

We now examine the total muon decay rate predicted by the V - A Law. That can be obtained by integrating 114, 116, or 117:

$$\lambda = 1/\tau_\mu = G^2W_0^5/(6\pi^3\hbar^7c^6). \quad 118.$$

We wish to see how closely the observed mean-life $\tau_\mu = 2.22 \pm 0.02 \mu\text{sec}$. is reproduced by using the same coupling strength as is needed in the nuclear β -decay. The problem has some ambiguity, however. The symbol $G = \sqrt{2}g_C\gamma$ was introduced in the expression for the V - A Law of nuclear β -decay, 62, after neglecting possible differences of the vector and pseudovector

coupling strengths. We might as well have defined $G = \sqrt{2}g|C_A|$ instead. This would be immaterial if the nuclear β -decay data conformed to the simple expectations of the V - A Law, i.e. if using the latter for analyzing the data yielded $C_A = -C_V$ within experimental accuracy. Actually, as was seen in the subsection on Fermi and GT Radiations, $|C_A|^2 = (1.47 \pm 0.06)|C_V|^2$ emerges, instead of unity. The consequent vector coupling strength which can be derived from the comparative half life of the neutron is:

$$\sqrt{2}gC_V = \left[\frac{2\pi^3 \ln 2}{1 + 3|C_A|^2/|C_V|^2} \cdot \frac{\hbar/mc^2}{(ft)_n} \right]^{1/2} mc^2(\hbar/mc)^3 = (1.40 \pm 0.04)(10)^{-49} \text{ erg-cm.}^3 \quad 119.$$

The pseudovector coupling strength is $|C_A|/|C_V| = (1.21 \pm 0.03)$ times as great.

In the case of the muon, the V - A Law was applied without attempting to discriminate between vector and pseudovector coupling strengths. Indeed, once it is granted that only the left-handed states of neutrinos participate in Fermi interactions, then a distinction between a vector and pseudovector coupling becomes meaningless for muon decay. This is because the vector current $\psi_\mu \dagger \beta \gamma_\mu \phi_\nu$ and the pseudovector $\psi_\mu \dagger \beta \gamma_\mu \gamma_5 \phi_\nu$ used in a muon coupling form like 112, become identical when $\phi_\nu = \frac{1}{2}(1 + \gamma_5)\psi_\nu$ so that $\gamma_5 \phi_\nu = \phi_\nu$.

We proceed by trying first the nucleonic vector coupling strength of 119 for the muon, i.e. put $G = \sqrt{2}gC_V$ into 114:

$$\tau_\mu = 3 \frac{(ft)_n}{\ln 2} \left(1 + 3 \frac{|C_A|^2}{|C_V|^2} \right) \left(\frac{m_e c^2}{W_0} \right)^5 = 2.30 \pm 0.15 \text{ } \mu\text{sec.} \quad 120.$$

This calculated value agrees very well with the observations, while putting $G = \sqrt{2}g|C_A|$ would have given only $1.6 \text{ } \mu\text{sec.}$, well outside the uncertainties. This significant fact, that the muon decay coupling strength equals the vector, rather than pseudovector, coupling strength of the nuclear decay was pointed out by Feynman & Gell-Mann (34). What they make of this will be discussed in the last section.

So far, in considering the muon decay, this discussion has only followed out the implications of a natural generalization of the V - A Law, by which currents $\phi_a \dagger \beta \gamma_\mu \phi_b$, generated by the transformations of the "left-handed" components $\phi = \frac{1}{2}(1 + \gamma_5)\psi$ of the states, are coupled to each other. A neutrino-antineutrino distinction, as if divorced from the discrimination by helicity, and the principle of lepton conservation have been maintained. The transformation currents were written as if generated in $n \leftrightarrow p$, $e \leftrightarrow \nu$ and $\mu \leftrightarrow \nu$ transformations. It was mentioned that the coupling 113, which is written as if $e \leftrightarrow \mu$ and $\nu \leftrightarrow \nu$, is equivalent to 112 ($e \leftrightarrow \nu$, $\mu \leftrightarrow \nu$) when only currents are coupled, as in the V - A Law. The results agree very closely with experimental observations, even as to absolute magnitude, if we suppose the vector part of the V - A coupling is unmodified in the nuclear β -decay process, and it is a modification of the axial part which is responsible for deviations of the latter process from the V - A Law.

Full use is made of the information about the muon decay only if we consider also what alternative picture will fit the data equally well. In the picture used so far, the positive muons were treated as antimuons. We might try changing it only in the particular way that the positive muons are to be treated as the "normal" ones, so that the positive muon decay constitutes a capture of electrons out of negative-energy states

$$\mu^+ + e^- \leftrightarrow \nu + \nu, \quad 121.$$

with two like neutrinos emerging, when consistency with lepton conservation is maintained. This plainly leads to a contradiction of the data on the muon spectrum, if the idea is also preserved that only left-handed neutrinos are involved. The point is that like neutrinos cannot be emitted codirectionally if they also have parallel spins, because of the Pauli principle. The consequence is a spectrum with a vanishing end point intensity ($\rho=0$), in contradiction to the observations of a maximum end-point intensity.

The objection found here to the emission of like neutrinos when they are also alike in helicity obviously holds regardless of the muon vs. antimuon question, i.e. even when the lepton conservation principle is abandoned. On the other hand, when one admits neutrinos of both helicities, as in the extreme of lepton nonconservation represented by a Majorana neutrino $\bar{\nu} \equiv \nu$, then codirectional neutrinos of opposite helicity are possible. The muon decay is consistent with the two-component neutrino theory, whether one speaks of a neutrino plus an antineutrino of opposite helicity, or of a Majorana neutrino capable of both helicities.

The alternatives just mentioned may be viewed as "extremes," in the sense already discussed, of lepton conservation vs. nonconservation. By replacing ϕ_ν with $\frac{1}{2}(1+\gamma_5)(1+DC)\psi_\nu$, as in the coupling 82 one could investigate (69) intermediate degrees of lepton nonconservation ($0 < |D| < 1$). This can change the expectations for muon decay because two neutrinos are involved. It would provide another parameter through which closer agreement between measurements and theory would be possible. However, the agreement for $|D|=0$ or 1 is close enough already, so that one will have to be wary as to the significance of small improvements of agreement by these means.

PIONIC EFFECTS IN FERMI INTERACTIONS

In the subsection The $V-A$ Law, reference was made to certain "renormalization effects" on the states of nucleons which can be expected to influence their behavior in Fermi interactions. The strong interactions of nucleons with the pion field makes them oscillate between the neutron and proton states, each attended by some complementary pion cloud. For example,

$$n \leftrightarrow p + \pi^- \leftrightarrow n + \pi^0 \leftrightarrow n + \pi^+ + \pi^- \leftrightarrow \dots \text{etc.} \quad 122.$$

The reality of this type of phenomenon is attested by the essential part it plays in the pion decay as it was discussed above. It is appropriate to reopen

the subject at this point, after we have examined the muon decay, because no nucleons, hence none of these pionic effects, intrude in the latter process. There is now available a basis of comparison of Fermi interactions with and without the pionic effects.

Before considering in the next subsection the empirical measure of the effects which the comparison of the muon and nucleon decays may give, it will be well to acquire an idea of the a priori theoretical expectations. The earliest attempts (12a to d) to treat the complex problem were naturally quite drastically simplified. They were comparisons of nucleonic states before and after the pion field is "turned on." First, a "bare nucleon" was assumed, i.e. its state was taken to be completely specified by a pure Dirac spinor, such as is used to describe the neutrino or muon, except for proper allowances for charge and mass differences. It is just such nucleon states which are presumed in the treatment of the neutron decay as presented above. This had been done despite, for example, the well-known fact that nucleons have magnetic moments differing substantially from those expected of pure Dirac particles. Second, "physical nucleon" states were assumed which are mixtures of types such as indicated in 122. Some measure of the relative probabilities of the various components of the mixture ought to be derivable from known facts about pion-nucleon interactions, e.g., the differences they cause in the nucleon magnetic moments. Actually, such data give ambiguous information, because of the intrusion of divergent integrals, much like the ones mentioned in connection with the pion decay. Certain procedures for "cutting off" the divergent, high-momentum parts of the integrals have led to fairly successful correlations of many pion-nucleon interaction phenomena. It is the "physical nucleon" states derived from these somewhat arbitrary procedures which were put to use in the β -decay problem here.

Typical results were obtained by Ross (12d), after a preliminary exploration by Finkelstein & Moszkowski (12a). They are given as ratios $\langle 1 \rangle / \langle 1 \rangle_0$ of Fermi matrix elements and $\langle \sigma \rangle / \langle \sigma \rangle_0$ of GT matrix elements evaluated for "physical nucleon" and "bare nucleon" states:

$$\begin{aligned} \langle 1 \rangle / \langle 1 \rangle_0 &= 1 - \frac{1}{3}P_{11} - \frac{1}{3}P_{10}, \\ \langle \sigma \rangle / \langle \sigma \rangle_0 &= 1 - \frac{1}{3}P_{11} - \frac{1}{3}P_{10}. \end{aligned} \tag{123}$$

These results apply, more strictly, to the free neutron decay, since the presence of neighboring nucleons, as in a nucleus, is ignored. P_{11} is the fraction of the time the nucleon spends attended by a pion cloud having one unit of angular momentum and one unit of "isotopic spin." The simplest component of this mixed state has one pion, in a p -state as required for parity conservation during strong interactions, since the pion field is pseudoscalar. The expression P_{10} is a fraction, allowing for two or more pions with a total angular momentum of one unit or a total isotopic spin of one unit. The pion-nucleon interaction data, as evaluated by the "cut-off" procedure mentioned above, yield roughly $P_{11} \approx 0.6$ and $P_{10} \approx 0$. With these numbers, the ratios 123 become $1/5$ and $7/15$, respectively. That corresponds to a

"renormalization" of the vector coupling constant C_V which measures the Fermi transitions via $\langle 1 \rangle$, to one-fifth its unrenormalized value! The pseudovector coupling constant C_A for the GT transitions via $\langle \sigma \rangle$ is reduced by $7/15$. Consequently $|C_A|/|C_V| = 7/3$ is the ratio of the renormalized coupling constants, if the ratio is unity, as in the $V-A$ Law, before the renormalization by the pionic effects. It should be compared with the observed ratio $|C_A|/|C_V| \approx 1.2$, as reported in 30. That result certainly gives no assurance that it is on the right track! Of course, the crude estimations employed should not be expected to yield at all quantitative results. They are quoted only because no essentially better ones for the specific problem here seem to be available, yet the effects in question are fully expected to be important ones.

An approach apparently less compromised by oversimplifications is afforded by the "dispersion-theoretic" methods developed by Goldberger and others. For instance, the recoils of the nucleons, when they emit the pion clouds, are not explicitly neglected, as in the above-quoted attempt. On the other hand, the dispersion-theoretic methods have not proved applicable to the problem of the renormalizations of C_A and C_V , or the ratio $|C_A|/|C_V|$.

Goldberger & Treiman (70) were able to evaluate another effect, however. They showed that the pion field should not only change the effective magnitudes of the Fermi interactions, but also the effective forms. First, the vector (V) part of the β -coupling is effectively supplemented with a "gradient" form of coupling, i.e., one which is proportional to the momentum difference in the neutron and proton states of the transforming nucleon. Second, the pseudovector (A) part of the β -interaction is supplemented with a coupling which can be simulated by a pseudoscalar (P) form such as was discussed in a preceding subsection. Thus, a " $V-A$ Law," which couples pure Dirac spinor states, becomes effectively a " $V + (\text{gradient}) - (A + cP)$ " Law, when the nucleonic states are modified by their strong interactions with the pion field.

The two form modifications, symbolized by " (gradient) " and " cP ," both disappear in the limit of vanishing nucleonic momenta and so should be more conspicuous in muon-nucleon interactions (see 96), in which the nucleons recoil more appreciably, than in the electron emissions by nucleons. Goldberger & Treiman were able to show that the " (gradient) " supplementation of the vector coupling will probably be too small to be detectable even in muon capture by nucleons. The outcome for the pseudoscalar ($\sim "cP"$) modification of the pseudovector coupling was more interesting. The authors were able to evaluate it by using the data on pion-decay, which process involves state amplitudes which can be related to those appearing in muon capture or electron-decay, through the dispersion-theoretic forms. It turns out that the effective pseudoscalar coupling strength is proportional to the mass of the emitted or captured lepton, and that, in muon capture, it is eight times as strong as the remaining pseudovector (A) coupling! This changes quite drastically the way expectations for muon capture are to be

derived, but the analogous effect in ordinary β -decay is only the fraction $8/207$ as great. Pseudoscalar coupling even in strengths comparable with vector or pseudovector couplings has already proved difficult to detect (see the subsection Pseudoscalar β -Coupling); hence the pionic modification of the coupling forms in ordinary β -decay seems negligible at present. Apparently, the only really important pionic influences in nuclear β -decay which remain are the possible absolute renormalizations of the vector and pseudovector coupling constant C_V and C_A .

A FEYNMAN—GELL-MANN THEORY

Already noted in the subsection Muon Decay was the close agreement between the coupling strength needed to give the observed muon lifetime, and the vector coupling strength in nuclear β -decay. Muon decay involves no nucleons; hence there are no strong pion-nucleon interactions to cause an effective renormalization of the muon-decay coupling strength. Yet, at least the vector coupling strength of nuclear β -decay coincides with it very closely. This empirical measure of the pionic effect on the nuclear vector coupling indicates that it is negligible! Of course, this interpretation is based on the presumption of a universal Fermi interaction; i.e. both the processes being compared are generated according to the same fundamental law. Considering the coincidence of the forms $V-A$ needed for both processes, as well as the coincidence of strengths discussed here, the case for the presumption seems strong.

The empirical conclusion of the preceding paragraph is difficult to accept at face value. It is hard to understand why a strong interaction with the pion field does not inhibit the "electron emitting powers" of the nucleon substantially, relative to the muon's. The neutron must spend a substantial part of its existence as a proton plus negative pion cloud, and only in a neutron state should it emit negatrons. The understanding of the fact that the neutron has a large magnetic moment is based on such a picture, as are many other facets of nucleonic behavior. It is true that none of these effects can yet be reliably calculated. (The crude estimates quoted in the preceding subsection lead to an expectation of a weakening of the nucleon's effective vector coupling strength by a factor 5!) Nevertheless, it does not seem premature to look for explanations other than just that the pionic effects are not there! Feynman & Gell-Mann (34), who first pointed out this situation, have also advanced a theory which may account for it.

The conservation of the nucleon's vector coupling strength, during its virtual oscillations into states attended by pion clouds, can be considered analogous to the conservation of its "electromagnetic coupling strength," as measured by its total electric charge. The latter is accounted for by the fact that the pions are themselves charged, and so keep the charge of the total "physical nucleon" invariant. This situation is formalized by calculating electromagnetic effects as resulting from a conserved (divergenceless) current, in which the Dirac current, $j_\mu = \bar{\psi}\gamma_\mu\psi$, is supplemented with a pion

current, $i(\phi_x^* \nabla_\mu \phi_x - (\nabla_\mu \phi_x)^* \phi_x)$. To explain the conservation of the vector β -coupling strength in the same way, the nucleon transformation current $J_\mu = \bar{\psi} \tau_\pm \gamma_\mu \psi$ of 31 must be supplemented with a pion transformation current. One must suppose that the pions carry whatever "electron-emitting power" leaves the nucleon, when it emits the pion cloud! One attributes "Fermi charge" to them.

The best information on the pion-nucleon interaction indicates that nucleons emit pion clouds in such a way as to conserve isotopic spin. When the latter variable is included in the description of the nucleon state, then the electromagnetic, Dirac current becomes $j_\mu = \bar{\psi}(\frac{1}{2} + \tau_3) \gamma_\mu \psi$ where $\tau_3 = \pm \frac{1}{2}$ in the proton and neutron states, respectively. Only the part $\bar{\psi} \tau_3 \gamma_\mu \psi$ is involved together with the pion cloud, and is unconserved by itself, in the presence of the pion field. What is conserved, as the nucleon oscillates among its virtual states, is the current vector in "charge space":

$$J_\mu = \bar{\psi} \tau \gamma_\mu \psi + i[\phi_x^* T \nabla_\mu \phi_x - (\nabla_\mu \phi_x)^* T \phi_x]. \quad 124.$$

Here τ and T are the isotopic spin vectors of magnitude $\tau = \frac{1}{2}$ for the nucleon, and $T = 1$ for the pion (which has three charge states: $T_3 = 0, \pm 1$). It is $J_{3\mu}$, with τ_3 and T_3 , which contributes to the electromagnetic current. It is $J_{\pm\mu}$, with $\tau_\pm = \frac{1}{2}(\tau_1 \pm i\tau_2)$ and $T_\pm = \frac{1}{2}(T_1 \pm iT_2)$, to which the vector β -coupling is now presumed proportional ($C_V \bar{\psi} \tau_\pm \beta \gamma_\mu \psi_n$ of the coupling 47 is now replaced by $C_V J_{\pm\mu}$!).

The modification of the nucleonic current vector, which is to enter the β -coupling, into the divergenceless one J_μ which includes pion currents, does not alter the expectations for the allowed nuclear β -decay as reported in the first parts of this review. This emerges formally because nucleonic recoils are negligible in the "allowed approximation," and the net pion current will be proportional to such recoils. It can also be understood on the same basis as the fact that the proton can be treated as a point charge in low-energy electromagnetic interactions; the pion cloud merely redistributes the charge over a region which is small compared to low-energy wavelengths.

A test of the Feynman—Gell-Mann theory in nuclear β -decay necessarily involves looking at effects for which the nucleonic recoils become appreciable. Such are the effects classified as "forbidden transitions," and "forbidden corrections" to allowed transitions. It is the latter type of effect which Gell-Mann (71) has suggested for experimental investigation and for which he was able to provide a very clever mode of estimating what is to be expected (by taking further advantage of the analogy to the electromagnetic coupling). Unfortunately, the requisite experiment, involving the detection of a small departure of an observed β -spectrum from the statistical shape, is not an easy one and no definitive result has yet been announced.

A point of uncertainty in the Feynman—Gell-Mann theory remains. It has been concerned only with the vector part of the β -coupling, for which the comparison with the muon decay had fairly definite implications. The theory

has nothing to say about a comparable intrusion of the pion's "Fermi charge" into the pseudovector (A) part of the coupling. One should probably not expect as complete a removal of the pionic renormalization effect as in the vector coupling. The ratio of C_A to C_V does deviate from the $V-A$ Law. However, a pion bearing "Fermi charge" is only too likely to have some influence also on the pseudovector part of the physical nucleon's β -coupling. There has apparently not yet developed sufficient insight into the relationship between the V and A parts, aside from the fact that they add up so as to produce roughly left-handed nucleonic states, to lead to a definitive answer.

One may still argue that the pseudovector part of the coupling should not have pion "Fermi charge" effects added to it because of such success as it has had in explaining the pion decay. This is a process in which the vector coupling plays no role. However, the success of the pion decay theory may be just as invariant to the addition of the pion's "Fermi charge" as is the allowed nuclear β -decay.

It should perhaps still be mentioned that the Feynman—Gell-Mann theory of the vector coupling does lead to a new expectation for pion decay. The "Fermi charge" \equiv "electron-emitting power" which the theory attributes to the pion leads to the expectation of such direct processes as $\pi \rightarrow \pi^0 + e + \nu$. Comparatively little energy is released in the latter; hence it is difficult for it to compete with the usual $\pi \rightarrow \mu + \nu$ decay mode, or even $\pi \rightarrow e + \nu$.

On the whole, it seems necessary to conclude that even if there is a successful detection of such a β -spectrum deviation as is required in the Gell-Mann experiment, its interpretation will be subject to uncertainty as long as the questions concerning the pseudovector part of the coupling remain.

LITERATURE CITED

1. Konopinski, E. J., and Langer, L. M., *Ann. Rev. of Nuclear Sci.*, **2**, 261 (1953)
2. Lee, T. D., and Yang, C. N. *Phys. Rev.*, **104**, 254 (1956)
3. Wu, C. S., Ambler, E., Hayward, R. W., Hoppes, D. D., and Hudson, R. P., *Phys. Rev.*, **105**, 1413 (1957)
4. Hermannsfeldt, W. B., Allen, J. S. and Stähelin, P., *Phys. Rev.*, **107**, 641 (1957)
5. Goldhaber, M., Grodzins, L., and Sunyar, A. W. *Phys. Rev.*, **109**, 1015 (1958)
6. Fermi, E., *Z. Phys.*, **88**, 161 (1934)
- 7a. Lee, T. D., and Yang, C. N., *Phys. Rev.*, **105**, 1671 (1957)
- 7b. Landau, L., *Soviet Phys. JETP*, **5**, 336 (1957)
- 7c. Wigner, E. P., *Revs. Modern Phys.*, **29**, 255 (1957)
- 7d. Salam, A., *Nuovo cimento*, **5**, 229 (1957)
- 8a. Schwinger, J., *Phys. Rev.*, **91**, 720 (1953)
- 8b. Lüders, G., *Kgl. Danske Videnskab. Selskab*, **28** (1954)
- 8c. Pauli, W., *Niels Bohr and the Development of Physics* (Pergamon Press, London, Engl., 1955)
- 9a. Postma, H., Huiskamp, W. J., Miedema, A. R., Steenland, M. J., Tolhoek, H. A., and Gorter, C. J., *Physica*, **23**, 259 (1957)

- 9b. Ambler, E., Hayward, R. W., Hoppes, D. D. and Hudson, R. P., *Phys. Rev.*, **110**, 787 (1958)
10. Sosnovskii, A. N., Spivak, P. E., Prokof'ev, Yu. A., Kutikov, I. E. and Dobrynin, Yu. P., *Soviet Phys. (JETP)*, **35**, 739 (1959)
- 11a. Gerhart, J. B., *Phys. Rev.*, **109**, 897 (1958)
- 11b. Van der Leun, C. Doctoral thesis, Utrecht University, Utrecht, Netherlands, (1958)
- 12a. Finkelstein, R. J., and Moszkowski, S. A., *Phys. Rev.*, **95**, 1695 (1954)
- 12b. Gerschtein, S. S., and Zel'dovich, Ya. B., *Soviet Phys. (JETP)*, **2**, 576 (1956)
- 12c. Stech, B., *Z. Physik*, **145**, 319 (1956)
- 12d. Ross, M., *Phys. Rev.*, **104**, 1736, (1956)
13. Frauenfelder, H., Bobone, R., von Goeler, E., Levine, N., Lewis, H. R., Peacock, R. N., Rossi, A., and De Pasquali, G., *Phys. Rev.*, **106**, 386 (1957)
14. De Waard, H., and Poppema, O. J., *Physica*, **23**, 597 (1957)
15. Langevin-Joliot, H., Marty, N., and Sergent, P., *Compt. rend.*, **244**, 3142 (1957)
16. Cavanagh, P. E., Turner, J. F., Coleman, C. F., Gard, G. A., and Ridley, B. W., *Phil. Mag.*, **2**, 1105 (1957)
17. Alikhanov, A. I., Yeliseyev, G. P., Liubimov, V. A., and Ershler, B. V., *Soviet Phys. (JETP)*, **34**, 541 (1958)
18. De-Shalit, A., Cuperman, S., Lipkin, H. J., and Rothen, T., *Phys. Rev.*, **107**, 1459 (1957)
- 19a. Frauenfelder, H., Hanson, A. O., Levine, N. Rossi, A., and De Pasquali, G., *Phys. Rev.*, **107**, 643 (1957)
- 19b. Benczer-Koller, N., Schwarzschild, A., Vise, J. B., and Wu, C. S., *Phys. Rev.*, **109**, 85 (1958)
- 20a. Schopper, H., *Phil. Mag.*, **2**, 710 (1957) *Fortschr. Phys.*, **5**, 581 (1957)
- 20b. Boehm F., and Wapstra, A. H., *Phys. Rev.*, **106**, 1364; **107**, 1202 (1957)
- 20c. Steffen, R. M., *Proc. Rehovoth Conf. Nuclear Structure*, **1957**, 419 (1958)
- 20d. Lundby, A., Patro, A. P., and Stroott, J. P. *Nuovo cimento*, **6**, 745 (1957); **7**, 891 (1958)
- 21a. Deutsch, M., Gittelman, B., Bauer, R. W., Grodzins, L., and Sunyar, A. W., *Phys. Rev.*, **107**, 1733 (1957)
- 21b. Boehm, F., Novey, T. B., Barnes, C. A., and Stech, B., *Phys. Rev.*, **108**, 1497 (1957)
- 22a. Hanna, S. S., and Preston, R. S., *Phys. Rev.*, **108**, 160 (1957)
- 22b. Frankel, S., Hansen, P. G., Nathan, O., and Temmer, G. M., *Phys. Rev.*, **108**, 1099 (1957)
23. Page, L. A., and Heinberg, M., *Phys. Rev.*, **106**, 1220 (1957)
24. Kistner, O. C., Schwarzschild, A., and Rustad, B. M., *Phys. Rev.*, **104**, 154 (1956)
25. Robson, J. M., *Phys. Rev.*, **100**, 933 (1955)
26. Hermannsfeldt, W. B., Burman, R. L., Stäbelin, P., Allen, J. S., and Braid, T. H., *Bull. Am. Phys. Soc.*, **4**, 77 (1959); a confirmation of the He⁶ result was reported by Pleasonton, F., Johnson, C. H., and Snell, A. H., *Bull. Am. Phys. Soc.*, **4**, 78 (1959)
- 27a. Maxson, D. R., Allen, J. S., and Jentschke, W. K., *Phys. Rev.*, **97**, 109 (1955)
- 27b. Good, M. L., and Lauer, E. J., *Phys. Rev.*, **105**, 213 (1957)
- 27c. Alford, W. P., and Hamilton, D. R., *Phys. Rev.*, **105**, 673 (1957)
- 28a. Rustad, B. M., and Ruby, S. L., *Phys. Rev.*, **97**, 991 (1955).

- 28b. Wu, C. S., and Schwarzschild, A., *Columbia Univ. Rept. CU-173* (1958) (Unpublished)
- 29a. Lauterjung, K. H., Schimmer, B., and Maier-Leibnitz, H., *Z. Physik*, **150**, 657 (1958)
- 29b. Barnes, C. A., Fowler, W. A., Greenstein, H. B., Lauritsen, C. C., and Nordberg, M. E. *Phys. Rev. Letters*, **1**, 328 (1958)
30. Burgy, M. T., Krohn, V. E., Novey, T. B., Ringo, G. R., and Telegdi, V. L., *Phys. Rev.* **110**, 1214 (1958); *Phys. Rev. Letters*, **1**, 324 (1958)
31. Clark, M. A., Robson, J. M., and Nathans, R., *Phys. Rev. Letters*, **1**, 100 (1958)
32. Boehm, F., and Wapstra, A. H., *Phys. Rev.*, **109**, 456 (1958)
33. Ambler, E., Hayward, R. W., Hoppes, D. D., and Hudson, R. P., *Phys. Rev.*, **110**, 787 (1958)
34. Feynman, R. P., and Gell-Mann, M., *Phys. Rev.*, **109**, 193 (1958)
35. Marshak, R. E., and Sudarshan, E. C. G., *Phys. Rev.*, **109**, 1860 (1958)
36. Sakurai, J. J., *Nuovo cimento*, **7**, 649 (1958)
37. Critchfield, C. L., *Phys. Rev.*, **63**, 417 (1943)
38. Jensen, J. H., and Stech, B., *Z. Physik*, **141**, 175 (1955)
39. Jackson, J. D., Treiman, S. B., and Wyld, H. W., *Phys. Rev.*, **106**, 517 (1957)
40. Tolhoek, H. A., and de Groot, S. R., *Physica*, **17**, 81 (1951)
41. Cowan, C. L., Reines, F., Harrison, F. B., Kruse, H. W., and McGuire, A. D., *Science*, **124**, 103 (1956)
- 42a. Muehlhause, C. O., and Oleksa, S., *Phys. Rev.*, **105**, 1332 (1957)
- 42b. Carter, R. E., Reines, F., Wagner, J. J., and Wyman, M. E., *Phys. Rev.*, **113**, 280 (1959)
- 43a. King, R. W., and Perkins, J. F., *Phys. Rev.*, **112**, 963 (1958)
- 43b. Reines, F., and Cowan, C. L., *Phys. Rev.*, **113**, 273 (1959)
44. Majorana, E., *Nuovo cimento*, **14**, 171 (1937)
45. Davis, R., *Phys. Rev.*, **97**, 766 (1955)
46. An excellent summary of Double β -Decay has been prepared by Primakoff, H., and Rosen, S. P. (To be published)
47. Cowan, C. L., Harrison, F. B., Langer, L. M. and Reines, F., *Nuovo cimento*, **3**, 649 (1956)
48. Konopinski, E. J., and Mahmoud, H., *Phys. Rev.*, **92**, 1045 (1953)
- 49a. Pauli, W., *Nuovo cimento*, **6**, 204 (1957)
- 49b. Enz, C. D., *Nuovo cimento*, **6**, 250 (1957)
- 49c. Kahana, S., and Pursey, D. L., *Nuovo cimento*, **6**, 1469 (1957)
- 50a. Serpe, J., *Physica*, **18**, 259 (1952)
- 50b. McLennan, J. A., *Phys. Rev.*, **106**, 821 (1957)
- 50c. Case, K. M., *Phys. Rev.*, **107**, 307 (1957)
51. Lee, T. D., and Yang, C. N., *Phys. Rev.*, **105**, 1671 (1957)
52. Landau, L., *Nuclear Phys.*, **3**, 127 (1957)
53. Salam, A., *Nuovo cimento*, **5**, 299 (1957)
54. Weyl, H., *Z. Physik*, **56**, 330 (1929)
55. Pauli, W., *Handb. Physik*, **24**, I, 226 (1931)
- 56a. Puppi, G., *Nuovo cimento*, **5**, 505 (1948)
- 56b. Klein, O., *Nature*, **161**, 897 (1948)
- 56c. Lee, T. D., Rosenbluth, M., and Yang, C. N., *Phys. Rev.*, **75**, 905 (1949)
- 56d. Tiomno, J., and Wheeler, J. A., *Revs. Modern Phys.*, **21**, 144 (1949)

- 57a. Fazzini, T., Fidecaro, G., Merrison, A. W., Paul, H., and Tollestrup, A. V., *Phys. Rev. Letters*, **1**, 247 (1958)
- 57b. Impeduglia, G., Plano, R., Prodell, A., Samios, N., Schwartz, M., and Steinberger, J., *Phys. Rev. Letters*, **1**, 249 (1958)
58. Ruderman, M., and Finkelstein, R., *Phys. Rev.*, **76**, 1458 (1959)
59. Love, W. A., Marder, S., Nadelhaft, I., Siegel, R. T., and Taylor, A. E., *Phys. Rev. Letters*, **2**, 107 (1959), after a theoretical prognosis by Jackson, J. D., Treiman, S. B., and Wyld, H. W., *Phys. Rev.*, **107**, 327 (1957)
60. Goldberger, M. L., and Treiman, S. B., *Phys. Rev.*, **110**, 1178 (1958)
61. Lederman, L. M., Booth, E. F., Byfield, H. and Kessler, J., *Phys. Rev.*, **83**, 685 (1951)
62. Treiman, S. B., and Wyld, H. W., *Phys. Rev.*, **101**, 1552 (1956)
- 63a. Bouchiat, C., and Michel, L., *Phys. Rev.*, **106**, 170 (1957)
- 63b. Kinoshita, T., and Sirlin, A., *Phys. Rev.*, **107**, 593 (1957); **108**, 844 (1957)
- 63c. Larsen, S., Lubkin, E., and Tausner, M., *Phys. Rev.*, **107**, 856 (1957)
64. Michel, L., *Proc. Phys. Soc. (London)*, **A63**, 514 (1950)
- 65a. Rosenson, L., *Phys. Rev.*, **109**, 958 (1958)
- 65b. Sargent, C. P., Rinehart, M., Lederman, L. M., and Rogers, K. C., *Phys. Rev.*, **99**, 885 (1955)
- 65c. Crowe, K., *Bull. Am. Phys. Soc.*, **2**, 206 (1957)
66. Plano, R. J., and LeCourtois, A., *Bull. Am. Phys. Soc.*, **4**, 82 (1959)
67. Garwin, R. L., Lederman, L. M., and Weinrich, M., *Phys. Rev.*, **105**, 1415 (1957)
68. Culligan, G., Frank, S. G. F., and Holt, J. R., *Bull. Am. Phys. Soc.*, **4**, 81 (1959)
69. Friedman, M. H., *Phys. Rev.*, **106**, 387 (1957)
70. Goldberger, M. L., and Treiman, S. B., *Phys. Rev.*, **111**, 354 (1958)
71. Gell-Mann, M., *Phys. Rev.*, **111**, 312 (1958)

HIGH-ENERGY NUCLEAR REACTIONS^{1,2}

By J. M. MILLER

Department of Chemistry, Columbia University, New York, N. Y.

AND

J. HUDIS

Department of Chemistry, Brookhaven National Laboratory, Upton, Long Island, N. Y.

1. INTRODUCTION

The present review is concerned primarily with the inelastic interactions between complex nuclei and nucleons with energies in excess of about 100 Mev. The interactions of lower-energy pions and muons with complex nuclei will be considered only briefly, and heavy-ion interactions not at all. Attention will be focussed on the product nuclei that remain after the inelastic collisions and on the nucleons and nuclei that are emitted. Elementary-particle production will not be considered except insofar as it influences the properties of the residual nuclei and the emitted nucleonic particles.

Previous reviews of high-energy nuclear reactions include those by Templeton (205), Rudstam (182), and Lindenbaum (122). The theoretical framework within which these reactions have been discussed is presented in Section 3 of a recent review by Feshbach (48).

The characteristic difference between low- (<50 Mev) and high- (>100-Mev) energy nuclear reactions is illustrated in Figure 1. There, the cross section for the formation of a particular mass-number product is plotted against the mass number (mass-yield curve) for 40-, 480-, and 3000-Mev protons incident upon bismuth. Typically, nearly all of the products of the low-energy reaction are spread over just a few mass numbers; the products from high-energy bombardment, on the other hand, are spread over many mass numbers and, indeed, essentially all products with mass numbers less than that of the target are formed with measurable cross sections.

Reactions induced by high-energy particles are usually (and sometimes quite arbitrarily) divided into four categories: spallation, in which nucleons or small clusters of nucleons are emitted from the struck nucleus; fission, in which the struck nucleus divides into two or more roughly equal masses; fragmentation, in which chunks of nuclear matter are split off from the struck nucleus in a fast process; and secondary reactions, in which a particle that is emitted in spallation interacts with another nucleus in the target. In terms of the mass-yield curve at 480 Mev presented in Figure 1, those products with mass number between 160 and 209 may be considered as spallation products, those with mass number between 60 and 140 as fission products, and those with mass number greater than that of the target as secondary

¹ The survey of literature pertaining to this review was concluded in February, 1959.

² This work was supported in part by the U. S. Atomic Energy Commission.

products. The products with mass numbers between 20 and 40 observed in the 3-Bev bombardment are thought to result from fragmentation. It should be emphasized at this point that the above categories are not at all mutually exclusive, in that a target nucleus that has been struck by an incident particle may, for example, first emit several particles in a spallation reaction, and may then still undergo fission; or, an excited fragmentation product will probably emit several nucleons in the process of de-excitation.

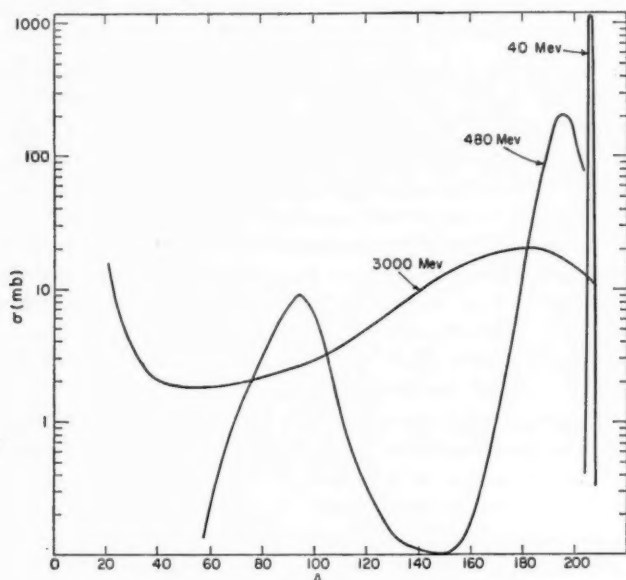


FIG. 1. Mass-yield curves for the proton bombardment of bismuth. The 40-Mev curve was taken from Bell & Skarsgard (14); the 480-Mev curve was constructed from data of Hunter & Miller for 380-Mev protons on bismuth (88), Kalamian *et al.* for 660-Mev protons on Bi (100), and Vinogradov *et al.* for 480-Mev protons on bismuth (209); the 3000-Mev curve was constructed from data of Wolfgang *et al.* for 3000-Mev protons on Pb (215).

In Sections 5 through 8 of this review, there are detailed discussions of spallation, fission, secondary reactions, and fragmentation, respectively. Section 2 contains a brief description of the experimental methods that have been employed and of their limitations. Section 3 gives a discussion of the theoretical framework and models employed in the analysis of high-energy reactions. Section 4 presents information on the total inelastic cross section at high energies. In section 9 the present state of knowledge in the field will be summarized and some of the outstanding problems sketched. Finally, in Table II which appears at the end of the article an attempt is made to give a complete listing of experimental investigations of high-energy nuclear reactions that fall within the framework of this article. No attempt is made

at completeness of references within the body of the text; rather, only representative investigations are referred to.

2. EXPERIMENTAL METHODS

The techniques used in the investigation of high-energy nuclear reactions include radiochemistry, mass spectroscopy, nuclear emulsions, and counters.

Radiochemical methods are used to determine the formation cross sections of radioactive nuclides. Very briefly, the technique involves the irradiation of a target with a known number of particles, chemical separation and purification of the desired element, and the determination of the number of radioactive atoms present in the purified sample by some sort of radiation detection apparatus. The inherent experimental difficulties of this method usually lead to results good only to ~ 20 to 30 per cent.

Recently Gordon & Friedman (69) have applied the technique of mass spectroscopy to the determination of formation cross sections in their study of the yields of cesium isotopes from gold irradiated with 3-Bev protons. This method of course is not limited to radioactive products with reasonable half lives but may be used to determine yields of very-long-lived and stable species. The mass spectrometric determination of rare gas production previously applied to He^3 and He^4 (137) has recently been extended to other rare gases and to Bev energies (186).

By means of nuclear emulsions, the investigation of nuclear reactions may be attacked from another direction. Instead of looking at the accumulation of product nuclides resulting from a large number of interactions, one looks at individual reactions and may determine the relative number, nuclear charge, energy, and angular distribution of charged particles emitted during the reaction. Emulsions may be used in two ways—as detectors for particles emitted from a target, or they may serve as both detector and target. Perfilov and his coworkers [e.g. (170)] have been especially active with the latter technique and have developed procedures by which emulsions may be loaded with salts of uranium, bismuth, and tungsten thereby extending the usefulness of plate work beyond reactions in the usual emulsion nuclei. Some disadvantages of plate work include the difficulty of estimating absolute cross sections, that of preparing emulsions which are suitable for the recording of both very-high- and very-low-energy particles from the same reactions, and, of course, the fact that the neutrons emitted in a reaction are not detected.

The counter telescope method may also be used to determine the energy and angular distribution of emitted charged particles by allowing the particles to pass through a group of counters which define a direction with respect to the incident beam. The advantages of this technique over nuclear emulsion work include the greater freedom in choice of targets, the possibility of determining coincidences between various charged particles, greater ease of distinguishing between particles such as H^1 , H^2 , H^3 , He^3 , and He^4 , and the possibility of neutron detection.

3. MODEL AND THEORY

3.1 General statement.—The theoretical framework within which high-energy reactions have usually been analyzed was first discussed by Heisenberg (78) and by Serber (187). A complete review of the theoretical situation in high-energy reactions of complex nuclei in terms of the optical model has recently been given by Feshbach (48).

In general, the model employed divides high-energy reactions into two phases: an initial-interaction phase in which the incident high-energy particle strikes the target nucleus (characterized by mass number A^0 and atomic number Z^0) and ejects a number of particles by direct interaction leaving a residual excited nucleus (characterized by A' , Z' , excitation energy U' , and angular momentum I); this is followed by the de-excitation of the excited residual nucleus A' , Z' , either through the emission of particles and photons (often called evaporation) or through break-up into two or more fragments of comparable mass leaving the final product nucleus or nuclei.

The initial interaction will lead, in general, to a variety of residual nuclei A' , Z' , each with a spectrum of excitation energies; this will, in turn, lead to the spectrum of final products which, as seen in Figure 1, is characteristic of high-energy reactions. The emission of a few high-energy particles (energies greater than 50 to 100 Mev) in each inelastic interaction at high energies is also consistent with this picture. For example, Bernardini, Booth & Lindenbaum (19) found an average of about 0.75 proton emitted with energies above 30 Mev subsequent to each interaction of a 360-Mev proton with one of the heavy nuclei (Ag or Br) in a photographic emulsion; these directly ejected particles are often called knock-on particles. It should be mentioned at this point that some knock-on particles may also be emitted with lower energies and thus are difficult to distinguish experimentally from the particles emitted in the second or evaporation phase of high-energy reactions. The separation of the lower-energy particles into two groups has been based upon the difference in the angular distributions expected for evaporation and knock-on particles.

The de-excitation of the residual excited nuclei that remain after the knock-on process is envisaged as occurring in a manner similar to that of the excited compound nucleus that figures in the Bohr model for low-energy nuclear reactions. Thus it is expected, and is observed, that the characteristics of some of the particles emitted in high-energy reactions are sensitive to parameters such as binding energies and Coulomb barriers and, in short, are similar to those for particles emitted in low-energy reactions. These are the "evaporated" particles.

With this two-step picture, the cross section for the formation of a product nucleus A , Z (excluding products of secondary reactions) in the bombardment of a target A^0 , Z^0 with a particle q with kinetic energy E , may be expressed as:

$$\sigma(A, Z | A^0, Z^0, q, E) = \sum_{A', Z', I} \int_0^\infty \sigma(A', Z', U', I | A^0, Z^0, q, E) \eta(A, Z | A', Z', U', I) dU \quad 1.$$

where $\sigma(A', Z', U', I|A^0, Z^0, q, E)$ is the differential cross section for the formation, in the knock-on step, of the residual nucleus A', Z' with spin I and excitation energy in the interval dU at U , and $\eta(A, Z|A', Z', U', I)$ is the probability that the product nucleus A, Z remains after the de-excitation of that residual nucleus by the emission of particles and photons. Formally, both fission and fragmentation processes are described by expression 1 if the summation is taken over all nuclei produced in the knock-on phase including fragmentation products, and if the η function includes the probability of fission at each step in the de-excitation of the residual excited nucleus. The spin I is included for completeness; no analysis to date has made any attempt to include it in the calculations. Attention will be given now to the detailed models and assumptions on which estimates of the σ and η functions are based.

3.2 Knock-on phase.—The first assumption that underlies the analysis of the initial interactions in high-energy reactions is that the motion of the incident nucleon within the target nucleus can be treated in terms of a succession of two-body collisions between the incident nucleon and the individual nucleons in the target nucleus and that the subsequent motion of the struck nucleons can be treated in the same way (multiple scattering). Further, if the energy of the incident nucleon or of the struck nucleons in the nucleus is high enough, it is assumed that these collisions can be considered as collisions between free nucleons (impulse approximation). Thus, the incident nucleon generates an intranuclear cascade and the problem becomes a stochastic one in which each step is described by the properties of nucleon-nucleon collisions within nuclear matter. The fact that the collisions occur within nuclear matter manifests itself through the Pauli principle (collisions leading to occupied states are forbidden), the momentum distribution of the nucleons in the nucleus, and the change in the kinetic energy of the incident nucleon as it crosses the nuclear boundary. The validity of these assumptions has been examined in detail by Lax (118), Chew and co-workers (33, 34), and Ashkin & Wick (2). Intuitively, though, it is clear that these assumptions require that the wavelength of the fast nucleon (its effective size) should be small compared to the internucleon distance in the nucleus and that the kinetic energy of the fast nucleon should be large compared to the potential energy felt by nucleons within nuclear matter. These requirements are doubtless met by nucleons with energies in excess of 100 Mev. The intractability of the problem in the absence of these simplifying assumptions has encouraged their use—with considerable success—at nucleon energies where their validity, however, is not immediately clear [see, for example, the "frivolous" model of Lane & Wandel (114)].

If the motion of the incident nucleon within the struck nucleus is treated classically, then, as shown by Fernbach, Serber & Taylor (47), the inelastic cross section for a high-energy particle incident upon a nucleus with a sharp boundary may be expressed in terms of the nuclear radius R and the mean free path of the incident particle in nuclear matter λ :

$$\sigma = \pi R^2 \left[1 - \frac{\left(1 + 2 \frac{R}{\lambda}\right) \exp\left(-2 \frac{R}{\lambda}\right)}{2 \frac{R^2}{\lambda^2}} \right]. \quad 2.$$

Under the impulse approximation, the mean free path is given in terms of the effective cross section for the interaction of the incident particle with neutrons, $\bar{\sigma}_{qn}$, and with protons, $\bar{\sigma}_{qp}$:

$$\lambda = \frac{\frac{4}{3}\pi R^3}{Z\bar{\sigma}_{qp} + N\bar{\sigma}_{qn}}. \quad 3.$$

These effective cross sections differ from the free-nucleon cross sections because of two factors: the Pauli exclusion principle which makes occupied states inaccessible after scattering, and the momentum distribution of the nucleons within the nucleus. These two points have been fully discussed by Goldberger (67).

The stochastic nature of the problem within the framework of the model and assumptions just described suggests the use of a Monte Carlo calculation to simulate the intranuclear cascade and to estimate $\sigma(A', Z', U', I | A^0, Z^0, q, E)$. The pattern for this treatment of the problem was set by Goldberger (67), and followed by Bernardini *et al.* (20); Morrison *et al.* (153); McManus *et al.* (138); Meadows (139); Combe (35); Rudstam (182); Ivanova & P'ianov (94); Nikol'skii *et al.* (160); and Metropolis *et al.* (146, 147). All of these authors used essentially the same nuclear model: a Fermi momentum distribution of nucleons contained in a uniform-density nucleus with a square-well potential energy. There are differences among the calculations of these various authors in the values given to nuclear radii, potential-well depth, the energy below which cascade particles are assumed to be captured, and the treatment of reflections at the nuclear surface. The calculations of Metropolis *et al.* (146, 147), having been performed on the MANIAC electronic computer, are the most complete in that they give the problem a three-dimensional relativistic treatment, include meson production and participation in the intranuclear cascade, treat a number of target nuclei and a number of incident energies up to 1.8 Bev, and follow many more cascades for each set of initial conditions than were followed in the calculations of the other authors. Such calculations, in addition to predicting the spectrum of excited nuclei remaining after the intranuclear cascade, will also give the differential cross sections for the energy and angular distributions of knock-on particles. Typical results of these Monte Carlo calculations are shown in Figures 2 and 3 taken from the papers of Metropolis *et al.* (146, 147). The histograms shown in Figure 2 illustrate the spectra of excitation energies remaining in residual nuclei of various mass numbers formed in the cascades generated by 460- and 1840-Mev protons incident upon Cu^{64} . The average excitation energies deposited by protons of various energies incident upon Al, Cu, Ru, and U nuclei are shown

in Figure 3. The relatively rapid increase in excitation energy with incident energy above 400 Mev is ascribed by the authors to the onset of meson production in the nucleon-nucleon collisions. They suggest that the relatively large cross section for meson-nucleon scattering (the positive pion-proton scattering cross section goes to about 200 millibarns at the peak of the resonance), coupled with the possibility of meson absorption by nuclear matter, makes the meson an efficient carrier of excitation energy from the incident nucleon to the struck nucleus. Pi-meson absorption was assumed to

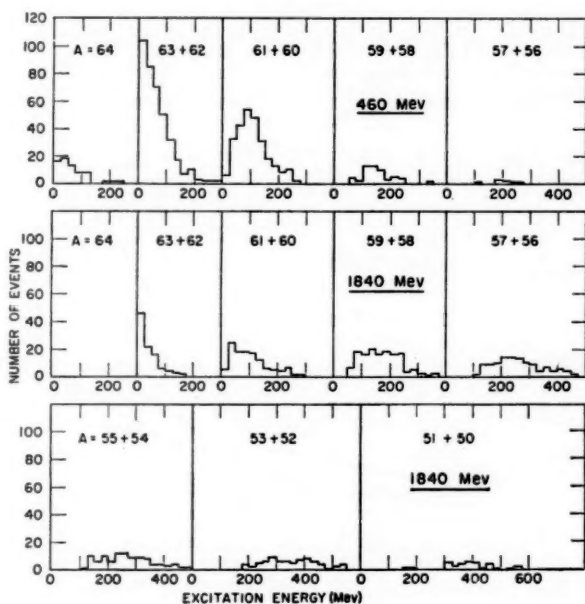


FIG. 2. Calculated excitation energy spectra for different cascade products from the bombardment of Cu^{64} with protons of 460-Mev and 1840-Mev incident energy, taken from Metropolis *et al.* (147).

occur through the interaction of the pion with two nucleons within the nucleus as had been suggested by Frank *et al.* (55). This approach was also used in the calculations in which pions were the incident particles.

Some comparisons between the results of these calculations and corresponding experimental studies will be made in the later sections of this review. At this point it may be remarked that, in the main, the agreement between the results calculated in this manner and the experimental data is quite good. However, no systematic study of the sensitivity of the calculated results to the input parameters and model has as yet been made, and until that is done it is not clear whether the agreement comes primarily from the

statistical aspect of the problem or whether the agreement with experiment speaks for the validity of the details of the model.

The difficulties with the various Monte Carlo calculations are in two categories. As Metropolis *et al.* (147) point out, better input information about the diffuse nuclear boundary, pion-nuclear potential energy, dynamics of pion production, and perhaps other quantities, is certainly required and would probably go a long way toward rectifying some of the discrepancies between observed and calculated results. But these corrections clearly do not alter the spirit of the calculation. However, observations such as Sørensen's

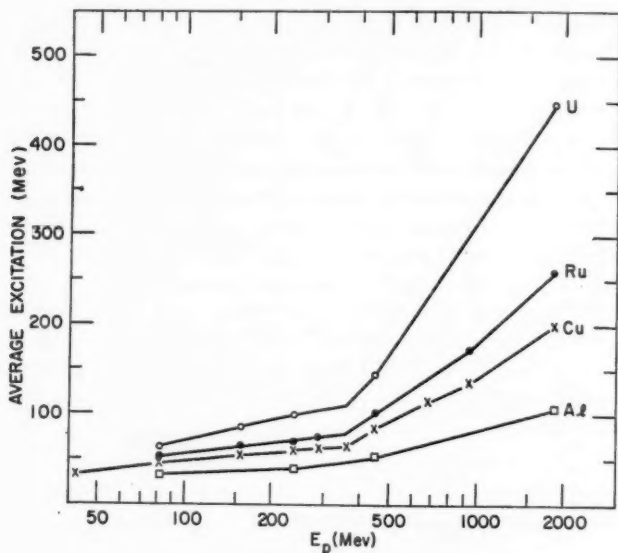


FIG. 3. Calculated average excitation energy in residual nucleus, plotted as a function of incident proton energy for four target elements, taken from Metropolis *et al.* (147).

(195) in which he found very energetic Li^8 particles emitted in very-high-energy reactions suggest that interactions between a high-energy nucleon and a cluster of nucleons acting in concert are also of significance. A recent analysis by Glassgold, Heckrotte & Watson (60a) of the collective excitations of nuclear matter presents another approach to the interpretation of high-energy interactions which naturally includes excitations of clusters of nucleons. In their formalism, these excitations would come about through the establishment, by a very-high-energy incident particle, of a "shock wave" within the struck nucleus.

3.3 Evaporation phase.—Evidence that a second type of process must be

important in the emission of particles subsequent to inelastic interactions at high energies comes from two sources:

The shapes of the energy spectra of the low-energy charged particles (black prongs) detected in photographic emulsions that were exposed either to cosmic rays or to artificially accelerated particles are at least qualitatively consistent with those expected for the emission of particles from excited nuclei and inconsistent with those expected for direct emission through the knock-on process. For example, the evaporation theory calculation of

TABLE I
RELATIVE YIELDS OF ISOBARIC SPALLATION PRODUCTS

	Ti ⁴⁵	V ⁴⁷	Cr ⁴⁸	Cr ⁴⁹	Mn ⁵¹	Fe ⁵²	Co ⁵⁵	Ni ⁵⁶	Refer- ence
	Ca ⁴⁵	Sc ⁴⁷	V ⁴⁸	V ⁴⁹	Cr ⁵¹	Mn ⁵²	Fe ⁵⁵	Co ⁵⁶	
V+170 Mev <i>p</i>	1.9	0.6	0.009						(182)
Mn+170 Mev <i>p</i>	4.5	1.1	0.05			0.015			(182)
Co+170 Mev <i>p</i>		1.2	0.03			0.015			(182)
Fe+340 Mev <i>p</i>	6.6	2.9	0.08	0.32	0.10	0.05			(184)
Co+370 Mev <i>p</i>	5.3			0.27	0.15	0.02	0.14		(15)
Cu+340 Mev <i>p</i>	6.2				0.20	0.02	0.20		(12)
Cu+2200 Mev <i>p</i>	2.3	0.8	0.05	0.16	0.07	0.04	0.12		(58)
Zn+340 Mev <i>p</i>	4.2		0.04		0.13	0.02			(218)
As+380 Mev <i>p</i>	2.5	1.9	0.04	0.28	0.06	0.01	0.11	0.0004	(38)
Cr ⁵³ +<40 Mev α						0.03			(151)
Fe ⁵⁴ +<40 Mev α							0.14	0.014	(152)
Ti ⁴⁶ +<40 Mev α			0.03	2					(177)

Le Couteur (120) for the energy spectrum of low-energy (<30 Mev) singly charged particles agrees quite well with the observations of Harding *et al.* (75).

The second source of evidence is found in the ratios of the production cross sections of isobaric (constant-mass number) spallation products. In Table I the relative yields of several isobaric spallation products are shown for a variety of targets and incident particles. We see that these ratios, which are reliable to at best 20 or 30 per cent, are indeed remarkably independent of bombarding conditions. Even more striking are the data given in Table I which show that the relative yields of the isobaric pairs Cr⁴⁸-V⁴⁸ and Fe⁵²-Mn⁵² are the same, whether these products arise from low-energy reactions (Ti⁴⁶ or Cr⁵⁰ plus 40-Mev He⁴ ions) or high-energy reactions. As discussed by Halpern (74) and by Belmont & Miller (15), this constancy can occur only if some process is operative which makes the relative probabilities of proton and neutron emission much more sensitive to nuclear properties than they are in the knock-on process.

All analyses of particle evaporation from excited residual nuclei remaining after the intranuclear cascade have used the statistical assumption and the formalism first developed by Weisskopf (212) for the compound nucleus model of Bohr (24). These analyses, then, start with the well-known expression of Weisskopf for the probability per unit time that a particle of type i with binding energy B_i and spin s_i is emitted in the energy interval $d\epsilon_i$ at an energy ϵ_i from a nucleus with excitation U :

$$W(\epsilon_i)d\epsilon_i = \frac{2s_i + 1}{\pi^2 \hbar^3} \mu_i \sigma_i(\epsilon_i) \epsilon_i \frac{\rho'(U - B_i - \epsilon_i)}{\rho(U)} d\epsilon_i \quad 4.$$

where $\rho(U)$ is the density of energy levels of the original nucleus at excitation energy U , $\rho'(U - B_i - \epsilon_i)$ is the density of energy levels of the nucleus remaining after the emission of particle i with kinetic energy ϵ_i , μ_i is the reduced mass of the system after emission, and $\sigma_i(\epsilon_i)$ is the cross section for the exact inverse of the emission process.

The cross section for the inverse process is usually approximated by the continuum theory cross section for the capture of particle i with kinetic energy ϵ_i by the residual nucleus in its ground state. It is in this term that the effect of the Coulomb barrier upon the emission of charged particles explicitly appears.

Much of the uncertainty in the use of the Weisskopf formalism for the analysis of the emission of particles from excited nuclei arises in the selection of an explicit expression for the level densities of the excited nuclei; the literature and the confusion on this point are both growing. Most investigations use conventional statistical-mechanical techniques and result in an expression for the level density in terms of the nuclear temperature τ , excitation energy U , and entropy S :

$$\rho(U) = \frac{e^S}{\tau \left(2\pi \frac{dU}{d\tau} \right)^{1/2}} \quad 5.$$

Approximations that are introduced into the formalism (22) leading to expression 5 are not very good for low excitation energies and, for reasonable nuclear models, lead to the absurd result of an infinite level density in the region of the ground state. In nearly all analyses of the evaporation of particles from excited nuclei, the nonexponential dependence upon excitation energy is essentially ignored. This occurs automatically at high excitation energies because of the relatively slow variation of the nonexponential term. Expression 5 is quite general, and a particular nuclear model must be chosen before an explicit dependence of level density upon excitation energy may be obtained. The usual assumption is to take

$$U = a\tau^n \quad 6.$$

and this expression, together with the thermodynamic definition of temperature, gives

$$S = \frac{n}{n-1} (aU^{n-1})^{1/n} \quad 7.$$

This results in an expression for the level density in the following form:

$$\rho(U) = \frac{1}{\sqrt{2\pi n}} \left(\frac{a}{U^{n+1}} \right)^{1/(2n)} \exp \left(\frac{n}{n-1} a^{1/n} U^{(n-1)/n} \right). \quad 8.$$

In most applications of Equation 4, " n " of Equations 6 and 8 is taken as two (which corresponds to a noninteracting Fermi gas), and the energy dependence of the preexponential factor of Equation 8 is ignored:

$$\rho(U) \approx \exp(2a^{1/2}U^{1/2}). \quad 8a.$$

The quantity " a " is, in principle, determined by the nuclear model [see, for example, reference (22)]; in practice " a " is often taken to be a parameter the value of which is to be experimentally determined. In a discussion of the experimental determination of " a ," Igo and Wegner (90) point out that experimental determinations of " a " fall into two classes: those that give $a = 0.11A$ (where A is the mass number of the nuclide) and those that give $a = 2$, independent of mass number. This unfortunate anomaly is as yet unresolved.

Hurwitz & Bethe (89) have pointed out that level-density expressions of the form of Equation 8 must be modified in order that the dependence of level density upon the odd, or even, or magic character of the neutron and proton numbers may be taken into consideration. Their analysis of the problem leads to the suggestion that the excitation energy in Equation 8 be measured not above the ground state of the nuclide but rather above a characteristic level which would be the ground state if special effects such as pairing and shell perturbations did not exist. Thus, in the investigation of the evaporation of particles from excited nuclei, the level density is often taken as [see, for example, Belmont & Miller (15)]:

$$\rho(U) = C \exp[2a^{1/2}(U - \delta)^{1/2}] \quad 9.$$

where C is taken as dependent upon mass number but not upon excitation energy, and δ is the difference in energy between the characteristic level and the ground state [see Cameron (28) for a detailed discussion of δ].

Le Couteur (120); Yamaguchi (220); Fujimoto & Yamaguchi (59); Jackson (95); Rudstam (182); and Dostrovsky, Rabinowitz & Bivins (44) have used Equation 4 in the theoretical investigation of the evaporation of particles from excited nuclei remaining after the intranuclear cascade is over, that is, the estimation of η in Equation 1. The problem is again essentially a stochastic one in that the initial nucleus, characterized by A' , Z' , and U' , has a probability of emitting a particle of type i with kinetic energy ϵ_i which is proportional to the expression in Equation 4 (normalization is accomplished by integrating Equation 4 over the energy spectrum for each particle i and summing over all types of particles, i); this emission, in general, leads to a new nucleus A'' , Z'' , and U'' , whose behavior is again governed

* The expression " a " as used by Igo and Wegner is four times the " a " of Equation 8.

by a set of equations of the type given in expression 4. Thus the problem is one of an "evaporation cascade" and it, too, may be treated by the Monte Carlo method. The first four investigators cited above attempted to give an analytic solution to the problem by what amounts to an averaging process; in the latter two investigations, Le Couteur's formulation of expression 4 was used in a Monte Carlo treatment of the evaporation cascade. The calculation of Dostrovsky *et al.* (44) is the most complete since their use of an electronic computer for following the Monte Carlo cascades made it feasible to follow many more cascades and thus to improve the statistical accuracy of their results. In all of these calculations performed to date an explicit form of the level density expression which smooths over fluctuations in the level density among isobars has been used. Since these fluctuations are decisive in the determination of relative isobaric yields, these calculations cannot be expected to yield reliable estimates of them.⁴ The calculations are quite useful, though, for predicting the average number of the various types of particles emitted from highly excited nuclei, for giving the distribution of these numbers about their average, and for predicting the energy spectrum of the emitted particles at energies above the Coulomb barrier cut-off. They thus are useful for computing $\sum_Z \eta(A, Z | A' Z' U')$.

Competition between fission and evaporation of particles from nuclei along the path of the evaporation cascade has been investigated by Pate (165) and by Dostrovsky, Fraenkel & Rabinowitz (43). These investigations suffered from the lack of a reliable quantitative description of the fission process which would give the probability per unit time that a nuclide with a given excitation energy fissions into given fission products. The results of these calculations will be discussed in Section 6.5.

Hudis & Miller (87) have used the evaporation theory formalism to calculate the cross sections for the production of Be⁷ in the proton bombardments of copper, silver, and gold. The agreement between their rather approximate calculation and the experimental results indicates the usefulness of considering particles such as lithium and beryllium as evaporated fragments.

The use of a statistical theory for the analysis of the de-excitation of highly excited nuclei (often at excitations of several hundred Mev) is open to serious criticism. The criticism may be stated in different ways, but what it amounts to is the fact that as the excitation energy increases, the mean-life of the nucleus between particle emissions decreases, while the time required for the equilibration of the excitation energy increases. This can mean, for example, that the characteristics of the "*n*th" emitted particle are not independent of those of the "*(n-1)*th" particle. It also means that

⁴ Dostrovsky, Fraenkel & Friedlander (42a) have recently shown that experimental isobaric-yield ratios can be approximately reproduced by Monte Carlo evaporation calculations if level densities are computed according to Equation 9, with δ values reflecting pairing and shell effects.

there is really no sharp division between a knock-on process and evaporation process as is generally assumed. Nevertheless, there has been success in the use of the formalism described for the estimation of the energy spectra of black prongs and for the estimation of mass-yield curves.

4. TOTAL INELASTIC CROSS SECTION

The total inelastic cross section for the interaction of high-energy particles with complex nuclei may be measured in either of two ways: measurement of the attenuation of the beam by inelastic interactions, or measurement of the cross sections of each of the products of the inelastic interaction.

The first method suffers from the difficulty met in separating the beam attenuation by inelastic events from that caused by elastic events. The differentiation is generally accomplished by observing the apparent cross section as a function of the solid angle subtended by the detector at the absorber and also by observing the energy spectrum of the detected particles. The main difficulty comes, of course, from the inelastic events in which little excitation energy is transferred to the struck nucleus.

The second method is unreliable largely because of the difficulty encountered in measuring the cross sections for the production of all of the products. When radiochemical techniques are used, there is the difficulty in assaying the stable products; in photographic-emulsion studies there are the two problems of separating the events in heavy and in light nuclei from each other and of correcting for those events that do not have charged-particle emission. These uncertainties make the second method considerably less reliable than the first.

The energy dependence of the inelastic cross section, as measured by the attenuation method (149), is illustrated in Figure 4; the curves in the figure are those computed by Metropolis *et al.* (146). It is to be noticed that the inelastic cross sections shown in Figure 4 are close to the geometric cross sections corresponding to a nuclear radius $r = 1.3 \times 10^{-13} A^{1/3}$. The calculated cross sections (see Eq. 2) will be slightly smaller than geometric because the nuclear model used implies a finite probability for a nucleon to traverse a nucleus without making a collision; this latter phenomenon has been termed transparency.

Radiochemical determinations of inelastic cross sections are most apt to be reliable for heavy elements. For them, the high Coulomb barrier assures a predominance of neutron evaporation, and the spallation products are very likely to be found on the neutron-deficient side of stability rather than in the stability valley as occurs with the lighter targets. In this connection, it is of interest to compare a radiochemical determination of the inelastic cross section of bismuth with *ca.* 400-Mev protons with that determined by the attenuation method. A cross section of about 1.3 barns may be deduced from the spallation study of bismuth by Hunter & Miller (88) and the fission study of bismuth by Jodra & Sugarman (96). This value is to be compared

with that of 1.5 barns found by Millburn *et al.* (149) in their attenuation experiments.

The inelastic interaction cross sections for composite bombarding particles, which have been discussed in detail by Millburn *et al.* (149) and by Heckrotte (76), are again nearly geometrical if the finite size of the bombarding particle as well as nuclear transparency are taken into consideration.

5. SPALLATION

As has already been mentioned, spallation reactions are those in which nucleons or small clusters of nucleons are emitted from struck nuclei in the

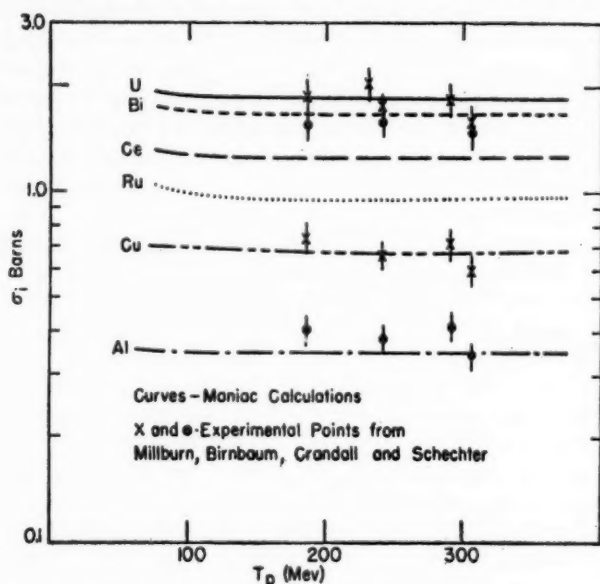


FIG. 4. Comparison of calculated (146) inelastic proton-nucleus cross sections with experimental values (149). Figure taken from Metropolis *et al.* (146).

knock-on and in the evaporation phases of high-energy nuclear reactions. In this section, an attempt will be made to give some picture of the distributions of spallation products as they depend upon target, energy of incident particle, and type of incident particle. These distributions will then be compared, wherever possible, with the results of the calculations described in the previous sections. To that end, in the following two subsections the relative yields of isobaric spallation products and the mass-yield distributions will be discussed. Although the mass-yield distribution is the one that is, at this point, more easily compared with theory, the construction of a mass-yield curve nearly always requires the estimation of unmeasured production cross sections. Thus, it is better first to examine the isobaric distributions

in order that a guide for estimating unmeasured cross sections may be available.

5.1 Relative yields of isobaric spallation products.—The ratios of cross sections for the production of several pairs of isobaric products in reactions of protons of various energies with several different targets are given in Table I. Since nearly all of the nuclides listed there decay at least partly by electron capture, considerable experimental errors are to be expected in those experiments in which the x-rays were detected with conventional Geiger-counting setups. Errors from this source are expected to make the numbers in Table I reliable to perhaps a factor of two when comparisons between results from different laboratories are made.

Despite this experimental uncertainty, three characteristic features of isobaric yields are evident from the data: (a) There can be a large preference for one isobaric product over another, even in the instance of neighboring isobars. This is particularly true for even-mass-number products and is well exemplified at mass numbers 48 and 52. Odd-mass-number products show the same effect to a smaller degree. (b) The relative yields of isobaric spallation products are nearly independent of target as long as the isobars are at least a few mass and atomic numbers away from the target. The relative isobaric yields at mass number 51 from the bombardment of iron, cobalt, copper, zinc, and arsenic with 340-to 370-Mev protons provide a good example of this characteristic. (c) The relative isobaric yields from a given target appear to be fairly insensitive to the energy of the incident particle. The data for cobalt and for copper targets show no change within about a factor of two or three when the bombarding energy goes from 170 to 370 Mev for the former and from 340 to 2200 Mev for the latter.

It is worthy of mention that the above three comments obtain even though the individual cross sections vary over a large factor: the cross section for producing Mn^{52} varies from 0.70 millibarns for arsenic bombarded with 380-Mev protons to 31 millibarns for 170-Mev protons on cobalt.

These three characteristic features of the relative isobaric cross sections are qualitatively what is to be expected as a consequence of the evaporation phase of nuclear reactions. The decisive importance of the evaporation process in the determination of relative isobaric yields is emphasized by the data in the last three lines of Table I. There it may be seen that the ratios observed in what are characteristically low-energy reactions proceeding through the compound-nucleus mechanism are essentially the same as those observed in high-energy reactions. The divergences that occur, for example, at mass numbers 49 and 56 probably reflect the fact that in the low-energy reactions the evaporation cascades start from a given excited compound nucleus, whereas in the high-energy reactions the evaporation cascades start from a spectrum of excited nuclei. The large differences between the formation cross sections of Mn^{52} and Fe^{52} and between Cr^{48} and V^{48} that are observed for both low- and high-energy reactions doubtless arise from

the same cause: the lower energy level density in the even-even nuclides as compared to the odd-odd nuclides.

The insensitivity to target is probably a reflection of two factors: (a) the ratio of the average numbers of neutrons and protons emitted in the intranuclear cascade (146, 147) is not very different from that corresponding to nuclear stability and hence the evaporation chain, for all targets, starts from nuclei not too distant from stability; and (b) the distributions of the same isobaric products resulting from the evaporation of particles from two different excited nuclei are not significantly different provided that the two initial excited nuclei are not very distant from the line of stability and that the evaporation chain is not too short. The insensitivity of the observed isobaric ratios to bombarding energies indicates—and this is borne out in the Monte Carlo calculation (146, 147)—that the distribution in A' , Z' , U' of excited progenitors of a given set of isobaric products is nearly independent of the bombarding energy.

While there are few instances in which relative yields of more than two isobaric products have been measured, the general form of the isobaric-yield curve for spallation products with $45 < A < 70$ may be inferred from existing data. For odd-mass-number spallation products with Z at least one unit and A at least three or four units less than those of the target, the most probable charge for a given mass-number product is usually one greater than or equal to that for beta stability. The isobaric-yield curve then falls off by about a factor of between 3 and 10 for odd-mass-number products on either side of the most probable product. The even-mass-number products exhibit a somewhat different behavior in that the major part of the isobaric yield appears to be shared between two neighboring isobars: one stable and the other with atomic number one greater. As is seen in Table I, the isobaric-yield curve may fall off from the broad maximum quite rapidly with increasing atomic number; less is known about the behavior on the other side of the maximum.

This description is quite crude and it must be remembered that the isobaric-yield curves, particularly those for even mass numbers, will exhibit irregularities because of the factors mentioned in connection with Equation 9. Indeed, it is just these factors that cause the differences between even- and odd-mass products.

Rudstam (182) has discussed the isobaric yield in terms of a gaussian distribution. Both the odd- and even-mass products may be included if the maximum of the gaussian occurs near the appropriate atomic number for odd-mass products and between the two appropriate atomic numbers for even-mass products.

Although there are few data on relative isobaric yields from heavier target nuclei and from other types of incident particles, it is clear that, for example, in Winsberg's (213) investigation of the interaction of 122-Mev negative pions with iodine, the final distribution of products is governed by the evaporation of particles from excited nuclei. Further, Lindner & Osborne

(125) found that the ratio of the production cross sections for Pa^{227} and Th^{227} from the proton bombardment of U^{238} stays essentially constant at a value ranging between three and four as the proton energy is varied from 100 to 340 Mev. These same authors also found that the ratio of yields of Ac^{224} and Ra^{224} is the same, within experimental error, from a Th^{232} target as it is from U^{238} . These few results lend support to the generalizations indicated for lighter targets and incident protons.

While it is safe to conclude that as a first approximation the relative isobaric yields of spallation products are not very sensitive to targets and to the type and energy of the incident particles the spallation data from 2.2-Bev protons on copper (58) and 450-Mev neutrons on copper (135) suggest that for neutrons and for Bev protons there may be a tendency toward a slight increase in the probability of forming the more neutron-excess isobaric products. Clarification of this point, however, must await further experiments.

5.2 Mass-yield curves for spallation products.—The determination of the cross sections for the formation of all of the products of a given mass number in a spallation reaction requires, as mentioned before, the estimation of the production cross sections for the long-lived and stable products. The uncertainty introduced by this procedure is probably rather unimportant for heavy targets because for them the isobaric-yield distribution peaks fairly far over on the neutron-deficient side of stability and thus the contribution from stable products is relatively unimportant. For lighter targets, the information presented in the previous subsection is of considerable help in determining the shape of the mass-yield curve.

As an example of the mass-yield curve for the spallation of a heavy element, one may consider the results of the investigation by Hunter & Miller (88) of the spallation of bismuth by 380-Mev protons. Their experimental results are presented in Figure 5 together with the mass-yield curve (the cross-hatched area) calculated by them on the basis of the two Monte Carlo calculations of the knock-on (147) and evaporation processes (44). As was pointed out by the authors, the calculation really refers to 450-Mev protons, which probably explains the divergence between the calculated and experimental values for low-mass-number products. Other than that, the agreement between the experiment and theory is gratifying. The general way in which the mass-yield curve for bismuth would change with the energy of the incident protons has been indicated in Figure 1.

The previous discussion of relative isobaric yields suggests that the best way to interpolate the formation cross sections for stable isotopes formed in the spallation of lighter targets would be through the use of evaporation theory in a form that would include the special factors which strongly influence energy level densities within several Mev of the ground state. Since such a detailed analysis of the consequences of evaporation theory is not yet available, two approximate methods have been employed: (a) An empirical approach, suggested by Rudstam (182), which essentially assumes that the

mass-yield curve for spallation decreases exponentially and that relative isobaric yields have a gaussian distribution centered about some most probable atomic number (nonintegral) which varies smoothly with mass number; and (b) An attempt to predict the detailed consequences of the evaporation cascade through a combination of the use of approximate evaporation theory calculations and relative isobaric yields found in low-energy reactions [see, for example, Belmont & Miller (15)].

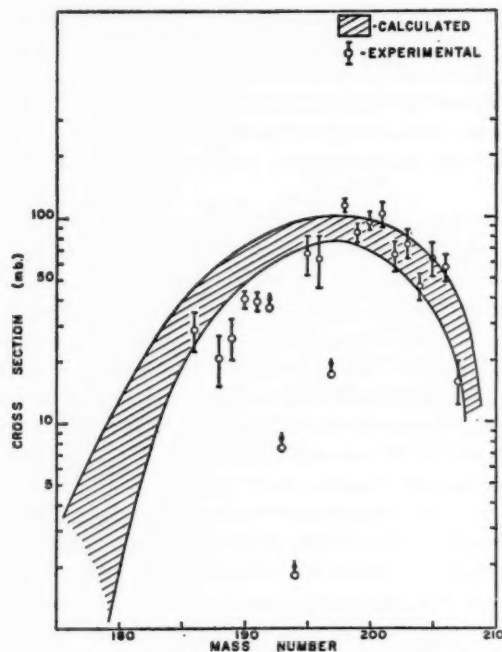


FIG. 5. Mass-yield data of Hunter & Miller (88) for 380-Mev protons on bismuth compared with calculations of Metropolis *et al.* (147) and Dostrovsky *et al.* (44). Figure taken from (88).

The most intensive study of the spallation of light-element targets has been done with copper (see Table II at the end of this chapter). Although the facts that copper has two stable isotopes of comparable abundance and that the difficulty of interpolating yields in the vicinity of the magic number 28 make the construction of a mass-yield curve from these data difficult, it is worthwhile comparing the curves which have been constructed with those predicted by calculation. The comparison between theory and experiment (including interpolated results) is shown in Figure 6 taken from Friedlander (56) who used data from (12, 58, 146, 147). The agreement between theory and experiment displayed in Figure 6 is rather good. Using a different inter-

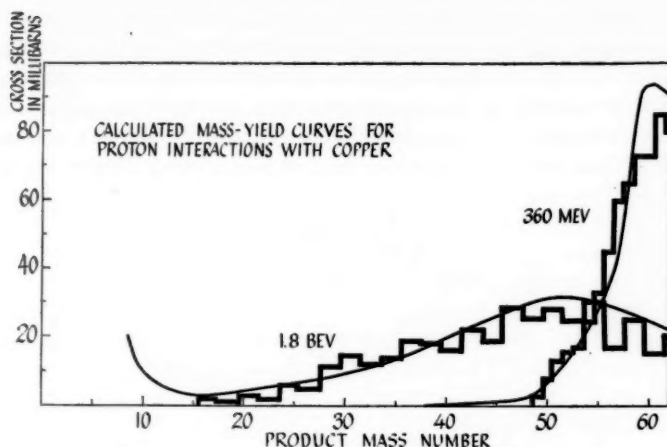


FIG. 6. Mass-yield curves of Batzel, Miller & Seaborg (12) and Friedlander *et al.* (58) for 340-Mev and 2200-Mev proton bombardment of copper respectively, compared with those calculated by Metropolis *et al.* (146, 147). Figure taken from Friedlander (56). Histograms are calculated data.

polation procedure, Barr (7) has arrived at a mass-yield curve that is in slightly less satisfactory agreement with theory.

5.3 *Excitation functions for spallation reactions.*—The study of excitation functions—variation of production cross section with incident energy—is a simple and often very useful means of investigating the mechanism of nu-

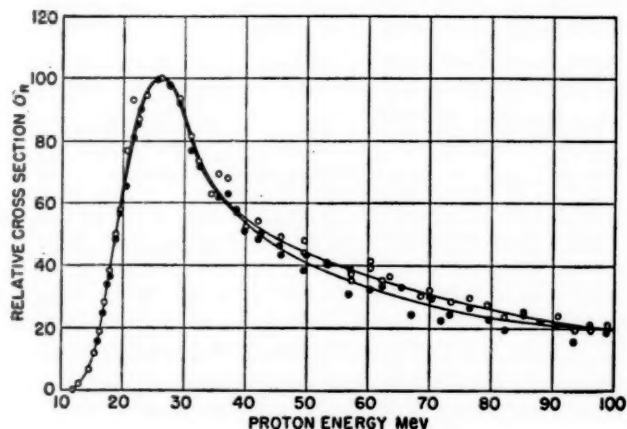


FIG. 7. Excitation functions for the reaction $\text{Co}^{58}(p, pn)\text{Co}^{58,58m}$ taken from Sharp *et al.* (191). Solid points are Co^{58} , open circles are Co^{58m} . The peak cross sections are 270 mb for Co^{58} and 400 mb for Co^{58m} (191).

clear reactions. The excitation functions for spallation reactions may be divided into two classes: those for which the threshold is in the region where the Bohr compound-nucleus formalism is still applicable (<40 Mev), and those with thresholds in the knock-on region (>60 Mev). Figure 7, taken from a paper by Sharp, Diamond & Wilkinson (191), affords a good example of the first class. In this figure it is seen that the cross section for a typical

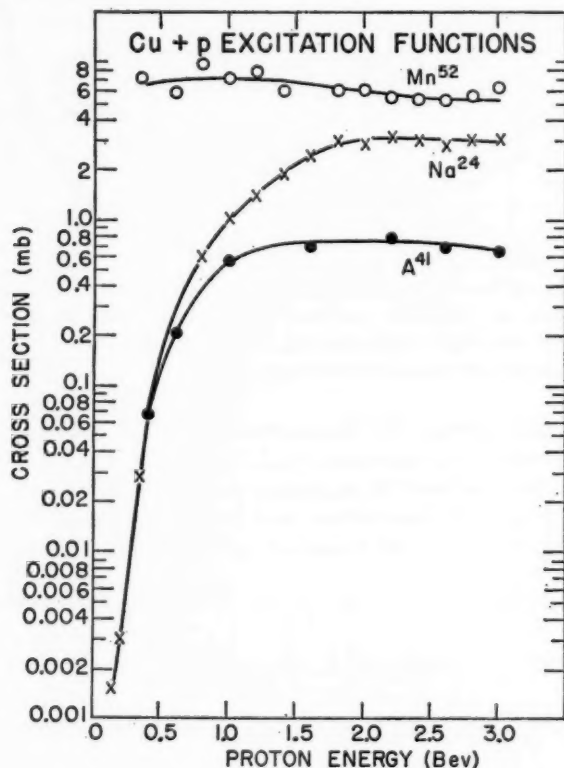


FIG. 8. Excitation functions for the production of Na^{24} , Ar^{41} , and Mn^{52} from copper targets irradiated with protons, from Miskel *et al.* (152a).

low-energy reaction, (p, pn), rises sharply to a maximum and then declines rapidly because of increased competition from other reactions which become energetically possible as the energy is raised. The tendency towards leveling off at higher bombarding energies is what is expected as the knock-on interaction replaces that of compound-nucleus formation.

The excitation functions for some high-energy spallation reactions of copper are shown in Figure 8 taken from the data of Miskel *et al.* (152a). In contrast to the sharply peaked curve observed at low energies it can be seen that the cross sections which result from high-energy reactions, after

rising to a maximum, either level off or diminish gradually as the energy of the incident particle is raised. The energy region included in Figure 8 is such that only the tail of the Mn excitation function is shown. The gradual decrease in cross sections past the excitation function peaks is expected from the previous discussion of spallation reactions for two reasons. (a) As can be seen from Figure 3, most of the incident particle energy is dissipated as kinetic energy of the knock-on particles; hence the main effect of increasing bombarding energy is merely to increase the kinetic energy of the outgoing particles. (b) To the extent that increasing the bombarding energy does cause new competing reactions to occur, they occur at the expense of all the other reactions and therefore no one of them decreases markedly.

5.4 *Simple spallation reactions.*—Simple high-energy reactions such as (p, n) , (p, pn) and $(p, 2p)$ provide a rather severe test of the various theoretical analyses of spallation reactions, since both the intranuclear and the evaporation cascades are small and so the effect of improper input information will not be smeared out by the random processes as it is for larger cascades. The comparison between theoretical and experimental results has been made and discussed by Metropolis *et al.* (147) and by Caretto & Friedlander (29). The former have shown that for the $\text{Ni}^{64}(p, n)\text{Cu}^{64}$ reaction, the shape of the excitation function and the absolute values of the cross section were well reproduced by the theory. While the shapes of the excitation functions for the (p, pn) and $(p, 2p)$ reactions were predicted by the calculations fairly well, the values predicted for the cross sections were generally too low by a factor of two or three. This rather significant discrepancy is probably connected with the unrealistic model used in the Monte Carlo knock-on calculation: a sharp nuclear boundary with no diffuse edge, and an energy distribution of nucleons within the nucleus given by the Fermi distribution. An extensive study of (p, pn) cross sections by Markowitz *et al.* (133) suggests that this reaction may be very sensitive to the details of the energy distribution of the more loosely bound nucleons within the nucleus.

5.5 *Photographic-emulsion studies of spallation reactions.*—The energy and angular distributions of charged particles emitted in spallation reactions may be conveniently studied through the use of sensitive photographic emulsions. Comparisons of this type of study with predicted results show remarkably good agreement (146, 147). Comparisons between spallation reactions investigated by the emulsion and radiochemical techniques are rather difficult to make. Qualitatively, though, there is agreement between the form of the mass-yield curve for 350- to 400-Mev protons incident upon targets of mass ~ 60 and the observation of Bernardini, Booth & Lindenbaum (21) that the black-prong number distribution is essentially flat for from one to three black prongs and then falls rapidly for higher prong numbers.

6. FISSION

Over the past decade or so, it has been found that in addition to the well-known fission of the heaviest elements with low-energy neutrons, any

nucleus can be made to fission provided it is supplied with sufficient excitation energy [cf., Spence & Ford (196)]. In this review attention will be focussed upon the aspects of the problem peculiar to fission induced by high-energy particles and the reader is referred to a recent review by Leachman (119) as well as to the comprehensive review by Halpern (74a) in this volume for the details of the mechanism of the fission process which are important to the computation of $\eta(A, Z|A', Z', U')$ where the product A, Z is a fission product. It should immediately be mentioned that the analysis of high-

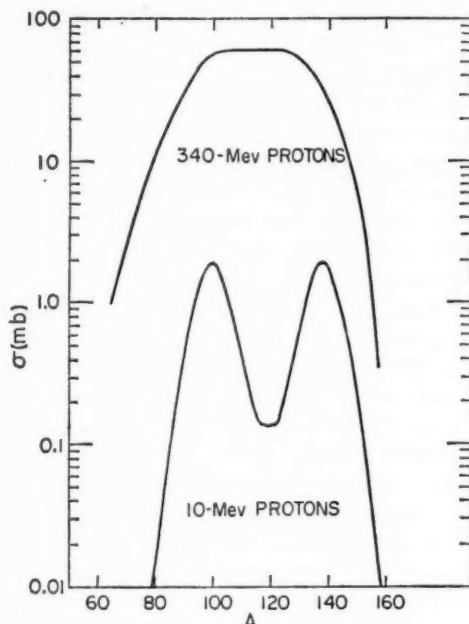


FIG. 9. Mass-yield curves for proton-induced fission of U^{238} , taken from Stevenson *et al.* (199).

energy fission experiments, as well as those at low energies, is made difficult by the fact that no successful computation of this quantity exists.

6.1 Mass-yield curve for the fission process.—The mass-yield distribution for the fission process has been examined by many investigators who agree quite well in their conclusions. The marked difference between the mass-yield distributions for low- and high-energy fission is illustrated in Figure 9 taken from the paper of Stevenson *et al.* (199). There it is seen that the well-known double-peaked mass distribution, characteristic of low-energy fission, changes over to a single-peaked distribution characteristic of high-energy fission. These investigators also found that the single-peaked distribution grows wider with increasing bombarding energy. The increase in width occurs

at the expense of the symmetry of the curve; it starts to bulge out toward the low-mass-number side. There is also evidence that the peak of the high-energy fission mass-yield distribution moves slowly to lower mass numbers as the energy of the incident proton increases (96). As is seen in Figure 1, when the energy of the incident particle is further increased to the order of a Bev, the fission-yield curve has merged with that for spallation and the single-peaked distribution is no longer discernible.

6.2 Total fission cross sections.—Total fission cross sections have been found, as might be expected, to be very sensitive to the nature of the target and to bombarding energy for all but the heaviest elements. Kruger & Sugarman (106) found, for example, that the total fission cross section with 450-Mev protons ranged from a few millibarns for Ho^{165} to 670 millibarns for Th^{232} . Jodra & Sugarman (96) found the proton-induced fission cross section of bismuth to rise steadily from threshold to 450 Mev where it has a value of 200 millibarns. Stevenson *et al.* (199) observed, on the other hand, that the fission cross section for U^{238} rose very rapidly to essentially the value of the geometric cross section once the threshold had been passed; this is typical behavior for the heaviest elements.

While the remarks that have just been made describe the general features of total fission cross sections, it must be added that there are often large discrepancies among the determinations of this quantity. For example, for 350-Mev bismuth fission, Jodra & Sugarman (96) and Biller (23), both using radiochemical techniques, find values of 170 millibarns and 240 millibarns, respectively; at the same energy, but using an ionization chamber, Steiner & Jungerman (197) find a value of about 240 millibarns. These values are to be contrasted with those found by Perfilov *et al.* (170), who, using a loaded-photographic-emulsion technique, quote a value of 90 millibarns at 460 Mev, a factor of two lower than that given in (96) at 410 Mev. Clearly, absolute values of high-energy fission cross sections are not easy to determine.

6.3 Relative isobaric yields of fission products.—Before sketching the experimental results on the study of the relative isobaric yields of fission products, it is well to point out that the form of this distribution is not necessarily entirely governed by the fission process; the evaporation of particles from the excited primary fission fragments may alter the primary distribution. The investigation of the reactions of 340-Mev protons with U and Th by Lindner & Osborne (125) suggests that for the heaviest elements fission may compete successfully with particle emission all along the evaporation cascade, and thus each primary fission fragment may well have sufficient excitation energy to evaporate a few particles. However, a study of the angular correlation between fission fragments and neutrons in uranium fission by Skyrme & Harding (194) indicates that the post-fission evaporation of particles is small. For the fission of elements in the vicinity of bismuth by protons of several hundred Mev, it is likely that many neutrons must be emitted before fission can compete at all successfully with particle emission; thus, fission is apt to occur toward the end of the evaporation

cascade and it is not likely that there will be much excitation energy in the primary fission fragments available for the further evaporation of particles. In the fission of elements such as silver, existing data (71, 105) suggest that the isobaric distribution from fission is entirely governed by the evaporation of particles from the excited primary fission fragments. This is suggested by the observation that the relative yields of isobaric fission products in the region of mass numbers 50 to 60 formed in the fission of silver are very similar to those found for the spallation of nuclei such as cobalt, copper, zinc, and arsenic where these relative yields are determined by the evaporation cascade. Considering the high fission barriers of silver and of any of its possible cascade products, it is not surprising that fission occurs only at high excitations and with small probability.

The relative yields of isobaric products arising from the high-energy fission of the heaviest elements were investigated and other data on this subject reviewed in a recent paper by Pate, Foster & Yaffe (166). They found that the isobaric-yield distribution broadens with increasing bombarding energy and that the peak moves closer to stability from the neutron-excess side. For protons of several hundred Mev, the distribution has a width at half maximum of about three units of charge, and the peak is about one position removed from stability.

There are not enough data on isobaric fission product yields for the construction of an isobar distribution curve for the high-energy fission of elements in the vicinity of bismuth. There are enough data, though, to locate the position of the peak of this distribution curve; it is found on the neutron-excess side of stability and seems to move toward stability as the bombarding energy increases [see for example (96)].

There is, at this time, no theoretical prediction of the charge distribution in the fission act which agrees with experiment. In light of this situation, workers in the field have tended to discuss the charge distribution in fission in terms of two models that are suggested by the data: equal charge displacement, and unchanged charge distribution. In equal charge displacement, first suggested by Glendenin *et al.* (61) for low-energy fission, the most probable nuclear charges for complementary fission fragments are equally removed from the most stable nuclear charges corresponding to their masses. In unchanged charge distribution, first suggested by Goeckerman & Perlman (63) for high-energy fission, the most probable neutron-to-proton ratio of the fragments is the same as that of the parent fissioning nucleus. In both models, the distribution of charge has been assumed to be gaussian. Although unchanged charge distribution was first invoked in the interpretation of the data obtained in high-energy fission, there is evidence that equal charge displacement is a better description of the situation for the high-energy fission of U and Th (165).

6.4 Energetics of high-energy fission.—Two interesting questions about the high-energy fission process are those of the energy release and the excitation energy that has been deposited in the struck nucleus in events that lead to fission.

It has been found [see, for example (200)] that the kinetic energy of a given fission product decreases with increasing bombardment energy. This observation has been interpreted to mean that the partner of a given fission product gets lighter as the bombardment energy goes up.

By means of a measurement of the ranges of fission fragments, Porile & Sugarman (174) have found that the average deposition energies in the 450-Mev fission of bismuth and tantalum are 160 and 190 Mev, respectively, reflecting the increasing difficulty of causing fission in the excited cascade products as the mass of the target nucleus decreases. Perfilov *et al.* (170) through the study of the angle between fission fragments in loaded nuclear emulsions irradiated with 460-Mev protons deduce values of 190 Mev and 340 Mev as the average pre-fission excitation energies for bismuth and tungsten, respectively.

6.5 Dependence of fission probability upon excitation energy and nuclear type.—All of the characteristics of high-energy fission that have just been described would be predicted by Equation 1 if $\eta(A, Z|A', Z', U')$ were known for the fission process. Knowledge of the η function for fission would come, in turn (see discussion in Sect. 3.3), from an analysis of fission-evaporation cascades starting from the various nuclei A', Z', U' , if one knew $P(A, Z, U|A_i, Z_i, U_i)$, the probability per unit time that nucleus A_i, Z_i with excitation energy U_i fission into the product A, Z with excitation U . The subscript i refers to any nucleus formed during the fission-evaporation cascade, and the probability function P would have to be evaluated for all such nuclei. This probability function is the counterpart for the fission process of Equation 4 for particle evaporation. Unfortunately, no successful theoretical treatment of fission that would yield this function exists. This situation has prompted several investigators to solve the integral Equation 1 for the η function through the use of experimental values of $\sigma(A, Z)$ and theoretical estimates of $\sigma(A', Z', U'|A_0, Z_0, q, E)$, and then to unscramble the evaporation-fission cascade leading to η in order that they may evaluate $P(A, Z, U|A_i, Z_i, U_i)$. Clearly, this is a formidable task!

The task is somewhat more tractable if the incident particle is below 40 Mev so that compound-nucleus formation can be assumed and the fission-evaporation cascade is at most about three or four steps long. Investigation of this simpler situation has, indeed, proved useful [see, e.g. the survey by Vandebosch & Huizenga (208)] and has shown that the " P " function is, in the low-energy region, nearly independent of excitation energy once past the fission threshold. It has also been shown that P depends upon A_i and Z_i in a manner that is reminiscent of the dependence upon the fissionability parameter Z^2/A described by Bohr & Wheeler (25). The success at lower energies has encouraged a few investigators to look into the situation in the high-energy region where estimates of $\sigma(A', Z', U'|A_0, Z_0, q, E)$ are obtained from calculation (146, 147) and the evaporation-fission cascades may be many steps in length.

Using Monte Carlo calculations for the intranuclear (147) and evaporation (44) cascades, Pate (165) has successfully interpreted the data of Lav-

rukhhina & Krasavina (115) on the 450-Mev fission of U^{238} by assuming that "fission . . . begins to compete effectively with particle emission when the Z^2/A value is greater than about 36, in a fashion independent of energy." On the other hand, Shamov (189), analyzing the same data with the help of rough estimates of the intranuclear cascade, concludes that the fission probability is dependent upon the excitation energy. Batzel (10), in an unpublished analysis of the results of Lindner & Osborne (125) on the 340-Mev spallation of U^{238} , finds, in agreement with Pate (165), that the fission probability is not energy dependent.

A detailed Monte Carlo evaporation-fission calculation by Dostrovsky *et al.* (43), using an energy-dependent fission width derived from the formalism of Bohr & Wheeler (25), has had success in predicting total fission cross sections for several nuclides; but it remains to be seen how successful it is in treating other more detailed data from high-energy reactions with heavy nuclei.

The fact that different investigators have arrived at two very different conclusions about the energy dependence of P is perhaps not too surprising in light of the results of the knock-on cascade calculations. As may be seen from Figures 16 and 17 of (147): (a) For a given target nucleus, the average excitation energy \bar{U}' of a given product of the knock-on cascade A' , Z' is remarkably independent of the energy of the incident particle once an effective threshold has been passed; and (b) The average excitation energy of a given knock-on product increases with the number of knock-on particles emitted. From (a) one would conclude that the excitation energy spectrum of a primary cascade product $A'Z'$ is substantially independent of bombarding energy except in the immediate region of its effective threshold. From (b) one would conclude that the same nuclide $A'Z'$, formed during the evaporation-fission cascade from other primary knock-on products, may have an excitation-energy spectrum which varies slowly with the incident particle energy. From these conclusions it follows that the excitation-energy spectrum of a nuclide $A'Z'$ varies slowly, if at all, over most of the range of incident particle energies. Hence, unless it accidentally happens that the P function for a given nuclide is changing rapidly just in the small region of excitation energies where the excitation spectrum is also changing relatively rapidly, the energy variation of P will be obscured.

7. LIGHT-PARTICLE EMISSION

7.1 General.—Some of the earliest information about high-energy nuclear reactions came from the study of nuclear emulsions irradiated with cosmic rays (75, 195). In addition to protons, alpha particles and heavier particles such as lithium, beryllium, and boron fragments were observed. More recently, nuclear-emulsion studies with high-intensity beams of monoenergetic particles combined with improved techniques of charge and energy identification have brought forth a picture, which if still not clearly understood, is at least statistically more meaningful than the early cosmic-ray work (3a,

128, 156, 157). To summarize the results of emulsion work on the emission of light particles, the following may be stated: (a) The number of light particles with $Z \geq 2$ increases with increasing energy of the irradiating particle. (b) The yield of light particles is a descending function of the charge $-\sigma_{He} > \sigma_{Li} > \sigma_{Be} > \sigma_B$. (c) A large fraction of the light particles observed is emitted isotropically, and the energy spectra for the various particles are consistent with nuclear temperatures deduced from other work. (d) There are always a fair number of particles emitted with less energy than would be expected from a reasonable estimate of the Coulomb barrier. (e) There are usually some light fragments, emitted largely in the forward direction, which have energies higher than can be explained by any simple picture.

Statements (a), (b), and (c) indicate that the evaporation mechanism as described in Section 3.3, if extended to include heavier particles, will probably account for the formation cross section, energy distribution, and isotropy of most of the light fragments. As mentioned earlier, the radiochemically determined yields of Be^7 from copper, silver, and gold targets irradiated with 1- and 2-Bev protons have been at least partially explained by an evaporation process in a calculation by Hudis & Miller (87).

Explanations of observation (d) are all based upon redefinition of what is a "reasonable Coulomb barrier." Bagge (3) has suggested that at high excitations the effective Coulomb barrier may be reduced considerably by large-amplitude surface oscillations. Further, the possibility that the particles may be evaporated towards the end of a long evaporation chain when both the Coulomb barrier and nuclear temperature may be much lower than has been assumed must also be considered.

At the present time, the results mentioned in (e) cannot be explained by any reasonable evaporation mechanism, and new high-energy processes such as fragmentation (see Sect. 8) are believed responsible. The yields of light nuclides such as H^3 , He^3 , He^4 , and He^6 found in high-energy nuclear reactions should also be explained by the formalism of Section 3.3 if an evaporation mechanism is important in their formation. Rowland & Wolfgang (181) mention that their experimental yields of He^6 from various targets irradiated with 1- to 3-Bev protons seem to be in rough agreement with that expected from an evaporation mechanism. Schaeffer (186), however, has shown that the ratio of He^3/H^3 from iron irradiated with 0.18- to 3.0-Bev protons is always about a factor of two higher than calculated. Similarly, Curry, Libby & Wolfgang (40) find that their observed formation cross sections for tritium production at BeV energies are much lower than calculated.

Denisenko *et al.* (41) have investigated the interaction of 560- to 660-Mev protons with uranium nuclei by emulsion techniques and have observed triple-pronged events in which one of the partners is a light fragment ($Z \leq 11$). The cross section for this ternary-fission type reaction rises rapidly between 560 and 660 Mev but is only a small fraction of the binary fission cross section even at 660 Mev ($\sigma_{\text{binary}}/\sigma_{\text{ternary}} = 200$).

7.2. *Secondary reactions.*—Any particle or nuclide arising from the inter-

action of the irradiating particles with target nuclei may, of course, subsequently interact with other target nuclei. These secondary reactions may be investigated radiochemically if the resulting nuclides have a charge greater than the combined charge of target nucleus and bombarding particle. These investigations are experimentally quite difficult because of the low formation cross section of secondary products, and great care must be taken with target purity. In addition, the results of these studies are difficult to evaluate unambiguously, since the observed yield of a particular secondary reaction depends on three quantities, none of which is known precisely, if at all. These are the cross section for the formation of the secondary particle in the primary interaction, the energy distribution of these secondary particles, and the excitation function for the formation of the observed product from the interaction of the secondary particle with the target nuclei.

In order to explain the observed yields of iodine isotopes in the 335-Mev proton bombardment of tin, Marquez & Perlman (136) came to the conclusion that the secondary lithium fragments had surprisingly large formation cross sections and high kinetic energies (>80 – 100 Mev) and must, therefore, have been produced by some kind of "direct ejection" mechanism. However, more recent work by Kuznetsova *et al.* (111) on the same reaction indicates much lower cross sections for the iodine isotopes and, therefore, a much lower average kinetic energy for the secondary lithium fragments. In addition, the experimental work and extensive calculations on the secondary reactions initiated by 380-Mev protons in gold led Metzger & Miller (148) to conclusions similar to those of Kuznetsova *et al.* (111).

8. FRAGMENTATION

Finite yields of nuclides with masses between 18 and 32 have been observed from heavy targets such as Ta (158), Au (134), Th (117), and U (54) with incident proton energies as low as 340 Mev. The mass-yield curves from most of these experiments indicate that the yield of light nuclides cannot be completely accounted for by the fission process described in Section 6. Porile & Sugarman (175) came to the same conclusion for at least part of the yield of Cu^{67} resulting from the irradiation of Bi^{209} with 450-Mev protons. A similar lack of agreement between the general characteristics of the high-energy fission process and experiment was found by Kruger & Sugarman (106) for the fission yields of Ho^{165} irradiated with 450-Mev protons.

The failure of the combined fission-spallation mechanism to describe observed mass-yield curves becomes much more apparent as the energy of the irradiating particle is raised to the Bev region. The mass-yield curve for $\text{Pb} + 3$ -Bev protons shown in Figure 1 indicates the gross changes observed between 480 Mev and 3 Bev. A very similar pattern has been observed by Grover (73) in the 5.7-Bev proton irradiation of tantalum. A more detailed investigation of the yields of light nuclides shows that they are produced in interactions which have high thresholds (see Fig. 10), that the values of the

individual formation cross sections are of the order of millibarns for bombarding energies between 1 and 6 Bev, and that the yields along an isobaric chain tend to peak on, or a little to the neutron-excess side of, stability (30).

A violent mechanism of nuclear disintegration—fragmentation—has been hypothesized by Wolfgang *et al.* (215) to explain the above observations. It

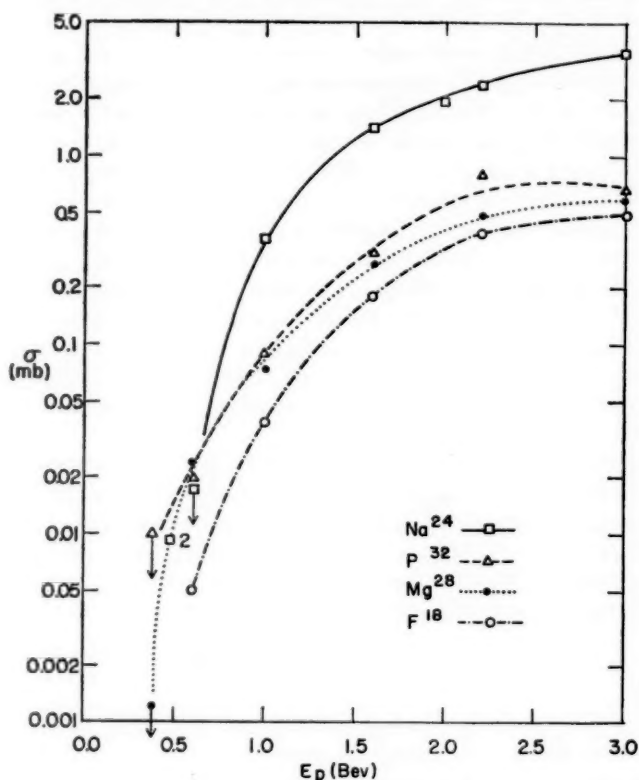


FIG. 10. Excitation functions for the production of F^{18} , Na^{24} , Mg^{28} , and P^{32} from lead targets irradiated with Bev protons, taken from Wolfgang *et al.* (215).

should be noted that the necessity or possibility of a new mechanism of nuclear disintegration at high bombarding energies had been suggested by earlier workers: Heisenberg (79); Marquez and Perlman (136); and Sørensen (195), among others. Fragmentation has been described as a rapid break-up of an excited nucleus which takes place in a time short compared to the time required for the equilibration of energy throughout the nucleus. The same energy-deposition mechanism which was introduced to explain the high yield of spallation products 15 to 20 mass numbers away from the target, namely meson production, scattering, and reabsorption, is believed re-

sponsible for fragmentation. Elementary pion-nucleon cross sections indicate that there is a very good probability that the meson-nucleon reactions mentioned—production, scattering, absorption—take place in a restricted zone of the nucleus, thus giving rise to local hot spots. It is suggested that these hot spots cause the break-up into fragments. The “shock-wave” approach of Glassgold *et al.* (60a) mentioned in Section 3.2 may provide an alternative mechanism.

The process would result in two fragments, one large and one small, both highly excited, with neutron-to-proton ratios similar to that of the struck nucleus. Particle evaporation would be expected to follow the fragmentation process. Since the light partner is quite neutron-rich, de-excitation would probably proceed by neutron emission toward the stability valley, followed by neutron and proton emission down the valley. Thus, peak yields of light fragmentation partners would indeed be expected to lie either on, or to the neutron-excess side of, stability. Because of the increased Coulomb barrier, de-excitation of the heavy fragment would probably go by neutron evaporation across the stability valley into the region of neutron-deficient nuclides. Thus the fragmentation mechanism may also account for a large fraction of the observed yields of neutron-deficient nuclides 15 to 75 mass numbers away from the target nucleus and may explain the atypical behavior of the 3-Bev mass-yield curve (Fig. 1) in the region of $A \approx 150$ to 200.

A determination of the excitation functions for the formation of Na^{24} and F^{18} from various targets between 1 and 6 Bev by Caretto, Hudis & Friedlander (30) suggests that fragmentation seems to be an important mechanism for the production of light nuclides from heavy targets, $Z > 70$. The rapid increase of fragmentation yields from Ta to U targets at a given energy, however, remains unexplained.

9. SUMMARY

Some idea of the progress in the field of high-energy nuclear reactions may be obtained by comparing the results discussed in this review with those ably covered by Templeton (205) six years ago. The type of calculation outlined in Section 3 appears to affirm the original picture given by Serber (187) and to be in agreement with experimental determinations of spallation yields in the few-hundred-Mev region. Although there are still many unanswered questions concerning details of the spallation mechanism, such as variation of isobaric yields with distance from the target and with type and energy of incident particles, and disagreement between calculated and experimental results for yields of simple reactions such as p , pn , etc., it seems safe to say that the model used appears to be in substantial agreement with a large body of data. The problem of high-energy fission, on the other hand, is still largely unsolved. It is known that as the energy of the incident particle is increased, lighter and lighter targets may be made to fission and that the preferred mode of scission is symmetric; but details about fission characteristics of specific nuclei excited to hundreds of Mev are lacking. Theoretical

approaches to the problem have not gone far in clearing up the picture since two very different fission mechanisms, energy-dependent and energy-independent, can both be made to agree with experimental results. More refined calculations and more experiments which yield specific data about the fissioning nuclides, recoil ranges for example, should help.

The situation as the energy of the incident particle is raised into the Bev region is more complicated and confused. This fact is not surprising when it is realized that the possibility now arises that on occasion the nucleus may momentarily have an excitation energy equal to its total binding energy. Under these circumstances it may seem a little foolish to think of a mechanism which provides a neatly defined sequence of events: knock-on cascade followed by an evaporation-fission cascade.

Where the mass-yield curve corresponds to spallation yields only, the same mechanism and calculations which were worked out for the lower-energy reactions, but now including meson processes, give good agreement with experimental results. The fission picture, though, is completely obscured by a lack of any obvious fission peak in the mass-yield curve resulting from Bev-proton irradiation of heavy targets. Instead, it is apparent from the experimental results that all mass numbers below that of the target may be produced with cross sections which are similar to each other within an order of magnitude.

The greatest change in the experimental mass-yield curve for heavy elements irradiated with Bev protons compared to that for a few-hundred-Mev particles is in the mass region $6 < A < 30$. At Bev energies, products in this mass region are formed with appreciable cross sections whereas they have extremely low cross sections or are completely absent in lower-energy irradiations. These products may be formed by a new mechanism different from knock-on, evaporation, and fission, in which, it has been suggested, mesons play an important role.

This confused state of nuclear reactions in the Bev region is neither surprising nor discouraging if it is remembered that this field is just six or seven years old. As a matter of fact, this review article comes at a time at which it bears much the same relationship to nuclear reactions at Bev energies as did Templeton's article to lower-energy reactions, and the similarity as to the amount and type of experimental results available is surprising. Information is now available about the gross features of the mass-yield curves for a variety of targets irradiated with Bev protons, but relatively few experiments have been performed to test specific points of proposed mechanisms. Undoubtedly many more refined and specific experiments, e.g. experiments that give information on the recoil properties of product nuclei, will be done in the following years to help clarify our picture of this field.

Finally, the rapid improvement in high-speed electronic computers has made it possible to do theoretical calculations of nuclear processes on a scale previously impossible. There will undoubtedly be many experiments performed in the next few years which will supply better input information for these calculations.

TABLE II
COMPILATION OF HIGH-ENERGY NUCLEAR REACTION STUDIES*

Target	Incident Particle and Energy (Mev)	Products	Laboratory	Comments	Reference
Be	p 335	Be ⁷	UCRL	also C, Al, Cu, Ag, Au	(136)
	p 330	H, He, Li, B	UCRL	σ 's and momenta	(6)
	p 40-160	Be ⁷	Harwell		(185)
	p 156	Be ⁷	Harwell		(178)
B	p 0-100	C ¹¹	Harvard	also C, Al, S	(83)
C	p 1000-3000	Be ⁷	BNL	also Al, Cu, Ag, Au	(4)
	p 2000, 3000	C ¹¹	BNL	abs. σ	(39)
	p 400-3000	C ¹¹	BNL		(216)
	p 1000-2850	He ⁴	BNL	also Al, Cu, Ag, Pb	(181)
	p 450, 2050	H ²	BNL and Chicago	also N, O, Mg, Al, Fe, Ni, Ag, Pb	(40)
	p 980	sp.	Birmingham	also N, O, F	(204)
	p 200-950	C ¹¹	Birmingham	abs. σ	(27)
	p 150-660	C ¹¹	USSR		(176)
	p 461	C ¹¹	Chicago	abs. σ	(180)
	p 105-350	C ¹¹	UCRL	abs. σ	(36)
	p th-340	C ¹¹	UCRL	abs. σ	(1)
	p 340	Li ⁸	UCRL	also N, Ne, Ar, Kr, Xe	(219)
	p 335	Be ⁷	UCRL	also Be, Al, Cu, Ag, Au	(36)
	p 330	H, He, Li, B	UCRL	σ 's and momenta	(6)
	p 32-156	Be ⁷	Harwell		(42)
	p 60-140	C ¹¹	UCRL		(221)
	p 0-100	C ¹¹	Harvard	also Al, B, S	(83)
	d 0-195	C ¹¹	UCRL		(206)
	d 85-190	C ¹¹	UCRL	abs. σ	(36)
	d 190	Li ⁸	UCRL	also N, Ne, Ar, Kr, Xe	(219)
	α 0-390	C ¹¹	UCRL		(206)
	α 380	C ¹¹	UCRL	abs. σ	(36)
	α th-380	C ¹¹	Livermore		(123)
	n 90	sp.	UCRL	cl. ch.	(101)
	n 90	sp.	UCRL	also C-S	(104)
N	p 400, 3000	p, pn	BNL	also F, Fe, Ni, Cu, Zn, Mo, Ta	(133)
	p 2200	H ²	BNL	also O	(52)
	p 450, 2050	H ²	BNL	also C, O, Mg	(40)
	p 980	sp.	Birmingham	also C, O, F	(204)
	p 340	Li ⁸	UCRL	also C, Ne, Ar, Kr, Xe	(219)
	d 190	Li ⁸	UCRL	also C, Ne, Ar, Kr, Xe	(219)
	n 90	sp.	UCRL	also C-S	(104)
	π^- 145	C ¹¹	Chicago	also O	(206b)
O	p 2200	H ²	BNL	also N	(52)
	p 450, 2050	H ²	BNL and Chicago	also C, N, Al, Mg, Fe, Ni, Ag, Pb	(40)
	p 980	sp.	Birmingham	also C, N, F	(204)
	p 420	F ¹⁸	Chicago	also F, Al, Cl, Cu, Ag, Au	(134)
	n 90	sp.	UCRL	also C-S	(104)
	π^- 145	C ¹¹	Chicago	also N	(206b)
F	p 280-3000	p, pn	BNL	also N, Fe, Ni, Cu, Zn	(133)
	p 980	sp.	Birmingham	also C, N, O	(204)
	p 420	F ¹⁸	Chicago	also Al, O, Cl, Cu, Ag, Au	(134)
Ne	p 340	Li ⁸	UCRL	also C, N, Ar, Kr, Xe	(219)
	d 190	Li ⁸	UCRL	also C, N, Ar, Kr, Xe	(219)
Na	p th-120	F ¹⁸ , Na ²³	Harvard	also Mg	(143)

* In column 1 target materials are arranged according to atomic number. In column 2, under incident particle and energy, excitation functions are indicated by the spread in the energy, i.e., 40-160 Mev; th stands for threshold. In column 3 the range of mass numbers of observed products is indicated where possible, i.e., $18 < A < 140$. Some abbreviations used are sp. (spallation products); fission (fission products); fission frag. (fission fragments), usually in emulsions; σ_f (fission cross section). In column 4 the university or laboratory where the work originated is specifically indicated where possible; otherwise country of origin is given. In column 5, under comments, additional target elements irradiated in the same work are listed, as well as techniques used other than radiochemistry. Some abbreviations used are abs. (absolute); cl. ch. (cloud chamber); emul. (emulsion); spec. (spectrometer); prods. (products); ang. dist. (angular distribution); det'n (determination).

Target	Incident Particle and Energy (Mev)	Products	Laboratory	Comments	Reference
Mg	p 450, 2050	H ³	BNL and Chicago	also C, N, O, Al, Fe, Ni, Ag, Pb	(40)
	p 300-660	H ³	USSR	also Pb, Bi, Au, Sn, Al, etc.	(110)
	p th-120	F ¹⁸ , Na ²⁴	Harvard	also Na	(143)
	p 70, 100	Na ²²	Harvard		(144)
	d 0-190	F ¹⁸ , Na ²² , Na ²⁴	UCRL		(9)
	n 90	sp.	UCRL	also C-S	(104)
Al	p 1000-6000	F ¹⁸ , Na ²⁴	BNL and UCRL	also Cu, Ag, Ta, Pb, U, Au	(30)
	p 1000-3000	Be ⁷	BNL	also C, Cu, Ag, Au	(4)
	p 400-3000	sp.	BNL		(57)
	p 1000-2850	He ⁴	BNL	also C, Cu, Ag, Pb	(181)
	p 450, 2050	H ³	BNL and Chicago	also C, N, O, Mg, Fe, Ni, Ag, Pb	(40)
	p 120-660	H ³	USSR	also Pb, Bi, Sn, Au, Mg, etc.	(110)
	p 150-660	Na ^{22,24}	USSR		(176)
	p 420	F ¹⁸	Chicago	also F, C, Cu, Ag, Au, O	(134)
	p 105-350	Na ²⁴	UCRL	abs. σ	(36)
	p 32-350	Na ²⁴	Livermore		(82)
	p 30-350	Na ²⁴	Livermore	abs. σ	(198)
	p 335	Be ⁷	UCRL	also Be, C	(136)
	p 0-100	F ¹⁸ , Na ^{22,24}	Harvard	also C, B, S	(83)
	d th-190	Na ²⁴	Livermore	abs. σ	(11)
	d 85-190	Na ²⁴	UCRL	abs. σ	(36)
	d 30-190	Na ²²	Livermore		(179)
	α 380	Na ²⁴	UCRL	abs. σ	(36)
	α th-380	Na ²⁴	Livermore		(124)
	n ~370	sp.	Chicago	also Cu	(135)
	n 90	sp.	UCRL	also C-S	(104)
S	p 0-100	C ¹¹	Harvard	also C, Al, B	(83)
	n 90	sp.	UCRL	also C-S	(104)
Cl	p 45-430	Na ²⁴ , Mg ²⁴ , P ³² , S ³⁶	Carnegie Tech.		(98)
	p 420	F ¹⁸	Chicago	also O, F, Al, Cu, Ag, Au	(134)
Ar	p 340	Li ⁸	UCRL	also C, N, Ne, Kr, Xe	(219)
	d 190	Li ⁸	UCRL	also C, N, Ne, Kr, Xe	(219)
Sc	p th-100	Sc ^{44,46m}	Harvard	also Br, Co	(142)
V	p 60-240	28 < A < 49	Rochester		(77)
	p 170	24 < A < 49	Uppsala	also As, Co, Mn	(182, 183)
	d 190	Mn ^{52,56}	UCRL	also Cr-Sr	(26)
Mn	p 170	31 < A < 48	Uppsala	also As, Co, V	(182, 183)
	d 190	Mn ^{52,56}	UCRL	also Cr-Sr	(26)
Fe	p 160-6200	H ³ , Ar ³⁷	BNL, Harvard		(53)
	p 400, 3000	p, p ⁿ	BNL	also N, F, Ni, Cu, Zn, Mo, Ta	(133)
	p 160, 430, 3000	He ³ , He ⁴ , Ar ³⁶ , Ar ³⁸	BNL		(186)
	p 220	H ³	BNL		(51)
	p 450, 2050	H ³	BNL and Chicago	also C, N, O, Mg, Al, Ni, Ag, Pb	(40)
	p 340	H ³ , He ³ , He ⁴	Durham, and Oxford		(137)
	p 340	22 < A < 56	UCRL		(184)
	p 50-177	H ³	CERN		(62)
	d 190	Mn ^{52,56}	UCRL	also Cr-Sr	(26)
Co	p 370	11 < A < 58	Columbia		(15)
	p 370	Fe ^{53,55}	Columbia and BNL	also Cu	(150)
	p 60-240	33 < A < 58	Rochester		(211)
	p 170	31 < A < 57	Uppsala	also V, Mn, As	(182, 183)
	p th-100	Co ^{57,58m}	Harvard	also Br, Sc	(142)
	p 0-100	48 < A < 58	Harvard		(191)
	d 190	Mn ^{52,56}	UCRL	also Cr-Sr	(26)
Ni	p 400, 3000	p, p ⁿ	BNL	also N, F, Fe, Cu, Zn, Mo, Ta	(133)
	p 450, 2050	H ³	BNL and Chicago	also C, N, O, Al, Mg, Fe, Ag, Pb	(40)

Target	Incident Particle and Energy (Mev)	Products	Laboratory	Comments	Reference
Ni	<i>d</i> 190	Mn ^{52,56}	UCRL	also Cr-Sr	(26)
Cu	<i>p</i> 1000-6000	F ¹⁸ , Na ²⁴	BNL and UCRL	also Al, Ag, Ta, Pb, Au, U	(30)
	<i>p</i> 5700	3 < <i>A</i> < 66	UCRL	also <i>p</i> , <i>pn</i> and <i>p,pπ</i> ⁺ study	(7)
	<i>p</i> 1000-3000	Be ⁷	BNL	also Al, C, Ag, Au	(4)
	<i>p</i> 280-3000	<i>p, pn</i>	BNL	also N, F, Fe, Ni, Zn, Mo, Ta	(133)
	<i>p</i> 1000-2850	He ⁶	BNL	also C, Al, Ag, Pb	(181)
	<i>p</i> 2200	7 < <i>A</i> < 64	BNL		(58)
	<i>p</i> 2200	Ga ^{66,67,68} , Ge ^{66,67,68} , As ^{71,72}	BNL		(207)
	<i>p</i> 980	18 < <i>A</i> < 64	Birmingham		(178a)
	<i>p</i> 660	H ³	USSR	also Pb, Bi, Sn, Mg, Al, etc	(110)
	<i>p</i> 120-660	Na ²⁴ , P ³²	USSR	also La, Au, Th	(117)
	<i>p</i> 660	32 < <i>A</i> < 64	USSR	also La, Bi	(155)
	<i>p</i> 480	11 < <i>A</i> < 68	USSR	also Bi	(210)
	<i>p</i> 420	F ¹⁸	Chicago	also O, F, Al, Cl	(134)
	<i>p</i> 100-440	Ni ⁵⁸	Chicago		(60)
	<i>p</i> 370	Cu, F ¹⁸ , Na ²⁴ , K ⁴²	Columbia		(72)
	<i>p</i> 370	Fe ^{53,55,59}	Columbia and BNL	also Co	(150)
	<i>p</i> 340	22 < <i>A</i> < 65	UCRL	measured recoil ranges of spallation products	(13)
	<i>p</i> 340	22 < <i>A</i> < 65	UCRL		(12)
	<i>p</i> 335	Be ⁷	UCRL	also Be, C, Al, Ag, Au	(136)
	<i>p</i> th-100	Cu ^{61,62,64} , Zn ^{62,63}	Harvard		(140)
	<i>p</i> 90	48 < <i>A</i> < 64	Livermore		(222)
	<i>d</i> 280	11 < <i>A</i> < 68	USSR	also Bi	(210)
	<i>d</i> 0-190	52 < <i>A</i> < 65	UCRL		(8)
	<i>d</i> 190	22 < <i>A</i> < 65	UCRL		(12)
	<i>d</i> 190	Mn ^{52,56}	UCRL	also Cr-Sr	(26)
	<i>d</i> 190	48 < <i>A</i> < 64	Livermore		(222)
	<i>α</i> 190, 380	22 < <i>A</i> < 65	UCRL		(12)
	<i>n</i> ~370	45 < <i>A</i> < 65	Chicago	also Al	(135)
	<i>n</i> 90	48 < <i>A</i> < 64	Livermore		(222)
Zn	<i>p</i> 400, 3000	<i>p, pn</i>	BNL	also N, F, Cu, Ni, Fe, Mo, Ta	(133)
	<i>p</i> 660	H ³	USSR	also Pb, Bi, Sn, Al, etc.	(110)
	<i>p</i> 340	24 < <i>A</i> < 67	UCRL		(218)
	<i>d</i> 190	Mn ^{52,56}	UCRL	also Cr-Sr	(26)
	<i>π</i> ⁻ 122	Cu ⁵⁸⁻⁶⁷	Chicago		(206a)
As	<i>p</i> 380	42 < <i>A</i> < 75	Columbia		(38)
	<i>p</i> 49, 103, 170	56 < <i>A</i> < 74	Uppsala	also V, Mn, Co	(182, 183)
	<i>d</i> 190	49 < <i>A</i> < 75	UCRL		(85)
	<i>d</i> 190	51 < <i>A</i> < 75	UCRL		(86)
	<i>d</i> 190	Mn ^{52,56}	UCRL	also Cr-Sr	(26)
Br	<i>p</i> th-100	Br ^{80,80m}	Harvard	also Co, Sc	(142)
	<i>d</i> 190	Mn ^{52,56}	UCRL	also Cr-Sr	(26)
	<i>π</i> ⁻ 122	68 < <i>A</i> < 78	Chicago		(203)
Kr	<i>p</i> 340	Li ⁸	UCRL	also C, N, Ne, Ar, Xe	(219)
	<i>d</i> 190	Li ⁸	UCRL	also C, N, Ne, Ar, Xe	(219)
Y	<i>p</i> 240	68 < <i>A</i> < 89	Rochester		(31)
Mo	<i>p</i> 280-3000	<i>p, pn</i>	BNL	also N, F, Fe, Ni, Cu, Zn, Ta	(133)
AgBr	<i>p</i> 6200	Li, Be	Japan		(156)
	<i>p</i> 6200	Z > 3	Japan		(157)
	<i>p</i> 5700	Li ⁸	Birmingham		(68)
	<i>p</i> 950	Li ⁸	Birmingham		(154)
	<i>p</i> 560-660	fiss. frag.	USSR	also U	(41)
	<i>p</i> 350-660	Z > 4	USSR		(128, 129)
	<i>n</i> 395	Z > 2	USSR		(193)
	cosmic rays	Li ⁸	England		(84)
	cosmic rays	3 < Z < 10	London		(171)
	cosmic rays	He, Li	Bristol		(195)
Ag	<i>p</i> 1000-6000	F ¹⁸ , Na ²⁴	BNL and UCRL	also Al, Cu, Ta, Au, Pb, U	(30)
	<i>p</i> 1000-3000	Be ⁷	BNL	also C, Al, Cu, Au	(4)

Target	Incident Particle and Energy (Mev)	Products	Laboratory	Comments	Reference
Ag	p 1000-2850	He^4	BNL	also C, Al, Cu, Pb	(181)
	p 450, 2050	H^2	BNL and Chicago	also C, N, O, Al, Mg, Fe, Ni, Pb	(40)
	p 660	H^3	USSR	also Pb, Bi, Sn, Mg, Al, etc.	(110)
	p 480	$11 < A < 106$	USSR		(107)
	p 420	F^{18}	Chicago		(134)
	p 388	$43 < A < 73$	Columbia	also O, F, Al, Cl, Au, Cu	(71)
	p 340	$7 < A < 107$	UCRL		(105)
	p 335	Be^7	UCRL	also Be, C, Al	(136)
	d 280	$11 < A < 106$	USSR		(107)
	α 550	$11 < A < 106$	USSR		(107)
	π^-	Pd, Rh, Ru	Chicago		(64)
In	p 2000-6000	$In^{109-115}, Cd^{107-115},$ Be^7	UCRL		(159)
Sn	p 170-660	$I^{120-126}, Te^{118}$	USSR	secondary reactions	(111)
	p 660	H^3	USSR	also Pb, Bi, Mg, Al, etc.	(110)
	p 335	$I^{120-126}$	UCRL	secondary reactions	(136)
Sb	p 660	H^3	USSR	also Al, Pb, Bi, Mg, Au, etc	(110)
	d 50-190	$87 < A < 121$	UCRL		(127)
	α 380	$87 < A < 121$	UCRL		(127)
I	p 250-6200	$I^{120-126}$	UCRL		(113)
	p 100-660	$I^{120-126}$	USSR		(112)
	p 240	$100 < A < 126$	Rochester		(46)
	α 250-720	$I^{120-126}$	UCRL		(113)
	π^- 122	$107 < A < 127$	Chicago		(213)
	μ^-	$Te^{118-127}, Sb^{122-124}$	Chicago		(214)
Xe	p 340	Li^8	UCRL	also C, N, Ne, Ar, Kr	(219)
	d 190	Li^8	UCRL	also C, N, Ne, Ar, Kr	(219)
Cs	p 240	$95 < A < 132$	Rochester		(49)
	p 60-240	$117 < A < 133$	Rochester		(50)
La	p 120-660	Na^{24}, P^{32}	USSR	also Cu, Au, Th	(117)
	p 660	$32 < A < 95$	USSR		(116)
	p 480	$106 < A < 134$	USSR	also Cu, Bi	(155)
Ce	p 400-3000	Ce^{141}, La^{141}	BNL		(29)
Ho	p 450	$59 < A < 115$	Chicago	also Th, Bi, Re, Au, Ta	(106)
Ta	p 1000-6000	Na^{24}	BNL, UCRL	also Al, Cu, Ag, Au, Pb, U	(30)
	p 5700	$7 < A < 181$	UCRL		(73)
	p 280-3000	p, pn	BNL	also N, F, Fe, Ni, Zn, Cu, Mo	(133)
	p 660	$165 < A < 173$	USSR		(70)
	p 450	$59 < A < 115$	Chicago	also Bi, Au, Th, Re, Ho	(106)
	p 450	$47 < A < 129$	Chicago	recoils, also Bi	(174)
	p 340	$24 < A < 178$	UCRL		(158)
	α 400	$72 < A < 133$	UCRL	also Bi, Pb, Ti, Pt	(172)
					(172)
W	p 460, 660	fiss. frag.	USSR	also U, Bi	(169, 170)
	p 660	fiss. frag.	USSR	emul., also U, Bi	(188, 190)
	d 280	$24 < A < 185$	USSR		(109)
	n 380	σf	USSR	also Pt, Au, Ti, Pb, Bi, Th, U	(65, 66)
	π^-	fiss. frag.	USSR	emul., also U, Bi	(169, 170)
	π^- slow	fiss. frag.	USSR	emul., also U, Pb	(168)
Re	p 450	$59 < A < 115$	Chicago	also Th, Bi, Au, Ta, Ho	(106)
Pt	α 400	$72 < A < 133$	UCRL	also Bi, Pb, Ti, Ta	(172)
	n 380	σf	USSR	also W, Au, Ti, Pb, Bi, Th, U	(65, 66)
	n 84	σf	UCRL	also Au-Bi, Th	(102)
Au	p 1000-6000	F^{18}, Na^{24}	BNL, UCRL	also Al, Cu, Ag, Ta, Pb, U	(30)
	p 1000-3000	Be^7	BNL	also C, Al, Cu, Ag	(4)
	p 3000	Cs, Ba, Rb	BNL	mass spec.	(69)
	p 660	H^3	USSR	also Pb, Bi, Sn, Mg, Al, etc.	(110)
	p 120-660	Na^{24}, P^{32}	USSR	also Cu, La, Th	(117)
	p 450	$59 < A < 115$	Chicago	also Th, Bi, Re, Ta, Ho	(106)
	p 420	F^{18}	Chicago	also O, F, Al, Cl, Cu, Ag	(134)
					(134)

Target	Incident Particle and Energy (Mev)	Products	Laboratory	Comments	Reference
Au	p 380	$Tl^{195-202}, Pb^{188-202}$	Columbia		(148)
	p 100-340	σf	UCRL	also U, Th, Bi	(197)
	p 335	Be^7	UCRL	also Be, C, Al, Cu, Ag	(136)
	n 380	σf	USSR	also W, Pt, Ti, Pb, Bi, Th, U	(65, 66)
	n 84	σf	UCRL	also Pt-Bi, Th	(102)
Hg	π^- 122	$78 < A < 139$	Chicago		(202)
Tl	d 200	$72 < A < 133$	UCRL	also Bi, Pb, Pt, Ta	(172)
	α 400	$72 < A < 133$	UCRL	also Bi, Pb, Pt, Ta	(172)
	n 380	σf	USSR	also W, Pt, Au, Pb, Bi, Th, U	(65, 66)
	n 84	σf	UCRL	also Pt-Bi, Th	(102)
Pb	p 1000-6000	Fr^{18}, Na^{34}	BNL, UCRL	also Al, Cu, Ag, Ta, Au, U	(30)
	p 600-3000	$18 < A < 140$	BNL		(215)
	p 1000-2850	He^4	BNL	also C, Al, Cu, Ag	(181)
	p 450, 2050	H^2	BNL, Chicago	also C, N, O, Mg, Al, Fe, Ni, Ag	(40)
	p 120-660	H^3	USSR	also Bi, Au, Sn, Mg, Al, etc.	(110)
	p 480	$At^{208-210, 211}$	USSR	secondary reactions, also Bi	(108)
	p 12-85	(p, pxn) prods.	McGill	also Bi	(14)
	d 200	$72 < A < 133$	UCRL	also Bi, Ti, Pt, Ta	(172)
	d 190	$45 < A < 149$	UCRL	also Bi	(63)
	α 400	$72 < A < 133$	UCRL	also Bi, Ti, Pt, Ta	(172)
	n 380	σf	USSR	also W, Pt, Au, Ti, Bi, U	(65, 66)
	n 100	$72 < A < 133$	UCRL	also Bi, Ti, Pt, Ta	(172)
	n 84	σf	UCRL	also Pt-Bi, Th	(102)
	π^- slow	fiss. frag.	USSR	emul., also W, U	(168)
Bi	p 50-2200	$Sr^{91}, Ba^{129}, Ba^{130m}$	Chicago and BNL	recoils	(200)
	p 220	$66 < A < 203$	BNL	recoils	(201)
	p 660	$134 < A < 209$	USSR		(100)
	p 300-660	H^1	USSR	also Pb, Al, Sn, Mg, Au, etc	(110)
	p 480, 660	$59 < A < 208$	USSR	also Cu, La	(155)
	p 460, 660	fiss. frag.	USSR	emul., also W, U	(169, 170)
	p 660	fiss. frag.	USSR	emul., also W, U	(188, 190)
	p 480	$At^{208-210, 211}$	USSR		(100)
	p 480	$24 < A < 209$	USSR	also U, Th	(209)
	p 480	$176 < A < 206$	USSR	also Cu	(210)
	p 375, 450	$198 < A < 209$	Chicago		(18)
	p 75-450	$61 < A < 131$	Chicago		(96)
	p 450	$59 < A < 115$	Chicago	also Th, Au, Re, Ta, Ho	(106)
	p 450	$56 < A < 133$	Chicago	recoils, also Ta	(174)
	p 450	$Cd^{115-116m}$	Chicago	recoils	(173)
	p 450	$Ga^{72-73}, Sr^{91-92}, Cd^{115-117}$	Chicago	recoils	(217)
	p 340	$45 < A < 133$	UCRL		(23)
	p 380	$186 < A < 207$	Columbia		(88)
	p 100-340	σf	UCRL	also U, Th, Au	(197)
	p 12-85	(p, xn) prods.	McGill	also Pb	(14)
	d 50-200	$72 < A < 133$	UCRL	also Pb, Ti, Pt, Ta	(172)
	d 190	$45 < A < 149$	UCRL	also Pb	(63)
	α 400	$72 < A < 133$	UCRL	also Pb, Ti, Pt, Ta	(172)
	n 120, 380	σf	USSR	also W, Pt, Ag, Ti, Pb, Bi, U	(65, 66)
	n 100	$72 < A < 133$	UCRL	also Pb, Ti, Pt, Ta	(172)
	n 84	σf	UCRL	also Pt-Pb, Th	(102)
	π^-	fiss. frag.	USSR	emul., also W, U	(169, 170)
Th	p 120-660	Na^{34}, Pn	USSR	also Cu, La, Au	(117)
	p 480	$24 < A < 210$	USSR	also U, Bi	(209)
	p 450	$59 < A < 115$	Chicago	also Bi, Au, Re, Ta, Ho	(106)
	p th-348	$Pa^{237-239}$	UCRL	also U	(145)
	p 100-340	$210 < A < 232$	Livermore	also U	(125)
	p 50-340	$66 < A < 139$	Livermore	also U	(126)
	p 100-340	σf	UCRL	also U, Bi, Au	(197)
	p 160	$At^{210-211}$	Orsay	secondary reactions, also Pb	(121)
	p 45, 80, 155	$Sr^{91-92}, Ag^{113-115}, Ba^{139}$	Harvard	ang. dist., also U	(141)
	p 8-87	$U^{130-132}, Te^{132}$	McGill		(166)
	d th-194	$Pa^{237-239}$	UCRL	also U	(145)
	d 0-190	Pa^{233}, Pa^{239}	Livermore	also $(d, 2n)$ and $(d, 4n)$ from U^{238}	(37)
	d 50-190	$66 < A < 139$	Livermore	also U	(126)
	α th-388	$Pa^{237-239}, U^{239-238}$	UCRL	also U	(145)
	α 50-380	$66 < A < 139$	Livermore	also U	(126)

Target	Incident Particle and Energy (Mev)	Products	Laboratory	Comments	Reference
Th	n 380	σf	USSR	also W, Pt, Au, Ti, Pb, Bi, U	(65, 66)
	n 84	σf	UCRL	also Pt-Bi	(102)
U	p 6200	Cu ⁶⁷ , Mo ⁹⁹ , Ag ¹¹¹	UCRL	σ 's and recoil ranges	(5)
	p 1000-6000	F ¹⁹ , Na ²⁴	BNL, UCRL	also Al, Cu, Ag, Ta, Au, Pb	(30)
	p 5700	$7 < A < 66$	UCRL		(32)
	p 5700	$52 < A < 212$	UCRL		(192)
	p 560-660	fiss. frag.	USSR	emul.	(41)
	p 140-660	σf	USSR	emul.	(91, 94)
	p 660	fiss. frag.	USSR	emul., ang. dist.	(130, 131)
	p 660	fiss. frag.	USSR	emul., ang. dist.	(163, 164)
	p 630	$134 < A < 177$	USSR		(167)
	p 460, 660	fiss. frag.	USSR	emul., also W, Bi	(169, 170)
	p 660	fiss. frag.	USSR	emul., also Bi, W	(188, 190)
	p 480	$24 < A < 210$	USSR	also Th, Bi	(209)
	p 460	σf	USSR	emul.	(93)
	p 450	fiss. frag.	USSR	emul.	(162)
	p th-348	Pa ^{237, 239}	UCRL	also Th	(145)
	p 340	$24 < A < 236$	UCRL		(54)
	p 70-340	$89 < A < 140$	Livermore		(80)
	p 100-340	$223 < A < 238$	Livermore	also Th	(125)
	p 50-340	$66 < A < 139$	Livermore	also Th	(126)
	p 100-340	σf	UCRL	also Th, Bi, Au	(197)
	p 10-340	$90 < A < 157$	Livermore		(199)
	p 335	$89 < A < 140$	UCRL	range det'n.	(45)
	p 170	$65 < A < 140$, Th ^{237, 238}	CERN		(103)
	p 45, 80, 155	Sr ^{91, 92} , Ag ¹¹³⁻¹¹⁵ , Ba ¹³⁹	Harvard	ang. dist., also Th	(141)
d	0-190	Np ²³⁸ , Np ²³⁹	Livermore	also (d, 2n) and (d, 4n) on Th ²³²	(37)
d	19-190	$89 < A < 140$	Livermore		(80)
d	20-190	$89 < A < 140$	Livermore		(81)
d	50-190	$66 < A < 139$	Livermore	also Th	(126)
d	20-190	$90 < A < 157$	Livermore		(199)
α	50-380	$89 < A < 140$	Livermore		(80)
α	50-380	$66 < A < 139$	Livermore	also Th	(126)
α	380	$55 < A < 239$	UCRL		(161)
n	44, 180, 460	fiss. frag.	USSR	emul.	(16, 17)
n	120, 380	σf	USSR	also W, Th, Pt, Au, Ti, Pb, Bi	(65, 66)
π^+	300	fiss. frag.	USSR	emul.	(41)
π^+	280	σf , light frag. $Z \geq 4$	USSR	emul.	(92)
π^-		σf	UCRL	emul.	(97)
π^- slow		fiss. frag.	USSR	emul.	(16, 17)
π^-		σf	USSR	emul.	(132)
π^-		fiss. frag.	USSR	emul., also W, Bi	(169, 170)
π^- slow		fiss. frag.	USSR	emul., also Pb, W	(168)
μ^-		σf	UCRL	emul.	(97)

LITERATURE CITED

1. Aamodt, R. L., Peterson, V., and Phillips, R., *U. S. Atomic Energy Commission Document, UCRL 1400* (1951)
2. Ashkin, J., and Wick, G. C., *Phys. Rev.*, **85**, 686 (1952)
3. Bagge, E., *Ann. phys.*, **33**, 389 (1938)
- 3a. Bailey, L. E., *U. S. Atomic Energy Commission Document, UCRL 3394* (1956)
4. Baker, E., Friedlander, G., and Hudis, J., *Phys. Rev.*, **112**, 1319 (1958)
5. Baltzinger, C., *U. S. Atomic Energy Commission Document, UCRL 8430* (1958)
6. Barkas, W. H., and Tyren, H., *U. S. Atomic Energy Commission Document, UCRL 1914* (Berkeley, Calif., 1952)
7. Barr, D. W., *U. S. Atomic Energy Commission Document, UCRL 3793* (Berkeley, Calif., 1957)
8. Bartell, F. O., Helmholz, A. C., Softky, S. D., and Stewart, D. B., *Phys. Rev.*, **80**, 1006, (1950)
9. Bartell, F. O., and Softky, S. D., *Phys. Rev.*, **84**, 463 (1951)
10. Batzel, R. E., *U. S. Atomic Energy Commission Document, UCRL 4303* (1954)
11. Batzel, R. E., Crane, W. W. T., and O'Kelley, G. D., *Phys. Rev.*, **91**, 939 (1953)
12. Batzel, R. E., Miller, D. R., and Seaborg, G. T., *Phys. Rev.*, **84**, 671 (1951)
13. Batzel, R. E., and Seaborg, G. T., *Phys. Rev.*, **79**, 528 (1950)
14. Bell, R. E., and Skarsgard, H. M., *Can. J. Phys.*, **34**, 745 (1956)
15. Belmont, E., and Miller, J. M., *Phys. Rev.*, **95**, 1554 (1954)
16. Belovitskii, G. E., Romanova, T. A., Sukhov, L. V., and Frank, I. M., *Zhur. Eksptl. i Teoret. Fiz.*, **28**, 729 (1955); *Atomic Energy Research Estab. Lib. Transl.*, 612 (1955)
17. Belovitskii, G. E., Romanova, T. A., Sukhov, L. V., and Frank, I. M., *Soviet Phys. JETP*, **2**, 493 (1956)
18. Bennett, W. E., *Phys. Rev.*, **94**, 997 (1954)
19. Bernardini, G., Booth, E. T., and Lindenbaum, S. J., *Phys. Rev.*, **85**, 526 (1952)
20. Bernardini, G., Booth, E. T., and Lindenbaum, S. J., *Phys. Rev.*, **88**, 1017 (1952)
21. Bernardini, G., Booth, E. T., and Lindenbaum, S. J., *Phys. Rev.*, **85**, 826 (1952)
22. Bethe, H. A., *Revs. Modern Phys.*, **9**, 69 (1937)
23. Biller, W. F., *U. S. Atomic Energy Commission Document, UCRL 2067* (Berkeley, Calif., 1953)
24. Bohr, N., *Science*, **86**, 161 (1937)
25. Bohr, N., and Wheeler, J. A., *Phys. Rev.*, **56**, 426 (1939)
26. Bonner, N. A., and Orr, W. C., *Phys. Rev.*, **76**, 140 (1949)
27. Burcham, W. E., Symonds, J. L., and Young, J. D., *Proc. Phys. Soc. (London)*, **A68**, 1001 (1955)
28. Cameron, A. G. W., *Can. J. Phys.*, **36**, 1040 (1958)
29. Caretto, A. A., and Friedlander, G., *Phys. Rev.*, **110**, 1169 (1958)
30. Caretto, A. A., Hudis, J., and Friedlander, G., *Phys. Rev.*, **110**, 1130 (1958)
31. Caretto, A. A., and Wiig, E. O., *Phys. Rev.*, **103**, 236 (1956)
32. Carnahan, C. L., *U. S. Atomic Energy Commission Document, UCRL 8020* (Berkeley, Calif., 1957)
33. Chew, G. F., and Goldberger, M. L., *Phys. Rev.*, **87**, 778 (1952)
34. Chew, G. F., and Wick, G. C., *Phys. Rev.*, **85**, 636 (1952)
35. Combe, J., *Nuovo cimento*, **3**, 5182 (1956)
36. Crandall, W. E., Millburn, G. P., Pyle, R. V., and Birnbaum, W., *Phys. Rev.*, **101**, 329 (1956)

37. Crane, W. W. T., and Iddings, G. M., *U. S. Atomic Energy Commission Document, MTA48* (Livermore, Calif., 1953)
38. Cumming, J. B., *U. S. Atomic Energy Commission Document, N.Y.O. 6141* (1954)
39. Cumming, J. B., Friedlander, G., and Swartz, C. E., *Phys. Rev.*, **111**, 1386 (1958)
40. Currie, L. A., Libby, W. F., and Wolfgang, R. L., *Phys. Rev.*, **101**, 1557 (1956)
41. Denisenko, G. F., Ivanova, N. S., Novikova, N. R., Perfilov, N. A., Prokofieva, E. I., and Shamov, V. P., *Phys. Rev.*, **109**, 1779 (1958)
42. Dickson, J. M., and Randle, T. C., *Proc. Phys. Soc. (London)*, **A64**, 902 (1951)
- 42a. Dostrovsky, I., Fraenkel, Z., and Friedlander, G. (Submitted to *Phys. Rev.*)
43. Dostrovsky, I., Fraenkel, Z., and Rabinowitz, P., *Proc. Intern. Conf. Peaceful Uses Atomic Energy, IInd Conf. Geneva, 1958*, Paper 1615 (1959)
44. Dostrovsky, I., Rabinowitz, P., and Bivins, R., *Phys. Rev.*, **111**, 1659 (1958)
45. Douthett, E. M., and Templeton, D. H., *Phys. Rev.*, **94**, 128 (1954)
46. Dropsky, B., *Nuclear Reactions of Iodine with 240-mev Protons* (Doctoral thesis, Univ. of Rochester, Rochester, N. Y., 1953)
47. Fernbach, S., Serber, R., and Taylor, T. B., *Phys. Rev.*, **75**, 1352 (1946)
48. Feshbach, H., *Ann. Rev. Nuclear Sci.*, **8**, 49 (1958)
49. Fink, R. W., and Wiig, E. O., *Phys. Rev.*, **94**, 1357 (1954)
50. Fink, R. W., and Wiig, E. O., *Phys. Rev.*, **96**, 185 (1954)
51. Fireman, E. L., *Phys. Rev.*, **97**, 1303 (1955)
52. Fireman, E. L., and Rowland, F. S., *Phys. Rev.*, **97**, 780 (1955)
53. Fireman, E. L., and Zähringer, J., *Phys. Rev.*, **107**, 1695 (1957)
54. Folger, R. L., Stevenson, P. C., and Seaborg, G. T., *Phys. Rev.*, **98**, 107 (1955)
55. Frank, R. M., Gammel, J. L., and Watson, K. M., *Phys. Rev.*, **101**, 891 (1956)
56. Friedlander, G., *Hearings on the Physical Research Program before the Subcommittee on Research and Development of the Joint Committee on Atomic Energy, Eighty-Fifth Congress, Second Session*, 61 (1958)
57. Friedlander, G., Hudis, J., and Wolfgang, R. L., *Phys. Rev.*, **99**, 263 (1955)
58. Friedlander, G., Miller, J. M., Wolfgang, R. L., Hudis, J., and Baker, E., *Phys. Rev.*, **94**, 727 (1954)
59. Fujimoto, Y., and Yamaguchi, Y., *Progr. Theoret. Phys. (Kyoto)*, **4**, 468 (1950); **5**, 76 (1950); **5**, 787 (1950)
60. Fung, S., and Turkevich, A., *Phys. Rev.*, **95**, 176 (1954)
- 60a. Glassgold, A. E., Heckrotte, W., and Watson, K. M., *Ann. Phys.*, **6**, 1 (1959)
61. Glendenin, L., Coryell, C. D., and Edwards, R. R., *Phys. Rev.*, **75**, 337 (1949)
62. Goebel, K., *European Organization for Nuclear Research Report, CERN 58-2* (Geneva) (1958)
63. Goeckermann, R. H., and Perlman, I., *Phys. Rev.*, **76**, 628 (1949)
64. Goishi, W., and Libby, W. F., *Phys. Rev.*, **104**, 1717 (1956)
65. Gol'danskiĭ, V. I., Pen'kina, V. S., and Tarumov, E. Z., *Soviet Phys. JETP*, **2**, 677 (1956)
66. Gol'danskiĭ, V. I., Tarumov, E. Z., and Pen'kina, V. S., *Doklady Akad. Nauk S.S.S.R.*, **101**, 1027 (1955)
67. Goldberger, M. L., *Phys. Rev.*, **74**, 1268 (1948)
68. Goldsack, S. J., Lock, W. O., and Munir, B. A., *Phil. Mag.*, **2**, 149 (1957)
69. Gordon, B. M., and Friedman, L., *Phys. Rev.*, **108**, 1053 (1957)
70. Gorodinskiĭ, G. M., Murin, A. N., Prokovskii, V. N., and Preobrazhenskii, B. K., *Izvest. Akad. Nauk S.S.S.R. Ser. Fiz.*, **21**, 1004 (1957)
71. Greenberg, D. H., *U. S. Atomic Energy Commission Document, NYO 6140* (1954)

72. Greenberg, D. H., and Miller, J. M., *Phys. Rev.*, **84**, 845 (1951)
73. Grover, J. R., *U. S. Atomic Energy Commission Document, UCRL 3932* (1957)
74. Halpern, I., *Phys. Rev.*, **97**, 1327 (1955)
- 74a. Halpern, I., *Ann. Rev. Nuclear Sci.*, **9**, 245 (1959)
75. Harding, J. B., Lattimore, S., and Perkins, D. H., *Proc. Roy. Soc. (London)*, **A196**, 325 (1949)
76. Heckrotte, W., *Phys. Rev.*, **95**, 1279 (1954)
77. Heining, C. G., and Wiig, E. O., *Phys. Rev.*, **101**, 1074 (1956)
78. Heisenberg, W., *Naturwissenschaften*, **25**, 749 (1937)
79. Heisenberg, W., *Z. Physik*, **126**, 569 (1949)
80. Hicks, H. G., and Gilbert, R. S., *Phys. Rev.*, **100**, 1286 (1955)
81. Hicks, H. G., Stevenson, P. C., Gilbert, R. S., and Hutchin, W. H., *Phys. Rev.*, **100**, 1284 (1955)
82. Hicks, H. G., Stevenson, P. C., and Nervik, W. E., *Phys. Rev.*, **102**, 1390 (1956)
83. Hintz, N. M., and Ramsey, N. F., *Phys. Rev.*, **88**, 19 (1952)
84. Hodgson, P. E., *Phil. Mag.*, **42**, 207 (1951)
85. Hopkins, H. H., *Phys. Rev.*, **77**, 717 (1950)
86. Hopkins, H. H., and Cunningham, B. B., *Phys. Rev.*, **73**, 1406 (1948)
87. Hudis, J., and Miller, J. M., *Phys. Rev.*, **112**, 1322 (1958)
88. Hunter, E. T., and Miller, J. M., *Phys. Rev.* (To be published)
89. Hurwitz, H., Jr., and Bethe, H., *Phys. Rev.*, **81**, 898 (1951)
90. Igo, G., and Wegner, H., *Phys. Rev.*, **102**, 1364 (1956)
91. Ivanova, N. S., *Soviet Phys. JETP*, **4**, 365 (1957)
92. Ivanova, N. S., *Zhur. Eksptl. i Teoret. Fiz.*, **34**, 1381 (1958)
93. Ivanova, N. S., Perfilov, N. A., and Shamov, V. P., *Doklady Akad. Nauk S.S.S.R.*, **103**, 573 (1955); *U. S. Atomic Energy Commission Transl.*, 2307 (1955)
94. Ivanova, N. S., and P'ianov, I. I., *Soviet Phys. JETP*, **4**, 367 (1957)
95. Jackson, J. P., *Can. J. Phys.*, **34**, 767 (1956)
96. Jodra, L. G., and Sugarman, N., *Phys. Rev.*, **99**, 1470 (1955)
97. John, W., and Fry, W. F., *U. S. Atomic Energy Commission Document, UCRL 2113* (Berkeley, Calif., 1953)
98. Jones, J. W., *U. S. Atomic Energy Commission Rept.*, NYO 6627, Contract A.T. (30-1)-844 (May, 1956)
99. Jungerman, J., *Phys. Rev.*, **79**, 632 (1950)
100. Kaliamin, A. V., Murin, A. N., Preobrazhenskii, B. K., and Titov, N. E., *Atomic Energy (U.S.S.R.) (English Transl.)*, **4**, 196 (1958)
101. Kellogg, D. A., *U. S. Atomic Energy Commission Document, UCRL 1899* (Berkeley, Calif., 1952)
102. Kelly, E. L., and Wiegand, C., *Phys. Rev.*, **73**, 1135 (1948)
103. Kjelberg, A., and Pappas, A. C., *Nuclear Phys.*, **1**, 322 (1956)
104. Knox, W. J., *Phys. Rev.*, **75**, 537 (1949)
105. Kofstad, P. K., *U. S. Atomic Energy Commission Document, UCRL 2265* (Berkeley, Calif., 1953)
106. Kruger, P., and Sugarman, N., *Phys. Rev.*, **99**, 1459 (1955)
107. Kurchatov, B. V., Mekhedov, V. N., Borisova, N. I., Kuznetsova, M. Ya., Kurchatova, L. N., and Christyakov, L. V., *Conf. Acad. Sci. U.S.S.R., Peaceful Uses Atomic Energy, Moscow* (1955); *U. S. Atomic Energy Commission Transl.*, 2435, Part 2, 111-24 (1955)

108. Kurchatov, B. V., Mekhedov, V. N., Christyakov, L. V., Kuznetsova, M. Ya., and Solov'ev, V. G., *Soviet Phys. JETP*, **8**, 40 (1959)
109. Kurchatov, B. V., Mekhedov, V. N., Kuznetsova, M. Ya., and Kurchatova, L. N., *Conf. Acad. Sci. U.S.S.R. Peaceful Uses Atomic Energy, Moscow* (1955); *U. S. Atomic Energy Commission Transl.*, 2435, Part 2, 79-84 (1955)
110. Kuznetsov, V. V., and Mekhedov, V. N., *Joint Inst. for Nuclear Research, Moscow, Lab. of Nuclear Problems*, NP 6901 (1958)
111. Kuznetsova, M. Ya., Mekhedov, V. N., and Khalkin, V. A., *U. S. Atomic Energy Commission Transl.*, 3258 (1957) (From a publication of the Joint Institute of Nuclear Research, U.S.S.R.)
112. Kuznetsova, M. Ya., Mekhedov, V. N., and Khalkin, V. A., *Soviet Phys. JETP*, **34**, 759 (1958)
113. Ladenbauer, I. M., *U. S. Atomic Energy Commission Document*, UCRL 8200 (1958)
114. Lane, A. M., and Wandel, C. F., *Phys. Rev.*, **98**, 1524 (1955)
115. Lavrukhina, A. K., and Krasavina, L. D., *J. Nuclear Energy*, **5**, 236 (1957)
116. Lavrukhina, A. K., Krasavina, L. D., and Pozdnyaikov, A. A., *Doklady Akad. Nauk S.S.S.R.*, **119**, 56 (1958)
117. Lavrukhina, A. K., Moskaleva, L. P., Krasavina, L. D., and Grechishcheva, I. M., *Atomnaya Energ.*, **3**, No. 10, 285 (1957)
118. Lax, M., *Rev. Modern Phys.*, **23**, 287 (1951)
119. Leachman, R. B., *Proc. Intern. Conf. Peaceful Uses Atomic Energy, IInd Conf., Geneva, 1958*, Paper 665 (1959)
120. Le Couteur, K. J., *Proc. Phys. Soc. (London)*, **A63**, 259 (1950)
121. Lefort, M., Simonoff, G., and Tarrago, X., *Compt. rend.*, **248**, 216 (1959)
122. Lindenbaum, S. J., *Ann. Rev. Nuclear Sci.*, **7**, 317 (1957)
123. Lindner, M., and Osborne, R. N., *Phys. Rev.*, **91**, 1501 (1953)
124. Lindner, M., and Osborne, R. N., *Phys. Rev.*, **91**, 342 (1953)
125. Lindner, M., and Osborne, R. N., *Phys. Rev.*, **103**, 378 (1956)
126. Lindner, M., and Osborne, R. N., *Phys. Rev.*, **94**, 1323 (1954)
127. Lindner, M., and Perlman, I., *Phys. Rev.*, **78**, 499 (1950)
128. Lozhkin, O. V., *Soviet Phys. JETP*, **6**, 273 (1958)
129. Lozhkin, O. V., and Perfilov, N. A., *Soviet Phys. JETP*, **4**, 790 (1957)
130. Lozhkin, O. V., Perfilov, N. A., and Shamov, V. P., *Soviet Phys. JETP*, **2**, 116 (1956)
131. Lozhkin, O. V., Perfilov, N. A., and Shamov, V. P., *Doklady Akad. Nauk S.S.S.R.*, **103**, 407 (1955); *U. S. Atomic Energy Commission Transl.*, 2296 (1955)
132. Lozhkin, O. V., and Shamov, V. P., *Zhur. Eksptl. i Teoret. Fiz.*, **28**, 739 (1955); *Atomic Energy Research Estab. Lib. Transl.*, 636 (1955)
133. Markowitz, S., Rowland, F. S., and Friedlander, G., *Phys. Rev.*, **112**, 1295 (1958)
134. Marquez, L., *Phys. Rev.*, **86**, 405 (1952)
135. Marquez, L., *Phys. Rev.*, **88**, 225 (1952)
136. Marquez, L., and Perlman, I., *Phys. Rev.*, **81**, 953 (1951)
137. Martin, G. R., Thomson, S. J., Wardle, G., and Mayne, K. I., *Phil. Mag.*, **45**, 410 (1954)
138. McManus, H., Sharp, W. T., and Gellman, H., *Phys. Rev.*, **93**, 924 A (1954)
139. Meadows, J. W., *Phys. Rev.*, **98**, 744 (1955)

140. Meadows, J. W., *Phys. Rev.*, **91**, 885 (1953)
141. Meadows, J. W., *Phys. Rev.*, **110**, 1109 (1958)
142. Meadows, J. W., Diamond, R. M., and Sharp, R. A., *Phys. Rev.*, **102**, 190 (1956)
143. Meadows, J. W., and Holt, R. B., *Phys. Rev.*, **83**, 47 (1951)
144. Meadows, J. W., and Holt, R. B., *Phys. Rev.*, **83**, 1257 (1951)
145. Meinke, W. W., Wick, G. C., and Seaborg, G. T., *J. Inorg. & Nuclear Chem.*, **3**, 69 (1956)
146. Metropolis, N., Bivins, R., Storm, M., Turkevich, A., Miller, J. M., and Friedlander, G., *Phys. Rev.*, **110**, 185 (1958)
147. Metropolis, N., Bivins, R., Storm, M., Miller, J. M., Friedlander, G., and Turkevich, A., *Phys. Rev.*, **110**, 204 (1958)
148. Metzger, A. E., and Miller, J. M., *Phys. Rev.*, **113**, 1125 (1959)
149. Millburn, G. P., Birnbaum, W., Crandall, W. E., and Schechter, L., *Phys. Rev.*, **95**, 1268 (1954)
150. Miller, J. M., and Friedlander, G., *Phys. Rev.*, **84**, 589 (1951)
151. Miller, J. M., Friedlander, G., and Markowitz, S., *Phys. Rev.*, **98**, 1197 A (1955)
152. Miller, J. M., and Houck, F. S., *Bull. Am. Phys. Soc.*, **2**, 60 (1957)
- 152a. Miskel, J. A., Perlman, M. L., Friedlander, G., and Miller, J. M., *Phys. Rev.*, **98**, 1197 A (1955)
153. Morrison, H., Muirhead, H., and Rosser, W. G. V., *Phil. Mag.*, **44**, 1326 (1953)
154. Munir, B. A., *Phil. Mag.*, **1**, 355 (1956)
155. Murin, A. N. Preobrazhenskii, B. K., Yutlandov, I. A., and Yakimov, M. A., *Conf. Acad. Sci. U.S.S.R. Peaceful Uses of Atomic Energy, Moscow*, (1955); *U. S. Atomic Energy Commission Transl.*, 2435, Part 2, 101-10 (1955)
156. Nakagawa, S., Tamai, E., Huzita, H., and Okudaira, K., *J. Phys. Soc. Japan*, **12**, 747 (1957)
157. Nakagawa, S., Tamai, E., and Nomoto, S., *Nuovo cimento*, **9**, 780 (1958)
158. Nervick, W. E., *Phys. Rev.*, **97**, 1092 (1957)
159. Nethaway, D. R., *U. S. Atomic Energy Commission Document, UCRL 3628* (Berkeley, Calif, 1957)
160. Nikol'skii, B. A., Kudrin, L. P., and Ali-Zade, S. A., *Soviet Phys. JETP*, **5**, 93 (1957)
161. O'Connor, P. R., and Seaborg, G. T., *Phys. Rev.*, **74**, 1189 (1948)
162. Ostroumov, V. I., *Doklady Akad. Nauk S.S.S.R.*, **103**, 409 (1955); *Atomic Energy Research Estab. Lib. Transl.*, 692 (1955)
163. Ostroumov, V. I., and Filov, R. A., *Zhur. Ekspl. i Teoret. Fiz.*, **33**, 1335 (1957)
164. Ostroumov, V. I., and Perfilov, N. A., *Soviet Phys. JETP*, **4**, 603 (1957)
165. Pate, B. D., *Can. J. Chem.*, **36**, 1707 (1958)
166. Pate, B. D., Foster, J. S., and Yaffe, L., *Can. J. Chem.*, **36**, 1691 (1958)
167. Pavlotskaia, F. I., and Lavrukhina, A. K., *Soviet Phys. JETP*, **34**, 732 (1958)
168. Perfilov, N. A., and Ivanova, N. S., *Soviet Phys. JETP*, **2**, 433 (1956)
169. Perfilov, N. A., Lozhkin, O. V., and Shamov, V. P., *Doklady Akad. Nauk S.S.S.R.*, **103**, 417 (1955); *U. S. Atomic Energy Commission Transl.*, 2304 (1955)
170. Perfilov, N. A., Ivanova, N. S., Lozhkin, O. V., Ostroumov, V. I., and Shamov, V. P., *Conf. Acad. Sci. U.S.S.R. Peaceful Uses—Atomic Energy, Moscow*, (1955); *U. S. Atomic Energy Commission Transl.*, 2336, 79 (1955)
171. Perkins, D. H., *Proc. Roy. Soc. (London)*, **203A**, 399 (1950)

172. Perlman, I., Goeckermann, R. H., Templeton, D. H., and Howland, J. J., *Phys. Rev.*, **72**, 352 (1947)
173. Porile, N. T., *Phys. Rev.*, **108**, 1526 (1957)
174. Porile, N. T., and Sugarman, N., *Phys. Rev.*, **107**, 1410 (1957)
175. Porile, N. T., and Sugarman, N., *Phys. Rev.*, **107**, 1422 (1957)
176. Prokoshkin, Iu. D., and Tiapkin, A. A., *Soviet Phys. JETP*, **5**, 148 (1957)
177. Raleigh, D. O., *Excitation Functions from the Alpha-Particle Bombardment of Ti^{48}* (Doctoral thesis, Columbia Univ., New York, N. Y., 1958)
178. Randle, T. C., Dickson, J. M., and Cassels, J. M., *Phil. Mag.*, **42**, 665 (1951)
- 178a. Reasbeck, P., and Warren, J. E., *J. Inorg. Nuclear Chem.*, **7**, 343 (1958)
179. Ring, S. O., and Litz, L. M., *Phys. Rev.*, **97**, 427 (1955)
180. Rosenfeld, A. H., Swanson, R. A., and Warshaw, S. D., *Phys. Rev.*, **103**, 413 (1956)
181. Rowland, F. S., and Wolfgang, R. L., *Phys. Rev.*, **110**, 175 (1958)
182. Rudstam, G., *Spallation of Medium Weight Elements* (Doctoral thesis, NP-6191, Univ. of Uppsala, Uppsala, Sweden, 1956)
183. Rudstam, G., *Phil. Mag.*, **44**, 1131 (1953)
184. Rudstam, G., Stevenson, P. C., and Folger, R. L., *Phys. Rev.*, **87**, 358 (1952)
185. Salter, D. C., and Bird, L., *Phil. Mag.*, **44**, 1305 (1953)
186. Schaeffer, O. A., and Zähringer, J., *Z. Naturforsch.*, **13a**, 346 (1958)
187. Serber, R., *Phys. Rev.*, **72**, 1114 (1947)
188. Shamov, V. P., *Doklady Akad. Nauk S.S.S.R.*, **103**, 593 (1955); *U. S. Atomic Energy Commission Transl.*, 2308 (1955)
189. Shamov, V. P., *Soviet Phys. JETP*, **6**, 268 (1958)
190. Shamov, V. P., and Lozhkin, O. V., *Zhur. Eksp. i Teoret. Fiz.*, **29**, 286 (1955); *Atomic Energy Research Estab. Lib. Transl.*, 653 (1955)
191. Sharp, R. A., Diamond, R. M., and Wilkinson, G., *Phys. Rev.*, **101**, 1493 (1956)
192. Shudde, R. H., *U. S. Atomic Energy Commission Document, UCRL 3419* (Berkeley, Calif., 1956)
193. Sidorov, V. M., and Grigoriev, E. L., *Soviet Phys. JETP*, **6**, 906 (1958)
194. Skyrme, D. M., and Harding, G. N., *Nuovo cimento*, **9**, 1082 (1958)
195. Sörensen, S. O. C., *Phil. Mag.*, **42**, 188 (1951)
196. Spence, R. W., and Ford, G. P., *Ann. Rev. Nuclear Sci.*, **2**, 411 (1953)
197. Steiner, H. M., and Jungerman, J. A., *Phys. Rev.*, **101**, 807 (1956)
198. Stevenson, P. C., Hicks, H. G., and Folger, R. L., *U. S. Atomic Energy Commission Document, UCRL 4371* (Livermore, Calif., 1954)
199. Stevenson, P. C., Hicks, H. G., Nervik, W. E., and Nethaway, D. R., *Phys. Rev.*, **111**, 886 (1958)
200. Sugarman, N., Campos, M., and Wielgoz, K., *Phys. Rev.*, **101**, 388 (1956)
201. Sugarman, N., Duffield, R. B., Friedlander, G., and Miller, J. M., *Phys. Rev.*, **95**, 1704 (1954)
202. Sugarman, N., and Haber, A., *Phys. Rev.*, **92**, 730 (1953)
203. Sugihara, T. T., and Libby, W. F., *Phys. Rev.*, **88**, 587 (1952)
204. Symonds, J. L., Warren, J., and Young, J. D., *Proc. Phys. Soc. (London)*, **A70**, 824 (1957)
205. Templeton, D. H., *Ann. Rev. Nuclear Sci.*, **2**, 93 (1953)
206. Thornton, R. L., and Senseman, R. W., *Phys. Rev.*, **72**, 872 (1947)
- 206a. Turkevich, A., and Fung, S. C., *Phys. Rev.*, **92**, 521 (1953)

- 206b. Turkevich, A., and Niday, J. B., *Phys. Rev.*, **84**, 1253 (1951)
- 207. Turkevich, A., and Sugarman, N., *Phys. Rev.*, **94**, 728 (1954)
- 208. Vandenbosch, R., and Huizenga, J. R., *Proc. Intern. Conf. Peaceful Uses Atomic Energy, IInd Conf., Geneva, 1958*, Paper 688 (1959)
- 209. Vinogradov, A. P., Alimarin, I. P., Baranov, V. I., Lavrukhina, A. K., Baranova, T. V., Pavlotskaya, F. I., Bragina, A. A., and Yakovlev, Yu. V., *Conf. Acad. Sci. U.S.S.R. Peaceful Uses of Atomic Energy, Moscow* (1955); *U. S. Atomic Energy Commission Transl.*, 2435, Part 2, 65-78 (1955)
- 210. Vinogradov, A. P., Alimarin, I. P., Baranov, V. I., Lavrukhina, A. K., Baranova, T. V., and Pavlotskaya, F. I., *Conf. Acad. Sci. U.S.S.R. Peaceful Uses of Atomic Energy, Moscow*, (1955); *U. S. Atomic Energy Commission Transl.*, 2435, Part 2, 85-100 (1955)
- 211. Wagner, G. D., and Wiig, E. O., *Phys. Rev.*, **96**, 1100 (1954)
- 212. Weisskopf, V., *Phys. Rev.*, **52**, 295 (1937)
- 213. Winsberg, L., *Phys. Rev.*, **95**, 198 (1954)
- 214. Winsberg, L., *Phys. Rev.*, **95**, 205 (1954)
- 215. Wolfgang, R. L., Baker, E. W., Caretto, A. A., Cumming, J. B., Friedlander, G., and Hudis, J., *Phys. Rev.*, **103**, 394 (1956)
- 216. Wolfgang, R. L., and Friedlander, G., *Phys. Rev.*, **96**, 190 (1954)
- 217. Wolke, R. L., and Gutmann, J. R., *Phys. Rev.*, **107**, 850 (1957)
- 218. Worthington, W. J., Jr., *U. S. Atomic Energy Commission Document, UCRL 1627* (Berkeley, Calif., 1952)
- 219. Wright, S. C., *Phys. Rev.*, **79**, 838 (1950)
- 220. Yamaguchi, Y., *Progr. Theoret. Phys.*, **5**, 142 (1950)
- 221. Chupp, W. W., and McMillan, E. M., *Phys. Rev.*, **72**, 873 (1947)
- 222. Coleman, G. H., and Tewes, H. A., *Phys. Rev.*, **99**, 288 (1955)

TECHNETIUM AND ASTATINE CHEMISTRY^{1,2}

BY EDWARD ANDERS

*Department of Chemistry and Enrico Fermi Institute for Nuclear Studies,
University of Chicago, Chicago, Illinois*

INTRODUCTION

Technetium and astatine were the first "missing" elements to be synthesized by man [Perrier & Segrè (1); Corson, MacKenzie & Segrè (2)]. Both can be said to occur in nature only in the widest sense of the term: astatine as a short-lived rare branch product in the decay of the uranium and thorium radioactive series (3), and technetium as a spontaneous-fission product in uranium ores (4). The instability of astatine is not unexpected since all nuclides above Bi²⁰⁹ are either α or β unstable. In the case of technetium, the existence of stable isotopes of molybdenum and ruthenium at masses 97 and 99, respectively, precludes the occurrence of stable technetium nuclides.

Of the isotopes of technetium, no less than four have been used for tracer studies: 60 day Tc^{95m}, 4.2 day Tc⁹⁶, 91 day Tc^{97m}, and 6 hr. Tc^{99m}. The half life and radiations of the latter isotope make it particularly suited for this purpose. Three other isotopes, of masses 97, 98, and 99, have half lives $>10^5$ yr. and can therefore be used to study the chemistry of the element on a macroscale. The best-known of these is 2.12×10^5 yr. Tc⁹⁹. It is produced in fission with a yield of ~ 6 per cent and has been available in weighable quantities since 1946.

In the 22 years since the discovery of technetium, our knowledge of its chemistry has increased considerably. Yet the sum total of our knowledge is woefully small compared to that available for rhenium some 15 to 25 years after its discovery [Gmelin (5); Druce (6)]. It would seem that this lack of progress is attributable to two principal causes. First, much of the work on technetium has never received regular publication and has remained unknown and inaccessible to the majority of scientists. There is a wealth of information locked up in technical reports of the U. S., Canadian, and British Atomic Energy Projects and in unpublished doctoral theses, manuscripts, and papers presented at meetings of scientific societies. Two excellent manuscripts by Boyd, Larson & Motta (7) and Fried & Hall (8) may be cited as examples. Some of these reports have been declassified after delays of 7 to 10 years; others, dealing with subjects as innocuous as the tracer chemistry of technetium, e.g. (9), were classified and have remained so for reasons not obvious to the uninitiated. Second, the high price of technetium (currently \$17,000 per g.) has made the element virtually inaccessible to university sci-

¹ The survey of the literature pertaining to this review was concluded in March, 1959.

² This work was supported in part by the U. S. Atomic Energy Commission.

entists, particularly those outside the United States. It is unfortunate that the present price policy, justified as it may be on economic grounds, has put the university scientists under a severe handicap relative to their colleagues at government laboratories. Though it is perfectly feasible to conduct chemistry on a milligram scale, there is little incentive to do so when another laboratory can repeat the work on a 10-g. scale. One must wonder to what extent this consideration has actually retarded progress in the field.

The history of astatine has been rather different. The first isotopes to be discovered, 7.5 hr. At²¹¹ and 8.3 hr. At²¹⁰, still are and will probably remain the longest-lived isotopes of this element. For this reason, all information on the chemistry of astatine has been derived from radiochemical studies of 10^{-10} to 10^{-14} M solutions. Few workers have been attracted to the field, and our knowledge is even less complete than in the case of technetium. Again, a considerable amount of information is buried in unpublished reports and manuscripts.

This reviewer has attempted to cover the period since 1948 with some degree of thoroughness, although earlier papers have been included when of particular importance. Some excellent reviews of earlier vintage are available, e.g. (5, 10, 11, 12) on Tc, and (11, 13, 14) on At. No attempt has been made to discuss the isotopes of Tc and At, since all relevant data can be found in the tables of Strominger, Hollander & Seaborg (15) as well as in the papers of Boyd (16) and Hyde (17) on Tc and At, respectively.

CHEMISTRY OF TECHNETIUM

The metal.—Technetium metal can be prepared by reduction of the sulfide with hydrogen at 1100°C. (8, 18). A purer product is obtained by hydrogen reduction of ammonium pertechnetate³ at 500–600°C. (19) or by electrodeposition from 2N H₂SO₄ in the presence of fluoride ions (20). The metal has a density of 11.49 and crystallizes in a hexagonal close-packed structure with an average metallic radius of 1.358 Å (21). No evidence for polymorphism was found at pressures up to 100,000 kg./cm.² (22). The metal is slightly paramagnetic (23) and becomes superconductive below 11.2°K. (24). It melts at 2140 ± 20°C. under atmospheric pressure (25).

The optical (26, 27, 28) and x-ray (29, 30, 31) emission spectra have been measured. The first and second ionization potentials are 7.28 and 15.26 ev, respectively (32). The third ionization potential has been estimated as 31.9 ev (33) and the work function as 4.4 v. (34).

Technetium metal dissolves in nitric acid, aqua regia, and hot, concentrated sulfuric acid. It is insoluble in hydrochloric acid and, in contrast to rhenium, in neutral or alkaline hydrogen peroxide (18, 19).

Oxidation state +7.—This is the most thoroughly characterized oxidation

³ No consensus of opinion seems to exist concerning the nomenclature of technetium anions. We shall use the long form, "pertechnetic" and "pertechnetate," rather than the short form, "pertechnic" and "pertechnate."

state of technetium. The yellow, crystalline heptoxide is obtained by burning technetium metal in dry oxygen at 400°–600°C. (35). Its melting and boiling points are 119.5° and 311°C., respectively. It is not isomorphous with rhenium heptoxide and differs from it in other respects as well. For example, solid Tc_2O_7 shows electrical conductivity just below its melting point but is nonconductive in the liquid state. Rhenium heptoxide shows the opposite behavior (36). The reasons for these differences are not understood.

Technetium heptoxide dissolves in water to give a colorless solution of HTcO_4 from which red-black crystals of the anhydrous acid can be prepared by evaporation (35, 36). The vapor pressures of HTcO_4 and Tc_2O_7 have been measured (36). Numerous pertechnetetic acid salts have been prepared, e.g. NH_4TcO_4 , KTcO_4 , AgTcO_4 , CsTcO_4 , tetraphenylarsonium pertechnetate, and nitron pertechnetate. Most of these salts are more soluble than the corresponding perrrhenates and perchlorates (37) though the last two have a low enough solubility to permit their use as gravimetric weighing forms. The ammonium, potassium, and silver salts have the CaWO_4 structure (38). Potassium pertechnetate melts at 540°C. and sublimes at $\sim 1000^\circ\text{C}$. without decomposition (39). When contaminated with $(\text{NH}_4)_2\text{SO}_4$, NH_4TcO_4 decomposes on heating (8, 40), but pure NH_4TcO_4 has been sublimed without apparent decomposition in the preparation of β -ray spectrometer sources (41).

The metal-oxygen distance in the TcO_4^- ion is about 1.75 Å (38), compared to 1.97 Å in ReO_4^- (42). This trend in bond distances is rather surprising in view of the greater stability of the perrrhenate ion, and the proposed equality of the ionic radii of Tc^{7+} and Re^{7+} [0.56 Å according to Ahrens (43)].

The optical absorption spectrum of pertechnetate ion has been measured. The molar absorbances at 2440 and 2875 Å are 6100 and 2320, respectively (44). The spectrum is very similar to those of the isoelectronic species ReO_4^- , MnO_4^- , and RuO_4 (8, 12).

It was found by Cartledge that pertechnetate ion is a most effective corrosion inhibitor (45 to 49). When kept in solutions containing as little as 5 to 50 p.p.m. of TcO_4^- , mild carbon steels do not corrode at temperatures up to at least 250°C.

The brown-black heptasulfide can be prepared by precipitation from solutions 2 to 4 *N* in HCl or H_2SO_4 by means of hydrogen sulfide (18, 40). The precipitation is sluggish and incomplete under some conditions, particularly if the technetium is not all in the +7 state (18, 50). Many of the precautions required in the precipitation of rhenium (51, 52, 53) are equally applicable to technetium.

Two oxyhalides of Tc (VII) have been reported. Pertechnetyl chloride, TcO_3Cl , is formed when 12 *M* HCl is added to a solution of KTcO_4 in 18 *M* H_2SO_4 (39) and may be extracted into inert solvents such as CCl_4 , CHCl_3 , or C_6H_{14} . The oxyfluoride, TcO_3F , appears to form by the reaction of HTcO_4 or Tc_2O_7 with UF_4 (54).

Information on the electron density distribution in several technetium compounds has been obtained by means of 6 hr. Tc^{99m} [Bainbridge, Goldhaber & Wilson (55, 56)]. Since the half life of this nuclide is governed by a highly internally converted transition of extremely low energy (2 kev), the decay rate should be affected by the electron density near the nucleus. It was found that the decay constant in KTcO_4 was 0.27 ± 0.01 per cent larger than in Tc_2S_7 . An appreciably smaller effect was later obtained by Dzhelepov & Kraft (57).

Oxidation state +4.—This oxidation state has been fairly well characterized. The black dioxide TcO_2 can be obtained by pyrolysis of NH_4TcO_4 (8). It has the MoO_2 structure (38, 58). Its dihydrate has been prepared by electrolytic reduction of pertechnetate solutions (59) or by hydrolysis of TcCl_6^- . At trace concentrations, pertechnetate in dilute sulfuric acid solutions is reduced to a tetravalent state by hydrazine, hydroxylamine, ascorbic acid, and stannous chloride. This state shows the behavior expected of the hydrated dioxide (50). The dioxide can be oxidized to pertechnetate by HNO_3 , Ce (IV), or alkaline H_2O_2 . At elevated temperatures, it reacts with oxygen to give Tc_2O_7 .

The disulfide TcS_2 has been prepared by heating Tc_2S_7 with sulfur in a sealed tube for 24 hr. at 1000°C . and removing the excess sulfur by vacuum sublimation (8). It is isomorphous with ReS_2 (38).

The blood-red, crystalline tetrachloride has been prepared by Knox *et al.* (60) by heating Tc_2O_7 and CCl_4 in a sealed tube. Its magnetic properties have not been determined.

Like its congeners, technetium forms hexahalogen complexes in the +4 oxidation state. The golden-yellow K_2TcCl_6 may be prepared by reduction of TcO_4^- with KI in concentrated HCl (8, 23). A simpler synthesis is based on the fact that strong HCl itself will reduce TcO_4^- to TcCl_6^- (4). The reaction is slow; even in 13 *N* HCl, 1 hr. is required at room temperatures (50). Potassium hexachlorotechnetate (IV) is isomorphous with K_2ReCl_6 (38, 58) and has a magnetic moment of 4.3 Bohr magnetons. The paramagnetic resonance spectrum of $\text{K}_2\text{Tc}^{99}\text{Cl}_6$ has been measured (61). By analogy with rhenium (62, 63) one may expect a number of mixed chloro-hydroxo complexes of Tc (IV). It is interesting to note that Boyd has indeed observed gradual changes in the absorption spectrum of K_2TcCl_6 in 3 *N* HCl (12). In neutral solution, hydrolysis to TcO_2 is rapid and complete. The TcCl_6^- ion is extracted by isobutanol, by chloroform in the presence of tetraphenylarsonium ion (4), and by other organic liquids and amines (12). It coprecipitates with thallium and α - α' dipyridyl hexachlororhenates (50). Hexachlorotechnetate (IV) is oxidized to pertechnetate by H_2O_2 in acid or alkaline solution and by HNO_3 (50, 60). The preparation of K_2TcBr_6 and K_2TcI_6 has been reported (39).

Oxidation states +6 and 5.—The chemistry of technetium in its remaining oxidation states is not too well understood. As is the case with rhenium

and manganese, the +5 and +6 oxidation states are harder to prepare than the +4 state. Gerlit (50) obtained Tc (VI) by hydrazine reduction of cold, alkaline pertechnetate solutions. Since his experiments were carried out with 6 hr. Tc^{99m} , the compound could not be isolated but had to be characterized by radiochemical techniques. It is neither extracted by ketones or pyridine nor precipitated by ferric hydroxide, but it is carried quantitatively by molybdenum 8-hydroxyquinolate, and silver and lead molybdate. In the presence of dioximes, it can be extracted into inert solvents such as chloroform. At an OH^- concentration of 0.02 to 0.05 *N* the compound slowly disproportionates to Tc (VII) and Tc (IV) in the ratio of $\sim 2:1$. The above facts are consistent with its identification as TcO_4^- .

Another oxidation state of technetium has been observed in the reduction of TcO_4^- to TcCl_6^- by 6–8 *M* HCl. At 100°C., the reaction is complete in ~ 12 hr. During the first 2 hr., an intermediate oxidation state forms that extracts into hexone with a partition coefficient of >30 (compared to ~ 11 for TcO_4^-), absorbs light strongly at 2350 Å (molar absorbance, $\epsilon \approx 3 \times 10^4$), and forms a red complex with thiocyanate (4). Crouthamel (64) showed that this complex ($\epsilon = 52,200$ at 5130 Å) is attributable to Tc (V). He also obtained evidence for the formation of Tc (VI), (V), and (IV) in the potentiometric titration of TcO_4^- by Ti (III) in 12 *M* H_2SO_4 . In this medium, Tc (VI) disproportionates within 3 to 4 minutes to Tc (V) and Tc (VII), whereas Tc (V) disproportionates to Tc (VII) and Tc (IV) within an hour. In 2 *M* H_2SO_4 or HCl, saturated with $(\text{NH}_4)_2\text{SO}_4$ and NH_4Cl , respectively, a red color (absorption maximum ~ 5000 Å) was observed at the stoichiometric endpoint of Tc (V). No such color was observed in 10 to 12 *M* acid. It is interesting to note that although pure NH_4TcO_4 is colorless, pertechnetate preparations having a pink to reddish color were reported by all early workers in the field (18, 65, 66), and an absorption spectrum measured by Parker *et al.* (66) shows a distinct maximum at ~ 5000 Å. A pink substance was also obtained in the oxidation of electrodeposited TcO_2 by NaClO (67). Moreover, Fried & Hall (8) described a volatile, dark purple oxide of technetium, obtained by the action of O_2 on Tc metal at 400°–1000°C. Analysis of two samples of this oxide gave O/Tc ratios of 3.07 and 3.02, respectively. The assignment of an oxidation state lower than +7 to this oxide was further justified by the observation that it did not yield NH_4TcO_4 when treated with H_2O and NH_3 but required addition of H_2O_2 . A further study of this problem would be highly desirable.

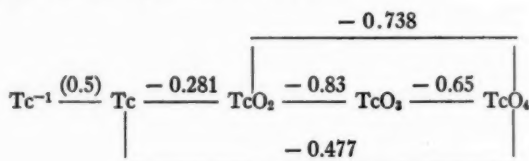
Oxidation state +3 and unidentified lower states.—Thomason has prepared a green solution containing Tc (III) by controlled cathode potential electrolysis of TcO_4^- in a phosphate buffer at pH 7 (68). It is easily oxidized by air to Tc (IV). Gerlit (50) reports that an oxidation state lower than (IV) is obtained in the reduction of TcO_4^- by Zn in concentrated HCl. This state does not coprecipitate with thallium hexachlororhenate (IV) from hydrochloric acid solutions, with rare earth or alkaline earth oxalates from weakly

acid or neutral solutions, or with copper and zinc sulfides from weakly acid solutions. It is carried quantitatively by iron and zirconium hydroxides and by the sulfide, hydroxide, and 8-hydroxyquinolate of manganese. It is readily oxidized by oxygen, hydrogen peroxide, and nitric acid. Although Gerlit interprets this oxidation state as Tc (II), the above evidence definitely does not rule out its assignment to Tc (III).

The cationic nature of these species has not been demonstrated, nor have any other cationic states of Tc been identified with any certainty. Flagg & Bleidner (69) reported that solutions of electrodeposited Tc (TcO_2 ?) in dilute acids, and pertechnetate solutions treated with HCl or SnCl_2 were absorbed on basic alumina columns, indicating reduction to a cation. Boyd, Larson & Motta (70) conducted electromigration experiments on TcO_4^- solutions in 4 M H_2SO_4 . Their results indicated the presence of both cationic and anionic species, but since pure ReO_4^- solutions gave the same results, the evidence is not conclusive. Some adsorption on cation exchange resin was observed for TcO_4^- solutions in 1–2N H_2SO_4 and 0.25–0.75 N HNO_3 (70, 71), but the exchange was irreversible and may have been caused by precipitation of TcO_2 on the resin. A thorough investigation of the lower oxidation states of Tc is needed badly.

Nelson *et al.* (23) have prepared two paramagnetic chlorides or oxychlorides of unknown oxidation state by chlorination of TcO_2 at 300°C. A blue and a brown compound volatilizing at 80°–90° and 500°C., respectively, were obtained; because of difficulties in the analysis, their composition was not determined.

The oxidation potential diagram of technetium is shown below. Most of the data result from the exacting work of Boyd, Cobble, Cartledge, and their associates at Oak Ridge National Laboratory though it is interesting to note that Flagg and Bleidner in 1945 came within 0.07 v. of the correct value for the Tc/TcO_4^- potential by measurements of the critical deposition potential at concentrations of 10^{-12} M. An estimated value for the speculative (–I) state has also been included (12).



A summary of the known thermodynamic properties of technetium is given in Table I.

ANALYTICAL CHEMISTRY OF TECHNETIUM

In many respects, the analytical behavior of Tc is similar to that of Re. Both form stable XO_4^- anions that give insoluble salts with large cations;

TABLE I

THERMODYNAMIC PROPERTIES OF TECHNETIUM AND SOME OF ITS COMPOUNDS AT 298.16°K. [FROM (12)]

Compound	$-\Delta H_f^\circ$ (kcal./mole)	S° (cal./mole deg)	$-\Delta S_f^\circ$	$-\Delta F_f^\circ$ (kcal./mole)
Tc (c)	0.0	7.4 ± 0.2	0.0	0.0
Tc (g)	—	43.26 ± 0.01	35.9 ± 0.2	—
TcO ₂ (c)	103.7 ± 2.0	14.9 ± 0.5	41.5 ± 0.5	91.4 ± 2.0
TcO ₃ (c)*	129.0 ± 5.0	17.3 ± 0.6	63.1 ± 0.6	110.2 ± 5.0
Tc ₂ O ₇ (c)	266.1 ± 2.6	45.8 ± 2.0	140.9 ± 2.0	224.1 ± 2.6
HTcO ₄ (c)	167.4 ± 1.3	33.3 ± 2.0	87.7 ± 2.0	141.3 ± 1.3
TcO ₄ ⁻ (aq)	173.0 ± 1.3	46.0 ± 0.1	75.0 ± 0.1	150.6 ± 1.3
KTcO ₄ (c)	242.5 ± 1.5	39.74 ± 0.10	78.9 ± 1.0	219.0 ± 1.5
K ₂ TcCl ₆ (c)	—	49.5 ± 1.0	117.6 ± 1.0	—

* Only estimated values are available for this compound (36).

both form volatile heptoxides; and both form acid-insoluble heptasulfides. However, there are subtle differences between the two elements that can cause them to behave very differently under certain conditions. The vapor pressure of Tc₂O₇ (36) is much higher than that of Re₂O₇ at low temperatures (e.g. 10^{-1} mm. at 100°C., compared to $\sim 3 \times 10^{-5}$ mm. for Re₂O₇). In contrast to rhenium, technetium (VII) is, therefore, easily lost upon evaporation of acid solutions unless a reducing agent is present or the evaporation is conducted at a low temperature. Ignorance of these factors has led to a multitude of conflicting statements concerning the volatility of technetium.

Other important properties of Tc (VII) are its relatively greater ease of reduction and the slowness of some intermediate steps in the reduction process. Pertechnetate ion is reduced to a lower oxidation state by hydrochloric acid, thiocyanate ion (64), and by organic impurities present in tetraphenylarsonium chloride (72), anion exchange resin (73), and some organic solvents. Yet the complete reduction to Tc (IV) is slow, and by analogy with rhenium (63) a multiplicity of reaction products may be expected. Unless precautions are taken to maintain technetium in the appropriate oxidation state, erratic results will be obtained.

Many radiochemical procedures for Tc have been developed (1, 4, 12, 50, 74, 75). All of these may be resolved into a small number of basic operations, e.g. distillation, sulfide precipitation, etc. In order to avoid the repetition that a discussion of the complete procedures would entail, only a discussion of these basic operations will be given.

Distillation.—Because of the volatility of Tc₂O₇, technetium may be co-distilled with acids. Perchloric acid gives good yields and even a partial separation from rhenium (66, 76) but carries RuO₄ quantitatively. Molybde-

num is carried to a significant extent, unless complexed by phosphoric acid (56, 77). Sulfuric acid (74) gives a clean separation from Ru (78), but the yields of Tc are occasionally very poor as a result of its reduction by trace impurities in the acid (7, 67, 70). Much more reproducible results are obtained in the presence of oxidizing agents [e.g. Ce (IV), HNO_3 , CrO_3 , etc.]), but since RuO_4 distills under these conditions, it has to be removed in a separate step. Because of the great difference in vapor pressures of the heptoxides at low temperatures, Tc may be separated from Re by repeated alternating evaporations with HNO_3 and HCl (79). One may also take advantage of the greater ease of reduction of Tc to separate it from Re. When 6N HCl is distilled into 80 per cent H_2SO_4 at $180^\circ\text{--}200^\circ\text{C}$., Re volatilizes, while most of the Tc stays behind [Perrier & Segrè (74)]. Separation factors of up to 50 have been obtained by this procedure [Morgan & Sizeland (71)].

Sublimation.—Technetium heptoxide may be separated from molybdenum trioxide by fractional sublimation at $\geq 300^\circ\text{C}$. (8, 74).

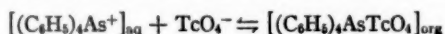
Precipitation as sulfide.—As little as 3 mg./l. of technetium may be precipitated by H_2S from 4 M H_2SO_4 (40, 70). At lower concentrations, the sulfides of Pt, Re, Cu, Mn, and many other elements may be used as carriers. Detailed studies on the optimum conditions for coprecipitation have been made (70, 71, 74, 80). Thioacetamide (67) or sodium thiosulfate (50, 53) may be used to advantage instead of hydrogen sulfide.

Many other elements in this region of the periodic table precipitate under the same conditions, so that the method is more useful for purposes of concentration than separation. However, the lower oxidation states of Tc do not precipitate with H_2S in strongly acid solutions, and one may, therefore, separate Tc from Re by conducting the precipitation in a medium that reduces Tc (VII), e.g. ≥ 6 N HCl (50, 70, 74).

Precipitation of insoluble pertechnetates.—Pertechnetate forms slightly soluble salts with large cations e.g. Tl^+ , Ag^+ , Cs^+ , nitron, and $(\text{C}_6\text{H}_5)_4\text{As}^+$. At 0°C ., precipitation with the last-mentioned reagent is feasible at concentrations as low as 5 mg. Tc/l. (37). At lower concentrations, any of the XY_4^- anions may be used as carriers: e.g. ReO_4^- , ClO_4^- , IO_4^- , and BF_4^- (50, 78, 81). In basic solutions, molybdenum does not interfere. Decontamination from other fission products is excellent: a single-step β -decontamination factor of 10^5 has been reported. The principal remaining contaminants are Zr, Nb, and Ru (81). Coprecipitation with $(\text{C}_6\text{H}_5)_4\text{AsReO}_4$ is probably the fastest known separation method for Tc; when, milking 5 sec. Tc^{102} from 11.5 min. Mo^{102} , Flegenheimer & Seelmann-Eggebert (82) were able to precipitate and filter the sample in 5 to 6 sec.

Removal of the technetium from the organic precipitate may be accomplished by wet combustion, by electrolysis in concentrated H_2SO_4 , or by passing an alcohol solution of the precipitate through an anion exchanger in the chloride form. The organic cation passes through the exchanger, while the pertechnetate is adsorbed and may be subsequently eluted by HClO_4 (12, 19).

Solvent extraction.—Considerable work has been done on the solvent extraction behavior of pertechnetate ion. Goishi & Libby (83) found that pyridine extracts TcO_4^- from 4 *N* NaOH solution with a partition coefficient of 778. Perrhenate and permanganate are extracted to a similar degree. Pertechnetate also extracts into chloroform in the presence of tetraphenylarsonium ion (72). The equilibrium constant for the reaction:



is $\sim 3 \times 10^6$. The decontamination from fission products should be at least as good as in the precipitation reaction, if care is taken to remove iodine before extraction. Trivalent gold as chloro- or bromoaurate is also extracted and must be removed by reduction with H_2O_2 , or by distillation.

Extraction of TcO_4^- into hexone, butex, and other solvents has also been investigated (4, 71, 84). Of particular interest are the recent extensive studies of Gerlit (50) and Boyd & Larson (85). Gerlit investigated the extraction of Tc, Re, Mo, and Ru into 21 organic solvents, from acid, alkaline, and neutral solutions. In acid solution, alcohols, ketones, and tributyl phosphate are the best extractants for ReO_4^- and TcO_4^- ; in basic solution, ketones and cyclic amines. Many possible separations of Tc from Ru and Mo may be inferred from his data. Boyd & Larson conducted an exceedingly thorough study of 34 solvents and found that tertiary amines as well as quaternary ammonium salts gave the largest partition coefficients. Strongly basic solvents (e.g. amines) extract TcO_4^- as an "-onium" salt, whereas solvents of lower basicity extract either free pertechnetic acid or an inorganic pertechnetate (50, 85, 86).

Back-extraction of the technetium into the aqueous phase may be accomplished in several ways. In some cases, a pH change will suffice; in others, displacement by another anion such as perchlorate, nitrate, or bisulfate is most effective. A third possibility was pointed out by Gerlit: the partition coefficient in a given oxygen-containing solvent may be decreased sufficiently by addition of a nonpolar solvent to permit quantitative back-extraction into the aqueous phase.

The principal disadvantage of all extraction methods is the inevitable introduction of organic matter which may reduce TcO_4^- and cause difficulties in subsequent steps.

Chromatography.—Pertechnetate and perrhenate ions are very strongly adsorbed by most anion exchangers (70, 71, 87, 88) and may be separated by ion-exchange chromatography. The ratio of the distribution coefficients is ~ 1.6 to 2, i.e. comparable to adjacent rare earths. Good separations therefore require some care and tend to be slow (≥ 3 hr.). Among the ions used as elutriants are thiocyanate (89, 90), perchlorate (4, 73, 91, 92), and nitrate (88). Perchlorate ion gives the best separations and interferes least with subsequent operations. Because of some peculiarities of commercial resins, the highest practically attainable separation factors are 10^4 – 10^5 (73). Molybdenum is also adsorbed by anion exchange resins and may be eluted

by hydroxide (92, 93), oxalate (90), or hydrochloric acid (94). Separation factors of $>10^3$ should be readily attainable.

Technetium can also be separated from molybdenum by paper chromatography (95). The separation from rhenium is incomplete under most conditions, except when Tc is selectively reduced by HCl (96).

Miscellaneous methods.—Technetium may be separated from molybdenum by extracting the latter into ether from 6 N HCl (74) or precipitating it with Pb^{++} , Ag^+ , 8-hydroxyquinoline, or α -benzoinoxime (1, 69, 80). Although the separation factors are low ($\sim 10^2$), these methods are rapid and offer advantages in certain situations. Electrodeposition from 2 N NaOH solutions will separate macroamounts of Tc from Mo and Re (59). A good separation from Re may be obtained by reducing Tc (VII) with concentrated HCl and coprecipitating the Tc (IV) with $Fe(OH)_3$. The Tc is oxidized to the +7 state by dissolving the precipitate in concentrated HNO_3 , and the Fe^{3+} is removed by precipitation with ammonia (50). Another separation from rhenium is based on the fact that Tc, but not Re, will form a complex with phthalocyanin (97). The copper complex may be used as a carrier in this reaction. Technetium and ruthenium may be separated by distilling RuO_4 in a chlorine stream (98) or by reducing RuO_4 or RuO_4^- to RuO_2 by means of alcohol or formaldehyde (74, 76). Separation factors of the order of 10^2 have been obtained by the latter procedure.

Assay methods.—Even the long-lived isotopes of Tc can be readily determined by means of their radioactivity. The specific activity of Tc^{99} is 37.8 d/min. per 10^{-9} g., an amount that is easily detectable despite the softness of its radiation. An even smaller amount of the longer-lived Tc^{98} , e.g. 2.6 d/min. or 5×10^{-10} g., has been measured by β - γ coincidence counting (99). Neutron activation analysis gives even higher sensitivities for these two isotopes, i.e. 2×10^{-11} g. and 1×10^{-12} g., respectively (4, 67, 91), although the method is not without its pitfalls.

In the absence of Cr and Re, the strongest lines in the optical emission spectrum of Tc are sufficiently free from interference to be used for its identification. As little as 10^{-8} g. of Tc may be detected (100). The strong absorption of TcO_4^- in the ultraviolet has been used for its quantitative determination (8), and the red thiocyanate complex of Tc (V) should serve this purpose even better (64). A polarographic method sensitive to 5×10^{-8} g. has also been reported (101). All these methods are subject to interferences, and should be employed with caution.

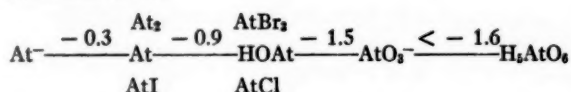
For gravimetric determinations, tetraphenylarsonium pertechnetate is most satisfactory although the sulfide may be used with proper precautions (40).

CHEMISTRY OF ASTATINE

From its position in the periodic table, one may expect astatine to resemble iodine fairly closely, though some second-order differences should

exist. For example, the +7 oxidation state of astatine should be somewhat less stable and the electropositive character of the lower oxidation states more pronounced than in the case of iodine. Unfortunately, the chemistry of iodine on a tracer scale occasionally differs greatly from its macrochemistry (102, 103). Not only do new ionic species appear at low concentrations, but the situation is further complicated by reactions with ever-present impurities, by adsorption effects, and by radiocolloid formation. These facts must be kept in mind when attempting to interpret the behavior of astatine at low concentrations.

At least four oxidation states of astatine are known at present: a (-1) state that coprecipitates with AgI; a zero state that is extractable into organic solvents; a (+5) state that carries on insoluble iodates; and an intermediate state (+3?) that neither extracts into organic solvents nor carries on insoluble iodates. A tentative oxidation potential diagram has been suggested by Appelman (104).



Oxidation state 0.—When astatine is isolated from a bismuth target by volatilization, it shows many properties expected of the zero oxidation state. It is volatile from glass surfaces at room temperature but is strongly adsorbed by metals such as silver, gold, and platinum. Adsorption by silver remains high at 325°C., indicating the formation of a stable compound (105). Astatine (0) is soluble in nitric acid and is generally used in this form for tracer studies.

Astatine zero extracts readily from nitric acid solutions into organic solvents such as C_6H_6 or CCl_4 . The partition coefficients are rather variable and depend mainly on the type of impurities present. If the organic phase containing At (0) is washed repeatedly with dilute HNO_3 , the partition coefficient approaches a limiting value (e.g. 90 for CCl_4). Most of the astatine can be back-extracted into the aqueous phase by 0.1 *M* NaOH, probably because of hydrolysis to the (-1) and a higher state (105). However, it has not been possible to decide on the basis of present evidence whether the extractable species is At_2 or At.

With the exception of At (0) and interhalogen compounds, none of the other oxidation states extract into inert organic solvents. It is, therefore, possible to study the reactions of At (0) by exposing it to oxidizing, reducing, and complexing agents and by observing any changes in the partition coefficient.

This method has been used in a qualitative way by Johnson, Leininger & Segrè (105). A decrease of the partition coefficient was observed with the following reagents. (a) Reducing agents, such as SO_2 or H_3AsO_3 . Evidently, At (0) is reduced to At^- . The reaction with H_3AsO_3 is slow at room tempera-

ture. (b) Some halogens or halogen compounds, e.g. Br_2 , I^- , and HCl . Presumably, interhalogen compounds are formed. In the case of Br_2 , oxidation to an intermediate state, e.g. HAtO_2 , is an alternative possibility, and the reaction is further complicated by extreme photosensitivity (104). (c) Oxidizing agents, e.g. $\text{S}_2\text{O}_8^{2-}$, IO_3^- , Fe^{3+} , and Hg^{++} . The reaction with the first two reagents is slow and leads to a state that coprecipitates with insoluble iodates, presumably AtO_3^- . The reaction with Fe^{3+} produces an intermediate state that is neither extracted by organic solvents nor coprecipitated with AgIO_3 . Recently, Appelman (104) has shown that the apparent oxidation by Fe^{3+} is actually a photochemical reaction. No further information is available on the reaction with Hg^{++} , but it would seem that a weakly ionized HgAt_2 or a complex such as HgAt_4^{2-} is more likely a product than a higher oxidation state of astatine.

It is also significant that Fe^{2+} reduces higher states of astatine to At (0), but not to At^- (105). Distillation experiments from a variety of media (e.g. HNO_3 , HCl , HClO_4 , H_2SO_4 , etc.) indicate that the nonvolatile states of astatine present in most of these solutions can be reduced to volatile At (0) by Fe^{2+} (105).

The electrodeposition of At from HNO_3 and H_2SO_4 has been studied (105). Both anodic and cathodic deposition was observed, but the nature of the deposited species could not be established. A potential of -0.7 v. for the At^-/At_2 couple has been calculated by Haissinsky (109). The first ionization potential of astatine has been estimated as 9.2, 10.4, or 9.65 ev (33, 106, 107, respectively) and the second as 20.1 ev. (33). The ground state frequency of the At_2 molecule has been estimated as $172.9 \pm 4.3 \text{ cm}^{-1}$ (108).

Interhalogen compounds.—When the extraction is conducted in the presence of a redox buffer, the results are much more reproducible and lend themselves to quantitative interpretation. If the redox buffer is a halogen couple, e.g. I^-/I_2 , the dominant species are interhalogen compounds such as AtI and AtI_2^- . The former extracts into CCl_4 with a partition coefficient of 6, while for the more polar AtBr a value of 0.04 is obtained (104). Appelman has also succeeded in measuring equilibrium constants for many reactions involving compounds of astatine with other halogens, and one may await the publication of his results with interest.

Neumann (110, 111) has studied the extraction of astatine from HCl solutions. A neutral and a negatively charged species seem to be present in solutions that have been oxidized with HNO_3 or Cl_2 . By analogy with iodine, the species have been tentatively designated AtCl and AtCl_2^- , respectively, although the experimental evidence is equally consistent with an assignment to AtCl_3 and AtCl_4^- , respectively. In $\geq 3M$ HCl , AtCl_2^- is the principal species. It extracts readily into isopropyl ether but not into CCl_4 or benzene.

Oxidation state (-I).—When treated with strong reducing agents such as Zn or SO_2 in acid and Na_2SO_3 in basic solution, At (0) is reduced to what appears to be At^- , as indicated by electromigration experiments and copre-

cipitation with AgI (2, 105). The astatide ion is expected to show strong ultraviolet absorption at ~ 3000 Å (112). The ratio of the diffusion coefficients $D_{I^-}/D_{At^-} = 1.41 \pm 0.02$ in 1 per cent NaCl solution containing 1.2×10^{-3} M KI and 4×10^{-3} Na₂SO₃ (113). Some indications for the formation of a volatile hydride have been obtained (2).

Oxidation state +3.—This oxidation number has been tentatively assigned to a very nondescript state of astatine that does not coprecipitate with AgI, extract into organic solvents, or carry on insoluble iodates. It is produced by the action of moderately strong oxidizing agents, e.g. Br₂ or vanadium (V) on At (0) (14, 104, 105), and by the photochemical oxidation of At (0) in the presence of Fe (III). There is no evidence to suggest that the same species is produced in all these reactions. Anion-exchange studies of astatine would be highly desirable.

Oxidation states +5, +7.—When At (0) solutions are treated with strong oxidizing agents, such as Cr₂O₇²⁻, S₂O₈²⁻, Ce (IV), Cl₂, IO₄⁻, and NaBiO₃, a state is formed that does not extract into CCl₄, but is quantitatively carried on silver, lead, and barium iodates and lanthanum hydroxide (14, 104, 105). Since no activity was carried by potassium periodate, it is possible that perastatate ion was not produced under any of these conditions. However, in view of the bewildering variety of periodate anions (114) a definite conclusion cannot be drawn without further evidence. An ionic radius of 0.62 Å for At⁷⁺ has been calculated (43).

Organic chemistry of astatine.—Because of the limited range and high specific ionization of α -radiation, astatine-labeled compounds are ideally suited for localization of radiation within cells. Hughes *et al.* have, therefore, prepared several organic compounds of astatine of potential biological usefulness (115, 116, 117). Astatobenzene, *p*-astatobenzoic acid, and astatinated serum albumin were obtained by the diazo reaction; astatinated ovalbumin and γ globulin, by direct astatination in the presence of KI₃; and astatinated tyrosine, by reaction of astatine and N-iodosuccinimide. The product resembled the corresponding iodine compound in each case.

Neumann (110) observed that both benzene and phenol reacted with AtCl, but the products were not identified.

Analytical chemistry of astatine.—Astatine can be isolated from bismuth targets by volatilization at 300–700°C. It condenses at liquid-air to dry-ice temperatures and may be purified by resublimation at room temperature and collected in HNO₃, NaOH, or on a silver foil (2, 105, 117, 118). If a target material other than Bi is used (e.g. Au), it may be dissolved in molten Pb or Bi (119). Special precautions are sometimes required to prevent subsequent radiocolloid formation (120, 121).

Alternatively, the bismuth target may be dissolved in HNO₃, the solution made 8 M in HCl, and the astatine extracted into isopropyl ether (110, 118). Other methods, involving precipitation of bismuth as the phosphate, have been described (122).

Many coprecipitation reactions of astatine are known. Astatine (0) is

carried quantitatively by the sulfides of Bi, Hg, Ag, and Sb; rather less completely by HgO , $\text{Fe}(\text{OH})_3$, $\text{Al}(\text{OH})_3$ and $\text{La}(\text{OH})_3$; and not at all by PbCl_2 and TlI (2, 105). It also coprecipitates with PdI_2 , Te, and Ag in the presence of SO_2 (2, 122). Even the reactions given in the first paper of Corson, MacKenzie & Segrè were sufficient to permit the separation of At from all known elements.

A rapid separation of At from Po, Bi, and Pb may be effected by adding 2 per cent tributyl phosphate to an astatine solution in isopropyl ether and contacting it with $2M \text{HNO}_3$ – $4M \text{HCl}$. Only astatine remains in the organic phase under these conditions (118).

Methods for the quantitative determination of At have been described (122, 123). The astatine is coprecipitated with tellurium, or deposited on metallic silver, and determined by α -counting. Good results are also obtained by liquid scintillation counting (124), or by x-ray counting.

Biological effects.—Like iodine, astatine is selectively concentrated in thyroid tissue. Extensive studies of the subject have been made by Hamilton *et al.* (120, 121, 125, 126).

LITERATURE CITED

1. Perrier, C., and Segrè, E., *J. Chem. Phys.*, **5**, 712 (1937)
2. Corson, D. R., MacKenzie, K. R., and Segrè, E., *Phys. Rev.*, **57**, 672 (1940)
3. Hyde, E. K., and Ghiorso, A., *Phys. Rev.*, **90**, 267 (1953)
4. Alperovitch, E., *Contribution to the Problem of Naturally Occurring Technetium* (Doctoral thesis, Columbia Univ., New York, N. Y., January, 1954)
5. *Gmelin's Handbuch der anorganischen Chemie, System-Nr. 69/70, Manganese. Rhenium*, 8th Ed. (Verlag Chemie, Berlin, 154 pp., 1955)
6. Druce, J. G. F., *Rhenium* (University Press, Cambridge, Engl., 92 pp., 1948)
7. Boyd, G. E., Larson, Q. V., and Motta, E. E., *Isolation of Milligram Quantities of Long-Lived Technetium from Neutron Irradiated Molybdenum* (Unpublished manuscript, 1954); see also *U. S. Atomic Energy Commission Document, AECD-2151* (1948)
8. Fried, S., and Hall, N. F., *Chemistry of Technetium* (Presented at Spring Meeting Am. Chem. Society, April 1950); see also *Phys. Rev.*, **81**, 741 (1951)
9. Boyd, G. E., Motta, E. E., and Larson, Q. V., *U. S. Atomic Energy Commission Report, MonC-99* (April 1, 1947)
10. Hackney, J. C., *J. Chem. Educ.*, **28**, 186 (1951)
11. Segrè, E., *I. nuovi elementi chimici*, 21-30, 41-54, *Conf. Donegani* (Accademia Nazionale dei Lincei, Rome, Italy, 118 pp., 1953)
12. Boyd, G. E., *J. Chem. Educ.*, **36**, 3 (1959)
13. Bagnall, K. W., *Chemistry of the Rare Radioelements*, 97-102 (Academic Press, Inc., New York, N. Y., 177 pp., 1957)
14. Hyde, E. K., *J. Chem. Educ.*, **36**, 15 (1959)
15. Strominger, D., Hollander, J. M., and Seaborg, G. T., *Revs. Mod. Phys.*, **30**, 585 (1958)
16. Boyd, G. E., *Record of Chem. Progr.*, **12**, 67 (1951)
17. Hyde, E. K., *J. Phys. Chem.*, **58**, 21 (1954)
18. Fried, S., *J. Am. Chem. Soc.*, **70**, 442 (1948)
19. Cobble, J. W., Nelson, C. M., Parker, G. W., Smith, W. T., Jr., and Boyd, G. E., *J. Am. Chem. Soc.*, **74**, 1852 (1952)
20. Parker, G. W. [Private communication quoted in Boyd, G. E., *J. Chem. Educ.*, **36**, 3 (1959)]
21. Mooney, R. C. L., *Acta Cryst.*, **1**, 161 (1948)
22. Bridgman, P. W., *Proc. Am. Acad. Arts Sci.*, **84**, 117 (1955)
23. Nelson, C. M., Boyd, G. E., and Smith, W. T., Jr., *J. Am. Chem. Soc.*, **76**, 348 (1954)
24. Daunt, J. G., and Cobble, J. W., *Phys. Rev.*, **92**, 507 (1953)
25. Parker, G. W., *U. S. Atomic Energy Commission Report, ORNL-1260* (May, 1952)
26. Timma, D., *J. Optical Soc. Am.*, **39**, 898 (1959)
27. Meggers, W. F., and Scribner, B. F., *J. Research Natl. Bur. Standards*, **45**, 476 (1950)
28. Meggers, W. R., *Spectrochim. Acta*, **4**, 317 (1951)
29. Burkhart, L. E., Peed, W. F., and Saunders, B. G., *Phys. Rev.*, **73**, 347 (1948)
30. Marmier, P., Blaser, J. P., Preiswerk, P., and Scherrer, P., *Helv. Phys. Acta*, **22**, 155 (1949)
31. Rogosa, G. L., and Peed, W. F., *Phys. Rev.*, **100**, 1763 (1955)

32. Moore, C. E., *Atomic Energy Levels, Vol. III, NBS Circular 467* (U. S. Govt. Printing Office, Washington 25, D. C., 1958)
33. Finkelnburg, W., and Humbach, W., *Naturwissenschaften*, **42**, 35 (1955)
34. Michaelson, H. B., *J. Appl. Phys.*, **21**, 536 (1950)
35. Boyd, G. E., Cobble, J. W., Nelson, C. M., and Smith, W. T., Jr., *J. Am. Chem. Soc.*, **74**, 556 (1952)
36. Smith, W. T., Jr., Cobble, J. W., and Boyd, G. E., *J. Am. Chem. Soc.*, **75**, 5773 (1953); **75**, 5777 (1953)
37. Parker, G. W., and Martin, W. J., *U. S. Atomic Energy Commission Document, ORNL-1116* (1952)
38. Zachariasen, W. H. [Private communication to G. E. Boyd, quoted in Boyd, G. E., *J. Chem. Educ.*, **36**, 3 (1959)]
39. Busey, R. H., and Larson, Q. V., *U. S. Atomic Energy Commission Document, ORNL-2584* (1958)
40. Rulfs, C. L., and Meinke, W. W., *J. Am. Chem. Soc.*, **74**, 235 (1952)
41. Wu, C. S. (Personal communication, Sept., 1950)
42. Cobble, J. W., *J. Chem. Phys.*, **21**, 1443 (1953)
43. Ahrens, L. H., *Geochim. Cosmochim. Acta*, **2**, 155 (1952)
44. Boyd, G. E. (Private communication, February, 1959)
45. Cartledge, G. H., *J. Am. Chem. Soc.*, **77**, 2658 (1955)
46. Cartledge, G. H., *Corrosion*, **11**, 335t (1955)
47. Cartledge, G. H., *J. Phys. Chem.*, **59**, 979 (1955)
48. Cartledge, G. H., *J. Phys. Chem.*, **60**, 28 (1956)
49. Sympton, R. F., and Cartledge, G. H., *J. Phys. Chem.*, **60**, 1037 (1956)
50. Gerlit, J. B., *Proc. Internat. Conf. Peaceful Uses of Atomic Energy, Geneva, 1955*, **7**, 145 (1956)
51. Geilmann, W., and Lange, F., *Z. anal. Chem.*, **126**, 321 (1943)
52. Geilmann, W., Wiechmann, F., and Wrigge, F. W., *Z. Anal. Chem.*, **126**, 418 (1943)
53. Geilmann, W., and Bode, H., *Z. anal. Chem.*, **130**, 222 (1950)
54. Sites, J. R., Baldock, C. R., and Gilpatrick, L. O., *U. S. Atomic Energy Commission Document, ORNL-1327* (1952)
55. Bainbridge, K. T., Goldhaber, M., and Wilson, E., *Phys. Rev.*, **84**, 1260 (1951)
56. Bainbridge, K. T., Goldhaber, M., and Wilson, E., *Phys. Rev.*, **90**, 430 (1953)
57. Dzhelepov, B. S., and Kraft, O. E., *Vestnik Leningrad. Univ.*, **10**, No. 8, *Ser. Mat. Fiz. i Khim.*, No. 3, 97 (1955)
58. Magneli, A., and Anderson, G., *Acta Chem. Scand.*, **9**, 1378 (1955)
59. Rogers, L. B., *J. Am. Chem. Soc.*, **71**, 1507 (1949)
60. Knox, K., Tyree, S. Y., Jr., Srivastava, R. D., Norman, V., Bassett, J. Y., Jr., and Holloway, J. H., *J. Am. Chem. Soc.*, **79**, 3358 (1957)
61. Low, W., and Llewellyn, P. M., *Phys. Rev.*, **110**, 842 (1958)
62. Maun, E. K., *Investigations in the Chemistry of Rhenium* (Doctoral thesis, Calif. Inst. of Technol., Pasadena, Calif., 1949)
63. Maun, E. K., and Davidson, N., *J. Am. Chem. Soc.*, **72**, 2254 (1950)
64. Crouthamel, E. C., *Anal. Chem.*, **29**, 1756 (1957)
65. Motta, E. E., Boyd, G. E., and Larson, Q. V., *Phys. Rev.*, **72**, 1270 (1947)
66. Parker, G. W., Reed, J., and Ruch, J. W., *U. S. Atomic Energy Commission Document, AECD-2043* (1948)
67. Anders, E. (Unpublished data, September, 1951)

68. Thomason, P. F., *U. S. Atomic Energy Commission Document, ORNL-2453* (1958)
69. Flagg, J. F., and Bleidner, W. E., *J. Chem. Phys.*, **13**, 269 (1945)
70. Boyd, G. E., Larson, Q. V., and Motta, E. E., *U. S. Atomic Energy Commission Document, AECD-2151* (1948)
71. Morgan, F., and Sizeland, M. L., *United Kingdom Atomic Energy Authority Report AERE C/M 96* (1950)
72. Tribalat, S., and Beydon, J., *Anal. Chim. Acta*, **8**, 22 (1953)
73. Sen Sarma, R. N., Anders, E., and Miller, J. M., *J. Phys. Chem.*, **63**, 559 (1959)
74. Perrier, C., and Segrè, E., *J. Chem. Phys.*, **5**, 712 (1937)
75. Krohn, N. A., *U. S. Atomic Energy Commission Document, CF-54-7-196* (1954)
76. Glendenin, L. E., *Nat. Nuclear Energy Ser., Div. IV-9*, Paper 258, 1542 (1951)
77. Mihelich, J. W., Goldhaber, M., and Wilson, E., *Phys. Rev.*, **82**, 972 (1951)
78. Glendenin, L. E., *Natl. Nuclear Energy Ser., Div. IV-9*, Paper 259, 1545 (1951)
79. Sugarman, N., and Richter, H., *Phys. Rev.*, **73**, 1411 (1948)
80. Jacobi, E., *Helv. Chim. Acta*, **31**, 2118 (1948)
81. Parker, G. W., and Martin, W. J., *U. S. Atomic Energy Commission Document, ORNL-870* (1950)
82. Flegenhimer, J., and Seelmann-Eggebert, W., *Proc. Intern. Conf. Peaceful Uses of Atomic Energy, Geneva, 1955*, **7**, 152 (1956)
83. Goishi, W., and Libby, W. F., *J. Am. Chem. Soc.*, **74**, 6109 (1952)
84. Johns, D. H., *Tracer Studies on Technetium Separations* (Doctoral thesis, Univ. of Wisconsin, Madison, Wis., 1954)
85. Boyd, G. E., and Larson, Q. V., *U. S. Atomic Energy Commission Document, ORNL-2159* (1956)
86. Boyd, G. E., and Larson, Q. V., *U. S. Atomic Energy Commission Document, ORNL-2584* (1958)
87. Kraus, K. A., and Nelson, F., *Proc. Intern. Conf. Peaceful Uses of Atomic Energy, Geneva, 1955*, **7**, 113 (1956)
88. Huffman, E. H., Oswalt, R. L., and Williams, L. A., *J. Inorg. & Nuclear Chem.*, **3**, 49 (1956)
89. Atteberry, R. W., and Boyd, G. E., *J. Am. Chem. Soc.*, **72**, 4805 (1950)
90. Hall, N. F., and Johns, D. H., *J. Am. Chem. Soc.*, **75**, 5787 (1953)
91. Alperovitch, E., and Miller, J. M., *Nature*, **176**, 299 (1955)
92. Boyd, G. E., and Larson, Q. V., *J. Phys. Chem.*, **60**, 707 (1956)
93. Fisher, S. A., and Meloche, V. W., *Anal. Chem.*, **24**, 1100 (1952)
94. Kraus, K. A., Nelson, G. F., and Moore, G. E., *J. Am. Chem. Soc.*, **77**, 3972 (1955)
95. Lederer, M., *Anal. Chim. Acta*, **12**, 146 (1955)
96. Levi, M., and Lederer, M., *J. Inorg. & Nuclear Chem.*, **4**, 381 (1957)
97. Herr, W., *Z. Naturforsch.*, **9a**, 907 (1954)
98. Gile, J. D., Garrison, W. M., and Hamilton, J. G., *U. S. Atomic Energy Commission Document, UCRL-1419* (1951)
99. Anders, E., *Phys. Rev.*, **110**, 427 (1958)
100. Slavin, M. (Personal communication, November, 1952)
101. Miller, H. H., *U. S. Atomic Energy Commission Document, ORNL-1880* (1955)
102. Kahn, M., and Wahl, A. C., *J. Chem. Phys.*, **21**, 1185 (1953)
103. Good, M. L., and Edwards, R. R., *J. Inorg. & Nuclear Chem.*, **2**, 196 (1956)
104. Appelman, E. H. (Private communication, October, 1958 and March, 1959)

105. Johnson, G. L., Leininger, R. F., and Segrè, E., *J. Chem. Phys.*, **17**, 1 (1949)
106. Varshni, T. P., *Z. Physik.*, **135**, 512 (1953)
107. Piccardi, G., *Atti accad. Nazl. Lincei* [6] **6**, 428 (1927)
108. Majumdar, K., and Varshni, Y. P., *Indian J. Phys.*, **28**, 103 (1954)
109. Haissinsky, M., *Comité intern. thermodynam. et cinét. electrochim.*, *Compt. rend. réunion*, 1951, 218 (1952); *Chem. Abstr.*, **46**, 1857a (1942)
110. Neumann, H. M., *J. Inorg. & Nuclear Chem.*, **4**, 349 (1957)
111. Neumann, H. M. (Private communication, March, 1959)
112. Platzman, R. L., and Franck, J., *Research Council Israel, Spec. Publ. No. 1*, 21 (1952)
113. Durbin, P. W., *U. S. Atomic Energy Commission Document, UCRL-3013* (1955)
114. Sidgwick, N. V., *The Chemical Elements and their Compounds*, 1237-39 (Oxford University Press, Oxford, Engl., 1703 pp., 1950)
115. Hughes, W. L., and Gitlin, D., *U. S. Atomic Energy Commission Document BNL-314* (1954); see also *Federation Proc.*, **14**, 229 (1955)
116. Hughes, W. L., and Klinenberg, J., *U. S. Atomic Energy Commission Document, BNL-367* (1955)
117. Hughes, W. L., Smith, E., and Klinenberg, J., *U. S. Atomic Energy Commission Document, BNL-406* (1956)
118. Barton, G. W., Jr., Ghiorso, A., and Perlman, I., *Phys. Rev.*, **82**, 13 (1951)
119. Burcham, W. E., *Proc. Phys. Soc. (London)*, **67A**, 555 (1954)
120. Hamilton, J. G., Parrott, M., Johnston, M., and Durbin, P. W., *U. S. Atomic Energy Commission Document, UCRL-2418* (1953)
121. Parrott, M., Garrison, W. M., Durbin, P. W., Johnston, M., Powell, H. S., and Hamilton, J. G., *U. S. Atomic Energy Commission Document, UCRL-3065* (1955)
122. Aten, A. H. W., Jr., Doorgeest, T., Hollstein, U., and Moeken, H. P., *Analyst*, **77**, 774 (1952)
123. Garrison, W. M., Gile, J. D., Maxwell, R. D., and Hamilton, J. G., *Anal. Chem.*, **23**, 204 (1951)
124. Basson, J. K., *Anal. Chem.*, **28**, 1472 (1956)
125. Hamilton, J. G., and Soley, M. H., *Proc. Natl. Acad. Sci. U. S.*, **26**, 433 (1940)
126. Hamilton, J. G., Asling, C. W., Garrison, W. M., and Scott, K. G., *The Accumulation, Metabolism, and Biological Effects of Astatine in Rats and Monkeys* (Univ. of California Press, Berkeley, Calif., 1953)

SOLVENT EXTRACTION IN RADIOCHEMICAL SEPARATIONS^{1,2}

BY HENRY FREISER

Department of Chemistry, University of Arizona, Tucson, Arizona
AND

GEORGE H. MORRISON

Research Laboratories, Sylvania Electric Products, Inc., Bayside, New York

The last several years have seen a reawakening appreciation of the value of solvent extraction separations processes both on analytical and process scales. Separations by solvent extraction are simple, convenient, clean, and applicable equally well to carrier-free tracer and macro amounts of materials. They usually require apparatus as uncomplicated as a separatory funnel and may readily be adapted to remote handling procedures.

A variety of separations techniques have been applied to the problems of isolation and radiochemical purification of nuclides. General descriptions and recent surveys of radiochemical separations can be found in references (1) through (5). Although all of the separation methods mentioned are of great importance to the radiochemist, solvent extraction is particularly well suited to the purification of many radioisotopes since, after several extractions of a substance, the final product is usually relatively free from extraneous impurities which may be present when other separation procedures are employed. Also, if the isotope of interest has a short half life, a rapid separation is essential and extraction procedures have proved invaluable. Most of the extractions employed in radiochemistry are based on previously developed conventional analytical extractions, and the recent book by the authors (6) offers a comprehensive treatment of the subject of extraction as applied to inorganic analysis. In addition to covering the principles and practical aspects of the technique, procedures for the extraction of the elements are presented. The review by the authors (7) in *Analytical Chemistry* surveys the latest developments in the field.

CLASSIFICATION OF SOLVENT EXTRACTION SYSTEMS

Most metal salts are strong electrolytes that are relatively insoluble in organic solvents and soluble in water because of its ability to solvate the ions as well as because of its high dielectric constant. Since it is usually necessary to transform the hydrated metal ion into an uncharged complex in order to extract it into an organic solvent, it is convenient to classify metal extraction systems on the basis of the nature of the extractable metal

¹ The survey of literature pertaining to this review was completed in December, 1958.

² Among the abbreviations used in this chapter are: EDTA (ethylenediaminetetraacetic acid); HDGP (dioctylphenyl orthophosphoric acid); TBP (tributyl phosphate); TTA (thenoyltrifluoroacetone).

complex involved. Thus, two broad categories of metal complexes—chelates and ion association complexes—may be distinguished. These categories are utilized in the classification scheme outlined in Table I (7). The names applied to the systems are indicative of the reagents used to achieve complex formation.

Under chelate extraction systems are included only those involving uncharged chelates. Since charged chelates must pair with oppositely charged ions to form extractable species, these are properly classified with the ion association systems. It may be noted that the chelate systems are divided in groups based on the size of the chelate ring formed.

The ion association systems are classified according to the charge of the metal-containing ion. Systems containing the metal in the anion may sometimes be referred to in terms of the "onium" cation with which it is associated. With "oxonium" systems are encountered extractions in which the solvent plays an important role, namely, participation in complex formation. Such systems are usually characterized by the need for an oxygen-containing solvent (such as an alcohol, ether, ester, ketone, etc.) for successful extraction. Furthermore, the basicity of the solvent molecule will be an important factor in determining its efficacy in extraction. Thus, the extraction of iron (III) as chloroferric acid may be accomplished more readily with ethyl ether as solvent than with the more weakly basic dichloroethyl ether.

There is some degree of overlap in "onium" usage since some systems containing the metal in the cation may also be referred to in this way. As a case in point might be cited the nitrate extraction systems, such as that of uranyl nitrate. The extraction of uranyl nitrate into oxygen-containing solvents proceeds through the formation of a complex in which solvent molecules are coordinated to the uranyl cation. Again solvent basicity is a determining factor in ease of extraction. As more basic solvents are employed, inert diluents may be tolerated. Trialkylphosphine oxides, considered a separate system, form such strong oxonium complexes that the reagent is used in tenth-molar solution in a hydrocarbon diluent.

PRINCIPLES OF SOLVENT EXTRACTION

Distribution law.—The classical distribution law which describes as constant the ratio of solute concentrations in each of two immiscible solvents must be modified when the solute participates in chemical interactions in either solvent. Since this is almost invariably the case in metal extractions, it is important to distinguish between the constant distribution coefficient K_D , which characterizes the distribution of a particular species essentially identical in either phase, and the distribution ratio D , the stoichiometric ratio of concentrations including all forms of the component of interest in each of the respective phases. One of the major objectives of solvent extraction theory is to develop expressions based on considerations of the various chemical equilibria involved in extraction permitting the prediction of the variation of D values with the extraction conditions.

TABLE I
METAL EXTRACTION SYSTEMS (7)

	<i>Reactive Grouping</i>
I. Chelate Systems	
A. 4-membered ring systems	
1. Dialkylthiocarbamates	$-\text{N}-\text{C}-\text{S}^{(-)}-$
2. Xanthates	$-\text{S}=\text{C}-\text{S}^{(-)}-$
B. 5-membered ring systems	
1. <i>N</i> -Benzoylphenylhydroxylamine	$-\text{O}=\text{C}-\text{N}-\text{O}^{(-)}-$
2. Cupferron	$-\text{O}=\text{N}-\text{N}-\text{O}^{(-)}-$
3. α -Dioximes	$-\text{N}=\text{C}-\text{C}=\text{N}^{(-)}-$
4. Dithizone	$-\text{N}-\text{N}=\text{C}-\text{S}^{(-)}-$
5. 8-Quinololins	$-\text{N}=\text{C}-\text{C}-\text{O}^{(-)}-$
6. Toluene-3,4-dithiol	$-(^{(-)})\text{S}-\text{C}=\text{C}-\text{S}^{(-)}-$
7. Catechol	$-(^{(-)})\text{O}-\text{C}=\text{C}-\text{O}^{(-)}-$
C. 6-membered ring systems	
1. β -Diketones and hydroxycarbonyls	$-\text{O}=\text{C}-\text{C}=\text{C}-\text{O}^{(-)}-$
a. Acetylacetone	
b. Thenoyltrifluoroacetone (TTA)	
c. Morin	
d. Quinalizarin	
2. Nitrosonaphthols	$-\text{O}=\text{N}-\text{C}=\text{C}-\text{O}^{(-)}-$
3. Salicylaldoxime	$-\text{N}=\text{C}-\text{C}=\text{C}-\text{O}^{(-)}-$
D. Polydentate Systems	
1. Pyridyl-azo-naththol (PAN)	$-\text{N}=\text{C}-\text{N}=\text{N}-\text{C}=\text{C}-\text{O}^{(-)}-$
II. Ion Association Systems	
A. Metal contained in cationic member of ion-pair	
1. Alkylphosphoric Acids	
2. Carboxylic Acids	
3. Cationic chelates	
a. Phenanthrolines	
b. Polypyridyls	
4. Nitrate	
5. Trialkylphosphine Oxides	
B. Metal contained in anionic member of ion-pair*	
1. Halides (GaCl_4^-)	
2. Thiocyanates ($\text{Co}(\text{CNS})_4^-$)	
3. Oxyanions (MnO_4^-)	
4. Anionic chelates ($\text{Co}(\text{Nitroso R salt})_3^{3-}$)	

* The cation member associated with these metal-containing anions is usually of an "onium" type such as (a) oxonium, e.g., ROH_2^+ , R_2OH^+ , R_2COH^+ ; (b) ammonium, e.g., RNH_3^+ , $\cdots \text{R}_4\text{N}^+$; (c) arsonium, R_4As^+ ; (d) phosphonium, R_4P^+ ; (e) stibonium, R_4Sb^+ ; (f) sulfonium, R_2S^+ .

Process of extraction.—With all metal extraction systems, chelate and ion association alike, three aspects of the extraction process may be discerned: (a) formation of an extractable metal species in the aqueous phase, (b) distribution of the extractable complex, and (c) chemical interactions of the complex in the organic phase. Of these, only the first step will be considered here.

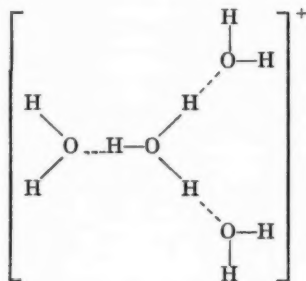
Formation of an uncharged complex.—This step involves all reactions pertaining to the formation of an extractable metal complex in the aqueous phase. This complex may be formed either by co-ordination with monodentate or polydentate (chelating) ligands or by ion pairing. The former type conforms to the general relation



where M^{n+} is an n -charged metal cation and R^- is an anion of a suitable co-ordinating agent. If R^- has significant proton affinity (i.e. it is the conjugate base of a weak acid) then its concentration and, therefore, the extent of complex formation will be pH-dependent. Reactions other than the ionization of the weak acid HR will also affect the course of the extraction if, as with the reaction of M^{n+} with a competing complexing agent, the concentrations of any of the species in Equation 1 are thereby affected.

Ion pairing follows the formation of a charged metal complex (via co-ordination) in a manner to give an uncharged species. Thus, a metal such as copper (I) which forms a cationic chelate with neocuproin will form an extractable complex when this cation pairs with an anion such as perchlorate; viz. $[\text{Cu}(2,9\text{-dimethylphenanthroline})_2]^+ [\text{ClO}_4]^-$ whereas the extraction of manganese (VII) as $[\text{C}_6\text{H}_5]_4\text{As}^+ [\text{MnO}_4]^-$ illustrates the incorporation of the metal in the anionic partner of the ion pair.

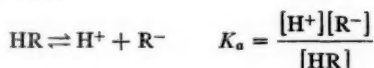
Of particular interest in this category is the extraction of such acid species as $[\text{H}^+, \text{FeCl}_4^-]$ and $[\text{H}^+, \text{GaCl}_4^-]$ obtained in the extraction of metals from concentrated hydrogen halide solutions. Recent work by Tuck & Diamond (8) explains the special need for basic oxygen-containing solvents in terms of the ability of the hydronium ion to hydrogen-bond with water molecules to form H_9O_4^+ ,



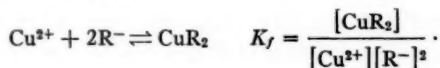
whose stability depends on its ability to co-ordinate with solvent molecules. Hence, the basicity and steric availability of the oxygen in solvents used in such extractions are more important than are their dielectric constants.

Quantitative treatments of extraction equilibria.—The feasibility of describing accurately the dependency of the course of an extraction upon the various experimental parameters depends on the extent to which the many extraction equilibria are understood. For example, in the extraction of Cu^{2+} by TTA (symbolized as HR, a weak acid) the equilibria associated with the following reactions in aqueous phase leading to metal complex formation must be considered:

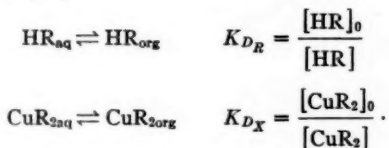
(a) Ionization of TTA



(b) Metal Chelate Formation



In addition, the distribution equilibria of both the chelate CuR_2 and the reagent HR come into play.



On the basis of all these equilibria it is possible to derive an expression for the distribution ratio D , viz:

$$D = \frac{K_f K_a^2 K_{D_R}}{K_{D_X}^2} \frac{[\text{HR}]_0^2}{[\text{H}^+]^2}$$

From this expression, it may be correctly predicted that the slopes of the log D vs pH or log $[\text{HR}]_0$ curves are each two and that D is here independent of $[\text{Cu}^{2+}]$. Furthermore, knowledge of the values of the equilibrium constants would permit complete description of D . An interesting recent example of the corollary approach of using solvent extraction behavior to elucidate reactions and equilibria of interest may be found in a paper by Peppard *et al.* (9). Examination of the extraction of tracer levels of rare-earth cations by HDGP (dioctylphenyl orthophosphoric acid) in toluene revealed a linear dependence of log D upon both pH and $[\text{HDGP}]_0$, each with a slope of 3. From this behavior the equation

$$D = K [\text{HDGP}]_0^3 / [\text{H}^+]^3$$

reminiscent of the Cu-TTA equation was derived. However, the HDGP was known from other studies to be essentially completely dimerized in the toluene phase. Hence, if HDGP ionized to H^+ and $(\text{DGP})^-$ the expected dependency of log D on log HDGP would be a line of slope 3/2. This having been ruled out by the extraction data, an alternative postulate was presented that was consistent with the data, namely, that the dimer ionized as a mono-

$$\begin{array}{c} \text{GO} \quad \text{O-HO} \quad \text{OG} \\ \diagdown \quad \diagup \quad \diagdown \quad \diagup \\ \text{P} \quad \text{O} \quad \text{P} \\ \diagup \quad \diagdown \quad \diagup \quad \diagdown \\ \text{GO} \quad \text{O} \quad \text{OG} \\ \quad \quad \quad \left(\frac{M}{3} \right) \end{array}$$

H

$(C_2H_5)_2N-C \begin{matrix} S \\ | \\ S^-, Na^+ \end{matrix}$

Li Be B C N O F Ne

Na Mg Al Si P S Cl Ar

K Ca Sc Ti V Cr Mn Fe Co Ni Cu Zn Ga Ge As Se Br Kr

Rb Sr Y Zr Nb Mo Tc Ru Rh Pd Ag Cd In Sn Sb Te I Xe

Cs Ba La Hf Ta W Re Os Ir Pt Au Hg Tl Pb Bi Po At Rn

Fa Ra Ac

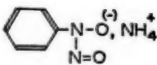
Ce Pr Nd Pm Sm Eu Gd Tb Dy Ho Er Tm Yb Lu

Th Pa U Np Pu Am Cm Bk Cf E Fm Mv Io2 Io3

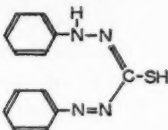
FIG. 1. Elements extractable with sodium diethyldithiocarbamate. The number under an element symbol indicates the pH value at which the element can be completely extracted.

a chloroform solution of diethylammonium diethyldithiocarbamate. Copper can be separated from many elements at a pH 3.5 in the presence of ammonium citrate by extraction into a chloroform solution of diethyldithiocarbamate (16). Uranium-233 produced in irradiated thorium has been separated from all alpha-emitters but the short-lived bismuth-212 by extraction with sodium diethyldithiocarbamate out of a solution saturated with ammonium nitrate and having a pH 2.5–3.0; methylisobutylketone was used as solvent (17).

Cupferron and related reagents.—Figure 2 summarizes the known cupferron extractions. Recent work includes the extraction of thorium, zir-

H		Cupferron																He	
Li Be																		B C N O F Ne	
Na Mg																		Al Si P S Cl A	
7																		2	
K	Ca	Sc	Ti	V	Cr	Mn	Fe	Co	Ni	Cu	Zn	Ga	Ge	As	Se	Br	Kr		
			-0.3	-0.3		7	-0.3	4	4	-0.3	4								
Rb	Sr	Y	Zr	Nb	Mo	Tc	Ru	Rh	Pd	Ag	Cd	In	Sn	Sb	Te	I	Xe		
			-0.3	<0	-0.4						7	0	-0.3	-0.3					
Cs	Ba	La	Hf	Ta	W	Re	Os	Ir	Pt	Au	Hg	Tl	Pb	Bi	Po	At	Rn		
			-0.3	<0	-0.3						7		3	0					
Fa		Ra	Ac																

Dithizone



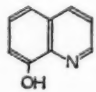
H																	He
Li	Be											B	C	N	O	F	Ne
Na	Mg											Al	Si	P	S	Cl	Ar
K	Ca	Sc	Ti	V	Cr	Mn	Fe	Co	Ni	Cu	Zn	Ga	Ge	As	Se	Br	Kr
					~11	6	7	8	1	8							
Rb	Sr	Y	Zr	Nb	Mo	Tc	Ru	Rh	Pd	Ag	Cd	In	Sn	Sb	Te	I	Xe
									~10	~10	13	8	6				
Cs	Ba	La	Hf	Ta	W	Re	Os	Ir	Pt	Au	Hg	Tl	Pb	Bi	Po	At	Rn
									2	~10	~10	3	8.5	~2	~10		
Fr	Ra	Ac															

Ce Pr Nd Pm Sm Eu Gd Tb Dy Ho Er Tm Yb Lu
Th Pa U Np Pu Am Cm Bk Cf E Fm Mv 102 103

FIG. 3. Elements extractable by dithizone. See caption of Figure 1 for explanation of numbers.

8-Quinolinols.—(See Fig. 4.) The distribution of thorium, uranium, and lanthanum between water and chloroform solutions of various 5,7-dihalo-8-quinolinols has been studied (24). Extraction with the dihalo derivatives can be achieved at somewhat lower pH values than is possible with 8-quinolinol itself. Uranium-233 can be separated from thorium and all alpha-emitters as the 8-quinolinol chelate in methylisobutylketone when EDTA is used to mask thorium and other metals (25). Alimarin & Gibalo (26) use an isoamyl alcohol solution of 8-quinolinol to separate niobium from tantalum in a solu-

8-Quinolinol



H																	He
Li	Be											B	C	N	O	F	Ne
Na	Mg											Al	Si	P	S	Cl	Ar
K	Ca	Sc	Ti	V	Cr	Mn	Fe	Co	Ni	Cu	Zn	Ga	Ge	As	Se	Br	Kr
Rb	Sr	Y	Zr	Nb	Mo	Tc	Ru	Rh	Pd	Ag	Cd	In	Sn	Sb	Te	I	Xe
Cs	Ba	La	Hf	Ta	W	Re	Os	Ir	Pt	Au	Hg	Tl	Pb	Bi	Po	At	Rn
													8.5	4			
Fr	Ra	Ac															

Ce Pr Nd Pm Sm Eu Gd Tb Dy Ho Er Tm Yb Lu
Th Pa U Np Pu Am Cm Bk Cf E Fm Mv 102 103

FIG. 4. Elements extractable by 8-quinolinol. See caption of Figure 1 for explanation of numbers.

[illegible]

FIG. 5. Elements extractable by acetylacetone. See caption of Figure 1 for explanation of numbers.

tion at pH between 6 and 9 containing citrate or tartrate. For separating niobium from tungsten, these authors change only the organic solvent, using chloroform in place of isoamyl alcohol. Bruninx & Irvine (27) extracted niobium away from tantalum using 5,7-dichloro-8-quinolinol in nitrobenzene, amylacetate, or β -chloroethyl ether at a pH of 10.

β -Diketones.—(See Fig. 5 and 6.) The extraction behavior of uranium and a number of other metals with acetylacetone has been studied (28). EDTA will mask the extraction of copper, bismuth, and lead but will not

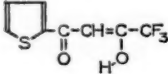
																TTA																									
H																			He																						
Li	Be																																								
6																																									
Na	Mg																	B	C	N	O	F	Ne																		
																		Al	Si	P	S	Cl	A																		
																		55																							
K	Ca	Sc	Ti	V	Cr	Mn	Fe	Co	Ni	Cu	Zn	Ga	Ge	As	Se	Br	Kr																								
8	15															2	35																								
Rb	Sr	Y	Zr	Nb	Mo	Tc	Ru	Rh	Pd	Ag	Cd	In	Sn	Sb	Te	I	Xe																								
>10		>6	-0.8																																						
Cs	Ba	La	Hf	Ta	W	Re	Os	Ir	Pt	Au	Hg	Tl	Pb	Bi	Po	At	Rn																								
		-0.8																35	4	2	15																				
Fa	Ra	Ac																																							
>5																																									
																		Ce	Pr	Nd	Pm	Sm	Eu	Gd	Tb	Dy	Ho	Er	Tm	Yb	Lu										
																																		>3,4							
																		Th	Pa	U	Np	Pu	Am	Cm	Bk	Cf	E	Fm	Mv	102	103	3,4									
																		0.8 < 0 > 3																-0.3	-0.3	3.5	35	2.5	3		

FIG. 6. Elements extractable by thenoyltrifluoroacetone. See caption of Figure 1 for explanation of numbers.

affect that of uranium. Vanadium (29) and chromium (30) can be extracted with acetylacetone.

Recent work with TTA includes the highly selective extraction of zirconium from concentrated nitric acid solutions (31), the extraction of neptunium (32), plutonium (33), cerium (34), and protactinium (35) from strong mineral acid media.

Nitrosonaphthols.—Thorium, uranium, and lanthanum can be separately extracted with proper pH control when either 1-nitroso-2-naphthol or 2-nitroso-1-naphthol in chloroform is used as extractant (24). Uranium can be selectively extracted away from vanadium and iron with EDTA-masking at a pH of 7.0 to 7.5 and with 1-nitroso-2-naphthol in isoamyl alcohol (36) as solvent.

Other chelating agents.—Dyrssen (37) has reviewed the use of a number of chelating agents for the extraction of lanthanide and actinide elements; these included a group of polydentate chelating agents designated as di(salicylal)-alkylene-diimines which have been used to extract uranium away from trivalent lanthanide elements. Cheng (38) has selectively extracted uranium with the aid of EDTA-masking using pyridyl-azonaphthol in *o*-dichlorobenzene. Harris & Freiser (39) have applied pyridyl-azonaphthol extractions to copper, zinc, nickel, and manganese.

ION ASSOCIATION SYSTEMS

Alkylphosphoric acids.—One of the most recent extraction systems to be investigated involves the use of the dialkylphosphoric acids as complexing agents (40). Figure 7 summarizes those elements that have already been extracted under a variety of conditions. Scadden & Ballou (41) have investigated the extraction properties of both carrier-free and macro-concentrations of fission product elements using dibutylphosphoric acid in di-*n*-butyl ether.

H																He	
Li Be														B C N O F Ne			
Na Mg														Al Si P S Cl A			
K	Ca	Sc	Ti	V	Cr	Mn	Fe	Co	Ni	Cu	Zn	Ga	Ge	As	Se	Br	Kr
Rb	Sr	Y	Zr	Nb	Mo	Tc	Ru	Rh	Pd	Ag	Cd	In	Sn	Sb	Te	I	Xe
Cs	Ba	La	Hf	Ta	W	Re	Os	Ir	Pt	Au	Hg	Tl	Pb	Bi	Po	At	Rn
Fr Ra Ac																	
<div style="border: 1px dashed black; padding: 2px; display: inline-block;">Ce Pr Nd Pm Sm Eu Gd Tb Dy Ho Er Tm Yb Lu</div>																	
Th Pa U Np Pu Am Cm Bk Cf E Fm Mv Io2 Io3																	

FIG. 7. Elements extracted in alkylphosphoric acid system. Solid blocks—appreciably extracted; broken blocks—partially extracted.

They were able to separate Zr and Nb from each other and from nearly all other fission products. The use of di-(2-ethylhexyl)-phosphoric acid for the fractionation of the lanthanides using a carrier solvent such as toluene has been reported (42), and it has also been possible to separate Bk (IV) from the remainder of the actinide elements (43). The use of this reagent for the extraction of U and V has been previously demonstrated (44).

Dioctylphosphoric acid has been used to isolate carrier-free Y^{90} , La^{140} , Ce^{144} , Pr^{143} , and Pr^{144} (45). Tracer-level Ce^{144} is selectively extracted away from other lanthanides by 0.30 to 0.75 *M* di-2-ethylhexylphosphoric acid in

H																He																												
Li	Be															B	C	N	O	F	Ne																							
Na	Mg															Al	Si	P	S	Cl	Ar																							
K	Ca	Sc	Ti	V	Cr	Mn	Fe	Co	Ni	Cu	Zn	Ga	Ge	As	Se	Br	Kr																											
Rb	Sr	Y	Zr	Nb	Mo	Tc	Ru	Rh	Pd	Ag	Cd	In	Sn	Sb	Te	I	Xe																											
Cs	Ba	La	Hf	Ta	W	Re	Os	Ir	Pt	Au	Hg	Tl	Pb	Bi	Po	At	Rn																											
Fa	Ra	Ac																																										
															Ce	Pr	Nd	Pm	Sm	Eu	Gd	Tb	Dy	Ho	Er	Tm	Yb	Lu																
															Th	Pa	U	Np	Pu	Am	Cm	Bk	Cf	E	Fm	Mv	102	103																

FIG. 8. Elements extracted in carboxylic acid system.

heptane out of 10 *M* nitric acid. With the reagent in toluene solution, it was possible to extract Y^{90} away from Sr^{90} out of 0.1 *M* hydrochloric acid, and La^{140} away from Ba out of 0.05 *M* HCl.

Carboxylic acids.—Solutions of carboxylic acids in organic solvents have been found to be effective in extracting several metals out of alkaline aqueous solutions, and those elements that have been shown to extract under a variety of conditions are given in Figure 8.

The use of carboxylic acids as extractants of particular interest to radiochemists has only recently been fully appreciated, and recent work by Hök-Bernström (46, 47, 48) further emphasizes the importance of reagents such as salicylic, cinnamic, 3,5-dinitrobenzoic, and methoxybenzoic acids for the extraction of U (VI), Pu (IV), Th (IV), and La (III), the most promising solvent being methyl isobutyl ketone. Separations that have been achieved include Th from La and Th from U. Perfluorocarboxylic acids have been used to separate cations in charge groups (49).

Cationic chelates.—Heterocyclic polyamines such as the phenanthrolines and polypyridyls have been used to a limited extent in extraction. In this system the metal ion forms a cationic chelate with the reagent, and the neutral extractable species is formed by association of the positive complex

with an anion. Thus, tris-phenanthroline iron (II) perchlorate has been found to be moderately extractable into chloroform and other solvents, but most satisfactorily into nitrobenzene (50). The Co complex of 2,2',2''-terpyridyl has also been extracted into nitrobenzene, and only Cu, Fe, and larger amounts of Ni interfere (51). The use of alkylated phenanthrolines such as 2,9-dimethylphenanthroline (52) in these reactions has resulted in the formation of a Cu (I) complex that can be easily and highly selectively extracted with the higher alcohols such as amyl and hexyl alcohols.

Nitrate.—One of the most valuable extraction systems for the separation of elements of interest to atomic energy programs is the nitrate system. As

H																He	
Li Be											B C N O F Ne						
Na Mg											Al Si P S Cl A						
K	Ca	Sc	Ti	V	Cr	Mn	Fe	Co	Ni	Cu	Zn	Ga	Ge	As	Se	Br	Kr
Rb	Sr	Y	Zr	Nb	Mo	Tc	Ru	Rh	Pd	Ag	Cd	In	Sn	Sb	Te	I	Xe
Cs	Ba	La	Hf	Ta	W	Re	Os	Ir	Pt	Au	Hg	Tl	Pb	Bi	Po	At	Rn
Fr Ra Ac																	
Ce	Pr Nd Pm Sm Eu Gd Tb Dy Ho Er Tm Yb Lu																
Th	Pa	U	Np	Pu	Am	Cm	Bk	Cf	E	Fm	Mv	102	103				

FIG. 9. Elements extracted in nitrate system. Solid blocks—appreciably extracted; broken blocks—partially extracted.

early as 1842 it was found that uranyl nitrate dissolved readily in ethyl ether, and this fact was used in the purification of U from pitchblende (53). Other early studies included the separation of U from V (54) and the concentration of the rare-earth elements in the analysis of U ores (55). With the discovery of the enhancement of the extraction of U by means of salting-out agents (56, 57), the process has assumed great importance in recent years.

Those elements that are extracted in the nitrate system under various conditions are shown in Figure 9. In addition to U (VI), Am (VI), Np (VI), and Pu (VI), other elements which extract well as nitrate complexes include Ce (IV), Au (III), Fe (III), Sc (III), Pa (IV), and Th (IV). Solvents that have been used extensively in the extraction of nitrates include ethyl ether, tributyl phosphate, and methyl isobutyl ketone.

Early work showed that tributyl phosphate was very effective in extracting Ce, Tl, and U nitrates from nitric acid solutions (58). More recently McKay *et al.* (59 to 63) have made an intensive study of the use of tributyl phosphate as an extracting solvent for actinide and fission product nitrates. Among the elements that were found to extract appreciably were Zr, Ce, Pu

(IV) and (VI), and Th. The system can be used to extract and separate Y and the lower lanthanides (La-Gd) also. In extraction of trace level quantities out of nitric acid solutions into TBP the ease of extraction increased in the order Pu (IV) > Np (IV) > Th, but reversed for the metals in the higher oxidation state, i.e., U (VI) > Np (VI) > Pu (VI) (64). Sato (65) has determined distribution ratio data for uranyl nitrate into TBP (65). Separation factors as high as 2 have been attained for successive lanthanides. In all of the studies, the effects of nitric acid concentration and salting-out agents were evaluated. In an extension of earlier work (66) Peppard *et al.* (67) have further investigated the fractionation of the trivalent lanthanides as a function of tributyl phosphate concentration, nitric acid concentration, and atomic number and have observed a nonmonotonic ordering of the lanthanides. A study by Wendlandt & Bryant (68) of the solubilities of a large number of metal nitrate salts in pure tributyl phosphate reveals many more possibilities for the separation of elements.

Methyl isobutyl ketone has been employed as a solvent for U and Pu recovery from fission products (69). In this extraction the separation of the desired products from the fission products is influenced by solvent purity, salting strength, acidity, temperature, and the presence of minor components in the system. Rydberg & Bernström (70) determined the distribution ratios of U (VI), Pu (IV) and (VI), Th (IV), Zr (IV), La (III), Ca, and Na between methyl isobutyl ketone and aqueous solutions of varying nitric acid and calcium nitrate concentrations. As a result of this study, possible methods are presented for the separation of U and Pu from certain fission products. Maeck *et al.* (71) have developed a highly selective extraction method for uranium using aluminum nitrate, tetrapropylammonium nitrate in an acid-deficient solution, and hexone as solvent.

Limited work has been done on the separation of fissionable materials from fission products in the nitrate system with other solvents such as pentaether, isopropyl ether, dibutyl cellosolve, and many alcohols (69).

Trialkylphosphine oxides.—A study of the uranium-extracting ability of a series of organophosphorus compounds has shown that U may be quantitatively extracted from nitrate solutions with a 0.1 *M* alkylphosphine oxide solution in kerosene or carbon tetrachloride when *n*-octyl, *n*-decyl, *n*-dodecyl, or 3,5,5-trimethylhexylphosphine oxides are employed (72). Vanadium (V) also can be quantitatively extracted with 0.6 *M* trioctylphosphine oxide in kerosene.

The great potentiality of the alkylphosphine oxides as analytical extractants is evident from studies of Mann & White (73), who examined the extraction behavior of many metal ions in acid media using a 0.1 *M* solution of either tri-*n*-octylphosphine oxide or 2-ethyl-*n*-hexylphosphine oxide in cyclohexane. The extraction behavior of the elements in this system under a variety of conditions is summarized in Figure 10.

Halides.—The extraction of elements from hydrochloric acid solutions to ethyl ether has been in the past one of the most studied systems, starting with the work of Rothe in 1892 on the extraction of iron. Comprehensive studies

Among the recent chloride studies of interest to radiochemists are the behavior of protactinium, using diisopropyl ketone (74, 75); astatine, using ethyl ether (76); and polonium, using diisopropyl ketone (77). Chloride extractions have been made with tributyl phosphate as solvent, and very promising separations have been noted. Thus, Peppard *et al.*, have separated thorium, protactinium, and uranium in one case (78) and scandium, thorium, and zirconium in another study (79). Another detailed study of the distribution of zirconium has been reported (80).

FIG. 10. Elements extracted in trialkylphosphine oxide system. Solid blocks—appreciably extracted; broken blocks—partially extracted.

Investigation of the other halide systems has increased in recent years, and comprehensive studies have been made of the extraction of metals from hydrofluoric acid solutions to ethyl ether (81, 82), from hydrobromic acid solutions to ethyl ether (83, 84, 85) and methylisobutyl ketone (86), and from hydriodic acid (87), or potassium iodide and sulfuric acid solutions (88), to ethyl ether. Those elements that extract in the fluoride, bromide, and iodide systems with the use of various solvents and acid concentrations are shown in Figures 12, 13, and 14. It is evident that a number of different separations are possible depending upon the choice of halide. An interesting observation has been made on the extractability of the alkali metals as polyiodides with nitromethane as solvent (89). Although not completely successful, attempts were made to separate the respective alkali metals from each other with the use of mixed solvents.

Thiocyanates.—The use of alkali thiocyanates as complexing reagents for the colorimetric estimation of a number of metals is well known, and more

H																	He				
Li	Be															B	C	N	O	F	Ne
Na Mg																Al	Si	P	S	Cl	A
K	Ca	Sc	Ti	V	Cr	Mn	Fe	Co	Ni	Cu	Zn	Ga	Ge	As	Se	Br	Kr				
Rb	Sr	Y	Zr	Nb	Mo	Tc	Ru	Rh	Pd	Ag	Cd	In	Sn	Sb	Te	I	Xe				
Cs	Ba	La	Hf	Ta	W	Re	Os	Ir	Pt	Au	Hg	Tl	Pb	Bi	Po	At	Rn				
Fr Ra Ac																					
Ce Pr Nd Pm Sm Eu Gd Tb Dy Ho Er Tm Yb Lu																					
Th Pa U Np Pu Am Cm Bk Cf E Fm Mv 102 103																					

FIG. 11. Elements extracted in chloride system. Solid blocks—appreciably extracted; broken blocks—partially extracted.

recently advantage has been taken of the extractability of some of these complexes into organic solvents as a means of separation. An intensive study of the distribution of many metal thiocyanates to ethyl ether has been made (90), and the results of this study as well as a number of others employing different solvents, concentrations, etc. are summarized in Figure 15. The use of tributylamine in the extraction of metal thiocyanates by amyl acetate has recently been described and definitely involves an ammonium rather than the oxonium cation (91, 92).

Oxyanions.—Certain metals which form oxyanions may be further complexed by association with large organic cations to form uncharged species

H																	He				
Li	Be															B	C	N	O	F	Ne
Na Mg																Al	Si	P	S	Cl	Ar
K	Ca	Sc	Ti	V	Cr	Mn	Fe	Co	Ni	Cu	Zn	Ga	Ge	As	Se	Br	Kr				
Rb	Sr	Y	Zr	Nb	Mo	Tc	Ru	Rh	Pd	Ag	Cd	In	Sn	Sb	Te	I	Xe				
Cs	Ba	La	Hf	Ta	W	Re	Os	Ir	Pt	Au	Hg	Tl	Pb	Bi	Po	At	Rn				
Fr Ra Ac																					
Ce Pr Nd Pm Sm Eu Gd Tb Dy Ho Er Tm Yb Lu																					
Th Pa U Np Pu Am Cm Bk Cf E Fm Mv 102 103																					

FIG. 12. Elements extracted in fluoride system. Solid blocks—appreciably extracted; broken blocks—partially extracted.

senate, vanadate, and polyvanadate have been prepared and their extractions into chloroform studied (96).

Anionic chelates.—An interesting recent development in extraction concerns the utilization of anionic chelate-formers such as nitroso-R salt, 7-iodo-8-quinolinol-5-sulfonic acid (ferron), and sulfosalicylic acid. These form negatively charged metal chelates which can pair with cations such as tributylammonium, tetraphenylarsonium, and tetraphenylphosphonium ions to give rise to extractable species (91, 97, 98, 99). Magnesium is reported to form an anionic complex, with three molecules of 8-quinolinol, which pairs with butylammonium ion to give a chloroform-extractable species (100). Similarly, an anionic 8-quinolinol complex of uranium has been described as combining with tetra-alkylammonium ions (101).

H																	He				
Li	Be															B	C	N	O	F	Ne
Na	Mg															Al	Si	P	S	Cl	A
K	Ca	Sc	Ti	V	Cr	Mn	Fe	Co	Ni	Cu	Zn	Ga	Ge	As	Se	Br	Kr				
Rb	Sr	Y	Zr	Nb	Mo	Tc	Ru	Rh	Pd	Ag	Cd	In	Sn	Sb	Te	I	Xe				
Cs	Ba	La	Hf	Ta	W	Re	Os	Ir	Pt	Au	Hg	Tl	Pb	Bi	Po	At	Rn				
Fa	Ra	Ac																			
			Ce	Pr	Nd	Pm	Sm	Eu	Gd	Tb	Dy	Ho	Er	Tm	Yb	Lu					
			Th	Pa	U	Np	Pu	Am	Cm	Bk	Cf	E	Fm	Mv	102	103					

FIG. 15. Elements extracted in thiocyanate system. Solid blocks—appreciably extracted; broken blocks—partially extracted.

APPARATUS

Laboratory extractions.—In the laboratory, three basic types of liquid-liquid extractions are generally utilized, namely, batch, continuous, and countercurrent distribution methods. In general, conventional laboratory apparatus used for solvent extraction may be employed with low-level radioactive material. Appropriate shielding should be employed for materials of high activity, and extractors have been modified to provide maximum remote control. Since a large sample of extractors used for inorganic separations (6) and organic extractions (102) has been described, only a few of the more recent and interesting modifications for use with highly radioactive samples are mentioned here. With regard to batch extraction, the separatory funnel still remains the most used and simplest type of apparatus with greatest applicability to analytical problems.

Continuous extractions are particularly useful when the distribution ratio is relatively small, since a large number of batch extractions would normally be necessary to effect quantitative separation. Most continuous-extraction devices operate on the same general principle, which consists of distilling the extracting solvent from a boiler flask and condensing it and passing it continuously through the solution being extracted. The extracting liquid separates out and flows back into the receiving flask, where it is again evaporated and recycled while the extracted solute remains in the receiving flask. When the solvent cannot easily be distilled, a continuous supply of fresh solvent may be added from a reservoir.

High efficiency in continuous extraction depends on the viscosity of the phases, the value of the distribution ratio, and the relative volumes of the two phases, to mention a few of the more important factors. One practical method of improving the efficiency is to insure as high an area of contact as possible between the two liquids. As the extracting solvent passes through the solution, fritted-glass discs, small orifices, baffles, and stirrers may be used to bring the two immiscible layers in closer contact.

An interesting modification of the conventional continuous ether extractor, where the solvent is recycled by distillation and condensation and dispersed in the aqueous phase by means of a sintered-glass disc, provides for the handling of highly radioactive solutions (103). As shown in Figure 16, a train has been attached to the bottom of the extraction chamber to permit sampling and removal of the aqueous phase by means of a remotely controlled pump, following the extraction. The expended aqueous phase is pumped into a shielded active-waste container, and the extractor can then be used for another extraction. The apparatus has been used to separate uranium in irradiated samples by extraction of the nitrate with ethyl ether after the addition of salting-out agents. Beta and gamma fission product activities ranging from a few hundred milliroentgens to several hundred roentgens per hour have been handled conveniently.

A reservoir type of continuous extractor for use with chelating agents has been designed by Meinke & Anderson (104) for the separation of highly radioactive materials. Although the apparatus was developed for the extraction with thenoyltrifluoroacetone of macro amounts of thorium from highly radioactive fission products present after cyclotron bombardment, it is readily adaptable to many other types of problems. As shown in Figure 17, all manipulations are adaptable to remote control and most of the functions are automatic, so that the apparatus can be well shielded. The extractor consists of a tube containing a sintered-glass disc. Several overflow tubes allow the adaptation of the extractor to varying amounts of solution to be extracted. The inlet tube below the sintered disc, F, is connected to the chelate reservoir, E, with flexible tubing. The tubes sealed onto the extractor at G permit the insertion of micro pH electrodes into the solution to be extracted. The stopcock at A controls the flow of nitrogen gas, which is used to lift the extract from the extractor to the small trap bulb, C, where it then falls by

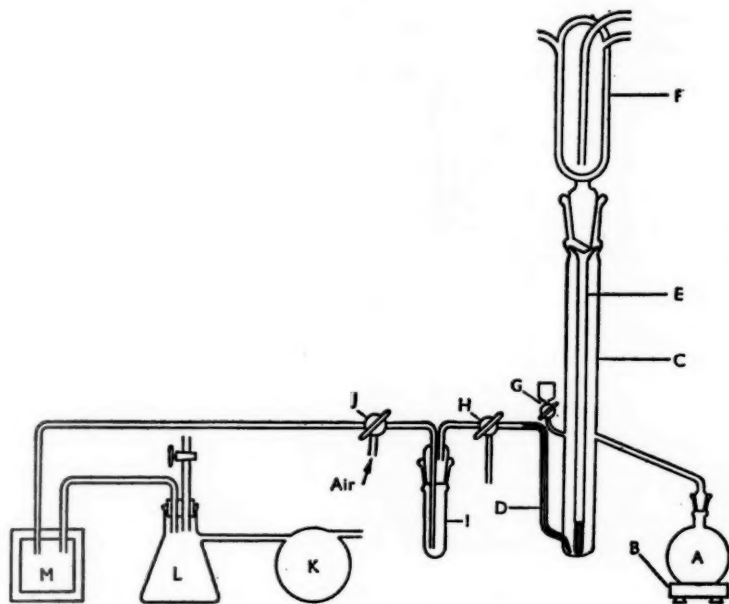


FIG. 16. Continuous ether extractor (93).

A = 500-ml. Florence flask

B = hot-plate

C = extractor, length about 40 cm., made from Pyrex-glass tubing having an outside diameter of 21 mm. The ether overflow arm is attached to the extractor 11 cm. from the bottom and is made from 12-mm. Pyrex-glass tubing and is about 15 cm. long

D = drain tube

E = ether-dispersing tube

F = condenser

G = sample entrance tube

H = three-way stopcock

I = raffinate-aliquot tube

J = parallel oblique stopcock

K = mechanical pump

L = safety bottle

M = shielded liquid-active-waste container

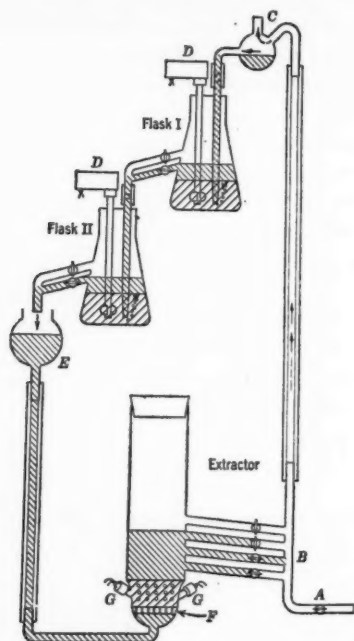


FIG. 17. Continuous extractor for use with chelating agents (94). This extractor is readily adaptable to remote control operation.

- A = Stopcock on nitrogen gas inlet
- B = Overflow tubes
- C = Trap
- D = Stirring motors
- E = Chelate reservoir
- F = Sintered disc
- G = Micro pH electrodes

gravity into flask I. Small stirring motors, D, furnish sufficient agitation for the stripping and washing taking place in flasks I and II.

The third method of extraction, discontinuous countercurrent distribution, is employed for the fractionation of materials whose distribution ratios are very similar, and it involves the carrying out of many individual extractions rapidly and in sequence. Although the technique has been applied with great success to the fractionation of organic compounds (102), only recently has it been applied to inorganic separations. Thus, Peppard *et al.* have used countercurrent distribution to fractionate the rare earths (66) and to separate thorium, scandium, and zirconium, using tributyl phosphate as solvent (79). Another application is the separation of metals using acetylacetone (105). With regard to apparatus, most of the extractors involve a design of

tube operating by decantation based on that originally developed by Craig and co-workers (106), and the technique lends itself to remote control operation.

Moore (107) has separated uranium and plutonium from thorium, rare earths, zirconium, niobium, and ruthenium in hydrochloric acid solutions by extraction into tri(iso octyl)amine dissolved in xylene or methyl isobutyl ketone.

LITERATURE CITED

1. Stevenson, P. C., and Hicks, H. G., *Ann. Rev. Nuclear Sci.*, **3**, 221 (1953)
2. Glendenin, L. E., and Steinberg, E. P., *Ann. Rev. Nuclear Sci.*, **4**, 69 (1954)
3. Finston, H. L., and Miskel, J., *Ann. Rev. Nuclear Sci.*, **5**, 269 (1955)
4. Meinke, W. W., *Anal. Chem.*, **28**, 736 (1956)
5. Meinke, W. W., *Anal. Chem.*, **30**, 686 (1958)
6. Morrison, G. H., and Freiser, H., *Solvent Extraction in Analytical Chemistry* (John Wiley & Sons, Inc., 278 pp., New York, N. Y., 1957)
7. Morrison, G. H., and Freiser, H., *Anal. Chem.*, **30**, 632 (1958)
8. Tuck, D. J., and Diamond, R. M., *Proc. Chem. Soc.*, 236 (1958)
9. Peppard, D. F., Mason, G. W., Driscoll, W. J., and Sironen, R. J., *J. Inorg. & Nuclear Chem.*, **7**, 276 (1958)
10. Irving, H. M., Andrew, G., and Risdon, E. J., *J. Chem. Soc.*, 541 (1949)
11. Bolomey, R. A., and Wish, L., *J. Am. Chem. Soc.*, **72**, 4483 (1950)
12. Hague, J. L., Brown, E. D., and Bright, H. A., *J. Research Natl. Bur. Standards*, **47**, 380 (1951)
13. Foreman, J. K., Riley, C. J., and Smith, T. D., *Analyst*, **82**, 89 (1957)
14. Harvey, B. G., Heal, H. G., Maddock, A. G., and Rowley, E. L., *J. Chem. Soc.*, 1010 (1947)
15. Maynes, A. D., and McBryde, W. A. E., *Anal. Chem.*, **29**, 1259 (1957)
16. Abson, D., and Lipscomb, A. G., *Analyst*, **82**, 152 (1957)
17. Hardwick, W. H., and Moreton-Smith, M., *Analyst*, **83**, 9 (1958)
18. Fritz, J. S., Richard, M. J., and Bystroff, A. S., *Anal. Chem.*, **29**, 577 (1957)
19. Alimarin, I. P., and Gibalo, I. M., *Doklady Akad. Nauk S.S.S.R.*, **109**, 1137 (1956); *Chem. Abstr.*, **51**, 4860c (1957)
20. Dyrssen, D., *Acta Chem. Scand.*, **10**, 353 (1956)
21. Hartner, B., and Freiser, H., *Conf. Anal. Chem. and Appl. Spectroscopy* (Pittsburgh, Pa., March, 1958)
22. Iwantschegg, G., *Angew. Chem.*, **69**, 472 (1957)
23. Bagnall, K. W., and Robertson, D. S., *J. Chem. Soc.*, 509 (1957)
24. Dyrssen, D., Dyrssen, M., and Johansson, E., *Acta Chem. Scand.*, **10**, 106 (1956)
25. Clayton, R. F., Hardwick, W. H., Moreton-Smith, M., and Todd, R., *Analyst*, **83**, 13 (1958)
26. Alimarin, I. P., and Gibalo, I. M., *Vestnik Moskov. Univ., Ser. Mat., Mekh., Astron., Fiz. i Khim.*, **11**, 185 (1956); *Chem. Abstr.*, **51**, 17342A (1957)
27. Bruninx, E., and Irvine, J. W., in *Radioisotopes in Scientific Research*, **II**, 232 (Pergamon Press, New York, N. Y., 1958)
28. Krishen, A., and Freiser, H., *Anal. Chem.*, **29**, 288 (1957)
29. McKaveney, J. P., and Freiser, H., *Anal. Chem.*, **30**, 526 (1958)
30. McKaveney, J. P., and Freiser, H., *Anal. Chem.*, **30**, 1965 (1958)

31. Moore, F. L., *Anal. Chem.*, **28**, 997 (1956)
32. Moore, F. L., *Anal. Chem.*, **29**, 941 (1957)
33. Moore, F. L., and Hudgens, J. E., *Anal. Chem.*, **29**, 1767 (1957)
34. Smith, G. W., and Moore, F. L., *Anal. Chem.*, **29**, 448 (1957)
35. Bouissieres, G., and Vernois, J., *Compt. rend.*, **244**, 2508 (1957)
36. Alimarin, I. P., and Zolotov, Y. A., *Z. Anal. Khim.*, **12**, 176 (1957); *Chem. Abstr.*, **52**, 165d (1958)
37. Dyrssen, D., *Svensk Kem. Tidskr.*, **68**, 212 (1956)
38. Cheng, K. L., *Anal. Chem.*, **30**, 1027 (1958)
39. Harris, O. E., and Freiser, H., *Conf. Anal. Chem. and Appl. Spectroscopy* (Pittsburgh, Pa., March, 1958)
40. White, J. C., *U. S. Atomic Energy Commission Report, CF-57-2-37* (Feb. 8, 1957)
41. Scadden, E. M., and Ballou, N. E., *Anal. Chem.*, **25**, 1602 (1953)
42. Peppard, D. F., Mason, G. W., Maier, J. L., and Driscoll, W. S., *J. Inorg. & Nuclear Chem.*, **4**, 334 (1957)
43. Peppard, D. F., Moline, S. W., and Mason, G. W., *J. Inorg. & Nuclear Chem.*, **4**, 344 (1957)
44. Blake, C. A., *U. S. Atomic Energy Commission Report, ORNL-1903* (May 13, 1955)
45. Peppard, D. F., Mason, G. W., and Moline, S. W., *J. Inorg. & Nuclear Chem.*, **5**, 141 (1957)
46. Hök-Bernström, B., *Acta Chem. Scand.*, **10**, 163 (1956)
47. Hök-Bernström, B., *Acta Chem. Scand.*, **10**, 174 (1956)
48. Hök-Bernström, B., *Svensk Kem. Tidskr.*, **68**, 34 (1956)
49. Mills, G. F., and Whetsel, H. B., *J. Am. Chem. Soc.*, **77**, 4690 (1955)
50. Margerum, D. W., and Banks, C. V., *Anal. Chem.*, **26**, 200 (1954)
51. Miller, R. R., and Brandt, W. W., *Anal. Chem.*, **26**, 1968 (1954)
52. Cahler, A. R., *Anal. Chem.*, **26**, 577 (1954)
53. Peligot, E., *Ann. chim. et phys.*, **5**, 1 (1842)
54. Pierle, C. A., *Ind. Eng. Chem.*, **12**, 60 (1920)
55. Hoffman, J. I., *J. Wash. Acad. Sci.*, **38**, 233 (1948)
56. Hecht, F., and Grünwald, A., *Mikrochemie ver. Mikrochim. Acta*, **30**, 279 (1943)
57. Furman, N. H., Mundy, R. J., and Morrison, G. H., *U. S. Atomic Energy Commission Report, AECD-2938* (1949)
58. Warf, J. C., *J. Am. Chem. Soc.*, **71**, 3257 (1949)
59. Alcock, K., Bedford, F. C., Hardwick, W. H., and McKay, H. A. C., *J. Inorg. & Nuclear Chem.*, **4**, 100 (1957)
60. Best, G. F., McKay, H. A. C., and Woodgate, P. R., *J. Inorg. & Nuclear Chem.*, **4**, 315 (1957)
61. Healy, T. V., and McKay, H. A. C., *Trans. Faraday Soc.*, **52**, 633 (1956)
62. Hesford, E., McKay, H. A. C., and Scargill, D., *J. Inorg. & Nuclear Chem.*, **4**, 321 (1957)
63. Scargill, D., Alcock, K., Fletcher, J. M., Hesford, E., and McKay, H. A. C., *J. Inorg. & Nuclear Chem.*, **4**, 304 (1957)
64. Alcock, K., Best, G. F., Hesford, E., and McKay, H. A. C., *J. Inorg. & Nuclear Chem.*, **6**, 328 (1958)
65. Sato, T., *J. Inorg. & Nuclear Chem.*, **6**, 334 (1958)

66. Peppard, D. F., Faris, J. P., Gray, P. R., and Mason, G. W., *J. Phys. Chem.*, **57**, 294 (1953)
67. Peppard, D. F., Driscoll, W. J., Sironen, R. J., and McCarty, S., *J. Inorg. & Nuclear Chem.*, **4**, 326 (1957)
68. Wendlandt, W. W., and Bryant, J. M., *J. Phys. Chem.*, **60**, 1145 (1956)
69. Bruce, F. R., *Proc. Intern. Conf. Peaceful Uses Atomic Energy, Geneva, 1955*, **7**, 100, 128 (1956)
70. Rydberg, J., and Bernström, B., *Acta Chem. Scand.*, **11**, 86 (1957)
71. Maick, W. J., Booman, G. L., Elliott, M. C., and Rein, J. E., *Anal. Chem.*, **30**, 1902 (1958)
72. Blake, C. A., Brown, K. B., and Coleman, C. F., *U. S. Atomic Energy Commission Report, ORNL-1964* (1955)
73. Mann, C. K., and White, J. C., *Anal. Chem.*, **30**, 989 (1958)
74. Golden, J., and Maddock, A. G., *J. Inorg. & Nuclear Chem.*, **2**, 46 (1956)
75. Goble, A., Golden, J., and Maddock, A. G., *Can. J. Chem.*, **34**, 284 (1956)
76. Neumann, H. M., *J. Inorg. & Nuclear Chem.*, **4**, 349 (1957)
77. Cairo, A. E., and Maddock, A. G., *Proc. Intern. Conf. Peaceful Uses Atomic Energy, Geneva, 1955*, **7**, 331 (1956)
78. Peppard, D. F., Mason, G. W., and Gergel, M. V., *J. Inorg. & Nuclear Chem.*, **3**, 370 (1956)
79. Peppard, D. F., Mason, G. W., and Maier, J. L., *J. Inorg. & Nuclear Chem.*, **3**, 215 (1956)
80. Levitt, A. E., and Freund, H., *J. Am. Chem. Soc.*, **78**, 1545 (1956)
81. Kitahara, S., *Kagaku Kenkyusho Hôkoku*, **25**, 165 (1949)
82. Bock, R., and Herrmann, M., *Z. anorg. u. allgem. Chem.*, **284**, 288 (1956)
83. Wada, I., and Ishii, R., *Bull. Inst. Phys. Chem. Research (Tokyo)*, **13**, 264 (1934)
84. Wada, I., and Ishii, R., *Sci. Papers Inst. Phys. Chem. Research (Tokyo)*, **34**, 787 (1938)
85. Bock, R., Kusche, H., and Bock, E., *Z. anal. Chem.*, **138**, 167 (1953)
86. Denaro, A. R., and Occleshaw, V. J., *Anal. Chim. Acta*, **13**, 239 (1955)
87. Kitahara, S., *Kagaku Kenkyusho Hôkoku*, **24**, 454 (1948)
88. Irving, H., and Rossotti, F. J. C., *Analyst*, **77**, 801 (1952)
89. Bock, R., and Hoppe, I., *Anal. Chim. Acta*, **16**, 406 (1957)
90. Bock, R., *Z. anal. Chem.*, **133**, 110 (1951)
91. Ziegler, M., Glemser, O., and Petri, N., *Z. anal. Chem.*, **153**, 241 (1956)
92. Ziegler, M., Glemser, O., and Petri, N., *Z. anal. Chem.*, **154**, 81 (1957)
93. Tribalat, S., *Anal. Chim. Acta*, **3**, 113 (1949)
94. Beeston, J. M., and Lewis, J. R., *Anal. Chem.*, **25**, 651 (1953)
95. Tribalat, S., and Beydon, J., *Anal. Chim. Acta*, **6**, 96 (1952); **8**, 22 (1953)
96. Ziegler, M., and Glemser, O., *Angew. Chem.*, **68**, 522 (1957)
97. Ziegler, M., and Glemser, O., *Angew. Chem.*, **68**, 411 (1956)
98. Ziegler, M., and Glemser, O., *Z. anal. Chem.*, **153**, 246 (1956)
99. Ziegler, M., and Glemser, O., *Z. anal. Chem.*, **157**, 19 (1957)
100. Umland, F., and Hoffman, W., *Anal. Chim. Acta*, **17**, 237 (1957)
101. Clifford, W. E., *U. S. Atomic Energy Commission Report, RMO-2623* (June, 1956)

102. Craig, L. C., and Craig, D., *Techniques of Organic Chemistry* **3**, Part I (Weissberger, A., Ed., Interscience Publishers, Inc., New York, N. Y., 1956)
103. Jensen, K. J., and Bane, R. W., *Analyst*, **82**, 67 (1957)
104. Meinke, W. W., and Anderson, R. E., *Anal. Chem.*, **24**, 708 (1952)
105. Krishen, A., *Solvent Extractions with Acetylacetone* (Doctoral thesis, Univ. of Pittsburgh, Pittsburgh, Pa., 1957)
106. Craig, L. C., Hausmann, W., Ahrens, E. H., Jr., and Harfenist, E. J., *Anal. Chem.*, **23**, 1326 (1951)
107. Moore, F. L., *Anal. Chem.*, **30**, 908 (1958)

NUCLEAR FISSION¹

BY I. HALPERN

Department of Physics, University of Washington, Seattle, Washington

The first comprehensive review of the subject of nuclear fission appeared very shortly after the discovery of the fission process itself. The paper of Bohr & Wheeler (1) was as much a preview as a review. It told experimenters what they might look for and what they should find. It provided a framework and a language for the discussion of the fission process that, with few changes, is in use today. In the 20 years that have passed since the paper of Bohr & Wheeler, there have been few really significant contributions to our basic understanding of the fission process. It is in some ways awesome to compare the tremendous development of the applications of nuclear fission in this period with the slow growth of our understanding of its fundamental features.

It would be unfair to imply that nothing new has happened in fission in all this time. There has been a large amount of very fine experimental work, especially in recent years, and considerable progress has been made in the correlation of these experiments. If one is willing to lean only lightly on the available theory, it is possible to see the relationships of certain aspects of fission to others. This review was written in this spirit, i.e., from a phenomenological point of view. Some aspects of the theory of atomic nuclei that seem especially relevant to fission, and are consequently often called "fission theory," are treated briefly where they appear to apply.

The author has benefited from the analyses of the fission process that have been published from time to time by Wheeler and his co-workers (2, 3, 4). In recent years there have been some other reviews of fission (5, 6), the most comprehensive of which are the review by Whitehouse (7), the 1956 Chalk River Report (8), the Russian review of the same year (9), and Leachman's paper at the 1958 Geneva Conference (10).

The present review consists of two parts. The first is concerned with the probability that a nucleus will undergo fission. The second part has to do with the nature of the fission process as it is characterized by the distributions in mass, charge, energy, and angle of the fission products.

PART I. THE PROBABILITY OF FISSION

1. SPONTANEOUS-FISSION HALF LIVES

It seems safe enough to discuss fission as a mode of decay of a genuine compound nucleus, there being no evidence for any "direct" fission reactions. In examining the dependence of the fission probability on the properties of the compound nucleus, it is convenient first of all to think of the ex-

¹ The literature which was surveyed for this review was published before January, 1959.

citation energy. The fission of nuclei in their ground states (spontaneous fission) was first observed by Flerov & Petrzhak in uranium (11), and in recent years it has been studied in a number of nuclear species. Generally the probability of spontaneous fission is found by measuring the fission rate in a sample of known weight with an ionization chamber. The techniques are similar to those normally used to determine the half lives for alpha decay.

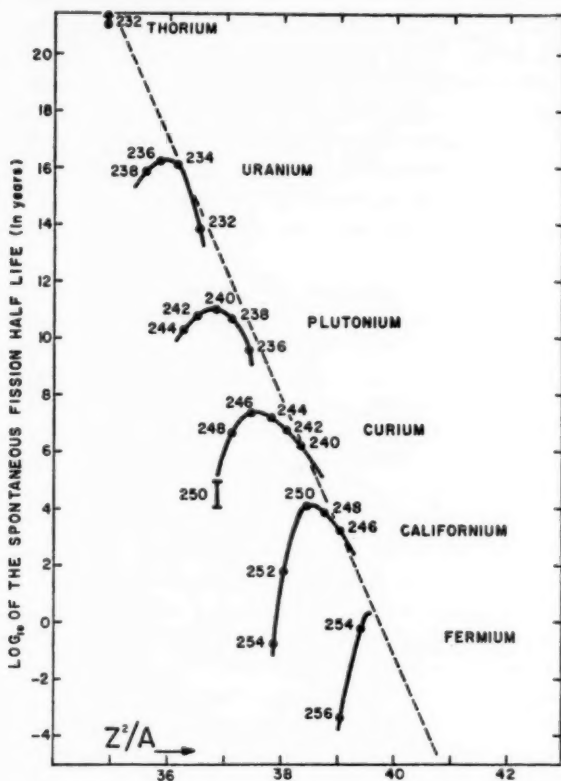


FIG. 1. Spontaneous-fission lifetimes of even-even nuclei. With the exception of the points for Cm^{250} (14) and Th^{232} (15) the data are those compiled by Hyde & Seaborg (16).

It is found that the fission decay rates vary by many factors of 10 between nuclides which lie close to each other in the isotope chart, and one must therefore be especially careful about the purity of samples used in spontaneous-fission measurements.

In Figure 1 the measured half lives for a number of species have been plotted against Z^2/A [Seaborg (12) and Whitehouse & Galbraith (13)]. According to the simple liquid-drop model of fission (which will be discussed

later), the fissionability is expected to depend on the atomic weight A and the atomic number Z of a nuclide through the combination Z^2/A . It is seen from the figure that although the data points distribute in a regular pattern, the spontaneous-fission half life does not depend on the value of Z^2/A alone. It should also be mentioned that the points in the figure give the data for only one class of nuclides, the even-even nuclides. There exist rather fewer data for other types of nuclides, and these indicate (Table I) that odd- A nuclides have abnormally long lifetimes compared to even-even nuclides.

TABLE I
SPONTANEOUS-FISSION HALF LIVES OF ODD- A NUCLIDES

Isotope	Half Life (Years)*
Pa^{231}	$\geq 1 \times 10^{16}$
U^{233}	$\geq 3 \times 10^{17}$
U^{235}	2×10^{17}
Np^{237}	$\geq 4 \times 10^{16}$
Pu^{239}	5.5×10^{16}
Am^{241}	$\geq 1.4 \times 10^{13}$
Bk^{249}	6×10^8
Cf^{249}	1.5×10^9
E^{253}	$\geq 7 \times 10^5$
Fm^{255}	20

* References to the original literature can be found in Hyde & Seaborg (16).

2. THE PENETRATION OF THE FISSION BARRIER

It is possible to understand some of the main features of Figure 1 in a semiquantitative way. Although fission in all heavy elements is exothermic, the main force between two potential fission fragments at short distances is the attractive nuclear force; only at larger distances does the Coulomb repulsion dominate. This difference in the dependence of the attractive and repulsive parts of the force between the fragments on the separation distance gives rise to a potential barrier, just as in the problem of alpha decay. And, as in alpha decay, the penetrability of this barrier is the dominant factor determining the lifetime τ . If one ignores the changes which take place in the future fragments during the barrier penetration, the penetrability is proportional to

$$p = \exp \left(- \frac{2}{\hbar} \int \sqrt{2M(V-E)} dr \right)$$

where M is the reduced mass of the two separating fragments and $V-E$ is their "negative kinetic energy" at the separation r . The range of integration extends over the barrier thickness b . Since very little is known about the shape $V(r)$ of the barrier, it is convenient to imagine that it is a parabola

$V = \frac{1}{2}K (\tau - \tau_{\text{peak}})^2$ which has been turned upside down. Then the exponent is simply

$$-\frac{2\pi}{\hbar} \sqrt{\frac{M}{K}} E \quad \text{or} \quad -\frac{b}{2} \frac{\pi}{\hbar} \sqrt{2ME}.$$

Here E is just the energy deficit of the two-fragment system measured from the top of the barrier. It is the so-called "fission threshold" (Sect. 4). In order to see whether the penetrability computed with this expression has a reasonable value let us determine the size of b that is needed to fit the measured lifetime of, say, U^{238} . The value of E for U^{238} appears to be about 5.8 Mev (Table II in Sect. 4). If one neglects the relatively constant and not too large factors which multiply p in the expression for the lifetime, the value of the exponent corresponding to the measured lifetime of U^{238} is roughly 100. It is assumed here that the lifetime for $E=0$ would be of the order of a nuclear crossing time, $\sim 3 \times 10^{-21}$ sec. (Actually the measured values of τ near $E=0$ are about 10^{-15} sec., but there are special reasons for this which are discussed in Sect. 5.) The value of b implied by the given value of the exponent is 15×10^{-13} cm. This happens to be very nearly the diameter of a fission fragment, a length which is certainly a reasonable value for the barrier thickness. It appears then that a barrier of sensible thickness can account for the spontaneous-fission half life of U^{238} in terms of its measured fission threshold.

It is seen in Figure 1 that, with increasing Z , nuclei tend to have shorter lifetimes. This fact reflects the increasing strength in these nuclei of the Coulomb repulsion relative to the nuclear attraction, a change which acts to decrease the value of the product $\sqrt{Mb^2E}$ appearing in the penetrability exponent. Thus for Cm^{240} , where the lifetime is 10^{10} times smaller than for U^{238} , the value of Eb^2 would be six-tenths of that in U^{238} . One may wonder how much of this decrease in Eb^2 is to be ascribed to each of the factors E and b^2 . There exists, at present, no clear, quantitative answer to this question either from theory or from experiment. Since it seems hardly possible to measure b^2 , an experimental answer would have to come through a measurement of the fission threshold. But in Cm^{240} (or in any of the other heavier isotopes in Fig. 1) the spontaneous fission rate is too great to permit the observation of a fission threshold, even with the most intense fluxes presently available. Fission thresholds of the heavy elements can be inferred from the measured fissionabilities of these elements (Sect. 6), but such estimates are probably still too unreliable to be combined with spontaneous-fission τ 's to give E and b^2 separately.

The straight line in Figure 1 is meant to indicate the average rate at which the log of the lifetime falls off as Z^2/A increases. It corresponds to the relation

$$b\sqrt{AE} = 60(46 - Z^2/A) \quad 1.$$

where E is the fission threshold in Mev and b is the barrier thickness in units of 10^{-13} cm.

Although Equation 1 may be useful for making rough estimates of still unmeasured half lives, it would be risky to extrapolate it too far. According to the liquid-drop model (1) [and some generalizations of it (17)], $b\sqrt{AE}$ should go as $(\text{const.} - Z^2/A)^{2.5}$ when Z^2/A has values close to that of the limiting constant. It is seen, as this last expression would imply, that an envelope to the parabolic curves which have been drawn through the data does actually show some curvature. It would be inadvisable nevertheless to take the 2.5-power law too seriously. For small extrapolations of the data it is probably best to make use of the apparently regular variations of half life with Z^2/A for "corresponding" isotopes of the different elements (18). The much more difficult and uncertain problem of making distant extrapolations to extremely heavy nuclei has recently been examined in some detail by Werner & Wheeler (19).

It should be emphasized that there is no evidence in Figure 1 that Z^2/A is a particularly appropriate parameter as regards the fission half life. Had one chosen simply Z for the abscissa, the data would have looked at least as tightly organized as they do now. The choice of Z^2/A is motivated by the liquid-drop model. Although a plot against any reasonable abscissa would need "corrections" to get all of the data points onto a single curve, one can hope that with the appropriate choice of abscissa such corrections would be simple and would make good physical sense. Swiatecki has taken the view that Z^2/A does qualify as the best parameter to describe fission lifetimes and that the "corrections" needed to bring the data onto a common curve arise from small single-particle effects (20). His correction recipe, although plausible, is neither particularly simple nor unique. He raises the values of the logarithms of τ by an amount proportional to δM , where δM is a correction to the "liquid-drop" mass of an isotope which arises from shell structure. It happens to be largest for the heaviest isotopes of an element. Swiatecki's procedure provides a "corrected" τ that does vary smoothly with Z^2/A , but despite the reasonable qualitative arguments that underlie the procedure, it is, when all is said and done, rather empirical. This is indicated in part by its failure to anticipate the revision in the accepted value of the Th^{232} half life from 10^{18} years to greater than 10^{21} years (15).

In a similar spirit Newton (20a) and Wheeler (3) suggested that the anomalously long lifetimes of odd- A isotopes result from a single-particle effect. The main point [first emphasized by Bohr (21)] is that a fissioning system passes through the saddle-point distortions so slowly that the nucleonic levels there are rather sharply defined. It is assumed that for neighboring nuclei (be they odd or even) the lowest state at the saddle is roughly at the same height above the actual ground state. In even-even nuclei, the lowest nucleonic state has a spin of zero at all distortions because of the pairing of spins and so the saddle-point "ground state" is accessible to the nucleus as it distorts from the true ground state. In an odd nucleus, on the other hand, the spin of the lowest state changes from point to point as the nucleus distorts. The lowest saddle-point state which has the same spin as the undistorted ground state will in general lie above the saddle-point ground state.

Since the total angular momentum of the nucleus does not change during fission, it is clear that the effective barrier for odd- A nuclei would be higher than that for even- A nuclei. The extra height, which Wheeler calls the "specialization energy," must be about one Mev if it is to account for the life-time hindrances ($\sim 10^6$) observed for the odd- A nuclei. This implies that the lowest accessible saddle-point state in an odd- A nucleus must differ from the saddle-point ground state by having different spins for some of the individual nucleons and not only by having different amounts of collective rotation. In the latter situation the "specialization energy" could be much lower than 1 Mev. The analysis requires, therefore, that there be rather little mixing of different types of states which have the same total angular momentum. This would be consistent with what is known of the nature of low-lying states in heavy nuclei.

From studies of fission at moderate energies one can learn whether there are any odd-even differences in the fission barrier beyond those attributable to the specialization energy. The implications of such studies are not yet altogether clear (see Sect. 6).

3. THE LIQUID-DROP MODEL

The liquid-drop model has already been mentioned several times. Its main features will now be outlined, at least in so far as spontaneous fission is concerned. The model has served since its introduction by Bohr & Wheeler (1) and by Frenkel (22) as the basic conceptual framework for the fission problem. The point of this model is to replace the actual Hamiltonian of the nucleus with a simple classical approximate Hamiltonian which hopefully has the essential properties of the true one and can be used in specific calculations and more generally for thinking about the fission process.

In its most basic form the model for the fissioning nucleus is a uniformly charged incompressible drop of liquid. The liquid is taken to possess a surface tension which is independent of the shape of the drop and of its temperature. The underlying idea here is that those energy changes occurring during the fission process which are caused by the nuclear forces resemble very much the surface-tension-connected energy changes in a drop of liquid which is changing its shape.

To see the reasonableness of this association, one recalls that the total binding energy of a heavy nucleus is roughly proportional to the number of nucleons in the nucleus rather than to the square of this number. This implies that each nucleon interacts effectively with a number of nucleons which is small compared to the total number of nucleons in the nucleus. It is reasonable to think of this small number of nucleons as the near neighbors, and one must therefore distinguish between nucleons that happen to be on the surface and other nucleons. The surface nucleons, having less than their full complement of neighbors, contribute less to the total binding than do the interior nucleons. One may write the total energy of the nucleus in its ground state $V_N + T + V_C$, where T is the kinetic energy of the nucleons

and the subscripts on the potential energies stand for "nuclear" and "Coulomb." In line with the preceding account of the nuclear forces, it is reasonable to assume that V_N can be split into two terms, one proportional to the nuclear volume, the other to the nuclear surface area: $V_N = -V_0[v - \gamma s]$. Here V_0 is the potential energy per unit volume of nucleons in the interior of the nucleus. The second term is the surface "correction" term. The coefficient γ measures by how much the average potential energy is reduced for a surface nucleon compared to an interior nucleon. In a similar way it can be shown (23) that the kinetic energy of the nucleons can be split into two terms: $T = T_0[v - \epsilon s]$. The total energy of the nucleus can therefore be written

$$v(T_0 - V_0) + s(\gamma V_0 - \epsilon T_0) + \frac{1}{2} \iint \frac{\rho_i \rho_j}{|r_i - r_j|} dv_i dv_j$$

where the last term is the Coulomb energy.

In the simplest treatment of the drop model it is assumed that all nuclear distortions take place at constant volume. In such distortions, the first term in the energy plays no role and can be forgotten. In evaluating the last term, it is assumed that the charge density is the same throughout the nuclear volume. The coefficient of the surface term is not determined from separate estimates of γ , V_0 etc. It is determined from the so-called "surface term" in one of the semiempirical mass formulas. To the extent that the choice of terms which are included in a mass formula is arbitrary, so is the meaning of the surface energy term and its value. It is as much with hope as with conviction that one writes the energy change in a nucleus brought about by a great distortion as the sum of a Coulomb term and a term which is simply proportional to the surface area, with the proportionality coefficient determined from an ordinary mass formula.

For a stable nucleus it is clear that the sum of the surface and Coulomb energy changes, $\Delta E_S + \Delta E_Q$, must be positive for any small distortion from equilibrium. But it can be shown that for certain distortions of a drop, the (negative) Coulomb term overtakes the surface term if the distortion is increased beyond a certain amount. For example, let us imagine that the nuclear drop is spherical to start with and that as it begins to stretch for fission it takes on axially symmetric shapes which are given by the simple expression

$$r = R_0[1 + \alpha_2 P_2(\cos \theta)] \quad 2.$$

where r is the radial coordinate of the surface of the drop at the angle θ to the symmetry axis, and α_2 , which is assumed to be rather small in the application of Equation 2, is a measure of the stretch of the drop in the axial direction. It can be shown that as the drop stretches, the Coulomb energy changes by $\Delta E_Q = -\frac{1}{2} E_{Q0} \alpha_2^2$. This expression is correct to lowest order in α_2^2 , and E_{Q0} is the Coulomb energy in the original spherical state. The corresponding surface energy change is $\Delta E_S = +\frac{3}{2} E_{S0} \alpha_2^2$. It follows that

for the drop to be stable against the α_2 distortion, it is necessary that $x = E_{Q0}/2 E_{S0}$ be smaller than one.

It is also easy to show that ΔE_Q for the division of the drop into two identical drops is $(2^{-2/3} - 1) E_{Q0} = -0.74 x E_{S0}$ and that the corresponding value of ΔE_S is $(2^{1/3} - 1) E_{S0} = +0.26 E_{S0}$. The energy released in such a division is $(0.74 x - 0.26) E_{CO}$, so that for x larger than about $\frac{1}{3}$ but less than 1, the final shapes here have less energy than the starting shape even though small distortions of the original sphere tend to increase its energy. It is clear that for fission which begins with an α_2 type of distortion there exists some minimum energy, a fission threshold energy, which must be supplied to the drop to bring it to the critical shape from which it can fly apart on its own.

Certainly one of the first things that one would like to do with the drop model is to find the fission threshold B_f and the corresponding distortion or, better, to find the thresholds and distortions if there happen to be a number of different shapes, each leading in its own way to fission. Even for the simple uniformly charged incompressible liquid drop, this remains an unsolved problem. In order to describe an arbitrary distortion one needs an infinite number of parameters and, in principle, the problem is that of locating those distortions which have *extremum* values with respect to all of these parameters. In practice, one tries to guess plausible shapes for the critical deformations and to choose coordinates that represent these in the simplest possible way. If one finds a "saddle point" by doing this limited type of problem it seems, however, that there is no simple way to know how close it is in shape or in energy to the true lowest saddle point of a liquid drop.

The fact that the simple charged liquid drop is apparently complex enough so that one does not know how it fissions is only one of the problems in the application of the drop model to nuclear fission. A second class of problems arises when one questions the relevance of the model to various aspects of the fission of an actual nucleus. Some reasons to question the relevance of the model can be made clearer by considering some of the magnitudes involved. The Coulomb energy of the drop which one takes to represent a nucleus is $\frac{3}{8} (Ze)^2/R$ where R is the radius of the nucleus. For U^{238} , this energy is roughly 830 Mev. One can obtain the surface energy for U^{238} from one of the mass formulas, and it is about 520 Mev. This makes the parameter x equal to about 0.8 for U^{238} . Since $x = E_{Q0}/2 E_{S0}$, and since E_{Q0} and E_{S0} are proportional to Z^2/R and $4\pi R^2$ respectively, it follows that x is proportional to Z^2/R^3 and thus to Z^2/A . The species for which x is equal to one is the species which is just unstable against fission. Its value of Z^2/A must be $1/0.8$ times that of U^{238} or about 45. The fact that the limiting value of Z^2/A in the empirical Equation 1 happens to be close to 45 is no particular evidence for the validity of the drop model. According to the model (1), the left side of Equation 1 should be proportional to the 2.5 power rather than the first power of $[(Z^2/A)_{\text{lim}} - Z^2/A]$. If the data of Figure 1 are fitted

to a 2.5-power law, they require a value of $(Z^2/A)_{lim}$ which is much larger than 45.

To examine the relative magnitudes of some of the energies involved in fission, let us imagine that the sequence of shapes assumed during U^{238} fission is reasonably approximated by Equation 2, at least up to distortions approaching that of the saddle point. Then one can obtain a very rough estimate of the saddle-point distortion by setting the fission threshold $B_f = 5.8$ Mev equal to $\frac{1}{2} \alpha_2^2 [2E_{so} - E_{q0}]$. With the aforementioned values, $E_{so} = 520$ Mev and $E_{q0} = 830$ Mev, this gives $\alpha_2^2 = \frac{1}{7}$. The corresponding ΔE_Q during the stretching is about 23 Mev and ΔE_S is 29 Mev. Although the liquid drop is not being treated in a consistent way here, these estimates are adequate to show that the distortion energy at the saddle point comes in as a small difference between two rather large energies. A small error in either of these energies can bring about great changes in the estimated threshold energy and distortion. Moreover, "small" energies that are normally overlooked in the drop model may actually be relatively important as regards fission. Such normally neglected energies include those associated with nuclear compressibility (24), the uneven distribution of charge in the nuclear volume (25), and the polarizability of the charge distribution (26). It must also be kept in mind that the nuclear level structure is not fine-grained compared to the 6 Mev of the fission threshold, so that one may certainly expect nonclassical effects associated with individual nuclear states (21).

In general, when one introduces a model for some physical phenomenon it is either because the implications of the model are easy to calculate although the ultimately necessary corrections may not be, or because it is the other way round. The drop model seems to have neither virtue. It does not yield its implications readily nor is it easy to know what modifications are required to make it an effective description of fission. The model has so far found most of its application in discussions of the probability of fission and the mass distribution of low-energy fission (Sect. 13), but in neither area has it been particularly successful. Probably the main implication of this fact is that fission is a very complicated process.

4. FISSION CROSS SECTIONS NEAR THRESHOLD

The slope of the excitation curve below the barrier.—It is not possible to observe fission at excitation energies between the ground state and about 5 Mev. In this energy range, nuclear lifetimes are determined by the probability of electromagnetic de-excitation. Electromagnetic lifetimes are of the order of 10^{-15} sec., and it is only for excitations about equal to the fission barrier height that the fission lifetime becomes as short as this.

The fission cross sections σ_f will first be examined as far below the barrier as they have been measured. Here as in spontaneous fission, their character should be dominated by the penetrability $\exp(-E/E_P)$, where E_P is $(\hbar/2\pi)\sqrt{K/M}$ (Sect. 2) and E is the energy deficit from the top of the

barrier. Assuming that the penetrability varies more rapidly with E than any other factor in the fission width Γ_f and that Γ_f varies faster with E than the total decay width Γ_T or the total reaction cross section σ_R , it follows that $d \ln \sigma_f / dE \cong -1/E_P$. It is of interest to see whether the measured excitation functions have the implied exponential character and, if so, whether the observed values of E_P are consistent with the corresponding values obtained in the analysis of spontaneous fission.

Although results from threshold region measurement have already been used in connection with spontaneous fission measurements (Sect. 2), it is by no means obvious that this was correct to do. One could imagine that the barrier which is effective in spontaneous fission is unrelated to that in threshold fission. (This would mean that different types of distortions are involved in the two kinds of fission.) Such a situation would arise if part of the fission barrier were very tall and thin, say 200 Mev high and 2×10^{-13} cm. thick, and if another part were low but fat, say 6 Mev high but 20×10^{-13} cm. thick. Clearly the first part of the barrier would be used in spontaneous fission because the penetrability is lowest through it, and the second part will be important in the threshold region as well as at somewhat higher excitation energies. To be sure, this is a very unrealistic example but it was meant only to demonstrate that one cannot be certain, *a priori*, that the barrier which was discussed in Sect. 2 also applies at higher energies. The best evidence that it actually does apply is that (a) the distribution functions of fragment masses, kinetic energies, etc. which one observes in spontaneous fission seem to be very similar to those observed at the threshold and at higher energies (Part II); (b) one can, with some success, use a barrier whose width and height are adjusted to fit threshold fission data to compute the penetrability at the energy of spontaneous fission.

It is to check this second point that the dependence of σ_f on energy in the threshold region will be examined. According to the spontaneous-fission data, E_P for U^{238} and neighboring nuclei is about 60 kev. Now E_P characterizes the parabolic barrier that would have the same penetrability as the actual barrier. It is seen from Figure 2 that if the same barrier is used in spontaneous as in threshold fission, the effective parabolic barrier is narrower for threshold fission. A narrower barrier corresponds to a somewhat higher value for E_P . One would estimate that $E_P \cong 85$ kev should be appropriate for the threshold region. With this value one is led to expect that σ_f should change by a factor of 10 for every 0.2 Mev change in excitation energy.

The average photofission cross sections in Th^{232} and in U^{238} below the threshold have been measured by Katz and his co-workers (27) [Fig. 3(a)], and the average slopes seem to be in fair accord with our estimate of E_P . Whether the differences between the two curves in Figure 3(a) are an indication that the considerations here are much too simple, or whether they are primarily a reflection of the well-known difficulties of measuring photo-cross sections with continuous x-ray spectra is hard to say. Although the

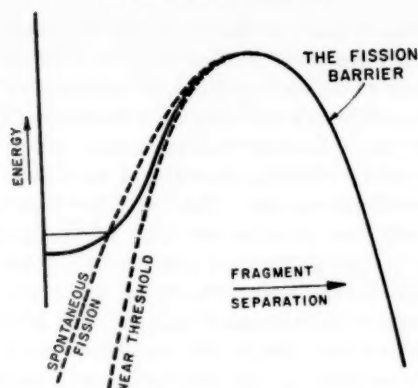


FIG. 2. A diagram to show that the effective parabolic barrier is narrower for threshold fission than for spontaneous fission.

threshold region can be studied with particles as well as with photons, the photons have the advantage that they probably do not produce as large a variety of angular momentum states as the particles. In future work this may prove to be useful enough to offset the inherent technical troubles associated with photons.

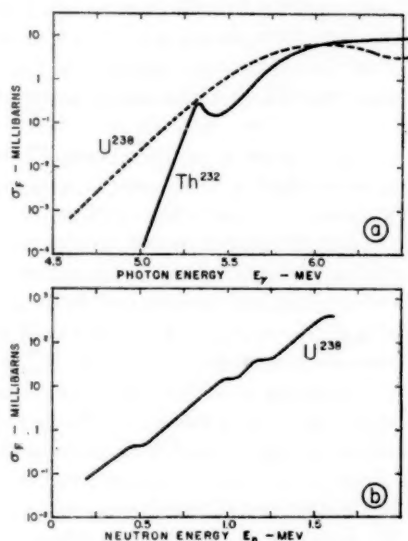


FIG. 3. (a) Low-energy photofission cross sections according to Katz *et al.* (27) (b) A low-energy neutron-fission cross section according to Ennis (28). Lamphere has reported similar curves (30).

Neutron studies have another disadvantage compared to photon studies. They can be used only for those nuclear species where the fission threshold lies above the neutron emission threshold. In addition to the implied restriction to compound nuclei with odd numbers of neutrons, this circumstance is accompanied by the following disadvantage. Since $\sigma_f = \sigma_R \cdot \Gamma_f / \Gamma_T$, the energy dependence of σ_f will be proportional to that of Γ_f only if σ_R and Γ_T vary very slowly with energy. This may be true when Γ_T is mostly Γ_γ , the photon width, but it is hardly true when Γ_n , the neutron width, becomes the largest part of Γ_T . Since Γ_n increases rapidly with energy above the neutron emission threshold, there is reason to expect that the slope of a curve of $\ln \sigma_f$ vs. energy may be smaller in neutron bombardments than in those photon bombardments which are performed below the threshold for neutron emission. Moreover, Γ_n will not, in general, increase smoothly with excitation but, as Bohr (21) and Wheeler (4) pointed out, can increase in fairly sudden jumps at those energies where neutron emissions to new levels in the residual nucleus become possible. Such jumps are visible in the measurements of Ennis (28) for U^{238} (Fig. 3). Cranberg finds that the bumps seen by Ennis occur approximately where inelastic scatterings of neutrons to new levels become possible (29), and this provides some confirmation for the view of Wheeler and Bohr. It is to be noted that, even on the smooth parts of the excitation curve, the slope is somewhat smaller than that implied by the estimated value of E_P . Ennis has also measured σ_f in Np^{237} , and here there happen to be no bumps on the fast rising part of the curve (28) and the cross section increases by a factor of 10 for each $\frac{1}{2}$ Mev. This is slightly faster than the rate in U^{238} . Everything considered, it would seem that the observed behavior of σ_f in low-energy neutron fission and photofission is consistent with the idea that the same barrier is being penetrated as that in spontaneous fission.

Incidentally, the reduction of σ_f at the threshold for neutron emission has been observed in photofission, too, where it appears to be a strong effect [Winhold (31); Katz (27); Schmitt (32); Baz (33)].

The shape of the excitation curve at barrier energies.—As the bombarding energy approaches the barrier height in a study of below-barrier fission the behavior of the cross section should be expected to depart from the behavior characterized by $d \ln \sigma_f / dE = -1/E_P$ for a number of reasons. (a) The expression which has been used here for the penetrability, $p = \exp(-E/E_P)$, can be shown to be the limiting form for small p of a more general expression for the penetrability (2), $P = (1 + 1/p)^{-1}$. The latter expression is valid in the energy region of the threshold itself ($E=0$), and there it changes more slowly with energy than p . (b) When the penetrability begins to change slowly with excitation energy, there are other factors upon which σ_f depends that may begin to play a role in its energy dependence. Such a factor is the one which measures the chance of concentrating an amount of energy U_f on the fission oscillation rather than on other degrees of freedom. This factor probably has a form something like $e^{-U_f/T}$. Strictly speaking, σ_f will be pro-

portional to an integral over U_f up to the full nuclear excitation energy $\int_{E_{\text{exc}}} e^{-U_f/T} P(U_f) dU_f$. When p is small, P is roughly $e^{-E/E_P} = e^{(U_f - B_f)/E_P}$ where B_f is the barrier height. Then σ_f turns out to be approximately proportional to $e^{(E_{\text{exc}} - B_f)/E_P}$ as already assumed in the earlier discussion. One gets this simple result because E_P is much smaller than the value of the nuclear temperature T which applies near the threshold. In the immediate neighborhood of the threshold, where the rate of change of P with energy decreases, both factors $e^{-U_f/T}$ and P may begin to be of comparable importance in determining the dependence of σ_f on excitation energy. At even higher excitation energies, the fissions take place with $P \sim 1$, and $e^{-U_f/T}$ becomes the dominating factor (see Sect. 6 and 7). (c) Another complication that confuses the energy dependence of σ_f in the immediate neighborhood of the threshold has to do with the already mentioned approximate discreteness of nucleonic levels in the saddle-point region. Each level acts like a new and separate threshold. As the excitation energy is increased from below the threshold, σ_f rises more or less abruptly as each new nucleonic level or channel becomes available for fission. These sudden increases in σ_f correspond to the sudden decreases in σ_f which have been blamed on the discreteness of the neutron channels competing with fission. For a number of reasons these steps which one expects in σ_f as a result of the saddle-point nucleonic structure should be rounded. One such reason has already been mentioned. The penetrability does not change abruptly from 0 to 1 as one reaches the top of a barrier. Instead it requires an energy interval of the order of E_P for the penetrability to change significantly. Another reason for the rounding is that the nucleonic levels in the saddle-point region have an energy which varies continuously over the pass. Associated with this variation is a band of collective levels like those familiar from molecular structure. Depending on their nature and their spacing, these levels can also be responsible for a certain amount of blurring of the steps in σ_f .

Some of these complications are especially pertinent in the interpretation of measurements recently performed at threshold energies with deuterons. Charged particles can be used in threshold studies only if they are involved in "direct interactions" since a compound nuclear reaction of a charged particle and a heavy nucleus leads to an excitation energy well above the threshold. By measuring the ratio of (d, pf) to (d, p) events as a function of proton energy, Stokes, Northrop & Boyer were able to find the probability for fission as a function of the excitation energy which is brought into the target nucleus by the stripped-off neutron (34). Their measurements extended well into the negative-kinetic-energy region for these "incident" neutrons (Fig. 4), and their results show that the fission probability increases sharply at certain energies. Apparently the effects that tend to round the steps in σ_f are not so serious that they destroy all of the structure in the excitation curves. The "negative energy" sides of the curves were analyzed by the authors into sums of functions, each of which had the form of $P = (1 + 1/p)^{-1}$ with a normalization chosen to fit the data. The authors

associate the lowest P curve with the rotational band of levels based on the saddle-point ground state. The second P curve corresponds to a level lying about one Mev above the lowest state and they suggest that this may be a vibrational level. The maximum value of the slope of a P curve which is normalized so that $\sigma_{\max} = 1$ can be shown to be $1/4E_P$ or, according to our previous estimate of E_P , about 3 Mev^{-1} . The measured maximum slopes are somewhat smaller than this, as one would of course expect them to be if there were washing-out effects of any kind.

Determinations of fission thresholds.—We have so far been concerned mostly with the slopes of the fission cross-section curves in the threshold region. It is probably of greater interest to obtain from these curves values

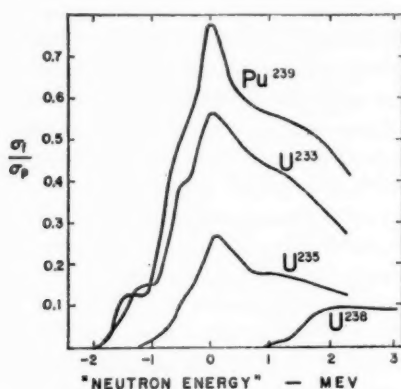


FIG. 4. The probability of fission in (d, p) reactions. The ordinate is the ratio of the (d, pf) cross section to the total (d, p) cross section which gives rise to protons with the same energy. The energy scale has been converted to the energy that the captured neutron contributes to the nucleus in excess of its own binding energy. The measurements are those of Stokes, Northrop & Boyer (34).

for the so-called "fission threshold." Since fission is extremely exothermic, the term "threshold" certainly does not mean the energetic threshold. Although it has been used to mean "the lowest excitation energy at which fission is observed," this proves to be an unreliable and otherwise rather useless definition. The most useful meaning for "threshold" would appear to be that suggested by Cameron (35). It is simply the excitation energy corresponding to the top of the fission barrier. As will be seen in a moment, this definition suffers from being hard to apply. In fact the procedures that one must use with this definition to obtain thresholds from the data generally lead to such uncertain results that one is prompted to wonder whether it is worth talking about thresholds at all. Despite the difficulties, an effort will be made to extract some values of thresholds from the available measurements. The main reason that one should make this effort is that in

any theoretical account of the relative fissionabilities of different species or the energy dependence of fissionability, the value of the fission threshold enters in a very natural way. So far, threshold measurements have been made only with three projectiles, deuterons, neutrons, and photons.

(a) The thresholds from (d, pf) measurements are those determined by Stokes *et al.* (34) from their lowest component penetrability curve for each element. The energy dependence of a penetrability curve is such that the curve reaches half its height at the threshold energy. The "thresholds" so defined are very easy to read off from the experimental curves and are listed in Table II.

(b) The thresholds from (n, f) reactions were estimated from the excita-

TABLE II
MEASURED FISSION THRESHOLDS

Nuclide	Reaction	Threshold (Mev)
Th ²³²	(γ, f)	5.8
Pa ²³³	(n, f)	6.2
Th ²³³	(n, f)	6.4
U ²³³	(γ, f)	5.4
U ²³⁴	(d, pf)	5.2
U ²³⁵	(n, f)	5.7
U ²³⁶	(d, pf)	5.8
U ²³⁷	(n, f)	6.3
Np ²³⁷	(γ, f)	5.6
U ²³⁸	(γ, f)	5.8
Np ²³⁸	(n, f)	6.0
U ²³⁹	(n, f)	6.2
Pu ²³⁹	(γ, f)	5.4
Pu ²⁴⁰	(d, pf)	4.7
Pu ²⁴¹	(n, f)	6.3
Am ²⁴¹	(γ, f)	6.0
Am ²⁴²	(n, f)	6.4

tion curves given in *Neutron Cross Sections* by Hughes & Harvey (36) and Hughes & Schwartz (37). They are the excitation energies at which the cross section is half way up its first major rise. It must be admitted at once that these "thresholds" may have very little connection to those determined from the (d, pf) reactions. For example, the lowest threshold in Pu²³⁹ (d, pf) was estimated to come at $E_n = -1.65$ Mev (Fig. 4). If one had happened to overlook the bump in the curve that comes at the far left, and instead had estimated the threshold to come halfway up the main peak, the estimate would have been raised by as much as one Mev. Thus one must, at the very least, be consistent in the attention that one pays to bumps in the excitation curve. But even if one were to make the unwarranted assumption that the

resolution in (n, f) measurements was sufficient to display all bumps, one would still have serious difficulties. For as has been shown, some bumps in the (n, f) curves are apparently caused by neutron inelastic scattering (Fig. 3). Since there is no safe way to tell one kind of bump from another by examination of the excitation curves, there is considerable uncertainty about all of the (n, f) threshold estimates. In general, they are probably systematically high compared to the (d, pf) thresholds. It should be remarked that the ambiguities referred to here would probably not be removed if the targets so far examined only by the (n, f) reaction were studied instead by the (d, pf) reaction. The interpretation of the excitation curves of the latter reaction also becomes difficult when $E_n > 0$.

(c) The (γ, f) thresholds were estimated from the excitation curves of Katz (27) in the same way that the (n, f) thresholds were estimated. Depending on the particular nuclide, these estimates may also suffer from neutron-emission complications. At the very least, they all suffer from the uncertainties associated with the use of a continuous bremsstrahlung spectrum. Finally, they tend to lie slightly higher than the "true" thresholds because, as one can tell from angular distribution measurements, threshold-energy photons bring in only spins of unity. For an even-even target the photo-threshold therefore corresponds to the lowest $1-$ state, not to the lowest saddle-point state which is presumably a $0+$ state. In the particle bombardments the input spin spectrum is very likely broad enough so that the true threshold state can be populated. The energy separation between photon- and particle-measured thresholds should therefore be the spacing between the ground state and the lowest $1-$ state at the saddle point. This spacing is probably several tenths of a Mev but is still poorly known.

If one plots the threshold values in the table against the values of Z^2/A for the fissioning nuclides, it is readily seen that, on the average, the threshold falls as Z^2/A increases. This is, of course, to be expected on the basis of Figure 1 and of the most general considerations according to the drop model. There is also a slight hint from the numbers of Table II that the thresholds of even-even nuclides may lie lower on the average than those of other nuclides. It is difficult to know how much of this apparent effect is true and how much of it may arise from possible systematic misestimates of the thresholds. If, as Swiatecki suggests (38), the even-even thresholds are truly lower (because of shell effects), this might account, in part, for the fact that the spontaneous-fission half lives of the even-even nuclides are lower than those of others (see Sect. 2).

It has already been remarked that the classical problem of locating the fission thresholds of a simple incompressible uniformly charged drop has not been solved. There do, however, exist threshold energy solutions for drops whose shapes are restricted to some special family. Clearly all such special solutions must provide an overestimate of the threshold, for by varying parameters which were kept fixed in such solutions, one would generally be able to reduce the computed threshold energy. A considerable amount of

work has been done with symmetric drops, that is, with axially symmetric drops which also have reflection symmetry about the midplane perpendicular to the axis. This work has recently been reviewed by Swiatecki (39). It is reasonable to ask whether the computed thresholds for these drops are larger than those in Table II. Unfortunately it is not possible to answer even this simple question unambiguously. The answer is very sensitive to the value of the surface tension chosen for the nuclear drop and, as already seen, there are some uncertainties which arise in the assignment of this parameter.

Even if the absolute values of significant physical quantities are hard to predict with the drop model, one might hope that the model would provide insights about trends and variations of such quantities. For example, Swiatecki has shown (17) that with some generality the threshold energy for symmetric drops should be proportional to the cube of $y = (Z^2/A)_{\text{lim}} - (Z^2/A)$ where $(Z^2/A)_{\text{lim}}$ is some constant (see Sect. 3). For the actual asymmetric fission that takes place at low energy, the drop model provides a correction term to be added to the one proportional to y^3 . Although the form of the y dependence of this new term is given by the theory, its size is not. If one now includes in the considerations some corrections for possible shell effects, it would appear that the implications which one has so far deduced from the drop model concerning fission thresholds are not sufficiently firm to be tested.

5. FISSION WITH SLOW NEUTRONS

The account of the probability of fission at successively higher excitation energies will now be interrupted for a consideration of the probability of fission following slow-neutron capture. The excitation energy of the compound nucleus formed in such capture is generally within one Mev of the fission threshold, sometimes above it, sometimes below it. As seen in the last section, this particular energy is often accessible with photons, fast neutrons, and in other ways. Slow-neutron fission, however, merits very special attention. In the first place, very many of the results to be discussed in Part II were obtained with slow neutrons. But perhaps more to the point is the fact that one can excite individual quantum states of the compound nucleus by using slow neutrons of well-selected energy. The comparison of these levels with regard to various features of the fission process has already provided important new insights (Sect. 13), and as techniques continue to develop, it is likely to provide many more.

Figure 5 shows the total cross section and the fission cross section as a function of slow-neutron bombarding energy in a nucleus typical of those which are readily fissionable with slow neutrons. The curves are for U^{235} and were obtained by Shore & Sailor with a crystal spectrometer (40). Similar measurements have been made with choppers using the time-of-flight technique. Among the recent measurements in this so-called resonance region are those reported by Fluharty (U^{233}) (41); Bollinger (Pu^{239}) (42); and Vladimirovsky (U^{233} , U^{235} , Pu^{239}) (43).

Even-even compound nuclei which are made by slow-neutron capture in the heavy elements decay with appreciable probability by fission or by photon emission only. It is seen from Figure 5 that the fission cross section is not everywhere proportional to the absorption cross section (the total cross section minus the scattering cross section). This implies that either the fission width or the photon emission width (or both) must be varying from level to level. By the fitting of Breit-Wigner curves to the resonances it has been shown that the photon emission width remains the same for all levels to within about ± 30 per cent (40, 44). The fission widths show considerable fluctuations.

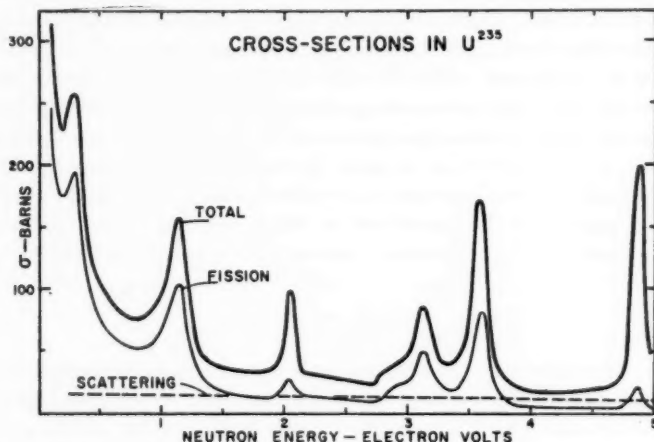


FIG. 5. Fission and total cross sections in U^{235} in the electron-volt region. The curves were taken from the work of Shore & Sailor (40).

The average values of the observed fission and capture widths for the lowest resonances are given in Table III for three nuclides. The average fission widths are about 0.1 eV and the radiative-capture widths are two to four times smaller. If the fission widths were only 10 times larger than they are it would have been difficult to find their values since it would no longer have been possible to resolve the separate levels. The fortunate fact that the fission widths are small enough to be measured provides the only situation, other than that in spontaneous fission, where absolute fission widths have been measured directly. The reason for this happy circumstance is, as Wheeler points out (1, 4) that the number of saddle-point channels available for fission from any one resonance state is a number close to 1. More specifically he shows that the number of available channels is equal to 2π times the average fission width divided by the level spacing. If more than 10 channels were "open" for fission in a nucleus excited to a typical slow-

neutron resonance state, then the resonance levels would become unresolved. This is presumably what happens at higher excitation energies.

One other piece of evidence for the small number of channels available in slow-neutron fission comes from the already mentioned fluctuations in fission width from resonance to resonance. The fission width of a particular resonance state depends on how its wave function happens to overlap with those of the transition states. If there were many states through which the nucleus could pass on its way to fission, the fission widths would be more or less the same for all levels for the same reason that photon emission widths are rather constant. The possible end states for photon emission are appar-

TABLE III
AVERAGE WIDTHS OF THE LOWEST SLOW-NEUTRON RESONANCES
(millivolts)

Nuclide	Γ_f	Γ_γ	Reference	Energy above Threshold (Mev)*
U ²³⁵	190	50	Fluharty <i>et al.</i> (41)	1.53
U ²³⁸	63	33	Shore & Sailor (40)	0.62
Pu ²³⁹	99	39	Bollinger <i>et al.</i> (42)	1.65

* Stokes *et al.* (*d, pf*) (34).

ently sufficiently many and sufficiently varied so that all compound levels of comparable energy have about the same average chance of emitting a photon. Figure 6 shows a plot of the integral fission width distribution for the lowest slow-neutron levels in U²³⁵. The theoretical curves in the figure are those from the statistical theory of level widths of Porter & Thomas (45). They involve the parameter C which corresponds to the number of available saddle-point channels. It is seen from the figure that C probably lies between one and four. The same sort of conclusion applies to the analyses which have been made of the levels of other fissionable nuclei. It should be pointed out here that the value of C which is determined by fitting the observed distribution of fission widths is expected to be a somewhat larger number than the "number of channels" determined from the size of the average fission width according to Wheeler. For example, if there happened to be three possible channels, each with equal but very poor transmission for fission, one would have very narrow resonances, and the total number of effectively open channels could be much smaller than one. Yet these small widths would fluctuate from resonance to resonance in a way that would correspond to $C=3$.

It is seen then that in slow-neutron fission only a few saddle-point chan-

nels are open. To be more precise in the description of how these channels are actually used in the fissions which proceed from a given resonance state, one would need to develop a theory of the motion of the nucleus into the saddle-point region. It appears from an analysis of the problem by Wilets (46) that near threshold there may not be sufficient coupling between particle and collective modes to maintain equipartition among all modes during this motion. Under these conditions, the average fission width turns out to be smaller than the one expected when only the number of available channels and their penetrabilities are taken into account.

From the fact that the measured fission width is ~ 0.1 ev it follows that

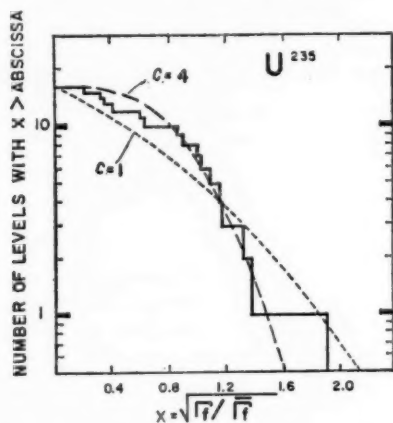


FIG. 6. The distribution of fission widths in U^{235} according to Havens (44). The histogram gives the integral distribution in fission width. It has been plotted in a way that facilitates comparisons with the theory of Porter & Thomas (45). The parameters C which label the theoretical curves give the effective numbers of end states or channels for the nuclear decay by fission. The data seem to require a value of C between 1 and 4.

the lifetime for fission is about 10^{-14} sec. Since the penetrability in slow-neutron fission is of order one and since a fissionlike oscillation of a nuclear drop should take $\sim 10^{-20}$ sec., it is clear that it takes about 10^6 times as long to concentrate the energy on a fission mode as it takes for the nucleus to fly apart once it has the energy. The reason for this long time is of course that there are many non-fission-producing degrees of freedom competing for the energy. This competition has already been mentioned in connection with the introduction of the factor $e^{-U_f/T}$ in Section 4. This quantity corresponds to the level spacing which enters as the factor in the above-mentioned connection between the fission width and the number of open fission channels.

Since the resonant states which are formed in slow-neutron capture can be grouped into two sets of states whose spins differ by one unit, it follows from the fact that spin is conserved during the fission process that the dif-

ferent resonant states will in general not fission through the same set of channels. In particular, the lowest saddle-point rotational band will be open only to states with one of the two possible spins of the resonant states because of the requirements of parity conservation. As Wheeler has emphasized (4) this suggests that if the lowest channel happens to be well separated from the others, an appropriate decomposition of the fission width distribution may help one classify the resonance states according to their spin.

There is no lack of measurements of fission cross sections with thermal neutrons. A sample of some of the results is given in Table IV. Fuller tables are given by Hughes & Schwartz (37) and by Hyde & Seaborg (16). Several

TABLE IV
THERMAL NEUTRON FISSION CROSS SECTIONS*

Nuclide	σ_f (Barns)	σ_f/σ_{abs}	Reference
U^{235}	518 ± 4		Bigham <i>et al.</i> (47)
	530 ± 8	0.90	Harvey & Saunders (48)
U^{238}	556 ± 6		Bigham <i>et al.</i> (47)
	576 ± 15	0.84	Harvey & Saunders (48)
	$542 \pm 4^\dagger$		Friesen <i>et al.</i> (49)
	$590 \pm 6^\dagger$		Saplakoglu (50)
	$623 \pm 14^\dagger$		Raffle as quoted in (44)
Np^{237}	0.019 ± 0.003	1×10^{-4}	Hyde & Seaborg (16)
Pu^{238}	18.4 ± 0.9	0.03	Hulet <i>et al.</i> (51)
Pu^{239}	779 ± 5	0.7	Bigham <i>et al.</i> (47) and Hyde & Seaborg (16)
Pu^{241}	1055 ± 8	0.8	Bigham <i>et al.</i> (47) and Hyde & Seaborg (16)
Am^{241}	3.13 ± 0.15	4×10^{-3}	Hulet <i>et al.</i> (51) and Hyde & Seaborg (16)
Am^{242}	6390 ± 500	0.75	Hulet <i>et al.</i> (51) and Hyde & Seaborg (16)
Am^{243}	< 0.072	$< 5 \times 10^{-4}$	Hulet <i>et al.</i> (51) and Hyde & Seaborg (16)
Am^{245}	1880 ± 150	0.9	Hulet <i>et al.</i> (51)

* See (16), (36), and (37) for more complete tables.

† Corrected from measurements at 2200 m./sec. to thermal measurements by a factor given in (48).

entries have been included in the table for the isotope U^{238} to show that there is still considerable uncertainty in the absolute values of the thermal cross sections. The values in the table are not particularly interesting from the viewpoint of the fission process. The large sizes of some of the cross sections have to do with the well-known large absorption cross sections for slow neutrons. The precise value of a particular absorption cross section will depend on the nearness to thermal energies of one of the resonances of the compound nucleus. Perhaps a bit more significant for the discussion of the fission process is the ratio of the fission cross section to the total absorption cross section (column 3). This ratio varies over a range of 10^4 for the nuclides in

the table. It is large for the targets which have an odd number of neutrons, since for them the capture of a neutron leads to an excitation energy above the fission threshold. The precise value of the ratio depends on the relative fission widths of those levels which happen to lie near the thermal energy. Since, as seen earlier, the fission widths fluctuate considerably from level to level, there is no particular meaning to be attached to the thermal-neutron value of the relative fission width.

6. FISSION AT MODERATE EXCITATION ENERGIES

Neutron fission and photofission.—When nuclei are excited to energies which are more than a few Mev above the fission threshold, it becomes impossible to measure the fission width directly. The levels are too broad, compared to their spacings, to be resolved, and it is of course not feasible to measure actual fission lifetimes, since they are shorter than 10^{-18} sec. One must be satisfied with a measurement of the relative fission width, Γ_f/Γ_T . It should be said here that the symbols Γ as they will be used in this section will refer to average level widths taken over many compound nuclear levels. The value of Γ_f/Γ_T can sometimes be obtained from a direct comparison of the fission and total cross sections, but sometimes it is easier to determine Γ_f/Γ_n where Γ_n is the average width for neutron emission. At the energies we are considering, the components of Γ_T other than Γ_f and Γ_n are negligible, so that $\Gamma_T \cong \Gamma_n + \Gamma_f$ and a measurement of the ratio between any two of these three quantities determines the relative values of all three of them.

The relative fission width shows enormously wide variations among the familiar fissioning species excited to the same energy. Huizenga has carefully compared fissionabilities at excitation energies of 3 to 4 Mev above the threshold (52), and some of the data in his compilation have been plotted in Figure 7. The data were obtained in neutron and photon bombardments only, and it appears from the figure that these two kinds of measurements give rather consistent results. In a later report (53) Vandenbosch & Huizenga used better values for the total reaction cross sections in the neutron bombardments than were used for Figure 7. This revision results in an increase of about 15 per cent in the neutron fission points and raises the question of a possible discrepancy between the neutron and photon data. This point will be considered further below.

Probably the most obvious regularity in Figure 7 is the increase of fissionability with decreasing mass number for a given element. This may come about in part because of increasing Z^2/A but also because of increasing neutron-binding energies as A decreases. Both factors favor fission over neutron emission. In order to estimate their relative importance, an effort will be made to account for the observed slope of the curve for uranium isotopes in the figure. The inset in Figure 7 is meant to illustrate the competition of fission with neutron emission from the excited compound nucleus. The width Γ_n for neutron emission is expected to be roughly proportional to $N_n \exp$

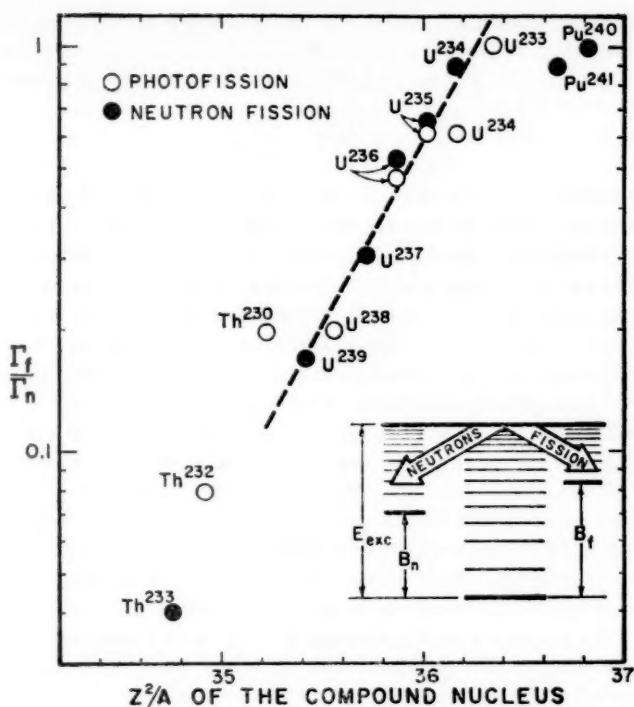


FIG. 7. The ratio of fission widths to neutron emission widths in low-energy neutron and photofission. The data were taken from the compilation of Huizenga (52) where references to the original papers are given.

$(-B_n/T)$ where N_n varies more slowly with energy than the exponential and B_n is the neutron binding energy. The temperature T increases with the excitation energy E_{exc} , but the validity of the expression for Γ_n does not depend sensitively on how T varies with excitation energy. Generally speaking, the validity of the formula improves the larger both the quantities $E_{exc} - B_n$ and $E_{exc} - T$. In the same spirit, the fission width Γ_f is expected to be proportional to $N_f \exp(-B_f/T)$ where B_f is the height of the fission barrier. Underlying the use of the same temperature T to describe both widths are the assumption that the quantity $B_n - B_f$ is much smaller than E_{exc} and the plausible assumption that the distorted nucleus at the saddle point has the same volume and hence the same energy dependence for its level density as a normal nucleus. It follows that

$$\frac{\Gamma_f}{\Gamma_n} = N e^{(B_n - B_f)/T} = N e^{\Delta/T} \quad 3.$$

where N_f/N_n has been replaced by N and $B_n - B_f$ by Δ . N should be a number of the order of unity, and it may have some slight energy dependence. (See

the more detailed discussion below.) In analyzing the data, it will be assumed for simplicity that N is the same for all fissionable nuclei. Then the slope of the line for uranium in Figure 7 expressed in terms of the mass number A is

$$\frac{1}{T} \left(\frac{dB_n}{dA} - \frac{dB_f}{dA} \right).$$

The mass tables of Cameron indicate that for uranium dB_n/dA is roughly -0.15 Mev per mass number for either the odd- A or the even- A isotopes considered separately (54). If one assumes that dB_f/dA is also the same for the odd isotopes of an element as for the even ones, then one must expect the odd isotopes to lie on a line in Figure 7 which is parallel to, but not necessarily coincident with that of the even isotopes. As nearly as one can tell, these two lines for uranium isotopes actually fall on one another. We shall return to this point later. An estimate for dB_f/dA must now be developed to see whether with a reasonable value of T one can account for the observed slope in Figure 7. This can be done for the uranium isotopes with fair accuracy on the basis of Table II. The uranium data there give $dB_f/dA = 0.19$ Mev per mass unit within an accuracy of about 25 per cent. It is instructive to make the same estimate in another way. It was seen that the average dependence of the spontaneous-fission half life on Z^2/A implies that $b\sqrt{AB_f} = 60 (46 - Z^2/A)$ (Sect. 2). If it is assumed, for example, that the barrier thickness b is the same for all fissioning species, then (since A is very nearly the same for all species), $B_f^{1/2}$ is proportional to $(46 - Z^2/A)$. This quantity changes by 9 per cent between U^{233} and U^{239} or by 1.5 per cent per mass unit. Hence B_f might be expected to change about 3 per cent or 0.18 Mev per mass unit. Had one made the more reasonable assumption that b is not constant but that all barriers have the same shape (i.e., $B_f \sim b^2$), then one would have found a variation of only 0.09 Mev per mass unit. When it is recalled that the envelope in Figure 1 is really not straight as this simple formula implies but that it curves, it becomes reasonable to use for dB_f/dA some value in between 0.09 and 0.18 Mev. For simplicity, 0.15 Mev is chosen. (This happens to make dB_f/dA of the same magnitude, but of opposite sign as dB_n/dA .) It is gratifying that the estimate from the spontaneous-fission data is not too far off from that based on the table of fission thresholds. According to these estimates the slope in Figure 7 is about half a result of the variation of neutron width with A , and half a result of the variation of the fission width. Altogether, $d/dA (\ln \Gamma_f/\Gamma_n) = 0.30/T$. The measured value of this slope is 0.38, implying that T must be ~ 0.8 . This is not an unreasonable value for the nuclear temperature at the excitation energies dealt with here.

Since apparently only half the mass-number dependence of Γ_f/Γ_n has to do with the fission width or with Z^2/A , one must not expect the data for different elements to lie on the same curve when Γ_f/Γ_n is plotted against Z^2/A . The thorium and plutonium data should lie on lines roughly parallel

to the uranium line to its left and right, respectively. This is because a plutonium isotope with the same value of Z^2/A as some uranium isotope is necessarily more neutron-rich with reference to the stable valley. It has a lower neutron-binding energy and therefore its Γ_f/Γ_n must be smaller. From the value of the change in B_n at constant Z^2/A from uranium to plutonium (0.7 Mev) (54), and the slope of the uranium line in Figure 7, it is easy to show that one would expect the plutonium line to be displaced 0.45 units of Z^2/A to the right of the uranium line. It can be seen that the locations of the points for Pu^{240} and Pu^{241} are in accord with this estimate. One can also see that in the neighborhood of the uranium line, the thorium data lie to the left, as expected, although the observed displacement is somewhat smaller than our rough estimate would lead us to expect.

Charged-particle-induced fission.—Values of Γ_f/Γ_n can be obtained from studies of charged-particle-induced fission also. Such values generally refer to higher excitation energies than have been considered so far because of the role of the Coulomb barrier for the incident charged particles. Vandenbosch & Huizenga have recently compiled a list of fission probabilities observed in various medium-energy charged-particle reactions (53). It is simplest to begin with an examination of the evidence from but a single representative type of reaction. The reaction most extensively studied is the $(\alpha, 4n)$ reaction, and the cross sections for a large number of targets have recently been collected by Vandenbosch & Seaborg (55). In a non-fissionable heavy nucleus the peak value of the $(\alpha, 4n)$ cross section is about 1.2 barns (56). In a fissionable nucleus it is smaller because of the competition from fission. Vandenbosch & Seaborg use the quantity $\bar{G}_n = [\sigma(\alpha, 4n)/1.2]^{1/4}$ to characterize the relative probability for neutron emission. Here $\sigma(\alpha, 4n)$ is the measured cross section in barns at its peak (which generally occurs slightly above 40 Mev), and \bar{G}_n is, therefore, a geometric mean value of Γ_n/Γ_f for the four neutron emissions involved in the $(\alpha, 4n)$ reaction. The observed values of \bar{G}_n for targets of even Z are shown in Figure 8.

The curves for \bar{G}_n which appear in Figure 8 were computed by finding, for a large number of targets, the product of the relevant four factors (one for each of the four neutron emissions), $\Gamma_n/\Gamma_f = (1 + \Gamma_f/\Gamma_n)^{-1}$. The quantity Γ_f/Γ_n was computed according to Equation 3 in terms of the quantities N , B_n , B_f and T . Although N may be somewhat energy dependent, this dependence should be nearly the same for all species; and since the experimental data being considered here all refer to comparable excitation energies, it is reasonable to set N equal to some constant, the same constant for all nuclear species. The choice $N=0.6$ provided the best fit to the uranium and plutonium data. The values of T were taken to be 1.5, 1.3, 1.0 and 0.7 Mev for the successive neutron emissions. The values of B_n were taken from the tables of Cameron (54), but odd-even differences were removed by averaging. The height of the fission barrier B_f was determined from Equation 1 with the assumption that all barriers have the same shape.

More specifically it was assumed that $B_f = 0.555 (46 - Z^2/A)$. The multiplying constant here was chosen to reproduce the measured threshold of U^{238} . The use of this formula like the use of average B_n values smoothes over any odd-even differences.

In this connection it is important to point out that B_n and B_f as they appear in Equation 3 are the effective values of these quantities for the purpose of measuring level densities. It was indicated earlier that on the average, the measured value of B_f may be lower for even-even nuclides than for others. The value of B_n for such nuclides is, on the other hand, higher. As Jackson has pointed out (57), the measured value of $B_n - B_f$ for an even-even nuclide

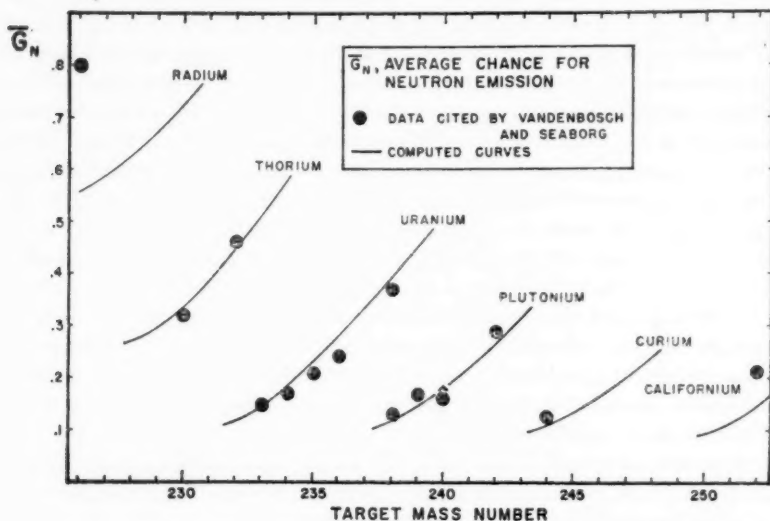


FIG. 8. The average chance that neutron emission occurs instead of fission in a number of elements. The data were all determined by Vandenbosch & Seaborg (55) from the sizes of $(\alpha, 4n)$ cross sections in fissionable elements. The labels and the abscissa here refer to the target element. The curves were computed as described in the text.

may be as much as 2 Mev larger than the measured value of this difference for an even-odd nuclide. In the interpretation of fission data, it is not feasible at present to begin with measured values of B_n and B_f and then to correct them to effective values. In the first place there are too few reliable measurements of B_f . Besides, the "corrections" to effective values involve considerable guesswork. Instead use is made of the observation that Γ_f/Γ_n seems to be independent of oddness or evenness in Figure 7. This is taken to imply that the "corrections" when properly applied manage very nearly to cancel the odd-even differences which appear in the measured values of $\Delta = B_n - B_f$. This would be what one would expect if oddness or evenness

had an effect on the position of ground states, but not on the positions of higher levels.

It is seen that the computations of \bar{G}_n , simple and rough as they are, are fairly successful in reproducing the observations. It is to be emphasized that there were no separate adjustments here for the different elements. They were all treated identically. The most serious discrepancy is for the radium bombardment. The reason that the calculated value of \bar{G}_n is as high as it is here (but not quite high enough) is that B_n is anomalously small for nuclides in this neighborhood. This has to do with the proximity of the 126-neutron shell. Measurements of fissionabilities of nuclides lighter than thorium (Sect. 8) suggest that part of the radium discrepancy here is attributable to a sharper rise in B_f with decreasing Z than is implied by Equation 1. Since this equation is based in the loosest way on spontaneous-fission data and since none of these data refer to elements lighter than uranium, one need not be too disturbed by a possible conflict between the equation and the radium measurements.

Two $(\alpha, 4n)$ cross sections have been measured for odd- Z targets (55). For Bk^{249} the measured value of \bar{G}_n was 0.27, the computed value, 0.18. For Am^{243} these values were 0.34 and 0.22 respectively. The relative discrepancy between measurement and computation here is larger than for any of the even- Z targets. This result and the abnormally long spontaneous-fission half lives of odd-odd nuclei suggest that odd- Z nuclei may somehow be intrinsically less fissionable than even- Z nuclei. Clearly, more experimental work is needed to determine the effects of oddness or evenness on fissionability.

Angular momentum and fissionability.—The fissionability data which have been obtained in charged-particle reactions other than the $(\alpha, 4n)$ reaction will not be examined here. Vandenbosch & Huizenga have shown that they are reasonably consistent with the implications of this reaction (53). It is of interest, however, to compare the data of Figures 7 and 8. If one computes Γ_f/Γ_n for the uranium isotopes in photon and neutron fission using the same procedure that was used to obtain the curves in Figure 8, it is found that one overestimates the observed values of Γ_f/Γ_n given in Figure 7 by a factor of about two. It is unlikely that this factor can be much, if at all, reduced by taking into account the possible energy dependence of the factor N in Equation 3. N probably decreases slowly as the excitation energy increases (Sect. 7) and we are looking for an effect that makes Γ_f/Γ_n larger rather than smaller at higher energies. The alpha particles which are responsible for the fissions considered in Figure 8 bring in much more angular momentum as well as more excitation energy than the neutrons and photons of Figure 7. This suggests that Γ_f/Γ_n may increase with the amount of angular momentum deposited in the nucleus. Such a possible connection between the relative fission probability and angular momentum was first emphasized by Pik-Pichak (58).

It is easy to understand the direction of the angular-momentum effect

and even to estimate its order of magnitude. Suppose that a nucleus happens to have some fairly large amount of angular momentum I and that it evaporates a neutron. Since the neutron is generally evaporated with only a small amount of energy and since it has a small mass, it does not remove much of the angular momentum from the nucleus. The angular momentum which remains in the residual nucleus is still $\sim I$. Associated with this angular momentum is some rotational kinetic energy; and in computing the probability for the neutron emission in terms of the density of states in the final nucleus, one should subtract from the excitation energy this unavailable rotation energy. Such a subtraction is equivalent to the addition of a term $I^2\hbar^2/2\mathfrak{I}$ to the neutron binding energy B_n . This added term represents approximately the minimum amount of energy that must be tied up in rotation when the angular momentum is I . For a highly excited nucleus, this minimum is achieved when the nucleus rotates as a whole, and then \mathfrak{I} is the so-called rigid-body moment of inertia. For a typical heavy nucleus $\hbar^2/2\mathfrak{I}$ has the value 2.5 kev.

The effective fission threshold is also raised because of the rotation but not as much as the neutron threshold. It is raised by $(\hbar^2/2\mathfrak{I}_s)I^2$ where \mathfrak{I}_s is the moment of inertia at the saddle point about an axis perpendicular to the fission axis. The quantity Δ is therefore increased by the amount

$$\frac{\hbar^2 I^2}{2} \left(\frac{1}{\mathfrak{I}} - \frac{1}{\mathfrak{I}_s} \right)$$

because of the rotation. Assuming that the elongation of the nucleus at the saddle point is such that $\mathfrak{I}_s = 2.5 \mathfrak{I}$, and using $\hbar^2/2\mathfrak{I} = 2.5$ kev, it follows that Δ is effectively increased by $1.5 I^2$ kev. In the $(\alpha, 4n)$ reaction studies of Figure 8, the average value of I^2 is about 250 so that Δ is increased by $\frac{1}{2}$ Mev. In the analysis of Figure 7 it was seen that Δ increases by 0.3 Mev and Γ_f/T_n changes by a factor of 1.4 when the mass number A changes by one unit. One would accordingly expect that Γ_f/T_n should be about 1.5 times larger for uranium isotopes which are produced in the $(\alpha, 4n)$ reactions than it is for the same isotopes produced in fission with low-energy neutrons. Considering the roughness of the present estimate, this conclusion is probably in adequate agreement with the observed factor of two which has been mentioned above.

It has also been mentioned in connection with Figure 7 that the neutron fission points may actually be about 15 per cent higher on the average than the photofission points. It is of interest to inquire whether this difference could possibly arise from angular-momentum effects. At the lower energies which are involved here [compared to those in the $(\alpha, 4n)$ reactions] it is probably more appropriate to use for $\hbar^2/2\mathfrak{I}$ a number like 7 kev instead of 2.5 kev. The former number is the one which applies to the rotation of heavy nuclei near the ground state (21). Using this value and the value $\overline{I^2} = 8$ for 3-Mev neutrons one expects Δ to be about 1/30 Mev higher for fis-

sion induced by such neutrons than for photofission at the same excitation energy. According to our rough estimates, this would correspond to a 5 per cent larger value of Γ_f/Γ_n in the neutron fission. This expected difference is rather smaller than the 15 per cent deduced from the analysis of the data by Vandenbosch & Huizenga (53). The most likely reason that the neutron-measured values of Γ_f/Γ_n are somewhat larger than those measured in photon-induced reactions is that the effective fission thresholds in photofission probably lie several tenths of a Mev above those in particle-induced fission (Sect. 4).

To learn something about the angular-momentum effect, it is probably most sensible at this stage to study it where it is large. This suggests that one compare the fission cross sections of heavy ions with the cross sections of lighter projectiles which one chooses to produce the same species of compound nucleus at the same excitation energy. Because of the high Coulomb barrier for heavy ions they can be used only at relatively high excitation energies. Nucleon-induced reactions at these energies tend to be complicated by "direct interactions" and it would therefore seem that it would be most fruitful to compare heavy ions with alpha particles or with other heavy ions.

Some fission measurements have already been made with heavy ions which can be related to the alpha-particle measurements of Figure 8. For example, Flerov has reported an excitation curve for the (C^{12} , $4n$) reaction in uranium (59) (Fig. 9). A peak value of about $65 \mu\text{b}$ was found for the cross section at the same energy at which the total (actually the fission) cross section was 0.08 barn. This makes $\bar{G}_n = 0.17$. The same compound nucleus at roughly the same excitation energy is produced at the peak of the (α , $4n$) reaction in Cm^{246} . Although this particular cross section has not actually been measured, it should be safe enough to take its value for \bar{G}_n from the computed curves in Figure 8. This value happens to be 0.17 or exactly the same as that in the corresponding heavy-ion measurement. The agreement is gratifying. Unfortunately it is not easy to estimate the small difference that one would expect in \bar{G}_n for the two bombardments arising from the angular-momentum effect. The heavy-ion bombarding energy here happens to be below the Coulomb barrier, and it is not a simple matter in this situation to estimate the average I^2 which the heavy ions deposit in the nucleus.

7. FISSION AT HIGH EXCITATION ENERGIES

The derivation of an expression for Γ_f/Γ_n .—In the last section it was assumed that Γ_f/Γ_n has the form $N e^{\Delta/T}$. There the primary interest was in comparing different species at comparable excitation energies. In this section we shall be more concerned with the energy dependence of Γ_f/Γ_n . For that reason it becomes important to understand what sort of energy dependence one might reasonably expect for the factor N . Before turning to the relevant data, we therefore "derive" the form $\Gamma_f/\Gamma_n = N e^{\Delta/T}$ from a simple

classical analogy and in so doing learn something about the possible structure of N .

We consider a classical particle in equilibrium with others in an enclosure from which it can escape. This particle will later be identified either with a neutron or with the degrees of freedom appropriate to fission. But in either case the model is an equilibrium model. If the fission saddle point is actually sometimes reached in a way that does not correspond to the continual interchange of energy between all of the degrees of freedom at some temperature T , then any equilibrium model will be inappropriate as a description of fission.

It is easy to show that a classical particle in a box of any number of dimensions has a probability of escape from a hole in the box which is pro-

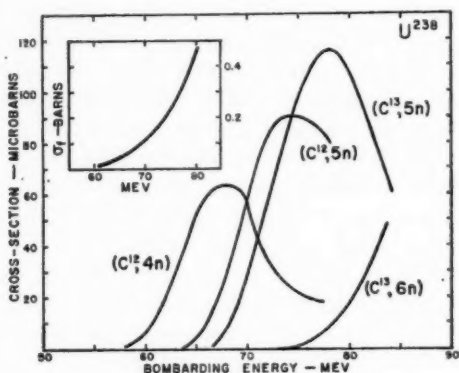


FIG. 9. Carbon cross sections on U^{238} reported by Flerov (59). As described in the text, these curves can be used to estimate fissionabilities of the compound nuclei which are formed.

portional to $T^{1/2}e^{-E_c/T}$. This is the Richardson equation for thermionic emission, and E_c is the work function for the particle in the region of the hole. It is assumed that away from the hole, E_c is infinite. The proportionality coefficients in this expression involve the ratio of the size of the hole to the volume of the box.

The top drawing in Figure 10 shows, by way of example, a particle in a two-dimensional box which happens to have a hole on one side. The particle which is about to escape should be imagined to collide from time to time with other particles in the box which represent other degrees of freedom of the system. For the simple case of a two-dimensional box, it is convenient to use the third dimension to represent the potential which confines the particle to the box. The second drawing from the top represents a box where the work function is E_c in the hole and infinite elsewhere. For a particle to escape, it must reach coordinates (x, y) within the hole and it must have a

kinetic energy, just before it gets there, which will be enough to carry it through the hole. In particular its kinetic energy in the direction perpendicular to the hole must be at least E_c .

The third drawing shows the situation where the work function varies quadratically with the distance from a point ($E_c = \frac{1}{2}Kr^2 + E_0$). Then in place of the factor $e^{-E_c/T}$ in the Richardson equation, we have $e^{-E_0/T}$ times

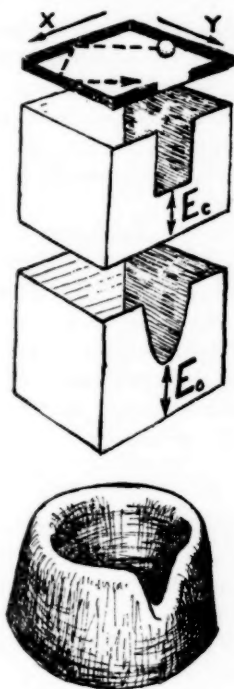


FIG. 10. Diagrams to explain how the probability of fission can be compared to the probability of escape of a particle from an enclosure (see text). In all figures, the enclosure is supposed to be two-dimensional, and the vertical dimension is used to represent the height of the energetic barrier at the edge of the enclosure. The parabolic opening in the box where the threshold is labelled E_0 corresponds to a typical saddle point.

$\int e^{-1/2kr^2/T} d\gamma = \text{const} \cdot T^{1/2} e^{-E_0/T}$ and the total escape probability becomes $\text{const} \cdot T e^{-E_0/T}$. The situation being described in this drawing is that of escape through a somewhat idealized "saddle point." The ash tray in the fourth drawing has perhaps a more realistic saddle point, and the probability for escape from it should be roughly (but not exactly) the same as that from the box in the third drawing.

In order to have a saddle point at all, one must be dealing with a problem which involves at least two dimensions. (In α -decay one usually considers only the radial coordinate and one therefore speaks of the barrier—but not of a saddle point.) In thinking about fission one often associates with y in Figure 10 the coordinate α_2 which measures the stretch of the nucleus. It must have at least a certain value if fission is to occur, but that is not enough. One often associates with x the coordinate α_3 which measures the asymmetry of the nucleus, and fission occurs with significant probability only when α_3 lies within certain particular limits. If there are other degrees of freedom in addition to α_3 which must likewise have their coordinates in some specified range in order for fission to occur, the problem just takes on more dimensions. It is, however, easy to show that if these other coordinates also have "quadratic work functions" then the escape probability is $T^{d/2}e^{-E_0/T}$ where d is the total number of dimensions essential to the fission distortion ($d=2$ in Fig. 10).

It is probably appropriate to use a Maxwell particle (as one does in deriving the Richardson equation) to describe fission. Fission is essentially a classical mode. On the other hand, in considering neutron emission it should be remembered that the neutrons are more like a Fermi gas than a Maxwell-Boltzmann gas. Under the circumstances their "thermionic emission" probability is more appropriately described by the Dushman equation rather than by the Richardson equation, and Γ_n is proportional to $T^2e^{-B_n/T}$.

From the foregoing it follows that

$$\Gamma_f/\Gamma_n \cong T^{(d-4)/2} e^{(B_n-B_f)/T} = T^{(d-4)/2} e^{\Delta/T} \quad 4.$$

where d is the "essential dimensionality" of the fission process. For the situation described in Figure 10, d is 2 and the factor so far called N is simply proportional to $1/T$. This form of Γ_f/Γ_n was first suggested by Fujimoto & Yamaguchi (60).

As long as the power of T in Equation 4 is some small number, then one must expect the energy dependence of Γ_f/Γ_n to be controlled mainly by the exponential as long as Δ is reasonably large. One should, for example, see very large changes in Γ_f/Γ_n in very fissionable (large- Δ) nuclei at low excitation energies. It is probably difficult to measure σ_f in very fissionable nuclei with the available fluxes of projectiles because of spontaneous fission. It should, however, be possible to examine the energy dependence of Γ_f/Γ_n in such nuclei by comparing the (γ, n) excitation curves with those in slightly lighter nuclei. One would assume here that the excitation curves for photon absorption are rather much the same in all heavy nuclei.

Fission cross sections as a function of energy.—Available data which have a bearing on the problem of the energy dependence of Γ_f/Γ_n will now be examined. It is convenient to consider these data in three separate classes: (a) the comparison of fission cross sections with total reaction cross sections as a function of energy; (b) the comparison of nonfission cross sections in

fissionable nuclei with total cross sections, and (c) the measurement of the angular correlation between fission fragments and fission neutrons. It must be said at the outset that the results of an examination of the data are disappointing. There are plenty of data and vast numbers of sensible guesses about what is happening to fissionability as a function of energy, but there are no clear answers. The major source of confusion arises from the nature of higher-energy reactions. At high energies, projectiles tend to deposit varying amounts of energy and momentum in nuclei, and they often eject a few nucleons in the process. This makes the rather subtle analyses required in the assessments of fissionabilities somewhat unreliable.

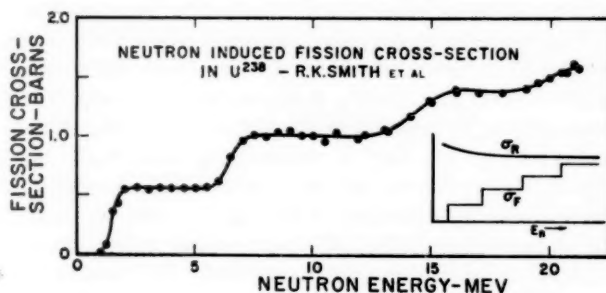


FIG. 11. The fast-neutron fission cross section in U^{238} according to Smith *et al.* (61). The inset is an idealization to show how the fission cross section σ_f increases suddenly at definite thresholds. By comparing σ_f to the total reaction cross section σ_R , one can, in principle, determine how fissionability varies with excitation energy.

Figure 11 shows the fission cross section in U^{238} determined by Smith, Henkel & Nobles (61). The most striking feature of the curve is its step-like character (idealized in the inset). The second step occurs when the U^{238} produced in the (n, n') reactions can be left with enough excitation energy to undergo fission. The next step occurs at the fission threshold for U^{237} and so on. The difficulty of obtaining information about the fissionabilities at the higher energies will be illustrated by a simple example. It is assumed that Γ_f/Γ_T has the not unreasonable values 0.13, 0.17, and 0.23 for U^{239} , U^{238} , and U^{237} respectively. It is further assumed that these values apply at all excitation energies. It is then an easy matter to predict fission cross sections. On the third step (~ 18 Mev), one should have $\sigma_f/\sigma_R = [0.13 + (0.87)(0.17) + (0.72)(0.23)] = 0.44$. But suppose that for some reason, fissionability falls to zero in the course of a few Mev at excitation energies above 16 Mev, then the first term would be missing in σ_f/σ_R , and one would have instead $\sigma_f/\sigma_R = [(0.17) + (0.83)(0.23)] = 0.36$. This represents only a 20 per cent change in the expected fission cross section. Although σ_f can be measured with an accuracy better than 20 per cent, it would still

be difficult to learn about the energy dependence of Γ_f/T_n from such a measurement. One would have to divide σ_f by σ_R , and it is somewhat more difficult to measure the total reaction cross section than it is to measure the fission cross section. Besides, at higher energies the measurements would be confused by the "direct interactions" which deposit amounts of energy in the nucleus which are at present not well known. Finally, one must be prepared to correct the observations for the change in angular-momentum deposit (Sect. 6) as the bombarding energy is changed. Only then can one extract the dependence of Γ_f/T_n on excitation energy. It is clear that it is not an easy matter to learn about Γ_f/T_n from the absolute values of the fission cross sections at different energies.

Nor is it easy to learn much from the qualitative character of curves like those in Figure 11. Even if Γ_f/T_n begins to fall off with increasing excitation energy, as Equation 3 would imply for nuclei with positive Δ , one would certainly still see the steplike character of the excitation curves. (In fact it should be all the more striking, the faster Γ_f/T_n falls off with energy.) One might expect to see the tops of the steps tilted if Γ_f/T_n decreases significantly in a 6-Mev interval, but even this effect should be somewhat obscured by the expected rounding of the steps. Although targets heavier than U^{238} should (according to Eq. 3) have a more energy-dependent Γ_f/T_n because they have larger values of Δ , they would not necessarily show this dependence more clearly through their excitation curves. In nuclei with large Δ and correspondingly large fissionability, σ_f approaches σ_R at all energies, and the steps would become a less significant and less instructive part of the excitation curve.

Recently, Manley (62) carefully examined the somewhat simpler but related problem of the consistency of the fission cross sections on the second steps in neutron fission curves with the fissionabilities determined from the first steps. His analysis of a number of fission excitation curves of this type leads him to conclude that Γ_f/T_n is either decreasing for the observed nuclides between the excitation energies of 9 and 15 Mev or that the total reaction cross section falls in this 6-Mev interval by an unlikely amount approaching 30 per cent. These conclusions would be even stronger if any amount of "angular-momentum effect" were included in the considerations.

If one were to continue to increase the bombarding energy in Figure 11 one would expect σ_f to continue to rise in steps asymptotically approaching the total reaction cross section. It is, therefore, curious that Steiner & Jungerman (63) have found that σ_f stays equal to 45 per cent of the reaction cross section in $Th^{232}(p, f)$ as the proton energy is varied from 100 to 340 Mev. Such a failure of σ_f to continue to increase with bombarding energy could be attributable to a number of causes other than a falling off of Γ_f/T_n . Among these are (a) the possibility that enough protons are ejected in the initial interactions so that many of the compound nuclei are formed with very low fissionabilities; (b) the fact that at high bombarding energies only a fraction of the incident energy is generally deposited in the nucleus.

As a result, there are fewer opportunities for fission than one might offhand expect. Fortunately, Metropolis *et al.* have recently published detailed Monte Carlo calculations of high-energy reactions (64) which can be used to compute fission cross sections for comparison with Steiner's actual measurements. The results of such calculations show that in order for the computations to give values of the cross section as low as the measured ones, one must assume that Γ_f/Γ_n drops off appreciably at higher excitation energies. But it must be admitted that there are those who remain unconvinced by such calculations. (For example, the reviewer is generally unconvinced by calculations of this type which are done by others.) The calculations usually contain a large enough number of uncertain estimates to make it difficult to ascertain how sensitive the conclusions are to the assumptions.

This same objection applies to the recent calculations of Dostrovsky *et al.* (65); of Shamov (66); and of Vandenbosch & Huizenga (53). They all calculate high-energy fission yields or yields of spallation products. The first two authors conclude that Γ_f/Γ_n does drop off with increasing energy, the latter that it does not necessarily.

Nonfission cross sections as a function of energy.—It has been pointed out that in the very heavy fissionable nuclei the measured values of σ_f turn out to be too close to values of σ_R to be fruitfully compared to them. It becomes more practical to determine relative fission probabilities from the excitation functions for the reactions other than fission. For example, we have already learned something about Γ_f/Γ_n from the $(\alpha, 4n)$ reactions (Sect. 6). If one could in addition make as careful measurements of the $(\alpha, 5n)$ excitation curves, a comparison of these two sets of curves should provide fairly direct information about Γ_f/Γ_n at the initial excitation energy of the compound nuclei in the $(\alpha, 5n)$ reaction.

For example, the excitation curves reproduced in Figure 9 are for reactions of carbon ions with U^{238} in which only neutrons are emitted (59). It has already been mentioned that the peak cross section of the $(C^{12}, 4n)$ curve corresponds to $\bar{G}_n = 0.17$ and is in good agreement with expectations based on the $(\alpha, 4n)$ measurements. The $(C^{13}, 5n)$ reaction has the property that after the first neutron emission the residual nucleus has the same excitation energy as the compound nucleus which is made in the $(C^{12}, 4n)$ reaction. If one overlooks the slight possible differences in the spin distributions of these two sets of Cf^{250} nuclei, one may write

$$\left(\frac{\sigma_{5n}}{\sigma_R}\right)_{78} = \left(\frac{\Gamma_n}{\Gamma_T}\right)_{78} \cdot \left(\frac{\sigma_{4n}}{\sigma_R}\right)_{67}. \quad 5.$$

The first and last ratios are evaluated at the peaks of the $(C^{13}, 5n)$ and $(C^{12}, 4n)$ excitation curves, and the subscripts refer to the bombarding energies at these peaks. The expression Γ_n/Γ_T at 78 Mev is therefore simply

$$\frac{(\sigma_{5n})_{78}}{(\sigma_{4n})_{67}} \cdot \frac{(\sigma_R)_{67}}{(\sigma_R)_{78}}.$$

The first factor is seen to be about two, and the second one can be obtained

from the fission cross sections measured by the same authors. It is about one-sixth. This makes $(\Gamma_n/\Gamma_T)_{78} = \frac{1}{6}$ for Cf^{251} . Unfortunately there are no measurements for this particular nuclide at other energies. The value is in good agreement with the formula $\Gamma_f/\Gamma_n = 0.6 e^{\Delta/T}$ which was used in the computations for Figure 8, but it would be risky to take this as evidence that Γ_f/Γ_n is dropping off with increasing T as this formula implies. It would seem, however, that a program of measurements of this type could provide more useful information about high-energy fissionabilities than any of the methods yet discussed. Flerov's scheme of using both C^{12} and C^{13} has the virtue that it is applicable to the study of a large number of nuclides. But even if one used only, say, C^{12} , it would be possible to bombard pairs of consecutive uranium or plutonium isotopes to learn about Γ_f/Γ_n in certain specific nuclides at a definite energy. Or one could study $\text{U}^{236} (\text{C}^{12}, 4n)$ and $\text{U}^{238} (\text{C}^{12}, 6n)$ to learn about the combination of nuclides Cf^{250} and Cf^{249} . Vandenbosch & Huizenga have used this "method of pairs" in analyzing a bombardment with alpha particles (53), and it might well be worth making careful measurements with alpha particles on a large number of nuclides. Although results obtained with alpha particles or with other light particles may not be as easy to interpret as the heavy-ion results (where the excitation curves are more classical in the compound nucleus sense), a consistent programmatic study might prove to be useful.

Neutron angular correlations and high-energy fissionability.—An interesting experiment has been performed on the problem of high-energy fissionability that is quite different in approach from any discussed up to this point. Harding & Farley have measured the angular correlation between fission fragments and evaporation neutrons which are emitted at the same time (67, 68). If the neutron evaporation precedes fission, the neutrons should be essentially isotropic with respect to the fragments. [There may actually be a slight correlation attributable to the effect of the nuclear rotation on the distributions of both fission fragments and neutrons (69).] If a neutron is emitted after fission, it will still come from the site of the target nucleus since fission fragments move too slowly for their displacements to be observable in the time required for neutron evaporation. But the velocity of the neutron will be affected. To its evaporation velocity \bar{v}_n will be added that of the moving fission fragment \bar{v}_f . As a result the neutron's angular distribution will be folded in the direction of the fragment. In addition, the neutron's energy spectrum in the laboratory system will become a function of the angle between it and the fission fragments. The average value of the ratio $|v_f|/v_n$ is perhaps 0.4 or larger even in high-energy bombardments so that the effects on both the angular and energy distributions should be easily measurable. Harding and Farley studied the angular distribution effect in a bombardment of uranium with 147-Mev protons. They found that the neutrons are emitted rather isotropically and that of the 13.1 neutrons which accompany each fission, on the average, apparently only 2.5 ± 1 neutrons are emitted from a moving fragment. The implication is clearly

that Γ_f/T_n has become very small indeed at the higher excitation energies. Although it would be possible to use a better neutron detector than the one used by Harding & Farley (theirs was insensitive below a cutoff energy of about 1 Mev) and although the interpretation of the experiment has occasioned a few misgivings (70), it does not appear that there was anything basically wrong either with the experiment or its interpretation. In view of its directness, the method of Harding & Farley has much to recommend it. It should prove especially applicable to studies of Γ_f/T_n in bombardments where compound nuclei are formed at definite excitation energies, for example in moderate-energy alpha-particle bombardments (71).

A few other types of studies of fissionability at high energy should be mentioned before this section is concluded. It has already been indicated that nucleon-induced fission studies become complicated at higher energies because of the transparency of nuclei to nucleons. Radiochemical and counter experiments performed under these conditions tend to give results which are superpositions of those from many different types of events. One can get a more differential view using photographic plates. For example, with plates one can hope to determine, for each event, the nuclear charge and excitation energy at the end of the collision-cascade part of the reaction. [See Ivanova (72); Ostroumov (73); and the review by Bromley (74).]

Fission at high excitation energy has also been extensively studied in experiments on the capture of π^- -mesons and in π^+ -meson bombardments [Perfilov, Ivanova, and others in their group (75 to 79)]. There have been measurements by Bernardini (80), Minarik (81), Jungerman (82) and their co-workers on high-energy photofission. None of these measurements will be discussed. Although they all shed some light on the interactions of mesons with complex nuclei, at the present stage of their interpretation they have rather little to say about the fission process itself.

It is well known that at higher bombarding energies, neutrons and other particles can be ejected from nuclei "directly." In the considerations discussed so far, fission has, however, been treated as though it occurs only in nuclei which are in thermal equilibrium. This view is probably reasonable since the coupling of incident nucleons to the collective fission modes is very likely small. Although "direct" fission is certainly possible in principle, no clear evidence for such fission has yet been found (see Sect. 15).

8. FISSION OF ELEMENTS LIGHTER THAN THORIUM

In this section the fission probabilities at medium and high energies of nuclides which are lighter than thorium will be examined. In the last section it was seen that according to Equation 3 one would expect Γ_f/T_n of the elements heavier than thorium (i.e., those with positive Δ) to decrease at high energy. There was some evidence that this is actually happening, but it was not altogether clear. According to Equation 3 one would expect, too, that the elements lighter than thorium (i.e., those with negative Δ) would have values of Γ_f/T_n which increase with excitation energy until the nuclear

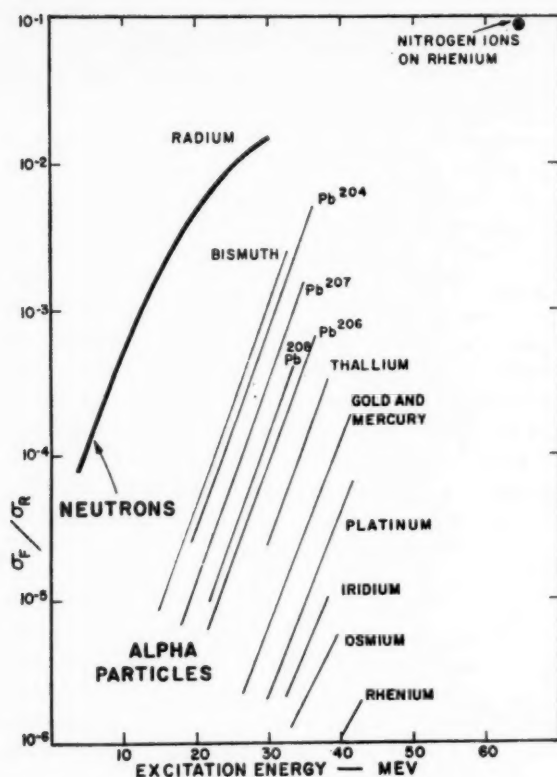


FIG. 12. The fission cross section divided by the total reaction cross section in a variety of bombardments. All of the lower curves represent data on alpha-particle bombardments by Fairhall & Neuzil (83). The radium measurement is that of Nobles & Leachman (84), and the nitrogen-on-rhenium point at the top is from the work of Druin *et al.* (85).

temperature is of the order of Δ . After that, Γ_f/Γ_n is expected to fall off, for these elements, just as for the heavier ones. Fairhall & Neuzil have recently given a very convincing demonstration that in the alpha-particle fission of bismuth and lighter nuclei, Γ_f/Γ_n does indeed increase rapidly with excitation energy (83). This can most easily be seen by means of an example from their data (Fig. 12). When Pb^{208} is bombarded to produce Po^{212} compound nuclei at 35-Mev excitation, the figure shows that the ratio of the fission to the total cross section σ_f/σ_R is 6×10^{-4} . If now a neutron is evaporated, one has the compound nucleus Po^{211} at an excitation energy of about 27 Mev. But this nucleus can also be produced directly in a bombardment of Pb^{207} and it is seen that σ_f/σ_R is then only 1×10^{-4} . It follows that most of the

fission produced in the bombardment of Pb^{208} with alpha particles happens before any neutrons are evaporated. (In drawing this conclusion it is assumed that the fissionabilities of the two 27 Mev Po^{211} nuclei which are involved in the argument are very nearly equal despite the fact that these nuclei must have somewhat different average amounts of angular momentum.) The essential point is that the fission excitation curves are very steep, whereas the spacing between curves for different isotopes of the same element is not very great. Therefore, one must attribute the increase of fissionability with bombarding energy to a dependence of fissionability on excitation energy rather than to the fact that the lighter isotopes of an element tend to be more fissionable (as in Fig. 7). One implication of this conclusion is that σ_f/σ_R in Figure 12 is very nearly equal to Γ_f/Γ_T for the compound nucleus which is made in the bombardment.

The examination of alpha-particle fission in heavy elements (Sect. 6) revealed that the data can reasonably well be represented by Equation 3 with $N=0.6$, namely by $\Gamma_f/\Gamma_n = 0.6 e^{\Delta/T}$. One way to see whether the (α, f) cross sections in the lighter elements form a consistent pattern with those in the heavier ones is to examine the applicability of this formula for Γ_f/Γ_n to the data in Figure 12. In the bombardment of gold, to take an example, Γ_f/Γ_n is 10^{-6} and 5×10^{-4} at 25 Mev and 40 Mev respectively (Fig. 12). The formula gives $\Gamma_f/\Gamma_n \cong 0.6$ at both energies.

One can at this point simply conclude that fission in the lighter elements is "different" from that in the heavier ones (and this viewpoint will be taken up briefly later). It is, however, important to see whether Equation 3 can be patched up in any simple way to bring the behavior in the two mass regions into some agreement. Almost the only quantity in the formula that can be tampered with very much is B_f because so little is known about it. One must imagine that in light elements B_f is actually considerably larger than it comes out to be according to the linear formula (Eq. 1). Only then could one hope to account for the smallness of the fission cross sections in these elements. It was seen earlier that even the spontaneous-fission data would be fitted better with a formula which would give larger values of B_f for the lighter elements than Equation 1 does. It was also seen that this same failing of Equation 1 shows up in the alpha-fission studies illustrated in Figure 8.

To determine better values for B_f in the light elements one may simply try to fit Equation 3 to the cross sections of Fairhall and Neuzil keeping $N=0.6$ as before. It should be remarked here that if one determines values of Δ (i.e. of B_f) by fitting Γ_f/Γ_n at some specific excitation energy, he may not be satisfied that this fit is meaningful unless the chosen value of Δ reproduces (within reason) the shape of the excitation function. Fortunately it does turn out that the family of curves, $\Gamma_f/\Gamma_n = 0.6 e^{\Delta/T}$, which are characterized by different values of Δ , does resemble the set of curves of Figure 12 to a fair degree. (In making this comparison it was assumed that $T^2 = E_{\text{exo}}/7.5$

where T and E_{exo} are in Mev.) It is clear that the computed cross sections rise sharply with energy for the same reason that they are small, namely because Δ is large and negative. The values of B_f which bring the computed curves into reasonable correspondence with the measured ones are roughly 28, 23, and 18 Mev for iridium, lead, and polonium compound nuclei. These "thresholds" are hardly small compared to the excitation energy as assumed in the derivation of Equation 3. It is therefore hard to know without a more detailed investigation whether the observations in Figure 12 are consistent (in terms of the *ideas* behind Eq. 3) with the observations in heavier elements. It seems safe to conclude, however, that if a simple, common account of fissionability can be developed for all elements it will require that the thresholds become very large for elements lighter than thorium. There is some hint from angular distribution measurements (Sect. 15) that this increase of fission thresholds occurs rather abruptly just below thorium, but this evidence is only qualitative.

The cross section for $\text{Ra}^{226}(n, f)$ has been measured by Nobles & Leachman in the energy range covered by Figure 12, and a smooth version of their excitation curve has therefore been plotted there (84). The average slope of this curve is only slightly smaller than that in the alpha-particle work. This may imply that the fission seen at the higher energies here can include some contributions from the fission of Ra^{226} and Ra^{225} although Ra^{227} fission is probably dominant.

A point from the nitrogen bombardment of rhenium has also been plotted in Figure 12 (85). At a bombarding energy as low as 80 Mev (excitation energy ~ 63 Mev), the fission cross section is already about 10 per cent of the total cross section. As one can see from the data compiled in Table V this makes it about 30 times larger than the cross section in nucleon-induced fission which leads nominally to the same compound nucleus at the same excitation energy. Even the (α, f) curves would have to continue to rise at the steep rate seen in Figure 12 to reach such fissionabilities at corresponding excitation energies. Pik-Pichak explains the high fissionability of the lead formed in $\text{Re}(\text{N}^{14}, f)$ on the grounds of the reduction of B_f by the angular momentum effect (58) (Sect. 6). Because the projectile here is a heavy ion, it turns out that the maximum angular-momentum deposit is about $30 \hbar$ even though the bombarding energy is only some 16 Mev above the barrier. But according to the rough estimate of Sect. 6 even this amount of angular momentum should not have too large an effect because of the way Γ_f/T_n depends on excitation energy. Since the angular momentum effect increases the effective value of Δ , it has its largest influence at low T (i.e., after the evaporation of neutrons). But in the lighter fissioning elements, Γ_f/T_n becomes negligibly small at just these energies. This fact prevents the angular-momentum effect from realizing its potentialities.

Perhaps a contributing reason for the high fissionability in heavy-ion bombardments is the fact that they give rise to compound nuclei which are

unusually neutron-poor (e.g., Pb^{199}). Although Figure 12 does not show a very strong variation with neutron poverty, this effect should increase with increasing poverty, and Pb^{199} is rather far out of the stable valley.

Fission has been observed in elements even lighter than the lightest one in Table V, for instance in copper [Batzel & Seaborg (90a)]. The cross sections here are very small, so small that it is difficult to "study" this fission. It might be worth trying to induce fission in these very light elements with heavy ions since they seem to be so effective in producing fission.

TABLE V
RATIOS σ_f/σ_R IN "LIGHT" ELEMENTS AT MEDIUM AND HIGH ENERGIES

Element of Compound Nucleus	Reaction and Bombarding Energy (Mev)						
	$(\alpha, f)^*$	(n, f)		(p, f)		$(N^{14}, f)^{\dagger\dagger}$	
	42	84†	120‡	380‡	~100§	~300	80
Silver						$0.3 \times 10^{-3} $	
Tungsten						$2 \times 10^{-3}\#$	
Gold	1×10^{-3}	1×10^{-3}	5×10^{-3}	10×10^{-3}			
Mercury	2.5×10^{-3}				5×10^{-3}	$30 \times 10^{-3}\S$	
Thallium	12×10^{-3}	1.6×10^{-3}	5×10^{-3}	10×10^{-3}			
Lead	10×10^{-3}	3×10^{-3}	10×10^{-3}	16×10^{-3}			9×10^{-3}
Bismuth	35×10^{-3}	10×10^{-3}	18×10^{-3}	37×10^{-3}			
Polonium	$\sim 50 \times 10^{-3}$				60×10^{-3}	$130 \times 10^{-3}\S^{**}$	
Astatine	250×10^{-3}						
Radon							40×10^{-3}

* Fairhall & Neuzil (83)

† Kelly & Wiegand (86)

‡ Gol'danskii *et al.* (87)

§ Steiner & Jungerman (63)

|| Denisenko *et al.* (88)

Nervik & Seaborg (89)

** Jodra & Sugarman (90)

†† Druin *et al.* (85)

In any case it seems clear that the region of the periodic table around lead deserves considerable further study. It could provide some useful information about the angular-momentum effect, about fission thresholds, and it might tell whether it is profitable to imagine that there is more than one kind of fission (Sect. 13). Although the cross sections in the lead region are small, they are large enough for many kinds of measurements. Offsetting the disadvantage of the small cross sections is the advantage that the fission which occurs in these elements tends to be "pure" in the sense that a single nuclide is responsible for most of the fission. One does not have to disentangle the effects of fissions occurring after neutron emission, at least if one stays with moderate bombarding energies.

PART II. DISTRIBUTIONS OF FISSION FRAGMENTS

We have been concerned with the problem of estimating the chance that a nucleus will undergo fission. We turn now to an examination of what it is that is undergone. In the absence of a unifying fission theory some other way must be found to organize a description of the fission process. It is convenient to make use of distribution functions of those quantities which are conserved in the course of fission. We shall begin by examining what happens to the energy released in fission. Then the distribution functions for the mass numbers and atomic numbers of the fragments will be taken up. Finally, the evidence which relates to the apportionment of angular momentum will be examined.

It should be admitted at this point that treatment of the integral probability for fission as a topic separate from the distribution functions was rather arbitrary although convenient. It could be that the discussion of fission probabilities would be simplified if one were to recognize that there is more than one kind of fission and that we have been dealing, in Part I, with superpositions of the different kinds (see Sect. 13).

9. THE ENERGY AVAILABLE FOR FISSION

For the purpose of discussing the energetics, one may imagine that fission happens in the three distinct stages illustrated in Figure 13. In the first stage, the fissioning compound nucleus splits into two fragments. These fragments are the excited residual nuclei formed in the fission act. They have the property that the sum of their atomic numbers, $Z_1 + Z_2$, is the atomic number Z_0 of the original nucleus. The corresponding relationship also holds for their atomic weights.

The second stage of the process may be thought to consist of the evaporation of neutrons and occasional charged particles (although the emission of charged particles should perhaps more appropriately be considered as part of the first stage; see Sect. 13). Toward the end of the second stage, photons are emitted, leaving as end products of this stage the nuclei (A_3Z_3) and (A_4Z_4) in their ground states. It is these nuclei that one observes as "the fission fragments" in counter experiments or in photographic emulsions. The radiochemist also sees these nuclei if their half lives for β -decay are not too short. More generally, the "fission products" of the chemist lie in the decay chain between these nuclides and the final stable nuclides (A_5Z_5) and (A_6Z_6) . There is a small probability for the emission of a "delayed neutron" in the course of the third stage, the β -decay stage, of the fission process.

The nuclei (A_1Z_1) and (A_2Z_2) are the primary residual nuclei that result from the fission process. It is true that they are essentially unobservable, for they are generally formed with sufficient excitation energy to decay by particle emission in less than 10^{-16} sec. Still, it is necessary to refer to them (in particular to the Q value for their production) in discussing the energy

released in the fission part of the process. The Q values for the production of nuclei drawn lower in the figure are important for the applications of fission, but because they involve the energetics of photon and neutron emission as well as of the fission act they are not particularly basic to fission. The Q value for the production of (A_1Z_1) and (A_2Z_2) is the sum of the kinetic energies and the excitation energies given to these fragments. It is often simply called "the energy release in fission," although as just noted, the practical energy

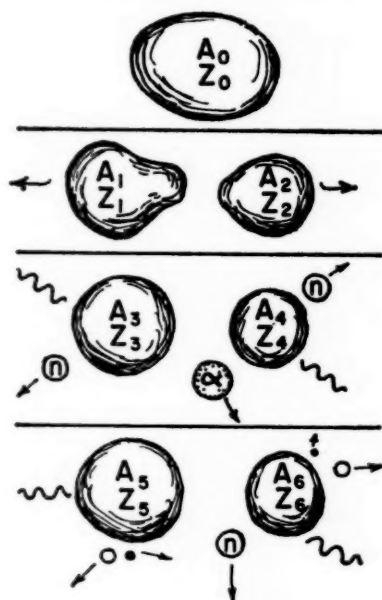


FIG. 13. Particles and radiations emitted in fission. For the purpose of introducing a consistent terminology, we imagine that the first stage of fission consists of a simple division of the original nucleus with no loss of particles or energy. These primary fission fragments then emit neutrons, photons and occasional α -particles ending up as the species A_3 and A_4 in their ground states. The final process is the beta decay (accompanied by photon and occasional delayed-neutron emission). The nuclei A_5 and A_6 are stable.

release is larger than this. The value of Q can be computed for any pair of "first" nuclei from their masses and the mass of the original fissioning nucleus. Unfortunately the masses of fission fragments are not always well known since some fragments lie rather far from the center of the stable valley of nuclides. The Q values given in Figure 14 were obtained with the help of Cameron's mass tables which involve certain reasonable extrapolations from measured masses (54). At each value of A_1/A_2 , the ordinate gives the largest Q for that mass ratio. (The Q is of course not uniquely determined by

A_1/A_2 since it also depends on Z_1/Z_2 .) There has been some slight smoothing of the curves in Figure 14 to remove odd-even oscillations. The peaks and other structure that can still be seen are connected with shell effects. These graphs are in essential agreement with the more critical examination of Q values in fission by Hay & Newton (91).

It is apparent from the curves that fission is energetically possible for a wide range of initial and final nuclei. The energy release in the symmetric fission of Os^{190} is only a little less than half that in Cf^{252} . In fact, symmetric

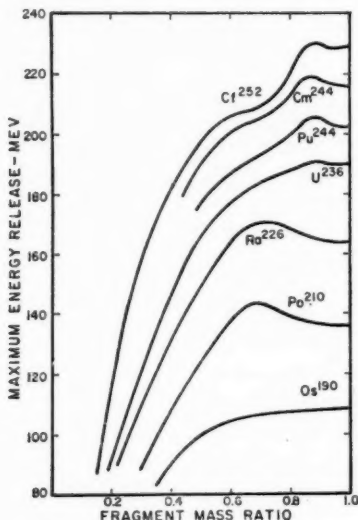


FIG. 14. Q values of fission. The maximum values of the energy release in spontaneous fission as a function of the mass ratio. Mass values were taken from Cameron's tables (54).

fission first becomes energetically impossible for nuclei which are roughly half as heavy as Os^{190} . It is also seen from the figure that for fragment mass ratios as large as 4:1, Q is still greater than 100 Mev for many species. Of course, since the final particles in fission are both charged, the Q values are not themselves the energies which determine the relative probabilities of different divisions in the fission process. One must at least subtract from each Q value some appropriate Coulomb energy between the fragments at the instant of their formation. Further consideration will be given later to the questions of possible effects of the energetics on the mass and charge distributions (Sect. 13 and 14).

10. THE KINETIC ENERGIES OF FISSION FRAGMENTS

In this and the next section the experimental information on each of the two parts of the fission Q value will be examined. These parts are the kinetic

energy E_K and the excitation energy E_X of the fragments (A_1Z_1) and (A_2Z_2). A measurement of the apportionment of Q between E_X and E_K can provide a rough picture of the fissioning system at the moment of scission. (By scission one usually means the stage in the fission act when the fragments are just far enough apart to be uninfluenced by each other's nuclear forces.) Suppose, for example, that scission does not occur until the nucleus is stretched far out like a hot dog and that the stretching has been fairly slow. Then the Coulomb energy between fragments would be much smaller than

TABLE VI
AVERAGE KINETIC ENERGY RELEASE IN FISSION

Compound Nucleus	Type of Fission	Method of Measurement	Author	E_K (Mev)	$E_K / \frac{Z^2}{A^{1/2}}$
Bj ²¹⁰	90 Mev n	Ion chamber	Jungerman & Wright (92)	142 ± 4	0.122
Th ²³⁰	Thermal n	Ion chamber	Smith <i>et al.</i> (93)	162 ± 4	0.123
Th ²³²	45 Mev n	Ion chamber	Jungerman & Wright (92)	168 ± 6	0.128
U ²³⁴	Thermal n	Time-of-flight	Stein (94)	163 ± 2	0.119
	Thermal n	Ion chamber	Smith <i>et al.</i> (93)	163 ± 2	0.119
U ²³⁸	Thermal n	Ion chamber	Smith <i>et al.</i> (93)	165 ± 2	
	Thermal n	Time-of-flight			0.121
		and Ion chamber	Leachman (95)	167.1 ± 2	
	Thermal n	Time-of-flight	Stein (94)	165 ± 2	
	Thermal n	Calorimetry	Leachman & Shafer (96)	167.1 ± 1.6	0.121
	Thermal n	Calorimetry	Gunn <i>et al.</i> (97)	166 ± 2	
U ²³⁵	45 Mev n	Ion Chamber	Jungerman & Wright (92)	158 ± 6	0.116
	90 Mev n	Ion Chamber	Jungerman & Wright (92)	160 ± 4	0.117
Pu ²⁴⁰	Thermal n	Time-of-flight	Stein (94)	172 ± 2	
	spont. f.	Ion Chamber	Smith <i>et al.</i> (93)	172 ± 2	0.121
Pu ²⁴³	Thermal n				
	spont. f.	Ion Chamber	Smith <i>et al.</i> (93)	174 ± 3	0.123
Cm ²⁴⁴	Spont. f.	Ion Chamber	Smith <i>et al.</i> (93)	185.5 ± 5	0.126
Cf ²⁵³	Spont. f.	Ion Chamber	Smith <i>et al.</i> (93)	185 ± 4	
		Time-of-Flight	Milton & Fraser (98)	181.9 ± 5	0.121
Fm ²⁵⁴	Spont. f.	Ion Chamber	Smith <i>et al.</i> (93)	176 ± 6	0.111

for fragments which are formed, say, as adjacent spherical droplets. Hence E_K would be small for the hot-dog fragments, and their excitation energy E_X would be correspondingly large. Another way to describe this difference is to note that there must be some E_X in the distortion of the hot-dog fragments which is absent in the spherical ones.

Table VI lists some measured average values for the total kinetic energies of fission fragments. The time-of-flight data have been corrected for neutron and photon emission so that they apply to the species (A_1Z_1) and (A_2Z_2) of Figure 13. The calorimetric data have been corrected for β -emission in addition. No particular corrections were made in the case of the high-energy neutron data. Here even the identity of the fissioning species is uncertain. The main point of including these data here together with the recent more

accurate data is that they show fairly clearly that the mean kinetic energy of fission fragments does not depend very sensitively on the initial excitation energy. This observation has been confirmed in a number of other measurements of kinetic energies (97a, 97b), and in measurements of fragment excitation energies (Sect. 11). It probably implies that the mean distance between fragments at scission is very nearly the same at all excitation energies. This conclusion follows from the fact that virtually all of the kinetic energy of the fission fragments arises from the Coulomb repulsion which acts between them after scission. The experimental evidence that very little kinetic energy of separation is picked up on the descent from the saddle point is given in the next section. It is pointed out there that roughly one neutron more is evaporated in association with the thermal-neutron fission of Pu^{239} than in spontaneous fission of the same nucleus (Pu^{240}). This would imply that the kinetic energy picked up in the thermal fission during the slide down from the saddle point is largely converted to internal energy as the separation proceeds. When the distortion reaches the point at which the spontaneous fission normally "emerges" from the barrier, the thermally fissioned nucleus also has virtually no kinetic energy of separation, but instead it has converted its extra energy into excitation energy, presumably because of the coupling of the separation "mode" to the internal modes in the nucleus.

There is no reason to expect that a larger fraction of the descent energy should remain kinetic energy if the nucleus happens to be more excited than the ones just considered. Besides, it should be at least as likely that the separation mode is in thermal equilibrium with other modes before it gets to the saddle point as after it does (see Sect. 7). It is therefore to be expected that even at high excitation energies the separation mode does not start out from the saddle point with a kinetic energy greater than the nuclear temperature. Even if there should happen to be some slight nonequilibrium effects so that the separation kinetic energy at the scission time is somewhat larger than one would estimate from the nuclear temperature, not all of this kinetic energy becomes kinetic energy between the fragments. Some of it remains kinetic energy in the separation direction within the fragments. It seems clear, then, that as the excitation energy of the fissioning nucleus is increased one should not expect a corresponding increase in the observed fragment kinetic energy arising from the separation kinetic energy which happens to be in the system before scission.

The fact that the observed kinetic energy is insensitive to excitation energy is, therefore, an indication that the Coulomb energy between fragments at scission does not depend strongly on the excitation energy of the system. Roughly speaking, the mean distance between the fragments at scission is, therefore, the same at all excitation energies. This observation suggests that fission kinetic-energy data (plus some plausible arguments) can be used to set an upper limit on the amount of thermal expansion of excited nuclei.

The last column of Table VI gives the observed values of \bar{E}_K divided by $Z^2/A^{1/3}$. With the exception of the point for fermium it is seen that these ratios certainly do not vary much from nucleus to nucleus. If all of the fissioning nuclei had the same assortment of shapes at scission, this is what one would expect since the Coulomb energy associated with any shape would scale as $Z^2/A^{1/3}$. One cannot safely turn this around to say that the near-constancy of the ratios in the last column indicates a similarity of shapes at scission for all nuclei. And yet such a similarity would not be unreasonable. Although one might expect appreciable differences in the saddle-point shapes, the more highly fissionable nuclei being less distorted from the normal nuclear shape, the shapes at the actual time of separation should be rather more similar for different nuclei.

It is of interest to compare the Coulomb energy between two adjacent spherical "fragments" with the observed values of \bar{E}_K . The potential energy between two spherical nuclei with $Z=46$ and $A=118$ (the symmetric fragments of U^{236}) is 202 Mev if they are just touching (where $r_0=1.5$ fermis has been used in the estimate of the nuclear radii). If one recomputes this energy for the mass ratio 1.3 instead of 1.0, the value is still as large as 198 Mev. These results are roughly 20 per cent greater than the value of \bar{E}_K measured for the thermal fission of U^{235} . It would appear that, on the average, the fragments, regarded as spheres, start to fly apart from 20 per cent further apart than just touching. It is, of course, not surprising that the fragments begin their motion apart from a somewhat stretched configuration of the fissioning nucleus.

It should be possible to learn something about the distribution of nuclear elongations at the scission point (where the separation kinetic energy is probably still very small as discussed above) by examining the width of the distribution in E_K . Milton & Fraser have used a time-of-flight arrangement to measure the distribution in E_K as a function of the mass ratio in the spontaneous fission of Cf^{252} (98). Their results are shown in Figure 15. The full widths of these distributions are about 20 Mev at half-maximum. A width of similar magnitude in U^{236} was found by B. L. Cohen and his co-workers (99). They used magnetic analysis in the detection of the fission fragments. Stein, who used a time-of-flight technique (94) to study U^{236} , found a slightly smaller width than Cohen. In any event, the widths of the E_K distributions are all fairly large and they, therefore, suggest that there is a considerable variation in the effective length of the fissioning nucleus at the time of scission.

Figure 15 also shows that the average kinetic-energy release decreases as the asymmetry of fission increases. If one imagines that the asymmetric fragments pinch off at the same separation as symmetric ones, one must expect that they will come apart with less kinetic energy. For a mass ratio of two, one would, with this assumption, expect the Coulomb energy at scission to be about $(2/3) Z \cdot (4/3) Z/Z^2$ as large as for symmetric fission. Z , here, is the atomic number of a typical symmetric fission fragment. This esti-

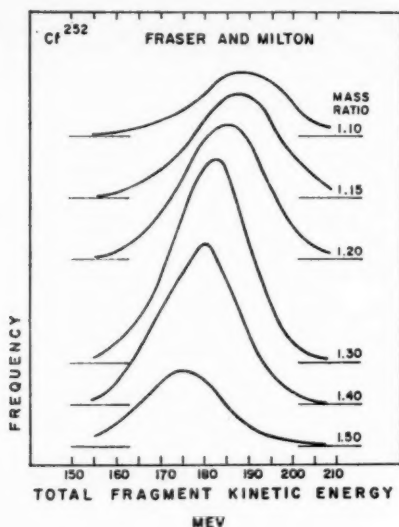


FIG. 15. The distribution of total fragment kinetic energies as a function of the fragment mass ratio according to the measurements of Milton & Fraser (98).

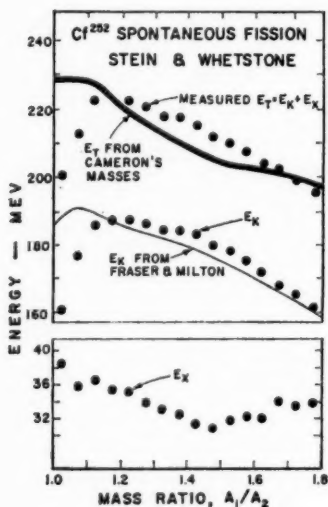


FIG. 16. Measured average values of the kinetic and excitation energies as a function of fragment mass ratio (100). The top curve shows to what extent the sum of these energies agrees with that expected on the basis of Q values determined from a mass formula (54). (See Fig. 14.)

mated reduction ($\sim 11\%$) of the kinetic energy of fragments having a 2:1 mass ratio is in moderately good agreement with the observations (Fig. 16). It may therefore be tentatively concluded that the scissions which give rise to the different mass ratios occur at very nearly the same time (i.e., the same elongation) in the fission process.

It should perhaps be mentioned here that in recent calculations of the fragment mass distribution according to a statistical model, Cameron has shown that this distribution is extremely sensitive to the relative values of the mean separations at scission for different mass ratios (Sect. 13). He finds, for example, that a 5 per cent difference in these separations for symmetric and asymmetric mass pairs can account, in his theory, for the well-known strong suppression of symmetric division in thermal fission. One reason for more and improved measurements of average values of E_K as a function of mass ratio is that they could provide a critical measure of the importance of statistical considerations in determining the nature of the scission process.

There is some indication that the average E_K is abnormally small for the very symmetric mass division (Fig. 16). This result is, however, somewhat uncertain because of the very low yield of these particular fragments in spontaneous fission. It will be interesting to see whether the very symmetric fragments have an anomalously low E_K in fissions induced at higher energies.

11. THE EXCITATION ENERGIES OF FISSION FRAGMENTS

The energy balance.—By subtracting the value of the average kinetic energy release from estimates of the total energy release Q , one can in principle determine the average excitation energies of the fragments. These energies can also be determined directly by measuring the numbers and energies of the photons and neutrons which are emitted during the de-excitation of the fragments. It is interesting to see how well the different parts of the energy release add up to the appropriate Q . Among other things, such checking up on the energy balance provides an estimate of the accuracies of the component measurements. The average energy release for the most probable fragment mass ratios in thermal-neutron fission of U^{235} is about 193 Mev (54). (The contribution of the captured neutron's binding energy is included.) The mean kinetic energy of both fragments is 166 Mev, implying that the total excitation energy of the fragments is 27 Mev. The average number of neutrons emitted in this fission is known to be very nearly 2.5, and the average binding energy and kinetic energy (in the center-of-mass system) of these neutrons are 5.5 and 1.5 Mev respectively. Thus the neutrons take away something over 17 Mev. Maienschein has recently found that about 7 Mev are carried off by prompt photons (112). Altogether this comes within 3 Mev of balancing the books. In view of the nature of the averages made, this is probably as good agreement as should be expected. A more differential examination of the energy balance in fission has recently

been made by Stein & Whetstone (100). They studied the energetics in the spontaneous fission of Cf^{252} as a function of fragment mass ratio, and their results are shown in Figure 16. The agreement here is only fair even if one discounts the discrepancy for a symmetric mass split. Although it is not clear at the moment where the major sources of the discrepancies lie (whether in the determinations of the masses, kinetic energies, or excitation energies), the coincidence types of measurements will probably prove to be powerful enough to provide for an early resolution of the energy balance problem.

Prompt-neutron spectra.—We turn now to a more detailed look at the spectra of the so-called "prompt" neutrons and photons. With some reservations, it may be said that the spectra indicate that neutrons and photons are "evaporated" from fragments, that is, they are emitted from nuclei in thermal equilibrium.

The neutrons are found to be emitted in times shorter than a few times 10^{-14} sec. (101), as one would expect in almost any case. If neutrons are "evaporated," their spectra should resemble those of neutrons normally emitted from middle-weight elements in compound nucleus reactions. Such spectra appear to be roughly Maxwellian with mean energies of about 4/3 Mev (102). Since the neutrons in fission are presumably evaporated from fragments still moving at the full speed which they acquire upon separation, the neutron spectrum will reflect the average kinetic energy (2/3 Mev per nucleon) of a fission fragment. The average laboratory energy of fission neutrons would be $\overline{P_L^2}/2m$ where the laboratory momentum $\vec{P}_L = \vec{P}_{c.m.} + \vec{P}_f$, is the sum of the neutron momentum in the fragment system and the laboratory momentum, per nucleon, of a fragment. If the reasonable assumption is made that the average value of $\vec{P}_{c.m.} \cdot \vec{P}_f$ is zero, then

$$\frac{1}{2m} \overline{P_L^2} = \frac{1}{2m} \overline{P_{c.m.}^2} + \frac{1}{2m} \overline{P_f^2}$$

which, according to the estimates just made, is $4/2 + 2/3 = 2$ Mev. This value is in good accord with the measured average neutron energy in the thermal fission of U^{235} . It is clear from the nature of the estimate that it should apply about equally well to low-energy fission in virtually all fissioning nuclei. In the very heaviest of these, like Cf^{252} , the average neutron energy might be expected to be slightly higher than in U^{235} since both the excitation and kinetic energies of the fragments are somewhat higher. Recent measurements by Hjalmar (103) and by Smith (104) show that the average energy of neutrons evaporated from Cf^{252} is about 10 per cent higher than that from U^{235} .

To compute the expected neutron spectra in detail, one should average over the excitation- and kinetic-energy distributions of the different fragments. It was found by Watt (105), Gurevich (106), and others that the observed spectra could be very well approximated by one computed on a somewhat simplified model. It is assumed that in the center-of-mass system

of each fragment the neutrons are emitted isotropically with the unique spectrum $\sqrt{E_n} e^{-E_n/T}$. It is further assumed that all fragments fly off with the same kinetic energy per nucleon, E_F . Then the laboratory spectrum can easily be shown to have the form $e^{-E_L/T} \sinh \sqrt{4E_L E_F/T^2}$ where E_L is the laboratory neutron energy. The two parameters in this function are T , which is $2/3$ of the mean evaporation energy and E_F , the mean contribution to the neutron energy from the fragment motion. For the spectrum from the thermal fission of U^{235} Watt obtains his best fit with $3/2 T = 1.5$ Mev and $E_F = 0.5$ Mev. Although these energies add up to the same value for the average neutron energy, 2 Mev, which was just estimated from the value of \bar{E}_K and from neutron spectra from nuclear reactions, the division into the center-of-mass part and the fragment motion part is different here. This difference is not to be too lightly dismissed, since Watt fits the observed fission neutron spectrum over a range in ordinate of $\sim 10^6$, and the values of his parameters are therefore quite well determined by the data. Besides, the measurements which were used by Watt and his evaluations of the parameters have recently been confirmed with improved techniques (107). It is because of the over-all precision of these measurements that it is challenging to give a quantitative theoretical account of the observed spectrum. Unfortunately, and despite the many studies which have been made of neutron "evaporation" from nuclei, the shapes of evaporation spectra are not yet well enough known to permit a critical examination of the Watt spectrum. Indeed, the best "evaporation spectrum" known (if all of it is really an evaporation spectrum) is probably just the one fitted by Watt. The measurements here extend beyond 16 Mev whereas those performed in ordinary nuclear reaction studies are already confused by so-called direct interactions at much lower energies.

Some confirmation of the essential ideas in the Watt formulation was provided by Fraser's observations of the angular correlation between fission fragments and neutrons (101). Fraser found a forward-folding of the neutrons along the fragment directions that seemed to be quantitatively consistent with the idea of neutron evaporation from fast moving fragments. Fraser's neutron counter was rather energy-insensitive, and by use of an energy-sensitive detector it becomes possible to examine the nature of the neutron emission more critically. With such a counter it is easier to learn, for example, whether the neutron emission is isotropic in the center-of-mass system. Recent measurements with a neutron time-of-flight counter do not seem to be altogether consistent with an evaporation model [Bowman & Thompson (108)]. It will probably be necessary to do some more measurements before the neutron problem will be resolved, but with the modern coincidence techniques these measurements should not be too difficult.

Another set of investigations that is consistent with an evaporation model (but is probably not inconsistent with a moderate amount of non-evaporative neutron emission) has to do with the distribution function for

the numbers ν of neutrons which are emitted per fission event. Many elements have been investigated, and calculations of the expected distributions have been given by Leachman (109); Cohen (99); Terrell (110); and others (111). Perhaps the simplest calculations are those of Terrell who assumes that the distribution function for the excitation energy of a fragment is Gaussian with a width that is the same for all fissioning species. He also assumes that the average binding and kinetic energies of emitted neutrons are the same in all fissions. A curve adapted from his analysis is shown in Figure 17. It is seen that the width of this curve is more or less consistent with the widths of Figure 15, assuming that it costs 7 Mev to evaporate a neutron. Such a consistency in the widths of the excitation- and kinetic-

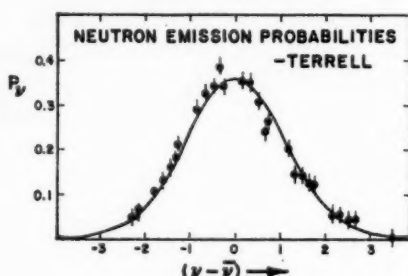


FIG. 17. The relative probabilities for emitting ν neutrons in a fission event when the average number of neutrons emitted per event is $\bar{\nu}$. The data points refer to observations on several different elements. References to the original literature are given in the paper by Terrell (110) from which this curve was taken.

energy distributions is to be expected, since the variation in the total energy release Q is small over the mass range which includes the most probable fragments. The fact that Terrell can fit such a large amount of data with a single universal curve shows to what extent the data are insensitive to details in the neutron emission process. Terrell indicates, for example, that information about the way in which the available excitation energy is shared between the two fragments of each pair is very difficult to extract from the data on neutron multiplicities. Fortunately there are other methods (to be discussed below) which provide fairly precise information on this interesting question. It would appear, however, that integral studies of neutron multiplicities are not likely to shed much light on the nature of neutron emission in fission.

Prompt-photon spectra.—It can be said at once that one would expect, on the basis of the usual picture of the de-excitation of excited nuclei, that the total energy released in photons per fission should be about the same for all targets. It should be slightly less than the binding energy of a neutron to a primary fission fragment, say, 4 to 5 Mev. The basis for this conclusion can

be seen with the help of Figure 18. The dots at the left represent the energy levels of the primary fission fragment, say (A_1Z_1) . This fragment (which is formed in some excited state) is assumed to decay to the right by a chain of neutron emissions until neutron emission is no longer energetically possible. Then a few photons are emitted, bringing the final nucleus to its ground state. (The nucleus at this stage corresponds to species A_3Z_3 of Fig. 13.) The sloping lines in Figure 18 represent the flow lines for the neutron evaporation. Their slope corresponds to the average kinetic energy taken off by neutrons. As the nucleus de-excites there is of course some diffusion at right angles to the flow lines because of the spread in neutron kinetic energy, but for purposes of the present argument it may be imagined that the flow

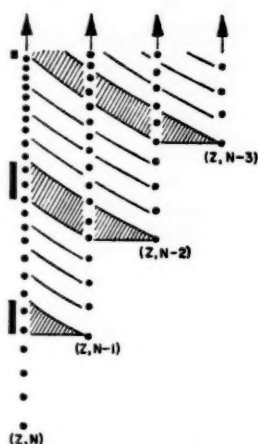


FIG. 18. A diagram to show the de-excitation of a fission fragment by neutron and photon emission. The fragment is produced in some excited state at the left and it transforms its way to the right roughly following one of the flow lines. If photons are emitted only when neutron emission is no longer possible, one would expect (see text) that the average energy emitted in photons per fragment is a little less than half a typical neutron binding energy.

takes place along the lines. For flow which takes place in one of the unshaded paths, the last step is the emission of photons whose total energy is on the average half the binding energy of a neutron. But if the fragment happens to be formed in one of the states marked with a black bar, the flow will take place in a shaded region and the final neutron evaporation will tend to leave the final nucleus in the ground state or some other rather low-lying state. At any rate, these fragments give rise to an abnormally small amount of photons. Because of the latter excitations the average energy emitted in photons from a fragment must be something less than half a binding energy.

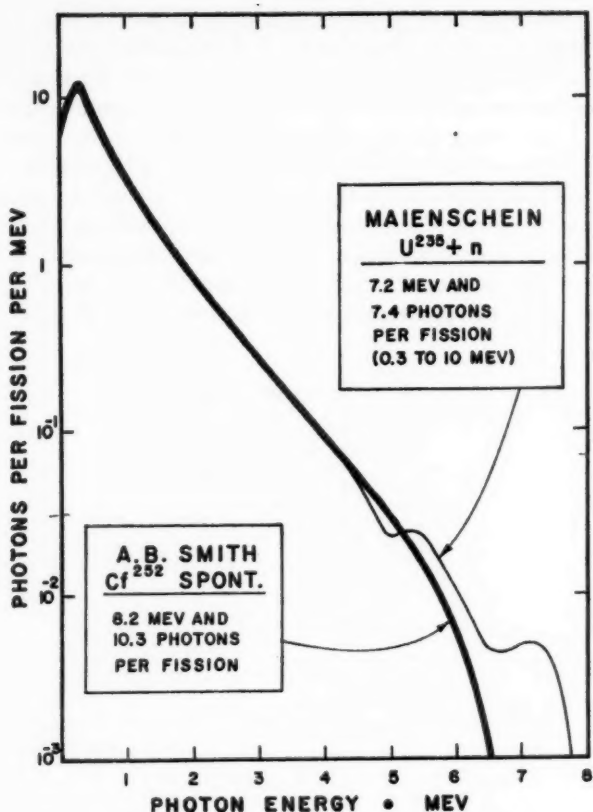


FIG. 19. Spectra of prompt fission photons. The spectrum obtained in the thermal fission of U^{235} (112) is apparently similar to that in the spontaneous fission of Cf^{252} (93).

Since there are always two fragments, the total photon energy should on the average be a bit less than a typical neutron-binding energy, or 4 to 5 Mev. This same conclusion was arrived at by Leachman (111). The prompt-photon spectra observed by Smith *et al.* (93) and by Maienschein *et al.* (112) are shown in Figure 19. Similar measurements have been reported by Bowman & Thompson (108). These measurements all agree that the total energy of emitted photons, per fission, is almost twice the estimated amount.

It is clear from Figure 19 that this discrepancy does not arise from the emission of some high-energy photons in competition with the neutron emission. Less than 2 per cent of the photons have energies greater than 2 Mev. In fact, it is seen that the spectrum "breaks" at roughly a neutron binding energy, as one would expect from the compound nuclear model represented

in Figure 18. There are also other results that support the view that photons are not emitted until the fragments have evaporated all of the neutrons that they can. In a study of fission photons with energies up to $\frac{1}{2}$ Mev, Skliarevskii found that these photons are virtually all emitted with a lifetime in the neighborhood of 1 μ sec. This is, of course, much longer than the lifetime for neutron emission. It is interesting in this connection to compare the mean energy (~ 1 Mev) of the photons emitted in fission with the mean energy (~ 2 Mev) of photons emitted in slow-neutron capture [Groshev (114)]. One would expect the capture spectra to be slightly harder since the first photon-emitting states here are all at about 7-Mev excitation. This energy is rather higher than that of the typical first photon-emitting state in the fission de-excitation, but one would not expect as large an effect on \bar{E}_γ from this difference in starting energies as one observes. In fact, it would seem from the shape and intensity of the observed spectrum that if one were to subtract from it a sizable soft component, the remaining part of the spectrum would be consistent with expectations based on Figure 18 both with regard to intensity and mean energy. The problem, then, may be to understand the origin of the extra soft component. Voitovetskii and his co-workers (115) and Skliarevskii (113) have found definite lines in this soft component. Voitovetskii suggests that these lines may arise from the de-excitation of similar rotational states in different fragments. It should be possible to learn whether fragments of particular masses are responsible for the soft photons. Since the lifetime for the emission of these soft photons was found to be $\sim 10^{-9}$ sec., they are emitted from the fragment after it has travelled an average distance of ~ 1 cm. from the fission origin. With the help of a collimating system like Skliarevskii's, it would be interesting to measure the masses of fragments in coincidence with soft photons.

One final piece of experimental information bearing on the nature of the prompt photon emission in fission comes from the studies of the angular distribution of the photons with respect to the fragments. The most recent study of such a distribution indicates that it is essentially isotropic (116). A few per cent more photons are emitted in the fragment direction in the center-of-mass system than at right angles to that direction. The sign of this small anisotropy is such as to indicate that the radiation comes from charge which is revolving around the fission symmetry axis (if we assume that we are dealing with electric dipole radiation). This would correspond to radiation from nucleonic rather than rotational transitions.

It is clear that there are some fundamental problems associated with the emission of photons in fission. As a number of authors point out, one of the difficulties standing in the way of their early resolution, from the experimental side, is the ever-present background of fission neutrons.

The dependence of $\bar{\nu}$ on energy and nuclear species.—It was mentioned in the previous section that the average kinetic energy of fission fragments is essentially independent of the excitation energy of the fissioning nucleus.

This implies that most of the excitation energy of the fissioning nucleus must find its way into the excitation energy of the fragments. To determine the division of the available energy between kinetic energy and internal fragment energy with the greatest precision, one should in fact measure the average fragment excitation energy rather than the kinetic energy. The for-

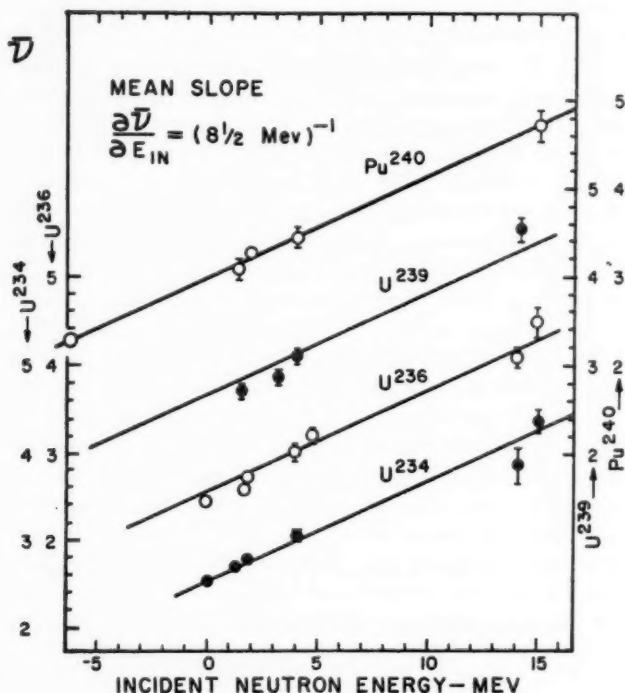


FIG. 20. The average number of neutrons emitted per fission in neutron-induced fission plotted as a function of the bombarding energy. Each curve is labelled according to the compound nucleus which is formed. The point at the left for Pu^{240} refers to spontaneous fission. References to the original literature can be found in the compilation of Leachman (10) from which these curves were taken.

mer energy is much smaller and provides better resolution for the determination of the energy division. As shown before, it takes ~ 7 Mev to evaporate a neutron from a fission fragment. This implies that $\bar{\nu}$, the average number of neutrons emitted per fission, should increase by unity for each 7-Mev increase of the bombarding energy if all of the "extra" available energy goes into fragment excitation energy. This seems to be approximately the case as can be seen from Figure 20 which was taken from the compilation of

Leachman (10). Some additional data and references are given in his report. It should be remarked that in the bombardments occurring at the highest energies in the figure, some of the fissions take place only after neutron emission. The prefission neutrons are included in the measurements of $\bar{\nu}$ and they tend to carry off perhaps a little more than 7 Mev per emitted neutron. Still, it would seem that the measured average slope, $\sim 8\frac{1}{2}$ Mev per neutron, is sufficiently different from 7 Mev per neutron to indicate that the fragment kinetic energy may be getting a small but finite share of the "extra" energy supplied to the nucleus. There is a slight hint from the work of Mostovaya (117) that this may be the case. In an ionization chamber comparison of Pu^{240} spontaneous fission with thermal fission of Pu^{239} , it is found that the average kinetic energy release in the spontaneous fission is perhaps 1 Mev less. Unfortunately this difference is hardly larger than the estimated precision of the comparison.

To explain the fact that virtually all of the bombarding energy in fission is converted into excitation energy of the fragments, one need only assume that the nuclear modes are very nearly in thermal equilibrium before the nucleus passes through the saddle point. As has already been pointed out (Sect. 10), the fact that the spontaneous fission point lies on the same curve as the other points (Fig. 20) implies that there must as well be thermal equilibrium on the descent from the saddle point, at least up to the point where a spontaneously fissioning nucleus emerges from the barrier. These considerations, which indicate that the motion of the nucleus past the saddle point is viscous or sticky, were first given by Wheeler. The liquid in the liquid-drop model is apparently more like taffy than like water. This description probably applies all the way up to the scission point. Geilikman has recently calculated some excitation energies of fission fragments on the basis of a liquid-drop model into which some viscosity was introduced (118). His results seem to depend on the nuclear species and on its starting energy in a qualitatively reasonable way.

Bondarenko, Kuzminov, and their co-workers have compiled a table of values of $\bar{\nu}$ for spontaneous fission (119) which is based both on actual spontaneous-fission measurements and on measurements performed at higher energies (see Table VII). The values of $\bar{\nu}$ from the latter measurements were "extrapolated" to spontaneous-fission energies with the help of curves like those in Figure 20. These authors also computed the values of $\bar{\nu}$ to be expected on the basis of estimates of the total energy release and the kinetic energy release in fission. Their results are in good agreement with the actual measurements.

Although measurements of average energy releases and of $\bar{\nu}$ have led to some new ideas about the fission process (e.g., the viscosity in the descent from the saddle), it is clear that measurements of a more differential character should be even more powerful. One of the first such measurements was Fraser's (101). Using a coincidence arrangement, he found that apparently

30 per cent more neutrons are emitted from the light fragment than from the heavy one in the thermal fission of U^{233} , U^{235} , and Pu^{239} . Recent measurements by Whetstone indicate that in the spontaneous fission of Cf^{252} about 5 per cent more neutrons are emitted from the light fragment (120). It is probably too soon to say whether one should attach any particular significance to the difference between Whetstone's results for Cf^{252} and Fraser's for

TABLE VII
 $\bar{\nu}$, THE AVERAGE NUMBER OF NEUTRONS EMITTED IN SPONTANEOUS FISSION*

Nuclide	$\bar{\nu}$
Th^{230}	$1.24 \pm 0.15^\dagger$
Th^{232}	$1.36 \pm 0.15^\dagger$
U^{234}	$1.63 \pm 0.15^\dagger$
U^{236}	$1.58 \pm 0.15^\dagger$
U^{238}	2.30 ± 0.20
U^{239}	$1.71 \pm 0.15^\dagger$
Np^{238}	$1.67 \pm 0.15^\dagger$
Pu^{238}	2.17 ± 0.20
Pu^{239}	2.28 ± 0.10
Pu^{240}	2.23 ± 0.05
Pu^{242}	2.28 ± 0.13
Am^{242}	$2.42 \pm 0.15^\dagger$
Cm^{242}	2.59 ± 0.11
Cm^{244}	2.82 ± 0.09
Bk^{249}	3.72 ± 0.16
Cf^{246}	2.92 ± 0.19
Cf^{252}	3.84 ± 0.12
Cf^{254}	3.90 ± 0.14
Fm^{254}	4.05 ± 0.19

* This table was adapted from the one by Bondarenko *et al.* where references to the original literature are given (119). A similar table is given by Hyde & Seaborg (16).

† These values are extrapolations from measurements made with thermal or fast neutrons.

lighter elements. In any case, it is quite significant that both authors find that the light fragment emits most of the neutrons. It indicates, contrary to expectations, that the light fragment is more excited than the heavy one at scission. If the excitation energy of the fragments comes mostly from the distortion energy at scission and if the light and heavy fragments have similar shapes at that time, one would expect somewhat more energy in the heavy fragment. Moreover, whatever energy there is in the nucleon excita-

tion at scission should be divided in proportion to A and should, therefore, also go mostly with the heavy fragment.

It was assumed in this last argument that the mean neutron binding energies are roughly the same in the light and heavy fragments and that the amount of energy which is taken off by photons is also the same for both fragments. These would seem to be reasonable assumptions.

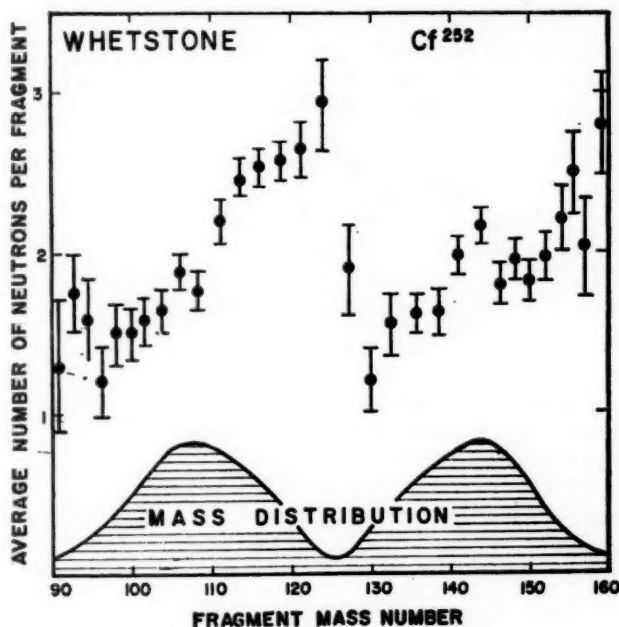


FIG. 21. The average number of neutrons emitted per fission as a function of the mass of the fragment from which the neutrons come. The data were obtained in a coincidence measurement using the time-of-flight technique (120).

In pursuing the problem of neutron emission as a function of fragment mass, Fraser & Milton found an even more surprising result than the slightly larger neutron yields from the light fragment. They found that about three times as many neutrons are emitted from the light as from the heavy fragment in near-symmetric fission and that it is almost the other way around in very asymmetric fission (121). Whetstone has recently confirmed the existence of this curious effect by observations on Cf^{252} (120). His results are given in Figure 21. The total number of neutrons which are emitted from a given mass pair is not very sensitive to the mass ratio, as already seen (Fig. 16), but the apportionment of excitation energy between fragments is apparently extremely sensitive to mass ratio. One lesson from Figure 21 is, as Vladi-

mirskii has put it, that symmetric fission is not really symmetric (122). For when a pair of fragments are produced with nearly equal masses, the slightly lighter fragment has perhaps three times as much excitation energy as the heavier one. Under the circumstances, the heavy fragment must be produced in a rather undistorted (spherical) state. This suggests, as first pointed out by Whetstone (123), that fission into the various different mass ratios can be imagined to take place from a common starting shape which has a moderately long neck and is asymmetric. The ball on the left side of the dumbbell (Fig. 22) is as heavy as the other ball and the bar put together. In this picture, symmetric fission would arise from a cutting off along *A*. The heavy fragment would come off with very little excitation energy because

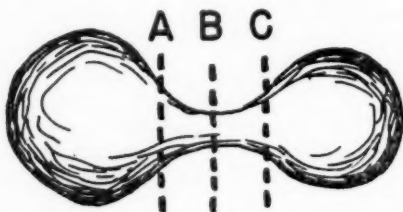


FIG. 22. A model of the nucleus just before scission. If one of the potential fragments is always larger than the other, there may be a simple way to understand the results of Fig. 21. (See text.)

of its nearly spherical shape. If fission happens to occur at the more likely spot *B*, then one has asymmetric fission with roughly equal excitations (from the distortions) in each fragment. Scission at *C* corresponds to very asymmetric fission, and in this case it is seen that the light fragment should be formed with very little excitation energy, just as it evidently is. This picture is consistent with the earlier observation that the elongation at scission is roughly the same for symmetric and asymmetric divisions, and it certainly gives a simple qualitative account of the results of Figure 21. For each type of cut (*A*, *B*, or *C*), the actual pinch-off can occur at different times, as this asymmetrical system is stretching. This would have the effect of introducing a spread in the fragment excitation energies (and a complementary spread in the kinetic energies). Pursuing this kind of view, Vladimirovskii was led to look for some reason for the asymmetry in Figure 22. He suggests that the large-sphere-end of the nucleus tends to remain fixed in size during fission because of the energy associated with certain "outer nucleons" of high angular momentum which it contains (122). He points out that this special stability of the heavy fragment may be related to the uniformity in the size of this fragment among the different fissioning species (see Sect. 13). One has to examine the problem in more detail to see to what extent this suggestion may be quantitatively reasonable.

12. BETA DECAY AND DELAYED NEUTRON EMISSION FROM FISSION FRAGMENTS

Within a microsecond after the fission act, the "final" fragments A_3Z_3 and A_4Z_4 (Fig. 13) are in their ground states. These fragments are, on the average, some four beta decays away from the stable valley of the nuclides, and with a half life of a millisecond or more they decay toward the truly final stable fragments A_6Z_6 and A_6Z_6 . In the course of the decay, β -particles, neutrinos, photons and, occasionally, delayed neutrons are emitted. From the practical point of view these radiations contribute to the energy release in fission and their contributions should be added to the kinetic and excitation energies so far discussed. Detailed information about the β -decay of fission fragments is of course not only of interest to those concerned with the construction of nuclear reactors. It is of fairly fundamental interest in nuclear physics because it can be used to determine the masses of nuclides which are further away from the stable valley than those which can be produced by ordinary means. To the radiochemist who studies the fission process, the detailed knowledge of the β -decay chains is especially important. He needs this information in order to interpret his measurements in terms of the charge and mass distributions of fission (Sect. 13, 14). Despite all of these good reasons to consider the radioactive decay of fission fragments, we shall not do so here. The decays take place too late after the occurrence of fission to provide much information about the actual fission process itself.

For information and references about the β -decay chains in fission, the reader is referred to the recent article by Katcoff (124) and the table of isotopes of Strominger *et al.* (125). For a comprehensive treatment of the occasional (delayed) neutron emission along the decay chain one may refer to the reviews of Keepin (126, 127).

13. THE MASS NUMBERS OF FISSION FRAGMENTS

Division into more than two fragments.—Generally a nucleus undergoing fission divides into two fragments of comparable size. There are indications that very rarely (perhaps one time in 10^4 or less) there is division into three large fragments (128). The rarity of such "tripartition" or ternary fission cannot be understood simply from energetic considerations. In fact the total energy release can be larger for tripartition than for normal binary fission. However, the minimum kinetic energy that must be carried off by fragments in tripartition is also somewhat larger. It is probably most reasonable to assume the $E_X = E_T - E_K$ gives the best measure of fission probability, at least as far as energy is concerned. Simple estimates indicate that there should be a considerable overlap between the range of E_X in binary fission and that expected for ternary fission. This would imply that tripartition is suppressed more by the difficulties of organizing the nucleus for the more complicated division than by any considerations of the energies of final states.

The name "ternary fission" is sometimes applied to fission into two normal heavy fragments plus a high-energy alpha particle. In the thermal-neutron fission of U^{235} the ratio of such ternary events to normal events is roughly 1 to 300 (129). If it were true that these alpha particles were evaporated from the moving fragments, the name "ternary fission" would certainly be inappropriate. But the indications are that at least most of the fission alpha particles are not evaporated from fragments. One can make a rough estimate of the expected number of evaporated alpha particles from the ratio of (γ, α) to (γ, n) yields in photonuclear reactions (130). This estimate is at least 10 times lower than the observed probability of the ternary fission. Fulmer & Cohen point out, too, that there are more low-energy alpha particles in the observed spectrum than one could legitimately expect if they were evaporated (129). Perhaps the best indication that they are not evaporated is their angular distribution with respect to the fission fragments (128). They come off in a fairly tight distribution centered at about 80° to the light fragment. These observations on the energy and angular distributions are consistent with a picture in which the alpha particle is the spray in the fission act. It is a droplet which is left floating between the separating fragments. In a completely symmetric division, the droplet would remain standing stock-still in the middle, quite undetectable. But if the alpha particle is formed off-axis or with some off-axis momentum, it will be pushed out by the separating fragments essentially at right angles to the axis. It is clear that the observed alpha-particle spectra and angular distributions must give some measure of the phase space occupied by the alpha particles when they are made. The alpha particles, rare as they are, may therefore prove to be a very useful probe for exploring the nuclear configuration at scission. A number of measurements of the alpha-particle yield as a function of excitation energy, nuclear species, and fragment kinetic energy have recently been undertaken (131, 132).

It should perhaps be explicitly remarked that the alpha-particle emission was ignored in the considerations of the energetics in fission (Sect. 11) because the average energy carried off by alpha particles is less than 0.1 Mev per fission (129).

From time to time the suggestion has been made that fragments somewhat heavier than alpha particles occur as the third particles in ternary fission. According to the best evidences such ternary fission is extremely rare if it occurs at all [Flynn (133)].

The mass distribution in thermal-neutron fission.—We turn now to the mass distribution of normal two-fragment fission. The major technique used for the measurement of mass yields has been radiochemistry (134). By means of chemical separations and more-or-less standard counting techniques, one can determine the yields of the nuclides whose mass numbers are A_1 and A_2 (Fig. 13) and whose atomic numbers are only slightly smaller than Z_1 and Z_2 . That is, one can measure the yields of radioactive species which lie

toward the end of their β -decay chains. Since one generally wants to interpret the measurements in terms of the yields which obtain at the stage (A_3, A_4), it is necessary to make a few corrections to the measured data. One must correct for interruptions of the β -decay chains (by stable nuclides), for delayed neutron emission, and for the amount of "direct" yield of products which lie farther down the chain than the nuclide being measured. For ther-

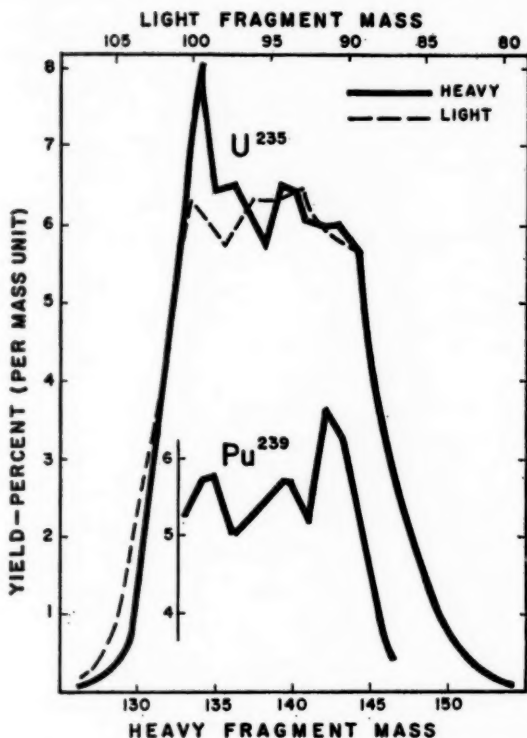


FIG. 23. The cumulative yields of different mass numbers in thermal fission. The yields are expressed in per cent per mass number, normalized to 100 per cent for the light and heavy peaks separately. The data for these figures were taken from the recent critical examination of mass distributions by Katcoff (124). References to the original literature are given in his work.

mal-neutron fission these corrections are generally small compared to uncertainties introduced by counting errors and by the lack of detailed knowledge of the β -decay systematics. In general, radiochemical mass-yield determinations have accuracies no better than about 10 per cent. Recently mass spectrometry has been introduced as a technique for measuring fission product mass distributions, and here the accuracy is normally a few times

better [Thode and his co-workers, cf. (135)]. Although time-of-flight techniques can also be used to measure mass distributions, they do not have the mass resolution of the other methods, principally because of the complications arising from the emission of prompt neutrons (94).

Perhaps the best measured mass distribution is that for the thermal-neutron fission of U^{235} . Figure 23 is a plot of this distribution which is based on the recent compilations of Katcoff (124). The distribution for the "light peak" has been plotted to overlap with that of the "heavy peak" in such a way that the sum of the masses at any value of the abscissa is 233.5. This number is the average mass of the system after 2.5 neutrons have been evaporated. It is seen that the yields of complementary fragments are in fair agreement. The centers of the light and heavy peaks occur at roughly $A=95$ and $A=139$, indicating that the mass of one of the fragments tends to be about half again as large as that of the other. The amount of division into nearly-equal-size fragments is negligible and does not even appear on the figure.

Fine structure.—The irregularity on the tops of the peaks is called "fine structure" and some of it may be attributable to shell effects which lead to greater chances for the formation of certain mass pairs than for the formation of neighboring mass pairs. If this were, however, the only cause of fine structure, the yields of corresponding light and heavy masses would be expected to be exactly the same. It has been suggested by Glendenin that the peak at $A=134$ may be caused by an abnormal amount of neutron emission from fragments which would otherwise have become nuclei with $A=135$ or $A=136$ (136, 137). Such an effect would be attributable to unusually low neutron-binding energies for nuclei with these particular masses and would therefore also be connected in some way with the nuclear shell structure. Although in principle this suggestion of "neutron emission fine structure" could be independently and rather directly checked by counter measurements like the one whose results appear in Figure 21, such measurements do not yet have the necessary resolution. It is probably easier to study fine structure with counters by examining the mass distributions themselves rather than the neutron emission. Stein's counter measurements with U^{235} do not show the peak at $A=134$, but his resolution seems to be only on the edge of being able to show it (94).

It is interesting that the "fine structure" in the thermal fission of Pu^{239} is significantly different from that in U^{235} (Fig. 23) and also that the peak at $A=134$ is virtually all gone when U^{235} is made to fission by 14-Mev neutrons (138). These facts suggest that some of the fine structure may be a "noise" connected more with the slight ups and downs in the single-particle structure than with major shell effects.

The average mass ratio in the fission of different species.—In comparing the low-energy mass distributions for different species, one is struck by the fact that the mass ratio for the most probable division is not the same for all

targets. This is illustrated in Figure 24 where the masses at the centers of the light and heavy peaks have been plotted as a function of the mass number of the fissioning nucleus. With the exception of the triangles (see below), the plotted points refer to thermal-neutron fission and to spontaneous fission. It is seen that the heavy-fragment "primary" mass stays very nearly con-

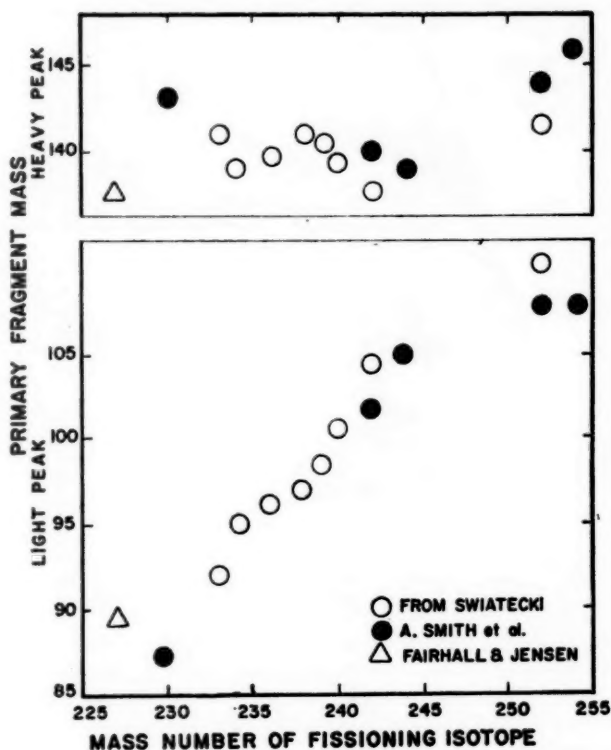


FIG. 24. The mass numbers at the centers of the light and heavy mass peaks in low-energy fission. The open circles are from the compilation of Swiatecki (139). The closed circles are from the more recent measurements of Smith *et al.* (93) and the triangles are from the study of radium fission by Jensen & Fairhall (140).

stant and that therefore the light mass alone reflects the changing mass of the target. Preliminary measurements by Sugihara indicate that this constancy in the mass of the heavy fragment may persist to isotopes as light as polonium (141). The corresponding mass ratio in this case would then be 2.0 (compared to about 1.3 for californium, the heaviest element investigated so far). Such a determined persistence of the heavy-fragment size would indicate that it may have a fundamental rather than incidental re-

lation to the fission process. Whether this general favoring of a particular heavy mass is related to the apparent favoring mentioned toward the end of Sect. 11 in connection with neutron emission is not yet clear.

Shapes of mass distribution curves.—The triangles in Figure 24 are based on the measurements of Jensen & Fairhall shown in Figure 25 (140). They

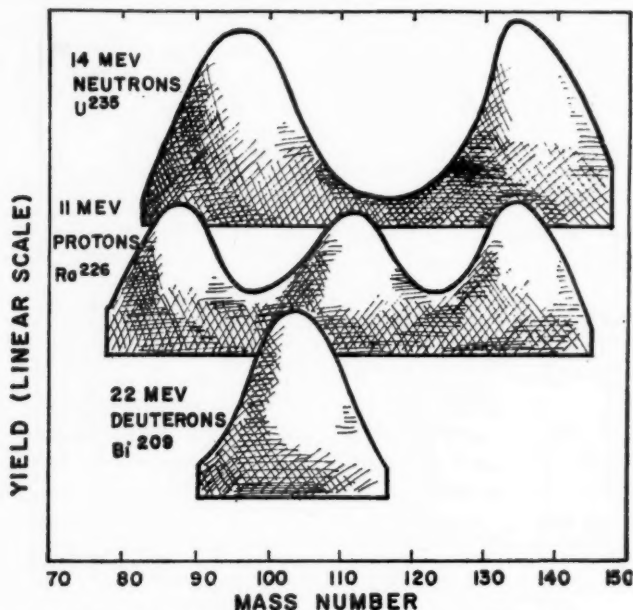


FIG. 25. Mass distributions in fission at moderately low energies. As the atomic number of the target decreases, the relative importance of "symmetric fission" increases. The curves are based on measurements by Fairhall (142) (Bi^{209}), Jensen & Fairhall (140) (Ra^{226}) and on data compiled by Katcoff (124) (U^{235}). The cross sections decrease rapidly as the atomic number of the target decreases.

refer to the outer peaks on the radium curve. Inasmuch as these points fit in well with those observed in "normal" binary fission, it seems appropriate to associate these outer radium peaks with the familiar asymmetric fission.

The central peak in radium is probably to be associated with the single peak that Fairhall has found in bismuth fission at moderate energies (142). These single peaks, the so-called symmetric peaks, are much narrower than the symmetric distributions which are observed in high-energy fission of the heavy elements. The latter distributions (Fig. 26) are often thought to come about simply from a general washing out of detail at higher energies. Not only does the "valley" fill in as the energy is increased, but the sides of the

distributions also spread out somewhat. It is not unreasonable that whatever it is that makes low-energy fission asymmetric becomes less compelling as the nucleus is heated up. Incidentally, it can be seen in Figure 26 that the narrow single-peaked bismuth curve also spreads out as the bombarding energy is increased. The widths of the mass distributions in higher-energy

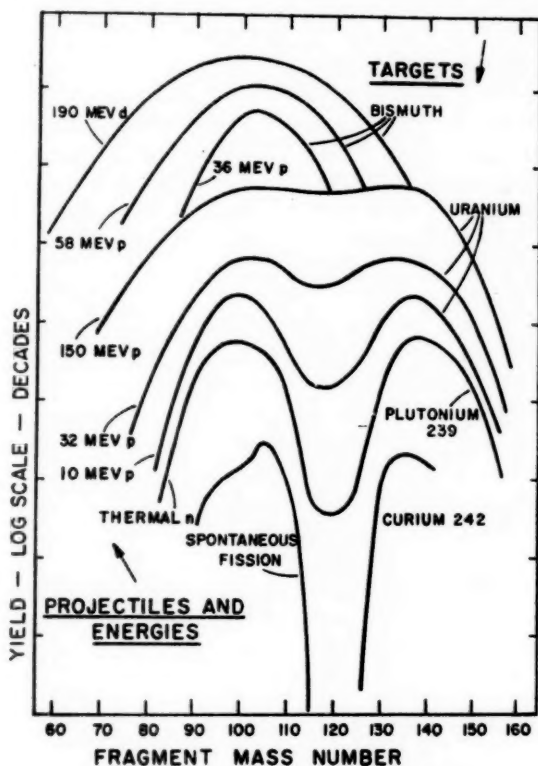


FIG. 26. Shapes of mass distributions to show their dependence on the bombarding energy and on the nature of the fissioning species. The measurements were performed by a number of different people: Curium [Steinberg & Glendenin (143)]; plutonium [see Katcoff (124)]; uranium [Stevenson *et al.* (144)]; and bismuth [Sugihara (141); Goeckermann & Perlman (145)].

bombardments are in all cases too large to be accounted for simply by the spread of deposition energies and the associated spread in the number of particles emitted either before or after fission. The large increase in widths at higher energies must be a more fundamental feature of the fission process.

"Symmetric" vs. "asymmetric" fission.—The occurrence of a narrow symmetric peak in some species at low energy and, especially, the fact that such a

peak can be observed together with asymmetric fission in radium suggest that it may be reasonable to think of symmetric fission as a "type" or "mode" of fission distinct from asymmetric fission. Such a view receives some support from the observation that the energy dependence of the "filling in of the valley" in heavier targets resembles the total fission excita-

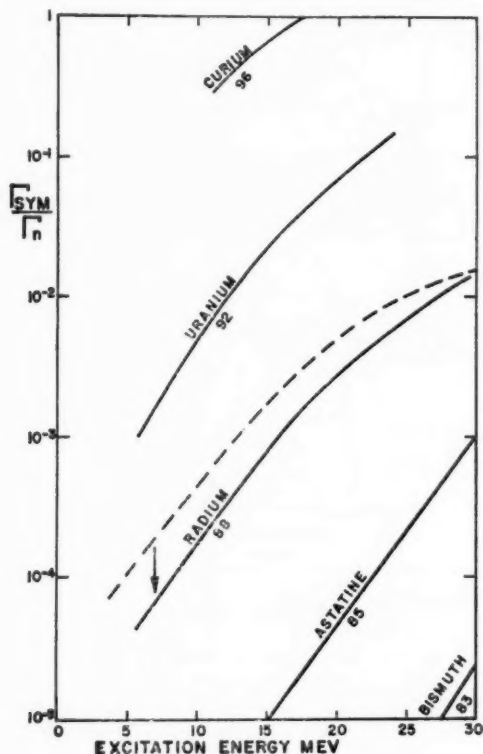


FIG. 27. The ratio of the symmetric-fission width to the neutron emission width. The lowest two curves are based on the work of Fairhall & Neuzil (83). The radium data are those of Nobles & Leachman (84). The uranium data were obtained in Los Alamos and were given in the report by Hemmendinger (147). The curium curve is based on the work of Glass (148). (See text.)

tion curves in the light targets, like bismuth, where the mass distribution is symmetric at all energies. That is, it may be possible to introduce some simplicities in the analysis of mass distributions in heavy targets if one regards them as a superposition of symmetric and asymmetric parts. A view point of this sort was recently advanced by Jensen & Fairhall (146).

In Figure 27 we have tried to indicate the quantitative similarities between the growth of "symmetric" fission with energy for a number of dif-

ferent species. The lower curves are taken from Figure 12 except that the radium curve was corrected as shown to remove the contributions which the "asymmetric fission" makes to the total fission cross section. The quantity $\Gamma_{\text{sym}}/\Gamma_n$ for the uranium curve was computed from the rate of filling in of the valley which was observed by the Los Alamos Radiochemistry Group (147). It was assumed here that $\Gamma_{\text{sym}}/\Gamma_{\text{asym}}$ is given by the valley-to-peak ratio and that over the entire range of excitation energies with which we are concerned, $\Gamma_f = \Gamma_{\text{sym}} + \Gamma_{\text{asym}} = \frac{1}{2}\Gamma_n$ (Fig. 7). The curium curve comes from the valley-to-peak data of Glass *et al.* on the alpha-particle bombardment of plutonium (148). It has been assumed here that $\Gamma_f/\Gamma_n = 5$ (Fig. 8) and that all of the symmetric yield comes from fission before neutron evaporation. These are all somewhat questionable although reasonable assumptions. If one accepts them, it is seen that the filling in of the valley in the fission of heavy targets has about the same energy dependence as the "light"-element symmetric fission. Moreover, the different curves are spaced in a reasonably regular way as a function of the atomic number of the fissioning nucleus.

It should not be too hard to establish whether it is meaningful or useful to think of symmetric and asymmetric fission as distinct "modes," associated perhaps with quite different saddle-point shapes. One would try to see whether these two "types of fission" exhibit differences other than those which were used to define them. One would compare typical symmetric fission (say low-energy alpha-induced fission of bismuth) with typical asymmetric fission (say low-energy fission of U^{235}) with regard to the kinetic-energy distributions, the emission of neutrons and some of the other types of distributions which have been discussed.

It should be pointed out, while we are on the subject, that although it had been known for a long time that the mass symmetry in heavy elements increases with the bombarding energy, it was recently shown clearly for the first time that this increase arises from an increase in mass symmetry with excitation energy. In an investigation of thorium and other targets using protons with good energy resolution, Bowles, Brown & Butler found the following effect (149, 150). As the bombarding energy was increased and a threshold was reached where fission following the emission of some definite number of neutrons became energetically possible, the increment of (very low-energy) fissions that came in was essentially purely asymmetric. The symmetric part of the mass distributions which one observes at higher bombarding energies apparently comes only from fissions which occur at higher excitation energies. There have been, in the past, a number of comparisons of "peak-to-valley" ratios as a function of bombarding energy where many nuclear species were considered together (151). Because the relative amount of fission after the emission of one or more neutrons depends on the fissionability of a species and because the mass distribution depends on the excitation energy, such comparisons are too integral and should not be expected to give comparable results for different targets. With the work of Butler and his

co-workers, it becomes possible to get a rough idea of the peak-to-valley ratio in Pa^{233} and its neighbors as a function of excitation energy. Making use of some reasonable estimates of Γ_f/Γ_n as a function of energy in the different protactinium isotopes, one finds that the curve in Figure 28 leads to a good reproduction of the observed dependence of the ratio of peak to valley on bombarding energy. The analysis is not precise enough to give very detailed information. But it is probably safe enough to say that in isotopes near Pa^{233} the probabilities for symmetric and asymmetric mass division are

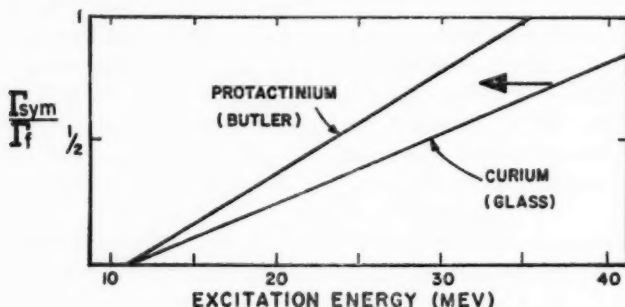


FIG. 28. The ratio of the mass-symmetric part of the fission width to the total fission width. The protactinium curve was constructed to fit the data of Bowles *et al.* (149) giving the ratio of symmetric to asymmetric yields as a function of bombarding energy in $p+\text{Th}^{232}$. If it is assumed that the curve in this figure applies to all Pa isotopes and if one uses reasonable estimates of Γ_f/Γ_n for these isotopes, one can reproduce the results of (149). The curve for curium is based on the measurements of Glass *et al.* (148) on $\alpha+\text{Pu}^{239}$ and the assumption that most of the fission occurs before neutron emission since Cm^{243} is very fissionable. This assumption leads to an overestimate in the amount of asymmetric fission at the higher energies. The arrow shows how one must move the top of the curve to correct it. Within the precision of these analyses, the ratio $\Gamma_{\text{sym}}/\Gamma_f$ behaves in the same way with energy for protactinium and curium and presumably for elements in between.

roughly equal at an excitation energy of 23 Mev and that it takes about 10 Mev for the mass distribution to change its character from essentially asymmetric to essentially symmetric. In the same figure we have plotted the peak-to-valley changes in the alpha-particle fission of Pu^{239} as a function of excitation energy. Actually the data refer to the measurements (148) as a function of bombarding energy, but the fissionability of the compound nucleus Cm^{243} is so large that only a small fraction of the observed fissions is preceded by neutron emission. At the higher bombarding energies one cannot, however, be very sure about the relative contribution to the asymmetric component from fission which takes place after neutron emission. The arrow shows the direction in which the upper part of the measured curve must be

moved to allow for the contributions of fission after neutron emission, but it is hard to know just how far to move the curve. In any case it would seem from the closeness of the two lines in Figure 28 that the ratio between symmetric and asymmetric fission yields varies with energy in very nearly the same way for the common heavy nuclides.

It is apparently true that the ratio of the total fission width to the neutron width in heavy targets does not change very rapidly with energy at low energies (Sect. 6). Figure 28 then implies that $\Gamma_{\text{asym}}/\Gamma_n$ probably drops off with increasing energy. It is unfortunately very difficult to learn about this particular ratio at high excitation energies because it is hard to know how to subtract from measured mass distributions the large contributions to σ_{asym} of those fissions which occur only after the emission of neutrons.

An unwarranted but simple summary of the foregoing description of the mass distribution is that it may be reasonable to think of fission in terms of two modes, symmetric and asymmetric. Each may have to do with relatively unrelated nuclear distortions so that they compete with each other in the same sense that they compete with neutron evaporation. The symmetric component increases regularly with energy and with the atomic number of the fissioning nucleus. Less is known about the energy dependence of the asymmetric component; but as far as atomic numbers go, it seems to become very improbable for elements with $Z < 88$ (radium). Recent observations by Fairhall & Neuzil that the mass distribution in the alpha-particle fission of gold is wider than it is in bismuth may be a hint that asymmetry becomes popular again as one gets away from the closed shells on the lighter side (83).

The essential difference between the two-mode view of fission which has just been described and a one-mode view is that the latter view involves only one saddle. It is to that extent a simpler view. Since here symmetric and asymmetric divisions use the same saddle, one can imagine that the nature of the mass distribution is determined only after passage through the saddle (as one does in the statistical theory described below). It is entirely possible, however, that there is some predisposition to certain divisions already at the saddle. In the one-saddle view the regularity of Figure 27 is of course not taken as evidence for an independent symmetric mode. The regularity would be blamed on the similarity of behavior of fissioning nuclei according to Figure 28 (which has to be accounted for in any case) and the improbability of low-excitation-energy fission in lighter elements (Sect. 8). Probably the triple-humped curve for radium in Figure 25 puts the most strain on a one-mode view, but even here there are ways of accommodating to the data. In view of the latitudes still available to both the one- and two-mode descriptions, it is probably not too fruitful at present to be concerned with the distinction between them.

In trying to understand at what stage in the fission process the mass distribution is determined, one would like to know how the distribution

depends on the starting state, that is, on the original quantum state of the fissioning nucleus. A number of separate distinguishable starting states are available only for fissions induced by neutrons with energies in the electron-volt range. Prompted by the ideas of Wheeler and Bohr, there have recently been a number of measurements in which the mass distributions for different resonant states (Fig. 5) have been compared. Since these states arise from the combination of an $l=0$ neutron with the target nucleus, it is clear that they can be grouped into the two sets having a total angular momentum half a unit higher and half a unit lower than the target in its ground state. If the nuclear shape at the saddle point is sensitive to the value of the total angular momentum and if the final mass distribution is sensitive to the nuclear shape at the saddle point, then one could expect a dependence of the mass distributions on the angular momentum. In the specific example of U^{235} , Wheeler suggests that the 3- states which are formed when a neutron is captured might pass through a fission channel in which there is an asymmetry in the nuclear shape (4). Consequently, one might expect a suppression of the symmetric part of the mass distribution. Measurements have so far been made with U^{233} [Regier (152); Roeland (153)] and with U^{235} [Roeland (153); Los Alamos (154); Nasuhoglu (155)] using various techniques. In each case the distribution for some group of resonance or epithermal neutrons was compared with that for thermal neutrons. The different measurements do not agree beyond indicating that the ratio of symmetric to asymmetric fission does not change by a very large amount when the incident neutron energy is changed. To pursue these investigations, it would be desirable to examine a large number of resonances in a single nucleus in order to see whether the observed mass distributions actually are of just two kinds. If there happened to be more variety it might tell something about the number of different channels open to states of a given angular momentum. If one could independently determine to which spin state the different resonances in slow-neutron fission belong, that too would be helpful. But it is apparently difficult (156).

In a study of low-energy photofission, Schmitt & Duffield have found an effect that may be connected to the role of saddle-point levels on the mass distributions (32). They found that the Cd^{117} yield in uranium fission goes through a very sharp peak at 6 Mev. Since this peak happens to occur very near the neutron-binding energy in U^{238} , Wheeler has suggested that when neutron emission first becomes possible it may happen to compete preferentially with that fission channel which leads to symmetric (Cd^{117}) fission (4). This would explain the falling side of the peak. One would have to find some separate explanation for the fact that at the same energy, the Cd^{117} yield in the fission of Th^{232} is about 100 times smaller. It would be useful to know whether other symmetric fragments in U^{238} fission show the same sharp peak as Cd^{117} . If not, it may indicate that the spike is connected with some sort of "fine structure" (which is somehow not nearly so "fine" as the usual fine structure).

Explanations of the mass distributions.—Having examined in some detail a number of features of the observed mass distributions, we return to the obvious and fundamental question, "Why is low-energy fission in heavy elements asymmetric?" The essential facts about the asymmetry are these: (a) It is a striking effect. (In thermal fission, division into symmetric mass pairs happens only about 10^{-3} times as often as division into the most probable pair.) (b) It is a simple effect. (The mass distribution consists of two rather smooth humps. The fine structure is very much smaller than the main two-hump structure.) (c) It is a rather universal effect. (The low-energy mass distributions are very much the same for all heavy elements.) In view of these features one cannot help feeling that there must be some single, simple explanation of the asymmetry. It is no doubt this feeling, plus the fact that no explanations (simple or involved) have as yet achieved a fairly general acceptance, that keeps the mass distribution problem in the "popular puzzle" class. It is hard for anyone who first hears about the problem not to begin to look at once for the explanation, and it is entirely possible that the proper explanation has already been eloquently given. If so, it still remains buried in the "noise" of the many suggested explanations.

The present review will unfortunately be limited to a rather superficial survey of some of these explanations much as the subject deserves a critical and thorough examination. Certainly the first place to look for an explanation is in the liquid-drop model. It has already been pointed out that the implications of the model are not easy to determine, but the indications seem to be that the shape of the drop at the lowest saddle point is symmetric. Nossoff (157) and Businaro & Gallone (158) have indicated that within the framework of the drop model it is, however, entirely possible that a strong asymmetry can develop between the saddle point and the actual rupture of the nucleus. It is Swiatecki who has continually emphasized the gap between our understanding of the drop model and our needs for applications of the model to fission. He himself has done more than anyone to help close this gap (17, 39, 159). In a recent study he has pointed out that even after a nucleus has passed through the "binary fission" saddle, there is a chance that it can assume distortions associated with division into three (or even more) fragments (159). The three-fragment shape may, however, fail to perform both of its intended divisions, giving rise to one large fragment and one small one. It would seem, however, that if this were the basis for the asymmetry in fission, the large fragment would usually find itself with more excitation energy (because of its greater distortion) than the small fragment. This apparently does not happen, as already mentioned (Sect. 11).

Hill has emphasized that an examination of the potential-energy surfaces associated with drop model distortions may not be an adequate way to explore the consequences of the model. It overlooks possibly important dynamic effects (159a). Using a drop with a particularly simple shape, Inglis has studied some aspects of the dynamics of droplet fission (160). He finds a slight favoring of asymmetry which is associated with the lower reduced

mass for an asymmetric split, but he points out that the magnitude of the effect is too small to account for the observed asymmetry in fission.

Swiatecki, Maris, and others have called attention to the possibility that the classical droplet model may perhaps be made more realistic as a description of fission if it is modified to take nuclear compressibility and actual nuclear charge distributions into account (24, 25). The inclusion of some of these features seems to favor asymmetry in a qualitative way, but they have not been adequately explored quantitatively.

In addition to those attempts at explanations of the mass distribution which involve only classical considerations of some sort of liquid drop, there have been some which rely on single-particle effects. There have been, for example, many suggestions based on magic numbers. The fission fragment which marks the inside edge of the heavy mass peak (seen in Fig. 24 to be much the same for all nuclei) has very nearly 82 neutrons and 50 protons. When symmetric fission occurs, these shells must be broken up and this is held by some to account for its suppression. In a similar way it has been suggested that for fission to be probable, one fragment must contain a full shell of 50 neutrons and the other fragment must contain an 82-neutron shell. Asymmetric fission must in this view become rare when there are fewer than 132 neutrons in the fissioning nucleus. This seems to be the case. But one would also imagine that the mass peaks would then be wider for heavier nuclei than they are for nuclei which have only a few neutrons more than 132. This does not agree with the observations. It has been suggested by Hill (161) and by Curie (162) that the inner shells in the shell model have a particular spatial integrity and that a core like Ca^{40} is preserved intact inside one of the fragments. The asymmetry then arises from a statistical division of the remaining nucleons between a second fragment and the one with the magic core. Most of the "magic number" accounts of the asymmetry have merely called attention to certain numerology without exploring the possible physical processes through which the numbers might come to play a particularly important role.

A more fully developed view of the fission process which emphasizes the role of shell structure is that of Fong (163). His approach is based on the idea that the motion in fission is very slow (see Sect. 11). More precisely, it is assumed that the various degrees of freedom in the fissioning nucleus remain in thermal equilibrium all the way to scission and that the distributions of mass and charge are determined simply by the numbers of states energetically available at the scission time. Fong computes the densities of available states which correspond to different mass division by estimating the amount of excitation energy in the nucleus at the scission time and by using neutron-capture cross sections to tell him how the level density varies as a function of fragment mass. He finds that he can reproduce the thermal-fission mass distribution curve for U^{235} very well, and he attributes his success to shell structure effects. Because of the shell structure, the masses of the potential fragments are such that about 5 Mev more excitation energy is

available for asymmetric fission than for symmetric fission. This small amount of extra energy manages to have so dramatic an effect as the suppression of symmetric fission by a factor of 600 because it enters the problem in the exponent of a level density. This is one of the attractive features of Fong's theory, namely that he finds a natural "amplifier" that can blow up some not too large effect to account for the striking peak-to-valley ratio. Fong has not given any comparisons of his recipe with other mass distributions. One might, for example, be concerned that he would be unable to account for the observation that the "valley" rises above the asymmetric peaks at higher energies since, in his formulation, the most probable modes at any one energy should apparently remain most probable at all energies. Perring & Story have used Fong's parameters to compute the mass distribution to be expected in the thermal fission of Pu^{239} and they find that their results are not even qualitatively like the observations (164). Perhaps the most difficult evidence to accommodate to Fong's viewpoint is that relating to the numbers of prompt neutrons as a function of the fragment mass (Fig. 21). In a consistent statistical view of fission, this number of neutrons should be a rough measure of the average excitation energy of each fragment mass at scission. For maximum probabilities one would expect the division of excitation energy between fragments to be about equal and it is apparently far from that. In an independent assessment of the possible role of statistical considerations in fission, Newton has decided that Fong's level density formulae do not sufficiently reflect shell structure effects and that if they did, this would to some extent nullify the benefits that Fong reaps from shell effects in his computations of the energy releases (165). In Newton's view, purely statistical considerations cannot provide an explanation of the basic mass distributions although they can certainly be responsible for some observable effects.

More recently Cameron has done a calculation along the lines of Fong and Newton, using a newer set of nuclear masses and newer level densities (166). Again it would appear that statistics alone cannot account for the mass distribution. Cameron introduces nonstatistical ideas by making the separation distance R between the fragments at scission some specified function of the mass ratio. This function is determined empirically to fit the observed mass distribution and it is left to the future to determine its physical origin. Since Cameron is willing to allow his chosen function to vary with the nuclear species and with the excitation energy of the fissioning nucleus, he has essentially introduced an infinite number of arbitrary, empirically determined parameters. Under the circumstances he points out that the criteria for the reasonableness of his procedure are that his functions should be simple and smooth and that they should vary regularly from element to element. Furthermore, once one has picked a function for, say, thermal fission of U^{235} , one must be able to account for the kinetic energy distributions, the dependence of neutron emission on mass ratio, and all of the other observed features of fission that were not used in picking the function R .

Cameron indicates that a number of observed distributions in fission do seem to correlate with each other from this point of view.

In a sense, then, Cameron's calculations suggest that it requires a combination of statistical, single-particle effects and collective effects (those responsible for his mass ratio dependence on R) in order to account for the asymmetric mass distribution. Such a view has also been suggested by some who have entered the problem from the collective side, that is with the drop model. For example, in looking for a possible origin of the instability against asymmetry past the saddle point, Geilikman has suggested that the extra energy release which is associated with asymmetric fission because of single-particle effects tends to make it easy for asymmetric oscillations to appear (167). The idea is that such oscillations might grow sufficiently in amplitude between the saddle point and scission to account for the double-humped mass distribution. It is not yet clear to what extent Cameron and Geilikman are saying similar things from different starting viewpoints or, for that matter, whether either approach is essentially on the right track. The problem of explaining the "universal" double-humped mass distribution has become more complicated since this distribution has been found not to be so universal after all (Fig. 25). One must now demand of any proposed theory of the mass distribution that it explain the rapid disappearance of asymmetric fission in elements lighter than radium.

14. THE DISTRIBUTION OF NUCLEAR CHARGE BETWEEN FRAGMENTS

If one were to make a plot of the distribution of fragment atomic numbers which appear in, say, the thermal-neutron fission of U^{235} one would find that it looks almost exactly like the double-humped curve which describes the mass distribution. The point is that nuclear matter is not very polarizable, and to a good approximation each fragment gets a share of protons which is proportional to its share of nucleons. Actually, as numerous studies have shown, the specific charge is not exactly the same for all fragments. The detailed examination of the charge distribution has been carried out mainly by radiochemical means, and so far at least, it seems not to have provided any major insights about the nature of the fission process.

The problem of the nuclear charge distribution as it is usually formulated is to learn how to characterize the most probable charge Z_p for any fragment mass number and to find the width of the distribution about this most probable charge. As one must expect, the most probable fragments turn out to be rather neutron-rich. They lie well outside of the valley of stable nuclides and they decay with short half lives. Our information about the nuclear charge distribution comes from observations of species which happen to lie closer to the stable valley than the most probable fragments. Since such fragments are generally produced by the β -decay of fragments having lower Z , as well as directly in fission, their measured yields are not true "primary" yields. But in some of the β -decay chains there happens to be a break because of the existence of a neutron-rich stable nuclide or because a member

of the decay chain occurs in the gas phase and can be easily removed. Then it becomes possible to measure the primary yield of some particular fragment. There are, however, very few examples of chains with interruptions, and in studies of the charge distribution the available data are usually all lumped together. That is, one assumes that for all fragment atomic weights, the distribution in nuclear charge has exactly the same shape and width. One tries to find a recipe which gives the most probable charge Z_p as a function of atomic weight in such a way that all of the measured independent yields fall onto a single universal Gaussian curve which is a function of $(Z - Z_p)$. Here Z is the charge of the primary fragment before it starts its β -decay.

It is not too difficult to estimate roughly how Z_p should go with A . It has already been pointed out that if one ignores nuclear polarizability, the ratio of neutrons to protons should be the same in both fragments of a pair. This would also be what one would find if scission took place before the charges had a chance to readjust even if, for some reason, they ultimately would. On the other extreme, one can assign to the nuclei a reasonable polarizability (on the basis of the "symmetry" term in the mass formula) and assume that there is equilibrium of the internal charge distribution at the time of scission [Present (26)]. One could compute Z_p according to this sort of picture by finding the Z division for which the total fragment excitation energy is a maximum [Fong (163)]. If one overlooks for the moment the dependence of the total kinetic energy on the division of Z , one would expect the most probable division to be one where the β -decay chain to the stable valley is shorter for the light fragment. (To understand this, one must remember that the sum of the β -decay chains is the same for all fragment pairs of a given A_3 and A_4 and that the sides of the valley of nuclides are steeper for the lighter masses.) To take the dependence of fragment kinetic energy on the Z division into account, it is assumed that the separation at which scission takes place does not depend on the Z division. Then the kinetic energy which is given to the fragments is less, and the excitation energy more, for smaller charges of the light fragment just estimated. In fact, if one folds the "kinetic energy effect" together with the "valley steepness effect" assuming all the time that the most probable charge division is the one which provides the largest excitation energy release, then this most probable division turns out to have the property that the β -decay chain lengths are roughly equal for the light and the heavy fragment. The idea that Z_p corresponds to equal chain lengths for complementary fragments was first suggested on altogether empirical grounds by Glendenin (168).

There are a number of points that should be made about "the equal chain length" rule for locating Z_p . In the first place it is important to emphasize that its predictions differ from the "equal specific charge" rule (based on the assumed absence of polarizability) by less than one charge unit throughout the mass region where measurements have been made. Yet because the charge distributions are very narrow (Fig. 29), it is possible to discriminate

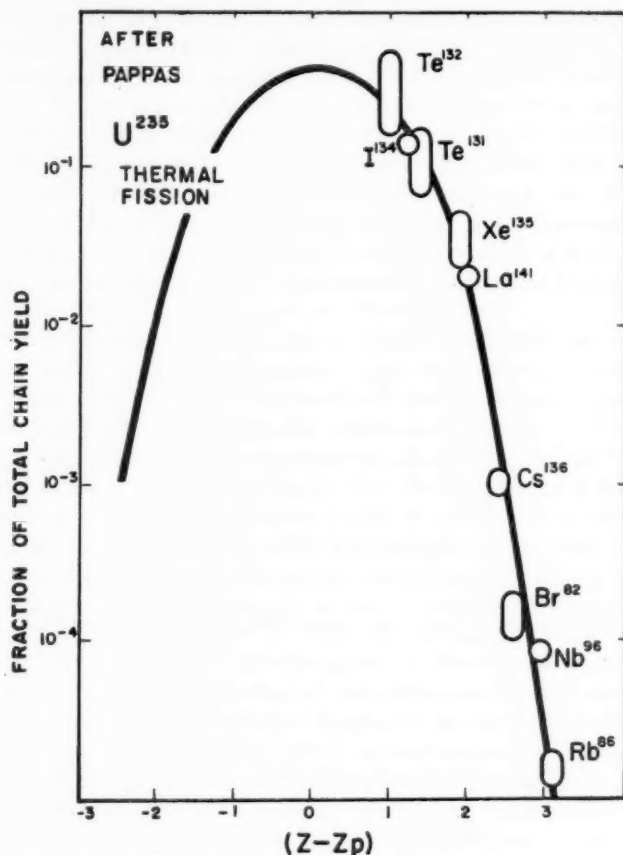


FIG. 29. The nuclear charge distribution of fission fragments. The curve gives the independent yield of fission fragments as a function of the difference between the atomic number Z of each fragment and the corresponding value of Z_p , the atomic number of that fragment with the same mass which has the largest yield. The implication of the fit of the data to the curve is that if Z_p is chosen properly, the charge distributions of all fragments can be represented on a simple universal curve. The data given were compiled by Pappas (169).

between the two rules by experiment, and for low-energy fission the first rule seems to be definitely better. This is gratifying since it would seem to be the better rule on physical grounds. A second point about the equal-charge-displacement or equal-chain-length rule is that because it defines Z_p in terms of the location of the stable valley and because the charge distribution curve is very narrow, it requires that one locate the center of the stable valley to within about 0.2 unit of Z or better. This can be done only if one is willing to be somewhat arbitrary. The empirical rule begins to lose

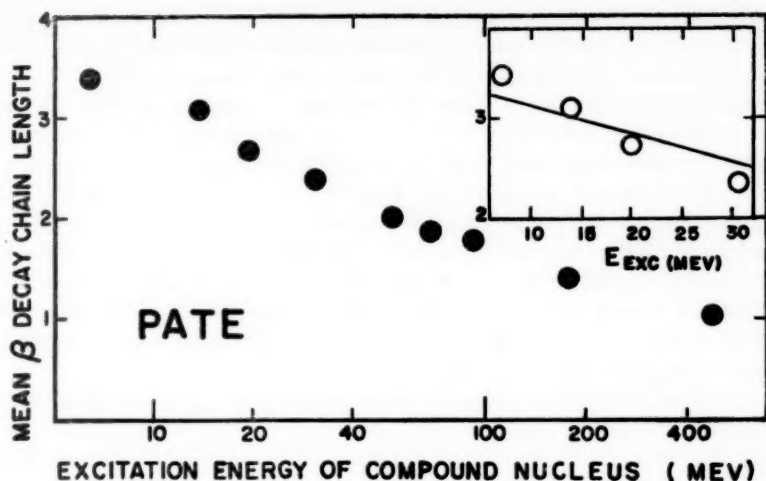


FIG. 30. The average distance of independently formed fission fragments from the stable valley in units of Z . The data here were collected by Pate (170) and refer to different elements. The abscissa is the bombarding energy plus the binding energy of the incident particle. It is called the energy of the compound nucleus, but it is not meant to imply that compound nuclei are always formed. The inset compares the energy dependence of the lower-energy data to the expectations. (See text.)

some of its simplicity if one must supply, along with it, a special and discontinuous plot of the stable valley [Pappas (169)]. In applying the rule, one must decide whether it applies to the fragments (A_1, A_2) before neutron emission or the fragments (A_3, A_4) after neutron emission because the relative distances from the stable valley can be rather different for these two sets of fragments (see Fig. 21). The final point about the equal-charge-displacement rule is that, unfortunately, it seems to have evolved in the literature from a rough empirical description (which should consequently be expected to hold only qualitatively and tentatively and which should ultimately be justified in terms of some physical considerations) to a real "theory." It is often referred to as the equal-charge-displacement "postulate" or even "mechanism," and "corrections" are applied to it as though it were a bonafide, although approximate, theoretical account.

As the bombarding energy is increased, more neutrons are emitted in fission, and the most probable charge-to-mass ratio of the resulting fragments (A_3, A_4) is higher. The fission fragments observed by the radiochemist are therefore found to lie closer and closer to the stable valley as the energy is increased until at high enough energies one even finds positron emitters among them. This effect is shown in Figure 30 where the distance from the stable valley (measured in units of Z) at the peaks of the measured charge distributions is given as a function of the excitation energy [Pate

(170)]. It is easy to show that if ΔN neutrons are removed from a neutron-rich nuclide, the nuclide moves $\Delta Z = (dZ/dA)\Delta N$ units closer to the stable valley where dZ/dA is measured along the valley. Using the facts that on the average $dZ/dA = 0.4$ in the region of the fission fragments and that it takes an excitation energy increase of 17 Mev (Fig. 20) to have each fragment emit another neutron, one finds that the starting slope in Figure 30 should be about $\frac{1}{40}$ charge unit per Mev. The inset shows that the data actually fall off somewhat faster than this, but perhaps the discrepancy is within the combined uncertainties of the data and the estimate. The observation that the mean chain length is 2.4 units shorter for the 480-Mev bombardment than for thermal fission implies that the mean deposition energy at 480 Mev is roughly 2.4×40 Mev, a figure which is in fair agreement with other estimates of the same quantity (64).

The observed width of the Gaussian curves which give the distribution of nuclear charges around the most probable value is roughly 0.9 unit of charge for thermal fission. The curves become somewhat wider for higher bombarding energies, as one would expect from the spread in deposition energies alone. It is easy to understand on the basis of any "equilibrium" or statistical model why the curve should be as narrow as it is. For then the probability for fission into a given pair of fragments will be proportional to a product of level densities or to $\exp [2(E_1 + E_2)/T]$ where E_1 and E_2 are the excitation energies of the fragments and T is their mean nuclear temperature (171). For the most probable charge division between the fragments for a particular mass division, $(E_1 + E_2)$ takes on its largest value. If now ΔZ protons of one of the fragments are exchanged with the same number of neutrons in the other, $(E_1 + E_2)$ decreases by $C(\Delta Z)^2$ or by $C(Z - Z_p)^2$. The coefficient C is a measure of the so-called symmetry energy which is related to the nuclear polarizability. One can very easily evaluate it with the help of Newton's tables of fission-fragment masses (91). It is about 1.6 Mev. Then, with the reasonable value $T = 1$ Mev, the charge distribution should be proportional to $\exp (-3.2[Z - Z_p]^2) \cong \exp (-[Z - Z_p]^2/2(0.4)^2)$. The implied width of the charge distribution is 0.4 units of Z or only half as wide as the observed width. A more detailed calculation with the statistical theory has been carried out by Fong who finds the same sort of discrepancy (163). In view of the complications in the way excitation energy is actually distributed between fragments (indicated by Fig. 21), it is not surprising that the width estimated on the basis of an idealized statistical model turns out to be somewhat narrower than the observed one (Fig. 29). Everything considered it would seem, however, that the charge distributions are to be understood in terms of statistical considerations connected with some sort of thermal equilibrium. It was seen that energetics probably also plays a role in determining the distribution of fragment size or mass but that its role there is not yet clear (Sect. 13).

Nuclear charge distributions have been measured with techniques other than the usual radiochemical ones. For example, the mass spectrograph has

been useful here, as it has been for the determination of mass distributions (135). Another technique involves the use of a gas-filled magnetic spectrometer [Cohen & Fulmer (172)]. This method has the virtue compared to the other measurements that it gives the width of the charge distribution for a single mass. It also sees "both sides" of the distribution, i.e., the fast decaying side as well as the side on which the chemical measurements are made. It is gratifying that the width measured by Cohen and Fulmer is consistent with that based on the other measurements. Finally, one should mention the recent measurements of prompt x-rays from fission fragments [Skliarevskii (113); Carter (173)]. With an improvement in resolution this type of study may provide a way, through coincidence measurements, of determining values of Z_p as a function of the mass division.

15. THE ANGULAR DISTRIBUTIONS OF FISSION FRAGMENTS

Anisotropies at low excitation energies.—Angular anisotropies of fission fragments with respect to an incident beam were first seen in photofission (174). It was found that, for photon energies extending a few Mev above the fission threshold, more fragments are emitted at right angles to the beam than in other directions. Recent measurements by Katz show that very close to the threshold, the anisotropy (i.e., the ratio of maximum to minimum differential cross sections as a function of angle) can become as large as 10 or 20 (27). Such large anisotropies are found only in even-even targets; the odd- A targets give isotropic distributions.

The angular distribution of fission fragments reflects the way in which the struck nuclei divide up the angular momentum which is given to them by the incident particles. That part of this angular momentum which is "converted" into the orbital angular momentum between fragments is seen in the angular distributions. The rest of the angular momentum becomes part of the individual spins of the fragments. It was clear from the early measurements that for some reason virtually all of the angular momentum which is brought into a nucleus by near-threshold photons goes into the orbital angular momentum. It was also clear from the angular distributions that one was dealing with electric dipole absorptions and that the amount of angular momentum which was introduced was only one unit and that it was directed, as one would expect, along the beam. The main problem was to understand why almost all of the angular momentum went into the orbital motion, for it could easily be shown that a more-or-less equitable distribution of the momentum between orbit and spin would have resulted in a rather isotropic angular distribution (31). The orbital motion can manage to get the lion's share of the angular momentum if there is, for some reason, a premium on the pairing of individual nucleon spins during the fission process. This idea was developed by Bohr (21) and independently by Strutinski (175). Bohr's suggestion that the motion through the saddle is slow enough so that nucleonic states are reasonably well defined has already been mentioned. The lowest states at the saddle point in an even-even nucleus are

assumed to resemble the lowest rotational band in a normal (only slightly distorted) even-even nucleus. This band is characterized by $K=0$ where K is, as usual, the projection of the total angular momentum I on the nuclear symmetry axis. As a result of a dipole absorption it is possible to excite a 1^- rotational level belonging to this band. Apparently the fissioning nucleus rotates in this state as it passes through the saddle point, and finally it snaps apart along the symmetry axis with its angular momentum still perpendicular to the symmetry axis. In this way one can see qualitatively the origin of the observed angular distribution.

At higher photon energies, other types of 1^- states can and do come into play at the saddle point. In some of these states, \vec{I} is oriented along the symmetry axis and the fact that the fissions may occur through many different types of 1^- channels tends to make the angular distributions increasingly more isotropic as the incident energy is raised. One can understand in similar terms the observation mentioned above that the angular distributions in the photofission of odd- A targets appear to be isotropic even at low energy. The assortment of different types of states begins to come in at lower energies in such nuclei than it does in even-even nuclei. Besides, the random orientation of the target spin gives rise to a corresponding randomness of the compound nuclear spin orientation which also tends to make the distributions from odd- A targets isotropic.

There have recently been a number of detailed measurements of angular distributions in the photofission of U^{238} and Th^{232} . Lazareva and her co-workers find that at a synchrotron energy of 9.4 Mev, there is an indication in the angular distribution of an electric quadrupole component about half as big as the dipole component (176). At this energy there happens to be a dip in the total fission cross section which is apparently connected with the onset, at a somewhat lower energy, of competition from neutron emission. The authors suggest that this competition works against dipole fission preferentially and that therefore the quadrupole quanta have a chance in this one energy interval to show that they are being absorbed. Lazareva's measurements were made with photographic plates but Katz, using counters, finds no evidence for any quadrupole contribution to the angular distribution (27). There have also been some other measurements (177), but the question of the possible quadrupole absorption remains unresolved. The interest in this particular problem comes as much from trying to understand the photon-absorption mechanisms in nuclei as it does from the desire to learn about the nucleonic level structure at the saddle point.

In addition to the photofission work there have been at least two other kinds of angular distribution studies near the fission threshold. Henkel & Brolley have found that in the neutron fission of thorium just above the threshold, the angular distribution of fragments shows a peaking at 90° to the beam (178). This peak quickly disappears as the energy is raised (Fig. 31). As will be seen in detail below, the distributions in particle-induced fis-

sion are normally peaked back and forth along the beam. This is what one would expect if the orbital motion between the fragments obtains a fair share of the angular momentum contributed by the projectile. But Wilets & Chase have pointed out that very close to the threshold, ideas like "fairness" (which is essentially a statistical consideration) do not apply (179). Depending on the particular properties of the available channels or saddle-point states, one can get the anisotropy to go one way or the other. In fact, unless the value of K which characterizes the lowest rotational band (chan-

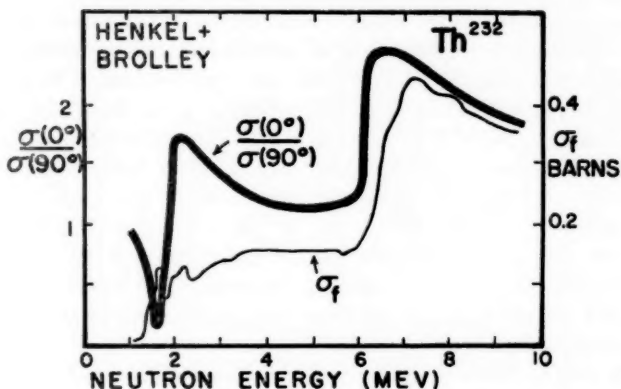


FIG. 31. The anisotropy and the fission cross section in fast-neutron fission of thorium as a function of bombarding energy (178).

nel) at the saddle point is zero or $\frac{1}{2}$, there should be a greater differential cross section at 90° than at 0° . The suppression of the 0° yield can be understood from the fact that 0° is necessarily perpendicular to the angular momentum vector when an even-even target is struck by a particle. Therefore, the nuclear symmetry axis (which presumably becomes the fragment separation axis) cannot be lined up along 0° when K , the projection of \vec{I} along it, remains finite.

One important point that one learns from the very large sizes of the fragment anisotropies which are observed near the threshold is that the nucleus apparently does not reorient its symmetry axis with respect of \vec{I} once it passes the saddle point. Arguments have already been given (Sect. 11) which indicate that the descent from the saddle is slow and that there is continual interchange of energy between different degrees of freedom. Somehow the rotation of the nucleus seems to be exempt from this interchange; otherwise we could not see as sharp angular distributions as we do. This exemption must reflect the large moment of inertia that the nucleus has by the time it reaches the saddle point (the nucleus is stretched out and is hard to turn) and it also indicates that the nucleus probably retains an

appreciable amount of axial symmetry in the descent from the saddle. (Such symmetry would keep the nucleons from exchanging angular momentum with the rotational collective modes.)

Still another kind of near-threshold angular distribution measurement was carried out with thermal neutrons and aligned nuclei [Dabbs, Roberts & Parker (180)]. Preliminary results on U^{233} indicate an isotropic distribution. This result is somewhat surprising but it may be attributable to the fact that with thermal neutrons one is already too far away ($\sim 1\frac{1}{2}$ Mev, Sect. 4) from the threshold to see an appreciable anisotropy.

In principle one can also study distributions in the threshold region by means of coincidence experiments in which inelastic scattering or other "direct interactions" are used to deposit the required energy in the nucleus. One might then rely on the angular distribution of the scattered particles in the chosen energy interval to provide some information about the amount of angular momentum which has been deposited in the nucleus (181).

Anisotropies at medium excitation energies.—In the so-called medium-energy region (i.e., up to several tens of Mev) angular distributions have been studied with protons [Cohen (182)]; with neutrons [Henkel & Brolley (178)] and [Blumberg (183)]; and with deuterons and alpha particles [Coffin & Halpern (184)]. Some of the more striking features of the observations can be summarized:

(a) The fragments come off with greatest probability forward and backward along the beam.

(b) The anisotropies observed in alpha-particle bombardments are larger than those seen in deuteron bombardments, and these in turn are larger than those seen in proton bombardments.

(c) The anisotropies are roughly as large in odd- A targets as in even-even targets (in contrast to the situation in low-energy photofission).

(d) In neutron fission the anisotropy is found to increase sharply whenever a threshold is reached where it becomes energetically possible for fission to occur in the residual nucleus which is left behind after the evaporation of some definite number of neutrons (Fig. 11).

(e) As the bombarding energy increases, the average anisotropy (taken over intervals of ~ 10 Mev) changes only slowly.

(f) The anisotropy is not the same for all fragment masses. It is largest for the most asymmetric masses (182, 185). This effect was also seen in photofission [Fairhall (186)].

(g) The anisotropy decreases as the value of Z^2/A of the target increases.

By making use of some of the ideas of Bohr and Mottleson (21) and of Strutinski (175), it has been possible to give a semiquantitative explanation of these and other observations [Halpern & Strutinski (187); Griffin (188)]. The angular distribution of fission fragments must depend on two quantities: the angular momentum \vec{I} introduced by the projectile, and the fraction of it that is turned into orbital momentum between the fragments. This frac-

tion can be characterized with the help of the parameter K , where K is now the projection of \vec{I} on the separation axis between fission fragments. For example, if one assumes that the nucleus has axial symmetry and that $K=0$, the fragments will necessarily be emitted at right angles to \vec{I} . That is, under these conditions all of \vec{I} gets used for the orbital motion of the fragments.

Although the average $|\vec{I}|$ is something controlled from the outside (by the choice of the projectile and its energy), the distribution of K in a given situation is presumably determined by the nucleus itself. It was seen earlier that the projections of \vec{I} on the symmetry axis are pretty well frozen in after the saddle point. One may therefore assume that the observed K 's (inferred from the angular distributions) are characteristic of some point in the fission process near the saddle point. One may imagine that the K of a given fission event is "picked" by the nucleus in the following way. The excitation energy is exchanged back and forth among degrees of freedom until either fission occurs or a neutron is emitted. During the period of energy exchanges, the nucleus distorts several times, almost but not quite reaching the saddle point. Each time it approaches the saddle, the nucleus does so with a value of K which is not necessarily the same as the one it had the last time. The nucleons and collective rotation have had plenty of time to exchange angular momentum and change K . In this view the values of K with which the nucleus passes through the saddle point depend essentially on the K spectrum of the states in the saddle-point region itself.

It can be shown from elementary statistical considerations or from classical arguments which should be valid at moderately high excitation energies that the most reasonable type of K spectrum is Gaussian. The classical argument, advanced by Strutinski (187), runs as follows. The distribution in K should be given by a Boltzmann factor $\exp [-E_{\text{rot}}/T]$ where

$$E_{\text{rot}} = \frac{\hbar^2}{2\mathfrak{I}_{\parallel}} K^2 + \frac{\hbar^2}{2\mathfrak{I}_{\perp}} (I^2 - K^2).$$

Here \mathfrak{I}_{\perp} and \mathfrak{I}_{\parallel} are the moments of inertia of the nucleus in the saddle-point region perpendicular and parallel to the symmetry axis. (At high enough temperatures they are presumably the "rigid-body" moments.) It is seen that the implied K distribution for a given T is Gaussian and that the average value of K^2 is

$$K_0^2 = T \frac{\mathfrak{I}_{\perp}\mathfrak{I}_{\parallel}}{\mathfrak{I}_{\perp} - \mathfrak{I}_{\parallel}} \frac{1}{\hbar^2}. \quad 6.$$

In trying to account for the above-mentioned observations concerning medium-energy distributions, it is of course most reasonable to begin by introducing as few arbitrary parameters as possible. One should see how far one can get in explaining the different kinds of observations on the basis of a single simple story. In this spirit, we overlook the probable slight dependence of \mathfrak{I}_{\perp} and \mathfrak{I}_{\parallel} on nuclear species and assume that K_0^2 is the same

function of excitation energy (measured from the saddle-point ground state) for all of the nuclear species which have been investigated. It is also assumed in accord with Equation 6 that K_0^2 does not depend on $|\vec{I}|$ (except that K must not exceed $|\vec{I}|$).

If I_0^2 is the average value of I^2 introduced in a given bombardment, then I_0^2 and K_0^2 together determine the angular distribution of the fragments. It

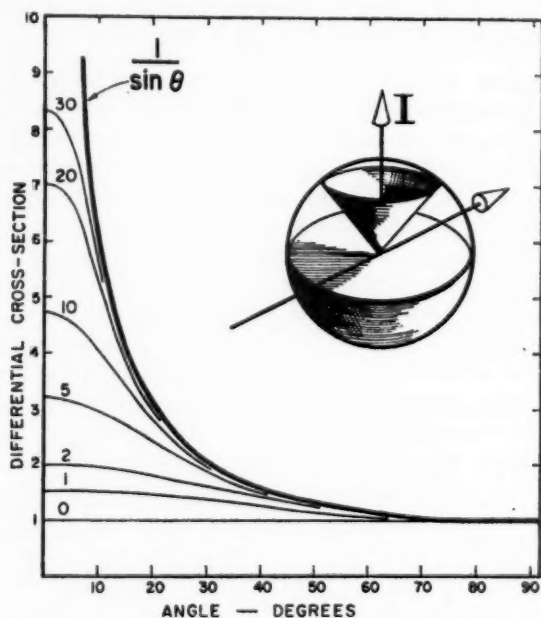


FIG. 32. Angular distributions of fission fragments. If a beam of particles is incident upon a target from left to right (see inset) it introduces into nuclei angular momenta \vec{I} which are oriented at right angles to the beam. If these nuclei undergo fission in such a way that the projection of \vec{I} on the fission direction is K , the fragments will come off in a cone whose half angle is $\cos^{-1} K/I$. To obtain the angular distribution for a given species one must average over the K and \vec{I} distributions in the problem. Typical angular distributions are shown in this figure. They are characterized by the parameter $P = \frac{1}{2}(I_0^2/K_0^2)$ where I_0^2 and K_0^2 are average values of I^2 and K^2 [Halpern & Strutinski (187)].

is only a geometry problem (187) to find the angular distribution which corresponds to given values of I_0^2 and K_0^2 . Typical computed angular distributions are shown in Figure 32. They are characterized by values of the parameter $P = \frac{1}{2}I_0^2/K_0^2$. It is seen that they are all peaked forward (and backward). The larger I_0 is with respect to K_0 , the more the distribution looks like

$1/\sin\theta$. This feature can be understood in simple classical terms. Let us take the polar axis of a nucleus (regarded as a sphere) parallel to the direction of the incident beam. The vectors \vec{I} will then lie in the equatorial plane, and if the fission takes place perpendicular to \vec{I} (as one would expect for a simple classical model) then the fragments should come off with equal probability at all polar angles in the longitude plane which is perpendicular to \vec{I} . Since all such planes are equally likely to occur, the angular distribution of fragments will be proportional to the density of intersections of uniformly spaced longitudes and latitudes on the sphere, or to $1/\sin\theta$.

We have, then, explained the observation (a). It is important to notice from Figure 32 that if one wants to measure K_0 one must be able to make observations at small angles. It is seen, for example, that the ratio of differential cross sections at 45° to 90° is very nearly the same for all large values of P , namely $\sim\sqrt{2}$.

Observation (b) is also easy to understand since the heavier projectiles bring in more I_0 for a given excitation energy (or K_0) than the lighter ones.

The third observation says that there is apparently no washing out of anisotropies by the random spin distribution of odd- A targets. It can be shown from geometrical considerations that as long as the spin of the target is small compared to both I_0 and K_0 , it should have very little effect.

The fourth observation, concerning the sudden increases of anisotropies at certain energies, is illustrated by the experimental results given in Figure 31. It is seen that at 6 Mev, where the $(n, n'f)$ reaction becomes energetically possible and where, as a result, σ_f increases suddenly, the anisotropy also increases sharply. From the trend of the anisotropy just below 6 Mev, it is clear that the fissions of the (n, f) reaction must be essentially isotropic above 6 Mev. Since the average anisotropy from the combination of (n, f) and $(n, n'f)$ reactions is rather large, that caused by the $(n, n'f)$ fissions alone must be very large indeed. This implies that $P = \frac{1}{2}I_0^2/K_0^2$ is very large for these fissions, and this in turn means that K_0^2 must be very small. This conclusion is certainly consistent with experience from the photofission experiments. From those experiments we learned that near threshold there is an extreme pairing of spins (i.e., K_0^2 tends to become zero), and in the neutron experiment under discussion we are again dealing with a variety of threshold fission.

It is also significant that the neutron evaporation does not reduce the effective value of I_0^2 excessively as a result of the random reorientations of \vec{I} which must occur as the neutrons leave. It can be shown (just as in the third point) that as long as the angular momenta which are carried off by neutrons are small compared to I_0 they hardly reduce the anisotropies.

The fifth observation reflects the fact that I_0^2 and K_0^2 both increase in rather much the same way with bombarding energy. The empirically determined energy dependence of K_0^2 is given in Figure 33.

The sixth point is very provocative. It suggests that there may be a connection between the K distribution at the saddle point and the mass distribution. It was shown, however, that this need not be the case, at least on the basis of present evidence (31, 187). The observed correlation between mass and angular distributions could arise from the fact that

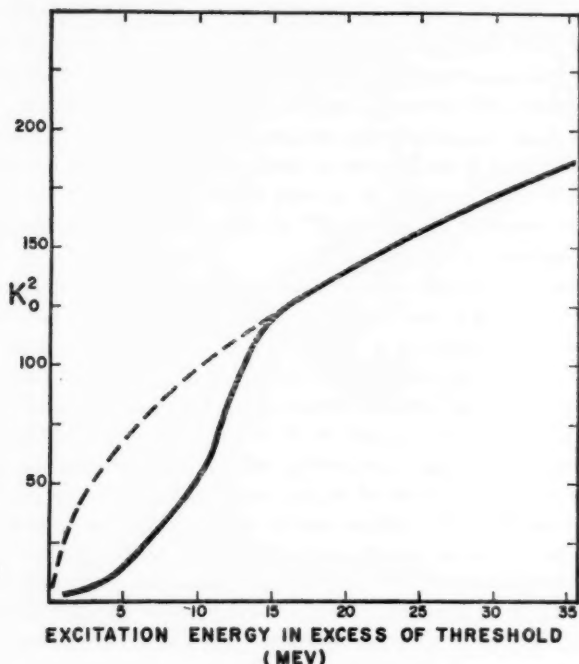


FIG. 33. K_0^2 as a function of the nuclear excitation energy measured from the fission threshold. K_0 gives the average projection of the total angular momentum upon the symmetry axis of a nucleus which is stretched to the saddle-point shape. It is one of the two parameters involved in the computation of fragment angular distributions according to Fig. 32. The curve given here was determined empirically but it fits simple theoretical estimates at the high-energy end [Halpern & Strutinski (187)].

symmetric fissions occur mostly before neutrons are evaporated, that is, when K_0^2 is still large. They therefore tend to be isotropic. The fissions which occur after the evaporation of many neutrons are very asymmetric in mass and, because of the low K_0^2 , very anisotropic. The observed correlation can therefore come about because of the complexity introduced by neutron evaporations followed by fission. In order to establish whether there really is some basic connection between mass and angular distributions, one should probably look for these correlations in a bombardment with 3-Mev neutrons.

The fact (g) that the anisotropy decreases as Z^2/A increases has also been explained to be something of an accident (187). Some data showing this effect are given in Figure 34. The curve drawn through the alpha-particle data has been computed using the foregoing formulation. The reason that Pu^{239} has a small anisotropy is, according to these calculations, simply that it is very fissionable and that most of the fissions therefore occur when K_0^2 is still large. In the lighter elements, relatively more fission occurs after neutron emission and, therefore, with lower values of K_0^2 and correspondingly larger anisotropies.

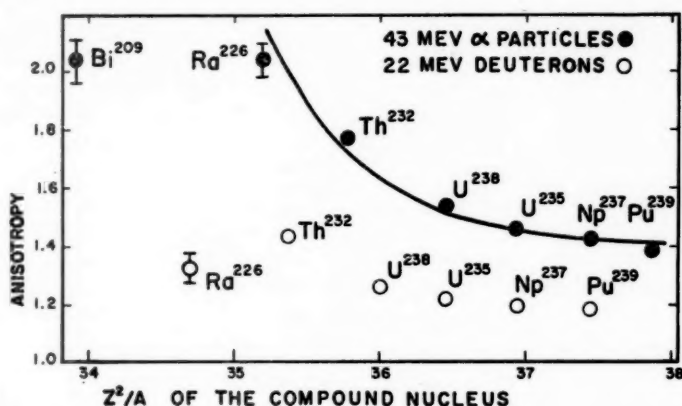


FIG. 34. The fission fragment anisotropy as a function of Z^2/A of the compound nucleus formed. The measured points are labelled according to the target nucleus. The data are those of Coffin & Halpern (184).

In this connection there is an interesting anomaly in the data. The ratio of Ra^{226} to Th^{232} anisotropies was well measured for both alpha-particle- and deuteron-induced fission, and it is larger than unity for the former and smaller for the latter. This suggests that in the deuteron fission of radium, the contribution of the highly anisotropic fissions which follow neutron evaporation is suppressed. This would be reasonable if the nuclei involved here had a fission probability which depended on excitation energy like those in Figure 12, i.e., if the fissionability became very small at low excitation energies. In the alpha-particle fission of radium, the dependence of fissionability on excitation energy is apparently more similar to that generally seen in the heavy elements, where it varies only slowly with energy. If this difference in (α, f) and (d, f) anisotropies in radium bombardments arises, as suggested, simply from the nature of the energy dependence of the fissionability, it is remarkable that this dependence changes its character so suddenly in terms of the change in nuclear species.

This explanation of the anomalously small anisotropy of the deuteron fission of radium in terms of the excitation functions is at first glance some-

what inconsistent with the observed rather large anisotropy in the fission of bismuth with alpha particles. It is clear from Figure 12 and the interpretation which has been given of those curves that the alpha-particle fission of bismuth occurs mostly in the original compound nucleus rather than in the nuclei which appear only after neutron emission. For this reason one might expect the anisotropy here to be very low. In particular, one might ask why the anisotropy in the alpha-particle fission of bismuth should be any larger than it is in plutonium. In plutonium, fission also occurs mostly in the original compound nucleus (because it is so very fissionable), and the bombarding energy is of course the same as in the bismuth fission so that I^2 is very nearly the same. The point must be that K_0^2 is much smaller in the bismuth fission. This is not too hard to understand on the basis of Equation 6. In bismuth the fission threshold is apparently very high (Sect. 8). Therefore the excitation energy relevant for the determination of K_0^2 is correspondingly small and T in Equation 6 can be very small. Moreover at low excitation energies, the moments of inertia in Equation 6 take on values smaller than the rigid-body values and for this reason, too, K_0^2 is small for bismuth. This last effect is illustrated by the empirically found departure from the linear dependence of K_0^2 on T (T goes as $E_{\text{exo}}^{1/2}$) that one can see at the lower end of Figure 33. There is also another reason that K_0^2 may be low for the lighter nuclei. The saddle-point configuration for these nuclei should be somewhat more stretched than for the heavy ones, and $\mathfrak{I}_\perp - \mathfrak{I}_\parallel$ in the denominator of Equation 6 should, therefore, be larger. Quantitative considerations show, however, that this should only be a small effect. To this extent K_0^2 is independent of the nuclear species but depends only on the excitation energy (through T and through $\mathfrak{I}_\perp \mathfrak{I}_\parallel / \mathfrak{I}_\perp - \mathfrak{I}_\parallel$) just as assumed.

One implication of the foregoing considerations is that the anisotropy in the deuteron fission of bismuth should probably be larger than that in radium. That is, the anisotropy curve for deuterons (Fig. 34) should rise again from its dip at radium as one goes to yet lighter nuclei. There should probably be a corresponding dip in anisotropy between radium and bismuth in the alpha-particle fission curve, but this one would be hard to establish because the required targets are unavailable.

Incidentally, the values of K_0^2 are generally large enough in, say, alpha-particle bombardments that only a small fraction of I appears in the angular distribution of the fragments. The rest is divided between the fragments in the form of internal spin. It is not surprising therefore that the production of high-spin isomers among the fragments increases as the bombarding energy goes up (189). It would be interesting to study the production of such isomers in small- I as well as in large- I situations, for example, in the giant resonance photofission of even-even nuclei. Here I is only unity, and if high-spin fragments are still present, one might be able to learn something about the distribution of the nucleonic angular momentum at the time of scission.

Anisotropies at high excitation energies.—There have been a number of investigations of fission angular distributions at energies near 100 Mev and higher. The new heavy-ion experiments seem to give reasonably large anisotropies, as one would expect (190). The anisotropies induced in high-energy nucleon bombardments are generally small. One curious effect has showed up. In high-energy proton bombardments the anisotropy in uranium and thorium seems to favor 90° instead of 0° and 180° [Lozhkin (191); Meadows (192); Faissner (193); Sugarman (193a)]. Strutinski (194) and Halpern (195) suggested that this may arise from the fact that relatively many encounters of a high-energy nucleon and a nucleus take the following form. The fast nucleon passes through the heavy nucleus, hitting one or two nucleons into a direction at right angles to its path. These "soft" nucleons travel through the nucleus, playing the role of a beam of particles which is "incident" at right angles to the original beam. They therefore give "inverted" anisotropies.

One final type of angular distribution experiment should be mentioned. Fairhall has compared the ratio of symmetric to asymmetric fission at 0° and 180° in a 43-Mev alpha-particle bombardment (196). If there were a difference in this ratio it could possibly indicate the existence of some "fast" or "direct" fission. Within his errors ($\sim 5\%$) Fairhall has found no effect. Similar results have recently been reported by Protopopov & Eismont in a bombardment with 14-Mev neutrons (197). This problem is also being studied by Faissner in high-energy fission induced by protons (193). He uses photographic plates and he hopes to be able to distinguish the light from the heavy fragment tracks so that he can measure their angular distributions separately.

By way of conclusion I shall make one guess and one comment. It should be clear that there still exist many unsolved fundamental problems in fission physics. The guess is that the important experimental developments in the near future are likely to come from the new coincidence techniques rather than from radiochemistry, the technique that has probably been the most useful so far. Radiochemistry sees the fragments rather late in the process, after too many things have happened, and it sees them in too integral a way. The experiments that examine correlations of different aspects of fission (like that of Fig. 21) seem to show the most promise for providing incisive information about the fission act.

The comment I would like to make has to do with an apparent exclusiveness of research in fission. It is certainly understandable that for historical and practical reasons much of fission work should be going on in the large national laboratories. But rather little work is being done outside of them. One could hope that this would change, for fission physics has itself been changing from a separate isolated branch of nuclear physics (or chemistry) to one in which there are many connections, on many levels, to other parts of nuclear physics.

The author is indebted to a number of his colleagues for stimulating

discussions of various aspects of the fission problem. These colleagues include A. W. Fairhall, J. H. Manley, B. Mottleson, W. J. Nicholson, E. P. Steinberg, V. M. Strutinski, and L. Wilets. Dr. Wilets has kindly and critically read this entire manuscript. This work was begun at CERN while the author was holding a National Science Foundation Postdoctoral Fellowship, and he would like to thank both organizations for their support. He would like to thank J. Allred for providing early copies of the papers on fission which were reported at the 1958 Geneva conference. Finally he must thank Roberta Rohde whose help in preparing the manuscript was indispensable.

LITERATURE CITED

1. Bohr, N., and Wheeler, J. A., *Phys. Rev.*, **56**, 426 (1939)
2. Hill, D. L., and Wheeler, J. A., *Phys. Rev.*, **89**, 1102 (1953)
3. Wheeler, J. A., in *Niels Bohr and the Development of Physics*, 163-84 (McGraw-Hill Book Co., Inc., New York, N. Y., 1955)
4. Wheeler, J. A., *Proc. Intern. Conf. Nuclear Reactions, Amsterdam*, 1103-14 (1956)
5. Spence, R. W., and Ford, G. P., *Ann. Rev. Nuclear Sci.*, **2**, 399 (1953)
6. Wilets, L., *Proc. Rehovoth Conf. Nuclear Structure, 1957* (North-Holland Publishing Co., 1958)
7. Whitehouse, W. J., *Progr. in Nuclear Phys.*, **2**, 120 (1952)
8. *Proc. Symposium on Phys. of Fission, CRP-642A* (Atomic Energy of Canada, Ltd., Chalk River, Ontario, 1956)
9. "Physics of Nuclear Fission," *Atomnaya Energ.*, Suppl. 1 (Bradley, J. E. S., Transl., Pergamon Press, New York, N. Y., 1958)
10. Leachman, R. B., Paper P/2467, *Proc. Intern. Conf. Peaceful Uses Atomic Energy, 2nd Conf.* (Geneva, 1958)
11. Flerov, G. N., and Petrzhak, K. A., *Phys. Rev.*, **58**, 89 (1940)
12. Seaborg, G. T., *Phys. Rev.*, **85**, 157 (1952)
13. Whitehouse, W. J., and Galbraith, W., *Nature*, **169**, 494 (1952)
14. Huizenga, J. R., and Diamond, H., *Phys. Rev.*, **107**, 1087 (1957)
15. Flerov, G. N., Kochkov, D. S., Kobkin, V. S., and Terent'ev, V. V., *Soviet Phys. "Doklady,"* **118**, 79 (1958)
16. Hyde, E. K., and Seaborg, G. T., *Encyclopedia of Phys.*, **42**, 205-308 (Springer-Verlag, Berlin, Germany, 1957)
17. Swiatecki, W. J., *Phys. Rev.*, **101**, 651 (1956)
18. Ghiorso, A., Paper P/718, *Proc. Intern. Conf. Peaceful Uses Atomic Energy* (Geneva, 1955)
19. Werner, F. G., and Wheeler, J. A., *Phys. Rev.*, **109**, 126 (1958)
20. Swiatecki, W. J., *Phys. Rev.*, **100**, 937 (1955)
- 20a. Newton, J. O., *Progr. in Nuclear Phys.*, **4**, 234 (1955)
21. Bohr, A., Paper P/911, *Proc. Intern. Conf. Peaceful Uses Atomic Energy* (Geneva, 1955)
22. Frenkel, J. A., *Zhur. Ekspl. i Teoret. Fiz*, **9**, 641 (1939)
23. Wilets, L., *Rev. Modern Phys.*, **30**, 542 (1958)
24. Swiatecki, W. J., *Phys. Rev.*, **83**, 178 (1951)
25. Maris, Th. A. J., *Phys. Rev.*, **101**, 502 (1956)

26. Present, R. D., *Phys. Rev.*, **72**, 7 (1947)
27. Katz, L., Baerg, A. P., and Brown, F., Paper P/200, *Proc. Intern. Conf. Peaceful Uses Atomic Energy, 2nd Conf.* (Geneva, 1958)
28. Ennis, M. E., reported by A. Hemmendinger, Paper P/663, *Proc. Intern. Conf. Peaceful Uses of Atomic Energy, 2nd Conf.* (Geneva, 1958)
29. Cranberg, L., and Levin, J. S., *Phys. Rev.*, **109**, 2063 (1958)
30. Lamphere, R. W., *Phys. Rev.*, **104**, 1654 (1956)
31. Winhold, E. J., and Halpern, I., *Phys. Rev.*, **103**, 990 (1956)
32. Schmitt, R. A., and Duffield, R. B., *Phys. Rev.*, **105**, 1277 (1957)
33. Baz, A. I., and Smorodinsky, Ya. A., Paper P/2472, *Proc. Intern. Conf. Peaceful Uses Atomic Energy, 2nd Conf.* (Geneva, 1958)
34. Stokes, R. H., Northrop, J. A., and Boyer, K., Paper P/2472, *Proc. Intern. Conf. Peaceful Uses Atomic Energy, 2nd Conf.* (Geneva, 1958)
35. Cameron, A. G. W., *Proc. Symposium on Phys. of Fission, CRP-642A*, 189 (Atomic Energy of Canada, Ltd., Chalk River, Ontario, 1956)
36. Hughes, D. J., and Harvey, J. A., *U. S. Atomic Energy Commission Document, BNL 325* (1955)
37. Hughes, D. J., and Schwartz, R. B., *U. S. Atomic Energy Commission Document, BNL 325* (1955); 2nd Ed. (1958)
38. Swiatecki, W. J., *Phys. Rev.*, **101**, 97 (1956)
39. Swiatecki, W. J., *Phys. Rev.*, **104**, 993 (1956)
40. Shore, F. J., and Sailor, V. L., Paper P/648, *Proc. Intern. Conf. Peaceful Uses Atomic Energy, 2nd Conf.* (Geneva, 1958)
41. Fluharty, R. G., Moore, M. S., and Evans, J. E., Paper P/645, *Proc. Intern. Conf. Peaceful Uses Atomic Energy, 2nd Conf.* (Geneva, 1958)
42. Bollinger, L. M., Cote, R. E., and Thomas, G. E., Paper P/687, *Proc. Intern. Conf. Peaceful Uses Atomic Energy, 2nd Conf.* (Geneva, 1958)
43. Vladimirovsky, V. V., Kirpichnikov, I. V., Panov, A. A., Radkevich, I. A., and Sukhoruchkin, S. I., Paper P/2221, *Proc. Intern. Conf. Peaceful Uses Atomic Energy, 2nd Conf.* (Geneva, 1958)
44. Havens, W. W., Jr., and Melkonian, E., Paper P/665, *Proc. Intern. Conf. Peaceful Uses Atomic Energy, 2nd Conf.* (Geneva, 1958)
45. Porter, C. E., and Thomas, R. G., *Phys. Rev.*, **104**, 483 (1956)
46. Wilets, L., University of Washington (To be published)
47. Bigham, C. B., Hanna, G. C., Tunncliffe, P. R., Campion, P. J., Lounsbury, M., and MacKenzie, D. R., Paper P/204, *Proc. Intern. Conf. Peaceful Uses Atomic Energy, 2nd Conf.* (Geneva, 1958)
48. Harvey, J. A., and Sanders, J. E., in *Progr. in Nuclear Energy*, **1**, 52 (1956)
49. Friesen, W. J., Leonard, B. R., Jr., Seppi, E. J., and White, F. A., *Bull. Am. Phys. Soc.* [Ser. II], **1**, 249 (1956)
50. Saplakoglu, A., Paper P/1599, *Proc. Intern. Conf. Peaceful Uses Atomic Energy, 2nd Conf.* (Geneva, 1958)
51. Hulet, E. K., Hoff, R. W., Bowman, H. R., and Michel, M. C., *Phys. Rev.*, **107**, 1294 (1957)
52. Huizenga, J. R., *Phys. Rev.*, **109**, 484 (1958)
53. Vandebosch, R., and Huizenga, J. R., Paper P/688, *Proc. Intern. Conf. Peaceful Uses Atomic Energy, 2nd Conf.* (Geneva, 1958)
54. Cameron, A. G. W., *A Revised Semi-Empirical Mass Formula, CRP 690* (Atomic Energy of Canada, Ltd., Chalk River, Ontario, 1957)

55. Vandenbosch, R., and Seaborg, G. T., *Phys. Rev.*, **110**, 507 (1958)
56. John, W., Jr., *Phys. Rev.*, **103**, 704 (1956)
57. Jackson, J. D., in *Proc. Symposium on Phys. of Fission, CRP-642A*, 125 (Atomic Energy of Canada, Ltd., Chalk River, Ontario, 1956)
58. Pik-Pichak, G. A., *Zhur. Eksptl. i Teoret. Fiz.*, **34**, 341 (1958); Transl., *Soviet Phys. JETP*, **7**, 238 (1958)
59. Flerov, G. N., in *U. S. Atomic Energy Commission Document, ORNL 2606* (1958)
60. Fujimoto, Y., and Yamaguchi, Y., *Progr. Theoret. Phys.*, **5**, 76 (1950)
61. Smith, R. K., Henkel, R. L., and Nobles, R. A., quoted by Hemmendinger, A., Paper P/663, *Proc. Intern. Conf. Peaceful Uses Atomic Energy, 2nd Conf.* (Geneva, 1958)
62. Manley, J. H., Los Alamos Sci. Lab. (Private communication)
63. Steiner, H. M., and Jungerman, J. A., *Phys. Rev.*, **101**, 807 (1956)
64. Metropolis, N., Bivins, R., Storm, M., Turkevich, A., Miller, J. M., and Friedlander, G., *Phys. Rev.*, **110**, 185 (1958)
65. Dostrovsky, I., Fraenkel, Z., and Rabinowitz, P., Paper P/1615, *Proc. Intern. Conf. Peaceful Uses Atomic Energy, 2nd Conf.* (Geneva, 1958)
66. Shamov, V. P., *Zhur. Eksptl. i Teoret. Fiz.*, **33**, 346 (1957); Transl., *Soviet Phys. JETP*, **6**, 268 (1958)
67. Harding, G. N., and Farley, F. J. M., *Proc. Phys. Soc. (London)*, **A69**, 853 (1956)
68. Skyrme, D. M., and Harding, G. N., *Nuovo cimento*, **9**, 1082 (1958)
69. Ericson, T., and Strutinski, V., *Nuclear Phys.*, **8**, 284 (1958)
70. Marquez, L., *Proc. Phys. Soc. (London)*, **A70**, 546 (1957)
71. Drake, D., Univ. of Washington (Private communication)
72. Ivanova, N. S., and P'ianov, I. I., *Zhur. Eksptl. i Teoret. Fiz.*, **31**, 416 (1956); Transl., *Soviet Phys. JETP*, **4**, 367 (1957)
73. Ostroumov, V. I., *Doklady Akad. Nauk. S.S.S.R.*, **103**, 409 (1955)
74. Bromley, D. A., in *Proc. Symposium on Phys. of Fission, CRP-642A*, 65 (Atomic Energy of Canada, Ltd., Chalk River, Ontario, 1956)
75. Perfilov, N. A., Lozhkin, O. V., and Shamov, V. P., *Zhur. Eksptl. i Teoret. Fiz.*, **28**, 655 (1955); Transl., *Soviet Phys. JETP*, **1**, 439 (1955)
76. Lozhkin, O. V., and Shamov, V. P., *Zhur. Eksptl. i Teoret. Fiz.*, **28**, 739 (1955); Transl., *Soviet Phys. JETP*, **1**, 587 (1955)
77. Perfilov, N. A., and Ivanova, N. S., *Zhur. Eksptl. i Teoret. Fiz.*, **28**, 732 (1955); Transl., *Soviet Phys. JETP*, **2**, 433 (1956)
78. Ivanova, N. S., *Zhur. Eksptl. i Teoret. Fiz.*, **31**, 693 (1956); Transl., *Soviet Phys. JETP*, **4**, 597 (1957)
79. Ivanova, N. S., Ostroumov, V. I., and Filov, R. A., Paper P/2039, *Proc. Intern. Conf. Peaceful Uses Atomic Energy, 2nd Conf.* (Geneva, 1958)
80. Bernardini, G., Reitz, R., and Segrè, E., *Phys. Rev.*, **90**, 573 (1953)
81. Minarik, E. V., and Novikov, V. A., *Zhur. Eksptl. i Teoret. Fiz.*, **32**, 241 (1957); Transl., *Soviet Phys. JETP*, **5**, 253 (1957)
82. Jungerman, J. A., and Steiner, H. M., *Phys. Rev.*, **106**, 585 (1957)
83. Fairhall, A. W., and Neuzil, E. F., Univ. of Washington (To be published)
84. Nobles, R. A., and Leachman, R. B., *Nuclear Phys.*, **5**, 211 (1958)
85. Druin, V. A., Polikanov, S. M., and Flerov, G. N., *Zhur. Eksptl. i Teoret. Fiz.*, **32**, 1289 (1957); Transl., *Soviet Phys. JETP*, **5**, 1059 (1957)
86. Kelly, E. L., and Wiegand, C., *Phys. Rev.*, **73**, 1135 (1958)

87. Gol'danskii, V. I., Pen'kina, V. S., and Tarumov, E. Z., *Zhur. Eksptl. i Teoret. Fiz.*, **29**, 778 (1955); Transl., *Soviet Phys. JETP*, **2**, 677 (1956)
88. Denisenko, G. F., Ivanova, N. S., Novikova, N. R., Perfilov, N. A., Prokoffieva, E. I., and Shamov, V. P., *Phys. Rev.*, **109**, 1779 (1958)
89. Nervik, W. E., and Seaborg, G. T., *Phys. Rev.*, **97**, 1092 (1955)
90. Jodra, L. G., and Sugarman, N., *Phys. Rev.*, **99**, 1470 (1955)
- 90a. Batzel, R., and Seaborg, G. T., *Phys. Rev.*, **82**, 607 (1951)
91. Hay, I. W., and Newton, T. D., *Atomic Energy of Canada, Ltd., CRP Rept., TPI-87* (Chalk River, Ontario, 1956)
92. Jungerman, J., and Wright, S. C., *Phys. Rev.*, **76**, 1112 (1949)
93. Smith, A. B., Fields, P. R., Friedman, A. M., Cox, S., and Sjoblom, R. K., Paper P/690, *Proc. Intern. Conf. Peaceful Uses Atomic Energy, 2nd Conf.* (Geneva, 1958)
94. Stein, W. E., *Phys. Rev.*, **108**, 94 (1957)
95. Leachman, R. B., *Phys. Rev.*, **87**, 444 (1952)
96. Leachman, R. B., and Schafer, W. D., *Can. J. Phys.*, **33**, 357 (1955)
97. Gunn, S. R., Hicks, H. G., Levy, H. B., and Stevenson, P. C., *Phys. Rev.*, **107**, 1642 (1957)
- 97a. Sugarman, N., Campos, M., and Wielgoz, K., *Phys. Rev.*, **101**, 388 (1956)
- 97b. Douthett, E. M., and Templeton, D. H., *Phys. Rev.*, **94**, 128 (1954)
98. Milton, J. C. D., and Fraser, J. S., *Phys. Rev.*, **111**, 877 (1958)
99. Cohen, B. L., Cohen, A. F., and Coley, C. D., *Phys. Rev.*, **104**, 1046 (1956)
100. Stein, W. E., and Whetstone, S. L., Jr., *Phys. Rev.*, **110**, 476 (1958)
101. Fraser, J. S., *Phys. Rev.*, **88**, 536 (1952)
102. Graves, E. R., and Rosen, L., *Phys. Rev.*, **89**, 343 (1953)
103. Hjalmar, E., Slätis, H., and Thompson, S. G., *Phys. Rev.*, **100**, 1542 (1955)
104. Smith, A. B., Fields, P. R., and Roberts, J. H., *Phys. Rev.*, **108**, 411 (1957)
105. Watt, B. E., *Phys. Rev.*, **87**, 1037 (1952)
106. Gurevich, I. I., and Mukhin, K. N., *Rept. Akad. Nauk. S.S.S.R.*, 1951 quoted in "Physics of Nuclear Fission," *Atomnaya Energ.*, Suppl. 1 (Bradley, J. E. S., Transl., Pergamon Press, New York, N. Y., 1958)
107. Cranberg, L., Frye, G., Nereson, N., and Rosen, L., *Phys. Rev.*, **103**, 662 (1956)
108. Bowman, H. R., and Thompson, S. G., Paper P/652, *Proc. Intern. Conf. Peaceful Uses Atomic Energy, 2nd Conf.* (Geneva, 1958)
109. Leachman, R. B., *Phys. Rev.*, **101**, 1005 (1956)
110. Terrell, J., *Phys. Rev.*, **108**, 783 (1957)
111. Leachman, R. B., and Kazek, C. S., Jr., *Phys. Rev.*, **105**, 1511 (1957)
112. Maienschein, F. C., Peelle, R. W., Zobel, W., and Love, T. A., Paper P/670, *Proc. Intern. Conf. Peaceful Uses Atomic Energy, 2nd Conf.* (Geneva, 1958)
113. Skliarevskii, V. V., Fomenko, D. E., and Stepanov, E. P., *Zhur. Eksptl. i Teoret. Fiz.*, **32**, 256 (1957); Transl., *Soviet Phys. JETP*, **5**, 220 (1957)
114. Groshev, L. V., Demidov, A. M., Lutsenko, V. N., and Pelekhov, V. I., Paper P/2029, *Proc. Intern. Conf. Peaceful Uses Atomic Energy, 2nd Conf.* (Geneva, 1958)
115. Voitovetskii, V. K., Levin, B. A., and Marchenko, E. V., *Zhur. Eksptl. i Teoret. Fiz.*, **32**, 263 (1957); Transl., *Soviet Phys. JETP*, **5**, 184 (1957)
116. Hoffman, M., *Bull. Am. Phys. Soc.* [II], **3**, 6 (1958)
117. Mostovaya, T. A., Paper P/2031, *Proc. Intern. Conf. Peaceful Uses Atomic Energy, 2nd Conf.* (Geneva, 1958)

118. Geilikman, B. T., Paper P/2473, *Proc. Intern. Conf. Peaceful Uses Atomic Energy, 2nd Conf.* (Geneva, 1958)
119. Bondarenko, I. I., Kuzminov, B. D., Kutsayeva, L. S., Prokhorova, L. I., and Smirenkin, G. N., Paper P/2187, *Proc. Intern. Conf. Peaceful Uses Atomic Energy, 2nd Conf.* (Geneva, 1958)
120. Whetstone, S. L., quoted in Leachman, R. B., Paper P/2467, *Proc. Intern. Conf. Peaceful Uses Atomic Energy, 2nd Conf.* (Geneva, 1958)
121. Fraser, J. S., and Milton, J. C. D., *Phys. Rev.*, **93**, 818 (1954)
122. Vladimirkii, V. V., *Zhur. Ekspl. i Teoret. Fiz.* **32**, 822 (1957); Transl., *Soviet Phys. JETP*, **5**, 673 (1957)
123. Whetstone, S. L., Los Alamos Sci. Lab. (Private communication)
124. Katcoff, S., *Nucleonics*, **16**, 78 (April 1958)
125. Strominger, D., Hollander, J. M., and Seaborg, G. T., *Rev. Modern. Phys.*, **30**, 585 (1958)
126. Keepin, G. R., *Progr. in Nuclear Energy*, **1**, 191 (1956)
127. Keepin, G. R., *J. Nuclear Energy*, **7**, 13 (1958)
128. Perfilov, N. A., in "Physics of Nuclear Fission," *Atomnaya Energ.*, Suppl. 1 (Bradley, J. E. S., Transl., Pergamon Press, New York, N. Y., 1958)
129. Fulmer, C. B., and Cohen, B. L., *Phys. Rev.*, **108**, 370 (1957)
130. Erdős, P., *The Emission of Alpha Particles from Nuclei Excited by Gamma Rays*, (Doctoral thesis, Eidgenössische Technische Hochschule, Zurich, Switzerland, 1957)
131. Nobles, R. A., Los Alamos Sci. Lab. (Private communication)
132. Nicholson, W. J., Univ. of Washington (Private communication)
133. Flynn, K. F., Glendenin, L. E., and Steinberg, E. P., *Phys. Rev.*, **101**, 1492 (1956)
134. Steinberg, E. P., and Glendenin, L. E., Paper P/614, *Proc. Intern. Conf. Peaceful Uses Atomic Energy* (Geneva, 1955)
135. Fritze, K., McMullen, C. C., and Thode, H. G., Paper P/187, *Proc. Intern. Conf. Peaceful Uses of Atomic Energy, 2nd Conf.* (Geneva, 1958)
136. Glendenin, L. E., *Phys. Rev.*, **75**, 337 (1959)
137. Glendenin, L. E., Steinberg, E. P., Ingrham, M. G., and Hess, D. C., *Phys. Rev.*, **84**, 860 (1951)
138. Wahl, A. C., *Phys. Rev.*, **99**, 730 (1955)
139. Swiatecki, W. J., *Phys. Rev.*, **100**, 936 (1955)
140. Jensen, R. C., and Fairhall, A. W., *Phys. Rev.*, **109**, 942 (1958)
141. Sugihara, T. T., *Ann. Progr. Rept.*, NYO 7759 (Clark Univ., Mass, 1959)
142. Fairhall, A. W., *Phys. Rev.*, **102**, 1335 (1956)
143. Steinberg, E. P., and Glendenin, L. E., *Phys. Rev.*, **95**, 431 (1954)
144. Stevenson, P. C., Hicks, H. G., Nervik, W. E., and Nethaway, D. R., *Phys. Rev.*, **111**, 886 (1958)
145. Goeckerman, R. H., and Perlman, I., *Phys. Rev.*, **76**, 728 (1949)
146. Jensen, R. C., and Fairhall, A. W., *Bull. Am. Phys. Soc.* [II], **2**, 378 (1957)
147. Los Alamos Radiochemistry Group quoted by Hemmendinger, A., Paper P/663, *Proc. Intern. Conf. Peaceful Uses Atomic Energy, 2nd Conf.* (Geneva, 1958)
148. Glass, R. A., Carr, R. J., Cobble, J. W., and Seaborg, G. T., *Phys. Rev.*, **104**, 434 (1956)
149. Bowles, B. J., Brown, F., and Butler, J. P., *Phys. Rev.*, **107**, 751 (1957)
150. Butler, J. P., Bowles, B. J., and Brown, F., Paper P/6, *Proc. Intern. Conf. Peaceful Uses Atomic Energy, 2nd Conf.* (Geneva, 1958)

151. Jones, W. H., Timnick, A., Paehler, J. H., and Handley, T. H., *Phys. Rev.*, **99**, 184 (1955)
152. Regier, R. B., Burgus, W. H., Smith, J. R., and Moore, M. S., *Bull. Am. Phys. Soc.* [II], **3**, 6 (1958)
153. Roeland, L. W., Bollinger, L. M., and Thomas, G. E., Paper P/551, *Proc. Intern. Conf. Peaceful Uses of Atomic Energy, 2nd Conf.* (Geneva, 1958)
154. Los Alamos Radiochemistry Group, *Phys. Rev.*, **107**, 325 (1957)
155. Nasuhoglu, R., Raboy, S., Ringo, G. R., Glendenin, L. E., and Steinberg, E. P., *Phys. Rev.*, **108**, 1522 (1957)
156. Fox, J. D., Zimmerman, R. L., Hughes, D. J., Palevsky, H., Brussel, M. K., and Chrien, R. E., *Phys. Rev.*, **110**, 1472 (1958)
157. Nossorff, V. G., Paper P/653, *Proc. Intern. Conf. Peaceful Uses Atomic Energy* (Geneva, 1955)
158. Businaro, U. L., and Gallone, S., *Nuovo cimento*, **1**, 629 (1955)
159. Swiatecki, W. J., Paper P/651, *Proc. Intern. Conf. Peaceful Uses Atomic Energy, 2nd Conf.* (Geneva, 1958)
- 159a. Hill, D. L., Paper P/660, *Proc. Intern. Conf. Peaceful Uses Atomic Energy, 2nd Conf.* (Geneva, 1958)
160. Inglis, D. R., *Ann. Phys.*, **5**, 106 (1958)
161. Hill, R. D., *Phys. Rev.*, **98**, 1272 (1955)
162. Curie, D., *Compt. rend.*, **235**, 1286 (1952)
163. Fong, P., *Phys. Rev.*, **102**, 434 (1956)
164. Perring, J. K., and Story, J. S., *Phys. Rev.*, **98**, 1525 (1955)
165. Newton, T. D., in *Proc. Symposium on Phys. of Fission, CRP-642A* (Atomic Energy of Canada, Ltd., Chalk River, Ontario, 1956)
166. Cameron, A. G. W., Paper P/198, *Proc. Intern. Conf. Peaceful Uses Atomic Energy, 2nd Conf.* (Geneva, 1958)
167. Geilikman, B. T. (Private communication from V. M. Strutinski, Atomic Energy Lab., Moscow, Russia)
168. Glendenin, L. E., Coryell, C. D., and Edwards, R. R., Paper 52 in *Natl. Nuclear Energy Series, Div. IV*, **9** (1951)
169. Pappas, A. C., Paper P/881, *Proc. Intern. Conf. Peaceful Uses Atomic Energy* (Geneva, 1955)
170. Pate, B. D., Foster, J. S., and Yaffe, L., *Can. J. Chem.*, **36**, 1691 (1958)
171. Blatt, J. M., and Weisskopf, V. F., *Theoretical Nuclear Physics*, 371 (John Wiley & Sons, Inc., New York, N. Y., 1952)
172. Cohen, B. L., and Fulmer, C. B., *Nuclear Phys.*, **6**, 547 (1958)
173. Carter, R. E., Wagner, J. J., and Wyman, M. E., quoted in Paper P/665, *Proc. Intern. Conf. Peaceful Uses Atomic Energy, 2nd Conf.* (Geneva, 1958)
174. Winhold, E. J., Demos, P. T., and Halpern, I., *Phys. Rev.*, **87**, 1139 (1952)
175. Strutinski, V. M., *Zhur. Ekspl. i Teoret. Fiz.*, **30**, 606 (1956); Transl., *Soviet Phys. JETP* **3**, 638 (1956)
176. Baz, A. I., Kulikova, N. M., Lazareva, L. E., Nikitina, N. V., and Semenov, V. A., Paper P/2037, *Proc. Intern. Conf. Peaceful Uses Atomic Energy, 2nd Conf.* (Geneva, 1958)
177. Faissner, H., and Gönnewein, F., *Z. Physik*, **153**, 257 (1958)
178. Henkel, R. L., and Brolley, J. E., Jr., *Phys. Rev.*, **103**, 1292 (1956)
179. Wilets, L., and Chase, D. M., *Phys. Rev.*, **103**, 1296 (1956)

180. Dabbs, J. W. T., Roberts, L. D., and Parker, G. W., *Bull. Am. Phys. Soc.* [II], **3**, 6 (1958)
181. Bodansky, D., Halpern, I., Manley, J. H., and Nicholson, W. J., *Ann. Prog. Rept., Univ. of Washington Cyclotron*, 35 (1957)
182. Cohen, B. L., Ferrell-Bryan, B. L., Coombe, D. J., and Hullings, M. K., *Phys. Rev.*, **98**, 685 (1955)
183. Blumberg, L., Los Alamos Sci. Lab. (Private communication from J. H. Manley)
184. Coffin, C. T., and Halpern, I., *Phys. Rev.*, **112**, 536 (1958)
185. Hickenlooper, M. P., and Fairhall, A. W., *Ann. Progr. Rept., Univ. of Washington Cyclotron*, 27 (1957)
186. Fairhall, A. W., Halpern, I., and Winhold, E. J., *Phys. Rev.*, **94**, 733 (1954)
187. Halpern, I., and Strutinski, V. M., Paper P/1513, *Proc. Intern. Conf. Peaceful Uses Atomic Energy, 2nd Conf.* (Geneva, 1958)
188. Griffin, J. J., *Bull. Am. Phys. Soc.* [II], **3**, 337 (1958); (Private communication)
189. Hicks, H. G., and Gilbert, R. S., *Phys. Rev.*, **100**, 1286 (1955)
190. Alexander, J., Lawrence Radiation Lab., Berkeley, Calif. (Private communication)
191. Lozhkin, O. V., Perfilov, N. A., and Shamov, V. P., *Zhur. Eksptl. i Teoret. Fiz.*, **29**, 292 (1955); Transl., *Soviet Phys. JETP*, **2**, 116 (1956)
192. Meadows, J. W., *Phys. Rev.*, **110**, 1109 (1958)
193. Faissner, H., and Schneider, H., *Physik Verhandl.*, **10**, 1959
- 193a. Sugarman, N., Univ. of Chicago (Private communication)
194. Strutinski, V. M., Atomic Energy Lab., Moscow, Russia (Private discussions)
195. Halpern, I., *Nuclear Phys.*, **11**, 522 (1959)
196. Fairhall, A. W., Univ. of Washington (Private communication)
197. Protopopov, A. N., and Eismont, V. P., *Soviet J. Atomic Energy*, **4**, 194 (1958)

ADVANCES IN ELECTRONICS ASSOCIATED WITH NUCLEAR RESEARCH¹

BY H. W. KENDALL

Department of Physics, Stanford University, Stanford, California

1. INTRODUCTION

The scope of the present article has been restricted to discussions of four areas of advance in nuclear electronic instrumentation: (a) semiconductor electronics, (b) photomultipliers, (c) fast time measurements, (d) instrumentation for complex experiments. The widespread use of semiconductors in computer construction has not yet been repeated in the field of nuclear instrumentation, although for many problems they are far more satisfactory than vacuum tubes. Section 2 includes a brief summary of the important properties of transistors and fast semiconductor diodes with references to explicit circuit designs which would be useful for several phases of nuclear and high-energy research. Section 3 summarizes the properties of photomultiplier tubes, particularly as they affect short time resolution, while Section 4 discusses recent advances in the techniques of the measurement of times shorter than 10 nsec.² Section 5 outlines some of the applications of computer-type techniques to the storage and analysis of information from complex experimental equipment.

2. SEMICONDUCTOR DEVICES

Although semiconductor diodes have been in widespread use in nuclear instrumentation for a number of years, transistors are used at present only rarely. Their application to computers was recognized soon after their development and in the past few years high-speed logical elements have been designed whose small size, modest power requirements, and reliability exceed the performance expected from the finest vacuum-tube designs. The increasing complexity of the instrumentation associated with large particle accelerator experiments, and their great operating cost, put the reliability of equipment at a great premium. Fortunately the computer designers have solved successfully a number of problems similar to those encountered in nuclear instrumentation, and there is a large body of design information that can easily be adapted to nuclear problems.

It seems likely that within a few years the major portion of nuclear instrumentation will be almost entirely transistorized: with this in mind, this section will be devoted to a discussion of the properties of transistors that are important in the design and construction of many of the familiar types

¹ The survey of literature pertaining to this review was concluded in March, 1959.

² We use the abbreviation nsec. (nanosecond = 10^{-9} second).

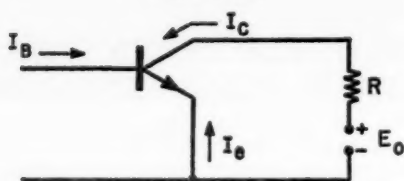


FIG. 1. $n-p-n$ transistor in the common-emitter configuration.

of nuclear counting equipment. Data on some of the newer high-speed semiconductor diodes are included.

Properties of transistors.—A number of books treat transistor theory and advanced circuit design in detail (1 to 5). Hunter (2) gives many references to papers published to 1956.

The important low-frequency properties of a transistor can be examined using the common-emitter configuration as an example (Fig. 1). We use the notation of Millman & Taub (5). Positive currents flow into the transistor elements. The ratio of the change in collector current to change in emitter current for constant base-collector voltage is called α :

$$\alpha = [\Delta I_c / \Delta I_e]_{V_{cb} \text{ const.}}$$

With this definition the base current can be written

$$I_b = - (I_c + I_e)$$

which, in terms of α becomes

$$I_b = -I_{co} - (1 - \alpha)I_e$$

where the constant current I_{co} is called the "reverse saturation collector current," or, frequently, the "collector-base saturation current." Clearly I_{co} is the current which flows into the base circuit when the emitter current is zero. It has its origin in thermally-produced electron-hole pairs in the back-biased base-collector junction. It is nearly independent of the base-collector potential and has an exponential temperature dependence. The current I_{co} changes approximately 10 per cent for a 1°C . rise in temperature. To first approximation the α of the transistor is independent of temperature, but a change in I_{co} shifts the operating point of the circuit and, depending on the external impedance in the base circuit, can cause a change in the base-emitter bias which will be amplified by the dc gain of the configuration. If the consequent rise in collector current and dissipation is sufficiently large, the heat generated at the collector may be enough to increase I_{co} and to initiate a regenerative effect giving rise to "thermal runaway." The thermal time constant of the collector of even the largest transistors is of the order of milliseconds (for a high-frequency transistor it may be a fraction of a microsecond), so that thermal runaway usually destroys the transistor.

The base current can be expressed in terms of the collector current:

$$I_b = -\frac{I_{co}}{\alpha} + \frac{1 - \alpha}{\alpha} I_e = -\frac{I_{co}}{\alpha} + \left(\frac{1}{\beta}\right) I_e$$

where β is the current gain in the common emitter configuration, and the emitter base voltage is small compared with the collector-base voltage. As α is usually in the range 0.94–0.99, the current gain β can be as large as 100 and sometimes more.

When the base current is zero there remains a collector current $I_c = +I_{co}/(1-\alpha)$ which may be relatively large for transistors with α near unity. If an external source supplies a current $-I_{co}/\alpha$ to the base, the collector current will be zero and the transistor is "cutoff." Increasing the base current from this back-biased condition will bring the transistor into the "active region," in which the collector current is substantially independent of the base-collector voltage and depends only on the base current. When the collector current is sufficiently high so most of the voltage E_0 appears across the load R , the transistor is in saturation. The collector-emitter voltage V_{ce} can be very low for a transistor in saturation, e.g., for a saturated 2N501, $V_{ce} < 0.05$ volt. This voltage is sufficiently low that a second transistor in the configuration of Figure 1, driven from the collector, will be substantially cutoff, a property extremely useful in transistor switching circuits. The region of saturation is loosely described as a three-way short circuit between the three transistor elements, although the base current is substantially less than the collector or emitter currents. In both cutoff and saturation, the transistor dissipates very little power, one of the attractive features of its use as a switch.

Maximum ratings are established for both voltages and currents in normal transistor operation. Unlike vacuum tubes, transistors do not tolerate large transient overloads, and circuits must be designed with care so that maximum transistor ratings are not exceeded. The collector-emitter voltage is limited by avalanche breakdown, Zener breakdown, or punch-through [Hunter (2, pp. 4-2, 10-3)]. For low-frequency transistors, V_{ce} is usually limited by one of the first two. High-frequency transistors, of the surface-barrier type, with thin base regions, are limited by punch-through, in which electrical narrowing of the base region allows the collector to "touch" the emitter. Drift transistors may be limited by avalanche breakdown. Typical maxima for V_{ce} are in the range 20 to 40 volts; special transistors may be rated to 100 volts or higher. Inverse bias on the base-emitter junction can cause breakdown, and it is frequently necessary to diode-clamp the junction to prevent excess back bias.

Maximum ratings of both peak and average collector dissipation should be observed. The thermal time constant of the collector of a transistor switch may be so short that switching transients can cause thermal damage to the junctions. Switching a large current into a resistive or capacitive load can couple energy capacitively to the base; this energy is amplified, increasing the power dissipated at the collector. Switching inductive loads may give rise to transient over-voltages which can exceed $[V_{ce}]_{max}$ (6).

The mean life of a transistor operated conservatively can be extremely long: 10^4 to 10^5 hr. can be expected from most modern transistors. Certain

types, such as the surface-barrier high-frequency transistors, are very sensitive to high ambient temperature. Under these conditions the thin base region diffuses into the neighboring material and disappears. This can occur even during storage at above-normal temperature. Diffused-base transistors are not as subject to this type of ageing and are the transistor of choice for long-period reliability in high-speed circuits.

Conservative circuit design includes care both in the cooling of transistors by appropriate heat sinks or positioning, and dc biasing for stability

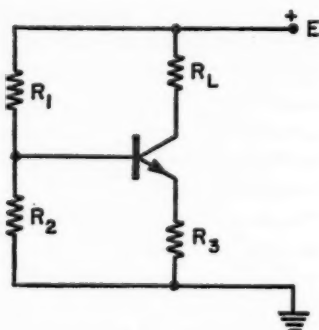


FIG. 2. *n-p-n* transistor, dc biasing circuit.

against thermal runaway. A stability factor S can be defined [DeWitt & Rossoff (3, p. 147 ff.)] where

$$S = dI_c/dI_{co}.$$

For the common biasing circuit used in many ac amplifiers (Fig. 2), it is easily shown that

$$S \cong \frac{1 + (R_3/R_B)}{(1 + \alpha) + (R_3/R_B)}, \quad \text{where } R_B = \frac{R_1 R_2}{R_1 + R_2}.$$

Maximum stability occurs for values of S near unity. As the emitter bias resistor is decreased relative to R_B , S approaches $(1 - \alpha)^{-1}$ which corresponds to full amplification of I_{co} by the common-emitter transistor configuration. The criterion above is conservative; DeWitt & Rossoff (3) give a more complete analysis. Schenkerman (7) has published nomographs from which S may be estimated for a range of circuit and cooling configurations.

The uniformity of the structure of a transistor is closely connected with its performance, and nuclear radiations can be expected to alter the structure and thus affect the performance. In many circumstances it is necessary to operate transistorized equipment in a region of high nuclear radiation flux, and studies have been made (8) to determine the effect of radiation on transistor properties. Two principal effects occur for γ -ray and neutron irradiation: (a) a decrease of the minority carrier lifetime, and (b) the conversion of p -type to n -type semiconductor. Effect (a) results in a permanent decrease in

the common-emitter current gain β , and effect (b) tends to reduce the punch-through voltage. Both effects may be accompanied by an increase in I_{co} .

The high-frequency thin base transistors appear to be the most resistant to radiation: a number of 2N501 transistors tested by neutron irradiation showed approximately a 20 per cent decrease in β after irradiation with $\sim 10^{13}$ neutrons/cm.², with lower-frequency transistors showing the same effect after irradiation with $\sim 10^{12}$ neutrons/cm.² Different radiations could be expected to cause widely varying degradation of transistor performance, but not much information on this subject is available.

When a transistor is used as an amplifier or switch for pulses with high-frequency components, the transistor can no longer be treated as a device with a constant α and instantaneous transmission. Discussions of transistor equivalent circuits at high frequency (2, 3) are complicated by the fact that the complex representation of the transistor elements depends not only on the frequency but also on the dc operating point, which is in turn dependent on circuit configuration, collector temperature, and transistor power dissipation. For medium or large signals the small-signal equivalent circuits are useful only for orientation; the more exact equations become too nonlinear to be practical for design purposes. The frequency dependence of α in the small-signal approximation can be written

$$\alpha = \frac{\alpha_0}{1 + (\omega/\omega_\alpha)}$$

where α_0 is the dc value of α , and $f_\alpha = \omega_\alpha/2\pi$ is the " α -cutoff frequency." The quantity f_α , the α -cutoff frequency in the common-emitter configuration, is frequently used as a criterion for the high-frequency performance of a transistor. The collector current response (5, p. 587) to an input signal at the base depends not only on the quantity f_α of the equivalent collector current generator but also on time constants of the type $(r_b + R)C_c$, where r_b is an equivalent base resistor, R is the load resistance, and C_c is the collector capacitance which results from the presence of charge carriers in the base. The number of charge carriers in the base is in turn determined by the emitter current which may depend on the dc operating point. It is clear that an iterative procedure would be required to solve a frequency-dependent circuit configuration, and these do not always converge with a reasonable speed. This example neglects other frequency-dependent parameters and is intended only to illustrate the complexities of high-frequency analysis.

There are a number of types of transistors available. Three classes of high-frequency transistors are (a) surface-barrier, (b) diffused-base, and (c) drift transistors. Type (a) is constructed by electrolytic etching of the base to form a thin base region. These are becoming obsolete because of their high rate of thermal deterioration and the low maximum value of V_{ce} consequent on the thin base region. The two remaining types are not very different. Diffused-base transistors have moderately high values of f_α but do not have the high-frequency characteristics of the drift transistors. The drift

transistors have a built-in accelerating field in the base region which augments the usual diffusion process in transferring charge to the collector. Their high-frequency properties are complicated by changes in this field, and f_{α} is not as satisfactory a high-frequency parameter as for (a) and (b). The active elements of some drift transistors made by photoetching processes have the shape of a small truncated cone; these have become known as MESA-type transistors.

The maximum frequency of oscillation f_{\max} is frequently specified for drift transistors; this represents the highest frequency for which the unit will deliver usable power and is a measure of the gain-bandwidth product for the transistor. At this frequency it has unit power gain.

The frequency at which the transistor delivers half its dc power gain is frequently called the " β -cutoff frequency." Above this frequency the power gain decreases at 6 db per octave, reaching unity at approximately f_{α} . The maximum frequency of oscillation f_{\max} is usually much higher than f_{α} . The construction of a high-frequency transistor determines the exact relation between these quantities and the form of the corrections to the simple frequency dependence of α stated above.

The output impedance of a transistor as an emitter follower is extremely low, is independent of the type of transistor to first approximation, and varies inversely with the collector current (9). Similar to the cathode follower, the output impedance is $1/g_m$ in parallel with the emitter resistor, where g_m is the effective transconductance, defined as in vacuum tube practice. The transconductance is given approximately by

$$g_m \cong 21 \times I_c \text{ (ma/v.)}$$

where I_c is the collector current. One- to 2-ma collector current is sufficient to establish an emitter follower output impedance of a few ohms.

The input impedance of an emitter follower depends on the value of the emitter load. If the load R is large compared to $1/g_m$, the input impedance is

$$Z_{in} \cong \beta^2 R.$$

Transistor electronics for nuclear detectors.—The small size of transistors and the high speed of the newer units make them well adapted to circuits which amplify and select pulses from nuclear radiation counters. Their low input resistance is a disadvantage if they are used as amplifier input stages driven by photomultipliers, as there is no integration of the photomultiplier anode current pulse, and the output signal may be inconveniently short. Feedback circuits having a high input resistance have been designed which will integrate a photomultiplier anode current pulse. The decay constant of the integrated pulse is determined by passive elements. Three circuits of this type have been discussed by Anzalone (10), Graveson & Sadowski (11), and by Chase (12). These circuits have rise times which are long compared with the rise time of the photomultiplier anode current pulse or have near-unity gain which depends on the load impedance imposed on the preamplifier. An

integrating preamplifier with a fast rise capability coupled with a gain-of-four amplifier with a 3-ohm output impedance has been designed at Stanford (13) (Fig. 3). Using Philco 2N501 transistors, miniature resistors, and condensers, it can be constructed using printed-circuit techniques on a chassis $\frac{3}{4}$ -in. wide by 2 in. long and is suitable for use with large counter arrays from which the time of arrival of events must be preserved to less than 10 nsec. With an integration time of $1.5 \mu\text{sec.}$ and an over-all bandwidth greater than 50 mc./sec., it generates a pulse which can be conveniently amplified by conventional "slow" linear amplifiers for pulse-height analysis, or delay-line

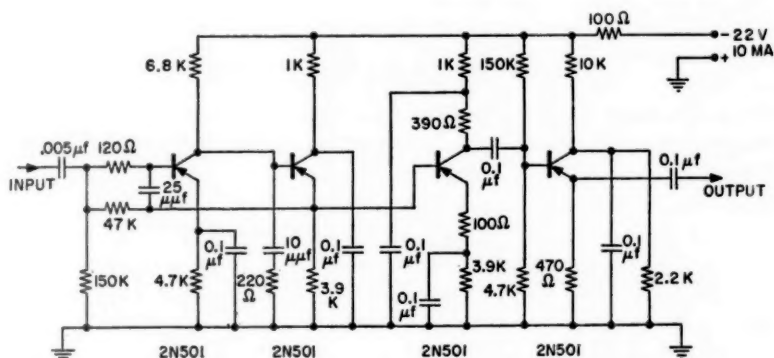
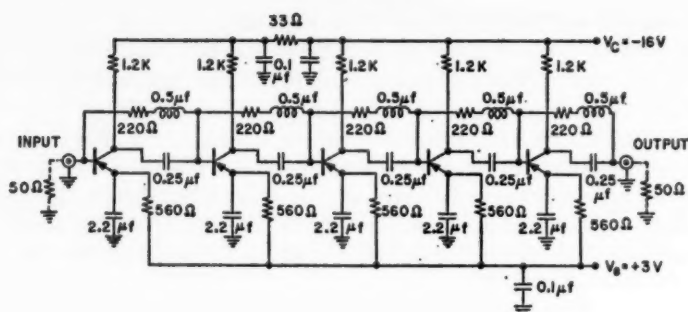


FIG. 3. Photomultiplier integrator-preamplifier. See text for discussion of circuit.

clipped for fast coincidence measurements. Increased gain can easily be realized with this unit at the expense of the rise time of the output pulse. This preamplifier has a maximum output pulse of approximately one volt with good overload characteristics, determined by the cutoff level of the third transistor from the left in Fig. 3. The 2N501 transistor is frequently used in this and similar circuits. It has an α -cutoff frequency greater than 150 mc./sec., is relatively low in cost; with a saturation collector voltage less than 0.05 volt, it is well adapted to direct-coupled high-speed computer logic. A summary of the electrical properties of the 2N501 has been published by the manufacturers (14), who also include a number of typical and useful switching and binary circuits.

To construct linear amplifiers (15) with bandwidths significantly greater than 80 mc./sec., it is necessary to use transistors whose α -cutoff frequency is greater than ~ 300 mc./sec. All those available at present have been listed by Tulchin (16); all are $p-n-p$ germanium transistors. The low power ratings of the fast transistors limit the output pulse amplitude which is available. This maximum pulse is usually about one volt at a 100-ohm impedance level, which is unsatisfactory for many applications.

A transistor amplifier has been designed by de Broekert & Scarlett (17) using five WE M2039 transistors in cascade (see Fig. 4). With a voltage gain



WIDEBAND TRANSISTOR AMPLIFIER

FIG. 4. Wideband transistor amplifier (17). The author appreciates permission by R. Scarlett to reproduce this circuit. The properties of this amplifier are discussed in the text.

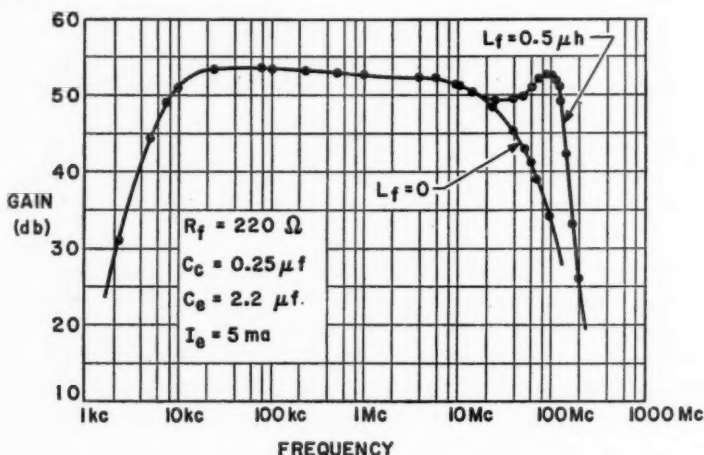


FIG. 5. Frequency response of the wideband transistor amplifier (17) shown in Fig. 4.

of 350 from 8 to 120 mc./sec. (Fig. 5), it has a maximum output pulse height of one volt. Peaking for optimum transient response would reduce the bandwidth. Exceeding vacuum-tube distributed line amplifiers in gain but lacking their large pulse capabilities, amplifiers such as this should be useful in amplifying the small pulses from ultra-fast coincidence circuits before presentation to the diode discriminators which are frequently used to reject single events. The phase shift of signals amplified by a drift transistor is appreciable and causes instability if feedback loops are established around two or more transistors of an ultra-wide-band transistor amplifier. The voltage gain of a single stage is sufficient so that it is practical to use negative feedback around

each transistor. A degree of stabilization is thus available in a transistor amplifier at frequencies for which a vacuum-tube amplifier would have to be operated with no feedback.

Transistor discriminators have not yet reached speeds comparable to those of the fast amplifiers. The circuit configurations are similar to usual vacuum-tube practice (5) with transistorized equivalents of the Schmidt circuit or one-shot multivibrators (2, 3). A number of circuits have been published (12, 18, 19, 20).

Conventional multivibrator circuits in the quiescent state customarily have one transistor biased to cutoff, and a second in saturation. During a cycle of operation the transistors must be switched either into or out of saturation from their quiescent operating point. The amount of charge stored in the base region of a saturated transistor is appreciable, and delays are always introduced in trigger circuits or flip-flops by the necessity of establishing or eliminating this saturation charge. Frequently the collector of a transistor can be clamped to prevent saturation, either with semiconductor diodes or by using transistors, with a resulting increase in the speed and complexity of the circuit. Analyses of the regeneration process in junction transistor multivibrators have been published by Pederson (21), who treats the inertia effects of transistor saturation during turn-on and turn-off cycles. Suran (22) gives designs for three clamped multivibrators with pulse widths of about 1 μ sec. and rise times longer than 20 nsec. The newer fast transistors should allow much improvement in multivibrator performance.

A number of binary scalers have been constructed which will operate with sine-wave input at over 50 mc./sec., but these have not yet been adapted to scaling of random pulses arriving at mean rates comparable to 5×10^7 pulses/sec. The nuclear scaling equipment described by Chase (12) contains a simple 10 mc./sec. binary scaler using surface-barrier transistors in the Higinbotham-coupled configuration. With more control of the saturation characteristics, circuits of this kind will operate well for pulse pairs separated by less than 60 nsec. Baldinger (23) has constructed a transistorized scale of two which will operate at 20 mc./sec. Transistor coupling to the emitters of a two-transistor binary serves to control saturation effects.

Fast coincidence circuits of great simplicity can be constructed using fast transistors. Although over-all resolving times below 5 nsec. are not feasible at present, the reliability and compactness of a semiconductor coincidence-trigger circuit, as with the preamplifiers, makes large counter arrays and n -tuple coincidences far more feasible for resolving times of 10 nsec. and longer than with vacuum-tube circuitry.

The simple coincidence circuit (24) in Figure 6 is basically a transistorized Rossi circuit. The transistors are operated nearly saturated and are driven off by positive input pulses. A circuit of this type operates with a shorter resolving time if the input pulses have a negative undershoot to re-establish the base saturation charge density. With 2N501 transistors care should be taken not to exceed the inverse base-emitter rating of 2 v.

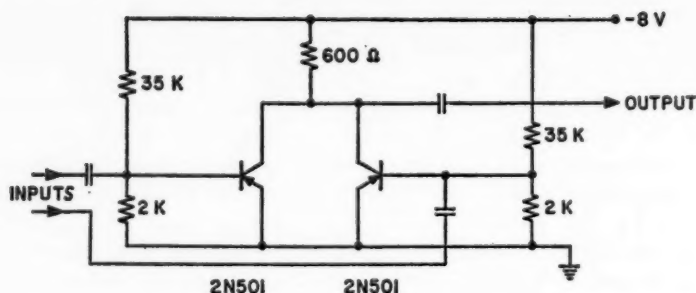


FIG. 6. Transistorized coincidence circuit (24). The two transistors are connected in the Rossi configuration.

More complex circuits using coincidence-operated trigger generators have been discussed by Fitch (25) and Miller (26). Both have resolving times of about 10 nsec. The trigger circuits operate on pulses of less than 1 v. amplitude. The Fitch trigger circuit generates a 2 v. pulse with a width of 35 nsec.

Fast semiconductor diodes.—In the past year a number of very fast diodes have become available whose minority carrier density during conduction is so low that their back resistance is re-established very quickly when suddenly back-biased from the conducting state. This property makes them particularly suitable for discrimination of fast pulses. Among the fastest of these is the Qutronics Q6-100, which "clears" in less than 1 nsec. It has excellent dc characteristics. The properties of a few of the faster diodes (27) are shown in Table I.

TABLE I
FAST SEMICONDUCTOR DIODES*

Diode	R_{forward}		V_{reverse} at 100 μ a	I_{reverse} at 10 v.	Recovery† 250 Ω cct.
	1 ma	11 ma			
IN34A	40 Ω	90 Ω		10 μ a	2–3 nsec.
1N116	15 Ω	25 Ω		10 μ a	
1N82A	20 Ω	40 Ω	1 v.		<1 nsec.
Qutronics Q6-100	10 Ω	20 Ω	7.5 v.		<1 nsec.
G7A	10 Ω	20 Ω	1 v.		<1 nsec.

* Taken from data of F. Evans, "Useful Diodes for Millimicrosecond Circuits," File No. 6C4-4, ref. (27).

† Recovery is measured by cutting off a forward current of 15 ma with a fast voltage step function. The recovery time is the time required for the voltage drop across the diode to reach a stable value.

Transistors in computer-type circuits.—Reference has been made to large counter arrays and complex coincidence circuitry which appear more and more to be necessary for the low-yield experiments connected with the large particle accelerators. (See Sect. 4 for a discussion of complex instrumentation.) The techniques of digital computer design are applicable to these and to similar problems; many of the operations such as gating, detecting coincidences, and coding, storage, and read-out of information are common to computers and to complex experimental apparatus. Millman & Taub (5, Chap. 13) give an elementary summary of computer operations in terms of vacuum-tube circuits; Chapter 18 discusses the application of transistors to these same operations; both chapters have extensive references to papers before 1956. A review of transistor techniques applied to complex transistor switching systems is included in the paper by Yokelson, Cagle & Underwood (28) on semiconductor circuit design philosophy.

The successful operation of computer-type instrumentation involves the compatibility of a large number of building blocks. Most of these circuits use transistors solely as switches, and control of saturation becomes an important element in speed of operation. There are a number of configurations in common use for coupling stages. The low saturation voltage of many of the faster transistors makes direct coupling practical. A minimum number of components is required, but transistor performance tolerances become more stringent. Henle & Walsh (29) have published a survey of the problems of transistor switching in computer circuits, discussing in detail a number of coupling methods. They also give detailed analyses of many familiar transistor circuits, including the useful complementary emitter follower, a unity-gain, noninverting stage with a low-output impedance for pulses of either polarity. This circuit, like the complementary symmetry pull-pull amplifier, has no vacuum-tube analogue. It is useful for driving capacitive or low-resistance loads when it is necessary to preserve both the rise and fall times of fast pulses.

Transistor oscillators can be constructed whose frequency stability compares with that of vacuum-tube circuits. The nonmicrophonic characteristic of transistors makes such circuits well adapted to proton resonance magnetic field measurements (30, 31).

The temperature dependence of transistor properties introduces drift problems when they are used in dc amplifier circuits. As is the case with vacuum-tube circuits, drift cannot be distinguished from a change in signal amplitude, and hence the signal-to-drift ratio is unresponsive to negative feedback. Careful compensation can alleviate the problem, as can operation at low emitter currents [as shown by Lindsay & Woll (32)], but conventional chopper techniques are perhaps a more satisfactory solution. A hybrid (vacuum tube plus transistor) circuit for the precise control of a magnetic field (33) makes use of dc-coupled transistor techniques using power transistors to control a large magnet current.

Low-frequency transistorized amplifiers are unaffected by the drift

problems associated with dc amplifiers. Noise figures for selected transistors are comparable with those of vacuum tubes, and transistorized low-frequency amplifiers can be constructed to operate successfully from low-level sources. Some of the problems of noise in low-frequency feedback transistor amplifiers have been studied by Avery & Bowes (34) in the construction of an amplifier for infrared spectrometer signals.

3. PHOTOMULTIPLIERS

Short time resolution has become one of the important modern nuclear techniques. Needed not only in the study of the characteristic times of nuclear processes, it is required in the measurement of particle velocity as in time-of-flight techniques or rejection of background as in counter telescopes. Photomultipliers remain the weakest link in the instrumentation of short-time measurements by counter techniques save when scintillator materials of long phosphor decay time are used. The arrival of a fast particle at a Cerenkov counter can generate a light pulse at a photomultiplier lasting a very small fraction of a nanosecond, even using an appreciable thickness of radiator. Electronic analysis of electrical pulses can furnish time information for a single pulse with a time inaccuracy in the range $(5-8) \times 10^{-11}$ sec. With the best commercially available photomultipliers, the time of arrival of the light pulse from the detection of a single particle in a Cerenkov counter can be determined to no better than about 2 nsec. although under some circumstances this figure may be reduced by a factor of three. However, by using additional criteria in selecting the pulses, e.g., selecting only those events giving an approximately uniform pulse height, and by analyzing a large number of events to average over fluctuations in the detection equipment, it has been possible to measure shorter times. Using techniques of this kind with scintillation counters, Sunyar (35) has been able to measure directly the flight time of γ -rays over 1-cm. path.

The difficulties of this type of measurement are very great, and the techniques are not well adapted to routine use, particularly when the time of arrival of each pulse must be determined. Significant improvement of photomultipliers could make the measurement of these times very much easier.

The sources of timing errors in a counter are several. Light from an event in a Cerenkov counter reaches the photomultiplier in a very short time; but scintillators, having an exponentially decaying light output, introduce additional timing fluctuations. An analysis of the effect of these fluctuations in terms of the scintillator characteristics is given by de Waard (36). Although photoelectrons are emitted from the photocathode with negligible time delays, they are not emitted with uniform velocities nor in a uniform direction. Upon emission they are swept by an accelerating field in the direction of the electron multiplier structure. The nonuniformity of direction is not as severe in loss of timing information as is the initial distribution of velocity, although both contribute to the variations in electron transit time to the first multi-

plier dynode. A nonuniform accelerating field can also contribute to this variation, as can differences in path length from different parts of the photocathode to the first dynode. Frequently, these two difficulties are encountered together, the fields being weakest over those portions of the photocathode farthest from the first dynode. Timing errors introduced in this region of a photomultiplier are commonly larger than those contributed by the multiplier structure itself. Some additional time spreading occurs in the multiplier structure. This spreading has its origin also in unequal transit times for electrons emitted from various parts of the dynodes and, as before, to both nonuniform geometry and nonuniform accelerating fields. For a uniformly illuminated cathode this contributes to the output pulse rise time. For a non-uniformly illuminated cathode it can change the time of arrival of the output pulse (see below). Contributions to the transit time-spread from the cathode-first dynode region and the multiplier structure have been measured for a number of photomultipliers by Greenblatt (37).

The use of a spherical photocathode reduces the variation in electron path lengths in the region between the photocathode and the first dynode and also facilitates shaping the accelerating field to reduce variations in the electron velocities. A significant reduction in the transit time-spread arising in the photocathode-first dynode region, even in the older tubes, can be made by using only the center region of the photocathode. Curves giving the transit time differences for electrons originating at different radial distances from the centers of RCA photomultipliers 6810, 6810A, 7046, and 7264, have been published (38) and are useful in estimating the improvement to be gained by masking.

An additional source of time jitter that can limit the time resolution of Cerenkov counters is occasionally important. If the Cerenkov radiator is of limited thickness or, from the design of the optical system, the light collection efficiency is poor, there may be on the average only a few photoelectrons emitted from the photocathode. With a photomultiplier having a hemispherical photocathode and a shaped accelerating field in the cathode-first dynode region, the transit time spread of photoelectrons in reaching the first dynode may be less than 0.8 nsec. However, photoelectrons emitted from different portions of the cathode strike the first dynode in different regions [and some may in fact miss it altogether, resulting in regions of reduced sensitivity on the photocathode surface (38)]. The time variation which can be expected as a result of transit time differences in the first few multiplier dynodes depends on the magnitude of the fluctuations of position of the photoelectrons emitted from the photocathode. These fluctuations are large for very weak illumination. The electron shower from a single electron striking the first dynode is collimated during traversal of the early dynodes so that transit time-spread from the range of initial starting points increases until the showers have spread to cover essentially the whole dynode surfaces. Measurements of these spreads indicate that with hemispherical-cathode

photomultipliers and shaped fields, dynode transit time variations of as much as 1 nsec. may occur, for photoelectrons emitted along different portions of a line on the photocathode perpendicular to the dynode axes. If the extreme edges of the photocathode are not masked, the spread may be appreciably greater.

Photomultipliers in which the number of photoelectrons has large fluctuations generate an output pulse whose accuracy of arrival time is no better than 1 nsec., even when the initiating light pulse is much shorter than 1 nsec. This effect is usually not considered in evaluating the expected performance of a counter but constitutes an important limit on the timing accuracy obtainable from counters with low light output, even with the best photomultipliers.

Morton, Matheson & Greenblatt (39) and Morton (40) have described an experimental photomultiplier which reduces the over-all time spread, compared with presently available tubes, by as much as two to three orders of magnitude. Photomultipliers are now available whose over-all transit time spread is of the order of a few nsec. (38); one, the RCA 7046, has a photocathode diameter of 5 in. and a window of ultraviolet-transmitting glass to extend the short-wavelength response to 250 μ . This tube is particularly useful for coincidence telescopes, for the electron transit time can be adjusted over a range of several nsec. by varying the photocathode-first dynode potential, keeping the relative potential of the focusing electrode constant with respect to the dynode and photocathode. This convenient feature speeds the alignment of coincidence circuits, as a narrow continuous range of delays can be introduced by changing this potential (41).

The fastest commercially available photomultiplier is manufactured in France, the 14-stage 56AVP described by Pietri (42).³ The output pulses have a half-amplitude width of 2 nsec. and have an approximately Gaussian shape. The conventional 14-stage photomultiplier, for example the RCA 6810A, has an output pulse with a low-amplitude "tail" lasting many times longer than the duration of the main pulse. This introduces a dead time into coincidence circuits whose pulse-shaping is done by cutting off a high-gain pentode. Measurements of the short time interval distribution between pulse pairs arriving in the same counter will be biased by this dead time. A Gaussian-shaped pulse reduces the difficulty as much as is consistent with the rise-time properties of the photomultiplier.

Mack & Kirsten (43) have listed specifications of over 50 types of photomultipliers, with a number of curves on cathode transit time differences for a number of photocathode shapes. The output pulse shapes for an input light pulse of short duration are given plus data on cathode sensitivities, gain, and saturation and overload characteristics. Much of this information is not available elsewhere or widely distributed in the literature, so this is a useful reference.

³ Available as Amperex 56AVP from Amperex Corp., Hicksville, L. I., New York.

4. MEASUREMENT OF SHORT TIMES

A number of improvements have been made recently which substantially reduce the difficulties in routine fast-coincidence measurements for times shorter than 10 nsec. Extremely fast pulse transformers are available making it no longer necessary to match the output pulse polarities of one piece of equipment to the input properties of the next, for pulses can be inverted with unity gain and an increase in rise time of the order of 3×10^{-11} sec. Vernier chronotrons have been constructed whose sensitivity to small time displacements exceeds the performance necessary to time-analyze the outputs of most radiation detectors. Oscilloscopes are now able to reproduce transient pulse behavior for times shorter than 0.3 nsec. In this section we describe many of these improvements and give references to some useful compilations of information on components and equipment.

Fast amplifiers and trigger circuits.—The performance of available fast amplifiers has not increased in recent years. The single design for pulse rise times less than 5 nsec. remains the distributed or chain amplifier (44). The most familiar are the Hewlett-Packard 460AR and 460BR, although several others are commercially available. These have a rise time of 2.6 nsec. and delay times of 18 and 21 nsec., respectively. The amplifier gains are adjustable but unstabilized, depending on both the line voltage and the condition of the vacuum tubes. For the 460AR the input impedance is 200 ohms and the output impedance 280 ohms. The input and output impedances of the 460BR are both 200 ohms. It is frequently convenient to use connecting cables whose impedances would cause serious mismatch. The use of resistors for proper termination causes a serious loss of signal amplitude, particularly when used to match to 50-ohm cables. The ease with which small transformers can be constructed (see next section) makes it possible to match the amplifier line impedances to most cables having impedances in the range 40 to 200 ohms. There is less dissipation of energy in these than with resistive terminations, and therefore less decrease in pulse amplitude. The transformers do not degrade the pulse rise times significantly. An example taken from the *UCRL Counting Handbook* (45) is a transformer used to couple the output of a Hewlett-Packard 460AR amplifier to a load of 125 ohms. Using a resistor to match the 280-ohm amplifier output impedance to the load limits the output voltage to -6 v. A trifilar wound transformer on a Ferroxcube 102-208F12 core increases the output to -9 v. The transformer is constructed by forming four turns with each of three pieces of No. 27 wire on the ferrite core. These windings are connected in series so as to form a 3:2 turns ratio autotransformer. The transformer can be mounted in a 125-ohm connecting plug (45) or mounted inside the amplifier. A transformer of similar construction but of 5:4 ratio will match the 125-ohm input cable to the 200-ohm input grid line of the 460AR amplifier. Equipped with two such transformers the 460AR amplifier has a gain of 10 from a 125-ohm input impedance to a 125-ohm load. The amplifier rise time is increased about 2.5 per cent and the pulse delay from input to output increased about 1 nsec.

An extensive evaluation of the performance of these amplifiers with and without impedance transformers has been reported in the *Counting Handbook* (45), including an investigation of their overload properties; as in the case of cable characteristics and photomultipliers, much of the information is not available elsewhere.

No important improvements have been made recently in the performance of fast trigger circuits. Variations of the secondary-emission pentode Moody discriminator circuit (46) have output pulse rise times greater than 5 nsec. In spite of stabilization of the quiescent current in the pentode, the pulse rise time may still fluctuate since the rise time depends on the tube transconductance over the entire region from the quiescent operating point to saturation, and stabilization of the quiescent current hence cannot entirely

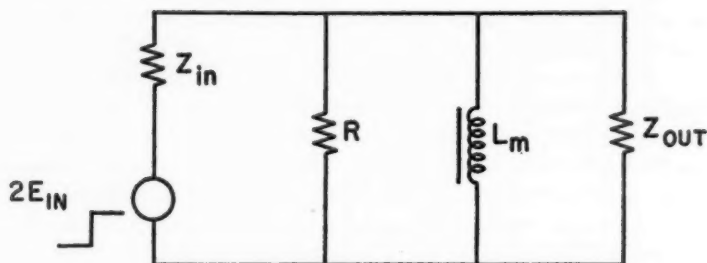


FIG. 7. Equivalent circuit for fast pulse transformers, useful for finding the "droop" of a transmitted pulse. See text for typical values of the circuit parameters.

determine the circuit properties during regeneration. Brown (47) has analyzed the gain-bandwidth product of series-connected double vacuum-tube amplifiers; his analysis indicates they may be useful if used in the construction of fast trigger circuits.

Fast passive elements.—Transformers have a number of useful characteristics in high-speed circuitry. The most useful is their ability to transform the impedance of a pulse or to invert a pulse. The dc isolation of the primary and secondary allows the dc levels of the input and output to be selected arbitrarily, and the low dc resistance of the windings makes them well adapted for introducing pulses into circuits carrying direct currents. The use of ferrites has greatly increased the usefulness of transformers in the nanosecond range, for their high bulk resistance ($\sim 10^7$ times greater than some magnetic alloy core materials) greatly lessens the magnitude of eddy currents. Millman & Taub (48) discuss the high-frequency equivalent circuits of high-speed pulse transformers.

The design and performance of several small transformers are given by Mack & Evans (45); from this we reproduce Figure 7, a simple equivalent circuit for the low-frequency response of a transformer matching impedance Z_{in} to Z_{out} following step-function excitation. This equivalent circuit is use-

ful for times after 1 nsec. from the application of the input pulse and may be used to calculate the droop of a flat-topped pulse and the pulse reflection coefficients. For N_p the number of primary turns and N_s the number of secondary turns, and L_m the magnetizing inductance, the magnetizing time constant T_m is $T_m \approx 2L_m/Z_{in}$ and $Z_{out} \approx (N_s/N_p)^2 Z_{in}$. The droop (ratio of pulse amplitude at $t=T$ to the amplitude at $t=0$) of a flat-topped driving pulse of width T is then $\approx 2L_m T/Z_{in}$, where L_m depends on the core properties and the number of primary turns. For small ferrite "pot" cores, e.g., Ferroxcube core 400T750-3C2 (48), $L_m \approx 1.0 N_p^2$ (μh); it is less for toroidal cores. Reflection caused by R is $\approx -Z_{in}/2R$, while reflection from an error in N_p/N_s is $\approx \frac{1}{2}[Z_{out}/Z_{in}](N_p/N_s)^2 - 1]$. For the Ferroxcube core mentioned above, $L_m \approx 0.86 N_p^2$ μh enry, and $R \approx 34 N_p^2$ ohm. The rise times of these transformers are in the range 0.3–0.5 nsec.

An interesting transformer design is in use at Princeton (49). It makes use of the fact that a pulse from a transmission line may be inverted by transposing the shield and center conductor at the line output [Lewis & Wells (46)]. The low-frequency properties of the transformer are determined by the signal transit time outside the shield, from the output to input. This transit time may be increased by a large factor by increasing the inductance in the return path. Winding the cable on a toroidal ferrite core is the most satisfactory method of accomplishing this for pulse widths below 50 nsec.; a hybrid core (ferrite and permalloy) can be used for transmission of pulses of width between 10 and 100 μsec . The high-frequency response of the transformer is simply the response of the cable itself, which in general is sufficiently good that the rise time of the transformer is negligibly small. Two or more such transformers, connected in parallel at the input, may be series connected at the output to form an impedance transformer.

A number of new semiflexible transmission cables are available whose wide bandwidth allows fast pulses to be transmitted long distances with little high-frequency attenuation and thus little increase in rise time. The usual polyethylene-insulated coaxial cables (such as RG-53/U) can make a substantial contribution to the rise time of a photomultiplier pulse in lengths greater than 200 to 300 ft. As the rise time of a cable varies as the square of its length (50), a long transmission cable may introduce serious pulse distortions. With the larger particle accelerators it is usually not convenient to operate fast coincidence circuits near the particle detectors, so that wide-band transmission lines are in common use to transmit pulses to the control centers. Typical of these are the 50-ohm Styroflex semi-flexible cables,⁴ which have rise times (depending on the cable diameter) from 1.2×10^{-12} to 1.2×10^{-11} sec. in 100-ft. lengths.

Coincidence systems and time analyzers.—A great many circuits have been developed for the prompt or delayed coincidence analysis of pulses, for which the characteristic times are shorter than 10 nsec. The early work has been

⁴ From Phelps-Dodge Copper Products Co., New York.

reviewed by Bell (51), Bay (52), and more recently by de Waard (53). The shortest time resolution obtained in the earlier work was accomplished by some variation of the fast-slow system (51) because the finite rise times of photomultiplier pulses make the timing very sensitive to pulse height, and it was necessary to use pulse-height selection to eliminate undesirable time jitter. In the measurement of the lifetimes of nuclear excited states, it is usually no disadvantage to restrict the usable range of pulse heights and frequently it is necessary in order to reject interfering radiations. For the multiple fast coincidences that are required in the operation of a counter telescope the situation is reversed: it becomes very important to accept a wide range of pulse amplitudes for coincidence analysis, in part because the desired counting rates are low, and in part because it is desirable to have a high counting efficiency. This places an added burden on a fast coincidence circuit: it should not be significantly pulse-height sensitive. Coincidence counters used with pulsed accelerators occasionally operate with background counting rates higher than 10^7 sec., so that, in addition, the coincidence circuit dead times may be an important limitation.

The conventional 6BN6 double-coincidence circuit, in which narrow pulses are presented to the two control grids, is, like the Garwin circuit (53), inherently amplitude sensitive. This sensitivity can be decreased by operating the tube at lower plate voltage than normal for this tube. The tube then saturates with smaller signals on the control grids so that from the cutoff condition 1 v. signals are sufficient to reach saturation output current. Green & Bell (54) report coincidence resolving times of less than 1 nsec. with a circuit of this design.

It is customary to over-drive circuits of this type in order to define accurately the time at which the input signals turn the tube on completely. Pulses with excessive base width can increase the effective resolving time by an order of magnitude, and control of the pulse width is usually necessary. Generating the required positive pulse by using a negative pulse from a photomultiplier to cutoff a high-gain pentode with delay-line pulse shaping at the anode is satisfactory; the long-base photomultiplier pulse then introduces a dead time which may be as long as 5 to 20 nsec. without, however, increasing the resolving time. The 6810A type phototubes generate pulses having long bases (see Sect. 3).

Increasing the speed of data taking and averaging many instrumental fluctuations are accomplished by the use of a time analyzer (53). Slow pulse-height analysis of output of a 6BN6 coincidence circuit or of the Bell circuit (55) in effect measures the time overlap of the coincident pulses, by overlap-to-charge conversion, and is capable of a time resolution for delayed coincidence experiments better than 0.01 nsec. when sufficient data are available for an analysis of the edges (or drop-off) of the resolving time curve. A time analyzer makes only a small improvement in the time accuracy with which the single coincidence may be determined, although the multichannel display is

more convenient. A similar circuit of the overlap-to-charge conversion principle is used to time-analyze pulses from a cooled, unactivated NaI γ -ray counter (56).

A multichannel time analyzer using a 20 mc./sec. crystal oscillator gated on and off by the pulses whose time displacement is to be measured has recently been constructed (57). Time analyzers using this principle of operation are limited by the difficulty of constructing reliable vacuum-tube scalers capable of operating faster than about 20 mc./sec. Only a few vacuum-tube scaler circuits of this speed have been published (58), and it appears the next advances will be by the application of solid-state amplifiers (see Sect. 2).

The Vernier chronotron has very high time resolution achieved by circulating two "coincident" pulses in a pair of circular delay lines of slightly different lengths. The relative time of arrival of the pulses is compared at the line inputs each revolution, and the time one pulse overtakes the other defines an interval from the starting of the cycle which is dependent on the initial time displacement of the two events. Using the 6810A with scintillation detectors, Lefevre & Russell (59) and Lefevre & Brown (59a) have achieved a prompt coincidence-resolving time curve with a width at half maximum of less than 1 nsec.

The time sorter described by Gatti and co-workers (60, 61) operates on a different principle. Pulses from two counters are used to shock-excite two LC resonant circuits whose resonant frequencies ω_1 and ω_2 are low compared with the reciprocals of the pulse widths, yielding wave trains whose relative phase at the start depends on the time positions of the centroids of the initiating pulses; the phases are relatively insensitive to the pulse amplitudes, providing the induced amplitude is large compared with residual excitation of the resonant circuit. The initial phase angle of the difference frequency $\omega_1 - \omega_2$ is equal to this relative phase angle of the wave trains ω_1 and ω_2 . Hence a time shift of the initiating pulses of t seconds will result in a time shift T of the difference wave given by $T = t\omega_1/(\omega_1 - \omega_2)$, a time shift which can be determined by measuring the interval to the first zero crossing of this difference wave. As the time dilation factor $\omega_1/(\omega_1 - \omega_2)$ can be of order 100, conventional slow electronics are sufficient to determine T . This technique, as with the Vernier chronotron, yields coincidence-resolving times below 1 nsec. and is one of the few instruments with which one can determine the relative times of arrival of two pulses alone to such high accuracy. Unfortunately it has a long dead time and so is unsuitable in its present form for use with high counting rate channels.

It is interesting to note that in three recent meson experiments using counter telescopes, all requiring the shortest resolving time, the data were recorded on film using fast oscilloscopes, and timing and pulse amplitude determinations were made by analysis of the traces (62 to 62b). Fluctuations in the operating points of a few components of a fast multichannel coincidence circuit can lead to the loss or incorrect interpretation of data, and the

reliability of extremely fast vacuum-tube electronics is not always sufficiently high to give confidence in its proper operation for low-counting-rate experiments of great difficulty.

Test equipment and monitors.—The construction of circuits capable of responding to very fast pulses has been accompanied by the development of test equipment of comparable speed. Light sources of sub-nanosecond rise time, fast pulse generators, and wide-band oscilloscopes, all become necessary for the design and repair of fast counting and coincidence circuits. Kerns, Kirsten & Cox (63, 63a) have described an extremely fast light pulser with a light rise time less than 0.5 nsec. The fall from peak to half-peak amplitude is less than 1.5 nsec., with intensity adjustable over two decades using crossed polarizers, and over a factor of 10^6 by altering the voltage applied to the light source. An electrical pulse of equivalent rise time is available for synchronizing auxiliary equipment.

Lewis & Wells (46) describe the generation of fast electrical pulses by the discharge of a charged transmission line center-conductor into a second line initially uncharged. Two different designs using relays with mercury-wetted contacts are described by Cox (64). They have rise times of less than 0.5 nsec., output voltages up to 100 v., and pulse widths adjustable from less than 1 nsec. to greater than 1 μ sec.

For observing pulses with rise times less than about 2 nsec., it is not feasible to use oscilloscopes with conventional distributed amplification, for in order to achieve usable electron beam deflection the electrons must spend a minimum time in the cathode ray tube deflection system, and this transit time determines maximum frequency response. An oscilloscope is available commercially⁵ (65) whose beam is deflected by a traveling-wave deflection system (66). The rise time is approximately 0.1 nsec. The electron beam can be focused to a spot about one thousandth of an inch in diameter, so even small deflections of the beam can yield useful information. A similar instrument has been described by Winningstad (67).

5. COMPLEX INSTRUMENTATION AND DATA HANDLING

When the number of data channels in an experiment becomes very large, data handling itself becomes a problem. An increasing number of experiments involves an amount of data so large that manual transcription becomes tedious and simple-arithmetic data reduction so lengthy that it is economical to search for techniques to process the bulk of the information by computer methods. Depending on the experiment, if the number of channels exceeds some number in the range from 30 to 300, the data-handling problem may be quite severe. With the increase in reliability of modern computers and computer techniques there is less prejudice against their use in data handling and data reduction.

Within an experiment it frequently is convenient to use computer tech-

⁵ Manufactured by Edgerton, Germeshausen and Grier, Inc., Boston, Mass.

niques to combine information so that only the combined output is accepted for storage. For example, a two-scintillator counter telescope can be arranged to give pulses proportional to the differential energy loss and total energy of a fast charged particle. Electronic multiplication of these pulse magnitudes yields a pulse whose height can be used to identify the mass of the incident particle. The magnitude of this pulse then becomes the information of interest. Briscoe (68) has described circuits which can form this product in a few microseconds.

A large number of data channels is frequently necessary when it is desired to store all the information furnished by even a simple experiment. Birk, Braid & Detenbeck (69) have constructed a two-dimensional pulse-height analyzer which records correlated number pairs on punch tape. There are $(127)^2$ channels available for storage. A similar two-dimensional analyzer using a magnetic drum storage with 3072 storage channels has been constructed by Chase (70). These devices are used principally to record correlated pulse-height information, for example from NaI(Tl) counters detecting γ -rays in coincidence; and usually only limited numbers of channels, determined by inspection, are of quantitative interest. A computer would be required to analyze the output data provided instruments of this kind were used to their fullest capacities.

Experiments are under construction at Princeton (71), Berkeley (72), and Stanford (73) which involve data reduction by either IBM-650 or -704 computers with no manual transcription of the information from the experimental apparatus. In all cases the apparatus punches either tape or cards which can subsequently be read directly into a digital computer. It appears that increasing use will be made of the large computers in proportion to the increase in complexity of new experiments.

LITERATURE CITED

1. *The Transistor* (Bell Telephone Laboratories, Inc., New York, N. Y., for Western Electric Co., Inc., November 15, 1951)¹
2. Hunter, L. P., Ed., *Handbook of Semiconductor Electronics* (McGraw-Hill Book Co., Inc., New York, N. Y., 650 pp., 1956)
3. DeWitt, D., and Rossoff, A. L., *Transistor Electronics* (McGraw-Hill Book Co., Inc., New York, N. Y., 381 pp., 1957)
4. "Transistor Issue," *Proc. IRE (Inst. Radio Engrs.)*, **46** (1958)²
5. Millman, J., and Taub, H., *Pulse and Digital Circuits* (McGraw-Hill Book Co., Inc., New York, N. Y., 1956)
6. Lin, H. C., and Jordan, W. F., Jr., *IRE Trans. on Electron Devices*, **ED-6**, 79 (1959)
7. Schenkerman, S., *Electronics*, **31**, 122 (1958)
8. Keister, G. L., and Stewart, H. V., *Proc. IRE (Inst. Radio Engrs.)*, **45**, 931 (1957)
9. Baldinger, E., *Nuclear Instr.*, **2**, 193 (1958)
10. Anzalone, P., *Electronic Design*, 38 (June 1, 1957)
11. Graveson, R. T., and Sadowsky, H., *IRE Trans. on Nuclear Sci.*, **NS-5**, 179 (1958)
12. Chase, R. L., *Brookhaven Natl. Lab. Quart. Progr. Rept.*, 1 Oct.-31 Dec. 1957, 29-30 (Unpublished)³
13. Cutler, L., *Transistorized Integrator-Amplifier for Photomultiplier* (Stanford University, unpublished)
14. "2N501 Application," *Appl. Rept. No. 330* (Lansdale Tube Co. [Division of Philco Corp.], Lansdale, Pa.)
15. Griswold, D. M., and Cadra, V. J., *IRE Natl. Conv. Record*, **4**, Part 3, 49 (1958)
16. Tulchin, H., *Electronics*, **57** (1959)
17. de Broekert, J. C., and Scarlett, R. M., *Stanford Electronics Lab. Tech. Rept.*, No. SEL 514-1, 15 January, 1959 (Unpublished)
18. Hamilton, D. J., *IRE Trans. on Circuit Theory*, **CT-5**, 69 (1958)
19. Armstrong, H. L., *Electronics*, **31**, 96 (1958)
20. Zaglio, E., *Nuovo cimento*, **6**, 512 (1957)
21. Pederson, D. O., *IRE Trans. on Circuit Theory*, **CT-2**, 171 (1955)
22. Suran, J. J., *Proc. IRE (Inst. Radio Engrs.)*, **46**, 1260 (1958)
23. Baldinger, E., and Santchi, P., *Nuclear Instr.*, **2**, 128 (1958)
24. Deutsch, M. (Private communication)
25. Fitch, V., in "The Second Symposium on Advances in Fast Pulse Techniques for Nuclear Counting," *U. S. Atomic Energy Commission Rept.*, UCRL-8706 (Unpublished)
26. Miller, R. W., *Rev. Sci. Instr.* (In press)
27. File CC4-4(3), "The Counting Handbook," *U. S. Atomic Energy Commission Report*, UCRL-3307 (Unpublished)⁴
28. Yokelson, B., Cagle, W., and Underwood, M., *Bell System Tech. J.*, **37**, 1125 (1958)

¹ Selected reference material on characteristics and applications.

² This issue contains papers covering a wide range of transistor development.

³ The author wishes to thank W. Higinbotham for furnishing a copy of this report.

⁴ The author appreciates permission of Dr. R. Mack to reproduce portions of this Handbook.

29. Henle, R. A., and Walsh, J. H., *Proc. IRE (Inst. Radio Engrs.)*, **46**, 1240 (1958)
30. Singer, J. R., and Johnson, S. D., *Rev. Sci. Instr.*, **30**, 92 (1959)
31. Garwin, R., Patlach, A., and Reich, H., *Rev. Sci. Instr.*, **30**, 79 (1959)
32. Lindsay, J. E., and Woll, H. J., *RCA Rev.*, **19**, 433 (1958)
33. Garwin, R. L., Hutchinson, D., Penman, S., and Shapiro, G., *Rev. Sci. Instr.*, **30**, 105 (1959)
34. Avery, D. G., and Bowes, R. C., *J. Sci. Instr.*, **35**, 212 (1958)
35. Sunyar, A. W. (Private communication)
36. De Waard, H., *Nuclear Instr.*, **2**, 74 (1958)
37. Greenblatt, M. H., *IRE Trans. on Nuclear Sci.*, **NS-5**, 13 (1958)
38. Widmaier, W., *IRE Trans. on Nuclear Sci.*, **NS-5**, 114 (1958)
39. Morton, G. A., Matheson, R. M., and Greenblatt, M. H., *IRE Trans. on Nuclear Sci.*, **NS-5**, 98 (1958)
40. Morton, G. A., in "The Second Symposium on Advances in Fast Pulse Techniques for Nuclear Counting," *U. S. Atomic Energy Commission Dept., UCRL-8706* (Unpublished)
41. Richter, B. (Personal communication)⁵
42. Pietri, G., in "The Second Symposium on Advances in Fast Pulse Techniques for Nuclear Counting," *U. S. Atomic Energy Commission Dept., UCRL-8706* (Unpublished)
43. Sect. CC8-2, CC8-3, CC8-4, "The Counting Handbook," *U. S. Atomic Energy Commission Report, UCRL-3307* (Unpublished)
44. Ginzton, E. L., Hewlett, W., Jasberg, J., and Noe, J., *Proc. IRE (Inst. Radio Engrs.)*, **36**, 956 (1948); see also Ref. (46)
45. Sect. CC2-3, CC2-4, "The Counting Handbook," *U. S. Atomic Energy Commission Report, UCRL-3307* (Unpublished)
46. Lewis, I., and Wells, F. H., *Millimicrosecond Pulse Techniques*, 232-34 (McGraw-Hill Book Co., Inc., New York, N. Y., 310 pp., 1954)
47. Brown, M., *Rev. Sci. Instr.*, **30**, 169 (1959)
48. Millman, J., and Taub, H., *Pulse and Digital Circuits*, Chap. 253-85 (McGraw-Hill Book Co., Inc., New York, N. Y., 1956)
49. O'Neill, G. K. (Private communication)
50. Kirsten, F., in Sect. CC2-2, "The Counting Handbook," *U. S. Atomic Energy Commission Report, UCRL-3307* (Unpublished)⁶
51. Bell, R. E., *Ann. Rev. Nuclear Sci.*, **4**, 93 (1954)
52. Bay, Z., *Nucleonics*, **14**, 56 (1956)
53. de Waard, H., *Nuclear Instr.*, **2**, 73 (1958)
54. Green, R. E., and Bell, R. E., *Nuclear Instr.*, **3**, 127 (1958)
55. Sunyar, A. M., *Bull. Am. Phys. Soc., Ser. [II]*, **2**, 137 (1957)
56. Beghian, L. E., Kegel, G., and Scharenberg, R., *Rev. Sci. Instr.*, **29**, 753 (1958)
57. Hillas, A. M., and Tennant, R. M., *Nuclear Instr.*, **3**, 344 (1958)
58. Collinge, B., and Huxtable, G., *Nuclear Instr.*, **3**, 116 (1958)
59. Lefevre, H., and Russell, J., *IRE Trans. on Nuclear Sci.*, **NS-5**, 146 (1958)
- 59a. Lefevre, H., and Brown, J., *Rev. Sci. Instr.*, **30**, 159 (1959)
60. Gatti, E., in "The Second Symposium on Advances in Fast Pulse Techniques for Nuclear Counting," *U. S. Atomic Energy Commission Document, UCRL-8706* (Unpublished)

⁵ The author appreciates a discussion of this feature with Dr. Richter.

⁶ This contains specifications of most of the wide-band transmission lines.

61. Cottini, C., and Gatti, E., *Nuclear Instr.*, **2**, 88 (1958)⁷
62. Impeduglia, G., Plano, R., Prodell, A., Samios, N., Schwartz, M., and Steinberger, J., *Phys. Rev. Letters*, **1**, 249 (1958)
- 62a. Fazzini, T., Fidecaro, G., Merrison, A. W., Paul, H., and Tollestrup, A. V., *Phys. Rev. Letters*, **1**, 247 (1958)
- 62b. Anderson, H. L., Fujii, T., Miller, R. H., Tau, L., *Phys. Rev. Letters*, **2**, 53 (1959)
63. Kerns, Q., and Kirsten, F., *Rev. Sci. Instr.*, **30**, 31 (1959)
- 63a. Kerns, Q., Kirsten, F., and Cox, G., Sect. CC8-30, "The Counting Handbook," *U. S. Atomic Energy Commission Report, UCRL-3307* (Unpublished)⁸
64. Section CC10-1, "The Counting Handbook," *U. S. Atomic Energy Commission Report, UCRL-3307* (Unpublished)
65. Germeshausen, K., Goldberg, S., and McDonald, D., *IRE Trans. on Electron Devices*, **ED-4**, 152 (1957)
66. Patten, R. B., in "The Second Symposium on Advances in Fast Pulse Techniques for Nuclear Counting," *U. S. Atomic Energy Commission Document, UCRL-8706* (Unpublished)
67. Winningstad, C. N., *Rev. Sci. Instr.*, **29**, 578 (1958)
68. Briscoe, W. L., *Rev. Sci. Instr.*, **29**, 401 (1958)
69. Birk, M., Braid, T. H., and Detenbeck, R. W., *Rev. Sci. Instr.*, **29**, 203 (1958)
70. Chase, R. L., "A Two-Dimensional Kicksorter with Magnetic Drum Storage," *Brookhaven Natl. Lab. Rept., No. 3838* (Unpublished)⁹
71. Fitch, V. L. (Private Communication)
72. Mack, D. (Private communication)
73. Oeser, J. (Private communication)

⁷ This contains references to earlier papers.

⁸ Both (63) and (63a) should be consulted.

⁹ W. Higinbotham very kindly furnished a copy of this report.

HIGH-TEMPERATURE PLASMA RESEARCH AND CONTROLLED FUSION¹

By R. F. POST

University of California, Lawrence Radiation Laboratory, Livermore, California

INTRODUCTION

The astrophysicists who, in the 1930's, unraveled the mystery of the origin of energy production by the sun and stars unwittingly set the stage for one of today's most intriguing, difficult, and promising fields of research. The investigation of the behavior of totally ionized gases or "plasmas" at ultra-high temperatures is a field of experimental research not yet a decade old. But it is already seen to be one of enormous promise—and one of equally great difficulty.

Stimulus for intensive experimental research into the properties of high-temperature plasmas came first from the appreciation that such studies could lead to a practical means for the controlled release of nuclear fusion energy. The realization of this possibility could be of incalculable value to humanity, as a future source of power, because of the essentially limitless reserve of the primary fusion fuel, deuterium, the potentially low cost of power from such a source, and the absence of radioactive waste products in its utilization.

Because of its association with the general question of nuclear energy, and possibly because of a lack of early appreciation of the extreme difficulty of the problem, work in this field has been, until recently, for the most part carried out in government-sponsored laboratories and under tight secrecy restrictions. Happily, this latter trend has now reversed. Perhaps in part stimulated by an open prediction, at the first (1955) Geneva Conference on the Peaceful Uses of Atomic Energy, by Dr. H. Bhabha that "... a method will be found for liberating fusion energy in a controlled manner within the next two decades," the second Geneva Conference on the Peaceful Uses of Atomic Energy, in 1958, saw the complete declassification of controlled-fusion information by the member nations of the U.N. and the beginning of a healthy and spirited interchange of information on this field of research. As wisely remarked at the conference in the paper by L. A. Artzimovich on *Research on Controlled Thermonuclear Reactions in the USSR*, "This problem seems to have been created especially for the purpose of developing close cooperation between the scientists and engineers of various countries. . . ." This sentiment was voiced again at the same conference by Edward Teller who said, in his paper on U. S. fusion work, "I see a very fruitful field of research for physicists, for groups of physicists, for scientists in a whole country and for scientists in the whole world."

¹ The survey of literature pertaining to this chapter was concluded in July, 1959.

Voluminous though it was, the information on high-temperature plasma research released at the 1958 Geneva Conference showed clearly that, as with an iceberg, only superficial details are now seen, and the major part of the work in this field is yet to be done before even the feasibility of obtaining power from controlled fusion can be demonstrated. It seems therefore likely that other, wholly unrelated applications will be realized before this can be done.

The problem which is to be solved if high-temperature plasmas are to be studied or their practical application contemplated can be simply stated. It is that one should heat and hold confined within electromagnetic "walls" a tenuous ionized gas at kinetic temperature of tens or hundreds of millions of degrees. To be effective, the confinement must be operative for an appreciable fraction of a second, or longer, implying that the particles must be able to execute thousands or even millions of periodic motions within the confinement volume before they are lost. Because, as will be seen, such high-energy particles will only very slowly undergo deflections by their mutual collisions, the motion of each particle should be predictable from well-known equations of motion of charged particles, so that the entire problem is, in principle, solvable from elementary considerations.

Why is it then that a field for which all the basic physical laws are well understood is so intractable? The answer to this question probably has several parts. First, although plasma is itself the most elementary form of matter, the breadth of phenomena which are important in the behavior of high-temperature plasmas as produced in the laboratory is exceedingly large. To cite a few: (a) Atomic processes, such as ionization, excitation, and charge exchange may compete and interplay in a complicated way. (b) The fact that the plasma particles are charged means that a variety of complicated transport phenomena will occur, arising from near and "distant" collisional interactions of the plasma particles, coupled through their Coulomb fields. (c) Beside the more obvious collisional encounters between the individual charged particles of the plasma, the long-range nature of Coulomb forces gives rise to a host of "co-operative" (or more usually "unco-operative"!) phenomena, evidenced through a wide variety of electrostatic, oscillatory, or unstable behavior. This situation is complicated by the fact that, of necessity, the high-temperature plasma is almost invariably immersed in, and strongly coupled to, a magnetic field. Thus, although the individual particles' motions are all predictable from the electromagnetic fields in which they move, the fields can themselves be strongly influenced by the particles.

A second reason for the difficulty of experimental work in this field is traceable to the crucial role of technology. The performance of significant experiments has usually first required a substantial extrapolation of some technology, or even the development of previously nonexistent techniques. For example, to produce the rapidly rising and enormous electrical currents required in some experiments, new developments in electrical energy storage and switching have been required. Some experiments which require the

achievement of exceedingly antiseptic vacuum conditions have had to be preceded by intense research into the general problems of ultravacuums and surface physics. The problem of physical measurements on plasmas has required that many new instruments and techniques be developed.

But perhaps the most important factor of all in limiting the rate of progress toward understanding phenomena in high-temperature plasma is the essential way in which both the experimental study and the problem of successful generation and confinement of a high-temperature plasma are found to be intertwined. In a sense, in order to be able to understand and to solve the problems, one has to have solved them already. This linking between creation of the system and its study is rarely encountered in as acute a form in any other branch of physics. This fact, together with the complexity of possible modes of behavior of a plasma, has meant that detailed understanding and even conceptual advances have proceeded by painfully slow steps from experiment to experiment, with little or no probability of a "break-through" into an area of rapid advance. The lesson that careful study and understanding must yet proceed hand in hand up a long and arduous path has been sometimes forgotten in contemplating the glamor of the final objectives of the research, but its validity is not thereby lessened.

PHYSICAL PROCESSES IN A HIGH-TEMPERATURE PLASMA

The great variety and simultaneous importance of the various physical processes which can occur in a high-temperature plasma are a challenge both to the experimentalist and to the theoretical physicist working in the field. (It is at the same time a source of dismay to one who is trying to present an orderly review of the subject.) It is of minor comfort to know that the basic equations—i.e., Maxwell's equations, the equations of motion of charged particles, the equations of statistical mechanics, the theory of nuclear reactions, and the quantum theory are all well validated and understood. Problems arise not at this level but rather when these separate disciplines are all relevant to a single situation, so that the equations are thereby coupled.

To fathom a complicated problem it must be somehow separated into its parts. This is not easy to do for plasma, but some degree of conceptual separation of the problem is possible along the following lines: One obviously can divide the behavior of plasma into those processes which are primarily particle-like and those which are largely the result of collective interactions. This division is aided by the fact that, necessarily, experiments on high-temperature plasmas in the laboratory are usually confined to the use of plasmas of relatively low particle density, so that rarely are more than two particles of the plasma involved in any single elementary physical event. With this division firmly in mind a coherent picture of plasma behavior can be formed.

Generally speaking, the hopes for practical application of high-temperature plasma research to the production of power from controlled fusion are wrapped up in searching for means to reach a favorable competition between

particle-like processes in the plasma, at the same time avoiding the catastrophe which can result from co-operative effects. On the one hand, simple collisional processes are important in determining the probability of fusion reactions as compared with the probability of dissipation of the plasma or its internal energy by collisional diffusion or by elementary radiation processes. On the other hand, looking at the problem of obtaining nuclear power from a plasma one sees that collective interactions in the plasma play essentially no role in promoting nuclear reactions but can act rapidly to dissipate the plasma or its energy. Thus one might say that the game of searching for practical ways to produce a high-temperature plasma is often one of searching for ways to minimize the "mob" aspects of the plasma, and at the same time to maximize the probability of the desired interactions between its individual members.

In the section to follow, the most important particulate processes in a high-temperature plasma will be briefly reviewed, in order to establish the order of magnitude of competing effects. It is important to understand these processes since they are very potent in determining the physical conditions which must be achieved in any serious study of a high-temperature plasma.

PARTICULATE PROCESSES

Ionization.—The formation of a plasma results from the ionization of a gas of neutral atoms. In a low-density, high-temperature plasma, ionization comes about primarily from collisions between energetic electrons and neutral gas atoms. Since ionization itself releases a new electron, the possibility of the familiar cascade gas discharge process exists and is an important consideration in the initiation of some high-temperature plasmas where very high electrical currents are used. The cross section σ_i for the ionization of simple atoms is reasonably well predicted by Born approximation calculations (1). A convenient simplified representation of this calculation is given by the expression:

$$\begin{aligned}\sigma_i &= \frac{\pi e^4}{\chi^3} b f(u) = \sigma_0 f(u) \text{ cm}^2. & 1. \\ f(u) &= \frac{\epsilon}{u} \log_e u, & u = \frac{W}{\chi} \\ f(\epsilon) &= 1.\end{aligned}$$

Here W is the energy of the incident electron and χ is the ionization potential in ergs. The constant b is approximately 0.2 for simple atoms. Figure 1 shows a relative comparison between an ionization function of the general form of expression 1 and the experimentally measured values for hydrogen and other elements.

Typical values of the cross section for ionization of simple atoms (such as hydrogen) by electrons predicted by Equation 1 lie in the range of 10^{-16} to 10^{-17} cm.² An ionizing electron will necessarily have a velocity of about 3×10^8 cm./sec. or more. Thus the product $\sigma_i v$ is typically about 3×10^{-8} to 3×10^{-9} cm.² sec.⁻¹ In high-temperature plasma experiments, final plasma

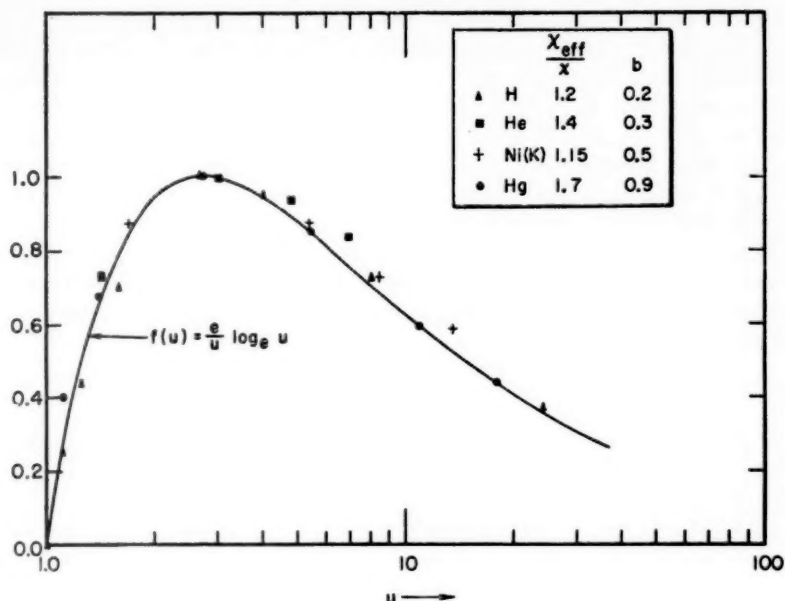


FIG. 1. Ionization cross-section function $f(u)$, compared with experimental data. Ionization potential also used as fitting parameter.

densities of 10^{14} to perhaps 10^{16} particles per cm^3 are of interest. One must therefore conclude that under these conditions the ionization rate of a neutral atom $n_e \sigma_i v$ (where n_e is the electron density) will usually be very high, corresponding to lifetimes for ionization of the order of $1 \mu\text{sec.}$ or less. On the other hand, if the initial plasma density is very low, as it may be in some approaches, the rate of ionization may become low enough to give rise to serious difficulties, some of which will be mentioned later.

Coulomb collisions.—The dominant interparticle collision process in a high-temperature plasma is Rutherford scattering, i.e., elastic scattering arising from the mutual Coulomb electrostatic fields of the charged particles of the plasma. Such processes lead to the deflection of and energy exchange between the particles of the plasma. They are important because they determine the basic rate of all collisional transport processes in the plasma. Since the effective range of the electrostatic forces between charged particles is infinite, in order properly to define "collisions" between charged particles in a plasma it is customary to divide the available range of impact parameters into three regions: (a) the "close-collision" region, where the interaction between two colliding particles is sufficiently strong to lead to large discontinuous deflections or energy exchanges; (b) the "distant-collision" region, where deflection or energy exchange between particles is an essentially continuous process arising, for any given particle, from the integrated effect of

small but uncorrelated "collisions" with the many particles which are "distant" yet close enough to lie within a characteristic distance (the Debye shielding length λ_D); (c) the region of collective or plasma interactions, lying outside the Debye sphere. From this latter region will arise electric and magnetic fields as a result of macroscopic charge separation and electric currents flowing in the plasma. For these phenomena to arise, correlated and coupled motion of the plasma particles is essential, and from such effects stems most of the complexity of plasma behavior.

Returning to the particular question of collisional effects, the cross section for process (a) above, i.e. for "large" deflections by collisions between particles of equal mass and equal charge can be simply estimated and is given by the value

$$\sigma_c \approx \frac{\pi Z^4 e^4}{W^2} \text{ cm.}^2 \quad 2.$$

Here Ze must be interpreted as the effective charge seen by each particle as it approaches the other to within the classical distance of minimum approach, $r_c = Z^2 e^2 / W$. Thus unless the colliding charged particles are each completely stripped ions, Z will, in effect, be a function of W . If W is expressed in kev,

$$\sigma_c \approx 6 \times 10^{-20} \frac{Z^4}{W^2} \text{ cm.}^2 \quad 3.$$

A similar calculation can be made for (b), the effect of "distant" collisions between equal-mass particles. In this case the answer will depend on the shape of the particle-energy distributions. Chandrasekhar (2) and Spitzer (3) have calculated these effects in detail. For purposes of estimation, however, an approximate expression will suffice. For collisions between equal mass, equal-charge particles of similar mean energy, the integrated effect of distant collisions produces a dispersion in angle (or in energy) which can be represented by an effective cross section. Thus for a "large" deflection, the cross section for those distant collisions is, approximately,

$$\sigma_d \approx \frac{\pi Z^4 e^4}{W^2} \left[\frac{\log \Lambda}{2} \right] \text{ cm.}^2 \quad 4.$$

where $\Lambda = \lambda_D / r_c$. It turns out that $\lambda_D \gg r_c$ and in fact $\log \Lambda \approx 20$ in most cases, and

$$\sigma_d \approx 10\sigma_c \approx 6 \times 10^{-19} \frac{Z^4}{W^2} \text{ cm.}^2 \quad 5.$$

Thus distant collisions are about one order of magnitude more important than close collisions in producing particle deflections.

The fact that many particles are simultaneously involved in the "distant" collisions can be seen from Figure 2. This figure presents

$$\lambda_D = \sqrt{\frac{kT_e}{4\pi n_e e^2}}$$

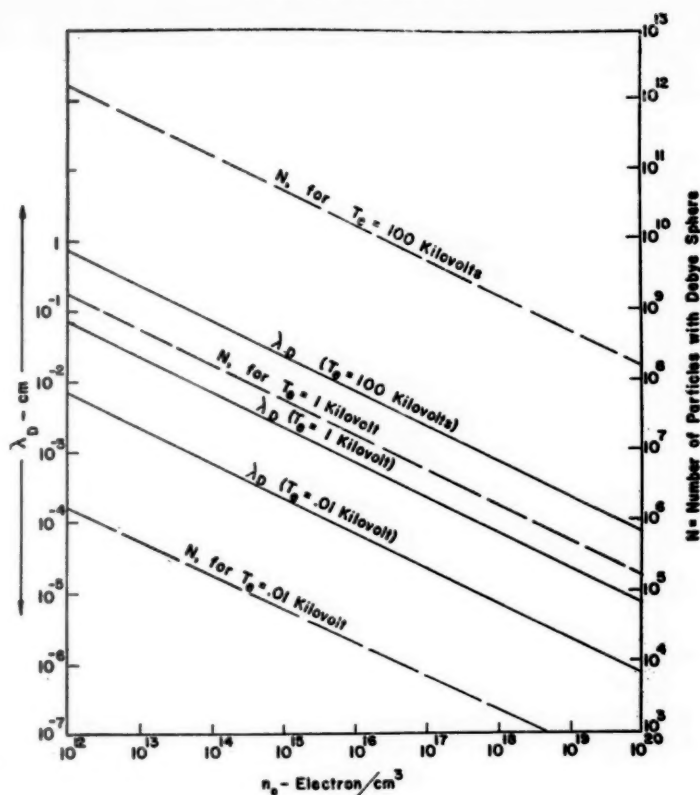


FIG. 2. Mean free path for distant collision ($2D$) and number of electrons in a Debye sphere (N) plotted against electron density.

as a function of n_e for various values of T_e . Here T_e is given in kilovolts (1 kev kinetic temperature = $kT = 1.16 \times 10^7$ K.). Corresponding to the given values of n_e and λ_D , the number of electrons in a Debye sphere is also plotted. This number can be seen to be quite large for typical densities and temperatures. Although the representation achieved is nevertheless probably reasonably satisfactory, it is one of the weaknesses of present plasma theory that it treats the collisional interactions between a given charged particle and each of its many neighbors within a Debye length as separate, uncorrelated "events," even though many such events may be occurring simultaneously.

The effect of distant collisions with ions of known energy distribution in producing deflections of a given ion can be more precisely stated in terms of the "relaxation times" of Chandrasekhar. For an ion of velocity v colliding with a Maxwellian distribution of similar ions at a kinetic temperature kT , the cumulative effect of distant collisions will cause an angular deflection θ , the mean square value of which will grow linearly with time as

$$\bar{\theta}^2 = t/t_D$$

6.

where

$$t_D = \frac{M^2 v^3}{8\pi n Z^4 e^4 \log \Lambda} \left(\frac{1}{H(x)} \right) \text{ sec.},$$

$$x^2 = \frac{1}{2} \frac{M v^2}{kT}$$

and $H(x)$ is a slowly varying function of x which is about equal to 0.5 for typical values of x . The values of $H(x)$ are tabulated (after Chandrasekhar) in Table I.

TABLE I
VALUES OF $H(x)$

x	$H(x)$
0.6	0.421
0.8	0.534
1.0	0.629
1.2	0.706
1.4	0.766
1.6	0.813
1.8	0.849
2.0	0.876
2.5	0.920
3.0	0.944
4.0	0.969

With $H(x)=0.5$ and with M expressed in units of the proton mass ($M = A M_P$), t_D can be written in terms of the particle energy W , in kilovolts:

$$t_D = 1.8 \times 10^{10} \left(\frac{A^{1/2}}{Z^4} \right) \frac{W^{3/2}}{n} \text{ sec.} \quad 7.$$

When $\bar{\theta}^2$ is set equal to 1, t_D can be seen to define the scattering time for a "large" deflection. This condition is also nearly the same as that for the time required to introduce an rms energy dispersion $\sqrt{\Delta E^2}$ about equal to the original energy. These two effects will be considered interchangeably in the discussions to follow.

Some general remarks can be made about these interparticle Coulomb scattering cross sections and rates. First, their rapid Z dependence provides one of the many reasons why high-temperature plasma research is almost always carried out with elements of low atomic number, such as hydrogen or helium. Secondly, the relatively rapid dependence of the scattering cross section on particle energy means that the role of Coulomb scattering may vary enormously during the course of a single experiment, if the plasma

energy varies also with time. For example, in some experiments, the initial ion energies might be only a few electron volts, at which times the Coulomb scattering cross section would be two or three orders of magnitude larger than any other competing cross section (such as ordinary gas kinetic scattering). But if the final ion energies increase to, say, 10 kev, the scattering cross section (for low- Z ions) would drop to less than 10^{-4} of typical atomic cross sections.

In addition to encounters between like particles, collisions between ions and electrons can play an important role in a plasma. Despite their small mass relative to the ions, the electrons of a plasma can substantially influence the energy of the plasma ions by collisional interactions, because of their greater mobility.

Two distinctly different phenomena are to be distinguished here. First, whatever the initial ion energy, the effect of randomly directed collisional impulses from the electrons will be to generate an energy dispersion about the mean value of the ion energy at a rate which is relatively independent of the ion energy itself. Second, whenever the ion possesses a mean energy larger than the mean electron energy, a "dynamical friction" between the moving ion and the electrons will arise, which will monotonically slow down the ion until energy equipartition occurs. For energetic ions, both of these phenomena will be operative at the same time, and their competition will determine the actual energy history of an ion in its electron environment.

The first phenomenon is most important if the plasma ions have a lower mean energy than the electrons. In this case the effect of the elementary impulses delivered by electrons within the Debye sphere is to "heat" the ion, at a rate which theory indicates is not sensitive to the shape of the electron energy distribution. This process is of practical importance in situations where the plasma ions are to be heated by contact with higher-temperature electrons.

On the other hand, if the ion possesses an energy which is large compared to the mean electron energy, the dynamical friction effect will become dominant and will eventually slow the ion to the same mean energy as the electrons. In this case, however, theory shows that the electrons which are most important in determining the rate of energy transfer from ion to electrons are those with velocities comparable to or less than the ion velocity. But note that for situations where the mean energy of the ions is not too high compared to the electron energy distribution, the number of electrons possessing a velocity equal to or less than that of the ionic velocity is a small fraction of the total number and their energy is very small compared to the mean. Thus the theoretical result obtained for dynamical friction will be sensitively dependent on the detailed shape of the electron energy distribution at the low-energy end. In calculations of the dynamical friction a Maxwellian distribution is usually assumed. There are, however, reasons why this assumption may not be a valid one in the non-equilibrium plasmas encountered in the laboratory. An example is the effect which the dynamical

friction itself may have on the distribution through the "heating" of these low-energy electrons which it produces. Also, it has recently been shown theoretically that the rates of energy transfer between electrons and ions may be modified by factors of about two in the presence of a strong magnetic field (4). Unfortunately, none of these theoretical predictions has been investigated experimentally, so that the possibility exists that large discrepancies will be found between present theoretical transfer rates and those actually encountered. This could have an important bearing on some proposed experiments and on their interpretation.

The presently accepted electron-ion transfer rates (not including the effect of a magnetic field) can be derived from the previously mentioned work of Chandrasekhar or Spitzer. For an ion of charge Z and mass M moving in a cloud of electrons at temperature T_e , the expression takes the simple form (5)

$$\left(\frac{dW}{dt}\right)_{ei} = 4\pi\sqrt{2} \log \Lambda \frac{n_e Z^2 e^4}{(\pi m k T_e)^{1/2}} \left(\frac{m}{M}\right) \left(1 - \frac{W}{\frac{3}{2} k T_e}\right) \text{ erg sec.}^{-1} \quad 8.$$

This expression contains both of the transport effects mentioned above.

For ion energies small compared to the mean electron energy, ion heating through the generation of a dispersion of ion energies with an rms value $W = \sqrt{\Delta W^2}$ will occur. The rate, as predicted by Equation 8 in the limit of $W \ll \frac{3}{2} k T_e$ is

$$\left(\frac{dW}{dt}\right)_{ei} = 2.8 \times 10^{-12} \left(\frac{Z^2}{A}\right) \frac{n_e}{T_e^{1/2}} \text{ kev/sec.} \quad 8.1$$

where W and T_e are in kilovolts. This same expression will also apply, approximately, to the rate of generation of a dispersion in energy about the mean of the energy of a higher-energy ion with $W > \frac{3}{2} k T_e$.

The theoretical range of validity of 8 at high ion energies is limited to those cases where the ion velocity is less than the mean electron velocity, i.e., where

$$W < \left(\frac{M}{m}\right) \left(\frac{3}{2} k T_e\right).$$

For ion energies in excess of this value, the velocity distribution of the electrons becomes of less importance, the dynamical friction completely dominates, and the transfer rate approaches a rate which is independent of the electron temperature and is given by

$$\left(\frac{dW}{dt}\right)_{ei} = -\frac{4\pi}{\sqrt{2}} \log \Lambda \frac{n_e Z^2 e^4}{M^{1/2}} \left(\frac{M}{m}\right) \frac{1}{W^{1/2}}. \quad 9.$$

This rate of loss of ion energy is clearly independent of the electron temperature or velocity distribution function. Thus at the two limits, i.e., either for $W \ll \frac{3}{2} k T_e$, or $W \gg (M/m) (\frac{3}{2} k T_e)$, the transfer rates are not appreciably sensitive to the shape of the electron energy distribution function.

Unfortunately, most of the physically interesting cases lie well between these two limits.

In the intermediate range, where dynamical friction is important, expression 8 given above takes the form

$$\frac{1}{W} \frac{dW}{dt} = -1.8 \times 10^{-12} \frac{n_e (Z^2/A)}{T_e^{3/2}}, \text{ sec.}^{-1} \quad 8.2$$

with A being the atomic weight of the ion relative to hydrogen, and T_e in kilovolts. This yields the integrated expression for the decrease of W through dynamical friction:

$$W = W_0 e^{-t/t_e}$$

where

$$t_e = 5.5 \times 10^{11} \frac{T_e^{3/2}}{n_e} \left(\frac{A}{Z^2} \right) \text{ sec.} \quad 10.$$

and T_e is in kev.

If the electron temperature is low, t_e may become quite small compared to the mean ion-ion collision time t_D . For example, if $n_e = 10^{14}$ and $T_e = 0.010$ kev then for protons ($A = Z = 1$) satisfying the condition $W < 1836 (\frac{1}{2} k T_e)$, i.e., $W < 27$ kev, the time constant for energy loss by dynamical friction is $t_e = 5.5 \mu\text{sec}$. By contrast, if the mean proton energy is, for example, 10 kev, the corresponding ion-ion scattering time t_D as calculated from Equation 7 is roughly 6 msec. At an electron temperature of 1 kev the two times become about equal, and at an electron temperature of 10 kev, t_e is about 30 times t_D (for protons). Corresponding to these three different characteristic times, three "mean free paths" for energy degradation can be defined. These are, for the examples above: $\lambda_e = 780$ cm. ($T_e = 10$ ev), $\lambda_D = 8.5 \times 10^6$ cm., $\lambda_e = 2.5 \times 10^7$ cm. ($T_e = 10$ kev). These distances are all obviously large compared to apparatus dimensions.

Inspection of the above relations shows that, as far as energy-dispersion effects of the ions are considered, in contrast to dynamical friction, the small mass of the electrons relative to ions implies that ion-ion collisions are relatively far more important in producing energy dispersion and deflection of the ions than are electron-ion collisions. The relative rates of these two processes may be estimated from a comparison of 8.1 and 7. These predict the appropriate rates of dispersion in ion energy as, respectively,

$$\left(\frac{dW}{dt} \right)_{ii} = 2.8 \times 10^{-12} \left(\frac{Z^2}{A} \right) \frac{n_e}{T_e^{1/2}} \quad 8.1$$

and

$$\left(\frac{dW}{dt} \right)_{ee} \approx \frac{W}{t_D} = 0.55 \times 10^{-10} \left(\frac{Z^4}{A^{1/2}} \right) \frac{n_i}{W^{1/2}}. \quad 7.1$$

Since $n_i = Z n_e$ in a plasma composed of electrons and ions of charge Z ,

in this case the ratio of these two rates is

$$\frac{\left(\frac{dW}{dt}\right)_{ei}}{\left(\frac{dw}{dt}\right)_{ii}} = \frac{5.1 \times 10^{-2}}{(A^{1/2}Z^2)} \left(\frac{W}{T_e}\right)^{1/2}. \quad 11.$$

For protons, the two rates do not reach equality until the ion energy has reached $(5.1 \times 10^{-2})^{-2} = 380$ times the electron temperature.

The entire question of energy transfer rates between ions and electrons is one of great importance in high-temperature plasma research, since in many cases these rates are critical in determining the relative importance of other processes, such as the rate of loss of energy from the plasma by radiation (which arises solely from the electrons) or the rate of "cooling" of ions which are exposed to low-temperature electrons, such as those which might be associated with a low-temperature arc. Yet at this date essentially no experimental data exist on these fundamental processes. In addition, theory itself has not been refined to include some effects which may be important, for example, the likely existence of distortions of the electron energy distribution from a Maxwellian, caused by the energy transfer itself, and by other processes.

Bremsstrahlung and excitation radiation.—Radiation provides a direct cooling mechanism for a high-temperature plasma. Fortunately for the experimenter, the rates of radiation from such plasmas, at the particle densities used in the laboratory, are far less than the Planck or black-surface value.

For example, if the temperature were 10 kev (1.17×10^8 °K.), the Planck value would be about 10^{21} watts/cm.², an almost inconceivably large rate of energy loss. But the fact that a tenuous plasma is optically very "thin" over almost all of its emission spectrum means that its radiation is much reduced compared to the Planck value. Nevertheless, great care must be taken to minimize even these residual radiation losses, to keep them from overwhelming the means for heating the plasma and keeping it hot.

Considering collisional processes only, there exist three mechanisms for radiation from the plasma. The first of these is the ordinary bremsstrahlung or x-ray generation which occurs when the plasma electrons are deflected by encounters with the ions. The second mechanism is a similar radiation which occurs when electron-electron collisions occur. This process vanishes in the classical (nonrelativistic) limit but may become important for very high electron temperatures. The third mechanism which can occur, and one which under some circumstances may completely dominate the radiation losses, is what will be here dubbed "excitation radiation," i.e., radiation which results from the collision of electrons with partially stripped ions, with the production of excited states and subsequent reradiation.

(a) *Electron-ion bremsstrahlung:* The magnitude of the radiation loss from electron-ion bremsstrahlung is usually obtained by integration of the

nonrelativistic radiation loss expression, as given by Heitler (6)

$$\frac{dw}{dx} = -\frac{16}{3} n_i Z^2 \bar{\phi} m c^2$$

$$\bar{\phi} = \frac{r_0^2}{137} = \frac{e^4}{\hbar m c^3} = 5.7 \times 10^{-28} \text{ cm.}^2 \quad 12.$$

Use of this simple expression introduces some errors at low and high plasma energies, but the corrections are not large. Writing

$$\frac{dw}{dt} = \frac{dw}{dx} v_e$$

and integrating over the electron velocity distribution (assumed Maxwellian) one obtains an expression for the bremsstrahlung power loss per unit volume:

$$p_{ei} = \frac{32}{3} \sqrt{\frac{2}{\pi}} \frac{e^6}{\hbar m^{3/2} c^3} n_e n_i Z^2 (kT)^{1/2} \text{ ergs cm.}^{-3} \quad 13.$$

$$= 0.48 \times 10^{-30} n_e n_i Z^2 T_e^{1/2} \text{ watts cm.}^{-3} \quad 14.$$

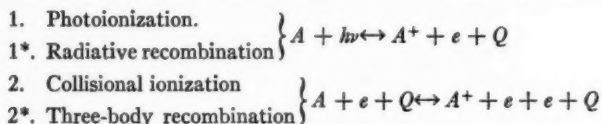
if T_e is expressed in kilovolts.

(b) *Electron-electron bremsstrahlung*: In the nonrelativistic limit, electron-electron collisions would give rise to no bremsstrahlung losses, since the dipole moment of the colliding system is zero in this limit. However, relativistic effects can become sufficiently important at high electron temperatures to produce appreciable radiation losses from electron-electron collisions. This process has been recently calculated in various degrees of approximation by several investigators. Not all of the calculations agree, and few papers on the subject have been published at this date. Stickforth (7) has performed detailed calculations on the effect. His results may be simply stated as a ratio of electron-electron to the ordinary electron-ion bremsstrahlung for $Z=1$. These ratios ($e-e/e-i$) are, for Maxwellian electron distributions, 0.06 at $kT_e=25$ kev, 0.13 at $kT_e=50$ kev, 0.34 at $kT_e=100$ kev, and 0.64 at $kT_e=150$ kev. At all but the highest temperatures the predicted increase is small. This encourages one to believe that the additional radiation losses arising from electron-electron collisions will not represent a substantial effect, except for systems where the electron temperature is inordinately high.

(c) *Excitation radiation*: Although it is customary to assume that all ions in a high-temperature plasma will become completely stripped of their bound electrons, this assumption is unwarranted for the tenuous plasmas produced in the laboratory. Furthermore, even where the primary constituent of the plasma is of low atomic number, the fact that the absolute density of the plasma is so low means that it is essentially impossible to keep it from being partially contaminated by some higher- Z impurities. Such impurities are usually derived from occluded material on the vacuum-chamber walls. For example, in a chamber of usual dimensions, if the plasma density were 10^{14} particles/cm.³, the release of only a few per cent of the adsorbed impurity

atoms in a single atomic monolayer on the chamber walls could make the impurity-atom density about equal to the original plasma particle density!

The calculation of the degree of stripping of a small component of high- Z atoms immersed in a tenuous plasma must proceed along different lines from those usually employed. The usual method of calculation involves what are essentially thermodynamic equilibrium arguments, as embodied in the so-called Saha equation (8). In a plasma in complete thermodynamic equilibrium between the particles and the radiation field, the final state of ionization is determined by detailed balancing between pairs of processes:



However, in a tenuous plasma the radiation field does not reach its equilibrium value and the density is usually too low for 2^* to be important. Thus 1 and 1^* and 2 and 2^* do not balance. The final state of ionization is therefore primarily determined by a balance between 1^* and 2. The importance of this type of ionization equilibrium in tenuous plasmas, such as the sun's corona, has been discussed by Wooley & Allen (9) and by Elwert (10).

It should be noted that since 1, 1^* , 2, and 2^* depend in different ways on the plasma density, the state of ionization predicted by the Saha equation is a function of density, tending to higher states of ionization at lower densities. However, 1^* and 2 depend in the same way on density, so that the state of ionization which is predicted for a low-density, nonequilibrium plasma is independent of density.

The state of ionization predicted for the nonequilibrium low-density plasma is substantially lower than that predicted by the Saha equation. The cross sections for processes 1^* and 2 for all possible states of ionization of high- Z atoms are not well enough known to permit accurate calculations; furthermore, the competition between the two processes will also be somewhat dependent on the detailed shape of the electron distribution function, since 1^* and 2 do not have the same dependence on electron energy. However, in some cases which are of particular interest, the physical situation is sufficiently simple to permit reasonably reliable calculations to be made.

One case of interest is the limiting one of atoms which have been stripped down to a single bound electron. Figure 3 presents curves for various elements which give the probability, as a function of electron temperature (Maxwellian electron distribution assumed), that the ion of that element will retain one or more bound electrons. It will be seen that even elements with as low an atomic number as oxygen will not become completely stripped until quite high temperatures are reached. Higher-atomic-number atoms may never become completely stripped. For comparison, a similar curve for oxygen at a typical density, as computed from the Saha equation, is also

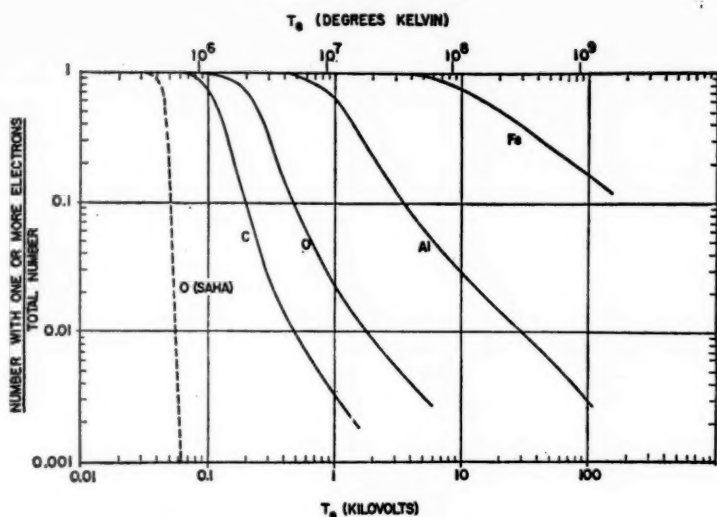


FIG. 3. Atom fraction containing one or more electrons as a function of electron temperature.

shown. The gross difference between the results of the two methods of calculation is apparent.

Figure 4 presents another type of "stripping curve," plotted in this case as a function of atomic number. The curves shown represent the locus of points for which the mean probability is 50 per cent that the ion in question exists in the plasma at the temperature indicated. Two lines are shown, the upper one being for the one-electron ions of Figure 3, so that the points shown are the same as those found by drawing a line across Figure 3 at the 0.5 level. The lower curve gives similar information, but for three-electron (lithiumlike) ions. These ions, as will be explained below, are of particular interest because of their radiation properties.

It should be recognized that the stripping curves calculated above represent steady-state values of the ionization. However, high states of ionization are only reached by step-by-step ionization processes and so it may require an appreciable time for the steady state to be reached. Thus it may often be true in laboratory experiments that the time scale of the experiment is such that the degree of ionization reached will be substantially less than that predicted in steady state. However, by the same method outlined above, transient stripping curves can also be calculated, and it is thus possible to evaluate the importance of these effects.

Once the state of ionization of the ions is known, the rate of production of excitation radiation can be determined. For the usual low-impurity densities

which are of practical interest, this calculation consists merely in evaluating the rate of collisional excitation of the bound electrons and equating this rate to the subsequent spontaneous photon-emission rate. What one discovers immediately is that at low and intermediate temperatures this process may be many orders of magnitude more important in producing radiation energy losses than the bremsstrahlung. Of course, if the electron temperature can

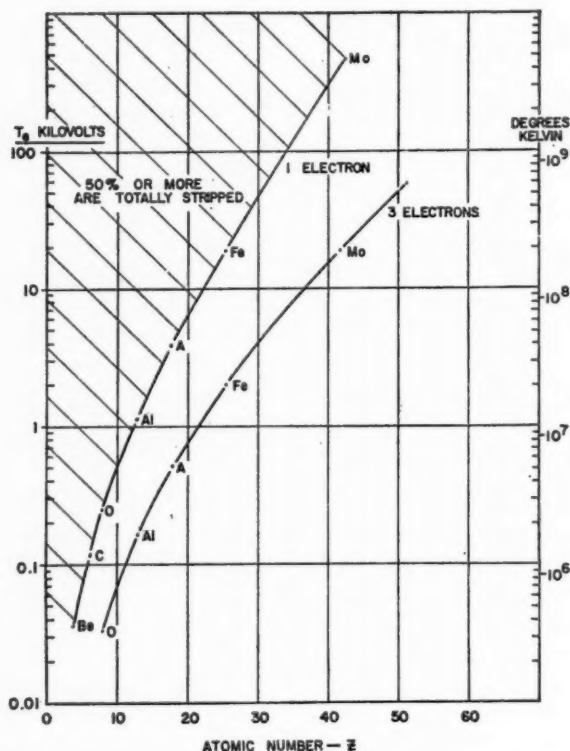


FIG. 4. Stripping temperatures for one- and three-electron ions as functions of atomic number. The curves represent the loci of points for which the mean probability is 50 per cent that the ion in question exists at the electron temperature shown.

be made sufficiently large and if steady-state conditions are attained, then the stripping may become sufficiently complete to reduce the excitation radiation to a low level. Nevertheless, excitation radiation can represent an enormous energy-loss mechanism under some circumstances.

Figure 5 presents the results of some calculations on the intensity of excitation radiation to be expected from selected impurity atoms. The results are given only for two particular ionization states—the one-electron and

three-electron ions previously considered. The one-electron ion is interesting because it represents the hardest incompletely stripped state. The three-electron ion is particularly interesting because it also is a relatively hardy ion and because its outer electron possesses a strong, low-lying $2S-2P$ resonance transition which has an excitation energy equal to $2(Z-2)$ electron-volts. Thus, for example, oxygen VI, a three-electron ion, will emit a

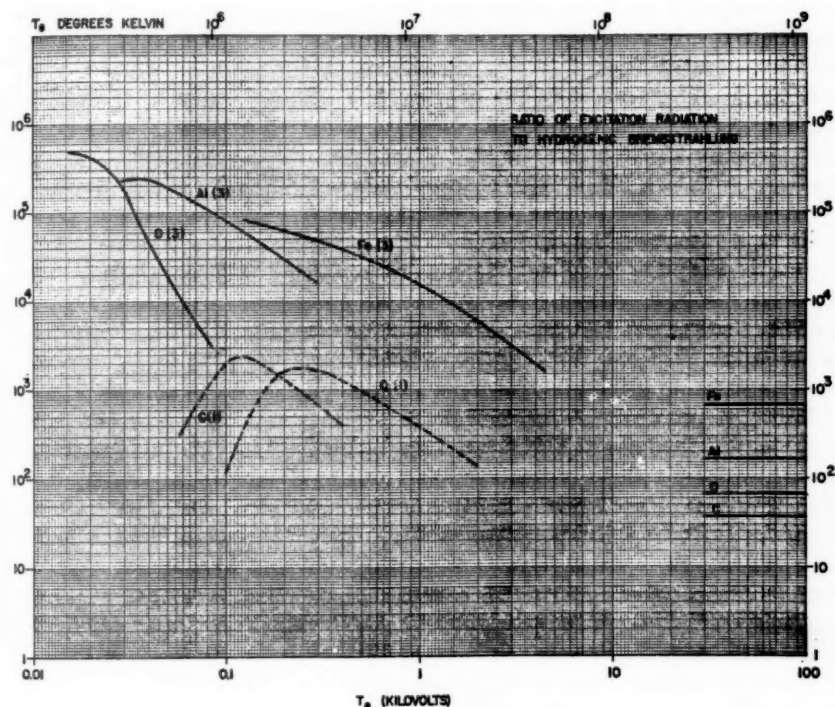


FIG. 5. Ratio of excitation radiation to hydrogenic bremsstrahlung.

strong resonance line at 12 ev (1032 Å), in the vacuum ultraviolet. The next excited state lies far above this line, at about $2.3(Z-2)^2$ ev or 83 ev above the ground state. The ionization potential is of course, even larger compared to the first level.

In the figure, the steady-state excitation-radiation intensities are presented as ratios (on an atom-for-atom basis) to the electron-ion bremsstrahlung rate for a hydrogen plasma. The curves represent the combined effect of the calculated variation of excitation probability with electron temperature and the steady-state abundances of the indicated ions. Since approximate theoretical expressions were used to calculate the ionization and excitation probabilities, some quantitative errors must be anticipated.

It is apparent from Figure 5 that in some cases radiation rates 10^5 to 10^6 times the bremsstrahlung rate can be encountered. To take an example, consider a hydrogenic plasma with a small contamination of aluminum. Assume that the electron temperature is 10^6 °K. and the electron density is 10^{16} cm $^{-3}$. Equation 12 then predicts that the electron-hydrogen-ion bremsstrahlung loss will be approximately 15 watts per cm. 3 Figure 5 shows that the three-electron ionic state of aluminum would be emitting at a rate approximately 10^6 times that of hydrogenic bremsstrahlung at this temperature. Other adjacent states of ionization, not included in this calculation, would make an additional contribution. Therefore, a hydrogenic plasma at 10^6 °K. containing a contamination of 1 per cent of aluminum would be expected to lose energy at a rate in excess of about 10^3 times the bremsstrahlung loss or at more than 15,000 watts per cm. 3 This is probably a large enough energy loss rate to have a substantial effect on the energy balance of the plasma.

It can be seen from the figure that the role of excitation radiation is greatest at low temperatures, and as higher temperatures are reached the degree of stripping rises and the rate of excitation radiation falls greatly. This is a fortunate circumstance for the future of plasma research but may provide little solace for those experimenters who presently find themselves restricted to the lower-temperature part of the curve.

The horizontal lines at the right of the figure indicate the asymptotic values of bremsstrahlung losses from the various ions. It can be seen from this that in steady state the extra radiation emitted as excitation radiation should become relatively unimportant above about 10^8 °K. However, it should be remembered that, particularly for ions of very high Z , the transient degree of ionization may be substantially less than the steady-state value so that the rate of excitation radiation actually emitted may be substantially larger than that indicated by these curves.

At densities of partially stripped impurity ions greater than about 10^{15} cm. $^{-3}$, the excitation radiation from plasmas of the dimensions used in laboratory experiments will begin to be influenced by self-absorption effects. At densities of about 10^{17} cm. $^{-3}$ these effects will become sufficiently pronounced to transform the losses from a volume to a surface character and to broaden the emission lines into rough trapezoidal shapes. At these densities the radiation losses are predicted to increase slightly less than linearly with the volume (as the $\frac{3}{4}$ th power) and will vary only as the square root of the impurity density, rather than linearly. Impurity densities this high, however, would give rise to enormous absolute radiation fluxes.

Charge exchange.—Under some circumstances of interest in high-temperature plasma research, the plasma density may be low enough so that the ionizing ability of the plasma is relatively small. Under these circumstances neutral atoms of thermal velocity, arising perhaps from the vacuum chamber walls, may penetrate the plasma and survive long enough to provide a serious loss mechanism through the process of charge exchange or charge transfer. As the name implies, charge transfer results in the capture, by an ion, of an

electron from a passing neutral atom. In high-temperature plasmas confined by electromagnetic fields, such a mechanism leads to a decrease in the purity of and a loss of energy from the plasma, since charge exchange between a fast ion and a slow neutral impurity atom leads to the formation of a fast neutral—which can immediately escape the confining fields—leaving behind a “cold” impurity ion in its place.

The plasma densities below which charge exchange losses within the plasma volume are possible may be estimated from the ionization cross sections given earlier. If the ionization cross section of Equation 1 is multiplied by v and integrated over a Maxwellian distribution, an expression can be derived for $\langle\sigma v\rangle_i$, the mean electronic ionization rate parameter. This parameter will be found to have a maximum value of about 10^{-8} cm.³ sec.⁻¹, occurring when the electron temperature in ev is about equal to the ionization potential. Above its maximum, $\langle\sigma v\rangle_i$ falls off slowly with increasing electron temperature. To estimate the electron density below which a slow neutral atom may penetrate the plasma of usual dimensions, one calculates the lifetime against ionization of the atom and multiplies by its thermal velocity. If the distance found this way is comparable to the plasma dimensions, neutrals will be able to penetrate. As a rough example, at $n_e = 10^{12}$, the mean lifetime for ionization is $(n_e \sigma v)^{-1} \approx 10^{-4}$ sec. The velocity of a thermal oxygen atom is about 5×10^4 cm./sec. Thus the mean free path for the oxygen atom would be about 5 cm. in the plasma, and charge exchange losses could begin to become serious. At $n_e = 10^{11}$, this distance becomes 50 cm., and most laboratory plasmas would be ineffective in preventing the penetration. At a density of 10^{14} , however, $\lambda = 0.5$ mm., and the neutral population in the interior of the plasma would be microscopic.

The relative seriousness of having a population of neutrals within the plasma depends on the charge exchange lifetime of the high-energy ions. Unfortunately, at the ion energies of greatest potential interest in high-temperature plasma research, say roughly between 2 and 200 kev, the charge exchange cross sections σ_{10} , are large, and the lifetimes are correspondingly short. Typical values of σ_{10} are 10^{-16} cm.² so that over the above energy range $\langle\sigma_{10} v\rangle$ may be 10^{-8} cm.³ sec.⁻¹ or more and is thus as large or larger than $\langle\sigma v\rangle_i$. This value is to be compared with that for scattering of the ions, calculated from Equation 7. For 10-kev protons $\langle\sigma v\rangle_{\text{scat}} = 1/n t_D \approx 2 \times 10^{-12}$ cm.³ sec.⁻¹ or almost four orders of magnitude less. Also, as will be seen from a later section, $\langle\sigma_{10} v\rangle$ is typically some eight to nine orders of magnitude larger than the values of the corresponding rate parameter for nuclear fusion reactions.

Ion lifetimes against charge exchange can be calculated if the neutral density is known. For example, if the neutral pressure is 10^{-8} mm. Hg, $n_0 \approx 3 \times 10^{10}$ atoms/cm.³ and $t_{10} = n_0 \sigma_{10} v^{-1} \approx 3$ msec.

The implications of these remarks is that, although charge exchange losses will represent at most a surface effect for high-temperature plasmas of densities greater than about 10^{13} , they can represent a serious inhibiting

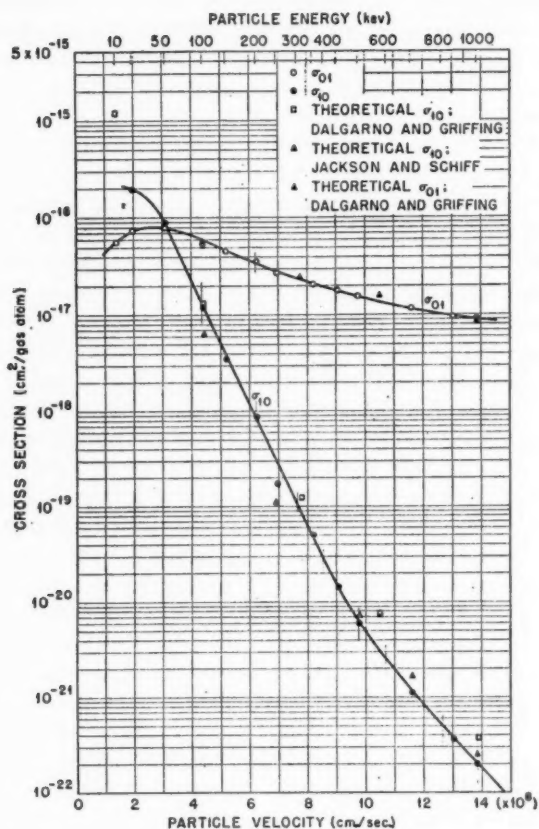
UNCLASSIFIED
ORNL-LR-DWG 15939

FIG. 6. The charge transfer cross section per atom of gas traversed as a function of particle velocity and energy. Hydrogen atoms and ions in hydrogen gas.

mechanism for the build-up or long-time confinement of lower-density plasmas.

In some methods of generating a high-temperature plasma, particularly those which involve the injection and accumulation of high-energy ions, it is inevitable that during the build-up the plasma density will pass through a low-density regime. In such cases three general approaches exist for combating charge exchange losses. The first is the obvious one of improving the system vacuum. The second approach is to perform the build-up operation in a time short compared to the charge exchange lifetime, so that the plasma density rapidly exceeds the critical value above which ionization processes dispose of the neutrals. The third general approach is to take advantage of

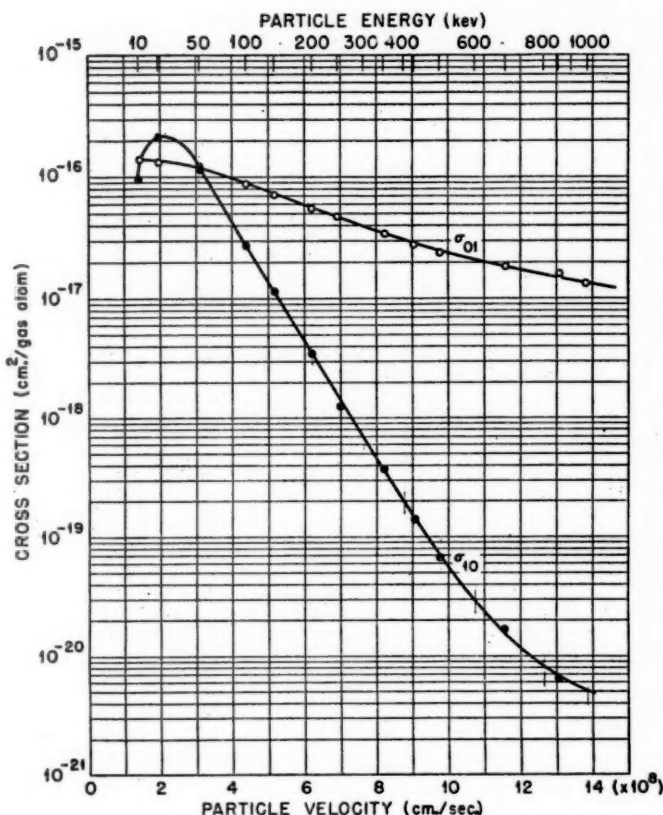
UNCLASSIFIED
ORNL-LR-DWG 15938

FIG. 7. The charge transfer cross section per atom of gas traversed as a function of particle velocity and energy. Hydrogen atoms and ions in helium gas.

the fact that at very high ion energies the charge exchange cross section begins to drop rapidly with energy, whereas the ionizing ability of the ions themselves remains large. This latter approach will be discussed at greater length in connection with experimental work.

To illustrate the dependence of the charge exchange cross section on energy and on type of neutral atom, curves taken in various gases from the work of Stier & Barnett (11) which show the values of σ_{10} for protons in various gases are shown in Figures 6 to 9. Also shown on their curves are the ionization cross sections σ_{01} for the probability of ionization of fast hydrogen atoms passing through the indicated gases.

Nuclear reactions.—In terms of their influence on the behavior of a high-

temperature plasma, nuclear fusion reactions would normally play a completely secondary role. Yet, it is the possibility that such reactions could be made energetically self-sustaining when produced through the agency of a confined hot plasma that provides the greatest stimulus for the study of plasma properties. If it had turned out that a nuclear fusion reaction could

UNCLASSIFIED
ORNL-LR-DWG 15937

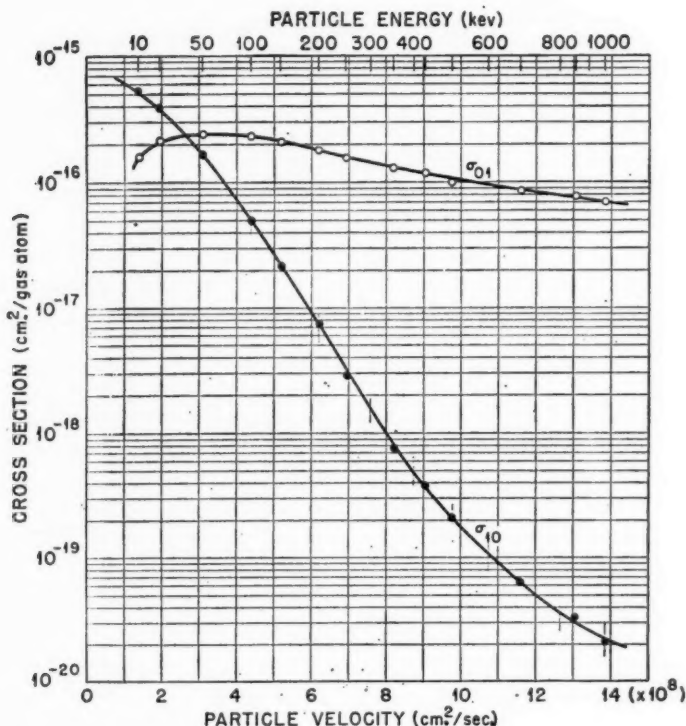


FIG. 8. The charge transfer cross section per atom of gas traversed as a function of particle velocity and energy. Hydrogen atoms and ions in nitrogen gas.

be found with a cross section, say 10⁶ times as large as any presently known, power from controlled fusion would probably have been realized long before now. It is the smallness of the reaction cross sections that makes the problem look hard—even in theory. In order to place the magnitude of the reaction cross section in proper perspective with other competing effects, a brief summary will be given.

Consider two species of ions capable of reacting with each other by mutual collisions. If the particle densities of the ions are n_1 and n_2 , respec-

tively, the numbers of reactions per unit volume will be

$$R_{12} = n_1 n_2 \langle \sigma v \rangle_{12} \quad 15.$$

where $\langle \sigma v \rangle_{12}$ is the product of the reaction cross section and the relative velocity of ion types 1 and 2, averaged over the distribution of their relative velocities. Note that since a high-temperature plasma need not exist in a

UNCLASSIFIED
ORNL-LR-DWG 15936

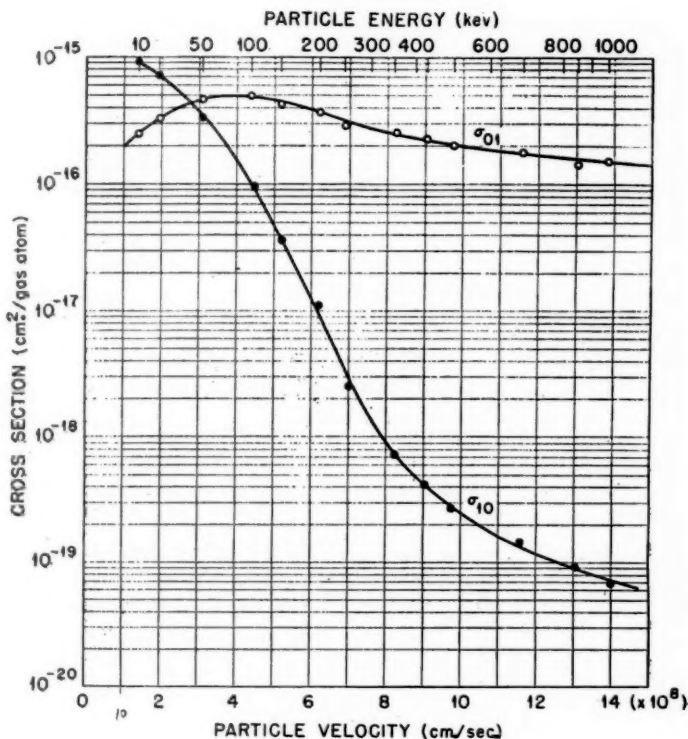


FIG. 9. The charge transfer cross section per atom of gas traversed as a function of article velocity and energy. Hydrogen atoms and ions in argon gas.

state of kinetic equilibrium among its constituent particles, there is no need to assume that 1 and 2 have the same velocity or energy distribution; there are circumstances where practical advantages would accrue from choosing widely different velocity distributions for 1 and 2. However, most calculations of $\langle \sigma v \rangle$ have been made under the assumption that the plasma ions are characterized by a single mean energy and, usually, by a Maxwellian velocity distribution.

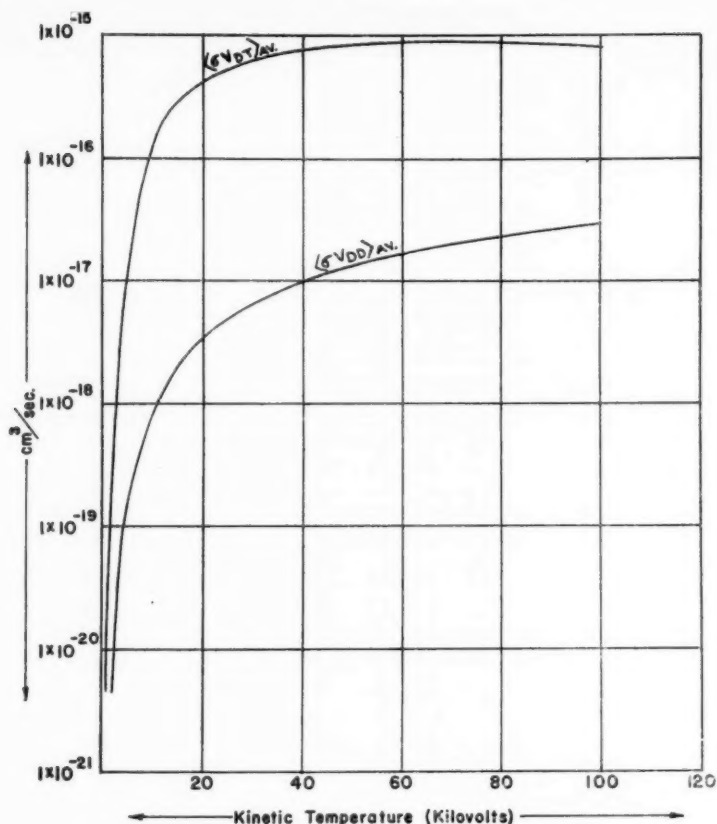
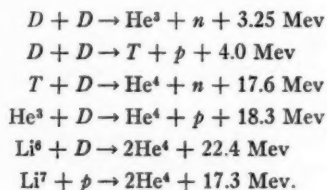


FIG. 10. Calculated $\langle \sigma v \rangle$ values for DD and DT reactions.

The main reactions of interest as possible sources of fusion energy are tabulated below:



Of these the DD , TD , and He^3D reactions are the most important. Using the measured cross sections, various investigators have calculated $\langle \sigma v \rangle$ values for the above reactions. Figure 10 presents the values of $\langle \sigma v \rangle$ for the TD and for the sum of the DD reactions for ion kinetic temperatures up to 100 kev. Table II reproduces some of the calculations of Thompson (12).

Whether these reactions can sustain themselves against losses depends, of course, on the environment within which they are conducted. A necessary but not sufficient condition for a self-sustaining reaction can be obtained by comparing the energy release of the reactions with radiation losses. The fact that $\langle\sigma v\rangle$ generally varies much more rapidly with temperature than do the radiation losses means that the nuclear reaction will only be able to support itself against radiation losses above a certain temperature, sometimes called the "Ideal Ignition Temperature" (IIT). If only bremsstrahlung losses are considered in competition with the nuclear energy release, the IIT is independent of n_i since both vary in the same way with plasma density. Accord-

TABLE II
THOMPSON'S RESULTS (12) FOR AVERAGE VALUES OF σv FOR SEVERAL
THERMONUCLEAR REACTIONS AT A SERIES OF TEMPERATURES

Temperature Kev	10^{-2}	10^{-1}	1	10	100
He^3D	2.3×10^{-79}	4.7×10^{-48}	1.5×10^{-26}	7.4×10^{-20}	4.5×10^{-16}
TT	2.5×10^{-86}	1.6×10^{-34}	1.4×10^{-24}	9.8×10^{-21}	—
$\text{Li}^6\text{D}(\rho)$	1.0×10^{-86}	1.1×10^{-47}	6.5×10^{-30}	1.8×10^{-20}	1.3×10^{-16}
$\text{Li}^6\text{D}(n)$	6.0×10^{-93}	1.1×10^{-49}	6.1×10^{-30}	3.9×10^{-21}	1.9×10^{-17}

ing to the usual method of counting only charged reaction products in the balance, the IIT comes out to be about 4 kev for the TD reaction, and about 35 kev for the DD reaction. The concept of the IIT is only mentioned here to emphasize its artificiality. Since many other loss mechanisms can exist besides bremsstrahlung and since the usual definition of the IIT assumes equality between electron and ion temperature, the values of the IIT should be viewed merely as rough lower limits to the required operating temperatures. However, the concept is useful in showing that, for example, in the case of the simple DD reaction, the energy balance situation is so marginal that any appreciable additional loss mechanism would be sufficient to upset it. It seems almost certain that effective use of the DD reaction will require the use of a fuel cycle involving the reaction products, and possibly other means for improving the over-all efficiency of the reaction.

Again let it be emphasized that since the calculated power balance is often marginal, the basic transport phenomena in the plasma which control the rate of energy and momentum transfer between ions and ions, and ions and electrons will play a crucial role in determining whether or not a positive power balance can be established with the reaction in question.

COLLECTIVE PROCESSES

In an ordinary atomic or molecular gas, complex collective phenomena such as shocks, turbulence, or various other instabilities of flow can occur.

However, as the density of such a gas is reduced, all collective phenomena vanish because the coupling afforded by collisions becomes less important and the mean free path of the particles becomes comparable with the dimensions of the system. Not so with an ionized gas. As a result of the long-range nature of the Coulomb force, the presence of collective effects is not dependent for its existence on collisional coupling and persists even in the limit of infinite mean free path. Furthermore, the fact that the particles of a plasma are electrically charged gives rise to new effects for which there are no analogies in a classical gas, since the plasma is a dynamic, electrically conducting fluid capable of interacting with and producing electromagnetic fields.

Since the understanding of collective effects in even ordinary gases has developed only slowly over many years, it seems clear that the whole manifold of new effects possible in a plasma will preclude any comprehensive understanding of its behavior for years to come. But despite the formidable nature of this task, substantial theoretical advances have been made in the last few years in formulating the basic equations and in extracting many interesting predictions from them as to various possible modes of behavior of a plasma. Unfortunately, few of these predictions, and in most cases only the simplest ones, have been subjected to experimental confirmation. The origin of one of the difficulties of experimental work, i.e., the coupled nature of the problem and its investigation, has been discussed earlier. Because of the existing deficiencies of understanding, in a survey article such as this one can do little more than to present some of the basic equations as they are now understood and try to summarize isolated predictions which can be made from them. In the following section some of the basic equations of motion of a plasma will be briefly reviewed. Because nearly all high-temperature plasma research is perforce carried out in an environment of strong magnetic fields, this aspect of the problem will be emphasized.

Equations of motion: general.—There exists, in principle, a straightforward method for calculating the whole panoply of collective behavior in plasma. This would be to solve for the self-consistent motion of each plasma particle in the total electromagnetic field produced by the motion of all of its neighbors and by the influence of known external charges and currents. If a solution were known at any time, the future evolution of the plasma system could be predicted. Like many other examples in physics, this ambitious prescription fails because of its generality. Except in special cases, systems composed of 10^{17} or so charged particles are just too complicated to be analyzed in this manner. Nevertheless, there is much to be learned from this "kinetic theory" type of approach, especially since it rests on a firm intuitive base in the limit of strong external fields and low plasma density—the familiar case encountered in the analysis of particle accelerators.

The general equation of motion of a single charged particle of mass M and charge Z in a given external electromagnetic field is

$$M \frac{dv}{dt} = Ze \left(E + \frac{v}{c} \times B \right). \quad 16.$$

In the general case, the orbits predictable from this equation can be arbitrarily complicated. A great simplification results in the limit of strong magnetic fields, weak electric fields, and velocities such that $v/c \ll 1$. In this limit the motion of the charged particle is helical in nature, so that at any instant of time a "guiding center" can be defined. Superposed on this helical motion there will be various drift motions, expressible as motions of the guiding center. These guiding-center drifts will arise from the action of the electric field and from spatial inhomogeneities of the magnetic field. They have been treated extensively by Gunn, Alfvén, Spitzer, and others and will only be briefly listed here.

The simplest but most fundamentally important drift arises when there is a component of \mathbf{E} perpendicular to \mathbf{B} . In this case, a simple transformation of co-ordinates to a frame moving at the velocity $c[(\mathbf{E} \times \mathbf{B})/B^2]$ renders \mathbf{E} zero in that frame so that the motion is again helical. Thus the guiding centers of both positive and negative particles will drift in the same direction at the velocity $v_0 = c(E/B)$ independent of their mass or charge. This drift is an essential mechanism in many aspects of the collective behavior of a plasma, including its instabilities. One way of describing its origin is to identify the drift with the fact that a plasma, being a highly compressible conducting fluid, tends to move and to distort so that the local electric field everywhere within the plasma (in its local frame of reference) is zero.

If the magnetic field is inhomogeneous, other drift motions occur. A gradient of magnetic field perpendicular to the direction of the field produces a drift of magnitude

$$v_b = \frac{\rho_e v_{\perp}}{2} \frac{\nabla_{\perp} B}{B} \text{ cm. sec.}^{-1} \quad 17.$$

where ρ_e is the radius of curvature of the particle orbit and v_{\perp} is its rotational velocity component. This drift arises simply because of the difference of radius of curvature of the path of the particle as it rotates in the field. The drift is therefore perpendicular both to the field and the direction of the gradient and is oppositely directed for positive and negative charges. It thus can give rise to an electric current and to electrostatic fields, from the resulting charge separation.

If particles are moving in helical paths along the field lines, the curvature of these field lines will produce centrifugal accelerations which will also produce a drift. This drift, which is perpendicular to the field direction and to a plane containing the local radius of curvature of the field lines, is also oppositely directed for positive and negative charges and can give rise to currents and charge separations. The magnitude of the centrifugal drift is

$$v_c = \frac{v_{\parallel}^2}{R\omega_e} \quad 18.$$

where ω_e is the gyromagnetic or cyclotron angular frequency of rotation of the particle in the field and R is the local radius of curvature of the magnetic field lines.

The centrifugal drift is an example of a more general "gyroscopic" drift that can be expected to occur whenever the plasma particles are subjected to a force which is perpendicular to the local direction of the magnetic field. Another example is the drift v_g which will occur in the presence of a gravitational field. Since in a gravitational field a helically moving particle will lie in a region of lower potential energy at the bottom of its orbit circle than when it is at the top, it will be moving faster at this point than at the top. Thus its radius of curvature will be longer below than above, and a drift will result. The magnitude of this drift velocity is

$$v_g = \frac{g_{\perp}}{\omega_c} \quad 19.$$

where g_{\perp} is the component of g which is perpendicular to the direction of the magnetic field and ω_c is the gyromagnetic angular frequency of the particle. The quantity v_g is oppositely directed for electrons and ions, being much larger for the latter. It is found that v_g is usually too small to be of any practical importance in plasma research, being of order 10^{-4} cm./sec. for a proton in a magnetic field of 10^4 gauss. It is, however, of heuristic importance in the understanding of certain plasma instabilities which will be discussed and may play a role in geophysical phenomena.

It is well-nigh impossible to study a plasma in the laboratory without encountering magnetic field gradients and therefore encountering the drifts v_b and v_c . Since either can give rise to charge separation effects, unless care is taken in the choice of the field geometry, electrostatic fields within the plasma can be set up which will cause the $\mathbf{E} \times \mathbf{B}$ drift v_0 to occur, leading to a rapid escape of the plasma. Examples of this effect will be cited in a later section.

Equations of motion: adiabatic invariants.—A more precise way to state the restrictions which have been placed on the equation of motion 16, in deriving the drift motions v_0 , v_b , and v_c , is to note that they are equivalent to requiring that the fractional variations in the magnetic and electric fields in space shall be small over distances of the order of the diameter of the particle orbit and also that they shall vary sufficiently slowly with time so that the fractional variation during a time equal to the reciprocal of the angular frequency of the particle is small. This "adiabatic hypothesis" is well satisfied in many cases and forms a powerful starting point for analysis. Mathematically stated, the conditions on the magnetic field variations are that

$$\lambda_B = \left| \frac{\nabla B}{B} \right|^{-1} \gg \rho_0 = B \frac{v_{\perp}}{\omega_c} = \frac{M v_{\perp} c}{ZeB} \quad 20.$$

$$t_B = \left| \frac{1}{B} \frac{\partial B}{\partial t} \right|^{-1} \gg \omega_c^{-1} = \frac{Mc}{ZeB}. \quad 21.$$

It is clear that both conditions are much more easily satisfied for electrons than for positive ions. As a matter of fact, it is difficult to achieve situations which will violate the conditions as applied to electrons. To illustrate this

point, if $B = 10^4$ gauss and the particle energy is 10^4 volts, then 20 implies, for electrons, that $\lambda_B \gg 0.034$ cm. It would take a steep field gradient indeed to violate this condition. Similarly, for electrons, 21 requires that $t_B \gg 5.7 \times 10^{-12}$ sec., a condition which would be almost impossible to violate, except through the agency of some very high-frequency plasma oscillation. On the other hand, protons under the same circumstances would satisfy the conditions for adiabatic behavior only if $\lambda \gg 1.5$ cm. and $t_B \gg 1.1 \times 10^{-8}$ sec.; these are substantially more restrictive conditions but still often satisfied. Of course, at low B values the conditions 20 and 21 are less likely to be satisfied, since both vary as $1/B$.

The conditions for adiabatic behavior given above have an important consequence. Under these conditions the angular momentum of motion of the particle around its guiding center remains constant as it moves along the field lines, and the magnetic moment $\mu = W_{\perp}/B$ is a so-called adiabatic invariant of the motion (13). The adiabatic invariance of μ to all orders in an expansion in powers of $\epsilon = \rho_e/\lambda$ has been proved by Kruskal (14), Hertwech & Schluter (15), and others. In effect these authors show that the maximum value of the magnitude of the fractional fluctuations in magnetic moment, $|\delta\mu/\mu|$, which occur as a particle moves from region to region in the field can be expected to be expressible in a form such as

$$\left| \frac{\delta\mu}{\mu} \right|_{\max} = ae^{-b/\epsilon} \quad 22.$$

where a and b are "constants" appropriate to the detailed shape of the field in which the particle is moving. Although the values of a and b are not quantitatively predicted by theory, numerical calculations (16) in specific cases indicate that a and b are typically about equal to 1. It follows that for all $\epsilon = \rho_e/\lambda$ less than about 0.1 the value of μ should remain very nearly constant, in the absence of perturbing forces (such as collisions). There is additional evidence that the normal variations in μ may be cyclic and not random, so that μ will remain bounded throughout the motion. The general validity of this picture of the constancy of μ over periods as long as 10^{13} revolutions of the particles (in this case electrons) is being verified in detail by experiments which are now being conducted (17) and is an important recent development in the understanding of charged-particle dynamics.

One important consequence of the constancy of μ is that it implies that a charged particle will maintain constant magnetic flux through the plane of its helical orbit as it moves. Thus, in coursing through a varying magnetic field, each charged particle (if adiabatic) maintains a constant flux through its orbit circle. In many situations this implies that the plasma as a whole will preserve flux as it moves, so that in moving from a region of weak field into a strong field or in being subjected to an increasing magnetic field, the plasma will compress in obedience to the flux conditions. This behavior is also intimately related to the E/B drift velocity mentioned earlier, since in maintaining constant flux the plasma particles are moving so as to trans-

form the local E field to zero in their frame of reference. This concept can be generalized to yield another adiabatic invariant of the motion, for magnetic fields slowly varying in time.

The fact that a spiraling particle possesses a magnetic moment implies that, in moving in the presence of a field gradient, it experiences a force

$$F = -\mu \nabla B. \quad 23.$$

The constancy of μ implies that this can equally well be written as

$$F = -\nabla(\mu B) \quad 24.$$

showing that (μB) acts as a potential. Thus, in moving along field lines into a region of increasing magnetic field, a charged particle may be reflected. This is the familiar "magnetic mirror" effect, dating back to Störmer's pioneer work in the reflection of cosmic rays by the earth's field.

An important consequence of Equation 24 is that it shows that it is possible to trap charged particles between regions of strong magnetic field by taking advantage of this force. Since, at the point of reflection, the entire energy of the particle resides in rotatory motion, the trapping condition is merely that

$$\mu B_{\max} > W \quad 25.$$

where B_{\max} is the least maximum of the two regions of strong field bounding the central region. Equation 25 will be discussed in more detail in a later section in connection with one of the possible methods of magnetically confining a hot plasma, the "Mirror Machine."

The magnetic moment is not the only adiabatic invariant applying to the motion of charged particles in a magnetic field. If particles are trapped and execute periodic orbits along the field lines, as in the example above, then another important invariant governs the motion. This invariant is the action integral, i.e., the integral of the parallel component of momentum, taken along the path of the guiding center of the particle. This integral, familiar to students of classical mechanics as a special case of Liouville's theorem, is:

$$\oint p_{\parallel} du = A = \text{constant}$$

The complete validity of A as an adiabatic invariant for fields which vary slowly during the period of one reflection has only recently been established. The existence of this invariant has important practical consequences. It can be used to demonstrate that nearly adiabatic particles, in performing periodic trapped motions within a given region of space, even though slowly drifting, will continue to move on certain well-defined surfaces and will not show any tendency to "walk" radially in the field, provided it satisfies certain rough conditions of symmetry. This circumstance, first put forth by Teller (18), has been borne out by the findings of the Argus experiment (19) concerned with the trapping of "man-made" charged particles in the earth's magnetic field above the stratosphere.

For purposes of computing the essential details of the motion of trapped particles where the trapping magnetic field changes its intensity or shape slowly with time, the two adiabatic invariants can be combined into a single useful integral (20). If u_1 and u_2 denote the co-ordinates (measured along a field line) of the "high-water marks" of a trapped particle, then the evolution of these high-water marks is determined by the equation

$$[B(0, t)]^{1/2} \int_{u_1}^{u_2} (R_M - R)^{1/2} du = S = \text{constant}. \quad 26.$$

Here $B(0, t)$ is the minimum value of the magnetic field within the trapped region ($u=0$, by definition), $R(u, t)$ is the ratio of the magnetic field at u to that at $u=0$ and R_M is the value of R at u_1 and u_2 (the same at both). The equation may also be written as an integral over R , which is sometimes more convenient to use. It is

$$[B(0, t)]^{1/2} \int_{R_M(1)}^{R_M(2)} (R_M - R)^{1/2} \frac{du}{dR} dR = S. \quad 27.$$

This latter expression can be used to derive an integral expression for Teller's invariant surface. Considering any two adjacent orbits (a) and (b) which lie on this surface and are characterized by the same value of S and R_M , one obtains by subtraction the result that the following integral must vanish for any pair of orbits lying on Teller's surface

$$\int_{R_M(1)}^{R_M(2)} (B_M - B)^{1/2} \left[\left. \frac{du}{dB} \right|_a - \left. \frac{du}{dB} \right|_b \right] dB = 0. \quad 28.$$

For systems of axial symmetry, the surface corresponds to the usual "flux surface" (i.e., a surface of rotation generated by rotating the magnetic lines about the axis). For approximately axially symmetric systems, such as the earth's field, the surface will also deviate from axial symmetry but, according to Teller's hypothesis, will still close on itself.

The method of analysis of plasma behavior by the use of adiabatic invariants is a powerful one which is coming into increasing use. As well as being useful for treating quasi-static situations, it can be applied to instability problems [see e.g. Rosenbluth & Longmire (21)]. It is probably the best one available for treating problems of plasma confinement, which will be touched on in a later section.

Pressure balance and the macroscopic equations.—To obtain an equation describing the collective properties of a plasma it is necessary to find a way to sum over the motions of the individual particles properly, retaining the important features of the system and eliminating higher order terms. Macroscopic plasma equations derived in this way are therefore approximations and do not provide a comprehensive representation. The starting point for most equations is the Boltzmann equation (22). [See (3) for a discussion of the deviation of macroscopic equations from the Boltzmann equation.] The Boltzmann equation is essentially a continuity equation which predicts the

evolution with time of the distribution function of each class of particles in the plasma under the influence of the force fields in which the particles move. Written for the i -particle component (i.e., electrons or one class of ions) the B equation is

$$\frac{df_i}{dt} + \mathbf{v} \cdot \nabla f_i + \left(\frac{\mathbf{F}_i}{M_i} \right) \cdot \nabla_{\mathbf{v}} f_i = \left(\frac{df_i}{dt} \right)_{\text{coll}}. \quad 29.$$

Specifically, $f_i(\mathbf{r}, \mathbf{v}, t) dxdydzdv_xdv_ydv_z$ is the number of particles which are in the indicated element of phase-volume at the point of 6-dimensional phase-space denoted by \mathbf{r}, \mathbf{v} . The quantity \mathbf{F}_i is the external force acting on the i th class of particles. The term $(df_i/dt)_{\text{coll}}$ represents the effect of collisions in causing the diffusion of f_i in phase-space, and generally will contain complicated integrals over phase-space.

The usual approximation in treating a high-temperature plasma problem by means of the Boltzmann equation is to set $(df_i/dt)_{\text{coll}} = 0$, thus ignoring slow changes in the system caused by collisions. This procedure is acceptable for obtaining quasi-static equilibria and for calculating non-equilibrium effects which are rapid (but not *too* rapid) compared to collision frequencies. Written this way, Boltzmann's equation is merely Liouville's equation—an equation of continuity in phase-space.

The Boltzmann equation provides a nearly rigorous means for deriving the macroscopic equation of momentum balance in a plasma. Physically, however, it is more informative to write down the equation from first principles and refer to the rigorous derivation for verification. In a manner similar to that used by Spitzer, we shall write down a total momentum- or force-balance equation for a volume element of each of two classes of particles (electrons and ions) and obtain the final equation by combination. Thus for the force-balance equation:

for ions:

$$-n_i M_i \dot{\mathbf{v}} + n_i e Z \mathbf{E} + n_i \frac{eZ}{c} \mathbf{v}_i \times \mathbf{B} - \nabla \cdot \mathbf{P}_i - n_i M_i \nabla \phi + \alpha(\mathbf{v}_e - \mathbf{v}_i) = 0 \quad 30.$$

for electrons:

$$-n_e m \dot{\mathbf{v}}_e - n_e e \mathbf{E} - n_e \frac{e}{c} \mathbf{v}_e \times \mathbf{B} - \nabla \cdot \mathbf{P}_e - n_e m \nabla \phi - \alpha(\mathbf{v}_e - \mathbf{v}_i) = 0. \quad 31.$$

Here the first term represents the inertial force; the second the force from the electric field; the third the force from the magnetic field; the fourth the divergence of the pressure (stress) tensor giving momentum transfer by particle flux [see (3) for a discussion of the stress tensor]; the fifth the gravitational force; and the sixth the dynamical friction force from relative motion of electron and ions, with α to be determined by collision equations.

In a plasma of other than vanishing density, one finds $n_e = Z n_i$ very nearly. Thus, adding 30 and 31 one obtains

$$-\rho \dot{\mathbf{v}} + \frac{1}{c} \mathbf{J} \times \mathbf{B} - \nabla \cdot \mathbf{P} - \rho \nabla \phi = 0 \quad 32.$$

where

$$\begin{aligned}\rho &= n_i Z m + n_e M, \text{ the mean density} \\ P &= P_e + P_i, \text{ the total plasma pressure} \\ v &= \frac{m Z v_e + M v_i}{m Z + M}, \text{ the net mass velocity} \\ J &= n_e e Z (v_i - v_e), \text{ the electric current density.}\end{aligned}$$

The gravitational force is usually totally negligible, and the acceleration terms are small except for very rapidly varying forces. Thus, for quasi-static cases Equation 32 reduces to

$$\nabla \cdot P = \frac{1}{c} J \times B \quad 33.$$

showing that the pressure (stress) tensor must be balanced by electrodynamic forces from currents flowing in the plasma. This points up the non-equilibrium nature of the magnetic confinement of a plasma, since currents imply dissipation of energy, which must either be supplied by diffusion of the magnetic field into the plasma or by a continuous influx of new particles.

Multiplying 30 by M and (31) by $(-m)$ and adding, a current equation is obtained (gravitational force ignored)

$$\frac{M}{e} \dot{v} - \frac{m}{n e^2} j + E + \frac{v}{c} \times B - \frac{1}{n e} \nabla \cdot P_i - \frac{\alpha}{n^2 e^2} j = 0. \quad 34.$$

The inertial J and dynamical friction terms are usually small, so that 34 becomes an equation from which E can be determined

$$E + \frac{v}{c} \times B - \frac{1}{n e} \nabla \cdot P_i = 0. \quad 35.$$

If there is no net mass motion or mass rotation ($v=0$) then

$$E = -\frac{1}{n e} \nabla \cdot P_i. \quad 36.$$

Equation 32 can be used to yield a simple and informative pressure balance equation. An axially symmetric "natural" co-ordinate system is chosen, in which the direction of the co-ordinate also is related to the local direction of the field lines as shown in Figure 11.

The unit vector n lies in the direction B , t is directed toward the axis as shown, and p lies tangent to the flux surface. In this co-ordinate system the pressure tensor takes on the diagonal form

$$P = \begin{pmatrix} P_{\parallel} & 0 & 0 \\ 0 & P_{\perp} & 0 \\ 0 & 0 & P_{\perp} \end{pmatrix} \quad 37.$$

corresponding to two equal "perpendicular pressure" components P_{\perp} at right angles to the field line, and a "parallel pressure" component P_{\parallel} along

FIG. 11. Unit vectors n and t in relation to field line.

the field lines. P may also be written in the form

$$P = P_+ \Pi + P_- nn \quad 38.$$

where

$$P_+ = P_{\perp} \quad \text{and} \quad P_- = P_{\parallel} - P_{\perp}.$$

Thus

$$P = \begin{pmatrix} P_{\perp} & 0 & 0 \\ 0 & P_{\perp} & 0 \\ 0 & 0 & P_{\perp} \end{pmatrix}^* + \begin{pmatrix} P_{\parallel} - P_{\perp} & 0 & 0 \\ 0 & 0 & 0 \\ 0 & 0 & 0 \end{pmatrix}^{\dagger} \quad 39.$$

* P_+ = ordinary scalar pressure of magnitude P_{\perp}

† P_- = parallel pressure only, magnitude $(P_{\parallel} - P_{\perp})$

Thus expression 33 becomes

$$\begin{aligned} \Delta \cdot P &= \nabla \cdot (P_{\perp} \Pi + (P_{\parallel} - P_{\perp}) nn) \\ &= [\nabla P_+ + \nabla \cdot (P_- nn)] = J \times B. \end{aligned} \quad 40.$$

Two separate pressure-balance equations are obtained where the parallel and perpendicular components of this equation are combined. Now $J \times B$ is \perp to B , so that the \parallel component of 40 is zero, i.e.

$$\begin{aligned} (\nabla \cdot P) \cdot n &= 0 = [\nabla P_+ + \nabla P_- + \nabla \cdot (P_- nn)] \cdot n \\ &= \nabla P_+ \cdot n + \nabla P_- \cdot n + P_- (\nabla \cdot n) + (n \cdot \nabla) n \cdot n. \end{aligned} \quad 41.$$

But

$$n = \frac{B}{|B|}$$

so that

$$\begin{aligned} \nabla \cdot n &= \frac{1}{|B|} \nabla \cdot B - \frac{1}{B^2} B \cdot \nabla B \\ &= -\frac{\nabla B}{B} \quad \text{since} \quad \nabla \cdot B = 0. \end{aligned}$$

Also $[(n \cdot \nabla) n] \cdot n = 0$. Thus the parallel equation is

$$(\nabla \cdot P)_{\parallel} = 0 = \nabla P_+ + \nabla P_- + P_- \left[-\frac{\nabla B}{B} \right]_{\parallel} \quad 42.$$

i.e.

$$\nabla P_{\parallel} \Big|_{\parallel} = - (P_{\perp} - P_{\parallel}) \frac{\nabla B}{B} \Big|_{\parallel}. \quad 43.$$

The p component can be obtained in a similar way. Here the equation is

$$[\nabla \cdot P] \cdot p = - \frac{1}{c} [J \times B] \cdot p. \quad 44.$$

Since $\nabla \times B = (4\pi/c) J$, one obtains

$$\begin{aligned} \left[\nabla \left(P_{\perp} + \frac{B^2}{8\pi} \right) \right]_{\perp} &= \left[\frac{B^2}{4\pi} + (P_{\perp} - P_{\parallel}) \right] [(n \cdot \nabla) n] \\ &= \left[\frac{B^2}{4\pi} + (P_{\perp} - P_{\parallel}) \right] \frac{1}{R} \end{aligned} \quad 45.$$

where R is the radius of curvature of the magnetic lines, negative if the lines are concave toward the axis, positive if they are convex.

Equation 43 and 45 define the required conditions for a magnetostatic pressure balance in an axially symmetric field of arbitrary configuration. If $P_{\perp} = P_{\parallel}$ these equations reduce to the ones for a scalar pressure given by Spitzer. Note that it is not possible to support a pressure-gradient parallel to a field line if the pressure is a scalar.

Equation 45 is an important equation for the whole field of high-temperature plasma research, since it shows the manner in which a magnetic field can support a radial plasma pressure gradient, and thus shows how a plasma can be confined by a static magnetic field. In any region of the field which is parallel to the axis (such as the central region of a long solenoid), the right-hand side of 45 vanishes and the resulting equation yields

$$P_{\perp} + \frac{B^2}{8\pi} = \text{constant} = \frac{B_0^2}{8\pi}. \quad 46.$$

The presence of a plasma pressure component p_{\perp} therefore results in a diamagnetic depression of the field strength inside the plasma by an equal amount.

This shows that the diamagnetism of the plasma is to be identified with the \perp -component of the pressure. This in turn can be traced to the net magnetic moment per unit volume, derivable from the individual magnetic moments μ of the particles.

It is often convenient to measure the confined-particle pressure in units of the external magnetic pressure (energy density) to yield the dimensionless unit

$$\beta \equiv \frac{P_{\perp}}{(B_0^2/8\pi)}. \quad 47.$$

With this definition, 46 takes the form

$$= 1 - \left(\frac{B}{B_0} \right)^2. \quad 46.1$$

The parameter β can obviously never exceed unity, since $\beta=1$ corresponds to complete exclusion of the magnetic field from the interior of the plasma. In many cases other considerations, such as the onset of hydro-magnetic instabilities, will limit the allowable values of β even further. Thus β is both an index of the degree of trouble to be expected in the magnetic confinement of a plasma and a measure of the efficiency of utilization of the magnetic field in confining the plasma.

For any given applied external magnetic field it is possible to find an infinity of possible solutions to 43 and 45, which serve merely to define the required relationship between P_{\perp} , P_{\parallel} , and B in order to produce magnetostatic equilibrium. However, other physical conditions imposed on the system will usually limit the number of physically possible solutions. For example, one factor controlling the allowed solutions will be collisional diffusion. In the presence of diffusion losses the decaying plasma will automatically tend to take up a particular distribution, corresponding to the lowest-mode solution to the equation of diffusion of the plasma in the magnetic field. Another factor controlling the allowed solutions will be the onset of hydro-magnetic instabilities alluded to in the discussion of the parameter β . Examples of these limitations will be discussed in connection with plasma instabilities.

Diffusion of a plasma across a magnetic field.—It has been shown that it is possible to sustain a pressure gradient in a plasma only if currents flow within the plasma. The existence of persistent currents must imply that the entropy of the system is increasing, since ordered currents flowing in a conducting medium must result in the transformation of ordered energy into disordered energy, unless the medium is a superconductor. If a plasma system is isolated within a confining magnetic field and no sources of particles or energy are present, then the entropy change of the plasma must be accompanied by an outward diffusion across the magnetic field. The energy to maintain the persistent currents must in this case come from an incoming flow of magnetic-field energy as the two fluids, plasma and magnetic field, intermingle. This situation resembles very much the diffusion of a suddenly applied magnetic field into an ordinary conductor. The initial penetration of the field into the conductor is prevented by a pattern of eddy currents. As the eddy currents decay, the field penetrates into the conductor. A plasma is also a conductor, a conducting fluid, and a similar description can be given of the penetration of magnetic field into a plasma. The energy to maintain the eddy currents in the case of the plasma cannot be derived from the internal energy of the plasma itself, since this would constitute a violation of the Second Law of Thermodynamics. The presence of internal sources of energy or of particles could, of course, allow the attainment of a steady state.

The physical laws for the diffusion of a plasma across a magnetic field are most easily understood on the particle picture if the diffusion is visualized as the result of a continuous random-walk process of the plasma particles. Collisional encounters with neighboring particles serve to displace the guid-

ing center of a particle a distance of the order of the cyclotron radius of curvature of the particle per "large" scatter. The composite behavior of the plasma is then the summation of these individual effects. The mean distance that a given particle may diffuse from its original starting point per unit time will thus be proportional to the square root of the number of steps per unit time and to the length of each step. The diffusion rate is thus reduced either if (a) the density is reduced or if (b) the magnetic field is increased. It is also intrinsically more rapid for ions than for electrons, because of their larger orbit radii.

Returning now to the macroscopic picture of plasma diffusion across a field, we see that interparticle collision processes, since they are dominated by the energy-dependent Coulomb cross section, will occur only at a very slow rate in a low-density, high-temperature plasma. This means that the rates of decay of persistent plasma currents, originating in the dynamical friction effects associated with these collisions, may be very slow. Thus, if it is controlled by collisional processes alone, the velocity of diffusion of a plasma across a magnetic field would be correspondingly slow. This fact, of course, is the key assumption in all proposed methods of using "magnetic bottles" to establish a self-sustaining nuclear fusion reaction.

No general treatment of the problem of plasma diffusion across a magnetic field has been given. This is true in part because of the difficulty of the problem and the variety of situations possible. But another reason is that, according to the most recent theories, the intrinsic rates of diffusion of ions and electrons across a field are generally not the same, so that charge separation effects can be expected to occur, with the possibility of static electric fields within the plasma. No adequate way of treating the effect of such fields has been developed, so the existing treatments only strictly apply to those few cases where electric fields caused by charge separation can be ignored, either because their limiting values can be shown to be small compared to other quantities of interest, or because it can be shown that they cannot build up to their limiting values. An example of the last-mentioned case would be one in which the charge separation effects were nullified by the flow of new charges along the magnetic field lines from outside the system.

Spitzer (3) has given an expression for the diffusion drift velocity of a plasma across a magnetic field in the limit of very low β (magnetic field only slightly perturbed by the presence of the plasma). It is derived from the macroscopic electrical conductivity of a plasma, and applies to a plane plasma or to one of cylindrical geometry where the plasma radius is large compared to particle-orbit diameters. This expression is useful for estimating the magnitude of the diffusion effects but does not include some higher-order effects which will be discussed below. Spitzer's expression may be written as

$$v_d = - \frac{c}{\sigma} \frac{\nabla P_{\perp}}{B^2} \quad 49.$$

where σ is the transverse electrical conductivity of the plasma in cm^{-1}

(emu). With Spitzer's value for σ , Equation 49 becomes

$$v_d = -\frac{4}{3} \frac{(2\pi m_e c^2)^{1/2}}{(kT_e)^{3/2}} c e^2 Z \log \Lambda \frac{\nabla P_\perp}{B^2} \text{ cm. sec.}^{-1} \quad 50.$$

Inserting the definition of β and expressing T_e in kilovolts, one obtains

$$v_d = -\frac{260}{T_e^{3/2}} \frac{Z \nabla \beta}{(1-\beta)} \text{ cm. sec.}^{-1} \quad 51.$$

At high temperatures this corresponds to a very slow velocity and a correspondingly small outward flux of particles. This total flux is given by $F_P = n v_d = n_i (1+Z) v_d$. If the electron temperature and ion temperature are T_i and T_e , respectively, and the ion temperature is written as $T_i = \alpha T_e$, then since

$$\beta = \frac{n_e k T_e + n_i k T_i}{B_0^2 / 8\pi} = n_e k T_e \frac{1 + \alpha Z^{-1}}{B_0^2 / 8\pi},$$

$$F_d = -\frac{3.2 \times 10^9}{T_e^{3/2}} \left(\frac{1+Z}{\alpha+Z} \right) Z B_0^2 \frac{\nabla \beta^2}{(1-\beta)} \text{ particles cm}^{-2} \text{ sec.}^{-1} \quad 52.$$

The corresponding kinetic-energy flux is $Q_d = \overline{W} F_d$. Since $\overline{W} = \frac{1}{2}(1+\alpha)kT_e$,

$$Q_d = -\frac{0.78 \times 10^{-6}}{T_e^{3/2}} \left[1 + \frac{1+\alpha Z}{\alpha+Z} \right] Z B_0^2 \frac{\nabla \beta^2}{(1-\beta)} \text{ watts cm.}^{-2} \quad 53.$$

To take an example, if $B_0 = 10^4$ gauss, $\alpha = Z = 1$, and $T_e = 10$ kev, then $F_d = 10^{15} \nabla \beta^2 / (1-\beta)$ particles cm.⁻² sec.⁻¹ and $Q_d = 5.0 \nabla \beta^2 / (1-\beta)$ watts/cm.² If $\beta = 0.1$, setting $\nabla \beta^2 \approx \beta^2 / L$ with $L = 10$ cm. for example, then $F_d \approx 1.1 \times 10^{12}$ particles/cm.²/sec. and Q_d would be only 5 mw/cm.² These loss rates are exceedingly small and illustrate the potential effectiveness of a strong magnetic field in inhibiting the diffusion of a plasma. Unfortunately it has not yet been possible, as far as is known, to set up any experimental situation in a high-temperature plasma where these predicted low rates could be experimentally verified. Other phenomena, such as instabilities, impurity effects, or other loss mechanisms, have always dominated the situation so that these theoretical diffusion losses would be undetectably small by comparison.

Examination of Spitzer's expression for the diffusion shows that the diffusion originates entirely from electron-ion collisions and that ion-ion collisions, which might be expected to be far more important, because of their large cyclotron orbit diameter, in fact make no contribution to the diffusion. Spitzer (3), Simon (22), and Longmire & Rosenbluth (23) have discussed this apparent paradox and have shown that like-particle collisions make no contribution to the diffusion in first order of an expression in powers of the orbit diameter over the gradient length, because of a fortuitous cancellation of moments, but that they do contribute in higher order. Also, although charge separation effects do not appear in first order, they do in higher order and may give rise to important, and as yet uncalculated, physical effects.

Longmire and Rosenbluth's result for the diffusion flux of particles of

type (1) arising from collisions with those of type (2) is as follows (to first order and in one dimension):

$$F_1(2) = \frac{4}{3} \left(\frac{2\pi m e^2}{kT} \right)^{1/2} \left(\frac{e e_2^2}{B^2} \right) \log \Lambda \left\{ \left(1 + \frac{e_1}{e_2} \right) n_1 \frac{\partial n_2}{\partial x} - \frac{\partial}{\partial x} n_1 n_2 \right\}. \quad 54.$$

The quantities e_1 and e_2 are the respective charges; m is the reduced mass $m_1 m_2 / m_1 + m_2$. In first order, no charge separation is predicted by 54, since it is readily verified that the net charge flux is zero, i.e., $e_1 F_1(2) + e_2 F_2(1) = 0$ in an originally neutral plasma.

For $m_2 \ll m_1$, i.e., for the diffusion arising from electron-ion collisions, Equation 54 reduces to Spitzer's expression 50. But, in addition, it predicts some interesting physical effects not predicted by 50. For example, consider the diffusion of a small, high- Z , thermalized impurity component immersed in a hydrogenic plasma of constant density. Taking $m_2 = M_p$ and the impurity mass $m_1 = A M_p$, one finds that Equation 54 predicts that the rate of diffusion of impurity ions into the hydrogenic plasma is independent of their charge! Furthermore, for the same gradient of impurity density, the diffusion proceeds at a rate which is substantially faster than "normal" diffusion rates (for example as predicted by Equation 50). The factor of increase is $[A/(A+1)]^{1/2} (M_p/m_e)^{1/2}$, i.e., about 37 for $A=3$, for example.

At the same time, the presence of a very small percentage of impurity ions could substantially enhance the velocity of diffusion of, say, a hydrogenic plasma. This is because ion-ion collisions between nonidentical ions can now become important since the first-order moments do not cancel for this type of collision. If both the hydrogen-ion and impurity components have the same spatial distribution then one finds from expression 54 that the presence of a small high- Z ion component of particle density ϵ times the particle density of hydrogen ions would be expected to produce a diffusion flux which would be

$$\left\{ \epsilon \left[\left(\frac{A}{A+1} \right) \frac{M_p}{m} \right]^{1/2} \frac{Z(Z-1)}{2} \right\} \quad 55.$$

times as great as the "normal" $e-i$ diffusion flux. Thus, stripped oxygen ions ($A=16$, $Z=8$) would produce a rate 1160 ϵ times the normal rate, so that an oxygen impurity component of only 0.1 per cent would about double the diffusion rate, as compared to the normal value.

If the collisions between identical particles ($e-e$ or $i-i$) are to be considered, then the flux predicted by 54 formally vanishes and higher derivatives must be retained in the derivation. In this case Longmire and Rosenbluth's results take the form

$$F_1(1) = \frac{8}{15} \left(\frac{\pi m_1 e^2}{kT} \right)^{1/2} \left(\frac{e e_1^2}{B^2} \right) \left(\frac{m_1 k T c^2}{e_1 B^2} \right) \log \Lambda \left\{ n_1^2 \frac{\partial}{\partial x} \left(\frac{1}{n_1} \frac{\partial^2 n_1}{\partial x^2} \right) \right\}. \quad 56.$$

Since $F_1(1)$ is seen to vary as $m_1^{3/2}$, the contribution of $e-e$ collisions to the diffusion as predicted by 56 is seen to be negligible compared to $i-i$ col-

lisions. These will, in turn, normally be small compared to the $e-i$ value of 54, the ratio being given approximately by

$$\frac{F_i(i)}{F_i(e)} \approx \left(\frac{R_i}{D}\right)^2 \left(\frac{M_i}{m_e}\right)^{1/2} \quad 57.$$

where R_i is the gyromagnetic radius of the ion and D a characteristic distance over which the density changes substantially. As long as $R_i \ll D$, expression 57 will be small. However, the presence of the mass ratio term means that unless (R_i/D) is small compared to $(m_e/M_i)^{1/4}$, i.e., small compared to about 0.15 for protons, the fluxes $F_i(i)$ and $F_i(e)$ will be of the same order. Thus if $B = 10^4$ gauss, for example, if the proton energy were 10^4 ev, then $R_i = 1.45$ cm. and D would have to be large compared to 10 cm.

The diffusion predicted by 56 does not follow the usual form of diffusion laws and clearly vanishes unless the particle-density variation is of quadratic or a higher power in the space co-ordinates.

It should be clearly emphasized that little if any experimental confirmation exists for the theoretical self-diffusion rates predicted by 50, 54, or 56. In those few cases where diffusion rates of plasma particles have been measured, as in the work of Simon and Spitzer (24, 24a), the plasma has been immersed in a large neutral-particle background and the diffusion has been dominated by ion-neutral collisions. In other cases, where the plasma was more completely ionized, as for example in the Princeton Stellarator experiments (49), other effects, such as instabilities, have dominated so that the observed diffusion was much more rapid than the "classical" values. Verification or refutation of these theoretical results must, therefore, still await the experimental achievement of a quiescent and highly ionized plasma.

Waves and oscillations in a plasma.—One striking manifestation of collective effects in a plasma is its ability to support oscillations and to propagate waves which have no classical analogues. The detailed anatomy of these waves and oscillations is very complicated, and no attempt will be made in this article to do other than sketch their gross characteristics. The reader is referred to the now voluminous literature on the subject for further details.

Generally speaking, one way of classifying waves in a plasma is on the basis of relative frequency of the oscillation. If the frequency of a stimulated oscillation is so low that it is less than the collision frequency of the particles, and if the dimensions of the plasma system are large compared to a mean free collision path, an ordinary sound wave can be propagated through a plasma. Under most circumstances of interest these requirements are not satisfied, however, and sound waves will not be propagated. However, all other waves in a plasma are basically electromagnetic in nature and are therefore propagated through the interplay of charges, currents, and magnetic fields in the plasma, and collisions play a secondary role.

The presence of a magnetic field and the electrically conducting nature of a plasma introduce a kind of coupling between the particles which permits

the existence of a new kind of low-frequency wave—the Alfvén or hydromagnetic wave. Since the plasma and the magnetic field tend to move together (see the earlier discussion of $E \times B$ drift and the flux-preserving character of the individual-particle motions), a wave, similar in some cases to an elastic wave in a crystal, can be propagated through a plasma immersed in a magnetic field. Heuristically speaking, the magnetic-field lines act as elastic bands, "loaded" with the mass density of the plasma, so that the velocity of propagation depends both on the magnetic stress tensor and on the total mass density of the plasma but is independent of the charge or energy of the plasma particles. For simple waves of this type propagated in the direction of the field lines, the wave velocity is given by the expression:

$$v_a = \sqrt{\frac{B^2}{4\pi\rho}} \text{ cm. sec.}^{-1} \quad 58.$$

The index of refraction of these waves (c/v_a) is seen to be

$$\nu = \sqrt{\frac{2\rho c^2}{(B^2/8\pi)}} \quad 59.$$

i.e., the square root of twice the density of mass energy divided by the density of magnetic-field energy. In most plasmas $\nu \gg 1$ corresponding to rather slow waves. For example if $B = 10^4$ gauss, $n_i = 10^{14}$ protons/cm.³, then $\nu = 270$ so that $v_a = 10^8$ cm./sec. In the limit of low plasma density or high magnetic fields the correct limiting expression for ν shows that $\nu \rightarrow 1$, and the wave becomes an ordinary electromagnetic wave.

Carrying forward this theme, one can easily show that the indicated low velocity of propagation of these waves can be identified with the fact that the plasma exhibits a high dielectric constant for low-frequency disturbances. The magnitude of this dielectric constant is

$$\epsilon = 1 + \frac{2\rho c^2}{(B^2/8\pi)}. \quad 60.$$

The Alfvén velocity follows from 60 in the limit $\epsilon \gg 1$.

In a simple situation, such as the propagation along a cylindrical column of plasma, the hydromagnetic waves can be of types similar to some of those which would be propagated along an elastic rod. Thus torsional and compressional waves can be propagated, with a large variety of possible radial velocity distributions, determined by the frequency, the mode of excitation, and the boundary conditions (25).

Simple Alfvén waves can exist up to a limiting frequency approximately defined by the cyclotron frequency of the ions in the plasma, at which point the wave becomes highly dispersive and another type of analysis must be applied. In this new regime "ion waves" can be excited which, in principle, permit resonance energy to be exchanged effectively between the ions and the oscillating electromagnetic field. It is hoped to take advantage of this fact in some proposed plasma-heating methods (26).

At frequencies above the ion cyclotron frequency, the plasma ions can no longer respond adiabatically to the fluctuating wave fields. For this regime the effects of motion of the electron cloud relative to the essentially stationary ions become of importance. But such relative motions will generally produce a charge separation and, therefore, a restoring electric field. This is the regime of the electrostatic plasma oscillation. In simple cases, such as for oscillations along magnetic field lines, these waves represent simply the possible oscillations of the electrons about the equilibrium charge position. In the simplest theory of these oscillations they are of fixed frequency, namely at the Langmuir or plasma frequency

$$\begin{aligned}\omega_p &= \sqrt{\frac{4\pi n_e e^2}{m}} \quad \text{radians/sec.} \\ &= 5.7 \times 10^4 n_e^{1/2}.\end{aligned}\quad 61.$$

Such an oscillation cannot properly be defined as a "wave" since it corresponds to a nonpropagating disturbance of arbitrary physical dimensions. However, J. J. Thomson & G. P. Thomson (27), Landau (28), Bohm & Gross (29), and others have shown that the effect of thermal velocities is to introduce a dispersion relation between frequency and wavelength of these simple (longitudinal) electrostatic oscillations. As derived by Bohm and Gross this takes the following form:

$$\frac{\omega^2}{k^2} = \frac{\omega_p^2}{k^2} + \frac{3kT_e}{m_e}.\quad 62.$$

If $kT_e \rightarrow 0$, this reduces to 61. Using the definition of the Debye length $\lambda_D = \sqrt{kT/\pi 4n_e e^2}$, 62 can be rearranged in the form:

$$\left(\frac{\lambda_D}{\lambda}\right)^2 = \frac{1}{12\pi^2} \left[\left(\frac{\omega}{\omega_p}\right)^2 - 1 \right].\quad 63.$$

For $\lambda \gg \lambda_D$, the frequency of oscillation must be close to ω_p . However, as $\lambda \rightarrow \lambda_D$ (or more exactly, $\lambda \rightarrow 4\pi^{1/2}\lambda_D$ as shown by Bohm and Gross), so that the plasma oscillation wavelength becomes comparable to the shielding distance, a limiting frequency is reached at $\omega_e^2 = (3\pi/4)\omega_p^2 \approx 2\omega_p^2$. Thus the frequency range of these oscillations is relatively narrow, being confined to a range less than an octave above the plasma frequency.

If this limiting frequency ω_e is larger than the electron cyclotron frequency, $\omega_c = eB/mc$, then the plasma is transparent to all waves of higher frequency, which are discernible as ordinary electromagnetic waves, propagating through a dispersive medium with a limiting index of refraction equal to $1 - \omega_p/\omega^2$. As a result of the definitions of ω_e and ω_c , the condition $\omega_e > \omega_c$ can be written as

$$n_e mc^2 > (B^2/8\pi)\quad 64.$$

i.e., the condition is equivalent to the requirement that the mass-energy density of the electrons exceeds the magnetic-energy density. If this condition

is not satisfied, the plasma will still exhibit a strong resonance anisotropy in its wave propagation characteristics for wave frequencies in the vicinity of the electron cyclotron resonance.

Resonance dispersion of an electromagnetic wave propagating through a plasma will occur whenever the direction and propagation velocity of the wave are such that an electric field in resonance with one of the elementary-particle motions can occur. Thus, as in the example just given of waves in the vicinity of electron gyromagnetic resonance, energy exchange effects will be large between the electrons and a circularly polarized electromagnetic wave rotating in the same direction as the electrons, and large dispersion in the propagation of this "extraordinary" wave will occur. The ordinary wave will, however, interact only weakly, so that it will be propagated freely through the plasma (along the field lines).

Plasma waves of the kinds which have been described are not only of academic interest but are also of importance to other aspects of plasma behavior. They may, for example, play a role in certain kinds of unstable behavior of a plasma, and they also strongly influence the nature of the radiation which can be emitted by the plasma at frequencies below the plasma frequency. Parenthetically, it is worth remarking that the amount of radiation which can be emitted by a quiescent high-temperature plasma in the microwave and long-wave length, infrared part of the spectrum is sharply limited by the Rayleigh-Jeans value and thus does not usually comprise an appreciable energy loss.

Plasma instabilities.—Again because the problem of confinement is the central one of high-temperature plasma research, the most intensive theoretical and experimental work of this field has gone into a study of the problem of instabilities. Theoretically, except for simple cases, the problem is very difficult, the treatments are involved, and the physical assumptions made in order to treat the problem are incomplete and often unrealistic. No attempt will be made in this article to detail the voluminous work in this field, but some of the more important results to date will be briefly reviewed.

In our present understanding of the instabilities of a plasma, at least two general classes into which they fall are now discernible. The first of these is the "interchange" or hydromagnetic instabilities which are loosely to be identified with the tendency of the plasma, as a hot gas, to expand against the magnetic field. In so doing it finds ways, in effect, to displace the magnetic field lines and escape through the region of weakened fields thus created. The clue to the possibility of this kind of instability is, therefore, to discover those situations in which a physically allowed outward perturbation of the plasma from its position of pressure equilibrium with the magnetic field will result in a weakening of the field in the vicinity of the perturbations, thus allowing the instability to grow and propagate. The name "interchange" instability arises from the concept, first put forth by Teller (30), of the growth of such instabilities by the mechanism of progressive in-

finitesimal interchanges of plasma between (a) regions of higher plasma and lower magnetic-field energy density and (b) adjacent regions of low relative plasma pressure and higher magnetic intensity. If any such displacement can be found which results in an expansion of the plasma without a compensating increase in the magnetic energy, it can be assumed that such a displacement will continue to grow, drawing its energy from the internal energy of the plasma via the expansion.

The second general class of instability mechanisms now understood to be operative in a high-temperature plasma might be called "velocity-space instabilities." These are instabilities associated with particular deviations of the plasma particle distributions from isotropic, Maxwellian form. They can be traced to the strong tendency of a nonequilibrium system to approach an equilibrium state, by attempting to minimize what might be called "pressure gradients in velocity space," analogous to the previously described tendency of the plasma to obliterate pressure gradients in co-ordinate space, i.e., to expand. Some of these velocity-space instabilities are associated with streaming flow in the plasma, such as that which occurs when a heavy electrical current is passed through the plasma. Generally speaking, being of velocity-space origin, instabilities of this type could occur even in an infinite plasma. In occurring in a finite plasma, this type of instability could be expected also to affect the confinement, because of its potentially strong effects on the particle motions.

(a) Interchange instabilities: The basic concept of the interchange instability is that a system of plasma and magnetic field in hydrostatic equilibrium is unstable against any infinitesimal perturbation which can be shown to leave the magnetic-field energy unchanged while allowing the plasma to undergo a net negative change in potential energy. The pioneer paper on this subject was written by Kruskal & Schwarzschild (31) who discussed the instability of the surface of a semi-infinite plasma supported from below against the force of gravity by a uniform magnetic field. In this paper they showed that the plasma surface would be unstable against any small ripple of the surface, in exactly the same way that the surface of a heavy liquid, supported from below against gravity by a gas, is unstable, even though it is in pressure equilibrium (try it with an inverted glass of water sometime). This classical or "Taylor" instability was shown by Kruskal & Schwarzschild to occur in the same way and at the same rate in the plasma case. However, for present purposes, the most important result of their paper was the elucidation of the physical mechanism of the growth of the instability. It was shown that the mechanism depended on charge separations induced by the oppositely directed drifts of velocities, v_θ , of positive ions and electrons under the combined influence of the magnetic field and the force of gravity. (See Eq. 19.) This charge separation produces an electric field which then continues to "drive" the instability through the mechanism of the $E \times B$ drift of Equation 17. This mechanism, i.e., a drift-induced charge separation, followed by a self-perpetuating $E \times B$ drift, is a common

denominator of every variety of interchange instability. This does not, however, imply that all situations where drifts and charge separation occur are unstable, since the signs of the final drift may be such as to oppose the original displacement. This is, for example, the case if the sign of g is reversed (i.e., the field lies above the plasma) in the Taylor-Kruskal-Schwarzschild-instability.

In a magnetically confined plasma the most important drifts producing charge separation are the centrifugal and gradient- B drifts v_e and v_b , respectively (Eq. 18 and 17). Since both of these effects originate from the presence of curved magnetic lines, whether or not a given field plasma configuration is stable depends on whether the combined effect of these drifts is to produce a self-perpetuating $E \times B$ drift or not. Since it is impossible to construct a finite confinement volume without encountering curved lines, the test is relevant to every case.

Rosenbluth & Longmire (21) have applied the above particle drift concepts to the problem of calculating hydromagnetic instabilities and have been able to deduce a criterion for the stability of a system of plasma and magnetic field against hydromagnetic disturbances, in the limit of $\beta \ll 1$. As applied to an axially symmetric system (either infinite or periodic) this can be written as an integral over a system period, along any field line of the system to which the criterion is to be applied. Thus the criterion for stability is that

$$\int \frac{(P_{\parallel} + P_{\perp})}{rRB^2} dl > 0 \quad 65.$$

Here r is the distance of the line of force from the axis of symmetry, and R is the local radius of curvature of the line, which will in general vary along the path of integration. The quantity R is counted as positive if the center of curvature lies outside the plasma and vice versa. The quantities P_{\parallel} and P_{\perp} have their usual definition as the plasma pressure components perpendicular and parallel to the field direction respectively.

It will be informative to consider some examples of the application of this result. First, it is to be noted that a uniform field ($R = \infty$) is neutrally stable, independent of the relative values of P_{\parallel} and P_{\perp} . (This will not turn out to be true when velocity-space instabilities are considered.) Second, a plasma system where the field curvature is everywhere toward the plasma is unstable under all conditions. An example is the confinement of a plasma solely by means of currents flowing in the plasma itself. This will be discussed in connection with the "pinch effect." In this case the instability had been earlier predicted in the papers of Kruskal & Schwarzschild and has been later and independently predicted by many other investigators. In this case the instabilities take the form of a necking off (sausage instability) or a violent helical distortion ("kink" or "corkscrew" instability).

Another case of considerable practical interest is that of a long axial field of periodically alternating strength, so that the field lines resemble a string

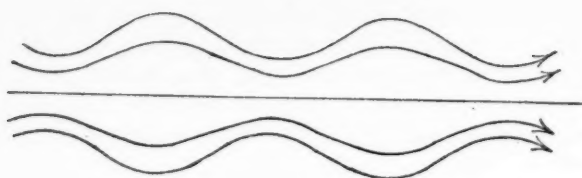


FIG. 12. Lines of force in an axial field of periodically alternating intensity.

of sausages, as shown in Figure 12. Such a field could be produced by a suitably chosen set of external coils.

In this case R is alternately positive and negative and it is not clear a priori whether the system is stable. Except for special cases where the variation of $(P_{\parallel} + P_{\perp})$ is such as to weight the regions of positive R sufficiently, such a system is predicted to be unstable, although it is clear that the instability is of a weaker degree than the pinch example above, where the magnetic field and the plasma are so intimately related that any motion of the plasma has an immediate and direct effect on the magnetic field. In the present case, the magnetic field originates from external metallic conductors and the instability cannot appreciably influence the confining field.

If the field consists of a periodic system of cusp-shaped regions, as shown in Figure 13, R will be everywhere positive and the system should be stable. This system presents certain practical difficulties, however. Such systems have been suggested, independently and in slightly different form by Tuck, by Grad (32), and by other investigators.

The stability criterion 65 sheds no light on the nature of the instabilities which would be expected to occur when it is violated. Such information must be obtained from a more detailed analysis. The most intensive work of this kind has been done by Bernstein *et al.* of the Princeton University group (33). They have shown that for the periodic "sausage" field example above and for other related cases the most likely form the instability will take is that of a fluted column, as shown in section in Figure 14. This instability, like other hydromagnetic instabilities of the interchange type, is predicted to grow at essentially the thermal speed of the ions. In a hot plasma this corresponds to a very rapid growth.

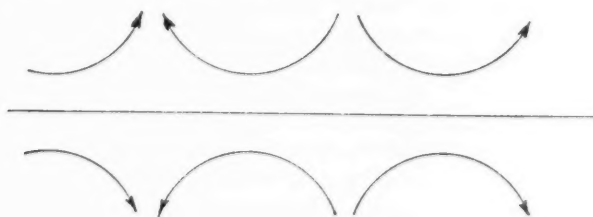


FIG. 13. Cusp-shaped magnetic field.

Since it has been shown in theory that most of the simplest magnetic-field geometries are likely to be hydromagnetically unstable, ways have been sought to shape the fields so that these instabilities might be suppressed. The analysis of these types of problems has turned out, not surprisingly, to be even more difficult than the development of stability criteria. Rather than to attempt to detail the many specific configurations which have been investigated, it appears more worthwhile simply to point out the basic principle which is common to all the methods of constructing theoretically stable configurations and let the reader pursue the details for himself in the literature.²

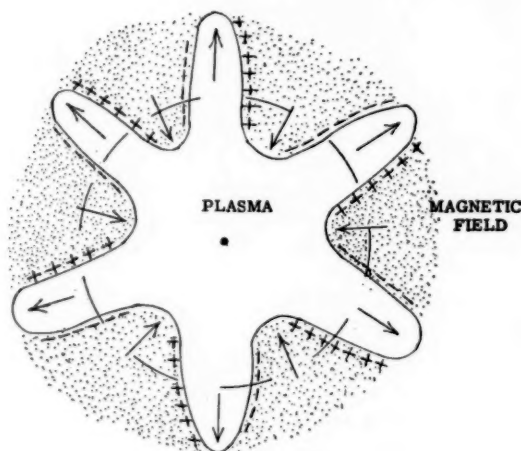


FIG. 14. Flute instability.

The basic principle by which a hydromagnetically unstable configuration can be rendered stable (in theory), as first elucidated by the Princeton group, is to introduce a sufficient degree of shear into the field configuration. Thus, if one considers the confining magnetic field (as in the sausage-shaped case above, for example) as made up of concentric shells of field lines, the stabilization prescription is to modify the field so that the lines in successive shells do not lie parallel to each other—i.e., so that they possess a shear. This effect could clearly be accomplished in the above example if a conductor were placed on the axis and a current passed through it. Since the magnetic field of this conductor falls off with radius in a manner different from the field produced by the external coils, a sheared field would be automatically produced. In many cases, however, it would not be possible to introduce a physical conductor into the interior of the confinement chamber, even on the axis, and other means of producing sheared fields must be sought. The

² For example, numerous papers in the *Proceedings of the Second International Conference for Peaceful Uses of Atomic Energy*, Volume 31 and 32.

Princeton group has shown that this is possible even for the closed toroidal geometry of the Stellarator, by use of special sets of helical windings on the outside of the confinement chamber.

Why a shear field should stabilize against interchange instabilities is easy to see. The field lines of successive flux shells cannot then simply displace uniformly to allow the plasma to pass between the lines but must undergo a more complicated distortion. If the shear is sufficient, this will require an increase in the magnetic energy which will exceed the plasma-pressure energy released in the expansion, thus inhibiting its occurrence. Roughly speaking, one has succeeded in making a basket-weave-like pattern of elastic field lines which is patently less pervious to the plasma than a bundle of parallel field lines.

It is clear from the theory of shear stabilization and from the physical picture which has been presented that such a procedure will only be effective if the value of β , the relative plasma pressure, is not too large. Perturbation of the applied field by the presence of the plasma always tends to destroy the shear and thus to render the system less stable. Thus, for any shear-stabilized system there will exist a critical value β_c above which instability will result. The actual value of β_c will, of course, depend greatly on the system under consideration, but typical values might range between 0.05 and 0.3.

Other possible methods of stabilizing against hydromagnetic disturbances exist. In general, they are based on finding ways to "stiffen" the reaction of the confining fields against perturbations by the distorting plasma. One such effect will be noted in connection with the Mirror Machine, an example of a device where the field lines leave the plasma and may be anchored in external conductors.

At this point it is worth pointing out that despite the prodigious theoretical effort which has been made to investigate this problem, only the most obvious features of hydromagnetic stability theory have been experimentally corroborated. Subtleties, such as whether or not there exist flute instabilities of a plasma confined by external fields or, even if they exist, whether they can be stabilized by shear fields, have not been explored. This is in part because of the difficulty of the problem, and in part because these theoretically weak instabilities have apparently often been obscured by much more violent disturbances of nonhydromagnetic origin. Furthermore, the theory has not yet been extended to include the effect of static electric fields, collisional damping, and the effect of finite orbit size, all of which are present in a real plasma and which may play an important role.

(b) Velocity-space instabilities: The hydromagnetic instabilities which have been discussed owe their origin to a strong tendency for the plasma to seek a state of higher entropy in co-ordinate space. Similar effects can be expected to exist in the realm of velocity space. Streaming motion, pressure anisotropy, and abnormal deviations in the energy dependence of the particle distribution functions all represent degrees of order which, since they represent states of low entropy, may allow instabilities to develop. These types of

instabilities have only recently been appreciated as being potentially important in the achievement of confined plasmas, since in the past the tendency was to blame any observed instability on hydromagnetic effects. It is now fairly clear, however, that velocity-space instabilities may explain some of the puzzling behavior of confined plasmas for which there is no simple hydromagnetic explanation.

One of the earliest predicted velocity-space instabilities is the one associated with unstable electrostatic plasma oscillations discussed by Bohm & Gross (34). Their analysis which applies to an "infinite" plasma with no magnetic field present shows that an initial perturbation can grow into an unstable oscillation of the plasma if the electron distribution function has a peak at a velocity which is substantially above the mean electron velocity—i.e., that a special group of high-energy electrons is present. If there are a sufficient number of these high-energy electrons (they need not comprise a very large fraction of the total number of electrons) the amplitude of the plasma waves will be expected to build up until they extract a sufficient amount of energy from the special group to eliminate the peak. Physically, the basic interaction mechanism arises from the fact that the anomalous electrons can become trapped in the trough of a plasma wave which moves with the same velocity as these electrons. In this way a continuous transfer of energy is possible between particles and waves. The requirement that such waves shall grow is merely that the transfer from the electrons is able to overcome the damping effect of collisions. This is possible provided the temperature is high enough and if the resonant wave has a wavelength appreciably greater than a Debye length. At shorter wavelengths the phenomenon known as "Landau damping" occurs and rapidly attenuates the wave. This latter effect is just a result of the disappearance of co-operative effects for distances shorter than a Debye wavelength.

Wave-particle interactions of the type just described are the simplest example of velocity-space instabilities in a plasma. When the plasma is immersed in a magnetic field, many new classes of waves become possible, and it can be expected that each will carry the potential of being excited by an appropriate anomalous particle velocity distribution. A wide variety of these possible wave-particle reactions has been discussed by Akhiezer *et al.* (35) in a recent paper. However, in these cases, the magnetic field constrains the particles to move in ways that may not be generally compatible with setting up a resonant interaction, so that even more special conditions may be imposed on the exciting streams. Harris (36) has treated the unstable electrostatic oscillations of a plasma immersed in a uniform magnetic field. Since he finds that the wavelengths of these unstable oscillations are relatively small, his analysis may also apply to more general cases. In Harris' case the stimulation of the oscillations arises from an assumed anisotropy of the electron velocity distribution, since free streaming is not possible (except along magnetic lines) in the presence of the magnetic field. Provided a sufficient degree of anisotropy exists in the electron distribution, Harris finds a formal condition (in

terms of the Nyquist diagram) for growing oscillations. It also can be shown from his work that in all cases the plasma will be stable against these oscillations, i.e., they cannot grow if the condition

$$\left(\frac{\omega_p}{\omega_{ce}}\right)^2 < 1 \quad 66.$$

is satisfied. This condition can be written, from the definitions of the quantities, as equivalent to the condition

$$\frac{n_e mc^2}{2(B^2/8\pi)} < 1 \quad 67.$$

i.e., the mass energy-density of the electrons must be less than twice the energy-density of the magnetic field. This condition can also be written so as to define a critical β -value for the electrons, by defining

$$\beta_e = \frac{n_e k T_e}{(B^2/8\pi)},$$

so that 66 becomes

$$\beta_e < 2 \frac{k T_e}{mc^2}. \quad 68.$$

This is a fairly stringent condition, especially at low electron energies. Lastly, further manipulation of 66 shows that it is equivalent to the condition that

$$\frac{\bar{r}_e}{\lambda_D} < 1 \quad 69.$$

i.e., the mean gyromagnetic radius of the electrons should be less than the Debye length. The physical significance of this condition is presumably that Landau damping becomes important when it is satisfied and guarantees the stability.

It is not at this time clear what the effect of these unstable oscillations might be on a confined plasma. They may do no more than to provide an additional mechanism (besides collisions) for smoothing out directional anisotropies in the velocity distribution of the plasma electrons. In many confinement schemes this would be of little consequence. In others, such as the pinch effect, however, which are critically dependent on the existence of flowing electron streams, the presence of such a randomizing mechanism could have serious consequences.

It is to be expected that the hydromagnetic modes of wave motion of a plasma may also experience particle-wave stimulation under the proper circumstances and exhibit velocity-space instabilities. The condition for the generation of such unstable hydromagnetic waves can be determined by examination of the dispersion relation for these waves in an infinite medium. If the direction of propagation of these waves with respect to the direction

of B is θ , then following Chandrasekhar, Kaufman & Watson (37) the condition for stability against such waves takes the form

$$\beta(1 - \eta) \cos^2 \theta + \frac{\beta}{2} \left(1 - \frac{1}{\eta}\right) \sin^2 \theta + 1 > 0 \quad 70.$$

Here

$$\beta = \frac{P_{\perp}}{(B^2/8\pi)} \quad \text{and} \quad \eta = \frac{P_{\perp}}{P_{\parallel}}.$$

When $\theta=0$ (propagation parallel to B) this condition defines a critical β for $P_{\perp} > P_{\parallel}$, since it becomes

$$\beta < \frac{1}{\frac{P_{\perp}}{P_{\parallel}} - 1}, \quad P_{\perp} > P_{\parallel}. \quad 71.$$

When $\theta=\pi/2$ (propagation perpendicular to B) the condition defines a critical β for the case $P_{\parallel} > P_{\perp}$. This is

$$\beta < \frac{1}{\frac{P_{\parallel}}{P_{\perp}} - 1}, \quad P_{\parallel} > P_{\perp}. \quad 72.$$

Note that neither of these conditions imposes any limitation on the stability for a scalar pressure, $P_{\perp} = P_{\parallel}$. Condition 71 can be combined with Equation 43 for the pressure-balance condition along magnetic lines to yield an interesting condition which reflects the restrictions imposed by both. The assumption is made that the regions of field are substantially larger than the unstable wavelengths of interest. In such a case the combined condition for stability becomes:

$$\left| \frac{\nabla P_{\parallel}}{P_{\parallel}} \right| < \frac{1}{\beta} \left| \frac{\nabla B}{B} \right|, \quad P_{\perp} > P_{\parallel}. \quad 73.$$

The reason for the existence of conditions such as 71 and 72 can be given a simple physical explanation. When $P_{\perp} > P_{\parallel}$ and expression 71 is not satisfied, the development of any momentary localized weakening of the field would result in creating a trapping region between two mirrors. This would result in an increased local population of particles with an excess of rotational energy, and thus in a further depression of the field which might then grow and burst, like a bubble. This kind of velocity-space instability has, therefore, sometimes been called a "mirror" instability.

The instability associated with failure to satisfy 72 with $P_{\parallel} > P_{\perp}$ has been called the "firehose instability" because of its close analogy with the well-known instability of high-pressure hose. In this case, the development of a local bending of the field lines results in the development of centrifugal force component (arising from the parallel motions associated with P_{\parallel}) which will lead to a growth of the field distortion.

The examples which have been given represent a few special cases of

what must be a very general class of plasma instabilities. It appears that instabilities of this type seem usually to be associated with a critical β -value below which they are either absent or grow too slowly to be of consequence, so that in many cases they should be avoidable by proper choice of physical conditions. However, in some confinement methods, such as the simple pinch, it is essential that a nonisotropic flow exist to sustain the confining fields. In these cases, velocity-space instabilities appear to present a potentially insuperable problem.

BASIC FORMS OF THE "MAGNETIC BOTTLES"

It has already been emphasized that the study of a high-temperature plasma cannot be separated from the problem of providing adequate confinement. Thus, to undertake any such study it is always necessary to invent or adopt some particular configuration of electromagnetic fields which can be seen to be able, at least in principle, to supply this confinement. The general approach which seems most nearly capable of satisfying these requirements is the "magnetic bottle"—i.e., a confinement region "constructed" from a pattern of static or quasi-static magnetic field lines. The assumption that this is the most promising general approach has been implicit in most of the discussion in this article. It is the author's opinion that other possible approaches which have been suggested, such as the use, alone, of intense radiofrequency fields for confinement, or various electrostatic confinement schemes, fall seriously short of satisfying the quantitative requirements of this problem, even though they may appear to be qualitatively feasible.

In this section some of the basic forms of magnetic bottle which have been proposed and which are being investigated will be briefly described. It would not be feasible to detail the manifold variations on these basic schemes which are also under study, but these variations usually involve details rather than any concepts basically different from those embodied in their ancestors.

A few years ago it was possible to make a simple division of all magnetic bottles into two distinct classes. This division was on the basis of whether the confining field was either (a) generated entirely by currents flowing within the plasma (the pinch effect) or (b) generated by currents flowing in external metallic conductors. Today this distinction is disappearing, particularly with regard to method (a), so that a considerable degree of crossbreeding can be detected. It is nevertheless instructive to act as if the division still existed and to discuss magnetic bottles from this viewpoint. For a more complete survey of the historical development of these approaches, the reader is referred to the excellent book of Bishop (38).

THE PINCH EFFECT

The earliest investigated, and what at first appeared to be the simplest and most promising "magnetic bottle" was based on the electrical phenome-

non known as the "pinch effect," the self-constriction of a current-carrying fluid. The first theoretical work on the pinch effect in a plasma was done by Bennett (39) although the effect had been recognized in liquid conductors for many years. Bennett's theory provided the pressure-balance equation for the pinch, i.e.,

$$I^2 = 2Nk(T_i + T_e). \quad 74.$$

In this equation, I = the total current in the discharge (ab amp) and N is the total number of ions ($Z=1$), or electrons, per centimeter in the pinched column. Note that nowhere in this relation does the physical dimension or the radial density distribution of the particles appear. These parameters are therefore presumably free to be determined by other physical conditions and constraints in the plasma, such as diffusion. If reasonable numbers are put in for N , T_i , and T_e , one will find that the currents required to sustain pressure equilibrium are quite large. For example, suppose $T_i = T_e = 10$ kev and $N = 10^{16}$ cm.⁻¹, appropriate to a column of 10 cm. diameter at a mean density of about 10^{14} cm.⁻³. In this case $I = 250,000$ amp.

In concept, the use of the pinch effect to produce a magnetic bottle is exceedingly simple. Starting with a chamber full of neutral gas, one would merely, in principle, initiate a discharge in the gas and then pass a high current through the discharge, thus constricting it and heating it by compressional and resistive heating effects. This simple concept was the basis of the first high-temperature plasma experiments initiated in England, in Russia, and in the United States. It was soon discovered, however, that this picture is grossly oversimplified, and the pinch is now known to be a much more complicated phenomenon than was first thought. Thus, the first simple idea of the pinch has undergone a continuous process of evolution until it is today hardly recognizable as a descendant. For this reason, a discussion of the pinch effect as a magnetic bottle must be somewhat historical in nature.

The first experimental observation of the pinch seems to have been made by Ware (40) in 1951; he found also that although a pinch could be created, it had a very transient existence. Ware's experiments were conducted in a toroidal chamber, the pinch current being induced into the plasma by transformer action. This was done in order to eliminate the losses of particles and energy which would be expected to occur if physical electrodes would be used. Figure 15 shows a sketch of such a toroidal pinch tube.

The experimental facts of Ware's work and of similar work by Tuck *et al.* (41) in this country and Kurchatov (42) in Russia were that, although a momentary pinch of the discharge plasma could be created, its duration was only about 1 μ sec., after which time the column was observed to break into violent turbulence and dissipated itself on the walls of the chamber. This was just the sort of behavior predicted by Kruskal & Schwarzschild (31). The instabilities observed were found to be either of the "kink" or the "sausage" type mentioned earlier.

If the motivation for pinch research had been merely that of the academic

pursuit of interesting plasma phenomena, the discovery of these instability effects would not have been a source of dismay but would merely have heightened one's interest in what otherwise might have been dull and uninformative behavior. However, in all cases, the research efforts in the various countries were being driven by the hope that they would lead to fusion power; thus the discovery of these violent instabilities came as an unpleasant shock. Confronted with their existence, research in the United States sought to explore two possible ways out of the dilemma. One, the so called "dynamic

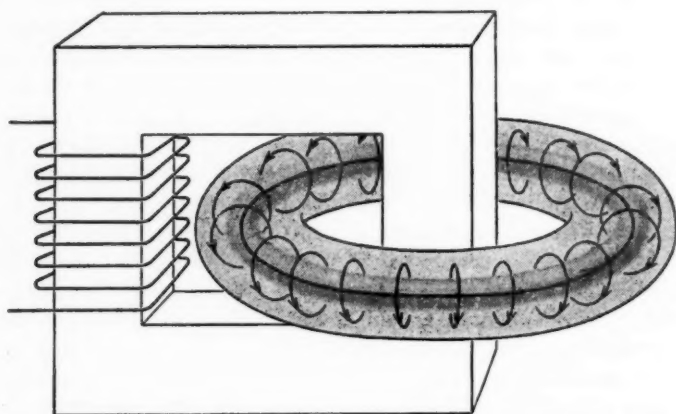


FIG. 15. Doughnut-shaped pinch tube is made by threading a transformer core through a hollow ring containing plasma. Current through the winding at left causes a strong induced current in the plasma, which is then pinched by its own circular magnetic field.

pinch" (which might also be called the "hit-and-run" approach) would be to attempt to make the pinch so extreme and to have it occur so rapidly that a high temperature would be achieved and energy-reproducing fusion reactions obtained before the instabilities disrupted the plasma. Thus experiments were started, at about the same time in this country and in Russia, using a simple cylindrical discharge column, connected to powerful condenser banks of very low internal inductance.

The theory of such a dynamic pinch was worked out by Rosenbluth (43) at about the time the experiments were being performed. A similar result was derived in Russia. Rosenbluth predicted that in simple cases the pinching column would collapse inward with a radial velocity given by the expression

$$\dot{r} = \sqrt{\frac{4}{4\pi\rho} \frac{c^2 E^2}{}} \text{ cm. sec.}^{-1} \quad 75.$$

where E is the applied electric field and ρ the instantaneous density of the plasma column. The energy given to the ions is, of course, proportional to $(\dot{r})^2$, but for interesting values of \dot{r} to be obtained, Equation 75 implies that very large values of E be reached, not high enough, however, to dismay the hopeful experimenters.

In the first experiments in the United States, performed by Baker at the University of California Radiation Laboratory and by Tuck's group, the experimenters were delighted to discover that when deuterium gas was used in the discharge, a short burst of neutrons was observed, in apparent confirmation of the fact that the dynamic pinch was capable of producing thermonuclear temperatures. However, through patient analysis, triggered by the paradoxical fact that too many neutrons were being observed to be consistent with theory, it was found that the origin of the neutrons could be traced to nonthermonuclear particle-acceleration processes associated with the ubiquitous instabilities (44). Thus died most of the hopes for achieving thermonuclear reactions from the simple dynamic pinch. Nevertheless, the intense effort to explore this phenomenon had resulted in a great increase in the sophistication of understanding of dynamic and of instability behavior in plasmas, and in the development of many new and powerful experimental methods for analyzing the plasma behavior.

The second possible way of overcoming the fundamental weakness of the pinch effect as a magnetic bottle was the obvious one of trying to inhibit or eliminate the instabilities. This led to the investigation of the effect of combining an imposed axial magnetic field with the self-field of the current-carrying plasma, as a means of "stiffening" the plasma and thus inhibiting the growth of instabilities. Early experiments by Baker and his collaborators (45) show that even a weak axial field strongly suppressed the "sausage" instability; there was certainly reason to hope that a combination of fields could be found that would be stable against all instability modes. The first complete theories of this, the so-called "stabilized pinch," were worked out independently by Rosenbluth (46), Shafranov (47), and Tayler (48). These theories predicted that, provided certain restrictive conditions on the ratio of diameters of the pinch column and a surrounding metallic shell and on the relative strength and distribution of the axial and transverse magnetic fields were satisfied, the column should be stable. (Unfortunately, the theory also showed that only a small amount of "pinching" would be allowable, thereby introducing certain technical problems in how to heat the plasma.) Although first experiments with this new approach indicated that some stabilization was achieved and seemed to corroborate the theory, a closer look has shown more subtleties than have been expected and has cast serious doubts on the feasibility of the whole approach. This question is, however, still under active study, since the great discrepancies between the theory and the actual behavior of the plasma are not understood.

Thus, the pinch effect, which has been the earliest and by all odds the

most intensively investigated of all "magnetic bottles," has constantly had to evolve and to change in response to the discovery of more and more complex plasma behavior, which destroys its effectiveness as a confinement system. Whether there is any possible way to cope with these effects or whether they are inherent in any scheme which depends heavily on self-fields for confinement is not clear, but the present picture is a bleak one, at least for fusion purposes. For pure science, however, this same behavior provides a wealth of subtle hydromagnetic effects which are worthwhile to seek out and understand for their own sake.

THE STELLARATOR

Lyman Spitzer (49) of Princeton University is responsible for conceiving a very different and promising type of magnetic bottle, which he has dubbed "the Stellarator." As the name implies, the Stellarator is a device in which it is proposed to carry out nuclear fusion reactions in steady state. The Stellarator concept is a proposed method of plasma confinement involving the use of an externally produced longitudinal magnetic field in a confinement chamber of toroidal topology. Although the possibility of the use of a simple torus with externally generated fields as a magnetic bottle had been one of the earliest thoughts in this field (Fermi, Kerst, Landshoff, Teller, R. R. Wilson, and Tuck, 1946), it was at that time already appreciated that the simple torus would not work. The difficulty was seen to arise from the fundamental drifts of the particles, occasioned by the curvature and outwardly directed field gradients in the torus (see discussion of centrifugal and gradient B drifts, p. 411). These drifts were seen to be the origin of charge separation effects in the plasma which would create an uncanceled internal electric field and thus rapidly propel the plasma (by $E \times B$ drift) to the outer wall of the chamber.

In 1951, Spitzer showed how this difficulty could be avoided, in principle, by a simple geometric change. He showed that if the single torus were to be twisted into a "figure 8," the drifts alluded to would no longer be cumulative but would cancel, in first approximation, so that confinement should be possible. Although the Stellarator, like the pinch, has been forced by the problem of instabilities to evolve into more complex forms, the basic Stellarator effect present in the single "figure 8" has remained as a crucial element. Spitzer's "new twist" introduced the concept of the "rotational transform" which was shown to be an essential element to the achievement of equilibrium confinement in an endless tube. Suppose that one considers sectioning the confinement chamber at any point. If this is done one will "see" the ends of the many lines of magnetic force displayed, arranged in successive magnetic shells or tubes of force, as shown in Figure 16. If one now fastens his attention on any given shell, an interesting property of the magnetic lines lying on this shell emerges. Consider the line labeled 1 in the sketch. If the section is that of a simple torus, then if line 1 is traced around the torus and back to the sectional plane, it will be found to form a

circle closing on itself. But if the torus has been distorted, for example into Spitzer's "figure 8," then when line 1 is traced around it will be found to return not at point 1 but at some other point, say 2. Continued tracing of the line will send the line through a series of points, such as 3, etc., so that a single line will be found to trace out an entire magnetic surface. One line, and one only, will close on itself in one revolution. This is the magnetic axis *A*.

This apparently academic property of magnetic lines has immediate practical importance for plasma confinement. First, because of the rotation

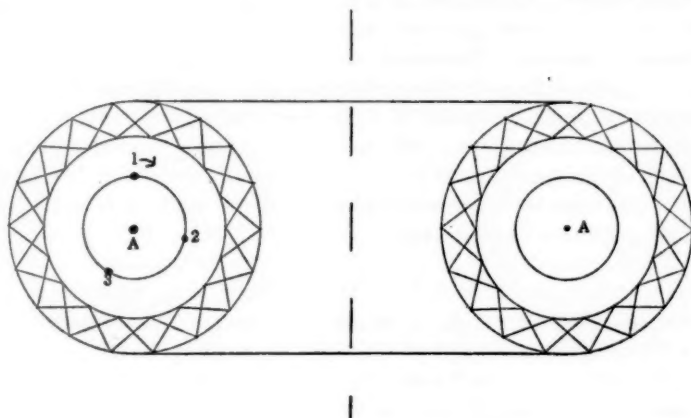


FIG. 16. Stellarator—Rotational Transform.

of the lines, the individual-particle drifts which occur with respect to these lines remain on the magnetic surfaces also and do not approach the walls. This is the microscopic picture of Stellarator confinement. Second, the asymmetric charge separation effects which are associated with the single torus can no longer occur, since charge can freely flow along lines of force to any part of a given magnetic surface. Thus a static pressure equilibrium can be reached. This is the picture of confinement on the macroscopic scale.

To test these ideas it was necessary to solve the practical problems of creating and heating the plasma to be confined. The experimental approach to this problem, begun in 1952, has been to ionize the gas and preheat it by inducing in it an electrical current (just as in the toroidal pinch experiments, but weaker). Following this, it was intended further to heat the plasma by the use of localized pulsations of the magnetic field—so-called "magnetic pumping."

In carrying out this program, however, the Princeton physicists have again uncovered unsuspected facets of the behavior of a plasma. None of the heating operations has worked as well as had been hoped, and the plasma has managed to escape in exasperatingly short times, before having reached

more than a small fraction of the predicted temperatures. Again it is clear that instabilities, possibly of several kinds, are playing a dominant role in the behavior of the present experimental Stellarators. The conviction that this was so, reached as long ago as 1954, is what has stimulated the impressive theoretical effort at Princeton on the general problem of hydromagnetic instabilities. These studies have led to a considerable revision of the original "figure 8" idea, until the present Stellarators are visualized as race-track-shaped objects around which are wound an inner group of helical conductors (the "stabilizing windings") and outer, confining-field windings. It is not yet known whether the present scheme will work or not, because of the difficulty of achieving the required plasma conditions. Impurity, recombination, and other atomic phenomena involving particle exchange with the walls seem to occur (probably abetted by instabilities) and they obscure the situation.

Despite the great difficulty of achieving the high-temperature plasma required to test the Stellarator principle properly, it is clear that its concept represents a fundamental advance in plasma physics, and it is the only idea yet put forth which shows theoretical promise for the steady-state confinement of plasma in an endless tube.

THE MIRROR MACHINE

The theoretical fact that a uniform magnetic field should be very effective for inhibiting the diffusion of a plasma across its lines of force but is obviously completely ineffective for preventing flow along the lines was the stimulus for the invention of the Stellarator and its toroidal predecessor. But if a way could be found to "plug" the ends of such a field, an attractive confinement scheme might result. Since the elementary-particle drifts in an axially symmetric magnetic field are also axially symmetric, in the equilibrium state no tendency for charge separation results. This is likely to have a salutary effect on the stability problem.

One way to cork the ends of a uniform field has been discussed (p. 396) in connection with one of the fundamental phenomena exhibited by a plasma in a magnetic field—the magnetic-mirror effect. The use of a magnetic mirror on either end of a confinement region then provides a possible way to establish a plasma confinement zone.

Starting with this basic notion, the author has proposed some specific ways of employing magnetic mirrors to create, heat, and confine a high-temperature plasma, and formed a group, in 1952, to begin to explore the use of the magnetic-mirror effect for plasma confinement. These ideas collectively came to be known as the "Mirror Machine" (50) and have formed the basis for a continued and extensive experimental and theoretical program under the author's direction at the Lawrence Radiation Laboratory (51). First confinement experiments, carried out in 1952 and 1953, although primitive, showed qualitatively that the principle was sound. Later work has centered around the problem of achieving higher temperatures and longer confinement times.

The Mirror Machine differs in some important ways from either of the magnetic bottles discussed earlier. First, the confining magnetic lines are not closed within the plasma or the confining volume but pass out of the plasma region at the ends and enter the walls of the confinement chamber. Second, because of this fact, particles can be lost from the confinement volume by the process of diffusion in velocity space. That is to say, because confinement by mirrors depends on a pitch-angle relationship for the particles, deflection of a particle into an unfavorable pitch angle will result in its loss through the mirror. For this reason, collisions play a crucial role in Mirror Machine confinement. Roughly speaking, a single large-angle deflection of any particle, the characteristic time for which is given by Equation 7, will result in the loss of that particle through the mirror. Since the inter-particle collision cross sections drop rapidly with increasing energy, this puts a premium on achieving a high plasma temperature in the Mirror Machine. The numbers are such that at ion temperatures of 50 to 100 kv. confinement times of acceptable duration would be predicted, albeit substantially shorter than the corresponding theoretical confinement times of the Stellarator. Since the electrons of the plasma are, for comparable energies, much more rapidly scattered than the ions, then, as always in other similar situations in a plasma, a positive plasma potential will be expected to arise, so as to restore equality of the loss rates of positive and negative charges. This also differs from the corresponding situation in the Stellarator.

Within this general framework the experimental work at Livermore has gone forward to try to confine a low-density, but very hot, plasma between mirrors. The philosophy has been, first, to get one's feet wet—but one toe at a time, so to speak. The starting point for the studies has been the fact that, in the absence of co-operative and collisional effects, trapped adiabatic (i.e., small orbit-diameter) particles can rigorously be shown to remain trapped between mirrors for indefinite periods of time. Thus, a plasma of sufficiently low density should also approximate this situation and should exhibit a confinement time which is limited only by collisional effects and not by the much shorter instability growth times. The starting condition at the beginning of an experiment has thus always been that the confinement chamber is highly evacuated. Into this chamber charged particles are then injected to form the initial plasma, which may be of very low density if desired. This approach is to be contrasted with that employed in all pinch studies and in the Stellarator program, where the starting conditions have, perforce, landed the experiment immediately in the midst of fully developed plasma conditions, with little opportunity (especially in the case of the pinch) of building up from a low initial density.

Perhaps because of this, or one of the other differences mentioned, the Mirror-Machine experiments at Livermore have not yet encountered the catastrophic instabilities of the pinch or the Stellarator; and confinement times measured in milliseconds have been seen, apparently limited only by simple collision processes which are seen to diminish in importance as

higher temperatures are reached. The predicted instability growth times would be only a few microseconds and are thus much shorter than the observed confinement times. But the story is only beginning to be told, and unpleasant surprises may yet lie in store. In other recent experiments where the mirror principle is employed, such as the Scylla shock-magnetic compression experiment at the Los Alamos Scientific Laboratory (52) or the similar work of Kolb at the Naval Research Laboratory (53), the duration of the experiment (a few microseconds) has usually been too short to tell whether instabilities are present or not.

In carrying out most of the Livermore Mirror experiments the method of adiabatic magnetic compression described earlier in connection with the adiabatic invariants of particle motion between mirrors (p. 397) has been employed as a tool to trap, manipulate, and heat an injected low-energy plasma. The most difficult technical problem has been that of injection, a general problem for systems of this kind (to be later discussed in greater length). Difficult though the experiments have been, they have shown that the principle of plasma confinement by mirrors is basically sound, and that the method is one of great flexibility. On the other hand, it is clear from the nature of the velocity-space losses of the Mirror Machine that even if these losses are not in excess of the theoretical values, the fusion power balance achievable by a simple open-ended Mirror Machine would be marginal, and obtainable only at quite high ion temperatures.

THE ASTRON

Although it has not yet received any experimental test, the Astron proposal of Nicholas Christofilos (54) deserves mention as a basically different form of magnetic bottle. The Astron achieves a synthesis of some of the features of all three of the previously discussed bottles, pinch, Stellarator, and Mirror Machine, by introducing a new element into the plasma, a current sheet of helically moving relativistic electrons. Basically the idea is: (a) First, an axially symmetric longitudinal field with weak end-mirrors would be created within an internally evacuated confinement chamber. This would be done with external coils. (b) Next, heavy current pulses of electrons of many millions of electron volts and in the form of a precisely collimated beam would then be injected and trapped, so as to create a current sheet of circling electrons. The strength of this current sheet would then be built up until it actually reversed the direction of the field between it and the axis, thus creating a toroidal pattern of closed magnetic lines passing through the electron layer. (c) Into this *mélange* would be injected cold gas, to be ionized and heated by energy drawn from the electron layer. (d) Continued injection of both fast electrons and cold gas would permit a steady-state thermonuclear reaction to be set up.

Needless to say, there is a host of formidable practical and theoretical questions to be answered before one can say whether or not the Astron principle is sound. However, preliminary experiments are now underway at

Livermore to try to drive a wedge into the problem. Present studies are concerned entirely with the problem of electron injection, which is fundamental to the Astron concept and is very difficult in its own right.

MISCELLANY

Space simply does not permit a description of all of the variations on the three basic confinement methods (pinch, Stellarator, and Mirror Machine) which are under study or have been suggested. In this country they go under such names as "Triax Pinch" (55), "Homopolar" (55), "Ixon" and "Picket Fence" (56), "Hard Core Pinch" (57), "Helical Mirror Machine" (58), and others. These devices generally are aimed either at improvements in the basic geometry to improve stability (Triax, Picket Fence, Hard Core, and the helical Mirror Machine), at forced rotation of a plasma as a possible heating method (Homopolar), or as an aid to reducing mirror losses (Ixon). Variations of these kinds may well contain elements which are important in solving some of the problems of the simple geometries from which they were derived. Only time will tell whether these devices are of primary or only academic interest.

THE INJECTION PROBLEM

Although it is primarily a technical problem, no discussion of high-temperature plasma research would be adequate without some discussion of what can be called "the injection problem." This is the general problem of creating or capturing the charged particles of the plasma within a magnetic bottle. It arises because of a fundamental problem; namely, if one has been able to construct a magnetic bottle which is effective in preventing the escape of a plasma from its interior, he has at the same time created a situation which is equally effective in excluding other charged particles from penetrating the bottle from the outside. No magnetic bottle can escape this problem, but the methods of coping with it are very different. Basically the only way to circumvent it is to change "something" in a nonconservative way while the injection is going on. To be more specific, the "something" could be (a) the magnetic field strength (familiar from the example of the betatron or synchrotron), (b) the state of charge of the injected particles, or (c) the classical trajectory of the particle, by collisions or co-operative effects in a plasma.

Injection method (b) is practiced, in an almost trivial way, in the present pinch and Stellarator work, where the starting conditions are those of a neutral gas within the confining chamber, containing all the particles which are to be used in the experiment. These are ionized and heated to form the plasma. But the problem of replenishing these particles during the confinement, if need be, would be a nontrivial one.

Methods (a) and (c) have been employed in the past in the Mirror-Machine work at Livermore and in other experiments. In the Livermore work, the general method has been to inject streams or bursts of plasma into

the confinement volume through co-operative effects, while the magnetic field is weak, and then capture these bursts by increasing the strength of the field. This method is simple in principle but allows only a single packet of plasma to be captured per compression.

Method (b), change-of-charge injection, is the essential component of the Oak Ridge injection experiment, DCX (59), and the Russian OGRA experiment (60). In DCX, after the original suggestions (by York of the Livermore laboratory and independently by Luce of Oak Ridge), 600-keV molecular (H_2^+ or D_2^+) ions are curved in through the fringing field at the midplane of a short DC Mirror confinement chamber. These ions are broken into atomic ions and neutral atoms by being passed through an unusual carbon discharge discovered by Luce. A large fraction of the original beam is thus trapped, because of the fact that the atomic ions, having only half the kinetic energy, move in smaller orbits and cannot readily escape. In these experiments the use of such high ion energies is largely dictated by a desire to take advantage of the reduced charge exchange cross sections which are characteristic of these energies. The present experiments are aimed primarily at investigating the trapping process and the vacuum pumping properties of the trapped ions and are not visualized as being capable of producing a full-blown thermonuclear plasma. This is in part because the machine size and length are such that the orbits of the trapped ions are very nonadiabatic, and only orbits which circle the axis are bound magnetically.

The OGRA experiment in Russia also uses molecular-ion injection at the midplane of a Mirror Machine, but the machine in this case is quite long (36 ft. between mirrors), and the ions are to be brought in at an oblique angle so that they may travel back and forth between the mirrors many times before returning to strike the injector nose. It is hoped that breakup and trapping will occur on residual gas in the machine, followed by breakup on the already trapped particles. There are indications that breakup arcs, perhaps similar to the DCX arc, may also be employed.

At the Livermore laboratory, Lauer, Gibson & Lamb (61) following earlier suggestions made by Colgate and, independently, by Brobeck, have examined theoretically the possibility of injecting beams of very fast atoms (up to 1 MeV) into a Stellarator or a Mirror Machine and trapping them on the residual gas. They conclude that this may be possible if certain restrictive vacuum conditions are satisfied. At present Damm and Post are preparing to test the injection of a 20-keV atom-beam into a small Mirror-Machine beam [the ALICE experiment—for Adiabatic, Low-Energy Injection and Capture Experiment (!)]. Here the initial breakup mechanism is to be a low-density "background plasma."

These various "change-of-charge" injection experiments all illustrate a trend toward an injection philosophy which has been long recognized as of great promise because, as well as accomplishing injection (if it works!), it would also solve or alleviate the heating problem, since the trapped ions would already possess large kinetic energies. It is the author's opinion that

this trend will continue and grow, finding its way into virtually all of the proposed approaches.

Finally, the reason for dwelling on the injection problem is that it is fundamental to the whole question of creating a high-temperature plasma and because in many cases (for example, in the Mirror Machine) it is the main technological bottleneck which slows the pace of study and understanding of confined plasmas.

WHERE ARE WE?

Often-repeated platitudes in the early days of high-temperature plasma research toward controlled fusion were that "this is one of the most difficult research problems ever undertaken," or, "a long-range project," or "one-in-a-million long shot." Yet despite the apparent awareness of the pitfalls, the lure of the final objective was so great that some of the traditional scientific precautions were by-passed in hopes of leapfrogging into an early solution. With the infinite wisdom of hindsight to help us, we now see that a more fundamental attack on the problem, concentrating first on basic physical constants and processes, followed by systematic critical experiments to bring experiment and theory into rapport, with little or no regard to such will-of-the-wisp goals as "the first thermonuclear neutrons," would probably have put us farther along the way of understanding than we now are. Although someone has defined plasma as "that which cannot be understood," 10 years from now physicists may well be wondering what all the present confusion about plasma behavior was about; such is the power of a concentrated scientific attack on the problem.

On the subject of a high-temperature plasma, what can we now say that is experimentally or theoretically on solid ground, and, can therefore, be used as a yardstick to measure progress to date and to estimate the distance yet to go? I prefer to cast the answer to this question in terms of an abbreviated summary of the most recent experimental and theoretical work on the three main approaches mentioned in the previous section. This will necessarily exclude some excellent associated work (such as shock tube research) but will encompass most of our present understanding. The experimental facts which will be discussed are generally available in the literature; their interpretation will be colored by the author's own opinions.

PINCH EFFECT

First, let us summarize the status of the "pinch effect," the most widely and intensively studied of all approaches. For many years and in many laboratories, physicists have been passing enormous, transient discharge currents through gases in linear and toroidal chambers, making at least one thing clear: plasmas can, indeed, conduct very high electrical current densities! Also, with an amazing regularity, almost every apparatus variant tried has yielded fusion neutrons in numbers essentially independent of size, topology, geography—everything but peak current. This applies to appa-

ratus as large as the British Zeta (62) and as small as the Los Alamos Perhapsatron P-4 (63) and its equivalents in many other laboratories. Although preliminary evidence, especially in Zeta, seemed to indicate that the neutrons had resulted from the achievement of true plasma temperatures at the lower fringe of those of interest for thermonuclear reactions, further careful study has in every case indicated that the neutrons could be traced to reactions occurring between a very small fraction of the ions of the plasma, colliding with a gas target composed of the rest of the plasma. At kinetic temperatures of a few times 10^6 °K. which, it was thought, had been achieved, the theoretical neutron yield from thermonuclear reaction is numerically the same as that which would result if a small (1 part in 10^6) group of the ions were to be somehow accelerated to 10 kev and then collided with the rest of the plasma. In all of the pinch experiments which yield neutrons there have been obvious signs that active instabilities were present. It therefore now seems clear that, without exception, neutrons from pinches, of whatever variety, have resulted from runaway or stochastic acceleration processes in the current carrying channel.

The second important fact of pinch research which has emerged is that in all cases, the production of an intense discharge current is always accompanied by an energy loss rate from the discharge which is many orders of magnitude larger than predicted by diffusion theory or by bremsstrahlung considerations. It appears that there may be several mechanisms operative in this effect, whose relative importance may change from experiment to experiment. The end result is the same: an enormous electrical energy input is required merely to maintain the current, and this energy all ends up at the walls of the discharge tube, without heating the plasma beyond a relatively low indicated temperature. Two mechanisms seem to be the most important ones, although others may also play a role. Colgate (64) has obtained evidence that runaway electrons of 3 to 5 kev, escaping from the plasma by some nonadiabatic process (such as, possibly, driven plasma oscillations), can account for a large energy loss. These electrons, which tend to "run away" in the axial-pinch electric field, are probably responsible for carrying most of the electric current, yet comprise only a small fraction of the total charge. Thus their continued loss is easily replenished from other low-energy members of the electron distribution. Colgate and Phillips (65) have also obtained some evidence that, especially after the first microsecond or so, radiation losses in the vacuum-ultraviolet are intense. This leads one to consider the impurity excitation radiation mechanism (see pp. 379-84) as the only likely source of this radiation, especially because the wall bombardment effects are so intense at this time.

There is every evidence, therefore, that "nature abhors a pinch" as much as she does a vacuum and that a fundamental change in the philosophy of the pinch is needed to eliminate these difficulties. There seem to be at least two directions in which this is being attempted. One is the study of what has been called a "hard-core" pinch (57), i.e., a discharge in which most of

the current may be carried by a solid central conductor, so that the plasma is trapped between this conductor and the axial field produced by an external coil. This configuration, in which the plasma may carry only a small part of the total current, can hardly be called a "pinch" any more but may still represent a necessary evolutionary development of the genus. The familiar and probable behavioral resemblance between a toroidal hard-core pinch and a "stabilized" Stellarator is rather close, although they have evolved from entirely different initial concepts.

The second kind of attack on the ills of the pinch is to attempt some form of dynamic stabilization, through the use of alternating fields (56). There is at this time no evidence that such a procedure can or cannot be made to work.

The two worst problems today for the pinch, therefore, seem to be (a) instabilities and (b) impurities. There is evidence that these problems are coupled—i.e., wall bombardment caused by instabilities causes the release of impurities. Thus, solution of one problem may greatly improve the other.

Despite the vicissitudes which have been met by the pinch experimenters, some very impressive and careful experimental work has been done in this field. For example (and there are many) the magnetic-probe data and analysis of Lovberg at Los Alamos (66) seem to be in the best tradition of experimental physics.

STELLARATOR EXPERIMENTS

Much of what has just been said about the pinch also would seem to apply to the Princeton Stellarator experiments, with an important difference. The similarity extends to the fact that in all of the heating and confinement experiments to date, instabilities, apparently largely traceable to the presence of the induced unidirectional "ohmic" heating current, have caused the plasma to be lost at a very rapid rate (decay times of order 100 μ sec.). This loss again aggravates the impurity problem, despite the great care that has been taken to achieve clean vacuum conditions. The impurity problem may, however, have two aspects in the Stellarator experiments. In addition to the radiation losses occasioned by high-Z impurities, another effect seems to exist, particularly when hydrogen is used as the initial gas. This phenomenon, called "pump-out" by the Princeton group, results in the rapid depletion of the gas in the confinement chamber during the experimental pulse. Apparently the gas is buried in the walls as a result of recombination and, possibly, charge-exchange processes going on in the plasma, which create a flux of fast, neutral atoms.

The most important difference between the Stellarator and pinch-effect experiments is that these probably extraneous difficulties have prevented a true test of the actual Stellarator confinement principle. When finally tested, it might prove to be very good indeed, by contrast with simple pinch confinement, which has been tried and found wanting. In the Princeton experiments (49) there seems to have been a constant close rapport between experimental

results and theoretical effort, and many of the facets of the work are very impressive. As one of many examples, the analytical and experimental work of Stix (26) on ion cyclotron waves and heating has been a model of careful work.

THE MIRROR MACHINE

By comparison with the pinch work, the amount of effort on the Mirror Machine has been quite small. This must be in part attributed to the unorthodox way (from a thermonuclear-plasma standpoint) in which the confinement is supposed to work and to the obvious fact that even the theoretical margin of safety to produce a self-sustaining reaction is clearly small. Furthermore, because of the rapid energy dependence of mirror losses and the deleterious role of charge exchange losses, it is not easy to perform a mirror experiment, starting merely with a chamber full of gas. This means the injection problem is encountered early, and in full force. Until fairly recently, the only extensive work on mirror confinement seems to have been done at Livermore. In the last year or so, however, increasing emphasis is being placed on this method in many parts of the world.

At Livermore, as has been noted earlier, the main emphasis has been on heating and confinement studies. To summarize briefly the work to date, transient plasma streams (duration a few microseconds) have been trapped and compressed in magnetic-mirror fields which start with low fields (i.e., of order 20 gauss) and increase about 1000-fold or more over a period of a few hundred microseconds. This compression process has been shown to produce a small spindle of plasma (diameter 1 to 2 cm.) which remains confined for several milliseconds, decaying with typical initial time constants of about 1 msec. The behavior of this confined plasma has been deduced primarily from diagnosis of effects produced by the heated electrons. It has been shown that the electron component of the plasma has reached a temperature of about 20 kev (2×10^8 °K.) and a final density of 10^{13} to 10^{14} cm⁻³. This means that the peak plasma pressure represented by those electrons has been about 1 atm. or more, representing a β -value approaching 0.08. In these experiments, the initial electron temperature was about 10 ev, so that the observed final electron temperatures were in rough agreement with the predicted magnetic compression ratio (1000:1). But the ion energy, being limited by the initial low magnetic field, is thought not to have exceeded 1 kev (10^7 °K.). Direct measurements of the plasma ion composition and final temperature are now being attempted. As far as can be told, the observed rates of particle loss for the bulk of the plasma are in agreement with the rate expected from particle collisions, and no evidence for gross instabilities has been seen. However, the small size of the plasma column, and the fact that the electron temperature is much higher than the ion energies mean that one cannot draw general conclusions about mirror stability from these experiments. Nevertheless, it is heartening to find even one "special" case of plasma confinement where stability over fairly long periods of time can be demon-

strated. Since the field configuration of the mirror is theoretically unstable by hydromagnetic criteria, the fact of the observed stability has been rationalized by noting that in the Mirror Machine the flux lines pass out of the plasma and enter a conducting surface, thus are "tied" at the ends. This effect, if it exists, would exert a strong stabilizing influence on the plasma by preventing the free interchange of adjacent lines. It is by no means clear, however, that this explanation is the correct one for the observed stability. It is somewhat ironic that the magnetic bottle with the largest theoretical leakage rate should exhibit the most stable behavior.

A great deal of additional effort has been expended in the Mirror Machine program in trying to find improved solutions to the injection problem, which remains the number-one technical barrier in the way of making better physical measurements and increasing the plasma temperature. Only when this is accomplished will it be possible to make definitive tests of the stability and confinement properties of the Mirror Machine.

On other experiments employing the mirror principle the objectives have been often quite different from those at Livermore. In the DCX experiment at Oak Ridge, the main emphasis is on the method of molecular ion trapping as a plasma "ignition" scheme, and plasma effects have thus far been of secondary importance. In the Los Alamos Scylla shock-compression work, the compression times have been too short for mirror action to have been of much importance. As these and other similar experiments evolve, however, they will also, no doubt, shed light on mirror confinement.

CONCLUSION

The reader will no doubt have noticed that although the words "controlled fusion" appear in the title of this article, very little space has been devoted to discussing fusion power. This was by no means done for the purpose of minimizing the eventual importance of achieving controlled fusion, but rather in order to underscore the importance of "high-temperature plasma research" at this phase of the effort. For this reason, although a wealth of valid and worthwhile material exists on the reaction physics, the scaling laws, and many of the practical aspects of fusion power, it was thought that this material did not properly belong in a review article such as this one. All of us are convinced of the promise of fusion power—what we need to do now is to bring its solution nearer by the only method sure to work—the scientific method applied to a fundamental study of the physics of high-temperature plasmas.

LITERATURE CITED

1. Massey, H. S. W., and Burhop, E. H. S., *Electronic and Ionic Impact Phenomena*, 141 (Oxford University Press, London, Engl., 1952)
2. Chandrasekhar, S., *Principles of Stellar Dynamics* (University of Chicago Press, Chicago, Ill., 1942)
3. Spitzer, L., *Physics of Fully Ionized Gases* (Interscience Publishers, Inc., New York, N. Y., 1956)
4. Tannenwald, L. M., *Phys. Rev.*, **113**, 1396 (1959); Rosenbluth, M. (Private communication)
5. Johnson, M. H. (Unpublished)
6. Heitler, W., *Quantum Theory of Radiation* (Oxford University Press, London, Engl., 1954)
7. Stickforth, J., *Bremsstrahlung Losses in a Hydrogen Plasma at Temperatures Above 10^8 °K.* (To be published)
8. Saha, M., *Phil. Mag.*, **40**, 472 (1940)
9. Wooley, R., and Allen, C., *Monthly Notices Roy. Astron. Soc.*, **108**, 292 (1948)
10. Elwert, G., *Z. Naturforsch.*, **7a**, 432 (1952)
11. Stier, P. M., and Barnett, C. F., *Phys. Rev.*, **109**, 355 (1958)
12. Thompson, W. B., *Proc. Roy. Soc. (London)*, **B70**, 1 (1957)
13. Alfven, H., *Cosmical Electrodynamics* (Oxford University Press, London, Engl., 1950)
14. Kruskal, M., *The Gyration of a Charged Particle* (Princeton University Report NYO-7903, March, 1958)
15. Hertwech, F., and Schluter, A., *Z. Naturforsch.*, **12a**, 844 (1957)
16. Garren, A., Riddell, R. J., Smith, L., Bing, G., Henrich, L. R., Northrop, T. G., and Roberts, J. E., *Proc. Intern. Conf. Peaceful Uses Atomic Energy, 2nd Conf., Geneva, 1958*, **31**, 65 (1959)
17. Gibson, G., and Lauer, E., *Bull. Am. Phys. Soc.*, **II**, **3**, 412 (1958)
18. Teller, E., *Proc. Intern. Conf. Peaceful Uses Atomic Energy, 2nd Conf., Geneva, 1958*, **31**, 27 (1959)
19. Christofilos, N., *Bull. Am. Phys. Soc.*, **II**, **4**, 216 (1959)
20. Post, R. F., *U. S. Atomic Energy Commission Report, TID-7503* (October, 1955); *Proc. Intern. Conf. Peaceful Uses Atomic Energy, 2nd Conf., Geneva, 1958*, **32**, 245 (1959)
21. Rosenbluth, M., and Longmire, C., *Ann. Phys.*, **1**, 120 (1957)
22. Simon, A., *Phys. Rev.*, **100**, 1557 (1955)
23. Longmire, C., and Rosenbluth, M., *Phys. Rev.*, **103**, 507 (1956)
24. Simon, A., *Proc. Intern. Conf. Peaceful Uses Atomic Energy, 2nd Conf., Geneva, 1958*, **32**, 343 (1959)
- 24a. Spitzer, L., *Proc. Intern. Conf. Peaceful Uses Atomic Energy, 2nd Conf., Geneva, 1958*, **32**, 190 (1959)
25. Newcomb, W., *The Hydromagnetic Waveguide* (Stanford Univ. Press, Stanford Calif., 1957)
26. Stix, T. H., *Proc. Intern. Conf. Peaceful Uses Atomic Energy, 2nd Conf., Geneva, 1958*, **31**, 125 (1959)
27. Thomson, J. J., and Thomson, G. P., *Conduction of Electricity Through Gases*, **2**, 353 (Cambridge University Press, London, 1933)
28. Landau, L., *J. Phys. U.S.S.R.*, **10**, 25 (1946)
29. Bohm, D., and Gross, E. P., *Phys. Rev.*, **75**, 1851 (1949)

30. Teller, E., *U. S. Atomic Energy Commission Report, TID-7503* (October, 1955)
31. Kruskal, M., and Schwarzschild, M., *Proc. Roy. Soc. (London)*, **A223**, 348 (1954)
32. Grad, H., *Proc. Intern. Conf. Peaceful Uses Atomic Energy, 2nd Conf., Geneva, 1958*, **31**, 190 (1959)
33. Bernstein, I., Frieman, E., Kruskal, M., and Kulsrud, R., *Proc. Roy. Soc. (London)*, **A244**, 17 (1958)
34. Bohm, D., and Gross, E. P., *Phys. Rev.*, **75**, 1864 (1949)
35. Akhiezer, A., Fainberg, Y. B., Sitenko, A. G., Stepanov, K., Kurilko, V., Gorbatenko, M., and Kirochkin, U., *Proc. Intern. Conf. Peaceful Uses Atomic Energy, 2nd Conf., Geneva, 1958*, **31**, 99 (1959)
36. Harris, E., *Phys. Rev. Letters*, **2**, 34 (1959)
37. Chandrasekhar, S., Kaufman, A., and Watson, K., *Proc. Roy. Soc. (London)*, **A245**, 435 (1958)
38. Bishop, A. S., *Project Sherwood* (Addison-Wesley Publishing Company, Inc., Cambridge, Mass., 1958)
39. Bennett, W. H., *Phys. Rev.*, **45**, 890 (1934)
40. Ware, A. A., *Phil. Trans. Roy. Soc. (London)*, **A243**, 863 (1951)
41. Tuck, J. L., Burkhardt, L. C., Dunaway, R. E., Mather, J. W., Phillips, J. A., Sawyer, G. A., Stratton, T. S., and Stovall, E. J., Jr., *J. Appl. Phys.*, **28**, No. 5 (1957)
42. Kurchatov, I. V., *Atomnaya Energ.*, **3**, 65 (1956)
43. Rosenbluth, M., *U. S. Atomic Energy Commission Document, LA-1850* (1954)
44. Colgate, S., *Proc. Conf. Gaseous Discharge Phenomena, Venice* (June, 1957)
45. Anderson, O., Baker, W., Colgate, S. A., Furth, H. P., Ise, J., Jr., Pyle, R. V., and Wright, R., *Phys. Rev.* **109**, 612 (1958)
46. Rosenbluth, M., *U. S. Atomic Energy Commission Document, LA-2030* (1956)
47. Shafranov, V., *Atomnaya Energ.*, **1**, 33 (1956)
48. Tayler, R., *Proc. Phys. Soc. (London)*, **B70**, 31 (1957)
49. Spitzer, L., *Proc. Intern. Conf. Peaceful Uses Atomic Energy, 2nd Conf., Geneva, 1958*, **32**, 181 (1959)
50. Post, R. F., *U. S. Atomic Energy Commission Document, UCRL-4231* (1954)
51. Post, R. F., *Proc. Intern. Conf. Peaceful Uses Atomic Energy, 2nd Conf., Geneva, 1958*, **32**, 245 (1959)
52. Elmore, W., *Proc. Intern. Conf. Peaceful Uses Atomic Energy, 2nd Conf., Geneva, 1958*, **32**, 337 (1959)
53. Kolb, A., *Proc. Intern. Conf. Peaceful Uses Atomic Energy, 2nd Conf., Geneva, 1958*, **31**, 328 (1959)
54. Christofilos, N., *Proc. Intern. Conf. Peaceful Uses Atomic Energy, 2nd Conf. Geneva, 1958*, **32**, 279 (1959)
55. Anderson, O., Baker, W., Ise, J., Jr., Kunkel, W. B., Pyle, R. V., and Stone, J. M., *Proc. Intern. Conf. Peaceful Uses Atomic Energy, 2nd Conf., Geneva, 1958*, **32**, 150, 155 (1959)
56. Tuck, J. L., *Proc. Intern. Conf. Peaceful Uses Atomic Energy, 2nd Conf., Geneva, 1958*, **32**, 3 (1959)
57. Colgate, S., and Furth, H. P., *U. S. Atomic Energy Commission Document, UCRL-5392* (1959)
58. Post, R. F., *U. S. Atomic Energy Commission Report, TID-7520*, 59 (1956)
59. Barnett, C. F., Bell, P. R., Luce, J. S., Shipley, E. D., and Simon, A., *Proc. Intern. Conf. Peaceful Uses Atomic Energy, 2nd Conf., Geneva, 1958*, **31**, 298 (1959)

60. Kurchatov, I. V., *J. Nuclear Energy*, **8**, 168-75 (1958)
61. Gibson, G., Lamb, W. A. S., and Lauer, E. J., *Proc. Intern. Conf. Peaceful Uses Atomic Energy, 2nd Conf., Geneva, 1958*, **32**, 275 (1959)
62. Thoneman, P., Butt, E. P., Carruthers, R., Dellis, A. N., Fry, D. W., Gibson, A., Harding, G. N., Lees, D. J., McWirtter, R. W. P., Pease, R. S., Ramsden, S. A., and Ward, S., *Nature*, **181**, 217 (1958)
63. Honsker, J., Karr, H., Osher, J., Phillips, J. A., and Tuck, J. L., *Nature*, **181**, 231 (1958)
64. Colgate, S., *Proc. Intern. Conf. Peaceful Uses Atomic Energy, 2nd Conf., Geneva, 1958*, **32**, 123 (1959)
65. Phillips, J. (Private communication)
66. Burkhardt, L., and Lovberg, R., *Proc. Intern. Conf. Peaceful Uses Atomic Energy, 2nd Conf., Geneva, 1958*, **32**, 29 (1959)

FAST REACTORS¹

BY LEONARD J. KOCH

Argonne National Laboratory, Lemont, Illinois
AND

HUGH C. PAXTON

Los Alamos Scientific Laboratory, Los Alamos, New Mexico

At the first Geneva Conference on the Peaceful Uses of Atomic Energy, Zinn pointed out that fast-neutron reactors promise to extend the world's energy resources tremendously by the efficient utilization of U^{238} , the abundant isotope in natural uranium (1). Though U^{238} will not fuel a reactor directly, it can be converted to Pu^{239} which, like U^{233} and U^{235} , is an effective fuel. By a peculiarity of nature, this conversion is especially efficient in reactors with high effective neutron energy, in other words, fast reactors. Once produced, of course, the Pu^{239} can be used to fuel any reactor type, of which fast and thermal reactors represent the extreme range of neutron energy. Jungnell & Lundquist call attention to a combination of these reactor classes that is particularly attractive for nuclear power based on a natural uranium supply (2).

The potentiality of fast reactors, as well as their special problems, can best be shown by a comparison with their thermal counterparts (3). The most striking difference between these reactor types results from the large contrast in the significant neutron cross sections, some of which are listed in Table I (4, 5, 6). Illustrated are nuclear parameters for the fuels U^{233} , U^{235} , and Pu^{239} ; for the so-called fertile materials U^{238} and Th^{232} ; and for representative structural materials, the coolant sodium, and collected fission products. Moderators, such as water, heavy water, beryllium, and graphite, which are essential to neutron thermalization, are not included because significant quantities cannot be tolerated in fast reactors.

Of the η neutrons produced per neutron absorbed by fuel, one neutron is required to maintain the fission chain reaction, and the remaining $\eta-1$ neutrons are absorbed by fertile U^{238} or Th^{232} , and by coolant and structural materials, or escape from the reactor. Neutron capture by fertile material regenerates fuel (Pu^{239} from U^{238} , and U^{233} from Th^{232}); and the number of new fuel nuclei produced per fuel nucleus destroyed, a measure of the efficiency of this process, is called the breeding ratio (where the fuel species does not change) or conversion ratio (where a new fuel is produced). For practical utilization of U^{238} and Th^{232} the breeding ratio should be greater than unity.

In the case of a thermal reactor, where there are negligible fissions produced in the fertile material by fast neutrons, the breeding ratio cannot ex-

¹ The survey of literature pertaining to this review was concluded in February, 1959.

TABLE I
NUCLEAR PARAMETERS FOR FAST* AND THERMAL† REACTORS

	Fuel						
	U ²³⁵		U ²³⁸		Pu ²³⁹		
	Fast	Thermal	Fast	Thermal	Fast	Thermal	
σ_f (barns)	1.44	582	2.20	527	1.78	746	
ν	2.52	2.47	2.59	2.51	2.98	2.90	
σ_c/σ_f	0.152	0.19	0.068	0.102	0.086	0.38	
$\eta-1$	1.18	1.07	1.42	1.28	1.74	1.10	
Fertile Material							
	U ²³⁸		Th ²³²				
	Fast	Thermal	Fast	Thermal			
σ_f (barn)	0.112	0	0.025	0			
ν	2.61	—	2.34	—			
σ_c (barn)	0.160	2.71	0.174	7.56			
Other Representative Materials							
	Fe		Na		Zr	Effective fission-product pair	
	Fast	Thermal	Fast	Thermal	Thermal	Fast (5)	Thermal (6)
$\sigma_c/\sigma_f(U^{235})$	6.1×10^{-3}	4.4×10^{-3}	1.80×10^{-3}	0.87×10^{-3}	0.31×10^{-3}	~ 0.08	~ 0.07
$\sigma_c/\sigma_f(U^{238})$	4.0×10^{-3}	4.8×10^{-3}	1.18×10^{-3}	0.96×10^{-3}	0.34×10^{-3}	—	~ 0.06
$\sigma_c/\sigma_f(Pu^{239})$	4.9×10^{-3}	3.4×10^{-3}	1.46×10^{-3}	0.68×10^{-3}	0.24×10^{-3}	—	~ 0.08

σ_f = microscopic-fission cross section

σ_c = microscopic-capture cross section

ν = number of neutrons produced per fission

$\eta = \nu / [1 + \sigma_c(\text{fuel})/\sigma_f(\text{fuel})]$ = number of neutrons produced per neutron absorption by fuel

* Fast-neutron parameters are averaged over the typical reactor spectrum of Figure 5.

† Thermal-neutron parameters are appropriate to 0.025 ev (4).

ceed $\eta-1$. As Table I indicates, $\eta-1$ for U^{235} in a thermal reactor is sufficiently large to achieve excess breeding in an efficient practical system. Fast-reactor neutron economy, however, is enhanced by fissions in U^{238} (to a lesser degree for Th^{232}), so that the breeding ratio is not necessarily limited to $\eta-1$. Fast reactors with fertile U^{238} may be expected to have a breeding ratio of about 1.7 when fueled with Pu^{239} , and a conversion ratio of approximately 1.2 with U^{235} .

It will be noted that Pu^{239} is the most attractive fuel for fast reactors, while U^{235} is the most favorable for thermal systems. The development of fast power reactors is being directed toward the use of plutonium as the reactor fuel even though essentially all of the work accomplished to date in this country (and plans for the immediate future) has involved U^{235} as an interim fuel.

Table I also indicates the source of the problems associated with achieving an efficient and economically practical fast power reactor. Because of the small fission cross section, high fuel concentrations are necessary in the fast-reactor core to achieve criticality with resultant small core volume to minimize the fissionable material requirements. A primary objective in fast reactors, therefore, is to achieve the highest possible power density in the reactor core. To obtain the high thermal performance required, the fuel must be finely divided (short heat transfer path) to limit the temperature gradient within it.

A problem associated with the high fuel enrichment concerns the utilization, or burn-up, of the fuel per reactor cycle. In thermal reactors, the fraction of fissionable atoms is small (of the order of 0.7 to 3 per cent of the fuel alloy), while in fast reactors the fraction of fissionable atoms is very large, in the range of 25 to 50 per cent of the fuel alloy. If the operating cycle is limited by radiation damage of the fuel elements, then the consumption of fissionable atoms before reprocessing is much greater in a thermal reactor than in a fast reactor. There are, however, some compensating considerations. Larger amounts and variety of alloying additions can be tolerated in a plutonium-fueled fast reactor to achieve a greater degree of radiation damage resistance in the fuel and thus increase the burn-up which can be achieved. This is possible because of the relatively larger fraction of excess neutrons that can be lost by parasitic absorption without significant loss in breeding ratio. Similarly, appreciable fission-product poisoning can be accommodated, so that crude and potentially inexpensive processing methods which do not completely remove fission products may be employed.

The fast-reactor fuel element, therefore, must be of small physical cross section to permit high thermal performance and must be of relatively simple design to allow inexpensive recycling. Fortunately, the fast reactor can tolerate the use of relatively conventional structural materials, such as stainless steel, so that expensive low capture-cross-section materials, such as zirconium, may be avoided.

It is somewhat difficult to evaluate differences in the control and stability characteristics of thermal and fast reactors. The prompt neutron lifetime in fast reactors is considerably shorter (approximately a factor of 100) than in thermal reactors, which results in a correspondingly shorter period² at prompt critical. Below prompt critical, the control and kinetics characteristics of the reactors are similar (7, 8, 9). Another significant difference is the automatic protection against reactivity transients afforded by the inherently large negative temperature coefficient of most thermal reactors, whereas in the case of fast reactors, protection against instability requires judicious design.

² Reactor period is the e -folding time for fission rate (or power). Below delayed critical (the steady-state power condition), the period is negative; above, it is positive and decreases as reactivity is added. At prompt critical (where promptly emitted neutrons alone would be sufficient to sustain a fission-chain reaction), the period is dangerously small, ranging from milliseconds for fast reactors to tenths of second for thermal reactors.

In summary, the primary advantage of fast power reactors is the high neutron efficiency which can be obtained, though at the expense of high fuel enrichment. The result is a large breeding ratio and efficient utilization of the abundant U^{238} isotope. Major engineering problems are involved, however, in the design of fast-neutron power reactors; they are associated with: (a) high power density in the reactor core and the attendant heat transfer considerations, (b) frequent and simple fuel recycling at low cost, and (c) considerations of reactor kinetics.

EXPERIENCE WITH FAST-NEUTRON SYSTEMS FAST-REACTOR PROGRAMS

The United States, Britain and Russia have active fast-reactor programs in progress. Other countries have modest study and evaluation efforts under way, with plans to extend these efforts at the earliest possible time. All of these programs are directed primarily toward the application of fast reactors for central-station power plants. For this application, fast reactors must meet the requirements of economic as well as technical feasibility.

A chronology of fast reactors is given in Table II. This listing includes reactors which have been completed, those under construction, and others planned for the immediate future; critical and subcritical facilities are not included. The programs of the various countries are similar in many respects. Experimental reactors are constructed first to obtain basic information and to learn the fundamental characteristics of the reactor system. These are followed by "prototype reactors" which tend to emphasize engineering aspects of the system and attempt to resolve the practical problems associated

TABLE II
COMPARISON OF FAST REACTORS

	Power (kw.) (thermal)	Coolant	Fuel (1st loading)
<i>U.S. Fast Reactors</i>			
Clementine	25	Hg	Pu (metal)
EBR-I	1,400	NaK	U^{235} (metal)
EBR-II	62,500	Na	U^{235} (metal)
Enrico Fermi	300,000	Na	U^{235} (metal)
<i>U.S.S.R. Fast Reactors</i>			
BP-2	100	Hg	Pu (metal)
BP-5	5,000	Na	Pu (oxide)
BH-50	200,000	Na	Pu-U (oxide)
<i>U.K. Fast Reactors</i>			
Dounreay	60,000	NaK	U^{235} (metal)

with useful power generation from fast reactors. The third step appears to be the construction of "developmental reactors" which may be defined as first generation power plants.

The following description of the reactor programs of the three countries briefly covers pertinent characteristics and the significance of each reactor to the program.

United States program.—The first fast reactor to operate in the United States was Clementine at Los Alamos in 1948 (10). It contained a plutonium metal core surrounded by a natural uranium reflector and included an island of natural uranium within the core. The fuel elements were plutonium clad with steel, and the reactor was cooled with mercury. It was primarily a fast-neutron irradiation facility and generated about 25 kw. of heat. It was dismantled in 1954 after the rupture of one of its fuel elements.

The second U.S. fast reactor was the EBR-I constructed by Argonne National Laboratory at the National Reactor Testing Station in Idaho in 1951 (11). This reactor is fueled with highly-enriched-uranium metal clad with stainless steel. The enriched core is surrounded by a natural-uranium blanket. The reactor is cooled with sodium-potassium alloy (NaK) and operates at moderately high temperature. The heat transported from the reactor is employed to generate steam to drive a turbine generator producing approximately 200 kw. of electrical power. This was the first nuclear plant to produce electrical power and is in operation at the present time. The second core of this reactor was damaged as the result of a partial melt-down during a transient experiment in 1956. The reactor internals were replaced at the time of the third fuel loading which was designed primarily to investigate more thoroughly the kinetic characteristics of the reactor system (12). This program will be followed by a plutonium loading of the reactor.

Although the EBR-I is a complete reactor and power system, it is a reactor experiment and not a prototype of a power plant. Information from it and from fast critical assemblies (to be described later) was used in the design of EBR-II, a prototype power plant. The EBR-II, now under construction by Argonne at the National Reactor Testing Station in Idaho, will generate 20 Mw. of electricity (13, 14). The rated thermal power of 62.5 Mw. will correspond to a maximum power density in the core in excess of 1 Mw. per l. of core volume and a thermal flux greater than 1,000,000 Btu per sq. ft. hr. The maximum sodium coolant velocity in the core will exceed 25 ft. per sec., and the mean outlet temperature of sodium from the reactor will be 900°F. This level of thermal performance is considered to be attractive for full-scale central-station power plants. In addition the EBR-II will include a fuel processing and fabrication plant to demonstrate an integrated fuel cycle.

The EBR-II will be operated first with an enriched-uranium loading containing approximately 5 weight-per cent synthetic-fission-product elements simulating the equilibrium concentration of unremoved fission products that are left by the purification process. Later, the reactor will be loaded with a fuel alloy containing a plutonium-U²³⁸-synthetic-fission-product alloy. The

EBR-II will be operated on a true plutonium- U^{238} breeding cycle at the earliest possible opportunity and thus will contribute to the primary objective of developing a plutonium-fueled fast power breeder.

The U.S. fast-power-reactor program also includes a full-scale developmental power plant. This is the Enrico Fermi Atomic Power Plant under construction by the Power Reactor Development Company at Monroe, Michigan (15, 16). It will generate 100 Mw. of electricity which will be distributed by the Detroit Edison Company through its utility distribution system. This plant will be fueled with enriched uranium metal alloyed with molybdenum. The thermal performance of the reactor is comparable to the EBR-II, but the fuel will be processed by conventional aqueous methods. It will provide badly needed experience in a full-scale plant operated by a utility organization in a commercial distribution system. This type of operation is expected to provide reliable data with respect to the operating costs and reliability of fast power reactors for central-station power plants.

Still in the planning stage at Los Alamos is LAMPRE, an advanced fast-reactor concept utilizing molten plutonium-iron eutectic as fuel, tantalum for containment of the fuel, and sodium as coolant (17). A 1-Mw. experiment presently under design at Los Alamos will not include any fertile material and will be simplified as much as possible by employing a steel reflector and borated-graphite neutron shield. There are many basic problems involved in this concept not the least of which are those relating to materials and their environment.

Russian program.—The U.S.S.R. program is philosophically similar to the U.S. program as can be seen by comparing the reactors listed in Table II (18, 19). The first experimental reactor was BP-2, constructed in 1956, which operated at 100 kw. thermal. It was fueled with plutonium metal and was cooled with circulating mercury. It was recently replaced by BP-5, a 5000-kw. sodium-cooled reactor fueled with sintered plutonium oxide that is canned in stainless steel. BP-5 is considered an engineering test reactor and only a small portion of the reflector contains uranium, the major part consisting of nickel. Though this eliminates the possibility of conducting over-all breeding experiments in the reactor, it is contended that breeding information from critical experiments is adequate. Materials tests in BP-5 are expected to develop the engineering data required for the design of a prototype fast-breeder-reactor power station.

The next step in the U.S.S.R. program will be the design and construction of a prototype plant that has been designated BH-50. The design parameters and preliminary conceptual designs for this plant have been described by Leipunsky and co-workers (19). It will be a 200-Mw. thermal, 50-Mw. electrical plant, sodium cooled, fueled with plutonium and containing a U^{238} blanket. It will be a true prototype power plant. No specific plans for fuel cycle have been stated other than that various plutonium alloys are under investigation. In addition to U^{238} as a diluent of the plutonium, inert additions such as barium and iron are being considered to enhance further the radiation

TABLE III

CHARACTERISTICS OF PROTOTYPE AND DEVELOPMENTAL FAST REACTORS

	EBR-II	Enrico Fermi	BH-50
Thermal Power (Mw.)	62.5	300	200
Core Diameter (in.)	19	30.5	25.5
Core Height (in.)	14.2	31	25.5
Coolant	Na	Na	Na
Coolant Outlet Temp. (°F.)	900	800	900
Avg. Power Density (kw./l.)	890	850	800
Avg. Heat Flux (Btu/hr.-ft. ²)	680,000	696,000	665,000
Coolant Velocity (ft./sec.)	26	32	19.5
Maximum Neutron Flux (cm. ⁻² sec. ⁻¹)	3.7×10^{15}	9×10^{15}	9×10^{15}
Core Composition—Volume %			
Fuel Alloy	31.8	27.9	47
Structure	19.5	24.9	13
Coolant	48.7	47.2	40

stability of fuel. It is postulated that the loss in breeding gain will be relatively small and could be more than offset if the performance of the fuel is improved sufficiently.

The U.S.S.R. program also includes the preliminary plans for a large full-scale central-station power plant. This plant has been designated BH-250 and would have a thermal power rating of 1,000,000 kw. The formulation of details of this plant is awaiting experience with BH-50.

British program.—To date, the United Kingdom program has emphasized the development of fundamental fast-reactor data from numerous critical experiments. The first U.K. reactor, being constructed at Dounreay, Scotland, can be described as a combined reactor experiment and preliminary prototype reactor (20, 21). The design power rating of 60 Mw. thermal is quite high for a first plant as compared with the initial U.S. and U.S.S.R. reactors. Although approximately the same size as the EBR-II, the structure of this reactor is more nearly like an enlarged version of EBR-I. It is cooled with NaK, and the uranium-chromium alloy is contained in individual fuel rods. Although the Dounreay reactor is identified as a reactor experiment, a relatively large power rating was selected to provide experience applicable to large systems.

Comparison of the three prototype and developmental reactors which have been described above (EBR-II, Enrico Fermi, and BH-50) reveals some interesting similarities that are summarized in Table III.

FAST CRITICAL ASSEMBLIES

Although the few fast-neutron power producers that have been planned tend to fall within a restricted compositional range, this may be more a

matter of expediency than necessity. Regardless, designers of such systems can and do use information from almost any fast-neutron assembly. In spite of the fact that detailed neutronics calculations with high-speed computing machines are more straightforward and a priori more reliable for fast systems than for those of lower neutron energy,³ they still must be checked against a wide range of compositions before they can be applied with confidence to the preliminary design of reactors. Step-wise checks of groups of nuclear parameters that are input data for such calculations uncover difficulties more certainly than any number of over-all checks. For example, cross sections associated with fuel are confirmed by comparing calculations with observations on a critical assembly consisting only of fuel. Once fuel alone is understood computationwise, parameters for fertile material may be checked against observations on systems that are simple fuel—fertile material mixtures. Then effects of reflection, and dilution with various structural materials and coolants, may be studied progressively.

Experiences with the elementary fast-neutron assemblies that have helped establish the general features of fast power reactors are reviewed in the following section.

Los Alamos critical assemblies.—At the Los Alamos Scientific Laboratory, early fast-neutron investigations stimulated construction of the Clementine reactor. Shortly afterward, experiments began on the first of a series of simple metal critical assemblies. One assembly, called Topsy, consisted of a roughly spherical U^{235} -metal core in a thick natural-uranium reflector (22); like others of the series, it was uncooled, so limited to very low power operation. At one stage, a nickel reflector replaced the natural uranium, and during another period there was a spherical plutonium-metal core in natural-uranium reflector (called Popsy). With the enriched uranium—normal uranium system, effects of core-shape variation, core-density change, and core dilution with U^{238} were studied. The Topsy assembly machine was retired in 1956, to be replaced by another more stable machine (Flatop).

The next of this series, Godiva, was essentially a critical bare sphere of highly-enriched uranium metal (23). After a lengthy survey of properties including its behavior under super-prompt-critical conditions, its principal function became the generation of short, intense, prompt "bursts" for irradiation purposes. When its five-year life was ended in 1957 by an accidentally large burst, Godiva was replaced by a new U^{235} assembly (Godiva II) designed specifically to serve as a burst-irradiation facility (24, 25).

Then followed a group of temporary cylindrical uranium-metal systems (the Jemima series), built up of interleaved plates of enriched uranium and

³ Cross sections vary more wildly over the neutron spectral ranges of so-called thermal and intermediate reactors than they do for fast systems. In particular, troublesome compromises that are required for handling cross-section resonances are minimal (though not absent) in fast-reactor computations.

normal uranium. The first three were unreflected, with average U^{235} contents of $53\frac{1}{2}$ w/o (per cent by weight), $37\frac{1}{2}$ w/o, and 29 w/o (26). A later assembly consisted of a core averaging $16\frac{1}{4}$ w/o U^{235} , and a 3 in.-thick natural-uranium reflector.

The latest simple metal assembly is Jezebel, bare, nearly spherical plutonium (27, 28). A survey of its properties has been completed, and it is planned to substitute U^{233} metal for the plutonium as soon as parts can be fabricated.

Subcritical assemblies.—It is appropriate, here, to interrupt this account of fast critical systems, and mention numerous subcritical metal assemblies at Los Alamos and the University of California Radiation Laboratory at Livermore that have been built up to sizes sufficient for reliable extrapolations to critical (29). These supplement significantly the information available from actual critical assemblies, particularly in dependence of critical mass upon shape, reflector material, and thickness, and intercomparisons of U^{235} , U^{233} , and Pu^{239} critical masses in similar reflectors.

Also contributing to the knowledge of fast-neutron systems were highly subcritical uranium-metal exponential columns at the Oak Ridge National Laboratory, Argonne, and Los Alamos (30, 31). In these columns, the U^{235} content of the uranium ranged from normal (0.7 w/o) to 31 w/o. Measurements indicated that undiluted uranium cannot be made critical with U^{235} content less than about $5\frac{1}{2}$ w/o, and provided estimates of critical quantities of pure uranium at $6\frac{1}{2}$ w/o and 9 w/o U^{235} , and of uranium between $14\frac{1}{2}$ w/o and 31 w/o U^{235} diluted with iron and aluminum.

Argonne critical assemblies.—In 1955, after experience with EBR-I, the Argonne National Laboratory put into operation its ZPR-III machine for assembling a wide variety of "zero-power" nuclear mock-ups of fast reactors (32). So far, the fuel has been U^{235} and the fertile material U^{238} ; aluminum at reduced density represents sodium coolant, and stainless steel the structure. Uranium in the core has contained from $11\frac{1}{2}$ to 93 w/o U^{235} . A representative reflector is ~ 12 in.-thick uranium depleted in U^{235} , with small quantities of stainless steel and aluminum. In one series of experiments core shapes were varied, and another was designed to show the influence of a modestly-moderating admixture of carbon. Other measurements established the relatively minor effects of inhomogeneities. In addition to general surveys, ZPR-III has been used for specific nuclear mock-ups of the EBR-II and Enrico Fermi Reactors. It is planned to extend ZPR-III studies to plutonium-fueled systems as the next phase of the program.

British critical assemblies.—In the United Kingdom fast-reactor program the Dounreay reactor was preceded by measurements on two zero-power assemblies at Harwell, Zephyr (since 1954) and Zeus (1955–1957). Zephyr (33, 34) has a small plutonium-fueled core of variable composition. One version consisted of nearly equal volumes of plutonium, natural uranium, and nickel (the material in which the plutonium is canned). The original reflector

was full-density normal uranium next to the core, surrounded by close-packed uranium rods. In a later version, graphite replaced the high-density uranium.

Zeus was a larger, U^{235} -fueled, assembly, essentially an adjustable zero-power mock-up of the Dounreay reactor (34). Various core arrangements contained about 12 v/o U^{235} (v/o means per cent by volume), an equal quantity of aluminum (the canning material), 19 to 36 v/o U^{238} , ~ 29 v/o void, and various proportions of iron, niobium, nickel, and vanadium. In one version, graphite was substituted for the latter group of diluents and part of the U^{238} , to simulate a uranium-carbide or -oxide core. The reflector consisted of 65 tons of natural uranium with intermixed iron and aluminum.

Russian critical assemblies.—The early assemblies, BP-1 (1955) and the BP-3 modification (1957), initiated the U.S.S.R. fast-reactor experimental program. BP-1 was a flexible assembly with core consisting of close-packed plutonium-metal rods canned in steel (18, 19). The early reflectors were either dense uranium (normal or depleted) or copper, 10 in. thick, but with an added prism extending the thickness to 40 in. on one side. In the later version, BP-3, an intermediate portion of the uranium reflector was replaced by close-packed uranium rods in water.

FAST-REACTOR NEUTRONICS

EXPERIMENTAL DATA FROM FAST ASSEMBLIES

Critical size.—The most obviously useful information about a critical system is a description of composition, shape, and size. For checking computations, it is usually desirable to correct the actual system (influenced by supports, subdivisions, controls, etc.) to an idealized critical configuration. Measurements of effects of perturbations, such as changes in shape, degree of homogeneity, and quantity of incidental diluents and reflecting materials, can guide corrections of this type. Examples of descriptions of critical assemblies and of their idealized counterparts are given in Table IV (35). As this listing suggests, spherical systems are easiest to compute, but cylinders are more practicable to construct and adjust. Consequently, sphere-cylinder conversions are of general interest. Figure 1 shows measured shape-conversion factors for enriched uranium-metal cores, both diluted and undiluted, in uranium reflectors of several thicknesses (26, 29, 32). Also generally useful are intercomparisons of various reflector materials, as illustrated by Figure 2, which shows reflector effects on the critical mass of spherical enriched uranium. (Shapes of the curves relating critical mass to reflector thickness will, of course, be different for larger, dilute cores.) Figure 3 gives critical masses of dense Pu^{239} and U^{233} relative to those of U^{235} in similar reflectors.

Perturbation data.—A particularly useful type of perturbation measurement gives the reactivity change associated with the insertion of a sample of material into a cavity within a critical assembly (26). Results for various positions in the assembly may be analyzed to give effective absorption and

TABLE IV
ELEMENTARY FAST CRITICAL ASSEMBLIES

Actual assembly		Idealized spherical assembly	
Description	Critical mass of fuel in core (kg.)	Description	Critical mass of fuel in core (kg.)
<i>U²³⁵-U²³⁸ undiluted</i>			
Godiva: bare approx. sphere of Oy (93.9), * $\rho(U^{235}) = 17.59$ gm./cm. ³	~48.7 (variable)	bare Oy (93.9) sphere, $\rho(U^{235}) = 17.59$ gm./cm. ³	48.7 U ²³⁵
Topsy: Oy (94.1) pseudosphere ($\frac{1}{4}$ in. cubic units), $\rho(U^{235}) = 17.60$ gm./cm. ³ , in thick U (natural).	16.38	Oy (94.1) sphere, $\rho(U^{235}) = 17.60$ gm./cm. ³ , in 9.0 in. thick U (natural) at 19.0 gm./cm. ³	16.28 U ²³⁵
Jemima Oy (53.6): bare cylinder of interleaved 10.5 in. dia. Oy (93.4) and U (natural) plates, $\rho(U^{235}) = 10.02$ gm./cm. ³ †	86.8	bare, homogeneous Oy (53.6) sphere, $\rho(U^{235}) = 10.02$ gm./cm. ³	75.0 U ²³⁵
Jemima Oy (37.7): bare cylinder of interleaved 10.5 in. dia. Oy (93.4) and U (natural) plates, $\bar{\rho}(U^{235}) = 7.07$ gm./cm. ³	100.7	bare, homogeneous Oy (37.7) sphere, $\rho(U^{235}) = 7.07$ gm./cm. ³	92.4 U ²³⁵
Jemima Oy (29.0): bare cylinder ~11.5 in. dia. built up of plates and blocks of Oy (93.4) and U (natural), $\bar{\rho}(U^{235}) = 5.45$ gm./cm. ³	123.0	bare, homogeneous Oy (29.0) sphere, $\rho(U^{235}) = 5.45$ gm./cm. ³	109.3 U ²³⁵
Oy (16.25) in 3 in. U: cylinder 15 in. dia. of interleaved 15 in. dia. Oy (93.4) and U (natural) plates, $\bar{\rho}(U^{235}) = 3.05$ gm./cm. ³ , in 3 in. thick U (natural)	112.5	homogeneous Oy (16.25) sphere, $\rho(U^{235}) = 3.05$ gm./cm. ³ , in 3.0 in. thick U (natural) at 19.0 gm./cm. ³	108.0 U ²³⁵ (~196 for bare sphere)
<i>U²³⁵-U²³⁸ diluted</i>			
ZPR-III, No. 6F: core approx. sphere built up of small plates in drawers, 29.9 v/o † Oy (46.5), 31.4 v/o Al, 12.3 v/o ss‡, 26.4 v/o void; thick reflector 83.5 v/o U (depleted)§, 2.3 v/o Al, 7.3 v/o ss, 6.9 v/o void.	131.1	homogeneous spherical system of same composition, reflector ~30 cm. thick; in core, $\rho(U^{235}) = 2.62$ gm./cm. ³	133.3 U ²³⁵
ZPR-III, No. 9A: core approx. sphere built up of small plates in drawers, 49.7 v/o Oy (23.4), 21.5 v/o Al, 14.2 v/o ss, 14.6 v/o void; thick reflector 83.5 v/o U (depleted), 7.3 v/o ss, 9.2 v/o void.	146.2	homogeneous spherical system of same composition, reflector ~30 cm. thick; in core, $\rho(U^{235}) = 2.19$ gm./cm. ³	150.6 U ²³⁵

* Oy (93.9) signifies uranium enriched to 93.9 w/o U²³⁵.

† v/o means per cent by volume.

‡ w/o means per cent by weight.

§ $\bar{\rho}$ means core-average density.

|| U (depleted) means U with below-normal U²³⁵ content.

‡ ss means stainless steel (type 304).

TABLE IV (Continued)

Actual assembly		Idealized spherical assembly	
Description	Critical mass of fuel in core (kg.)	Description	Critical mass of fuel in core (kg.)
ZPR-III, No. 11: cylindrical core built up of small plates in drawers, 81.2 v/o Oy (11.6), 9.15 v/o ss, 9.65 v/o void; thick reflector 83.5 v/o U (depleted), 7.3 v/o ss, 9.2 v/o void.	240.6	homogeneous spherical system of same composition, reflector ~30 cm. thick; in core $\rho(U^{235}) = 1.78 \text{ gm./cm.}^3$	253.6 U^{235}
Zeus, No. 1: hex. cylindrical core of Al tubes filled with Oy (45) and U, and rods of Ni, Mo, Nb, ss; reflector 65 tons U (natural) rods in Al cans, borated graphite outside.	203.2	homogeneous spherical core 49.1 v/o Oy (25.5), 5.8 v/o Nb, 2.6 v/o Ni, 11.9 v/o Al, 30.6 v/o void; reflector ~25 in. thick, 64 v/o U (natural), 27 v/o Al, 9 v/o void.	~190 U^{235}
<i>Pu^{239}-U^{235} undiluted</i>			
Jezebel: bare approx. sphere of Pu with minor diluents, made of several Ni-plated parts.	16.57 Pu	bare sphere of Pu^{239} , $\rho(Pu^{239}) = 15.56 \text{ gm./cm.}^3$	16.22 Pu^{239}
Popsy: 2 Ni-plated hemispheres of Pu with minor diluents, in thick U (natural).	5.78 Pu	sphere of Pu^{239} , $\rho(Pu^{239}) = 15.67 \text{ gm./cm.}^3$ in 9.5 in. thick U (natural)	5.74 Pu^{239}
<i>Pu^{239}-U^{235} diluted</i>			
Zephyr: core of $\frac{1}{2}$ in. dia. Pu rods canned in Ni, loaded in hexagonal array into a cylindrical U (natural) matrix and surrounded by a thick U (natural) blanket.	14.7 Pu	spherical core of 49.6 v/o Pu^{239} at 15.8 gm./cm. ³ , 32.7 v/o U (natural), 9.9 v/o Ni, 0.5 v/o Cu, 7.3 v/o void; reflector ~14 in. thick U (natural) at 19.0 gm./cm. ³	~14.0 Pu^{239}
<i>U^{235} and Th^{232} (subcritical extrapolations to critical)</i>			
10 kg. U^{235} in U: 2 Ni-plated hemispheres of U^{235} (98.25 w/o) $\frac{1}{2}$ in 0.96 in. thick U (natural).	9.70	spherical core of 9.705 kg. U^{235} and 0.172 kg. $U^{235} + U^{238}$ in 0.885 in. thick U (natural) at 18.9 gm./cm. ³ ; core radius 5.04 cm.	9.70 U^{235}
10 kg. U^{235} in Oy: 2 Ni-plated hemispheres of U^{235} (98.25 w/o) in 0.49 in. thick Oy (93.3).	9.70	spherical core of 9.705 kg. U^{235} and 0.172 kg. $U^{235} + U^{238}$ in 0.458 in. thick Oy (93.3) at 18.8 gm./cm. ³ ; core radius 5.04 cm.	9.70 U^{235}
7.5 kg. U^{235} in U: 2 Ni-plated hemispheres of U^{235} (98.25 w/o) in 2.098 in. thick U (natural).	7.47	spherical core of 7.468 kg. U^{235} and 0.133 kg. $U^{235} + U^{238}$ in 2.090 in. thick U (natural); at 18.9 gm./cm. ³ ; core radius 4.60 cm.	7.47 U^{235}
7.5 kg. U^{235} in Oy: 2 Ni-plated hemispheres of U^{235} (98.25 w/o) in 0.778 in. thick Oy (93.3).	7.47	spherical core of 7.468 kg. U^{235} and 0.133 kg. $U^{235} + U^{238}$ in 0.780 in. thick Oy (93.3) at 18.8 gm./cm. ³ ; core radius 4.60 cm.	7.47 U^{235}
Oy in Th: Oy (93.9) sphere, $\rho(U^{235}) = 17.5 \text{ gm./cm.}^3$, in 1.81 in. thick Th at 11.48 gm./cm. ³	34.7	same as actual	34.7 U^{235}

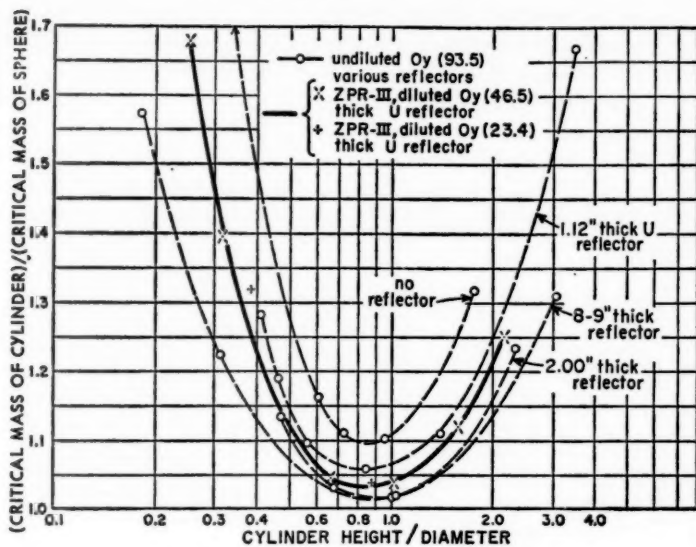


FIG. 1. Dependence of critical mass upon cylindrical core shape for various fast-neutron systems. The ZPR-III assemblies are described in Table IV.

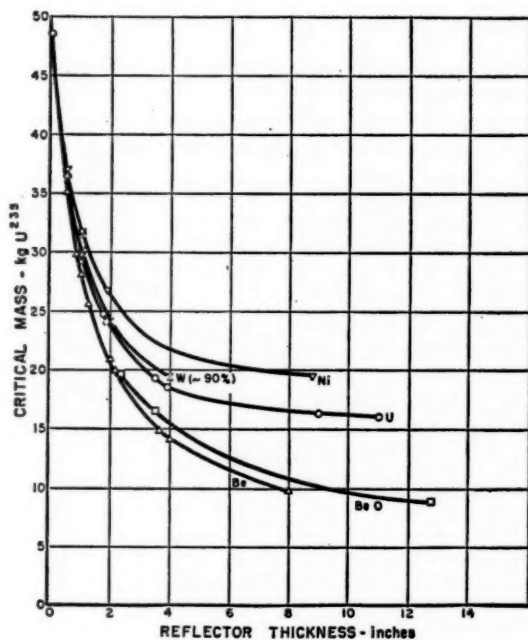


FIG. 2. Critical masses of spherical highly-enriched uranium cores in various reflectors.

transport cross sections⁴ for the perturbing material. Integration throughout the assembly and adjustment of core size to maintain a critical condition give a dilution exponent that describes the way in which the critical mass changes as the system is diluted uniformly with the perturbing material. Effective absorption and transport cross sections and dilution exponents are given in Table V for various materials in Jezebel (bare Pu), Godiva (bare U^{235}), and Topsy (U^{235} in natural U), and corresponding cross sections appear in Table VI for Zephyr (diluted Pu^{239} in natural U) and Zeus (diluted U^{235} in natural U) (34).

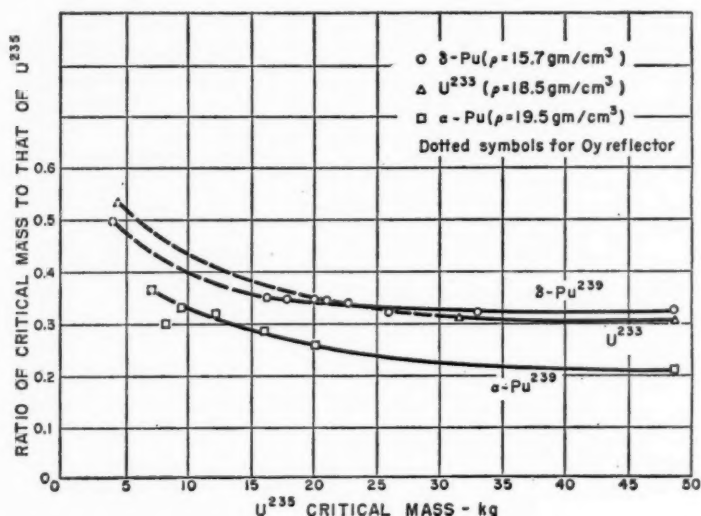


FIG. 3. Spherical critical masses of metallic Pu^{239} and U^{233} relative to those of U^{235} in reflectors of the same composition and thickness.

Spectral characteristics.—Critical-mass data are insufficient to verify details of computational schemes that are expected to give information such as breeding ratio and changes in a power reactor's behavior during its operational life. Ideally, neutron-flux spectra throughout a reactor are the sort of details for which experimental confirmation is desired. Apart from the external (leakage) flux, spectra are so difficult to measure (36) that so-called "spectral indices" are used to characterize them. These spectral indices are relative neutron-activation rates of detectors with differing sensitivities to neutron energy, such as: $\bar{\sigma}_f(U^{235} \text{ or } Pu^{239})/\bar{\sigma}_f(U^{238})$, $\bar{\sigma}_f(Np^{237} \text{ or } U^{234})/\bar{\sigma}_f(U^{238})$,

⁴ This "absorption" cross section represents capture cross section (minus fission, if appropriate) adjusted by a term representing the effect of energy degradation by scattering. The corresponding transport cross section, on the other hand, is undistorted, so is useful for checking the values used in detailed calculations.

TABLE V
SELECTED MATERIAL REPLACEMENT RESULTS FOR
TOPSY, GODIVA, AND JEZEBEL

Element (x)	Density gm.- atom/cm. ³	Topsy (Oy 94% in U)			Godiva (bare Oy 94%)			Jezebel (bare Pu)		
		$\bar{\sigma}_a(x)^*$ barn	$\bar{\sigma}_{tr}(x)^\dagger$ barn	Dilution exponent [‡] $n(x)$	$\bar{\sigma}_a(x)^*$ barn	$\bar{\sigma}_{tr}(x)^\dagger$ barn	Dilution exponent [‡] $n(x)$	$\bar{\sigma}_a(x)^*$ barn	$\bar{\sigma}_{tr}(x)$ barn	Dilution exponent [‡] $n(x)$
C	0.185	-0.022	2.13	0.86	-0.028	2.17	1.02	0.016	2.15	1.30
O		-0.013	2.20					0.023	2.22	
Al	0.100	-0.006	2.12	1.04	-0.006	2.14	1.51	0.033	2.30	1.61
Cr	0.138	0.015	2.41	0.98						
Mn	0.135	0.009	2.70	0.95						
Fe	0.137	0.020	2.29	1.01	0.006	2.29	1.28	0.050	2.44	1.45
Ni	0.152	0.066	2.77	1.02	0.056	2.65	1.22	0.111	2.77	1.39
Cu	0.141	0.035	2.68	0.99	0.022	2.73	1.18	0.074	2.83	1.37
Zr	0.071	0.022	3.87	1.02				0.070	4.10	1.51
Nb	0.092	0.068	3.99	1.01						
Mo	0.106	0.032	4.58	0.89				0.105	3.99	1.33
Ta	0.092	0.155	3.91	1.12				0.232	4.34	1.48
W	0.105	0.097	4.40	0.99				0.182	4.60	1.30
Th	0.049 ₈	0.069	4.48	1.08	0.017	4.92	1.46	0.141	5.00	1.66
U ²³⁸	0.080	-3.22 ₈								
U ²³⁵	0.080	-1.89 ₁ †			-1.86 ₂ †			-1.82 ₈	5.3	
U ²³³	0.080	-0.228	5.10†		-0.299	5.0†		-0.238	5.1*	
Pu ²³⁹		-3.63 ₈			-3.56 ₁			-3.60 ₉ *	5.3	
Pu ²⁴⁰		-2.58						-2.34		
Void				1.20			2.00			2.00

* $\bar{\sigma}_a(x) = \bar{\sigma}_c(x) - \bar{\sigma}_f(x) - \Delta\gamma\bar{\sigma}_s(x)$, where $\bar{\sigma}_c$ and $\bar{\sigma}_f$ are capture and fission cross sections (suitably averaged), $\Delta\gamma$ is the increase in neutron effectiveness per central scattering and $\bar{\sigma}_s$ is scattering cross section. (See footnote 4.)

† $\bar{\sigma}_{tr}$ is an effective transport cross-section. (See footnote 4.)

‡ The critical mass of a system diluted by the volume fraction $F(x)$ of element x , $m_c(x)$, is related to the critical mass of the undiluted system $m_c(0)$, according to $m_c(x)/m_c(0) = 1 - F(x)^{-n}$; $F(x) \ll 1$. If $\rho_0(x)$ is the normal density of x in gm.-atom/cm.³,

$$n(x) = 1.20 - \rho_0(x) [0.735 \bar{\sigma}_{tr}(x) - 12.82 \bar{\sigma}_a(x)], \text{ for Topsy;}$$

$$n(x) = 2.00 - \rho_0(x) [2.25 \bar{\sigma}_{tr}(x) - 14.27 \bar{\sigma}_a(x)], \text{ for Godiva;}$$

$$n(x) = 2.00 - \rho_0(x) [1.846 \bar{\sigma}_{tr}(x) - 9.964 \bar{\sigma}_a(x)], \text{ for Jezebel.}$$

‡ These values are used for normalization.

and $\bar{\sigma}_f(\text{Pu}^{239})/\bar{\sigma}_f(\text{U}^{235})$, where cross sections are flux averages. These ratios (or other combinations of them) may be supplemented by others involving effective neutron-capture cross sections, such as $\bar{\sigma}_{n,p}(\text{Al}^{27})$ and $\bar{\sigma}_{n,p}(\text{Fe}^{56})$.⁵ Table VII lists observed central spectral indices for various assemblies (35), Figure 4 shows variations of U²³⁵ fission rate with radius for typical systems, and Figure 5 illustrates the way in which a spectral index depends upon

⁵ As U²³⁵ is fissioned by neutrons of any energy, but U²³⁸ only by neutrons above ~ 1 Mev, the magnitude of $\bar{\sigma}_f(\text{U}^{238})/\bar{\sigma}_f(\text{U}^{235})$ characterizes the portion of the neutron spectrum above ~ 1 Mev; similarly, $\bar{\sigma}_f(\text{Np}^{237})/\bar{\sigma}_f(\text{U}^{235})$ indicates the portion above ~ 0.4 Mev, the fission threshold of Np²³⁷. $\bar{\sigma}_f(\text{U}^{238})/\bar{\sigma}_f(\text{Pu}^{239})$ changes primarily with differing portions of (fast) spectra between ~ 0.1 Mev and ~ 0.3 Mev. $\bar{\sigma}_{n,p}(\text{Al}^{27})$ and $\bar{\sigma}_{n,p}(\text{Fe}^{56})$ have thresholds of ~ 4.6 Mev and ~ 7.3 Mev.

TABLE VI
SELECTED MATERIAL REPLACEMENT RESULTS FOR ZEUS AND ZEPHYR

Element (x)	Zeus (No. 1)		Zephyr (No. 1)	
	$\bar{\sigma}_a(x)^*$ barn	$\bar{\sigma}_{tr}(x)$ barn	$\bar{\sigma}_a(x)^*$ barn	$\bar{\sigma}_{tr}(x)$ barn
C	-0.013	2.8	0	2.4
O	-0.010	3.2	0	2.5
Na	-0.003	3.5	0.021	2.9
Al	0.010	3.2	0.026	2.7
Cr	0.020	—	0.035	2.6
Mn	0.012	3.4	0.023	2.8
Fe	0.022	2.9	0.055	2.9
Ni	0.040	3.5	0.093	3.2
Cu	0.037	3.7	0.074	3.2
Zr	0.029	5.7	0.040	4.6
Nb	0.092	5.0	0.141	4.9
Mo	0.068	5.1	0.105	4.4
Ta	0.250	5.4	0.265	4.3
W	0.117	4.7	0.174	4.9
Hg	0.079	—	0.120	4.9
Th	0.133	6.7	-0.169	5.8
U	0.018	5.8	-0.124	5.1
U ²³³	-3.380	—	-3.32	6.5
U ²³⁵	-1.890	10.9	-1.850	6.1
U ²³⁸	0.032	—	—	—
Pu ²³⁹	-3.380	—	-3.660	4.8

* The same effective absorption cross section as in Table V. (See footnote 4.)

spectral shape. It may be added that the capture (n, γ) cross section $\bar{\sigma}_c(\text{U}^{238})$, or $\bar{\sigma}_c(\text{Th}^{232})$, is of particular importance in estimating breeding ratio (or conversion ratio):

$$BR = \frac{\text{rate of neutron capture in fertile nuclei}}{\text{rate of disappearance of fuel nuclei}}$$

Rossi alpha.—A final quantity which has utility for checking computation is Rossi alpha (α_r), the reciprocal of the pile period that an assembly would have in the absence of delayed neutrons (37). Below prompt critical, α_r is negative and $e^{\alpha_r t}$ represents the decay in fission rate that would be observed after a sharp pulse of neutrons is introduced into an assembly but during a time interval much shorter than any delayed-neutron period. Significantly above prompt critical, $1/\alpha_r$ is just the pile period, for then fission-rate growth is described by $e^{\alpha_r t}$. Table VIII gives α_r at delayed critical for

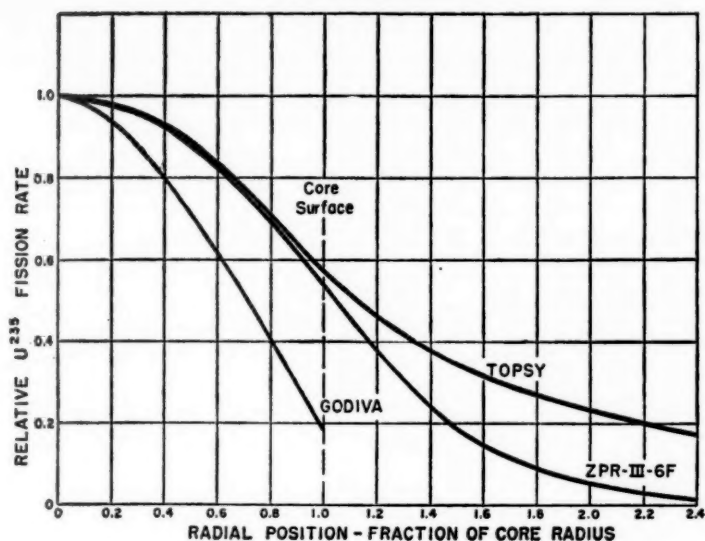


FIG. 4. U^{235} fission rate distributions in typical spherical fast-neutron systems. The assemblies are described in Table IV.

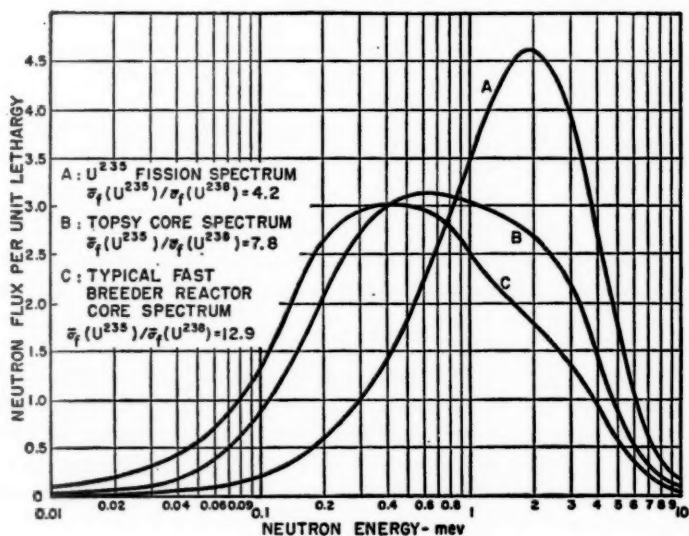


FIG. 5. Typical fast-neutron spectra. The ordinates represent flux per unit logarithmic energy increment. Topsy is described in Table IV.

TABLE VII
CENTRAL SPECTRAL INDICES OF VARIOUS ASSEMBLIES
(assemblies are described in Table IV)

	$\frac{\bar{\sigma}_f(U^{235})}{\bar{\sigma}_f(U^{238})}$	$\frac{\bar{\sigma}_f(Np^{237})}{\bar{\sigma}_f(U^{238})}$	$\frac{\bar{\sigma}_f(Pu^{239})}{\bar{\sigma}_f(U^{238})}$	$\frac{\bar{\sigma}_{\alpha,\gamma}(U^{238})}{\bar{\sigma}_f(U^{235})}$
<i>U²³⁵-U²³⁸ undiluted</i>				
Godiva (bare Oy-94)†	6.5	5.1	1.42	0.076
Topsy (Oy-94 in thick U)	7.3	5.2	1.40	0.080
Jemima Oy-53½ (bare cyl.)	8.7	5.3	~1.3	~0.089
Jemima Oy-37½ (bare cyl.)	10.8	5.9	—	—
Jemima Oy-29 (bare cyl.)	13.	—	—	—
Oy-16 in 3 in. U (cyl.)	18.2	7.1	—	—
<i>U²³⁵-U²³⁸ diluted</i>				
ZPR-III, No. 6F (30 v/o Oy-46½)	14.5	—	—	0.084
ZPR-III, No. 9A (50 v/o Oy-23½)	19.6	8.4*	1.30	—
ZPR-III, No. 11 (81 v/o Oy-11½, cyl.)	26.	8.3*	1.17	—
Zeus, No. 1 (49 v/o Oy-25½, cyl.)	16.4	—	1.27	0.107
<i>Pu²³⁹-U²³⁸ undiluted</i>				
Jezebel (bare Pu)	5.0	4.6	1.49	—
Popsy (Pu in thick U)	5.7	—	1.41	0.082
<i>Pu²³⁹-U²³⁸ diluted</i>				
Zephyr, No. 1 (cyl.)	7.8	4.7	1.35	0.086

* Values are for $\bar{\sigma}_f(U^{234})/\bar{\sigma}_f(U^{238})$; $\bar{\sigma}_f(U^{234})$ and $\bar{\sigma}_f(Np^{237})$ are similar.

† Oy-94 signifies uranium enriched to 94 w/o U²³⁵.

several fast assemblies, and corresponding values of $\Delta k/\Delta\alpha_r$,⁶ the mean life-time of prompt neutrons within an assembly (35). This quantity enters computations of the effects of super-prompt-critical reactor accidents.

A COMPUTATIONAL SURVEY OF SIMPLE FAST REACTORS

Type of computation.—Computational methods particularly suited to fast systems have been reviewed by Okrent, Avery & Hummel (26) and by Codd, Shepherd & Tait (38). Detailed methods solve, to various degrees of approximation, the transport equation that describes the propagation of neutrons within reactor materials. For geometrically simple systems, the most realistic solution is given by Carlson's S_n method, which requires modern, high-performance computing machines (39). The S_n computations take into

⁶ The expression k is the neutron-reproduction index, the average number of "daughter" fissions per fission. Its fractional increment measures reactivity.

TABLE VIII

ROSSI ALPHA AND PROMPT-NEUTRON LIFETIMES OF VARIOUS ASSEMBLIES

(assemblies are described in Table IV)

	Rossi alpha at delayed critical (sec. ⁻¹)	Effective delayed- neutron fraction	Prompt- neutron lifetime (sec.)
<i>U²³⁵-U²³⁸ undiluted</i>			
Godiva (bare Oy-94)	- 1.10 × 10 ⁶	0.0068	0.62 × 10 ⁻⁸
Topsy (Oy-94 in thick U)	- 0.37 × 10 ⁶	0.0073*	2.0 × 10 ⁻⁸
Jemima Oy-53½ (bare cyl.)	- 0.63 × 10 ⁶	0.0076*	1.2 × 10 ⁻⁸
Jemima Oy-37½ (bare cyl.)	- 0.46 × 10 ⁶	0.0079*	1.7 × 10 ⁻⁸
Jemima Oy-29 (bare cyl.)	- 0.37 × 10 ⁶	0.0080*	2.2 × 10 ⁻⁸
Oy-16 in 3 in. U (cyl.)	- 0.175 × 10 ⁶	0.0081†	4.1 × 10 ⁻⁸ †
<i>U²³⁵-U²³⁸ diluted</i>			
ZPR-III, No. 6F (30 v/o Oy-46½)	- 9.85 × 10 ⁴	0.0073*	7.4 × 10 ⁻⁸
ZPR-III, No. 9A (50 v/o Oy-23½)	- 9.0 × 10 ⁴	0.0073*	8.1 × 10 ⁻⁸
ZPR-III, No. 11 (81 v/o Oy-11½, cyl.)	- 10.4 × 10 ⁴	0.0074*	7.1 × 10 ⁻⁸
Zeus, No. 1 (49 v/o Oy-25½, cyl.)	—	0.0070	7 × 10 ⁻⁸
<i>Pu²³⁹-U²³⁸ undiluted</i>			
Jezebel (bare Pu)	- 0.65 × 10 ⁶	0.0020	0.31 × 10 ⁻⁸
Popsy (Pu in thick U)	- 0.20 × 10 ⁶	—	—
<i>Pu²³⁹-U²³⁸ diluted</i>			
Zephyr, No. 1 (cyl.)	—	0.0028	—

* Estimated from $\bar{\sigma}_f(U^{235})/\bar{\sigma}_f(U^{238})$ and delayed-neutron yields.

† Estimated for bare sphere with composition of core.

account the distribution of neutrons in energy (by subdivision into groups) and the angular dependence of neutron scattering (the "n" of S_n indicates the number of angular subdivisions). At present, the S_n method is used only for spheres (or infinite cylinders or infinite slabs) and can accommodate spherically-symmetric inhomogeneities. The less-detailed multigroup diffusion theory, which applies quite well to large, dilute fast reactors, is available in a form that is applicable to systems with axial symmetry. As we have some empirical guidance concerning the effects of shape changes (Fig. 1) and reflector distortions (Fig. 2, 3, and $\bar{\sigma}_{tr}$ from Tables V and VI), we shall confine our attention to results of S_n calculations on spherical systems⁷ (35, 40, 41).

⁷ While thus limiting ourselves, we should recognize the value of simplified "hand"-computation methods for understanding certain features of fast assemblies. Examples are: the constant-buckling relations of diffusion theory and asymptotic

TABLE IX
COMPUTED VS. EXPERIMENTAL PARAMETERS OF VARIOUS ASSEMBLIES
(assemblies are described in Table IV)

	Radius of equivalent spherical core (cm.)		$\bar{\sigma}_f(U^{235})/\bar{\sigma}_f(U^{238})$ at center	
	Expt.	Calc.	Expt.	Calc.
<i>U²³⁵-U²³⁸ undiluted</i>				
Godiva (bare Oy-94)*	8.71	8.67	6.5	6.4
Topsy (Oy-94 in thick U)*	6.04	5.98	7.3	7.0
Jemima Oy-53½ (bare cyl.)*	12.14	12.13	8.7	8.6
Jemima Oy-37½ (bare cyl.)*	14.62	14.77	10.8	10.5
Jemima Oy-29 (bare cyl.)*	16.85	17.28	~13.	12.4
Oy-16 in 3 in. U (cyl.)	20.4	20.64	18.2	18.3
<i>U²³⁵-U²³⁸ diluted</i>				
ZPR-III, No. 6F (30 v/o Oy-46½)*	23.0	22.8	14.5	12.0
ZPR-III, No. 9A (50 v/o Oy-23½)	25.4	25.4	19.6	17.1
ZPR-III, No. 11 (81 v/o Oy-11½, cyl.)	32.4	32.5	26.	24.3
<i>Pu²³⁹-U²³⁸ undiluted</i>				
Jezebel (bare Pu)*	6.29	6.25	5.0	5.4
Popsy (Pu in thick U)*	4.44	4.43	5.7	6.2
<i>U²³³ and Th²³² (subcritical)</i>				
10 kg. U ²³³ in U	5.04	5.00	—	5.3
10 kg. U ²³³ in Oy-93	5.04	5.02	—	5.2
7.5 kg. U ²³³ in U	4.60	4.55	—	5.5
7.5 kg. U ²³³ in Oy-93	4.60	4.55	—	5.2
Oy-94 in 1.8 in. Th	7.80	7.64	—	6.5

* Used for adjustments of S_n parameters within their ranges of experimental error.

The present aim is to picture the way in which fast-reactor properties depend upon core composition, where the reflector is a fixed, reasonable mixture of fertile material, structural material, and coolant. Because of insufficient experimental data, we must settle for a computational survey and shall use results of S_4 calculations with cross sections and other input parameters established by Hansen (35) and Roach (42).

Before proceeding, we should have information about the reliability of the computed data that will be used. For this purpose, Table IX compares

transport theories for approximating shape conversions, simplified two-energy group analysis for estimating the effectiveness of delayed neutrons relative to prompt neutrons, and neutron-economy considerations for obtaining fuel concentrations below which critical conditions cannot be attained.

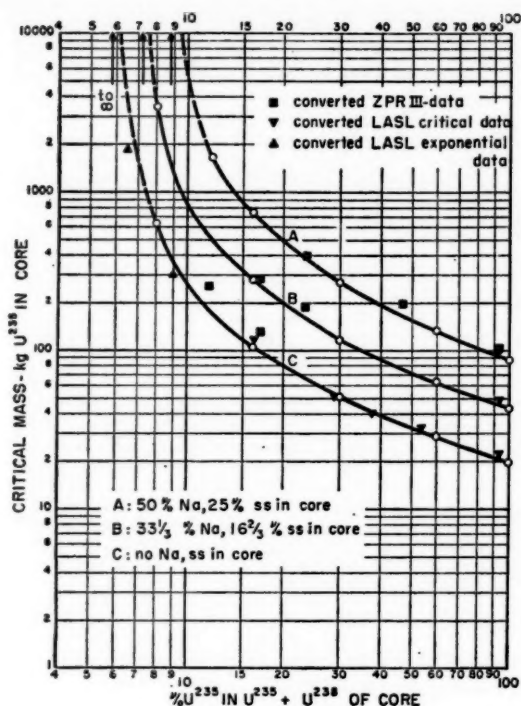


FIG. 6. Computed critical masses of spherical fast systems with U^{235} fuel and U^{238} fertile material. The reflector is 20 in. thick and consists of 40 v/o depleted U, 40 v/o Na, and 20 v/o stainless steel. The added points are converted ANL and LASL experimental data (see text for conversion method).

experimental data from Argonne and Los Alamos assemblies with results of the S_4 calculations. Checks are good enough and sufficiently general to establish reasonable confidence in computations on U^{235} - U^{238} systems, but we cannot be as certain about systems in which Pu^{239} or U^{233} is the fuel, or Th^{232} the fertile material.

The survey.—Though much more detail is available from the S_4 calculations, our survey will be limited to: (a) critical mass of fuel in the core, (b) critical volume of the core, and (c) breeding ratios with actual and infinite reflectors. The extent to which breeding ratio suffers as the result of neutron leakage or from capture in inert diluents may be inferred from the latter. These results are shown in Figures 6 to 8 for U^{235} - U^{238} cores with various degrees of dilution, in Figures 9 to 11 for Pu^{239} - U^{238} cores, and Figures 12 to 14 for U^{233} - Th^{232} cores (Th replaces the U in reflectors of the latter group). A point on each of the figures for Pu^{239} illustrates the consequence of replacing U^{238} by Th^{232} .

The added points on Figure 6 represent idealized data adjusted to ap-

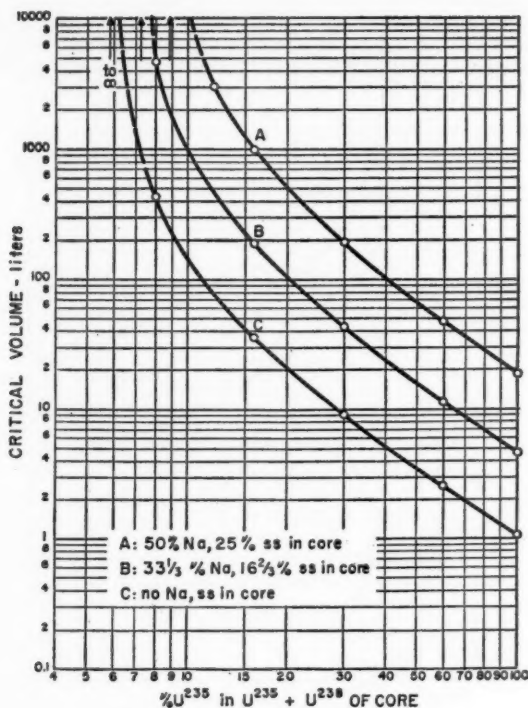


FIG. 7. Computed critical volumes of spherical fast systems with U^{235} fuel and U^{238} fertile material. The reflector is as described for Figure 6.

appropriate core and reflector compositions by means of the Topsy empirical relations of Table V. Fair agreement with the computed curves suggests general utility of this type of conversion—improvement would be expected if dilution exponents from assemblies such as Zeus or ZPR-III were to replace the Topsy values for the more dilute ranges. At least tentatively, then, the data of Table V may be used for judging the effects of replacing stainless steel and sodium by other diluents. For example, iron at normal density is equivalent (reactivity-wise) to stainless steel (304) at 0.97 normal density, nickel at 1.05 density, molybdenum at 0.61 density, or zirconium at 1.05 density. Added to these relations is a ZPR-III observation that sodium is equivalent to aluminum at 0.58 density. Finally, Tables V and VI may serve as a guide for estimating reactivity changes associated with fission-product accumulation and other compositional changes that occur during reactor operation.

Some general features of the summary curves, and their influence on power-reactor design, are: (a) The limiting critical concentration of fuel in the fuel-fertile combination (where the critical size becomes infinite) is

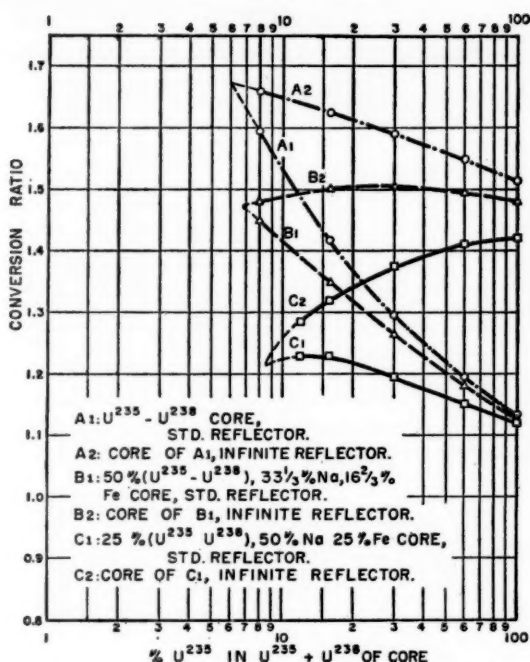


FIG. 8. Computed initial conversion ratios for spherical fast systems with U^{235} fuel and U^{238} fertile material. The lower set of curves is for the reflector described in the caption of Figure 6. The upper set applies to systems with infinite reflector of the same composition.

influenced somewhat, but not strongly, by inert diluents. (b) As the limiting critical concentration is approached, critical fuel mass and core size increase rapidly, and the breeding ratio changes relatively slowly. Practical upper limits to size and fuel inventory impose a lower limit of about 10 per cent fuel in fuel-plus-fertile material. (c) With thorium reflectors of the thickness chosen, breeding ratio suffers as the result of excessive neutron leakage. Thickening the reflector or surrounding it with a nonabsorbing reflector such as graphite will improve this situation. See, for example, the supporting evidence of Table X.

As steps are taken from an idealized fast-reactor concept toward a practical power-reactor design, so-called "detailed" neutronic calculations are found to be inadequate to describe the influence of engineering features. For preliminary design studies, additional guidance may be obtained from empirical relations (such as illustrated for shape changes, reflector changes and material replacements) and from specialized computations. But finally a detailed nuclear mock-up or zero-power proof test is required before design may be considered to be fixed.

TABLE X

COMPUTED EFFECTS OF ADDING REFLECTOR TO U^{235} - Th^{232} SYSTEMS

(standard reflector composition: 40 v/o Th, 40 v/o Na, 20 v/o stainless steel)

Core	Reflector		Core radius (cm.)	Initial breeding ratio
	Thickness of standard composition	60 cm. outer graphite		
12 v/o U^{235} , 88 v/o Th	32 cm.	none	22.6	0.77
	50 cm.	none	22.3	1.08
	50 cm.	present	22.3	1.34
	infinite	none	(22.3)	1.47
8 v/o U^{235} , 92 v/o Th	50 cm.	none	32.0	1.18
	50 cm.	present	31.9	1.35
	infinite	none	(31.9)	1.47
4 v/o U^{235} , 46 v/o Th, 33½ v/o Na, 16½ v/o ss	50 cm.	none	53.1	1.18
	50 cm.	present	53.0	1.31
	infinite	none	(53.0)	1.39
2 v/o U^{235} , 23 v/o Th, 50 v/o Na, 25 v/o ss	50 cm.	none	89.1	1.15
	50 cm.	present	88.9	1.28
	infinite	none	(88.9)	1.28

FAST-REACTOR ENGINEERING

Coolants and heat transfer.—Conventional coolants, such as water or hydrocarbons, cannot be employed in fast reactors because of the moderating effect of hydrogen. Fortunately, liquid metals such as mercury, sodium-potassium alloy (NaK), and sodium are effective heat-transfer media and do not degrade neutrons objectionably (as illustrated for sodium in Fig. 5). A review of the more advanced fast reactors reveals that sodium is now the favored coolant, although some of the early reactors employed mercury, and others use NaK, because of simplified technology. The pertinent physical properties of the three fast-reactor coolants are compared in Table XI.

The properties of sodium that make it a superior heat-transfer fluid are high heat capacity and exceptional thermal conductivity. NaK is inferior to pure sodium in these characteristics, but its lower melting temperature simplifies the requirements on the coolant systems. It is for this reason that NaK is employed in EBR-I and the Dounreay reactor, and its use provides experience which is also applicable to systems for chemically-similar sodium. A supplement to the *Liquid Metals Handbook* is devoted entirely to sodium and NaK (43).

TABLE XI
APPROXIMATE PHYSICAL PROPERTIES OF FAST-REACTOR
LIQUID-METAL COOLANTS

	Hg	Na	NaK*
Density at 570°F. (lb./ft. ³)	805.0	54.0	50.0
Melting point (°F.)	-38.0	208.0	12.0
Boiling point (°F.)	675.0	1620.0	1440.0
Sp. heat at 570°F. (Btu/lb.-°F.)	0.032	0.312	0.224
Thermal conductivity at 390°F. (Btu/hr.-ft.-°F.)	7.0	46.0	15.0

* Eutectic mixture (22% Na—78% K).

The principal problems that must be overcome in the development of sodium coolant systems arise from the moderately high melting temperature (97°C.) of sodium and its chemical activity, particularly with oxygen and

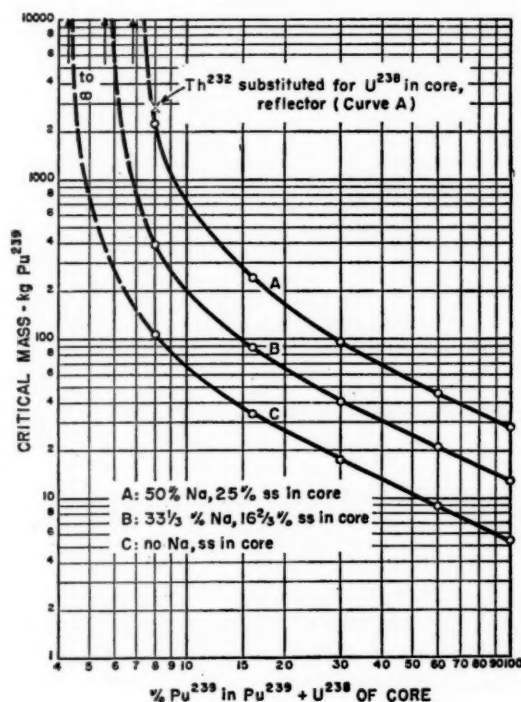


FIG. 9. Computed critical masses of spherical fast systems with Pu^{239} fuel and U^{238} fertile material. The reflector is 20 in. thick and consists of 40 v/o depleted U, 40 v/o Na, and 20 v/o stainless steel. The added point shows the effect of substituting Th^{232} for U^{238} in core and reflector.

water. Experience of the past 10 years has shown not only that these problems can be overcome, but also that the pumping characteristics of sodium are excellent, its neutron-induced activity can be accommodated, and its corrosion properties are quite acceptable if it is kept free of contaminants (particularly oxygen) (44, 45). The poor lubricating qualities of sodium and its chemical activity lead to the requirement for careful engineering design of components with moving parts, such as pumps and valves. Seals and

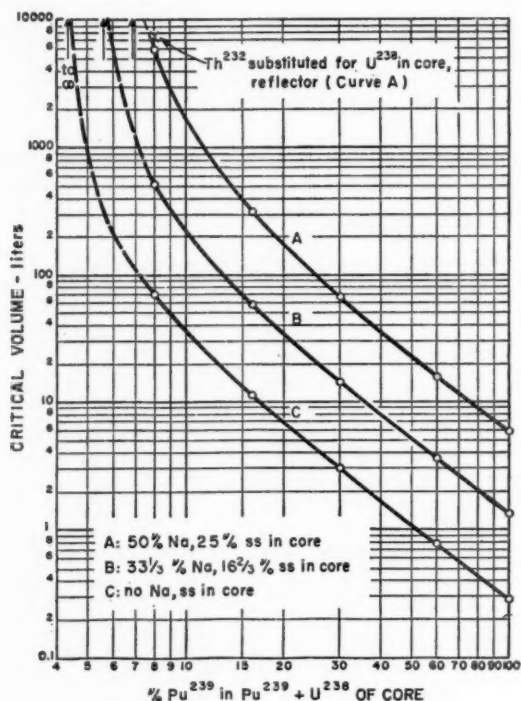


FIG. 10. Computed critical volumes of spherical fast systems with Pu²³⁹ fuel and U²³⁸ fertile material. The reflector is as described for Figure 9.

bearings are particularly complex and must be blanketed by inert gas to isolate sodium from the atmosphere. Electromagnetic pumps, heat exchange equipment of high thermal performance, instrumentation such as electromagnetic flow meters and leak-tight pressure sensing devices, and piping systems have now been developed in sizes and for operating temperatures which are of interest for large-scale reactor applications. At present all of these components are custom-engineered for the particular application. Satisfactory tests have been conducted on systems of 5000 gal.-per-min. capacity, operating at temperatures up to 900°F.; but long-term plant ex-

perience, similar to that which now exists for water cooled systems, must await the operation of the reactors under construction.

It has been seen in Table III that high heat fluxes and high coolant velocities are typical of fast reactors, consequences of necessarily great power density. Low coolant velocity implies high temperature rise of the coolant and excessive thermal stresses in the coolant system (because of the small heat capacity of fast-reactor cores and the high thermal conductivity of

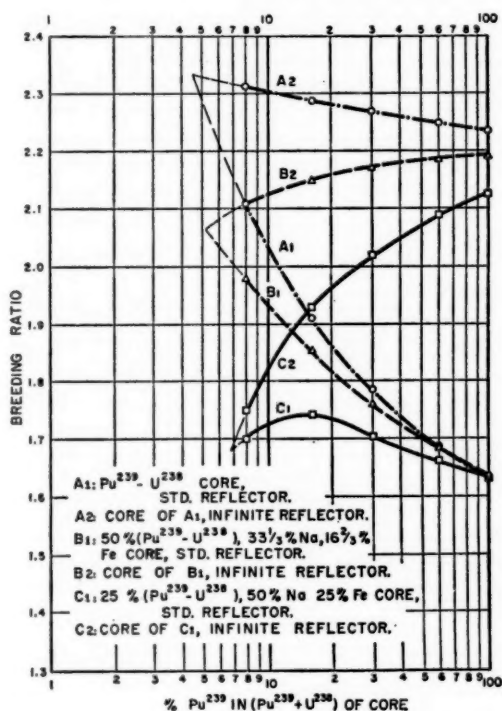


FIG. 11. Computed initial breeding ratios of spherical fast systems with Pu^{239} fuel and U^{238} fertile material. The lower set of curves is for the reflector described in the caption of Figure 9. The upper set applies to systems with infinite reflector of the same composition.

sodium, power-level changes are reflected rapidly in temperature changes of coolant-system components). On the other hand, velocities are limited by the attainable pressure that can be applied to the coolant and by the attendant pumping power. Consequently, for very large reactors, it will be necessary to compromise between low coolant velocity and high temperature rise. The restrictiveness of this compromise can be eased by taking advantage of the fact illustrated by Figure 1, that the height to diameter ratio of reactor cores can be considerably less than unity without appreciable sacrifice in

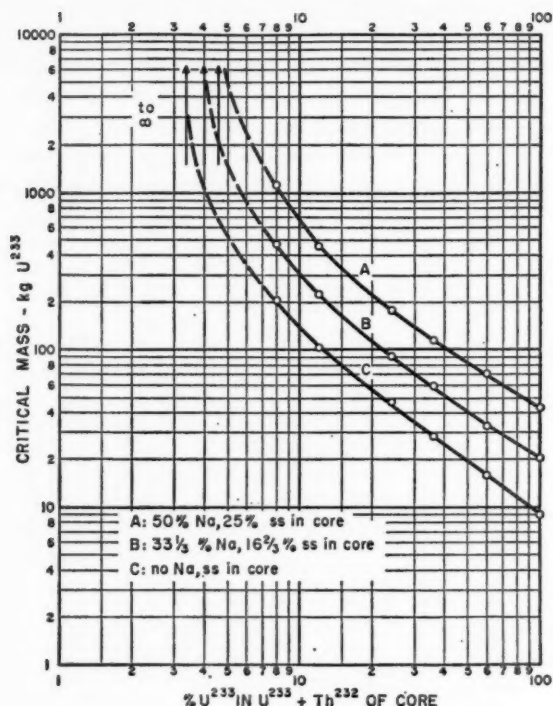


FIG. 12. Computed critical masses of spherical fast systems with U^{235} fuel and Th^{232} fertile material. The reflector is 20 in. thick and consists of 40 v/o Th, 40 v/o Na, and 20 v/o stainless steel.

critical mass. Reduction in core height becomes increasingly important for large reactors as the coolant temperature rise is nearly proportional to the height, all other factors being equal (coolant flow area, coolant flow velocity, power density, etc.). It can be anticipated that future large reactor cores will tend toward a height-to-diameter ratio below the 0.8 to 0.9 optimum indicated by Figure 1. It may be noted that the EBR-II core has a height-to-diameter ratio of approximately 0.75 (14).

Control and kinetics.—As has been stated, the control characteristics of fast reactors and of thermal reactors are very similar below prompt critical (8). The reactivity effects of temperature, fuel burn-out, and fission-product build-up are much smaller in fast reactors, but controls are correspondingly less effective because of the smaller neutron-capture cross sections of absorbers. Control is effected in fast reactors by movement of absorbers, fuel, or reflector. Practical considerations limit such controls to approximately 5 per cent to 10 per cent in reactivity as compared with absorption control of 10 per cent to 20 per cent in thermal reactors.

It is considered essential in power reactors to have a negative temperature coefficient and negative power coefficient of reactivity in order to achieve inherent self-limiting power characteristics. These are easily obtained in most thermal reactors. In fast reactors, the temperature coefficient is determined by thermal expansion of the fuel, structure, and coolant, of which the most significant parameter is the expansion of the fuel as it occurs instantaneously with an increase in power. It is extremely important, therefore, in the design of fast-reactor fuel elements to provide for expansion of the fuel in a manner which produces a negative reactivity effect on the reactor.

Though the early EBR-I cores had a negative temperature coefficient, under certain abnormal operating conditions they exhibited a "prompt positive temperature coefficient." This effect was observed during rapid changes in coolant-flow rate or power level and was attributed to "bowing" of the fuel elements (0.448 in. diameter) as a result of differential heating. Because of the shape of the neutron-flux distribution in the core (Fig. 4), an off-axis fuel element tended to heat nonuniformly around its circumference, the surface toward the center of the reactor having the higher temperature. This resulted in axial bowing of the fuel element toward the center of the reactor, tending to compact the core and increase reactivity. With a rapid change in temperature of the fuel elements, this effect should occur first, followed by a slower over-all expansion of the coolant and structure. So this reactor

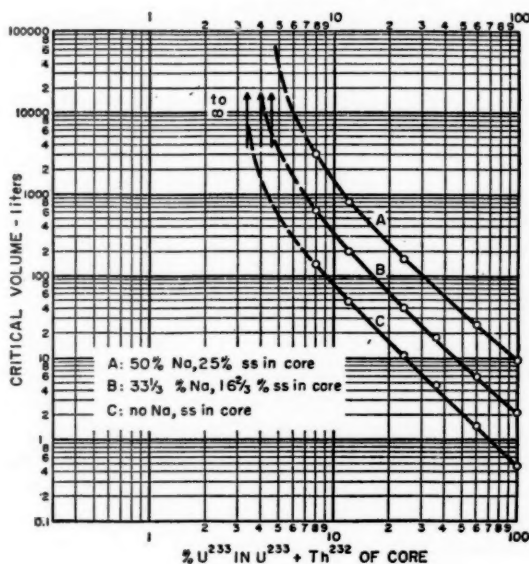


FIG. 13. Computed critical volumes of spherical fast systems with ^{233}U fuel and Th^{232} fertile material. The reflector is as described for Figure 12.

should exhibit first a transient positive temperature coefficient followed by the proper negative temperature coefficient. During a series of experiments without coolant flow which were conducted to measure this effect, an excessive power rise was permitted which resulted in a partial melt-down of the core. The reactor internals were dismantled and replaced by a core of revised design which permitted physical constraint of the fuel elements to prevent bowing. Tests on this core have confirmed that the prompt positive tem-

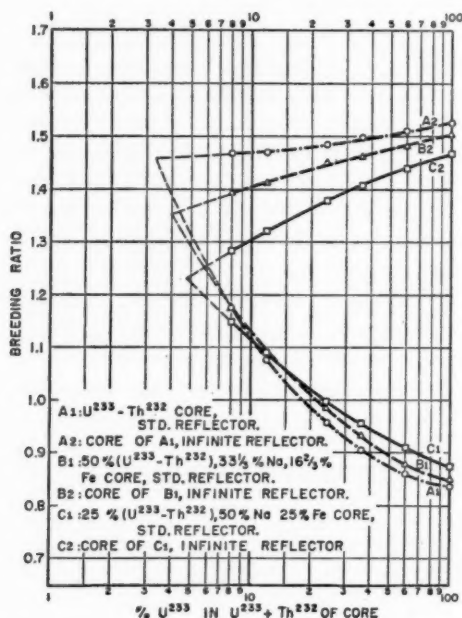


FIG. 14. Computed initial breeding ratios for spherical fast systems with U^{235} fuel and Th^{232} fertile material. The lower set of curves is for the reflector described in the caption of Figure 12. The upper set applies to systems with infinite reflector of the same composition.

perature coefficient in the EBR-I was attributable to the postulated bowing phenomena (12) and could be eliminated by proper design.

In the Enrico Fermi Reactor and EBR-II there are long, small-diameter fuel elements (approximately 0.145 in. fuel diameter) that are free to expand lengthwise, and inward bowing is prevented by contacting fins. The lengthwise expansion of each fuel pin has a negative effect on reactivity while radial expansion has essentially no effect (14, 16). The Dounreay fast reactor employs relatively large-diameter fuel elements, and perforated transverse plates within the reactor core prevent inward bowing (46).

Transient accident considerations.—Because of dilution by coolant and

structure, fast reactors contain the equivalent of several critical masses of compact fuel. The reactor therefore can conceivably be reassembled into a more efficient geometry, becoming super-prompt critical. Although it is difficult to postulate the circumstances under which the fuel may so rearrange itself, it is more difficult to prove that compaction is impossible. A series of events which might lead to such a super-prompt critical rearrangement involves the melt-down of the fuel in the absence of coolant, in a manner such that a large part of the core collapses under gravity into the remainder. This process has been given considerable theoretical attention (21, 25, 47, 48), with the result that there has been major design emphasis on the integrity of the sodium-coolant system and the prevention of coolant loss.

Melt-down of fuel in the presence of sodium coolant is a more complex phenomenon because of the possible "dispersing effect" of the sodium as a result of boiling and turbulence. The melt-down of EBR-I resulted in a dispersed, spongy mixture of uranium, stainless steel, and NaK with a reduced density near the center of the reactor (49). Results of analysis suggested that sodium agitation had forced the molten fuel outward from the hottest, nearly central region of the core. The emphasis on cooling reliability has been extended to the period after shutdown during which fission-product-decay heat must be removed. In the Dounreay reactor, parallel circuits of extreme reliability provide forced-convection cooling under almost any conceivable circumstance. The U. S. fast-power-reactors employ natural-convective circulation of the coolant after reactor shutdown with systems designed to function under all anticipated conditions.

In addition to the theoretical analysis of the fuel-melt-down problem, an extensive experimental program is centered about the transient reactor test facility (TREAT) that has been constructed recently at Arco, Idaho (50). TREAT is a pulsed, graphite-moderated reactor that is designed to melt metal fuel elements without damage to itself. Experimental facilities are provided for study of the melting process of elements with or without sodium coolant and under various power-transient conditions.

Fuel cycle considerations.—A major obstacle to economic power from fast-reactor central-station power plants appears to be the cost of the fabricating and reprocessing fuel. Although the plutonium-fueled fast breeder will produce an excess of plutonium from inexpensive U^{238} , it is necessary to convert the plutonium to usable form. Plutonium is produced to greatest extent in the blanket, while it is consumed primarily in the core. In the process of burning plutonium, it must be cycled through the reactor core many times, and part of the plutonium produced in the blanket must be added to the core to compensate for that which is burned out. The existing processing methods, both for core and blanket, impose prohibitive costs on the power produced. Two possibilities for improvement present themselves for the heterogeneous reactors that are presently under development: (a) to increase the permissible burn-up of the fuel within the reactor, thus reducing the frequency of the cycle, and (b) to reduce the cost of the fuel cycle.

High fuel burn-up implies the development of elements that are extremely resistant to radiation damage, while retaining a fuel density that is large enough to satisfy other fast-reactor requirements. Metal fuels of various alloy compositions have been explored as well as nonmetallic types such as oxides or carbides (51 to 57). Alloys, which have been stressed in this country, have the advantage of potentially high fuel density, whereas the ceramics which form the fast-oxide-breeder proposal of the Knolls Atomic Power Laboratory (and appear to play a part in the U.S.S.R. program) may prove to have superior radiation resistance. Operating experience well beyond that available at present will be required to establish the most economical approach. Even fuel burn-up of the order of 2 per cent per cycle seems unlikely to lead to economically competitive power without simplification of processing methods.

An attempt at such simplification is illustrated by the integrated reactor-fuel cycle concept for EBR-II. The pyrometallurgical fuel-process cycle that will be employed appears to be attractive for highly enriched, highly irradiated fuels (58). It consists of an oxidative-slugging, melt-refining process which removes only those fission products which volatilize at the melting temperature of uranium and those fission products whose oxides are more stable than uranium oxide. The fission-product elements whose oxides are less stable than uranium oxide are not removed and are recycled with the metal fuel. Oddly enough, these elements, which include ruthenium, molybdenum, niobium, technetium, and zirconium, appear to enhance the radiation stability of the alloy (for this reason, it has been proposed that these elements be included in the initial fuel loading). Since they are radioactive species, subsequent fabrication of the fuel must be accomplished by remote control in shielded facilities; so the buildup of trans-plutonium isotopes can be accommodated without long cooling periods. As purification is accomplished by retaining the irradiated fuel in the molten metal phase, the use of solvents which are unstable under radiation is avoided. This will permit the processing of short-cooled irradiated fuel and thus reduce the fuel inventory required in the system. The EBR-II process cycle is designed to accommodate fuel after 15 days' cooling as contrasted to the probable 180 days' cooling which would be required with conventional aqueous processing methods. Although the cost attributable to fuel holdup is not as great as direct fuel-processing costs, it remains significant.

ADVANCED CONCEPTS

The advanced fast-reactor concept LAMPRE at Los Alamos promises reduced fuel-cycle costs through direct processing of its molten plutonium-iron fuel. Such a fuel has superior heat-transfer properties, resists radiation damage, and is compatible with high-temperature operation (17, 59).

An interesting concept which has been given only preliminary consideration is a fast reactor cooled by boiling mercury. The mercury would be employed in a direct-cycle turbine-generator system, and a very compact auxil-

iary power unit could result. A more advanced concept along these lines, involving a similar arrangement with boiling sodium substituted for the mercury, could lead to an extremely high-temperature cycle.

Safety considerations have stimulated investigation of the coupled fast-thermal reactor concept, one version of which consists of a fast core with a thermalizing reflector (such as beryllium) sandwiched between two uranium blankets. Avery and co-workers at the Argonne National Laboratory have reported for this arrangement a prompt-neutron lifetime comparable to that of thermal reactors, with only moderate loss in breeding ratio (60). Other versions are being investigated at Harwell and in the U.S.S.R. (18, 34).

Although the primary goal of the various fast-reactor programs has been the efficient utilization of U^{238} in central-station power plants, other applications have not been completely overlooked. Among the characteristics of fast reactors that make them particularly attractive for other uses are their potentially small size and the permissible latitude in the selection of structural materials and coolants. (The thick blanket surrounding fast-power-reactor cores that is required to achieve a high breeding ratio is not essential for power generation.) These suggest that fast reactors may be useful as compact, high-temperature power sources such as remote power stations, power units for space application, and heat generators for ultra-high-temperature chemical processing.

ACKNOWLEDGMENT

We wish to express gratitude to D. B. Hall, Gordon E. Hansen, W. H. Roach, and R. D. Smith for essential contributions to this review.

LITERATURE CITED*

1. Zinn, W. H., "Review of Fast Power Reactors," *U.N. Paper 814* (1955)
2. Jungnell, D., and Lundquist, S., "Suitable Types of Reactors for the Development of Nuclear Power Supply Based on Natural Uranium as Fuel," *U.N. Paper 155* (1958)
3. Weinberg, A. M., "Survey of Fuel Cycles and Reactor Types," *U.N. Paper 862* (1955)
4. Hughes, D. J., and Schwartz, R. B., *Brookhaven Natl. Lab. Rept., BNL-325* (1958)
5. Greebler, P., Hurwitz, H., Jr., and Storm, M. L., *Nuclear Sci. and Eng.*, **2**, 334 (1957)
6. Walker, W. H., *Atomic Energy of Canada, Ltd., Chalk River Report, CRPP-634* (1956)
7. Keepin, G. R., Wimett, T. F., and Zeigler, R. K., *J. Nuclear Energy*, **6**, 1 (1957)
8. Keepin, G. R., and Wimett, T. F., *Nucleonics*, **16**, 86 (1958)
9. "Reactor Physics Constants," *U. S. Atomic Energy Commission Document, ANL-5800* (1958)
10. Journey, E. T., *Nucleonics*, **12**, 28 (1954)
11. Lichtenberger, H. V., Thalgott, F. W., Kato, W. Y., and Novick, M., "Operating Experience and Experimental Results Obtained from an NaK-Cooled Fast Reactor," *U.N. Paper 813* (1955)
12. Thalgott, F. W., Boland, J. F., Brittan, R. O., Carter, J. C., McGinnis, F. D., Novick, M., Okrent, D., Sandmeier, H. A., Smith, R. R., and Rice, R. E., "Stability Studies on EBR-I," *U.N. Paper 1845* (1958)
13. Barnes, A. H., Koch, L. J., Monson, H. O., and Smith, F. A., "The Engineering Design of EBR-II, A Prototype Fast Neutron Reactor Power Plant," *U.N. Paper 501* (1955)
14. Koch, L. J., Monson, H. O., Simmons, W. R., Levenson, M., Verber, F., Hutter, E., Jaross, R. A., Spalding, T. R., Simanton, J. R., and Lovoff, A., "Construction Design of EBR-II: An Integrated Unmoderated Nuclear Power Plant," *U.N. Paper 1782* (1958)
15. Amorosi, A., Donnell, A. P., and Wagner, H. A., "A Developmental Fast-Neutron Breeder Reactor," *U.N. Paper 491* (1955)
16. Amorosi, A., and Yevick, J. G., "An Appraisal of the Enrico Fermi Reactor," *U.N. Paper 2427* (1958)
17. Kiehn, R. M., King, L. D. P., Peterson, R. E., and Swickard, E. O., "A Proposal for a One-Megawatt Reactor Experiment Utilizing a Molten Plutonium Fuel," *U.N. Paper 445* (1958)
18. Leipunsky, A. I., Abramov, A. I., Andreev, V. N., Baryshnikov, A. I., Bondarenko, I. I., Galkov, V. I., Golubev, V. I., Gulko, A. D., Guseinov, A. G., Kazachkovsky, O. D., Kozlova, N. V., Krasnoyarov, N. V., Kuzminov, B. D., Morozov, V. N., Nikolaev, M. N., Smirenkin, G. N., Stavitsky, Iu. Ya., Ukraintsev, F. I., Usachev, L. N., Fetisov, N. I., and Sherman, L. E., "Studies in the Physics of Fast Neutron Reactors," *U.N. Paper 2038* (1958)

* References denoted *U. N. Papers* are papers presented at the International Conferences on the Peaceful Uses of Atomic Energy at Geneva. The year given in each case is the year the conference was held.

19. Leipunsky, A. I., Grabin, V. G., Aristarkhov, N. N., Bondarenko, I. I., Kazachkovsky, O. D., Lubimtsev, O. L., Pashkov, S. A., Pinkhasik, M. S., Renne, K. K., Stavitsky, Iu. Ya., Ukraintsev, F. I., and Usachev, L. N., "Experimental Fast Reactors in the Soviet Union," *U.N. Paper 2129* (1958)
20. Kendall, J. W., and Fry, T. M., "The Dounreay Fast Reactor Project," *U.N. Paper 405* (1955)
21. Cartwright, H., Tatlock, J., and Matthews, R. R., "The Dounreay Fast Reactor—Basic Problems in Design," *U.N. Paper 274* (1958)
22. White, R. H., *Nuclear Sci. and Eng.*, **1**, 53 (1956)
23. Peterson, R. E., and Newby, G. A., *Nuclear Sci. and Eng.*, **1**, 112 (1956)
24. Wimett, T. F., and Orndoff, J. D., "Applications of Godiva II Neutron Pulses," *U.N. Paper 419* (1958)
25. Stratton, W. R., Colvin, T. H., and Lazarus, R. B., "Analysis of Prompt Excursions in Simple Systems and Idealized Fast Reactors," *U.N. Paper 431* (1958)
26. Okrent, D., Avery, R., and Hummel, H. H., "A Survey of the Theoretical and Experimental Aspects of Fast-Reactor Physics," *U.N. Paper 609* (1955)
27. Paxton, H. C., *Nucleonics*, **13**, 10, 48 (1955)
28. Graves, G. A., Hansen, G. E., and Wood, D. P., "The Use of Los Alamos Critical Assembly Facilities in a Nuclear Training Program," *U.N. Paper 1047* (1958)
29. Graves, G. A., and Paxton, H. C., *Nucleonics*, **15**, 90 (1957)
30. Beyer, F. C., Bryan, R. H., Hummel, H. H., Lennox, D. H., Martens, F. H., Reardon, W. A., Rosenzweig, N., Smith, A. B., and Spinrad, B. I., "The Fast Exponential Experiment," *U.N. Paper 598* (1955)
31. Brolley, J., Byerley, F., Feld, B., Olds, A., Scallettar, R., Slotin, L., and Stewart, R., *Neutron Multiplication in a Mass of Uranium Metal, CF-1627* (Clinton Laboratories, Oak Ridge, Tenn., 1944)
32. Long, J. K., Loewenstein, W. B., Branyan, C. E., Brunson, G. S., Kirn, F. S., Okrent, D., Rice, R. E., and Thalgott, F. W., "Fast-Neutron Power Reactor Studies with ZPR-III," *U.N. Paper 598* (1958)
33. Holmes, J. E. R., McVicar, D. D., Rose, H., Smith, R. D., and Shepherd, L. R., "Experimental Studies on Fast Neutron Reactors at A.E.R.E.," *U.N. Paper 404* (1955)
34. Smith, R. D., and Sanders, J. E., "Experimental Work with Zero Energy Fast Reactors," *U.N. Paper 39* (1958)
35. Hansen, G. E., "Properties of Elementary Fast-Neutron Critical Assemblies," *U.N. Paper 592* (1958)
36. Redman, W. C., and Roberts, J. H., "Some Current Techniques of Fast-Neutron Spectrum Measurements," *U.N. Paper 597* (1958)
37. Orndoff, J. D., *Nuclear Sci. and Eng.*, **2**, 450 (1957)
38. Codd, J., Shepherd, L. R., and Tait, J. H., *Progress in Nuclear Energy*, **I**, Chap. 9 (Pergamon Press Ltd., London, Engl., 1956)
39. Carlson, B. G., and Bell, G. I., "Solution of the Transport Equation by the S_n Method," *U.N. Paper 2386* (1958)
40. Okrent, D., and Loewenstein, W. B., "The Physics of Fast Power Reactors—A Status Report," *U.N. Paper 637* (1958)
41. Kiehn, R. M., *Nuclear Sci. and Eng.*, **4**, 166 (1958)

42. Roach, W. H., *Nuclear Sci. and Eng.* (In press)
43. Jackson, C. B., Miller, R. R., Werner, R. C., Tidball, R. A., Grantz, H. E., and Lee, R. E., *U. S. Atomic Energy Commission Document, TID-5277* (July 1, 1955)
44. Trocki, T., Bruggeman, W. H., and Crever, F. E., "Sodium and Sodium-Potassium Alloy for Reactor Cooling and Steam Generation," *U.N. Paper 123* (1955)
45. Smith, F. A., "Sodium Technology for Nuclear Power Plants," *U.N. Paper 2291* (1958)
46. Ackroyd, R. T., Kinchin, G. H., Mann, J. E., and McCullen, J. D., "Stability Considerations in the Design of Fast Reactors," *U.N. Paper 1462* (1958)
47. McCarthy, W. J., Jr., Nicholson, R. B., Okrent, D., and Jankus, V. Z., "Studies of Nuclear Accidents in Fast Power Reactors," *U.N. Paper 2165* (1958)
48. Bethe, H. A., and Tait, J. H., *U.K. Atomic Energy Authority Document, US-UK Reactor Hazard Meeting, RHM(56)/113* (1956)
49. Kittel, J. H., Novick, M., and Buchanan, R. F., *Nuclear Sci. and Eng.*, **4**, 180 (1958)
50. Freund, G. A., Iskenderian, H. P., and Okrent, D., "TREAT, A Pulsed Graphite-Moderated Reactor for Kinetic Experiments," *U.N. Paper 1848* (1958)
51. Billington, D. S., "Radiation Damage in Reactor Materials," *U.N. Paper 744* (1955)
52. Kittel, J. H., and Paine, S. H., "Effect of Irradiation on Fuel Materials," *U.N. Paper 1890* (1958)
53. Eldred, V. W., Greenough, G. B., and Leech, P., "Fuel Element Behaviour Under Irradiation," *U.N. Paper 50* (1958)
54. Barnes, R. S., Churchman, A. T., Curtis, G. C., Eldred, V. W., Enderby, J. A., Foreman, A. J. E., Plail, O. S., Pugh, S. F., Walton, G. N., and Wyatt, L. M., "Swelling and Inert Gas Diffusion in Irradiated Uranium," *U.N. Paper 81* (1958)
55. Weber, C. E., "Radiation Stability of Core Components Containing the Fissile Atoms U^{235} and B^{10} ," *U.N. Paper 1862* (1958)
56. Turner, C. J., and Williams, L. R., "The Manufacture of Fuel Elements for the Dounreay Fast Reactor," *U.N. Paper 44* (1958)
57. Davidson, J. K., *U. S. Atomic Energy Commission Document, KAPL-1701* (1957)
58. Schraidt, J. H., and Levenson, M., "Developments in Pyrometallurgical Processing," *U.N. Paper 1795* (1958)
59. Hall, D., "Plutonium Fuels for Fast Reactors," *U.N. Paper 2021* (1958)
60. Avery, R., Branyan, C. E., Brunson, G. S., Cohn, C. E., Fischer, G. F., Hummel, H. H., Kato, W. Y., Kirn, F. S., Meneghetti, D., Thalgott, F. W., and Toppel, B. J., "Coupled Fast-Thermal Power Breeder Critical Experiment," *U.N. Paper 2160* (1958)

ECONOMICS OF NUCLEAR POWER^{1,2}

BY JAMES A. LANE

Oak Ridge National Laboratory, Oak Ridge, Tennessee

INTRODUCTION

The fission of one gram of nuclear fuel, valued at about \$15, results in the release of about 78 million Btu of heat which is equivalent to the heat generated in the burning of three tons of coal. In addition to this heat, enough excess neutrons are also released in the fission process so that it is theoretically possible to produce a gram or so of new nuclear fuel (worth perhaps \$12) by capturing the neutrons in the relatively cheap "fertile" materials, Th²³² or U²³⁸. Thus U²³⁵ or other nuclear fuels constitute a potential source of energy equivalent on an economical basis to coal at about \$1 per short ton. It is this prospect for cheap fuel that makes nuclear power so attractive. The initiation and maintenance of a self-sustaining fission reaction, however, and the creation of an environment in which the majority of the excess neutrons is captured in fertile materials rather than in other materials require unique designs and operating conditions which lead to costs not encountered in conventional power plants. Because of this, the cost advantage of nuclear vs. fossil fuels is reduced. In addition, the cost of preparing the nuclear fuel so that it will withstand the effect of bombardment by the high-energy particles in the nuclear reactor and the cost of recovering unburned nuclear fuel and fertile material from spent radioactive fuel elements further reduce the economic advantages which nuclear fuels seem to have. As a matter of fact, the technical problems of building a safe and reliable nuclear plant and the high costs associated with the nuclear fuel cycle appeared to be so formidable in 1956-1957 that many who planned to build nuclear plants withdrew from the picture. Fortunately, the vigorous attack on the problem of reducing nuclear power costs continued during this time, and in 1958 there occurred a definite trend toward increased optimism with respect to the future of economic nuclear power. It is the purpose of this paper to review and analyze this trend.

NUCLEAR POWER FORECASTS

Forecasts of the growth of the United States nuclear power industry made during the past four years (1, 2) provide an index of the degree of optimism of their authors with respect to the prospects for economic nuclear power. As seen in Figure 1, the projections cover a very wide range, with more recent estimates tending to be on the conservative side.

¹ The survey of literature pertaining to this review was concluded in March, 1959.

² Among the abbreviations used in this chapter are: MwD (megawatt-day); Mwe (megawatts of electricity); Mw(th) (megawatts of heat); MwYe (megawatt-year of electricity); t (ton).

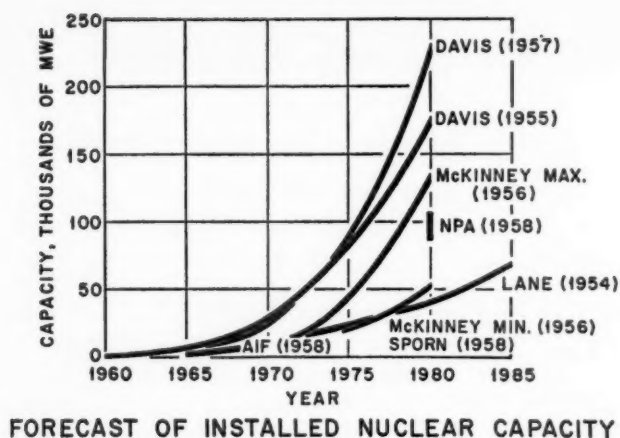
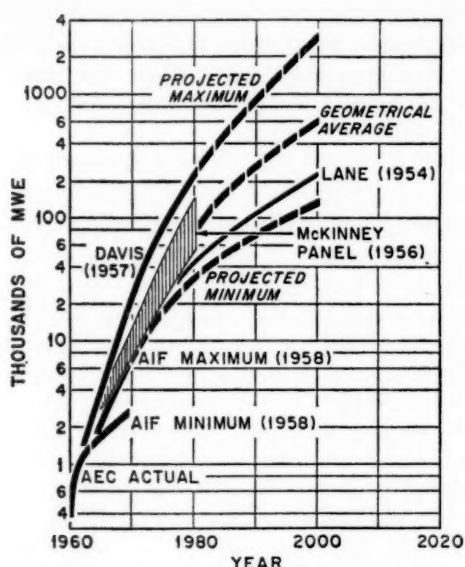


FIG. 1

Two methods² have been used to obtain the data represented by Figure 1. The first involves an estimate of the growth rate of the total electrical industry in the United States, usually projected at an annual expansion of from 4.3 to 7.0 per cent. This spread, in itself, results in a wide range of values, especially if the projection covers any appreciable period of time. Some fraction of this total growth is assumed to be taken up by nuclear plants. The over-all result is that projected nuclear power growths to the year 1980 vary by almost a factor of five.

The second approach to forecasting is based on an estimated market for electricity as a function of its cost, on the competitive "cost threshold" for nuclear power³ in various sections of the United States, and on the trend in nuclear power costs over the given period. Whether such an approach, which has been used in the forecasting studies carried out by the National Planning Association (1), is actually more meaningful than the "horseback" methods used by others is not clear at the present time. The most one can say with certainty is that nuclear power is making a positive, but slow, entry into the United States power picture and that at some future date, presumably by about 1975-1980, nuclear fuels will start to contribute substantially to our energy needs. Beyond 1980, the nuclear power industry will grow at a rate which depends on the availability and cost of nuclear source materials, the cost of nuclear power, and the need for power. Extrapolation of projected growth rates beyond 1980 is very uncertain; however, the range of such extrapolations may be used as an index of possible future requirements of nuclear source materials. Longer-range projections, therefore, are shown in Figure 2 for both the maximum and minimum growth rates. The geometrical average of extrapolated growths also shown in

³ Defined as the cost that would enable nuclear power to capture a market share of one billion kilowatthours per year.



PROJECTED GROWTHS OF U.S. NUCLEAR POWER

FIG. 2

TABLE I
POTENTIAL NUCLEAR SHARE OF U. S. ENERGY CONSUMPTION
IN COMPETITIVE USES IN 1980*

Energy Consuming Category	Installed Capacity 10 ⁶ kw. (heat)		Energy Consumption 10 ¹² Btu		Nuclear Share of Total %
	Total	Nuclear	Total	Nuclear	
Electric power generation†	732	192	14,798	4,307	29
Industrial process and furnace heat	n.e.‡	53	20,740	1,454	7
Ship propulsion	122	23	2,064	491	24
Railroad locomotion	169	8	1,000	96	10
U. S. Navy	60	60	450	450	—
U. S. Air Force	n.e.	40	500	110§	—
Other military	n.e.	17	n.e.	100	—
Total	—	393	39,552	7,008	16**

* From (1).

† 65% plant factor for conventional plants, 75% plant factor for nuclear plants.

‡ n.e.—not estimated.

|| Assumes 25% load factor.

§ Based on 10% load factor.

** Civilian categories only.

Figure 2 will be used as a basis for long-range material requirements.

There is some indication that nuclear fuels will become an important factor in uses other than the production of electricity. Just how important these other uses are is illustrated by Table I taken from (1).

PROJECTED ANNUAL AND CUMULATIVE REQUIREMENTS OF NUCLEAR SOURCE MATERIALS

Annual requirements of nuclear fuels and fertile materials depend on: (a) the growth rate of the industry, (b) the distribution by reactor types, and (c) inventory and burn-up requirements of each type. It has already been seen how uncertain are the forecasts of the growth rate. The projected distribution by reactor type and specific requirements for each type are even more uncertain since reactor technology is developing too rapidly at the present time to permit a singling-out of any one reactor system as the best, or to project its long-range potential. However, an order-of-magnitude estimate of maximum future uranium and thorium needs may be obtained from maximum projected growth rates, using conservative estimates for inventory and burn-up requirements. Such an approach has been used by Cohen (3), who estimates that about 20,000 tons of 1.5 per cent enriched uranium per year will be needed by 1980 if all nuclear power plants are based on slightly enriched pressurized water reactors, or 60,000 tons per year of natural uranium if the nuclear power system is based on natural-uranium-fueled gas-cooled graphite reactors. Since it requires about 2.5 tons of natural uranium to produce 1 ton of 1.5 per cent enriched fuel, projected requirements for both types of reactors appear to be approximately equal. Cohen's study shows that in both cases the primary requirement for uranium arises from the inventory of fuel held up in the reactor and processing plants, rather than from the uranium that is actually consumed to produce power. It is worthwhile, therefore, to examine the question of nuclear fuel inventories in more detail.

REACTOR INVENTORY REQUIREMENTS

Reactor inventories, measured as tons⁴ of natural uranium per Mwe, depend on the heat removal capabilities of the cooling system, the neutron economy of the reactor, and its thermal efficiency. High specific powers (kilowatts of heat per kilogram of fuel) achieved at the expense of higher enrichment or lower thermal efficiency, therefore, do not necessarily result in the most efficient use of natural uranium. Out-of-pile inventories of fuel in fabrication plants, in storage, or in the various fuel processing plants also depend on these same variables, as the ratio of external to internal inventory decreases as the reactor fuel cycle increases. As shown in (3), this ratio is given by the ratio of residence time of fuel in process to residence time in reactor. For a fabrication time of 300 days and cooling and reprocessing time

⁴ The term t(ton) refers to short ton throughout this paper.

of 180 days, the ratio of the external to internal inventory is given by $480 Kf/T$, where K =specific power/t, f =plant load factor, and T =average fuel lifetime, in MwD/t. Including 20 per cent spare fuel elements, the ratio of total inventory to reactor inventory, $R=480 Kf/T+1.2$. For future nuclear plants, fuel cycles of 15,000 MwD/t, specific powers of 40 Mw(th)/t, and 0.8 plant factor may be projected. On this basis, $R=2.2$, giving a total inventory of $2.2 \times 1/40$ or 0.055 ton/Mw(th). At a thermal efficiency of 34 per cent, this corresponds to 0.16 ton/Mwe. As pointed out in (3), to achieve

TABLE II
INVENTORY REQUIREMENTS AND DISTRIBUTION OF REACTOR TYPES
IN FUTURE U. S. NUCLEAR POWER INDUSTRY

Reactor Type*	Moder- ator	Breeding Ratio	Fissile and Fertile Inventory per Mwe	Percentage of Total Nuclear Electric Capacity	
				1960- 1980	Plants Built After 1980
PWR, BWR	H ₂ O	0.75	0.16 ton 1.5% U ²³⁵	45	15
SGR, GCR	Graphite	0.60	0.30 ton 2% U ²³⁵	30	10
Organic or Gas Cooled	D ₂ O	0.82	0.20 ton 1.1% U ²³⁵	25	10
Thorium Converter	Graphite	1.00	2.5 kg. U ²³⁵ 0.2 ton thorium		15
Aqueous Thorium Breeder	D ₂ O	1.10	1.0 kg. U ²³⁵ or U ²³³ 0.3 ton thorium		15
Fast Breeder	None	1.45	4.8 kg. U ²³⁵ or Pu ²³⁹ 0.26 ton U ²³⁸		35

* PWR=pressurized water reactor; BWR=boiling water reactor; SGR=sodium cooled graphite reactor; GCR=gas cooled graphite reactor.

the above conditions may require natural uranium slightly enriched with U²³⁵ (or recycled plutonium) to about 1.5 per cent fissionable material. In this case, the equivalent inventory of natural uranium amounts to about 0.4 ton/Mwe. Projected inventories for other reactor types taken from data in the literature (4, 5, 6) are summarized in Table II.

DISTRIBUTION BY REACTOR TYPE

The distribution of reactor types is also shown in Table II for the year 1980 and for new plants built after 1980. This latter projection is based on

the assumption that after 1980, 30 per cent of the nuclear plants will be based on the U^{235} - Th^{232} - U^{233} fuel cycle, rather than on the U^{235} - U^{238} - Pu^{239} cycle. It is also assumed that half of the uranium-fueled plants built after 1980 will be based on fast breeders and the other half on approximately equal numbers of H_2O , graphite, and D_2O moderated reactors. The projected capacity of various reactor types in the years 1970 to 2000 is shown in Table III based on the average growth rate of Figure 2.

TABLE III
PROJECTED CAPACITIES OF VARIOUS U. S. POWER REACTOR TYPES, MWE.

Reactor Type	1970	1980	1990	2000
PWR, BWR	5,000	35,200	64,000	113,600
GCR, SGR	3,300	23,500	42,700	75,700
D_2O Moderated	2,700	19,300	38,500	71,500
Thorium-graphite	—	—	28,800	78,100
Thorium- D_2O	—	—	28,800	78,100
Fast Breeder	—	—	67,200	183,000
Total	11,000	78,000	270,000	600,000

Combining the data on inventories with the projected distribution results in an average inventory requirement up to 1980 of 0.60 ton of natural uranium or equivalent⁵ per Mwe. After 1980 the average inventory requirements may drop to about 0.33 ton natural uranium per Mwe plus 0.075 ton thorium per Mwe as a result of the construction of the more advanced reactor types.

REACTOR BURN-UP REQUIREMENTS

Uranium burn-up requirements in nonbreeder reactors with and without recycle of plutonium are discussed at some length in various Geneva Conference Papers (7 to 11). Data from these papers indicate that with recycle of plutonium the maximum utilization of natural uranium in slightly enriched light-water reactors amounts to about 6100 MwD/t, in graphite moderated reactors to about 7800 MwD/t, and in D_2O moderated reactors to about 20,000 MwD/t. On this basis, the average minimum burn-up requirement in solid-fuel converter reactors is estimated to be 0.065 ton of natural uranium per MwYe.

PROJECTED TOTAL REQUIREMENTS

Total cumulative and annual requirements for uranium and thorium calculated from the above data are summarized in Table IV. In making

⁵ Assuming recovery of 5 kg. U^{235} per ton of natural uranium in diffusion plant.

these calculations, it has been assumed that U^{233} can be substituted for U^{235} inventories in thorium breeders and converters on an equal basis, and Pu^{239} for U^{235} in fast breeders. Also, it has been assumed that 5 kg. of enriched U^{235} can be recovered from one ton of natural uranium by isotope

TABLE IV
PROJECTED REQUIREMENTS OF U. S. NUCLEAR SOURCE MATERIALS

	1970	1980	1990	2000
<i>Cumulative Inventories</i>				
Natural uranium, tons	6,600	46,700	87,500	156,000
Thorium, tons			14,400	39,000
Depleted uranium, tons			17,500	47,500
U^{233} or U^{235} , kg.			101,800	274,000
U^{235} or Pu^{239} , kg.			322,000	878,000
<i>Cumulative Consumption</i>				
Natural uranium, tons	2,900	29,000	68,000	167,000
<i>Fissionable Material Production</i>				
U^{233} , kg.			35,000	132,000
Pu^{239} , kg.			300,000	1,060,000
<i>Cumulative Net Requirement</i>				
Natural uranium, tons	9,500	76,000	175,000	315,000
Thorium, tons			14,400	39,000
<i>Annual Requirement</i>				
Natural uranium, tons	2,400	12,000	18,000	34,000
Thorium, tons			1,900	3,000

separation. Diffusion plant tails, moreover, are assumed to be sufficient to supply depleted uranium for fast breeder inventories.

PRODUCTION RATES AND RESERVES OF NUCLEAR MATERIALS

It is seen from the foregoing that if the United States civilian nuclear power industry grows at an average of projected rates, uranium requirements may be about 12,000 tons per year by 1980 and 34,000 tons by 2000, with an additional annual thorium requirement of 3000 tons by the year 2000. Total cumulative requirements by 2000 A.D. are 315,000 tons of uranium plus 39,000 tons of thorium. Can the raw-materials production facilities supply this much? According to Johnson (12) the answer is yes. The uranium plants today have a total combined capacity capable of processing 50 million tons of ore a year. The most rapid increase in production has occurred since 1955, at which time the total uranium production of non-

TABLE V
RESERVES OF LOW-COST URANIUM AND THORIUM*
(TONS)

Uranium		Thorium	
<i>Known Reserves</i>			
United States	230,000	United States	20,000
Canada	400,000	Canada	200,000
South Africa	400,000	India	150,000
France	25,000	Brazil	10,000
Other	20,000	Other‡	20,000
Subtotal	1,075,000		400,000
<i>Assumed Additional Reserves</i>			
1. <i>Geologic Estimates (known areas)</i>			
United States	350,000	United States	30,000
France	75,000	India	50,000
	—	Brazil	20,000
Subtotal	425,000		100,000
2. <i>Experience Factor</i>			
Other known producing areas	500,000§		—
<i>Potential Reserves</i>	2,000,000		500,000#
Total	4,000,000		1,000,000

* Approximately an average of \$10/lb. oxide in high-grade concentrates; non-Communist countries only.

† Argentina, Australia, Belgian Congo, Portugal.

‡ Australia, Burma, Indonesia, Indochina, Madagascar, Malaya, Southern Africa, Thailand.

§ Based on conservative nature of Canadian and South African estimates and general experience that ultimate production exceeds original estimates.

|| Within reasonable period in new areas—before year 2000; based on geologic data and discovery experience and assuming aggressive exploration.

Conjecture in absence of experience factor and with only tentative geologic information.

Communist countries was at an annual rate of 11,500 tons of U_3O_8 . Present production in the United States is about 15,000 tons of U_3O_8 per year, and the annual rate in 1960 should be in excess of 20,000 tons. The production rate of Canada, now about 13,000 tons, should exceed 15,500 tons in 1959. South African production is more than 6000 tons of U_3O_8 per year. These three sources can produce a total of about 42,000 tons of U_3O_8 per year and can expand if necessary. Thorium production rates, now less than 1000 tons

per year, can easily reach 5000 or more tons per year by recovery of thorium as a byproduct of Canadian uranium production. Mining and ore-processing facilities, therefore, appear to be more than adequate to support an average United States nuclear industry for the next 40 years.

Known or assumed reserves of low-cost uranium and thorium also appear to be adequate to support even a larger-scale nuclear power program for more than 40 years (13). This is shown by Table V in which it is estimated that reserves amounting to 1 to 2 million tons of low-cost uranium and 500,000 tons of thorium exist in non-Communist countries.

CAPITAL COSTS

Capital costs of first-generation and prototype plants are summarized in Table VI. Data plotted in Figure 3 indicate that costs for such plants generally follow the relation $\$/\text{kw.} = 2500 P^{-1/3}$ where P is in megawatts of net electrical capability. Costs for advanced systems shown in Table VII

TABLE VI
CAPITAL COSTS OF FIRST-GENERATION AND PROTOTYPE
NUCLEAR POWER PLANTS IN U. S.

Plant Name	Reactor Type	Net Capability, Mwe	Unit Cost, \$/kw. (net)	Status	Reference
Shippingport	PWR	100	725	Operating	(14)
Indian Point	PWR	151*	510	Construction	(15)
Yankee	PWR	134	415	Construction	(16)
APPR-1	PWR	1.9	2,000	Operating	(17)
APPR-1a	PWR	3	1,780	Construction	(18)
Dresden	BWR	180	>285	Construction	(19)
Elk River	BWR	15†	670	Construction	(20)
Northern States	BWR	62	463	Construction	(21)
SENN	BWR	150	387	Design	(22)
Kaiser-ACF	GCR	44	960	Design Study	(23)
Kaiser-ACF	GCR	215	410	Design Study	(24)
ORNL-GCR-2	GCR	225	372	Design Study	(25)
General Atomics	GCR	40	612	Design Study	(26)
Hallam	SGR	75	570	Construction	(27)
Piqua	OMR	11.4	770‡	Construction	(28)
Enrico Fermi	FBR	90	537	Construction	(29)
GNEC	CO ₂ -D ₂ O	50	517	Design	(30)
CVNPA	D ₂ O	17	1,000	Design	(31)
Chugach	SDR	10	1,110	Design	(32)

* 104 Mwe from oil-fired superheater not included.

† 7 Mw. from oil-fired superheater not included.

‡ Turbine plant cost added to bid price.

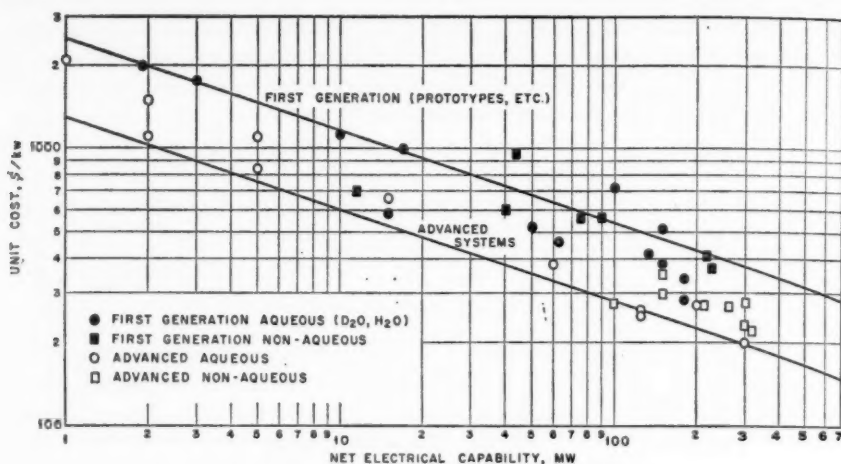


FIG. 3. Capital costs of nuclear power plants (excluding fuel).

and also plotted in Figure 3 show a reduction of almost a factor of two. The minimum capital costs projected for the best nuclear plants can be represented by $\$/kw. = 1300 P^{-1/3}$.

TABLE VII
ESTIMATED CAPITAL COSTS OF ADVANCED NUCLEAR POWER PLANTS

Plant Type	Net Capacity, Mwe	Unit Cost, \$/kw.	Reference
PWR (Package Reactors)	1	2,100	(33)
	2	1,500	(33)
	5	1,100	(33)
	125	250	(34)
BWR	2	1,100	(35)
	5	850	(36)
	15	666	(37)
	60	384	(38)
	200	275	(39)
	300	200	(39)
FBR	150	350	(40)
	300	280	(40)
Pebble Bed	125	254	(41)
SGR	150	300	(42)
	300	230	(42)
OMR	100	280	(28)
LMFR	315	225	(43)
Molten Fluoride	260	268	(44)
Natural Uranium—D ₂ O	200	275	(45, 46)
Thorium Breeder	315	285-407	(4)

FUEL CYCLE COSTS IN SOLID-FUEL REACTORS

Fuel cycle costs include: (a) the cost of enriching the uranium to the desired value, (b) the cost of converting the enriched UF_6 to the proper form (i.e., uranium metal, alloy, or oxide) for incorporation in fuel elements, (c) the cost of fabricating fuel elements, (d) the cost of recovering fissionable material (U^{233} , U^{235} , Pu^{239}) from spent fuel elements, and (e) the cost of converting products from the recovery plant to the desired form. Annual charges on fuel and fuel elements held up in the reactor and processing plants must be added to these costs, and credits for the value of recovered fissionable material subtracted. The net result, expressed in dollars per unit weight of material handled, divided by the number of net kilowatt hours of electricity produced per unit weight, gives the fuel costs. Therefore, the greater the exposure time—i.e., burn-up per cycle—the lower the conversion, fabrication, and processing costs in mills per kilowatthour. Reductions in nuclear fuel costs depend on minimizing factors which limit burn-up, such as failure of fuel elements as a result of radiation damage, or on maintaining the required ratio of fissionable material to neutron-absorbing material in the reactor.

Since with pure uranium metal excessive swelling occurs at burn-ups too low for economic power production (5), the trend in fuel element development has been toward the use of uranium compounds, such as UO_2 , uranium carbide, or uranium alloys with niobium or molybdenum. Most central-station power reactors are presently depending on the use of UO_2 clad with Zircaloy or stainless steel, in which case radiation damage limitations are less severe than is the problem of maintaining nuclear reactivity. Thus, the problem changes from a technical one to an economic balance between the costs of increasing the U^{235} enrichment to achieve long burn-up and the savings in conversion, fabrication, and reprocessing realized with long fuel exposure. However, uncertainties in the costs of carrying out each step of the fuel cycle, as well as uncertainties in the value of the fissionable material produced in the reactor, make it extremely difficult to determine the desired enrichment in any specific case. For a pressurized-water reactor, for example, almost a factor-of-three uncertainty in fuel cycle costs exists (47), brought about principally by the spread in estimated plutonium credits and fabrication charges. In this case, nuclear fuel costs including annual charges on inventories range from 2.3 to 6.4 mills/kwhr.

Similar fuel cost uncertainties are estimated by Herron *et al.* (11), as shown in Table VIII. Ranges of present unit fuel cycle costs vary from \$64 to \$102/kg. uranium for stainless-steel-clad metal alloy fuel elements to \$104 to \$219/kg. for zirconium-clad oxide fuel as shown in Table VIII. Possible reductions in unit fuel cycle costs are also shown in Table VIII.

In order that uncertainties in nuclear fuel costs should not hold up the sale of reactors or the development of economic nuclear power, individual manufacturers, as well as the United States Government, have been willing to assume the risk of fuel elements not meeting desired burn-ups. The General Electric Company, for example, is "guaranteeing" that fuel ele-

ments for Pacific Gas and Electric's boiling water reactor will achieve exposure times of 10,000 MwD/t (31). Similar guarantees, coupled with ceiling prices on the cost of fabricating stainless-steel- and Zircaloy-2-clad UO_2 fuel elements, have been given in connection with the United States—Euratom cooperative program (48, 49). With such guarantees, maximum fuel cycle

TABLE VIII
UNIT FUEL CYCLE COSTS IN SLIGHTLY ENRICHED
URANIUM-FUELED CONVERTER REACTORS*

Process	\$ /kg. U	
	Present	Long Range
UF_6 to UO_2 pellets	20-30	8-10
UF_6 to U metal (alloy)	15-18	3-7
Stainless-steel-clad oxide elements	25-75	15-50
Stainless-steel-clad metal elements	15-45	10-30
Zirconium-clad oxide elements	50-150	25-75
Zirconium-clad metal elements	25-75	12-35
Cooling and shipping	8	8
Separation of uranium, plutonium, fission products	20-25	15
Uranium nitrate to UF_6	5.60	3
Totals		
Stainless steel—oxide fuel elements	79-144	49-86
Stainless steel—metal fuel elements	64-102	39-63
Zirconium—oxide fuel elements	104-219	59-111
Zirconium—metal fuel elements	74-132	41-68

* From (11).

costs will be no more than 4.2 mills/kwhr. based on the breakdown shown in Table IX. These costs are based on achieving 10,000 MwD/t burn-ups in 0.25- to 0.5-in. diameter UO_2 fuel elements, enriched up to 3 per cent in U^{235} and fabricated at costs of \$100/kg. for stainless-steel cladding and \$150/kg. for zirconium cladding. Many experts believe that the difficulty in achieving these goals may not be great; however, actual construction and operating experience will be required to obtain a definitive answer to the fuel cycle problem. The main uncertainty is the degree of burn-up which will be realized for a given initial enrichment. As shown in Figure 4, both enrichment and exposure time have an important bearing on fuel costs.

A recent survey of initial fuel costs in large United States nuclear power stations (50), summarized in Table X, indicates that for the first three years of operation of these stations, solid-fuel cycle costs (assuming \$30 per gram credit for plutonium) will range from 3.5 to 7 mills/kwhr. excluding the Shippingport pressurized water reactor plant and the Enrico Fermi fast breeder plant.

TABLE IX
FUEL CYCLE COSTS FOR U. S.—EURATOM COOPERATIVE PROGRAM*

	Mills/kwhr.
Fuel inventory at 4%	0.6
U ²³⁵ burn-up	2.3
Fabrication	1.5
Chemical processing	0.3
Conversion of UNH to UF ₆	0.1
Transportation and insurance	0.3
	5.1
Plutonium credit at \$12 per gram less \$1.50 per gram for conversion to metal	0.9
	4.2

* From (49).

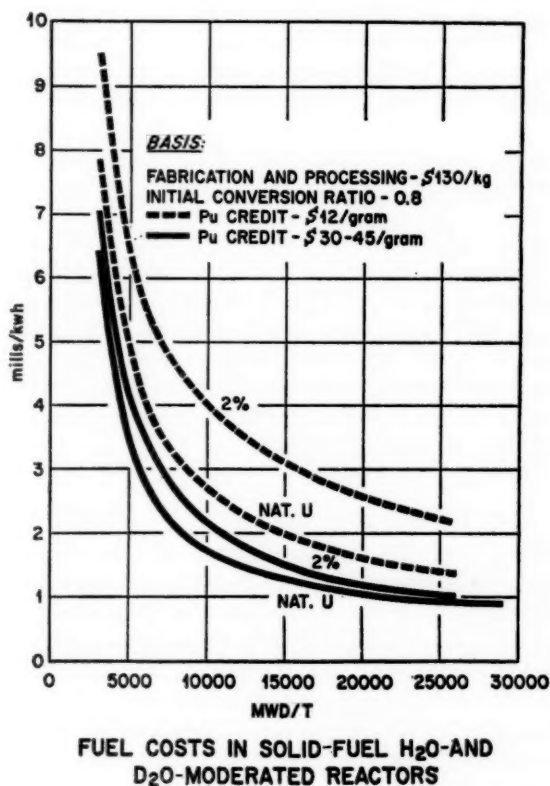


FIG. 4

TABLE X
INITIAL FUEL COSTS OF LARGE U. S. NUCLEAR POWER PLANTS*

	Nuclear Plant				
	Shippingport	Enrico Fermi	Consolidated Edison	Yankee	Dresden
Average enrichment, %	93% seed 0.7% blanket	27% core 0.36% blanket	5%	3%	1.5%
Average burn-up, MwD/t	140,000+2,940	9,160+916	15,200	6,800	10,000
Fuel cycle costs, mills/kwhr.					
Inventory	3.22	2.86	1.62	1.16	1.14
Fabrication	26.47	5.42	2.36	3.52	2.20
Reprocessing	1.04	2.55	0.27	0.74	0.53
Replaceable controls, etc.	2.13	0.04	0.05	0.08	0.14
Uranium burn-up	2.43	2.67	2.65	2.00	1.45
Plutonium credit	1.81	3.68	—	2.50	1.97
Total	33.48	9.86	6.95	5.00	3.49

* From (50).

OUTLOOK FOR FUEL COST REDUCTIONS

Reductions in fuel cycle costs are anticipated (51) through advances in technology such as increasing the power output per unit of total fuel and fertile-material inventory from 10 to 20 kw./kg. and increasing the burn-up per cycle from 10,000 MwD/t to 15,000 MwD/t and achievement of 1000°F. steam temperatures. Such improvements may reduce fuel cycle costs in some reactors to the range of 1.7 to 2.2 mills/kwhr. by 1970. The "rock bottom" fuel cycle cost for future solid-fuel converter reactors appears to be about 1.5 mills/kwhr. (52) as shown in Table XI.

FUEL CYCLE COSTS IN FLUID-FUEL REACTORS

An alternative approach to the problem of achieving low fuel cycle costs involves the development of fluid-fuel reactors in which the uranium, thorium, or both are in solution or suspension in the coolant. In this manner one eliminates problems of failure of solid-fuel elements because of radiation damage and the need for replacing fuel elements because of loss of reactivity. Such problems are exchanged for those introduced by the fact that fuel-coolant combinations are more difficult to handle than coolant alone as a result of their radioactivity and corrosiveness. The cost of remote maintenance operations in future large-scale fluid-level reactors, and thus the cost

TABLE XI
PROJECTED FUEL CYCLE COST FOR FUTURE D₂O MODERATED
PLUTONIUM RECYCLE REACTORS

Item	Basis	Fuel Costs mills/kwhr.
Fuel inventory	0.3 ton natural U/Mwe, \$40/kg., 8% charge	0.12
D ₂ O inventory	0.5 ton/Mwe, \$61/kg., 8% charge	0.35
Fuel fabrication	\$55/kg. Zr-clad elements, 15,000 MWD/t cycle	0.43
Uranium burn-up	15,000 MWD/t natural uranium	0.30
Processing and shipping	\$24/kg.	0.18
Fuel and D ₂ O losses	2%	0.12
		<hr/> 1.50

of power in such reactors, can not be projected with any accuracy. Fluid-fuel cycle costs, however, can be estimated rather closely since such costs depend on economic considerations (i.e., neutron economy vs. processing cost), rather than on technical factors such as radiation damage.

Fuel costs in various types of homogeneous reactors are summarized in Table XII (4). It is seen from this table that fuel costs for the two-region reactors are lower than the "rock bottom" fuel cycle cost projected for solid-fuel reactors. Similarly, low fuel cycle costs are projected for the nonaqueous-fluid-fuel reactors as shown in Table XIII (53). The potential fuel cost of fluid fuels compared to solid fuels appears to be about 0.5 to 1.0 mill/kwhr. Whether such an advantage will be offset in the long run by increased maintenance costs of fluid-fuel reactors can only be answered by the construction and operation of relatively large-scale prototypes.

TABLE XII
FUEL COSTS FOR LARGE-SCALE HOMOGENEOUS REACTORS
(125 Mwe Capacity)

Fuel Cost, mills/kwhr.	Two-Region		One-Region Slurry	
	Solution Core	Slurry Core	ThO ₂	UO ₂ +PuO ₂
Fuel inventory at 4%	0.16	0.21	0.39	0.07
D ₂ O inventory plus losses at 12%	0.33	0.33	0.60	0.45
Uranium burn-up less fissionable- material credit	-0.29	-0.26	-0.04	0.48
Chemical processing	1.01	1.01	0.95	1.08
Total fuel cost	<hr/> 1.21	<hr/> 1.29	<hr/> 1.90	<hr/> 2.08

TABLE XIII
PROJECTED FUEL CYCLE COSTS FOR NONAQUEOUS-
FLUID-FUEL REACTORS (315 MWE)

Item	Mills/kwhr.			
	U ²³⁵ -Thorium Molten Salt Fuel	1.4% Enriched Molten Salt Fuel	U ²³⁵ -Thorium Single-Region Liquid Metal Fuel	U ²³⁵ -Thorium Two-Region Liquid Metal Fuel
Fuel and fertile-material use charge @4%	0.52	0.42	0.28	0.27
Bismuth or salt inventory @8%	0.09	0.10	0.13	0.11
Salt amortization	0.09	0.11		
U ²³⁵ burn-up	0.58	0.79	0.49	0.28
Processing and shipping	0.04*	0.23†	0.27	0.69
	1.32	1.65	1.17	1.35

* Processing at end of 9 yr.

† Processing at end of 4.5 yr.

NUCLEAR POWER COSTS

Nuclear power costs for first-generation plants are summarized in Table XIV. It is seen that, for most of the large-scale plants, power costs are in the range of 12 to 13 mills/kwhr. with the exception of Shippingport (64.4 mills/kwhr.), the gas-cooled D₂O-moderated reactors designed by DuPont (21 to 24.5 mills/kwhr.), and the Canadian D₂O reactors (5.8 to 8.7 mills/kwhr.).

Power costs for second-generation nuclear plants which might be put into operation in 1964-1965 are estimated at about 8 to 10 mills/kwhr., as shown in Table XV taken from (60) with data corrected to an 80 per cent instead of 70 per cent load factor.

Power costs for second-generation and advanced reactors of other types taken from data in the literature are summarized in Table XVI. It is seen here that costs in the range of 6.3 to 8.9 mills/kwhr. might be projected for such plants. Some of these types such as the gas-cooled pressurized-water or boiling-water reactors might be put into operation by 1970 and be competitive with many coal-fired plants in the United States.

LONG-RANGE OUTLOOK FOR NUCLEAR POWER COSTS

Many people are now optimistic about the prospects for low-cost nuclear power in the United States in the next 10 to 20 years. At the Geneva International Conference on Peaceful Uses of Atomic Energy in September, 1958, two of the top United States power reactor development experts, Davis &

TABLE XIV
ESTIMATED POWER COSTS IN FIRST-GENERATION
LARGE-SCALE NUCLEAR PLANTS

Plant	Reactor Type	Capacity, Mwe	Power Cost, mills/kwhr.	Reference
Yankee	PWR	134	13-14	(16)
Indian Point	PWR	255	13.2	(15)
Shippingport	PWR	100	64.4	(54)
Hallam	SGR	100	13-14	(55)
SENN	BWR	150	13-14	(22)
	GCR	215	12.1-13.4	(56)
D ₂ O moderated	Gas cooled	100	21-24.5	(57)
D ₂ O moderated	Organic cooled	150	8.7	(58)
Natural uranium	D ₂ O	200	5.8	(45)

Staebler, delivered a paper (59) in which it was stated that, in their considered judgment, economically competitive atomic power plants will be in operation in the United States by 1966 and abroad two years earlier. Similar optimism is revealed by Reichle (63) who predicts 6.5-mill power in some large-scale nuclear plants by 1980, and by Cohen (60) who predicts 6.3-mill power by 1971. Thus, the pessimism which prevailed a year ago in regard to economic power seems to have been replaced with a more optimistic outlook. The primary reason for this increased optimism has been the realization that in spite of high capital costs and high fuel costs in the first-generation power demonstration and prototype plants, foreseeable advances in technology will reduce unit costs to competitive levels.

TABLE XV
COMPARISON OF TOTAL POWER COSTS IN NUCLEAR PLANTS—1964 BASIS*

	Boiling Water		Sodium Graphite		Gas Cooled—Graphite	
					Natural	Enriched
Electrical capacity, Mw.	190	580	205	637	162	558
Plant capital charges at 80% load, 15%	4.8	4.2	5.7	4.5	8.1	5.0
First core capital charge	0.3	0.3	0.1	0.1	0.3	0.2
Net fuel cost (\$12 per gram of Pu credit)	3.0	3.0	2.9	2.9	3.3	2.3
Operation and maintenance	0.9	0.6	1.2	0.8	1.1	0.8
Total, mills/kwhr.	9.0	8.1	9.9	8.3	12.8	8.3

* From (60).

TABLE XVI
ESTIMATED POWER COSTS IN SECOND GENERATION
AND ADVANCED NUCLEAR PLANTS

Reactor Type	Capacity, Mwe	Power Cost	Reference
Future Shippingport	150	9.7	(54)
Second-generation OMR	100	10-11	(28)
Second-generation U ²³⁵ fueled fast reactors	300	9.7	(40)
Sodium-cooled beryllium- and graphite-moderated	205	8.9*	(61)
Gas-cooled pebble bed	125	7.5-8.1	(62)
Boiling-water reactor "Target Plants"	300-460	6.3-7.4	(60)
Liquid-metal-fueled reactor	3.5	6.9-7.2	(43)
Molten-fluoride-fueled	260	8.9	(44)

* Calculated from data in (61).

LITERATURE CITED¹

1. Teitelbaum, P. D., *Natl. Planning Assoc. Rept.*, 59 (1958)
2. Davis, W. K., Roddis, L. H., and Goodman, C., *Nucleonics*, 15, No. 9, 90 (1957)
3. Cohen, K., *Nucleonics*, 16, No. 1, 66 (1958)
4. Lane, J. A., MacPherson, H. G., and Maslan, F., *Fluid Fuel Reactors* (Addison-Wesley Publishing Co., Inc., Reading, Mass., 979 pp., 1958)
5. Dietrich, J. R., and Zinn, W. H., *Solid Fuel Reactors* (Addison-Wesley Publishing Co. Inc., Reading Mass., 844 pp., 1958)
6. Arnold, E. D., and Ullmann, J. W., *U. S. Atomic Energy Document*, ORNL-2698 (April, 1959)
7. Greebler, P., Harker, W. H., Harriman, J. M., and Zebroski, E. L., "Recycle of Plutonium in Low-Enrichment Light Water Reactors," *U. N. Paper 2167* (1958)
8. Eschbach, E. A., Granquist, D. P., and Lewis, M., "The Comparative Economics of Plutonium Fuel Utilization and U²³⁵ Fuel Utilization in Thermal Power Reactors," *U. N. Paper 1068* (1958)
9. Jungnell, D., and Lundquist, S., "Suitable Types of Reactors for the Development of Nuclear Power Supply Based on Natural Uranium as Fuel," *U. N. Paper 155* (1958)
10. Pigford, T. H., Benedict, M., Shanstrom, R. T., Loomis, C. C., Van Ommeslaghe, B., "Fuel Cycles in Single-Region Thermal Power Reactors," *U. N. Paper 1016* (1958)
11. Herron, D. P., Mash, D. R., and Webster, J. W., "Fuel Cycles for Nuclear Power Reactors," *U. N. Paper 1044* (1958)
12. Johnson, J. C., "Resources of Nuclear Fuel for Atomic Power," *U. N. Paper 1921* (1958)
13. *Uranium and Thorium Raw Material Supplies*, U. S. Atomic Energy Commission, Division of Raw Materials, October, 1958); See also (12)

¹ References denoted as U. N. Papers are papers presented at the International Conferences on the Peaceful Uses of Atomic Energy at Geneva. The year given in each case is the year the conference was held.

14. "Special Report on Shippingport," *Nucleonics*, **16**, No. 4, 61 (1958)
15. Milne, G. R., Stroller, S. M., and Ward, F. R., "The Consolidated Edison Company of New York Nuclear Electric Generating Station," *U. N. Paper 1885* (1958)
16. Webster, W., "The Yankee Atomic Project," *Proc. Management and Atomic Energy Conf.*, 349 (Chicago, Ill., Mar. 26-28, 1958)
17. Alco Products, Inc., Schenectady, N. Y., "Detailed Cost Report," *APPR Contract AT-(11-1)-318*
18. *Nucleonics*, **17**, No. 2, 57 (1959)
19. Joslin, M., "Economics of Dresden Nuclear Power Plant," *Proc. Management and Atomic Energy Conf.*, 361 (Chicago, Ill., Mar. 26-28, 1958)
20. *Nucleonics*, **16**, No. 6, 24 (1958)
21. Graham, C. B., Hall, R. J., Klecker, R. W., Klotz, C. E., and Michel, R. G., "Engineering Design of an Advanced Boiling Water Reactor," *U. N. Paper 1852* (1958)
22. *Nucleonics*, **16**, No. 10, 26 (1958)
23. Kaiser Engineers Division, Henry J. Kaiser Co., and Nuclear Products-Erco Division, ACF Industries, Inc., *U. S. Atomic Energy Commission Document, IDO-2023*, Rev. 1 (1958)
24. Kaiser Engineers Division, Henry J. Kaiser Co., and Nuclear Products-Erco Division, ACF Industries, Inc., *U. S. Atomic Energy Commission Document, IDO-2024*, Rev. 1 (1958)
25. "The ORNL Gas-Cooled Reactor," *U. S. Atomic Energy Commission Document ORNL-2500*
26. *The Forum Memo*, **5**, No. 12, 7 (Barlow, R., Ed., Atomic Industrial Forum, New York, N. Y., 1958)
27. *Nucleonics*, **15**, No. 10, 25 (1957)
28. Weisner, E. F., and Parkins, W. E., "Application of Organic Moderated Reactors to Central Station Power Plants," *U. N. Paper 606* (1958)
29. "Third Annual Nuclear Power Report," *Elect. World*, **149**, 77 (1958)
30. *Nucleonics*, **16**, No. 1, 17 (1958)
31. *Nucleonics*, **16**, No. 6, 25 (1958)
32. *The Forum Memo*, **5**, No. 4, 10 (Barlow, R., Atomic Industrial Forum, New York, N. Y., 1958)
33. Williams, D. G., "The Economics of Small Military Nuclear Power Plants," *Proc. Management and Atomic Energy Conf.*, 89 (Chicago, Ill., Mar. 26-28, 1958)
34. Shoupp, W. E., "Advanced Pressurized Water Systems," *Proc. Management and Atomic Energy Conf.*, 138 (Chicago, Ill., Mar. 26-28, 1958)
35. Mowll, J. U., "Power Requirements in Remote Areas," *Proc. Management and Atomic Energy Conf.*, 106 (Chicago, Ill., Mar. 26-28, 1958)
36. *Nucleonics*, **16**, No. 11, 19 (1958)
37. *Nucleonics*, **16**, No. 11, 25 (1958)
38. *Nucleonics*, **16**, No. 6, 25 (1958)
39. *Nucleonics*, **17**, No. 1, 49 (1959)
40. Griswold, A., "Economic Prospects for Fast Breeder Reactors," *Proc. Management and Atomic Energy Conf.*, 357 (Chicago, Ill., Mar. 26-28, 1958)
41. Sanderson and Porter, Engineers, and Alco Products, Inc., *U. S. Atomic Energy Commission Document, NYOO-8753*, **1** (May, 1958); *Nucleonics*, **16**, No. 8, 25 (1958)

42. "Task Force Review of Sodium Graphite Reactors," *U. S. Atomic Energy Commission Report* (Unpublished, 1958)
43. Williams, C., and Schomer, R. T., "Liquid Metal Fuel Reactor and LMFRE-I," *U. N. Paper 2355* (1958)
44. MacPherson, H. G., Savage, H. W., Briant, R. C., Jordan, W. H., Alexander, L. G., Boudreau, W. F., Breeding, E. J., Cobb, W. G., Kinyon, B. W., Lackey, M. E., Mann, L. A., McDonald, W. B., Roberts, J. T., Savolainen, A. W., Storto, E., VonderLage, F. C., Whitman, G. D., and Zasler, J., "Molten Fluoride Power Reactor," *U. N. Paper 605* (1958)
45. Smith, H. A., Walker, W. M., Williams, N. L., and Critoph, E., "A Study of a Full-Scale, Uranium and Heavy Water Nuclear Power Plant," *U. N. Paper 208* (1958)
46. MacKay, I. N., "The Canadian NPD-2 Nuclear Power Station," *U. N. Paper 209* (1958)
47. Kallman, D., Davidson, L., Holden, R. B., Klotzbach, R. J., Streifus, C. A., Stoller, S. M., De la Cruz, F., and Brennan, J. E., *Nucleonics*, **16**, No. 1, 50 (1958)
48. *The Forum Memo*, **5**, No. 7, 15 (Barlow, R., Ed., Atomic Industrial Forum, New York, N. Y., 1958)
49. Armand, L., Etzel, F., and Giordani, F., *A Target for Euratom* (Issued by Secretariat of Euratom Comm., May, 1957)
50. Edison Electric Institute, New York, N. Y., "Survey of Initial Fuel Costs of Large U. S. Nuclear Power Stations," *EEI Publ.*, 59-150 (December, 1958)
51. Cohen, K., and Zebroski, E., *Nucleonics*, **17**, No. 3, 63 (1959)
52. Lane, J. A., "The Need for the Continued Development of Fluid Fuel Reactors," *Atomic Energy in Industry*, 7th Conf., (Cleveland, Ohio, April 9, 1959)
53. Guthrie, C. E., *U. S. Atomic Energy Commission Memoranda*, ORNL CF-59-1-13 (January, 1959); *ORNL CF-59-2-82* (February, 1959)
54. Shoupp, W. E., "Advanced Pressurized Water Systems," *Proc. Management and Atomic Energy Conf.*, 138 (Chicago, Ill., Mar. 26-28, 1958)
55. Parkins, W. E., "New Results on the Sodium-Graphite Power Reactor Program," *Proc. Management and Atomic Energy Conf.*, 122 (Chicago, Ill., Mar. 26-28, 1958)
56. W. H. Zinn and Associates, *Power Reactor Technology*, **1**, 55 (1958)
57. Holmes, R. C., Bernath, L., and Hones, E. W., *A Preliminary Evaluation of Gas Cooling of Power Reactors Moderated by Heavy Water*, DP-307 (E. I. Du Pont de Nemours and Co., Savannah River Lab.)
58. McNelly, M. J., "A Heavy-Water Moderated Power Reactor Employing an Organic Coolant," *U. N. Paper 210* (1958)
59. Davis, W. K., and Staebler, U. M., "The United States Nuclear Power Program," *U. N. Paper 1076* (1958)
60. Cohen, K., and Zebroski, E. L., *Proc. Am. Power Conf.*, **XX**, 113 (Chicago, Ill., 1958)
61. Levy, S., Voorhees, B. G., Aline, P. G., and Cohen, K. P., "Advanced Design of a Thermal Sodium Cooled Reactor for Power Production," *U. N. Paper 604* (1958)
62. *Nucleonics*, **16**, No. 8, 25 (1958)
63. Reichle, L. F. C., *Proc. Am. Power Conf.*, **XX** (Chicago, Ill., 1958)

VERTEBRATE RADIOBIOLOGY (EMBRYOLOGY)¹

BY ROBERTS RUGH

Department of Radiology, Columbia University, New York, N. Y.

Ionizing radiations have effects on the embryo which they have on no other stage of development, namely, they cause teratologies or congenital anomalies which cannot be produced by any level of irradiation after hatching or birth. Further, because of the high preponderance of cells in transition from the primitive to the differentiated state, the sensitivity of the embryo is unique. At any moment it is a mosaic of actively differentiating centers, each highly susceptible to irradiation insult which may result in death of the embryo, fetus, or adult, or in the persistence of anomalies. An exposure of the embryo to as little as 25 r x-rays is to insult it in a manner and to a degree out of all proportion to the effects obtained with such an exposure of the adult organism, into which the embryo develops.

Further, the embryo possesses undifferentiated cells which appear to be relatively radioresistant and from which there can develop the variety of differentiated cells of the adult. Thus, even though there is severe destruction of differentiating cells, there will be other cells which can be diverted in the interest of topographical normality so that a recognizable organism may result, though deficient to varying degrees. We call these conditions stunting, microcephaly, micropthalmia, brachydactyly, etc. This power of redirecting the potentials of certain cells co-ordinated with the interests of the whole is known in embryology as "organismic" influence. It can save the embryo from complete destruction to the extent that undifferentiated cells are still available after the irradiation insult. But it must be emphasized that the embryo does not have the power to step up cell production to take care of the deficiency, so that irradiation insult of the embryo or fetus appears inevitably to result in deficiencies. The reason this has not always been apparent is that while the proportions of the fetal-irradiated newborn may be within normal limits, its overall size has not always been compared with the unirradiated controls.

This is not to deny that gross anomalies can be and are produced by irradiation of the embryo, anomalies which reflect insult at a time when vital processes are going on. The major process which is so highly susceptible to effect is gastrulation, probably the most critical phase in the development of any embryo. Any interference with this process will result in cephalic anomalies such as we find in the mouse (see below). Such interference can result from damage to cells clear back to the original fertilized egg, indicating probable imbalance of chromosomes.

The concept of "the embryo" must therefore change. It is not simply a

¹ The survey of literature pertaining to this review was concluded February 1, 1959.

miniature of the adult organism into which it will develop, but is a dynamic, tirelessly changing mosaic of metamorphosing parts all integrated into an overall pattern by "organismic" forces which are beyond the attack of ionizing radiations as long as the building blocks are adequate in number and are basically intact and there is no interference with dynamic processes. What ionizing radiations do to the embryo is to destroy those cells which happen to be in the most vulnerable stage of metamorphosis at the time of exposure, and the embryo at all times has an abundance of such cells.

As yet there has been no adequate study of the long term sequelae of embryonic or fetal-irradiation, as there has been for postnatal irradiation. It is conceivable that the embryonic gonad of the mouse, for instance, which begins to differentiate at about the twelfth day of gestation, may accumulate the effects of ionizing radiations in its constituent germ cells long before birth, and possibly even at a different mutation rate from the later germ cells of the adult. Further, cancer has been found in the fetus and the newborn so that the origin of this slowly developing malignancy may well start by insult to some of the peculiarly sensitive cells of the embryo or fetus at a very early stage. The higher incidence of leukemia among children than adults may have a causal relation yet to be revealed by such studies.

It must not be presumed that ionizing radiations have effects on the embryo which are peculiar to this type of insult. There are many radiomimetic drugs which, if administered to the pregnant mammal, will produce in the embryos and fetuses the same types of anomalies as those resulting from exposure to ionizing radiations. It is the embryo which reacts to insult, but it so happens that ionizing radiations appear to be the most effective, consistent, and potent agent in teratogenesis. Just because the anomalies are often phenocopies of anomalies caused by irradiation of ancestral gametes does not justify conjuring up a genetic (mutational) explanation when such phenocopies may be produced by surgical invasion of the embryo, as has been done in experimental embryology. Recent studies on mouse exencephalia bear this out, as will be reported below.

In emphasizing the peculiar sensitivity of the embryo and fetus to ionizing radiations, we must not lose sight of the fact that these same ionizing radiations are proving a boon to research, diagnosis, and therapy with post-natal organisms and that in general we are all the wiser and richer by virtue of radiology. Congenital anomalies can be reduced by cautioning all against embryonic and fetal exposures, and the "reproductive wastage which causes the loss of at least one-third of each generation" (1) may likewise be reduced. Since the last review of this sort on embryology (2) there have appeared a number of studies on embryos from worms to man. These will be reviewed briefly in the following pages.

MARINE ORGANISMS

Some years ago it was demonstrated that when the sea urchin *Arbacia* egg is x-irradiated and then fertilized by normal sperm, there is a delay in

the onset of cleavage directly related to the level of exposure. However, such delay could be reduced considerably if there was a delay in the insemination after irradiation, apparently giving the egg time to "recover" from the injury. In fact the word "recovery" was used in the title of the papers. In a recent repetition of these experiments (3) the so-called "recovery" of the normal cleavage rate was confirmed, but it was found that the eggs did not in fact recover in the sense that they were in any way normal, for they did not develop beyond the gastrula stage. Further, the so-called "protective" drug cysteamine also helped to reduce the cleavage time toward the normal, counteracting the delaying effect of ionizing radiations. However, such "protected" eggs failed to develop beyond gastrulation to plutei. Thus, while delay in fertilization did counteract the delaying effect of irradiation, there was no true "recovery" nor "protection" against the consequences of irradiation at the cellular level.

Studies on the egg of the snail *Helisoma* (4) showed that the one- and two-cell stages of resting eggs withstood from two to four times as much radiation as did embryos undergoing mitosis. The LD_{50} to hatching for resting cells was from 300 to 400 r while it was about 100 r for mitotically active cells. For the trochophore the LD_{50} was between 500 to 1000 r, so that resistance generally increased with embryonic age.

When the fertilized eggs of the parchment worm *Chaetopterus* were x-rayed to 255 r and up to 17,250 r, it was found that the lower levels of exposure slightly retarded cleavage (below 1000 r) and that abnormal trochophores developed, with severe ciliary defects, cytoplasmic blebs, and feeble movements. Exposures above 1000 r resulted in death of all by the trochophore stage. Still higher exposures resulted in the production of multipolar spindles, fragmented chromosomes, and karyokinesis without cytokinesis (5).

FISH

Salmon embryos in the "eye" stage were affected by 500 r, but it required 2500 r to arrest development of all. The gonads and hematopoietic systems were affected by as little as 250 r (6). In the trout (*Salmo gairdnerii*) the fertilized egg is by far the most radiosensitive (LD_{50} of 58 r) and as the embryo develops it becomes more resistant until it can tolerate 900 r x-rays (7).

In an effort to discover the mechanisms of exencephalia, found in the mouse and rat (see below), a study was made on the transparent embryo of the fish *Fundulus* (8). It was found that the early embryo could survive rather high levels of x-irradiation and yet develop, but without eyes, or head, or even anterior end. Such anencephalic larvae had pulsating hearts with connecting blood vessels and often containing corpuscles, and their body and tail muscles were functional. This finding supports the thesis that exencephalia and anencephalia may result from interference with the mechanics of gastrulation so that the cephalic structures are abnormal, reduced, or absent while the rest of the organism appears to be able to develop rather normally.

AMPHIBIA

The newly fertilized egg and the blastula stage of the frog embryo are the most radiosensitive as determined by the frequency of teratologies which follow exposure. The unfertilized egg, the late neurula and the older tadpole appear to be the most radioresistant. These differences were explained as caused by (a) movement of the gametic nuclei in syngamy, (b) high potency of the early blastomeres, and (c) the abundance of differentiating cells. An exposure of 300 r was tolerated at the late neurula stage because most of the important differentiations had occurred by this time. Anomalies following 180 r exposure of the earlier blastula included pycnosis and karyorrhexis of the differentiating cells, exogastrulation, edema, stunting, microcephaly, flexure, aneurogenic and amorphous development. Some embryos failed to develop heads, and notochords could not be found, but posterior structures appeared quite normal. Exposures of the early neurula caused the sloughing off of neural cells into the neurocoel, a finding which has since been reported for the mouse and rat. Apparently, ionizing radiations are most damaging to moving chromosomes, the kinetics of mitosis, and the metamorphosis or differentiation of embryonic cells (9).

X-irradiation of the clawed toad *Xenopus* in early embryonic stages resulted in microphthalmia, edema, chondrodystrophy, and polydactylia (10). When another toad *Bufo boves* was exposed to 250 r to 5000 r after metamorphosis, it was found that above 1000 r there was pycnosis in the nuclear layer of the retina, especially at 24 hr. after exposure. High environmental temperature after exposure increased the incidence of pycnosis, and this was attributed to the effect of temperature on metabolism (11).

Refrigeration of bullfrog *R. catesbeiana* tadpoles to 3°C. gave them a degree of "protection" against the immediate effects of ionizing radiations, but this "protection" lasted only as long as the temperature was depressed (12, 12a). It is claimed that larval salamanders show persistent benefit from refrigeration during x-irradiation (13).

When salamander larvae are x-irradiated with 200 r or more and certain organs are orthotopically transplanted to normal hosts, such organs tend not only to survive the irradiation but to develop rather better than they would have in the original donor environment (14). This was first pointed out (15) in a statement to the effect that certain organ anlagen may not be severely damaged, but the host, having some other vital organ system that is particularly radiosensitive at the time of exposure, succumbs and takes along with it the less affected or more resistant anlagen.

CHICK

The chick embryo is not only warm blooded but depends so much upon its extraembryonic structures for circulation and respiration that its radiosensitivity is quite particularly related to its stage of development, and this changes from hour to hour. The embryo itself is not as radiosensitive as is

its extraembryonic circulation (16), so that changes in sensitivity are related to changes in the yolk-sac circulation. Embryonic anlagen, when exposed to doses that would be expected to kill the chick embryo, will develop as if they had not been irradiated at all if transplanted to a normal host environment. Such organs as the eyes or limb buds have been shown to survive relatively high levels of exposure. But, here again exposure during early gastrulation and neurulation results in neuroblasts being sloughed off into the neurocoel, both at the level of the brain and spinal cord (16). This study was further confirmed (17) to show that it was the disintegration of the intraembryonic plexi rather than hemorrhage in 12-day chick embryos exposed to 800 r which resulted in their death. It has been claimed (18) that chick mesencephalic wall could be damaged indirectly by x-irradiation of other embryonic structures, but it must be pointed out that scattered radiations might be sufficient to damage neuroblasts at the stage exposed and, also, anoxia following damage to the extraembryonic circulation might well destroy mesencephalic neuroblasts.

Four-day chick embryos showed four causes of death, as the dose was lowered from 22,000 r to 800 r. First, there were scattered hemorrhages, largely between myotomes. Second, hemorrhage occurred in the extraembryonic coelom. Third, there was intraembryonic hemorrhage of the occipital region, and fourth, embryos survived from 3 to 9 days and died from a variety of causes, none very distinct (19). In an earlier study it was shown that, in acute death studies, the LD_{50} for the 2-day chick embryo was about 2000 r, for the 8-day embryo about 700 r, and for the 16-day embryo about 900 r. The maximum radiosensitivity occurred between 8 to 10 days (20). When the unincubated blastoderm or developing embryos to the 36-hr. stage were exposed to 600 r, the organs affected were the nervous system, sense organs, somites, and notochordal area (21). Some embryos were anencephalic (without brains or heads) as previously (9) described for amphibian embryos.

Cysteamine, used prior to irradiation of the chick embryo, afforded some protection but not if injected into the egg after exposure. Protection was best achieved after the circulatory system had begun to function (22). More recently seven other drugs have been tested, as well as cold, with only meth-ylamine being effective. The protection was attributed to effects on the blood vascular system rather than on the embryo itself (23).

When P^{32} was injected into the yolk of 2-day incubated chick eggs, it was found that the LD_{50} was 100 μ c. in two days, and 165 μ c. was 100 per cent lethal. Effects on the embryo were similar to those following exposure to x- or gamma rays and included decrease in mitosis, abundant pycnosis, tissue degeneration, clumping of chromosomes, fragmentation of chromatin and nuclei. The most sensitive anlagen were the neural tube, optic cup, dense mesenchyme of the gut wall, limb buds and branchial arches. The less actively differentiating organ anlagen such as of the heart, notochord, lens, and cephalic myotomes were rather resistant (24).

When P^{32} was injected into the egg of the chick before incubation, it

caused malformations of the central nervous system, eyes, notochord, and somites. Rosettes were formed in the brain, and in one 5-day embryo an encephalocoel was formed (25).

RATS

The first systematic study of x-irradiation effects on embryonic rats appeared in 1950 (26) closely followed by a study showing that the growing central nervous tissue of the rat embryo is selectively and extensively destroyed by x-rays, with little or no effect on other differentiating tissues (27). This fact was attributed to the abundance of highly sensitive neuroblasts, present in the brain, cord, some ganglia, and the retina. Exposures of less than 100 r had a deleterious effect on scattered areas of neural-differentiating tissue. It was pointed out that the embryonic neuroblasts, comprising the differentiating nervous system, were 2500 or more times as sensitive as the neurons of the adult into which they develop. Necrosis was evident within 2 hr. of x-irradiation, and by 24 hr. areas of liquefaction necrosis were found containing cellular debris. Phagocytosis within 6 hr. helped to clean up these areas, but often rosettes were seen to develop in neural tissue. These rosettes were misinterpreted later as neoplasms (28), but they were rarely seen after birth. Even with the grotesque brains of these fetally-irradiated rats, they were able to "crawl, then eat, climb, run, and bite, but their motor patterns seemed more jerky than normal controls" (29). Exposures of 150 r caused the rats to be stunted; many were without a corpus callosum, had a small hippocampus, and incompletely developed striatum. The ventricles were abnormal, and white matter of the cerebellum was reduced.

Soon thereafter it was shown that certain enzyme inhibitors (nitrogen mustard and triethylene melamine, for example) were able to bring about similar changes in rat embryos, so that these were called radiomimetic drugs (30). The emphasis was then placed on the embryo as a highly sensitive, reactive developmental state most responsive to highly penetrating ionizing radiations, but in a similar manner to almost any drastic insult. It was found that 40 r (and possibly 25 r) would necrotize some neuroblasts and the most sensitive region was the anterior striatal periventricular region and the angle of the lateral ventricles where the corpus callosum formed. With increasing levels of exposure to ionizing radiations, more regions of the developing central nervous system were affected. As development progressed, these parts of the embryo passed beyond the stage of radiosensitivity, so that it was first suggested that ionizing radiations might be useful in locating areas of high embryonic (differentiating) activity. According to this investigator there was no effect of x-rays on the rat embryo during the first eight days, prior to implantation, but by day 9 (when the neural groove is formed) exposures of 150 r could produce anencephalias. While neuroblasts in mitosis were affected, it appeared that even the intermitotic neuroblasts were more radiosensitive. This term "neuroblast" was used to mean the intermediate state between the highly radioresistant, primitive, abundant

neurectoderm and the even more resistant, mature neuron. This "-blast" stage is found in all tissue differentiations and it is likely that it will be found that "-blast" cells, whether neuroblast, erythroblast, myoblast, spongioblast, etc., will all be rather equally radiosensitive by virtue of being transitional. Any developing organ containing a goodly supply of these "-blast" cells will suffer more by x-irradiation than will its precursor or its successor. From the ninth day on in the rat embryo there are neuroblasts present, but they do not appear in the cerebellum until late in fetal or early in postnatal life, so that that structure is radiosensitive later than the parts of the neopallium. In another study (31) it was suggested that the explanation of the high sensitivity of the neuroblasts was that ionizing radiations inhibited enzymes with active sulfhydryl groups that are concerned with protein synthesis. Possibly many enzymes depend upon -SH for their activity as electron transfer catalysts (31). But it has also been suggested that ionizing radiations may indirectly affect the neuroblasts by causing the formation of short-lived oxidizing compounds in the cell water, and this would disturb the oxidation-reduction equilibrium of enzymes which had an easily oxydizable -SH prosthetic group (32), or upset the ratio of reduced to oxidized glutathione (33).

Following a study of hundreds of fetal rats x-irradiated at various levels and stages, the statement was made (34) that

the primitive differentiating cells of the nervous system are probably the mammalian cells most easily destroyed by ionizing radiations. In fetal and newborn rats and mice (and other animals) substantial numbers of these cells become morphologically necrotic in less than 4 hr. after as little as 40 r is given to the whole body of the mother or the newborn. The effect is a direct one of radiation on the cell, there being no evidence that secondary, humoral, maternal, vascular, or other factors are responsible (35).

Neurectoderm could be destroyed by 600 to 800 r; some neurons and oligodendroglia of the newborn were damaged by 1500 r while it required 15,000 to 20,000 r to destroy some adult neurons.

The time of x-irradiation of the rat embryo or fetus was more directly related to a specific anomaly than was the dose, but the severity of the anomaly depended somewhat upon the dose delivered. However, a gross teratology could be produced by even a low-level exposure timed to coincide with active differentiation. Eye defects, cerebral deletions, etc. could be produced by exposure to even 150 r at certain rather limited times in embryonic development (35). The irradiation-damaged cells of the embryo or fetus are beyond repair or recovery so that deletions result which we may experience as microphthalmia, microcephalia, anencephalia, etc., but these deletions may be obscured by the fact that the developing organism has remarkable powers of integrating the remaining undifferentiated, undamaged neurectoderm into the topographically normal but reduced whole organism (36).

Rat embryos prior to implantation (before eight days) can tolerate 300 to 400 r to the extent that those which reach delivery appear to be free of

teratologies (37). This may prove to be an oversight or species specific (see below). Beginning on the ninth day it appears that the rat embryo is highly radiosensitive as a result of the sudden appearance of many differentiating centers, so that 150 r will cause anencephaly and severe brain deficiencies and facial deformities. A day later the effects of irradiations are more on the eyes, on day 11 exposure causes hydrocephalus and spinal anomalies, and on day 12 forebrain anomalies follow. At higher levels of exposure, anomalies develop in the heart, vessels, and the urinogenital system (38). However, such results are not consistently found in every member of an exposed litter. Rat embryos exposed to 150 r at 10 to 14 days gestation showed a significant increase in dental caries, but this did not follow irradiation after day 18 (39).

The concept of postirradiation repair or regeneration has been emphasized as occurring in fetal rats and mice after about day 14 when the phagocytes first appear (40). Through phagocytosis the cellular detritus is removed, and the undamaged primitive cells somehow aid in the regeneration of the lost parts. As a result, if the animal is examined at birth it appears to have made a complete "recovery." However, direct comparisons with the controls will show that there is topographical reorganization of the undamaged parts so that the organism is without lost parts, but it is most certainly deficient in cells to such an extent that organ systems are reduced in size. This was not emphasized by the investigator. He claimed that cells which are particularly vulnerable to irradiation insult are at the peak of differential cytology, associated with marked sulfhydryl enzyme activity concerned with both nucleic acid and protein synthesis (41). He states (42)

The number and distribution of dead cells is usually far out of proportion to any malformation that might follow . . . the early brain and spinal cord of rats have a capacity to regulate and regenerate comparable to that described in other vertebrates. . . . In a given region destructive damage will be proportional to the number of cells in the radiosensitive state. . . . Restitution must come from the adjacent neuroectodermal proliferating area and recovery may be determined by whether that area is still at peak mitotic activity, or subsiding, or resting prior to producing another crop of migrating cells.

Little attempt was made to explain microphthalmia, microcephalia, or other neural deletions following embryonic x-irradiation, because emphasis was placed on the apparent "recovery" of the topographic whole. Nevertheless these teratologies are the most common sequelae of embryonic or fetal x-irradiation. They are examples of deletions.

Fetal irradiation exerted an influence on the biochemical structure of the brain of the rat after birth, and it is suggested that the malformations of the neonatal brain may not represent the ultimate structural deformity. Exposure of 150 r from five to nine days before birth caused telencephalic malformations in 89 per cent of the embryos (43).

It appears that x- rather than gamma rays depress the growth rate of fetal rats (44, 45). Also, x-rays more consistently produce morphological

defects than does the same quantity of gamma irradiation. Most of the damage is to the developing skeleton, the membranous bones showing excessive porosity and ossification defects (46). The lethal dose had previously (47) been shown to be 0.46 mc of P^{32} on day 6, or 1.29 mc on day 10 of the rat. With increasing embryonic or fetal age a higher level of injection of P^{32} was necessary to cause death, but all exposures used had a depressing effect on postnatal body weight (48).

Only one study has appeared dealing with possible chemical protection of fetal rats (49). Mercaptoethylamine (MEA) injected into pregnant rats on days 15 and 18 prior to exposure of their fetuses to 300 r x-rays afforded some "protection." In this instance protection meant better survival, but such survivors should be followed for some months to determine to what degree protection was effective. Mere survival is always enhanced if fetal-irradiated rodents are given to foster mothers to nurse, but the long-term sequelae of fetal x-irradiation have not been studied.

It is believed that levels of exposure of fetal rats below those which cause histological change may nevertheless elicit behavioral effects in the offspring. Rat embryos from 11 to 19 days exposed to high doses of 300 to 600 r later exhibited more nervousness than the controls, in the maze situation. There were teeth chattering, persistent scratching, face washing, defecation, and urination during the last days in the maze. Also, it has been found that the learning ability of rats, fetally irradiated, was decreased as a function of the dose given (50). There is currently an investigation into the behavior of fetal-irradiated rats as determined by certain standard tests as well as by the electroencephalogram. It is believed that human society is really more affected by the apparently normal than by the grossly abnormal, either of which may result from fetal x-irradiation, as proven by the rat.

MICE

While the mouse embryo has proven to be extremely useful in radiobiological studies, extrapolations from mouse to man are fraught with danger and are ill advised. Nevertheless, conclusions drawn from mouse (and rat) experiments are certainly suggestive and may short-cut the time until we may have conclusions for the human.

It has been contended (51) that pregnancy induced in dogs after large doses of x-irradiation tended to protect the dog against irradiation death, but a recent study with 210 pregnant mice failed to support the contention for these rodents (52).

There have been exhaustive studies on effects of x-rays on the mouse embryo in which it was contended that such effects as were found were not mediated through the mother but were the result of direct exposure of the embryo or fetus (53 to 56). The long list of irradiation-induced congenital anomalies has been widely published but few of the explanations of their origins have been supported by evidence. One series (54) includes a suggestion that uniformly distributed ionizations might bring about in the

embryo chromosome breaks in randomly hit nuclei sufficient to interrupt or impede mitosis, resulting in the death of the cell. The surviving but damaged cells might give rise to similar descendants or dead cells either of which might interfere with normal development, resulting in a teratology. There may be a threshold in terms of cell numbers (or percentage of cell numbers) which effect an anomaly, but the degree of the teratology may relate to the excess in this number. Some anomalies may be induced with 300 r, but not with 200 r.

An exhaustive study has been made in which it has been shown that trypan blue and lithium carmine injected into the pregnant mouse will induce anomalies similar to those caused by x-rays; accordingly, they are called radiomimetic substances producing phenocopies of genetically derived anomalies (57).

On the basis of exposures of 200 r or more, it has been stated (58) that the preimplantation mouse embryos are so radiosensitive that very few survive beyond 12 days gestation, but this exposure on day 10.5 has no effect. Such preimplantation embryos which come to term appear to be without teratologies. The highest incidence of induction of congenital anomalies occurs between days 6.5 and 12.5 in the mouse. After day 13.5 it is again difficult to produce congenital anomalies by x-irradiation. The greatest decrease in birth weight occurs following x-irradiation to 200 r at 11.5 days (58).

More recent studies (8) show that severe cerebral anomalies can be produced by as little as 50 r delivered to the fertilized but uncleaved egg of the mouse (at 0.5 days) and at any daily interval thereafter through day 9.0 (see Table I and plates). The incidence of this gross anomaly is increased with exposures above 50 r, but the incidence of uterine resorption is also increased, particularly during the first several days after conception. The position of the embryo in the uterus bears no relation to its probability of developing this anomaly, and thus far chemical protective agents have not prevented its development. There is size reduction of all litters exposed to 50 r before implantation, and it is presumed that, while such severe anomalies as exencephalia may not be seen in every member of a litter, certainly the other members carry cytological, histological, and behavioral effects which, while they allow survival, may well debilitate the animals during life. Thus, it has been demonstrated that long before the appearance of any organ anlage, 50 r exposure of the cleavage or other preimplantation stages may bring about gross defects in the central nervous system of mice. It has not been determined whether there is a threshold (lower than 50 r) for discernible effects on the central nervous system in preimplantation x-irradiation.

Attempts to explain congenital anomalies following embryonic irradiation, either on the basis of "critical periods" in development or of genetic effects, now seem to be questionable. The "critical period" for exencephaly is now known to be any time before neural differentiation. If chromosomal aberrations are considered as "genetic" (heritable mutations?), then almost all x-irradiations produce genetic effects in the sense that exposed chromo-

somes are invariably damaged if the exposure is adequate. Also, there is no justification for ascribing the effects of irradiation to genetic (somatic) changes, particularly because the same anomalies can be elicited by nutritional deficiencies which could hardly bring about "genetic" changes.

It is an observed fact that severely damaged cells of the embryo are phagocytized and there remain the less damaged or completely undamaged

TABLE I
X-IRRADIATION OF THE EARLY MOUSE EMBRYO (58a)

Embryonic Age	50 r				200 r			
	Total No. Im-plants	Per Cent "Nor-mal"*	Per Cent Re-sorbed	Per Cent Exen-cephaly	Total No. Im-plants	Per Cent "Nor-mal"*	Per Cent Re-sorbed	Per Cent Exen-cephaly
0.5	52	58.0%	42.0%	0.0%	29	33.0%	64.0%	3.0%
1.5	90	95.0%	5.0%	0.0%	57	88.0%	10.0%	2.0%
2.5	95	73.0%	24.0%	3.0%	98	44.0%	56.0%	0.0%
3.5	76	88.0%	9.0%	3.0%	122	54.2%	45.4%	2.4%
4.5	53	92.0%	8.0%	0.0%	49	94.0%	4.0%	2.0%
5.5	37	87.0%	17.0%	6.0%	78	87.0%	11.5%	1.5%
6.5	77	92.0%	8.0%	0.0%	85	90.0%	5.0%	5.0%
7.0	23	100.0%	0.0%	0.0%	27	92.0%	0.0%	8.0%
7.5	25	96.0%	0.0%	4.0%	29	97.0%	0.0%	3.0%
8.0	39	92.5%	2.5%	5.0%	35	51.0%	26.0%	23.0%
8.5	26	100.0%	0.0%	0.0%	26	62.0%	0.0%	38.0%
9.0	20	95.0%	5.0%	0.0%	26	54.0%	38.0%	8.0%
9.5	12	90.0%	10.0%	0.0%	20	95.0%	5.0%	0.0%
Totals	625				681			
Average		88.0%	10.0%	1.6%		73.0%	20.0%	7.0%

* The term "normal" is used to designate those fetuses which appear to be normal. It is presumed that some of them will show neurological dysfunctions since they are litter mates of exencephalies and resorptions. Also, the term "resorption" includes dead fetuses as well as evidences of complete resorption.

cells which may be incorporated by "organismic influences" into the proper topographical development of the embryo. Thus we can explain the regulatory powers of the "organism as a whole." An irradiated organ anlage which would be carried to death by other necrotic and vital parts of the embryo may be transplanted to a normal embryo and survive as a normal anlage. Further, within 4 hr. of exposure of any embryo certain areas can be seen discharging vast numbers of necrotic (pycnotic and dead) cells, leaving the anlage with a deficit with which to build the organ. This is the explanation

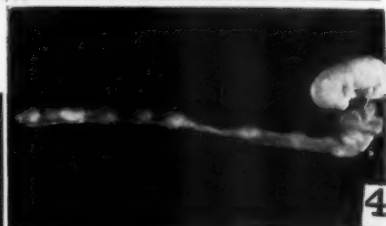


PLATE I

of the deficiencies that we call congenital anomalies following embryonic or fetal x-irradiation. To an embryologist this explanation is simple, and it is not necessary to conjure up genic action. Phenocopies which resemble the anomalies produced by irradiation of grandparental testes are produced by irradiation of the embryo, but this does not require an identical genic mechanism. The gap between the gene and the developmental process is still wide.

To take a specific example, the embryonic eye of the mouse begins to develop about day 12, and for several days thereafter the embryonic retina is very susceptible to x-irradiation insult. This was not evident in previous studies because the analysis was not made until after birth. However, when embryos were exposed to doses ranging from 50 to 300 r and studied histologically 4 hr. later, it was evident that the neural retina was severely damaged. In other embryos, examined 24 hr. after exposure, it was seen that there were abundant phagocytes aggregating in and near the retina and ingesting the dead and necrotic cells which had been neuroblasts of the retina. By 72 hr. the retina appeared to be re-formed, but it was shown that eyes of such mice at 2 mo. were microphthalmic to a degree related to embryonic exposure. For example, 150 r at 12.5 days reduced the eye volumes to 69 per cent, and 250 r at 12.5 days reduced eye volumes to 51 per cent of the controls. No study was made of the effect on visual acuity (59, 60, 61).

While clinicians often inquire whether embryonic or fetal x-irradiation

DESCRIPTION OF FIGURES 1-8, PLATE I

- FIG. 1. Entire litter of mice exposed to 200 r at 0.5 days postconception. One apparently normal, one exencephaly, and resorption sites.
- FIG. 2. Three members of litter of 11 receiving 200 r at 1.5 days, showing single exencephaly.
- FIG. 3. Entire litter (3) exposed to 50 r x-rays at 2.5 days.
- FIG. 4. Uteri of mouse exposed at 2.5 days after conception to 200 r x-rays, showing an apparently "normal" but stunted fetus and six resorption sites on the left side and three on the right.
- FIG. 5. Entire litter in position in uteri after receiving 50 r at 3.5 days.
- FIG. 6. Entire litter which received 200 r at 4.5 days, plus single control added (above) to show stunting effect of x-rays. Single exencephaly.
- FIG. 7. Litter of four which received 50 r at 5.5 days, with control at left. Note stunting of all, one exencephaly, and one abortive fetus.
- FIG. 8. Entire litter in position in uteri after receiving 200 r at 6.5 days, plus single normal control added (above). Note three exencephalies plus dead fetus.
-

These illustrations do not give any information relative to the frequency of these anomalies, only that they do occur. They never occur in otherwise normal pregnancies. Complete data will be published elsewhere under Rugh and Grupp. Fig. 1-16 will appear in (58a); Fig. 17-34 will appear in (58c); Fig. Suppl. 1-4 will appear in (58b).

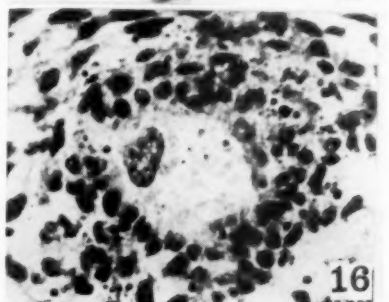
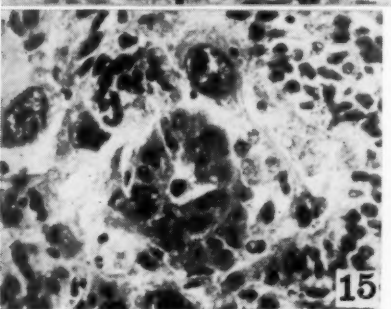
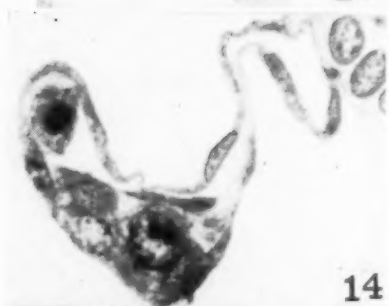
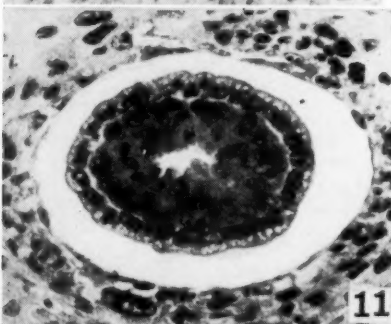
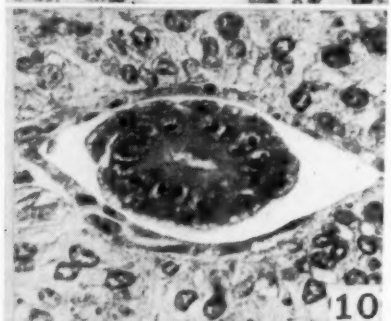
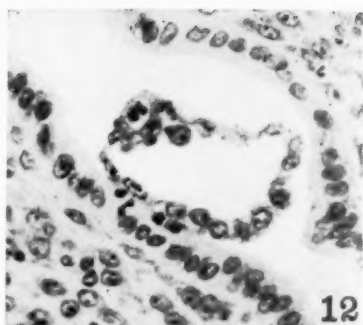
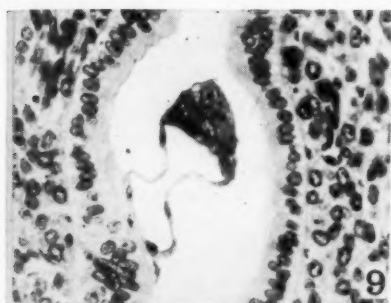


PLATE II

affects the fertility of the offspring, little work has been done in this area. In a recent paper it was shown that testes primordia are more radiosensitive than are ovarian primordia, as tested by subsequent fertility (62). In fact, it appears that the embryonic ovary is more resistant than is the adult ovary, which can be sterilized by 30 r and upwards. Exposures of the mouse embryos at 15.5 and 16.5 days to 50 to 200 r had little effect on the presumptive ovaries, but sterilized a considerable number of testes among the 500 mice exposed. Why there is a reversal of gonad sensitivity in the embryo as compared with the adult was not explained. Irradiation of embryonic gonad primordia established for each exposed gonad a level of fertility (or sterility) that was maintained throughout the life of the animal. There was no evidence of temporary sterility, or recovery of fertility, throughout the 9 mo. of study of reproductive activity of fetally-irradiated mice.

An exposure of 300 r at 9.5 days gestation of hybrid mice caused spina bifida, somite accumulation, bleb formation, tail malformations, coloboma, and hematomata (63); but if the exposure was fractionated at 30-min. intervals of 100 r each, the defects were greater than when the exposure was given in a single dose (64). Short interval fractionations were found to be the most hazardous to the embryos.

There is evidence that chemical "protection" of the mouse embryo is possible, using cysteamine before an exposure of 300 r on day 14.5. Not only did more mice survive the exposure, but those that were given protection showed a weight acceleration far greater than the untreated controls. Studies at the 17.5-day stage were even more convincing, and both cysteamine and cystamine afforded some protection in terms of survival and growth rate (65, 66, 67). It was pointed out that "protection" related to survival value alone and that there was no evidence of protection against the long term sequelae of irradiation. In this connection, it was also shown (68) that very low level exposures of the mouse embryo (10 r) would increase their 30-day

DESCRIPTION OF FIGURES 9-16, PLATE II

FIG. 9. Normal mouse blastula at 4.5 days in uterine cavity.

FIG. 10. Mouse embryo at 5.5 days showing thick inner embryonic ectoderm of egg cylinder.

FIG. 11. Mouse embryo at 6.5 days.

FIG. 12. Mouse embryo at 4.5 days (compare with Fig. 9) which was exposed to 200 r at 2.5 days. Note clumped chromosomes and enlarged cell of blastula.

FIG. 13. Similar to Fig. 12 but enlarged to show damage to nuclei.

FIG. 14. Oil-immersion view of mouse embryo at 4.5 days after 200 r x-rays at 2.5 days. Note free cell in blastocoel, swollen nucleus with paired nucleoli.

FIG. 15, 16. Resorbed embryos at 6.5 days (compare with Fig. 11) following 200 r x-rays. Note abundance of leucocytes (phagocytes) in vicinity, but no embryonic vestige.

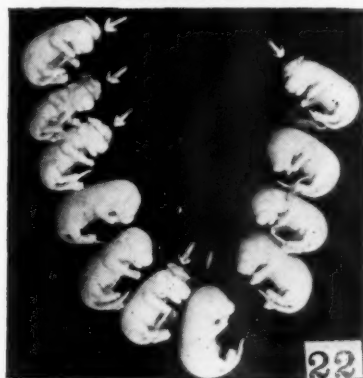
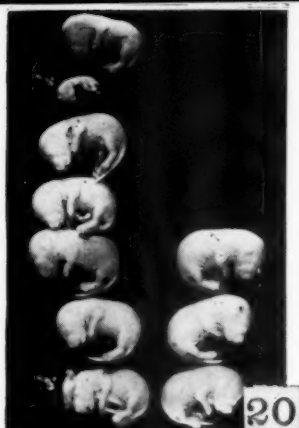
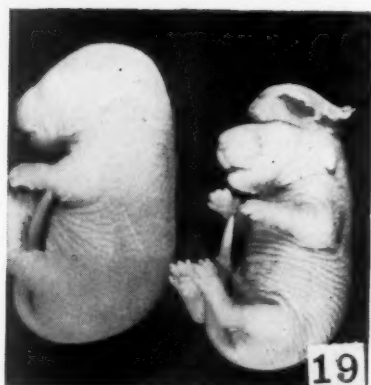
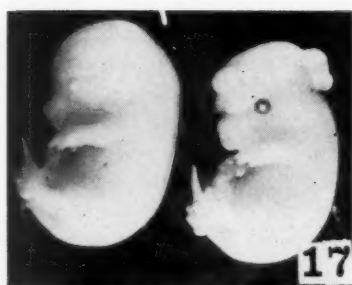


PLATE III

LD₅₀ when adults, while 25 r or more would reduce it; thus the low exposure tended to give the mice a small degree of immunization against the lethal effects of irradiation.

Radiiodine concentrates in the developing thyroid of the fetal mouse at 16 days (69) when the follicles first appear. Uptake is increased with gestational age, and neonatal growth is affected. It was also found that the reproductive activity of females irradiated by I¹³¹ in utero was reduced while the males were unaffected. Many fetally exposed mice developed chromophobe adenomas of the anterior pituitary glands at 9 to 12 mo., so that the treatment of pregnant human patients after the first trimester has been discouraged. But thiocyanate treatment of the pregnant mouse reduced the concentration of I¹³¹ in the fetal thyroids (70); methimazole (1-methyl-2-mercaptoimidazole) and thyrotropic hormones also alter the avidity of the fetal thyroid for radioiodine (71). Normally the fetuses collectively acquire the major part of any I¹³¹ into the pregnant mouse.

A contribution to embryological concepts has been made by drawing up a graph (72) of equivalent ages for the mouse and the human embryo which should be mentioned as very useful and instructive. While the mouse and human zygotes do not cleave before 24 hr., and implantation occurs in both at about 5.5 days, thereafter the rate of differentiation digresses in favor of the mouse which completes in the remaining 15 days what it takes

DESCRIPTION OF FIGURES 17-22, PLATE III

- FIG. 17. Two fetal mice from litter whose grandfather was a C57 black male that received 40,125 r to the testes and was then mated to normal CF1 white female. The F₁ litters were normal in appearance but when crossed with normal CF1 mice produced occasional exencephalies as seen here. This was probably attributable to chromosomal translocation which affects offspring after the first generation.
- FIG. 18. Litter mates with similar ancestry as in Fig. 1 showing range of anomalies caused by x-irradiation of germ cells of only one of the grandparents. Genetic factors involved.
- FIG. 19. Exencephaly in one member of a litter which was exposed to 200 r x-rays at 7.5 days gestation. This was caused by deletion of neuroblasts at the time of cerebral differentiation (phenocopy?)
- FIG. 20. Entire litter of mice at 18 days following exposure at 8.0 days gestation to only 50 r x-rays. Note exencephalia at position L 1, and failure to develop at position L 6; other litter members appear normal.
- FIG. 21. Section of head of mouse fetus with exencephaly showing brain protruding through the dorsal cranium where the mesenchyme failed to develop normal covering. Telocoels almost obliterated, and brain very abnormal.
- FIG. 22. Entire litter as found in uteri at 18 days following exposure to 200 r at 8.5 days gestation. Note total of 5 with exencephalia among litter of 11. Position in uterus unrelated to etiology of this teratology.

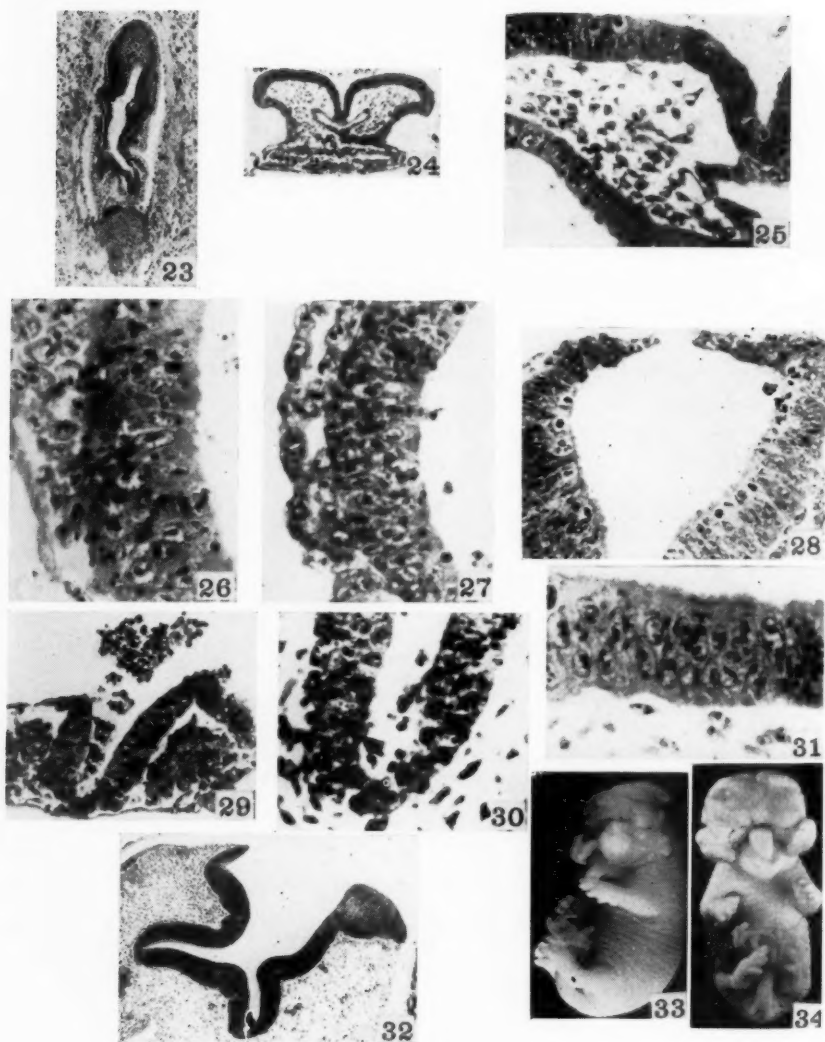


PLATE IV

the human embryo 260 days to accomplish. Nevertheless, the graph is of real value.

MAN

It seems that every x-irradiation-produced congenital anomaly found in the human has been produced in the mouse or the rat embryo by x-irradiation during embryonic or fetal life (73) (see Table II). Since it is possible to draw up a composite graph of normal development of mouse and of man (72), it may be justifiable to extrapolate from the mouse to man with regard to specific organ sensitivities if the word "probable" is interjected, indicating that the extrapolations are suggestive only. Since the mouse gestation period is 1/13 that of the human, mouse development is indeed telescoped with respect to that of the human. Further, it is now known that gastrulation and implantation occur at about the same time in the mouse and human, so that the latter two thirds of mouse development is further telescoped with respect to the rate of differentiation (see Table III).

DESCRIPTION OF FIGURES 23-34, PLATE IV

- FIG. 23. Section of normal mouse embryo at 7.5 days gestation showing thickened neur ectoderm.
- FIG. 24. Section through neural groove of mouse embryo at 7.5 days gestation at level of foregut.
- FIG. 25. High power view of neural groove neur ectoderm at 7.5 days gestation in the mouse, showing normal mitoses and abundant neur ectoderm and neuroblast cells.
- FIG. 26. Effect of 200 r x-rays 4 hr. after exposure at 7.5 days showing neur ectoderm severely damaged, with many pycnotic cells and very few intact neur ectoderm cells.
- FIG. 27. The condition of neur ectoderm 24 hr. after 200 r x-rays at 7.5 days gestation showing residual damage, some sloughed-off neuroblast cells in the amniotic cavity, but more normal cells than seen in the preceding stage.
- FIG. 28. Section through brain level 48 hr. after 200 r x-rays at 7.5 days gestation showing open cranial roof, but resumption of mitoses.
- FIG. 29. Section of neural groove 4 hr. after 200 r x-rays at 8.5 days showing many cells sloughed off into neurocoel, severely damaged neural ectoderm, but intact somite.
- FIG. 30. Condition of neural tube ectoderm 24 hr. after exposure to 200 r x-rays at 8.5 days gestation. Note severe damage.
- FIG. 31. Neural tube ectoderm 48 hr. after 200 r x-rays at 8.5 days gestation showing apparently normal cell activity.
- FIG. 32. Section of brain level of embryo developing exencephalia resulting from failure of the neural ectoderm to close above and cranial roof to form over the brain. Open brain cavity.
- FIG. 33, 34. Severe cerebral anomalies found in mice exposed to 150 r x-rays at 9.0 days gestation, affecting more than just the brain. Note rather normal appearance of body posterior to the head.

TABLE II
MAJOR ABNORMALITIES FOUND IN THE MAMMAL (HUMAN, MOUSE, RAT)
FOLLOWING FETAL X-IRRADIATION*

<i>Brain:</i>	<i>Skeleton:</i>
Anencephaly	Uniform reduction: Stunting
Porencephaly	Reduced skull dimensions
Microcephaly	Vaulted cranium
Encephalocoele (herniated brain)	Narrow head
Mongolism	Cranial blisters
Reduced medulla	Funnel chest
Cerebral atrophy	Congenital dislocation of hips
Mental retardation	Reduced and deformed tail
Idiocy	Overgrown and deformed feet
Neuroblastoma	Digital reductions
Deformities:	Calcaneo valgus
Narrow aqueduct	Abnormal limbs
Hydrocephalus	Syndactyly
Rosettes in neural tissue	Brachydactyly
Dilation of 3rd and 1st ventricles	Odontogenesis imperfecta
Spinal cord anomalies	Exostosis on proximal tibia
Reduction or absence of some cranial nerves	Metaphysis
	Amelogenesis
	Scleratomal necrosis
<i>Eyes:</i>	<i>Miscellaneous:</i>
Complete Absence-anophthalmia	Situs inversus
Microphthalmia	Hydronephrosis
Microcornia	Hydroureter
Coloboma	Hydrocoele
Deformed iris	Absence of kidney
Absence of lens and/or retina	Degenerate gonad
Open eyelids	Atrophy of lower extremities
Strabismus	Cutaneous depigmentation and hyperpigmentation
Retinoblastoma	Motorial disturbance of extremities
Hypermetropia	Increased probability of leukemia
Congenital glaucoma	Congenital heart disease
Partial albinism	Deformed ear
	Facial deformities
	Pituitary irregularity
	Dermatomal and myotomal necrosis

* These irradiation-induced anomalies have been reported in the works of Russell, Hicks, Miller, and Rugh for various mammalian fetuses, including the human.

TABLE III

CORRELATIONS IN DEVELOPMENT: MOUSE AND MAN DEVELOPMENTAL STAGE
IN HUMAN: ORGAN PRIMORDIA

Age in Days		Embryo, mm.	
Mouse	Man		
5	6		Implantation
	14	0.15	Germ layers, extra emb. membranes
	16	0.40	Primitive streak
8	20.5	1.5	Neural groove, blood islands, notochord
9	25.5	2.4	Cephalization, extensive vascularization, neural folds meet, primordia of sense organs, thyroid, limbs, muscles, pronephros, branch, arches, somites
10.5	28.5	4.2	Prim. brain w. vesicles, complete circulation, GI tract and derivatives, mesometanephros, vertebrae, 31 somites, yolk hemopoiesis
11.5	33.5	7.0	Genital ridge, heart, liver, mesonephros protuberant, limb and lung buds, 5 brain vesicles, all sense organs cardiac septa and 38 somites
12.5	36.5	9.0	Heart chambered, nerves and ganglia differentiating, thyroid anlagen bilobed
13.5	38.0	12.0	Sexless gonad primordia, liver hemopoiesis, brain flexures, limbs, thymus, GI tract actively differentiating
14.5	47.0	17.0	Cerebral hemispheres, corpora striatum, thalamus, blood vessels all actively differentiating, endocrine glands, peripheral and sympathetic nerves, eyes well formed
15.5	65.0	40.0	Cerebral cortex, intest. villi, thyroid follicles, first ossifications, sex differentiation with sex cords and germinal epithelium

Note: The highly radiosensitive neuroblasts are present throughout the embryo and fetus from about day 25 in the human (day 9 in the mouse) until some time after birth.

It is believed that implantation of the human embryo occurs at the sixth day, and, based upon rodent studies, it has been assumed that prior to this period in development it is highly radioresistant. However, very recent studies with the mouse embryo show that 50 r given even before the first cleavage (less than 0.5 day after conception) or on any day thereafter through day 9 may produce the very severe congenital anomaly of exencephalia (cerebral hernia), and it is certainly correct to presume that litter

mates of such anomalies may carry less graphic but similarly damaging results of x-irradiation (58a). On the basis of these studies it is now believed that x-irradiation hazards to the mammalian embryo exist from the instant of insemination at least through the period of organ differentiation, which is about 13 days in the mouse and somewhat later than 40 days in the human. We must therefore abandon the concept that sensitivity is related to the presence of anlagen, or that there are limited so-called critical periods for any particular organ system, and assume that the embryo at any stage prior to organ differentiation may be so disrupted by x-ray insult (as well as by radiomimetic insults) as to develop the congenital anomalies described. There are, then, at least three radiosensitive stages: the mature gamete (e.g., sperm) of the grandparent; the embryo prior to gastrulation and implantation; and the period of organ differentiation when the so-called "-blast" cells are so abundant. Once differentiation has been accomplished, it requires greater insult to produce any anomalies, and often this is impossible. In the case of neuroblast cells, these are present in the embryo from the earliest neural differentiation until several weeks after birth (cerebellum) so that neural sensitivity outspans all others. It has also been found (58b) that while 25 r alone will not produce severe exencephalies in the mouse, 50 r fractionated into two equal 25 r exposures at 2.5 and 7.5 days (during the predifferentiation stages) will occasionally result in exencephalies. If we assume that 25 r, then, are so damaging when given twice with such an extended intermediate span, we must likewise presume that each exposure alone must be damaging, even to a lesser degree. We have every reason to presume this applies as well to the human embryo.

Reliable human embryonic or fetal data, following x-irradiation, are rare (74) but, with the active cooperation of gynecologists and obstetricians and accurate records of all radiological examinations and treatments, we may shortly be able to present reliable statistical data. It is reported that exencephalia, for instance, occurs in about 1 in 4000 human births, but the more severe anencephalia (absence of brain or head) occurs about once in 1000 births. Thus far there has been no evidence to attribute these to embryonic x-ray insult, but as histories are better taken and examined, some correlation may be found. Data from Hiroshima and Nagasaki have been convincing. It has been found that there is a reduction in the head dimensions and evidence of retardation in children who were exposed in utero. The closer the pregnant Japanese woman was to ground zero, the more likely she was to have a microcephalic child, and mental retardation occurred in a high percentage of these children (75).

While both Japanese boys and girls showed stunting as a result of embryonic exposure to the atomic bomb, it appeared that the boys showed a reduction in head circumference while the girls not only showed this deficit but also reductions in average weight and height (76). Exposure during the second half of gestation was not so damaging, but the boys exposed during this period scored less in the Koga intelligence tests than did the girls (77,

77a). While neurological anomalies were found, none of the severe conditions described above for mice or rats have been found among children at either Nagasaki or Hiroshima. This may reflect poor survival value of those affected, since the data relate only to children delivered and surviving for the six to seven years subsequent to the atomic incident. Also, final analysis must be delayed until these children achieve adolescence at least, when other neurological effects may appear (78).

Microcephaly and mental retardation occurred most frequently among the 205 children exposed to the atomic bomb at Hiroshima, with congenital dislocation of the hips, mongolism, congenital heart disease, and hydrocoele as other effects (78). Among the children of 30 pregnant women exposed at Nagasaki, 23.4 per cent showed fetal mortality, 26 per cent neonatal or infant death, and among 16 surviving children 25 per cent showed mental retardation. The overall morbidity and mortality of atomic bomb exposure of human embryos was 60 per cent in this group, in contrast with 6 per cent for the unexposed general population. Exposure during the second or third trimester also resulted in greater percentage of fetal, neonatal, and infant mortality than among the controls. It is believed that these results are independent of trauma and burns from the bomb (79).

Microcephalic idiocy has long been attributed to the exposure of the human fetus to ionizing radiations (80, 81, 82), but there have also been reports of human fetal irradiation without obvious sequelae even though exposures were as much as 900 r at the fifth month, or 4790 r during the period of 90 to 112 days gestation, and the mothers' ovaries were sterilized (83, 84, 85). Subsequent examination of one of these cases indicated neurological symptoms that were not evident at 18 mo., which means that there is a wide range of so-called "normality" among infants and the necessity of awaiting a later stage in development when behavior and I.Q. tests may reveal more data.

The diagnostic x-ray examination of a pregnant woman at 4, 5, and 6 mo. was followed by delivery of a child showing a whole group of "congenital" anomalies such as microphthalmus, microcornea, syndactyly, brachydactyly, strabismus, hypermetropia, amelogenesis, and odontogenesis imperfecta (86). A castration case by radiation involved an unrecognized fourth month pregnancy in which instance it was estimated that the fetus received about 900 r. When the child was two years of age it showed atrophy of the lower extremities, areas of hyper- and dipigmentation, while an exencephalogram indicated hydrocephalus, porencephaly, and microcephaly. Psychometric tests revealed complete idiocy. Some 168 other and similar cases were reported (87) indicating that exposure to ionizing radiations at 4 to 5 mo. in the human had effects somewhat similar to those which follow 10.5 day gestation exposure in rats and mice. Exposure received in the first 2 mo. of pregnancy was said to result in 100 per cent damage, from 3 to 5 mo. caused 64 per cent damage, and 6 to 10 mo. some 23 per cent damage. Lumping together all such data may be misleading, but eventually, and with the cooperation of radiologists, gynecologists, and obstetricians, it will be possible

to determine more accurately the dosimetry and delivered dose, as well as the embryonic or fetal age in specific cases. Human data will be slow in accumulation but will eventually be available.

There has been a report (88) that there is a higher incidence of leukemia and cancer in offspring of mothers x-irradiated during pregnancy. Even roentgen pelvimetry has been suspect. In a later report (89) it was suggested that among 515 leukemia cases, following fetal irradiation, there appeared 15 mongolian idiots. There were also neoplasms of the brain, spinal cord, kidneys, suprarenals, lymph nodes, and other sites.

X-irradiation has been considered as a shock factor in the induction of human congenital defects, much like any traumatic, physiologic, or severe emotional stress (90). Even therapeutic irradiation of pregnant women has been considered as a factor in causing microcephaly and other defects in the fetus (91). Anencephalia has been reported in the human fetus (92, 93) but these cases have not been definitely attributed to ionizing radiations. And "from a genetic aspect every dose of radiation, no matter how small, to the embryo will cause damage" (94).

With further education and increasing awareness of the hazards of irradiation to the embryo or fetus, plus better technical methods of fluoroscopy, it should be expected that the offspring of radiologists will eventually not show any higher incidence toward genetic effects than that of the general medical population (95, 96). There is some doubt relative to the fertility data of radiologists, but in our modern society this factor is generally so controlled that statistical data are of no value. The radiologist has accepted the hazards of his profession, but these are being lessened rapidly.

Isotope data for the human embryo and fetus are rare. Two recent cases have been reported to show that pregnant women receiving large doses of I^{131} not only developed hypothyroidism, but that there was also congenital hypothyroidism in the offspring (97). Certainly there is no placental barrier to the transfer of isotopes to the fetus, and radiosodium has been used to test placental function (98). Since the human embryo or fetus is not available for experimental radiobiology, all data will come from accidental or inevitable exposures.

GENERAL SUMMARY AND CONCLUSIONS

The fertilized egg appears to be more radiosensitive than either gamete, probably because of interference with movements in syngamy. The embryo or fetus appears to be more radiosensitive than any postnatal stage, attributable in part to the presence of undifferentiated or differentiating organ anlagen. Anlagen of a specific organ may exhibit greater resistance than the adult organ (e.g., the ovary), but the embryo as a whole is subject to the induction of congenital anomalies which cannot be produced by any amount of irradiation after birth. There is no evidence of "recovery" of irradiation-damaged embryonic cells, but rather such cells may be phagocytized and removed, leaving an embryo with a deficit which may result in a deficient adult in terms of microphthalmia, microcephalia, stunting, etc.

"Congenital anomalies" may be brought about by x-irradiation insult at a period long before the onset of organ differentiation, e.g., at the one-celled (fertilization) stage. Exencephalia, or cerebral hernia, has been produced by 50 r at the 1.5 day stage in the mouse, prior to the first cleavage of the fertilized egg. It can be most readily produced by x-irradiation at 8.5 days but also by high level exposure of the grandparental sperm. The term phenocopy applies only to the final appearance, and does not allude to the method of derivation of the anomaly, which probably varies from purely genetic to interference with the movements of gastrulation. The term "critical period" for cerebral anomalies loses its significance when it extends over one-third of the gestation of the mouse.

Since the nervous system permeates all other systems, and the peculiarly radiosensitive neuroblasts are present over a long period of prenatal development, neurological teratologies have been emphasized in the literature. It is believed that any differentiating cell, of any tissue or organ, is more radio-sensitive than the formed tissue or organ.

It is possible that the so-called "protective" drugs may afford the embryo or fetus better survival value, but there is no evidence that they will protect the offspring from the usual sequelae of exposure to ionizing radiations. There is no explanation for the fact that within a litter there may be extreme variations in response to x-irradiation of the gravid uterus, beyond genotypic or biological variations. At the same time the outward appearance of normality within a litter (which shows some exencephaly) is no guarantee that the "normal" individual is in fact undamaged. Usually it is stunted, but it is predicted that it will also manifest neurological dysfunctions.

Congenital anomalies are not the exclusive province of exposure to ionizing radiations, for similar anomalies can be elicited by other insults, for example, by radiomimetic drugs and by nutritional deficiencies. The embryo is a mosaic of innumerable developmental potencies each with its specific sensitivity with respect to embryonic time, and irrespective of the nature of the insult. The time of irradiation will determine the nature of the congenital anomaly while the level of irradiation will determine the degree of divergence from the normal.

Human data are so fragmentary and confusing that no conclusions can be drawn. However, there is reason to believe that the human embryo is not exceptional and that the findings with other mammalian embryos may be, in general, extrapolated to the human until more accurate human data are available. This means that exposure of the human embryo should be avoided under all circumstances, particularly during early development (i.e., from the ninth day after the onset of menstruation, when fertilization could occur, to at least day 65 when the major organogenies have taken place). It is believed that gross congenital anomalies may result from exposures to ionizing radiations at any time from immediately after conception through at least the first trimester. It must be emphasized that this chapter has dealt with only the embryo and fetus. The data should not discourage either the radiol-

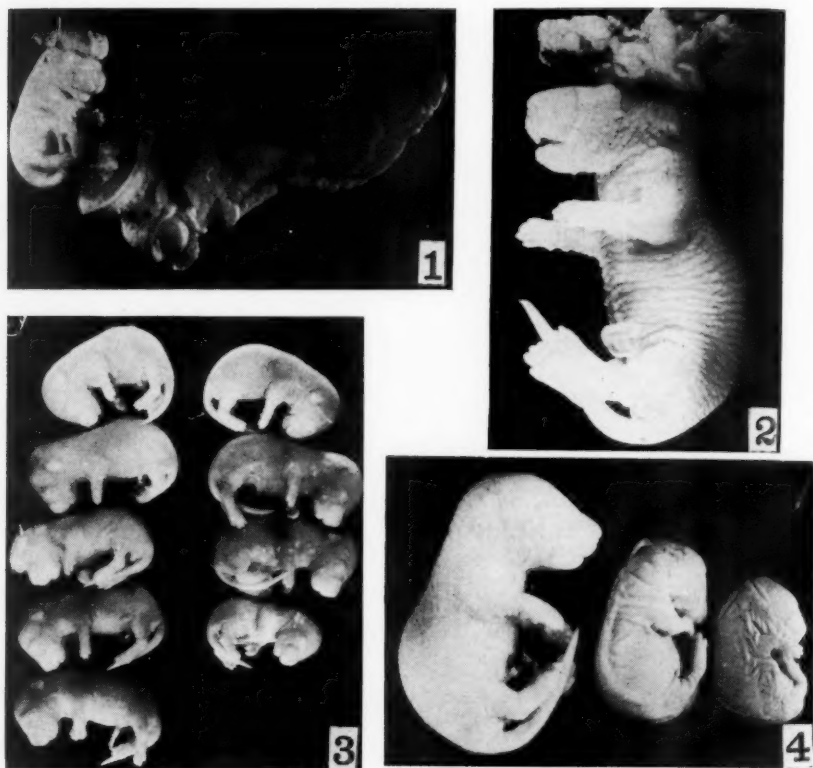


PLATE V

Supplement figures.—

- FIG. 1. Uteri of mouse exposed at 2.5 and 8.5 days gestation to 25 r each time, showing one horn with only resorbed embryos and the other horn with single fetus with exencephaly.
- FIG. 2. Effect of fractionating of 50 r into two 25 r components, delivered at 2.5 and 8.5 days gestation. Note grotesque exencephaly through dorsum of cranium.
- FIG. 3. Entire litter in position found in uteri, showing effect of fractionation of 50 r into two exposures of 25 r each 2 hr. apart on day 8.5. Single exencephaly, one grossly stunted, and others variously reduced in growth.
- FIG. 4. Similar to Fig. 3 but fractionation separated by 1 hr., total exposure 50 r in two 25 r doses. Part of litter only, showing two fetuses killed by the exposure.

ogists or the patient in the use of ionizing radiations for diagnosis or therapy of malignancies in the postnatal individual, where they may truly be life-saving.

SUPPLEMENT

Last-minute information is available on an extensive study in progress on exencephaly produced in the mouse embryo following x-irradiation at different stages of development, with fractionation of doses, and in combination with so-called "protective" drugs. It is possible at this time only to anticipate some of the findings.

The most radiosensitive period in embryonic development is prior to the first cleavage of the fertilized egg, or within 12 hr. of conception in the mouse. An exposure of 25 r will kill 38 per cent of the embryos in utero. Exposures down to 1 or 5 r are being tested, and a dose of 5 r increases uterine depth and resorption.

When 50 r are fractionated into two doses, given in all combinations from 0.5 to 8.5 days, exencephalies have also been produced. Certain combinations have a greater incidence of this anomaly, and of resorptions, with the greater percentages occurring if one of the fractions occurs at a very early stage of development. However, fractionations of 1 or 2 hr. interval between the 25 r exposures will also produce exencephalies (see Supplement Fig. 1 to 4 and description).

Preliminary evidence suggests that the protective drugs do in fact provide for greater percentage survival of embryos and do lessen to some extent the anomalies produced. Actual data will be forthcoming shortly. This project is being continued to determine to what extent the "apparently normal" litter mates of these irradiation-produced congenital anomalies are in fact "normal," the tests being with the electroencephalogram and by neurocytopathological studies.

LITERATURE CITED

1. Dublin, L. I., *Foetal, Infant and Early Childhood Mortality*, 11, Biological, Social and Economic Factors, UN Popul. Studies No. 13 (Dept. Social Affairs, UN, 44 pp., 1945)
2. O'Brien, J. P., *Ann. Rev. Nuclear Sci.*, **6**, 423 (1956)
3. Rugh, R., *Biol. Bull.*, **114**, 385 (1958)
4. Bonham, K., *Growth*, **19**, 9 (1955)
5. Henley, C., and Costello, D. P., *Biol. Bull.*, **112**, 184 (1957)
6. Welander, A. D., Donaldson, L. R., Foster, R. E., Bonham, K., and Seymour, A. H., *Growth*, **12**, 203 (1948)
7. Welander, A. D., *Growth*, **18**, 227 (1954)
8. Rugh, R., and Grupp, E. (In press)
9. Rugh, R., *J. Cellular Comp. Physiol.*, **43**, 39 (1954)
10. Schinz, H. R., and Fritz-Niggli, H., *Strahlentherapie*, **94**, 147 (1954)
11. Allen, B. M., *Anat. Record*, **128**, 514 (1957)
12. Allen, B. M., Schjeide, O. A., Hockwald, L. B., *Proc. Soc. Exptl. Biol. Med.*, **73**, 60 (1956)
- 12a. O'Brien, J. P., and Gozmerac, W. L., *Proc. Soc. Exptl. Biol. Med.*, **92**, 13 (1956)
13. LaHam, Q., and O'Brien, J. P., *Anat. Record*, **119**, 111 (1951)
14. Piatt, J., and Raventos, A., *J. Exptl. Zool.*, **124**, 167 (1953)
15. Rugh, R., *J. Morphol.*, **84**, 483 (1949)
16. Schneller, Sister M. B., *J. Morphol.*, **89**, 367 (1951)
17. Goldman, M., Glasser, S. R., and Tuttle, L. W., *U. S. Atomic Energy Commission Document, UR-296* (1955)
18. Tobin, M. J., and O'Brien, J. P., *Wasmann J. Biol.*, **10**, 1 (1952)
19. Boland, J., *Brit. J. Radiol.*, **27**, 324 (1954)
20. Karnofsky, D. I., Patterson, P. A., and Ridgeway, L. P., *Am. J. Roentgenol., Radium Therapy Nuclear Med.*, **64**, 280 (1950)
21. Reyes-Brion, M., *Arch. anat. microscop. morphol. exptl.*, **45**, 342 (1956)
22. Kirkmann, J. M., *Bull. Biol.*, **89**, 491 (1955)
23. Goffinet, J., *Arch. anat. microscop. morphol. exptl.*, **45**, 162 (1956)
24. Chapman, A. O., *J. Morphol.*, **95**, 451 (1954)
25. Chapman, A. O., and Latta, J. S., *Anat. Record*, **124**, 452 (1956)
26. Hicks, S. P., *Proc. Soc. Exptl. Biol. Med.*, **75**, 485 (1950)
27. Hicks, S. P., *Proc. Soc. Exptl. Biol. Med.*, **75**, 485 (1950)
28. Wilson, J. G., *Anat. Record*, **109**, 98 (1951; also Wilson, J. G., Brent, R. L., and Gordon, H. C., *U. S. Atomic Energy Commission Document, UR-183* (1951); *Cancer Research*, **12**, 222 (1952)
29. Hicks, S. P., *Proc. Soc. Exptl. Biol. Med.*, **75**, 485 (1950)
30. Hicks, S. P., *U. S. Atomic Energy Commission Document, AECU-2697* (1953)
31. Barron, E. G. S., and Dickman, S., *J. Gen. Physiol.*, **32**, 595 (1948)
32. Barron, E. G. S., *Enzymologia*, **11**, 201 (1951)
33. Danielli, J. F., and Davies, J. T., *Enzymologia*, **11**, 47 (1951)
34. Hicks, S. P., *Arch. Pathol.*, **55**, 302 (1953)
35. Hicks, S. P., *J. Cellular Comp. Physiol.*, **43**, 151 (1954)
36. Rugh, R., in *Radiation Biology* (Forssberg, A., and Errera, J., Eds., in press, 1959)
37. Hicks, S. P., *Arch. Pathol.*, **57**, 363 (1954)

38. Hicks, S. P., *Proc. Intern. Congr. Neuropathol., 4th Meeting Congr. (Brussels, 1957)*
39. Erzhoff, B. H., *Proc. Soc. Exptl. Biol. Med.*, **97**, 202 (1957)
40. Hicks, S. P., *Am. J. Pathol.*, **33**, 459 (1957)
41. Hicks, S. P., *Arch. Pathol.*, **57**, 363 (1954)
42. Hicks, S. P., *Proc. Intern. Congr. Neuropathol., 4th Congr. (Brussels, 1957)*
43. Riggs, H. E., McGrath, J. J., and Schwarz, H. P., *J. Neuropathol. Exptl. Neurol.*, **15**, 434 (1956)
44. Sikov, M. R., and Lofstram, J. E., *Radiology*, **69**, 274 (1957)
45. Sikov, M. R., and Noonan, T. R., *U. S. Atomic Energy Commission Document, UR-327* (1954)
46. Sikov, M. R., Lofstram, J. E., and Reston, J. F., *Radiation Research*, **7**, 449 (1957)
47. Schwarz, H. P., Riggs, H. E., Glick, C., McGrath, J., Cameron, W., Bayer, E., Dew, E., and Childs, R., *Proc. Soc. Exptl. Biol. Med.*, **80**, 467 (1952)
48. Sikov, M. R., and Noonan, T. R., *Radiation Research*, **7**, 541 (1957)
49. Maisin, H., Dunjic, A., Maldague, P., and Maisin, J., *Comt. rend. soc. biol.*, **149**, 1687 (1955)
50. Levinson, B., *J. Comp., and Physiol. Psychol.*, **45**, 140 (1952)
51. Rekers, R. E., *J. Lab. Clin. Med.*, **37**, 331 (1951)
52. Spalding, J. F., Strang, V. G., and Hawkins, S. B., *Radiation Research*, **8**, 222 (1958)
53. Russell, L. B., *Proc. Soc. Exptl. Biol. Med.*, **95**, 174 (1957)
54. Russell, L. B., and Russell, W. L., *J. Cellular Comp. Physiol.*, **43**, 103 (1954)
55. Russell, L. B., *J. Exptl. Zool.*, **114**, 545 (1950)
56. Russell, L. B., *J. Exptl. Zool.*, **131**, 329 (1954)
57. Murakami, U., *Folia Psychiat. et Neurol. Japon.*, **10**, 1-207 (1957)
58. Russell, L. B., and Russell, W. L., *Anat. Record*, **108**, 521 (1950)
- 58a. Rugh, R., and Grupp, E. J., *Neuropathol. and Exptl. Neurol.* (July, 1959)
- 58b. Rugh, R., and Grupp, E. (In press)
- 58c. Rugh, R., and Grupp, E., *Am. J. Roentgenol., Radium Therapy, and Nuclear Med.* (July, 1959)
59. Rugh, R., and Wolff, J., *Proc. Soc. Exptl. Biol. Med.*, **89**, 48 (1955)
60. Rugh, R., and Wolff, J., *Arch. Ophthalmol.*, **54**, 351 (1955)
61. Rugh, R., and Wolff, J., *Acta Med. Belg.*, 189 (1957)
62. Rugh, R., and Jackson, S., *J. Exptl. Zool.* (In press, 1958)
63. Aurebach, R., *Anat. Record*, **121**, 258 (1955)
64. Aurebach, R., *Nature*, **177**, 574 (1956)
65. Cronkite, E. P., Sipe, C. R., Eltholz, D. C., Chapman, W. H., and Chambers, F. W., Jr., *Proc. Soc. Exptl. Biol. Med.*, **73**, 184 (1950)
66. Rugh, R., and Wolff, J., *Radiation Research*, **7**, Abstr. 149 (1957)
67. Rugh, R., *Am. J. Physiol.*, **189**, 31 (1957)
68. Rugh, R., and Wolff, J., *Proc. Soc. Exptl. Biol. Med.*, **96**, 178 (1957)
69. Speert, H., Quimby, E. H., and Werner, S. C., *Surg., Gynec. Obstet.*, **93**, 230 (1951)
70. Rugh, R., and Clugston, H., *Endocrinology*, **58**, 8 (1956)
71. Rugh, R., and Booth, E., *J. Pediat.*, **44**, 516 (1954)
72. Otis, E. M., and Brent, R., *U. S. Atomic Energy Commission Document, UR-194* (1952)

73. Miller, R. W., *Pediatrics*, **18**, 1 (1956); also Rugh, R., *J. Pediat.*, **52**, 531-38 (1958)
74. Murphy, D. P., *Congenital Malformations* (J. B. Lippincott Co., Philadelphia, Pa., 127 pp., 1947)
75. Plummer, G., *Pediatrics*, **10**, 687 (1952)
76. Kawamoto, S., Hamada, M., Sutow, W., Reynolds, E., and Kuschner, J., *Atomic Bomb Casualty Commission Publ.* (1954)
77. Sutow, W. W., *Atomic Bomb Casualty Commission Publ.*, 1954 NYO-4428 (1953)
- 77a. Sutow, W. W., and West, E., *Am. J. Roentgenol. Radium Therapy Nuclear Med.*, **74**, 493 (1955)
78. Kawamoto, S., *Atomic Bomb Casualty Commission Publ.* (1955)
79. Yamazaki, J., Wright, S., and Wright, P., *J. Diseases Children*, **87**, 448 (1954)
80. Murphy, D. P., *Congenital Malformations* (J. B. Lippincott Co., Philadelphia, Pa., 127 pp., 1947)
81. Goldstein, L., and Murphy, D. P., *Am. J. Obstet. Gynecol.*, **18**, 189 (1929)
82. Dunlop, C. E., *Human Fertility*, **12**, 33 (1947)
83. Pinsonneault, G., *Union méd. Canada*, **8**, 945 (1949)
84. Hobbs, A. A., *Radiology*, **54**, 242 (1950)
85. Roland, M., and Weinberg, A., *Am. J. Obstet. Gynecol.*, **62**, 1167 (1951)
86. Pitter, J., and Svijsda, J., *Ophthalmologica*, **123**, 3861 (1952)
87. Basic, M., and Weber, D., *Strahlentherapie*, **99**, 628 (1956)
88. Stewart, A., Webb, J., Giles, D., and Hewitt, D., *Lancet*, **II**, 447 (1956)
89. Stewart, A., *Proc. Roy. Soc. Med.*, **50**, 251 (1957)
90. Streat, L. P., *Ärztl. Wochschr.*, **13**, 110 (1958)
91. Court-Brown, W. M., and Doll, R., *Med. Research Council Rept.* 9780, 87 (1956)
92. Erskine, C. A., *Acta Anat.*, **23**, 251 (1955)
93. Ford, E. H. N., *Acta Anat.*, **28**, 149 (1956)
94. Gyllensten, A. L., *Nord. Med.*, **59**, 846 (1958)
95. Macht, S. H., and Lawrence, P. S., *Am. J. Roentgenol. Radium Therapy Nuclear Med.*, **73**, 442 (1955)
96. Crow, J. F., *Am. J. Roentgenol. Radium Therapy Nuclear Med.*, **73**, 467 (1955)
97. Russell, C. P., Rose, H., and Starr, P., *Surg., Gynecol. Obstet.*, **104**, 560 (1957)
98. Clayton, C. G., Farmer, F. T., and Johnson, T., *Lancet*, **II**, 539 (1956)

BIOCHEMICAL EFFECTS OF IONIZING RADIATION^{1,2}

By MARGERY G. ORD AND L. A. STOCKEN³

Department of Biochemistry, Oxford University, Oxford, England

The year 1958 was notable for two international congress meetings: the Second International Congress of Atoms for Peace, in Geneva, Switzerland, and an International Congress for Radiation Research, in Burlington, Vermont, U.S.A. Since these two meetings alone made several hundred contributions to the biological aspects of the radiation syndrome, it is clear that this review can deal only in a very limited way with the literature of the biochemical effects of radiation. It is still to be regretted that although a vast amount of material has accumulated, the variation in radiation dose and time interval between exposure and observation precludes an integration of the data into a coherent story.

In this review the arrangement established by precedent will be followed and the information will be grouped into sections, each dealing with one topic. Such an arrangement has certain advantages but a solution of the problem might be more easily inspired if the data were considered in a chronological order. In this way the secondary reactions which take place in the whole animal could be clearly distinguished from the immediate damage and perhaps a connection established between the ionizing event, the formation of free radicals, and the primary biochemical lesion.

A very comprehensive review of the subject has recently been made by Errera (74) and there are others dealing with more limited aspects (84, 88, 93, 117, 125, 148, 155, 201, 244, 250).

CARBOHYDRATE METABOLISM

Absorption and liver glycogen levels.—It is generally agreed that absorption of glucose and other sugars is reduced in rats exposed to total-body radiation; this is mainly because of a delay in gastric emptying time (11, 87). Conflicting evidence has been reported when intestinal loops of irradiated animals are used, and it is likely that morphological changes in the intestinal cells and edema are factors in the decreased absorption rate (58, 75). It

¹ The survey of literature pertaining to this review was concluded in February, 1959.

² Among the abbreviations used in this chapter are: AET (S,2-aminoethylisothiuronium bromide hydrobromide); APT (S,3-aminopropylisothiuronium bromide hydrobromide); ATPase (adenosinetriphosphatase); BAL (2,3-dimercaptopropanol); DNase (deoxyribonuclease); DPN (diphosphopyridine nucleotide); FAc (sodium fluoroacetate); G₁ (presynthetic period in interphase); G₂ (postsynthetic period in interphase); RNase (ribonuclease); S (synthetic period in interphase); S_f (flotation rate expressed in negative Svedberg units); TBR (total-body radiation).

³ We wish to express our gratitude to Dr. L. H. Gray for considerable help with the section on the oxygen effect, to Mr. L. A. Biran for translation of Russian articles, and to Mr. A. Morris and Miss H. Minns for help with the bibliography.

should be noted, however, that no correlation could be established between the histological changes and the reduced glucose absorption in intestine taken from rats up to 17 days after exposure to 600 r TBR (57). Moss (186) compared the effects of local irradiation of the bowel with those after total-body exposure with the exteriorized bowel shielded. When the absorption from tied-off loops of the irradiated intestine was measured, a decreased disappearance of both glucose and arabinose was evident but when the bowel was shielded there was no alteration. Although there was a reduction in the organophosphates in the dried mucosa, since arabinose as well as glucose absorption was depressed it was thought that diffusion was a significant factor.

There have been relatively few contributions of late to the problem of the origin of hepatic glycogen which accumulates after whole-body exposure. It seems that the immediate fall (within 30 min.) in glycogen produced by supra-lethal doses is caused by adrenal stimulation, and the subsequent increase at 18 hr. follows from increased tissue breakdown. Lelievre (157) has extended his work on the glycogenolytic response to show a parallel increase in tissue and blood lactate concentrations after very high exposures. An interesting study of the effects of cortisone and x-radiation shows that in rats, at 24 hr., cortisone has a greater effect than 1300 r x-rays and that the two together cause the accumulation of more glycogen than either stimulus separately (162).

Some insight into the mechanism of increased glycogen deposition has been provided by the observations of Chaikoff and colleagues (110). They found that 4 hr. after irradiation of rats with 1000 r TBR, liver slices showed an increased rate of oxidation of both glucose and fructose, but after 24 hr. there was a marked incapacity to convert ^{14}C glucose to CO_2 , fatty acid, and glycogen while fructose metabolism was normal. Since the catabolic pathways of glucose and fructose are confluent below fructose diphosphate, the authors suggest the lesion is somewhere before the triose phosphate stage. It is of interest in this connection that the disturbance of peripheral glucose utilization following exposure of dogs to 250 to 600 r could be reversed (28) and the postradiation hyperglycemia in rabbits caused by 500 to 2000 r could be prevented by insulin (247).

Evidence supporting the view that tissue breakdown is responsible for the accumulation of glycogen has been obtained by direct measurement of weight loss in tissues of exposed rats and by a continuation of studies of excretion of amino acids following radiation (43). There was an increased output of taurine which was proportional to the dose received up to 250 r but thereafter no further increase took place. Urea levels also rose while creatinine was unaffected even with doses of 2000 r (123). Similar results were obtained by Pentz (205), and both groups of workers noted that adrenalectomy did not prevent the taurine excretion. The origin of the taurine is obscure; for, although Kit & Awapara (135) have shown that the free taurine concentration of lymphoid tissue is more than twice that of any amino acid, the demonstration by Pentz that combined thymectomy and splenectomy failed

to influence the taurine output makes it unlikely that destruction of lymphoid tissue is entirely responsible for the effect.

An extension to the earlier estimates of the free glycine pool has been made by Haberland *et al.* (95) and Lauenstein *et al.* (154) by the use of isotopically labelled phenylalanine and glycine. The results confirm the previous findings and are considered to be a direct measure of the extent to which tissue is broken down when rats are exposed to 756 r TBR. Morehouse & Searcy (184) followed the incorporation of ^{14}C glycine, alanine, and leucine into liver glycogen immediately after 1500 r. The greatest effect in fed rats was with alanine, but all the acids showed a much greater incorporation when the animals were starved.

Additional evidence for enhanced postradiation muscle catabolism comes from many studies of creatine excretion. Rats and monkeys had a marked creatinuria especially on the second day after exposure (76, 139, 266) but, on the other hand, dogs after 400 to 500 r showed no increase (4). From a long-term experiment with rats which had survived for 6 mo. following 1500 r γ -irradiation, the same authors concluded that radiation had no effect on creatine synthesis but produced damage to the tissue in which a significant part of the creatine was contained. Administration of methionine 30 min. after irradiation, but not before exposure, has been reported by Kumta *et al.* (142) to reduce the creatinuria in rats. Creatinine levels were unaffected.

The suggestion of muscle-protein breakdown tends to conflict with the failure to find evidence of immediate damage but this may be masked by small changes taking place in a tissue which makes a major contribution to the total cell population.

To summarize the experimental results, it appears that the increased hepatic glycogen at 24 hr. after radiation is not caused by a stimulation of the pituitary-adrenal axis per se [see (53) for an excellent review of the evidence relating to the hormonal work] but is caused by the breakdown of some as yet incompletely defined tissue and the subsequent storage of the carbon skeletons which are released.

More evidence for adrenal cortical changes comes from work on guinea-pig adrenal ascorbate levels which were reduced by 500 and 1000 r TBR but not by local irradiation (270). Rosenfield (221) studied the functional capacity of calf adrenals after 600 r γ -radiation. The glands were perfused with ACTH and oxygenated medium, and the maximal corticoid output over a 2 hr. period was measured. Twenty-four hours after exposure there was an increased output which returned to normal by 4 days and increased again preterminally. No abnormalities in the response to ACTH nor changes in steroid hydroxylating enzymes could be detected.

Glycolysis and respiration.—No change was observed in anaerobic glycolysis of mouse liver immediately after exposure to 60,000 r (156), but in the case of tumour cells 20,000 r given to human cervical uterine carcinoma reduced both respiration and anaerobic glycolysis by about 30 per cent (217).

A similar depression was found by Maass & Rathgen (170) when Yoshida

sarcoma, Jensen sarcoma, Walker sarcoma, and spleen slices were exposed *in vitro* to 10 to 20,000 r; liver slices on the other hand were unaffected. The same authors and their associates (171, 216) concluded that the reduced amount of DPN present in ascites tumour cells after exposure to the same dose was responsible for the reduced glycolysis. With low-energy x-rays (0.7 A; 40 kv.), 1000 r produced a 50 per cent depression of anaerobic fermentation by ascites cells in Ringer-phosphate. The inhibition was considerably reduced by the presence of catalase during irradiation (261, 261a).

There are some indications that effects on respiration and glycolysis can be induced by indirect means. Ebina & Kurosu (68) found only a small reduction in the glycolysis of ascites tumour cells which had been exposed to 500 and 1000 r; but when trivial concentrations of haematoporphyrin, which did not affect oxygen uptake, were added to the tumour suspension during irradiation *in vitro* with 7500 r, glycolysis was markedly reduced. An almost complete inhibition was produced by 66.6 μ g. (230). Silk, Hawtrey & Macintosh (234) measured the anaerobic glycolysis and O₂ uptake of Walker carcinoma, Ehrlich mouse ascites tumour, and Rous sarcoma in lymph taken from normal and x-irradiated dogs given 450 r 3 hr. previously. There was a depression of both glycolysis and respiration when bicarbonate-CO₂ was the medium, but when phosphate was employed the opposite result was obtained. If nonmalignant tissues were suspended in lymph from exposed dogs, the respiration was increased.

Snezhko (242) observed a depressed respiration in the brain of rabbits which had received 900 to 3000 r either to the head or whole body 1 hr. or in some cases as early as 5 to 10 min. previously. He also noted that there was an increased O₂ consumption in the brain when only the abdomen had been exposed.

Early effects on the respiration of tissues taken from animals exposed to moderate doses of radiation are uncertain. Many previous workers have reported a reduced respiration at times later than about 4 hr., but Szonyi & Várterész (251) found a twofold increase between 10 hr. and 15 days in the rate of respiration of homogenized duodenal mucosa from rats exposed to 600 r, and Hanel, Hjort & Purser observed an increased endogenous respiration of liver from rats given 450 r TBR (99). The oxygen consumption of rhesus monkeys is unaffected by 2500 r but is depressed by 5, 10, and 30,000 r TBR at 2 min. after radiation (38). It will be noticed that in order to demonstrate an immediate radiation response, very high doses are required and many authors have pointed out the difficulty of interpretation of data obtained by means of supralethal exposures. Effects produced by smaller doses require time to become manifest and are likely to be a secondary response.

FAT

Further data have been provided about the lipemia which follows exposure to near-lethal doses of x-radiation. In rabbits at 24 hr. the greatest increase was in neutral fat; phospholipid was increased by 140 to 190 per

cent and cholesterol by 70 to 80 per cent (168). In animals which died before 30 days there was no fall in lipid content at 48 hr., in contrast to those which ultimately survived. When a dose of 500 r was given to chick embryos at different stages of development, it produced increased concentrations of the S_f 10 to 30 lipoproteins which were correlated with reduced levels of the S_f 0 to 10 fraction. When 600 r were given on the day of hatching, the increased plasma lipid was shown to be caused by increased phospholipid together with the S_f 0-10 lipoproteins (227).

The interpretation of these results is difficult since the physiological significance of the lipid fractions is still being explored (82) and the radiation effects may be consequential to other changes in fat and carbohydrate metabolism. No alteration in quality or quantity has yet been demonstrated in liver lipids (6, 40, 48, 49, 50, 262) though incorporation of labelled precursors shows changes which seem to depend on the precursor and the conditions of the experiment—whether performed *in vitro* or *in vivo*. For example, the increased conversion of acetate $2-^{14}\text{C}$ into rat liver lipid and CO_2 was not demonstrated after irradiation of liver slices (124). In attempting to define the reasons for the higher incorporation *in vivo*, adrenalectomized, hypophysectomized, or pancreatectomized rats were used and it was again shown that complex interactions of the pituitary-adrenal axis were involved.

Cholesterol metabolism has been attracting some attention following the observation by Gould & Popjak (90) that it is the conversion of acetate to mevalonic acid which is accelerated after irradiation rather than the subsequent condensation of mevalonic acid to cholesterol. Further experiments (89) showed that the increased rate of acetate incorporation was present in rat adrenals. Again the uptake of mevalonic acid into cholesterol was similar in fed control and fasted irradiated animals, emphasizing that the controlling step in the biosynthesis, which is affected by x-radiation, is between acetoacetyl coenzyme A and mevalonic acid. Experiments with combinations of microsomes and supernatant fractions from livers of normal and irradiated rats have led to the suggestion (41) that there is a deficiency other than of the substrate in both fractions from livers of fasting rats. Paoletti, Paoletti & Garattini (203) used $1-^{14}\text{C}$ butyrate, as well as ^{14}C acetate and $2-^{14}\text{C}$ mevalonic acid, as precursors of cholesterol and fatty acid synthesis in *in vitro* experiments with liver slices taken from rats exposed to 3750 r 24 hr. previously. They found that butyrate incorporation, in contradistinction to that of the other acids, was unaltered. Mefferd, Webster & Nyman (177) exposed rats to 500 r TBR and mice to 425 r. ^{14}C acetate was injected at 0, 3, 6, 9, and 15 days after radiation, and in both species the specific activity of the cholesterol was down on the sixth day while that of the fatty acids was increased.

Other specific tissue lipids which have been examined include those of the skin, and a very careful analysis (229) of rabbit skin lipids 24 or 48 hr. after 4000 to 8000 r superficial irradiation failed to show any significant effects on various cholesterol, lecithin, or cephalin fractions.

Some further data have been presented on the formation of lipid peroxides following whole-body radiation (800 r) in rats (23). Homogenates of intestinal mucosa and bone marrow from control animals do not form peroxides when shaken aerobically but do so after the animals have been exposed. Ginzburg and co-workers found evidence for the presence of peroxide in rat spleen after 800, 1000, and 1200 r (86). Decreased ascorbate levels were taken as an indication of peroxide formation. Philpot and colleagues (207) have obtained more direct evidence of peroxide formation in irradiated mice and find that the LD₅₀ of auto-oxidized linoleic acid is only slightly higher than the amount found in mice after exposure to 950 r. They concluded that their results are consistent with the view that radiation toxicity is caused by the initiation of chain auto-oxidation of essential fatty acids producing lethal doses of peroxides in sites not reached by vitamin E. One difficulty, however, in accepting this idea is that they have failed to show similarity in the response of the whole animal to the effects of radiation and organic peroxides (220). The finding of a haemolytic factor, identified as an unsaturated fatty acid, in the livers of rats exposed to 500 and 1000 r, may be relevant in this connection (141). The suggestion of an interaction between peroxides and fatty acids or other compounds is supported by the work of Clubb & Wills (45) who showed that when the sulphhydryl enzyme succinic dehydrogenase was irradiated with 5000 r in the presence of emulsified linoleic acid there was a 66 per cent destruction of the enzyme.

PROTEINS AND PROTEIN METABOLISM

Alterations in the chemical properties of proteins by x-radiation *in vitro* are clearly established, and changes in tissue-protein levels occur, although usually as a consequence of other changes such as the destruction of lymphoid tissue.

The fall in γ -globulins is now well substantiated and has received additional support from the work of Werder, Hardin & Morgan (263) in mice after 300 r. The other serum protein fractions were unaffected. Rodionov and colleagues (219) studied the sulphhydryl content of soluble proteins in spleen and liver in rats after 600 to 700 r using amperometric titrations. They reported an immediate fall in sulphhydryl groups, which was maintained for several days; the extent of the fall was reduced by cysteine. Confirmation and extension of this work would be interesting. Changes in the electrophoretic properties of rabbit lens protein have been reported by Rupe and co-workers (223) but not until after the appearance of cataract.

Studies on protein synthesis using isotopically labelled precursors have confirmed the resistance of this process to x-radiation. Incorporation of ¹⁴C alanine by Yoshida ascites sarcoma cells and by liver homogenates was unaffected by 5000 r (24, 228) and this result was attributed to decreased glycolysis although the incorporation was blocked by 25 kr. Whitmore & Polard (265) have found that infectivity of T₁ phage was more radiosensitive than protein synthesis; their results were compatible with a long thin target

such as the double chain of DNA, which was 2.5μ in length for bacteria infection and 0.97μ for protein synthesis. In rye shoots, Sisakian & Kalacheva (235) found that 5000 r produced an activation in ^{14}C glycine incorporation into protein for the first 4 hr., followed by a return to normal. A dose of 10,000 r caused a fall of 15 to 25 per cent which gradually became more marked. The results were not attributable to alterations in the absorption of the glycine by the shoots.

ENZYMES

Changes in vivo.—Analysis of changes in enzyme activities after irradiation *in vivo* has been closely linked to established disturbances in related biochemical systems. The difficulties of interpretation of enzyme data with respect to cell death, altered cell population, and intracellular changes in distribution of enzymes have been considered elsewhere (201, 250).

Indications of increased protein catabolism leading to enhanced glycogen deposition, aminoaciduria, and creatinuria have already been referred to. Transamination is an essential link between protein and carbohydrate metabolism, and change in transaminase levels has, therefore, been investigated. Milch & Albaum (179) found that the glutamate-oxaloacetate transaminase level in rabbit serum rose after exposure. This has been confirmed in rabbits by Kessler and co-workers (129) and by Brent and colleagues (35). These two groups stress that there is little correlation between the rise in transaminase activity detectable by 5 hr. after radiation, the dose received, and the survival time. Brent *et al.* (35) failed to detect any similar increase in activity in rat serum, but they point out that technical difficulties as a result of the much higher level of enzyme in normal rats preclude observations of small effects and, in addition, there might be a true species difference in response between the animals. They also considered the origin of the increase; and since Brin & McKee had found little effect on transaminase whilst cells were intact (37), they thought it probable that the increase in serum level arose from destruction of radiosensitive cells although the enzyme concentration in such tissues is low. Petersen & Hughes were able to detect increases in both serum glutamate-oxaloacetate and glutamate-pyruvate transaminases within 6 hr. after 800 rads given to rats previously treated with CCl_4 (206).

Decreased levels of DNA after radiation have prompted examination of nucleases and it has been found that DNase II (optimum pH 5.6) in radiosensitive tissues is increased (62, 147). The change has been especially studied in spleen by Okada, Hempelmann, and their associates (193, 194, 195), and Okada has made a thorough study of inactivation of DNase *in vitro* (190, 191, 192). It was shown that the increase in DNase II activity in spleen was evident on a wet-weight basis but not per organ and that both DNase I and DNase II (136, 137) were increased in rat plasma and urine in the first 18 hr. after 350 and 700 r. Because of this rise in plasma level it was difficult to explain the rise in DNase II in spleen (and thymus) by

selective loss of inactive material in organ "pulp" after radiation. A contribution to the plasma DNase II from other sensitive tissues such as intestinal mucosa, which has a high concentration of this enzyme, may be important (201). An actual change in intracellular distribution of the enzyme was indicated from their later work (195); spleens from rats given 756 r 24 hr. before were homogenized, partly in 0.44 M sucrose and partly in distilled water. Normal spleens showed greater activity in water than in sucrose, but after irradiation the difference in activity between these two media was decreased although the total activity per mg. tissue from exposed spleen rose. Goutier-Pirrotte & Thonnard (92) had shown earlier that by 30 min. after 850 r rat spleen DNase II appeared to leak out of mitochondria and there are certain changes in its enzymological characteristics (91). These results have been interpreted (198) as evidence for sensitive structural changes in mitochondria as part of the immediate consequences of exposure [cf. (226)].

Recently Weymouth (264) has made a detailed study of DNase II and two RNases in mouse thymus after radiation. She concluded that the increases in activity found in the three enzymes cannot all be caused by changes in cell population. In rabbit skin, polynucleases, especially RNase, were decreased after 600 and 1200 r (128) but in guinea-pig skin after β -irradiation with 3000 rep there was a rise in RNase by 24 hr. (252). Roth & Eichel (222) have studied the distribution of rat spleen RNase after 700 r. Nuclear mitochondrial and microsomal fractions showed a relative loss in activity compared to that in the supernatant by 16 hr. when the total activity per mg. *N* had risen by 96 per cent. The shift was marked from the nucleus and appreciable from the mitochondria.

Smith & Low-Beer (241) have examined changes in uridylic and cytidylic acid dephosphorylases in rats 24 hr. after 325, 650, or 1300 r. Results were calculated on a wet-weight, dry-weight, and total-organ basis; and in spleen this led to markedly divergent effects. However, it appeared that in this organ uridylic acid dephosphorylase decreased but was increased in liver and pancreas; uridine phosphorylase and cytidylic acid dephosphorylase increased in spleen.

Variations in intestinal cholinesterase have been investigated because of the increase in motility of the gut after radiation, although it is usually believed that the two cannot be directly correlated (47). French & Wall (83) have confirmed that in rats and guinea pigs there is a fall in pseudocholinesterase 48 hr. after 650 and 250 r. In monkey intestine the enzyme was unaffected by 800 r. Lundin, Clemedson & Nelson (167) have shown a fall in pseudocholinesterase in guinea-pig plasma during the first 48 hr. after exposure, and Ponomarenko (209) reported a rise in various tissue cholinesterases in dogs shortly after 500 and 1000 r. Since the levels of pseudocholinesterase in plasma are related to liver changes and, in particular, are lowered by starvation, this response may well be secondary, and the changes in intestinal level may result from other and earlier damage to the cells.

The changes in DNase II already referred to have indicated mito-

chondrial damage; in the case of nuclei, catalase changes have been explained in a similar way. Creasey & Stocken (250) have shown a fall in catalase content of thymus nuclei from rats given 50, 200, or 1000 r 1 hr. previously. Irradiation of thymus nuclei *in vitro* also produced a loss in activity. Although generalized inhibition of catalase after radiation is no longer a tenable hypothesis, the possibility of its inactivation locally within the cell may be significant if intracellular peroxide formation is of any importance. Moreover, whilst the enzyme is apparently inactivated, this is linked with a loss of nuclear RNA, and catalase is known to be associated with RNA in yeast (122). It seems probable, therefore, that the fall in activity may result from dissociation of an essential enzyme-RNA linkage, so that these observations may provide another sensitive biochemical index of nuclear damage.

Irradiation of thymus nucleoprotein *in vitro* produced an increase in phosphatase activity with 0 to 100 r and a fall after 100 to 1000 r (253), and there was a fall in nuclear ATPase after irradiation of mouse Ehrlich ascites tumours *in vivo* (12).

Summarizing enzymological changes after x-radiation, there is still no good evidence that inactivation occurs as a primary biochemical event though it may result very directly from the primary biochemical changes.

Changes in vitro.—Much of the recent work on inactivation of enzymes *in vitro* has been concerned with radiochemical problems, protection, and the O₂ effect rather than with aspects that are immediately applicable to biochemical effects *in vivo*. Such papers will not, therefore, be considered here. Certain findings, however, are rather directly relevant; one is the report by Pihl, Lange & Eldjarn (208) that in their hands the two sulphydryl enzymes, muscle glyceraldehyde-phosphate dehydrogenase and alcohol dehydrogenase, have radiosensitivities *in vitro* such that the ionic yields are 0.02, in line with well-established values for nonsulphydryl enzymes, and are not, as claimed by Barron (13, 14) very much more susceptible with yields of about 1.0. Since inactivation of sulphydryl enzymes *in vivo* has failed to receive substantiation, this evidence of little difference in sensitivity *in vitro* between certain sulphydryl and nonsulphydryl enzymes seems to provide the final blow to the sulphydryl hypothesis of x-radiation damage.

More studies on the inactivation of trypsin *in vitro* have been reported (30, 31, 182) and Hutchinson and his colleagues (119, 120) have analysed the effects on yeast enzymes irradiated in wet and dry states and have calculated (119) that in yeast the average distance which a radical can diffuse is 30 Å if it reacts with large molecules at every encounter and a few hundred Å if the probability of collision is 10^{-3} . This estimate agrees closely with the one obtained by Butler and co-workers (42) from a study on the direct and indirect effects on DNA. They calculated the range of migration of free radicals without significant recombination to be 100 Å in solid DNA and in solutions from 1 per cent concentration upwards.

NUCLEOTIDE METABOLISM

The changes in compounds related to nucleotide metabolism arise partly from cell death and the interference in DNA metabolism and partly from the interference in the generation of ATP. Kritskii (140) followed the ^{14}C glycine incorporation into hypoxanthine in the livers of pigeons exposed to 2000 r. The rate was increased at 30 min. but by six days had fallen to a very low level. At all times there was an inhibition of incorporation into certain acids of the Krebs cycle, but the disturbance of substrates connected with purine biosynthesis was held to be the causative factor. There was no demonstrable effect when the livers were exposed to 80,000 r *in vitro*. A reduced ability to synthesize deoxyribose was found in spleen and kidney of rats exposed to 500 r TBR (174), and only the kidney had recovered by four days. The excretion of purine end-products by rats was proportional to the dose between 150 and 1000 r TBR, and the increase was not abolished by adrenalectomy (121).

It is now well established that whole-body irradiation uncouples oxidation and phosphorylation in mitochondria of spleen and thymus, and further evidence has been provided by van Bekkum (257) who found that, although the amounts were unchanged, the specific activities of ADP and ATP in spleen and thymus of rats at 4 hr. after 700 r TBR were reduced. From experiments with liver homogenates prepared from rats exposed to 650 r 3 hr. previously, Toropova concluded that the oxidative resynthesis of ATP was unaffected (254). Very much higher doses (up to 40,000 r) were used by Yost & Robson (269) who showed that in liver mitochondria *in vitro* oxidative phosphorylation was more sensitive than the cytochrome oxidase system. It is also of interest that UV irradiation of isolated liver mitochondria results in a preferential leakage of nucleotides, and there is no restoration of oxidative phosphorylation if the deficiency is made up from an exogenous source (25). In the Yoshida ascites sarcoma exposed to 25,000 r, a study of the stationary state relationships of ADP, ATP, and inorganic phosphate led Maass *et al.* (169) to the conclusion that the reduction in ATP was a consequence and not a cause of the inhibition of glycolysis.

The doses of radiation used in these experiments contrast sharply with those required to abolish nuclear phosphorylation in the radiosensitive tissues of the rat. One hundred roentgens given either *in vivo* or *in vitro* abolish the formation of labile phosphate, and this response is immediate (52). The general properties of nuclear phosphorylation have been investigated by Osawa, Allfrey & Mirsky (202) but the precise biochemical function of the nucleotides bound to the nucleus is not yet known. Suggestions as to the relation of this system to the synthesis of DNA especially in regard to radiosusceptibility have been discussed by Ord & Stocken (198).

NUCLEIC ACID AND NUCLEOPROTEINS

DNA and RNA.—The emphasis in the investigation of damage to nucleic acids and nucleoproteins has tended to shift from long- to short-term

effects, and more observations are being made of the incorporation of isotopically labelled precursors at various times in the mitotic cycle. These studies should aid in an understanding of the processes leading to nucleic acid synthesis in the cell and the initiating steps of cell division.

In general the recent work on the changes taking place in the content of nucleic acid (21, 26, 27, 44, 126, 161, 164, 173, 181, 255) in different tissues conforms with the earlier evidence showing that DNA is especially affected and that the reduced content is accompanied by a decreased rate of incorporation of isotopically labelled precursors into DNA and sometimes into RNA (107, 152, 197, 218). When a comparative study was made of the incorporation of ^{32}P and ^{14}C adenine into the acid-soluble, RNA, DNA, and lipid fractions of thymus glands from rats exposed 3, 12, 24, and 48 hr. previously to 100 r, Harrington & Lavik (102) found no change in either the acid-soluble or the lipid fractions. At 12 to 24 hr., ^{32}P incorporation into the RNA and DNA was about 60 per cent of the control values whereas in contrast to this the adenine incorporation was unaltered.

An interesting correlation of the changes in rabbit appendix and thymus following exposure to 1000 r total-body x-radiation has been made by Bishop & Davidson (27). The DNA content of appendix was reduced at 1 hr., above normal at 8 hr., and very markedly reduced at 24 hr. On the other hand, no change could be found in thymus. These authors noted an accumulation of deoxyriboside and deoxyribotide material which reached a peak at about 5 to 8 hr. after radiation. They suggested that the excess of DNA precursors and release of mitotic arrest were responsible for the increased amount of DNA present at this time in the appendix.

Chromatographic analysis of the purine and pyrimidine components in rat thymus at 1 hr. after 1000 r TBR showed a considerable increase in deoxycytidine and uridine phosphates (199). This increase, however, does not in thymus seem to lead to an increase in DNA synthesis since the same workers found a depression of about 50 per cent from 3 min. to 2 hr. in the incorporation of ^{32}P into DNA (197). Relevant to this is the observation by Pařízek *et al.* (204) that in the 24 hr. after exposure to low doses (50 to 300 r TBR), rats excrete an increased amount of deoxycytidine without a concomitant increase in thymidine.

Spectrophotometric, electrophoretic, and chemical analyses were used by Hess & Lagg to follow the changes in ribonucleoprotein content of calf and rabbit thymus during a period of 6 to 72 hr. after 200 to 760 r TBR γ -irradiation (109). The data show a progressive decrease both in respect of time and dosage but, on the other hand, when the electrophoretic pattern of extracts obtained from glands exposed *in vitro* to 982 r was compared with control extracts, no difference could be observed. A similar lack of effect on RNA was found by Ord & Stocken (200) who exposed a suspension of respiring thymocytes to 600 to 950 r γ -irradiation *in vitro* and showed that, while the incorporation of ^{32}P into DNA was inhibited, that into RNA was unchanged. These results resemble those found in the livers of animals exposed *in vivo*

where incorporation into DNA is reduced and that into RNA either unaffected or even slightly increased (218, 231). The explanation for the different response of the thymus *in vivo* and *in vitro* may be that the isolation process has damaged the thymocytes or that the secondary changes which take place in the whole animal are not present to influence the RNA metabolism *in vitro*.

More evidence for the difference in sensitivity at different times in the mitotic cycle has come from the work of Nygaard & Guttus (188). These authors irradiated the synchronously dividing slime mould, *Physarum polycephalum*, and after 6000 to 9000 r of x-rays given in interphase there was a more or less constant delay of the subsequent division. Comparison with the effects of irradiation at other times led them to the conclusion that the division process was the period of maximum sensitivity. Quastler & Sherman (214, 232) deduced from an autoradiographic study of ^3H thymidine incorporation into the crypt cells of the small intestine of mice that the G_1 period was about 10 hr., the S period about 7 hr., and the G_2 period about 1 hr. Moderate to heavy doses (800 to 3000 rads) blocked DNA synthesis for about 12 hr., and the period of DNA synthesis which followed was associated with only low levels of thymidine incorporation. There was then a second wave of abnormally high incorporation. When 800 rads were given, some of the cells divided; but with the higher dose there was no mitosis after either wave of DNA synthesis. In the glandular epithelium of the gastrointestinal tract of normal mice, the thymidine label was incorporated to half its maximum level within 10 min. of intraperitoneal injection, but if the mice were given 3000 rads the estimated rate of synthesis was reduced to 50 per cent at 15 min. and to zero at 2 hr. Two hundred rads produced a parallel but more slowly developing inhibition.

Bond, Fliedner & Cronkite (29) found ^3H thymidine uptake *in vitro* in bone marrow taken from dogs at 1 hr. after exposure to 250 r TBR was unchanged and 5000 rads given *in vitro* to human or dog marrow did not affect DNA synthesis greatly. The same authors (78) injected thymidine 30 min. before sacrifice of rats which had received 550 r and examined the marrow at 24, 72, and 168 hr. after radiation. They concluded that DNA synthesis was not markedly impaired in either primitive proliferative cells, the later myelocyte, or erythroid cells, and that the onset of mitosis in precursor cells may be delayed and the process may be imperfect. These results appear to conflict with those obtained by Lajtha *et al.* (153) who used ^{14}C formate labelling as an index of DNA synthesis and found that doses greater than 500 rads did depress synthesis in cells which had started synthesis, and small doses applied in G_1 reduced the number of cells entering S in a given time without affecting the rate of subsequent synthesis.

Beltz, Van Lancker & Potter (21) used ^{14}C orotic acid as a label for DNA synthesis in partially hepatectomized rats. In all cases (375, 750, 1500, and 3000 r at 6 to 12, 12 to 18, 18 to 24, and 24 to 30 hr. after operation) there was marked inhibition of DNA synthesis, but the smallest effect was again obtained when the animals were irradiated during the DNA-synthetic pe-

riod. These results agree with those of Kelly *et al.* (126) who used carbon tetrachloride poisoning instead of surgical hepatectomy.

Tumour cells and tissue culture seem to be gaining in popularity as systems for the study of radiation effects—especially in the nucleic-acid field. Kelly and co-workers (127) have shown that 800 r TBR did not depress ^{32}P incorporation into DNA of ascites cells until one day after exposure. They also showed that the cells continued to grow in size and to synthesize more DNA until they reached the octoploid state where the progress was arrested because mitosis was prevented. Similar results to these have been obtained by Dickson, Paul & Davidson (59) who exposed mouse fibroblasts in tissue culture to 800 r and found no alteration in the incorporation of ^{14}C formate into DNA or RNA up to 24 hr. following radiation. The formation of giant cells has been investigated in yeast by Spoerl & Looney (245, 246) who used x-rays, and by Harper, Pomerat & Kent (101) with 2000 to 4000 r γ -irradiation. In the mammalian system, giant cells were only obtained in the Chang strain of human conjunctiva whereas primary transplants of human conjunctiva, sclera, and iris and of monkey choroid, retina, corneal epithelium, and endothelium did not show this phenomenon. The authors considered that it was the continuous subculturing of cells which was responsible for the different response. There is the further possibility that when the cells have become fully conditioned to glycolysis as an energy source, irradiation fails to arrest DNA synthesis but does prevent mitosis.

Other evidence showing that little or no effect is produced by moderate doses of radiation on incorporation of labelled precursors into DNA of certain tumours has been obtained by Forssberg, Finlayson & Dreyfus (79) who gave adenine 2 min. after exposure of ascitic mice to 350 r and by Smellie *et al.* (236) who prepared a particle-free extract of ascites tumour cells which readily incorporates ^3H thymidine into DNA. This system was also unaffected by 500 r.

Of four ascites tumours examined by Harrington, Rauschkolb & Lavik (104), only incorporation into DNA of the tetraploid Ehrlich tumour was inhibited by 1000 r TBR. When irradiation was carried out *in vitro*, no inhibition of ^{32}P uptake was produced by as much as 10,000 r. It was then found (103) that an inhibition was caused if the ascites cells were allowed to come into contact with irradiated nontumour tissue. This led the authors to suggest that although irradiation may affect the DNA-synthetic process directly, certain secondary effects are also involved. Pertinent to this is the evidence obtained by Smellie, Thomson & Davidson (237) that formate incorporation into the nucleic acid purines of Ehrlich ascites cells *in vitro* is greatly stimulated by the addition of 5-amino-4-imidazolecarboxamide or by a soluble extract of mouse liver. These data would suggest that a dual insult is being offered to the *in vitro* preparation and that the radiation damage cannot be imposed on a system which is operating suboptimally.

If there are difficulties in the understanding of comparatively simple systems such as tissue culture and isolated cell preparations, the interpretation

of the mammalian response is even more uncertain and is not greatly advanced by reiteration of the statement that many of the changes may be the result, rather than the cause, of cell death. Cytological and genetic investigations have established the great radiosensitivity of chromosomes (213, 225); however, there are now a number of biochemical disturbances associated with the nucleus, with which impaired synthesis of DNA may be linked, which can be produced by less than 100 r. It is possible that these changes and those in chromosomes may soon be explicable in terms of a derangement in a single system which manifests its damage in a number of different ways. Light on the nature of this sensitive site is being shed not only from work already mentioned but also by contributions from the study of protection and of the oxygen effect.

Nucleoprotein.—Salganic (224) isolated nuclei from the thymus of calves and puppies exposed to 300 r and showed that incorporation of glycine- ^{14}C into protein was reduced and could be restored by addition of either homologous or heterologous DNA. These results agree with those obtained *in vitro* by Ficq & Errera (77) who used ^{14}C phenylalanine and exposed the isolated nuclei to 950 r x-rays. They noted a progressive loss in ability to incorporate the amino acid; and by 1 hr. there was an inhibition of 50 to 70 per cent which, too, could be partially released by the addition of either RNA or DNA. Harold & Ziporin (100) have also shown that protein synthesis is a prerequisite for resumption of DNA synthesis. Further evidence indicates that in recovery from radiation damage, RNA or protein synthesis is involved at an early stage. Bećarević (18, 19) observed the progress of restoration of catalase activity in yeast and at the same time measured the incorporation of 8^{14}C adenine and ^{14}C formate into RNA. A suitable dose of UV was administered to bring about partial inactivation of catalase activity and various adjuvants were then added to the system. Folic acid was required to restore the formate incorporation into RNA to normal levels, and this took place in the latent period before catalase activity was freely restored.

Previous attempts have failed to show that radiation *in vivo* modified some of the physical properties of DNA isolated fairly soon after exposure (197)⁴ but it has now been found by Vendrely and co-workers (260) that although the DNA content of pycnotic nuclei is unchanged, the nucleohistone is depolymerized. This nucleohistone was isolated by the customary procedures, and its chemical composition was identical with that obtained from nonirradiated animals.

Cole and Ellis (46, 172) studied the changes in mouse spleen after 810 to 850 r TBR. During the first 2 hr. after radiation the total deoxyribonucleoprotein remained constant but by 3 hr. there was a sharp fall which continued for 24 hr. During the 2 to 6-hr. interval there was a marked increase

⁴ Since the above was written, we have separated rat thymus DNA isolated 15 min. after 1000 r TBR by chromatographic analysis on Ecteola columns and have found a shift in the \bar{M}_w distribution of the component peaks.

in free polynucleotide which the authors ascribe to the action of proteases on deoxyribonucleoprotein. They further suggest that the polynucleotide remains intracellular until, as a result of cell lysis, it finds its way into the extracellular phase and is then degraded. Similar results were obtained with bone marrow (73). After 870 r the soluble deoxypolynucleotides reached a maximum value at 2 hr., and when marrow was taken from the rats immediately after radiation and incubated in phosphate buffer there was a steady increase which was greater than that in marrow taken from normal animals.

When ^{14}C formate was incubated *in vitro* with tissues taken after 17 hr. from rats exposed to 5000 r TBR, there was no change in the uptake into nucleoprotein of testes, while there was a decrease in the spleen and an increase in liver (215).

OXYGEN EFFECT

Analysis of the oxygen effect in recent years (69, 111, 268) has been mainly concerned with the physicochemical mechanisms by which death is produced and has lately focussed attention on the part played by organic free radicals, RO_2 , rather than HO_2 . A particularly useful review of physical and chemical mechanisms in the injury of cells by ionizing radiations has been provided by Howard-Flanders (117); and the influence of O_2 on the response to ionizing radiation of cells and tissues, and especially its importance in mammalian systems, has been lucidly and understandably summarized by Gray (93). Attempts are now being made to interpret the O_2 effect at the cellular level and, in particular, within the nucleus. This approach is extremely valuable since it emphasizes the similarities in behaviour of various systems and suggests characteristic properties of the O_2 -sensitive site which are beginning to find their counterparts in observations from other fields.

Ebert and associates (67) have been examining means by which the increased sensitivity in the presence of O_2 may be affected by changing the gaseous environment. Experiments have been carried out with suspensions of mouse Ehrlich ascites tumour cells, bean root tips, and *Shigella flexneri* Y6R, and their radiosensitivity studied in the presence of N_2 , H_2 , A, and other inert gases. The O_2 -dependent radiosensitivity was reduced 54 per cent by 110 atm. H_2 , 38 per cent by 110 atm. N_2 ; and in the presence of 21 atm. A the radiosensitivity was reduced to that normally found under anoxic conditions. Since O_2 utilization, as measured by haemoglobin reduction, was unaffected by the presence of these gases it was reasoned that the reduction in sensitivity did not result from an increased rate of utilization of O_2 . The effectiveness of the gases followed their partition between water and lipid and paralleled their anaesthetic potency. For this reason N_2O was later examined (66) with mouse Ehrlich ascites tumour cells. The radiosensitivity was reduced by 0.8 atm. N_2O in the presence of 0.2 atm. O_2 to the level in N_2 alone, and the authors concluded that the action of these gases might be to displace O_2 from a site, probably containing lipid, within the nucleus or associated with the nuclear membrane.

The biochemical nature of this site is still obscure. Haemoproteins might be implicated, but the existence of such compounds within the nucleus is certainly not proven although an O_2 requirement has been shown in certain synthetic processes occurring in isolated calf thymus nuclei (1). On the other hand, Moustacchi (187) has demonstrated that mutants of two strains of *E. Coli* (*E. Coli* B and *E. Coli* M.L.) in which the respiratory enzymes are either absent or less than 0.0002 of their concentration in the wild type show the same O_2 effects as the normal forms. Similarly, a cytochrome-deficient yeast has the same enhancement ratio as its wild type (93).

A related phenomenon which may throw light on the mechanism of the O_2 effect is that of sensitization, where NO is especially effective (116, 118). Gray and his colleagues (94) have found that Ehrlich ascites cells which were irradiated in the presence of NO and subsequently inoculated into mice showed reduced ability to produce tumours, compared to cells irradiated under anoxic conditions. Care was taken to subject control cells to the presence of NO for the same time as those irradiated, to eliminate any effects caused by toxicity. In four out of five pairs, growth of cells irradiated in NO showed a degree of damage as great as would have been sustained by cells which were aerobic at the time of irradiation. Erythrocytes were removed as completely as possible from the preparation before exposure so that NO was presumably reacting intracellularly.

Kihlman (130, 132), following the earlier work of Lilly and Thoday [cf. (160)], has made a study of the actions of cyanide on bean root tips and its radiosensitizing effect. Complex formation with Fe within the chromosome was offered as a possible explanation, and in a very interesting discussion the necessity for O_2 found for thymus nuclei (1) was correlated with this Fe site. In later work (131) the effects of cyanide, H_2S , and NO on the sensitivity of bean root chromosomes were compared and it was concluded that although NO can combine with cytochrome oxidase, the enhancing effect of this gas on radiation damage is, unlike that produced by H_2S and KCN, consistent with the idea of Howard-Flanders (117) that both O_2 and NO influence radiosensitivity by virtue of their affinity for free organic radicals.

Variations in O_2 effect shown by *E. coli* B have been traced by Alper & Gillies (2, 3) to dialyzable contaminants associated with the two different peptones (Oxoid and Difco) used in the growth media. The surviving fraction was smallest in the medium which was optimal for growth of the irradiated organisms. It was suggested that such factors might account for differences in O_2 -enhancement ratio reported from different laboratories. A deliberate attempt to reduce postradiation growth by incubation on a solid medium containing 5 μ g. chloramphenicol per ml. led to increased survival and was most effective after irradiation under anoxic conditions (85). It was therefore concluded that the enhancing effect of O_2 was exerted mainly on a fraction of the damage not affected by postirradiation conditions. In a rather similar experiment Kimball (133) has reported that streptomycin treatment after radiation reduced the incidence of recessive lethal mutations in para-

medium; the effect was found whether or not O_2 was present during exposure. Proctor (212) has made a detailed study of the effect of environmental conditions on the radiosensitivity of *B. thermoacidurans* spores. Their response was less complicated by external conditions than that of *E. Coli*. Moos, Mason & Nodiot (183) found that *E. Coli* B irradiated at 4° showed greater recovery when grown in liquid culture than when grown on slants.

PROTECTION

Descriptions of miscellaneous substances which can exert protective effects under certain conditions continue to amass. In recent years interest has focussed on three classes of compounds: the cysteine-cysteamine group; the amines, especially epinephrine and histamine; and the isothiuronium derivatives. The two explanations of their effects, reduction in intracellular O_2 tension or combination with free radicals, are still debated but the general view appears to favour anoxia as the main factor (93, 113). Thus, the interpretation of their actions is associated with the analysis of the effects of oxygen on radiosensitivity previously discussed. In the case of the cysteine-cysteamine group an additional factor in their protective action may be the formation of mixed disulphides with essential SH compounds, and more evidence for this hypothesis has been provided by Eldjarn & Pihl (70).

One of the most interesting reports has been that by Künkel and Schubert and their co-workers (143, to 146); they have recently been studying the mortality of dormice (*Glis glis*) exposed when hibernating. As has been reported for other mammals (63), hibernation defers the onset of death, but when the animals are returned to room temperature the usual effects of radiation become manifest, and the animals ultimately show the same mortality as those which were at room temperature during irradiation. Specific changes such as those in serum proteins also occur after return to room temperature. If cysteine is given to the irradiated group 21 days after irradiation when they are returned to ordinary temperature, survival increases and serum proteins, although initially altered, return to normal after a few days. Animals which are given ^{32}P whilst still hibernating show a 50 per cent reduction in incorporation into intestinal DNA, and when the mice go back to room temperature, ^{32}P uptake in unexposed animals rises towards the ordinary values at room temperature after 24 hr. In the irradiated group which received cysteine when returned to the warmth, the rate of ^{32}P uptake was identical to that in the uninjected dormice.

Rather similar experiments were performed with dried beans which were irradiated and then placed in nutrient solutions with and without cysteine; the inhibition of mitosis was then observed. Bull sperm were also exposed at 4° and their motility in suspensions with and without cysteine studied. The effect of cysteine when given some considerable time after exposure at a reduced temperature led the authors to conclude that there might be an unstable state in the cell immediately connected with the primary physical

effect of radiation during which the damage could still be influenced. This labile phase must be of a very short duration since Bacq and Philpot have treated mice within seconds after irradiation (5), but apparently it can be extended by a reduced metabolic level.

It would seem from the results with untreated hibernating dormice that x-radiation damage has been produced comparable to that in ordinary animals. The reduction in intestinal DNA synthesis which is detectable whilst the animal is hibernating recalls the impressions of Hornsey (114) that the intestine was less protected than the bone marrow when ordinary mice were irradiated at a reduced body temperature. The finding of effective cysteine treatment after radiation is potentially of great value but raises several points requiring elucidation. If the protective action of cysteine is attributed ordinarily to anoxia, the possibility of this mechanism obtaining in the experiments described seems remote. Data regarding O_2 tensions at the time of radiation and as a result of cysteine treatment would be most useful. It must also be noted that metabolic pathways in animals ceasing hibernation are changing from predominantly fat catabolism to carbohydrate breakdown, and cysteine may have special effects under these circumstances.

Analyses of the protective effects of the cysteine group at a biochemical level have been pursued by several groups. Hagen (96, 97) found that if cysteamine was administered to rats which were then immediately irradiated, no protective action was detectable on ^{32}P incorporation into regenerating liver if the exposure was during the synthetic period. If, however, the animals were exposed in the presynthetic period a protective effect was clearly apparent. Rather similar results were reported by Henke and co-workers (107) for DNA synthesis in the intestine. Rats were given 800 r, and 24 hr. later ^{32}P was injected intraperitoneally. The specific activity of DNA from untreated irradiated rats was 20 per cent of the control; from rats given cysteine before irradiation the specific activity was 40 per cent of the control, and the same fall in concentration of DNA occurred in the two groups of animals. It would seem that once the final, template stage of DNA synthesis is in progress, large exposures are required to reduce incorporation and it is more difficult to show a protective action of sulphhydryl compounds. Mole & Temple have analyzed the effects of cysteamine on mouse intestinal DNA content; they concluded that cysteamine reduced the initial damage produced by exposure but had no effect on recovery rates (181).

Goutier (91) has investigated changes in spleen DNase II in cysteamine-protected rats. For the first 48 hr. after exposure the activity per mg. *N* rose in a manner parallel to that in untreated rats but then fell again to the level found immediately after exposure. This reduction in activity was correlated with the rise in spleen DNA between 2 and 4 days after radiation also reported in rats given cysteamine.

General protection by cysteamine against irradiation from ^{60}Co was described in mice by Mewissen (178) and against local x-irradiation of the rectum in rats by Darcis & Hotterbeex (54). Davis and colleagues (55), Herve & Brumagne (108), and Wilson (267) found protection against the ef-

fects of β -radiation on rat skin and of x-rays by cysteine and cysteamine respectively. Smith (239) found that cysteine protected bone marrow against 800 r x-rays *in vitro*. Similar protection by cysteine and cysteamine against cutaneous effects of radiation were reported in Rhode Island chicks by Beaumariage (15). With chick fibroblast cultures, Oftedal (189) found that the cysteamine group did not prevent mitotic inhibition after irradiation but cysteamine had some beneficial effect on growth. Since this was not found with cysteine HCl or cysteamine HCl, it did not seem to be attributable to protection as usually described.

Studies on the rather complex responses of phage to irradiation have been continued, and Marcovich (175) has confirmed some of the effects at different stages of T₂ development. Only the extracellular stage and the latent period are modified by cysteamine.

Haley and colleagues (98) have tested the protective action of *dl*-6-8-dithiioctanoic acid to see if a naturally occurring dithiol would be protective as was recently reported for BAL by Doherty *et al.* (60). Although the time of death was delayed, the mice showed the same final mortality to 550 r as untreated animals.

In the analysis of the mode of protection exerted by the amine group—histamine, epinephrine, and the tryptamine derivatives—one of the most significant papers was that presented by van der Meer, van Bekkum & Cohen at Geneva on the production of anoxia as a common factor in epinephrine and histamine treatment (258). They measured the systemic blood pressure and spleen-O₂ tension in mice carefully controlled with respect to weight and sex. In 20 g. CBA mice, histamine is an extremely effective protector; 10 mg. produced 95 per cent survival with 675 r, lowered the blood pressure by 34 mm. Hg, and reduced the spleen-O₂ tension by 93 per cent. Five mg. gave 100 per cent survival, reduced the pressure by 43 mm. and the O₂ tension 77 per cent; and 0.1 mg. gave 5 per cent survival, a 20 mm. fall in blood pressure, and a 43 per cent drop in O₂ tension. Thirty micrograms of epinephrine caused a rise in blood pressure of 45 mm. and a fall in O₂ tension of 89 per cent, maintained for 23 min., whereas the same dose of noradrenaline gave only 5 per cent survival, raised the blood pressure by 40 mm., and caused a 48 per cent reduction in O₂ tension for no more than 8 min. These data were interpreted as strong evidence for the production of anoxia as the common factor in the protective actions of these compounds.

With the radioresistant Rhode Island chicks Beaumariage (16) could not detect any protective action of epinephrine against the lethal effects of 2000 r although Stearner and co-workers (248) had reported such an effect in the more sensitive White Leghorn chicks. Some protection was afforded by both epinephrine and histamine against cutaneous damage in Rhode Island birds (15).

Van der Brenk (32, 33) has been concerned with the roles of endogenous histamine and tryptamine liberation after radiation. Histamine depletion in rats by compound 48/80 reduced the mean survival time after 1000 r from 8.67 ± 4.10 days to 4.91 ± 1.04 days and caused more marked skin lesions

after local irradiation by 4000 r. Histological changes in mast cells produced by 48/80 were not the same as those produced by radiation. These findings argue strongly against the earlier ideas of Ellinger (71) that adverse radiation effects may be explained by the release of histamine. The fall in tissue content of histamine reported by Beaumariage & Lecomte (17) in rabbit skin and lungs 3 hr. after 700 r and the deleterious results of previous reduction in histamine content found by van der Brenk may be related to a physiologically advantageous release of histamine within tissues normally elicited after radiation, although Kiss (134) failed to detect any release of histamine after local exposure of rat skin, using the trypan-blue technique.

Both tryptamine and more particularly 5-hydroxytryptamine have a protective action, and by using antimetabolites of these compounds, for example *d*-lysergic acid diethylamide, van der Brenk & Elliott (34) have shown that in rats given 1000 r, antimetabolites of 5-hydroxytryptamine exerted no effects of their own but reduced the protection afforded by tryptamine and 5-hydroxytryptamine. Reserpine administration immediately before irradiation was slightly protective and the action was enhanced if iproniazid was given 24 hr. previously; if hydroxytryptamine was administered to reserpinized rats its effects were indistinguishable from those in animals not tranquilized. The authors, however, were not certain that all the protective effects which they found, for example that caused by the simultaneous action of reserpine and amine oxidase inhibition, which causes endogenous release of hydroxytryptamine, could be explained by decreased O_2 tension.

Continuing their work on the isothiuronium group, Doherty and his colleagues have studied the effects of the active derivative, 2-mercaptoethylguanidine hydrobromide in mice (256). They have also surveyed the protective actions of compounds structurally related to AET and its propylhomologue APT (61). The effects were assayed in mice. All the compounds intraguanylated similarly to AET and APT, but two types of activity were found. One class of derivatives was comparable to AET and APT in that protection was proportional to the amount administered up to exposures of 1500 r. The other type was effective at very low concentration but their protection could not be extended beyond 1100 r. One compound in this class, S,2-aminobutylisothiuronium bromide hydrobromide, showed stereoisomeric specificity which was traced to selective binding of one isomer at sensitive sites. The action of all the compounds was attributed to the penetration to these sensitive sites so that they were available there for neutralization of free radicals.

The Oak Ridge National Laboratory group also confirmed the protection afforded by AET to mouse bone-marrow cells irradiated *in vitro* (51, 238, 239), and Morkovin & Puck have demonstrated protection by AET of S3HeLa cell cultures. The mean lethal dose was raised from 96 r to 160 r by 0.4 mg./ml. (185).

Although the latest attacks on protection have been mostly along the lines already discussed, results from other methods continue to be reported. Studies on the effects of lowered metabolic rate, which are presumably at-

tributable to anoxia, have been extended. The delay produced by hibernation has already been referred to. Hornsey has given further details of the effects of hypothermia on the sensitivity of mice (115). A slight increase in survival in rabbits and guinea pigs through the chemical production of hypothermia has been reported by Matli (176). Conversely, heightened metabolic rates, resulting from thyroid or thyroxine treatment, have again been shown to increase the mortality (138, 210, 249).

The postradiation increase in DNase prompted Bacq and his colleagues (7, 8, 158) to investigate the effect on radiosensitivity of agents which might complex with Mg^{++} and so lower the concentration of this coenzyme for DNase I (neutral pH). The beneficial effect of several artificial chelating agents had already been described (9) and since citrate itself was ineffective it was decided to investigate the effect on sensitivity to sodium fluoroacetate which produces intracellular citrate accumulation in many tissues. Mice were used and FAc, given 5 or 2 hr. prior to exposure, reduced the mortality. (For 750 to 775 r, 21-day mortality resulted as follows: Controls 94 per cent, FAc-treated 40 per cent.) Citrate accumulation requires 30 to 60 min. before becoming evident, and injection of FAc immediately before or after radiation had no effect. Although these results are consistent with the idea of intracellular cation chelation as a protective factor, the authors point out (8) that serious physiological and biochemical consequences follow FAc poisoning and that other explanations, such as a fall in O_2 tension in the tissues, are possible.

In the course of this work it was observed that the sex difference in amount of citrate accumulated in the liver after FAc administration was reversed in mice compared to rats (64, 65, 196), so that males accumulated more than females (159). Van de Berg (22) also showed that cysteamine was able to reduce the accumulation of citrate in the livers of FAc-treated male rats after radiation, and since the effect was shown with cysteamine given 48 hr. after exposure it was attributed to a pharmacological action, possibly on the circulation.

In the case of yeast, chelation by ethylenediamine tetraacetate increased the radiosusceptibility (10). Autolyzed yeast extracts and RNA have been found by Detre & Finch to protect C3H mice (56), and Luchnik (163, 165) reported that in mice and peas such extracts had a slight curative action, proportional to their RNA content. Investigations into the beneficial effects of properdin and similar agents have been continued (81, 180, 240).

ELECTROLYTE SHIFTS

Possible changes in membrane permeability after exposure continue to be explored but to date alterations are only produced by rather high doses or as a result of actual cell breakdown. Studies on permeability changes of cell fractions with respect to electrolytes are virtually nonexistent; changes resulting in the leakage of enzymes from nuclei or from mitochondria have been referred to previously.

Ellinwood, Wilson & Coon (72) found an increased loss of K^+ from per-

fused rabbit heart irradiated *in vitro* with 500 to 2500 r. Breuer and his colleagues (36) examined the Na^+ , K^+ , Cl^- , and H_2O contents of rat spleen after 500 to 12,000 r TBR. There was a fall in K^+ and a rise in Na^+ , accompanied by tissue dehydration, but very little change in spleen chloride occurred. Heggen and co-workers (106) found marked changes in trace metal levels in rat spleen after 600 r. The increase in total iron confirms earlier reports by Ludewig & Chanutin (166). Kuzin & Ivanitskaia (149) studied the uptake of various radioactive colloids in rats 2, 24, and 48 hr. after 1000 r. In liver, colloid absorption was reduced at 2 hr. and markedly lowered by 48 hr. Increased uptake of $^{32}\text{PO}_4^{3-}$ and $^{131}\text{I}_2$ by rat liver after 800 r was shown by Shtern and colleagues (233). In their experiments it was not possible to remove all the blood from the liver before analysis of the acid-soluble phosphates, but the specific activity of this fraction compared with blood inorganic phosphate was approximately 200 per cent of the control value when the animals were injected intravenously immediately after exposure and killed 1 min. later. By the second and third day the permeability of the liver in irradiated animals declined. The results are similar to those found earlier by Forssberg & Hevesy in mice (80).

By means of a Thiry-Vella loop perfusion technique, which eliminates complications caused by gastric and intestinal motility, Vaughan & Alpen (259) have shown an increased permeability of dog intestine following exposure to 600 r.

In *E. Coli*, K^+ efflux was increased by irradiation; *E. Coli* B was more susceptible in this respect than *E. Coli* B/r (105). In yeast, K^+ loss was less sensitive than survival. Under anaerobic conditions more than 160 kr were required to produce K^+ leakage, with anaerobiosis at 0° , more than 300 kr (39).

SUMMARY

We regret that it has not been possible to include within this review all the recent papers in every field which is contributing to our knowledge of radiation biochemistry. Many aspects of long-term effects were discussed at Geneva and Burlington. Sparrow, Binnington & Bond (243) have published a complete bibliography of the effects of ionizing radiations on plants from 1896 to 1955, and the topic was also considered at a recent symposium (88). Lamerton and his associates (20) have given an account of their recent work on iron metabolism and erythropoiesis.

Perhaps the most interesting advances in the past year or so may be summarized under three headings. (a) There is the suggestion that recovery may be enhanced by postradiation treatment with cysteine. If this is confirmed it reopens the possibility of effective chemical treatment and prompts further examination of the biochemical effects of cysteine, especially in regard to its action on the different aspects of the nuclear lesion. (b) There are now many reports of the importance of cytoplasmic changes on the development of, and the recovery from, cell damage (74a, 150). Furthermore the derangements in fat and carbohydrate metabolism which are evident by 24 hr. are now being clarified in terms of tissue breakdown, where sites in addi-

tion to lymphoid tissue are probably involved. Adrenocortical influences on these changes are also becoming clearer. (c) Our understanding of the differential effects of x-radiation at different periods in the mitotic cycle and of the nature of the nuclear site affected has advanced mainly from the work of Ebert, Howard-Flanders, Kihlman, Lajtha and their colleagues. Unfortunately, at the present time chromosome damage cannot be directly equated to biochemical changes, but by the use of cell cultures and especially of synchronized preparations, some analysis of metabolic differences at different periods in the cell cycle is becoming possible. It is now firmly established (112, 115a, 151) that the period in interphase immediately preceding DNA synthesis is highly radiosensitive. Very recent work by V. R. Potter and his group (personal communication) has indicated that in regenerating liver essential enzymes for DNA synthesis, particularly thymidylate kinase, are made during G₁, and that the genesis of the kinase is radiosensitive. In relation to this discovery it is significant that R. L. Potter & Buettner-Janusch (211) have shown a block in the conversion of thymidine to thymidine nucleotides in rat spleen and thymus at intervals between 0 and 24 hr. after 800 r TBR.

It is to be hoped that a further study of these events and of nuclear phosphorylation will lead to an integration of the processes which set the stage for DNA synthesis. Success here should stimulate a more intensive attack on the biochemistry of the changes which precipitate division and of the mitotic process itself.

LITERATURE CITED

1. Allfrey, V. G., Mirsky, A. E., and Osawa, S., *J. Gen. Physiol.*, **40**, 451 (1957)
2. Alper, T., and Gillies, N. E., *Nature*, **181**, 961 (1958)
3. Alper, T., and Gillies, N. E., *J. Gen. Microbiol.*, **18**, 461 (1958)
4. Anderson, D. R., Joseph, B. J., Krise, G. M., and Williams, C. M., *Am. J. Physiol.*, **192**, 247 (1958)
5. Bacq, Z. M. (Personal communication)
6. Bacq, Z. M., Burg, C., Chevallier, A., and Heusghem, C., *J. physiol.*, **43**, 640 (1951)
7. Bacq, Z. M., Fischer, P., Herve, A., Liébecq, C., and Liébecq-Hutter, S., *Nature*, **182**, 175 (1958)
8. Bacq, Z. M., Fischer, P., and Herve, A., *Arch. intern. physiol.*, **66**, 75 (1958)
9. Bacq, Z. M., Herve, A., and Fischer, P., *Bull. acad. roy. méd. Belg.*, **18**, 226 (1953)
10. Bair, W. J., and Hungate, F. P., *Science*, **127**, 813 (1958)
11. Baker, D. G., and Hunter, C. G., *Radiation Research*, **9**, 660 (1958)
12. Bankowski, Z., and Vorbrodt, A., *Bull. acad. polon. sci., Ser. sci. biol.*, **5**, 245 (1957)
13. Barron, E. S. G., *U. S. Atomic Energy Commission Document*, AECD-2316 (1946)
14. Barron, E. S. G., Dickman, S., Muntz, J. A., and Singer, T. P., *J. Gen. Physiol.*, **32**, 537 (1948)
15. Beaumariage, M. L., *Le Sang*, **29**, 298 (1958)
16. Beaumariage, M. L., *Nature*, **182**, 803 (1958)
17. Beaumariage, M. L., and Lecomte, J., *Compt. rend. soc. biol.*, **151**, 1976 (1957)

18. Bečarević, A., *Biochim. et Biophys. Acta*, **25**, 299 (1957)
19. Bečarević, A., *Biochim. et Biophys. Acta*, **25**, 646 (1957)
20. Belcher, E. H., Harris, E. B., and Lamerton, L. F., *Brit. J. Haematol.*, **4**, 390 (1958)
21. Beltz, R. E., Van Lancker, J., and Potter, V. R., *Cancer Research*, **17**, 688 (1957)
22. van de Berg, A., *Arch. intern. physiol.*, **66**, 318 (1958)
23. Bernheim, F., Barber, A. A., Ottolenghi, A., and Wilbur, K. M., *Radiation Research*, **9**, 91 (1958)
24. Bettendorf, G., and Maass, H., *Strahlentherapie*, **106**, 263 (1958)
25. Beyer, R. E., and Kennison, R. D., *Biochim. et Biophys. Acta*, **28**, 432 (1958)
26. Biagnini, C., Gueritore, D., and Bellelli, L., *Radiation Research*, **9**, 92 (1958)
27. Bishop, C. W., and Davidson, J. N., *Brit. J. Radiol.*, **30**, 367 (1957)
28. Blokhin, N. N., Luganova, I. S., and Rotfel'd, L. S., *Intern. Abstr. Biol. Sci.*, **11**, 223 (1958)
29. Bond, V. P., Fliedner, T. M., and Cronkite, E. P., *Radiation Research*, **9**, 93 (1958)
30. de Bornier, B. M., *Compt. rend.*, **246**, 1081 (1958)
31. de Bornier, B. M., *Compt. rend.*, **246**, 2166 (1958)
32. van den Brenk, H. A. S., *Nature*, **180**, 1467 (1957)
33. van den Brenk, H. A. S., *Brit. J. Exptl. Pathol.*, **39**, 356 (1958)
34. van den Brenk, H. A. S., and Elliott, K., *Nature*, **182**, 1506 (1958)
35. Brent, R. L., McLaughlin, M. M., and Stabile, J. N., *Radiation Research*, **9**, 24 (1958)
36. Breuer, H., Knuppen, R., and Parchwitz, H. K., *Z. Naturforsch.*, **13b**, 741 (1958)
37. Brin, M., and McKee, R. W., *Arch. Biochem. Biophys.*, **61**, 384 (1956)
38. Brooks, P. M., Richey, E. O., and Pickering, J. E., *Radiation Research*, **6**, 430 (1957)
39. Bruce, A. K., *J. Gen. Physiol.*, **41**, 693 (1958)
40. Buchanan, D. J., Darby, W. J., Bridgforth, E. B., Hudson, G. W., and Efner, J. A., *Am. J. Physiol.*, **174**, 336 (1953)
41. Bucher, N. L. R., Loud, A. V., and McGarrahan, K., *Federation Proc.*, **16**, 17 (1957)
42. Butler, J. A. V., Pain, R. H., Robins, A. B., and Rotblat, J., *Proc. Roy. Soc. (London)*, **B149**, 12 (1958)
43. Caster, W. O., and Armstrong, W. D., *Proc. Soc. Exptl. Biol. Med.*, **91**, 126 (1956)
44. Caster, W. O., Redgate, E. S., and Armstrong, W. D., *Radiation Research*, **8**, 92 (1958)
45. Clubb, M. E., and Wills, E. D., *Biochem. J.*, **71**, 16P (1959)
46. Cole, L. J., and Ellis, M. E., *Radiation Research*, **7**, 508 (1957)
47. Conard, R. A., *Am. J. Physiol.*, **165**, 375 (1951)
48. Coniglio, J. G., Darby, W. J., Efner, J. A., Fleming, J., and Hudson, G. W., *Am. J. Physiol.*, **184**, 113 (1956)
49. Coniglio, J. G., Darby, W. J., Wilkerson, M. C., Stewart, R., Stockwell, A., and Hudson, G. W., *Am. J. Physiol.*, **172**, 86 (1953)
50. Cornatzer, W. E., Davison, J. P., Engelstad, O. D., and Simonson, C., *Radiation Research*, **1**, 546 (1954)
51. Cosgrove, G. E., Upton, A. C., Congdon, C. C., Doherty, D. G., Kimball, A. W., and Hollaender, A. H., *Radiation Research*, **9**, 103 (1958)

52. Creasey, W. A., and Stocken, L. A., *Biochem. J.*, **69**, 17P (1958)
53. Cronkite, E. P., and Bond, V. P., *Ann. Rev. Physiol.*, **18**, 483 (1956)
54. Darcis, L., and Hotterbeex, P., *Experientia*, **14**, 18 (1958)
55. Davis, A. K., Cranmore, D., and Alpen, E. L., *Radiation Research*, **9**, 222 (1958)
56. Detre, K. D., and Finch, S. C., *Science*, **128**, 656 (1958)
57. Detrick, L. E., Upham, H. C., Highby, D., Debley, V., and Haley, T. J., *Radiation Research*, **2**, 483 (1955)
58. Dickson, H. M., *Am. J. Physiol.*, **182**, 477 (1955)
59. Dickson, M., Paul, J., and Davidson, J. N., *Biochem. J.*, **70**, 18P (1958)
60. Doherty, D. G., Burnett, W. T., and Shapira, R., *Radiation Research*, **7**, 13 (1957)
61. Doherty, D. G., and Shapira, R., *Radiation Research*, **9**, 107 (1958)
62. Douglass, C. D., and Day, P. L., *Proc. Soc. Exptl. Biol. Med.*, **89**, 616 (1955)
63. Doull, J., and Dubois, K. P., *Proc. Soc. Exptl. Biol. Med.*, **84**, 367 (1953)
64. Dubois, K. P., Cochran, K. W., and Doull, J., *Proc. Soc. Exptl. Biol. Med.*, **76**, 422 (1951)
65. Dubois, K. P., Cochran, K. W., and Zerwic, M. M., *Proc. Soc. Exptl. Biol. Med.*, **78**, 452 (1951)
66. Ebert, M., and Hornsey, S., *Nature*, **182**, 1240 (1958)
67. Ebert, M., Hornsey, S., and Howard, A., *Nature*, **181**, 613 (1958)
68. Ebina, T., and Kurosu, M., *J. Natl. Cancer Inst.*, **20**, 1023 (1958)
69. Eidus, L. C., Kondakowa, N. W., and Otarowa, G. K., *Sowjetwissenschaft Naturwissenschaftliche Beitr.*, **10**, 1051 (1958)
70. Eldjarn, L., and Pihl, A., *Radiation Research*, **9**, 110 (1958)
71. Ellinger, F., *Schweiz. med. Wochschr.*, **81**, 61 (1951)
72. Ellinwood, L. E., Wilson, J. E., and Coon, J. M., *Proc. Soc. Exptl. Biol. Med.*, **94**, 129 (1957)
73. Ellis, M. E., and Cole, L. J., *Federation Proc.*, **17**, 366 (1958)
74. Errera, M., *Protoplasmatologia. Handbuch der Protoplasmaforschung*, 1-241 (Springer-Verlag, Vienna, Austria, 241 pp., 1957)
- 74a. Errera, M., Ficq, A., Logan, R., Skreb, Y. and Vanderhaeghe, F., *Proc. Intern. Conf. Peaceful Uses Atomic Energy, Geneva, 1958*, 15/P/1695 (1958)
75. Farrar, J. T., Small, M. D., Bullard, D., and Ingelfinger, F. J., *Am. J. Physiol.*, **186**, 549 (1956)
76. Federova, T. A., and Larina, M. A., *Intern. Abstr. Biol. Sci.*, **9**, 253 (1958)
77. Ficq, A., and Errera, M., *Exptl. Cell Research*, **14**, 182 (1958)
78. Fliedner, T. M., Cronkite, E. P., and Bond, V. P., *Radiation Research*, **9**, 114 (1958)
79. Forssberg, A., Finlayson, J. S., and Dreyfus, G., *Biochim. et Biophys. Acta*, **30**, 258 (1958)
80. Forssberg, A., and Hevesy, G., *Arkiv Kemi.*, **5**, 93 (1953)
81. Forssberg, A., Lingen, C., Ernster, L., and Lindberg, O., *Exptl. Cell Research*, **16**, 7 (1959)
82. Fredrickson, D. S., and Gordon, R. S., *Physiol. Revs.*, **38**, 585 (1958)
83. French, A. B., and Wall, P. E., *Am. J. Physiol.*, **188**, 76 (1957)
84. Fritz-Niggli, H., *Naturwissenschaften*, **45**, 557 (1958)
85. Gillies, N. E., and Alper, T., *Nature*, **183**, 237 (1959)
86. Ginzburg, M. B., Pandre, E. M., and Binus, N. M., *Biokhimiya*, **22**, 467 (1957)
87. Goodman, R. D., Lewis, A. E., and Schuck, E. A., *Am. J. Physiol.*, **169**, 242 (1952)

88. Gordon, S. A., *Quart. Rev. Biol.*, **32**, 3 (1957)
89. Gould, R. G., Bell, V. L., Lilly, E. G., and Popjak, G., *Radiation Research*, **9**, 121 (1958)
90. Gould, R. G., and Popjak, G., *Biochem. J.*, **66**, 51P (1957)
91. Goutier, R., *Radiation Research*, **9**, 122 (1958)
92. Goutier-Pirotte, M., and Thonnard, A., *Biochim. et Biophys. Acta*, **22**, 396 (1956)
93. Gray, L. H., 1957-58, *Lectures on the Scientific Basis of Medicine* (The Athlone Press, University of London, London, Engl., in press)
94. Gray, L. H., Green, F. O., and Hawes, C. A., *Nature*, **182**, 952 (1958)
95. Haberland, G. L., Schreier, K., Altman, K. I., and Hempelmann, L. H., *Biochim. et Biophys. Acta*, **25**, 237 (1957)
96. Hagen, U., *Radiation Research*, **9**, 125 (1958)
97. Hagen, U., and Ernst, H., *Proc. Intern. Conf. Peaceful Uses Atomic Energy, Geneva, 1958*, 15/P/991 (1958)
98. Haley, T. J., Flesher, A. M., and Komesu, N., *Nature*, **181**, 1405 (1958)
99. Hanel, H. K., Hjort, G., and Purser, P. R., *Acta. Radiol.*, **49**, 401 (1958)
100. Harold, F. M., and Ziporin, Z. Z., *Biochim. et Biophys. Acta*, **29**, 439 (1958)
101. Harper, J. Y., Jr., Pomerat, C. M., and Kent, S. P., *Z. Zellforsch. u. Mikroskop. Anat.*, **47**, 392 (1958)
102. Harrington, H., and Lavik, P. S., *Federation Proc.*, **16**, 192 (1957)
103. Harrington, H., and Lavik, P. S., *Cancer Research*, **17**, 38 (1957)
104. Harrington, H., Rauschkolb, D., and Lavik, P. S., *Cancer Research*, **17**, 34 (1957)
105. Harrison, A. P., Jr., Bruce, A. K., and Stapleton, G. E., *Proc. Soc. Exptl. Biol. Med.*, **98**, 740 (1958)
106. Heggen, G. E., Olson, K. B., Edwards, C. F., Clark, L. B., and Maisel, M., *Radiation Research*, **9**, 285 (1958)
107. Henke, H., Maass, H., and Schubert, G., *Strahlentherapie*, **106**, 253 (1958)
108. Herve, A., and Brumagne, J., *Experientia*, **14**, 12 (1958)
109. Hess, E. L., and Lagg, S. E., *Radiation Research*, **9**, 260 (1958)
110. Hill, R., Kiyasu, J., and Chaikoff, I. L., *Am. J. Physiol.*, **187**, 417 (1956)
111. Holmes, B. E., *Ann. Rev. Nuclear Sci.*, **7**, 89 (1957)
112. Holmes, B. E., and Mee, L. K., *Radiobiology Symposium, Liège, 1954*, 220 (Butterworth & Company, Ltd., London, Engl., 362 pp., 1955)
113. Hope, D. B., *Biochem. Soc. Symposium on Glutathione* (In preparation)
114. Hornsey, S., *Advances in Radiobiology*, 248 (Oliver & Boyd, Ltd., Edinburgh, Scotland, and London, Engl., 503 pp., 1957)
115. Hornsey, S., *Proc. Roy. Soc. (London)*, **B147**, 547 (1957)
- 115a. Howard, A., and Pelc, S. R., *Heredity Suppl.*, **6**, 261 (1953)
116. Howard-Flanders, P., *Nature*, **180**, 1191 (1957)
117. Howard-Flanders, P., *Advances in Biol. and Med. Phys.*, **6** (In press, 1958)
118. Howard-Flanders, P., and Jockey, P., *Radiation Research*, **9**, 131 (1958)
119. Hutchinson, F., *Radiation Research*, **7**, 473 (1957)
120. Hutchinson, F., Preston, A., and Vogel, B., *Radiation Research*, **7**, 465 (1957)
121. Jackson, K. L., and Entenman, C., *Proc. Soc. Exptl. Biol. Med.*, **97**, 184 (1958)
122. Kaplan, J. G., and Paik, W. K., *J. Gen. Physiol.*, **40**, 147 (1957)
123. Kay, R. E., Early, J. C., and Entenman, C., *Radiation Research*, **6**, 98 (1957)
124. Kay, R. E., Warner, W. L., and Entenman, C., *Radiation Research*, **9**, 137 (1958)
125. Kelly, L. S., *Progr. in Biophys. and Biophys. Chem.*, **8**, 144 (1957)

126. Kelly, L. S., Hirsch, J. D., Beach, G., and Palmer, W., *Cancer Research*, **17**, 117 (1957)
127. Kelly, L. S., Hirsch, J. D., Beach, G., and Petrakis, N. L., *Proc. Soc. Exptl. Biol. Med.*, **94**, 83 (1957)
128. Kerova, N. I., *Intern. Abstr. Biol. Sci.*, **9**, 253 (1958)
129. Kessler, G., Hermel, M. B., and Gershon-Cohen, J., *Proc. Soc. Exptl. Biol. Med.*, **98**, 201 (1958)
130. Kihlman, B. A., *J. Biophys. Biochem. Cytol.*, **3**, 363 (1957)
131. Kihlman, B. A., *Exptl. Cell Research*, **14**, 639 (1958)
132. Kihlman, B. A., Merz, T., and Swanson, C. P., *J. Biophys. Biochem. Cytol.*, **3**, 381 (1957)
133. Kimball, R. F., *Radiation Research*, **9**, 138 (1958)
134. Kiss, J., *Strahlentherapie*, **104**, 624 (1957)
135. Kit, S., and Awapara, J., *Cancer Research*, **13**, 694 (1953)
136. Kowlessar, O. D., Altman, K. I., and Hempelmann, L. H., *Arch. Biochem. Biophys.*, **52**, 362 (1954)
137. Kowlessar, O. D., Altman, K. I., and Hempelmann, L. H., *Arch. Biochem. Biophys.*, **54**, 355 (1955)
138. Krahe, M., and Kunkel, H. A., *Strahlentherapie*, **106**, 260 (1958)
139. Krise, G. M., Williams, C. M., and Anderson, D. R., *Proc. Soc. Exptl. Biol. Med.*, **95**, 764 (1957)
140. Kritskii, G. A., *Biokhymia* (English Transl.), **21**, 80 (1956)
141. Kudriashov, Iu. B., *Doklady Akad. Nauk S.S.S.R.*, **109**, 515 (1956)
142. Kumta, U. S., Gurnani, S. U., and Sanasrabudhe, M. B., *Experientia*, **13**, 372 (1957)
143. Kunkel, H. A., *Strahlentherapie, Sonderbande*, **38**, 17 (1958)
144. Kunkel, H. A., and Heckmann, U., *Strahlentherapie*, **106**, 256 (1958)
145. Kunkel, H. A., and Schubert, G., *Proc. Intern. Conf. Peaceful Uses Atomic Energy, Geneva, 1958*, 15/P/993 (1958)
146. Kunkel, H. A., and Schubert, G., *Radiation Research*, **9**, 141 (1958)
147. Kurnick, N. B., Massey, B. W., and Sandeen, G., *Radiation Research*, **9**, 141 (1958)
148. Kuzin, A. M., *Atompraxis*, **4**, 203 (1958)
149. Kuzin, A. M., and Ivanitskaia, E. A., *Biophysics*, **2**, 311 (1957)
150. Kuzin, A. M., and Schabadasch, A. L., *Proc. Intern. Conf. Peaceful Uses Atomic Energy, Geneva, 1958*, 15/P/2319 (1958)
151. Lajtha, L. G., Oliver, R., Berry, R., and Noyes, W. D., *Nature*, **182**, 1787 (1958)
152. Lajtha, L. G., Oliver, R., and Ellis, F., *Advances in Radiobiology*, **54** (Oliver & Boyd, Ltd., Edinburgh, Scotland, and London, Engl., 503 pp., 1957)
153. Lajtha, L. G., Oliver, R., Kumatori, T., and Ellis, F., *Radiation Research*, **8**, 1 (1958)
154. Lauenstein, K., Haberland, G. L., Hempelmann, L. H., and Altman, K. I., *Biochim. et Biophys. Acta*, **26**, 421 (1957)
155. Lebedinsky, A. V., *Proc. Intern. Conf. Peaceful Uses Atomic Energy, Geneva, 1958*, 15/P/2531 (1958)
156. Lelievre, P., *Compt. rend. soc. biol.*, **151**, 412 (1957)
157. Lelievre, P., *Compt. rend. soc. biol.*, **151**, 631 (1957)
158. Liébecq, C., and Liébecq-Hutter, S., *Arch. intern. physiol.*, **66**, 77 (1958)
159. Liébecq, C., and Liébecq-Hutter, S., *Experientia*, **14**, 216 (1958)

160. Lilly, L. J., *Exptl. Cell Research*, **14**, 257 (1958)
161. Lipkan, M. F., *Fiziol. Zhur. Akad. Nauk Ukr. R.S.R.*, **2**, 86 (1956)
162. Lowe, C. W., Rand, R. N., and Venkataraman, P. R., *Proc. Soc. Exptl. Biol. Med.*, **98**, 696 (1958)
163. Luchnik, N. V., *Biokhymia* (English Transl.), **21**, 139 (1956)
164. Luchnik, N. V., *Biokhymia* (English Transl.), **21**, 689 (1956)
165. Luchnik, N. V., *Biokhymia*, **23**, 146 (1958)
166. Ludewig, S., and Chanutin, A., *Am. J. Physiol.*, **166**, 384 (1951)
167. Lundin, J., Clemedson, C. J., and Nelson, A., *Acta Radiol.*, **48**, 52 (1957)
168. di Luzio, N. R., and Simon, K. A., *Radiation Research*, **7**, 79 (1957)
169. Maass, H., Hohne, G., Kunkel, H. A., and Rathgen, G. H., *Z. Naturforsch.*, **12b**, 553 (1957)
170. Maass, H., and Rathgen, G. H., *Strahlentherapie*, **103**, 668 (1957)
171. Maass, H., Rathgen, G. H., Kunkel, H. A., and Schubert, G., *Z. Naturforsch.*, **13b**, 735 (1958)
172. Main, R. K., Cole, L. J., and Ellis, M. E., *Nature*, **180**, 1285 (1957)
173. Mandel, P., Gros, C. M., Rodesch, J., Jaudel, C., and Chambon, P., *Advances in Radiobiology*, 59 (Oliver & Boyd, Ltd., Edinburgh, Scotland, and London, Engl., 503 pp., 1957)
174. Manoilov, S. E., Nemchinskaya, V. L., Alieva, A. Z., and Mytareva, L. V., *Biokhymia*, **22**, 1013 (1957)
175. Marcovich, H., *Radiation Research*, **9**, 149 (1958)
176. Matli, G., *Strahlentherapie*, **106**, 304 (1958)
177. Mefferd, R. B., Webster, W. W., and Nyman, M. A., *Radiation Research*, **8**, 461 (1958)
178. Mewissen, D. J., *Acta. Radiol.*, **48**, 141 (1957)
179. Milch, L. J., and Albaum, H. G., *Proc. Soc. Exptl. Biol. Med.*, **93**, 595 (1956)
180. Miya, F., Marcus, S., and Thorpe, B. D., *Proc. Soc. Exptl. Biol. Med.*, **99**, 757 (1958)
181. Mole, R. H., and Temple, D. M., *Nature*, **180**, 1278 (1957)
182. Monier, R., *Biochim. et Biophys. Acta*, **29**, 345 (1958)
183. Moos, W. S., Mason, H. C., and Nodiot, H., *Am. J. Roentgenol., Radium Therapy Nuclear Med.*, **80**, 122 (1958)
184. Morehouse, M. G., and Searcy, R. L., *Federation Proc.*, **16**, 223 (1957)
185. Morkovin, D., and Puck, T. T., *Radiation Research*, **9**, 155 (1958)
186. Moss, W. T., *Am. J. Roentgenol., Radium Therapy Nuclear Med.*, **78**, 850 (1957)
187. Moustacchi, E., *Ann. inst. Pasteur*, **94**, 89 (1958)
188. Nygaard, O. F., and Guttes, S., *Radiation Research*, **9**, 161 (1958)
189. Oftedal, P., *Nature*, **181**, 344 (1958)
190. Okada, S., *Arch. Biochem. Biophys.*, **67**, 95 (1957)
191. Okada, S., *Arch. Biochem. Biophys.*, **67**, 102 (1957)
192. Okada, S., *Arch. Biochem. Biophys.*, **67**, 113 (1957)
193. Okada, S., Gordon, E. R., King, R., and Hempelmann, L. H., *Arch. Biochem. Biophys.*, **70**, 469 (1957)
194. Okada, S., and Peachey, L. D., *J. Biophys. Biochem. Cytol.*, **3**, 239 (1957)
195. Okada, S., Schlegel, B., and Hempelmann, L. H., *Biochim. et Biophys. Acta*, **28**, 209 (1958)
196. Ord, M. G., and Stocken, L. A., *Proc. Soc. Exptl. Biol. Med.*, **83**, 695 (1953)
197. Ord, M. G., and Stocken, L. A., *Advances in Radiobiology*, 65 (Oliver & Boyd, Ltd., Edinburgh, Scotland, and London, Engl., 503 pp., 1957)

198. Ord, M. G., and Stocken, L. A., *Nature*, **182**, 1787 (1958)
199. Ord, M. G., and Stocken, L. A., *Biochim. et Biophys. Acta*, **29**, 201 (1958)
200. Ord, M. G., and Stocken, L. A., *Biochem. J.*, **68**, 410 (1958)
201. Ord, M. G., and Stocken, L. A., *Mechanisms in Radiobiology* (Academic Press, Inc., New York, N. Y., in preparation, 1959)
202. Osawa, S., Allfrey, V. G., and Mirsky, A. E., *J. Gen. Physiol.*, **40**, 491 (1957)
203. Paoletti, R., Paoletti, P., and Garattini, S., *Biochem. J.*, **71**, 4P (1959)
204. Pafizek, J., Arient, M., Dienstbier, Z., Škoda, J., *Nature*, **182**, 721 (1958)
205. Pentz, E. I., *J. Biol. Chem.*, **231**, 165 (1958)
206. Petersen, D. F., and Hughes, L. B., *Radiation Research*, **9**, 166 (1958)
207. Philpot, J. St. L., Horgan, V. J., Porter, B. W., and Roodyn, D. B., *Biochem. J.*, **67**, 551 (1957)
208. Pihl, A., Lange, R., and Eldjarn, L., *Nature*, **182**, 1732 (1958)
209. Ponomarenko, N. E., *Intern. Abstr. Biol. Sci.*, **11**, 224 (1958)
210. Pospíšil, M., and Novák, L., *Nature*, **182**, 1603 (1958)
211. Potter, R. L., and Buettner-Janusch, V., *Radiation Research*, **9**, 168 (1958)
212. Proctor, B. E., *Radiation Research*, **8**, 51 (1958)
213. Puck, T. T., Morkovin, D., Marcus, P. I., and Cieciora, S. J., *J. Exptl. Med.*, **106**, 485 (1957)
214. Quastler, H., and Sherman, F. G., *Radiation Research*, **9**, 169 (1958)
215. Rappaport, D. A., Siebert, R. A., and Collins, V. P., *Radiation Research*, **6**, 148 (1957)
216. Rathgen, G. H., and Maass, H., *Strahlentherapie*, **106**, 266 (1958)
217. Rathgen, G. H., Ullman, G., and Gerke, W., *Naturwissenschaften*, **45**, 423 (1958)
218. Richmond, J. E., Ord, M. G., and Stocken, L. A., *Biochem. J.*, **66**, 123 (1957)
219. Rodionov, V. M., Kedrova, E. M., and Marchenko, G. I., *Biokhymia*, **23**, 689 (1958)
220. Roodyn, D. B., and Philpot, J. St. L., *Radiation Research*, **9**, 172 (1958)
221. Rosenfield, G., *Am. J. Physiol.*, **192**, 232 (1958)
222. Roth, J. S., and Eichel, H. J., *Radiation Research*, **9**, 173 (1958)
223. Rupe, C. O., Monsul, R. W., and Koenig, V. L., *Radiation Research*, **8**, 265 (1958)
224. Salganic, R. I., *Biokhymia*, **23**, 377 (1958)
225. Sax, K., *Quart. Rev. Biol.*, **32**, 15 (1957)
226. Scherer, E., and Vogell, W., *Strahlentherapie*, **106**, 202 (1958)
227. Schjeide, O. A., Ragan, N., and Simons, S., *Radiation Research*, **9**, 327 (1958)
228. Schubert, G., Bettendorf, G., Kunkel, H. A., Maass, H., and Rathgen, G. H., *Strahlentherapie*, **106**, 483 (1958)
229. Schwarz, H. P., Dreisbach, L., and Kleschick, A., *Proc. Soc. Exptl. Biol. Med.*, **97**, 581 (1958)
230. Seelich, F., Pantlitschko, M., and Zakovsky, J., *Naturwissenschaften*, **44**, 586 (1957)
231. Sherman, F. G., and Almeida, A. B., *Advances in Radiobiology*, 49 (Oliver & Boyd, Ltd., Edinburgh, Scotland, and London, Engl., 503 pp., 1957)
232. Sherman, F. G., and Quastler, H., *Radiation Research*, **9**, 182 (1958)
233. Shtern, L. S., Rapoport, C. Ia., Gromakovskaia, M. M., and Zubkova, S. R., *Biophysics*, **2**, 188 (1957)
234. Silk, M. H., Hawtrey, A. O., and Macintosh, I. J. C., *Cancer Research*, **18**, 1257 (1958)

235. Sisakian, N. M., and Kalacheva, V. Y., *Biophysics*, **2**, 471 (1957)
236. Smellie, R. M. S., McArdle, A. H., Keir, H. M., and Davidson, J. N., *Biochem. J.*, **69**, 37P (1958)
237. Smellie, R. M. S., Thomson, R. Y., and Davidson, J. N., *Biochim. et Biophys. Acta.*, **29**, 59 (1958)
238. Smith, L. H., *Exptl. Cell Research*, **13**, 627 (1957)
239. Smith, L. H., *Radiation Research*, **9**, 185 (1958)
240. Smith, W. W., Alderman, I. M., and Gillespie, R. E., *Am. J. Physiol.*, **192**, 549 (1958)
241. Smith, K. C., and Low-Beer, B. V. A., *Radiation Research*, **6**, 521 (1957)
242. Snezhko, A. D., *Biophysics*, **2**, 70 (1957)
243. Sparrow, A. H., Binnington, J. P., and Bond, V. P., *Brookhaven Natl. Lab. Rept.*, No. 504 (BNL, L-103) (1958)
244. Spear, F. G., *Brit. J. Radiol.*, **31**, 114 (1958)
245. Spoerl, E., and Looney, D., *J. Bacteriol.*, **76**, 63 (1958)
246. Spoerl, E., and Looney, D., *J. Bacteriol.*, **76**, 70 (1958)
247. Steadman, L. T., and Grimaldi, A. J., *Univ. Rochester Rept.*, **205**, No. 6 (1952)
248. Stearner, S. P., Christian, E. J., and Brues, A. M., *Am. J. Physiol.*, **176**, 455 (1954)
249. Stein, J. A., and Griem, M. L., *Nature*, **182**, 1681 (1958)
250. Stocken, L. A., *Radiation Research*, Suppl. **1**, 53 (1959)
251. Szonyi, S., and Várterész, W., *Nature*, **179**, 51 (1957)
252. Tabachnick, J., and Weiss, J., *Radiation Research*, **9**, 281 (1958)
253. Tongur, V. S., Golubeva, N. P., Diskina, L. S., Spitkovskii, D. M., and Filipova, G. V., *Biophysics*, **2**, 461 (1957)
254. Toropova, G. P., *Doklady Akad. Nauk, S.S.S.R.*, **117**, 266 (1957)
255. Turovskii, V. C., *Intern. Abstr. Biol. Sci.*, **11**, 49 (1958)
256. Urso, P., Congdon, C. C., Doherty, D. G., and Shapira, R., *Blood*, **13**, 665 (1958)
257. van Bekkum, D. W., *Biochim. et Biophys. Acta*, **25**, 487 (1957)
258. Van der Meer, C., van Bekkum, D. W., and Cohen, J. A., *Proc. Intern. Conf. Peaceful Uses Atomic Energy, Geneva, 1958*, 15/P/556 (1958)
259. Vaughan, B. E., and Alpen, E. L., *Radiation Research*, **9**, 198 (1958)
260. Vendrely, R., Alfert, M., Matsudaira, H., and Knoblock, A., *Exptl. Cell Research*, **14**, 295 (1958)
261. Warburg, O., Schröder, W., Gewitz, H. S., and Völker, W., *Naturwissenschaften*, **45**, 192 (1958)
- 261a. Warburg, O., Schröder, W., Gewitz, H. S., and Völker, W., *Z. Naturforsch.*, **13b**, 591 (1958)
262. Weinman, E. O., Lerner, S. R., and Entenman, C., *Arch. Biochem. Biophys.*, **64**, 164 (1956)
263. Werder, A. A., Hardin, C. A., and Morgan, P., *Radiation Research*, **7**, 500 (1957)
264. Weymouth, P. P., *Radiation Research*, **8**, 307 (1958)
265. Whitmore, G., and Pollard, E. C., *Radiation Research*, **8**, 392 (1958)
266. Williams, C. M., Krise, G. M., Anderson, D. R., and Dowben, R. M., *Radiation Research*, **7**, 176 (1957)
267. Wilson, C. W., *Brit. J. Radiol.*, **31**, 100 (1958)
268. Wood, T. H., *Ann. Rev. Nuclear Sci.*, **8**, 343 (1958)
269. Yost, H. T., Jr., and Robson, H. H., *Biol. Bull.*, **113**, 198 (1957)
270. Zhorno, L. Ia., *Intern. Abstr. Biol. Sci.*, **10**, 41 (1958)

CELLULAR RADIOBIOLOGY^{1,2}

By K. C. ATWOOD

Department of Obstetrics and Gynecology, University of Chicago, Chicago, Illinois

This review is confined, where possible, to publications in 1958, and covers a range that is frankly eclectic. Such treatment seems appropriate for a field in which experiments with widely divergent objectives are unified only by the frequently irrelevant circumstance that they employ ionizing or ultraviolet radiations. As to the limitations implied in the term "cellular," experiments involving intact metazoans or chemical systems are mentioned where they seem to invite conjecture about events at the cellular level of organization. Some areas that will from time to time warrant separate reviews are omitted, such as the chromosomal cytology of induced neoplasms and irradiated mammalian cells in culture [e.g., Ford *et al.* (3); Puck (4)], whereas many omissions must be attributed to oversight.

In 1958 a new periodical was founded: *The International Journal of Radiation Biology*, edited by W. M. Dale and a distinguished board (5). The first International Congress of Radiation Research was held at Burlington, Vermont, in August, and its proceedings appeared as a supplement to *Radiation Research*. Books include *Radiation Biology and Medicine*, edited by Walter Claus (6); *Proceedings of the Second Conference on the Peaceful Uses of Atomic Energy* [reviewed by Loutit (7)], published by the United Nations Organization; *Report of the Scientific Committee on the Effects of Atomic Radiation* (8); and a volume on organic peroxides in radiobiology (9). Jagger (10) presents a penetrating review of photoreactivation, and Strauss (11) an illuminating discussion of the effects of transmutation of a radioisotope on the parent biomolecule.

RADIATION DAMAGE TO BIOMOLECULES

Nucleic acids—Paramagnetic resonance studies of irradiated nucleic acids and their constituents are reported by Gordy (12). Resonance patterns of DNA and RNA differ from those of their constituent nucleotides in being more sharply peaked and lacking a fine structure. The widely spaced patterns of deoxyguanosine and thymidine are conspicuously absent. It is Gordy's conjecture that the odd electron produced by ionization of the nucleic acids migrates from one ring side group to another. As a result of breakage in the chain, electrons may be trapped in isolated segments, in which migration into different ring groups cancels out the hyperfine structure. It is pointed

¹ The survey of literature pertaining to this review was concluded January 1, 1959.

² Among the abbreviations used in this chapter are: EDTA (ethylenediamine-tetra-acetic acid); kvp (kilovolts peak); LET (linear energy transfer); RBE (relative biological effectiveness); and UV (ultraviolet).

out that according to this hypothesis the unbroken nucleic acid chains are photoconductors.

The biological activity of DNA irradiated *in vitro* can at present be assayed only by virtue of its ability to effect bacterial transformations. Latarjet *et al.* (13) obtained soft x-ray inactivation curves of pneumococcus-transforming DNA with experimental refinements designed to eliminate indirect effect: a combination of freezing, 10 per cent yeast extract, and catalase. They point out that radicals in ice are sufficiently diffusible to form peroxides down to -100°C . and that reactions held in abeyance will in any case proceed upon thawing. It is therefore a mistake to assume that protective agents in the frozen state act solely on the direct effect. It is probably equally erroneous to assume with the present authors that the molecular environment is without influence on the direct effect. The inactivation curve shows at least two exponential components, the more sensitive of which is thought to represent hits outside the marker that hinder its incorporation into the bacterial genome, whereas the resistant component is inactivation of the marker itself. The respective molecular weights are 2.8×10^6 and 7×10^4 ; thus the size of the streptomycin resistance marker is placed between 1 and 2 per cent of the total DNA fiber [cf. Guild & DeFilippes, 1957 (14)].

Spin resonance in proteins.—Electron spin-resonance patterns of irradiated proteins have provided a new basis for the interpretation of radiation damage to proteins and for one of the types of oxygen effects. Gordy & Shields (15), in summarizing their investigations of irradiated proteins, point out the surprising feature that two pattern types predominate almost to the exclusion of all others: (a) a polyglycine doublet; (b) a field-dependent pattern of cysteine or cystine. In irradiated peptides and amino acids a large variety of other patterns is seen (16,17). The breakage of bonds within the protein may provide traps of the two characteristic types into which unpaired electrons have migrated from their site of formation. This implies that the breakage itself is produced on arrival of the migratory electron at a cystine or glycylglycine in the peptide chain. Orientation effects were seen in fibres such as silk and feathers. The patterns are surprisingly long-lived *in vacuo*, with variable but short lifetimes in the presence of oxygen. The extent to which the observed patterns represent a selection of long-lived configurations and to which other, transitory patterns are produced in solution where different mechanisms of radiation damage can occur remains to be seen. According to Blumenfeld & Kalmanson (18) denatured albumin traps many more electrons, as evidenced by greater amplitude of the diglycine doublet, than the native protein.

Dry systems.—Evidence has continued to accumulate that the modification of the primary mechanisms of radiation damage can be brought about in nonfluid systems by agencies similar to those that are effective in aqueous systems. Alexander & Toms (19) have used solid polymethyl methacrylate as a model system in which to study the protective effects of incorporated adjunctives on the fracture of the main polymer chain. They were able to con-

clude that energy must be transferred from the polymer to the protector and that the protective process is not mainly by means of interposition of the protector at the breakpoints. Aromatic compounds were generally able to protect in this system, whereas among the aliphatics only unsaturated or sulfhydryl compounds were protective. Braams *et al.* (20) have shown that the radiation sensitivity of dried enzymes to 40-Mev alphas is dependent on the manner of preparation. Cysteine or glutathione added to the solution from which the enzyme is dried will reduce the sensitivity to about one-half, while salt or acetate buffer may double the sensitivity. The quantities used were one to ten times that of enzyme.

The gamma sensitivity of a dry enzyme—and hence its apparent molecular weight by target theory—is shown by Sosa-Bourdouil *et al.* (21) to be somewhat dependent on the substrate with which it is assayed. Almond emulsin, a B-glycosidase, showed variations from mol. wt. 35,000 to 68,000 for hydrolysis of different glucosides. Synthetic activities gave values in the same range (22). The UV absorption peak of almond emulsin at 275 m μ was increased after 3.9×10^7 r. Infrared absorption, however, was unaltered.

Paramagnetic resonance studies with adjunctive agents in the solid state reveal that oxygen can transform the polyglycine doublet into a field-dependent pattern thought to arise from organic peroxide radicals. The field-dependent pattern attributed to cystine is quenched by oxygen. These observations suggest that enhancing agents such as oxygen may often act to modify direct alterations of biologically significant molecules. Carbonyl groups seem to protect compounds from this oxygen effect, and cysteinelike compounds may absorb some of the direct damage to proteins (15). The oxygen-dependent decay of irradiated nucleic acid resonance is very slow (12). Comparisons of the effects of adjunctives on resonance parameters with their effects on biological activities *in vivo* may, as Zimmer (23) points out, provide clues to the biomolecules involved—even though it is hardly possible that the biologically significant hits can contribute detectably to the signal. Ehrenberg & Ehrenberg (24) have progressed in this direction through studies on decay of signal amplitude in grass seeds of different water content. The radicals remaining after the initial rapid decay were decreased with decreasing water content, and the growth-inhibiting effect of the x-irradiation was proportional to the remaining radical concentration.

Irradiation of solutions.—Monier (25) shows that x-ray sensitizes dilute trypsin to reversible denaturation by urea. The sensitization itself, however, is not reversible. It is understandable that the breakage of one or two covalent bonds within the protein molecule could potentiate the later disruption of hydrogen bonds; sensitization should also result from irradiation in the dry state. Magnan de Bornier (26) determined the Michaelis-Menton constant for dilute trypsin solutions given 20,000 r of 90 kv. x-rays. It is significantly increased, showing a decreased affinity of enzyme for substrate. The decrease in over-all activity at this dose is slight; hence the alteration

of Michaelis-Menton constant may be largely independent of enzyme inactivation. A very interesting specific protection of tyrosinase by substrates is reported by Yost *et al.* (27). The enzyme activity on *p*-cresol or catechol is preferentially spared when the test substrate is present during gamma irradiation. The dose-effect curves for indirect trypsin inactivation show a more resistant minor component (28). This was interpreted to mean that the inactivated trypsin is a better protective agent than active or unirradiated trypsin. This hypothesis is reasonable because the denatured trypsin may act as a specific substrate for the intact enzyme, but direct experimental test of the possibility by means of mixtures was not made. It is also possible that the oxygen content of the solution may have been lowered after sufficient dose, the molecular population may have been initially heterogeneous, or partially inactivated molecules may be intrinsically more resistant because of exhaustion of the more sensitive sites, or of a target diminution resembling that proposed for DNA (13). Jayko & Garrison (29) measured protein carbonyl groups by the criterion of 2,4-dinitrophenylhydrazine retention on dialysis. They conclude that conversion of hydroxyl to carbonyl groups is one of the main effects of deuterium-beryllium neutron irradiation. The foregoing experiments concur in suggesting that subregions of the molecule may be mutually independent in the inactivation process.

Brinkman & Lamberts (30) have noted that 500 r of x-rays cause an immediate drop of 20 per cent in the viscosity of synovial fluid, suggesting the fragmentation of very long molecules (e.g., hyaluronic acid). The intradermal injection pressure is also immediately decreased, undoubtedly for the same reason. Rothschild *et al.* (31) decomposed ferriprotoporphyrin by gamma irradiation in dilute solution. The process is indistinguishable from oxidation with hydrogen peroxide or dilute permanganate.

Ultraviolet effects.—The discrepancy between the biological dose range and that in which degradation of typical biomolecules becomes obvious is even greater for UV than for ionizing radiations. Papers continue to be published dealing with effects of extremely large doses of UV on various organic materials. Larin (32) has observed that extremely large doses of 2537 Å UV destroy the electrophoretic pattern of human serum, changing it to a broad homogeneous peak. Hvidberg *et al.* (33) exposed K-hyaluronate solution to polychromatic UV from a high-pressure mercury lamp at 95 ergs/mm.²/sec. for 120 min. It showed a viscosity drop comparable to that produced by hyaluronidase. The high dose required here is in contrast to the sensitivity of synovial fluid viscosity to ionizing radiation. It is interesting that chondroitin sulfate remains unaffected. Serum oxidase, on the other hand, was found by Aprison (34) to be much more sensitive to UV than to x-ray. The decrease in enzyme activity of this copper-containing protein (ceruloplasmin) was directly correlated with the amount of copper removed, the normal copper content being 8 atoms/mol. with a mol. wt. of 151,000. The inactivation by UV is exponential, but it is not certain whether a molecule loses the copper atoms one at a time while retaining partial activity corresponding to the

residual number, or whether a denatured molecule loses all of its copper atoms at once.

THE OXYGEN EFFECT

The influence of oxygen on the end result of irradiation is complex; at least four components can tentatively be distinguished through the use of different experimental criteria: (a) oxygen-dependent production of reactive substances from water and low-molecular-weight solutes; (b) very short-lived O_2 -sensitive damages to biomolecules; (c) long-lived O_2 -sensitive damages, and (d) the dependence of repair processes on aerobic metabolism. As an example of (a), Adler (35) observes an aftereffect of irradiated medium on hemin-negative strain H_7 of *E. coli*. The effect is caused by hydrogen peroxide, and the absence of catalase in this strain is a necessary although not sufficient condition. Interestingly, the cells are not sensitive to H_2O_2 unless they have been irradiated. That the classical oxygen effect is probably quite independent of diffusible peroxides or aerobic metabolism is shown by Moustacchi (36) in a comparison of hemin-deficient *E. coli* and yeast mutants with the corresponding normal strains: no difference in O_2 effect is seen despite the absence of catalase. The possible role of HO_2 radicals and other reactive products whose yields are influenced by oxygen tension has been extensively discussed in previous reviews. Wood (37) has summarized the evidence against the HO_2 radical as mediator of the oxygen effect.

Very short-lived O_2 -sensitive damages have been discovered in *Shigella flexneri* by Howard-Flanders & Moore (38) with the aid of an ingenious device for rapid change of gaseous environment before or after irradiation. Within 10 msec. following a 7 msec. irradiation with 1.2-Mev electrons, the oxygen-sensitive lesion had disappeared. It is pointed out that none of the known features of the oxygen effect—in particular the relation of radiosensitivity to O_2 concentration (39) and to nitric oxide (40)—is inconsistent with the notion that a carbon radical in a large molecule is the typical O_2 -sensitive lesion. If this is so, the mean lifetime of the radical is estimated to be about 10^{-4} sec. without oxygen and 10^{-6} sec. in air.

A new appreciation of the uniformity of this aspect of the oxygen effect in different situations had been presaged by Howard-Flanders & Alper (41) when they found that the relation of O_2 concentration to radiosensitivity in *S. flexneri* is described by

$$\frac{S}{S_N} = \frac{K + m[O_2]}{K + [O_2]}$$

where S is the sensitivity at the concentration $[O_2]$, S_N the anoxic sensitivity, m the ratio of maximum to minimum sensitivities, and K the O_2 concentration at which the radiosensitivity is halfway between its minimum and maximum. This relation had been obscured in many instances by differences between the externally measured O_2 tension and that prevailing near the sites of damage. Kihlman (42) reveals the true relation between O_2 tension

and x-ray sensitivity of chromosomes in *Vicia* roots by use of the respiratory inhibitor cupferron (ammonium nitrosophenylhydroxylamine) to eliminate O_2 gradients. In the presence of inhibitor the constant K is greatly decreased so that the O_2 saturation curve for radiosensitivity is like that of *S. flexneri*. The maximum sensitivity is significantly increased by cupferron—an unexplained radiomimetic action probably similar to the cyanide effect studied in the same material by Lilly (43); cf. Kihlman, 1957 (1b); Kihlman, Merz & Swanson, 1957 (1c). Cyanide is radiomimetic only in the presence of oxygen and is a radiation enhancer only in its absence. Kirby-Smith & Dolphin (44) have encountered a rather peculiar O_2 -dependent intensity effect in the production of chromosome aberrations in *Tradescantia* microspores by 14-Mev electrons. When 400-rad doses were delivered in times varying from 100 to 10^{-6} sec., the aberration frequency decreased with decreasing time in air but not in N_2 . No significant change occurred in times below 5 sec. Preliminary experiments in high O_2 tension favor the hypothesis that a partial temporary anoxia is produced by a short irradiation. The oxygen tension in a sealed system would not, of course, be appreciably changed by 400 rads, unless already extremely low. But it is possible that if the lifetime of the O_2 -sensitive damage is short and diffusion is impeded, then a transitory local depletion in oxygen might result at high intensities. The time relations are somewhat different from those in Howard-Flanders & Moore's (38) experiments, but perhaps these differences can be accommodated. An exceptional aqueous system in which O_2 sensitivity is rather stable has been reported by Eidus *et al.* (45): the ATPase activity of myosin x-irradiated in anoxic solution further decreases when oxygen is admitted several hours later. Ebert *et al.* (46) have found that the O_2 effect on *Vicia* roots and ascites tumor cells is prevented by some gases under pressure. These include H_2 , N_2 , the noble gases, and the inert compounds N_2O (47) and cyclopropane. The mode of action is not yet worked out; the authors suggest that the adsorbed gas may render the site inaccessible to oxygen.

The oxygen effect is seen in dry systems; for example, Tallentire (48) reports it in dry *B. subtilis* spores [cf. Laser, 1956 (49)]. The influence of moisture content on sensitivity of barley seeds to x-rays is shown by Curtis *et al.* (50) to be entirely an aftereffect, with development of the major portion of the damage in the first 4 hr. (Curiously, the chlorophyll sector mutations did not show any aftereffect.) Adams & Nilan (51) find seeds with 8 per cent moisture to be O_2 -sensitive during this period following x-irradiation. Decay of spin resonance during the same period is reported (24). The question arises of whether the long-lived O_2 -sensitive damage in seeds of low water content can be identified with the short-lived damage in fully hydrated systems. Both types of O_2 sensitivity disappear with high LET. The usual absence of the long-lived O_2 sensitivity in wet systems and the ability of water to terminate immediately the sensitive period in dry systems suggest that water is the competitor of oxygen for the reactive radical. Howard-Flanders & Moore (38) present evidence that oxygen takes part in a com-

petitive reaction and point out that the hypothetical carbon radical formed by disruption of a C—H bond can be restored to its original state by obtaining a hydrogen ion and an electron, or a hydrogen atom. Under most conditions these are too scarce to compete effectively with oxygen; if they did, the oxygen effect would be strongly dependent on intensity—contrary to experience. If water is the competitor, the restoration of fixed carbon radicals would produce diffusible OH radicals, a distinct gain since many of these will terminate in harmless reactions. Finally, it is a matter of conjecture whether the breakage of chromosomes by O_2 alone, without radiation, reported by Conger & Fairchild (52) has some mechanism in common with the delayed oxygen enhancement of radiation injury; both require low moisture content.

The distinction between chromosome breakage and radiation-induced delay of chromosome rejoining became clear in 1954 (53). Subsequently Wolff & Luippold (54) showed that rejoining in *Vicia* requires aerobic metabolism, and is CO sensitive in *Tradescantia* (55). Anoxic suppression of rejoining between divided doses or at low intensities can therefore maintain the yield of two-break chromosome aberrations at the single acute dose level. Cohn (56) has studied CO inhibition of chromosome rejoining in onion root tips (from germinated seed). Fast and slowly rejoining components were detected, requiring 5 to 18 min. and 4 hr. respectively. Both components were inhibited by CO. It is not certain whether they can be identified with the fast and slow rejoining reported by Wolff & Luippold (1d), who attributed their fast (*ca.* 1 min.) component to ionic bonds; if so it negates the ionic bond hypothesis as Cohn (1e) previously pointed out. Recovery from heat sensitization of *Dahlbominus* (194) (discussed in another section) is CO sensitive. Doubtless, other O_2 -dependent postirradiation recovery processes will be discovered when new criteria are applied.

MICROBIAL SURVIVAL AND MUTATION

An outstanding compendium of the yeast work is provided by the symposium on this subject held at the International Congress of Radiation Research, comprising an introduction by Tobias (57), papers by Wood (37), Magni (58), Rothstein (59), and Beam (60), with invited discussion by James (61) and Mortimer (62). Wood's paper deals with primary mechanisms of radiation damage as evidenced by the influence of modifying agents on the radiosensitivity of haploid yeast. Rothstein discusses postirradiation biochemical changes; most interesting are the comparative sensitivities of the same substances inside and outside the cell, showing that the cell provides an extremely protective environment. Like these two papers, Magni's review of the genetic aspects of radiosensitivity in yeast and Beam's analysis of the role of divisional stage and metabolic history of the cell cannot be briefly summarized, but in company with Mortimer's (63) most recent paper on ploidy series they suggest a few general remarks.

The yeast case differs from others mainly in having a more complete

array of experiments designed to identify the prevailing causes of lethality. The high resistance of isolable biochemical functions and the dependence on ploidy implicate some sorts of damages to the genetic apparatus, but the precise nature of these is still far from clear. The paired-recessive lethal-defect hypothesis has dominated thinking in this field for the past decade, although it has been clearly untenable for the greater part of that time. The theoretical expression for survival according to this hypothesis was first given by Luria & Dulbecco in 1949 (64) as a model for the survival of phage-host multicomplexes in the hope of obtaining estimates of the number of genetic sites per phage. The expression was derived by Atwood & Norman (65) in the same year and its applicability to ploidy series explicitly stated. Tobias in 1952 arrived independently at the same model, which subsequently became so firmly entrenched as to be accepted without question by Wood (1a) as appropriate for a diploid organism whose haploid analogue has exponential survival. Yeast survival curves, however, do not usually give a precise fit to the model, and not even an approximate fit can be obtained for more than two ploidies at a time. The manner in which typical survival curves deviate from the model is in assuming a constant slope much sooner than the model would predict. Interestingly, it was this feature of the survival curves that finally led Dulbecco (66) to reject the model for the phage multicomplex case. It should be emphasized that the constant slope referred to is not necessarily the ultimate slope, since at very high doses unrelated processes of much higher multiplicity will supervene, as suggested by Beam (60) for the resistant stages in *Hansenula*.

Some years ago, Kimball applied his curve-fitting method (1f) to Pomper's extensive unpublished data on yeasts of different ploidies and found the recessive lethal parameter (i.e. the paired-site number) indistinguishable from unity in every case. This means that the multiplicity of the survival curve is of the same order as the ploidy, although the exact correspondence suggested by Lucke & Sarachek (67) is by no means general, and disagrees—for unknown reasons—with Mortimer's (63) data. The finding of multiplicity equal to the ploidy, although valid in specific cases, does not simplify the interpretation. Contrary to popular belief, no plausible model based on chromosomal injury has yet been proposed that predicts survival-curve multiplicity equal to the ploidy. The reason for the discrepancy between the foregoing results with Kimball's method and the *ca.* 30 paired sites estimated by others from similar curves is simple: Kimball's method estimates all three parameters from the same curve, whereas others have relied on the sensitivity parameter obtained from the haploid. If the model were correct in detail, both procedures would give the same results. Mortimer (63) finds a progressive increase in sensitivity from diploid to hexaploid, suggesting a dominant lethal process. The rather close proportionality of the LD_{10} to the reciprocal of the ploidy, however, must be regarded as fortuitous because the LD_{10} has no simple relation to any real parameter of the survival curves, which are differently shaped. Dominant and recessive lethal mutations can be

estimated in various ways: for example, by survival of the zygotes when one partner has been irradiated, and by the viability of the ascospores formed from such zygotes. Magni (58) shows that the results of such experiments do not account quantitatively for the lethal effect in terms of recessive and dominant lethal mutations. The picture is further complicated by the fact that the survival of polyploids is sometimes dependent on the manner in which they originate; that is, whether by fusion of haploids or by intrastain diploidization (63). In at least one instance (58) a single gene is in control of survival-curve shape changes during meiosis and sporulation. The failure to account for lethality in genetic experiments reveals a new component of the damage that is neither dominant nor recessive lethal mutation. Although situated in the genetic apparatus and subject to complementation by an undamaged chromosome set, this lesion is nonheritable. Other organisms do not necessarily resemble yeast in the relation of their ploidy to survival kinetics. Sparrow (68, 69) points to cases in the higher plants where radiation resistance continues to increase with ploidy. A ploidy series obtained in *Bombyx* by Tul'tseva & Astaurov (70) showed increased radiation resistance from diploid to tetraploid in some developmental stages, but in late larval stages the tetraploid seemed not as resistant as the diploid.

Woese (71) compares several spore-forming bacilli with respect to radiations of different LET. Survival curves of *B. subtilis*, *brevis*, and *mesentericus* are exponential whereas *B. cereus*, *mycoides*, and two strains of *megatherium* are multitarget. The same relation between cross-section parameter (for *B. megatherium*) and LET is obtained as previously reported by Donellan & Morowitz (1g) for *B. subtilis*. Woese suggests that some members of the genus *Bacillus* contain duplicate genetic material, whereas those that show exponential curves do not. Proctor *et al.* (72) report exponential survival of the spores of *Bacillus thermoacidurans* with Co^{60} gammas and 3-Mev cathode rays. Old spores seem to be more sensitive than young. Minimal changes were seen with oxygen, nitrogen, freezing, pH, ascorbate, and tomato juice content of the medium. Schwinghamer (73) has obtained survival curves for the urediospores of the phytopathogenic fungi *Melampsora lini*, the flax rust, and three *Puccinia* species, the wheat stem, oat stem, and oat crown rusts. Since these forms are not cultivable (past germination) *in vitro*, the lesion count on host plant seedlings was the criterion of viability. With ionizing radiation the ability to germinate on agar is much more resistant than the ability to infect the plant, germination remaining essentially 100 per cent until over 300 kr. With UV, x-ray, gamma, fast neutrons, and thermal neutrons the survival curves were essentially of the same form, showing a multiplicity of four for *Melampsora* and two for *Puccinia*. The urediospores are exactly binucleate and ostensibly haploid, although it is not known whether the chromosomes have already divided in the resting spore. With gamma and x-rays a second process of much higher multiplicity was seen above 80 kr. The *Puccinia* spores were about twice as resistant as *Melampsora* to ionizing radiations and 10 times as resistant to UV. Dryness usually enhances the

effect of UV (74), but in these spores exactly the reverse was found. Gafford (75) presents an analysis of Co^{60} gamma survival of uninucleate and multinucleate *Neurospora* conidia. The survival curves suggest that two different inactivation processes are taking place in hydrated spores, but only one of these in dry spores. Zelle *et al.* (76) find similar action spectra for UV mutation to streptomycin independence in *E. coli* SD-4 and purine independence in strain 82/r. The maxima are at the usual 2650 Å position. The action spectrum of mutation closely parallels that of inactivation of colony-forming ability, but a greater proportion of the mutagenic effect than of the lethal effect is photoreactivable in SD-4. The kinetics of photoreactivation were the same for inactivation and mutation, and the photoreactivable fractions were the same for all wavelengths tested from 2378 to 2967 Å, a finding not common to all systems (4). In SD-4 the number of surviving cells plated has no influence on the apparent number of mutants per survivor. In 82/r, however, the apparent number of mutants per survivor is greater when fewer cells are plated. This indicates that mutation on the plates plays a significant role in 82/r. Matney *et al.* (77) have studied the production of streptomycin-resistant or -dependent mutants in strain B/r by noncidal doses of UV. The bacteria were irradiated while on membrane filters at 2×10^8 cells per membrane. With a dose of 4 ergs/mm.², approximately 100 mutants per membrane were produced. Although this dose is noncidal for B/r, it kills 99 per cent of strain B cells. The growth period required for expression of the maximum number of mutants with noncidal doses was much shorter than with higher doses showing that the UV-induced lag in this system is independent of the mutations being scored [cf. Ryan and his co-workers (78, 79)]. Photoreactivation was possible for only a very short time.

Mutations to prototrophy in *E. coli* requiring arginine, methionine, or threonine were studied at very low x-ray doses by Demerec (80). Detection of reverse mutants was feasible at proportions of 10^{-11} . Spontaneous rates per 10^{10} were 10.8 in arginine-13; 15.6 in methionine-3; 2.3 in threonine-1. The doubling doses were 68 r, 98 r, and 85 r respectively. Lowest dose used was 8.5 r, highest 4750 r, with no evidence of a threshold. This paper confirms the fact that natural radiation accounts for only a small fraction of the spontaneous mutation rate. A complex locus in yeast-controlling induction of melizitase has been studied by Lindegren & Pittman (81). Seven alleles are known, differing in range of substrates capable of acting as inducers of the enzyme. Five of the alleles were obtained by UV irradiation of the wild type and all of these except the completely noninducible one showed spontaneous back-mutation on selective substrates. This noninducible allele was reverted by x-ray, however, but always in a single step without the production of intermediate alleles. Some x-ray-induced adenine-3B mutants of *Neurospora* are shown by de Serres (82) to be reversible by x-rays. The stable mutants in this series were characterized by abnormal linkage relations.

Alper & Gillies (83) report a variety of experiments that suggest to them that recovery following UV or ionizing radiations occurs on a medium sub-

optimal for growth. The addition of salt or peptone to the medium decreased the survival of strain B (but not of B/r, strain 86, *S. flexneri* and K12m-); and low pH increased survival. In contrast to the radiation effect, the survival vs. holding time at 52°C. showed no medium differential. The conclusion that recovery occurs under conditions suboptimal for growth seems wanting in generality, many exceptions having been found. Bair & Hungate (84) have noted a potentiation by EDTA (3×10^{-4} molar) of the growth-delaying effect of plutonium (0.5 mc./ml.) in liquid yeast cultures. EDTA alone was without effect and in the presence of EDTA less plutonium was found in cells than in the control cultures. The delaying effect of tritium added as T_2O at 90 mc./ml. was also potentiated by EDTA, but no effect of EDTA with single doses of external radiation could be shown. The addition of calcium did not counteract the EDTA effect. It seems possible, however, that other chelatable ions are involved and that some time is required to deplete the cell of the influential metals.

STATISTICAL MICROSCOPY

Statistical microscopy is the more general and descriptive term for target theory; it connotes the uses of radiation by which the size, number, shape, and intracellular location of functional microsystems may be deduced. Classical target theory did not include the counting of targets, but only the estimation of their physical dimensions. Following the early sensitive volume concept (e.g., Timofeef-Ressovsky; Zimmer), and the elaborate development of methods in this area by Lea, the discipline sank into temporary eclipse largely because the discovery of various ways of modifying radiation effects seemed to undermine its basic assumptions. Actually such new knowledge will, when properly taken into account, augment rather than impair the usefulness of radiation in revealing the organization of the living cell. A successful restatement of the theory seems imminent.

The vigorous recrudescence mounted by Pollard and his associates has continued in 1958 using LET dependence and electron penetration range. Analysis of the Newcastle disease virus has been extended with such methods by Wilson & Pollard (85). Newcastle disease virus was irradiated while dry and assayed for survival on monolayers of chick embryo fibroblasts. Electrons below 1 kv. gave no inactivation irrespective of dose, and this permits the conclusion that an insensitive outer coat of the virus is 230 Å thick. The cross section to 10-Mev protons and 4.3-Mev deuterons defines an inner sensitive region which, if spherical, is 560 Å in diameter. A larger cross section is presented, however, to 8.2-Mev alphas: 1020 Å diameter, if spherical. Secondary ionizations produced by delta rays perpendicular to the track were regarded as insufficient to explain the effect. The authors conjecture that multiple simultaneous ionization in the insensitive coat may result in the transfer of energy to the sensitive centers. Since the effect is observed with alphas yielding only 12 primary ionizations per 100 Å of track, the energy-transfer hypothesis might be put to experimental test by means of

low-voltage electron beams of high intensity that would create the same simultaneous ionization density in the external coat without reaching the sensitive center. Although the highest dose of nonpenetrant electrons used in the present experiment was about $2 \times 10^{11}/\text{cm}^2$, or about 16 electrons per Newcastle-disease-virus particle, the intensity was far from sufficient to mimic the alpha effect. It is estimated by the method of Woese & Pollard (1954) (86) that eight simultaneous ionizations in the insensitive coat are required in order to effect energy transfer. A matter of further conjecture is whether the target geometry itself may not account for this phenomenon. We may imagine the target as a constellation of points, a network or loose skein, so that particles of lower LET might sometimes traverse the region within the envelope of such structures without scoring a hit, whereas the alphas would almost inevitably produce an ionization within the significant structure if the general region were traversed. Further studies by Wilson (87) on the inactivation of the hemolysin located on the surface of Newcastle disease virus show no change in multiplicity of the dose-effect curves with different ion density. For this reason it seems more appropriate to regard the hemolysin sites as comprising 15 targets, each requiring one hit, than as a single target requiring 15 hits. The relation between the sensitivity parameter and the LET suggests that the target is not spherical, but flat, with a radius of 100 to 140 Å and perhaps 20 to 40 Å in thickness.

Preiss (88) has given a more detailed description of his experiments with low-voltage electron bombardment of the dry yeast cell in which invertase is located, on the basis of electron penetration range, in a shell between 500 and 1000 Å beneath the cell surface. A dose of 4×10^{14} electrons/ cm^2 inactivates practically all of the enzyme that is within reach of the electrons. A convincing methodological check was the reorientation of the cells and reirradiation. As expected, this further decreased the invertase activity.

Woese (89) has examined the survival curves of *Bacillus megatherium* spores under various conditions. In the LET range of 50 to 2000 ev/100 Å the survival-curve shape remains unchanged whether the spores are wet or dry, lysogenic or nonlysogenic. Because of the ineffectiveness of ion density in changing the multiplicity parameter of the survival curves, a multitarget theory is preferred to a multihit. No formula involving the exhaustive inactivation of uniform targets will fit the data. An excellent fit can be obtained, however, by the assumption of different sized targets; for example, 2 large and 16 small. The curves can also be fitted with the assumption of from 5 to 10 pairs of equal sized targets, the inactivation of both members of any pair being required for inactivation of the spore. The targets in any case must have a constant ratio of volume to cross-sectional area, for otherwise the curve shape would not be independent of ion density. The cross-section parameter continues to increase with increasing LET. A model requiring multiple simultaneous ionizations to explain the change in the cross-section parameter is rejected because a minimum requirement of eight ionizations would be necessary to fit the curves. An energy-transfer hypothesis is

capable of explaining the cross-section change, but may not be necessary. As in the case of the Newcastle-disease-virus-sensitive center, assumptions about the target geometry itself may accommodate this feature of the experimental data. The diffusion of radicals (which would almost automatically be invoked under normal conditions) is ruled out because of the dry state of the spores during irradiation.

Harm (90) has noted an increase in the sensitivity of intracellular T4 immediately postinfection by a factor of 1.6 over that of the free phage when soft x-rays are used. The gamma sensitivities under these conditions are equal, however. He explains this as a change in the target geometry after infection. It may be imagined that the DNA fibre in the free phage head is folded upon itself or closely packed in some manner that decreases the apparent sensitive volume to soft x-rays but not to gamma rays. Upon injection it may then unfold or separate. It is interesting that no such change is noticed with phage T2 (Latarjet, 1948, using very soft x-rays). This observation, made as it is in a liquid system, may have some bearing on the radical diffusion problem. Since in the rolled up or packed target inside the phage head the envelope of the diffusion distance will include a much smaller volume than it will when the DNA is straightened out, one would expect that radical diffusion would produce a postinfection increase in apparent sensitive volume even with radiation of low LET. The fact that this is not obtained with gamma rays suggests that radical diffusion is not an important cause of damage in this system. It will be recalled that *in vitro* studies have suggested that about half the damage to DNA in solution is indirect (91).

Various aspects of the T1 bacteriophage-host system have been studied by Whitmore & Pollard (92). Preinfection irradiation of the host inactivates the ability to form infective centers (i.e., the T1 capacity) and also the ability to form the phage-specific antigen which normally appears early in the latent period. The sensitivity of the capacity for specific antigen formation was 44 per cent of that for infective center formation. The free-phage antigen site is much less sensitive, with a 37 per cent dose of 1.5×10^6 r. The fact that the sensitivity of capacity continues to increase with increasing LET suggests that the target is of long thin shape rather than spherical. Pollard *et al.* (93) have noted that the host capacity of T1 is about 10 times more sensitive than free T1 (cf. the great resistance of T2 capacity). The survival curves of the infective centers show no multiplicity until at least 85 per cent of the latent period has elapsed, suggesting that capacity remains the predominant target until this time. The LET studies suggest a filamentous target requiring two simultaneous ionizations for its inactivation. The length of the filament for colony formation is 2700 μ ; for T1 capacity 48 μ ; for T2 capacity 1.8 μ ; the T1 initial monocomplex 55 μ . It appears that the sensitivity of the initial monocomplex slightly exceeds the sum of the sensitivities of the free T1 and the T1 capacity. The T1 capacities given in (92) and (93) differ by a factor of 20; the authors (92) attribute this to a difference in cultural conditions of the bacteria. Till & Pollard (94) have studied cross

reactivation and marker rescue in T1 (irradiated while dry) with relation to its LET dependence. Strain B/1 which is resistant to T1_p but not in T1_h was used as the indicator while free T1_h was irradiated. Change in the slope of the survival curve of T1_h with the T1_p carrier present, relative to the slope obtained in the absence of carrier, indicates cross reactivation. The cross-reactivated component became evident between 1 to 10 per cent survival. The hp₂ recombinants, also viable on B/1, parallel the cross-reactivated component. Thus, the mechanism of cross reactivation has the same cross section as that of recombinant formation. The ratio of cross section for cross reactivation to that of infectivity is 0.60, and is the same at all LET. Both cross sections increase linearly with LET up to at least 1200 ev/100 Å; hence, the targets must be very thin. The ratio of the cross sections is not dependent on the marker used in the carrier, nor on the multiplicity of carrier. Phenotypic mixing is unaffected by radiation; that is, the use of mixed indicator increased the h plaques to the same degree in the irradiated and control samples. The effect of irradiating the host was entirely independent of the foregoing phenomena; in other words, bacteria that retain capacity are equivalent to unirradiated bacteria in this system.

RADIATION EXPERIMENTS IN PHAGE REPLICATION

In the foregoing experiments (94) at doses where cross reactivation predominates, the distribution of burst sizes is clonal; in the control it is not. This suggests that replication of those portions of the damaged set that will appear in mature infective phage may be initiated at any time during the latent period by an event whose probability is proportional to the number of carrier prophage present. This initial event is probably a recombination; hence cross reactivation and marker rescue may be regarded as having a common cause. It is uncertain whether the phage-lethal hits must be eliminated by genetic exchange prior to replication or whether the defective phage can replicate although incapable of maturation into infective particles.

Epstein (95) has examined the question of whether the recombination that reactivates a multicomplex precedes replication. In his experiments a considerable control over the nature of the multicomplexes was achieved by an ingenious use of complementary markers. The crosses were made in a K12 host at low multiplicities, one parent containing an *r*-marker in the A-cistron and the other in the B-cistron. Under these conditions nearly all of the productive centers are double infections only. Recombination of unselected markers included in the crosses increased with UV dose as expected. Ultra-violet irradiation decreased the total yield in single-burst experiments and also decreased the participation of a given allele or its alternative in the reactivated complex. The marker knock-outs were proportional to dose, and the degree of clonality of particular recombinant types increased with dose. Finally, by means of premature lysis techniques the first particles to mature were found to have nearly as high a rate of recombination as those present at the natural time of lysis, that is to say, much above the recombination

rate of complexes formed from unirradiated phage. From these facts it was concluded that the reactivating recombination must occur before replication.

Epstein's results in the premature lysis experiments reopen the questions of whether the apparent increase in recombination caused by radiation is not merely the result of selection for the viable recombinants and also whether any of the phage-lethal hits are reactivable by mere complementation as in the case of the r -mutants in different cistrons. Such lethals would be difficult to detect because the autonomous hits requiring exchange for reactivation would, of course, be epistatic to them. Unfortunately it has not been possible to study the influence of multiplicity in a system where recombination is precluded.

Multiplicity reactivation in bacteriophage has been commonly regarded as an example of a fundamental difference in action between UV and ionizing radiations; it occurs extensively with UV but is negligible with ionizing radiations. Harm (90) reports that this relationship is characteristic only of phage irradiated in the extracellular state. The x-irradiation of multi-complexes leads to as much multiplicity reactivation as with UV, as much increase in recombinant frequency, and as much cross reactivation (where the monocomplex is x-irradiated prior to superinfection with unirradiated phage). Irradiation of phage and host separately does not produce these effects. Perhaps soft x-rays tend to produce multiple damages or crosslinks in the closely packed DNA fibre which preclude subsequent reactivation, whereas when the fibre is straightened out immediately after infection each traversing photoelectron would produce only a single damage. When the unirradiated phage precursor DNA in x-rayed complexes was caused to accumulate by means of treatment with chloramphenicol, marker rescue from the injured DNA was greatly increased. (Curiously enough this chloramphenicol-induced increase in marker rescue was not observed for UV-treated complexes unless the hosts had been irradiated prior to infection.) The dose to which these experiments could be carried was limited by decreasing plaque size, plaques being no longer visible in the neighborhood of 650 kr. This is probably a result of prolongation of the latent period until conditions on the indicator plate are no longer suitable for plaque formation. The dose-effect curves for marker rescue indicate that the early-step damage is not an all-or-none effect on injection but can be explained on the basis of fractional injection of a fragmented genome. The similarity of the reactivations following UV and x-irradiation of the multicomplexes suggests that they are the result of mechanical exchange of material rather than of chemical interactions. This implies that point changes in DNA will be similarly cross-reactivable no matter how they are produced. Flamand (96), for example, has reported the mutual reactivation of UV and formol treated Phi-N coliphage in stain W hosts.

In a splendid series of experiments Tomizawa (97) has further clarified the potentialities of UV-injured phage precursor DNA. The DNA accumulated in chloramphenicol-treated centers was UV irradiated. At four hits per

phage equivalent, DNA synthesis continued after irradiation, and phage matured when the centers were removed from chloramphenicol. More than half of the phage from such centers was noninfective but still possessed bacteria-killing ability. With 11 hits per phage equivalent, DNA synthesis did not continue after UV, and the particles that matured were nearly all noninfective. When these noninfective particles are formed from DNA labeled with P^{32} they are capable of transferring P^{32} activity to the progeny in mixed infections with normal particles. They are also capable of multiplicity reactivation, marker rescue, and photoreactivation in a manner comparable to free phage given the same UV dose. The fact that such noninfective particles are photoreactivable is of particular interest since they may be surmised to have passed through a nonreactivable period in the original host between the time of irradiation and maturation. When complexes with labeled parental phage were irradiated early in the latent period, few noninfective particles were produced, but much of the label was transferable. By means of variations in the time of labeling, the irradiated and unirradiated DNA could be differentially marked with P^{32} . In such experiments the irradiated and unirradiated DNA seemed to be mixed in the mature particles. Although infective particles did not preferentially contain unirradiated DNA (or vice versa), it was evident from transfer experiments that the noninfective particles carried phage-lethal hits in the irradiated portion of the DNA. Tomizawa arrived at the immensely satisfying conclusion that irradiated and unirradiated DNA can be mixed in phage and sorted out without loss of association between the lethal effects of UV and the phosphorous atoms of DNA. It is interesting that in this system the incorporation of heavily irradiated bacterial constituents into phage did not produce any noninfective particles. Similar experiments would be instructive in a system where capacity is much more sensitive.

Hill (98) has searched for possible interactions between UV and x-rays in bacteriophage T1 inactivation and has found none. The properties of the survivors of either radiation with respect to the other are identical to the properties of the unirradiated phage. The ratio of the plaques formed in light and dark remained constant. This absence of interaction simply indicates that at least one of the radiations has no detectable effect on the phage other than the production of phage-lethal hits. Since the UV survival curve shows a multiplicity greater than one, some of the UV survivors carry partial damages. The x-ray survival curve is exponential; hence, it is evident that the x-ray hit will be epistatic to the UV partial inactivation, while the x-ray survivors carry no partial inactivation and therefore cannot be expected to show any interaction with UV. Elkind & Sutton (99) find that UV reactivates soft x-rayed yeast, but only if the x-ray dose is sufficient to insure that the survivors were largely in the resistant divisional stage when irradiated. The effect is photoreversible and is independent of the sequence of irradiations. Whether analogous experiments in a phage system are possible is a matter for conjecture.

Symonds & McCloy (100) observed that the sensitivity to soft x-rays and P^{32} decay in T2 and T4 did not change during the first 5 min. of the latent period. With UV, however, the photoreactivable sector in T2 decreased from .67 to .45; in other words, with maximum photoreactivation the sensitivity of the T2 monocomplex does not change, while with no photoreactivation the complex appears to become more resistant to UV during the first 5 min. of the latent period. The authors explain this curious finding on the assumption that the events of the early portion of the latent period are all of a functional or nongenetic character and that the photoreactivable damage is all functional, while the nonphotoreactivable is both functional and genetic. Some experiments of Harm (101) suggest that these events of the first 5 min. of the latent period in T2 may be specifically related to the function of the u gene. This gene was shown by Streisinger (102) to account for the different UV sensitivities of T4 and T2. Harm shows that when T2 monocomplexes are infected at a multiplicity of three with T4 so highly inactivated as to preclude ordinary multiplicity reactivation, then the survival curve of the T2 phage becomes identical with that of T4. The T4 u gene leads to the restoration of a portion of the UV damage that is essentially all photoreactivable. At still higher UV doses the ability of T4 to produce a T4-like survival curve in T2 declines at a rate suggesting that the UV sensitivity of the u gene is about 1 per cent of the total phage sensitivity. A main objection to the terminology advanced by Symonds & McCloy (100) is the likelihood that the same damages that are photoreactivable, or erasable by the u gene, would otherwise require material exchange to eliminate them before replication. If this is so, the damages would have to be called genetic as well as functional.

SOME ASPECTS OF CHROMOSOMAL DAMAGE

The breakage and rejoining of chromosomes has been the subject of rather unrelated lines of inquiry, ranging from one extreme where the chromosomal effect is a mere index of radiation action to the other where radiation is merely a convenient means of producing chromosome breakage. Some of the problems remaining open to investigation are closely allied to more general questions of chromosome structure and function and some to the primary actions of radiation.

The question of the distance over which broken ends can rejoin in *Vicia* has been re-examined by Wolff *et al.* (103) in the light of the experimental finding that no interaction is apparent between neutron and x-ray-induced breaks. X-ray-induced breaks remain capable of interaction for at least 1/2 hr. after irradiation. A second dose given within this time results in a greater than additive yield of two-break exchange aberrations, showing that some of these aberrations involve a break from each of the radiation fractions. If the second dose is neutrons, the yield is simply additive; the neutrons apparently do not convert any of the x-ray-induced single breaks into two-break aberrations. Our explanation is that in nearly every instance of a

neutron-induced companion break within the interaction distance, the x-ray-induced break is redundant; that is, it would have been induced by the neutron-projected ionizing particle in any case. The same explanation applies to the linear dose-effect curve for neutron-induced two-break aberrations. If we knew the radius of energy transfer (by all mechanisms) from the track of the ionizing particle, this would permit an estimate of the maximum interaction distance. Lacking this, a maximum estimate was obtained in a different way: by first computing from reasonable assumptions the total breaks corresponding to a given aberration yield for the two types of radiation and for different values of the interaction distance. The aberration yield obtained from the total number of breaks in the combined irradiation is then seen to exceed additivity significantly unless the interaction distance is 0.3μ or less. I should like to direct attention to the site concept introduced in this paper. Since the interaction distance is very much smaller than the nuclear radius, we may speak of the average number of sites per cell at which chromosome strands lie within the interaction distance of each other. Other things being equal, the exchange yield is proportional to this number. Since the number may be expected to vary with ploidy, stage of mitotic cycle, and perhaps with external forces such as centrifugation, the concept will prove useful. A clue to the number of sites is supplied by the distribution of numbers of exchanges per cell. This distribution was formerly believed to be Poisson, but Atwood and Wolff [cited in (104)] find that its variance, both in *Tradescantia* and *Vicia*, is consistently smaller than that of a Poisson. This suggests that the number of sites is small and the distribution of sites is itself non-Poisson. It may be imagined that the juxtaposition of strands to form a site decreases their probability of forming other sites, a situation analogous to positive interference in crossing-over, but interchromosomal.

A puzzling aspect of chromosome exchanges has been the excess of metaphase dicentrics over anaphase bridges scored in the same material, fall-frees taken into account. Thoday (105) suggests that the production of additional breaks between the centromeres may explain such a discrepancy; it could, in principle, provided that these additional breaks are invisible in metaphase and part in anaphase. Conger (personal communication) finds a progressive decrease in bridge frequency between early and late anaphase in *Tradescantia*, suggesting that many of the bridges do, in fact, part. Schwartz & Murray (106) have revealed a novel feature of McClintock's classical breakage-fusion-bridge cycle in maize endosperm. Cycles were initiated either by x-irradiation of the endosperm or of pollen, or genetically by means of the activator-dissociator complex, then examined cytologically. Unexpectedly, the cycles are nearly all chromosomal, that is, of the double-bridge type. Moreover, they do not seem to be continuously propagated throughout the endosperm. Interruption of the cycle and conversion from chromatid to chromosome type by nondisjunction have been suggested by the authors. After the change to a chromosome cycle, two modes of progression are imaginable; either the broken double bridge rejoins before chromosome duplication, or both strands under-

go sister union and proceed as two independent chromatid cycles. In either case—but especially the latter—it is difficult to see how the double-bridge regime has any more stability than the single. By means of an ingenious marker system Fabergé (107) would have been able to detect a composite cycle—if it had occurred—formed by fusion of broken chromosomes from two simultaneous cycles initiated by Ac-Ds. The phenomenon was never observed to occur.

Jackson & Barber (108) compare the chromosome aberrations induced by 3000 r of x-ray in onion-root-tip cells (from germinating seeds) with those that appear spontaneously after aging of the seed. No remarkable difference was seen. In both cases the distributions of numbers of aberrations per cell were overdispersed, fitting the negative binomial better than the Poisson. Among the many imaginable reasons for this overdispersion, one is the change in dicentric frequency between metaphase and late anaphase already mentioned. If this change is brought about by the parting of bridges sometime during anaphase, an overdispersion will be caused as a result of intracell correlation of parting. It is interesting that terminal deletions, which form a large proportion of the aberrations scored, are also overdispersed. This finding of overdispersion is in contrast to the type of distribution found for metaphase exchanges alone (104). The aging effect on seeds, requiring a period of several years, seems to be quite erratic in its manifestations and must involve some as yet uncontrolled factors.

Seedling heights, survival, and pollen abnormalities were studied by Beard *et al.* (109) in the plants resulting from irradiation of seeds of barley, maize, mustard, and safflower with x-rays and thermal neutrons. The relation between plant height and amount of chromosome abnormality seems to be rather constant for a given radiation despite different sensitivities of the four species of plants; it is quite different when x-ray and neutron effects are compared. The bearing of such studies on the question of whether the lethal effects are chromosomal is problematical.

The possibility of bias introduced by mitotic delay in chromosome irradiation experiments is usually ignored, perhaps unwisely. Evans *et al.* (110) show that entry into metaphase is significantly delayed after doses of Co^{60} gammas within the range normally employed in chromosome breakage studies. A dose of 192 r given in aerated water caused a delay of 10 hr. The air-nitrogen ratio for the delay process was about 2 for cells 6 hr. or more from metaphase. Evidently one cannot rely on the time interval between irradiation and scoring of a cell in metaphase to determine the stage at which the cell was irradiated. More important, cells that were in different stages at irradiation may be scored simultaneously. The correction for delay will be difficult. On the one hand, the delay of cells in the same stage probably has a distribution, with greater variance at low dose; on the other, the difference in stage sensitivity will tend to synchronize the population after the initial depression of mitotic index. Whether our impressions of stage-specific effects would be substantially altered by a reinterpretation taking

into account the average delay is a matter of conjecture; let us hope not.

The stages of gametogenesis in *Lilium* can be distinguished by the bud length, hence irradiation in known stages is possible. Mitra (111) has done justice to the material in timing chromosome replication by means of the aberration types. Doses of 15 to 60 r of x-rays were used and the results analyzed at anaphase I. The most sensitive stages were preleptotene and late diplotene-diakinesis. Reciprocal translocations scored at late diplotene were the criterion of chromosome aberration, whereas dicentric chromatid bridges at anaphase accompanied by a single fragment signified chromatid aberrations. Irradiation prior to preleptotene produced only chromosome-type aberrations, whereas none of these are produced in zygotene or later. The chromatid breaks are produced from midpreleptotene until diakinesis. Subchromatid aberrations show a sudden increase at late pachytene and high frequency at diakinesis. Within 6 hr. of anaphase all the aberrations are of the subchromatid type. Evidently the chromosomes have divided before the time of pairing, a strong argument against hypotheses of crossing-over which require a duplication of chromosomes after pairing has occurred. Perhaps the only way to reconcile these findings with such a hypothesis is to assume that irradiation prior to duplication can lead to a chromatid break by injury to some chromosome precursor material. The time of chromosome reproduction indicated in these experiments corresponds to the time of DNA synthesis. The author points out two mysterious features of the subchromatid aberrations: first it is difficult to explain their failure to show up as chromatid aberrations at succeeding divisions and second, unlike chromatid aberrations, they increase during a period when there is no DNA synthesis and very little incorporation of labeled glycine. He suggests that the sensitivity to such aberrations may reflect a change in spatial relations of pre-existing units rather than the synthesis of new material.

The question of whether the oxygen effect is on breakage or rejoining, which now has a number of answers, is examined by Neary & Evans (112) who compare the relative frequencies of Co^{60} gamma-induced incomplete isochromatid and interchange aberrations in *Vicia* in air and N_2 . No differences are noted; the dose-effect curves are the same shape, with the N_2 /air dose ratio of about 2.5. The O_2 effect is judged in this instance to be on breakage since it is the same whether or not the aberrations involve rejoining. The absence of isochromatid breaks with nonunion both proximal and distal is cited in support of the potential-break theory of Revell (113). A more conventional explanation would be that isochromatid breaks at the same level are a rare coincidence with radiation of such low LET. Revell's theory derives its plausibility from being operationally indistinguishable in many respects from the usual breakage-first interpretation. Its merit rests on the extent to which any resemblance of induced exchange to meiotic crossing-over can be said to deepen our insight into the mechanisms of either process. Schacht (114) compares x-ray-induced crossing-over in the *Drosophila* male with reciprocal translocations. Translocations were about 17

times as frequent as crossovers. A majority of the crossovers were found in the 9 to 12 day brood; that is, in sperm from irradiated gonial cells. On the other hand, the majority of the translocations were recovered from the 3 to 9 day brood and hence probably induced in cells that were undergoing meiosis and spermatogenesis when irradiated. The question of whether an induced crossover is in reality a translocation between homologues has not been rigorously answered, but at least the opportunities for homologous and nonhomologous exchanges differ in their relations to the timing of the spermatogenic cycle.

Alexander (115) notes that translocations and dominant lethals produced with fission neutrons in *Drosophila virilis* males have linear dose-effect curves. The most sensitive time was 13 to 15 days before sampling, said to be a post-meiotic stage in that species. The RBE of these neutrons vs. x-rays varied from 6 in mature sperm to only 1.6 in meiotic cells. The rearrangements involved in detachments of attached x-chromosomes in *D. melanogaster* have been further studied by Parker with Hammond (116) and McCrone (117). X-ray-induced detachments show two-hit kinetics, with the sensitivity of the oocytes increasing for the first three days after eclosion, then remaining constant. Until three days of age, the rearrangements are mostly X-4 and X-Y (although translocations in general are extremely rare in oocytes), and with fractionated doses interaction is limited to 10 min. In older females the most frequent detachments are X-4 and X-2, with a few X-deletions, and rejoining is postponed until fertilization. The authors speculate that an arrest of oxidative metabolism in the unfertilized mature egg may prevent rejoining.

Bender (118) reports that loss of the ring X after x-irradiation is less frequent in oocytes than in sperm. Ring losses in sperm show a small but significant oxygen effect with x-rays, but not with gammas. In oocytes, the oxygen effect is larger with x-rays, but still absent with gammas. Bender conjectures that with the soft radiation, certain potential breaks become actual breaks more often in the presence of oxygen than in its absence, an explanation that does not seem to be useful in other contexts.

Experiments on RBE.—RBE experiments are merely incomplete target theory studies; the data are given, but their meaning unexplored. Two such studies, however, have brought out points of special interest. Conger *et al.* (119) have obtained RBE values for chromosome and chromatid aberrations in *Tradescantia* over a broad range of LET. A maximum is reached at about 60 keV/ μ followed by a decrease. The peak results from two opposing trends as LET increases: first, a decrease in the number of traversals per unit dose; second, an increase in the probability of breakage per traversal. The 14.1-MeV neutrons showed a markedly discrepant low RBE point in the plot of energy-average LET vs. RBE. These highly energetic neutrons are capable of projecting heavy particles as well as protons. The discrepancy arises from this heterogeneity of the projected particles, heavy particles contributing largely to biological effect, but very little to track length, whereas protons

of lower RBE contribute largely to track length. The average LET falls near the maximum effectiveness on the smoothed RBE curve, but the separate components fall far to either side. The RBE of the heavy-particle component was computed on the assumption that the proton RBE alone corresponds to its position on the smooth curve. When the radiation was thus resolved into its components, the discrepancy entirely disappeared.

The RBE of gamma rays, x-rays, 1-Mev and 14-Mev neutrons was determined by Edington & Randolph (120) for dominant lethals and sex-linked recessive lethals in *Drosophila*. Since the RBE was dose dependent in some of the dominant lethal comparisons, the 50 per cent hatchability level was chosen as the arbitrary standard. For recessive lethals a nonlinear dose-effect curve was noted for x-rays. The interpretation of the results depends on whether the track-average or energy-average LET is considered. In a case of a track-average LET, the RBE increases to 4.2 for dominant lethals and 1.6 for recessives with the 1-Mev neutrons that have the highest track average 46 kev/m. The 14-Mev neutrons on the other hand have the highest energy-average LET 75 kev/m., and if this is the criterion then the RBE rises to a maximum and declines. A situation similar to that noted by Conger *et al.* (119) must hold in this case; that is, the high-energy proton and heavy-particle components are being averaged and producing the anomalous relation between LET and RBE. This paper probably straightens out an old mystery: the discrepancy between the classical RBE values of Timofeef-Ressovsky and the modern values. Two factors seem to be involved: (a) the energy of the fast neutrons in the older experiments was probably much higher than the 3.9 Mev reported; (b) the irradiated flies in the older experiments were not mated for 48 hr., and this can decrease genetic damage. Other papers on RBE are (121, 122).

MUTAGENESIS IN HIGHER ANIMALS AND PLANTS

Mutation induction has ordinarily appeared to be independent of dose-rate, but Russell & Kelly (123) find a distinct intensity effect on specific locus mutation in mice in a comparison of acute x-irradiation and chronic gamma irradiation. Subsequently Russell *et al.* (124) confirmed the effect by showing that acute gamma and acute x-radiations are equally mutagenic to spermatogonia and both more effective than chronic gamma. In oocytes acute x-radiation is similarly more effective than chronic gamma radiation. At the same time the classical dose-rate independence of mutations in spermatozoa was confirmed. The gonial mutant frequency after an acute dose seems to persist indefinitely; hence it is unlikely that the explanation is in some long-term mechanism for getting rid of the mutations once they are induced. For spermatogonial cells it is imaginable that the answer to this problem can be found in the population dynamics of the germinal tissue. Acute dose mutations arise in a population of surviving cells that clearly has a very different initial composition from the steady-state population under

chronic dosage. The similar effect in oocytes, however, seems to call for some explanation that is not dependent on a heterogeneous population. The acute dose injury to the cell may lead to postirradiation conditions that increase the probability that latent damage to the gene will be consummated. Carter *et al.* (125) have initiated a low-dose chronic gamma study of specific locus mutations and dominant visibles in the mouse, but the data are still insufficient to permit conclusions.

An ingenious approach to the question of the origin of dominant lethal effects following ionizing radiation has been made by von Borstel (126) and permits conclusions which augment those derived from partial cell irradiation in the *Habrobracon* egg. The method is a comparison of the lethal syndrome in radiation-induced dominant lethal zygotes with that in genetically contrived aneuploids. The time of death falls into two main categories: in early embryogenesis, and following blastula formation. Both are produced by radiation, although the late deaths are characteristic of eggs irradiated in the first meiotic metaphase, and early deaths of prophase irradiation. The early effects are, of course, epistatic to the late; they predominate at high dose regardless of the stage irradiated. When aneuploidy was produced from translocation heterozygotes or from triploid females, the aneuploid zygotes were characterized by late death only; thus the very early lethality remains specifically inducible only with mutagenic agents. Similar results were obtained with *Drosophila*. The *Drosophila* zygotes simultaneously lacking X and Y chromosomes developed farther than those bearing radiation-induced dominant lethals. A detailed study of the stage at death of x-ray-induced embryo lethals in *Habrobracon* has been made by Whiting *et al.* (127). The dominant lethals die earliest in the haploid condition and death is delayed in the heterozygotes. Recessive lethals all exhibit the late death syndrome. The number of recessive lethals per gamete is not correlated with the stage at death when eggs are irradiated but does show a correlation in sperm. This seems to be related to the abundance of chromosome rearrangements induced in sperm in contrast to the scarcity in eggs. Such rearrangements produce aneuploidy following meiosis, and when numerous they somewhat reduce the average age at death. Lee (128) finds dominant lethals in honeybee sperm to show a similar dose-effect curve to that of *Drosophila* and *Habrobracon*. The induced dominant lethals caused early death. The proportion in irradiated sperm did not change after 1 yr. of storage. Fractionation effects were absent over a 1 hr. period and sperm inactivation required much larger doses than complete dominant lethal production.

Further studies on the interesting *R* locus in *Mormoniella* are reported by Caspari (129). This locus which affects eye color is unusually large by the criterion of radiation sensitivity, with an overall x-ray-induced mutation rate of about $7 \times 10^{-6}/r$. The locus is subdivisible into at least three cistrons designated *M*, *S*, and *O*. Mutation in *S* is about twice as frequent as in *O* with respect to the eye-color phenotype, whereas recessive lethals and sterile

factors are seven times as frequent. By contrast the mutants in *M* are very rare. With unfiltered 140 kvp x-rays, all classes of mutants in this locus show linear kinetics except dominant sterile, which is two-hit.

The germ cells of the early *Drosophila* embryo are situated at the polar cap of the egg where they may be irradiated with UV or treated with mutagenic chemicals. Altenburg (130) exposed this region to tertiary-butyl hydroperoxide vapor for 20 min. and produced *ca.* 5 per cent recessive lethals scored by Muller's sister technique. Reactivating light had no effect on this frequency. This experiment was apparently motivated by the report of Haas *et al.* (131) that UV-irradiated culture medium is made less mutagenic by visible light, perhaps because of destruction of organic peroxide mutagens. It is becoming increasingly evident that such diffusible poisons are not the usual mediators of UV damage (10). Proust (132) has used a novel method of exposure of *Drosophila* to UV. Ovaries dissected free were irradiated and then implanted in a new host bearing an ebony marker to insure detection of progeny from the transplant. Preliminary experiments suggested that damage to the ovaries was photoreactivable; hence subsequent experiments were done in red light. The Muller-5 method was adapted to the scoring of mutations in females by mating to Muller-5 males. A dose of 1420 ergs/mm.² gave 22 recessive lethals in 9 clones from 72 ovaries with 1064 chromosomes tested, an incidence of 2.1 per cent. Some exceptional F₁ Muller-5 males were found in clonal distributions. These were attributed to gonial attachments of the X chromosome taking place by heterochromatic crossing over.

The possibility that the genes of an organism can become resistant to mutation after long exposure to radiation was tested by Luning & Jonsson (133) by the use of Wallace's *Drosophila* populations 3 and 6; 3=control and 6=5 r/hr. of gamma for 6 yr. Lethals associated with rearrangements were not distinguished from point mutations in these experiments. The result is quite clear in showing no difference between the irradiated and control population with respect to acute dose mutagenesis.

Smith (134) has scored somatic mutation in petal-color heterozygotes of *Nicotiana* to afford a comparison of gamma-induced tumors. The somatic mutations increased linearly with the dose-rate of chronic gamma irradiation, but no evidence of induced tumors was found. The tumors that occurred spontaneously in interspecific hybrids appeared with unaltered frequency. In the Bracken fern, however, tumors which appear in the haploid prothalli were shown by Partanen (135) to increase linearly with the dose to the dormant spores. When spores received 16 kr of 136 kvp unfiltered x-rays, the subsequent tumor incidence was 26.5 per million as against 0.2 per million in the control. Howard (136) finds that 3 to 4 kr of x-rays can cause reassortment of the layers in periclinal chimeras of potato, a phenomenon that could easily be mistaken for mutation by the unwary. It is probably the result of cell death in the apical meristem followed by reconstitution of the layers from one or few cells.

POSTIRRADIATION BIOCHEMICAL CHANGES

Nucleic acids and nucleases.—A relation between protein and DNA synthesis similar to that established in bacteriophage systems has been reported in bacteria by Harold & Ziporin (137). Treatment with UV causes a temporary cessation of DNA synthesis. If protein synthesis is immediately blocked either by chloramphenicol or by amino acid deprivation of an auxotrophic mutant, resumption of DNA synthesis is prevented. If the blockade of protein synthesis is postponed until the end of the induction period, however, no effect on further DNA synthesis is noted for the first hour. Similar relationships were noted in bacteria treated with nitrogen or sulfur mustards (138). These agents stopped cell division and produced filamentous forms in strain B, and to a lesser extent in B/r. The duration of the transitory specific cessation of DNA synthesis was the same for strains B and B/r, although the survival was much less for B. The similarity in the delay period of B and B/r is in agreement with Kanazir & Errera (1954) (139). During the time of delayed DNA synthesis, acid-soluble deoxyribose accumulated, and leakage from the cells was noted with sulfur mustard but not with nitrogen mustard. The resumption of DNA synthesis was contingent on removal of the mustard and on conditions that allow protein synthesis; thus, deficient auxotrophs and cells treated with chloramphenicol or amino acid analogues did not resume synthesis. The DNA content of strains B and B/r was found by Harold & Ziporin (138) to be equal, in disagreement with a previous report of Morse and Carter (1949). Stuy (140) has examined the base composition of DNA synthesized following UV irradiation of strain B/r to a survival level of 0.3 per cent. This required 540 sec. at $600 \mu\text{w}/\text{cm}^2$ from a low-pressure germicidal lamp. In 55 min. following irradiation the turbidity increased 210 per cent while the survivors increased 260 per cent. No significant changes in DNA or RNA as percentage of dry weight were noted; hence, more than half of the DNA present was synthesized in cells that have been lethally irradiated. The base composition was found to be unchanged, in accord with reasonable expectations.

Some constituents of continuously x-irradiated yeast cultures were measured by Spoerl & Looney (141, 142). At 3.9 or 2 kr/hr. the cell number and dry weight approximately doubled within the first 2 hr. but thereafter increased very slowly at the lower dose-rate and remained constant at the higher, apparently arrested at a doublet stage. The dry weight slowly increased, but the trichloroacetic acid extract, lipid extract, and DNA showed little relative change, while polyphosphate increased more than the other constituents, and RNA less. Decreases in glucan, mannan, glycogen, and total carbohydrate were substantial. Experiments of this sort should be viewed with optimism; some day science may be sufficiently advanced to interpret them. Lajtha *et al.* (143) have followed the synthesis of DNA in human bone marrow cultures after x-irradiation, as evidenced by the incorporation of C^{14} -labeled formate. The result seems to depend on the posi-

tion of the cell in the mitotic cycle. When cells are in the synthetic period, 200 to 300 rads will not inhibit synthesis, although 500 rads or more give partial inhibition. The data can be interpreted to mean that about 50 per cent of the cells in the presynthetic stage are prevented from advancing to the synthetic stage by a dose of 200 to 300 rads. It was not possible, however, to decide whether a heterogeneous population or a uniform retardation by 50 per cent is involved. The authors believe that the effect is not related to chromosome damage or loss of cell viability, although the experiments do not seem to include any means of deciding such questions. A fair proportion of the cells must have lost reproductive ability at the doses used. Levin & Kritchevsky (144) find that giant cells produced in the HeLa strain with 1500 r of x-ray continue to incorporate P^{32} at a nearly normal rate. The trichloroacetic-acid-insoluble fraction contains the same proportion of the P^{32} activity in both the irradiated and the control cells.

Ord & Stocken (145) have shown that deoxyribotides accumulate in the x-rayed rat thymus to levels above the control. This seems to add to the evidence that where decrease in DNA synthesis occurs following irradiation, it cannot be attributed to a general shortage of precursors. Drášil & Soška (146), however, found that deoxyribonucleotides increased DNA synthesis in freshly explanted, irradiated guinea pig bone marrow, but not in unirradiated. Perhaps in such instances the enzymatic synthesis of "nonsense DNA" is involved rather than specific DNA replication. More likely, the alleged stimulation does not involve incorporation of the added nucleotides; if it did, then experiments with labeled nucleotides would show higher specific activity in DNA of irradiated cells than controls, a finding contrary to experience.

Enhancement of the release of nucleotides from rat liver mitochondria by enormous doses of UV has been reported by Beyer & Kennison (147). The nucleotide pattern differs from the spontaneous in having less ATP and in the presence of DPN which is absent from the control. When nucleotides are added back, the oxidative and phosphorylative activities of the particles are not, of course, restored. Changes in the RNase (pH 6 and 8) and DNase activities in mouse thymus after 160 r of x-rays have been studied by Weymouth (148). All were increased either on a per cell, per gram, or per DNA basis. The RNase that is active at pH 8 may have increased significantly on a per thymus basis. Peak increases between 24 and 72 hr. post-irradiation are followed by decline to subnormal levels by 168 hr. Changes in the ratio of thymocytes to stromal cells cannot, with simple assumptions, account for the behavior of all three of these enzymes simultaneously. Thymolysis with hydrocortisone also produced increases, but DNase and RNAase 8 were less augmented than with x-ray for equal thymic involution. Differential rates of unbinding, activation, proteolysis, leakage from dead cells, and removal from the gland may account for the independent behavior of these enzymes. Goutier & Goutier-Pirrotte (149) find that the DNase in rat spleen homogenates shows two components with pH optima 4.85 and

5.15 within 30 min. after x-irradiation, whereas the control shows a single optimum at pH 5.15. It would be interesting to compare purified DNase irradiated *in vitro*.

Other enzymes.—Postirradiation changes in the apparent amount of enzyme as measured by activity have been the subject of many reports in the past, but little is known of the processes involved except that radiation damage to the enzyme itself is of minor importance within the biologically interesting dose range. Enzyme activities are as frequently increased as decreased. Some experiments tending to implicate cell permeability are reported by Biraben & Delmon (150). Mouse liver arginase activity is decreased about 30 per cent within 45 min. after 700 r of x-ray. Pure arginase injected subcutaneously does not change the liver arginase activity in unirradiated mice but significantly increases it when injected after irradiation. Injected glutathione further augments the arginase activity in x-rayed, but not in control, mice. In view of Brinkman & Lamberts' (30) experiments on intradermal injection pressure, the release of the enzyme from the injection site may also be a factor of importance here. The inhibition of glycolysis and decrease in DPN level noted in Yoshida ascites tumor cells after 25 kr of x-rays by Rathgen & Maas (151) may be regarded as high-dose or postmortem effects: the dose is about 100 times lethal. Bettendorf & Maas (152) observe a depression of CO₂ production within 10 min. of 25 kr in the same system, followed by recovery within 1 hr. Glucose supplied immediately after x-ray is said to offset the depression of protein synthesis as measured by the criterion of C¹⁴ alanine uptake.

Schwimmer *et al.* (153) have found increased activities of phosphorylase, lactic dehydrogenase, and polyphenol oxidase in potato tubers following 11 to 14 kr of Co⁶⁰ gammas. They suggest that these increases may be brought about by a disturbance of the balance between enzyme synthesis and degradation and that in these instances the degradative processes may be more radiosensitive. A number of means are imaginable whereby this and other explanations of paradoxical enzyme activity increases might be tested experimentally.

Electrolyte transport.—Failure of electrolyte balance is an expected feature of moribund cells, but it is also seen as an isolated phenomenon with rapid onset and recovery. Tanada (154) reports a depression in the absorption rate of Ru⁸⁶ by mung bean roots within 1 min. after doses of soft x-rays in the 4000 r range given at a rate of about 2000 r/min. A minimum uptake rate was reached within 4 min. and complete recovery was obtained in 10 min. The second cm. sections of the root, initially highly resistant to this effect, become sensitive when soaked in deionized water. Calcium and magnesium ions decreased the sensitivity if they were always present but increased it if added only at the time of irradiation. An immediate drop in muscle resting potential with x-rays in the 10 to 80 kr range is described by Woodbury (155). The potential recovers slowly if potassium is supplied but continues to fall in potassium-free medium. The expected rate of fall upon inactivation

of the sodium pump was exceeded in the experiments. If the permeability constants used in the calculations are appropriate in this context, then we must assume not only defective sodium transport but also an increased permeability of the membrane to sodium.

In sufficient ammonium concentrations *E. coli* will lose potassium. Advantage has been taken of this effect by Harrison *et al.* (156) to study the potassium efflux rate in cell populations transferred to ammonium medium after x-irradiation. A protective effect is seen at high cell concentrations but it is not yet clear whether the causative interactions involve the irradiated medium or efflux products in the test medium. Retentivity (the reciprocal of the rate of potassium loss) decreases approximately exponentially with dose. It has not been determined whether the effect is all-or-none on the cells or whether an individual cell can show intermediate retentivity. The extent to which retentivity loss is secondary to cell death has not been worked out in detail. Eventual clarification of the mechanism of retentivity loss will be the more interesting because strain B/r is much more resistant to the process than B, suggesting that lethal hits and retentivity hits may more or less overlap. An especially valuable discussion of retentivity effects in yeast is given by Rothstein (59) including the kinetics, temperature effects, comparison of different radiations, relation of efflux to viability, and chemical effects on the membrane.

A shortening of erythrocyte lifetime that may possibly be related to defective electrolyte transport is reported by Sauerbier (157). When rabbit erythrocytes are x-rayed, labeled with Cr^{51} , and reinjected, a fraction of the cells are rapidly eliminated (within two days) followed by a slower decrease nearly parallel to the normal rate. Production of the rapidly eliminated fraction in the range 20 to 100 per cent at doses 10 to 230 kr seems to obey single-hit kinetics.

Photosynthetic systems.—Some effects of UV, gamma rays, and photodynamic action of intense visible light on photosynthetic systems were described in 1958. Gailey & Tolbert (158) describe the inhibition of greening of etiolated wheat seedlings by Co^{60} gamma rays. This process is rather resistant to ionizing radiation; a dose of 150 kr delayed chlorophyll synthesis for 10 hr. while 1220 kr caused permanent inhibition. Recovery does not occur if the plants are held in darkness but is initiated on short exposure to light and involves the same delay regardless of the duration of the previous dark period. Irradiation during the greening process produced a temporary cessation lasting about the same time as the initial delay. The time of onset of CO_2 fixation was unchanged except as secondary to chlorophyll deficiency. Normally CO_2 fixation begins 2 to 3 hr. after sustained greening, but when greening is delayed 2 to 3 hr., CO_2 fixation begins simultaneously. Evidently other processes prerequisite to establishment of CO_2 fixation are more radio-resistant than chlorophyll synthesis. About 100 kr of gamma radiation to the established system decreases CO_2 fixation [Zill & Tolbert (159)], whereas photolysis is unaffected except at much higher doses, where CO_2 fixation

shows a paradoxical increase. The distribution of label in photosynthetic products formed during the inhibited phase showed minimal changes, and the rate of CO₂ fixation returned to normal after 5 hr. Since these effects are markedly dependent on intensity they are not suitable for target theory analysis, yet it is clear that the apparent sensitive volume is very much smaller than the chloroplast.

Photolysis and CO₂ fixation were equally affected after UV treatment [Zill & Tolbert (159)] of 10,000 ergs/mm.² to chlorella or wheat seedlings (followed by immediate assay). The C¹⁴ distribution in the photosynthetic products showed an increase in phosphorylated compounds and a decrease in sucrose. Since uridine diphosphate glucose enters the synthesis of sucrose, the sucrose deficit is thought to be caused by destruction of uridine diphosphate which is known to be more labile to UV than is ATP.

Photodynamic actions.—Sironval & Kandler (160) find that the bleaching of chlorella by intense light involves an induction period after which carotene, chlorophyll-a, chlorophyll-b, and carotenols are destroyed in sequence. Oxygen is required both for induction and bleaching, and the induction process is dark-reversible. In killed cells no induction period is seen. The light intensities used in these experiments were of the order of 10⁵ lux.

Certain furocoumarins and related compounds that are known to sensitize the skin to long UV were found by Fowlks *et al.* (161) to sensitize bacteria also. One of the compounds active in this respect was 8-methoxypsoralen, a substance being marketed as an oral suntan pill. Becker (162) describes the effect of this substance in skin as the production of a stratum lucidum in locations where it does not usually occur. Excessive pigment retention in the stratum lucidum and the basal layer forms an effective screen against solar UV. A point of interest here is that the factors responsible for such specific actions of photosensitizing agents are poorly understood; the intracellular localization of the agent may prove to be a decisive factor. Cytotoxic effects on the Ehrlich ascites tumor are reported by Ludwig (163) to result from photodynamic action in eosin-sensitized mice up to 9 hr. before implantation of the tumor. The Strugger-positive criterion of cell damage was used, as described by Stenstrom *et al.* (164).

POSTIRRADIATION MORPHOLOGICAL CHANGES

A miscellany of reports on postirradiation cytomorphology have appeared in 1958. Pomerat *et al.* (165) have described giant cells produced in established tissue culture strains, and the absence of giant cells in primary explants. Pomerat believes giant cell formation is characteristic of established strains because these have aneuploid or polyploid chromosome numbers, whereas the unaltered cells from primary explants are usually diploid and euploid. Harper *et al.* (166) reach the same conclusion in comparing a variety of ophthalmic tissue explants to the established Chang strain from human conjunctiva. Pomerat *et al.* (167) find a similar relationship among tissue cultures from human amnion. If cell division is inhibited independently of

growth, it is reasonable to suppose that the growth rate of the nondividing cell will parallel that of the dividing cell from which it was produced, and indeed this is borne out in bacterial systems. The explanation of Pomerat's results may be simply that established tissue culture strains grow faster than primary explants.

Sherer & Vogell (168) report changes in mitochondrial morphology of liver, kidney, and spleen cells 1 hr. after 100 r of x-rays. These authors seem to believe that evidence of such changes can be seen in their electron micrographs. Nebel (169) has taken advantage of a sharpening effect on nuclear structures *ca.* 48 hr. after 1000 r of x-rays to obtain better electron micrographs of meiotic stages in mouse testis. Dose-effect curves for area growth of chick fibroblast or myoblast cultures are given by Trabert-van der Maesen & Frederic (170), who also describe loss of basophilia in the nucleolus within 1 hr. after an x-ray dose of 500 r. Mitosis at this time is nearly absent. Some cells may recover at 500 r, but with 1000 r the nuclear alterations persist. Changes progress more slowly in cells that have been irradiated at 20° than at 37°, but it is not clear whether the radiation must be administered at the time of the low-temperature period—probably not. Nucleolar changes in Walker carcinoma cells were followed for seven days postirradiation by Parchwitz & Wittekindt (171) by means of microspectrophotometric determinations of the ratio of RNA in the nucleolus and in an equivalent portion of cytoplasm. The normal mean value of this ratio was about 1.2. After 8000 r of x-rays, the distribution fluctuated slightly up to 9 hr. then became skewed to very high values, 2 to 9. These changes are very likely attributable to cell death.

Deering (172) has described in detail the well-known filamentous forms in *E. coli* strain B following UV irradiation. The length distribution of the filaments is attributable to a constant elongation factor operating on the length distribution of normal cells present at the time of irradiation. Filaments are difficult to distinguish until 90 min. after treatment. The number of dividing cells at any time before 90 min. can be obtained by extrapolation back from the growth-curve of plating units. The total number of cells prior to appearance of filaments is the sum of the number obtained by such an extrapolation and the subsequent filament count. This permits the interesting conclusion that all of the nondividing cells elongate. The filaments contain the same amounts of RNA and DNA per unit of cell-length as do normal cells. The 37 per cent dose for division ability in these experiments was 3 ergs/mm.² at 2652 Å, and the action spectrum was that of nucleic acid. Cell division remained photoreactivable within 20 min. following UV. Mandel *et al.* (173) describe a series of morphological alterations in proteus P18 caused by P³² in the medium. At first, L-forms with globular swellings were seen but normal forms eventually grew out. An interpretation of these cyclic changes might be aided by some knowledge of the stability of the secondary normal forms, and the effect of the used medium on fresh inocula. Korogodin (174) gives a detailed description of the morphology of moribund

yeast colonies after irradiation of resting diploid cells with Co^{60} gammas. In the control, the number of single cells decreases rapidly and the proportions of pairs and chains pass through transitory maxima. Within 12 hr. all of the colonies are discs. At 7.5 kr the sequence of events is the same, but the delays are prolonged. At 30 kr an appreciable proportion of the colonies cease growth as chains rather than discs, and at 112.5 kr the proportion reaching the disc stage is very small and most of the colonies stop growth as chains or pairs. From 200 to 400 kr all colonies stop as pairs and at 550 kr all fail to divide. Contrary to some previous reports, multicellular inactivation forms were also found with haploid cells.

PARTIAL CELL IRRADIATIONS

Partial cell experiments involving microbeams, microsurgical techniques, or natural separations of cell constituents provide some of the most direct means of recognizing the intracellular location of the radiation damage that is biologically significant by a given criterion. Too few of these instructive experiments were reported in 1958.

Iverson (175) has made use of nuclear transplantation techniques (similar to those of Ord and Danielli) in *Amoeba proteus* to compare sites of action of 2537 Å UV. After 1200 ergs/mm.² irradiated cytoplasm recovers in the presence of an unirradiated nucleus but is unable to repair an injured nucleus. An irradiated nucleus seems to have an injurious effect on normal cytoplasm. The main criterion of injury was the survival time, and the picture is unfortunately confused by the rather short survival times among controls. Thus, the shortening of survival in the various experiments, although statistically significant, is not as striking as it should be. The conclusions based on survival times, however, are supported by the results of methyl green-pyronine staining. Strangely enough the uptake of C^{14} phenylalanine is more depressed when cytoplasm alone is irradiated than when the whole cell is irradiated, cells with nucleus irradiation alone being intermediate in uptake between whole cell UV and controls [cf. Skreb & Errera (1h)].

Daniels & Vogel (176) have continued experiments with the large multinucleate amoeba *Pelomyxa* in which individuals lethally irradiated with ionizing radiations may be restored to reproductive viability by means of fusion with fragments of unirradiated individuals. When the contents of this amoeba are stratified by centrifugation, the heavy third, containing nuclei, is most active in restoring irradiated cells. The middle third, ostensibly anucleate, also gives a rather high frequency of restoration. The most likely explanation of Daniels' results is (in my opinion) that the frequency with which the middle fraction is effective represents the frequency with which it is contaminated with one or more nuclei. Alternatively, *Pelomyxa* may be organized in an unusual way, such that some extranuclear constituent is exhaustively inactivated at a lower dose than the nuclei.

An important role of the nucleolus in cell division is suggested by the experiments of Gaulden & Perry (177) on UV microbeam irradiation of

grasshopper neuroblasts. Permanent inhibition of mitosis was more frequent after nucleolar irradiation than after irradiation of a non-nucleolar region in the nucleus with the same microspot, particularly when early prophase cells were treated. Among cells that did divide, however, division was delayed to approximately the same extent in the nucleolar and non-nucleolar irradiations. Mitotic inhibition required irradiation of only one of the two nucleoli in the cell. The dose for the 3-sec. exposure of the microspot was 10^6 ergs/cm.², about 1500 times the dose necessary to produce spheration of the nucleolus with whole-cell irradiation, yet spheration was not seen. The authors suggest that this extremely high dose may denature the nucleolar material, thus preventing some of the morphological changes. It is especially significant that local injury practically anywhere on the chromosomes suffices to delay division; this is consistent with the enormous target size of the mitotic delay process to various radiations. With the microspot, division delay was frequently accompanied by a reversion in which the chromosomes assumed the appearance of an earlier mitotic stage. Reversion spreads throughout the entire nucleus, although initiated at a single point. [It will be recalled that chromosome paling and stickiness were obtained by Zirkle *et al.* (2b) in salamander epithelial cells only when part of a chromosome was in the microbeam.] Although these experiments imply an essential role of the nucleolus in the mitotic process, von Borstel & Rekemeyer (178) have shown that under certain conditions mitosis may proceed in the absence of the nucleolus. In a cross of attached X and attached XY *Drosophila* some of the zygotes contain autosomes only, and consequently no nucleolar organizer region. These lethal zygotes die after 10 to 12 nuclear divisions in the absence of a nucleolus. It should be remembered, however, that the insect egg contains chromosome precursor DNA in the cytoplasm and this may temporarily obviate certain functions that would otherwise be indispensable for mitosis. Indeed, the nucleolus is not visible in the normal zygote until after the twelfth mitosis (179).

Because of the positioning of its nucleus the newly laid *Habrobracon* egg is well suited to shielding experiments that distinguish between nuclear and cytoplasmic damage. Von Borstel & Rogers (180) have described the response of the cytoplasm of these eggs to alpha radiation. The LD₅₀ with nucleus shielded is 1.6×10^7 polonium alpha particles per egg with a survival curve of extremely high multiplicity, in contrast to the sensitive, single-hit survival with the nucleus exposed. Death occurs later in development with cytoplasmic than with nuclear irradiation, and morphological evidence of local damage is present. The appearance of the moribund embryos is similar to those that have received 2600 Å UV, and different from those receiving lethal doses of very short UV. Thus the organization of the cytoplasm is such that nonselective damage is equivalent, by this criterion, to NA damage.

RADIATION AS A QUASISENSORY STIMULUS

As Gray (181) has pointed out, a response to very small doses of ionizing radiation is to be expected in cells that are highly specialized sensory recep-

tors, if the normal stimulus involves the transformation of only a very small proportion of receptor molecules. The phosphene, a sensation of light produced by ionizing radiation in the vertebrate retina, has long been appreciated, and observations suggesting somewhat similar effects in lower organisms have been reported. *Daphnia* possesses two types of light-sensitive organ: the compound eye and the nauplius eye, which on the basis of behavioral and extirpation experiments are believed to respond to different portions of the visible spectrum. Baylor & Smith (182) observed downswimming in x-rayed *Daphnia*, a response that normally follows stimulation of the nauplius eye. No effects attributable to stimulation of the compound eye were seen. Similar behavior occurred in the presence of compounds with redox potential $+0.045$ v. or less. The x-ray effect is probably not attributable to irradiated water, since the response is immediate, the animals must be in the beam in order to respond, and no aftereffects or cumulative effects were apparent. Hug (183) has observed that land and water snails retract their feelers when irradiated with x, beta, or alpha radiations. The time between beginning of irradiation and the reflex response is inverse to the dose-rate above a threshold that may be as low as 5 r/sec. It is not yet known whether the summation process is referable to stimuli reaching the central nervous system or represents an accumulation of radiation products in the periphery.

Blondal (184) describes the behavior of mice at a dose-rate of 48 r per min. of x-rays (HVL 1.5 mm. Cu). A cessation of motor activity is noted when the dose has reached 500 to 600 r. This "inactivation" dose decreases with age; at 2 mo. it is slightly above the LD_{50} , whereas in older animals it is slightly below. The effect must be markedly dependent on dose-rate; experiments with different intensities, fractionated dose, and partial body irradiation would be instructive. Several behavioral criteria [Garcia *et al.* (185)] have suggested that much lower doses and intensities may constitute a noxious stimulus. As little as 30 r given at 5 r/min. induced saccharine aversion in rats. The retinal phosphene is apparently not involved, since ophthalmectomized animals responded.

Responses of bitterling to irradiated water are described by Heints (186); they probably involve olfactory stimulation. The dose, of the order of 10^{-4} r, is certainly the lowest for which a possibly valid biological effect has been claimed. The presence of organic material augmented the response, presumably through increased formation of detectable radiation products.

BENEFICIAL EFFECTS

Beneficial effects of radiation are nearly always subject to plausible explanation in terms of injury. Increased longevity in heavily irradiated female *Habrobracon*, for example, is tentatively attributed to cessation of egg production (A. R. Whiting, personal communication). Last year Cork (187) reported an apparent beneficial effect on viability in the beetle *Tribolium*. Park (personal communication) points out that these beetles are ordinarily heavily parasitized and that the host-parasite relation might be altered by radiation in a manner favorable to the host. For example, x-rays seem to

make rodents more resistant to *Plasmodium bergi*. The explanation worked out by Verain & Verain (188) is that the plasmodium prefers young erythrocytes and these are in short supply during the period of bone marrow depression. Inocula of parasitized blood given 2000 r *in vitro* had the same infectivity as unirradiated inocula.

A seemingly beneficial effect is seen in the flour mite *Tyroglyphus farinae* by Melville (189), based on the count of hatched and unhatched eggs at intervals following single doses of 5 to 10,000 r of gamma radiation. These doses increased the viability, but 40,000 r sterilized the population. One has the feeling that the criteria of viability in these cases are several steps removed from the real effects. Changes in the duration of different stages in the life cycle would be very misleading. Interactions are conceivable such that injurious effects on individuals would produce a stimulus to the population as a whole. Another possible instance of increased viability is given by Gross *et al.* (190) in the fish *Carassius carassius*. After 2 to 10,000 r x-rays, the 50-day survival at 3° C. was higher than in the control. On return to 15° C., irradiated fish die much more rapidly, however. The apparent beneficial effect is on the borderline of significance, and in view of the vicissitudes of piscine life tables it may be regarded with skepticism.

Since we are a step closer to primary actions in cells than in multicellular organisms, it is not surprising that beneficial effects at the cell level are reported less frequently and under more obscure circumstances. The x-ray stimulation of *Neurospora* conidia [Woodward & Clark, 1955 (191)] is an undoubtedly valid case; it may operate through augmentation of a normal activation mechanism that is destructive at the molecular level. Stimulation of growth of nodule bacteria is claimed by Sokurova (192) in response to the addition of U-233 fission products to the medium in concentrations of 1–2 mc./l. The low growth rate and yield of control cultures suggest that the medium is suboptimal; perhaps the fission product solution adds stimulatory trace elements, or perhaps by killing some cells it promotes reutilization of limiting factors by the survivors.

INSECT WHOLE-BODY RADIATION

The *Tribolium* case in the foregoing section cannot be regarded as typical; the radiation syndrome in insects presents variety. Although many insects are extremely resistant in the imaginal stage, *Calandra granaria* shows a marked reduction in 4-wk. survival of adults after a single dose of 5666 r of gamma rays, according to Jefferies & Cornwell (193). By the criteria of larval survival and fertility of the resultant adults, it appears that significant fractionation effects occur with larval irradiations 10 min. or more apart. This is an interesting time interval for fractionation effects—too long to involve primary actions and too short for many biological repair mechanisms. It is within the range of chromosome rejoining times, however. Baldwin (194) reports that the wasp *Dahlbominus* is sensitized to heat by a prior dose of 80,000 r of x-rays but not sensitized to x-rays by prior heating.

The recovery from sensitization proceeds 10 times faster at 32° than at 12°. Carbon monoxide completely inhibits this recovery, indicating a respiration-dependent repair mechanism.

If heat sensitization of DNA and protein (as demonstrable *in vitro*) is important in the insect, recovery may depend on synthesis of new molecules before the sensitized ones have deteriorated. Joly & Biellmann (195) have explored the possibility of radiation effects on the endocrine system that controls insect molting. A dose of 4700 r of x-ray given to *Locusta* at various times after the third molt reveals a critical period between the second and third day. X-irradiation before this time results in death before the fourth molt after a delay of up to two times normal, whereas x-ray after the critical period allows the fourth molt to proceed without delay. Shielding of the head and prothorax did not protect the insects; the effects were the same whether or not the endocrine glands were irradiated. Since the critical period coincides with cuticle synthesis and mitotic activity for the following molt, it was concluded that killing of epidermal cells constitutes the damage.

INSTRUMENTATION AND DOSIMETRY

Bertinchamps & Cotzias (196) offer a nomogram enabling dose-rate determinations at the center of spherical or cylindrical systems for 30 different isotopes of biological interest. Copies are available at Medical Research Center, Brookhaven National Laboratory, Upton, N.Y. Munro (197) describes the preparation and calibration of polonium-tipped microneedles. High dose measurement by means of gelation of styrene polyester plus inhibitor is proposed by Hoecker & Watkins (198), while Boag *et al.* (199) describe dosimetry based on UV absorption of irradiated plastics. Rozman & Zimmer (200) detect no saturation of plastic scintillators up to 10^4 rep/sec. and negligible damage up to 3×10^6 rep. Methylene blue dosimetry is re-discussed by Lafuente *et al.* (201). An extremely promising low-dose chemical system is given by Armstrong & Grant (202) based on fluorimetric measurement of salicylate produced from benzoate. The method is good in the range from 5 to 100 r.

LITERATURE CITED

- 1a. Wood, T. H., *Ann. Rev. Nuclear Sci.*, **8**, 343 (1958)
- 1b. Kihlman, B. A., *J. Biophys. Biochem. Cytol.*, **3**, 363-80 (1957)
- 1c. Kihlman, B. A., Merz, T., and Swanson, C. P., *J. Biophys. Biochem. Cytol.*, **3**, 381-91 (1957)
- 1d. Wolff, S., and Luippold, H. E., *Proc. Natl. Acad. Sci. U.S.A.*, **42**, 510-14 (1956)
- 1e. Cohn, N. S., *Genetics*, **41**, 639 (1956)
- 1f. Kimball, A. W., *Biometrics*, **9**, 201-11 (1953)
- 1g. Donellan, J. E., Jr., and Morowitz, H. J., *Radiation Research*, **7**, 71-78 (1957)
- 1h. Skreb, Y., and Errera, M., *Exptl. Cell Research*, **12**, 649-56 (1957)
- 2a. Powers, E. L., *Ann. Rev. Nuclear Sci.*, **7**, 63 (1957)
- 2b. Zirkle, R. E., Bloom, W., and Uretz, R. B., *Proc. Intern. Conf. Peaceful Uses Atomic Energy, Geneva, 1955*, **11**, 273-82 (1956)

3. Ford, C. E., Hamerton, J. L., and Mole, R. H., *Symposium on Genetic Approaches to Somatic Cell Variations*, Oak Ridge, Tenn., 235 (1958)
4. Puck, T. T., *Symposium on Genetic Approaches to Somatic Cell Variations*, Oak Ridge, Tenn., 287 (1958)
5. Dale, W. M., Ed., *The Intern. J. Radiation Biol.* (Taylor & Francis, Ltd., London, Engl.)
6. Claus, W. D., Ed., *Radiation Biol. and Med.* (Addison-Wesley Publishing Co., Inc., Reading, Mass., 944 pp., 1958)
7. Loutit, J. F., *Nature*, **182**, 1118 (1958)
8. *Rept. U. N. Sci. Comm. on Effects Atomic Radiation, General Assembly, Offic. Records; 13th Session, Suppl. No. 17(A/3838)* (New York, N. Y., 228 pp., 1958)
9. Haissinsky, M., Ed., *Organic Peroxides in Radiobiology* (Pergamon Press, London, Engl., 153 pp., 1958)
10. Jagger, J., *Bacteriol. Rev.*, **22**, 99 (1958)
11. Strauss, B. S., *Radiation Research*, **8**, 234 (1958)
12. Gordy, W., *Radiation Research*, Suppl. 1, 491-510 (1959)
13. Latarjet, R., Ephrussi-Taylor, H., and Rebeyrotte, N., *Radiation Research*, Suppl. 1, 417-30 (1959)
14. Guild, W. R., and DeFilippes, F. M., *Biochim. et Biophys. Acta*, **26**, 241 (1957)
15. Gordy, W., and Shields, H., *Radiation Research*, **9**, 611-25 (1958)
16. McCormick, G., and Gordy, W., *J. Phys. Chem.*, **62**, 783-89 (1958)
17. Shields, H., and Gordy, W., *J. Phys. Chem.*, **62**, 789-98 (1958)
18. Blumenfeld, L. A., and Kalmanson, E. A., *Akad. Nauk S.S.S.R., Biophys. Sect.*, **3**, 87-91 (1958)
19. Alexander, P., and Toms, D. J., *Radiation Research*, **9**, 509-24 (1958)
20. Braams, R., Hutchinson, F., and Dilip, R., *Nature*, **182**, 15-16 (1958)
21. Sosa-Bourdouil, C., Bonet-Maury, P., and Sosa, A., *Compt. rend.*, **246**, 1608-9 (1958)
22. Sosa-Bourdouil, C., Sosa, A., and Bonet-Maury, P., *Compt. rend.*, **246**, 2065-67 (1958)
23. Zimmer, K. G., *Radiation Research*, Suppl. 1, 519-29 (1959)
24. Ehrenberg, A., and Ehrenberg, L., *Arkiv Fys.*, **14**, 133-41 (1958)
25. Monier, R., *Biochim. et Biophys. Acta*, **29**, 345-49 (1958)
26. Magnan de Bornier, B., *Compt. rend.*, **246**, 2166-69 (1958)
27. Yost, H. T., Jr., Fitterer, D. W., Jr., and Goldin, H., *Radiation Research*, **9**, 411-21 (1958)
28. Magnan de Bornier, B., *Compt. rend.*, **246**, 1081-84 (1958)
29. Jayko, M. E., and Garrison, W. M., *Nature*, **181**, 413-14 (1958)
30. Brinkman, R., and Lamberts, H. B., *Nature*, **181**, 774-75 (1958)
31. Rothschild, M. C., Cosi, L., and Myers, L. S., Jr., *Nature*, **182**, 316 (1958)
32. Larin, N. M., *Nature*, **181**, 65 (1958)
33. Hvidberg, E., Kvorning, S. A., Schmidt, A., and Schou, J., *Nature*, **181**, 1338 (1958)
34. Aprison, M. H., *Arch. Biochem. Biophys.*, **78**, 260-64 (1958)
35. Adler, H. I., *Radiation Research*, **9**, 451-58 (1958)
36. Moustacchi, E., *Ann. inst. Pasteur*, **94**, 89-96 (1958)
37. Wood, T. H., *Radiation Research*, Suppl. 1, 333-46 (1959)
38. Howard-Flanders, P., and Moore, D., *Radiation Research*, **9**, 422-27 (1958)
39. Alper, T., and Howard-Flanders, P., *Nature*, **178**, 978 (1956)

40. Howard-Flanders, P., *Nature*, **180**, 1191-92 (1957)
41. Howard-Flanders, P., and Alper, T., *Radiation Research*, **7**, 518 (1957)
42. Kihlman, B. A., *Nature*, **182**, 730-31 (1958)
43. Lilly, L. J., *Exptl. Cell Research*, **14**, 257-67 (1958)
44. Kirby-Smith, J. S., and Dolphin, G. W., *Nature*, **182**, 270-71 (1958)
45. Eidus, L. Kh., Kondakova, N. V., and Otarova, G. K., *Biophysics (U.S.S.R.), English Transl.*, **3**, 197-201 (1958)
46. Ebert, M., Hornsey, S., and Howard, A., *Nature*, **181**, 613 (1958)
47. Ebert, M., and Hornsey, S., *Nature*, **182**, 1240 (1958)
48. Tallentire, A., *Nature*, **182**, 1024-25 (1958)
49. Laser, H., *CIBA Foundation Symposium, Ionizing Radiations and Cell Metabolism*, 106-(1956)
50. Curtis, H. J., Delihias, N., Caldecott, R. E., and Konzak, C. F., *Radiation Research*, **8**, 526-34 (1958)
51. Adams, J. D., and Nilan, R. A., *Radiation Research*, **8**, 111-22 (1958)
52. Conger, A. D., and Fairchild, L. M., *Proc. Natl. Acad. Sci. U. S.*, **38**, 290-99 (1952)
53. Wolff, S., and Atwood, K. C., *Proc. Natl. Acad. Sci. U. S.*, **40**, 187 (1954)
54. Wolff, S., and Luippold, H. E., *Science*, **122**, 231 (1955)
55. Wolff, S., and Luippold, H. E., *Genetics*, **43**, 493-501 (1958)
56. Cohn, N. S., *Genetics*, **43**, 362-73 (1958)
57. Tobias, C. A., *Radiation Research*, Suppl. 1, 326-31 (1959)
58. Magni, G. E., *Radiation Research*, Suppl. 1, 347-56 (1959)
59. Rothstein, A., *Radiation Research*, Suppl. 1, 357-71 (1959)
60. Beam, C. A., *Radiation Research*, Suppl. 1, 372-90 (1959)
61. James, A. P., *Radiation Research*, Suppl. 1, 391-93 (1959)
62. Mortimer, R. K., *Radiation Research*, Suppl. 1, 394-402 (1959)
63. Mortimer, R. K., *Radiation Research*, **9**, 312-26 (1958)
64. Luria, S. E., and Dulbecco, R., *Genetics*, **34**, 93-125 (1949)
65. Atwood, K. C., and Norman, A., *Proc. Natl. Acad. Sci. U. S.*, **12**, 696-709 (1949)
66. Dulbecco, R., *J. Bacteriol.*, **63**, 119-207 (1952)
67. Lucke, W. H., and Sarachek, A., *Nature*, **171**, 1014 (1953)
68. Sparrow, A. H., *Proc. Intern. Conf. Peaceful Uses Atomic Energy, 2nd Conf., Geneva, 1958*
69. Sparrow, A. H., *Radiation Research*, **9**, 187 (1958)
70. Tul'tseva, N. M., and Astaurov, B. L., *Biophysics (U.S.S.R.), English Transl.*, **3**, 183-89 (1958)
71. Woese, C. R., *J. Bacteriol.*, **75**, 5-8 (1958)
72. Proctor, B. E., Goldblith, S. A., Fuld, G. J., and Oberle, E. M., *Radiation Research*, **8**, 51-63 (1958)
73. Schwinghamer, E. A., *Radiation Research*, **8**, 329-43 (1958)
74. Kaplan, R. W., *Naturwissenschaften*, **42**, 184-85 (1955)
75. Gafford, R. D., *U. S. Air Force Publ. No. 57-61, USAF (Randolph Air Force Base, Texas, 1957)*
76. Zelle, M. R., Ogg, J. E., and Hollaender, A., *J. Bacteriol.*, **75**, 190-98 (1958)
77. Matney, T. S., Shankel, D. M., and Wyss, O., *J. Bacteriol.*, **75**, 180-83 (1958)
78. Ryan, F. J., Fried, P., and Schwartz, M., *J. Gen. Microbiol.*, **11**, 380-93 (1954)
79. Ryan, F. J., *Proc. Natl. Acad. Sci. U. S.*, **40**, 178-86 (1954)
80. Demerec, M., and Sams, J., *Science*, **127**, 1059 (1958)

81. Lindegren, C. C., and Pittman, D. D., *Nature*, **182**, 271-72 (1958)
82. de Serres, F. J., Jr., *Genetics*, **43**, 187-206 (1958)
83. Alper, T., and Gillies, N. E., *J. Gen. Microbiol.*, **18**, 461-72 (1958)
84. Bair, W. J., and Hungate, F. P., *Science*, **127**, 813 (1958)
85. Wilson, D., and Pollard, E. C., *Radiation Research*, **8**, 131-41 (1958)
86. Woese, D., and Pollard, E. C., *Arch. Biochem. Biophys.*, **50**, 354-67 (1954)
87. Wilson, D., *Radiation Research*, **8**, 142-49 (1958)
88. Preiss, J. W., *Arch. Biochem. Biophys.*, **75**, 186-95 (1958)
89. Woese, C. R., *Arch. Biochem. Biophys.*, **74**, 28-45 (1958)
90. Harm, W., *Virology*, **5**, 337-61 (1958)
91. Butler, J. A. V., *Radiation Research*, Suppl. 1, 403-16 (1959)
92. Whitmore, G., and Pollard, E. C., *Radiation Research*, **8**, 392-410 (1958)
93. Pollard, E. C., Setlow, J., and Watts, E., *Radiation Research*, **8**, 77-81 (1958)
94. Till, J. E., and Pollard, E. C., *Radiation Research*, **8**, 344-80 (1958)
95. Epstein, R. H., *Virology*, **6**, 382-404 (1958)
96. Flamand, J., *Compt. rend. soc. biol.*, **151**, 1269-71 (1958)
97. Tomizawa, J., *Virology*, **6**, 55-80 (1958)
98. Hill, R. F., *Radiation Research*, **8**, 46-50 (1958)
99. Elkind, M. M., and Sutton, H., *Science*, **128**, 1082-83 (1958)
100. Symonds, N., and McCloy, E. W., *Virology*, **6**, 649-68 (1958)
101. Harm, W., *Naturwissenschaften*, **45**, 391-92 (1958)
102. Streisinger, G., *Virology*, **2**, 1 (1956)
103. Wolff, S., Atwood, K. C., Randolph, M. L., and Luippold, H. E., *J. Biophys. Biochem. Cytol.*, **4**, 365-72 (1958)
104. Wolff, S., *Radiation Research*, Suppl. 1, 453-62 (1959)
105. Thoday, J. M., *Nature*, **181**, 932 (1959)
106. Schwartz, D., and Murray, C. B., *Proc. Intern. Genet. Symposia, Tokyo & Kyoto, 1956* (1957)
107. Fabergé, A. C., *Genetics*, **43**, 737-49 (1958)
108. Jackson, W. D., and Barber, H. N., *Heredity*, **12**, 1-25 (1958)
109. Beard, B. H., Haskins, F. A., and Gardner, C. O., *Genetics*, **43**, 728-36 (1958)
110. Evans, H. J., Neary, G. J., and Tonkinson, S. M., *Nature*, **181**, 1083 (1958)
111. Mitra, S., *Genetics*, **43**, 771-89 (1958)
112. Neary, G. J., and Evans, H. J., *Nature*, **182**, 890-91 (1958)
113. Revell, S. H., *Ann. N.Y. Acad. Sci.*, **68**, 802 (1958)
114. Schacht, L. E., *Genetics*, **43**, 665-78 (1958)
115. Alexander, M. L., *Genetics*, **43**, 458-69 (1958)
116. Parker, D. R., and Hammond, A. E., *Genetics*, **43**, 92-100 (1958)
117. Parker, D. R., and McCrone, J., *Genetics*, **43**, 172-86 (1958)
118. Bender, M. A., *Genetics*, **43**, 122-38 (1958)
119. Conger, A. D., Randolph, M. L., Sheppard, C. E., and Luippold, H. J., *Radiation Research*, **9**, 525-47 (1958)
120. Edington, C. W., and Randolph, M. L., *Genetics*, **43**, 715-27 (1958)
121. Bertram, C., and Hohne, G., *Strahlentherapie*, **106**, 269-72 (1958)
122. Spalding, J. F., Langham, W. H., and Anderson, E. C., *Radiation Research*, **8**, 322-28 (1958)
123. Russell, W. L., and Kelly, E. M., *Science*, **127**, 1062 (1958)
124. Russell, W. L., Russell, L. B., and Kelly, E. M., *Science*, **128**, 1546-50 (1958)
125. Carter, T. C., Lyon, M. F., and Phillips, R. J. S., *Nature*, **182**, 409 (1958)

126. von Borstel, R. C., *Proc. Intern. Congr. Genetics, 10th Congr., Montreal, 2*, 303 (1958)
127. Whiting, A. R., Caspari, S., Koukides, M., and Kao, P., *Radiation Research, 8*, 195-202 (1958)
128. Lee, W. R., *Genetics, 43*, 490-92 (1958)
129. Caspari, S. B., *Radiation Research, 8*, 273-83 (1958)
130. Altenburg, L. S., *Genetics, 43*, 662-64 (1958)
131. Haas, F., Clark, J. B., Wyss, O., and Stone, W. S., *Am. Naturalist, 84*, 261 (1950)
132. Proust, J., *Compt. rend., 246*, 986-89 (1958)
133. Lüning, K. G., and Jonsson, S., *Radiation Research, 8*, 181-86 (1958)
134. Smith, H. H., *Ann. N.Y. Acad. Sci., 71*, 1163-78 (1958)
135. Partanen, C. R., *Science, 128*, 1006-7 (1958)
136. Howard, H. A., *Nature, 182*, 1620 (1958)
137. Harold, F. M., and Ziporin, Z. Z., *Biochem. et Biophys. Acta, 28*, 492-503 (1958)
138. Harold, F. M., and Ziporin, Z. Z., *Biochem et Biophys. Acta, 28*, 482-91 (1958)
139. Kanazir, D., and Errera, M., *Biochim. et Biophys. Acta, 14*, 62 (1954)
140. Stuy, J. H., *J. Bacteriol., 76*, 668-69 (1958)
141. Spoerl, E., and Looney, D., *J. Bacteriol., 76*, 63-69 (1958)
142. Spoerl, E., and Looney, D., *J. Bacteriol., 76*, 70-74 (1958)
143. Lajtha, L. G., Oliver, R., Kumatori, T., and Ellis, F., *Radiation Research, 8*, 1-16 (1959)
144. Levin, S., and Kritchevsky, D., *Exptl. Cell Research, 15*, 422-23 (1958)
145. Ord, M. G., and Stocken, L. A., *Biochim. et Biophys. Acta, 29*, 201-2 (1958)
146. Drášil, V., and Soška, J., *Biochim. et Biophys. Acta, 28*, 667-68 (1958)
147. Beyer, R. E., and Kennison, R. D., *Biochim. et Biophys. Acta, 28*, 432-33 (1958)
148. Weymouth, P. P., *Radiation Research, 8*, 307-21 (1958)
149. Goutier, R., and Goutier-Pirrotte, M., *Compt. rend. soc. biol., 151*, 1445-48 (1958)
150. Biraben, J., and Delmon, G., *Compt. rend. soc. biol., 151*, 1507-9 (1958)
151. Rathgen, G. H., and Maass, H., *Strahlentherapie, 106*, 266-68 (1958)
152. Bettendorf, G., and Maass, H., *Strahlentherapie, 106*, 263-65 (1958)
153. Schwimmer, S., Weston, W. J., and Makower, R. V., *Arch. Biochem. Biophys., 75*, 425-34 (1958)
154. Tanada, R., *Radiation Research, 9*, 552-59 (1958)
155. Woodbury, J. W., *Exptl. Cell Research, Suppl. 5*, 547-59 (1958)
156. Harrison, A. P., Jr., Bruce, A. K., and Stapelton, G. E., *Proc. Soc. Exptl. Biol. Med., 98*, 740-43 (1958)
157. Sauerbier, W., *Strahlentherapie, 107*, 468-77 (1958)
158. Gailey, F. B., and Tolbert, N. E., *Arch. Biochem. Biophys., 76*, 188-95 (1958)
159. Zill, L. P., and Tolbert, N. E., *Arch. Biochem. Biophys., 76*, 196-203 (1958)
160. Sironval, C., and Kandler, O., *Biochim. et Biophys. Acta., 29*, 359-68 (1958)
161. Fowls, W. L., Griffith, D. G., and Oginsky, E. L., *Nature, 181*, 571-72 (1958)
162. Becker, S. W., *Science, 127*, 878 (1958)
163. Ludwig, F., *Compt. rend. soc. biol., 151*, 1117-18 (1958)
164. Stenstrom, K. W., Vermund, H., Musser, D. G., and Marvin, J. F., *Radiation Research, 2*, 180 (1955)
165. Pomerat, C. M., Kent, S. P., and Logie, L. C., *Z. Zellforsch. u. mikroskop. Anat., 47*, 158-74 (1957)

166. Harper, J. Y., Jr., Pomerat, C. M., and Kent, S. P., *Z. Zellforsch. u. mikroskop. Anat.*, **47**, 382-400 (1958)
167. Pomerat, C. M., Fernandes, M. V., Nakanishi, Y. H., and Kent, S. P., *Z. Zellforsch. u. mikroskop. Anat.*, **48**, 1-9 (1958)
168. Sherer, E., and Vogell, W., *Strahlentherapie*, **106**, 202-11 (1958)
169. Nebel, B. R., *Radiation Research*, Suppl. 1, 431-52 (1959)
170. Trabert-van der Maesen, M., and Frederic, J., *Compt. rend. soc. biol.*, **151**, 1608-11 (1958)
171. Parchwitz, H. K., and Wittekindt, E., *Strahlentherapie*, **106**, 282-88 (1958)
172. Deering, R. A., *J. Bacteriol.*, **76**, 123-30 (1958)
173. Mandel, P., Sensenbrenner, M., and Vincendon, G., *Nature*, **182**, 674-75 (1958)
174. Korogodin, V. I., *Biophysics*, **3**, 189-97 (1958) (Pergamon Inst. Transl.)
175. Iverson, R. M., *Exptl. Cell Research*, **15**, 268-70 (1958)
176. Daniels, E. W., and Vogel, H. H., Jr., *Proc. Intern. Conf. Peaceful Uses Atomic Energy, 2nd Conf., Geneva, 1958*
177. Gaulden, M. E., and Perry, R. P., *Proc. Natl. Acad. Sci. U.S.*, **44**, 553-59 (1958)
178. von Borstel, R. C., and Rekemeyer, M. L., *Nature*, **181**, 1597-98 (1958)
179. Sonnenblick, B. P., *Records Genetics Soc. Am.*, **16**, 52 (1947)
180. von Borstel, R. C., and Rogers, R. W., *Radiation Research*, **8**, 248-53 (1958)
181. Gray, L. H., *Radiation Research*, Suppl. 1, 73-102 (1959)
182. Baylor, E. R., and Smith, F. E., *Radiation Research*, **8**, 466-74 (1958)
183. Hug, O. D., *Strahlentherapie*, **106**, 155-60 (1958)
184. Blondal, H., *Nature*, **182**, 1026-27 (1958)
185. Garcia, J., Kimeldorf, D. J., and Hunt, E. L., *Brit. J. Radiol.*, **30**, 318-21, 354 (1957)
186. Heints, E., *Compt. rend.*, **246**, 1309-12 (1958)
187. Cork, J. M., *Radiation Research*, **7**, 551-57 (1957)
188. Verain, A., and Verain, A., *Compt. rend. soc. biol.*, **151**, 1164-66 (1958)
189. Melville, C., *Nature*, **181**, 1403-4 (1958)
190. Gross, C. M., Keiling, R., Bloch, J., and Vilain, J. P., *Compt. rend. soc. biol.*, **152**, 1187-90 (1958)
191. Woodward, V. W., and Clark, C. M., *Science*, **121**, 641-42 (1955)
192. Sokurova, E. N., *Mikrobiologiya*, **26**, 443-48 (AIBS Transl., 1957)
193. Jefferies, B. J., and Cornwell, P. B., *Nature*, **182**, 402-3 (1958)
194. Baldwin, W. F., *Radiation Research*, **8**, 17-21 (1958)
195. Joly, P., and Biellmann, G., *Compt. rend.*, **247**, 243-46 (1958)
196. Bertinchamps, A. J., and Cotzias, G. C., *Science*, **128**, 988-90 (1958)
197. Munro, T. R., *Exptl. Cell Research*, **15**, 529-36, 537-50 (1958)
198. Hoecker, F. E., and Watkins, I. W., *Intern. J. Appl. Radiation and Isotopes*, **3**, 31-35 (1958)
199. Boag, J. W., Dolphin, G. W., and Rotblat, J., *Radiation Research*, **9**, 589-610 (1958)
200. Rozman, I. M., and Zimmer, K. G., *Intern. J. Appl. Radiation and Isotopes*, **3**, 43 (1958)
201. Lafuente, B., Goldblith, S. A., and Proctor, B. E., *Intern. J. Appl. Radiation and Isotopes*, **3**, 119-124 (1958)
202. Armstrong, W. A., and Grant, D. W., *Nature*, **182**, 747 (1958)

AUTHOR INDEX

A

Aamodt, R. L., 190
 Abramov, A. I., 442, 446, 469
 Abson, D., 227
 Ackroyd, R. T., 466
 Adams, J. D., 558
 Adler, H. I., 557
 Agodi, A., 20
 Agranovitch, V. M., 11, 13
 Ahrens, E. H., Jr., 241
 Ahrens, L. H., 205, 215
 Aitken, M. J., 23
 Akhiezer, A., 19, 415
 Albaum, H. G., 529
 Alcock, K., 232, 233
 Alderman, I. M., 543
 Alexander, J., 335
 Alexander, L. G., 482, 490
 Alexander, M. L., 573
 Alexander, P., 554
 Alfert, M., 536
 Alford, W. P., 114
 Alfven, H., 395
 Alieva, A. Z., 532
 Alikhanov, A. I., 109
 Alimarin, I. P., 160, 192,
 194, 195, 227, 228, 230
 Aline, P. G., 490
 Ali-Zade, S. A., 68, 164
 Allen, B. M., 496
 Allen, C., 380
 Allen, J. S., 99, 114
 Allen, L., 2
 Allfrey, V. G., 532, 538
 Almeida, A. B., 534
 Alpen, E. L., 540, 544
 Alper, T., 538, 557, 562
 Alperovitch, E., 203, 206,
 207, 209, 211, 212
 Altenberg, L. S., 576
 Altman, K. I., 525, 529
 Ambler, E., 99, 100, 104,
 106, 119
 Amorosi, A., 442, 466
 Anders, E., 203-20: 207,
 209, 210, 211, 212
 Anderson, D. R., 525
 Anderson, E. C., 574
 Anderson, G., 206
 Anderson, H. L., 76, 361
 Anderson, O., 421, 427
 Anderson, R. E., 238
 Andreev, V. N., 442, 446, 469
 Andrew, G., 226
 Anzalone, P., 348
 Appelman, E. H., 213, 214,
 215
 Aprison, M. H., 556
 Araújo, J. M., 7, 14

Arient, M., 533
 Aristarkhov, N. N., 442,
 446
 Armand, L., 484, 485
 Armstrong, H. L., 351
 Armstrong, W. A., 587
 Armstrong, W. D., 524,
 533
 Arnold, E. D., 477
 Ashkin, J., 163
 Asling, C. W., 216
 Astaurov, B. L., 561
 Aten, A. H. W., Jr., 215,
 216
 Atteberry, R. W., 211
 Atwood, K. C., 553-92; 559,
 560, 569
 Aurebach, R., 507
 Austern, N., 2, 3, 8, 13
 Avery, D. G., 354
 Avery, R., 445, 446, 454,
 469
 Awapara, J., 524

B

Bacq, Z. M., 527, 540
 543
 Baerg, A. P., 254, 255,
 256, 260, 325, 326
 Bagge, E., 185
 Bagnall, K. W., 204, 227
 Bailey, L. E., 184
 Bainbridge, K. T., 206, 210
 Bair, W. J., 543, 563
 Baker, A. R., 2
 Baker, D. G., 523
 Baker, E., 167, 175, 176,
 177, 190, 191, 192, 193
 Baker, E. W., 160, 187,
 194
 Baker, W., 421, 427
 Baldin, A. M., 22
 Baldinger, E., 348, 351
 Baldock, C. R., 205
 Baldwin, W. F., 559, 586
 Ballou, N. E., 230
 Baltzinger, C., 195
 Bane, R. W., 238
 Bankowski, Z., 531
 Banks, C. V., 232
 Baranov, P. S., 23
 Baranov, V. I., 160, 192,
 194, 195
 Baranova, T. V., 160, 192,
 194, 195
 Barber, A. A., 528
 Barber, H. N., 571
 Barber, W. C., 18
 Bardon, M., 62, 85
 Barkas, W. H., 190
 Barker, F. C., 21
 Barnes, A. H., 441
 Barnes, C. A., 2, 110, 111,
 114
 Barnes, R. S., 468
 Barnett, C. F., 387, 428
 Barr, D. W., 177, 192
 Barron, E. G. S., 499, 531
 Bartell, F. O., 191, 192
 Barton, G. W., Jr., 215,
 216
 Barton, M. Q., 23
 Baryshnikov, A. I., 442,
 446, 469
 Basic, M., 515
 Bassett, J. Y., Jr., 206
 Bassi, P., 62
 Basson, J. K., 216
 Batzel, R., 285
 Batzel, R. E., 167, 176,
 177, 184, 191, 192
 Bauer, R. W., 110, 111
 Bay, Z., 360
 Bayer, E., 501
 Baylor, E. R., 585
 Baz, A. I., 256, 326
 Bazhanov, E. B., 23
 Beach, G., 533, 535
 Beam, C. A., 559, 560
 Beard, B. H., 571
 Beaumariage, M. L., 541,
 542
 Bécarevfc, A., 536
 Becker, S. W., 581
 Bedford, F. C., 232
 Beer, B. V. A. L., see
 Low-Beer, B. V. A.
 Beeston, J. M., 236
 Beghian, L. E., 361
 Behrends, R. E., 82
 Bekkum, D. W. van, 532,
 541
 Belcher, E. H., 544
 Bell, G. I., 454
 Bell, P. R., 428
 Bell, R. E., 160, 194, 360
 Bell, V. L., 527
 Bellelli, L., 533
 Belmont, E., 167, 169, 176,
 191
 Belovitskii, G. E., 195
 Beltz, R. E., 533, 534
 Benczer-Koller, N., 109
 Bender, M. A., 573
 Benedict, M., 478
 Bennett, W. E., 194
 Bennett, W. H., 419
 Berestetsky, V. B., 74
 Berg, A. van de, 543

- Berger, J. M., 2
 Berman, S. M., 67
 Bernardini, G., 162, 164, 179, 281
 Bernath, L., 489
 Bernheim, F., 528
 Bernstein, I., 412
 Bernström, B., 233
 Bernström, B. H., see Hök-Bernström, B.
 Berry, R., 545
 Bertinchamps, A. J., 587
 Bertozzi, W., 20
 Bertram, C., 574
 Best, G. F., 232
 Bethe, H. A., 5, 6, 7, 8, 13, 35, 168, 169, 467
 Bettendorf, G., 528, 579
 Beydon, J., 209, 211, 236
 Beyer, F. C., 445
 Beyer, R. E., 532, 578
 Biagini, C., 533
 Biellmann, G., 587
 Bigham, C. B., 265
 Bilenskii, S. M., 69
 Biller, W. F., 181, 194
 Billington, D. S., 468
 Bing, G., 395
 Binnington, J. P., 544
 Binus, N. M., 528
 Biraben, J., 579
 Bird, L., 190
 Birk, M., 363
 Birnbaum, W., 171, 172, 190, 191
 Bishop, A. S., 418
 Bishop, C. W., 533
 Bishop, G. R., 1
 Bivins, R., 164, 165, 166, 169, 170, 171, 172, 174, 175, 176, 177, 179, 183, 184, 279, 324
 Blake, C. A., 231, 233
 Blaser, J. P., 204
 Blatt, J. M., 5, 324
 Bleidner, W. E., 208, 212
 Blin-Stoyle, R. J., 73
 Bloch, C., 19
 Bloch, J., 586
 Blokhin, N. N., 524
 Blokhintsev, L. D., 76
 Blondal, H., 585
 Bloom, W., 584
 Blumberg, L., 328
 Blumenfeld, L. A., 554
 Boag, J. W., 587
 Bobone, R., 108, 111
 Bock, E., 234
 Bock, R., 234, 235
 Bodansky, D., 328
 Bode, H., 205, 210
 Boehm, F., 110, 111, 119, 124
 Bogdankevich, O. V., 22
 Bogolyubov, N. N., 31, 69
 Bohm, D., 408, 415
 Bohr, A., 253, 256, 272, 325, 328
 Bohr, N., 168, 183, 184, 245, 249, 250, 252, 262
 Boland, J., 497
 Boland, J. F., 441, 466
 Boldt, E., 62, 91, 92
 Bollinger, L. M., 261, 263, 316
 Bolomey, R. A., 226
 Bond, V. P., 525, 534, 544
 Bondarenko, I. I., 301, 302, 442, 446, 469
 Bonet-Maury, P., 555
 Bonham, K., 495
 Bonner, N. A., 191, 192
 Booman, G. L., 233
 Booth, E., 509
 Booth, E. T., 145, 162, 164, 179
 Borelli, V., 62
 Borello, D. A., 6
 Borisova, N. I., 193
 Bornier, B. M. de, 531, 555, 556
 Borstel, R. C. von, 575, 584
 Bouchiat, C., 147
 Boudreau, W. F., 482, 490
 Bouissieres, G., 230
 Bourdoul, C. S., see Sosa-Bourdoul, C.
 Bowes, R. C., 354
 Bowles, B. J., 313, 314
 Bowman, H. R., 265, 295, 298
 Boyd, G. E., 203, 204, 205, 206, 207, 208, 209, 210, 211, 212
 Boyer, K., 257, 258, 259, 263
 Braams, R., 555
 Bragina, A. A., 160, 194, 195
 Braid, T. H., 114, 363
 Brandt, W. W., 232
 Brandsen, B. H., 5
 Branyan, C. E., 445, 446, 469
 Breeding, E. J., 482, 490
 Breit, G., 3, 4
 Bremermann, H., 31, 33
 Brenk, H. A. S. van der, 541, 542
 Brennan, J. E., 483
 Brent, R., 509, 511
 Brent, R. L., 498, 529
 Breuer, H., 544
 Briant, R. C., 482, 490
 Bridgforth, E. B., 527
 Bridgman, P. W., 204
 Bright, H. A., 226
 Brin, M., 529
 Brink, D., 16
 Brinkman, R., 556, 579
 Brion, M. R., see Reyes-Brion, M.
 Briscoe, W. L., 363
 Brittan, R. O., 441, 466
 Broekert, J. C. de, 349, 350
 Brolley, J., 445
 Brolley, J. E., Jr., 326, 327, 328
 Bromley, D. A., 281
 Brooks, P. M., 526
 Brown, E. D., 226
 Brown, F., 254, 255, 256, 260, 313, 314, 325, 326
 Brown, G. E., 3, 19
 Brown, J., 361
 Brown, K. B., 233
 Brown, M., 358
 Brown, W. M. C., see Court-Brown, W. M.
 Bruce, A. K., 544, 580
 Bruce, F. R., 233
 Brues, A. M., 541
 Bruggeman, W. H., 462
 Bruin, M., 85, 86, 87, 90
 Brumagne, J., 540
 Bruninx, E., 229
 Brunson, G. S., 445, 446, 469
 Brussel, M. K., 316
 Bryan, R. H., 445
 Bryant, J. M., 233
 Buchanan, D. J., 527
 Buchanon, R. F., 467
 Bucher, N. L. R., 527
 Buettner-Janusch, V., 545
 Bullard, D., 523
 Burcham, W. E., 190, 215
 Burg, C., 527
 Burgus, W. H., 316
 Burgy, M. T., 75, 115
 Burhop, E. H. S., 370
 Burkhardt, G. H., 77, 78
 Burkhardt, L., 431
 Burkhardt, L. C., 419
 Burkhardt, L. E., 204
 Burman, R. L., 114
 Burnett, W. T., 541
 Busey, R. H., 205, 206
 Businaro, U. L., 317
 Butler, J. A. V., 531, 565
 Butler, J. P., 313, 314
 Butt, E. P., 430
 Byerley, F., 445
 Byers, N., 66
 Byfield, H., 145
 Bystroff, A. S., 227

C

- Cadra, V. J., 349
 Cagle, W., 353
 Cahler, A. R., 232
 Cairo, A. E., 234
 Caldecott, R. E., 558
 Caldwell, D. O., 62, 91, 92
 Cameron, A. G. W., 18, 169, 258, 268, 269, 287, 288, 292, 293, 319
 Cameron, W., 501

- Campion, P. J., 265
 Campos, M., 183, 194, 290
 Caretto, A. A., 160, 179,
 187, 188, 191, 192, 193,
 194, 195
 Carlson, B. G., 454
 Carnahan, C. L., 195
 Carr, R. J., 312, 313, 314
 Carruthers, R., 430
 Carter, J. C., 441, 466
 Carter, R. E., 134, 325
 Carter, T. C., 575
 Cartledge, G. H., 205
 Cartwright, H., 443, 467
 Carver, J. H., 2, 21
 Case, K. M., 139, 140
 Caspari, S., 575
 Caspari, S. B., 575
 Cassels, J. M., 77, 78,
 190
 Caster, W. O., 524, 533
 Cavanagh, P. E., 109,
 111
 Chaikoff, I. L., 524
 Chambers, F. W., Jr., 507
 Chambon, P., 533
 Chandrasekhar, S., 372,
 417
 Chanutin, A., 544
 Chapman, A. O., 497, 498
 Chapman, W. H., 507
 Chase, D. M., 327
 Chase, R. L., 348, 351,
 363
 Cheng, K. L., 230
 Chevallier, A., 527
 Chew, G. F., 29-60; 35,
 37, 39, 40, 41, 42, 43, 44,
 46, 47, 48, 50, 51, 54,
 55, 56, 57, 58, 163
 Chidley, B. G., 6, 12, 14,
 15
 Childs, R., 501
 Chinowsky, W., 62, 85
 Chizhov, V. P., 23
 Chou, H.-C., 76
 Chrien, R. E., 316
 Christian, E. J., 541
 Christian, R. S., 1
 Christofilos, N., 396, 426
 Christyakov, L. V., 193,
 194
 Chupp, W. W., 190
 Churchman, A. T., 468
 Chuvilo, I. V., 23
 Cieciura, S. J., 536
 Cini, M., 54, 58
 Clark, C. M., 586
 Clark, J. B., 576
 Clark, L. B., 544
 Clark, M. A., 75, 115, 119
 Claus, W. D., 553
 Clayton, C. G., 516
 Clayton, R. F., 228
 Clemedson, C. J., 530
 Clifford, W. E., 237
 Clubb, M. E., 528
 Clugston, H., 509
 Cobb, W. G., 482, 490
 Cobble, J. W., 204, 205,
 209, 210, 312, 313, 314
 Cochran, K. W., 543
 Codd, J., 454
 Coffin, C. T., 328, 333
 Cohen, A. F., 291
 Cohen, B. L., 291, 306,
 325, 328
 Cohen, J. A., 541
 Cohen, J. G., see
 Gershon-Cohen, J.
 Cohen, K., 476, 477, 486,
 488, 489, 490
 Cohen, K. P., 490
 Cohen, L. D., 21
 Cohn, C. E., 469
 Cohn, N. S., 559
 Cole, L. J., 536, 537
 Coleman, C. F., 109, 111, 233
 Coleman, G. H., 192
 Coley, C. D., 291
 Colgate, S., 421, 427, 430
 Collie, C. H., 23
 Collinge, B., 361
 Collins, V. P., 537
 Colvin, T. H., 444, 467
 Combe, J., 164
 Conard, R. A., 530
 Congdon, C. C., 542
 Conger, A. D., 559, 573, 574
 Coniglio, J. G., 527
 Conversi, M., 62, 83
 Cook, B. C., 18
 Coombe, D. J., 328
 Coombes, C. A., 83
 Coon, J. M., 543
 Cork, B., 83
 Cork, J. M., 585
 Cornatzer, W. E., 527
 Cornwell, P. B., 586
 Corson, D. R., 2, 203, 215,
 216
 Cortini, G., 20
 Coryell, C. D., 182, 321
 Cosgrove, G. E., 542
 Cosi, L., 556
 Costello, D. P., 495
 Cote, R. E., 261, 263
 Cottini, C., 361
 Courant, E. D., 19
 Court-Brown, W. M., 516
 Cowan, C. L., 133, 134,
 136
 Cox, G., 362
 Cox, S., 289, 298, 309
 Craig, D., 237, 240
 Craig, L. C., 237, 240,
 241
 Cranberg, L., 256, 295
 Crandall, W. E., 171, 172,
 190, 192
 Crane, W. W. T., 191, 194,
 195
 Cranmore, D., 540
 Crawford, F. S., Jr., 83
 Creasey, W. A., 531, 532
 Cresti, M., 83
 Crever, F. E., 462
 Critchfield, C. L., 129
 Critoph, E., 482, 489
 Cronkite, E. P., 507, 525,
 534
 Crosby, E. H., 18
 Crouthamel, E. C., 207,
 209, 212
 Crow, J. F., 516
 Crowe, K., 147
 Culligan, G., 148
 Cumming, J. B., 160, 167,
 187, 190, 192, 194
 Cunningham, B. B., 192
 Cuperman, S., 109
 Curie, D., 318
 Currie, L. A., 185, 190,
 191, 193, 194
 Curtis, G. C., 468
 Curtis, H. J., 558
 Cutler, L., 349
 Cziffra, P., 46
 Czyż, W., 4, 21

 D
 Dabbs, J. W. T., 328
 Dale, W. M., 553
 Dalitz, R. H., 61
 Danielli, J. F., 499
 Daniels, E. W., 583
 Danos, M., 14, 15
 Darby, W. J., 527
 Darcis, L., 540
 Daunt, J. G., 204
 Davidson, J. K., 468
 Davidson, J. N., 533, 535
 Davidson, L., 483
 Davidson, N., 206, 209
 Davies, J. T., 499
 Davis, A. K., 540
 Davis, R., 135
 Davis, W. K., 473, 489
 Davison, J. P., 527
 Day, P. L., 529
 de Berg, A. van, see
 Berg, A. van de
 de Bleij, V., 524
 de Bornier, B. M., see
 Bornier, B. M. de
 de Broekert, J. C., see
 Broekert, J. C. de
 Dedrick, K. G., 22
 Deering, R. A., 582
 DeFelippes, F. M., 554
 de Groot, S. R., see
 Groot, S. R. de
 de Hoffman, F., see
 Hoffman, F. de
 De la Cruz, F., 483
 Delhas, N., 558
 Dellis, A. N., 430
 Delmon, G., 579
 Demerec, M., 562
 Demidov, A. M., 299

- Demos, P. T., 325
 Denaro, A. R., 234
 Denisenko, G. F., 185, 192, 195, 285
 De Pasquali, G., 108, 109, 111
 der Brenk, H. A. S.,
 see Brenk, H. A. S. van der
 der Leun, C. V., see Van der Leun, C.
 der Maesen, M. T. van, see Trabert-van der Maesen, M.
 Derrick, G., 5
 DeSabbata, V., 1
 De Saussure, G., 5
 de Serres, F. J., Jr., see Serres, F. J., Jr., de
 De-Shalit, A., 109
 de Souza Santos, M. D., see Souza Santos, M. D. de
 D'Espagnat, B., 61, 76
 De Swart, J. J., 3, 4
 Detenbeck, R. W., 363
 Detre, K. D., 543
 Detrick, L. E., 524
 Deutsch, M., 110, 111, 351, 352
 Dew, E. 501
 De Waard, H., 109, 111, 354, 360
 DeWitt, D., 344, 346, 347, 351
 Diamond, H., 246
 Diamond, R. M., 177, 178, 191, 192, 224
 Dickman, S., 499, 531
 Dickson, H. M., 523
 Dickson, J. M., 190
 Dickson, M., 535
 Dienstbier, Z., 533
 Dietrich, J. R., 477, 483
 Dilip, R., 555
 di Luzio, N. R., see Luzio, N. R. di
 Diskina, L. S., 531
 Dobretsov, Yu. P., 68
 Dobrynin, Ya. P., 62, 75, 106, 134, 136
 Doherty, D. G., 541, 542
 Dolinsky, E. I., 76
 Doll, R., 516
 Dolphin, G. W., 558, 587
 Donaldson, L. R., 495
 Donellan, J. E., Jr., 561
 Donnell, A. P., 442
 Doorgeest, T., 215, 216
 Dostrovsky, I., 169, 170, 175, 176, 183, 184, 279
 Douglas, A. C., 5
 Douglass, C. D., 529
 Doull, J., 539, 543
 Douthett, E. M., 195, 290
 Dowben, R. M., 525
 Drake, D., 281
 Drážil, V., 578
 Dreisbach, L., 527
 Dreyfus, G., 535
 Driscoll, W. J., 225, 233
 Dropesky, B., 193
 Druce, J. G. F., 203
 Druin, V. A., 282, 284, 285
 Druin, V. A., 282, 284, 285
 Dublin, L. I., 494
 Dubois, K. P., 539, 543
 Duffield, R. B., 194, 256, 316
 Dulbecco, R., 560
 Dunaway, R. E., 419
 Dunjic, A., 501
 Dunlop, C. E., 515
 Durbin, P. W., 215, 216
 Durup, M., 553
 Dyrssen, M., 227, 228, 230
 Dyson, F. J., 31, 33
 Dzhelepov, B. S., 206

 E
 Early, J. C., 524
 Ebert, M., 537, 558
 Ebina, T., 526
 Edge, R. D., 21
 Edington, C. W., 574
 Edwards, C. F., 544
 Edwards, R. R., 182, 213, 321
 Efner, J. A., 527
 Eggebert, W. S., see Seelmann-Eggebert, W.
 Ehrenberg, A., 555, 558
 Ehrenberg, L., 555, 558
 Eichel, H. J., 530
 Eichler, J., 20
 Eidus, L. C., 537
 Eidus, L. Kh., 558
 Eisler, F., 62, 83
 Eismont, V. P., 335
 Eldjarn, L., 531, 539
 Eldred, V. W., 468
 Elkind, M. M., 568
 Ellinger, F., 542
 Ellinwood, L. E., 543
 Elliott, J. P., 20
 Elliott, K., 542
 Elliott, M. C., 233
 Ellis, F., 533, 534, 577
 Ellis, M. E., 536, 537
 Elmore, W., 426
 Eltholz, D. C., 507
 Elwert, G., 380
 Enderby, J. A., 468
 Engelstad, O. D., 527
 Ennis, M. E., 255, 256
 Enteman, C., 524, 527, 532
 Enz, C. D., 136
 Ephrussi-Taylor, H., 554, 556
 Epstein, R. H., 566
 Erdős, P., 21, 306
 Ericson, T., 280
 Ernst, H., 540
 Ernster, L., 543
 Erö, J., 20
 Errera, M., 523, 536, 544, 577, 583
 Ershler, B. V., 109
 Erskine, C. A., 516
 Erzhoff, B. H., 500
 Eschbach, E. A., 478
 Etzel, F., 484, 485
 Evans, H. J., 571, 572
 Evans, J. E., 261, 263

 F
 Fabergé, A. C., 571
 Fainberg, Y. B., 415
 Fairchild, L. M., 559
 Fairhall, A. W., 282, 285, 309, 310, 312, 315, 328, 333, 335
 Faissner, H., 326, 335
 Faris, J. P., 233, 240
 Farley, F. J. M., 280
 Farmer, F. T., 516
 Farrar, J. T., 523
 Fazzini, T., 76, 141, 142, 361
 Federbush, P., 58
 Federova, T. A., 525
 Feenberg, E., 77, 83
 Feinberg, G., 66, 67, 79
 Feld, B., 445
 Feld, B. T., 2, 23
 Feldman, G., 79
 Fermi, E., 64, 99, 122
 Fernades, M. V., 581
 Fernbach, S., 11, 13, 163
 Ferrari, A., 58
 Ferrell-Bryan, B. L., 328
 Ferrell, R. A., 18
 Ferrero, F., 20, 21
 Feshbach, H., 159, 162
 Fetsov, N. I., 442, 446, 469
 Feynman, R. B., 63, 64, 66, 67, 72, 73, 77, 82, 127, 129, 149, 153
 Ficq, A., 536, 544
 Fidecaro, G., 76, 141, 142, 361
 Fields, P. R., 289, 294, 298, 309
 Filippova, G. V., 531
 Filov, R. A., 195, 281
 Fink, R. W., 193
 Finch, S. C., 543
 Fink, R. W., 193
 Finkelburg, W., 204, 214
 Finkelstein, R., 141, 145, 146
 Finkelstein, R. J., 76, 82, 107, 151
 Finlayson, J. S., 535
 Finston, H. L., 221

- Fireman, E. L., 190, 191
 Fischer, C. R., 4
 Fischer, G. F., 469
 Fischer, P., 543
 Fisher, S. A., 212
 Fitch, V., 352
 Fitch, V. L., 363
 Fitterer, D. W., Jr., 556
 Flagg, J. F., 208, 212
 Flamand, J., 567
 Flanders, P. H., see Howard-Flanders, P.
 Flegenheimer, J., 210
 Fleming, J., 527
 Flerov, G. N., 246, 249, 273, 274, 279, 282, 284, 285
 Flesher, A. M., 541
 Fletcher, J. M., 232
 Flidner, T. M., 534
 Flowers, B. H., 20
 Fluharty, R. G., 261, 263
 Flynn, K. F., 306
 Foldy, L. L., 4, 5
 Folger, R. L., 167, 186, 191, 195
 Fomenko, D. E., 299, 325
 Fong, P., 318, 321, 324
 Ford, C. E., 553
 Ford, E. H. N., 516
 Ford, G. P., 180, 245
 Foreman, A. J. E., 468
 Foreman, J. K., 226
 Forkman, B., 20
 Forssberg, A., 535, 543, 544
 Foster, J. S., 182, 194, 323, 324
 Foster, R. E., 495
 Fowler, W. A., 114
 Fowlks, W. L., 581
 Fox, J. D., 316
 Fraenkel, Z., 170, 184, 279
 Franck, J., 215
 Frank, I. M., 195
 Frank, R. M., 165
 Frank, S. G. F., 148
 Frankel, S., 110
 Franzinetti, G., 61
 Franzini, P., 62, 83
 Fraser, J. S., 294, 295, 301, 303
 Fraser, J. W., 289, 291, 292
 Frauenfelder, H., 108, 109, 111
 Frayer, W., 38
 Frazer, W. R., 46
 Frederic, J., 582
 Frederickson, D. S., 527
 Freiser, H., 221-44; 221, 222, 225, 227, 229, 230, 237
 French, A. B., 530
 French, J. B., 21
 Frenkel, J. A., 250
 Freund, G. A., 467
 Freund, H., 234
 Fried, P., 562
 Fried, S., 203, 204, 205, 206, 207
 Friedlander, G., 160, 164, 165, 166, 167, 170, 171, 172, 174, 175, 176, 177, 178, 179, 183, 184, 187, 188, 190, 191, 192, 193, 194, 195, 279, 324
 Friedman, A. M., 289, 298, 309
 Friedman, L., 163, 193
 Friedman, M. H., 150
 Frieman, E., 412
 Friesen, W. J., 265
 Frisch, O. R., 61
 Fritz, J. S., 227
 Fritze, K., 308, 325
 Fritz-Niggli, H., 496, 523
 Fronsdaal, C., 82
 Fry, D. W., 430
 Fry, T. M., 443
 Fry, W. F., 195
 Frye, G., 295
 Fubini, S., 54
 Fujii, A., 83, 88
 Fujii, K., 65
 Fujii, S., 7, 14
 Fujii, T., 361
 Fujimoto, Y., 169, 276
 Fujita, J., 16, 17
 Fulco, J., 38
 Fuld, G. J., 561
 Fuller, E. G., 5, 15, 16, 22
 Fulmer, C. B., 306, 325
 Fulton, T., 79
 Fung, S. C., 192
 Furman, N. H., 232
 Furth, H. P., 421, 427, 430
 Furuichi, S., 84, 86, 90
- G
- Gafford, R. D., 562
 Gailley, F. B., 580
 Galbraith, W., 83, 246
 Galkov, V. I., 442, 446, 469
 Gallone, S., 317
 Gammel, J. L., 1, 3, 165
 Garattini, S., 527
 Garcia, J., 585
 Gard, G. A., 109, 111
 Gardner, C. O., 571
 Garren, A., 395
 Garrison, W. M., 212, 215, 216, 556
 Gartenhaus, S., 1
 Garwin, E. L., 21
 Garwin, R., 353
 Garwin, R. L., 148, 353
 Gasiorowicz, S., 58
 Gatti, E., 361
 Gatto, R., 58, 87, 88, 90
 Gauden, M. E., 583
 Geilikman, B. T., 301, 320
 Geilmann, W., 205, 210
 Gellman, H., 164
 Gell-Mann, M., 6, 8, 22, 61, 62, 63, 64, 66, 67, 72, 73, 77, 81, 82, 85, 83, 90, 91, 92, 93, 127, 129, 149, 153, 154
 Gergel, M. V., 234
 Gerhart, J. B., 106, 107, 113
 Gerke, W., 525
 Gerlit, J., 205, 206, 207, 209, 210, 211
 Germeshausen, K., 362
 Gershon-Cohen, J., 529
 Gershtein, S. S., 73, 76, 107
 Gewitz, H. S., 526
 Ghiorso, A., 203, 215, 216, 249
 Gibalo, I. M., 227, 228
 Gibson, A., 430
 Gibson, G., 395, 428
 Gilbert, R. S., 195, 334
 Gile, J. D., 212, 216
 Giles, D., 516
 Gill, R. G. S., see Summers-Gill, R. G.
 Gillies, N. E., 538, 562
 Gillispie, R. E., 543
 Gilpatrick, L. O., 205
 Ginzburg, M. B., 528
 Ginzton, E. L., 357
 Giordani, F., 484, 485
 Gitlin, D., 215
 Gittelmann, B., 110, 111
 Glass, R. A., 312, 313, 314
 Glasser, S. R., 497
 Glassgold, A. E., 11, 166, 188
 Glemser, O., 235, 237
 Glendenin, L. E., 182, 209, 210, 212, 221, 306, 308, 311, 316, 321
 Glick, C., 501
 Goble, A., 234
 Goebel, K., 191
 Goeckermann, R. H., 182, 193, 194, 311
 Goeler, E. von, 108, 111
 Goffinet, J., 497
 Goishi, W., 193, 211
 Gol'danskii, V. I., 23, 193, 194, 195, 285
 Goldberg, S., 362
 Goldberger, M. L., 6, 8, 22, 31, 33, 37, 39, 43, 50, 51, 58, 70, 73, 76, 81, 83, 144, 152, 163, 164
 Goldblith, S. A., 561, 587

- Goldbole, R. D., 23
 Goldemberg, J., 6
 Golden, J., 234
 Goldhaber, M., 99, 114, 206, 210
 Goldin, H., 556
 Goldman, M., 497
 Goldsack, S. J., 192
 Goldstein, L., 515
 Golubev, V. I., 442, 446, 469
 Golubeva, N. P., 531
 Gomes, L. C., 11, 23
 Gonella, L., 20
 Gönnewein, F., 326
 Good, M. L., 83, 114, 213
 Goodman, C., 473
 Goodman, R. D., 523
 Gorbatenko, M., 415
 Gorbunov, A. N., 5
 Gordon, B. M., 161, 193
 Gordon, E. R., 529
 Gordon, H. C., 498
 Gordon, R. S., 527
 Gordon, S. A., 523, 544
 Gordy, W., 553, 554, 555
 Gorodinskin, G. M., 193
 Gorter, C. J., 106
 Gottfried, K., 22
 Gould, R. G., 527
 Goutier, R., 530, 540, 578
 Goutier-Pirrotte, M., 578
 Gozmerac, W. L., 496
 Grabin, V. G., 442, 446
 Grad, H., 412
 Graham, C. B., 481
 Granquist, D. P., 478
 Grant, D. W., 587
 Grantz, H. E., 460
 Graves, E. R., 294
 Graves, G. A., 445, 446
 Graveson, R. T., 348
 Gray, L. H., 523, 537, 538, 539, 584
 Gray, P. R., 233, 240
 Grechishcheva, I. M., 186, 192, 193, 194
 Greebler, P., 437, 478
 Green, F. O., 538
 Green, R. E., 360
 Greenberg, D. H., 182, 192, 193
 Greenberg, L. H., 21
 Greenblatt, M. H., 355, 356
 Greenough, G. B., 468
 Greenstein, H. B., 114
 Griem, M. L., 543
 Griffin, J. J., 328
 Griffith, D. G., 581
 Grigoriev, E. L., 192
 Grigoryev, V. K., 75
 Grimaldi, A. J., 524
 Grisaru, M., 51
 Griswold, A., 482, 490
 Griswold, D. M., 349
 Grodzins, L., 99, 110, 111, 114
 Gromakovskaia, M. M., 544
 Groot, S. R. de, 133
 Gros, C. M., 533
 Groshev, L. V., 299
 Gross, C. M., 586
 Gross, E. P., 408, 415
 Grover, J. R., 186, 193
 Grünwald, A., 232
 Grupp, E., 495, 502, 503, 505, 514
 Guerritore, D., 533
 Guild, W. R., 554
 Gulko, A. D., 442, 446, 469
 Gunn, S. R., 289
 Gurevich, I. I., 68, 294
 Gurnani, S. U., 525
 Guselnov, A. G., 442, 446, 469
 Guth, E., 2, 3, 4
 Guthrie, C. E., 487
 Gutmann, J. R., 194
 Guttus, S., 534
 Gyllensten, A. L., 516
- H
- Haas, F., 576
 Haber, A., 194
 Haberland, G. L., 525
 Hackney, J. C., 204
 Hagen, U., 540
 Hague, J. L., 226
 Haissinsky, M., 214
 Halbert, E. C., 21
 Haley, T. J., 524, 541
 Hall, D., 468
 Hall, N. F., 203, 204, 205, 206, 207, 211, 212
 Hall, R. J., 481
 Halpern, I., 245-342; 167, 180, 256, 325, 328, 329, 330, 332, 333, 335
 Halpern, J., 2, 15, 18, 20
 Hamada, M., 514
 Hamerton, J. L., 553
 Hamilton, D. J., 351
 Hamilton, D. R., 114
 Hamilton, J. G., 212, 215, 216
 Hammond, A. E., 573
 Handley, T. H., 313
 Hanel, H. K., 526
 Hanna, G. C., 265
 Hanna, S. S., 110
 Hansen, G. E., 445, 446, 451, 454, 455, 456
 Hansen, P. G., 110
 Hanson, A. O., 2, 20, 109
 Hardin, C. A., 528
 Harding, G. N., 181, 280, 430
 Harding, J. B., 167, 184
 Hardwick, W. H., 227, 228, 232
 Harfenist, E. J., 241
 Harker, W. H., 478
 Harm, W., 565, 567, 569
 Harold, F. M., 536, 577
 Harper, J. Y., Jr., 535, 581
 Harriman, J. M., 478
 Harrington, H., 535
 Harris, E., 415
 Harris, E. B., 544
 Harris, O. E., 230
 Harrison, A. P., Jr., 544, 580
 Harrison, F. B., 133, 136, 137
 Hartner, B., 227
 Harvey, B. G., 226
 Harvey, J. A., 259, 265
 Haskins, F. A., 571
 Haslam, R. N. H., 18, 21
 Hausmann, W., 241
 Havens, W. W., Jr., 262, 264, 265
 Hawes, C. A., 538
 Hawkins, S. B., 501
 Hawtrey, A. O., 526
 Hay, I. W., 288, 324
 Hayward, E., 22
 Hayward, R. W., 99, 100, 104, 106, 119
 Heal, H. G., 226
 Healy, T. V., 232
 Hecht, F., 232
 Heckmann, U., 539
 Heckrotte, W., 166, 172, 188
 Heggen, G. E., 544
 Heinberg, M., 110, 111
 Heininger, C. G., 191
 Heinrich, F., 21
 Heints, E., 585
 Heisenberg, W., 162, 187
 Heitler, W., 379
 Helmholz, A. C., 192
 Hempelmann, L. H., 525, 529, 530
 Henke, H., 533, 540
 Henkel, R. L., 277, 326, 327, 328
 Henle, R. A., 353
 Henley, C., 495
 Henrich, L. R., 395
 Hermannsfeldt, W. B., 99, 114
 Hermel, M. B., 529
 Herr, W., 212
 Herrmann, M., 234
 Herron, D. P., 478, 483
 Hertwech, F., 395
 Herve, A., 540, 543
 Hesford, E., 232
 Hess, D. C., 308
 Hess, E. L., 533
 Heusghem, C., 527
 Hevesy, G., 544
 Hewitt, D., 516
 Hewlett, W., 357
 Hickenlooper, M. P., 328

- Hicks, H. G., 180, 181, 191, 195, 221, 289, 311, 334
Hicks, S. P., 498, 499, 500
Highby, D., 524
Hill, D. L., 245, 249, 256, 317
Hill, R., 524
Hill, R. D., 318
Hill, R. F., 568
Hillas, A. M., 361
Hintz, N. M., 190, 191
Hirsch, J. D., 533, 535
Hjalmar, E., 294
Hjort, G., 526
Hobbs, A. A., 515
Hockwald, L. B., 496
Hodgson, P. E., 192
Hoecker, F. E., 587
Hoff, R. W., 265
Hoffman, F. de, 35
Hoffman, J. I., 232
Hoffman, M., 299
Hoffman, W., 237
Hofstadter, R., 5
Hohne, G., 532, 574
Hök-Bernström, B., 231
Holden, R. B., 483
Hollaender, A., 562
Hollaender, A. H., 542
Hollander, J. M., 204, 305
Holloway, J. H., 206
Hollstein, U., 215, 216
Holmes, B. E., 537, 545
Holmes, J. E. R., 445
Holmes, R. C., 489
Holt, J. R., 148
Holt, R. B., 190, 191
Holthuisen, D. J., 85, 86, 87, 90
Hones, E. W., 489
Honsker, J., 430
Hope, D. B., 539
Hopkins, H. H., 192
Hoppe, I., 234
Hoppes, D. D., 99, 100, 104, 106, 119
Horgan, V. J., 528
Hornbostel, J., 83
Hornsey, S., 537, 540, 543, 558
Hotterbeex, P., 540
Houck, F. S., 167
Howard, A., 537, 545, 558
Howard, H. A., 576
Howard-Flanders, P., 523, 537, 538, 557, 558
Howland, J. J., 193, 194
Huang, K., 76
Hudgens, J. E., 230
Hudis, J., 159-202; 160, 167, 170, 175, 176, 177, 185, 187, 188, 190, 191, 192, 193, 194, 195
Hudson, G. W., 527
Hudson, R. P., 99, 100, 104, 106, 119
Huffman, E. H., 211
Hug, O. D., 585
Hughes, D. J., 259, 265, 316, 437, 439
Hughes, L. B., 529
Hughes, W. L., 215
Huiskamp, W. J., 106
Huizenga, J. R., 183, 246, 266, 267, 269, 271, 272, 279, 280
Hulet, E. K., 265
Hull, M. H., 4
Hullings, M. K., 328
Hulthén, L., 2, 3
Humbach, W., 204, 214
Hummel, H. H., 445, 446, 454, 469
Hungate, F. P., 543, 563
Hunt, E. L., 585
Hunter, C. G., 523
Hunter, E. T., 160, 171, 175, 176, 194
Hurwitz, H., Jr., 169, 437
Hutchin, W. H., 195
Hutchinson, D., 353
Hutchinson, F., 531, 555
Hutter, E., 441, 464, 466
Hutter, S. L., see Liebecq-Hutter, S.
Huxtable, G., 361
Huzita, H., 185, 192
Hvidberg, E., 556
Hyde, E. K., 203, 204, 215, 246, 247, 265, 302
- I
- Iddings, G. M., 194, 195
Igo, G., 169
Impeduglia, G., 76, 141, 142, 361
Ingelfinger, F. J., 523
Inglis, D. R., 317
Ingrham, M. G., 308
Ioffe, B. L., 65, 72, 77, 78
Irvine, J. W., 229
Irving, H., 234
Irving, H. M., 226
Ise, J., Jr., 421, 427
Ishii, R., 234
Iskenderian, H. P., 467
Ivanitskaia, E. A., 544
Ivanova, N. S., 161, 164, 181, 183, 185, 192, 193, 194, 195, 281, 285
Ivanter, I. G., 86, 90
Iverson, R. M., 583
Iwantscheff, G., 227
Iwata, K., 65
- J
- Jackson, C. B., 460
Jackson, J. D., 130, 131, 270
Jackson, J. P., 169
Jackson, K. L., 532
Jackson, S., 507
Jackson, W. D., 571
Jacobi, E., 210, 212
Jagger, J., 553, 576
James, A. P., 559
Jankus, V. Z., 467
Janusch, V. B., see Buettner-Janusch, V.
Jaross, R. A., 441, 464, 466
Jasberg, J., 357
Jauch, J. M., 34
Jaudel, C., 533
Jayko, M. E., 556
Jefferies, B. J., 586
Jensen, J. H., 129
Jensen, J. H. D., 12
Jensen, K. J., 238
Jensen, R. C., 309, 310, 312
Jentschke, W. K., 114
Jockey, P., 538
Jodra, L. G., 171, 181, 182, 194, 285
Johansson, E., 228
Johansson, S. A. E., 19, 20
John, W., 195
John, W., Jr., 269
Johns, D. H., 211, 212
Johnson, G. L., 213, 214, 215, 216
Johnson, J. C., 479
Johnson, M. H., 376
Johnson, S. D., 353
Johnson, T., 516
Johnston, M., 215, 216
Joliot, H. L., see Langevin-Joliot, H.
Joly, P., 587
Jones, J. W., 191
Jones, W. H., 313
Jongejans, B., 86, 87, 90
Jonsson, S., 576
Jordan, P., 21
Jordan, W. F., Jr., 345
Jordan, W. H., 482, 490
Joseph, B. J., 525
Joslin, M., 481
Jost, R., 31, 33
Jungerman, J., 289
Jungerman, J. A., 181, 194, 195, 278, 281, 285
Jungnell, D., 437, 478
Jurney, E. T., 441
- K
- Kahana, S., 136
Kahn, M., 213
Kalacheva, V. Y., 529
Kalbfleisch, G. R., 83
Kalliamin, A. V., 160, 194
Kallman, D., 483
Kalmanson, E. A., 554

- Kanazir, D., 577
 Kandler, O., 581
 Kao, P., 575
 Kaplan, J. G., 531
 Kaplan, R. W., 562
 Karnofsky, D. I., 497
 Karplus, R., 33, 58
 Karr, H., 430
 Katcoff, S., 305, 307, 308, 310, 311
 Kato, W. Y., 441, 469
 Katz, L., 6, 12, 14, 15, 18, 254, 255, 256, 260, 325, 326
 Kaufman, A., 417
 Kawaguchi, M., 4, 73, 83, 85
 Kawamoto, S., 514, 515
 Kay, R. E., 524, 527
 Kazachkovsky, O. D., 442, 446, 469
 Kazek, C. S., Jr., 296, 298
 Keck, J. C., 2
 Kedrova, E. M., 528
 Keepin, G. R., 305, 439
 Kegel, G., 361
 Kelling, R., 586
 Keir, H. M., 535
 Keister, G. L., 346
 Kellogg, D. A., 190
 Kelly, E. L., 193, 194, 195, 285, 574
 Kelly, L. S., 523, 533, 535
 Kendall, H. W., 343-66
 Kendall, J. W., 443
 Kennison, R. D., 532, 578
 Kent, D. C., 5
 Kent, S. P., 535, 581
 Kerns, Q., 362
 Kerova, N. I., 530
 Kessler, G., 529
 Kessler, J., 145
 Keszthelyi, L., 20
 Khalkin, V. A., 186, 193
 Khokhlov, Yu. K., 5, 6, 22
 Kiehn, R. M., 442, 455, 468
 Kihlman, B. A., 538, 557, 558
 Kikuta, T., 5
 Kimball, A. W., 542, 560
 Kimball, R. F., 538
 Kimeldorf, D. J., 585
 Kinchin, G. H., 466
 King, L. D. P., 442, 468
 King, R., 529
 King, R. W., 65, 134
 Kinoshita, T., 68, 147
 Kinyon, B. W., 482, 490
 Kirby-Smith, J. S., 558
 Kirkmann, J. M., 497
 Kirn, F. S., 445, 446, 469
 Kirochkin, U., 415
 Kirpichnikov, I. V., 261
 Kirsten, F., 359, 362
 Kiss, J., 542
 Kistner, O. C., 113
 Kit, S., 524
 Kitahara, S., 234
 Kittel, J. H., 467, 468
 Kiyasu, J., 524
 Kjellberg, A., 195
 Klecker, R. W., 481
 Klein, O., 65, 141
 Kleschick, A., 527
 Kliger, G. K., 23
 Klinenberg, J., 215
 Klotz, C. E., 481
 Klotzbach, R. J., 483
 Knoblock, A., 536
 Knox, K., 206
 Knox, W. J., 190, 191
 Knuppen, R., 544
 Kobkin, V. S., 246, 249
 Kobzarev, I. Yu., 86, 190
 Koch, H. W., 6
 Koch, L. J., 437-72; 441, 464, 466
 Kochkov, D. S., 246, 249
 Kodama, T., 84
 Koenig, V. L., 528
 Kofstad, P. K., 182, 193
 Kolb, A., 426
 Koller, N. B., see Benczer-Koller, N.
 Komar, A. P., 23
 Komesu, N., 541
 Kondakova, N. V., 558
 Kondakowa, N. W., 537
 Konopinski, E. J., 99-158; 61, 66, 75, 99, 105, 106, 130, 131, 136
 Konzak, C. F., 558
 Korogodin, V. I., 582
 Koukides, M., 575
 Kowlessar, O. D., 529
 Kozlova, N. V., 442, 446, 469
 Kraft, O. E., 206
 Krahe, M., 543
 Kramers, H. A., 30
 Krasavina, L. D., 183, 184, 186, 192, 193, 194
 Krasnoyarov, N. V., 442, 446, 469
 Kraus, K. A., 211, 212
 Krise, G. M., 525
 Krishen, A., 229, 240
 Kritchevsky, D., 578
 Kritskil, G. A., 532
 Krohn, N. A., 209
 Krohn, V. E., 75, 115
 Kronig, R., 30
 Kruger, P., 186, 193, 194
 Kruse, H. W., 133
 Kruskal, M., 395, 410, 412, 419
 Kudriashov, Iu. B., 528
 Kudrin, L. P., 164
 Kulchitsky, L. A., 23
 Kulikova, N. M., 326
 Kulrud, R., 412
 Kumatori, T., 534, 577
 Kumta, U. S., 525
 Kunkel, H. A., 525, 526, 528, 532, 539, 543
 Kunkel, W. B., 427
 Kurchatov, B. V., 193, 194
 Kurchatov, I. V., 419, 428
 Kurchatova, L. N., 193
 Kurilko, V., 415
 Kurnick, N. B., 529
 Kurosu, M., 526
 Kusche, H., 234, 236
 Kuschner, J., 514
 Kutikov, I. E., 62, 75, 106, 134, 136
 Kutsayeva, L. S., 301, 302
 Kuzin, A. M., 523, 544
 Kuzminov, B. D., 301, 302, 442, 446, 469
 Kuznetsov, V. V., 186, 191, 192, 193, 194
 Kuznetsova, M. Ya., 193, 194
 Kvorning, S. A., 556
- L
- Lackey, M. E., 482, 490
 Ladenbauer, I. M., 193
 Lafuente, B., 587
 Lagg, S. E., 533
 LaHam, Q., 496
 Lajtha, L. G., 533, 534, 545, 577
 Lamb, W. A. S., 428
 Lamberts, H. B., 556, 579
 Lambertson, G. R., 83
 Lamerton, L. F., 544
 Lamphere, R. W., 255
 Landau, L., 102, 408
 Landau, L. D., 65, 66, 139
 Lande, K., 62, 85
 Lane, A. M., 9, 163, 193
 Lane, J. A., 473-92; 477, 482, 486, 487
 Lange, F., 205
 Lange, R., 531
 Langer, L. M., 99, 105, 106, 130, 131, 136
 Langevin-Joliot, H., 109
 Langham, W. H., 574
 Larin, N. M., 556
 Larina, M. A., 525
 Larsen, S., 147
 Larson, Q. V., 203, 205, 206, 207, 208, 210, 211, 212
 Laser, H., 558
 Latarjet, R., 554, 556
 Latta, J. S., 498
 Lattes, C. M. G., 76
 Lattimore, S., 167, 184
 Lauenstein, K., 525
 Lauer, E., 395
 Lauer, E. J., 114, 428
 Lauritsen, C. C., 114
 Lauterjung, K. H., 114
 Lavik, P. S., 535
 Lavrukhina, A. K., 160, 183, 184, 186, 192, 193, 194,

- 195
Lawrence, P., S., 516
Lawson, R. D., 10
Lax, M., 163
Lazareva, L. E., 20, 22, 326
Lazarus, R. B., 444, 467
Leachman, R. B., 180, 245, 282, 284, 289, 296, 298, 300, 301, 312
Lebedinsky, A. V., 523
Lecomte, J., 542
LeCourtois, A., 147
Le Couteur, K. J., 167, 169
Lederer, M., 212
Lederman, L. M., 62, 85, 145, 147, 148
Lee, R. E., 460
Lee, T. D., 37, 61, 65, 66, 73, 76, 99, 102, 130, 139, 141
Lee, W. R., 575
Leech, P., 468
Lees, D. J., 430
Lefevre, H., 361
Lefort, M., 194
Lehmann, H., 31, 33, 34
Leibnitz, H. M., see Maier-Leibnitz, H.
Leikin, E. M., 20
Leininger, R. F., 213, 214, 215, 216
Leipunsky, A. I., 442, 446, 469
Leiss, J. E., 6, 21
Lelievre, P., 524, 525
Lennox, D. H., 445
Leonard, B. R., Jr., 265
Lerner, S. R., 527
Leun, C. V. der, see Van der Leun, C.
Levenson, M., 441, 464, 466, 468
Levi, M., 212
Levin, J. S., 256
Levin, S., 578
Levine, N., 108, 109, 111
Levinger, J. S., 1, 3, 4, 5, 6, 7, 8, 13, 14, 17, 19, 22
Levinson, B., 501
Levitt, A. E., 234
Levy, H. B., 289
Levy, M. M., 64
Levy, S., 490
Lewis, A. E., 523
Lewis, H. R., 108, 111
Lewis, I., 358, 359, 362
Lewis, J. R., 236
Lewis, M., 478
Libby, W. F., 185, 190, 191, 192, 193, 194, 211
Lichtenberger, H. V., 441
Liébecq, C., 543
Liébecq-Hutter, S., 543
Lilly, E. G., 527
Lilly, L. J., 538, 558
Lin, H. C., 345
Lindberg, O., 543
Lindgren, C. C., 562
Lindenbaum, S. J., 2, 159, 162, 164, 179
Lindner, M., 174, 175, 181
184, 190, 191, 193, 194, 195
Lindsay, J. E., 553
Lingen, C., 543
Lipkan, M. F., 533
Lipkin, H. J., 109
Lipscomb, A. G., 227
Littauer, R. M., 2
Litz, L. M., 191
Liubimov, V. A., 109
Livesey, D. L., 5
Llewellyn, P. M., 206
Lock, W. O., 192
Loewenstein, W. B., 445, 446, 455
Lofstrom, J. E., 500, 501
Logan, R., 544
Logie, L. C., 581
Logunov, A. A., 69
Lokan, K. H., 20, 21
Lokanathan, S., 67
Long, J. K., 445, 446
Longmire, C., 397, 404
Loomis, C. C., 478
Looney, D., 535, 577
Lopes, J. L., 6, 76
Loud, A. V., 527
Lounsbury, M., 265
Loutit, J. F., 553
Lovberg, R., 431
Love, T. A., 293, 298
Love, W. A., 77, 139, 144
Lovoff, A., 441, 464, 466
Low, F. E., 31, 37, 39, 40, 41, 42, 43, 47, 51, 56, 57
Low, W., 206
Low-Beer, B. V. A., 530
Lowe, C. W., 524
Lozhkin, O. V., 161, 181, 183, 185, 192, 193, 194, 195, 281, 335
Lubimtsev, O. L., 442, 446
Lubkin, E., 147
Luce, J. S., 428
Luchnik, N. V., 533, 543
Lucke, W. H., 560
Lüders, G., 104
Ludewig, S., 544
Ludwig, F., 581
Luganova, I. S., 524
Lundby, A., 110
Lundin, J., 530
Lundquist, S., 437, 478
Lüning, K. G., 576
Luria, S. E., 560
Lutsenko, V. N., 299
Luzio, N. R. di, 527
Lyon, M. F., 575
Luippold, H. E., 559, 569
Luippold, H. J., 573, 574
Maass, H., 525, 526, 528, 532, 533, 540, 579
McArdle, A. H., 535
McBryde, W. A. E., 226
McCarthy, W. J., Jr., 467
McCarty, S., 233
McCloy, E. W., 569
McCormick, G., 554
McCrone, J., 573
McCullen, J. D., 466
McDonald, D., 362
McDonald, W. B., 482, 490
McDonald, W. S., 2
McDowell, S. W., 54, 86, 89, 90
McGarrahan, K., 527
McGinnis, F. D., 441, 466
McGrath, J., 501
McGrath, J. J., 500
McGuire, A. D., 133
Macht, S. H., 516
Macintosh, I. J. C., 526
Mack, D., 363
McKaveney, J. P., 230
McKay, H. A. C., 232
MacKay, I. N., 482
McKee, R. W., 529
MacKenzie, D. R., 265
MacKenzie, K. R., 203, 215, 216
McLaughlin, M. M., 529
McLennan, J. A., 139, 140
McManus, H., 164
McMillan, E. M., 190
McMullen, C. C., 308, 325
McMurray, W. R., 23
McNelly, M. J., 489
MacPherson, H. G., 477, 482, 487, 490
McVicar, D. D., 445
McWirtter, R. W. P., 430
Maddock, A. G., 226, 234
Maesen, M. T. van der, see Trabert-vander Maesen, M.
Magnan de Bornier, B., see Bornier, B. M. de
Magnell, A., 206
Magni, G. E., 559, 561
Mahmoud, H. M., 66, 136
Maick, W. J., 233
Maienschein, F. C., 293, 298
Maier, J. L., 231, 234, 240
Maier-Leibnitz, H., 114
Main, I. G., 5
Main, R. K., 536
Maisel, M., 544
Maisin, H., 501
Maisin, J., 501
Majorana, E., 135
Majumdar, K., 214
Maki, Z., 65
Makower, R. V., 579
Maldague, P., 501
Malvano, R., 20, 21

- Mandel, P., 533, 582
 Mandelstam, S., 35, 37, 51, 52, 54, 55, 56
 Manley, J. H., 278, 328
 Mann, A. K., 21
 Mann, C. K., 233
 Mann, J. E., 466
 Mann, L. A., 482, 490
 Mann, M. G., see Gell-Mann, M.
 Mannelli, I., 62, 83
 Manoilov, S. E., 532
 Marchenko, E. V., 299
 Marchenko, G. I., 528
 Marcovich, H., 541
 Marcus, P. I., 536
 Marcus, S., 543
 Marder, S., 77, 139, 144
 Margerum, D. W., 232
 Maris, Th. A. J., 253, 318
 Mark, H., 10
 Markov, M. A., 61, 64, 80
 Markowitz, S., 167, 179, 190, 191, 192, 193
 Marmier, P., 204
 Marquez, L., 175, 186, 187, 190, 191, 192, 193, 194, 281
 Marshak, R. E., 1, 3, 4, 63, 64, 65, 73, 81, 90, 129
 Marshall, J. F., 2, 3, 4
 Martens, F. H., 445
 Martin, G. R., 161, 191
 Martin, W. J., 205, 210
 Marty, N., 109
 Marvin, J. F., 581
 Marx, G., 66
 Mash, D. R., 478, 483
 Maslan, F., 477, 482, 487
 Mason, G. W., 225, 231, 233, 234, 240
 Mason, H. C., 539
 Massey, B. W., 529
 Massey, H. S. W., 370
 Mather, J. W., 419
 Matheson, R. M., 356
 Matinian, S. G., 89, 90
 Matli, G., 543
 Matney, T. S., 562
 Matsudaira, H., 536
 Matsuyama, S., 51
 Matthews, R. R., 443, 467
 Maun, E. K., 206, 209
 Maury, P. B., see Bonet-Maury, P.
 Maxson, D. R., 114
 Maxwell, R. D., 216
 Mayer, M. G., 12
 Mayevsky, V., 76
 Mayne, K. I., 161, 191
 Maynes, A. D., 226
 Meadows, J. W., 164, 190, 191, 192, 194, 195, 335
 Medvedev, B. M., 31
 Mee, L. K., 545
 Mefferd, R. B., 527
 Meggers, W. R., 204
 Meinke, W. W., 194, 195, 205, 210, 212, 221, 238
 Mekhedov, V. N., 186, 191, 192, 193, 194
 Melkonian, E., 262, 264, 265
 Meloche, V. W., 212
 Melville, C., 586
 Menardi, S., 20
 Meneghetti, D., 469
 Merrison, A. W., 76, 141, 142, 361
 Merz, T., 538, 558
 Metropolis, N., 164, 165, 166, 171, 172, 174, 175, 176, 177, 179, 183, 184, 279, 324
 Metzger, A. E., 186, 194
 Mewissen, D. J., 540
 Michaelson, H. B., 204
 Michel, L., 67, 73, 147
 Michel, M. C., 265
 Michel, R. G., 481
 Middlemas, N., 23
 Miedema, A. R., 106
 Migdal, A., 5, 17
 Mihelich, J. W., 210
 Milch, L. J., 529
 Millburn, G. P., 171, 172, 190, 191
 Miller, D. R., 167, 176, 177, 192
 Miller, H. H., 212
 Miller, J. M., 159-202; 160, 164, 165, 166, 167, 169, 170, 171, 172, 173, 174, 175, 176, 177, 178, 179, 183, 184, 185, 186, 191, 192, 194, 209, 211, 212, 279, 324
 Miller, R. H., 361
 Miller, R. R., 232, 460
 Miller, R. W., 352, 511
 Millman, J., 344, 347, 351, 353, 358
 Milne, G. R., 481, 489
 Milone, C., 20
 Mills, G. F., 231
 Milton, J. C. D., 289, 291, 292, 303
 Minarik, E. V., 281
 Mirsky, A. E., 532, 538
 Miskel, J. A., 178, 221
 Mitra, S., 572
 Miya, F., 543
 Miyazawa, H., 50
 Moeken, H. P., 215, 216
 Mole, R. H., 533, 540, 553
 Moline, S. W., 231
 Monier, R., 531, 555
 Monson, H. O., 441, 464, 466
 Monsul, R. W., 528
 Mooney, R. C. L., 204
 Moore, C. E., 204
 Moore, D., 557, 558
 Moore, F. L., 230, 241
 Moore, G. E., 212
 Moore, M. S., 261, 263, 316
 Moos, W. S., 539
 Moravcsik, M., 46
 Morehouse, M. G., 525
 Moreton-Smith, M., 227, 228
 Morgan, F., 208, 210, 211
 Morgan, P., 528
 Morinaga, H., 21
 Morita, M., 5
 Morkovin, D., 536, 542
 Morowitz, H. J., 561
 Morozov, V. N., 442, 446, 469
 Morpurgo, G., 61
 Morrison, G. H., 221-44; 221, 222, 225, 232, 237
 Morrison, H., 164
 Morrison, P., 8, 13
 Mortimer, R. K., 559, 560, 561
 Morton, G. A., 356
 Moskaleva, L. P., 186, 192, 193, 194
 Moskowsky, S. A., 107, 151
 Moss, W. T., 524
 Mostovaya, T. A., 301
 Motta, E. E., 203, 207, 208, 210, 211
 Moustacchi, E., 538, 557
 Mowll, J. U., 482
 Muehlhause, C. O., 134
 Muirhead, H., 164
 Mukhin, K. N., 294
 Mundy, R. J., 232
 Munir, B. A., 192
 Munro, T. R., 587
 Muntz, J. A., 531
 Murakami, U., 502
 Murin, A. N., 160, 192, 193, 194
 Murphy, D. P., 514, 515
 Murray, C. B., 570
 Musser, D. G., 581
 Myers, L. S., Jr., 556
 Mytareva, L. V., 532

N

- Nadelhaft, I., 77, 139, 144
 Nakagawa, S., 185, 192
 Nakanishi, Y. H., 581
 Nambu, Y., 37, 39, 43, 51
 Nasuhoglu, R., 316
 Nathan, O., 110
 Nathans, R., 15, 18, 75, 115, 119
 Neary, G. J., 571, 572
 Nebel, B. R., 582
 Nelson, A., 530
 Nelson, C. M., 204, 205, 206, 208, 210
 Nelson, F., 211
 Nelson, G. F., 212
 Nemchinskaya, V. L., 532

Nereson, N., 295
 Nervick, W. E., 186, 193
 Nervik, W. E., 180, 181,
 191, 195, 285, 311
 Nethaway, D. R., 180, 181,
 193, 195, 311
 Neumann, H. M., 214, 215,
 234
 Neuzil, E. F., 282, 285,
 312, 315
 Newby, G. A., 444
 Newcomb, W., 407
 Newton, J. C., 249
 Newton, R. G., 4
 Newton, T. D., 288, 319,
 324
 Nicholson, A. F., 3
 Nicholson, R. B., 467
 Nicholson, W. J., 306, 328
 Nicolaev, F. A., 22
 Niday, J. B., 190
 Niggli, H. F., see Fritz-
 Niggli, H.
 Nikitina, N. V., 326
 Nikolaev, M. N., 442, 446,
 469
 Nikol'skiĭ, B. A., 68, 164
 Nilan, R. A., 558
 Nilsson, M., 20
 Nilsson, S. G., 16
 Nishijima, K., 73
 Nishijima, R., 61
 Nobles, R. A., 277, 282,
 284, 306, 312
 Nodiot, H., 539
 Noe, J., 357
 Nomoto, S., 185, 192
 Noonan, T. R., 500, 501
 Nordberg, M. E., 114
 Nordin, P., 82, 83
 Norman, A., 560
 Norman, V., 206
 Northrop, J. A., 257, 258,
 259, 263
 Northrop, T. G., 395
 Nossouff, V. G., 317
 Novák, L., 543
 Novey, T. B., 75, 110, 111,
 115
 Novick, M., 441, 466, 467
 Novikov, V. A., 281
 Novikova, N. R., 185, 192,
 195, 285
 Noyes, H. P., 54, 58
 Noyes, W. D., 545
 Nygaard, O. F., 534
 Nyman, M. A., 527

O

Oberle, E. M., 561
 O'Brien, J. P., 494, 496,
 497
 Occleshaw, V. J., 234
 O'Connor, P. R., 195
 Odian, A. C., 23
 Oehme, R., 31, 33, 39, 50,

51, 65
 Oeser, J., 363
 Oftedal, P., 541
 Ogawa, S., 84
 Ogg, J. E., 562
 Oginsky, E. L., 581
 Okada, S., 529, 530
 Okamoto, K., 6, 13, 15
 O'Kelley, G. D., 191
 Okonov, E. O., 61
 Okrent, D., 441, 445, 446,
 454, 455, 466, 467
 Okubo, S., 81, 90
 Okudaira, K., 185, 192
 Okun', L. B., 61-98; 61,
 65, 68, 72, 86, 89, 90,
 92, 93
 Olds, A., 445
 Oleksa, S., 134
 Oliver, R., 533, 534, 545,
 577
 Olson, K. B., 544
 Oneda, S., 85
 O'Neill, G. K., 2, 359
 Oppenheimer, J., 73
 Ord, M. G., 523-52; 523,
 529, 530, 532, 533, 534,
 536, 543, 578
 Orear, J., 82, 83
 Orndoff, J. D., 444, 452
 Orr, W. C., 191, 192
 Osawa, S., 538
 Osborne, L. S., 5
 Osborne, R. N., 174, 175,
 181, 184, 190, 191, 194,
 195
 Osher, J., 430
 Osokina, R. M., 20
 Ostroumov, V. I., 161,
 181, 183, 193, 194, 195,
 281
 Oswalt, R. L., 211
 Otarova, G. K., 558
 Otarowa, G. K., 537
 Otis, E. M., 509, 511
 Ottolenghi, A., 528

P

Paehler, J. H., 313
 Page, L. A., 110, 111
 Paik, W. K., 531
 Pain, R. H., 531
 Paine, S. H., 468
 Pais, A., 85, 90, 92
 Pal, Y., 62, 91, 92
 Palevsky, H., 316
 Palfrey, T. R., 23
 Palmer, W., 533, 535
 Pandre, E. M., 528
 Panov, A. A., 261
 Pantlitschko, M., 526
 Paoletti, P., 527
 Paoletti, R., 527
 Paolini, F. R., 20
 Pappas, A. C., 195, 322,
 323

Parchwitz, H. K., 544, 582
 Parizek, J., 533
 Parker, D. R., 573
 Parker, G. W., 204, 205,
 207, 209, 210, 328
 Parkins, W. E., 481, 482,
 489, 490
 Parrott, M., 215, 216
 Partanen, C. R., 576
 Pashkov, S. A., 442, 446
 Pate, B. D., 170, 182,
 183, 184, 194, 323, 324
 Patlach, A., 353
 Patro, A. P., 110
 Patten, R. B., 362
 Patterson, P. A., 497
 Patton, B. J., 21
 Paul, H., 76, 141, 142,
 361
 Paul, J., 535
 Pauli, W., 104, 136, 139
 Pavlotskaya, F. I., 160,
 192, 194, 195
 Paxton, H. C., 437-72; 445,
 446
 Peachey, L. D., 529
 Peacock, R. N., 108, 111
 Pease, R. S., 430
 Peaslee, D. C., 65
 Pederson, D. O., 351
 Peed, W. F., 204
 Peelle, R. W., 293, 298
 Peierls, R. E., 66
 Pelc, S. R., 545
 Pelekhov, V. I., 299
 Pelligot, E., 232
 Penfold, A. S., 6, 21
 Pen'kina, V. S., 193, 194,
 195, 285
 Penman, S., 353
 Penner, S., 21
 Pentz, E. I., 524
 Peppard, D. F., 231, 233,
 234, 235, 240
 Perfilov, N. A., 161, 181,
 183, 185, 192, 193, 194,
 195, 281, 285, 305, 306,
 335
 Perkins, D. H., 167, 184, 192
 Perkins, J. F., 134
 Perlman, I., 178, 182, 186,
 187, 190, 191, 192, 193,
 194, 215, 216, 311
 Perlman, M. L., 178
 Perrier, C., 203, 209,
 210, 212
 Perring, J. K., 319
 Perry, A. M., 2
 Perry, R. P., 583
 Petersen, D. F., 529
 Petersen, R. E., 442, 444,
 468
 Peterson, V., 190
 Peterson, V. Z., 2
 Petrakis, N. L., 535
 Petree, B., 15, 16
 Petri, N., 235, 237

- Petrzhak, K. A., 246
 Phillips, J., 430
 Phillips, J. A., 419, 430
 Phillips, R., 190
 Phillips, R. J. S., 575
 Philpot, J. St. L., 528
 P'ianov, I. I., 164, 195, 281
 Piatt, J., 496
 Piccardi, G., 214
 Pickering, J. E., 526
 Pierle, C. A., 232
 Pieroni, R. R., 6
 Pietri, G., 356
 Pigford, T. H., 478
 Pihl, A., 531, 539
 Plk-Pichak, 271, 284
 Pinkhasik, M. S., 442, 446
 Pinsonneault, G., 515
 Pirrotte, M. G., see Goutier-Pirrotte, M.
 Pitter, J., 515
 Pittman, D. D., 562
 Plail, O. S., 468
 Plano, R., 62, 76, 83, 141, 142, 361
 Plano, R. J., 147
 Platzman, R. L., 215
 Plummer, G., 514
 Polikanov, S. M., 282, 284, 285
 Polivanov, M. K., 31
 Polkinghorne, J. C., 73
 Pollard, E. C., 528, 563, 564, 565, 566
 Polubarinov, I. V., 65
 Pomeranchuk, I. Ya., 74
 Pomerat, C. M., 535, 581
 Ponomarenko, N. E., 530
 Pontecorvo, B., 65
 Pontecorvo, B. M., 92
 Popjak, G., 527
 Poppema, O. J., 109, 111
 Porile, N. T., 183, 186, 193, 194
 Porter, B. W., 528
 Porter, C. E., 263, 264
 Pospelov, A. N., 20
 Pospisil, M., 543
 Post, R. F., 367-436; 397, 424, 427
 Postma, H., 106
 Potter, R. L., 545
 Potter, V. R., 533, 534
 Powell, H. S., 215, 216
 Pozdnyakov, A. A., 193
 Preiss, J. W., 564
 Preiswerk, P., 204
 Prentki, J., 61
 Preobrazhenskii, B. K., 160, 192, 193, 194
 Present, R. D., 253, 321
 Preston, A., 531
 Preston, R. S., 110
 Price, G. A., 20
 Primakoff, H., 77, 83
 Proctor, B. E., 539, 561, 587
 Prodell, A., 62, 76, 83, 141, 142, 361
 Prokhorova, L. I., 301, 302
 Prokoffieva, E. I., 185, 192, 195, 285
 Prokof'ev, Yu. A., 62, 75, 106, 134, 136
 Prokoshkin, Iu. D., 190, 191
 Prokovskii, V. N., 193
 Protopopov, A. N., 335
 Proust, J., 576
 Puck, T. T., 536, 542, 553, 562
 Pugh, S. F., 468
 Puppi, G., 50, 62, 65, 141
 Purser, P. R., 526
 Pursey, D. L., 136
 Pyatt, K. D., 4
 Pyle, R. V., 190, 191, 421, 427
- Q
- Quastler, H., 534
 Quimby, E. H., 509
- R
- Rabinowitz, P., 169, 170, 175, 176, 183, 184, 279
 Raboy, S., 316
 Radkevich, I. A., 261
 Ragan, N., 527
 Raleigh, D. O., 167
 Ramsden, S. A., 430
 Ramsey, N. F., 190, 191
 Rand, R. N., 524
 Rand, S., 7, 10, 11, 12, 13, 14
 Randle, T. C., 190
 Randolph, M. L., 569, 573, 574
 Rapoport, C. Ia., 544
 Rappaport, D. A., 537
 Rathgen, G. H., 525, 526, 528, 532, 579
 Ratner, B. S., 20
 Rauschkolb, D., 535
 Raventos, A., 496
 Reardon, W. A., 445
 Reasbeck, P., 192
 Rebeyrotte, N., 554, 556
 Redgate, E. S., 533
 Redman, W. C., 450
 Reed, J., 207, 209
 Reed, L., 82, 83
 Regier, R. B., 316
 Reibel, K., 21
 Reich, H., 353
 Reichle, L. F. C., 489
 Rein, J. E., 233
 Reines, F., 133, 134, 136
 Reitz, R., 281
 Rekemeyer, M. L., 584
 Rekers, R. E., 501
 Renne, K. K., 442, 446
 Reston, J. F., 501
 Revell, S. H., 572
 Reyes-Brion, M., 497
 Reynolds, E., 514
 Rhodes, J. L., 21
 Riabinkin, V. I., 23
 Rice, R. E., 441, 445, 446
 Richard, M. J., 227
 Richey, E. O., 526
 Richmond, J. E., 533, 534
 Richter, B., 356
 Richter, H., 210
 Riddell, R. J., 395
 Ridgeway, L. P., 497
 Ridley, B. W., 109, 111
 Rigby, M., 77, 78
 Riggs, H. E., 500, 501
 Riley, C. J., 226
 Rinehart, M., 147
 Ring, S. O., 191
 Ringo, G. R., 75, 115, 316
 Risdon, E. J., 226
 Roach, W. H., 456
 Roberts, J. E., 395
 Roberts, J. H., 294, 450
 Roberts, J. T., 482, 490
 Roberts, L. D., 328
 Robertson, D. S., 227
 Robertson, H. H., 5
 Robins, A. B., 531
 Robson, H. H., 532
 Robson, J. M., 75, 113, 115, 119
 Roddis, L. H., 473
 Rodesch, J., 533
 Rodionov, V. M., 528
 Roeland, L. W., 316
 Roganov, V. S., 23
 Rogers, K. C., 147
 Rogers, L. B., 206, 212
 Rogers, R. W., 584
 Rogosa, G. L., 204
 Rohrllich, F., 34
 Roland, M., 515
 Romanova, T. A., 195
 Roodyn, D. B., 528
 Rose, H., 445, 516
 Rosen, L., 294, 295
 Rosenbaum, E. R., 61
 Rosenbluth, M., 65, 141, 397, 404, 411, 420, 421
 Rosenfeld, A. H., 61, 62, 82, 83, 85, 90, 91, 93, 190
 Rosenfield, G., 525
 Rosenson, L., 68, 147
 Rosenzweig, N., 445
 Ross, A. A., 10
 Ross, M., 107, 152
 Rosser, W. G. V., 164
 Rossi, A., 108, 109, 111
 Rossoff, A. L., 344, 346, 347, 351
 Rossotti, F. J. C., 234

Rotblat, J., 531, 587
 Rotfel'd, L. S., 524
 Roth, J. S., 530
 Rotherm, T., 109
 Rothschild, M. C., 556
 Rothstein, A., 559, 580
 Rowland, F. S., 179, 185,
 190, 191, 192, 193, 194
 Rowley, E. L., 226
 Rozman, I. M., 587
 Rubbino, A., 20
 Ruby, S. L., 114
 Ruch, J. W., 207, 209
 Ruderman, M. A., 33, 76,
 141, 145, 146
 Rudik, A. P., 65
 Rudstam, G., 159, 164,
 167, 169, 174, 175, 191,
 192
 Rugb, R., 493-522; 495,
 496, 497, 499, 502, 503,
 505, 507, 509, 514
 Rulfs, C. L., 205, 210,
 212
 Rupe, C. O., 528
 Russell, C. P., 516
 Russell, J., 361
 Russell, L. B., 501, 502,
 574
 Russell, W. L., 501, 502,
 574
 Rustad, B. M., 113, 114
 Rustgi, M. L., 3, 4, 5, 6,
 19
 Ryan, F. J., 562
 Rydberg, J., 233

S

Sachs, R. G., 91
 Sadowsky, H., 348
 Saha, M., 380
 Sailor, V. L., 261, 262,
 263
 Sakata, S., 64
 Sakurai, J. J., 62, 63, 65,
 66, 90, 129
 Salam, A., 66, 102, 139
 Salant, E. O., 83
 Salganic, R. I., 536
 Salter, D. C., 190
 Salzman, G., 50
 Samios, N., 62, 76, 83,
 141, 142, 361
 Sams, J., 562
 Sanasrabudhe, M. B., 525
 Sandeen, G., 529
 Sanders, J. E., 265, 445,
 446, 450, 469
 Sandmeier, H. A., 441, 466
 Santangelo, R., 62, 83
 Santchi, P., 351
 Santos, M. D. de S., see
 Souza Santos, M. D. de
 Saplakoglu, A., 265
 Sarachek, A., 560
 Sargent, C. P., 20, 147
 Sato, T., 232
 Sauerbier, W., 580
 Saunders, B. G., 204
 Savage, H. W., 482, 490
 Savolainen, A. W., 482,
 490
 Sawada, S., 86, 90
 Sawicki, J., 4, 19, 21
 Sawyer, G. A., 419
 Sax, K., 536
 Scadden, E. M., 230
 Scallettar, R., 445
 Scargill, D., 232
 Scarlett, R. M., 349, 350
 Schabadasch, A. L., 544
 Schacht, L. E., 572
 Schaeffer, O. A., 161, 185,
 191
 Schafer, W. D., 289
 Scharenberg, R., 361
 Schechter, L., 171, 172
 Schenkerman, S., 346
 Scherb, F., 23
 Scherer, E., 530
 Scherrer, P., 21, 204
 Schiff, L. I., 2, 3, 4
 Schimmer, B., 114
 Schinz, H. R., 496
 Schjeide, O. A., 527, 496
 Schlegel, B., 529, 530
 Schluter, A., 395
 Schmidt, A., 556
 Schmitt, R. A., 256, 316
 Schneider, H., 335
 Schneller, Sister M. B.,
 497
 Schnitzer, H., 50
 Schomer, R. T., 482, 490
 Schopper, H., 110
 Schou, J., 556
 Schraidt, J. H., 468
 Schreier, K., 525
 Schriever, B. D., 2
 Schröder, W., 526
 Schubert, G., 526, 528,
 533, 539, 540
 Schuck, E. A., 523
 Schwartz, D., 570
 Schwartz, M., 76, 83, 141,
 142, 361, 562
 Schwartz, N., 62
 Schwartz, R. B., 259, 265,
 437, 439
 Schwarz, H. P., 500, 501,
 527
 Schwarzschild, A., 109,
 113, 114
 Schwarzschild, M., 410,
 419
 Schwimmer, S., 579
 Schwinger, J., 66, 104
 Schwingamer, E. A., 561
 Scott, K. G., 216
 Scribner, B. F., 204
 Seaborg, G. T., 167, 176,
 177, 186, 192, 194, 195,
 204, 246, 247, 265, 269,
 270, 271, 285, 302, 305,
 307, 308, 310, 311, 312,
 313, 314
 Searcy, R. L., 525
 Seelich, F., 526
 Seelmann-Eggebert, W.,
 210
 Segrè, E., 203, 204, 209,
 210, 212, 213, 214, 215,
 216, 281
 Sehter, V. M., 64, 68, 79,
 82, 83
 Semenov, W. A., 326
 Sen Sarma, R. N., 209, 211
 Senseman, R. W., 190
 Sensenbrenner, M., 582
 Seppli, E. J., 265
 Serber, R., 162, 163, 188
 Sergeant, P., 109
 Serpe, J., 139, 140
 Serres, F. J., Jr., de,
 562
 Setlow, J., 565
 Seymour, A. H., 495
 Shafranov, V., 421
 Shamov, V. P., 161, 181,
 183, 184, 185, 192, 193,
 194, 195, 279, 281, 285,
 335
 Shankel, D. M., 562
 Shanstrom, R. T., 478
 Shapira, R., 541, 542
 Shapiro, G., 353
 Shapiro, I. S., 76
 Sharp, R. A., 177, 178,
 191, 192
 Sharp, W. T., 164
 Shepherd, L. R., 445, 454
 Sheppard, C. E., 573, 574
 Sherer, E., 582
 Sherman, F. G., 534
 Sherman, L. E., 442, 446,
 469
 Shevchenko, V. G., 23
 Shields, H., 554, 555
 Shipley, E. D., 428
 Shore, F. J., 261, 262,
 263
 Shoupp, W. E., 482, 489,
 490
 Shtern, L. S., 544
 Shudde, R. H., 195
 Sidgwick, N. V., 215
 Sidorov, V. M., 192
 Siebert, R. A., 537
 Siegel, R. T., 77, 139,
 144
 Signell, P. S., 1, 3
 Sikov, M. R., 500, 501
 Silk, M. H., 526
 Silva, E., 6
 Silvestrini, V., 62, 83
 Simanton, J. R., 441, 464,
 466
 Simmons, W. R., 441,
 464, 466
 Simon, A., 397, 404, 406,

- 428
 Simon, K. A., 527
 Simonoff, G., 194
 Simons, S., 527
 Simonson, C., 527
 Singer, J. R., 353
 Singer, T. P., 531
 Sipe, C. R., 507
 Sirlin, A., 68, 147
 Sironen, R. J., 225, 233
 Sironval, C., 581
 Sisakian, N. M., 529
 Sitenko, A. G., 19, 415
 Sites, J. R., 205
 Sizeland, M. L., 208, 210, 211
 Sjoblom, R. K., 289, 298, 309
 Skarsgard, H. M., 160, 194
 Skliarevskii, V. V., 299, 325
 Skoda, J., 533
 Skreb, Y., 544, 583
 Skyrme, D. M., 181, 281
 Skyrme, T. H. R., 61
 Slätis, H., 294
 Slavin, M., 212
 Slotin, L., 445
 Small, M. D., 523
 Smellie, R. M. S., 535
 Smirenkin, G. N., 301, 302, 442, 446, 469
 Smith, A. B., 289, 294, 298, 309, 445
 Smith, E., 215
 Smith, F. A., 441, 462
 Smith, F. E., 585
 Smith, G. W., 230
 Smith, H. A., 482, 489
 Smith, H. H., 576
 Smith, J. H., 23
 Smith, J. R., 316
 Smith, J. S. K., see Kirby-Smith, J. S.
 Smith, K. C., 530
 Smith, L., 395
 Smith, L. H., 541, 542
 Smith, M. M., see Moreton-Smith, M.
 Smith, R. D., 445, 446, 450, 469
 Smith, R. K., 277
 Smith, R. R., 441, 466
 Smith, T. D., 226
 Smith, W. T., Jr., 204, 205, 206, 208, 209, 210
 Smith, W. W., 543
 Smorodinsky, Ya. A., 61, 75, 256
 Snezhko, A. D., 526
 Softky, S. D., 191, 192
 Soga, M., 16
 Sokurova, E. N., 586
 Soley, M. H., 216
 Solnitz, F. T., 62, 82, 83
 Solov'ev, V. G., 194
 Sonnenblick, B. P., 584
 Sørensen, S. O. C., 166, 184, 187, 192
 Sosa, A., 555
 Sosa-Bourdouill, C., 555
 Soška, J., 578
 Sosnovskii, A. N., 62, 75, 106, 134, 136
 Souza Santos, M. D. de, 6
 Spalding, J. F., 501, 574
 Spalding, T. R., 441, 464, 466
 Sparrow, A. H., 544, 561
 Spear, F. G., 523
 Speert, H., 509
 Spence, R. W., 180, 245
 Spinrad, B. I., 445
 Spiridonov, V. M., 5
 Spitkovskii, D. M., 531
 Spitzer, L., 372, 398, 403, 404, 406, 422, 431
 Spivak, P. E., 62, 75, 106, 134, 136
 Spoerl, E., 535, 577
 Srivastava, R. D., 206
 Stabile, J. N., 529
 Staebler, U. M., 489
 Stafford, G. H., 2
 Stähelin, P., 99, 114
 Stakhanov, V., 82
 Stanghellini, A., 50, 54
 Stapleton, G. E., 544, 580
 Starr, P., 516
 Stavinski, V. S., 11, 13
 Stavitsky, Iu., Ya., 442, 446, 469
 Steadman, L. T., 524
 Stearner, S. P., 541
 Stech, B., 107, 110, 111, 129
 Steenland, M. J., 106
 Steffen, R. M., 110
 Stein, J. A., 543
 Stein, P. C., 23
 Stein, W. E., 289, 291, 292, 294, 308
 Steinberg, E. P., 221, 306, 308, 311, 316
 Steinberger, J., 62, 66, 67, 76, 83, 141, 142, 361
 Steiner, H. M., 181, 194, 195, 278, 281, 285
 Stenstrom, K. W., 581
 Stepanov, E. P., 299, 325
 Stepanov, K., 415
 Stephens, W. E., 20, 21
 Stevenson, M. L., 62, 83
 Stevenson, P. C., 167, 180, 181, 186, 191, 195, 221, 289, 311
 Stewart, A., 516
 Stewart, D. B., 192
 Stewart, H. V., 346
 Stewart, R., 445, 527
 Stickforth, J., 379
 Stier, P. M., 387
 Stix, T. H., 407, 432
 Stocken, L. A., 523-52, 523, 529, 530, 531, 532, 533, 534, 536, 543, 578
 Stockwell, A., 527
 Stokes, R. H., 257, 258, 259, 263
 Stoll, P., 21
 Stone, J. M., 427
 Stone, W. S., 576
 Storm, M., 164, 165, 166, 171, 172, 174, 175, 176, 177, 179, 183, 184, 279, 234
 Storm, M. L., 437
 Storto, E., 482, 490
 Story, J. S., 319
 Stovall, E. J., Jr., 419
 Stoyler, R. J. B., see Blin-Stoyler, R. J.
 Strang, V. G., 501
 Stratton, T. S., 419
 Stratton, W. R., 444, 467
 Strauss, B. S., 553
 Streat, L. P., 516
 Streater, R. F., 88
 Streifus, C. A., 483
 Streisinger, G., 569
 Stroller, S. M., 481, 483, 489
 Strominger, D., 204, 305
 Stroot, J. P., 110
 Strutinskii, V. M., 280, 325, 328, 329, 330, 332, 333, 335
 Stuy, J. H., 577
 Sudarshan, E. C. G., 63, 65, 73, 81, 90, 129
 Sugahara, Y., 84
 Sugarman, N., 171, 181, 182, 183, 186, 192, 193, 194, 210, 285, 290, 335
 Sugawara, M., 2, 3
 Sugihara, T. T., 192, 309, 311
 Suippold, H. E., 559
 Sukhoruchkin, S. I., 261
 Sukhov, L. V., 195
 Summers-Gill, R. G., 18
 Sunyar, A. W., 99, 110, 111, 114, 354, 360
 Suran, J. J., 351
 Surkova, L. V., 68
 Sutow, W., 514
 Sutow, W. W., 514, 515
 Sutton, H., 568
 Svijsda, J., 515
 Swanson, C. P., 538, 558
 Swanson, R. A., 190
 Swartz, C. E., 190
 Swiatecki, W. J., 249, 253, 260, 261, 309, 317, 318
 Swickard, E. O., 442, 468
 Symanzik, K., 31, 40, 42

Symonds, J. L., 190
 Symonds, N., 569
 Sympson, R. F., 205
 Szonyi, S., 526

T

Tabachnick, J., 530
 Taft, H. D., 82, 83
 Tait, J. H., 454, 467
 Takagi, S., 7, 14
 Tallentire, A., 558
 Tamai, E., 185, 192
 Tanada, R., 579
 Tanaka, S., 65
 Tannenwald, L. M., 376
 Tarrago, X., 194
 Tarumov, E. Z., 193, 194, 195, 285
 Tatlock, J., 443, 467
 Tau, L., 361
 Taub, H., 344, 347, 351, 353, 358
 Tausner, M., 147
 Tayler, R., 421
 Taylor, A. E., 77, 139, 144
 Taylor, H. E., see Ephrussi-Taylor, H.
 Taylor, J., 31, 33, 46
 Taylor, J. C., 73, 88
 Taylor, J. G. V., 21
 Taylor, T. B., 163
 Teitelbaum, P. D., 473, 474, 476
 Telegdi, V. L., 75, 115
 Teller, E., 396, 409
 Temmer, G. M., 110
 Temple, D. M., 533, 540
 Templeton, D. H., 159, 188, 193, 194, 195, 290
 Tennant, R. M., 361
 Terent'ev, V. V., 246, 249
 Terracini, O., 20
 Terrell, J., 296
 Deutsch, W. B., 81, 90
 Tewes, H. A., 192
 Thaler, R. M., 1, 3
 Thalgot, F. W., 441, 445, 466, 469
 Thirring, W. E., 6, 8, 22
 Thoday, J. M., 570
 Thode, H. G., 308, 325
 Thomas, G. E., 261, 263, 316
 Thomas, R. G., 263, 264
 Thomason, P. F., 207
 Thompson, S. G., 294, 295, 298
 Thompson, W. B., 390
 Thomson, G. P., 408
 Thomson, J. J., 408
 Thomson, R. Y., 535

Thomson, S. J., 161, 191
 Thoneman, P., 430
 Thonnard, A., 530
 Thornton, R. L., 190
 Thorpe, B. D., 543
 Tiapkin, A. A., 190, 191
 Ticho, H. K., 83
 Tidball, R. A., 460
 Till, J. E., 565, 566
 Timma, D., 204
 Timnick, A., 313
 Tiomno, J., 65, 141, 147
 Titov, N. E., 160, 194
 Titterton, E. W., 1
 Tobias, C. A., 559
 Tobin, M. J., 497
 Tocnaka, H., 62
 Todd, R., 228
 Tolbert, N. E., 580
 Tolhoek, H. A., 106, 133
 Tollestrup, A. V., 2, 76, 141, 142, 361
 Tomizawa, J., 567
 Toms, D. J., 554
 Toms, M. E., 1, 20
 Tongur, V. S., 531
 Tonkinson, S. M., 571
 Toppel, B. J., 469
 Toropova, G. P., 532
 Trabert-van der Maesen, M., 582
 Trebukhovskiy, Y. V., 75
 Treiman, S. B., 58, 70, 73, 76, 77, 81, 83, 85, 91, 130, 131, 144, 146, 152
 Tribalat, S., 209, 211, 236
 Tribuno, C., 20, 21
 Tripp, R. D., 62, 82, 83
 Trocki, T., 462
 Tuck, D. J., 224
 Tuck, J. L., 419, 427, 430, 431
 Tulchin, H., 349
 Tul'seva, N. M., 561
 Tunnicliffe, P. R., 265
 Turkevich, A., 164, 165, 166, 171, 172, 174, 175, 176, 177, 179, 183, 184, 190, 192, 279, 324
 Turner, C. J., 468
 Turner, J. F., 109, 111
 Turovskii, V. C., 533
 Tuttle, L. W., 497
 Tyree, S. Y., Jr., 206
 Tyren, H., 190
 Tzara, C., 6

U

Ullman, G., 525
 Ullmann, J. W., 477
 Umland, F., 237
 Ukraintsev, F. I., 442, 446, 469

Underwood, M., 353
 Upham, H. C., 524
 Upton, A. C., 542
 Uretsky, J., 46
 Uretz, R. B., 584
 Urso, P., 542
 Usachev, L. N., 442, 446, 469

V

Vaks, V. G., 77, 78
 van Bekkum, D. W., see Bekkum, D. W. van
 van de Berg, A., see Berg, A. van de
 Vandenbosch, R., 183, 266, 269, 270, 271, 272, 279, 280
 van der Brenk, H. A. S., see Brenk, H. A. S. van der
 Vanderhaeghe, F., 544
 Van der Leun, C., 106, 107, 113
 van der Maesen, M. T., see Trabert-van der Maesen, M.
 Van der Meer, C., 541
 Van Lancker, J., 533, 534
 Van Ommeslaghe, B., 478
 Varshni, Y. P., 214
 Várterész, W., 526
 Vaughan, B. E., 544
 Vendrely, R., 536
 Venkataraman, P. R., 524
 Verain, A(lice), 586
 Verain, A(ndré), 586
 Verber, F., 441, 464, 466
 Vermund, H., 581
 Vernois, J., 230
 Vilain, J. P., 586
 Villaca, S. S., 6
 Vincendon, G., 582
 Vinogradov, A. P., 160, 192, 194, 195
 Vise, J. B., 109
 Visscher, W. M., 18
 Vladimirovskii, V. V., 304
 Vladimirovsky, V. V., 75, 261
 Vogel, B., 531
 Vogel, H. H., Jr., 583
 Vogell, W., 530, 582
 Voitovetskii, V. K., 299
 Völker, W., 526
 Volkov, Yu. M., 23
 von Borstel, R. C., see Borstel, R. C. von
 VonderLage, F. C., 482, 490
 von Goeler, E., see Goeler, E., von
 Voorhees, B. G., 490
 Vorbrodt, A., 531

- W
Wada, I., 234
Wäffler, H., 21
Wagner, G. D., 191
Wagner, H. A., 442
Wagner, J. J., 134, 325
Wahl, A. C., 213, 308
Wakasa, A., 84
Walecka, J. D., 11, 23
Walker, W. H., 437
Walker, W. M., 482, 489
Wall, P. E., 530
Waloschek, P., 62
Walsh, J. H., 353
Walter, M., 21
Walton, G. N., 468
Wandel, C. F., 163, 193
Wapstra, A. H., 110, 119, 124
Wardle, G., 161, 191
Warf, J. C., 232
Warren, J., 190
Warren, J. E., 192
Warburg, O., 526
Ward, F. R., 481, 489
Ward, S., 430
Ware, A. A., 419
Warner, W. L., 527
Warshaw, S. D., 190
Watkins, I. W., 587
Watson, K. M., 165, 166, 188, 417
Watt, B. E., 294
Wattenberg, A., 23
Watts, E., 565
Webb, J., 516
Weber, C. E., 468
Weber, D., 515
Webster, J. W., 478, 483
Webster, W., 481, 489
Webster, W. W., 527
Wegner, H., 169
Weidmüller, H. A., 20
Weinberg, A., 515
Weinberg, A. M., 437
Weinberg, S., 73, 76, 81, 90
Weinman, E. O., 527
Weinrich, M., 148
Weinstein, R. M., 23
Weinstock, E. V., 20
Weisner, E. F., 481, 482, 490
Weiss, J., 530
Weiss, M. S., 15, 16
Weisskopf, V., 168
Weisskopf, V. F., 11, 23, 324
Welander, A. D., 495
Wells, F. H., 358, 359, 362
Wendlandt, W. W., 233
Wenzel, W. A., 83
Werder, A. A., 528
Werle, J., 90
Werner, F. G., 249
Werner, R. C., 460
Werner, S. C., 509
West, E., 514, 515
Weston, W. J., 579
Wetherell, A. M., 77, 78
Weyl, H., 139
Weymouth, P. P., 530, 578
Whalin, E. A., 2
Wheeler, J. A., 65, 141, 147, 183, 184, 245, 249, 250, 252, 256, 262, 265, 316
Whetsel, H. B., 231
Whetstone, A., 2
Whetstone, S. L., 302, 303, 304
Whetstone, S. L., Jr., 292, 294
White, F. A., 265
White, J. C., 230, 233
White, R. H., 444
Whitehead, C., 23
Whitehouse, W. J., 245, 246
Whiting, A. R., 575
Whitman, G. D., 482, 490
Whitmore, G., 528, 565
Wick, G. C., 61, 73, 163, 194, 195
Widmaier, W., 355, 356
Wiechmann, F., 205
Wiegand, C., 193, 194, 195, 285
Wielgoz, K., 183, 194, 290
Wigner, E. P., 102
Wiig, E. O., 191, 192, 193
Wilbur, K. M., 528
Wildermuth, K., 14
Wilets, L., 245, 251, 264, 327
Wilhelmsson, H., 20
Wilkerson, M. C., 527
Wilkinson, D. H., 1-28; 2, 7, 9, 11, 12, 13, 15, 16, 19, 20, 21
Wilkinson, G., 177, 178, 191
Williams, C., 482, 490
Williams, C. M., 525
Williams, D. G., 482
Williams, L. A., 211
Williams, L. R., 468
Williams, N. L., 482, 489
Wills, E. D., 528
Wilson, C. W., 540
Wilson, D., 563, 564
Wilson, E., 206, 210
Wilson, H., 23
Wilson, J. E., 543
Wilson, J. G., 498
Wilson, R., 1
Wilson, R. R., 3
Wimett, T. F., 439, 444
Winhold, E. J., 21, 256, 325, 328, 332
Winningstad, C. N., 362
Winsberg, L., 174, 193
Wish, L., 226
Wittekindt, E., 582
Wittern, H., 14
Woese, C. R., 561, 564
Woese, D., 564
Wolfe, H. B., 66
Wolfenstein, L., 76
Wolff, J., 505, 507
Wolff, S., 559, 569, 570, 571
Wolfgang, R. L., 160, 167, 175, 176, 177, 185, 187, 190, 191, 192, 193, 194
Wolke, R. L., 194
Woll, H. J., 353
Wong, D., 54, 58
Wong, H. S., 39, 54
Wood, D. P., 445
Wood, T. H., 537, 557, 559, 560
Woodbury, J. W., 579
Woodgate, P. R., 232
Woodward, V. W., 586
Woodward, W. M., 2
Wooley, R., 380
Wormald, J. R., 77, 78
Worthington, W. J., Jr., 167, 192
Wrigge, F. W., 205
Wright, P., 515
Wright, R., 421
Wright, S., 515
Wright, S. C., 190, 191, 192, 193, 289
Wu, C. S., 99, 100, 104, 109, 114, 205
Wyatt, L. M., 468
Wyld, H. W., 77, 130, 131, 146
Wyman, M. E., 134, 325
Wyss, O., 576, 562
Y
Yaffe, L., 182, 194, 323, 324
Yakimov, M. A., 192, 193, 194
Yakovlev, Yu. V., 160, 194, 195
Yamada, M., 5
Yamaguchi, Y., 169, 276
Yamazaki, J., 515
Yang, C. N., 37, 61, 64, 65, 66, 73, 76, 99, 102, 130, 139, 141
Yavor, I. P., 23
Yeliseyev, G. P., 109
Yergakov, V. A., 75
Yergin, P. F., 15
Yevick, J. G., 442, 466
Yokelson, B., 353
Yonezawa, M., 84, 86, 90
Yongejans, B., 85
Yost, H. T., Jr., 532, 556
Young, J. D., 190
Yutlandov, I. A., 192, 193, 194

Z

- Zachariasen, F., 3, 58, 88
89
Zachariasen, W. H., 205,
206
Zade, S. A. A., see
Ali-Zade, S. A.
Zaglio, E., 351
Zähringer, J., 161, 185,
191
Zakovsky, J., 526
Zasler, J., 482, 490
Zatsepina, G. N., 20
Zebroski, E., 486
Zebroski, E. L., 478, 488,
489, 490
Zeigler, R. K., 439
Zel'dovich, Ya. B., 37, 64,
73, 76, 77, 91, 92, 107
Zelle, M. R., 562
Zernik, W., 3, 4
Zerwic, M. M., 543
Zhorno, L. Ia., 525
Ziegler, M., 235, 237
Zimmer, K. G., 555, 587
Zimmerman, R. L., 316
Zimmermann, W., 31
Zinn, W. H., 437, 477, 483,
489
Ziporin, Z. Z., 536, 577
Zirkel, R. E., 584
Zobel, W., 293, 298
Zoboli, V., 62
Zolotov, Y. A., 230
Zubkova, S. R., 544

SUBJECT INDEX

A

- Acetylacetone
 - elements extractable by, 229, 240
- Adiabatic hypothesis of motion, 394-95
- Adrenal cortex
 - postradiation changes, 525, 545
- Alfvén wave, 407
- ALICE experiment, 428
- Alkylphosphoric acid system
 - elements extractable by, 230-31
- Alpha-particle anisotropies, 328, 333, 335
 - of bismuth, 334
 - decay and fission, 247
 - emission
 - in fission, 306
 - in heavy elements, 283
 - induced fission, 269-71, 272
 - measurements, 270, 273, 280, 282
 - of plutonium, 334
- Amines
 - protection against irradiation, 541-42
 - epinephrine, 451
 - histamine, 541, 542
 - tryptamine, 541-42
- Amino-aciduria
 - after radiation, 524
 - taurine excretion, 524-25
- S,2-aminoethylisothiuronium
 - protection against irradiation, 542
- Amoeba Pelomyxa
 - irradiation of, 583
- Amoeba proteus
 - nuclear transplantation in, 583
- Amplifiers
 - fast, 357-58
 - linear, 349
 - low-frequency transistorized, 353-54
 - photomultiplier integrating, 348-49
 - series-connected, 358
 - transistorized, 349-51
- Analyzers
 - two-dimensional pulse-height, 363
- Anencephalic larvae, 495
- Angular distributions; see individual particles
- Angular momentum effects, 271-73, 278, 284
- Anisotropy
 - alpha-particle, 328, 333, 335
 - fission-fragment, 325-35
- Anlagen, embryonic and radiation sensitivity, 514
- Anomalies
 - caused by nutritional deficiencies, 517
 - cerebral
 - in mouse egg, 502
 - congenital, 493, 494, 502, 503, 505, 511, 514, 517
 - "critical periods," 502-3, 517
 - in the embryo
 - phenocopies of, 494, 502, 505, 517
 - in frog blastula, 496
 - genetic changes, 503
 - in man, mouse, rat, 502, 512
 - in rat embryo, 499, 500
 - see also Radiation effects; and specific effects
- Anoxia
 - in irradiation, 539, 541
- Antineutrino
 - angular distribution of, 118
 - capture, 133-34
 - energy distribution of, 134
 - orientation of, 134
 - see also Neutrino
- Antiparticle, 139
- Argonne critical assemblies, 445
 - ZPR-III, 445, 447, 448, 454
- Argus experiment, 396
- Ascites tumor cells
 - DNA in, 535
 - irradiation of, 526, 532
 - and nitric oxide, 538
 - and nitrous oxide, 537
 - and oxygen effect, 537
- Assemblies, fast-critical, 443-46
 - critical mass
 - dependence on core shape, 449
 - spherical, 450, 457
 - of uranium cores, 449
 - critical size, 446
 - dilution exponent, 450
 - parameters, 456
 - perturbation data, 446, 450
 - prompt-neutron lifetimes, 455

- Rossi alpha, 452, 454, 455
- spectral characteristics, 450, 452
- Astatine
 - analytical chemistry of, 215, 216
 - back-extraction, 213
 - biological effects, 216
 - compared to iodine, 212-13, 214, 215, 216
 - history of, 204
 - organic chemistry of, 215
 - oxidation potential diagram, 213
 - radiochemical procedures for, 215-16
 - see also Astatine compounds
- Astatine compounds
 - interhalogen, 213, 214
 - organic, 215
 - oxidation states, 213-16
- Astron, 426-27

B

- Bacteriophage
 - host system, 565-66
 - irradiated, 565-66
 - multiplicity reactivation in, 567
 - postinfection sensitivity, 565
 - replication
 - and radiation, 566-69
 - and reactivation recombination, 566-67
 - sensitivity to soft x-rays, 569
 - sensitivity to ultraviolet rays, 569
- Baryon
 - decay of, 70, 71
- Beta coupling, 91-93, 107, 113, 121-22, 124, 130, 149, 152, 154, 155
- general V-A form, 126, 127
- for left-handed neutrinos, 125
- lepton nonconserving, 137
- pseudoscalar, 126, 145-46, 152-53
- V-A Law, 128
- Beta decay, 99-158
 - chain length in fission, 321-24
 - comparative half lives, 106-7, 132
 - double, 135-36, 137
 - of fission fragments, 305

ft-values of, 106-7, 132
 laws of, 99-155
 renormalization effects in,
 129, 150, 152-53
 selection rules, 107-7
 Bismuth, 310-11, 334
 anomalous anisotropy in
 fission, 334
 fission cross section for,
 181
 mass-yield curves for,
 160, 175, 176
 targets
 isolation of astatine from,
 215
 "-Blast" stage
 sensitivity to irradiation,
 499, 514
 in tissue differentiations,
 499
 Boltzmann equation, 397-98
 Breeding ratio, 437-38, 440,
 457, 459
 and neutron capture, 452
 for spherical fast systems,
 463-466
 Bremsstrahlung
 detection of electron polari-
 zation, 110, 115
 electron-electron, 378-79
 electron-ion, 378-79, 383-
 84
 Brink's Identity, 17
 British fast-reactor program,
 443
 critical assemblies, 445-
 46
 Zephyr, 445-46, 447, 452,
 454
 Zeus, 445, 446, 447, 452,
 454
 Dounreay reactor, 443,
 466
 British Zeta pinch apparatus,
 430
 Brueckner theory
 of nuclear matter, 11, 23
 Bullfrog R. catesbiana tad-
 poles
 irradiation of, 496
 refrigeration protection in,
 496

C

Californium 252
 spontaneous fission of, 291,
 292, 294, 298
 Carbohydrate metabolism,
 523-26
 glucose absorption, 523-25
 Carbon
 cross sections
 on uranium 238, 274
 Carbon monoxide
 inhibition of chromosome
 rejoining, 559

Carboxylic acids
 elements extracted with,
 231
 Carlson, B. G., method,
 454-57
 Cationic chelates
 in metal extraction, 231-
 32
 Cellular radiobiology, 553-
 87
 aspects of chromosome
 breakage, 569
 mitotic delay, 571-72
 bacteriophage replication
 radiation and, 566-69
 dosimetry, 587
 insect whole-body radia-
 tion, 586-87
 instrumentation, 587
 microbial survival and
 mutation, 559-63
 EDTA effect on, 563
 mutagenesis
 in higher animals and
 plants, 574-76
 oxygen effect, 557-59
 partial cell irradiations,
 583-84
 photosynthesis, 580-81
 postirradiation biochemical
 changes, 577-81
 postirradiation morphologi-
 cal changes, 581-83
 premature lysis techniques,
 566-67
 shielding experiments, 584
 statistical microscopy,
 563-66
 see also Radiation damage;
 and Radiation effects
 Centrifugal drift, 393, 411,
 422
 Cerenkov counters
 with photomultipliers, 354
 timing errors, 354-55
 Charge and spin variables,
 35-39
 Charge conjugation, 100-5
 CPT theorem, 104, 105
 "time reversal," 104
 noninvariance of beta proc-
 esses, 111
 operator for, 104, 125, 126
 and weak interactions, 65
 Charge distribution
 in fission, 182
 nuclear, 320-25
 at scission, 321
 Charge exchange
 cross sections
 hydrogen in argon gas,
 389
 hydrogen in helium gas,
 387
 hydrogen in hydrogen gas,
 386
 hydrogen in nitrogen gas,

388
 in high-temperature plas-
 mas, 384-87
 Charge separation
 in plasma, 393, 394, 403,
 404, 408, 510-11, 524
 gradient-B drifts, 411
 in Stellarator, 422, 423
 Chelate extraction systems,
 222, 223, 226-30
 Chick embryo
 irradiation of, 496-98
 Chirality transformation
 and weak interaction, 65
 Chloramphenicol
 blocking of protein syn-
 thesis, 577
 effect on radiosensitivity,
 567-68
 Chlorophyll synthesis
 delay of, 580
 Cholesterol metabolism
 after radiation, 527
 Cholinesterase variations
 after radiation, 530
 Chromatography, 211-12
 ion-exchange, 211
 paper, 212
 Chromosomes, irradiated
 aberrations
 chromatid, 572
 chromosome-type, 572
 isochromatid, 572
 in onion-root-tip cells,
 571
 overdispersion of, 571
 and plant height, 571
 subchromatid, 572
 two-break, 569-70
 breakage, 561-74
 double-bridge regime,
 570-71
 mitotic delay, 571-72
 mitotic inhibition of, 584
 and oxygen effect, 572
 RBE experiments, 573-74
 replication timing, 572
 Clementine fast reactor,
 441
 Cobalt
 excitation function
 for spallation reaction,
 177
 Cobalt 60 parity experiments,
 144
 angular distribution
 of beta rays, 103-4
 electron polarization,
 107-8
 Fermi-GT interference,
 106
 on oriented nuclei, 100-4
 spin change, 106
 Collective model
 of the absorption process,
 14-15
 of nuclear photo effect,

- 7, 17, 18
 Combined inversion
 and weak interaction, 65
 Common-emitter configura-
 tion, 344, 347
 Composite model hypothesis,
 93
 Compound nucleus model,
 168
 Continuous ether extractor,
 238, 239
 Conversion ratios (reactors),
 437, 452
 for spherical fast systems,
 459
 Copper
 extraction of, 224, 225,
 227
 fission of, 284, 285
 spallation of, 176-77, 178
 "Corkscrew" instability
 in pinch, 419
 of plasma, 411
 Coulomb collisions
 "close-collision" region,
 371, 372
 Debye shielding length,
 372, 408
 "distant-collision," 371-74
 "relaxation times," 373-
 74
 ion-ion, 377
 transport processes, 371
 between ions and electrons,
 375-78
 dynamical friction,"
 375-76, 377
 Coulomb energy, nuclear, 251
 between fragments, 291
 at scission, 290, 291, 293
 Counters
 coincidence
 transistorized, 360
 see also Cerenkov counter
 Counter telescope method
 of high-energy investiga-
 tion, 161
 Counter telescopes, 161
 in meson experiments,
 361-62
 two-scintillator, 363
 CPT theorem, 104, 105, 122
 Creatine excretion
 and muscle catabolism,
 525
 Critical assembly; see Ar-
 gone, British, Los
 Alamos, Russian crit-
 ical assemblies
 Cross sections
 inelastic
 of bismuth, 171
 for high-energy particles,
 163-64
 measurement, 171-72
 photonicuclear, 4, 5, 6, 8,
 19, 22
 pion-nucleon, 188
 radiative capture
 of protons for thermal
 neutrons, 2
 see also Fission cross
 sections
 Cupferron
 effect on radiosensitivity
 of chromosomes,
 558
 extraction with, 227
 Cysteamine protection
 against irradiation,
 540-41
 of chick embryo, 497
 from cobalt 60, 540
 of marine organism eggs,
 495
 of mouse embryo, 507-8
 in rat liver, 543
 of T2 phage, 541
 Cysteine
 and irradiation, 539-40,
 541, 544
- D
- Debye sphere, 372, 373, 375,
 408, 415
 Decays; see Beta decay;
 Leptonic decay; and
 Strange particles
 Deuterium
 in pinch effect, 421
 primary fusion fuel, 367
 Deuteron
 anisotropies of
 for deuteron-induced fis-
 sion, 333
 in medium-energy region,
 328
 bismuth fission, 334
 experimental deuteron cross
 sections, 4
 fission threshold studies,
 257-58, 259
 photodisintegration of, 1-
 5
 radium fission, 333-34
 Diamagnetism
 of high-temperature plasma,
 401
 Diethyldithiocarbamates
 metal extraction with,
 226-27
 β -Diketones
 metal extraction with,
 229-30
 Dilution exponent
 in reactors, 450, 451
 Dirac equation, 76, 84
 "Dirac" neutrino, 138-39
 Discriminators
 transistorized, 351
 Dispersion relations, 30,
 35, 49, 50
 derivation, 33
 for fixed angular momen-
 tum, 54
 at fixed momentum trans-
 fer, 47-51
 Mandelstam representa-
 tion, 51-59
 microscopic causality
 principle, 30
 nucleon-nucleon, 49
 pion-nucleon scattering,
 30-59
 pion-pion scattering, 51-
 52
 in plasma waves, 408,
 416
 reduction formula, 31
 substitution rule, 34-35
 subtractions in, 48
 see also Poles
 Distribution law
 of solute concentrations
 distribution coefficient
 K_D , 222
 distribution ratio D , 222,
 225, 238
 Dithizone
 elements extractable by,
 227-28
 DNA (deoxyribonucleic acid)
 marker rescue from,
 567
 radiation damage to, 565
 synthesis
 in ascites tumor cells, 535
 causes, 578
 and chromosome repro-
 duction, 572
 in hibernating animals,
 539, 540
 in human bone marrow,
 577-78
 and protein synthesis, 577
 radiation damage to, 531,
 532-36, 545
 DNase II
 radiation increase, 529-31
 Dogs, irradiation of, 501
 Dosimetry, 587
 Double-coincidence circuits,
 360, 362
 Dounreay reactor, 443, 460,
 466
 Drosophila
 irradiated, 575, 576
 Dry systems
 irradiation of, 554-55
 oxygen effect in, 558
 Dynamical friction
 between ion and electrons,
 375-76, 377, 398
- E
- E. coli B
 filamentous forms in, 582-
 83
 variations

in oxygen effect, 538-39
 Effective-mass
 nuclear, 13
 "Effective range" theory, 47
 Electricity
 growth rate
 of industry, 474
 Electrolyte balance
 failure of, 579-80
 Electrolyte shifts
 in irradiation, 543-44
 Electromagnetic waves
 in a plasma, 406, 407, 408
 resonance dispersion of, 409
 Electron
 and "adiabatic hypothesis," 394-95
 angular distribution, 103-4, 148
 density distribution
 in technetium compounds, 206
 -electron bremsstrahlung, 378-79, 383-84
 -ion bremsstrahlung, 378-79, 383-84
 -ion collisions, 404, 405
 -ion transfer rates, 376, 378
 in Mirror Machine, 432-33
 -neutrino correlation, 111-14, 117, 121-22, 132
 in Fermi versus GT radiations, 112
 in plasma, 375, 376-78, 415
 polarization, 107-11, 126-27
 bremsstrahlung detection of, 110, 115, 148
 runaway, 430
 see also Beta decay; Beta coupling; and Cobalt 60 experiments
 Electronics, nuclear; see Measurements, fast time; Instrumentation, complex; Semiconductor electronics; Photomultipliers; and Transistors
 Embryology
 differentiating centers, 493
 fertilized egg
 radiation sensitivity of, 516
 gastrulation susceptibility, 493
 irradiation of embryonic anlagen, 497
 man versus mouse, 509, 511-14
 nature of embryo, 493-94, 517
 "organismic" influences, 493, 494, 503

radiation-sensitive stages, 514, 519
 see also Radiation effects
 Energy-transfer hypothesis, 564-65
 Enrico Fermi Atomic Power Plant, 442, 445
 characteristics of, 443
 fuel elements, 466
 Enzymes
 radiation effects on, 529-31, 555, 578-79
 Equal-chain-length rule, 321-23
 Equal-specific-charge rule, 321-23
 Erythrocyte lifetime
 shortening of, 580
 Euratom program
 fuel cost table, 484, 485
 Evaporation cascade, 181-82, 183-84
 in high-energy reactions, 170, 173, 179
 in low-energy reactions, 173
 Evaporation spectrum, 295
 Excitation curves, fission
 analysis of, 278
 bumps in, 259-60
 comparison of, 279
 for photon absorption, 276
 shape at barrier energies, 256-58
 slope below fission barrier, 253-56
 Excitation radiation, 380-81
 intensities, 382-84
 in pinch effect, 430
 Saha equation, 380
 stripping temperatures, 382
 Exencephalia
 in fish *Fundulus*, 495
 human, 514
 in mouse embryos, 502, 503, 505, 506, 508, 509, 510, 511, 513, 514, 517, 519
 Extension rule, 47-48

F

Fast reactors
 accident considerations
 fuel melt-down problem, 467
 transient, 466-67
 TREAT, 467
 control and kinetics, 464-66
 coolants and heat transfer, 469-64
 engineering, 460-68
 "Fermi coupling," 106
 fuel cycle considerations, 467-68
 liquid-metal coolants, 461
 pyrometallurgical fuel-process cycle, 468
 see also Argonne, British, Los Alamos, and Russian fast reactors; and critical assemblies
 Fats
 radiation effects on, 526-29
 metabolism, 544-45
 Feedback circuits, 348
 Fermi-gas nuclear model, 13, 164
 Fermi selection rule; see Selection rules
 Fermi Theory of beta decay, 99, 100, 122-33
 coupling constant, 106
 flexibility of, 124
 restriction to left-handed states, 125-27
 V-A Law, 127-30
 Feynman-Gell-Mann current, 153-55
 beta-spectrum deviation, 155
 "Fierz Interference" terms in beta decay, 131
 "Firehose" instability, 417
 Fish
 Fundulus embryo, 495
 irradiation of, 495-96
 salmon embryos, 495
 trout eggs, 495
 Fission, 188-89, 245-336
 asymmetric, 311-17, 318, 320
 average mass ratios, 308-10
 binary, 306
 channels available for, 262-65
 in charged-particle bombardments, 269-71
 of copper, 284, 285
 as a "direct effect," 281, 335
 of elements lighter than thorium, 281-86
 energy available for, 286-88, 293-94
 excitation functions for, 256-58, 276, 278, 282
 fine structure in, 308, 316
 induced by
 charged particles, 269-73
 heavy ions, 280, 284
 mesons, 281
 neutrons (fast), 277-79
 neutrons (slow), 261-66
 neutrons (thermal), 290, 306-9
 liquid-drop model, 246-47
 mass distributions, 306-8, 313-15
 asymmetry of, 304
 dependence on excitation

- energy, 311, 313
 at moderate excitation
 energies, 266-73
 "modes" of, 313
 and neutron emission
 competition between,
 256, 266, 270, 272-73
 peak-to-valley ratios in,
 313-15
 photographic plate studies
 of, 281
 probability of, 183-84,
 245-86
 Q values of, 287-89
 of radium, 284
 resonances, 261, 262, 263
 shell structure in, 288,
 318, 319
 single-particle effects,
 249
 stages of, 286-88
 statistical theory of, 293,
 318-19
 symmetric, 293, 303-4,
 311-17, 319
 ternary, 305, 306
 see also Mass distribu-
 tions; Saddle point;
 Scission; Spontaneous
 fission; and following
 headings
- Fissionability**
 angular momentum and,
 271-73
 formula for, 267-68
 as function of energy,
 283
 high-energy, 280-81
 variation with excitation
 energy, 277-79, 333
- Fission barrier**
 dependence on Z^2A , 268
 heights of, 247
 effect of rotation on, 272
 in elements lighter than
 thorium, 283-84
 odd-even effects on, 269-
 71
 penetrability, 247-50,
 256, 257
 in spontaneous versus
 threshold fission, 254,
 255
 thickness of, 248
 see also Fission thresholds
- Fission cross sections**
 below barrier, 253-56
 for elements lighter than
 thorium, 282
 as function of energy,
 276-79, 273-81
 induced by
 heavy ions, 273
 neutrons (fast), 238, 255-
 56, 265-66, 277-79
 neutrons (slow), 265
 neutrons (thermal),
 265-66
 photons, 254-56
 in lead region, 285
 steps in, 277
 near threshold, 253-61
Fission excitation function,
 256-58, 282
 slope of, 254
- Fission fragments**
 angular correlation, 295
 angular distributions of,
 325-35
 from aligned nuclei, 328
 in alpha-particle bom-
 bardments, 333
 computations of, 330-31
 in deuteron bombard-
 ments, 333
 in direct interactions,
 328
 energy dependence of,
 325-35
 in neutron fission, 327
 theory of, 328-29
 at the threshold, 326-28,
 331
atomic numbers of, 320-
 21
 beta decay of, 305
 energy dependence of,
 323-24
 most probable, 321
 statistical theory of, 334
charge-to-mass ratio, 323
Coulomb energy between,
 291-93
de-excitation of, 297, 305
distance between
 at scission, 290
distance from stable val-
ley, 323-24
distributions of, 286-336
excitation energy of,
 293-305, 319
heavy fragment mass
 constancy of, 207-9
 hot-dog, 289
kinetic energies of, 288-
 93
 table, 289
mass distributions, 207-
 9, 305-20
 curves, shapes of, 310-
 11, 315, 320
 and liquid-drop model,
 317
 mass numbers of, 305-20
 measurements of, 324-25
 nuclear charge dis-
 tribution of, 320-25
- Fission, high-energy**, 159,
 179-84
 charge distribution in,
 182
 cross sections for, 181
 energetics of, 182-83
 mass-yield curve for,
 180-81
 low versus high-energy,
 180-81
 relative isobaric yields
 in, 181-82
- Fission neutrons**
 average energy of, 294
 delayed, 305
 energy distribution of,
 294-95
 linear dose-effect curves
 in *Drosophila virilis*
 males, 573
 numbers of, 295-96
 average, per fission,
 299-304
 average, table, 302
 dependence on excitation
 energy, 300-1
 dependence on fragment
 mass, 301-3
 in different elements
 300
 relative biological effect-
 iveness (RBE)
 versus x-rays, 573
 spectrum, 295
- Fission photons**
 angular distribution of,
 299
 and capture photons, 299
 emission time of, 298-99
 energy carried off by,
 288-89
 expected total energy of,
 296-98
 spectra of, 298-99
- Fission thresholds**, 248, 250,
 272
 determinations of, 258-
 61
 in deuteron bombardments,
 257-58, 259
 even-even, 260
 of heavy elements, 248
 increase of, 284
 liquid-drop model pre-
 dictions, 252, 260-61
 penetrability dependence
 on, 248
 in photofission and par-
 ticle-induced fission
 comparison of, 273
 seen in neutron fission,
 259-60
 seen in photofission, 260
 for spontaneous and in-
 duced fission
 comparison of, 254
 table of, 259
- Fission widths**
 in charged-particle bom-
 bardments, 269-71
 dependence on angular
 momentum, 271, 284
 dependence on channel
 spin, 265

- dependence on energy, 277-79, 282-83, 313
 - dependence on fission
 - barrier height, 267, 269
 - dependence on neutron binding energy, 267, 269
 - dependence on nuclear temperature, 267, 269
 - in elements lighter than thorium, 285
 - mass-symmetric part
 - ratio to total fission width, 314-15
 - odd-even effects, 271
 - for symmetric fission, 312
 - energy dependence of, 313
 - theory of, 266-67, 273
 - in uranium, 235, 263, 264
 - Fluoride systems
 - elements extracted in, 235
 - Fragmentation, 159, 185, 186-88
 - light-nuclide yields, 186-87
 - light particle emission, 185
 - mechanism, 187-88
 - secondary reactions, 185-86
 - Friction, dynamical
 - between ion and electrons, 375-76, 377, 398
 - Frog embryo
 - microcephaly in, 496
 - radiosensitivity of, 496
 - Fuels, nuclear
 - annual requirements of, 476
 - compared to coal, 473
 - cumulative requirements of, 476
 - in electricity production, 475
 - fuel cycle costs
 - burn-up per cycle, 483, 484
 - effect of burn-up on, 484-85
 - fabrication costs, 483, 484
 - in fluid-fuel reactors, 486-88
 - in homogeneous reactors, 487
 - for nonaqueous fluid-fuel reactors, 487, 488
 - projected, 487, 488
 - reductions in, 486
 - in solid-fuel reactors, 483-86
 - uncertainty, 483
 - in uranium-fueled converter reactors, 484
 - fuel cycle "guarantees," 483-85
 - other uses, 475-76
 - reactor fuel inventories, 476-77
 - future requirements, 477
 - Fundulus embryo
 - irradiation of, 495
 - Fusion power, 367, 368, 369-70, 388, 390, 433
 - DD, TD, and He^3D reactions, 390-91
 - from dynamic pinch, 421
 - from Mirror Machine, 426
- G**
- Gamma rays
 - polarization of, 115-16
 - see also Fission photons; and photon headings
 - "Gamow-Teller" selection rule (beta decay); see Selection rules
 - Giant cells, 581-82
 - in HeLa strain, 578
 - in mammalian system, 535
 - in yeast, 535
 - Giant resonances (photodisintegration), 648
 - collective model, 7, 14-15, 16-18, 20
 - of even-even nuclei, 334
 - in rare-earth regions, 15
 - widths, 16
 - sharpness of, 13, 14
 - shell or independent-particle model, 7-14, 15, 16-18, 20
 - as a single vibration, 14
 - splittings, 15, 16
 - widths of, 12-14, 16
 - G invariance
 - and weak interactions, 73
 - Glucose absorption
 - in irradiated rats, 523-24
 - Glycogen levels
 - of liver
 - in irradiated rats, 524-25
 - Godiva critical assembly, 444, 447, 450, 451, 454
 - G parity, 37, 39, 41
 - Gradient-B drifts
 - in plasma, 411
 - "Gyroscopic" drift
 - in plasma, 394
- H**
- Half lives
 - spontaneous-fission, 245-47, 249
 - of uranium 238, 248
 - see also Beta decay
 - Halides
 - in metal extraction
 - bromide systems, 236
 - chloride systems, 233-34, 235
 - fluoride systems, 235
 - iodide systems, 236
 - Hibernation
 - as protection against irradiation, 539, 540
 - High-energy reactions
 - comparison with low-energy reactions, 159-60
 - compilation of studies, 190-95
 - between complex nuclei and nucleons, 159-95
 - energy levels
 - density of, 168-69, 170
 - evaporation process, 162, 166-71, 175
 - light particles from, 170, 184-86
 - Monte Carlo calculations
 - in, 170
 - failure of fission-spallation mechanism, 186
 - Inelastic cross section, 163-64
 - knock-on process, 162-66, 167, 171, 184
 - Monte Carlo calculations
 - in, 164-66
 - residual excited nucleus
 - de-excitation of, 162
 - secondary reactions, 159
 - techniques in investigation, 161
 - yields of light nuclides, 185
 - see also Fission; Fragmentation; and Spallation
 - Human embryo
 - irradiation of, 511-16
 - major abnormalities after, 512
 - Hydrogenic plasma
 - diffusion velocity of, 405
 - Hydromagnetic waves, 407
 - unstable, 416
 - Hyperons
 - leptonic decay, 80-83
 - amplitude of, 81
 - theoretical rates of, 82
 - pionic sigma-hyperon decay, 79, 80
 - Hypothermia
 - protection against irradiation, 543
- I**
- Ideal ignition temperature, 391
 - Independent-particle model (IPM)
 - fast-nucleon emission, 19
 - Fermi-gas model, 13
 - harmonic oscillator, 7, 10, 16, 20

- of nuclear photo effect, 7-14, 15-23
 - raw calculations, 18, 20
 - rounded-edge well, 10
 - square well, 7, 9, 10, 11
 - transitions, 7-14, 17
 - from closed shells, 10
 - clustering of, 11
 - energy of, 11
 - nodeless to nodeless, 10
 - single-particle strength, 8, 10
 - see also fission headings
 - Insect whole-body radiation, 586-87
 - Instrumentation, complex, 343
 - computer techniques, 362-63
 - data handling, 362-63
 - two-dimensional pulse-height analyzers, 363
 - see also Measurements, fast time; Semiconductor electronics; Photomultipliers; and Transistors
 - Interference
 - of Fermi and GT radiation, 106, 121
 - Iodine
 - comparison with astatine, 212-13
 - interaction with pions, 174
 - isotope yields, 186
 - see also Halides
 - Ion association systems; see Solvent extraction
 - Ionization
 - equilibrium, 380
 - stripping curves, 380, 381
 - see also Plasma, high-temperature
 - Ionizing radiation; see Radiation effects
 - Ions
 - charge transfer, 384-85
 - collisions with electrons, 375-78
 - heavy
 - fission cross sections, 273
 - fission induced by, 284
 - fragment anisotropies, 335
 - high Coulomb barrier, 273
 - ion-ion collisions, 377, 405-6
 - pairing of, 224
 - see also Coulomb collisions; and Electrons
 - "Ion waves," 407
 - Iron complexes
 - and radiosensitivity, 535
- J
- Jezebel critical assembly, 445, 447, 450-51
- K
- "Kink" instability
 - in pinch, 419
 - of plasma, 411
 - K-meson decays, 83-91
 - charged and neutral, 90-91
 - interference effects in, 91
 - ratios and rates of, 85
 - "sliding ray" diagram, 88
- L
- Laboratory metal extractions
 - batch, 237-38
 - continuous extractors, 237, 238-40
 - ether type, 238, 239
 - reservoir type, 238, 240
 - countercurrent, 237, 240-41
 - rare-earth fractionation, 240
 - halides in, 233-35
 - Lagrangian interaction
 - isotopic spin change, 92
 - and matrix elements, 81
 - and selection rules, 91-93
 - of strongly interacting particles, 68-71
 - weak, 63, 65, 66, 67
 - LAMPRE fast reactor, 442, 468
 - "Landau damping," 415, 416
 - Langmuir frequency
 - of plasma oscillations, 408
 - Lead extraction, 226
 - Lead targets
 - irradiation of, 187
 - Leptonic decays
 - conservation of vector current, 71-73
 - G invariance, 73, 81
 - of K mesons and hyperons, 80-91
 - of mesons and baryons, 68-80
 - muon capture in hydrogen, 75-76
 - neutron decay, 73-75
 - of pions, 76-79
 - of strange particles, 78-80
 - see also Beta decay; Sakata model; and individual particles
 - Leptons, 105
 - conservation of, 136-38, 139, 145, 150
 - interaction between, 67-68
 - intermediate neutral, 135-36, 137
 - left-handed lepton states, 125-27
 - "leptonic charge," 66, 136
 - polarization, 131, 135
 - see also Beta decay; and Negatrons
 - Leukemia
 - as irradiation result, 516
 - Linear energy transfer (LET), 563, 564
 - in bacteriophage-host system, 565
 - dependence, 563, 566
 - effect on RBE, 573-74
 - and isochromatid breaks, 572
 - radiations of, 561
 - Liouville's equation, 396, 398
 - Lipemia
 - after x-radiation, 526-27
 - Lipids
 - after radiation, 526-28
 - Liquid-drop model, 246-47, 249
 - and fission mass distributions, 317-18
 - nuclear compressibility, 253
 - nuclear energy
 - dependence on distortion, 251
 - nuclear polarizability, 253
 - nuclear surface energy, 250, 251, 252
 - sticky liquid, 301
 - threshold predictions, 260-61
 - see also Fission; and Giant resonance
 - Lithium
 - in high-energy reactions, 166
 - Lorentz-invariance, 105
 - Los Alamos critical assemblies
 - Godiva, 444, 447, 450, 451, 453, 454
 - Jemima series, 444-45, 447, 454
 - Jezebel, 445, 450, 451
 - Topsy, 444, 447, 450, 451, 453, 454, 458
 - Low-energy reactions, 167, 173, 178
 - see also separate reaction headings
- M
- Macroscopic equations, 397
 - Magic nuclei, 15
 - effect on fission mass distribution, 318
 - Magnetic bottles, 403, 418-27
 - Astron, 426-27
 - confining field, 418
 - definition, 418
 - variations
 - Hard Core Pinch, 427
 - Helical Mirror Machine, 427
 - Homopolar, 427

Ixion, 427
 Picket Fence, 427
 Triax Pinch, 427
 see also individual forms
 Magnetic field shapes
 in fusion machines, 411-14
 Magnetic mirror, 396, 424
 see also Mirror Machine
 Magnetic moment
 of spiralling particle, 395, 396, 401
 Majorana exchange forces, 7, 18
 Majorana neutrino, 137-40
 Manganese extraction, 224
 MANIAC electronic computer, 164
 Man versus mouse, 511-14
 correlations in development, 513-14
 neuroblasts, 513
 Many-body treatment
 of nuclear matter; see Brueckner treatment
 Marker rescue, 566
 from injured DNA, 567
 of phage, 568
 Mass distributions
 and angular distributions
 correlation between, 332
 asymmetry of, 317, 319-20
 from different resonances, 316
 effect of compressibility on, 318
 effect of polarizability on, 318
 in low-energy photofission, 316
 magic numbers, 318
 single-particle effects on, 318
 see also Fission; and Fission fragments
 Mass spectrometry, 307
 Mass spectroscopy
 in high-energy investigation, 161
 Measurements, fast time, 343, 357-62
 coincidence systems, 359-60, 362
 fast amplifiers, 357-58
 fast pulse transformers, 357, 358
 fast trigger circuits, 358
 semiflexible transmission cables, 359
 rise times of, 359
 time analyzers, 360-62
 multichannel, 361
 Vernier chronotron, 361
 Mercaptoethylamine
 irradiation protection, 501
 Mercury
 as coolant
 in fast reactors, 460, 468

Mesons
 counter telescope experiments, 361-62
 decay of
 pseudoscalar, 69
 scalar, 70
 fission induced by, 281
 in high-energy reactions, 165, 189
 see also leptonic headings; Muon; and Pion
 Metabolism
 postradiation
 carbohydrate, 523-26, 544-45
 cholesterol, 527
 fat, 544-45
 nucleotide, 532
 protein, 528-29
 RNA, 534
 Metals; see Laboratory extractions; and Solvent extraction
 8-Methoxypsoralen, 581
 Methyl isobutyl ketone
 in metal extraction, 233
 Michel parameter, 67, 147, 150
 Microbeam irradiation
 of grasshopper neuroblasts, 583-84
 Microcephaly
 causes, 515
 in frog blastula, 496
 in Japanese children, 515
 Mirror Machine, 396, 414, 424-26
 adiabatic magnetic compression, 426
 ALICE experiment, 428
 heating and confinement studies, 432-33
 injection methods, 427-28, 429
 injection problem, 433
 Livermore experiments, 424-26
 present status, 432-33
 Scylla experiment, 426
 stability of, 433
 Molybdenum; see Technetium
 Monte Carlo calculations
 of evaporation process, 170, 174, 175, 183-84
 of high-energy reactions, 279
 of knock-on process, 164-66, 175, 179
 Mouse embryo
 cerebral anomalies, 502, 510, 511
 compared to human embryo, 509
 irradiation of, 501-11, 518
 major abnormalities, 512
 neuroectoderm, 510, 511
 neuroblast deletion, 508, 509

neuroblast sensitivity, 514, 517
 preimplantation, 502
 radiiodine
 in thyroid, 509
 testes primordia
 radiosensitivity of, 507
 sterilization, 507
 subsequent fertility, 507
 see also Exencephalia
 Multichannel time analyzer, 361
 Multicomplexes, irradiated, 566, 567
 Multiplicity reactivation
 in bacteriophage, 567, 568
 Multivibrators
 conventional circuits, 351
 junction transistor, 351
 Muon capture, 142, 144, 152
 in hydrogen, 75-76
 Muon decay, 67, 93, 100, 146-50
 coupling strength, 149, 153
 electron angular distribution in, 148
 energy spectrum, 147
 lifetime, 149
 polarization sign of, 77
 from polarized muon, 147
 spectrum, 89
 V-A Law in, 147-49
 Muons
 in K-meson decay, 83, 89, 90
 Mutation
 in higher animals and plants, 574-76
 intensity effect on
 in mice, 574
 resistance to, 576
 somatic
 and gamma irradiation, 576

N

"Natural" co-ordinate system, 399
 Negatrons
 capture of, 133
 decay, 133-34
 polarization of, 60, 107, 108, 110-11
 radiation of cobalt 60, 108, 111
 state of momentum, 127
 see also Beta coupling; and Beta decay
 Neutrino, 133-40
 angular distribution, 111, 118
 -antineutrino distinction, 134-36, 139, 140
 capture, 133-35
 "Dirac," 138-39
 four-component, 140

- left-handed, 125
 - "Majorana," 137-39, 150
 - polarization, 100, 111-13, 114, 115, 116
 - two-component theory, 138-40, 150
 - see also Antineutrino; Beta coupling; and Beta decay
 - Neutron cross sections
 - for reactors, 437, 439
 - see also Cross sections
 - Neutron decay, 73-75, 79, 113-14, 116-22
 - beta distribution from, 117, 121
 - Neutron detector, 280-81
 - Neutron-flux
 - distribution, 465
 - spectra, 450-52
 - Neutronics, fast-reactor, 446-60
 - experimental data, fast-assembly, 446-60
 - critical size, 446, 447-48
 - perturbation data, 446, 450
 - Rossi alpha, 452, 454, 455
 - spectral characteristics, 450, 452
 - Neutrons
 - angular correlations
 - with fission fragments, 280-81
 - angular distributions of
 - with aligned nuclei, 328
 - and chromosome breakage
 - x-ray-induced, 569-70
 - emission of, 270
 - dependence on fissionability, 313
 - effect on nuclear rotation axis, 331
 - probability for, 272
 - "thermionic emission" probability, 276
 - width, 256
 - fast
 - critical mass, 449
 - spectra, 453
 - fission, 267, 300, 327
 - fission cross sections, 255-56, 265-66
 - fission thresholds, 259-60
 - multiplicities of, 296
 - from pinches, 430
 - polarization of, 117-18
 - prompt
 - mean lifetimes of, 454, 455
 - neutron spectra, 294-96
 - thermal, 328
 - see also Fission neutrons
 - Newcastle disease virus
 - analysis of, 563-64
 - Nitrate extraction system
 - elements extracted in, 232-33
 - Nitric oxide
 - and radiosensitivity, 538
 - Nitrosonaphthols
 - metal extraction, 230
 - Nitrous oxide
 - radiosensitivity reduction by, 537
 - Nonfission cross sections
 - energy dependence of, 279-80
 - "Nonsense DNA," 578
 - Nuclear emulsions
 - in high-energy investigation, 161, 171, 181
 - with high-intensity beams, 184-85
 - of spallation reactions, 179
 - Nuclear photo effect; see Photodisintegration, nuclear
 - Nuclear power
 - capital costs
 - of advanced plants, 482, 488, 490
 - of first-generation prototype plants, 481-82, 484, 485
 - long-range outlook for, 488-90
 - for second-generation plants, 488, 489, 490
 - cheap fuel, 473
 - economics of, 473-90
 - forecasts, 473-76
 - of capacity, 474
 - electricity market estimate, 474-76
 - of growth, 474-76
 - growth rate of electrical industry, 474
 - production rates
 - of materials, 479-81
 - reactors, 476-78
 - reserves
 - of materials, 479-81
 - see also Fuels, nuclear
 - Nuclear power plants
 - capital costs of, 481-82, 484, 485, 488, 489, 490
 - initial fuel costs, 484, 486
 - table of, 486
 - total power costs in
 - estimate (1964), 489
 - Nuclear transplantation techniques, 583
 - Nucleases
 - postradiation biochemical changes, 577-81
 - after radiation, 529-31
 - Nucleic acids
 - irradiated, 553-54
 - postradiation changes, 577-79
 - synthesis, 577
 - Nucleolus
 - importance in all division, 583-84
 - loss of basophilia in, 582
 - RNA in, 582
 - Nucleon-nucleon potentials, 1, 3
 - deformed, 16
 - Gammel-Thaler, 1, 2, 3
 - Van Vleck, 13
 - velocity-dependent (effective mass), 13
 - Nucleon-nucleon scattering, 39
 - Nucleons
 - in fission, 250-51, 281
 - "soft," 335
 - Nucleoproteins
 - after irradiation, 533, 536-37
 - nucleohistone, 536
 - Nucleus, fissioning, 276, 280, 286-87, 290
 - compound
 - excitation energy of, 323
 - moment of inertia of, 272
 - polarizability of, 321
 - stickiness of, 300
- O
- "Onium" system, 222
 - "Optical theorem," 50
 - "Organismic" forces, 493, 494, 503
 - Oscillators
 - in multichannel time analyzer, 361
 - transistor, 353
 - Oscilloscope
 - for observing fast pulses, 362
 - Oxyanions
 - in solvent extraction, 235-37
 - Oxygen effect, 537-39, 557-59
 - carbon monoxide inhibition, 559
 - and carbon radical, 557, 559
 - on chromosome breakage or rejoining, 572
 - in dry systems, 558
 - E. coli B variations in, 538-39
 - and HO₂ radical, 557
 - inert gases
 - influences of, 537-38
 - ionic bond hypothesis, 559
 - and iron complexes, 538
 - within the nucleus
 - of a cell, 537
 - in oocytes, 573
 - and radiation, 537
 - on ring losses in sperm, 573
 - use of cupferron, 558
 - Oxygen saturation curve
 - of *Shigella flexneri*, 557, 558

- of Vicia root chromosomes, 557-58
- P
- "Parallel pressure components," 399, 400, 411, 412
- Paramagnetic resonance studies, 553, 555
- Parameters, nuclear
 - plutonium 239, 437
 - thorium 232, 437
 - uranium 233, 437
 - uranium 235, 437
 - uranium 238, 437
- Parchment worm Chaetoperus egg irradiation of, 495
- Parity, 100-5
 - and charge conjugation, 103, 104
 - operations, 103-5
 - space inversion, 103
 - Parity conservation, 102, 104, 124, 147, 148
 - effects of, 102
 - overthrow of, 100-3
 - mirror-image experiment, 101-2
 - violation of, 108, 139-40
 - see also Beta coupling; and Beta decay
- Partial cell irradiation, 583-84
- Particles, elementary, 61-67
 - masses and lifetimes of, 62
 - strong interactions, 64-65, 68-69
 - see also Sakata model
 - weak interactions of and charge conjugation, 65
 - and chirality transformation, 65
 - and combined inversion, 65
 - constant G, 63
 - and "leptonic charge," 66
 - between leptons, 67-68
 - nonconservation of parity in, 65
 - nonleptonic, 91-93
 - Universal Fermi interaction, 61-64, 66-67
 - see also Lagrangian interaction; and individual particles
- Perhapsatron pinch apparatus, 430
- Peroxide formation after radiation, 528, 531
- "Perpendicular pressure components," 399, 400, 411, 412
- Pertechnetate ion
 - as corrosion inhibitor, 205
 - optical absorption spectrum, 205
 - solvent extraction behavior, 211
- Perturbation theory, 34, 40, 41, 42, 47, 50, 51
 - conventional, 56
 - and weak interaction, 69, 76
- Phosphorus-32 injection in chick eggs, 497-98
- Phosphorylation
 - nuclear, 532
 - oxidative, 532
- Photocathodes
 - spherical, 355-56
- Photodeuterons, 21
- Photodisintegration, nuclear, 1-23
 - for deformed nuclei, 14-15
 - collective model, 14-15
 - Fermi gas model, 13
 - IPM, 15-16
 - of the deuteron, 1-5, 21
 - dispersion theory, 9
 - exchange forces, 8
 - low-energy data, 4
 - of very light nuclei, 5
 - see also Giant resonances
- Photodynamic action, 581
- Photo effect; see Photodisintegration
- Photofission, 254-56, 326
 - fission thresholds in, 260
 - fragment anisotropies, 325, 328, 331
 - giant resonance, 334
 - low-energy cross sections, 255
 - low-energy mass distributions in, 316
 - and neutron fission, 266-69, 272
 - quadrupole absorption and, 326
- Photographic plate studies of fission, 281
- Photomultiplier integrating amplifier, 358-59
- Photomultipliers, 343, 348, 354-56
 - Cerenkov counter detection, 354-55
 - fast passive elements, 358-62
 - fast types of, 356
 - and scintillators, 354
 - spherical photocathodes, 355-56
 - time difficulties, 354-56
- Photon
 - emission
 - end states for, 263
 - fission studies, 254-56
 - spectra in fission, 294, 296-99
 - widths, 256, 262
 - see also Fission photons; Gamma rays; and photo-headings above and below
- Photon scattering
 - elastic, 22
 - inelastic, 22
- Photopion production, 58
- Photoproduction of a pion, 2, 3
- Photoreaction; see Photodisintegration, nuclear
- Photoreactivation, 553
 - kinetics of, 562
 - of phage, 568, 569
- Photosynthesis, 580-81
- Pinch effect, 411, 412, 418-22, 425
 - "dynamic pinch"
 - with deuterium, 421
 - pinching column, 420-21
 - history of, 419-21
 - present status, 429-31
 - "hard-core" pinch, 430-31
 - Perhapsatron, 430
 - problems, 431
 - runaway electrons, 430
 - Zeta, 430
 - pressure-balance equation for, 419
 - "stabilized pinch," 421
- Pion
 - decays, 76-78, 79, 93, 100, 141-45, 155
 - electron to muon ratio, 143, 146
 - lifetime, 144, 145
 - polarization of products, 143
 - spectrum, 89
- Pion-nucleon interaction, 29-59
 - diagrams, 31
- Pion-nucleon scattering, 37, 49, 50, 57
 - low-energy, 56, 57
- Pion-photon vertex function calculation of, 58
- Pion-pion scattering, 29, 35-37, 41, 49, 50, 51-52, 54, 56-57, 58
- Plasma, high-temperature, 367-433
 - ALICE experiment, 428
 - collective physical processes, 391-418
 - action integral, 396
 - "adiabatic hypothesis," 394-95
 - adiabatic invariants, 394-97, 408
 - centrifugal drift, 393, 411
 - charge separation, 393
 - dielectric constant, 407
 - diffusion drift velocity,

- 403
 entropy change, 402, 414
 equations of motion, 392-94
 "extraordinary wave," 409
 "flux surface," 397
 gradient-B drifts, 411
 "guiding center," 393
 "gyroscopic" drift, 394
 "magnetic mirror," 396
 "Mirror Machine," 396
 plasma diffusion across a magnetic field, 402-6
 plasma frequency, 408
 radiation limits, 409
 see also Plasma instabilities; and Pressure balance equations
 diamagnetism of, 401
 difficulties in research, 368-69
 injection problem, 427-29, 433
 Oak Ridge DCX experiment, 428, 433
 partulate physical processes, 369-91
 charge exchange, 384-87
 DD, TD, and He³D reactions, 390-91
 electron-electron bremsstrahlung, 378, 379
 electron-ion bremsstrahlung, 378-79, 383-84
 electron-ion transfer rates, 376, 378
 "Ideal Ignition Temperature," 391
 ionization, 370-71, 380
 nuclear reactions, 387-91
 see also Coulomb collisions; and Excitation radiation
 Russian OGRA experiment, 428
 Scylla experiment, 428, 433
 see also Magnetic bottles
 Plasma instabilities, 409-18
 interchange instabilities, 409
 criterion for stability, 411, 412
 flute instability, 412-13
 physical mechanism of, 410
 "pinch effect," 411, 412
 sausage instability, 411, 419, 421
 shear field, 414
 suppression of, 413
 see also Stellarator
 velocity-space instabilities, 410, 411, 414-18, 425
 "firehose" instability, 417
 "Landau damping," 415
 "Mirror" instability, 417
 of Mirror Machine, 425, 426
 wave-particle interactions, 415
 Ploidy
 lethal radiation effects, 575
 radiosensitivity and, 559-61
 Plutonium
 as fast-reactor fuel, 467
 fission anisotropy of, 334
 Plutonium 239
 as reactor fuel, 437
 for fast reactors, 438
 Polarization
 in deuteron photo effect, 4
 see also individual particles; and rays
 Poles
 "backward" pion pole
 in neutron-proton scattering, 46
 coupling constants, 41-43
 pion-nucleon, 42, 51
 pion-pion, 55
 deuteron, 58
 "forward" pion poles, 46
 location of, 40-41
 in Mandelstam representation, 53
 "polology," 43-47
 "effective range" theory, 47
 extrapolation, 43-47, 51
 positions of, 45
 residues, 41-43, 45
 determination of scattering amplitudes, 44
 of deuteron pole, 43
 of nucleon pole, 51
 in scattering amplitudes, 39-47
 see also Perturbation theory
 Positrons
 emission of, 111
 polarization of, 110-11, 127
 see also Beta coupling; and Beta decay
 Potassium shift
 in irradiation, 543-44
 Pressure balance equations, 397-402
 Boltzmann equations, 397-98
 diamagnetic depression, 401
 "natural" co-ordinate system, 399
 "parallel pressure components," 399, 400, 411
 parameter β , 402
 "perpendicular pressure components," 399, 400, 411
 for pinch effect, 419
 pressure (stress) tensor, 398
 Proteins
 altered by radiation, 528-29, 554
 spin resonance in, 554
 Protein synthesis, 529, 536, 577
 blocking of, 577
 and glucose, 579
 resistance to x-radiation, 528
 Protons
 anisotropies, 328, 335
 in high-energy fission, 335
 see also High-energy reactions
 Prototrophy
 mutations in *E. coli* to, 562
 Q
 Quadrupole absorption, 326
 see also Photodisintegration; and nuclear and other photo- headings
 8-Quinolins
 extraction of metals, 228-29
 Q values
 of fission, 287-89, 293, 296
 R
 Radiation damage
 to bacteriophage-host system, 565-66
 to biomolecules, 553-57
 to DNA in solution, 565
 to dry systems, 554-55
 nuclear versus cytoplasmic, 584
 to nucleic acids, 553-54
 oxygen-sensitive damage, 557-59
 to proteins, 554
 recovery from, 562
 to yeast genetic apparatus, 559-60
 see also Oxygen effect
 Radiation effects
 adrenal cortical changes, 525
 amino-aciduria, 524-25
 anencephalia, 495
 in man, 514, 516
 in rat embryo, 499
 anoxia, 558
 beneficial, 585-86
 biochemical, 523-45
 on biomolecules, 553-57
 on "blast" cells, 499
 on carbohydrate metab-

olism, 523-26
 cerebral anomalies, 502
 on chick embryo, 496-98
 on cholesterol metabolism, 527
 chromosomal breakage, 569-74
 excess of metaphase dicentric, 570
 on creatine synthesis, 525
 cross reactivation, 555-66, 567
 on dogs, 501
 protection of pregnancy, 501
 dominant lethal effects, 575
 on *Drosophila*, 575
 electrolyte shifts, 543-44
 on electrolyte transport, 579-80
 and erythrocyte lifetime, 580
 on embryo, 493-519
 congenital anomalies, 493, 494, 502, 503, 505, 511, 514, 517
 at fertilization stage, 517
 during gastrulation, 493
 on embryonic amphibia, 496
 on embryonic rats, 498-501
 enhanced muscle catabolism, 525
 on enzymes, 529-31
 sulphydryl, 531
 trypsin, 531
 in vitro, 531
 in vivo, 529-31
 on fat, 526-29
 on fish, 495-96
 genetic
 on phage, 569
 on yeast, 599-60
 on germination ability, 561
 giant cell formation, 535
 on glucose absorption, 523-24
 on glycolysis, 525-26
 of ascites tumor cells, 526
 of mouse liver, 525
 on human embryo, 511-14
 exencephalia, 514
 stunting, 514-15
 "inactivation," 585
 on insects, 586-87
 on Japanese children, 514-15
 on lipids, 526-28
 on liver glycogen levels, 524-25
 major abnormalities
 in man, mouse, rat, 512
 in man, 511-16
 deficient adult, 516
 leukemia, 516

on marine organisms, 494-95
 marker rescue, 566
 from injured DNA, 567
 microcephalia, 499, 500, 574
 microphthalmia, 499, 500, 505
 on mitosis, 534, 535, 584
 on mouse embryo, 501-11
 mutagenesis, 574-76
 mutation of spores
 action spectrum of, 562
 mutations to prototrophy, 562
 on nucleic acid, 532-36
 on nucleoproteins, 533, 536-37
 oxygen effect, 537-39, 557-59
 peroxide formation, 528
 on photodynamic actions, 581
 on photosynthesis, 580-81
 on ploidy, 559-61
 postradiation biochemical changes, 559, 577-81
 increase in enzymes, 578-79
 increase in nucleotides released, 578-79
 postradiation morphological changes
 filamentous forms, 582
 giant cells, 581-82
 in mitochondria, 582
 multicellular inactivation forms, 583
 in the nucleolus, 582
 potassium shift, 543-44
 protection against, 495, 497, 501, 507, 517, 519
 by amines, 541-42
 anoxia in, 539, 541
 by cysteamine, 540-41
 by cysteine, 539-40, 541, 544
 by fluoroacetate, 543
 by hibernation, 539, 540
 by hypothermia, 543
 by reserpine, 542
 by S,2-aminoethylisothiuronium, 542
 by yeast, 543
 quasisensory stimulus, 584-85
 "recovery" from injury, 495, 500, 516
 sensitization to heat, 586-87
 ultraviolet, 556-57
 valuable, 494, 518-19
 on viscosity
 of synovial fluid, 556
 see also Embryology; Exencephalia; Mutation; and Ultraviolet effects
 Radiation sensitivity
 of chromosomes, 536, 538
 variations in, 537
 in mitotic cycle, 534, 545
 β -Radioactivity
 laws of, 99-155
 see also Beta coupling; and Beta decay
 Radiobiology; see Cellular radiobiology
 Radiochemical procedures
 for astatine, 215-16
 for technetium, 209-10, 212
 Radiochemical separations;
 see Solvent extraction
 Radiochemistry
 charge distribution examination, 320
 in high-energy investigation, 161, 171, 181
 of secondary reactions, 186
 mass-yield determination, 307
 measurement, 307, 335
 Radiiodine
 in fetal mouse thyroids, 509
 in pregnant women, 516
 Radiomimetic drugs, 494, 517
 in rat embryos, 498
 Radiomimetic insults, 514
 Radiosensitivity
 of bacteriophage, 565
 before fertilization of egg, 519
 of fertilized egg, 516
 oxygen saturation curve for, 557-58
 and ploidy, 559-61
 of yeast, 559-60
 genetic aspects of, 559-60
 see also Radiation damage; and Radiation effects
 Radium
 fission of, 271, 284, 333-34
 mass distribution in, 310-11, 315
 Rare-earth region
 photonuclear effect in, 14-16, 18
 Rat embryo
 irradiation of, 498-501
 anencephalia, 499
 microcephalia, 499, 500
 microphthalmia, 499, 500, 505
 neuroblasts, 498-99
 neurectoderm, 499
 postirradiation repair, 500

- Reactors
 burn-up requirements in, 478
 fuel cycle costs in, 483-86
 "developmental," 441
 fuel cycle costs in, 484
 in fluid-fuel reactors, 486-88
 in homogeneous reactors, 487
 in nonaqueous-fluid-fuel reactors, 487, 488
 in pressurized-water reactors, 483
 in uranium-fueled converter, 484
 fuel inventories, 476-77
 future distribution of
 by type, 477-78
 projected capacities of, 478
 thermal, 437-38, 464, 469
 parameters for, 439
 Reactors, fast-neutron, 437-69
 advanced concepts, 468-69
 compact high-temperature power, 469
 cooling by boiling mercury, 468
 fast-thermal reactor, 469
 LAMPRE, 468
 space application, 469
 ultra-high-temperature chemical processing, 469
 advantages of, 440
 compared to thermal reactors, 438-49
 control and stability, 439
 comparison of, 440
 computational survey of, 454-60
 effects of reflector on uranium-238, thorium-232 systems, 460
 S_n calculations, 454-57
 type of computation, 454-57
 critical volumes, 458
 cylindrical core shape
 dependence of critical mass on, 449, 463-64
 fast critical assemblies, 443-46
 British, 445-46
 Russian, 446
 see also individual laboratories and models
 fuel
 burn-up of, 438
 conversion ratio, 437
 critical concentration, 458-59
 cycle, 467-68
 fertile materials, 437, 444, 459
 radiation damage of, 438
 see also Fuel, nuclear
 parameters for, 439
 programs, 440-43
 see also individual countries
 prototype and developmental characteristics of, 443
 subcritical assemblies, 445
 uranium-metal exponential columns, 445
 see also Fast reactor engineering; Neutronics, fast-reactor; and Spherical fast systems
 Refrigeration
 during irradiation, 496
 Relative biological effectiveness (RBE), 574
 for chromosome and chromatid aberrations, 573
 classical versus modern, 574
 fission neutrons versus x-rays, 573
 Relaxation times
 in electron-ion collisions, 373-74
 Reservoir continuous extractor, 238-40
 Rhenium; see Technetium
 R locus in *Mormoniella*
 mutation rate of, 575-76
 RNA (ribonucleic acid)
 radiation damage to, 532-36
 and radiosensitivity, 543
 ratio in nucleolus, 582
 RNase decrease
 after irradiation, 530
 Rossi alpha, 452, 454
 table of, 455
 Rossi coincidence circuit, 351
 Russian critical assemblies
 BP-1, 446
 BP-3, 446
 Russian fast-reactor program, 442-43
 BP-2, 442
 BP-5, 442
 BH-50, 442-43
 BH-250, 443
 Russian OGRA experiment, 428
 Ruthenium; see Technetium
 S
 level structure of, 249-50, 257, 272, 274, 301, 316, 325-28
 of liquid drop, 252, 253
 one-saddle view, 315
 Saha equation, 380
 Sakata model, 64-65, 71, 72, 73, 91, 93
 Salamander larvae
 irradiation of, 496
 S, 2-aminoethylisothiouronium
 protection against irradiation, 542
 of S3HeLa cell cultures, 542
 Sausage instability
 in pinch, 419, 421
 of plasma, 411
 Scattering
 amplitude
 pion-pion, 48
 backward n-p, 46
 Coulomb, 374-75
 elastic
 of charged particles, 371
 proton-neutron, 11
 electron-electron, 109-10
 fast electron
 ion-ion, 377
 nucleon-antinucleon, 46
 nucleon-nucleon, 39, 46
 photon-nucleon, 58
 of photons, 22
 pion-nucleon, 47
 pion-pion, 29, 35-57, 41
 resonance, 115
 Scintillators
 timing fluctuations, 354
 Scission, 289, 290, 291, 309
 Coulomb energy
 between fragments, 290
 internal charge distribution at, 321
 mean separations at
 for different mass ratios, 293
 spin distribution at, 334
 Scylla Los Alamos experiment, 426, 433
 Sea-urchin *Arbacia* eggs
 irradiation of, 495
 Selection rules
 Fermi versus GT, 106-7
 "comparative half lives," 106, 132
 coupling strength, 107, 113, 121-22, 149, 152
 "ft-values," 106, 132
 for Lagrangian weak interaction, 91-93
 see also Electron-neutrino correlation
 see also Beta coupling; and Beta decay
 Semiconductor electronics, 343-54

semiconductor diodes, 343,
351
fast, 352
see also Transistors
Serum oxidase
radiosensitivity of, 556-57
Serum proteins
after radiation, 528, 539
Shell model; see Independent-
particle model (IPM)
Shigella flexneri
radiosensitivity of, 557, 558
Sievert's theorem, 3, 4, 6,
8
Snail Helisoma eggs
irradiation of, 495
Sodium
dispersing effect, 467
as fast-reactor coolant,
460, 461-63
-potassium alloy
as fast-reactor coolant,
460
Sodium fluoroacetate
and radiation sensitivity,
543
Solvent extraction, 221-41
apparatus, 237-41
see also Laboratory ex-
tractions
chelate systems, 222, 223,
226-30
cupferron, 227
diethyldithiocarbamates,
226-27
 β -diketones, 229-30
dithizone, 227-28
nitrosonaphthols, 230
8-quinolinols, 228-29
extraction equilibria
quantitative treatments
of, 225-26
extraction kinetics, 226
ion association systems
alkylphosphoric acids,
230-31
carboxylic acids, 231
cationic chelates, 231-32
extractions of anionic
chelates, 237
halides, 233-34
nitrate extractions, 232-
33
"onium" usage, 222
oxyanions, 235-37
trialkylphosphine oxides,
233, 234
metal extraction systems,
223
principles of, 222-26
distribution law, 222
process of, 224
formation of uncharged
complex, 224
"Source moments," 106
Space inversion, 103, 104
Spallation, 159, 172-79,

188-89
evaporation process in,
173
light-element targets,
176-77
excitation functions of, 177-
79
isobaric products
relative yields of, 167,
170, 172, 173-75
mass-yield distributions,
172, 175-77, 179
"Specialization energy," 250
"Spectral indices," 450
of fast assemblies, 454
Spherical fast systems
critical masses of, 461,
464
critical volumes of, 462,
465
initial breeding ratios of,
463, 466
initial conversion ratios
for, 459
see also Reactors
Spin resonance
in irradiating proteins, 554
Spin states
of leptons, 100
Splitting of photonuclear res-
onance, 15, 16
Spontaneous fission, 246-47,
309
lifetimes
of even-even nuclei, 246-
47, 249
odd-even differences,
247, 249
table of, 247
 Z^2A , 246-27, 249, 268
Spores
irradiation of, 561-62
survival curves of, 564
Statistical microscopy,
563-66
Stellarator, 406, 414, 425
"figure 8," 422-24
injection method, 427
"magnetic pumping," 423
present status, 431-32
"pump-out," 431
rotational transform, 423
"stabilizing windings," 424
Störmer's cosmic ray stud-
ies, 396
Strange particles
leptonic decays, 68-91
nonleptonic decays
 $\Delta T = 1/2$ rule, 92, 93
see also individual particles
Strong coupling
in "ordinary" particles,
pions and nucleons, 29-
59
Substitution rule
in dispersion relations,
34-35

Sulphydryl enzymes
in-vitro radiosensitivity of,
531
Sum-rule calculations
for nuclear photo effect,
4, 5-6, 7, 8, 13
Symmetry energy
nuclear, 324
see also Fission

T
Target theory, 563, 573-74,
581
Taurine
excretion of, 524-25
"Taylor" plasma instability,
410-11
Technetium
analytical chemistry of,
208-12
assay methods, 212
back-extraction, 211
distillation, 209-10
separation from molyb-
denum, 209-10, 211,
212
separation from rhenium,
209, 212
separation from ruthen-
ium, 210
ion-exchange separations,
211-12
oxidation potential diagram,
208
precipitation as sulfide,
210
radiochemical procedures,
209-12
removal from organic pre-
cipitate, 210
similarity to rhenium, 208-
9
solvent extraction, 211
thermodynamic properties
of, 209
see also Pertechnetate
ion; and Technetium
compounds
Technetium compounds, 205-
7, 210
insoluble pertechnetates
precipitation of, 210
oxidation states, 205-8,
210
thermodynamic properties
of, 209
unidentified lower states,
207-8
electromigration exper-
iments, 208
Teller, Edward
hypothesis of, 397
Teratogenesis, 494
Thenoyltrifluoroacetone
elements extractable by,
229

- Thermionic emission equation, 274
- Thiocyanates, alkali
as complexing reagents, 234-35
elements extracted in, 237
- Thorium
production rate, 480-81
projected requirements for, 478-79
reserves of, 480
- Thorium 232
as "fertile" material, 473
as reactor fuel, 437
- Thyroid
of fetal mouse, 516
avidity for radiiodine, 509
of pregnant women, 516
"Time reversal," 104, 119, 124
invariance to, 122
- Toads
Bufo boves, 496
clawed toad xenopus, 496
embryonic irradiation of, 496
- Topsy critical assembly, 444, 447, 450, 453, 454, 458
- Total-body radiation
of insects, 586-87
of rats, 523-24, 528
- Transaminases
postirradiation changes, 529
- Transformers, 357-59
fast pulse, 357
equivalent circuit for, 358-59
in high-speed circuitry, 358
- Transistors, 344-48
amplifiers
dc, 353
wideband, 349-51
collector current, 345, 347, 348
complementary emitter follower, 353
in computer-type circuits, 353-54
as switches, 353
cutoff, 345
 α -cutoff frequency, 347
 β -cutoff frequency, 348
cooling, 346
fast, 351
fast coincidence circuits, 351-52
high-frequency
diffused-base, 346, 347-48
drift, 347-48
surface-barrier, 345, 346, 347
multivibrator circuits, 351
nuclear detectors, 348-52
oscillators, 353
p-n-p germanium, 349
saturation, 345, 351, 353
transistor discriminators, 351
voltage limitations
avalanche breakdown, 345
punch-through, 345, 347
Zener breakdown, 345
"Transparency," 171
Transport processes
in plasma, 371
TREAT (transient reactor test facility), 467
Trialkylphosphine oxide system
elements extracted in, 233, 234
Tributylamine
in metal extraction, 235
Tributyl phosphate
in metal extraction, 233, 240
Trypsin; irradiated
inactivation in vitro, 531
- U
- Ultraviolet effects, 556-57
absorption
of irradiated plastics, 587
on DNA, 587-68
on Drosophila, 576
on E. coli B, 582-83
versus ionizing radiation, 567
on phage, 569
on rat liver mitochondria, 578
recovery from, 562-63
on serum oxidase, 556
survival curve, 568
versus x-radiation, 562-63, 567
on x-rayed yeast, 568
United States-Euratom program
fuel cycle costs
table of, 484, 485
United States fast-reactor program
Clementine, 441
EBR-I, 441, 460, 465-66, 467
EBR-II, 441-42, 443, 464, 466, 468
Enrico Fermi Atomic Power Plant, 442, 466
LAMPRE, 442, 468
Universal Fermi interaction, 61-64, 66-67, 89, 93, 140-55
charged vector meson
exchange of, 66
objection to, 76
pionic effects in, 150-53
primary, 66-67
see also Beta coupling
- Uranium
angular distribution effect
in 147-Mev bombardment, 280-81
burn-up requirements
in nonbreeder reactors, 478
compounds
in fuel development, 483
cores
in reflectors, 449
excitation curve
related to alpha-particle measurements, 273
extraction of, 226, 232, 233
half life of, 248
production rate, 479-80
projected requirements for, 476, 478-79
reserves of, 480
spontaneous fission of, 246
Z²A
of isotopes, 267, 268, 269
- Uranium 233
extraction of, 227, 228, 241
as reactor fuel, 437
for thermal systems, 438
- Uranium 235
content of uranium, 445
fission rate distributions, 453
fission widths in, 263, 264
mass distribution, 310-11, 318
as reactor fuel, 437, 459
thermal cross section, 265
thermal-neutron fission of, 293, 294, 298, 307, 308, 319
- Uranium 238
carbon cross sections on, 274
fast-neutron fission
cross section, 277-79
as fertile material, 459, 473
fission cross section for, 181
mass-yield curve for, 180
450-Mev fission of, 184
as reactor fuel, 437
- V
- V-A Law, 127-30, 140, 141, 152, 155
for muon decay, 147-49
Vernier chronotron, 361
Vertebrate radiobiology, 493-519
postirradiation regeneration
in fetal rats and mice, 500
see also Embryo; and Radiation effects
- Vicia roots
aberrations of, 572
aberration yield, 570

chromosome breakage, 569
radiosensitivity of, 557-58, 559

Virus structure
inferred
from radiation experiments, 563-64

W

Weak interactions; see Beta coupling; and Beta decay

Weak vector interaction
and electromagnetic interactions, 73
nonrenormalization of, 73

X

X-irradiation
of early mouse embryo, 503
"normal," 503, 517
of fetal rat, 500
growth rate, 500

versus gamma radiation, 574
-induced breaks in chromosomes, 569-70
-induced crossing over, 572-73
of multicomplexes, 567
of mung bean roots, 579
of muscle, 579
of pregnant mouse, 502
RBE versus fission neutrons, 573
ring losses after, 573
as shock factor, 516
survival curve, 568
of yeast, 568

Y

Yeast
bombardment of dry cell, 564
irradiated cultures
constituents of, 577

morphology of, 582-83
radiosensitivity of, 543, 559-60
recovery from radiation, 562-63
retentivity effects in, 580
survival curves, 560, 564
x-rayed
ultraviolet reactivation of, 568

Z

Z^2A , 246-47, 249, 266
of compound nucleus, 267
and fission barrier, 268
fission-fragment anisotropy of, 333
and fission threshold, 260
in liquid-drop model, 252-53
Zephyr critical assembly, 445-46, 447, 452, 454
Zeus critical assembly, 445-47, 452